Final Report

Natural and Artificial Systems for Recharge and Infiltration
"NASRI"

KompetenzZentrum Wasser Berlin (KWB gGmbH), Cicerostr.24, D-10709 Berlin, Germany

KOMPETENZZENTRUM
Wasser Berlin

The NASRI Team (members in each group in alphabetical order)

Dr. Birgit Fritz;

KompetenzZentrum Wasser Berlin (KWB gGmbH)

Andreas Deffke, Heidi Dlubek, Dr. Uwe Dünnbier, Patricia Luck, Elke Wittstock;

Berliner Wasserbetriebe

Dr. Gudrun Massmann, Bettina Ohm, Prof. Dr. Asaf Pekdeger, Dr. Thomas Taute;

Free University of Berlin, Dept. of Hydrogeology

Janek Greskowiak, Dr. Ekkehard Holzbecher, Dr. Christoph Horner, Prof. Dr. Gunnar Nützmann, Bernd Wiese;

Institute for Freshwater Ecology and Inland Fishery & Humboldt University of Berlin, Dept. of Geography

Britta Fanck, PD Dr. Thomas Heberer, Andy Mechlinski;

Technical University of Berlin, Dept. of Foodchemistry

Steffen Grünheid, Prof. Dr. Martin Jekel;

Technical University of Berlin, Dept. of Water Quality Control

Dr. Uta Böckelmann, Bianca Conradi, Prof. Dr. Ulrich Szewzyk;

Technical University of Berlin, Dept. of Microbiology

Dr. Hartmut Bartel, Dr. Ingrid Chorus, Dr. Gesche Grützmacher, Gabriele Wessel;

German Environmental Agency (UBA), Dept. of Water treatment

Dr. Dr. Halim Dizer, Prof. Dr. Juan Lopez-Pila, Dr. Regine Szewzyk;

German Environmental Agency (UBA), Dept. of Microbiology and Parasitology

Temporarily involved (e.g. Diploma thesis, student work, expert assistance and scientific exchange):
Marc Adam, Dr. Anat Bernstein, Dr. Frank Engelmann, Marcel Fischer, Susanne Frenzel, Charlotte Gahring, A. Hagemann, Uwe Hübner, Andrea Knappe, Dr. Claus Kofahl, Kerstin Leipnitz, Eberhard Licht, Oliver Menzel, Juliane Mohaupt, Cornelia Mundt, Alexander Nogeizig, Silke Phüringer, George Piques, Katalin Prausa, Doreen Richter, Stephanie Rögler, Jeannette Rümmler, Andrea Springer, Michael Voigt, Daniel Wicke, Philipp Wolf, Thomas Wollenhaupt, Sebastian Zülke.

Acknowledgements:

Contents:

This report consists of seven parts representing the results of the different working groups.

Introduction

Bank filtration, that is the abstraction of superficial groundwater in the proximity of and originating from nearby surface water, has long been used for drinking water preparation. Namely in Germany this technique is being used widely and it provides about 16% of the raw waters used for drinking water preparation [Kühn and Müller, 2000]. In particular, river bank filtration has a long tradition along the river Rhine [Sontheimer, 1980] and the river Elbe [Grischek et al., 2001]. Very recently, bank filtration meets growing interest worldwide as a (pre-) treatment technology in drinking water preparation that may be equally sustainable and cost effective, for example in the United States. Its importance on a global scale is expected to grow in as much, as groundwater resources decline and water demand continues to increase.

The quality of raw water obtained by bank filtration depends strongly upon the quality of surface waters, the hydrological and (hydro-) geochemical conditions of the subsurface and the residence time of the infiltrated waters. Moreover, the river sediment may significantly influence the groundwater quality [Doussan et al., 1997]. Physical processes (filtration, mixing. dilution), physico-chemical processes (dissolution and precipitation, ion-exchange and adsorption) and biological processes (transformation, oxidation and mineralization, reduction) alter the quality of the former surface water during passage of the subsurface [Kühn and Müller, 2000]. Moreover, bank filtration may act as a barrier against shock loads of contaminants, e.g. from accidental spills of chemicals into river waters [Malle 1994; Kühn and Müller, 2000].

Several benefical effects of bank filtration have been reported, among them reductions in COD, BOD, DOC and AOC [Kühn and Müller, 2000], a reduction of the content and an improved treatability of humic matter [Gerlach and Gimbel, 1999], reduction of microbes [Miettinen et al., 1997], removal of viruses [Havelaar et al., 1995], and reduction of trace organics (AOX), [Kühn and Müller, 2000], EDTA, certain naphthalene sulfonates, some pharmaceutically active substances (PhACs) [Sacher et al., 2001], fragrances and aromatic hydrocarbons [Juttner , 1999]. However, removal of trace organics need not be complete [Kühn and Müller, 2000] and infiltration of water via a river bank may become a source of groundwater contamination with trace organics [Mathys, 1994].

Despite considerable experiences with the use of (river) bank filtration in Germany [Jülich and Schubert, 2001] and the Netherlands [Hiemstra et al., 2001], present knowledge upon the processes occurring during bank filtration and their effects on water quality is still fragmentary and characterized by a 'black box'-approach. This limited understanding hampers:

- the optimisation of existing bank filtration processes,
- identification of surface water quality problems that cannot be eliminated by bank filtration,
- forecasts of the future development of bank filtration, namely under changing environmental and operational conditions,
- assessment of the role of bank filtration in partially closed water cycles,

- the identification of potential new sites suited for bank filtration and
- the assessment of raw water quality obtainable at other sites.

Thus, a concerted research action such as the one proposed in the following will improve understanding of bank filtration as a prerequisite for the future development of this natural and multi-barrier technology.

1.2   The Berlin Situation

Bank filtration has always been an important factor in the public water supply of the City of Berlin, which started in the second half of the 19th century with water works close to the River Spree and the Lake Tegel. Until today, bank filtration and groundwater recharge are inevitable components of the water supply, as all drinking water originates from local sources. About 75 % of the 220 Mill. m^3 per year of drinking water originate from bank filtration and water infiltration. All raw waters are aerated and passed through rapid sand filtration for removal of iron and manganese. There is no further treatment, neither for the removal of organic matter nor for disinfection prior to the distribution of the drinking water. Thus, a proper functioning of the natural filtration steps is essential to maintain the high drinking water quality in Berlin.

Recent studies on the hydrogeology and process performance of bank filtration in the Berlin area have shown, that the conditions of banks and underground passages vary widely, due to local differences and the operation of groundwater abstraction wells. Especially the Lake Tegel is an interesting case, due to the input of domestic and well-treated sewage with low dilution rates.

Recent investigations of the Technical University of Berlin in close cooperation with the Free University of Berlin on the fate of organic compounds have indicated, that the major environmental factors for the removal of trace organic pollutants are the retention time (range 1 – 6 month), the redox conditions and the level of organics in the surface water. The field observations are, however, very difficult to interpret due to varying water levels, variable redox status and poorly known flow-patterns.

It is presently not possible to quantify and describe the extent and kinetics of responsible mechanisms, especially concerning the biodegradation of trace organics. For example the antibiotic sulfmethoxazole is present in the lake at 250 ng/L and requires up to 3 – 4 months retention time (aerobic and anoxic conditions) to be completely removed. However, some bank filtration sites or groundwater recharge systems do not guarantee these long retention times, but sometimes less than a month. Other measures to control the trace organics in the Berlin water supply are, besides source control strategies, not available and thus, the underground passage is the only decisive step for the removal of poorly degradable contaminants.

1.3 Aims of the Research Program

As outlined above there is a clear need to understand and quantify the purification processes in bank filtration and groundwater recharge for those anthropogenic pollutants, which are difficult to avoid at the source and which pass through the wastewater treatment plants. Field studies are underway, but are not sufficient to draw the necessary conclusions for the suitable design and optimal operation of both important treatment and storage processes (using natural mechanisms to a wide extent).

A critical case of Berlin is the Lake Tegel with an indirect potable reuse system, which is also an interesting site for the worldwide aspects in water reclamation, applying soil-aquifer-treatment or aquifer storage and treatment. Other surface waters are either eutrophic with cyanotoxin problems or are containing variable amounts of treated domestic wastewater or run-off with pathogens.

This research program will cover traditional as well as novel requirements of drinking water preparation, that evolve from microbiological as well as chemical loads of surface water and which are to some extent, caused by the considerable portion of municipal wastewater in the surface waters of Berlin.

The provision with hygienically safe drinking water that is free from pathogens was one of the driving forces of public water supply and drinking water preparation. Recent reports outlined, that the removal efficiency for bacteria and viruses previously attributed to a soil or underground passage is not provided in all cases. The reasons for that are, however, yet unknown. As the surface water used for bank filtration is always more or less faecally contaminated, raw water hygiene remains an issue of investigation.

The growth of cyanobacteria in eutrophic surface waters and the release of cyanobacterial toxins (i.e. 'cyanotoxins') is usually seen as a problem of bathing water quality. However, the indirect use of surface water for drinking water preparation calls for a complete removal of cyanotoxins in bank filtration, of which the microcystins have been shown to be the most relevant group for Berlin. As microcystins are mostly contained within the cyanobacterial cells their removal by (bank) filtration processes may strongly be influenced by processes such as cell death and cell lysis.

In recent years, polar and poorly degradable organic pollutants are gaining increasing attention as a factor of water quality. Industrial chemicals as well as household products, certain pesticides and their polar metabolites and pharmaceutically active compounds are among these polar pollutants. These compounds are not necessarily removed in wastewater treatment and in drinking water preparation processes. In a water system like in the City of Berlin with its partly closed water cycles, the concentration of these compounds may increase slowly but continuously.

Dissolved organic matter levels may also increase in partly closed water cycles as effluent organic matter adds to the natural (groundwater) background. DOC removal in bank filtration is of particular importance when drinking water disinfection has to be performed. The load of organohalogens (AOX) in surface waters of Berlin has very different properties, depending on its

origin: besides a 'traditional' pool of chlorinated organics (AOCl) persistent iodinated compounds (AOI, x-ray contrast agents) are released from hospitals, whereas brominated and potentially labile organics (AOBr) are formed seasonally in the lakes.

One of the main research topics is the development of guidelines for optimal bank filtration and artificial recharge performance and design. In the past, knowledge of bank filtration and artificial recharge in Europe was growing and growing and is used widely, but no systematic analyses were done. Computer models and conceptual modelling can be used in order to understand the flow regime in the vicinity of well galleries taking into account the hydro-geological conditions, sediment layering and pumping regimes. Using the same concepts and simulation software, models can also be used for designing new well galleries or to manage existing ones with higher efficiency. When models of hydro-dynamical transport mechanisms are coupled with reaction models (biochemical, geochemical etc.) systematic model studies can be carried out to design well galleries for safe and reliable water supply using the natural cleaning mechanism of the existing aquifer system. Another high potential of these system analyses might be the possibility of simulating the behaviour of substances in the aquifer system. Every year new substances occur in the aquatic system and their reduction potential is not well known. Experiences through column studies and field investigations are often established and can be verified with models using changing biochemical and geochemical conditions. This allows us to implement this more general information within other hydro-geological systems that function as water supply systems.

1.4   Facilities for studies

The associated partners were able to provide all analytical capacities necessary for this project and experimental facilities in laboratory-scale (soil columns), an experimental field site (Marienfelde) and lake sites (Tegel and Wannsee) for studying bank filtration. For selected studies, an infiltration site (Tegel) was used. All three disciplines, hydrogeology, microbiology and chemistry, were involved in experiments at all four sites. It can be stated that the availability of all these facilities is unique in the world and provides excellent logistical conditions for research program.
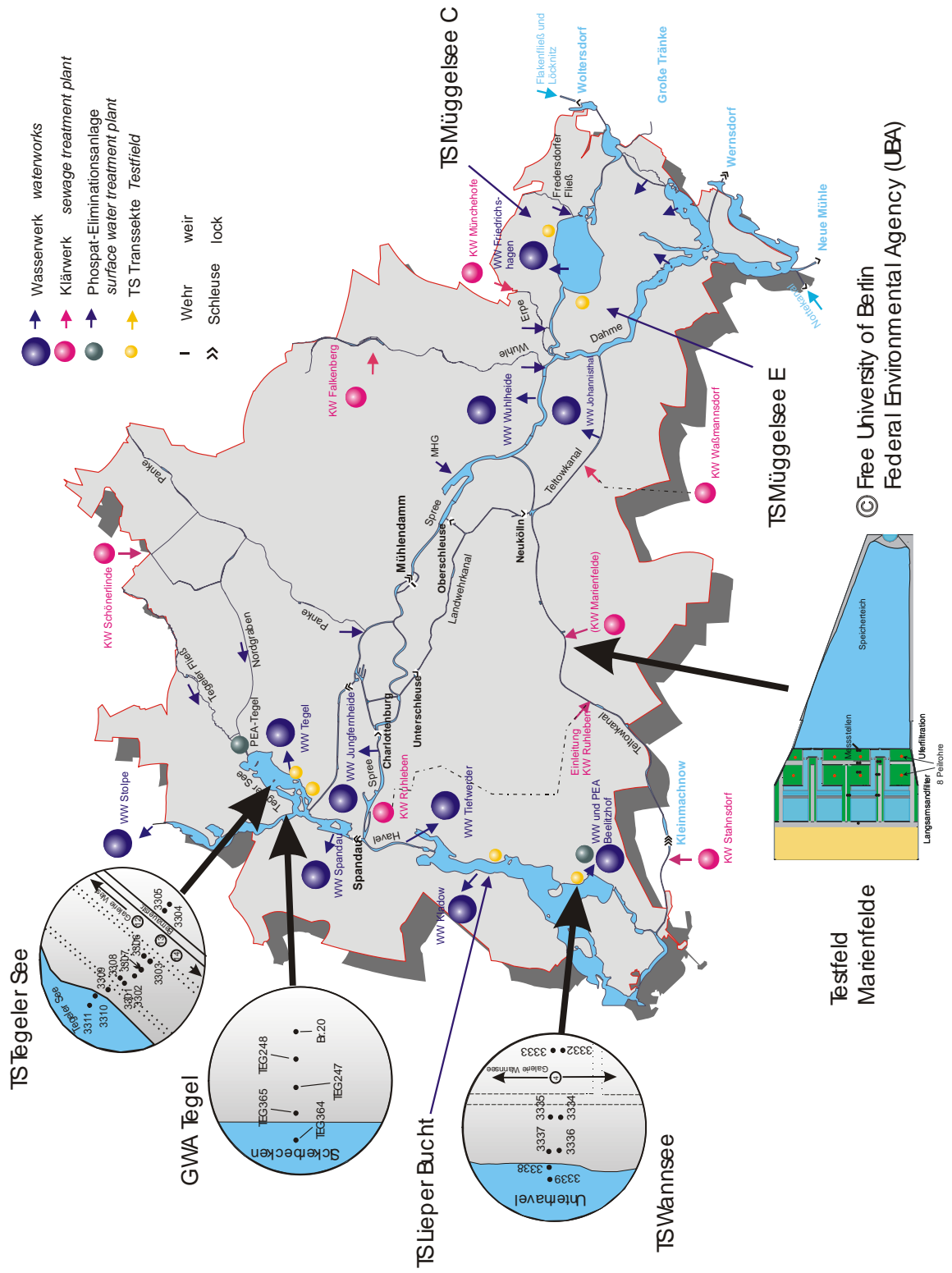
Figure 1 Water System of Berlin and Field sites used within the NASRI Project

1.3.1 Laboratory facilities

The studies in laboratories were either column-systems or related batch-experiments and are feasible and simple approaches for parameter studies on sorption or/and slow biodegradation of selected compounds.

At the UBA a total of 8 **large sediment columns** (description can be find in Part 4 "organics") of 5 m length was used there, that could be coupled in series to study long-term alterations in the groundwater over a period of several months. All column systems were equipped with systems to control the redox-conditions. These laboratory columns were used to study the removal of and metabolite formation from trace organic contaminants), to study the behaviour of bacteria and viruses, to study effects of operational conditions and to obtain basic data for the modelling.

Small column systems were used to study the influence of redox conditions and temperature effects (see also Part 4 "organics) on degradation reactions and special cores were used in clogging column experiments (see also Part 1 "hydrogeo") to observe the influence of the clogging zone. Investigations on the behaviour of bacteria and viruses often need special investigation, that why the scientist of the "bacteria" group used additionally their own column system (see Part 6 "bacteria").

1.3.2 Experimental site

The experimental site of the UBA at Berlin-Marienfelde consists of a storage pond with subsequent bank filtration and slow sand filtration (Figures 2 – 3) facilities (see also Part 5 "algae").
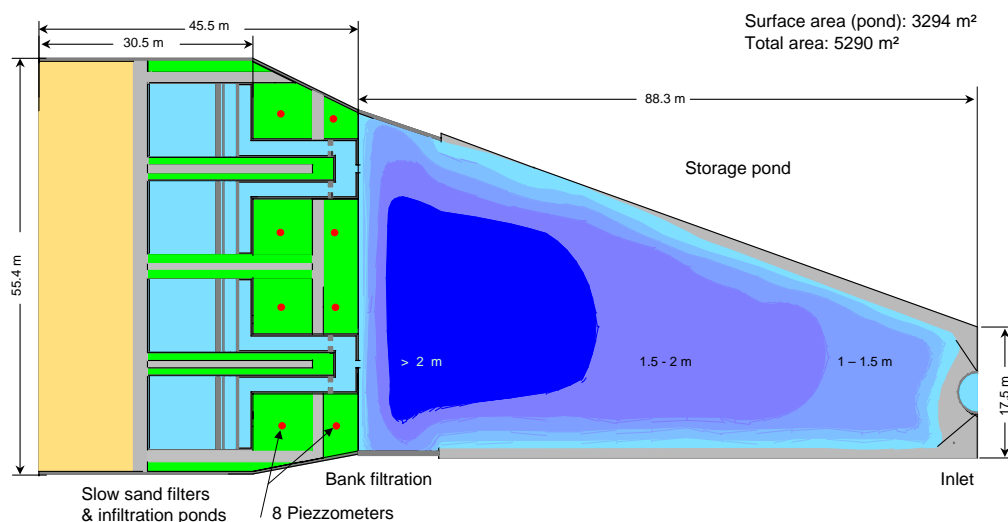

Figure 2: **Areal view of the storage pond system**

The storage pond system has a capacity of 7000 m^3 and a surface area of about 5,300 m^2 (Figure 1). From the storage pond, the water is conveyed into two slow sand filters and two open infiltration basins, each with a surface area of about 75 m^2 (Figure 1). Additionally, two subsurface

drains at a depth of about 5 m and 14 m and 36 m away from the bank line allow collecting bank filtrate. The parameters pH, O_2, electrical conductivity, temperature, redox potential, TOC, TN_b and fluorescence are measured and analysed continuously in flow-through mode controlled by a PC. The water from the drainage systems can be either pumped back to the inlet of the storage pond (recirculation) or discharged to the sewerage system (flow-through). The intake, and hence the flow, can be regulated via the pumping rate. Minimal flow rates are a few hundred litres per hour the achievable maximum is 40 m^3/h. The subsoil within the area of the bank filtration plants as well as the filling of the filter tanks consist of medium- or fine-grained sands and gravel of good permeability (average k_f value: $2*10^{-3}$ m/s). Accordingly, flow rates of between 0.5 m/d and 6 m/d can be set depending on the output of the pumps.
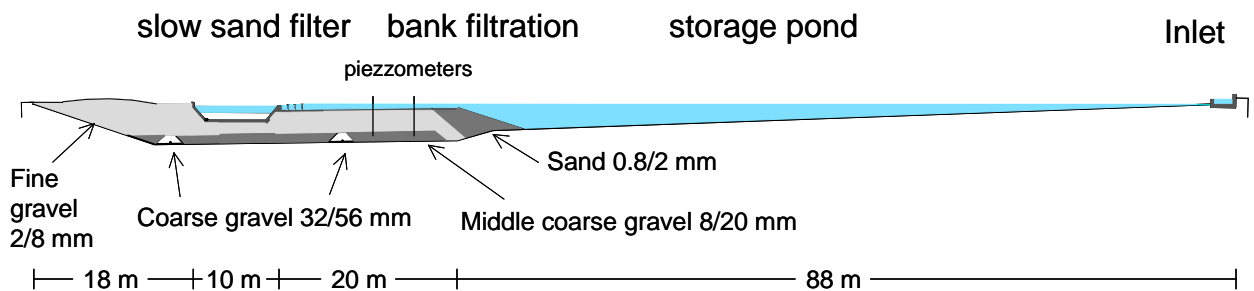
Figure 3: Cross section through the storage pond system.

As the facility is sealed towards the environment, experiments on the behaviour of substances that are hazardous to water during bank or slow sand filtration can be carried out on a field scale without any adverse environmental impacts. On the other hand, external conditions (scale factors, weather conditions) largely match those found in the real environment.

Figure 4: Schematic cross section through the bank filtration passage:

Approaches were made in the slow sand filter facilities and in enclosures which were installed in one of the open infiltration ponds (see Part 5 "algae", page 95). They were constructed as semi-technical scale filter columns that allowed experiments on a smaller scale and therefore under conditions easier to change and to control 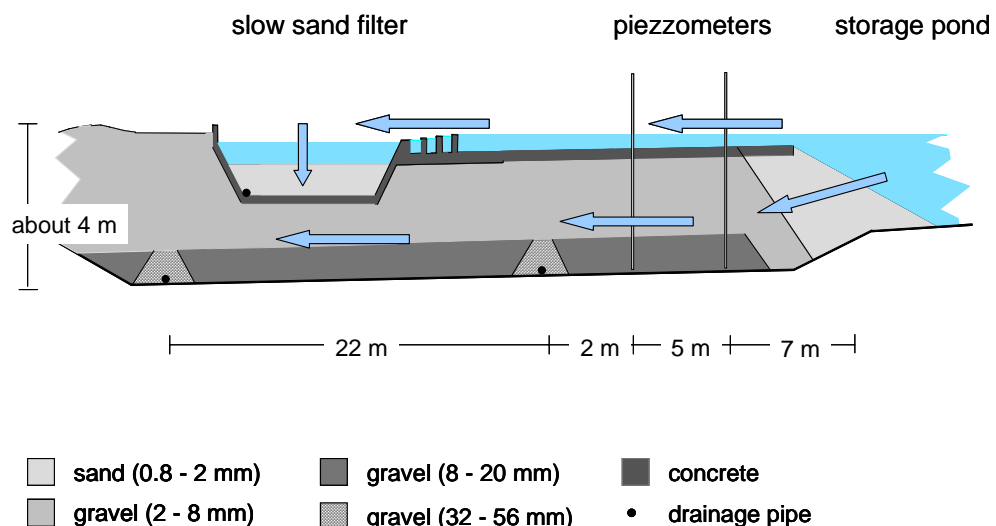than in the technical scale slow sand filters. Knowing that the travel times from the storage pond to the drain of the artificial bank filtration system are to fast led to the decision to do all experiments without the storage pond.

1.3.3   Lake Sites

Field studies took place at the banks of two surface waters in Berlin, the Lake Tegel located in the north-west of the city and the Lake Wannsee in the west. As previously mentioned, Lake Tegel is characterized by comparatively high portions of municipal wastewater effluents (around 30 % on average), that made this lake ideally suited to study specific effects of partly closed water cycles. Lake Wannsee is part of the River Havel and is situated downstream of the City of Berlin. Here, wastewater contents vary biannually due to the change of discharge of the wastewater treatment plant Berlin Ruhleben. Detailed knowledge on the hydrological situation at both sites was available and provided an ideal basis for modelling and for further investigations. There are numerous monitoring wells for sampling; upon completion up to 20 wells were available at each site, allowing a high spatial resolution in sampling. A detailed description of both bank filtration field sites and the artificial recharge transect with all the new observation wells can be find in Part 1 "hydrogeo".
The surface waters were also investigated and an extensive database is available.

Lake Tegel:

At this site, the bank filtrate is split into two layers, one of which stays close to the surface above the marl-layer under aerobic conditions. The other part of the filtrate penetrates deeper into the subsurface into an oxygen-free layer below the marl, where the drinking water well is located (well 13). Both layers can be sampled independently. Travel times of the groundwater are about 3 - 4 months for a 100 meters distance. Owing to a thick mud layer with low hydraulic conductivity at the lake sediment the majority of bank filtrate passes through the lakeshore.

Lake Wannsee:

Thw shallow groundwater layer at this site is well isolated from the deeper layers. This was confirmed by analysing the quality of the deep groundwater, which showed no measurable influence by surface water. Consequently, only the shallow wells were employed in this investigation. In addition, a new transect was drilled in the surrounding of well 3, who is on the right hand site of well 4. Like at Lake Tegel, a thick mud layer hampers infiltration into the lake bottom and the main flow path is through the lakeshore. The travel time to the raw water well (Br 4) was estimated to be 1 - 2 months.

1.3.4 Artificial Groundwater Recharge Facilities

The BWB are operating several recharge systems, either with untreated or pre-treated surface waters (Tegel, Spandau). The consortium has investigated quality aspects of groundwater recharge systems parallel to bank filtration. These investigations were performed at the infiltration site 'Saatwinkler Galerie' at Tegel Water Works. This groundwater aquifer consists of one sandy aquifer with partly embedded till layers.

A scheme of all sites is included within the report of the working group from the Freie University (Part 1 "hydrogeo").

1.5   Data management

Sampling of groundwater, surface water and drinking water from the abstraction wells started in May 2002 and has been continued monthly until August 2004. The sub department Services of the Berliner Wasserbetriebe organized and coordinated the sampling including arrangements for the management of facilities at the artificial recharge pond whereas the colleagues from the Laboratory department were responsible for the monthly sampling at the bank filtration field sites Tegel and Wannsee. All standard analyses were done at the Laboratory of the Berliner Wasserbetriebe. Special analyses (e.g. Isotopes, viruses, microcystin, some PhAC and Antibiotics) were carried out from the working groups of the Universities and the UBA.

The drilling of new boreholes at the field sites has been supported and financed from the Berliner Wasserbetriebe as well as the installation of several measurement devices.

The achieved data has been archived in the data base GeoDin$^{©.}$ This database allows combining chemical data, regional fixed geological data, the technical design and well construction data. The whole database is stored at the KompetenzZentrum Wasser Berlin.

1.6   Scientific Integration

With respect to our overall aim of developing guidelines more general knowledge of the bank filtration system is necessary. Therefore the modeling aspect was central in the project integration. All interpretation, data and measurements resulting from the investigations in Berlin were included into models. At the same time different systems (for example with different geology, management, water quality, climate) was included step by step to ensure that the acquired results are not specific for Berlin. In the end simulations could be made in the future for different systems worldwide.
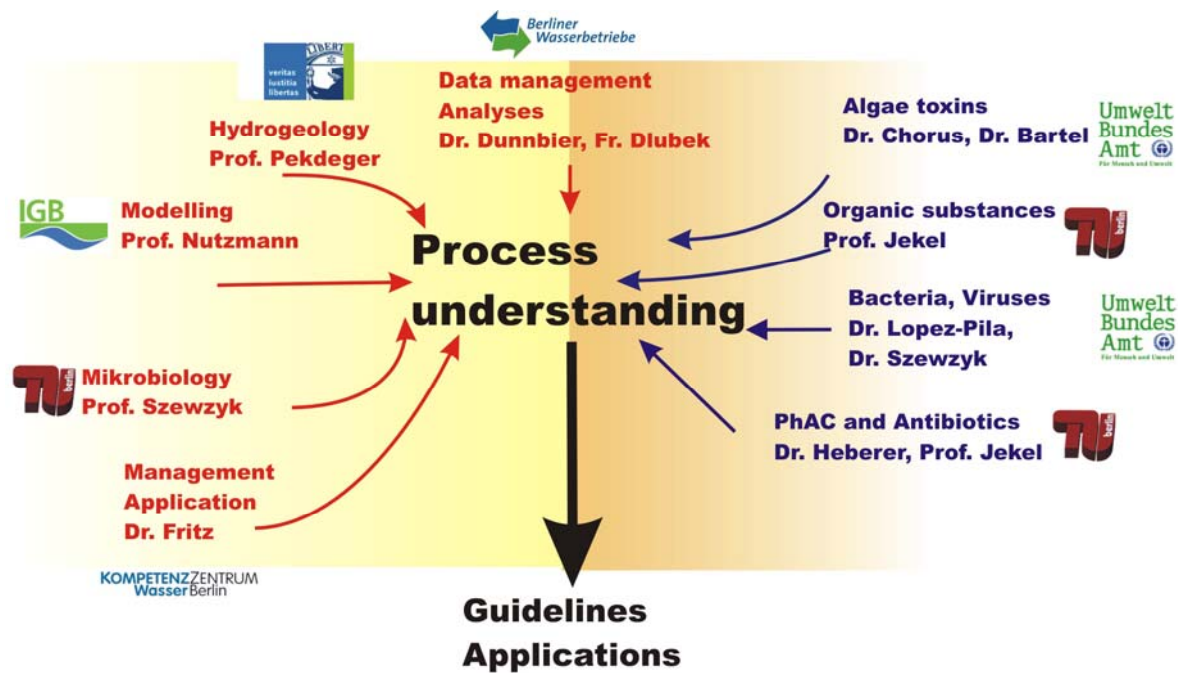
Figure 5: Scientific integration

1.7 References

Doussan C., Poitevin G., Ledoux E. and Delay M. (1997) River bank filtration: modelling of the changes in water chemistry with emphasis on nitrogen species. *J. Contam. Hydrol.* **25**, 129 - 156.

Gerlach M and Gimbel R. (1999) Influence of humic substance alteration during soil passage on their treatment behaviour. *Water Sci. Technol.* **40** (9), 231 - 239.

Grischek T., Worch E. and Nestler W. (2001) Is bank filtration under anoxic conditions feasible? In: *Proceedings of the International River Bank Filtration Conference* (Jülich W. and Schubert J., Eds.), IAWR Rheinthemen **4**, 57 - 65.

Havelaar A.H., Vanolphen M. and Schijven J.F. (1995) Removal and inactivation of viruses by drinking water treatment processes under full-scale conditions. *Water Sci. Technol.* **31** (5-6), 55 - 62.

Hiemstra P., Kolpa R.J., van Eekhout J.M.J.M., van Kessel T.A.L., Adamse E.D. and van Paassen J.A.M. (2001) Natural recharge of groundwater: bank filtration in the Netherlands. In: *Proceedings of the International River Bank Filtration Conference* (Jülich W. and Schubert J., Eds.), IAWR Rheinthemen **4**, 67 - 79.

Jülich W. and Schubert J., Eds. (2001) *Proceedings of the International River Bank Filtration Conference*, IAWR Rheinthemen **4**, 309 p.

Juttner F. (1999) Efficiacy of river bank filtration for the removal of fragrance compounds and aromatic hydrocarbons. *Water Sci. Technol.* **40** (6), 123 - 128.

Kühn W. and Müller U. (2000) Riverbank filtration - an overview. *Journal AWWA* **92**, 60 - 69.

Malle K.G. (1994) Accidential spills - frequency, improtance, control and coutermeasures. *Water Sci. Technol.* **29** (3), 149 - 163.

Mathys W. (1994) Pesticide pollution of ground and public drinking waters caused by articial groundwater recharge or bank filtration. *Zentralbl. Hyg. Umweltmed.* **196**, 338 - 359.

Miettinen I.T., Vartiainen T. and Martikainen P.J. (1997) Changes in water microbial quality during bank filtration of lake water. *Can. J. Microbiol.* **43**, 1126 - 1132.

Sacher F., Brauch H.-J. and Kühn W. (2001) Fate studies of hydrophilic organic micro-pollutants in riverbank filtration. In: *Proceedings of the International River Bank Filtration Conference* (Jülich W. and Schubert J., Eds.), IAWR Rheinthemen **4**, 139 - 148.

Sontheimer H. (1980) Experience with river bank filtration along the river Rhine. *Journal AWWA* **72**, 386.

NASRI: Natural and Artificial Systems for Recharge and Infiltration – Project summary

Type of Project: Project of the Kompetenzzentrum Wasser Berlin in cooperation with the Berliner Wasserbetriebe and six scientific working groups coming from different Berlin Research Institutes and Universities.

Duration: 2002 – 2005

Budget: cash 3,3 Mio € , total 6,89 Mio € (incl. overhead and in-kind contribution),

Funding: Berliner Wasserbetriebe and Veolia Wasser

Partner (Institution/responsible project leader/topic):

Umweltbundesamt (German Federal Environmental Agency)/ Dr. Chorus, Dr. Bartel
Retention and elimination of cyanobacterial toxins (microcystins) through artificial recharge and bank filtration

Umweltbundesamt (German Federal Environmental Agency)/ Dr. Lopez-Pila, Dr. Szewzyk
Using bacteriophages, indicator bacteria, and viral pathogens for assessing the health risk of drinking water obtained by bank filtration.

Berliner Wasserbetriebe/ E. Wittstock, H. Dlubek
Datamanagement, sampling, analyses, interpretation

Technische Universität / Prof. Jekel
Organic substances in bank filtration and artificial ground water recharge – process studies.

Technische Universität / Prof. Jekel , Dr. Heberer
Occurrence and fate of drug residues and related polar contaminants during bank filtration and artificial recharge.

Freie Universität Berlin / Prof. Pekdeger
Hydrogeological - hydrogeochemical processes during bank filtration and ground water recharge using a multi tracer approach.

IGB Leibniz-Institute of Freshwater Ecology and Inland Fisheries/ Prof. Dr. Nützmann
Integrated modelling concepts for bank filtration and artificial ground water recharge processes: coupled ground water transport and biogeochemical reactions.

Motivation and Aims of the Research Program

The main objective of the NASRI project (as expressed in the project proposal, 2001) was to develop a comprehensive process understanding to ensure the long term sustainability of bank filtration and artificial recharge keeping in mind future requirements and threats. In concordance with the stakeholders (Aims and needs of the BWB/Veolia, 2001), the identification of potential new sites and demonstration of potential transferability and application of results worldwide was added to the objectives.

1. A clear need was identified to <u>understand and quantify the purification processes in bank filtration and groundwater recharge</u> *(Process understanding)* in general and especially for those anthropogenic pollutants which are difficult to avoid at the source

and which pass through the wastewater treatment plants. This included the following agents:

  a. The growth of cyanobacteria in eutrophic surface waters and the release of <u>cyanobacterial toxins</u> ('cyanotoxins') is usually seen as a problem of bathing water quality. However, the indirect use of surface water for drinking water preparation calls for a complete removal of cyanotoxins in bank filtration.For Berlin the most relevant group of cyanotoxins are the liver-toxic microcystins. As microcystins are mostly contained within the cyanobacterial cells their removal by (bank) filtration processes may strongly be influenced by processes such as cell death and cell lysis.

  b. The provision with hygienically safe drinking water that is free from pathogens was one of the driving forces of public water supply and drinking water preparation. The removal efficiency for <u>bacteria and viruses</u> previously attributed to a soil or underground passage is not provided in all cases. As the surface water used for bank filtration is always more or less faecally contaminated, raw water hygiene remains an issue of investigation.

  c. The behaviour of <u>polar and poorly degradable organic pollutants</u> in BF and AR: Industrial chemicals as well as household products, certain pesticides and their polar metabolites and pharmaceutically active compounds are among these polar pollutants. These compounds are not necessarily removed in wastewater treatment and in drinking water preparation processes.

  d. <u>Dissolved organic matter levels</u> may also increase in partly closed water cycles as effluent organic matter adds to the natural (groundwater) background. DOC removal in bank filtration is of particular importance when drinking water disinfection has to be performed.

  e. The load of <u>organohalogens</u> (AOX) in surface waters of Berlin has very different properties, depending on its origin: besides a 'traditional' pool of chlorinated organics (AOCl) persistent iodinated compounds (AOI, x-ray contrast agents) are released from hospitals, whereas brominated and potentially labile organics (AOBr) are formed seasonally in the lakes.

2. The <u>development of planning support tools for optimal bank filtration and artificial recharge performance and design **(Transferability)**.</u>

  a. Computer models and conceptual modelling can be used in order to understand the flow regime in the vicinity of well galleries taking into account the hydro-geological conditions, sediment layering and pumping regimes.

b. Using the same concepts and simulation software, models can also be used for designing new well galleries or to manage existing ones with higher efficiency.

c. When models of hydro-dynamical transport mechanisms are coupled with reaction models (biochemical, geochemical etc.) systematic model studies can be carried out to design well galleries for safe and reliable water supply using the natural cleaning mechanism of the existing aquifer system. Another high potential of these system analyses might be the possibility of simulating the behaviour of substances in the aquifer system.

d. Experiences through column studies and field investigations can be verified with models using changing biochemical and geochemical conditions.

Facilities used for this project:

1. Experimental facilities in laboratory-scale: These laboratory columns were used to study the removal of and metabolite formation from trace organic contaminants, to study the behaviour of bacteria and viruses, to study effects of operational conditions and to obtain basic data for the modelling. This included:

   a. long soil columns to study long-term alterations in the groundwater over a period of several months

   b. short soil columns to study the influence of redox conditions and temperature effects (see also Part 4 "organics) on degradation reactions

   c. clogging column to observe the influence of the clogging zone

   d. batch experiments to be able to distinguish between adsorption and microbial degradation for substances where basic information is missing

3. Experimental field site including

   a. slow-sand filters

   b. enclosures

   c. artificial river system

4. Transects at two lake sites (Tegel and Wannsee) for studying bank filtration processes during the natural flow path

5. Transect at one artificial recharge site (Tegel) to study the differences between BF and AR.

All three disciplines, hydrogeology, microbiology and chemistry, were involved in experiments at all four sites. The availability of all these facilities is unique world-wide.

Main results

An extraction of main results of the research groups and overall interpretations are given in the following.

Process understanding: The most important result concerning process understanding is the definition of the influencing factors for the removal of substances. The NASRI results shows that the key factors are flow velocity, travel time, redox status and temperature.

- It can be stated that it is very important to determine <u>the flow paths and velocities at each individual site prior to investigations.</u>

- A reliable determination of the travel times at the field sites is only possible with the combination of different site appropriate tracers. The most reliable tracers for short travel times determined by the shift of seasonal variations are stable isotopes and trace substances (depending on waste water influence) with a monthly resolution. In Berlin stable isotopes, boron, gadolinium, chloride, potassium, are suited the best for travel time calculation.

- Tritium/Helium age dating has proven to be an adequate method for infiltrate of an age larger than half a year.

- Persistent trace substances can give additional information on the age of the infiltrating water, especially if surface water concentrations over time are known.

- Different <u>flow paths</u> can be established depending on geology, clogging zone establishment, well field design and management. The age of the different water types flowing to the drinking water well can therefore vary strongly. Travel times of several months ("young" bank filtrate) can be found in the same system with "older" bank filtrate with an age of up to serveral decades ("old" bank filtrate).

- The mixing of "young" and "old" infiltrate buffers locally and temporally restricted contaminations of lake water and gives therefore an additional safety.

- Usually <u>redox zones</u> are stratified horizontally in bank filtration systems (from the lake towards the well). In Berlin these stratification is established vertically (from the top to the depth) which is a result of both the vertical age stratification caused by the local hydrogeology which enables the water to infiltrate at the clogged shores only while inhibiting infiltration in the lake middle as well as of the water table oscillations triggered by the well pumping regime. *Important remark: Berlin lakes are very flat with slow water velocities and impermeable lake bottom sediments. This might be also the case for big rivers or lakes with less permeable sediments as it can be found often worldwide.*

- The redox system is influenced by the input of oxygen and the temperature of the infiltrating lake water.

- o Oxygen is introduced into the aquifer with the fluctuation of the depressing cone and not only brought in with the infiltrating water. This can be regulated with an adjusted well field management.
- o Very low temperatures lead to more aerobic redox conditions. Both very low and also high temperatures can have a negative effect on the cleaning capacity of the underground passage. Algae toxins as well as some organic trace substances show the best elimination at a medium temperature of about 15 °C, a long and cold winter can lead to a breakthrough of substances if the travel time is nor long enough. Hot summer temperatures can lower the degradation rate.

- The elimination of most substances is influenced primarily by the redox processes (see table) which can be regulated and designed in artificial recharge plants (in contrast to bank filtration sites) by using the pond implicating seasonal changes in well field management. For example the pond can be used only in winter time with faster travel times (higher pumping rates) resulting in better reduction of substances which show favorable degradation at aerobic conditions.

Fate and behavior of cyanotoxins, organic trace substances and pathogens: the investigation of the fate and behavior of those substances was needed in order to asses the long term sustainability of bank filtration systems.

- Cyanotoxin degradation is very efficient in bank filtration and AR systems.
    - o Redox conditions play a less important role than expected. Anaerobic degradation rates can be similar to those obtained under aerobic conditions.
    - o Temperature is the most important factor with the best elimination rates at temperatures greater than 15° C.
    - o The working hypothesis that a "worst-case" situation would be "fresh" sand (no earlier contact with toxins) and high filtration rates was falsified: surprisingly, degradation was better than expected and irreversible sorption to particles is proposed as explanation (requiring further verification).
    - o Elimination rates for cell-bound toxins are usually very high (> 99% within the first 10 cm), however, in some cases particle transport of cyanobacterial cells into the substrate was demonstrated and this led to longer term transport of intra-cellular MCYST.
    - o No accumulation of MCYST was found with cyanobacterial cells on the sediment surface.
    - o Microbiological degradation is the main elimination process. Half lives ranged from a few hours to days.

- o No MCYST was found in bank filtrate after more than two weeks of travel time.
- o Favorable conditions for MCYST elimination proved to be: low cyanobacterial cell density (i.e. biovolume < 5 mm³/L), sandy soil (medium to fine sand), intact clogging layer, temperatures > 10°C, travel time > 10 days.

- Organic trace substances do have different favorable conditions for elimination (see table).
  - o More than 50 analyzed substances were removed during bank filtration and artificial recharge.
  - o Only few are not removed efficiently (Sulfamethoxazole, Carbamazepine, Primidone, AMDOPH, Clofibric acid, Propyphenazone, AOI, 1,5 NDS)
  - o Soil column experiments validated the field site measurements.
  - o The Clogging zone is of major importance for degradation of organic trace substances.
  - o Degradation of DOC during the aerobic infiltration proved very efficient and rapid. LC-OCD measurements show very fast degradation of polysaccharide fraction during the first 20 cm and a partial degradation of other fractions during oxic conditions.
  - o No complete degradation of polysaccharides and partial removal of other DOC constituents at anoxic conditions.
  - o An underground passage of at least 4-5 months and anoxic/anaerobic conditions shows the best results.
  - o Anaerobic/anoxic conditions develop due to biodegradation of particulate organic matter in the infiltration zone.

- Bacteria and virus removal:
  - o Factors influencing elimination of viruses are:
    - ▪ Tenacity of Viruses
    - ▪ Composition of the soil (clay minerals)
    - ▪ Flow velocity, lower flow velocities allows higher elimination rates.
    - ▪ The existence of a clogging zone, especially the development of "Schmutzdecke" or interstitial colonization. If there is less microbial colonization than the elimination is worse than with adapted soil.
    - ▪ Hygienic quality of the surface water (limits?)
  - o E. coli and intestinal enterococci are no reliable indicators for human pathogenic viruses.
  - o Coliphages are acceptable indicators for pathogens and can be used to test the efficiency of bank filtration systems.

Models were calculated primary for data interpretation at the field sites as well as in the laboratory. In a second step, models were developed for planning purposes and potential transferability to new sites (see also point 2, Objectives, page 2).

- Different models helped to understand the processes taking place at the field sites and during laboratory experiments.

  o Conceptual modeling was done to calculate the exchange of mobile/immobile oxygen to be able to calculate oxygen kinetics within the soil columns needed for interpretation. Degradation of organic carbon was modeled as well as the adsorption reactions. For all those models MATLAB and PHREEQC was used. For bacteria and microcystins different retardation factors (depending on medium) could be calculated.

  o Flow and transport models were calculated as a tool for data interpretation at the field sites (defining the infiltration area, flow paths, travel times, mass balances, dependencies, mixing of different water types and influence of well field performance). This was the base for all degradation interpretations. They were also used for simulation of well field performances as pumping intervals and rates.

  o A user friendly software for soil column simulation was developed (Visual CXTFIT) which than was used from the scientists for the interpretation of their experiments.

- Reaction models were calculated to define the influences of temperature, redox changes and hydraulics on degradation rates. Multi species reaction and transport models led to a successful process simulation of Phenazone during the underground passage. This is a prerequisite for the simulation of potential behavior at other sites.

- A bank filtration simulator was developed as a tool for planning and design of new bank filtration sites especially for application in developing countries.

Conclusions

- Within the NASRI project a comprehensive process understanding has been developed successfully. The interaction of the identified main mechanisms was successfully demonstrated by models and simulations.

- No substance was found that might affect the long term sustainability of bank filtration and artificial recharge in the future. All substances detected in the surface water were eliminated, most substances were eliminated very efficient (up to 100%), some partly (> 50%), and only a few showed less removal efficiency (< 50%).

- Besides the models used for water quality calculation and interpretation a tool usable for planning new sites was developed. This first version of the bank filtration simulator was tested recently by UNESCO for planning bank filtration in Malawi and is also used in India (IDB-India project). Geochemical reactions and degradation processes will be added in the next update.

Outlook

- The NASRI project demonstrated that well field management has an important influence on raw water quality. The performance of the drinking water wells is influencing the whole bank filtration system as well as the seepage water and land site ground water inflow not only with respect to flow paths and patterns, but also by influencing degradation processes. Further research is needed to define best practice in well field management.
- Besides the successful project work at the settings in Berlin, the comprehensively integrated results serve as model for identifying "missing bricks" in general. Berlin has very favorable condition especially concerning the very good surface water quality. Some experimental results shows potential limits for the subsurface's cleaning capacity. Keeping also in mind that temperature is one key factor and that climate change might result in higher summer temperatures and longer and colder winters, investigations are needed in another climatic zone. To define the limits of bank filtration and to verify the process stability at higher contaminated surface waters in consequence of the NASRI outcomes research field sites in India were established.

Table: Summary of elimination rates of substances investigated within the NASRI project: low means < 50 %, medium up to 90%, good > 90% of the original concentration, no values are given if no investigation took place, ++ very efficient, + efficient, o inefficient, - no removal at all.

	Mean removal rate	Aerobic conditions	Anaerobic/anoxic conditions	Temperature dependency
PhAC				
AMDOPH	low	(-/o)	-	
Primidone	low	(-)	-	
Carbamacepine	low	(-/o)	-	
Propyhenazone	medium	+	-	
Clofibric acid	low	(-/o)	(-)	
Diclofenac	good	+	o	
Indomethacine	good			
Bezafibrate	good			
Antibiotic				
Sulfomethoxazole	good - medium	+	++	yes
Dehydroerythromicine	very good	+	++	
Clindmycine	very good	++	o	
Roxithromycin	very good	++	+	
Clarithromycine	very good	++	+	
Others				
Iopromide	very good	++	++	no
1,5-NDSS	no	-	-	
1,7-NDSS	very good	++	+	yes
2,7-NDSS	very good	++	+	yes
Cyanotoxins				
Microcystins	very good	++	++/+	yes

1

"Hydrogeological-hydrogeochemical processes during bank filtration and ground water recharge using a multi tracer approach"

"hydrogeo" group, Freie Universität Berlin

Responsible project leader: Prof. Dr. Asaf Pekdeger

Content:

List of Tables

List of Figures

11

1 LAKE TEGEL BANK FILTRATION SITE

1.1 Objectives

The main objective of the project was the detailed hydrogeological analysis of the bank filtration system at the target transects at Lake Tegel, Lake Wannsee and the artificial recharge pond 3 in Tegel (GWA) as well as at the semi-technical facilities in Marienfelde. The investigations aim for the general description of the hydrogeological, hydraulic, hydrogeochemical and hydrochemical conditions at the surface water/sediment/groundwater interface as well as within the aquifer at all sites studied on the basis of knowledge gained during previous investigations. Altogether, this will help to improve the knowledge on chemical processes accompanying infiltration including the retention of inorganic and organic compounds in both the saturated and the unsaturated zone close to the surface water source.

A major focus of the study is on the evaluation of spatial and temporal changes in water chemistry and quality depending on water flow paths and velocities which are extremely transient due to continuously changing pumping regimes of the production wells at all sites. The use of a combination of different tracers helped to derive travel times from the surface water to the productions wells, validate flow models and enable the calculation of the fraction of treated sewage in the bank-filtrate. Correlation between tracers and chemical parameters allows the subsequent estimation the retention and degradation of the (sewage bound) chemical compounds in the sediments.

Besides others, the main objective of the project phase was to get an overview on travel times, mixing proportions and the hydrochemical situation at the field-sites studied.

The key questions dealt with were:

- What are the travel times from the surface water to observation and production wells?
- What is the proportion of bank-filtrate (and likewise deeper and landside groundwater) in the production wells?
- What is the proportion of treated wastewater in the surface water and production wells?
- What are the hydrochemical conditions at the sites, in particular with regard to redox conditions?

This is important because:

- Only with the knowledge of the time-scales of the processes studied, a definition of rates is possible.
- It is important to differentiate between dilution and real removal of potential contaminants during bank filtration.

- In order to understand the behaviour of specific substances studied by all working groups, the hydrochemistry, in particular the redox-state of the systems has to be known.

1.2   Methods

1.2.1   Drilling of observation wells and recovery of sediment cores

The installation of additional groundwater observation wells was done in co-operation with the Zalf e.V. Müncheberg (Centre for Agricultural Landscape and Land Use Management) using a 1.5 ton drill with a hollow helical auger of the company NORDMEYER (figure 1), into which the wells were lowered after the drill had reached the desired depth. The observation wells are made of high density polyethylen (HDPE) pipes with a diameter of two inches (2"), topped by a 2" Cap ("Seba-Kappe"). The HDPE filter screens at the bottom have a length of two metres and a slit width of 0.3 mm and are usually followed by a 1 metre long unscreened "swamp" end and a 2" HDPE cone end. Using HDPE enables undistorted sampling of inorganic and organic water constituents.

Sediment cores were generally taken with vibrocoring rods containing a plastic liner, which were driven into the ground with the same NORDMEYER machine that was used for the well construction. The cores were stored in a deep freezer for subsequent analysis.

Figure 1: Snap shot of NORDMEYER drill (left) and recovered plastic liner containing aquifer sediment (right).

1.2.2   *Sampling*

From November 2001 to August 2005, groundwater sampling campaigns were conducted by BWB with initial support of the Free University of Berlin. Measurements for redox potential (E_h), pH, O_2, temperature (T) and electric conductivity were carried out in the field in a flow cell. Filtration with 0.45 μm membrane filters was done immediately after sample retrieval for analyses of cations and anions. Samples for cation analysis were preserved with concentrated nitric acid (HNO_3) to avoid the precipitation of Fe- and Mn-(hydr)oxides. Alkalinity samples were collected in glass bottles that were carefully filled without any air entrapment. Samples were stored at 4° C and full water analysis was generally performed one day after sampling.

1.2.3   *Sediment analysis*

Grain-size distribution, hydraulic conductivities

Sediment samples were sieved wet according to DIN 4022 using sieves of a mesh size of 8, 4, 2, 1, 0.500, 0.250, 0.125 and 0.063 mm. Prior to sieving, they were batched over night with sodium-hydrogen-phosphate as a dispersion agent.

Hydraulic conductivities (k_f-values) where calculated with the empirical formulas by HAZEN (1893) and BEYER (1964) using the kvs software (BUß, 1994).

After Hazen, the hydraulic conductivity, k_f, is:

$$k_f = C*(d_{10})^2$$

with: C = proportional factor = (0,7+0,03*t)/86,4=0,0116 at 10 °C (~groundwater temperature)

            t = temperature [°C]

            d_{10} = grain size of a sediment at the intersection with the 10% line of the sum curve [mm]

The formula is only valid when d_{60}/d_{10} is smaller than 5 (d_{60} is the grain size of a sediment at the intersection with the 60% line of the sum curve [mm]). BEYER (1964) modified the HAZEN formula by introducing different proportional factors for different d_{60}/d_{10} values. These formulas are only valid for sands with $0,06 < d_{10} < 0,6$.

Table 1: Proportional factors used for k_f estimation after BEYER.

d_{60}/d_{10}	C (range)	C (average)
1.0 ... 1.9	$(120 ... 105) \cdot 10^{-4}$	$110 \cdot 10^{-4}$
2.0 ... 2.9	$(105 ... 95) \cdot 10^{-4}$	$100 \cdot 10^{-4}$
3.0 ... 4.9	$(95 ... 85) \cdot 10^{-4}$	$90 \cdot 10^{-4}$
5.0 ... 9.9	$(85 ... 75) \cdot 10^{-4}$	$80 \cdot 10^{-4}$
10.0 ... 19.9	$(75 ... 65) \cdot 10^{-4}$	$70 \cdot 10^{-4}$
> 20.0	$< 65 \cdot 10^{-4}$	$60 \cdot 10^{-4}$

Iron- and manganese oxides and hydroxides

Fe(III)- and Mn(IV)-oxyhydroxides in the sediment were measured using ICP-AES (Jobin Yvon) after selective extraction with dithionite-citrate-hydrogencarbonate as a reducing agent (MEHRA & JACKSON, 1960). Both amorphous and crystalline Fe(III) and Mn(IV) minerals are dissolved by dithionite-citrate-hydrogen-carbonate, which is a strong reducing agent.

Two grams of freeze-dried sample were placed in a 100 ml centrifugal glass with 40 ml of 0.3 molar sodium-citrate-solution, 5 ml of 1 molar sodium-hydrogen-carbonate solution (Na-HCO$_3$) for pH buffering and 1 g of solid dithionite (Na$_2$S$_2$O$_4$) as a reducing agent. The solution was pre-heated at 80°C in a water bath to prevent oxidation prior to adding the solids. The solution was then stirred with a glass rod, centrifuged and decanted into a 100 ml graduated flask. This procedure was repeated once, thereby preheating the required additional solution in a beaker in the water bath and also adding it to the sediment in the water bath. The sediment was flushed afterwards with 10 ml 0.1 molar MgSO$_4$ solution. Before measuring the solution by AAS, it was acidified with 5 ml of 65 % HNO$_3$ (required because of strong citrate buffering). The remaining insoluble solid residue was flushed into the disintegration apparatus with nitric acid to obtain the total iron content of the sediment by summing both fractions. It was placed into the cabinet drier at 100 °C over night and replenished to 50 ml in a graduated flask.

Total cation contents

For total acid soluble solid phase contents of the cations Na, K, Ca, Mg, Fe, Mn and Al sediments were extracted by HNO$_3$ pressure elution (HEINRICHS, 1989).

Two gram of dried sediment were dissolved with 10 ml of nitric acid (HNO$_3$) and stored in a disintegration bomb over night. After leaching several times with distilled water, the sample was replenished to 50 ml in a graduated flask. The cations were then analysed by AAS. Those samples previously analysed for Mn(IV) and Fe(II) underwent HNO$_3$ pressure elution after dithionite-citrate-hydrogencarbonate reduction in order to get both Fe- and Mn-Oxides as well as the remaining fractions (adding up to total contents) from one sample.

Cation exchange capacity (CEC)

Cations are bound to ion exchanger in the soil and sediment. They can only go into solution via exchange with other cations present in the water. An ion exchanger is a substance with a positively or negatively charged surface. The charge is neutralised by ions with the opposite charge. The adsorbed ions form an ion coating. These ions are free to move and exchangeable. During exchange, ions on the surface of the exchanger are exchanged with ions in so-

lution. This is usually reversible and happens fast and stoichiometric. The process can be described by the laws of mass action. Ion exchanger can have a positive or negative surface charge. Clay minerals and humic substances are mainly negatively charged and are cation exchanger. The negative charge of clay minerals is caused by the partial isomorphic substitution of Si^{4+} by Al^{3+} in the crystal lattice. This is only partly balanced by the inclusion of positive ions in the crystal lattice. The charge of humic substances is depending on the pH. At a pH common in soils and sediments, they are negatively charged (LEWANDOWSKI et al., 1997 and therein). The CEC depends mainly on the amount and type of clay minerals, the amount and type of the organic material. The amount of silt and oxides has a minor influence on the CEC. The potential CEC_{pot} is measured at a constant pH of 8.1 (for example after MEHLICH), while the effective CEC_{eff} is the CEC at the actual soil pH. CEC_{eff} and CEC_{pot} are equal at a pH above 7-7.5. According to FÖRSTER & WITTMANN (1979), the CEC is 3-120 mmol(eq)/100g for different clay minerals, 10-24 mmol(eq)/100g for freshly precipitated Fe-Hydroxides, 11-34 mmol(eq)/100g for amorphous silica and 170-590 mmol(eq)/100g for humic acids in soils. Values for calcite are not given.

Cation exchange capacity was measured with the percolation method as CEC_{eff}. The exchange solution was produced by adding 25 g of $BaCl_2*2\ H_2O$ into a flask and filling it up to 1 l with distilled water. The re-exchange solution was made with 50 g $CaCl_2$ dissolved in 1 l of distilled water. Ten gram of quartz sand (p.a. annealed) were filled into a small PE column as a filter. Ten grams of mildly pounded sample sediment (only the fraction with a grain size < 2mm) were placed on top of the quartz sand. For replacement of the exchangeable cations by Ba^{2+} 75 ml of the exchange solution were added to the column in 5 portions of 15 ml and collected in a 250 ml flask. Afterwards, the column was flushed with distilled water and the flask was filled up to 250 ml. The displaced cations were measured by AAS. The pH has to be determined, because H^+ is accounted for in the budget calculations. For the re-exchange of the Ba^{2+} by Ca^{2+}, 100 ml of the re-exchange solution were added to the column in 4 portions of 25 ml each. The solution was collected in a 100 ml flask and filled to the marker with distilled water. The Ba^{2+} was analysed by ICP. The CEC_{eff} is the amount of Ba^{2+} re-exchanged in mmol(eq)/100g of sediment. Theoretically, the sum of the cations exchanged in the first run should be equal to the CEC. However, it is usually smaller because not all of the cations are measured (for example trace metals or NH_4^+ are missing). In sediments containing calcite the sum of the cations is often larger than the CEC, because some of the calcite is dissolved (KRETSCHMAR, 1991)

Pyrite and mono-sulphide content

Sulphide was extracted as acid volatile sulphide (AVS) using HCl and as pyrite (or CRS) using a Cr(II)Cl solution as extraction agent. AVS-sulphide includes mineral phases such as

Fe(II)-monosulphide (FeS), mackinawite ($Fe_{1-x}S$) and greigite (Fe_3S_4) (CORNWELL and MORSE, 1987; HSIEH and YANG, 1989; GAGNON et al., 1995). The extraction with Cr(II)Cl includes pyritebound S as well as AVS phases and elemental S (CANFIELD et al., 1986). In contrast to conventional methods the H_2S degassing in the acid environment was not blown out but transported into the Zn-acetate trap by passive diffusion over 48 h (HSIEH and YANG, 1989). After the precipitation of ZnS in the alkaline solution (pH 13), the amount of sulphide was measured iodometrically (HSIEH and YANG, 1989; GAGNON et al., 1995).

Organic and inorganic carbon content, total sulphur content

Organic and inorganic C as well as total S were determined with a C-N-S Analyser (CS-225, Leco Instruments GmbH). The sediment sample was crushed with an agate mortar and metallic aggregates (zinc, pure iron and wolfram chips) were added in a clay pan and placed in a burning chamber in an oxygen stream. The carbon or sulphur content was analysed via Infra-red (IR) detection.

To differentiate between organic and inorganic carbon, pre-treatment of the sample was necessary. The samples are weighted with the clay pans. 1 N HCl was added in order to destroy the carbonate fraction. After ablation of the excess acid, the remaining carbon can be analysed as before but with a chloride trap for the flue gas cleaning. It is equivalent to the organic carbon fraction of the sample. The inorganic carbon fractions, i.e. the carbonates are calculated by subtraction of the two values. The results are always averages of 3 measurements.

1.2.4   Water analysis

Standard chemistry

Both ions after sediment extraction as well as water samples from column or batch experiments and the suction cubs at the artificial recharge pond were analysed at the laboratories of the Free University of Berlin, using equipment listed in table 2.

Table 2: Overview on analytical instruments at the hydrogeology laboratory of the Free University of Berlin.

Parameter	Method	Type	Detection limit	Norm
B	ICP	Leemans	0.05 mg/l	
Ba^{2+}	ICP	Leemans	0.5 mg/l	
Br^-	IC	DX 100	0.5 mg/l	DEV (1986)
NO_3^-	IC	DX-100	0.5 mg/l	
Ca^{2+}	AAS/Flame	Perkin Elmer 5000	0.1 mg/l	DIN 38046-E3-1
Cl^-	IC	DX 100	1.0 mg/l	
Cu^{2+}	AAS/ Flame	Perkin Elmer 5000	0.05 mg/l	DIN 38046-E7/E21
Fe^{2+}	AAS/ Flame	Perkin Elmer 5000	0.1 mg/l	
HCO_3^-	Titration	DIN (1979)	1.0 mg/l	DIN 38409
I^-	Titration			DEV (1986)
K^+	Flame photometric	Eppendorf Elex 6361r	0.1 mg/l	DIN 38046-E3-14
Li^+	AAS/flame	Perkin Elmer 5000	0.05 mg/l	
Mg^{2+}	AAS/ flame	Perkin Elmer 5000	0.02 mg/l	DIN 38046-E3-1
Mn^{2+}	AAS/ flame	Perkin Elmer 5000	0.02 mg/l	
Na^+	Flame photometric	Eppendorf Elex 6361r	1.0 mg/l	DIN 38046-E3-14
NH_4^+	Quick test Colorimetric / Photometric	Dr. Lange/ MN / Merck	0.04 mg/l	
NO_2^-	Quick test Colorimetric / Photometric	Dr. Lange / MN / Merck	0.005 mg/l	
SiO_2	Photometric	Technicon Autoanalyser		DIN 38045-D21
SO_4^{2-}	IC	DX-100	1.0 mg/l	
Sr^{2+}	AAS/flame	Perkin Elmer 5000	0.02 mg/l	DIN 38046-E3-22
Zn^{2+}	AAS	Perkin Elmer 5000	0.05 mg/l	
DOC	Photometric	Technicon Autoanalyser	0.5 mg/l	

Stable isotopes

The stable isotope measurements of deuterium (D) and 18-oxygen (^{18}O) were carried out at the Alfred Wegener Institute, Research Unit Potsdam with a H_2 equilibration method for D/H ratios and a CO_2 equilibration method for $^{18}O/^{16}O$ ratios with a Finnigan MAT Delta-S mass spectrometer. After equilibration ten measurements were carried out for each sample. δD and $\delta^{18}O$ values were calculated using the commercial software ISODAT and reported in the standard δ notation representing per mil deviation relative to V-SMOW. The internal 1σ error is generally better than 0.8 ‰ for δD and better than 0.1 ‰ for $\delta^{18}O$. Details on the instrumentation, calibration and the measurement routine are described in (Meyer et al., 2000).

1.2.5 Tracer evaluation methods

Wastewater indicators and environmental tracers can be used to estimate either travel times from lake to production well or the proportion of bank filtrate in the production wells. For both purposes, conservative tracers (non-reactive and non-retarding) were used.

For studying the water movement, an appropriate tracer should show clear seasonality in the surface water or at least clear peaks at certain times of the year. Evaluating the peak shift from the surface water to a groundwater observation well yields travel times to the respective well. Oxygen and hydrogen isotopes show a typical seasonality in the surface water of Berlin with more negative values in winter. Tracers originating from wastewater show seasonality mainly because of dilution effects: The release of wastewater from the treatment plants is relatively constant throughout the year, while the natural discharge is much higher in winter. Therefore, the concentration of wastewater indicators is generally higher during summer. Locally, other effects may play a role too.

The fraction of treated wastewater at a sampling point in the surface water or in a production well is estimated from tracers in the well and in the end-members (for example the surface water and the background groundwater inland of a production well). The differences in concentration of the two end-members should ideally be large and concentrations should be stable with time. If the abstracted water is a mixture of surface water and background groundwater only, the percentage of bank filtrate in the well (*X*, given in %) is estimated by the following equation:

$$X[\%] = \frac{C_w - C_{GW}}{C_{SW} - C_{GW}} * 100$$

With C as the concentration of a suitable tracer in the groundwater (C_{GW}), well (C_w) or surface water (C_{SW}). If several filter screens exist in different aquifers the calculation is more difficult (for example at Wannsee).

Table 3 gives an overview on tracers used within this study, their origin, purpose of use and the difficulties associated with the use their use.

Table 3:Overview on most important major tracer applicable in Berlin.

Tracer:	Origin:	Useful for the interpretation of:	Difficulties:
δD, $\delta^{18}O$	surface water with seasonal variations (precipitation)	water movement, proportion of bank filtrate in raw water	none, conservative tracer
Temperature	surface water with seasonal variations	water movement	retarding
Cl^-, B	surface water with seasonal variations (WWTP)	water movement, proportion of bank filtrate in raw water	only if influence of saline groundwater can be excluded
Cl^-, Na^+, B	saline deeper groundwater	proportion of deeper saline ground-water	may vary strongly locally
SO_4^{2-}	dissolution of gypsum derived from building rubble in the shallow aquifer	proportion of shallow "native" groundwater	may vary strongly locally
Gd-DTPA	surface water with seasonal variations (WWTP)	water movement, proportion of bank filtrate in raw water	degradable
EDTA	surface water, effluent	water movement, proportion of bank filtrate in raw water	sometimes the background groundwater has also got very high concentrations
K	surface water with seasonal variations (WWTP)	water movement	Only if sorption on sediment can be excluded, Generally not behaving conservative
T/He	Surface water, through at-mospheric input	groundwater "age"	minimum age required is 6 months

The boxplots were done with available data from May 2002 to May 2005. Because some of the observation wells had only been sampled since January 2003 or had fallen dry in summer, the number of the samples varies and for some wells, only very few samples were analysed. When the concentrations analysed were below the detection limit, 0 was used in figures and for the boxplots.

1.2.6   Age dating

Samples were taken from selected wells for $T/^3He$ analysis. The analysis and data evaluation of the groundwater samples was carried out at the noble gas laboratory at the University of Bremen. The method uses the ratio of the concentration of radioactive tritium (^3H or T) and its decay product ^3He in the groundwater to determine the groundwater age. The "age" τ is the time passed since the water had its last contact with the atmosphere, in the present case, since the water infiltrated into the aquifer. It is defined as (TOLSTIKHIN & KAMENSKIY, 1969):

$$\tau = \frac{t_{1/2}}{\ln 2}\ln(1+\frac{^3He_{tri}}{^3H})$$

with: τ = age [a]

$t_{1/2}$ = half-life of ^3H (12.43 years)

$^3He_{tri}$ = fraction of total ^3He produced by ^3H decay [TU]

^3H = tritium concentration [TU]

Tritium is expressed in tritium units [TU]. One TU corresponds to a $T/^3H$ ratio of 10^{-18}. The natural ^3H concentration in the atmosphere is low (about 10 TU). In the 1950s and early 1960s the ^3H content in the atmosphere increased several orders of magnitude due to nuclear bomb testing. The concentrations have since been decreasing (figure2). The method has been used in many groundwater studies but only in STUTE et al. (1997), BEYERLE et al. (1999) and SÜLTENFUß & MASSMANN (2004) did the groundwater originate from bank-filtration.
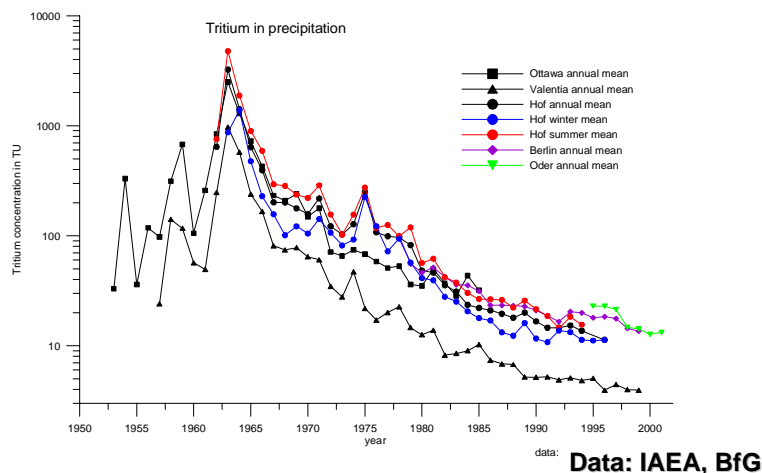
Figure 2: Tritium in the precipitation of several sites in the world (data source: IAEA, BfG).

1.2.7   *Stable isotopes of dissolved sulfate*

Samples for $\delta^{18}O$ and $\delta^{34}S$ of sulfate were collected in July 2004 and filtered with 0.45 µm membrane filters to avoid impurities. 2–3 ml of HCl were added and SO_4^{2-} was precipitated as $BaSO_4$ in the laboratory of the Free University of Berlin using the reagent $BaCl_2$. The $BaSO_4$ was caught on a filter and freed of the chloride content by rinsing with warm water. The filtered $BaSO_4$ was split in samples for $\delta^{18}O$ and $\delta^{34}S$ analysis and subsequently dried at 30 and 80 °C, respectively. All isotope results are reported as $\delta^{34}S$ and $\delta^{18}O$ values in per mil (‰), where:

$$\delta(‰)=[(R_{sample}/R_{standard}) -1]*1000$$

for $\delta^{34}S$ or $\delta^{18}O$, R = $^{34}S/^{32}S$ or $^{18}O/^{16}O$, respectively (Hoefs, 1997). $\delta^{34}S$ analyses of $BaSO_4$ and sulfides were performed after conversion to SO_2 in the presence of V_2O_5 and SiO_2 (YANAGISAWA & SAKAI, 1983) and subsequent determination of the sulfur isotope composition using a Finnigan MAT Delta E mass spectrometer at the isotope laboratory of the Institute of Mineralogy in Freiberg. For routine measurements an internal standard (SO_2), which is calibrated against the international IAEA-standard NBS 127, was used. Isotope values are reported relative to the international standard CDT. $\delta^{18}O$ values of $BaSO_4$ were determined on

Kommentar [GM2]:

22

CO_2 derived through reaction of $BaSO_4$ with graphite at a high temperature (RAFTER, 1967). Simultaneously generated CO was converted to CO_2 on a Ni-catalyst at 350 ^{O}C. After the complete conversion of CO to CO_2 all CO_2 gas was collected and analysed on a Finnigan MAT Delta plus mass spectrometer. As internal standard a synthetic $BaSO_4$ with a $\delta^{18}O$ value of 12.95‰ calibrated against the international IAEA standard NBS 19 was used. The reproducibility of the $\delta^{18}O$ analysis of $BaSO_4$ is usually better than ±0.2‰. $\delta^{34}S$ isotope values are reported relative to the international standard SMOW.

1.3 Results Lake Tegel Bank Filtration Site

1.3.1 Surface Water Investigations

Surface water investigations in the western part of the city were done within a student project (Doreen Richter, in cooperation with DFG project A. Knappe) in 2001 and 2002. Previous detailed surface water investigations at Lake Tege had been performed by HEIM et al. (2002) and FRITZ (2002). The necessity to take the surface water into consideration when investigating the bank filtration system arises from the fact that it is the source of the bank filtrate and therefore, hydrochemical variations have a large impact on the quality of the bank filtrate itself. Although the surface water was sampled within NASRI in front of the respective transects on a monthly basis, results only give very selective information for one particular point whereas results of the additional surface water investigations helped to understand the processes influencing the surface water quality and give an additional idea on its temporal and spatial variations.

The surface water contains a considerable amount of treated wastewater, since the natural base flow is low and 6 wastewater treatment plants (WWTP) are in operation. Indications of wastewater influence in the surface water are high concentrations of wastewater indicators such as Cl^-, Na^+, SO_4^{2-}, B, DOC or Gd-DTPA, high temperatures (in winter) and more negative isotopic signatures, because of the groundwater share (more negative isotopic signature) in the drinking water (KNAPPE et al., 2002, HEIM et al., 2002, MASSMANN et al., 2004)

Figure 3 shows maps of Cl^-, B and Gd concentrations and $\delta^{18}O$ values and in the surface water in July 2001 and December 2001 as two examples for the tracer distribution in summer and winter. In July, the base flow was the lowest in 2001/2002. Therefore, the spatial differences and absolute concentrations of wastewater indicators are larger in July 2001 as compared to winter months. The concentrations are highest (darkest colours) at the northern end of Lake Tegel, where the Nordgraben meets Lake Tegel and in the Teltowkanal, hence the proportions of WW are highest at these locations. It becomes clear that the transect Lake Wannsee is located in an transition area between Teltowkanal water flowing northwards into

23

Lake Wannsee and water of the Lower Havel, resembling the Spree water with lower propor-
tions of treated wastewater (compare chapter Wannsee). Figure 4 illustrates the approximate
proportions of treated wastewater calculated as percentage of WWTP discharge of the total
discharge at the respective gauging station (evaporation and abstraction disregarded). More
detailed calculations for previous years were done by SCHUHMACHER & SKRIPALLE (1999).
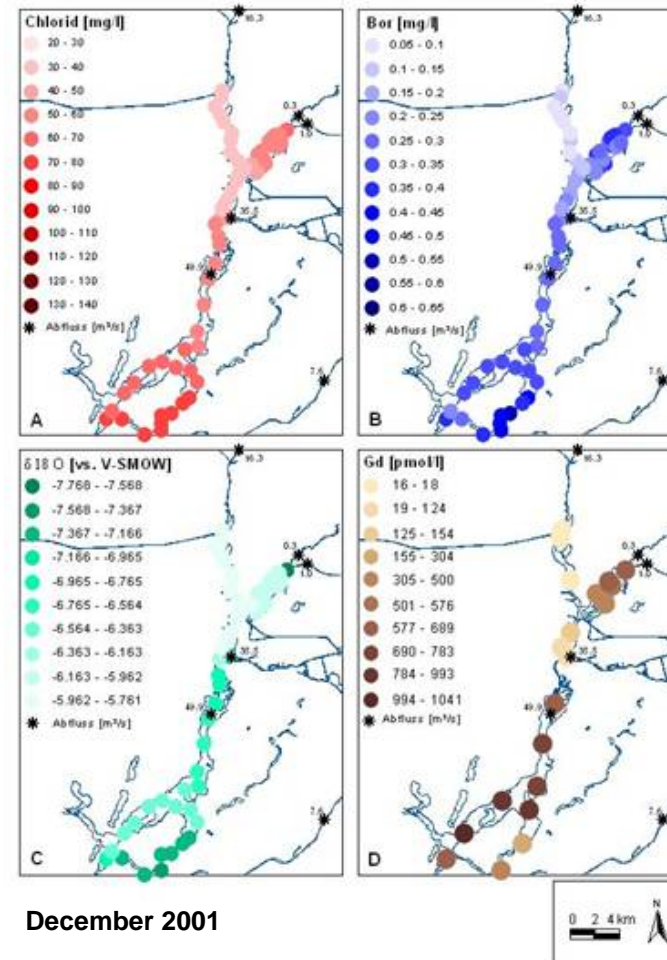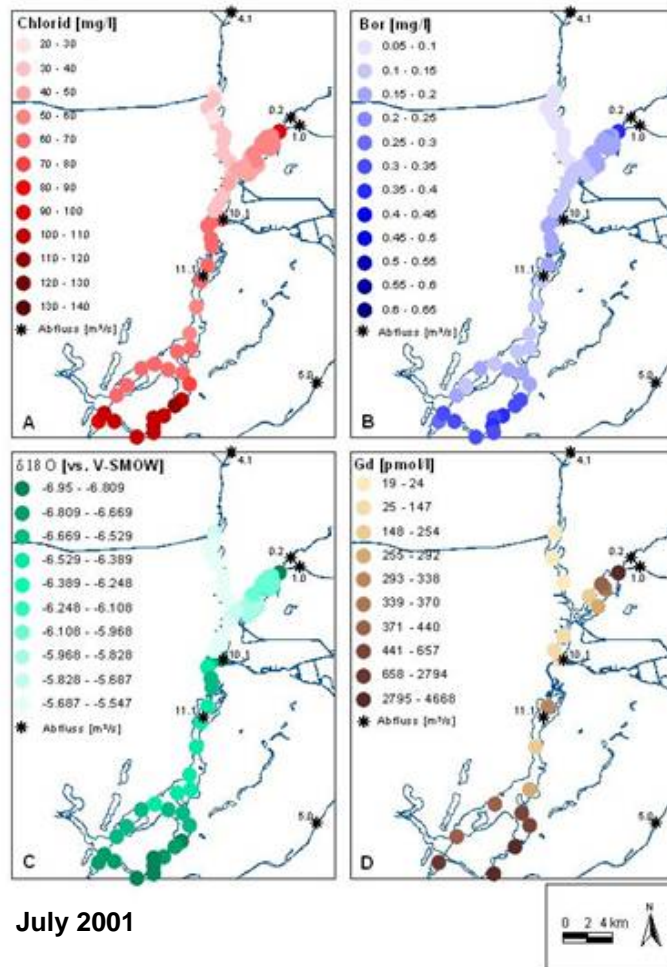
Figure 3: Exemplary comparison of distribution of wastewater indicators in the surface water system in summer and winter (RICHTER, 2003).

25
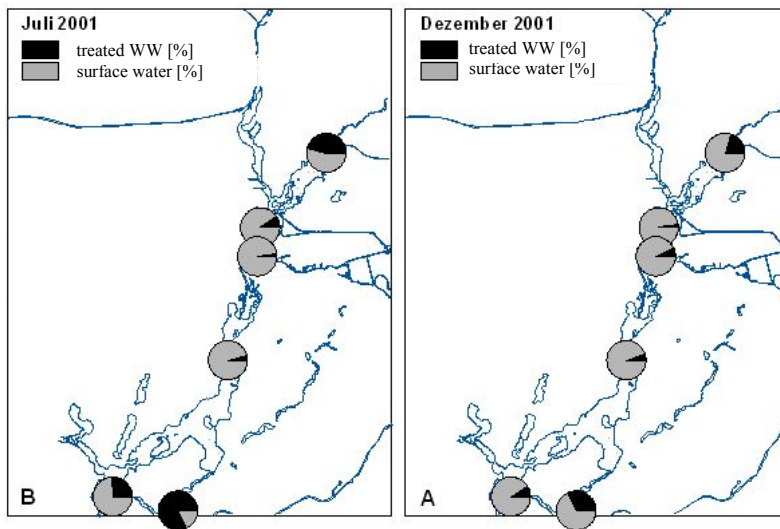
Figure 4: Exemplary proportion of treated wastewater in the surface water for summer and winter (RICH-TER, 2003).

The Nordgraben and the Tegeler Fließ (both small ditches) discharge into Lake Tegel after passing through the OWA phosphate elimination plant. The Tegeler Fließ water is only partly (but largely) flowing through the OWA and partly discharging directly into the lake. The Nordgraben carries a high load of treated WW from the WWTP Schönerlinde. A pipeline started operating in October 2001, pumping Upper Havel (Oberhavel) water into the OWA (in particular during summer months) to dilute the treated WW when the base flow is low in order to improve the surface water quality. The pipeline caused the proportion of WW in the OWA discharge to temporarily decrease from October 2001 onwards (figure 5). However, the total discharge of the WWTP Schönerlinde increased as well in the beginning of 2003, which is why the proportion of WW now resembles the original situation before October 2001 again (40 % WW). The components discharging into lake Tegel from the north (natural discharge Tegeler Fließ and Nordgraben, discharge WWTP Schönerlinde and added Oberhavel water share) as well as the percentage of WW in the total OWA discharge are shown in Figure 5. The sum of these components is not always perfectly equal to the values given for the total OWA discharge (black line), probably due to measurement errors and because the Tegeler Fließ only partly passes through the OWA. It can be seen that due to the higher share of Upper Havel water in summer, the proportion of treated WW in the OWA discharge in 2003 and 2004 was lower than in winter, which is the opposite of the "normal" situation (more dilution in winter), further complicating the evaluation of the tracer data.
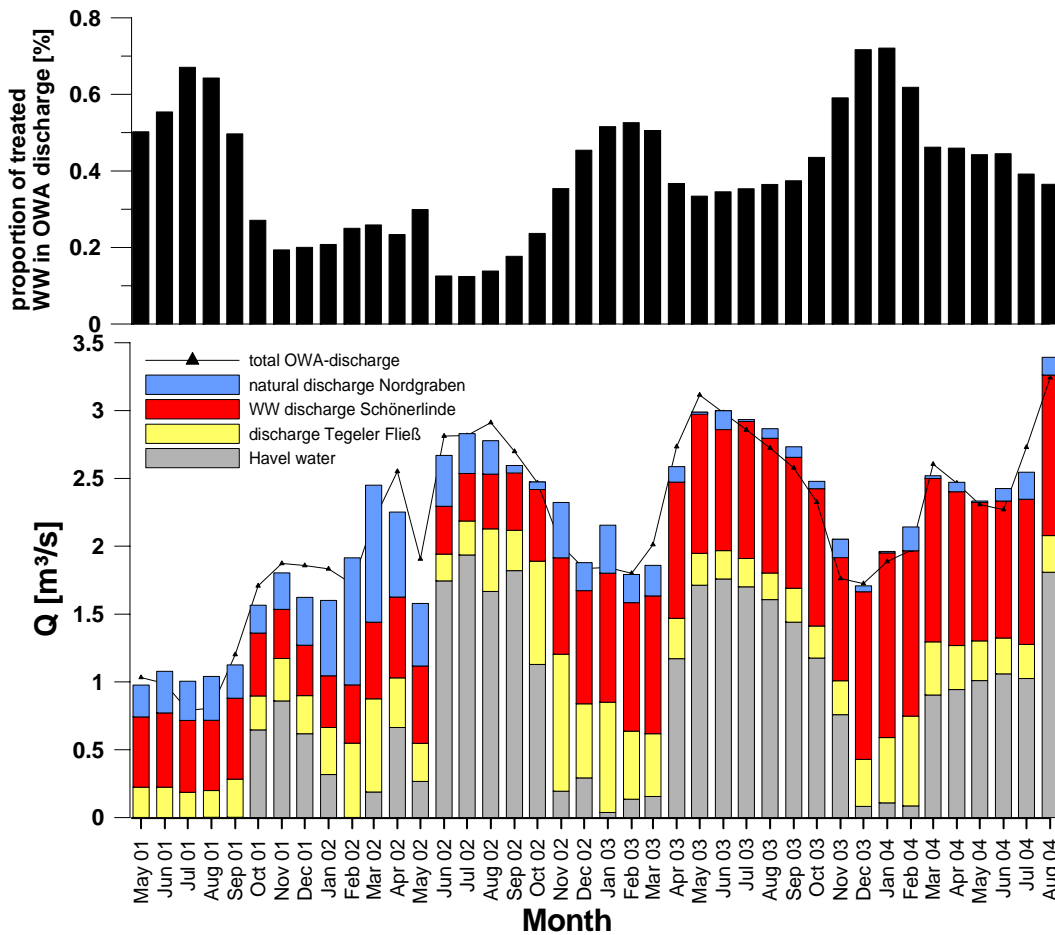
Figure 5: Total discharge of the OWA (black line) and discharge of components WWTP Schönerlinde (red bars), total discharge of Tegeler Fließ (yellow bars), calculated "natural" discharge of Nordgraben (blue bars, natural discharge Nordgraben = OWA inflow Nordgraben – discharge WWTP Schönerlinde) and Oberhavel input via pipe line). Data source: SENSTADT, 2001-2004 and BWB. Values are monthly averages.

Compared to Lake Wannsee, the conditions within the lake itself around the transect are more stable in terms of spatial distribution of the WW. The WW influence diminished with increasing distance from the OWA outlet (point 800, figure 6, right) but around the transect (point 310), the spatial variation at a certain time is small (figure 6, left).

27
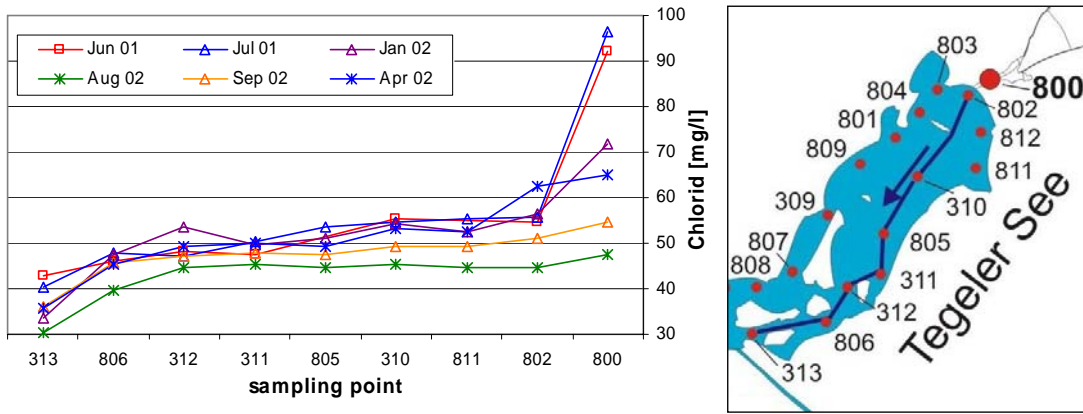
Figure 6: Chloride profiles throughout Lake Tegel during 6 sampling campaigns, sampling locations are given in the map to the right (RICHTER, 2003).
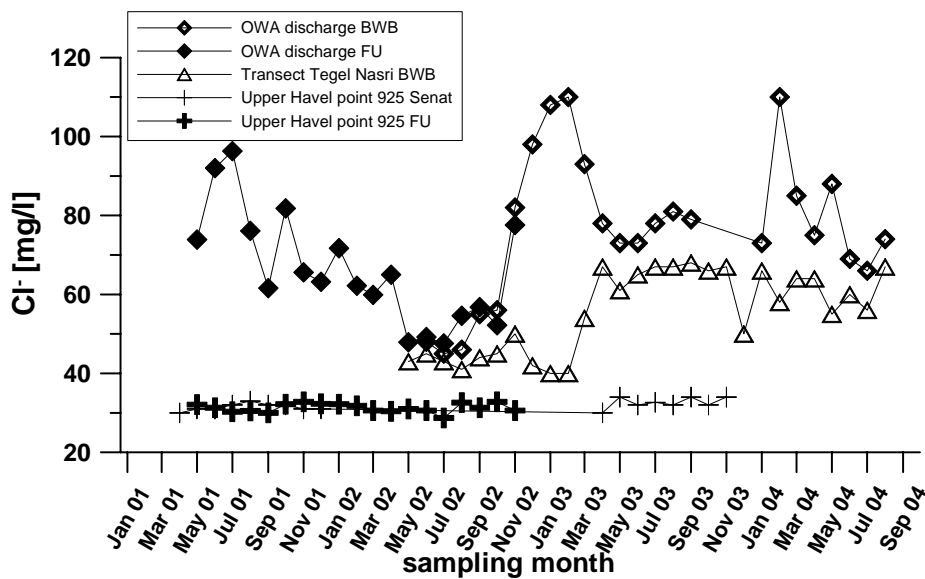
Figure 7: Cloride concentration in the surface water of the Upper Havel, Lake Tegel in front of the transect Tegel and Lake Tegel directly after the OWA outlet.

Figure 7 shows the chloride concentration in the Upper Havel (point 925), which is constantly low (~31 mg L^{-1}), Lake Tegel right after the OWA outlet (point 800, figure 6) and right in front of the transect Tegel. The sudden increase at the OWA outlet around December 2002 which coincides with the increased WW loads from Schönerlinde (figure 5) may be related to the increase in front of the transect about 4 months later. Using averages of this data-set, the proportion of treated WW in the surface water in front of the transect Tegel from May 2002 to August 2004 was ~21 % in average.

Principally, the concentrations of WW constituents are lower in winter, due to dilution with the larger natural discharge. The discharge of the WWTP's varies on a daily basis but does not show any seasonal fluctuations. The concentrations of wastewater bound substances in the effluent, for example chloride, do generally not show clear seasonalities (this is not true for specific substances, for example drug residues, which may be prescribed more often during certain times of the year). In contrast, the natural discharge is much higher in winter than it is in summer. However, as explained above, the changing conditions at Lake Tegel (figure 5) made the situations somewhat more complicated. In addition, the climatic situation was very different in 2002 compared to 2003. The combination of a very wet summer 2002 with lesser WW in the OWA discharge eliminated the typical summer peaks for most WW indicators, which were therefore of no use for the interpretation of travel time. Fortunately for the bank-filtration study, a clear minimum in February 2003 and a clear maximum in summer 2003 could be seen for most WW indicators which enables to define travel times at the transect.
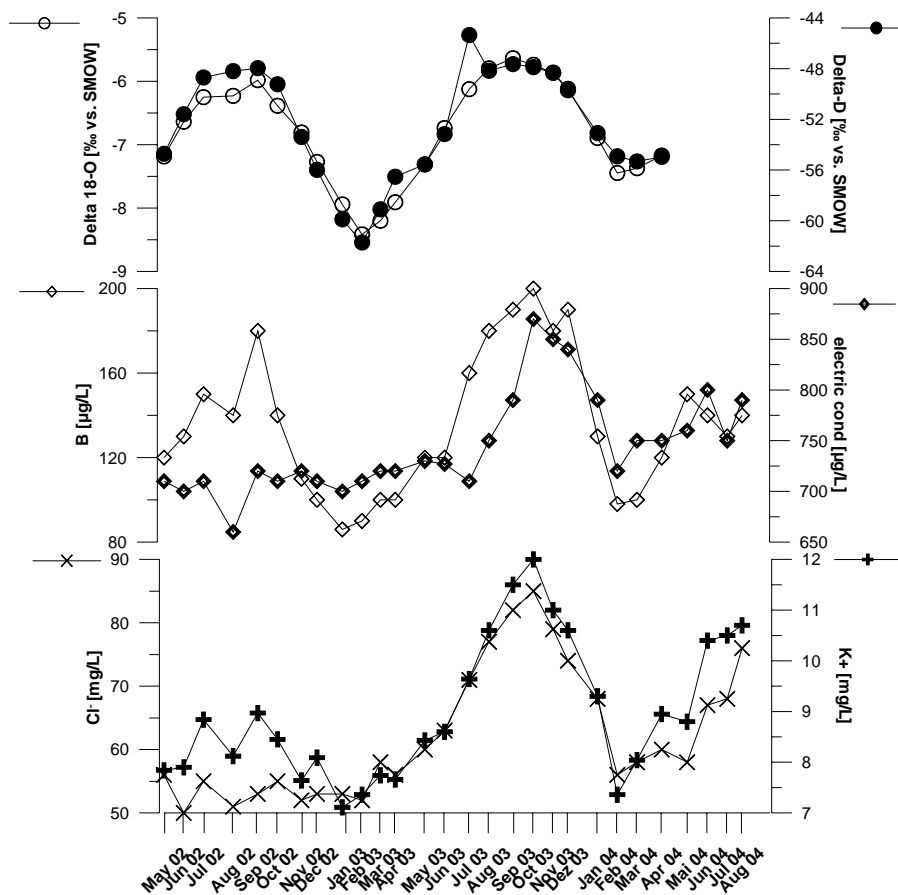
Figure 8: Stable isotopes, electric conductivity, B, Cl⁻ and K⁺ in Lake Tegel (data source: AWI + BWB).

1.3.2 Clogging layer

The bottom of Lake Tegel is covered with very thick layers of lacustrine sapropel. These mud sediments are characterized by low hydraulic conductivity (2.1E-07 to 2.8E-09 m/s; FRITZ et al., 2002). At the lake borders, adjacent to the shores, the lake bottom is free of these sediments. However, the sands present in these areas are still heavily clogged, resulting in a hydraulic conductivity of 5.4E-06 m/s (FRITZ et al., 2002). Despite decreasing infiltration capacity, the presence of the low conductivity sediments has two positive effects. First, their relatively low permeability slows down travel times from the lake to the production wells. Second, they are far more effective in removing contaminants than unclogged aquifer sands, as the high proportions of organic matter and the finer grained material increase the adsorption and reduction capacities of the sediments (e.g. HISCOCK & GRISCHEK, 2002). Several authors have found that the most significant chemical changes related to organic matter degradation take place during the first few meters of flow (e.g. JACOBS ET AL., 1988; BOURG & BERTIN, 1993; DOUSSAN et al, 1997).

Analysis of mud sediment cores, taken from Lake Tegel, (SIEVERS, 2001) revealed that at the upper parts of the mud profile, the organic carbon content exceeds 22 % and at a depth of 80 cm below the mud surface, the organic carbon content exceeds 17 % (figure 9). This extremely high organic content is expected to have a positive influence on the removal of certain undesirable contaminants by microbial activity.

One species, undesired in high concentrations in the drinking water and detected in the water resources of Berlin, is sulfate. Relatively high concentrations of sulfate have been sampled in the surface water systems of Berlin in the past. A maximum concentration of 175 mg/l was detected during the period between February 1998 and October 1999 in the main pond of Lake Tegel, and a maximum concentration of 184 mg/l was detected during the period between May 1998 and June 1999 in Lake Müggelsee (FRITZ, 2002). There is also a big concern that sulfate concentrations in the river Spree may strongly increase in the future since open pit mining upstream of Berlin was largely abandoned after 1990. The former open mines are currently flooded and will be used as storage ponds for the Spree in order to discharge water into the Spree when the base flow is low. Sulfate concentrations within the ponds are extremely high with up to 60 meq/l in 2000 (KOHFAHL, 2004) In the case of future Spree concentrations exceeding the drinking water limit, these cannot be diluted with groundwater because the groundwater itself (from first and second aquifer) contains sulfate in concentrations higher than drinking water limits over large areas of Berlin (SOMMER VON-JARMERSTEDT et al. 1998; PEKDEGER et al. 1998).

Reduction of sulfate during bank filtration is a natural process with the positive effect of reducing sulfate concentrations. Therefore, the study of sulfate reduction during bank filtration in the lake sediments around Berlin is of great interest. While SIEVERS (2001) could show

that sulfate disappears within a few decimetres within the mud (figure 9), sulfate concentrations in the groundwater are in the same order of magnitude as the surface water, indicating that only little water passes through the impermeable lacustrine sapropels.
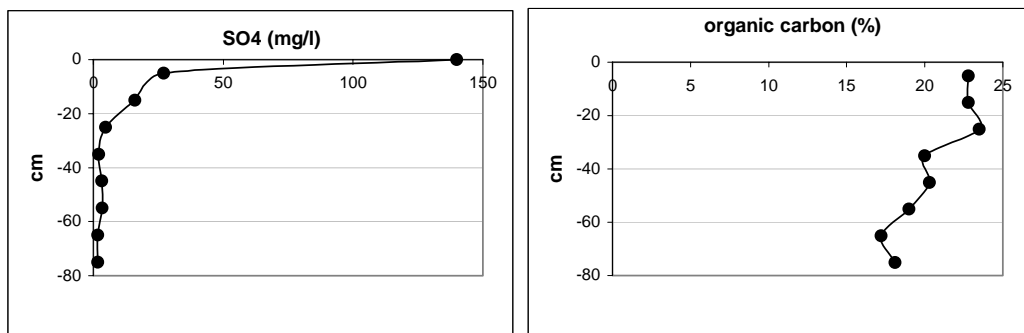
Figure 9: Sulfate in the pore water and organic carbon in the sediment of the mud sediment cores (SIEVERS, 2001).

Excursus: Modeling of sulfate reduction kinetics through a mud profile in Lake Tegel

Sulfate concentrations in the pore water of a 80 cm long mud core drilled in the bottom of Lake Tegel (SIEVERS, 2001, figure 9) were used to model sulfate reduction. Assuming that sulfate transport through the profile could be derived by diffusion and that the depletion in sulfate concentration was a consequence of redox reactions only, the geochemical computer program PHREEQC was used to fit first-order kinetic coefficients to the reduction process rates. The first-order coefficients obtained were 1.49×10^{-7} s^{-1} and 2.0×10^{-8} s^{-1} for the sections 0-10 and 10-40 cm below the mud surface, respectively. In the lowest 40 cm of the mud profile, 40-80 cm below the mud surface, steady-state concentrations were observed. The variation in the reduction rate constants in the upper 40 cm were suggested to be a consequence of the different types of organic compounds along the profile, rather than the total organic matter content. The steady-state concentrations at the lowest part of the profile are thought to be the consequence of either competition with other microbial populations or sulfide toxicity, a product of the sulfate reduction (figure 10).

31
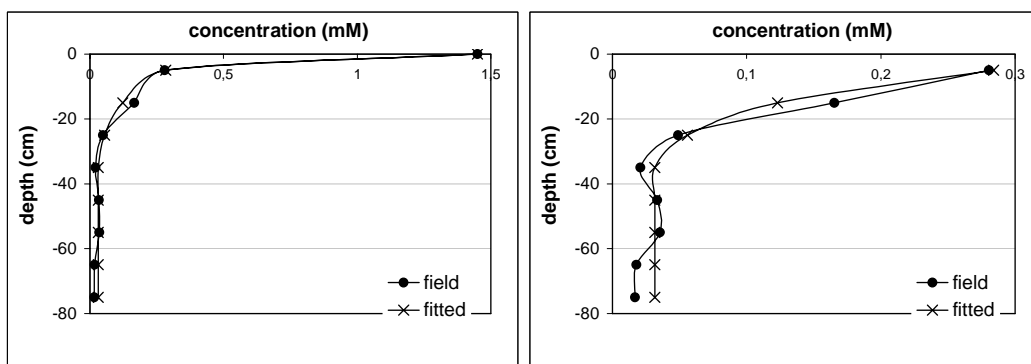
Figure 10: Sulfate concentration profile (full dots) and the fitted profile (crosses) using first-order kinetics. In the right figure the lake water concentrations were taken out in order toincrease the scale.

1.3.3 Aquifer sediments

The porous glaciofluvial sediments in the area are of Quaternary age (Saale glaciation; HAN-NAPPEL & ASBRAND, 2002). They consist of fine to coarse grained, but mainly medium sized sands. According to the Berlin terminology by LIMBERG AND THIERBACH (2002), both aquifers are part of the hydrogeological unit GWL 2 (qhol-qw). The aquifer is underlain by an aquitard of the Holstein interglacial at approximately 5 m below sea-level at both sites (HANNAPPEL & ASBRAND, 2002). A local aquitard, a glacial till of Saale age (local denotation qsWA) divides the aquifer in two (figure 11). The production well filter screens have been placed below the aquitard. However, the till is only partly present and was not encountered in drillings near the lake shore and below the pond. Therefore, the infiltration below the till is possible. The lithological cross section of FRITZ (2002) has been complemented with the new information (figures 11 and 14). Results from sieving analysis of samples taken at each lithological change (or at least every metre) of core TEG371UP) were added to figure 11. A relatively small variation from 1.5E-4 to 1.1E-03 m/s was observed, which is similar to hydraulic conductivities at the GWA Tegel.

Grain size distribution and hydraulic conductivities of core TEG371UP are shown in figure 12. In terms of the geochemical properties of the sediment, the unsaturated sediment zone (or, more precisely what was the unsaturated zone over a long period of time) differs from the sands below. At present, the unsaturated zone is much larger than it would be without pumping, at a water-table depth of 7-12 m below ground, depending on the pumping regime. Carbonate (inorganic carbon) appears from a depth of around 5.6 m onwards (figure 13) with a content of 0.16 to 1.3 weight %. The organic carbon content is low with 0.02-0.08 weight % (figure 13). With a few exceptions, the total iron content is 1-2 g/kg Fe (figure 13). The share of the reducible manganese fraction (Mn(hydr)oxides) seems to be getting slightly less with depth. In terms of total ion concentrations (HNO_3 extraction, figure 13), aluminium and iron are the main minor cations in the unsaturated sands, while calcium dominates within the saturated zone (figure 13).
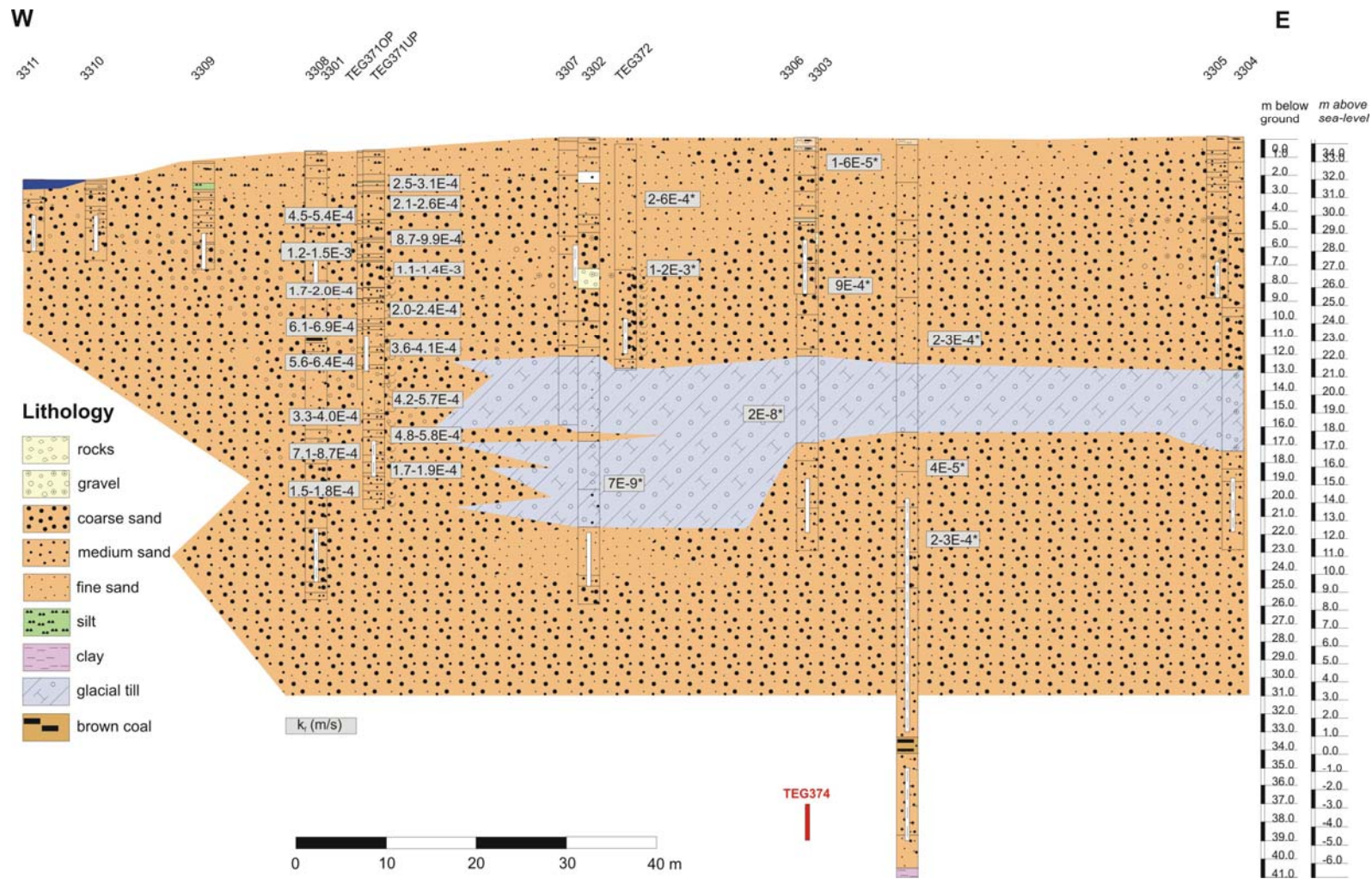
Figure 11: Geological cross-section of the transect Tegel with hydraulic conductivities from sieving of core TEG371UP. Values with* from Fritz (2002).
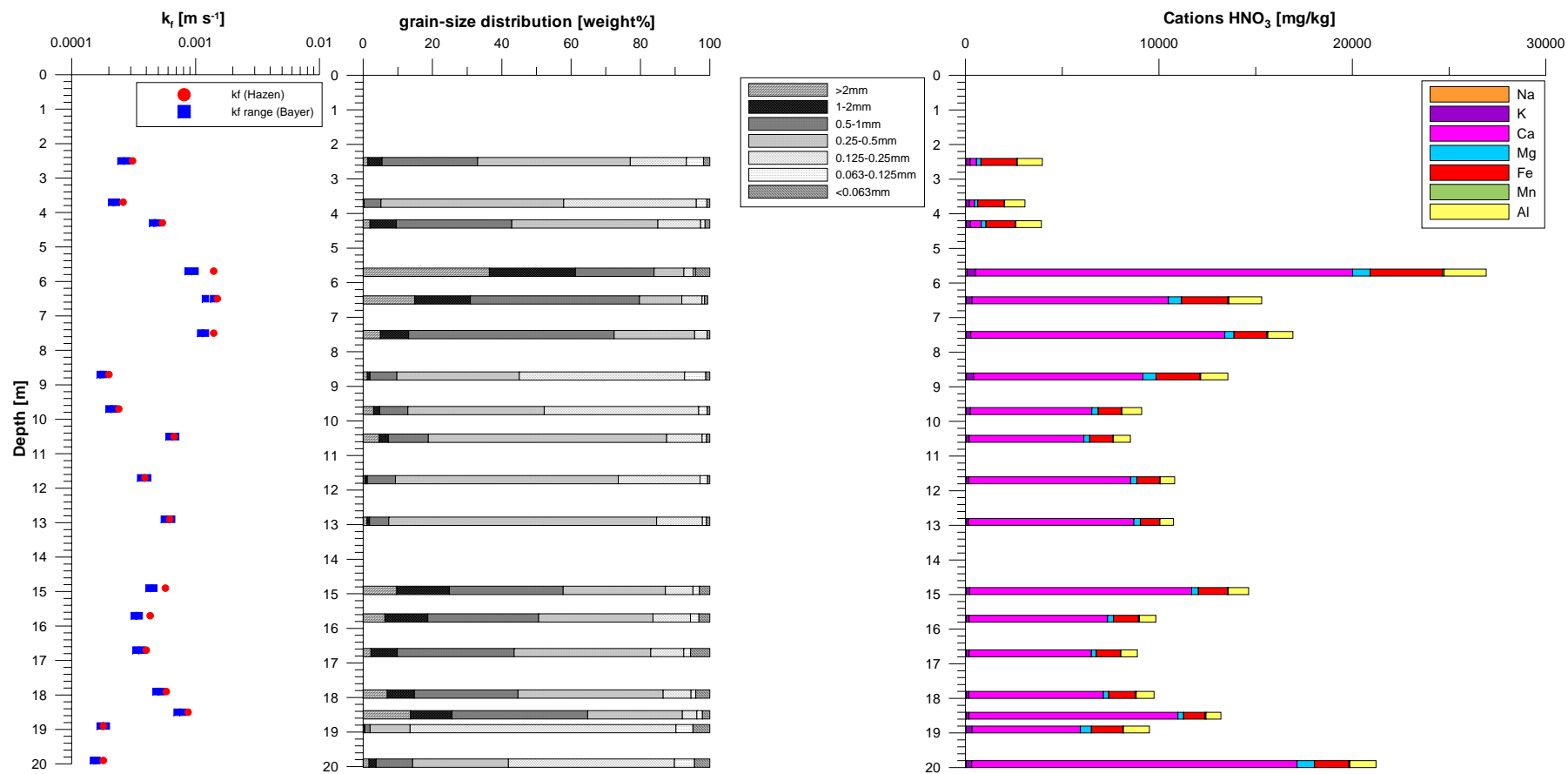
Figure 12: Hydraulic conductivities (k_f), grain-size distribution and cations from HNO_3 extraction in core TEG371UP.
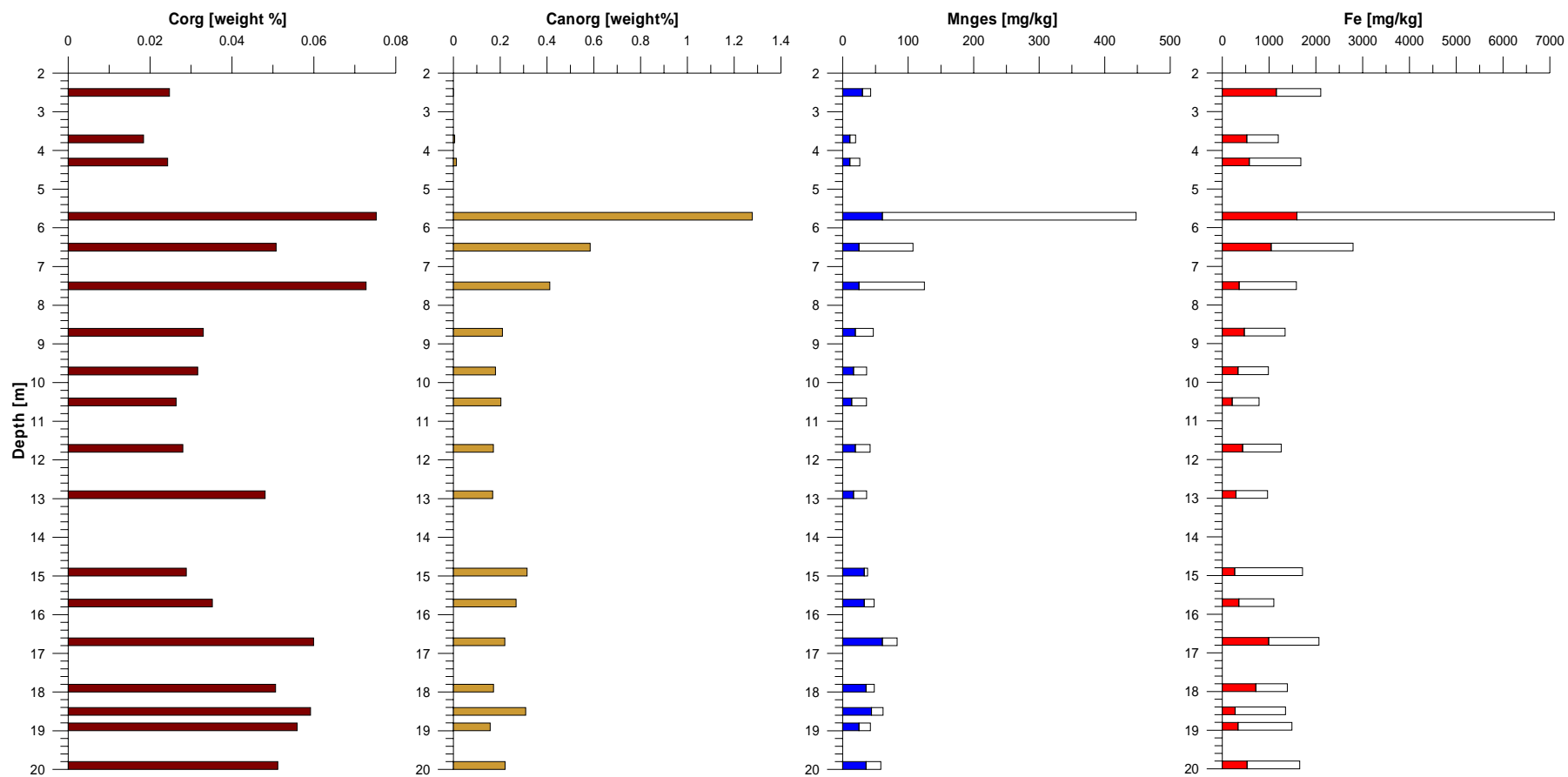
Figure 13: Organic and inorganic carbon content, Fe(III, red) and Fe(II, white), Mn(IV, blue) and Mn(II, white) content in core TEG371UP.

1.3.4 Hydraulic situation
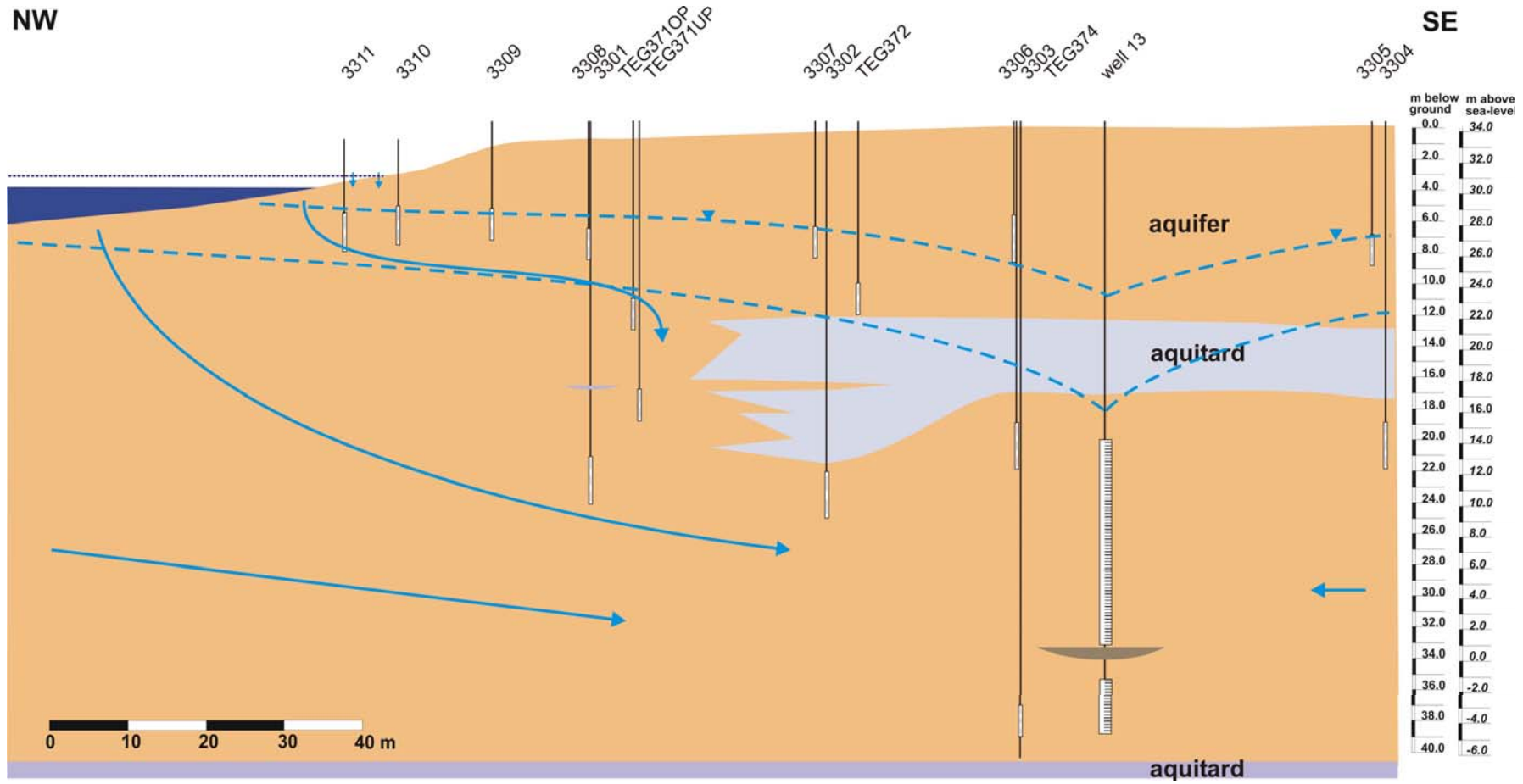
Figure 14: Simplified hydrogeological cross-section of transect Tegel, including the approximate location of the minimum and maximum surface and groundwater-level and exemplary flow-paths.

Figure 14 shows a simplified hydrogeological cross-section with approximate minimum and maximum surface- and groundwater levels as given by logger data between 2002 and 2004 (when well is in operation). All logger data available is presented in figure 15 for a first hydraulic overview. It reflects the fact that the summer 2003 was extraordinary dry and hot, causing a much larger groundwater drawdown and lower surface water level. In summer 2003, even the "deeper" shallow wells TEG372 and TEG371OP fell dry which means, since they have filter screens just above the till, that there was virtually almost no water above the till in the upper aquifer anymore.
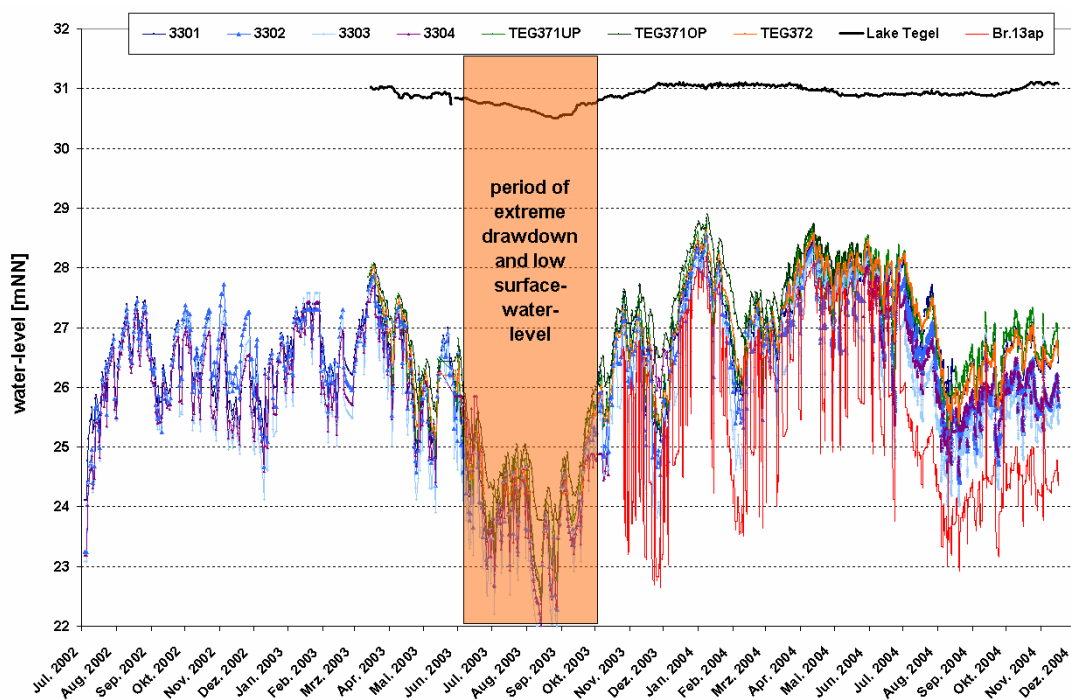
Figure 15: Available water-level data from data loggers at the transect Tegel. Lake Tegel is given in black at the top, while the red line is data from the piezometers in the gravel pack around the production well.

A steady-state 3-dimensional model of the site was constructed in the previous projects (FRITZ, 2002; EICHHORN, 2000). A simplified transient 2-dimensional model, simulating a number of pumping scenarios was developed by RÜMMLER (2003) in joint co-operation between the IGB and the FU on the basis of pumping test data from EICHHORN (2000). The aim was to understand how flow-paths, travel times and proportions of bank-filtrate vary depending on pumping rates and well regimes. Figure 16 shows the flow-paths of one scenario and is meant to give an idea on how flow-paths show a zigzag pattern due to alternating operation of the productions wells. But however strongly flow-paths may move, the following tracer evaluation still gives reasonable average values for residence times. But it has to be taken into account that the actual flow-path length may be larger than expected.

37
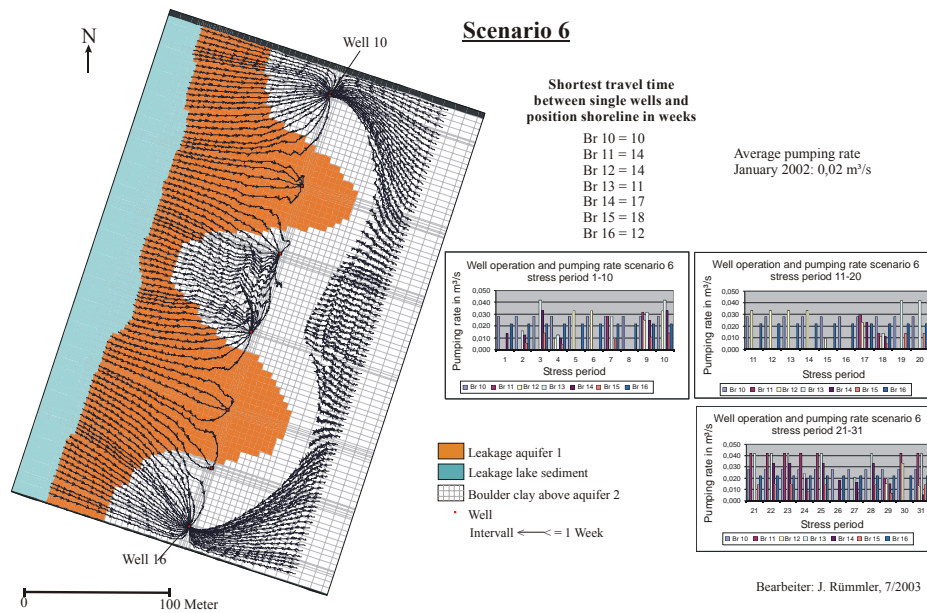
Figure 16: Flow-paths in a transient simulation with monthly alternation of wells 10, 12, 14, 16 and 10, 11, 15, 16 (RÜMMLER, 2003).

1.3.5 Tracer evaluation: Travel times/groundwater age

Breakthrough curves of potential tracers were sighted and a selection of the more suitable ones is shown below, divided into figures of the deeper (figures 17, 18) wells and a succession from shallower to deep (figures 19, 20) observation wells on one spot. Missing data is due to the fact that observation wells fell dry during summer months. For the approximation of travel times the shift of peaks or the shift of the increase or decrease of the concentration was used and estimated visually. Potassium, which appeared to be a suitable tracer at first, showed some retardation and was disregarded. Chloride breakthrough curves are also not shown, because they seem to fluctuate too strongly. The temperature, although not a conservative tracer, proved to be very useful and using a retardation factor of 2 seemed appropriate for the site. The stable isotopes, which are the most useful tracer for the determination of travel times since they are less vulnerable towards side-effects and are perfectly conservative, clearly show that the travel times have overall decreased, i.e. the flow velocities have increased within the time period of sampling. Therefore, rather then given just one value for travel time to a certain well, a range of travel times is given in the summary in figure 23, which is not due to uncertainty of the method but rather due to the fact that travel times did vary over the 2 years of sampling.

38
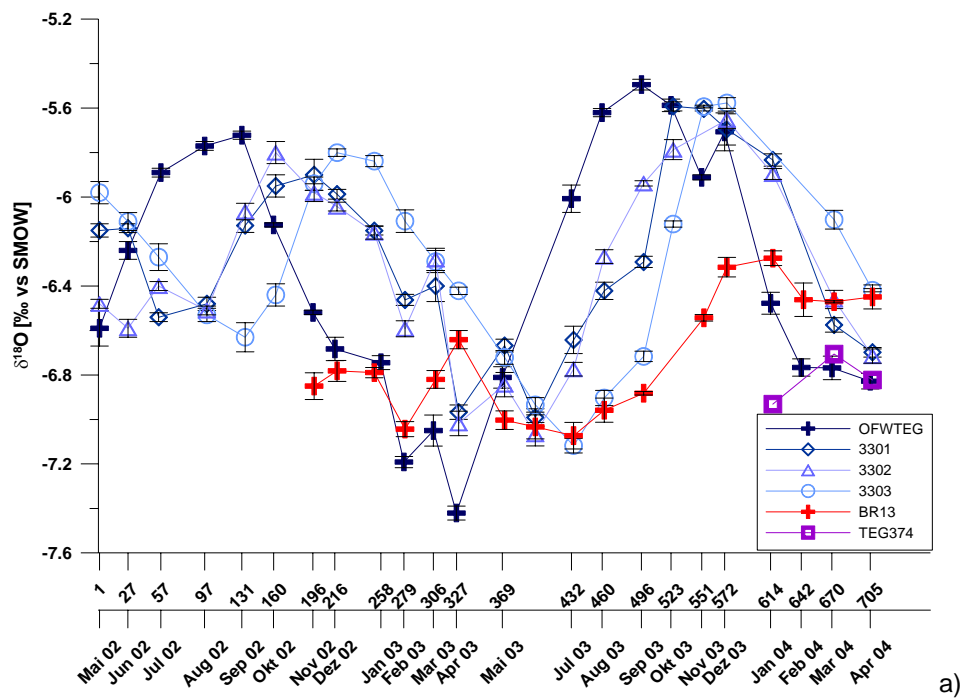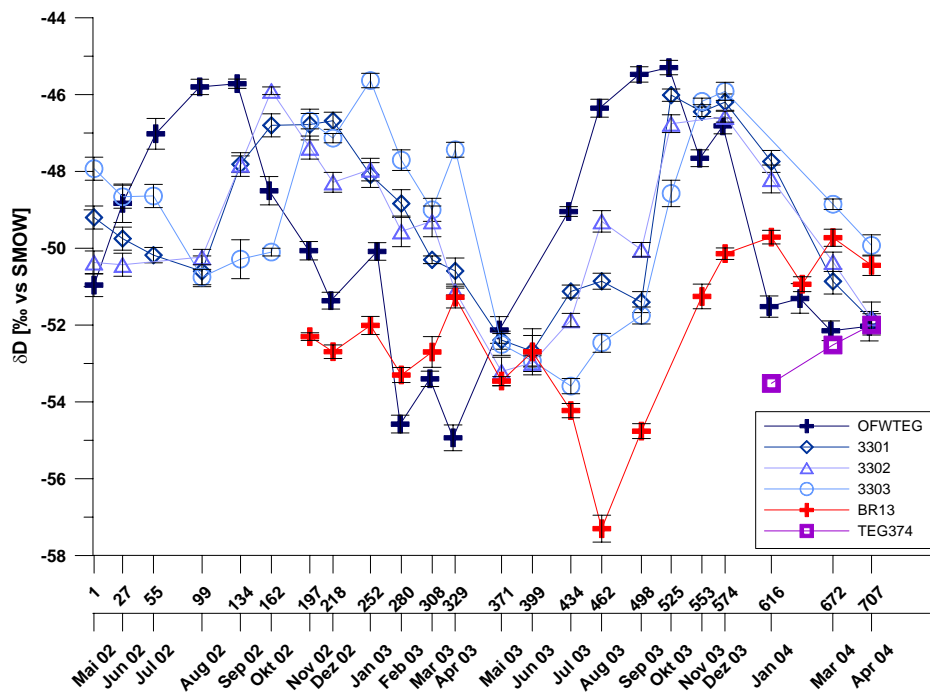
Figure 17: Breakthrough curves of $\delta^{18}O$ (a) and δD (b) in production well 13 (red symbols) and observation wells 3301, 3302, 3303 and TEG374 (compare figure 14). Data source: AWI. Month of sampling and days since start of NASRI are given on x-axis.
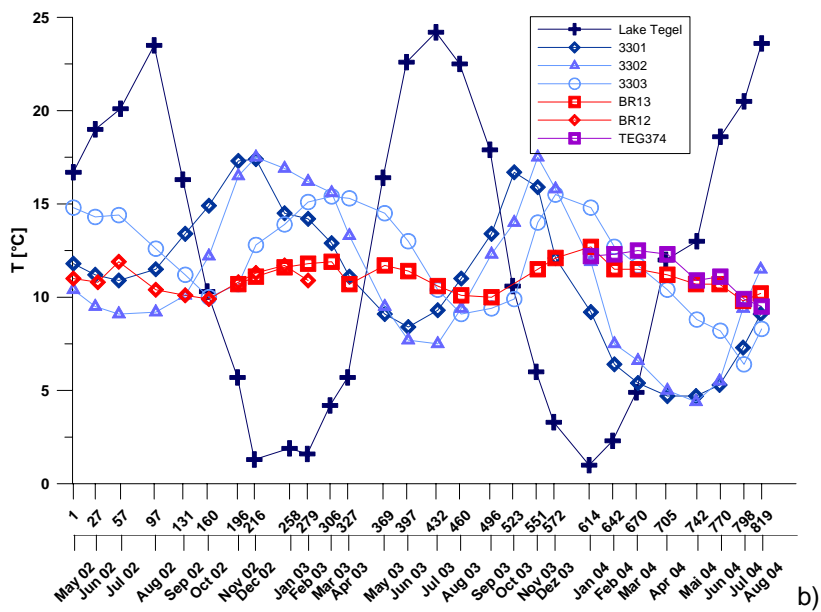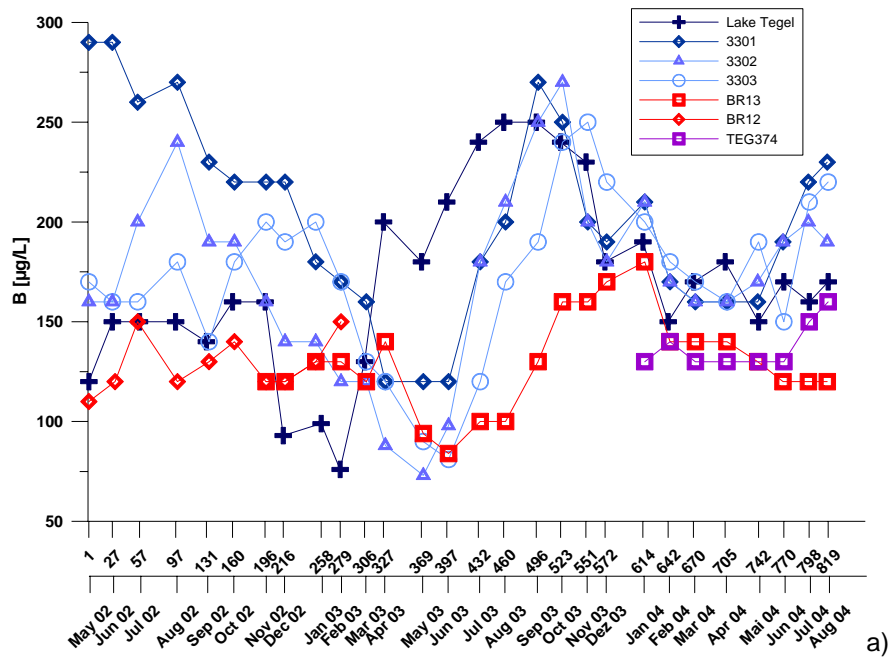
Figure 18: Breakthrough curves of B (a) and temperature (b) in production well 13 (red symbols) and observation wells 3301, 3302, 3303 and TEG374 (compare figure 14). Data source: BWB. Month of sampling and days since start of NASRI are given on x-axis.
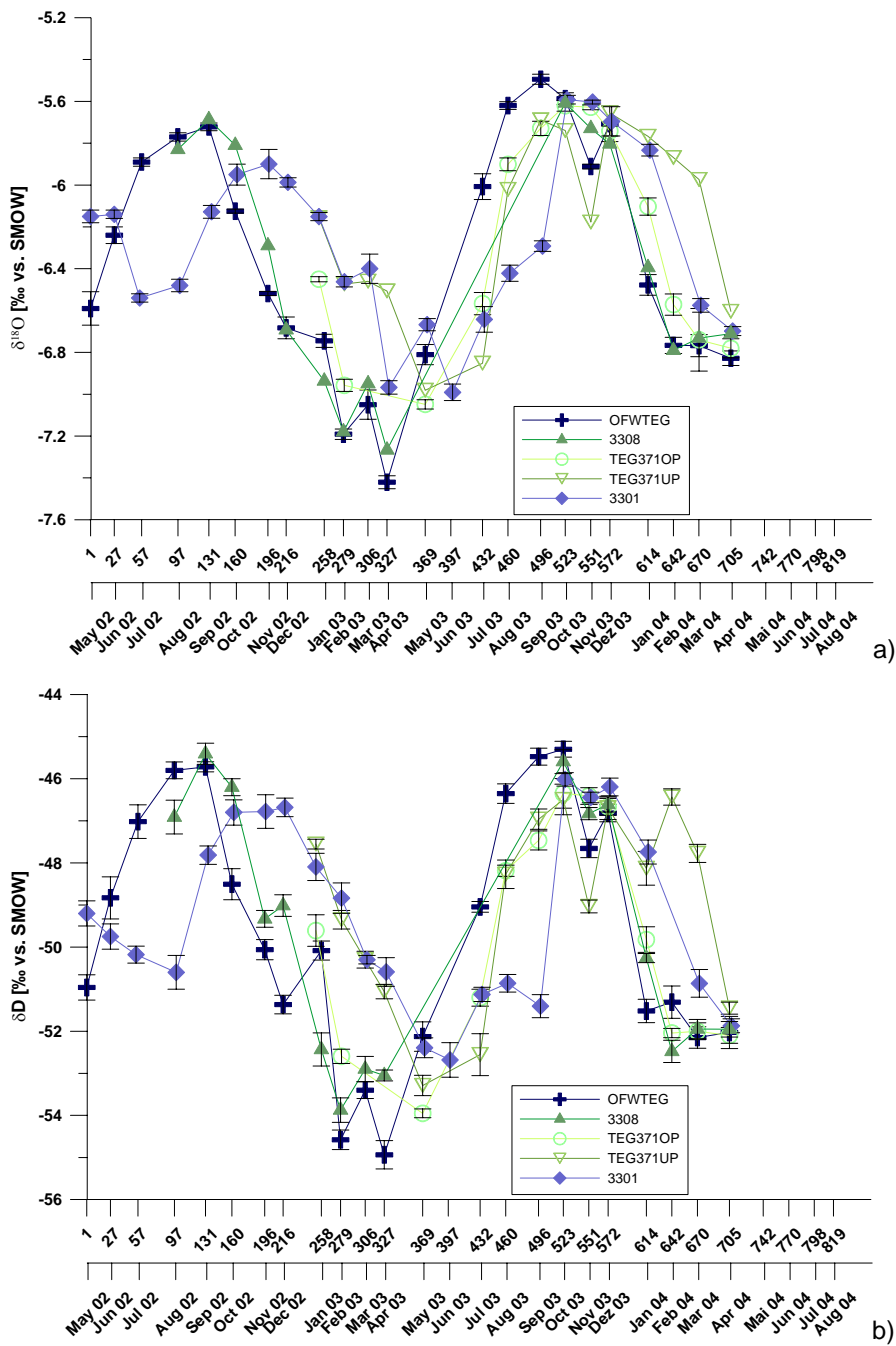
Figure 19: Breakthrough curves of $\delta^{18}O$ (a) and δD (b) from shallow (3308) to deep (3301) observation wells at one location (compare figure 14). Data source (AWI). Month of sampling and days since start of NASRI are given on x-axis.

41
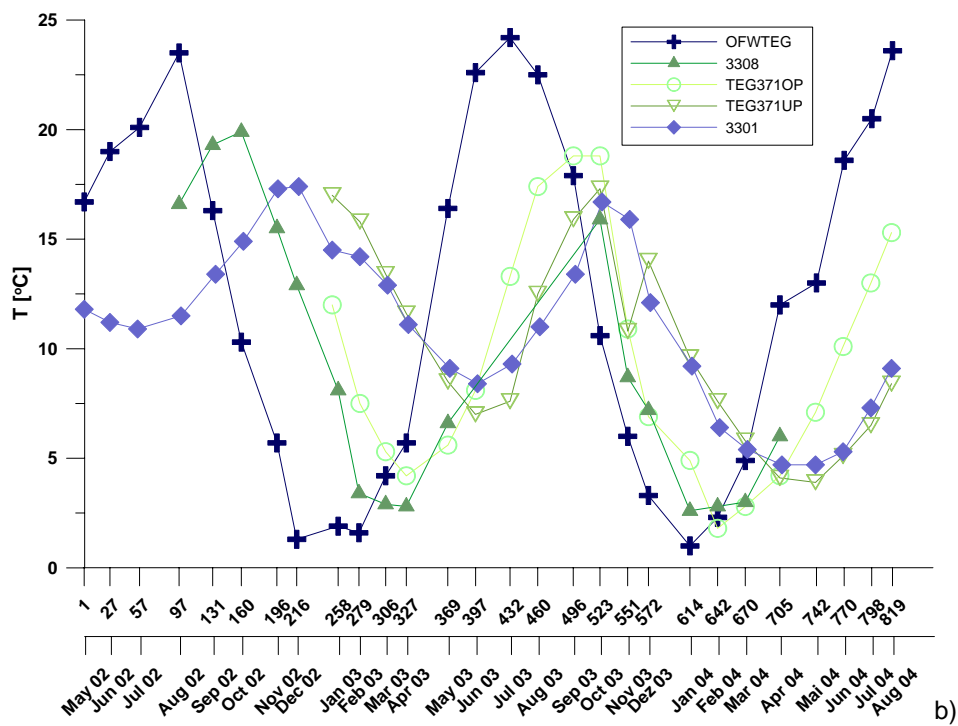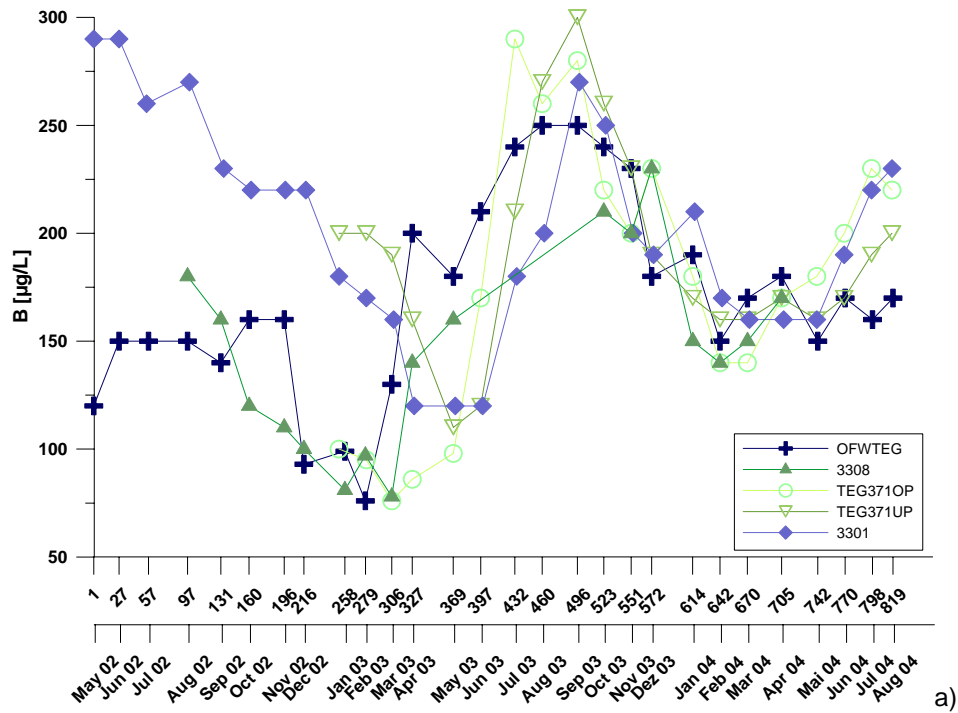
Figure 20: Breakthrough curves of δ^{18}O (above) and δD (below) from shallow (3308) to deep (3301) observation wells at one location (compare figure 14). Data source: BWB. Month of sampling and days since start of NASRI are given on x-axis.
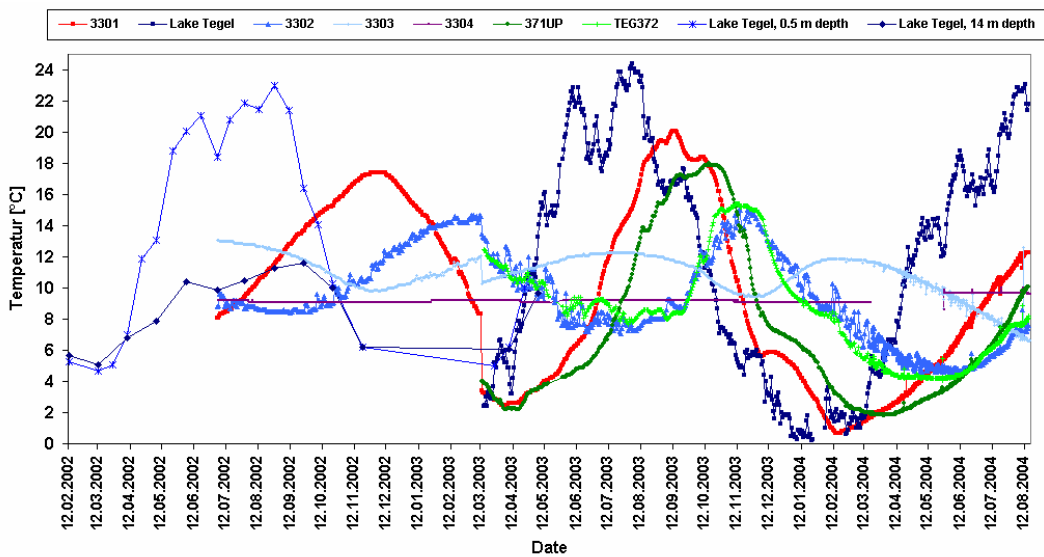
Figure 21: Temperature breakthrough curves registered with data loggers at the transect Tegel.

The temperature breakthrough curves from the data logger are shown in figure 21. With hourly measurements, they have a better resolution than the temperatures from monthly hydrochemical samplings. But, because the temperature sensor is combined with the pressure sensors, the logger are installed more or less at the same depth in all observation wells. Rather than reflecting the groundwater temperature of the filter screen depth, the curves are representative for the depth the loggers are installed in, which is usually shallower. Therefore, the data of the temperature logging cannot be directly compared with the chemical data from the filter of the observation wells. From comparison with the conventional tracers, the retardation factor (R) can be estimated from observation wells with shallow filters, where the logger is installed in the filter level which would result an R of 2 for TEG371OP, given as an example in figure 22.

43
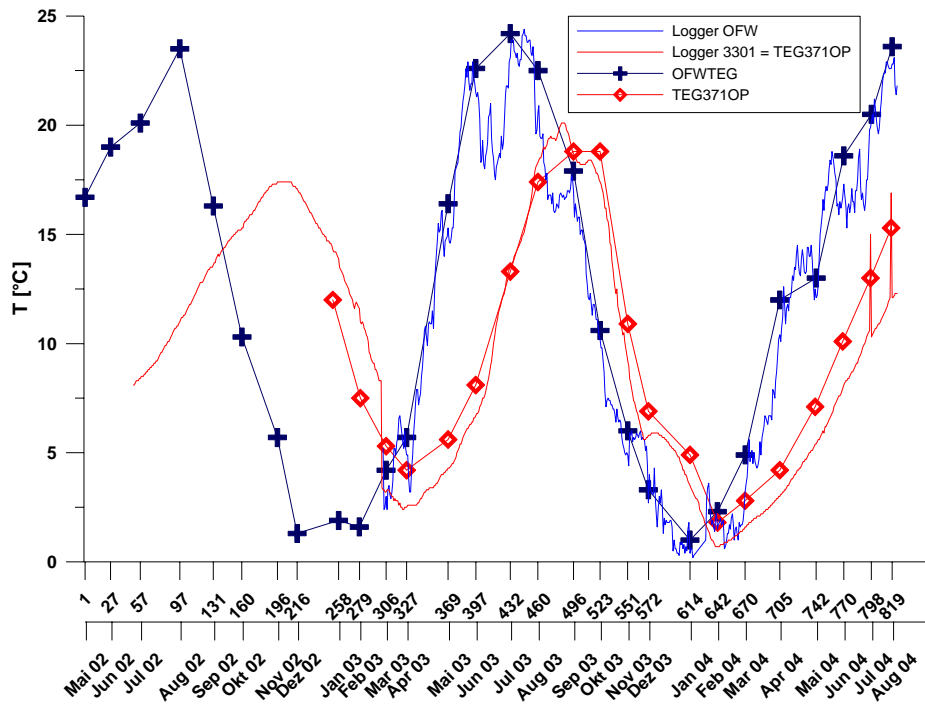
Figure 22: Logger data from Lake Tegel and observation well 3301, as well as temperature data from monthly sampling of Lake Tegel and TEG371OP. Month of sampling and days since start of NASRI are given on x-axis.

To obtain a better overview, the combined findings of the tracer evaluation are summarised in figure 23 (minimum and maximum travel times from May 2002 to August 2004 are given). The effective T/He age is shown in figure 24 (sampling took place in spring 2003).

Because observation wells between the lake and the production well except the very deep TEG374 show hardly any dampening of the amplitude of the input signal of the lake, they must largely consist of bank filtrate from the nearest shore, which should show an effective T/He age of <0.5 years (resolution of the method) as is the case for TEG371OP and 3303.

Although 3301 and 3302 resemble each other largely and have a similar dominating travel time, 3301 sometimes deviates strongly from the lake and 3302 with regard to some of the WW constituents (for example much higher B concentrations in summer 2002, figure 18a) which indicates that 3301 gets at least to a minor extent water from elsewhere and lies on a different flow path. The effective T/He age of 3301 is 1.7 years. If 100 % of the water of 3301 was originating from the direct lake shore, the effective age should be 0-0.5 years (resolution of the method for this site), like it is for TEG371OP and 3303. The effective T/He age is not a "real" age but the result of a mixture of T and ^{2}He of several water bodies. It does therefore not stand as a contradiction to the remaining tracer results. It only indicates that a (probably small) proportion of the water of 3301 is considerably older than 6 months. It is not possible

to say precisely how large this water volume is and what effective ages it is composed of. It does, together with results from some of the minor water constituents (see below), suggest that some water may be infiltrating around the islands within the lake or at the western lake side and is flowing beneath Lake Tegel, which is basically sealed as soon as the laccustrine sappropels become thick.

The background groundwater well 3304 (inland, data not shown) shows no seasonality because it does not contain bank filtrate. Therefore, a calculation of travel times does not make sense. The effective T/He age of observation well 3304 is 11.9 years.

TEG374 was installed in order to clarify remaining uncertainties concerning the vertical age stratification of the entire aquifer, since the former "deep" wells did not reach the lower parts of the aquifer. It was not possible to calculate a travel time for this well from tracer breakthrough curves, because TEG374 was only sampled over 7 months and appeared to show very little seasonality. The effective T/He age for this well is 25 years, which, together with the lack of seasonality, illustrates that there is a water component present in the lower aquifer that is decades, rather than months old. The fact that, for example the temperature, does still show a little seasonality does nevertheless show that TEG374 is probably not the end member of this old water component itself and might contain a lower percentage of water of a younger age. From its chemical composition, the water pumped from TEG374 is, however, clearly former surface water, even though one may argue that the name bank-filtrate might not be appropriate anymore.

The production wells themselves show a strongly dampened tracer signal due to mixing of bank filtrate with background groundwater and due to the fact that the long filter screen abstracts water of variable ages. However, when a signal is visible, it correlates to a dominant (or effective) travel time of 4-5 months. This shows that travel times have decreased compared to 1999-2000, when Fritz (2002) observed travel times of 6-8 months for the same well. The effective T/He age of well 13 was found to be 12.7 years which is even larger than the age of the background groundwater. Again, this clarifies that some of the abstracted water (namely the part flowing at the bottom of the aquifer) is considerably older than both, the "young" bank filtrate and the background groundwater.
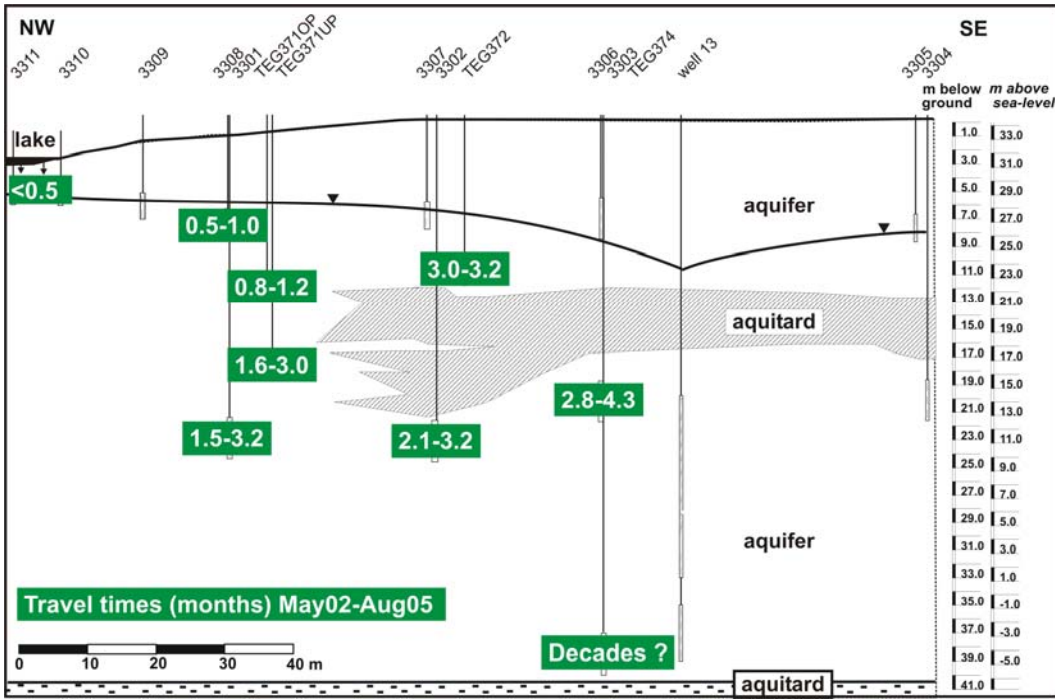
Figure 23: Summary of results from visual travel time estimation using breakthrough curves of $\delta^{18}O$, δD, B and temperature. Range of travel times observed from May 2002 to August 2004.
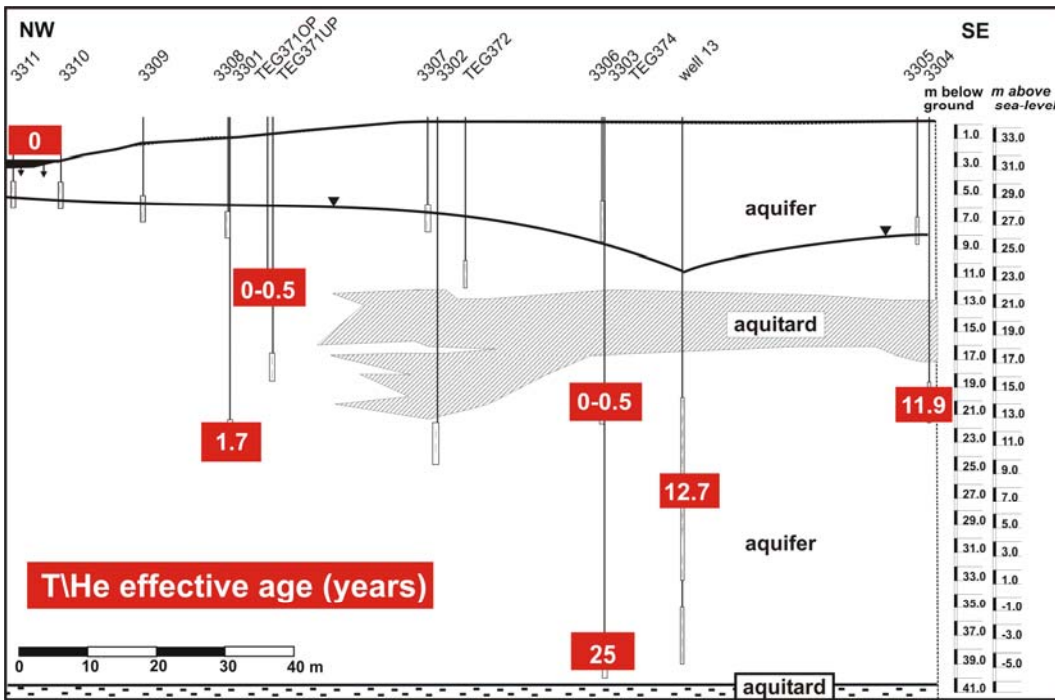
Figure 24: Effective T/He ages. Results do not necessarily represent travel times, since mixing of water alters the age.

1.3.6 Tracer evaluation: Mixing

Figure 25 shows that on a stable isotope scatter plot, the production wells 12, 13 and 14 lie between surface water and background groundwater. To calculate the proportion of bank-filtrate in the production wells, conservative tracer with a clear difference in concentration between groundwater and surface water and fewer seasonal variations are ideal. Average values of the background groundwater (3304), the surface water (or alternatively 3303) and the production wells of stable isotopes, K, EDTA and B which show a sufficient difference between groundwater and surface water (figure 26) were used to calculate the overall BF percentage in the production wells. The differentiation between old and young BF was not undertaken when these tracer were used, since the concentrations in the old BF resemble more or less those of the surface water average (despite lacking seasonality) for these substances (figures 27, 28).
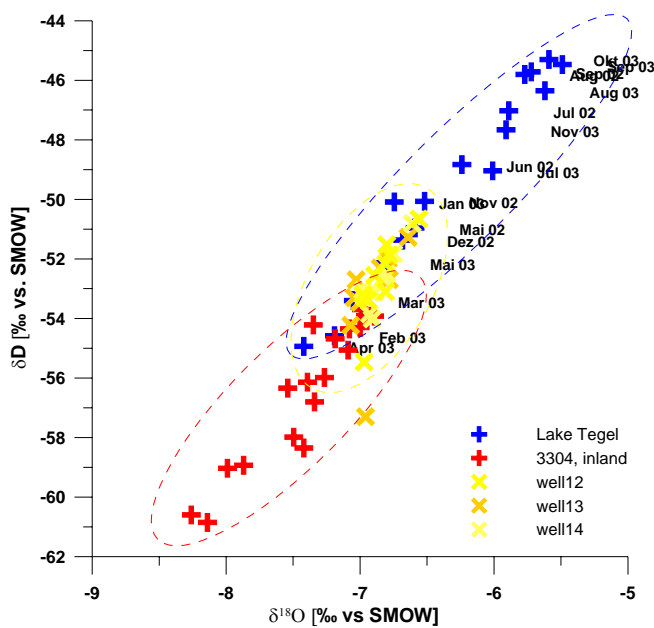
Figure 25: δD versus δ18O in surface water (blue), background groundwater (red) and abstracted water (yellow) in Tegel (May 2002-October 2003, data source: AWI).
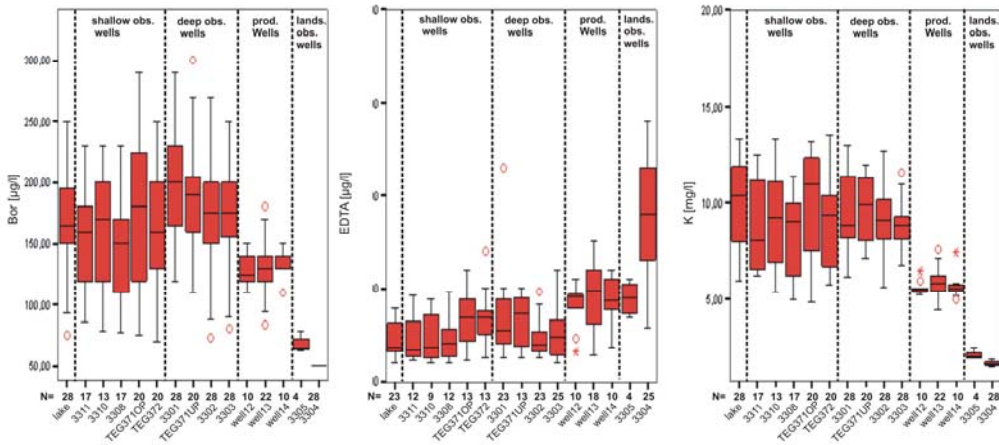
Figure 26: Boxplots for B, EDTA and K, illustrating the difference between the surface water and BF wells and the background groundwater, represented by 3304. Data from May 2002-August 2004, N = number of samples for respective well.

Some difficulties arouse. For example, the time-series show that all parameters strongly varied in the surface water over the period of sampling. Also, EDTA concentrations (figure 28) and isotope values (figure 27) in the background groundwater (3304) strongly changed in 2003 for unknown reasons, after having been more or less stable in the past (FRITZ, 2003). The isotope values increased to an extent that they even resembled surface water values in February 2003. The fact that the deeper, old BF and the production wells showed little seasonal variations suggested that it is more useful to use long-time averages only, rather then trying to calculate monthly percentages (because the time-lag which would have to be taken account for is not equal throughout the water column). The results of the calculations vary, depending on what parameter is used, whether concentrations of the lake water or 3303 are used for the calculations, whether or not the time offset was taken account for when calculating the average over a comparable time-period), what background groundwater concentration was assumed when concentrations were below detection limit (e.g. zero or detection limit of 50 µg/l for B) etc… Considering all these difficulties and choosing the most appropriate assumptions lead to a proportion of bank filtrate in well 13 of 58-69 % (for both young and old bank filtrate together).
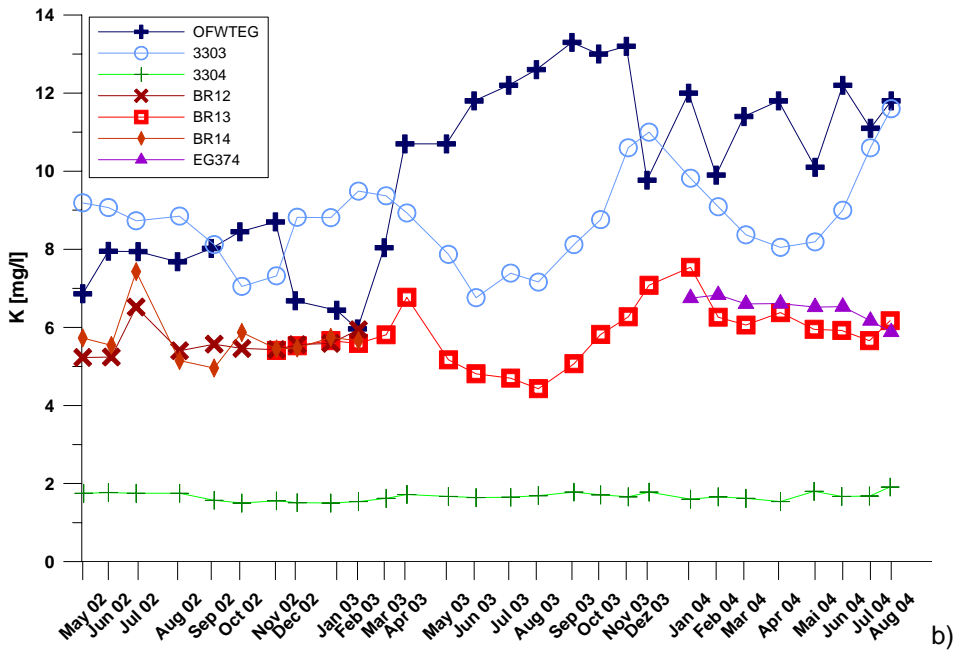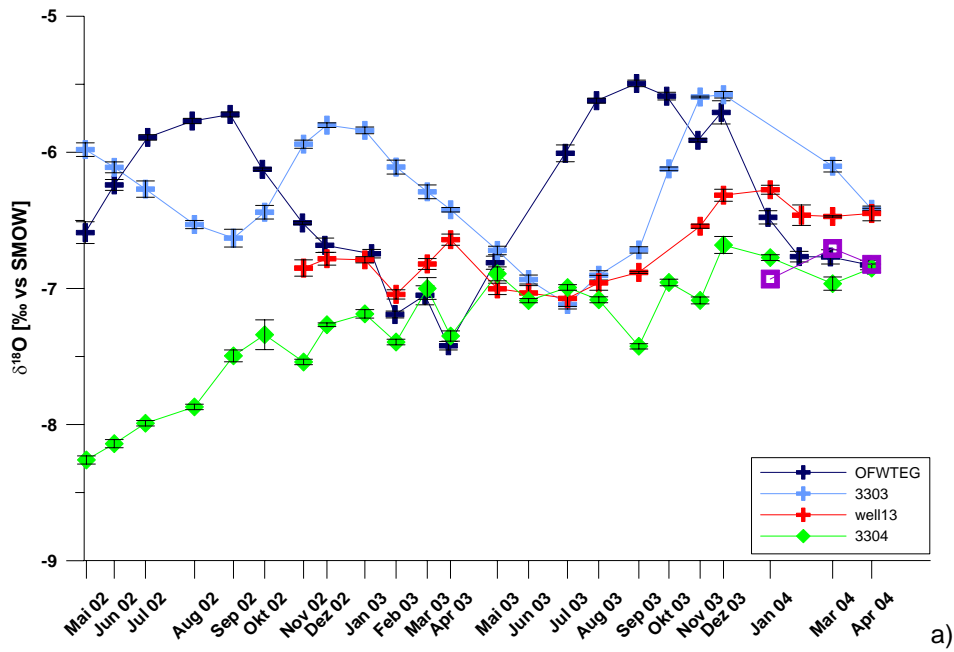
Figure 27: Time-series of δ18O (a) and K (b) in surface water, production wells and shallow observation wells 3303 & 3304 and deep observation well TEG374.
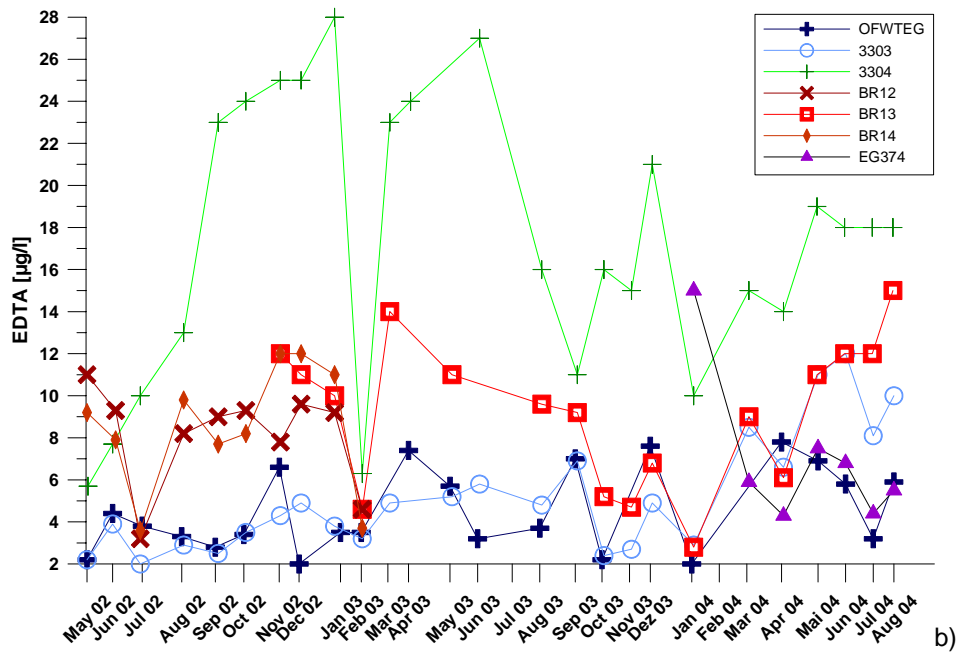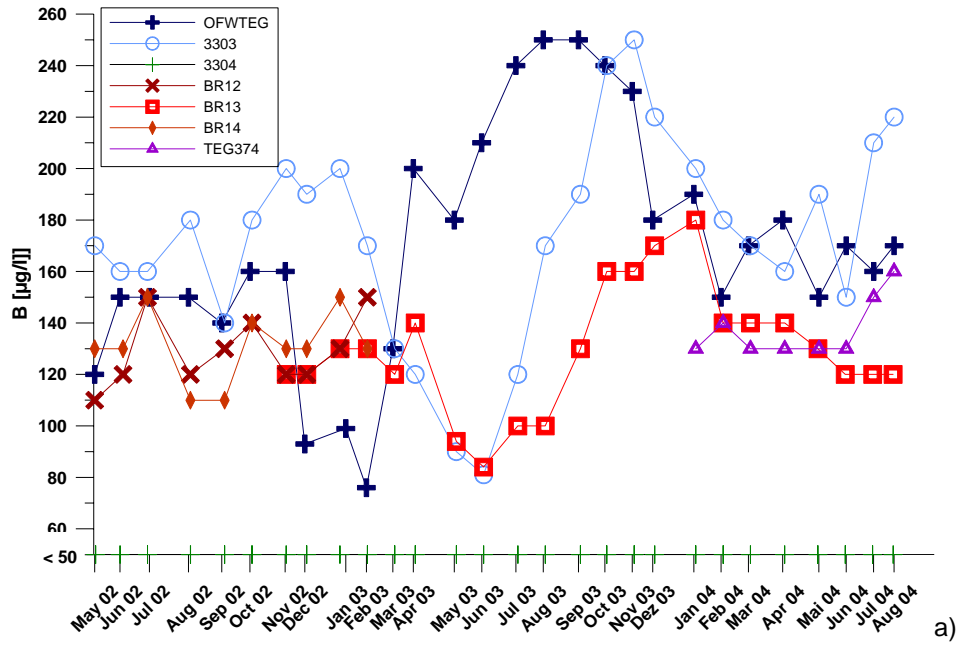
Figure 28: Time-series of δ18O (a) and K (b) in surface water, production wells and shallow observation wells 3303 & 3304 and deep observation well TEG374.
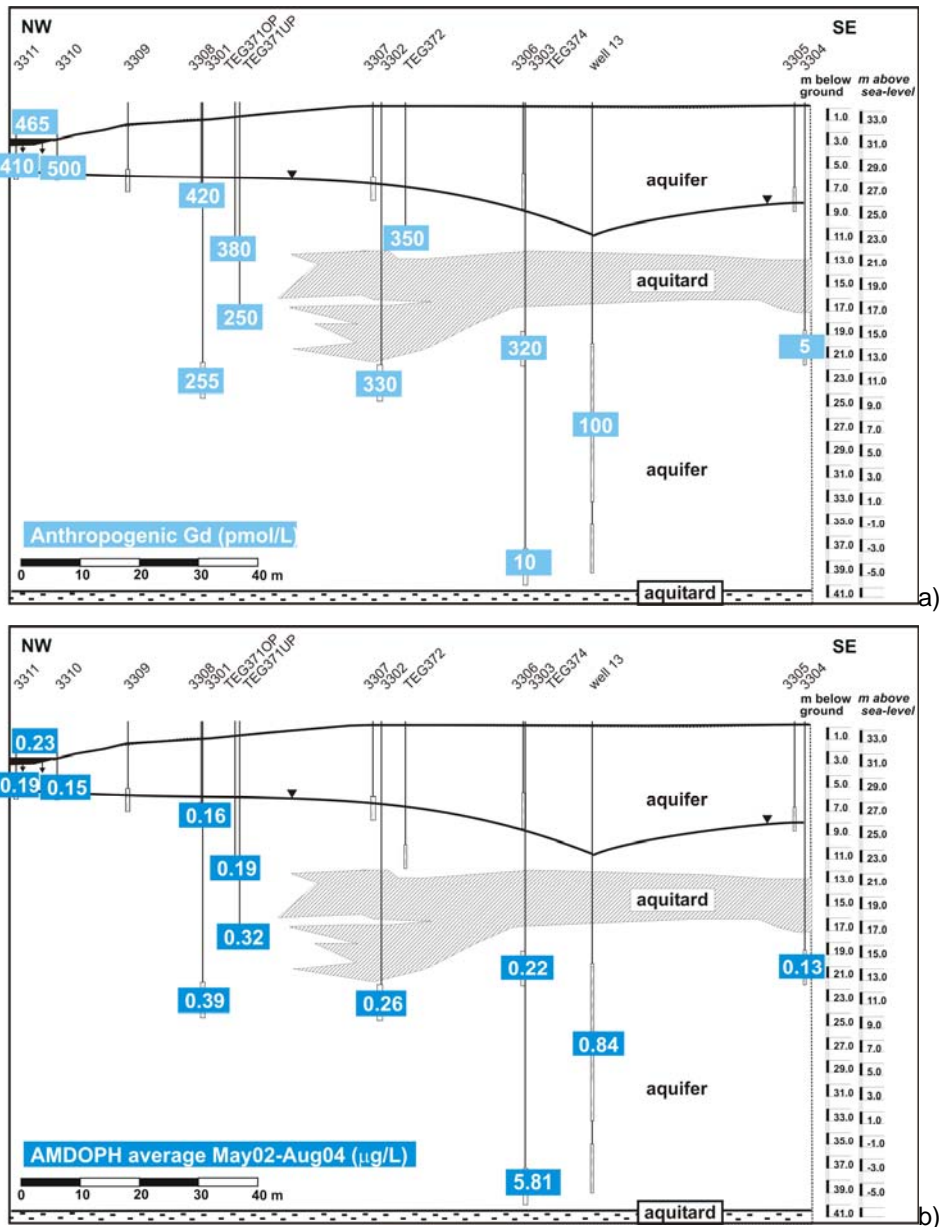
Figure 29: Average concentrations of Gd-DTPA (a) and AMDOPH (b) in wells at the transect Tegel.

Several facts indicated that the samples from the production wells (red colours in figures 27, 28) are not only a mixture of bank-filtrate encountered in the shallower parts of the aquifer (represented by observation wells 3301-3303; blue colours in figures 27, 28) and water from inland of the production wells (represented by observation well 3304; green colours in figures 27, 28).

1. The effective T/He age of 12.7 years of well 13, which is even older than the age of 3304 (11.9 years).

51

2. The fact that seasonal variations of all tracers in the production wells are rather small.

3. Most importantly: The fact that the production wells strongly differ from the "young" bank filtration wells with regard some of their minor water constituents. For example, some PhAC's, namely AMDOPH (figure 29a) and Phenazone are present in higher concentrations than in today's surface water, while others, for example Gd-DTPA (figure 29b) and Carbamazepine are present in much lower concentrations which cannot be explained by mixing of bank filtrate with background groundwater.

With the installation of the deep observation well TEG374 reaching the base of the aquifer it became clear that the deeper BF strongly differs from the shallow BF in some respects. Like the production wells, the seasonal tracer variations in the deeper groundwater are small, while the T/He age was 25 years. The concentrations of the minor water constituents mentioned under point 3 above differ even more strongly from the remaining wells. While the concentrations of AMDOPH (figure 29a) and Phenazone are even higher in TEG374 than in the production wells, the concentrations of Gd-DTPA (figure 29b) and Carbamazepine are very low or below detection. Hence, AMDOPH which appears to behave like a conservative tracer can be used to calculate the percentage of deeper, older BF in well 13 (~11 %). However, the time-series (figure 30) shows that the AMDOPH concentration in TEG374 also varies. In addition, the slight seasonal temperature variations indicate that TEG374 is not perfectly representative as an end-member for the deeper, old BF (assuming that this is decades old, it should not show any seasonal variations).
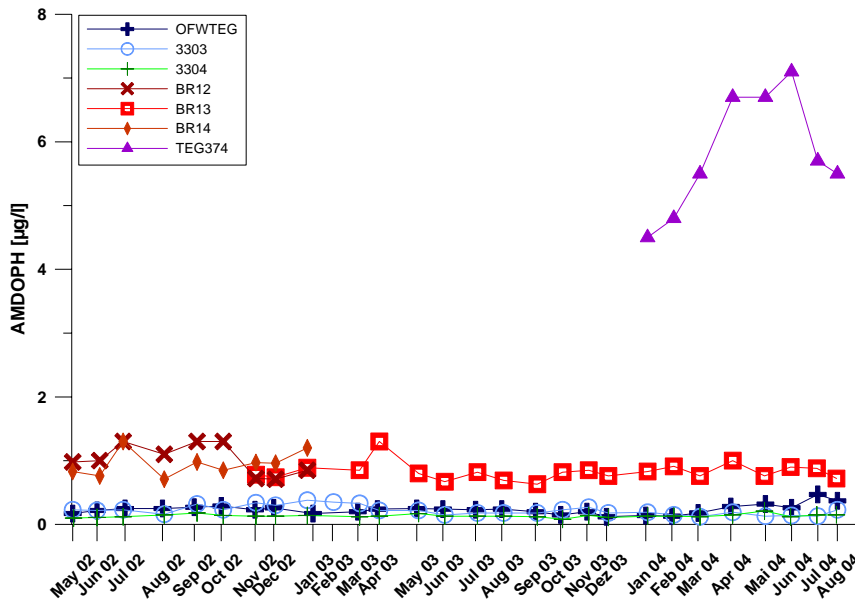
Figure 30: Time-series of AMDOPH in the production wells 12, 13 and 14, and the observation wells TEG374 (violet, deep BF), 3303 (light blue, shallow BF) and 3304 (green, inland) as wells as in Lake Tegel water (dark blue).

Therefore, with an average proportion of total BF of 58-69 % and an average proportion of deep, "old" BF of 11 %, an average of 47-58 % of the water in well 13 would be "young" BF, originating from the nearest shore in front of the transect.

All groundwater observation wells with the exception of the very deep TEG374 contain practically only (> 95%) young bank filtrate which infiltrated at the nearest shore which becomes apparent in the virtually undamped tracer breakthrough amplitudes (except of course for temperature) and the fact that the average concentrations for all non-reactive minor water constituents (e.g. AMDOPH) are similar to those of the lake. As mentioned above, 3301 and TEG371UP differ slightly from the remaining wells with regard to their T/He age which is slighly larger and also with regard to the concentrations of B or other tracer. Using average AMDOPH data to calculate the proportion of deep „old" bank filtrate (represented by TEG374) in 3301 would result in a value of 3 %, for TEG371 the percentage would be even lower. The calculation is based on the presumption that TEG374 is an end-member with regard to the deep, old BF.

Even though all of these calculations can not be precise due to the given limitations, they nevertheless give an idea on the order of magnitude of mixing proportions that can be expected.

1.3.7 Hydrochemistry at the transect

In terms of the hydrochemical properties at the transect, redox changes during infiltration are of particular importance, since they cause the appearance of the undesired metals Fe^{2+} and Mn^{2+} (BOURG & BERTIN, 1993), influence the behavior of a number of organic pollutants such as pharmaceutically active substances (HOLM et al., 1995), halogenated organic compounds (BOUWER & MCCARTHY, 1993; GRÜNHEID et al., 2004) and effect the pH and calcite solution capacity (RICHTERS et al, 2004).

Generally at Tegel, the deeper the well, the more reducing it is. In addition, wells located underneath the lake tend to be more reducing the further out into the lake they were installed. The observation wells from the upper aquifer above the till contain oxygen throughout most of the year while the deep observation wells are mostly anoxic or more precisely ferrous. Boxplots of the redox indicators are shown in figure 31. They show that the median of oxygen and nitrate is larger in the shallow observation wells than in the deeper observation and production wells, whereas these contain more ammonia, manganese and iron.
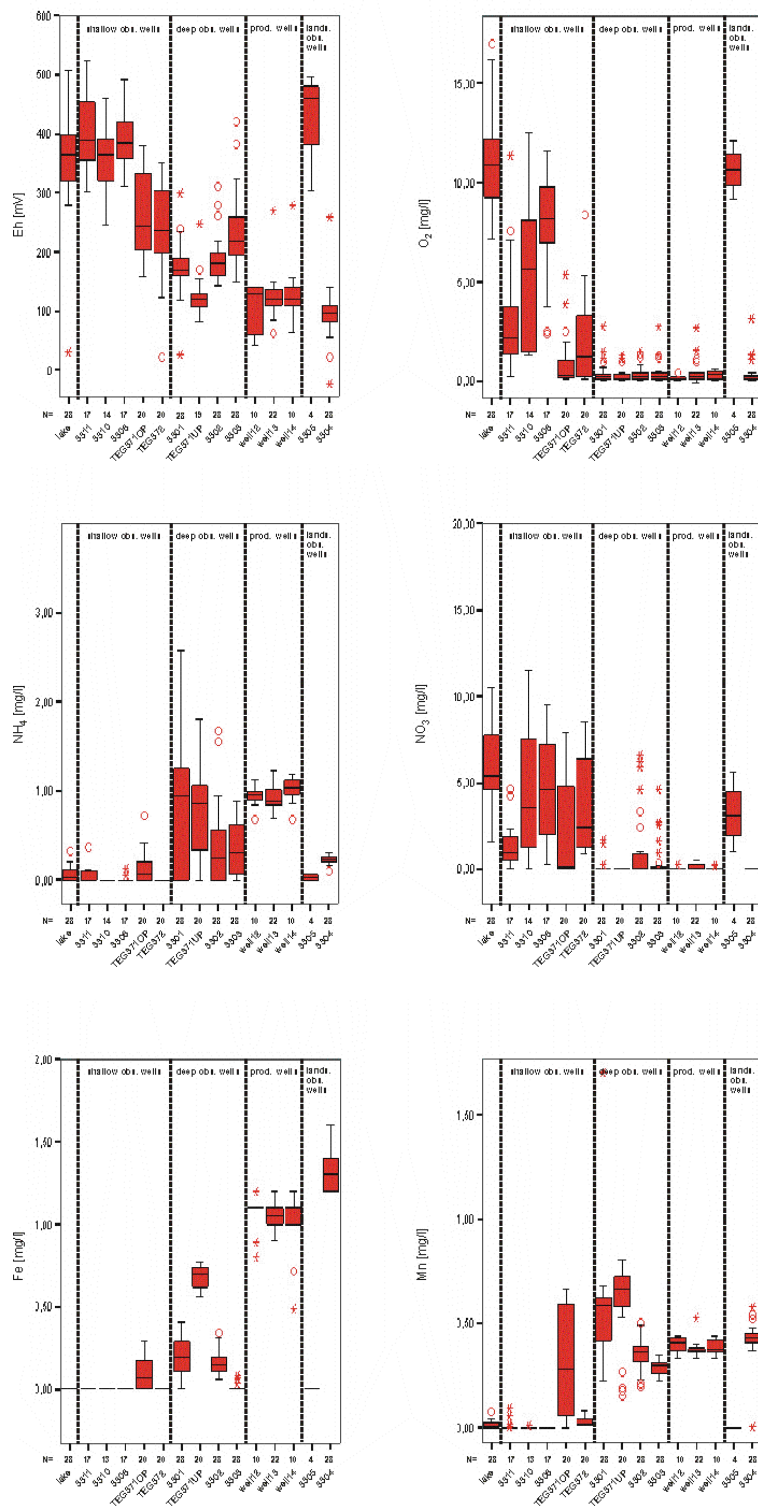
Figure 31: Boxplots of redox indicators Eh, O₂, NO₃⁻, NH₄⁺, Mn²⁺ & Fe²⁺ at the transect Lake Tegel.
Data from May 2002-August 2004, N = number of samples for respective well.
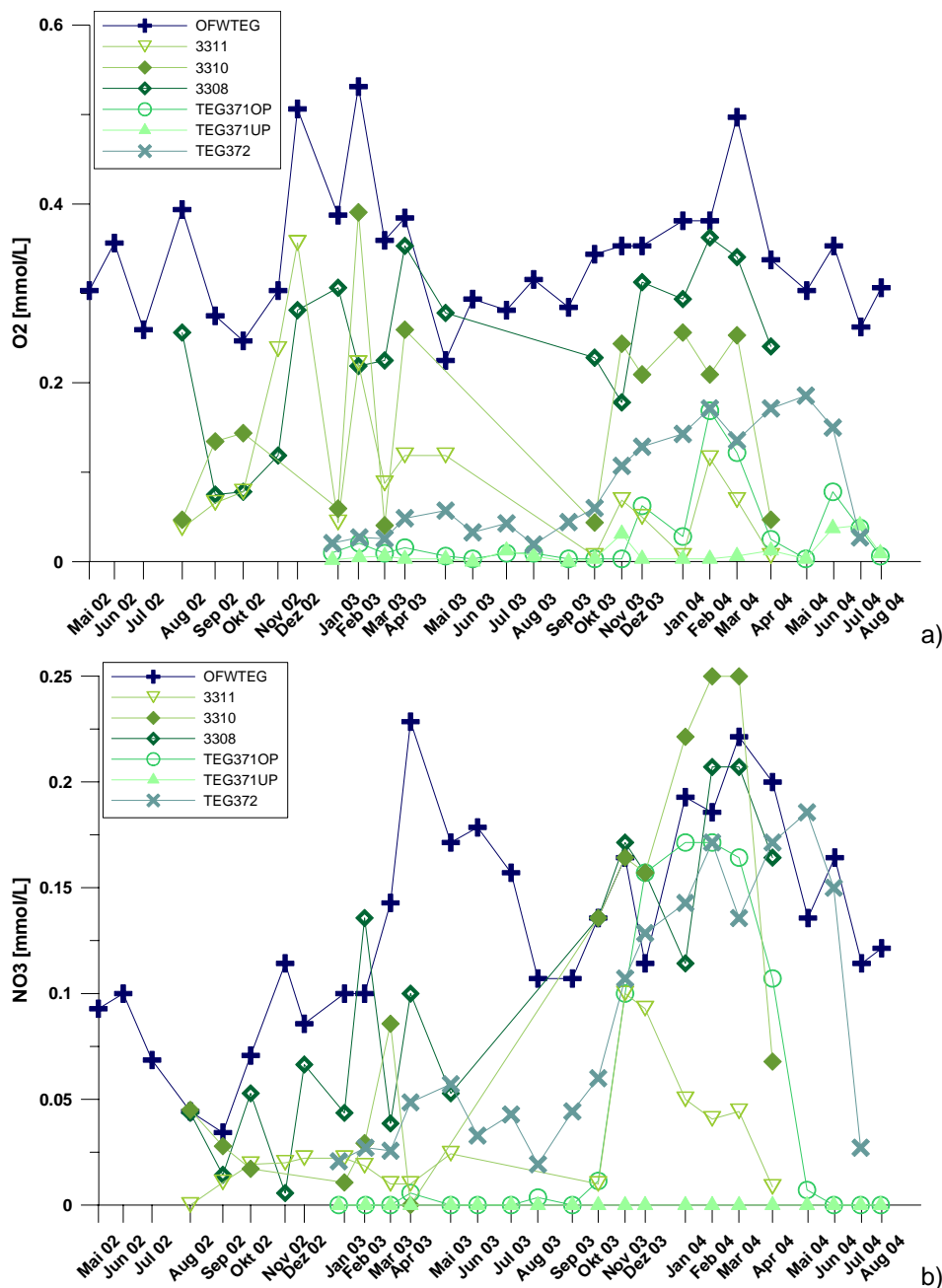
Figure 32: Oxygen and nitrate concentrations in the lake and the shallower observation wells at Transect Tegel. Data source: BWB.

However, the redox zones are not immobile and redox boundaries move seasonally. The younger bank filtrate (age < 5 months) undergoes strong seasonal temperature changes of up to 25 °C, depending on the distance from the lake. Because redox processes are microbially catalysed, these changes lead to differences in microbial activity (e.g. DAVID et al., 1997; PROMMER & STUYFZAND, 2005). As a result, oxygen and nitrate largely disappear in the very

shallow observation wells which do not fall dry at times when temperatures are highest (summer or autumn, depending on the respective time lag to the well). For some reason, nitrate concentrations in winter 2003/2004 were much higher in the shallow observation wells than in the previous year, even exceeding the concentrations in the lake itself (figure 32b).
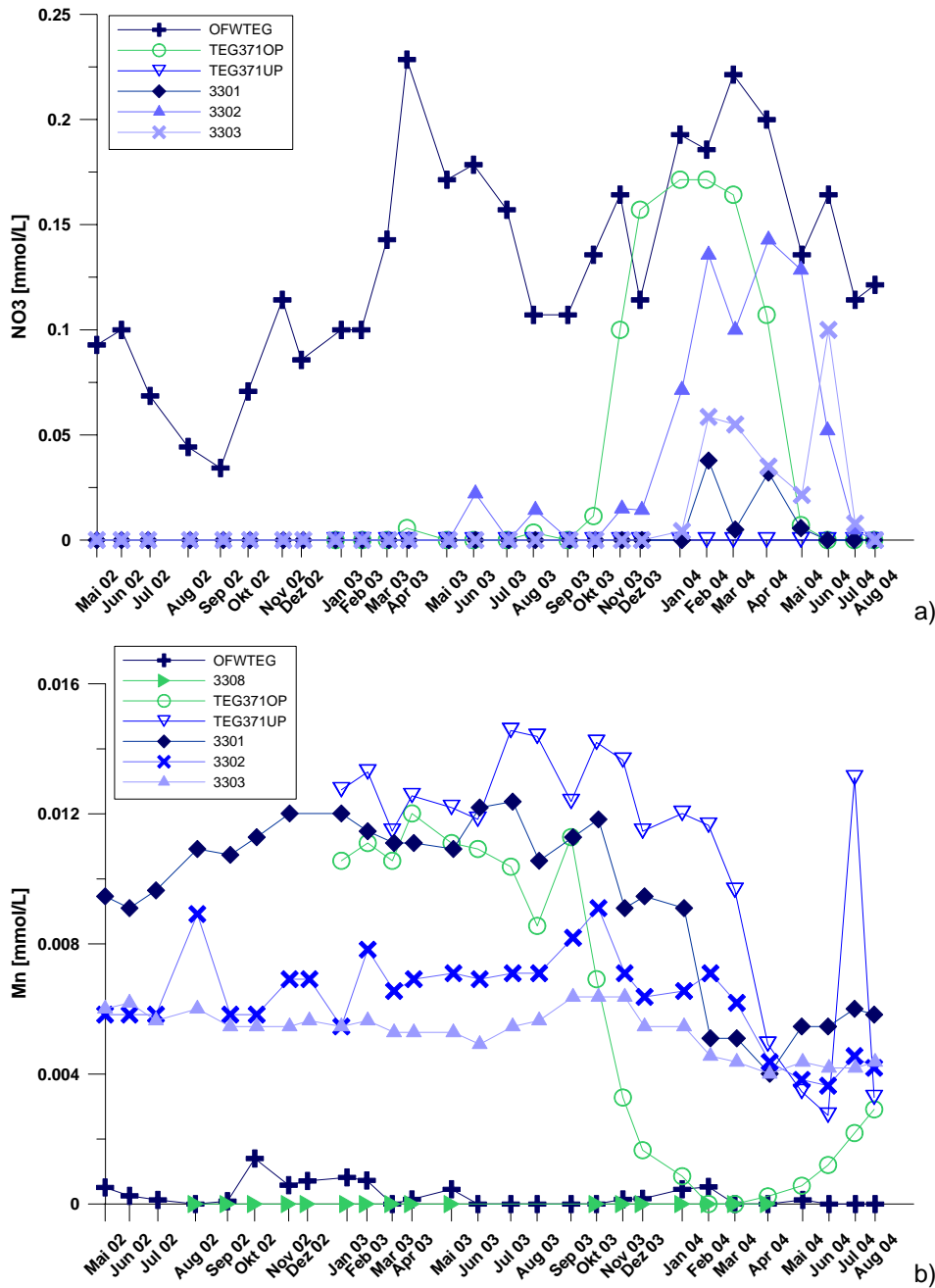
Figure 33: Time-series of nitrate and manganese in the deeper observation wells (and lake and the shallow wells 3308 and TEG371OP for comparison)

In addition, unlike in the previous years (FRITZ, 2002), nitrate was found to break through (with the respective time lag) into the deeper observation wells 3301, 3302 and 3303 (figure 33a), while manganese (figure 33b) and iron concentrations decreased at the same time. This shift of the redox zones towards less reducing conditions is probably related to the extreme drawdown in summer 2003, which exceeded the "normal" drawdown of previous years of about 3 metres. Another factor could be the fact that travel times have generally decreased from summer 2002 to summer 2003. None of these changes had any effect on the DOC concentration. Because of the time-lag, the effects are seen much later in winter 2003/2004. Redox zones as characterised by the disappearance of reactants (oxygen, nitrate, sulphate) or the appearance of reactants (iron, manganese) as suggested by CHAMP et al. (1979) were drawn into figure 34 for summer 2003 and winter 2004. Teg371UP tends to be more reducing than 3301 or 3302, probably due to locally deviating sediment properties (hydraulic conductivities and/or organic carbon content).
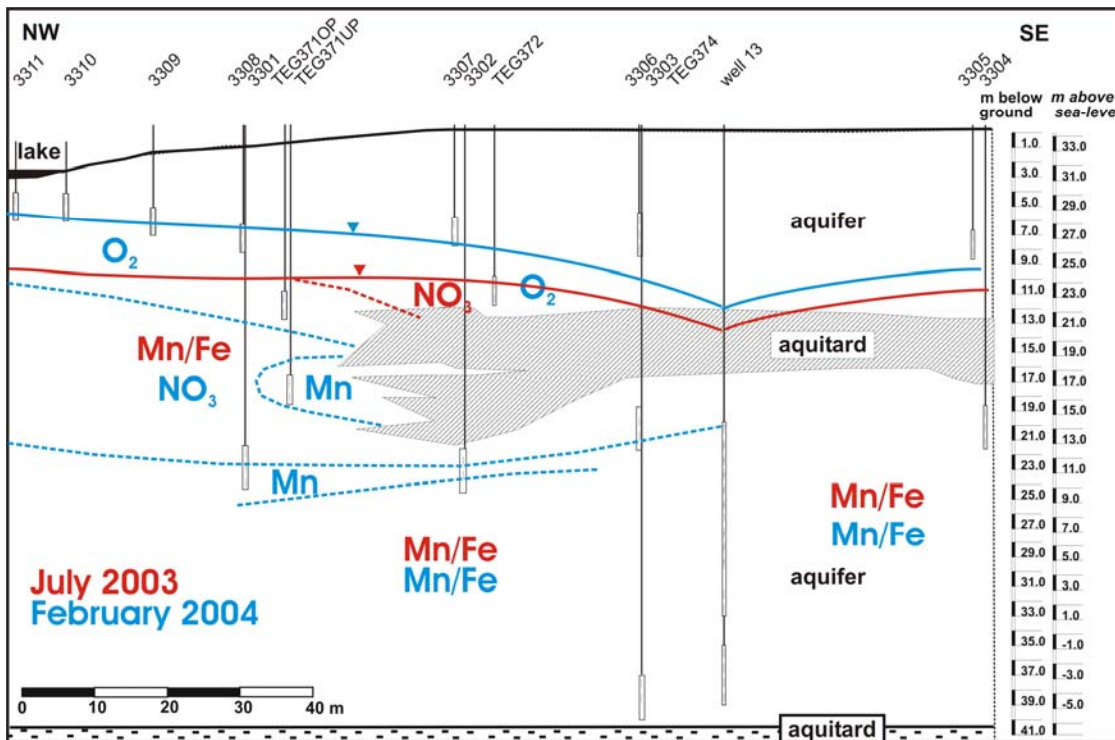
Figure 34: Approximate redox zoning as indicated by presence O_2, NO_3^-, Mn^{2+} and Fe^{2+} in July 2003 and February 2004.

The sulfate concentrations of the lake and the BF observation wells between lake and production well largely resemble each other with respect to sulfate concentrations and isotopic composition of sulfate (figure 35). Hence, a sulfidic redox milieu is never encountered. Only the sulfate concentrations of the deep observation well TEG374 appear to be a little lower at

times. In addition, the isotopic concentration of sulfate of TEG374 is slightly higher (the sulfate is heavier), which is an indicator for commencing sulfate reduction.
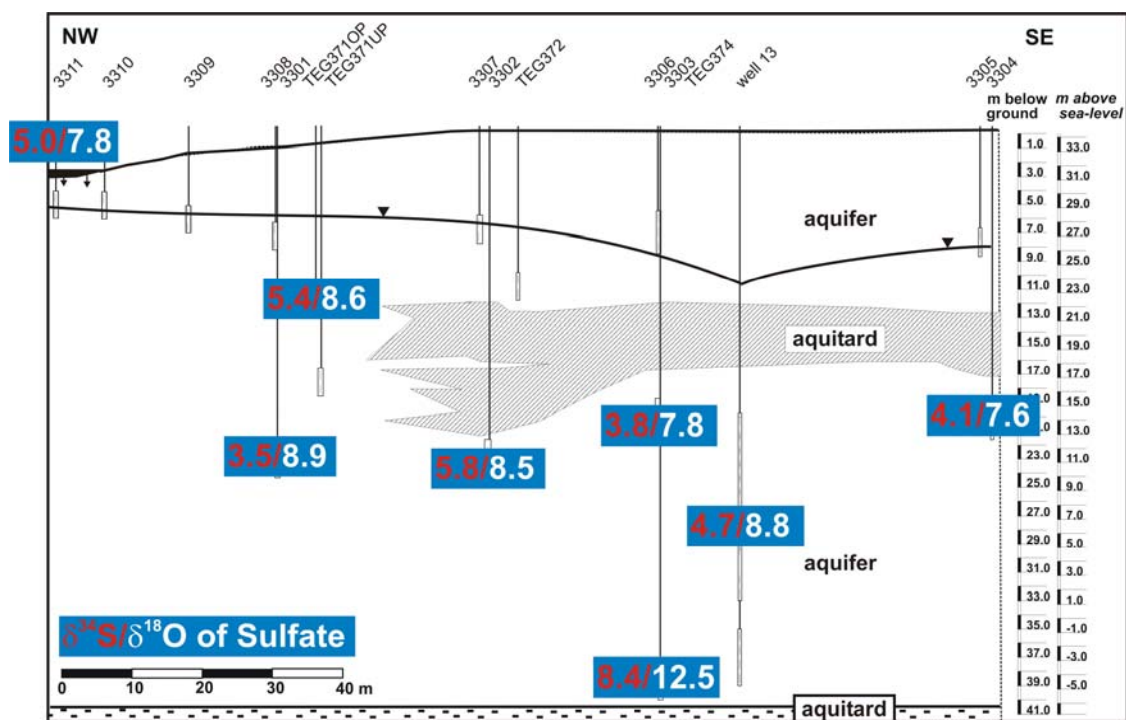
Figure 35: $\delta^{18}O$ [‰ vs. SMOW] and $\delta^{34}S$ [‰ vs. CDT] of sulfate from July 2004.

1.4   Major conclusions and summary Lake Tegel site

1.4.1   Surface water

- Lake Tegel is under the influence of Upper Havel water entering the lake from the south and treated WW from the WWTP Schönerlinde, which is discharging its effluent into the Nordgraben ditch.

- Evidence of elevated proportions of WW are elevated concentrations of WW indicators such as Cl^-, Na^+, SO_4^{2-}, B, DOC or Gd-DTPA, high temperatures (in winter) and more negative isotopic signatures and is most evident near the outlet of the surface water treatment plant (OWA).

- The surface water sampling point in front of the transect is sufficiently representative for the local surface water providing the source for the bank filtrate near the transect. The spatial variation of the surface water quality is relatively small.

- In average, the surface water in front of the transect contained approximately 21 % of treated WW between May 2002 and August 2004.

58

1.4.2　　　　Sediments / clogging layer

- Bank filtration mainly takes place near the lake shores, which is why sulfate concentrations of the bank filtrate resemble those of the surface water, despite the fact that sulfate is quickly reduced in the laccustrine sappropels covering the lake base.

- Modelling of a sulfate profile gave a fitted first-order constant for sulfate reduction in the uppermost 10 cm of the mud sediments profile is 1.49×10^{-7} s^{-1}. This value is 7.5 times higher than the fitted constant of 2.0×10^{-8} s^{-1} for the following section, 10-40 cm below the mud surface, which is expected to be a function of variations in the types of organic matter rather than variations in the total organic carbon content.

1.4.3　　　　Travel times

- The most useful tracer for travel time evaluation are stable isotopes, B and the temperature, for which a retardation factor of 2 is appropriate. Using wastewater indicators does only work if they show clear minima or maxima, which is not always the case. Even though the concentrations within the lake are more stable than for example at Lake Wannsee, some difficulties concerning the input signal remain. Using stable isotopes and temperatures, which are largely (even though not entirely) independent of the WW input and show clearer seasonalities is less problematic.

- The vertical age stratification of the bank filtrate within the quaternary aquifer is large.

- The shallow and semi-deep observation wells between the lake and the production well abstract mainly "young" bank filtrate of an age of a few months.

- The deepest observation well screened at the bottom of the aquifer contains "old " bank-filtrate that is decades rather than months old, probably originating from infiltration zones further west.

- The travel time of the bank-filtrate to well 13 on the shortest pathway is 4-5 months.

- The travel times have decreased in 2002/2003 compared to 1998/1999 (FRITZ, 2002).

1.4.4　　　　Mixing

- The most useful tracers for mixing calculations are stable isotopes, EDTA, B & K.

- The T/He age dating results, in combination with a lack in seasonality in the production wells, (and some chemical data) suggest that the production wells abstract a mixture of young bank-filtrate (several month old; 47-58 %), older bank-filtrate (decades old; 11 %), background groundwater (from inland of the well gallery; 31-42%) and possibly even a very small proportion of deeper groundwater from the underlying next aquifer.

- The background groundwater characteristics changed in 2003 (rising EDTA, δD and δ^{18}O values). The changes probably have to do with greater strain on gallery West, but exact origin is not certain.

1.4.5   *Hydrochemistry*

- All shallow wells contain oxygen throughout most of the year, while the deeper observation wells are generally post-oxic or, more precisely, ferrous as classified by BERNER (1981).
- The very deep parts of the aquifer show first signs of sulfate reduction.
- As it is the case at all other sites, the redox zones are transient. Variations are due to the seasonally varying microbial activity caused by the temperature changes and by hydraulic factors such as decreasing travel-times. In summer, higher temperatures generally lead to more reducing conditions, while winter conditions are less reducing. The differences may print through along the transect with a time-lag of several months in accordance to the travel times.

1.5 References

Beyer. W. 1964. Zur Bestimmung der Wasserdurchlässigkeit von Kiesen und Sanden aus der Kornverteilungskurve. Wasserwirtschaft Wassertechnik 14. 165-168.

Berner, R. A., 1981. A new geochemical classification of sedimentary environments. J. of Sed. Petr. 51(2), 359-365.

Beyerle, U., Aeschberg-Hertig, W., Hofer, M., Imboden, D. M., Baur, H. & Kipfer, R., 1999. Infiltration of river water to a shallow aquifer investigated with 3H/3He, noble gases and CFCs. J. of Hydr. 220, 169-185.

Bourg A.C.M. and Bertin C., 1993. Biogeochemical processes during the infiltration of river water into an alluvial aquifer. Environ. Sci. Technol. 27, 661-666

Bouwer, E. J. and McCarty, P. L. 1983. Transformations of halogenated organic compounds under denitrification conditions. Appl. Environ. Microbiol., 45(4), 1295–1299.

Bresser, R., 1995. 1-Methyl-2-phenylacetohydracid als potentieller Metabolit der Pyrazolin-Analgetika. Verlag Dr. Köster, Berlin

Buß. 1994. KVS - Programm zur Auswertung und graphischen Darstellung von Kornverteilungen

Canfield, D.E, Raiswell, R., Westrich, J.T., Reaves. C.M., Berner. R., 1986. The use of chromium reduction in the analysis of reduced inorganic sulfur in sediments and shales. Chem. Geol. 54. 149–155.

Champ, D.R., Gulens, J. and Jackson, R.E., 1979. Oxidation-reduction sequences in ground water flow systems. *Canadian Journal of Earth Sciences*, 16: 12-23.

Cornwell. J.C.. Morse. J.W. 1987. The characterization of iron sulfide minerals in anoxic marine sediments. Marine Chem. 22. 193–206.

David M.B., Gentry L. G., Smith K. M. and Kovacic D. A.,1997. Carbon, Plant, and Temperature Control of Nitrate Removal from Wetland Mesocosms. Transactions of the Illinois State Academy of Science, 90(3 and 4), 103-112.

Doussan C., Poitevin, G., Ledoux E., Delay M.,1997. River bank filtration: Modelling of the changes in water chemistry with emphasis on nitrogen species. J. of Cont. Hydrol. 25, 129-156)

Eichhorn 2000. Numerische Strömungsmodellierung der Uferfiltration am Tegeler See. Diplomarbeit Freie Universität Berlin.

Förster, U. & Wittmann, G.T.W., 1979. Metal pollution in the aquatic environment. 486 pp, Springer.

Fritz, B., 2002. Untersuchungen zur Uferfiltration unter verschiedenen wasserwirtschaftlichen, hydrogeologischen und hydraulischen Bedingungen. Dissertation, Freie Universität Berlin, Berlin, 203 pp.

Fritz, B., Sievers, J., Eichhorn, S., Pekdeger, A., 2002. Geochemical and hydraulic investigations of river sediments in a bank filtration system. In: P.J. Dillon (Editor), 4th International symposium on artificial recharge of groundwater. A.A. Balkema, Adelaide, pp. 95-100.

Gagnon. C.. Mucci. A.. Pelletier. E., 1995. Anomalous accumulation of acid-volatile sulphides (AVS) in a coastal marine sediment. Saguenay Fjord. Canada. Geochim. et Cosmochim. Acta 59. 2663–2675.

Grünheid, S., Schittko, S., Jekel, M. (2004). Behavior of bulk organics abd tace pollutants during bank filtration and groundwater recharge of wastewater impacted surface waters. Proceedings of the annual meeting of the Water Chemical Society, Bad Sarow, 75-80.

Hannappel, S., Asbrand, M., 2002. Entwicklung eines Hydrogeologischen Modells im unterirdischen Einzugsgebiet eines Wasserwerks im Lockergestein. *Schriftenreihe der Deutschen Geologischen Gesellschaft*, 24: 55-68.

Hazen. A., 1893. Some physical properties of sand and gravels with special reference to their use in filtration. Annual Report Mass. State Board of Health 24. 541-556.

Heim, B., Fritz, B. & Pekdeger, A., 2002. Remote sensing techniques and investigations of surface water used for artificial recharge. In: P.J. Dillon (Editor), 4th International symposium on artificial recharge of groundwater. A.A. Balkema, Adelaide, pp. 557-560.

Heinrichs. H. 1989. Aufschlußverfahren in der Analytischen Chemie. Laborpraxis 12. 1–6.

Hinspeter, S. 2001. Geochemisch – Isotopenhydrogeologische Untersuchungen zur Uferfiltration am Wasserwerk Beelitzhof – Wannsee. Diplomarbeit Freie Universität Berlin

Hiscock, K. M., Grischek, T.,2002. Attenuation of groundwater pollution by bank filtration. J. Hydrol. 266, 139-144.

Holm J.V., Rügge K., Bjerg P.L., Christensen T.H., 1995. Occurrence and Distribution of Pharmaceutical Organic Compounds in the Groundwater Downgradient of a Landfill (Grindsted, Denmark). Environ. Sci. Technol. 29(5), 1415-1420.

Hoefs, J.,1997. Stable Isotope Geochemistry, Springer, Berlin, 201 p.

Hsieh. Y.P.. Yang. C.H., 1989. Diffusion methods for the determination of reduced inorganic sulfur species in sediments. Limnol. Oceanogr. 34. 1126–1130.

Jacobs L.A., von Gunten H.R., Keil R., Kuslys M.,1988. Geochemical changes along a river-groundwater infiltration flow path: Glattfelden, Switzerland. Geochim. et Cosmochim. Acta 52, 2693-2706.

Knappe, A., Hubberten, H.-W., Pekdeger, A., Dulski, P., Möller, P.: A multi-tracer study on bank filtration processes in Berlin. In: Dillon, P. (Ed.): Management of Aquifer Recharge for Sustainability, Balkema, Adelaide, Australia, 2002, pp 239-244.

Kohfahl, C., 2004. The Influence of Water Table Oscillations on Pyrite Weathering and Acidification in Open Pit Lignite Mines, Column Studies and Modelling of Hydrogeochemical and Hydraulic Processes in the LOHSA Storage System, Germany, Dissertation, www.dissertation.de, in press.

Kretschmar, R.,1991. Kulturtechnisch-Bodenkundliches Praktikum, ausgewählte Laboratoriumsmethoden, eine Anleitung zum selbständigen Arbeiten an Böden. Christian-Albrechts-Universität Kiel, 7. Auflage.

Lewandowski, J., Leitschuh, S., Koß, V., 1997. Schadstoffe im Boden - Eine Einführung in Analytik und Bewertung. 339 S, Springer

Limberg, A., Thierbach, J., 2002. Hydrostratigraphie von Berlin-Korrelation mit dem Norddeutschen Gliederungsschema. Brandenburgische Geowiss. Beiträge, 9(1/2): 65-68.

Massmann, G., Knappe, A., Pekdeger, A., Richter, D. (2004). Investigating the influence of treated sewage in ground- and surface water using wastewater indicators in Berlin, Germany. Acta Hydrochim. et Hydrobiol. 32 (4-5), 336-350.

Mehra. O. P. and Jackson. M. L.. 1960. Iron oxide removal from soils and clays by a dithionite-citrate system buffered with sodium bicarbonate. Clays Clay Mineral. 5. 317-327

Meyer H., S.L., Wand U., Hubberten H.-W., and Friedrichsen H., 2000. Isotope Studies of Hydrogen and Oxygen in Ground Ice-Experiences with the Equilibration Technique. Isotopes Environ. Health Stud., 36: 133-149.

Pekdeger, A. Sommer.-von Jarmerstedt, C., 1998. Einfluß der Oberflächenwassergüte auf die Trinkwasserversorgung Berlins, Forschungspolitische Dialoge in Berlin - Geowissenschaft und Geotechnik, Berlin, pp. 33-41.

Prommer H. and Stuyfzand,2005. Identification of temperature dependent water quality changes during a deep well injection experiment in a pyritic aquifer. Environ. Sci. And Technol., in press

Rafter, T.A., 1967. Oxygen isotopic composition of sulfates. Part 1: a method for the extraction of oxygen and its quantitative conversion to carbondioxide for isotopic ratio measurements. New Zealand J. Sci. 10, 493–510.

Richter, D. 2003. Untersuchung des Gewässersystems von Spree und Havel im Berliner Westen mit Hilfe verschiedener Tracer. Diplomarbeit Freie Universität Berlin.

Richters L., Eckert P., Teermann I., Irmscher R.,2004. Untersuchung zur Entwicklung des pH-Wertes bei der Uferpassage in einem Wasserwerk am Rhein. Wasser Abwasser 145(9), 640-645.

Rümmler, 2003. 2-dimensionale-horizontal-ebene Simulation der grundwasserströmungsverhältnisse unter Uferfiltratbedingungen. Diplomarbeit Humboldt-Universität zu Berlin.

Schumacher, Skripalle, 1999. Arge Uferfiltration Detailbericht 1: Ermittlung der Uferfiltratanteile über die Abflussverhältnisse sowie die Durchflussaufteilung und Abwasseranteile im Berliner Gewässersystem bei Niedrigwasser für verschiedene Ableitungsvarianten der Klärwerke.- Abschlußbericht Uferfiltration Berlin: S 31

Senstadt, 2003. Öffentlichkeitsarbeit, Wasserwirtschaftliche Monatsberichte.

Sievers, J. 2001. Geochemische, hydrochemische und hydraulische Untersuchungen an Sedimentkernen aus dem Tegeler See.Diplomarbeit Freie Universität Berlin

Sommer-von Jarmersted, C., Kösters, E. & Pekdeger, A., 1998. Die Sulfat- und Chloridgehalte des Berliner Grundwassers.- Terra nostra 98/3: V341 - V342, Alfred- Wegener-Stiftung, Köln

Stute, M., Deák, J., Révész, K., Böhlke, J. K., Deseö, É., Weppernig, R. & Schlosser, P., 1997. Tritium /3He Dating of River Infiltration: An Example from the Danube in the Szigetköz Area, Hungary. Ground Water 35(5), 905-911.

Sültenfuß, J. and Massmann, G., 2004. Datierung mit der 3He-Tritium Methode am Beispiel der Uferfiltration im Oderbruch. Grundwasser, 9(4): 221-234.

Tolstikhin, I. N. & Kamenskiy, I. L., 1969. Determination of groundwater ages by the T-3He method. Geochemistry International 6, 810-811.

Yanagisawa, F., Sakai, H., 1983. Preparation of SO_2 for sulphur isotope ratio measurements by the thermal decomposition of $BaSO_4$–V_2O_5–SiO_2 mixtures. Anal. Chem. 55, 985–987.

1.6   Publications

Fritz, B., Massmann, G., A. Knappe, A. Pekdeger, 2003. Process studies in a bank filtration system in Berlin using environmental tracers. Hydroplus.

Greskowiak, J., Massmann, G., Wiese, B., Lewandowski, J., Hupfer, M., Nützmann, G., Pekdeger, A., 2004. Geochemical changes under alternating saturated and unsaturated conditions during artificial recharge via ponded infiltration of surface water. In: P.A.e. al. (Editor), Saturated and unsaturated zone - integration of process knowledge into effective models, Rome, Italy, pp. 157-163.

Greskowiak J., Prommer H., Massmann G., Johnston C.D., Nützmann G., Pekdeger A., in press. The Impact of Variably Saturated Conditions on Hydrogeochemical Changes during Artificial Recharge of Groundwater. Appl. Geochem.

Heberer, T., Michelinski, A., Fanck, B., Knappe, A., Massmann, G., Pekdeger, A., Fritz, B., 2004. Field Studies on the Fate and Transport of Pharmaceutical Residues in Bank Filtration. Ground Water Monitoring & Remediation, 24(2).

Massmann, G., Dünnbier, U., Greskowiak, J., Knappe, A. and Pekdeger, A., (2004). Investigating surface water - groundwater interactions with the help of sewage indicators in Berlin, Germany, Groundwater Quality 2004, Waterloo, Canada. IAHS Red Book series (in print).

Massmann G., Greskowiak J., Dünnbier U., Zuehlke S., Knappe A., Pekdeger A., submitted. The impact of alternating redox conditions ion groundwater chemistry during artificial recharge in Berlin, J. of Hydrol.

Massmann, G., Knappe, A., Pekdeger, A., Richter, D., 2004. Investigating the influence of treated sewage in ground- and surface water using wastewater indicators in Berlin, Germany. Acta Hydrochim. et Hydrobiol. 32 (4-5), 336-350.

Massmann, G., Knappe, A., Richter, D., Sültenfuß, J., Pekdeger, A.,2003. Application of Different Tracers to Evaluate the Flow Regime at Riverbank-Filtration Sites in Berlin, Germany. In: G. Melin (Editor). Riverbank Filtration - The Future is Now. Conference Proceedings, Cincinnati Ohio, USA, National Water Institute: 49-56.

2 Results Lake Wannsee Bank Filtration Site

The Wannsee bank filtration site consists of 2 transects running between the lake and well 4 and well 3 of the production well gallery Wannsee of the water works Beelitzhof (Figure 36). The second transect perpendicular to the adjacent production well 3 was constructed because previous studies could show that the proportion of bank filtrate in the production well 4 of the older transect 1 is particularly low. Altogether, 11 piezometers with a maximum depth of 25 m have been constructed within NASRI (see Figure 63 and Figure 64 for schematic cross sections).
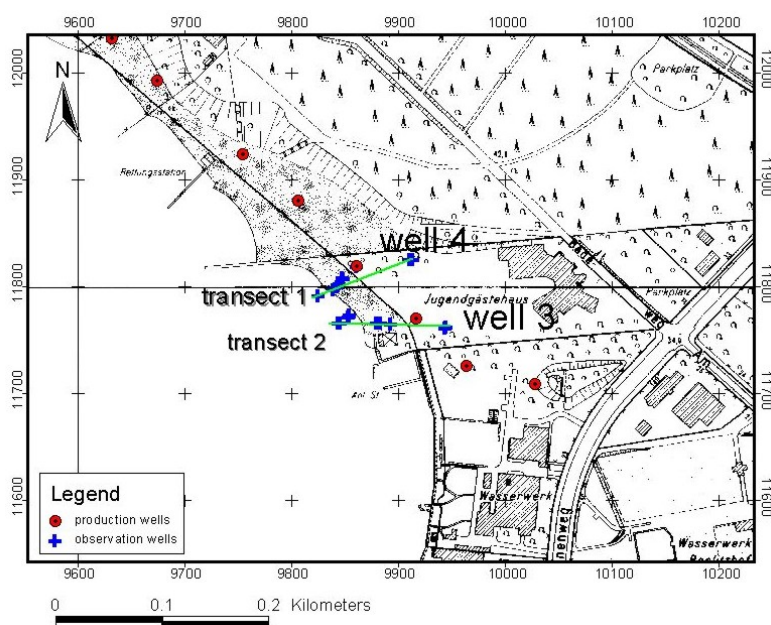
Figure 36: Location of the bank filtration transects 1 and 2 north of the water works Beelitzhof in southwest Berlin.

2.1 Surface water investigations

Lake Wannsee is an area where water from the Lower Havel (Unterhavel) with a comparatively low percentage of treated wastewater (WW) and Teltowkanal water with a rather high load of treated WW meet (Figure 37). The Teltowkanal water flows northwards through a chain of lakes ("Kleine Wannsee-Seenkette") into Lake Wannsee. In a surface water sampling campaign in 2001/2002 (Richter, 2003), samples were taken from the Upper and Lower Havel area within Berlin. Chloride (Cl^-) and Boron (B) concentrations of the relevant lower Havel, the Teltowkanal and lake Wannsee itself are shown in Figure 37, illustrating that the lake is a mixture of both sources. The figure also shows that the temporal variations in Cl^-

and B concentrations are rather large. The results of Richter (2003) also indicate that the transects are clearly under the influence of Teltowkanal water (compare figure 3, report part 1/Tegel).
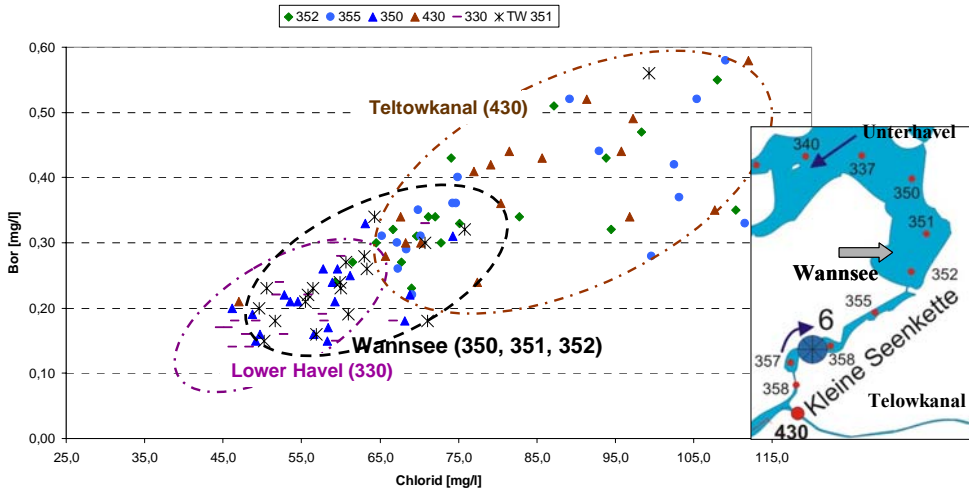
Figure 37: B versus Cl- in the lower Havel, the Teltowkanal and Lake Wannsee (data from 2001-2002; Richter, 2003).
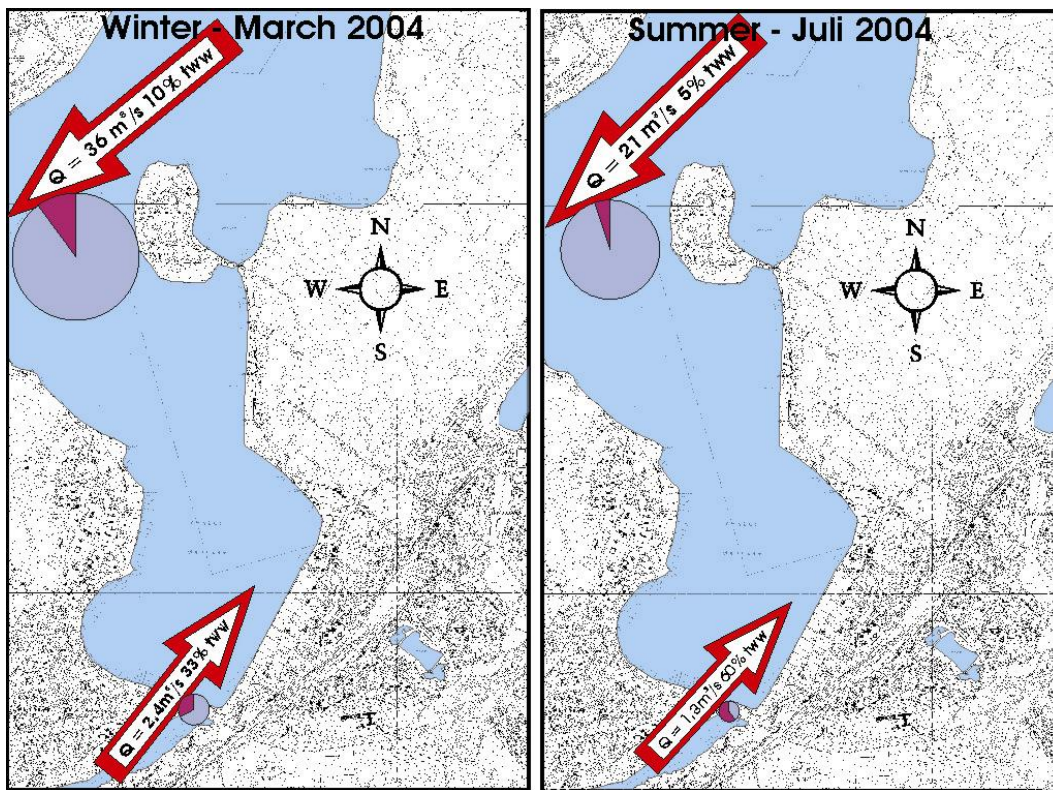
Figure 38: Compared proportions in summer and winter of the surface water runoff of lower Havel and "Kleine Seenkette" and their content of treated wastewater (TWW) (data source: wawimon/SenS & bwb).

Two surface water sampling campaigns were conducted during NASRI at Lake Wannsee in order to get an idea of the spatial variation of the concentration of relevant water constituents within the lake in summer and winter (March and July 2004). Figure 38 shows the monthly discharge of the lower Havel measured at the Frybrücke and Stössenseebrücke and of the "kleine Seenkette" at Alsenbrücke and the calculated proportion of treated wastewater in the corresponding water body during the time of sampling (March and July 2004). Because the WWTP Ruhleben discharges into the Teltowkanal in summer (between April and September), while it discharges into the Spree in winter, the percentage of wastewater in the Teltowkanal is considerably higher in summer. The proportions of treated wastewater were calculated as percentage of WWTP discharge of the total discharge at the respective gauging station (evaporation and abstraction disregarded). More detailed calculations for previous years were done by Schuhmacher & Skripalle (1999).

The distribution of electrical conductivities [µS/cm] and $\delta^{18}O$ [‰ vs. V-SMOW] in the surface water are shown as an example for March 2004 (Figure 39). High electrical conductivities and low $\delta^{18}O$ values are indicators for elevated WW proportions in the surface water (Knappe et al., 2002; Massmann et al., 2004). Figure 39 illustrates that at the time of sampling, the Teltowkanal water flowed north along the eastern lake border, with the largest WW concentrations present at this lake site. The lake is subject to relatively large spatial variations as a function of the mixing between lower Havel and Teltowkanal water. Figure 39 also clarifies that the surface water right in front of the transects shows a particularly large variability of the electrical conductivity and the $\delta^{18}O$ values. This constitutes a problem, because only one surface water sample was taken during NASRI sampling each month (in front of well 4), which is therefore not necessarily representative for the entire bank-filtration source. This may explain why the time-series of several potential tracer in the shallow observation wells within the lake show peaks appearing earlier than in the lake's time-series (e.g. TEG205 and TEG206, Figure 40). Because the transects are located in an area subject to large concentration gradients within the lake, 50 m further south concentrations may already be very different. In addition, transect 2 is not orientated perfectly perpendicular to the flow direction and it may receive water from 100 m further SE of the surface water sampling point.
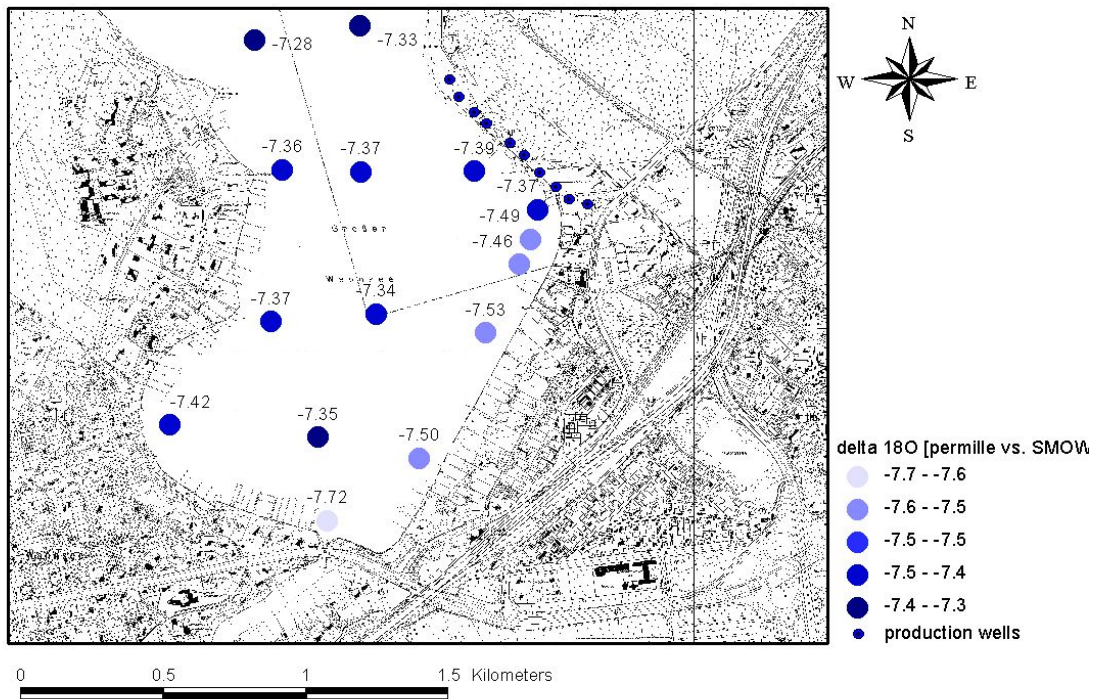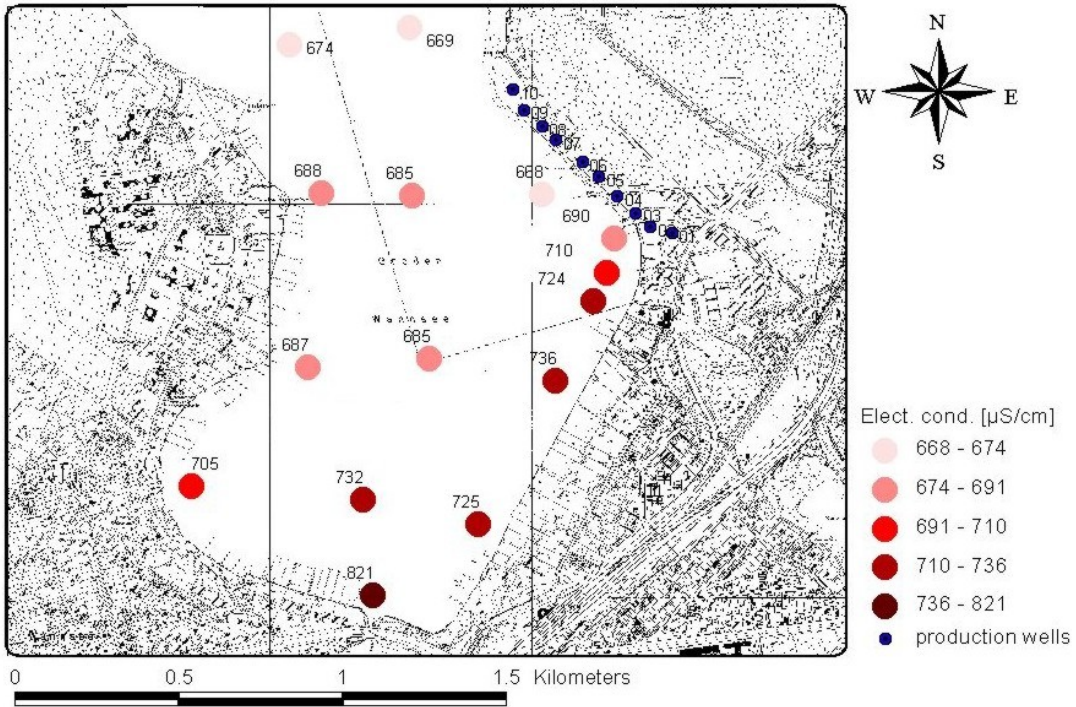
Figure 39: Electrical conductivity [µS/cm] and δ^{18}O [‰ vs. SMOW] in the surface water (sampling depth 0.2 m) in March 2004.
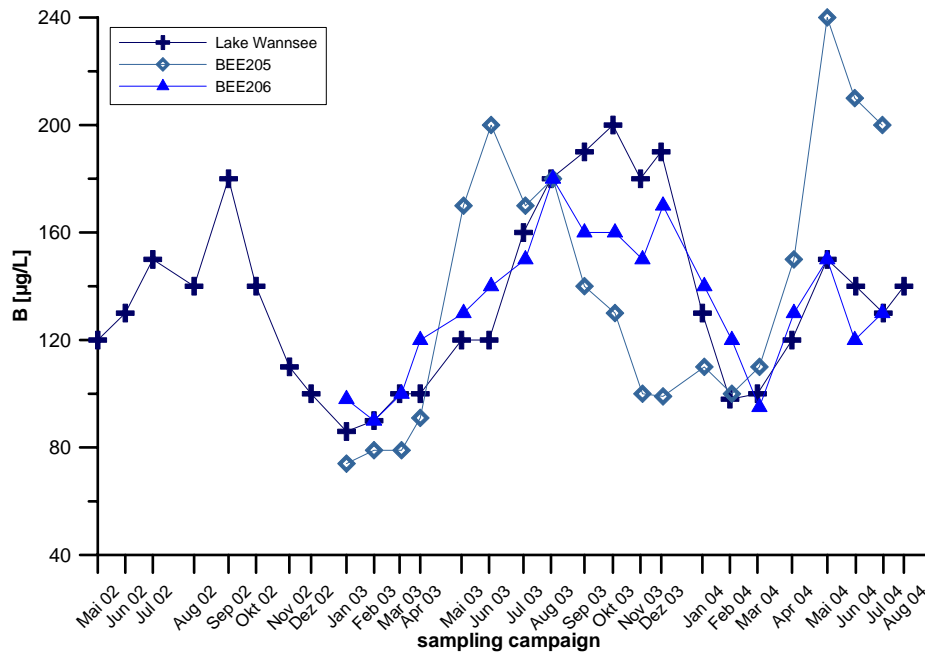
Figure 40: Time-series of boron (B) in shallow observation wells below the lake of transect 2. Dark-blue curve represents surface water sample (data source: BWB).

The northward flow direction of Teltowkanal water along the eastern lake border was not observed in July 2004. Exemplary comparison of temperature, electrical conductivity and MTBE distributions in the lake in March and July shows that in July, the electrical conductivity and the concentration of MTBE (and also: Cl^-, K^+, B, not shown) appear to be even higher along the western lake border. This may be caused by the fact that the various boat harbours at the eastern lake border are diffuse contaminant sources and may increase the concentration of these substances. Another possibility is that the flow patterns are temporally different. Winter temperature differences of almost 5 °C between the warmer Teltowkanal and the colder Havel water may cause the warmer water to flow on top. The sampling of the uppermost 0.2 m of the water column may thereby also not be representative for the entire water column.

Kommentar [GM5]: Das mit dem mixing ist irgendwie nicht ganz logisch, da insgesamt doch im Winter die Mischung (vertikal) in so einem See besser ist.

69
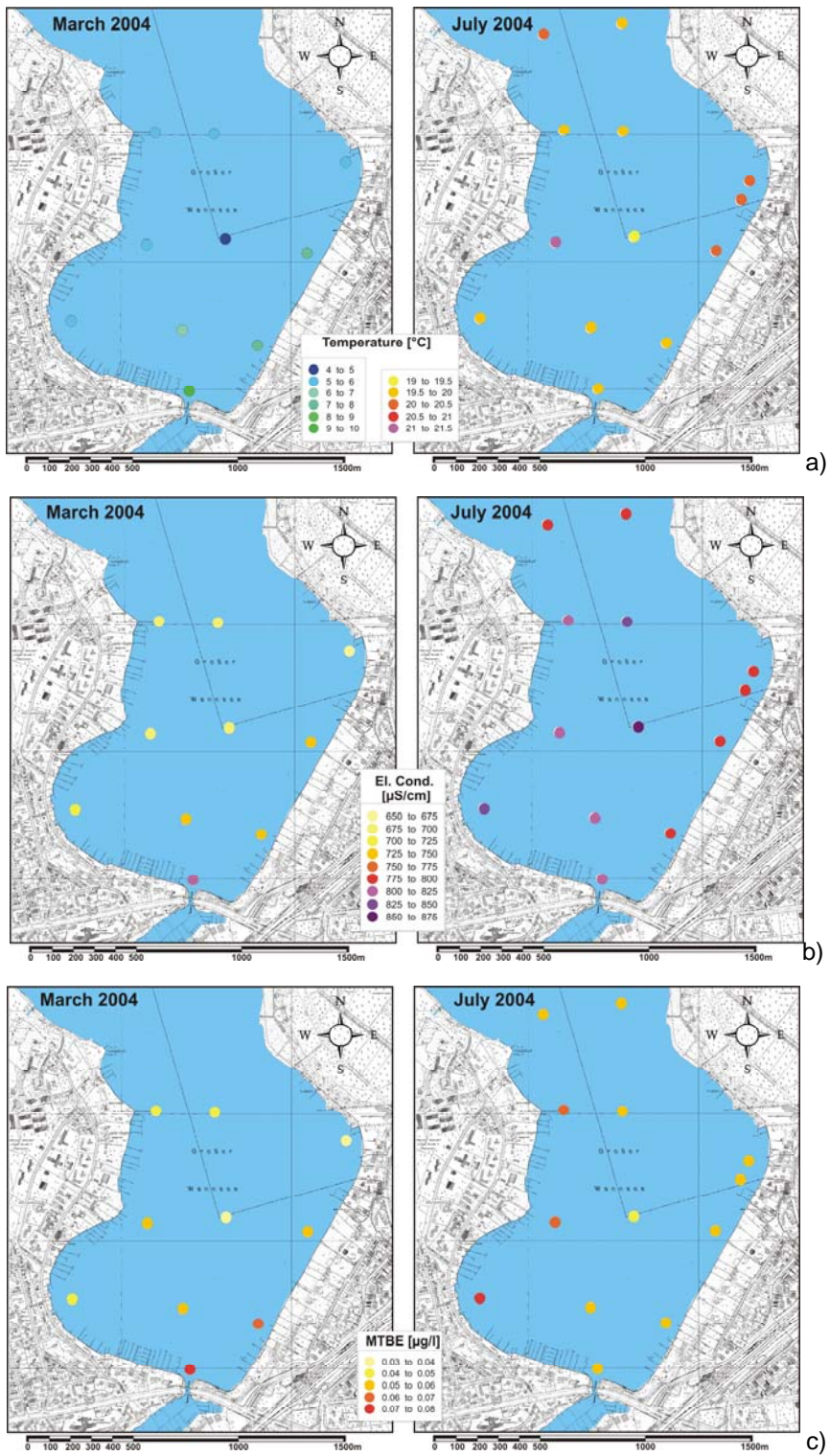
Figure 41: a) Temperature [°C]; b) electrical conductivity [µS/cm] and c) MTBE [µg/L] in the surface water in March (left) and July (right) 2004 at a depth of 0.2 m.

Figure 41 also illustrates that the electrical conductivity is generally higher in July than in March, owing to the seasonal influence (more dilution with natural discharge in summer) leading to the fact that the proportion of WW is higher in summer. The seasonal influence becomes clearest in the time-series of WW indicators (Figure 42). The very wet summer 2002 differs from the dryer summer 2003, which is why Cl⁻, Na⁺ (not shown), K⁺ and electric conductivity do not show the typical summer peak in 2002. Only EDTA (not shown), B and mainly the stable isotopes showed the expected peaks in summer 2002. The isotopic signal is more or less independent on the dilution with treated WW and a function of the temperature during the formation of the precipitation only, which is why the always show a seasonal effect. It is unclear why the time-series of the tracer differ from each other.
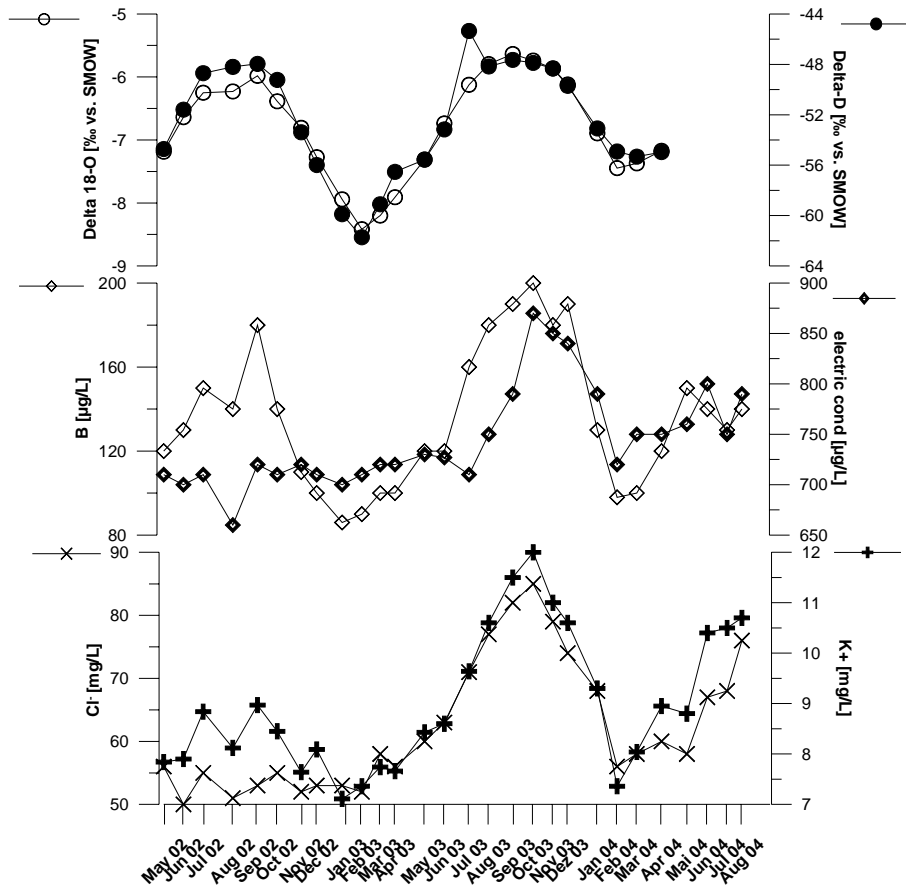
Figure 42: Stable isotope values, electrical conductivity, Cl⁻, K⁺, B and in the surface water of Lake Wannsee (data source: AWI & BWB).

2.2   Clogging layer

Figure 43 displays a geological cross-section at the field site Wannsee (SenS, 2000), reaching a depth of down to 100 meters below the lake surface. The sediments are mainly sands

71

incoherently interbedded with finer grained material, such as silts, clays and glacial tills. The lake base is mainly made of laccustrine sapropels with a thickness of close to 20 m, which were deposited during the Holocene. These sediments have a low hydraulic conductivity, thereby restricting the infiltration capacity. Only the lake margins, where the water depth is less than a few meters, the lake is underlain by sands.
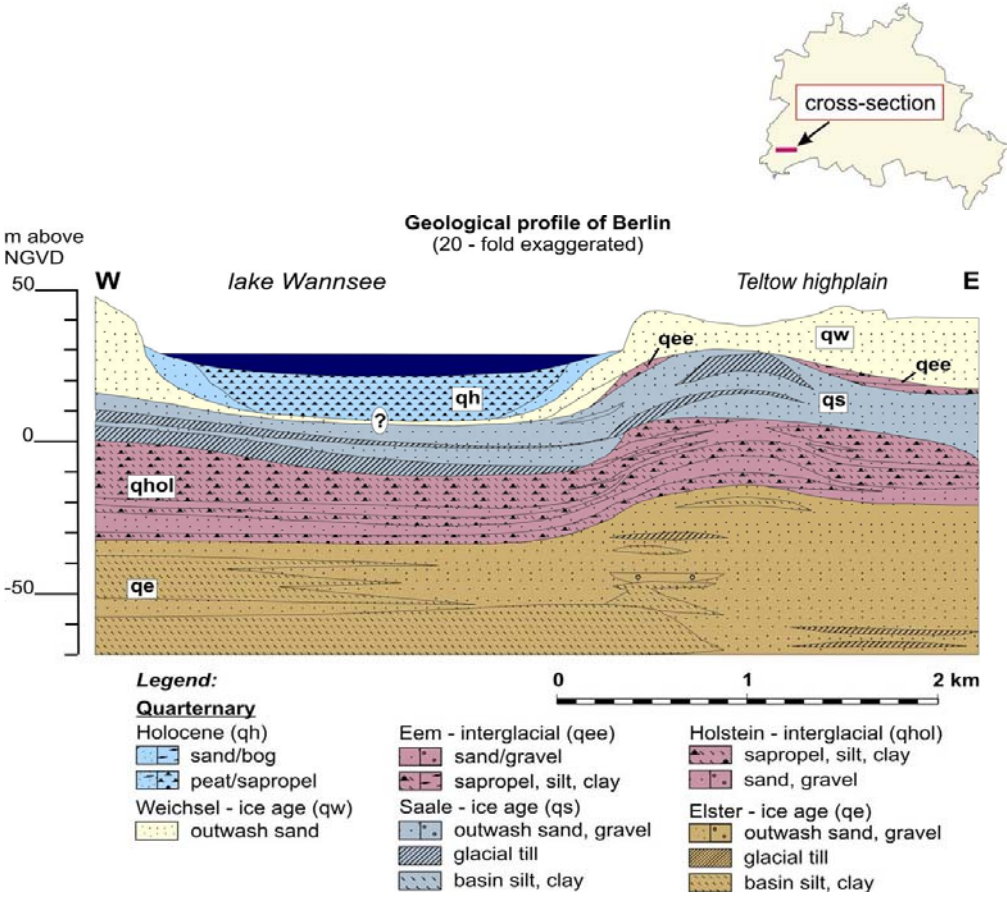
Figure 43: Geological cross-section of the Wannsee area in south-west Berlin (SenS 2000).

The presence, permeability, thickness and characteristics of the sediments covering the lake floor, i.e. the clogging layer, are of major importance for the behaviour of the entire bank filtration system, since they form the direct interface between surface water and groundwater. Several authors could show that the success of bank filtration schemes generally depends on microbial activity and chemical reactions which are mainly taking place in the very reactive clogging layer (Fritz et al., 2002; Hiscock and Grischek, 2002).

Because no previous detailed information existed at Lake Wannsee, the infiltration zone was investigated in greater detail. The investigations can be subdivided in 3 major parts:

1. Mapping of the infiltration zone with regard to the lithology, hydraulic conductivities and organic carbon content (including infiltration tests).

2. Drilling of several cores closer to the shore to determine the lithology as well as hydraulic and geochemical properties of the sediment in greater detail.

3. Column study with an undisturbed core from the lake shore to evaluate the hydrochemical changes directly at the surface water/ground water interface, in particular with regard to the redox chemistry.

Despite decreasing the infiltration capacity, the presence of the clogged sediments has two very positive effects: First, their relatively low permeability slows down the travel times from the lake to the well. Secondly, they are far more effective in removing contaminants than the unclogged sands of the aquifer because their adsorption and reduction capacities are larger owing to higher proportions of organic and/or fine grained material.

2.2.1 Mapping of the Wannsee lake sediments

Methods

The aim of the work was to map the extension of the area offshore of the relevant production wells at Lake Wannsee, in order to determine the extent of the zone where the surface water can infiltrate efficiently into the aquifer.

In August and October 2004, 180 disturbed sediment samples (Figure 44) were taken with a Van Veen-sediment dredge from a swimming platform at the grid points. Orientation on the lake was provided by several landmarks, so that each sampling place could well be fitted to the grid points. At each point, the recovered sediments were examined for the following criteria:

- grain size (finger test, DIN 4022)

- content of organic material (finger test, DIN 4022)

- colour

73

-   shell content

-   content of H_2CO_3 and H_2S (test with diluted HCl)
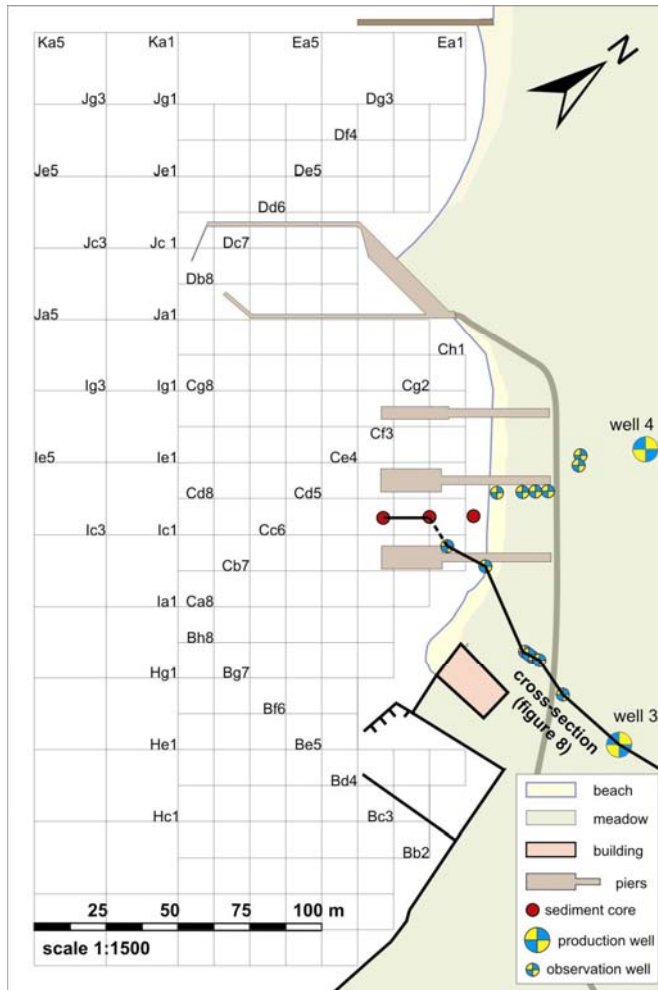
Figure 44: Sketch of the field site at lake Wannsee, showing the mapping grid in a 12.5 m raster (25 m outwards on the lake) with systematic naming of the grid points and the location of the cross-section presented in Figure 43.

In addition, the water depth was noted at each point by measuring the diving length of the dredge rope. The instability of the swimming platform inhibited the drilling of deeper cores by hammering or machine-driven methods. It was therefore not possible to map the thickness of the covering laccustrine sappropel layer.

Based on these findings, the sediments were classified according to the geopedological mapping instruction (AG Boden, 1996). In addition, the water depth was noted at each point by measuring the length of the dredge rope.

Grain-size distribution, which determines the hydraulic conductivity, as well as the organic carbon content, were determined in the laboratory with disturbed samples by sieving analyses, transient permeability experiments (Langguth & Voigt, 1980) and loss of ignition (for more detail see Nogeitzig, 2005).

Open-end tests were carried out in a narrow stripe along the bank of the lake (Figure 45). Tubes of PE material of one metre length were hammered softly 10 to 15 centimetres deep into the sediment. The volume of water (Q) seeping into the underground by gravity was monitored with a gauged flask and a stop watch in several intervals at each point and the hydraulic conductivity is calculated after Langguth & Voigt (1980).
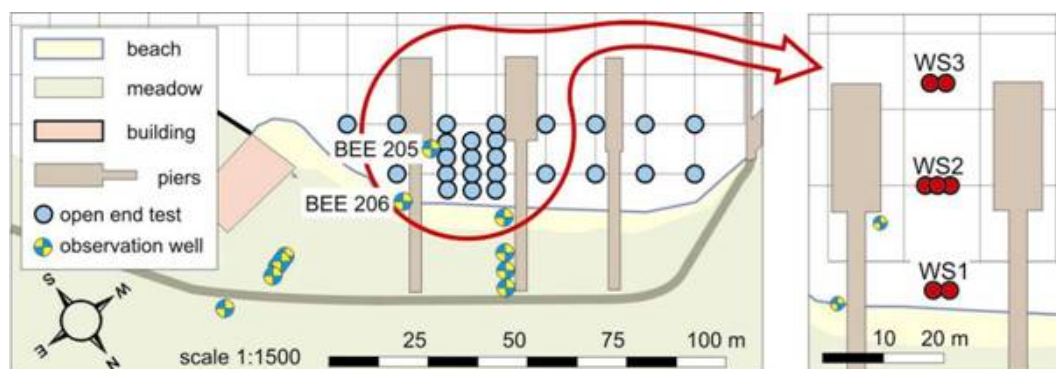
Figure 45: Infiltration experiments (open end tests) near the bankline of the lake (on the left), drilling places of the sediment cores taken for laboratory examinations (in detail on the right).

Results

Figure 46 displays the depth contours of the sediment surface below lake Wannsee. Within one hundred metres distance from the shoreline, the water depth is dropping from very shallow to more than eight metres where the sediment surface flattens out to a wide lacustrine basin, with maximum depths of about nine metres. Further in the northwest and in the southeast, the slope is less steep.
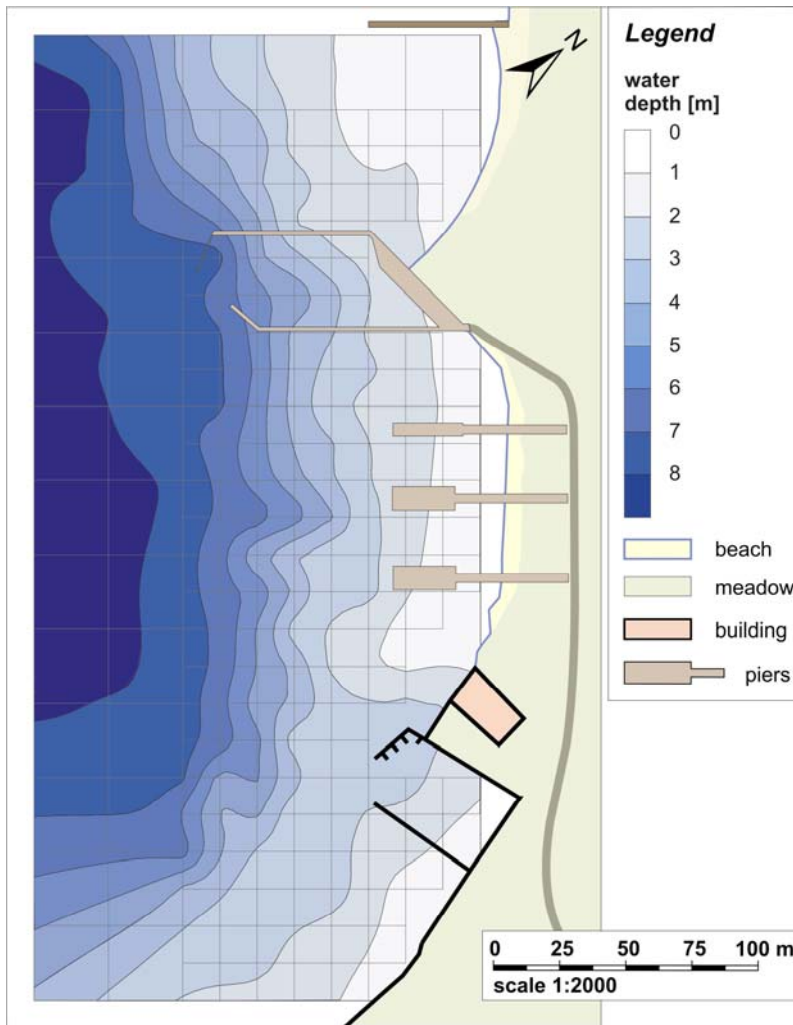
Figure 46: Map of the water depth in the field site at lake Wannsee.

The sediment samples of the mapping campaign are predominantly composed of fine grained sands with variable organic and inorganic carbon contents (Figure 47). In shallow water depths of down to two metres, the sands are coloured in light brown to greyish tones, and they are frequently covered by a film of green organic substances and interspersed with remnants of vegetation. Along with rising water depth from 2 to 6 metres, the colour of the sands is transiently changing from grey to darker olive-brown and dark grey tones. In a depth of more than 6 metres, their colour darkens to olive-black and black colours. The sands are generally getting finer grained with water depth. In a depth of more than 6 metres, fine grained sand sediments contain an increasing amount of silt. In a transitional depth between 6.5 and 7.5 metres, the sediments are composed of fine sand and silt in varying proportions, the latter dominates along with increasing water depth. In a depth of more than 7.2 metres, the packing density of the surface sediments changes from compact deposition to increas-

76

ingly lower packing densities. The granular structure is replaced by a watery, unconsolidated and non-granular structure of the sediments: At depths above 7 metres, laccustrine sapropels prevail.

With exception to the sand sediments in low water depths of < 2.5 metres, all samples contain minor amounts of sulphides, already noticeable by greyish colours. In depths to about 4.5 metres, the sands are settled by colonies of mussels which are a few centimetres thick. Along with rising depth, a layer of shells and detritus, increasingly crushed to finer fragments, replaces the mussel colonies. In depths exceeding 6 metres shells and shell detritus disappears; carbonate detritus of sand-grain size occurs within the sands on the sediment surface. The laccustrine sapropels contain carbonate in a fine-dispersed form.

The organic matter content (Figure 47) in the sands varies from 0.2 to almost 10 weight-percent with neither the presence of the mussel colonies, nor the water depth determining the amount of organic matter. The reason for the irregular distribution is possibly the depositional history of the sediments and the variable input of vegetation remnants from the land. In greater water depths, corresponding to the sedimentation of finer grained material, the amount of organic matter increases to values of regularly more than 10 weight-percent. The silty sediments mixed with laccustrine sapropels contain more than 10 weight-percent of organic matter (mostly > 15 weight-percent). The maximum content detected at the field site is 25.7 weight-percent in a loose, watery and unconsolidated laccustrine sapropel.
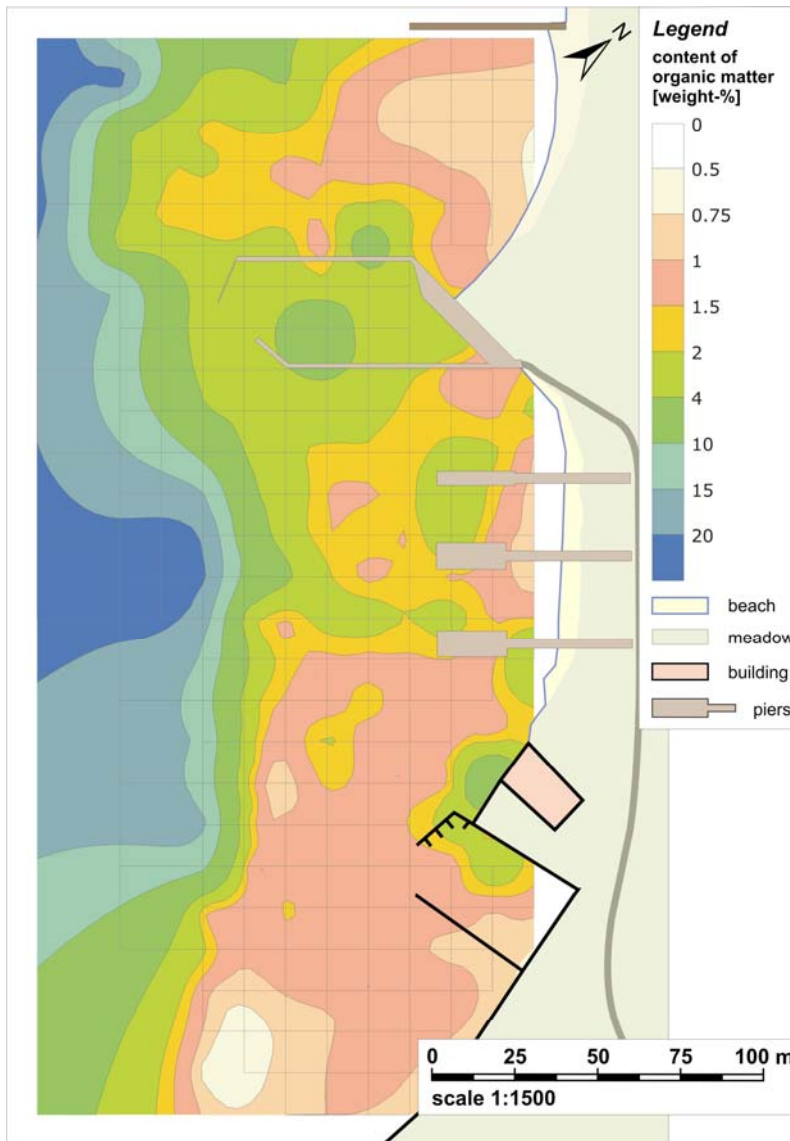
Figure 47: Map of organic carbon content of the lake bottom sediments.

Figure 48 shows the distribution of the hydraulic conductivity of the lake bottom sediments in derived from transient permeability tests of 79 samples. The hydraulic conductivity does not drop to small values in a stringent correspondence with the water depth. However, towards the basin edge, in more than seven metres water depth, the hydraulic conductivity rapidly decreases to values below $1*10^{-6}$ m/s. Figure 48 also displays the shape of an area where 28 additional open-end tests were conducted which is shown enlarged in Figure 49. The hydraulic conductivity of the sediments derived from the transient permeability tests are in the range of $1*10^{-6}$ to $5*10^{-5}$ m/s, whereas the open end tests resulted in distinctly lower values of $1*10^{-7}$ to $5*10^{-6}$ m/s. The differences are likely to be caused by the fact that the permeabil-

ity tests were conducted with disturbed samples, the vertical permeabilites are therefore expected to be lower than those given in Figure 48. The k_f-values derived from sieving are distinctly higher than those of corresponding permeability tests (Nogeitzig, 2005) and are likely to be the least representative. While hydraulic conductivity derived from sieving range from about $5*10^{-5}$ to $5*10^{-4}$ m/s, values from the corresponding tests range from $5*10^{-7}$ to $5*10^{-5}$ m/s. In addition, sediments below the lake bottom are unsaturated in the area where open end tests were conducted which further reduces the hydraulic conductivity.
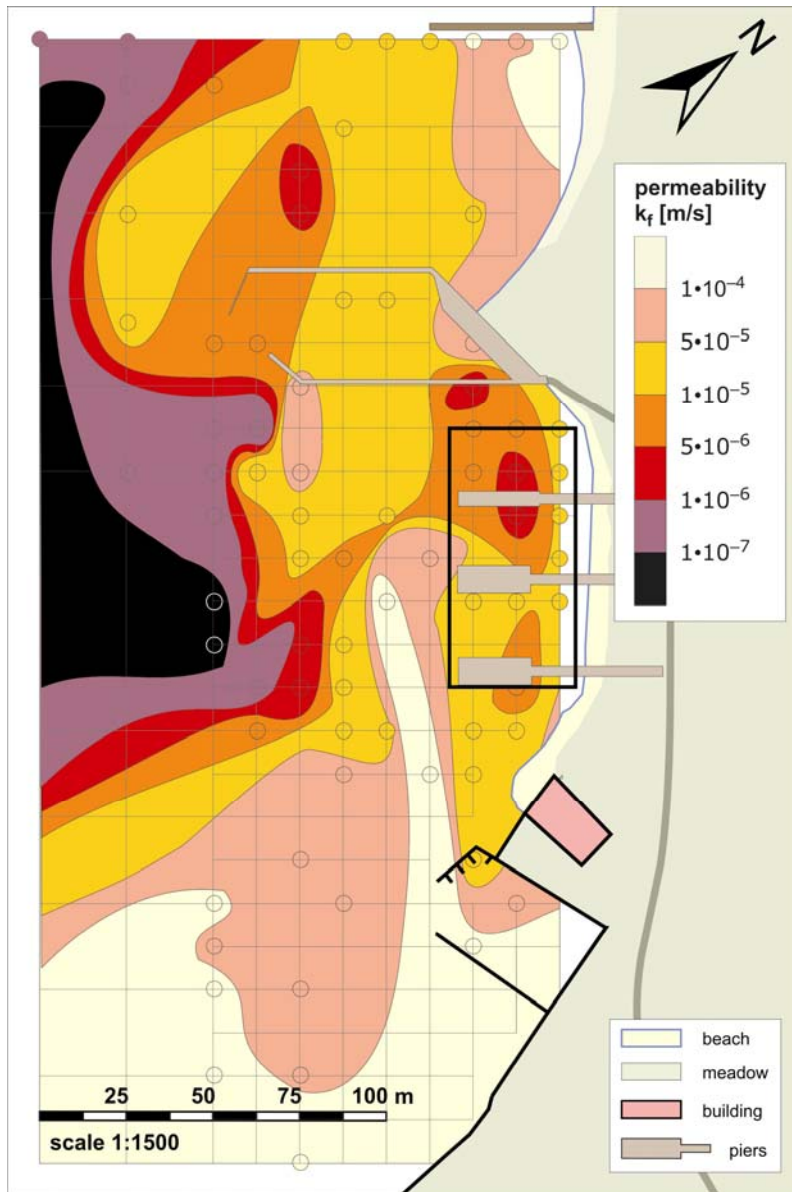
Figure 48: Map of the hydraulic conductivity at the field site, derived from transient permeability tests (small squares). The black rectangle is shown in Figure 49.

79
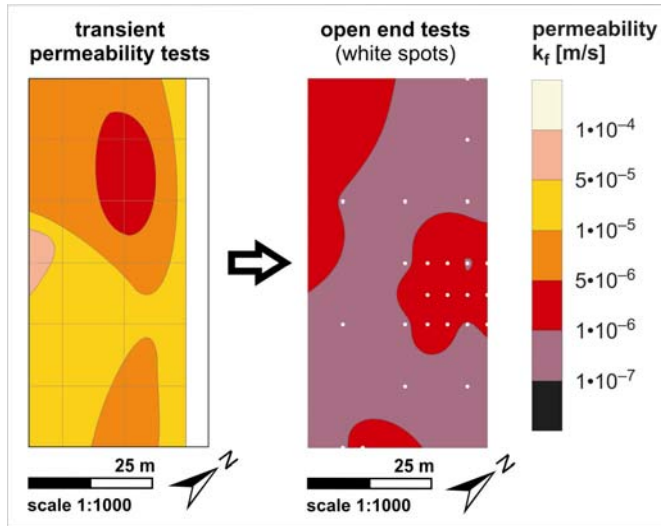
Figure 49: Enlargement given in figure 13 with hydraulic conductivities of the sediments derived from transient permeability tests (on the left) and from open end tests (on the right).

2.2.2   *Physical and geochemical characteristics of the Lake Sediments*

Methods

In January 2004, seven sediment cores were drilled in between two jetties of the aquatic sports centre of the Free University of Berlin in front of the wells 3 and 4 (Figure 50, location Figure 45). Two undisturbed sediment cores of approximately 1 m length were drilled each at three distances off the bank for sedimentological examinations. At the central place, the seventh sediment core was drilled and captured in a transparent liner of Perspex material for a column experiment. Table 1 provides an overview of the capture and to the destination of each sediment core. The cores from each location were drilled in < 0.5 m distance from each other. One core from each location was cut open for a lithological description (grain size distribution) and geochemical analysis (cation exchange capacity, organic carbon, inorganic carbon, total sulfur, pyrite, Fe- and Mn(hydr)oxide content). The second core at each distance was used to measure hydraulic conductivities by steady-state Darcy experiments (Langguth & Voigt, 1980).

Table 4: Overview of the drilling location and destination of the sediment cores. See also figure 8, figure 9 and figure 11 (on the right).

sediment core	distance from the bank	water depth	core category	destination
WS 1A, 1B	1.5 m	0.15 m	WS 1, 2, 3 A:	sediment chemistry
WS 2A, 2B, 2C	20 m	0.60 m	WS 1, 2, 3 B:	physical properties
WS 3A, 3B	40 m	2.30 m	WS 2 C:	column experiment

Figure 50: Taking cores from the drilling platform at Lake Wannsee.

Results

Figure 51 displays a lithological cross section from the shore to core location 3 (which is adjacent to observation well BEE205). The sediments are fine to medium sized sands containing strongly differing amounts of organic substances, such as remnants of vegetation fibres or pieces of coal. Thin layers of shells, broken shell detritus or gravel were also encountered. The grains-size distribution of core segments is shown in Figure 52. Coarse material is almost absent, while silt and clay occur at the bottom of WS 2B, the top of WS 1B and almost the entire core WS 3B in considerable proportions.
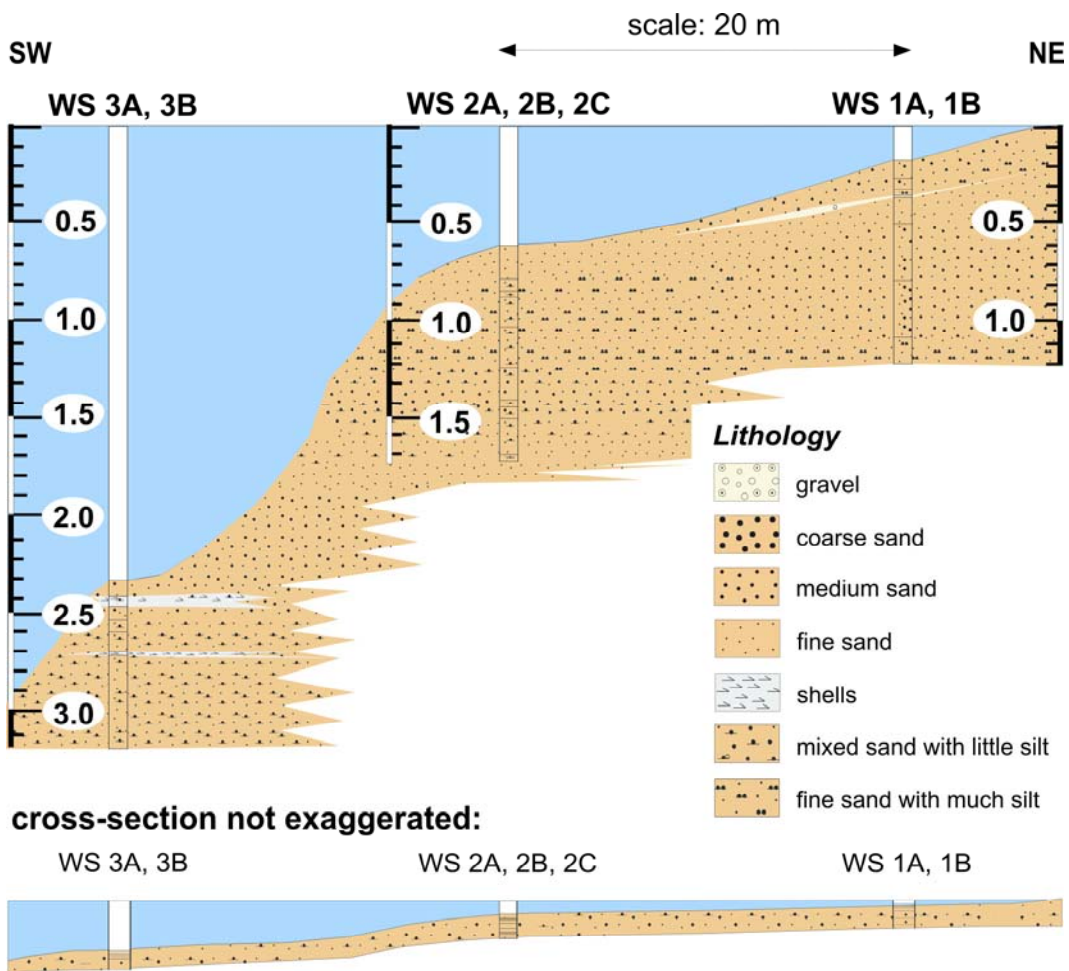
Figure 51: Cross-section of the drilling cores WS 1, WS 2 and WS 3, captured in 1.5, 20 and 40 m distance from the shoreline of the lake Wannsee.

The hydraulic conductivities from steady-state permeability tests (Figure 53) show variabilities between $1*10-4$ and $1*10-6$ m/s and appear to be greater than those obtained in the open-end tests (Figure 49). They seem to decrease from the shore (location W1) to the 40 m distant W3. They also appear to be lowest in the uppermost decimeters with an increasing trend with depth. Local finer grained layers (e.g. WS 2B, 80-100 cm depth) form an exception to this rule. Again, k_f-values derived from the grain size analyses are distinctly higher than those from steady-state permeability tests with undisturbed material and are less representative, since the disregard the clogging effect. It is not surprising that the open end tests deliver the lowest values for hydraulic conductivities. They are performed in the field under undisturbed condition, accounting for both grain-size distribution and packing effects. In addition, local layers such as in WS 2B with elevated silt and clay proportions are determining the vertical hydraulic conductivity, even though the remaining core may have a larger hydraulic conductivity.

However, even though the mapping and the core results revealed large heterogeneities in hydraulic conductivities and differences between the methods applied, the general trends became clear: The k_f-values decrease from values in the order of $10^{-4}/10^{-5}$ m/s close to the shore to $>10^{-7}$ m/s (and probably much less) within the basin, where water depths exceed 8 m and the organic carbon content is >20 weight-%.
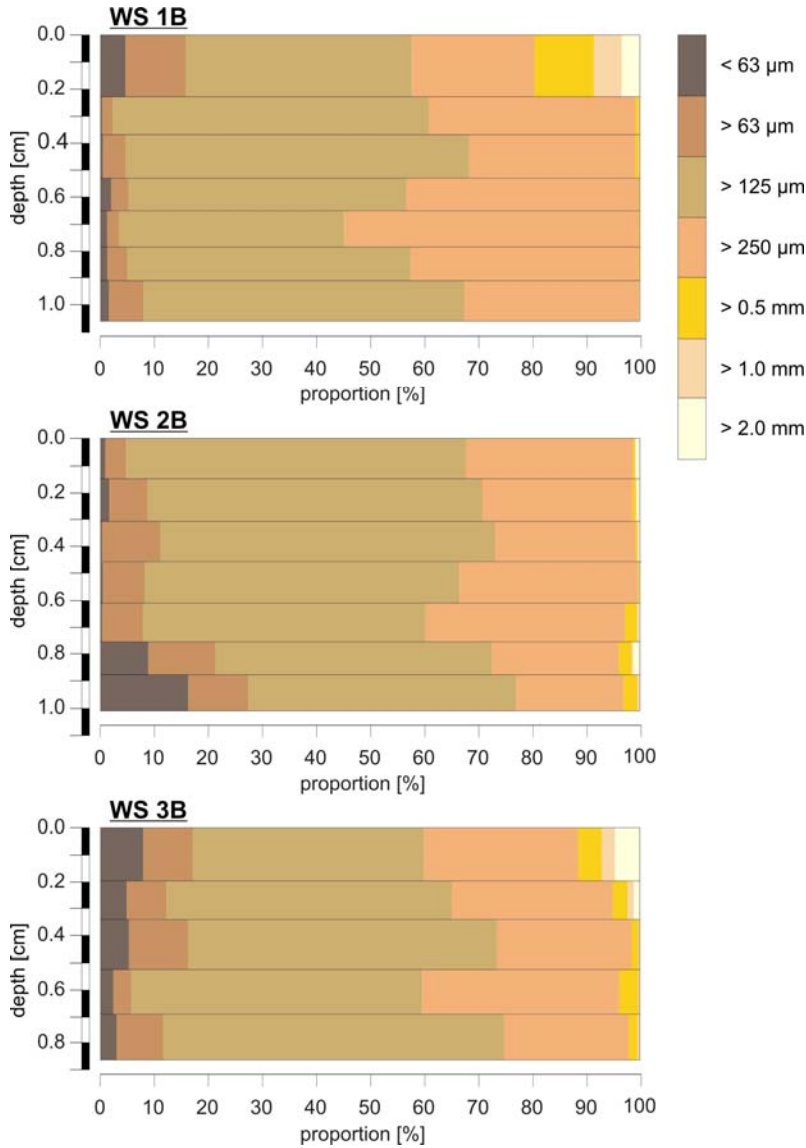
Figure 52: Grain size distribution of the drilling cores WS 1B, WS 2B and WS 3B in segments.
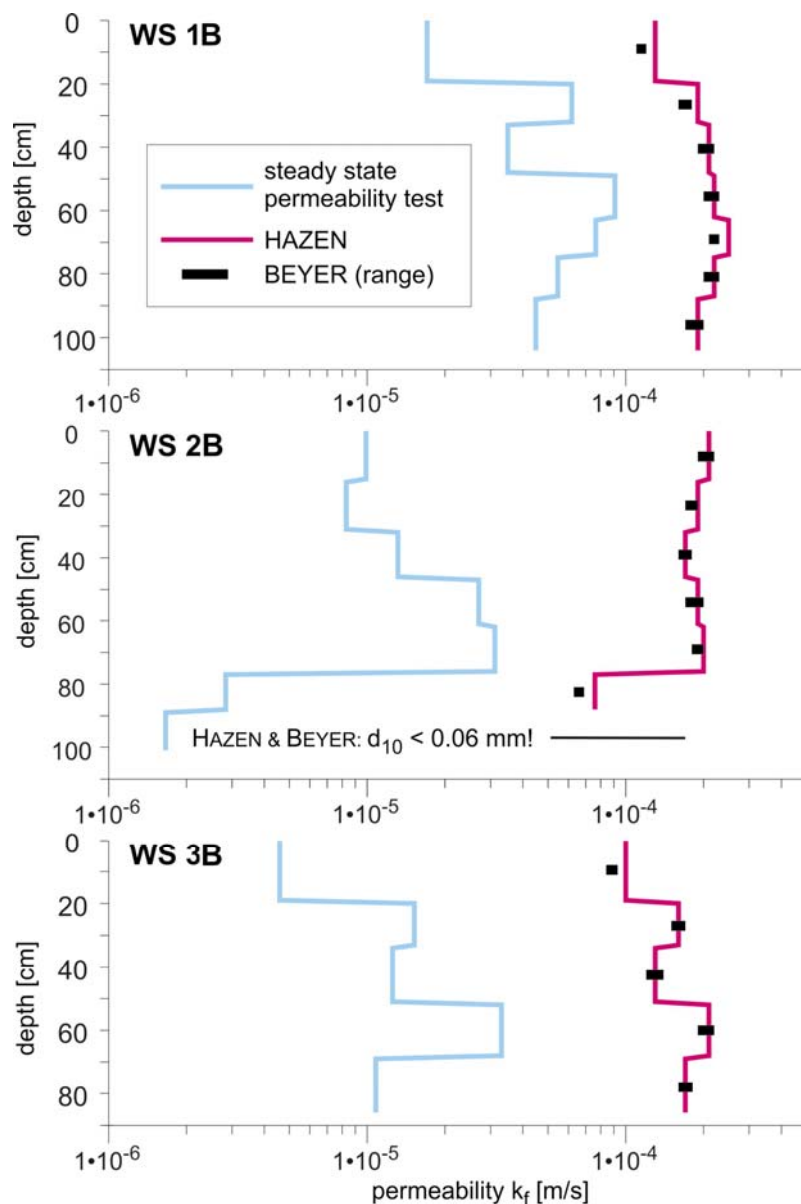
Figure 53: Results of the steady-state permeability tests show that the k_f-values range about one order of magnitude lower than the ones, derived from corresponding sieving analyses of the core segments WS 1, 2 and 3B.

The cores contain between 0.1 to 2 weight % organic carbon (Figure 54), with the exception of the uppermost decimeters of core WS 3A, containing up to 8 % of organic carbon. The sediments contain inorganic carbon as carbonate at an amount of up to 1 weight % C, with exception to the top layers of WS 1A and WS 3A and the bottom of WS 2A (Figure 54) with higher contents.
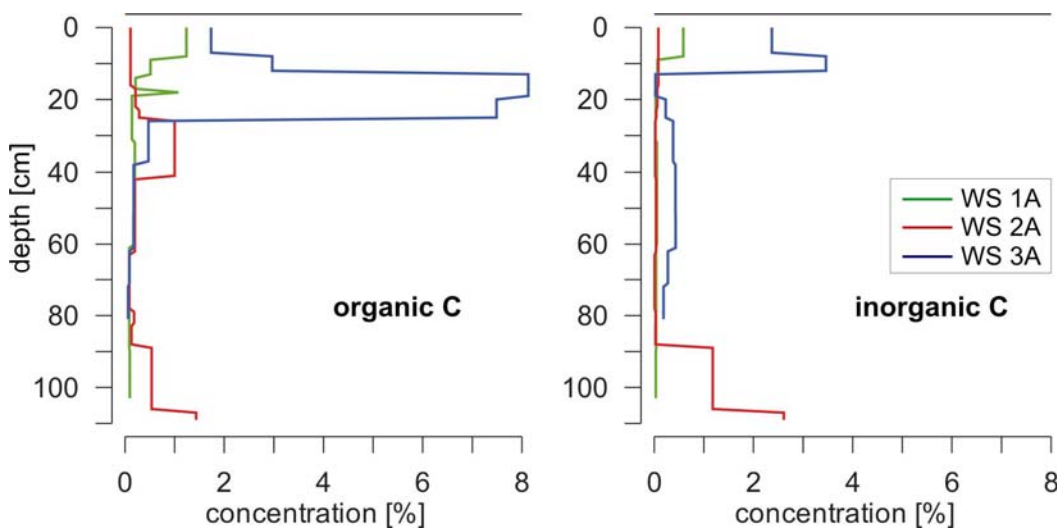
Figure 54: Distribution of organic C (left) and inorganic C (right) in the core segments WS 1,2 and 3A;

The concentrations of total sulphur and pyrite-S were measured in segments of the core WS 2A only; the proportion of pyrite-S varies in the range of about 10 to 35% of the total S in average (Figure 55).
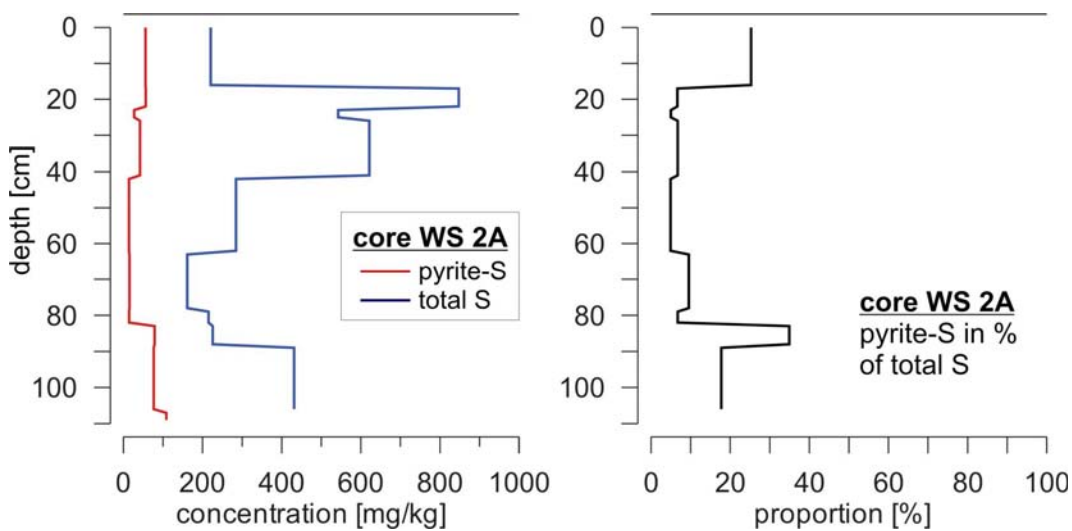
Figure 55: Distribution of pyrite-sulphur and total sulphur in the core WS 2A (left) and of the pyrite proportion of the total sulphur content (right).

The figures 29 displays the dithionite-reducible iron(III) and manganese(IV) contents and total iron and manganese contents within the three sediment cores. Dithionite-reducible iron(III) and manganese(IV) are present in sediments at considerable amounts. The ones of dithionite-reducible iron are varying in between of 200 to 1000 mg per kg, only the top of WS

3A and of WS 1A are containing values of up to 8800 mg/kg. The dithionite-reducible manganese contents are about one order of magnitude lower (Figure 56).
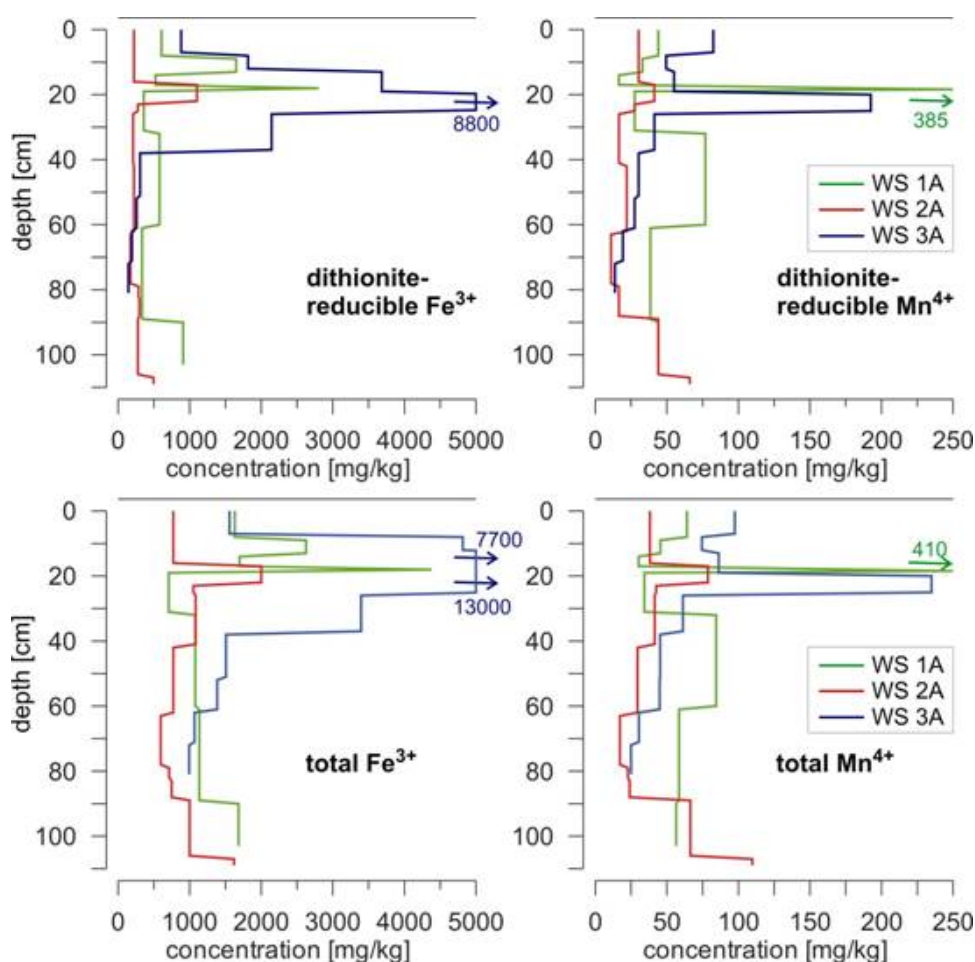
Figure 56: Distribution of the total (below) and of the dithionite-reducible (above) Fe(III) and Mn(IV) content in the cores WS 1, 2 and 3A.

The cation exchange capacity lies in the range of about 0.4 to 0.6 mmol-eq/100 g sediment (not shown).

2.2.3   Column study

Experimental set-up

The undisturbed core WS 2C of 0.99 m length was set up vertically in the laboratory at room temperatures of 20° to 22° C. The column was operated in downwards mode, using a pulsating pump. To simulate natural flow conditions, fresh surface water from Lake Wannsee was used which was stored in a container of 25 L volume and was bubbled with air by an aquarium air pump to retain constant saturation of oxygen. The aerated inlet water was led to the

column at super sufficient rate in order to avoid any drainage. The surplus of inlet water was branched off by an overflow outlet, which was fixed 20 cm above the sediment surface. Nine sampling ports to inlet water and outlet water were connected as water taps to the flexible pipes and as waterproof connections screwed into the Perspex tube of the column, which is shown in Figure 57. In addition, seven waterproof connections were screwed into the Perspex tube for the installation of O_2-probes directly in the sediment material. The outlet of the column was connected by flexible pipes of airtight Viton and glass material and fastened 40 cm above the bottom to set up a constant hydraulic gradient, forcing the inlet water to infiltrate at conditions similar to those at the drilling place at lake Wannsee (0.6 m water depth). In order to build up constant flow rates of the filtration water in the column, an additional pulsating pump was installed on 12th of August 2004 due to an irregularly and persisting rise of the flow rate.
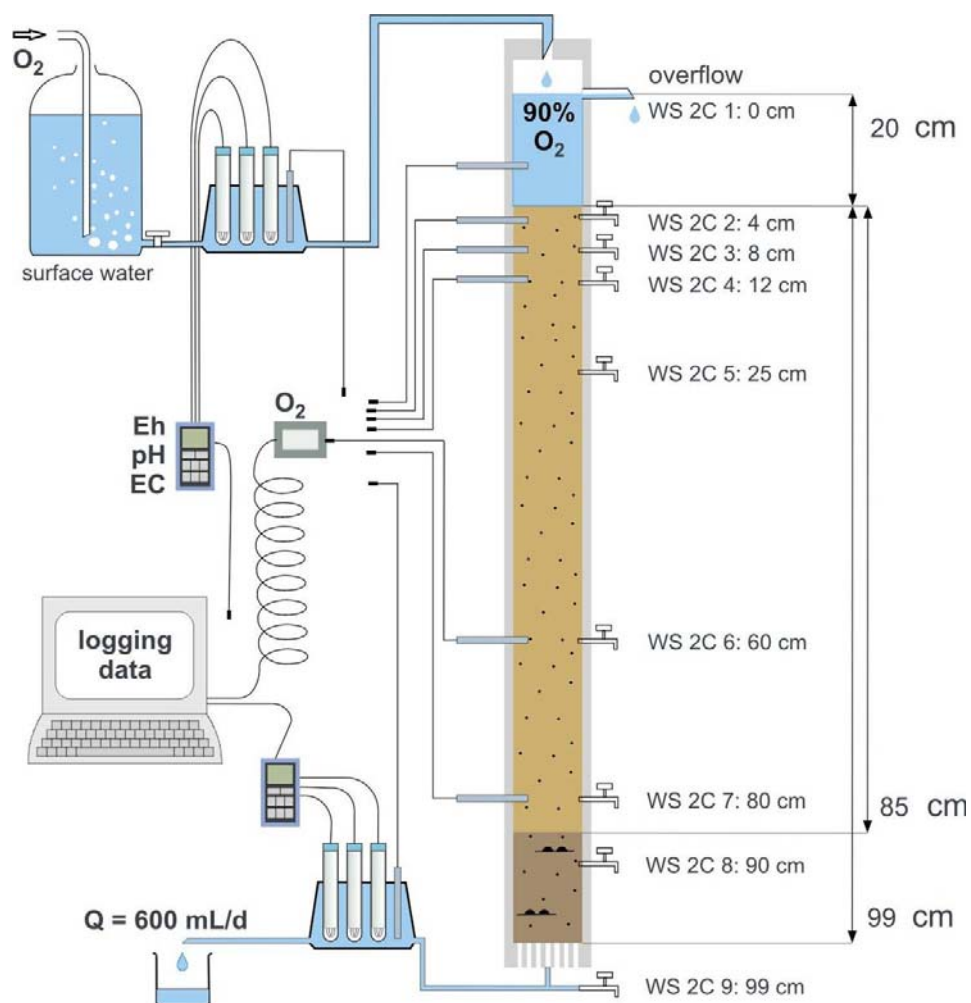
Figure 57: Column set up in the laboratory. Nine sampling ports and seven O_2-probes were installed.

The physicochemical parameters (pH-value, Eh-value and electric conductivity) of the filtrate water were measured in the inlet water and outlet water. Probes were installed into the flexible pipes of inlet and outlet. Sampling for cations (Na^+, K^+, Ca^{2+}, Mg^{2+}, Mn^{2+}, Fe^{2+}, NH_4^+,) and anions (Cl^-, HCO_3^-, SO_4^{2-}, NO_3^-, PO_4^{3-}, HS^-) and for dissolved organic carbon (DOC), took place monthly. O_2 was measured with seven luminescence probes (Presens 2003), placed directly into the sediment body inside the column.

Hydraulic properties

A tracer test was conducted from the 16th to the 26th of July 2004 by increasing the electrical conductivity with NaCl. The breakthrough curve was fitted using the analytical solution by (Ogata, 1970), which resulted in a flow velocity (v_a) of $6*10^{-6}$ m/s (or 0.52 m/d) and a dispersion coefficient (D_l) of $7.8*10^{-8}$ m²/s (0.0067 m²/d). The test was conducted at average flow rates of 600 ml/d, which, at an area of 0.035 m² would be equivalent to a Darcy velocity (v_f) of $1.8 \cdot 10^{-6}$ m/s. The effective porosity (n_e), equal to v_f/v_a would therefore be $\cong 30$ %.

However, these values (v_a and D_l) are only valid for the time period at which the tracer test was conducted, since the amount of water (Q) flowing through the column was not constant (Figure 58). Sampling extractions at the installed sampling ports contributed to the irregularities of the flow volumes. Temporally, entrapped gas was extracted with the water samples and new pathways were created. In order to stabilize the flow an additional pulsating pump was installed at the outlet on the 12th of August 2004 (day of operation 128). However, irregularities still persisted and Q varied between 200 and 1600 ml/d. The flow velocity therefore varied between 0.17 and 1.40 m/d within the experimental period. Even though this was not intended, it is not entirely unrealistic, since the flow velocity variations in the field will be comparatively high, due to variations in the pumping rates, the lake water level and the temperatures.
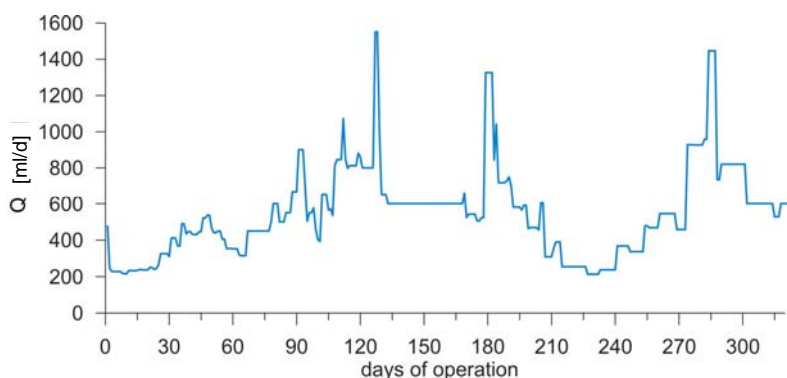
Figure 58: Temporal variations of the flow (Q) through the column.

Hydrochemistry

The electric conductivity (EC), pH and Eh (mV) measured regularly in the inflow and outflow are shown in Figure 59. Variabilities in the inflow are due to the tracer test performances, biological activity and evaporation in the fresh water container. Additionally, the surface water quality from the lake Wannsee, refilled at roughly monthly intervals, changes naturally.
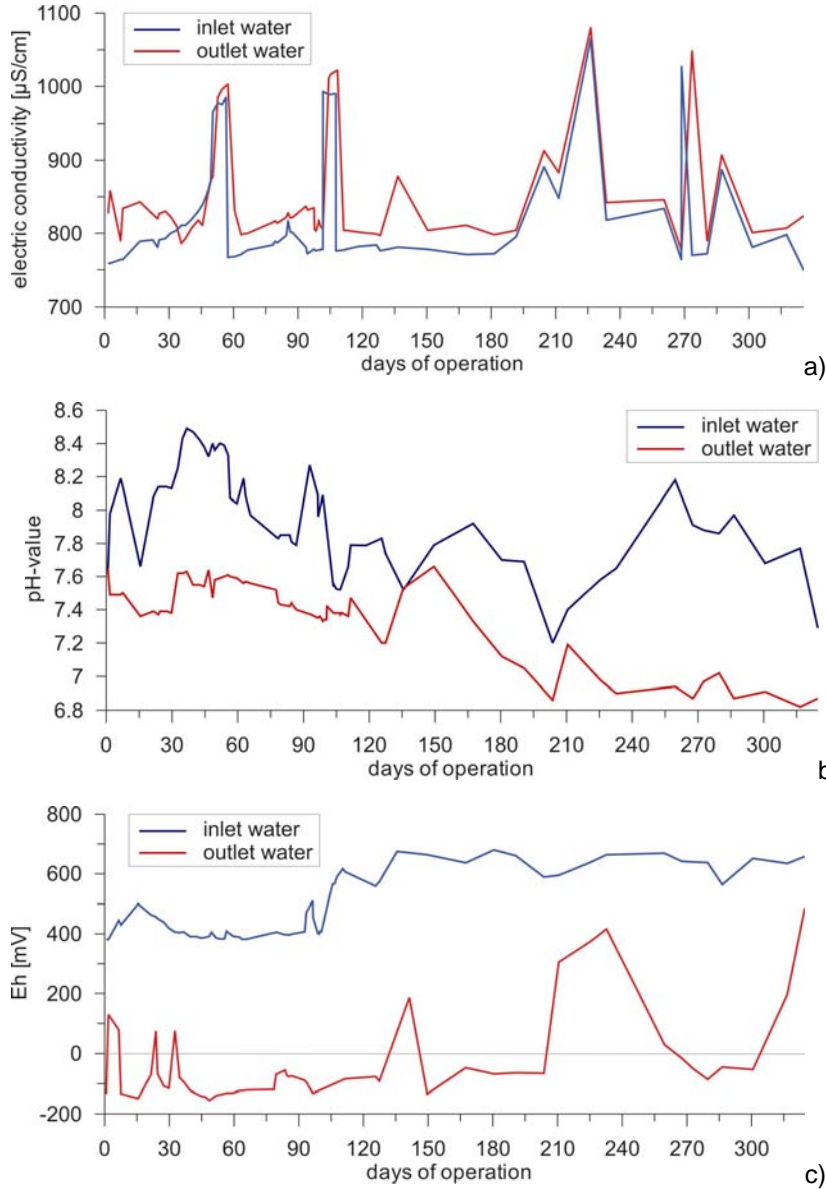
Figure 59: a) EC (µS/cm), b) pH and c) Eh (mV) values measured in inflow and outflow over the entire experimental period.

The ECs of the outflow were continuously slightly higher than those of the inflow, probably mainly caused by the dissolution of carbonates. The pH-value of the filtrate water persistently

decreased by 0.5 to 1.5 units from inflow to outflow which is due to biological activity of microorganisms producing CO_2. The redox potential strongly decreases within the column. The inflow is saturated with regard to oxygen, the Eh-value of the inlet water varies between +400 and +650 mV. Microbiological activity leads to a decrease of the Eh-value in the column to distinctly reducing conditions in the range of −100 to −150 mV. Elevated redox potentials in the outflow are likely to be the results of leakages in the outlet water pipe connections or measurement errors of the Eh-probes.

Figure 60 illustrates the development of the oxygen concentration at several depths within the column over the experimental period. It seems that quasi-steady state conditions were reached only towards the end of the experimental period. During the first 33 days of operation, oxygen was completely consumed in the uppermost four centimetres of the column. After one month, a change of color from darker grayish-black to light grey and brownish tones became visible in the sediments of the column, descending downwards from the top. After 3 months, oxygen was observed in 8 cm depth. More than 230 days were needed to detect oxygen in the depth of 12 cm. Over the entire experimental period, the oxidation of the sediments visibly advanced to a depth of more than 25 centimeters. However, oxygen did not reach the 60 and 80 cm probes. Because the column was stored stagnant for several months before it was set up, the sediments had become more reducing than under natural conditions and it took roughly 9 months before steady-state conditions were re-established.
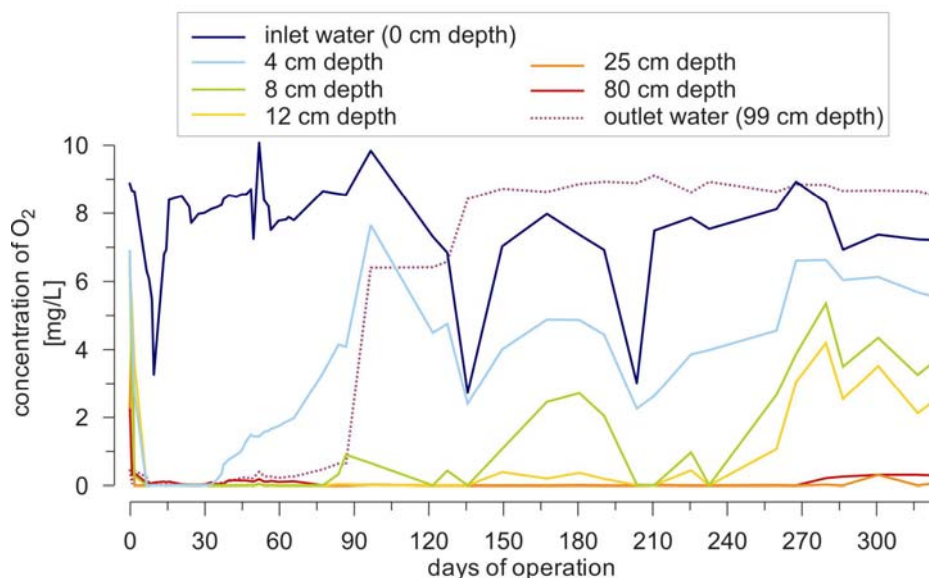
Figure 60: Oxygen concentrations at various depths in the column with time.

In Figure 61, the overall changes in the water chemistry from the inflow to the outflow of the column are shown as a mass balance (in mmol/L) over the entire experimental period. The median concentrations of the major ions and of the redox indicators are shown. The calcium,

magnesium and, most distinctly, the hydrogen carbonate concentrations are increasing during the sediment passage, most likely due to the dissolution of carbonate minerals caused by the slight pH drop. The gain of hydrogen carbonate is also a result of the microbial redox processes. The amounts of sodium, potassium, chloride and sulphate are decreasing insignificantly, considering their absolute concentration.
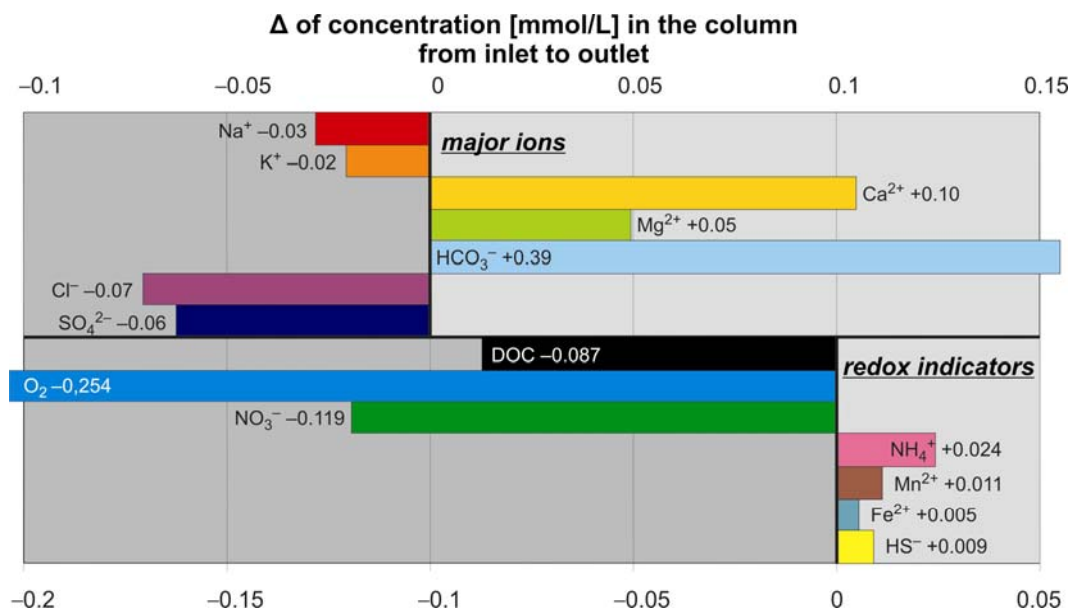
Figure 61: Concentration gains and losses of the water constituents from inflow to outlow.

Figure 61 additionally displays the gains and losses of the redox indicators (oxygen, nitrate, ammonia, manganese, iron and hydrogen sulfide) within the column. Roughly 15 % of the total dissolved organic carbon is oxidized in the column. Oxygen and nitrate are completely consumed while ammonium, manganese(II) and very low concentrations of iron(II) and hydrogensulfide are generated during the flow. Figure 62 shows the depth profiles of the redox indicators (median concentrations of the entire experimental period). Oxygen penetrates 25 cm into the sediment while nitrate reaches a depth of 90 cm. Manganese appears in 25 cm depth. An overlapping of the redox zones was observed. Hydrogen sulfide was only observed in the first few months and is therefore probably a relict of the stagnant storing period rather than a true indicator of sulfate reduction.
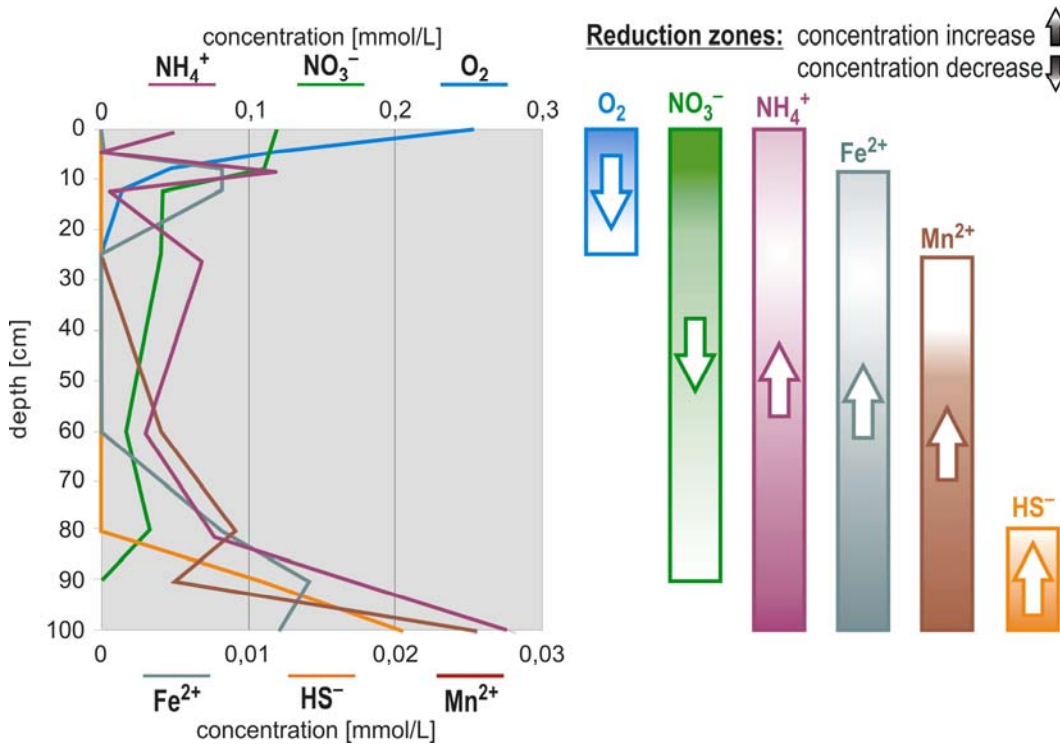
Figure 62: Depth profiles of the redox indicators (median concentration) and extent of the respective redox zone.

Hydrogeochemical Modeling

In order to get more detailed information about saturation indices of mineral phases and species distribution of the dissolved components hydrogeochemical calculations of analysed samples of the column study were carried out with Phreeqc-2. (version 1.5.09). The simulations were performed for samples with a complete number of analysed components and an electro balance error of less than 4 %. This reduced the data-set to a suit of 25. Since the samples taken from the in- or outflow of the column provided a more complete amount of analysed components, these samples were mainly used for the simulations. But nevertheless, analyses from all depths of the columns have been considered at least once.

If possible, the redox potential was defined in the Phreeqc-2 input file according to direct measurements. This was possible only for a number of samples of inflowing and outflowing water taken outside of the column. For water samples taken from the sample ports in the column, no redox measurements existed. In this case the redox potential was calculated by Phreeqc-2 using the measured redox couple N(-3)/N(5). Due to the fact that the redox couple is rarely in equilibrium, this may affect the accuracy of the results. In most cases the redox values calculated by Phreeqc were high in comparison with measured values of the outflowing water. This may be owing to the high concentrations of nitrate analysed in the column

The results of our calculations are compiled in Table 5. The simulations yielded slight over-saturation of calcite and aragonite in most samples. The rising alkalinities along the flow path are mainly the result of biodegradation of organic carbon and only to a lesser extent caused by calcite dissolution.

The calculated oversaturation of trivalent iron phases seems reasonable for in- and outflow-ing water with temporarily elevated measured redox values. With regard to the water in the column the authors suppose that calculated oversaturation of trivalent iron phases is a con-sequence of overestimated redox values and not reliable here. Furthermore the analytical results of the column study indicate mobilisation of iron and manganese which is in contrast to the results obtained with Phreeqc.

Gypsum and anhydrite never reach saturated conditions as a result of comparatively small concentrations which are always below 300 mg/l. Hence no reduction of sulphate occurs in our experiment, Pyrite keeps also permanently undersaturated.

Table 5: Calculated saturation indices (SI) for different mineral phases with Phreeqc.

depth	port name	date of analyses	pH	Eh (mV)	Electro neutrality (%)	SI Calcite	SI Aragonite	SI Dolomite	SI Siderite	SI Gypsum	SI Anhydrite	SI Goethite	SI Fe(OH)3	SI Pyrite
0	C1	11.01.2005	7.9	658	-3.5	0.42	0.27	0.11	-8.18	-1.36	-1.6	8.52	2.63	-211.83
0	C1	16.07.2004	8.2	426	-2.2	0.74	0.59	0.86	-5.17	-1.40	-1.64	8.35	2.46	-160.59
0	C1	28.07.2004	8.3	626	-2.2	0.83	0.68	1.02	-8.51	-1.36	-1.6	8.52	2.63	-211.96
0	C1	12.08.2004	8.1	592	-2.0	0.65	0.50	0.67	-8.16	-1.39	-1.62	8.05	2.16	-201.29
0	C1	03.09.2004	7.7	685	-1.7	0.29	0.14	-0.10	-8.48	-1.38	-1.62	8.33	2.44	-215.88
0	C1	22.07.2004	8.0	586	-1.1	0.58	0.44	0.54	-7.79	-1.40	-1.64	8.05	2.16	-197.68
0	C1	20.08.2004	7.9	696	0.8	0.46	0.31	0.24	-9.02	-1.39	-1.62	8.52	2.63	-223.09
0	C1	08.07.2004	8.4	657	4.0	1.01	0.86	1.37	-9.19	-1.36	-1.6	8.63	2.74	-222.3
4	C2	02.08.2004	8.0	0	-2.7	0.51	0.37	0.41	-3.27	-1.38	-1.62	8.05	2.16	-130.57
8	C3	30.07.2004	7.8	0	-2.5	0.36	0.22	0.11	-2.26	-1.40	-1.63	8.94	3.05	-129.76
12	C4	29.07.2004	7.5	0	-2.2	0.03	-0.12	-0.56	-2.93	-1.40	-1.64	7.98	2.09	-130.29
90	C8	09.05.2004	7.4	0	3.6	-0.03	-0.17	-0.72	-1.67	-1.30	-1.54	9.12	3.23	-128.15
100	C9	29.07.2004	7.7	0	-2.8	0.27	0.12	-0.09	-0.95	-1.33	-1.57	8.45	2.56	-104.34
100	C9	29.06.2004	7.6	-45	-2.3	0.16	0.02	-0.32	-0.12	-1.40	-1.63	4.24	-1.65	-34.85
100	C9	22.07.2004	7.5	-101	-2.1	0.07	-0.07	-0.48	-0.21	-1.42	-1.66	3.04	-2.85	-20.46
100	C9	12.07.2004	7.7	-97	-1.9	0.25	0.10	-0.11	-0.04	-1.38	-1.61	3.64	-2.25	-24.22
100	C9	22.12.2004	7.3	31	-1.0	-0.03	-0.18	-0.67	-0.52	-1.30	-1.53	4.64	-1.25	-49.04
100	C9	08.07.2004	7.5	-92	-1.0	0.13	-0.01	-0.34	-0.04	-1.34	-1.57	3.5	-2.39	-23.32
100	C9	11.01.2005	7.6	-88	-0.6	0.12	-0.03	-0.48	0.34	-1.33	-1.57	3.99	-1.9	-23.8
100	C9	09.05.2004	7.6	-138	-0.3	0.21	0.07	-0.25	0.22	-1.38	-1.62	3.14	-2.75	-13.67
100	C9	18.02.2005	7.4	203	0.5	-0.06	-0.21	-0.78	-0.94	-1.32	-1.55	7.35	1.46	-90.93
100	C9	20.08.2004	7.8	286	1.3	0.36	0.22	0.07	-1.47	-1.39	-1.62	8.94	3.05	-117.53
100	C9	03.09.2004	7.6	78	2.0	0.22	0.08	-0.18	0.54	-1.34	-1.58	7.08	1.19	-63.88
100	C9	17.11.2004	7.8	386	2.5	0.29	0.15	-0.06	-4.11	-1.28	-1.52	8.04	2.15	-143.34
100	C9	23.05.2004	7.6	-148	3.1	0.23	0.08	-0.17	0.12	-1.29	-1.53	2.95	-2.94	-11.56

2.3   Aquifer Sediments

The sediments encountered during the drilling campaign for the new observation wells at the Lake Wannsee transect 3 are fairly homogenous (depth < 26 m below ground). They mainly consist of fine- to medium sized sands of light greyish to brown colours. They are of glacial-fluvial origin (*Saale* to *Weichsel* glacial period). They are underlain by a finer grained, clayey organic rich aquitard of the *Holstein* interglacial period, which was not encountered during the new drilling. From previous drilling campaigns it is known that they can be expected around sea-level, which is equivalent to 35 m below ground at the site. Underlaying the Holstein are *Elster* sands, which are separated by an *Elster* silt aquitard. The production wells of the water works are screened above and below the *Holstein* aquitard as well as below the *Elster* silt. Lithological cross-sections of the transects Wannsee 1 and Wannsee 2 with available k_f data (from sieving) are shown in Figure 63 and Figure 64. Figures of the geochemical analysis of the core BEE202UP obtained during the drilling campaign are given in Figure 65 and Figure 66.
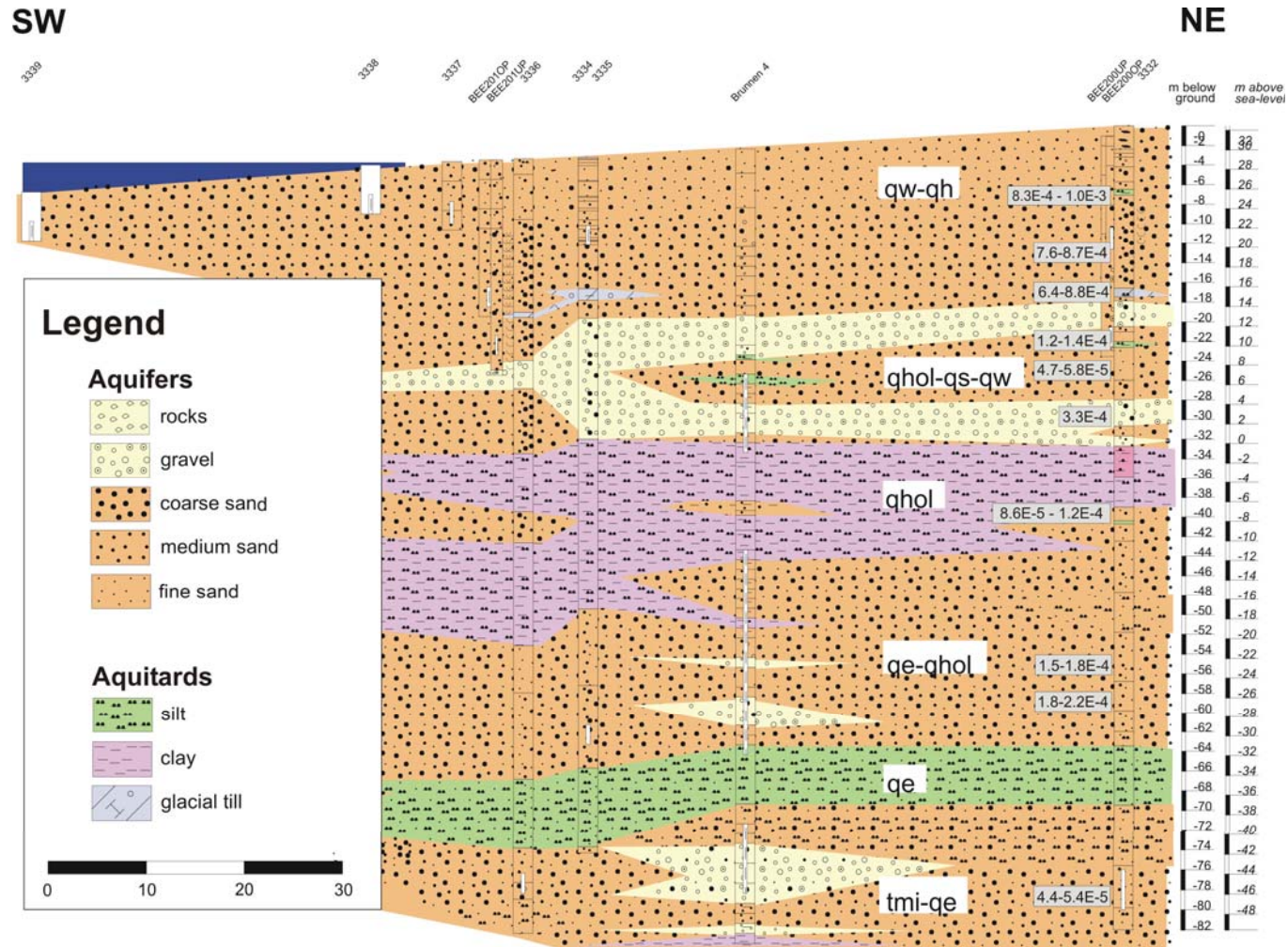
Figure 63: Lithological cross section of Wannsee 1 with k_f data of core 3332 (modified after Hinspeter, 2002).
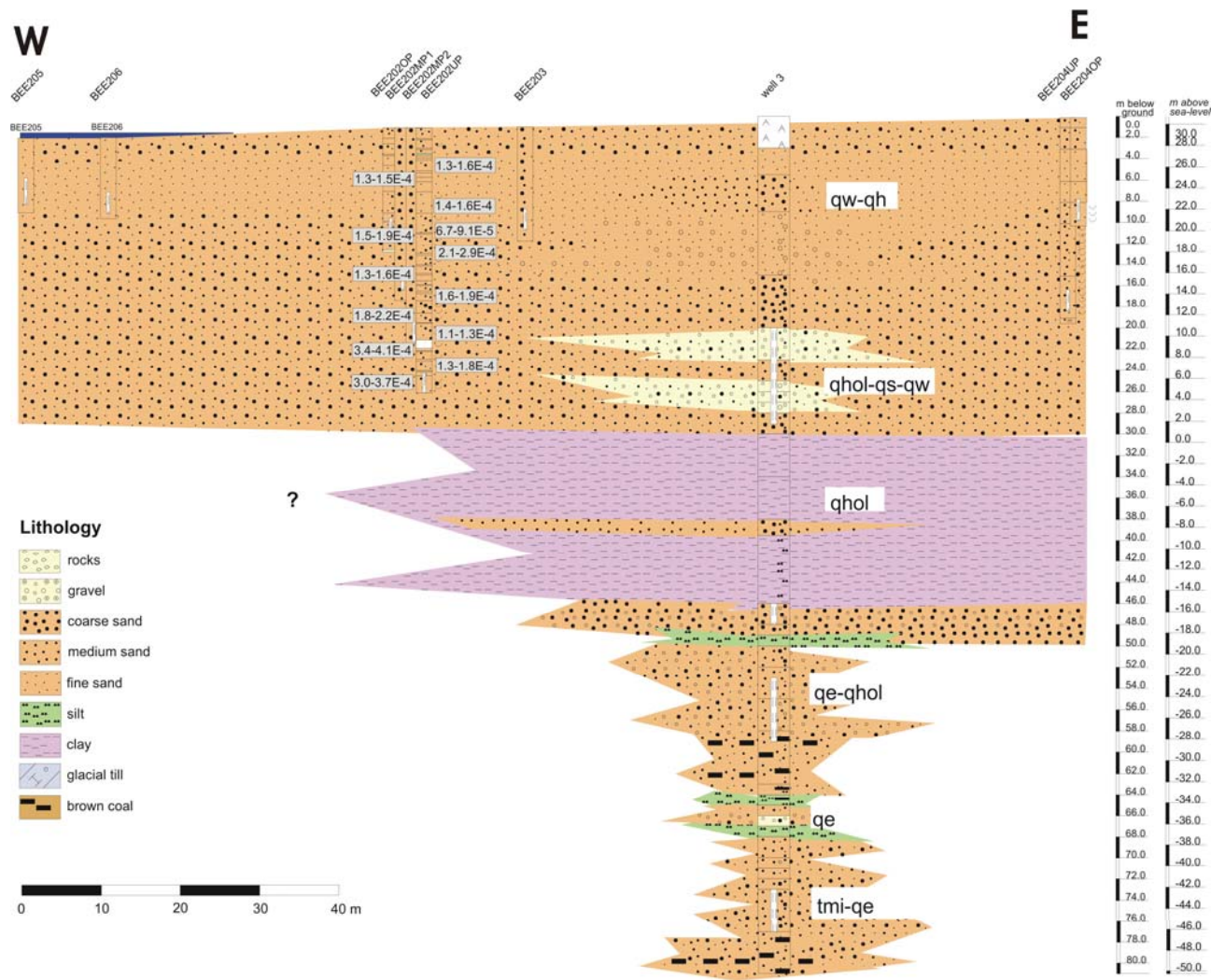
Figure 64: Lithological cross section of Wannsee 2 with k_f data of BEE202UP.
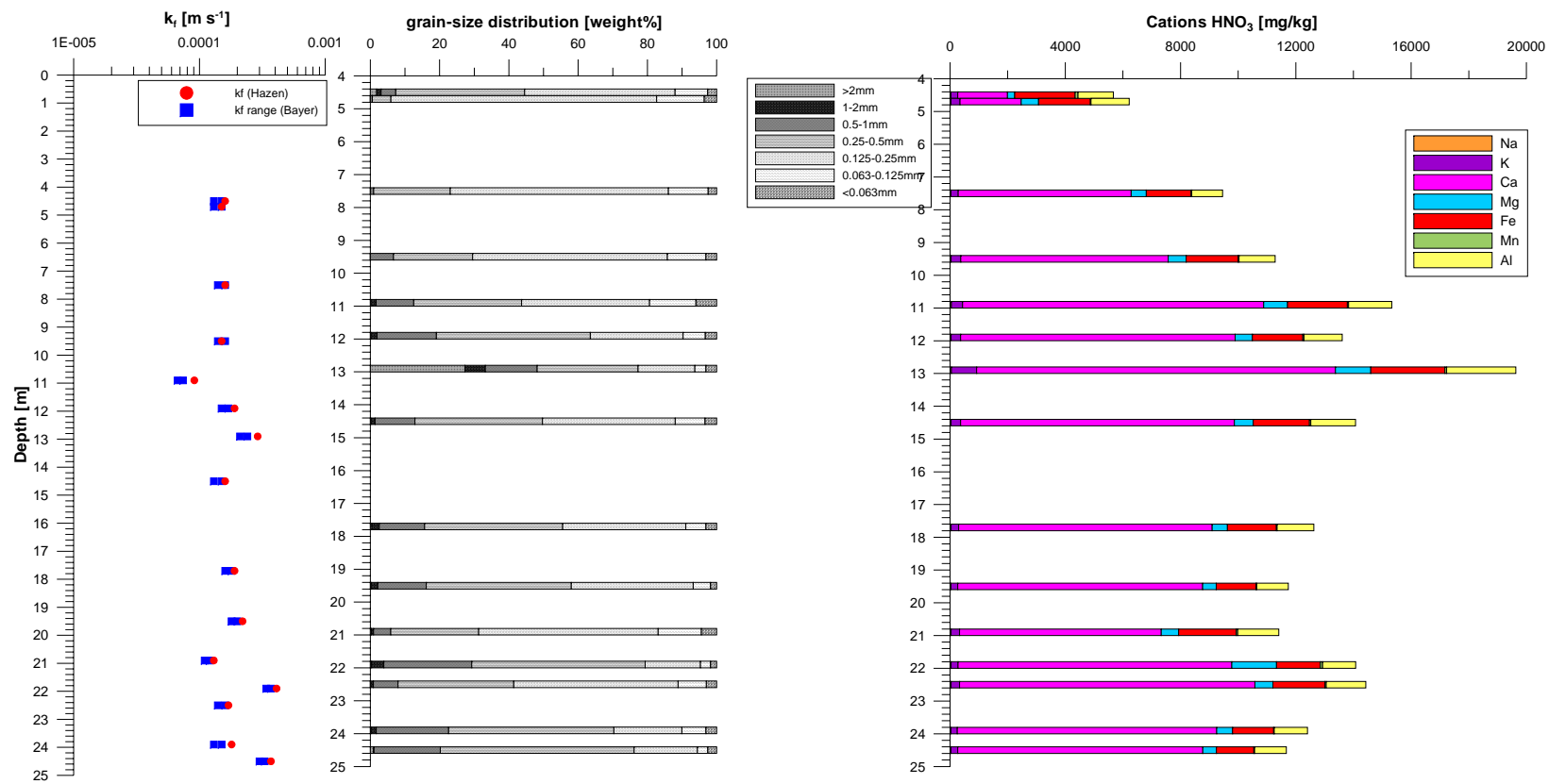
Figure 65: Hydraulic conductivities (k_f), grain-size distribution and cations from HNO_3 extraction in core BEE202UP.
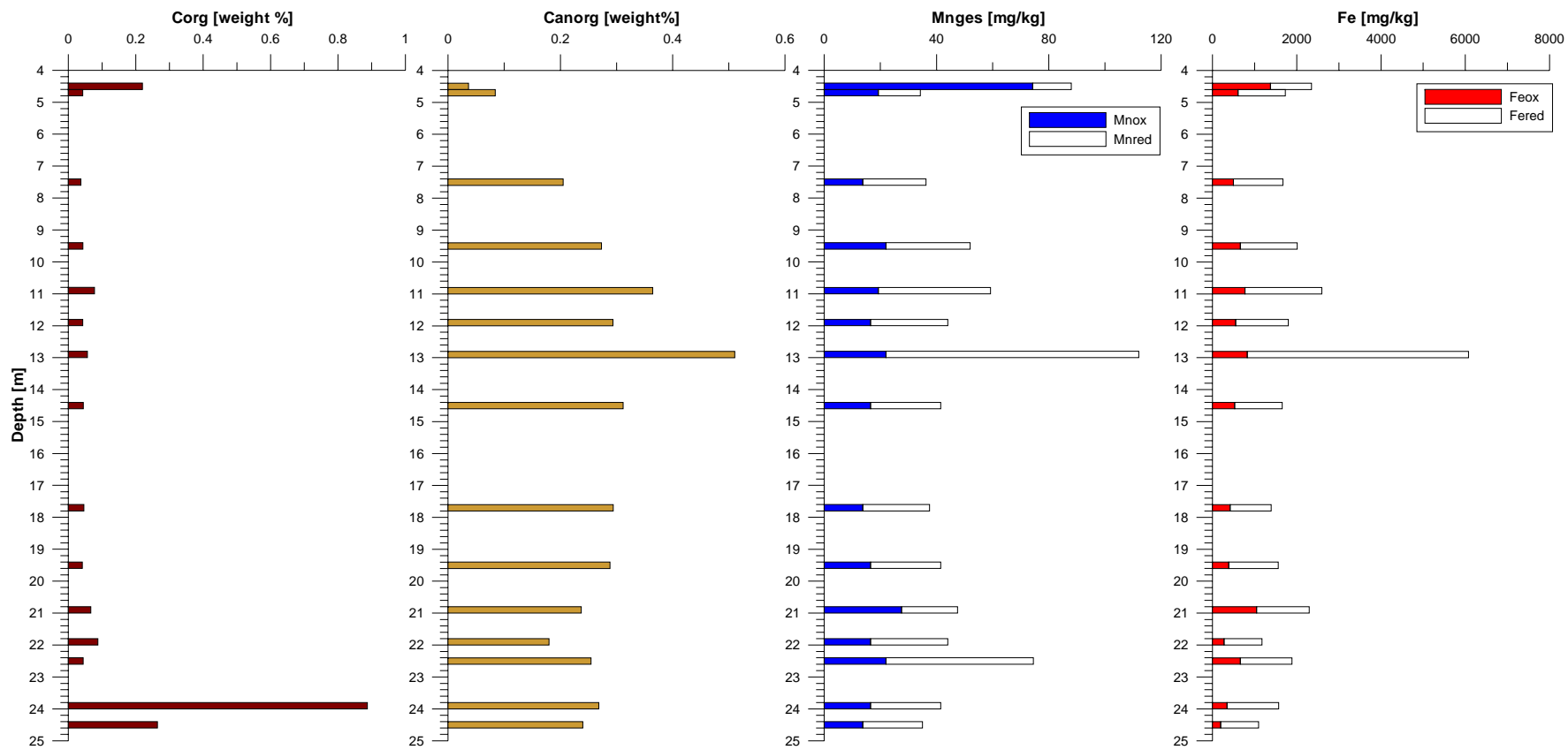
Figure 66: Organic and inorganic carbon content, Fe(III) and Fe(II), Mn(III) and Mn(II) content in core BEE202UP.

The sands of BEE202UP are fairly homogenous in terms of their hydraulic conductivity, which varied from $6.7*10^{-5}$ to $4.1*10^{-4}$ m/s (Figure 65). The hydraulic conductivities of the clogging layer are considerably lower (Figure 48, Figure 53), even though those values obtained from sieving are actually remarkably similar. The organic carbon content in the aquifer sands (Figure 66) is 0.04 to 0.26 weight %, with the exception of a sample containing 0.9 weight % organic C, because of small coal pieces. Compared to the uppermost decimetres of the lake sediments (Figure 47), the organic carbon content of the aquifer is low. All samples analysed contain inorganic carbon (carbonate) at amounts of 0.04-0.51 weight % C.

2.4 Tracer evaluation: Travel times/groundwater age

The Tritium/Helium (T/He) age dating results can give a first idea on the groundwater age, i.e. the average travel time from the surface to the sampling location; in the case of bank filtrate, from the lake to the relevant well. T/He dating was used to calculate the travel times of bank filtrate by Stute et al. (1997), Beyerle et al. (1999) and Sültenfuß & Massmann (2004). The combined T/He results of all sites are given in the Appendix.

Transect 1, which contains observation wells in the uppermost, but also in the lower aquifers, was dated with the T/He method in summer 2001. Instead of the calculated ages, Figure 67 shows Tritium (T) concentrations (TU) originating from atmospheric hydrogen bomb testing in the 1960s and radiogenic Helium-4 ($^4He_{rad}$) concentrations (Nml/kg) from the Uranium (U) and Thorium (Th) decay within the aquifer. If there is hardly any T left, because it has all decayed (pre-bombing age) or if there is no tritiogenic Helium present (Helium from the Tritium decay, He_{tri}) because the sample is very young and the T concentration is similar to that of the surface water, a reliable age cannot be given. Because the dated observation wells are either He_{tri}-free (i.e. very young as in the case for the shallower wells 3335, 3337, 3339) or T-free because they are very old (3332, 3334, 3336, wells screened below the Hostein aquitard), are precise age cannot be given.

If the Uranium and Thorium contents of the sediment were known, ^4He could be used to date the deeper groundwater (Beyerle et al., 1999). Because the U and Th contents are unknown, elevated concentrations of radiogenic ^4He can only be used as an indicator for a relatively "old" groundwater. The concentration of $2.8*10^{-4}$ Nml/kg the deepest observation well 3336 suggests that the water is not 99 years old (as calculated), but at least centuries old (pers. communication Sültenfuß, 2003). In both deeper aquifers, the groundwater is clearly considerably older than 50 years since T has already decayed and the ^4He values are high. Consequently, any "younger" substances (for example pharmaceutical residues or contrast agents) which were applied in the past decades only, should not be present in the 2 deeper aquifers. The deeper aquifers have not been sampled regularly within NASRI because they do not

belong to the bank-filtration system, which becomes clear when looking at the T/He data. A single sampling campaign conducted in March 2004 confirmed that the aquifers below the Holstein aquitard (wells 3332, 3334, 3336) do not contain any pharmaceutical residues or other substances (compare chapter 2.5).

In contrast to the deeper T/He results, the shallow wells reflect the atmospheric concentrations of T at the time of sampling, while radiogenic ^{4}He and tritiogenic ^{3}He could not be detected. The resulting calculated effective T/He age is 0 years, which is equivalent to less than 6 months, which is the resolution of the method at the site.
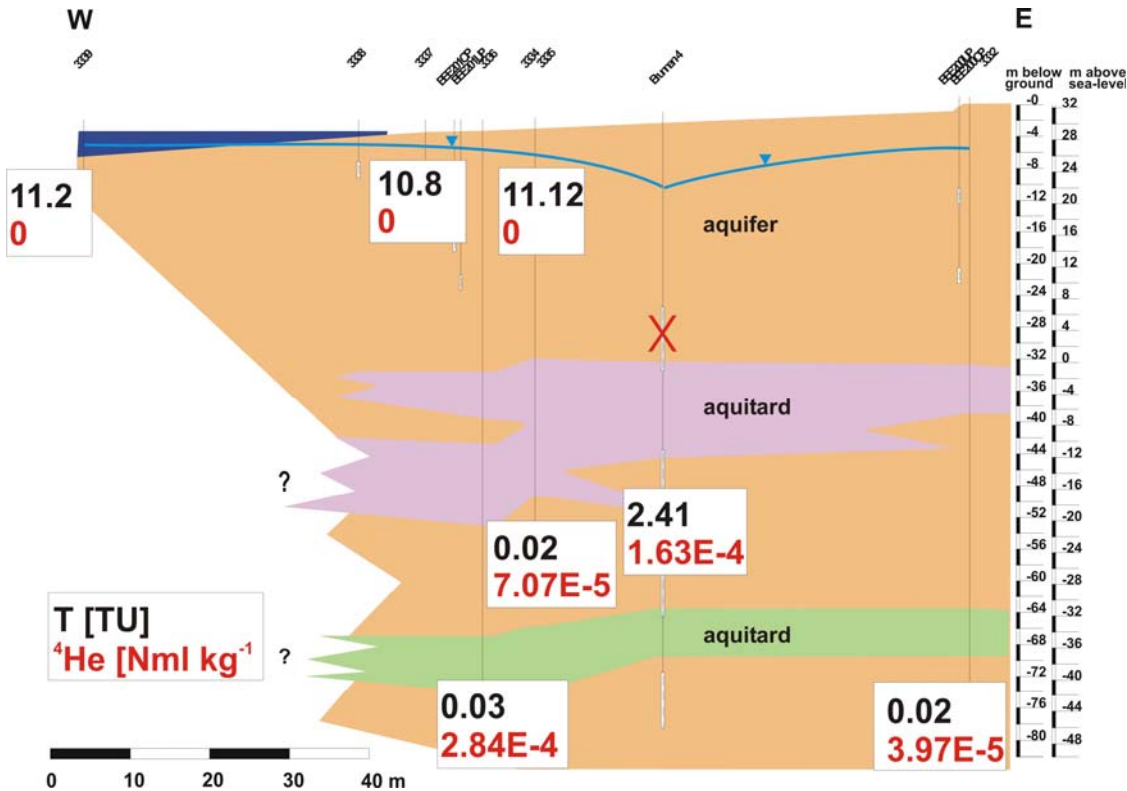
Figure 67: Tritium and radiogenic ^{4}He at Wannsee 2, sampling campaign summer 2001.

The production well is a mixture of all aquifers. The effective T/He age of well 4 is 25 years. This is not a "real" age in terms of an actual travel time but the results of mixing of water with distinctly different ages. A clear indicator of this (rather expectable) fact is the offset of well 4 from the precipitation input versus year curve. When plotting the "stable" tritium concentration (remaining T plus decayed tritiogenic He) of an unmixed sample against its calculated infiltration year, the sample should lie directly on the input curve given by the actual T concentration in the precipitation at the time. As shown in Figure 68, well 4 plots below the input curve as expected from its mixed nature. The T concentration of well 4 (2.4 TU) can be used for a mixing calculation. According to the T value, the production well 4 abstracts ~ 22 % of water

from the uppermost aquifer; a distinction between bank-filtrate and background groundwater from inland cannot be made. Therefore, results show that well 4 is not completely sealed. For simplicity, the deeper wells 3332, 3334 and 3336 were given an age of 1950 in Figure 68, even though they might be considerably older.
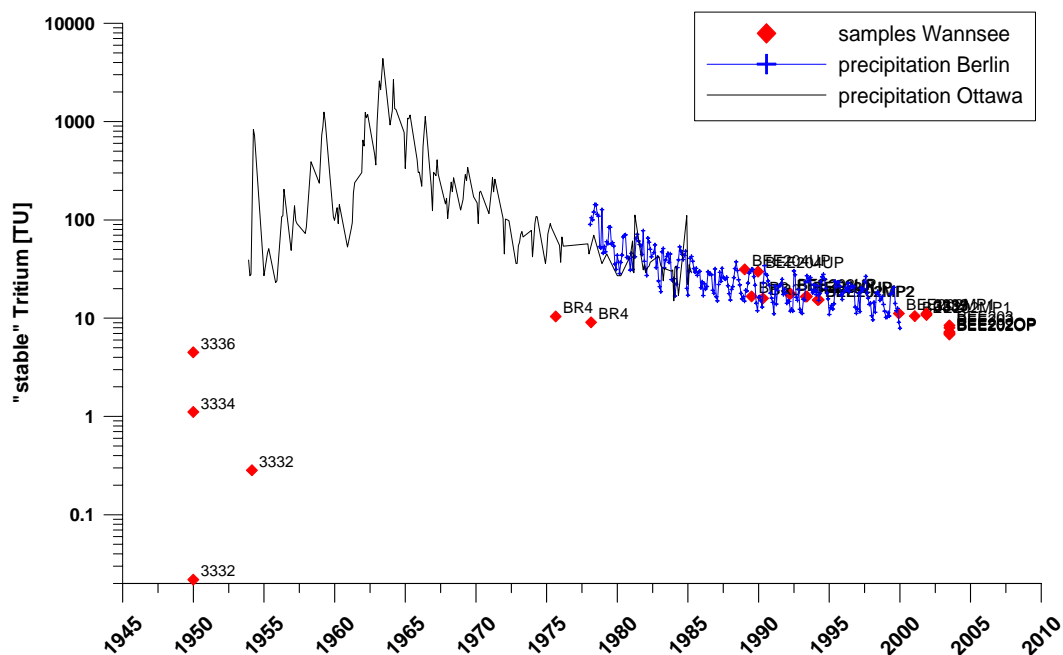
Figure 68: "Stable" T concentration (T+^{3}He$_{tri}$) versus calculated infiltration year for the Wannsee samples and time-series of T in the precipitation of Berlin and Ottawa (due to lack of data at the respective time in Berlin). Data source: IAEA, BfG.

Figure 69 presents the effective T/He ages of samples collected at transect Wannsee 2 in July 2003. The dating results showed that only the observation wells with the uppermost, shallowest filter screens contain "young" bank-filtrate (which is less than 6 months old). These are also the wells which show an almost undampened breakthrough of tracer curves. The T/He ages of the well group BEE202 with filter screens in 4 different depths of the up-permost aquifer (above the *Holstein* aquitard) increase from 0 to 10.7 years with depth. This clearly indicates that the groundwater in the uppermost aquifer shows a very strong vertical age differentiation, which had not been expected at first. The T/He-dating illustrates that wa-ter abstracted from the deeper observation wells (in the upper aquifer) is years to decades rather than months old. The same phenomenon was observed at the Lake Tegel bank filtra-tion transect. As in Tegel, this also explains the different composition of the bank filtrate re-garding a number of minor water constituents in the respective "layers" (compare chapter 2.5). It also indicates that bank filtrate must be flowing underneath the lakes, which are there-fore not water divides. Rather than flowing in 4 layers with different "real" travel times as indi-

cated by the coincidental number of filter-screens, it is likely that the bank filtrate is either "young" (< 6 months, originating from the nearest shore) or "old" (years to decades, originating from an opposing shore). Intermediate ages would be the result of mixing to variable degrees between these two sources. However, the use of particle tracking within the hydraulic model also suggested that the travel times of the two deeper wells (BEE202MP2 and BEE202UP) vary strongly between summer (8 and 13.5 years) and winter (0.24 and 3.75 years). The catchment areas of well 3 and 4 simulated in the hydraulic model varied seasonally but basically reached to the opposing south-western lake shore.

Production well 3 has a mean T/He age of 13.6 years, which is the result of mixing of water from 3 different aquifers (the two deeper aquifers are not shown in Figure 69) from 2 sides. The groundwater from the inland side displays a similar age.
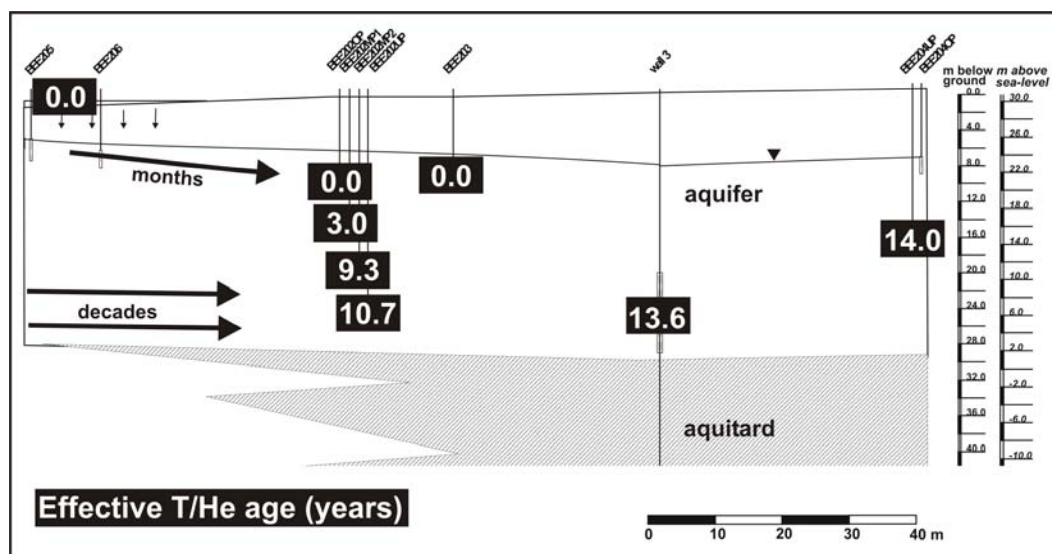
Figure 69: Effective T/He ages plotted at the position of the filter screen depth. Samples taken in July 2003.

The tracer evaluation with breakthrough curves turned out to be more complicated than expected. Isotope data of 2000/2001 and 2002/2003 shows that breakthrough curves of the shallow observation wells of transect 1 (3339, 3338, 3337 and 3335) and transect 2 (BEE205, BEE206, BEE202OP, BEE203) reflect the surface water signal, a clear indication that these wells contain young bank-filtrate. Because sampling of 3339, 3338 and 3335 was stopped in February 2003, data of 2000/2001 was added for reference. Figure 70 illustrates that residence times for the shallowest wells are rather low at this particular site. Travel times are around 20 days from the Lake to 3337, ~ 30 days to 3338, < 30 days to 3335 and 65 days to 3339. The travel times are shorter to the wells at the shore than to those below the lake which probably a consequence of the decreasing permeability of the sediments away

from the shore. Observation well 3335 is at approximately 2/3 of the way to the production well. Therefore, on the very shortest (shallowest) pathway, the travel time of the bank filtrate to well 4 is roughly 1.5 months.
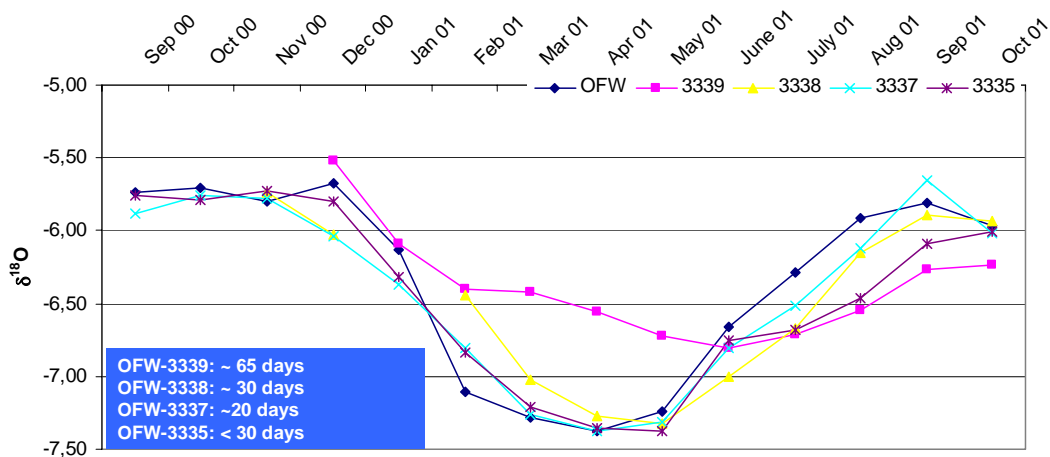
Figure 70: Isotope data from September 2000 to October 2001 (Hinspeter, 2002).

None of the remaining tracer (boron, chloride, potassium or EDTA) are of much use at the transect Wannsee 1. Potassium does not behave conservatively as it almost does in Tegel, EDTA fluctuates too in the input. The interpretation of Cl⁻ and B is difficult because of the lack of a clear peak in summer 2002 (sampling was stopped in winter 2003). The uncertainty of the input signal of the surface water of Lake Wannsee, caused by strong temporal and spatial variations was discussed earlier (chapter 2) and causes problems, for example in 3338 (transect 1) or BEE205 and BEE203 (transect 2). In the following, tracer breakthrough curves are shown for transect 2 only, which was sampled for much longer.

The breakthrough curves of the stable isotopes δD and $\delta^{18}O$ (Figure 71) and of Cl⁻ (Figure 71) show almost no delay from the lake to BEE206, while the temperature (Figure 72) is slightly off set. In contrast, the tracer break through about one month after peaking in the lake in BEE205, which is further out in the lake (Figure 69). The best estimates for travel times of the shallowest wells at Wannsee 2 are therefore ~1 month to BEE205 and less to BEE206 closer to the shore (maybe even less than 14 days) because of a better hydraulic conductivity of the clogging layer. BEE205 is located close to core 3B, while BEE206 is close to 1B (Figure 53), where hydraulic conductivities are about an order of magnitude higher. A better resolution can not be achieved with monthly sampling. The hydraulic model estimated travel times of a few days for both observation wells.
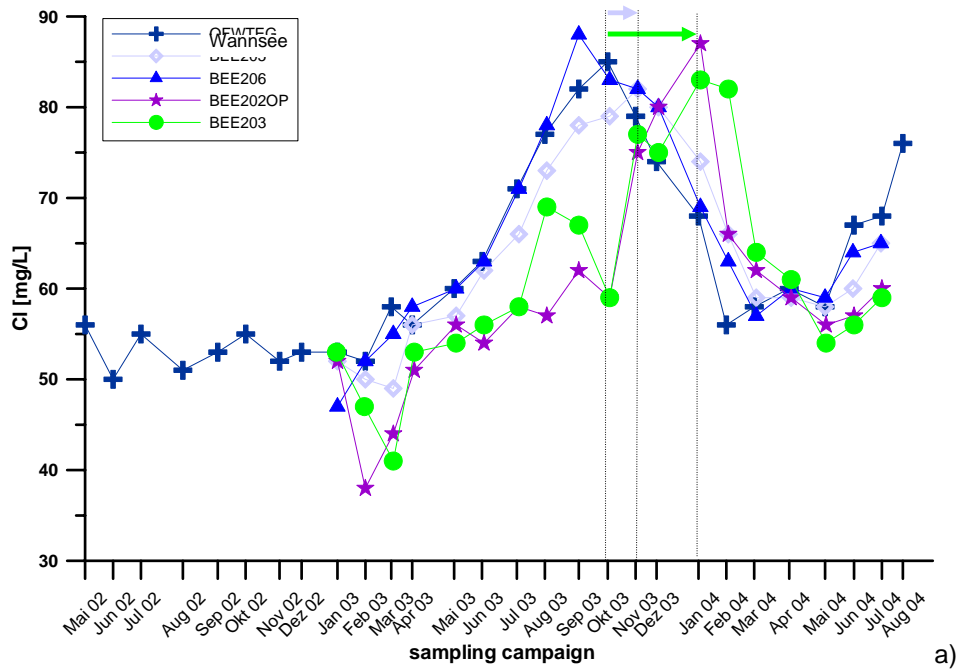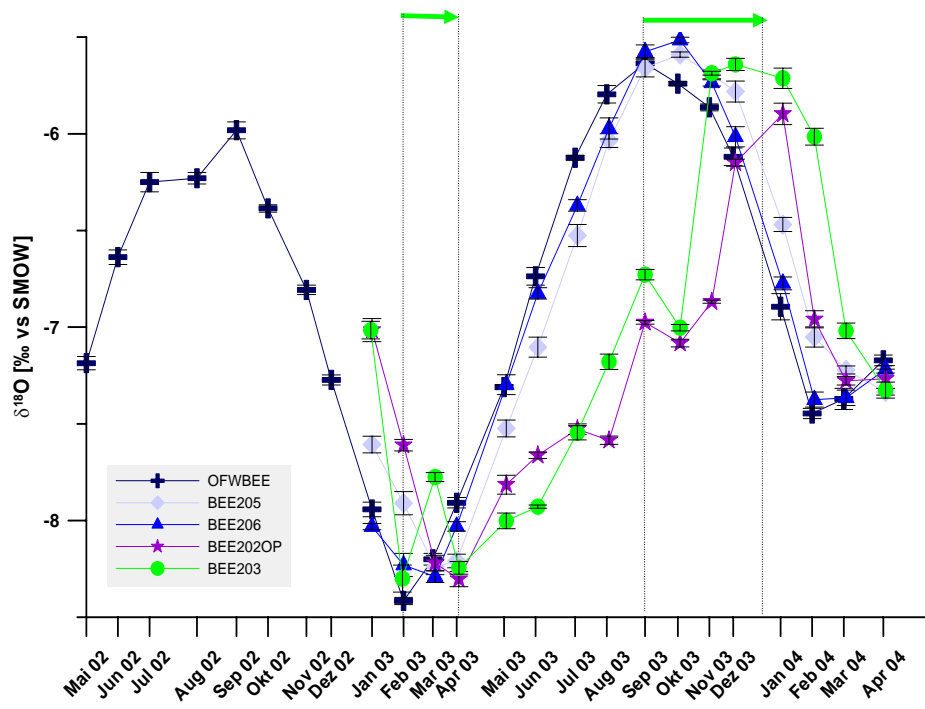
Figure 71: Time-series of Cl⁻ (a) and δ¹⁸O (b) in the shallow wells of transect 2 in Wannsee (Data source: BWB & AWI).
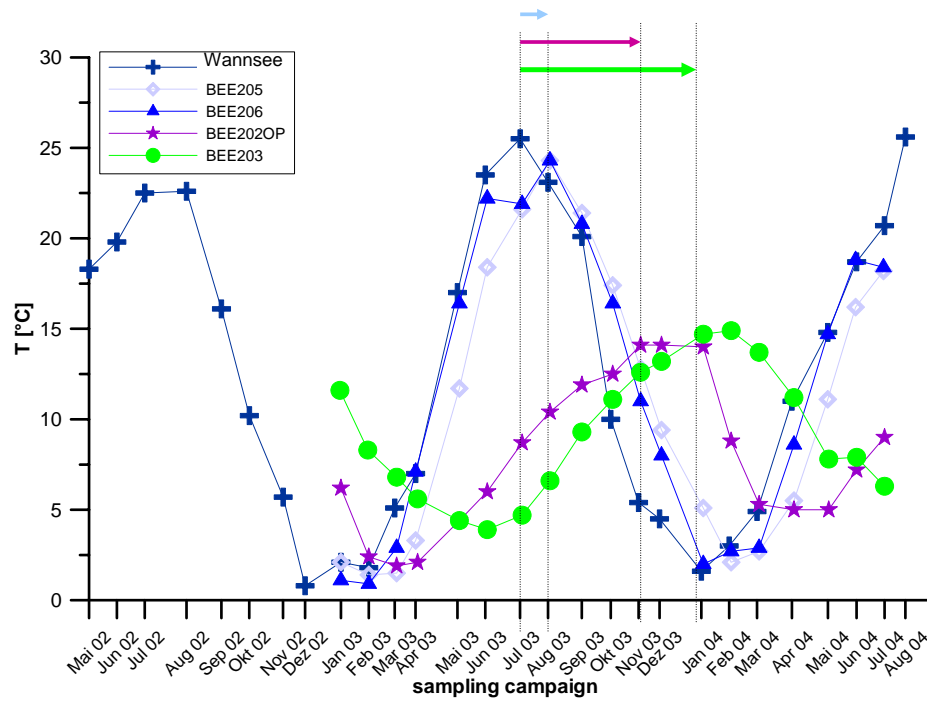
Figure 72: Time-series of temperature in the shallow wells of transect 2 in Wannsee. Note that temperature is retarding in comparison with a tracer, R ~ 2.1.

Breakthrough curves of BEE202OP and BEE203 are relatively similar to another, only the temperature shows a clear delay of BEE203 compared to BEE202OP. They both show an average time-lag of 2 and 4 months, depending on the time. Judging from Figure 71, it seems that the travel times are much longer in summer 2003 than in winter 2002/2003 and 2003/2004. The hydraulic model resulted in travel times of similar magnitudes, but with a tendency of longer travel times in winter (BEE202OP summer: 2 months, winter: 2.5 months; BEE203 summer: 2 months; winter 2.4 months). However, since BEE203 is about two thirds the way to the production well, the travel time on the fastest pathway is likely to be in the order of 3-6 months, depending on the hydraulic regime.
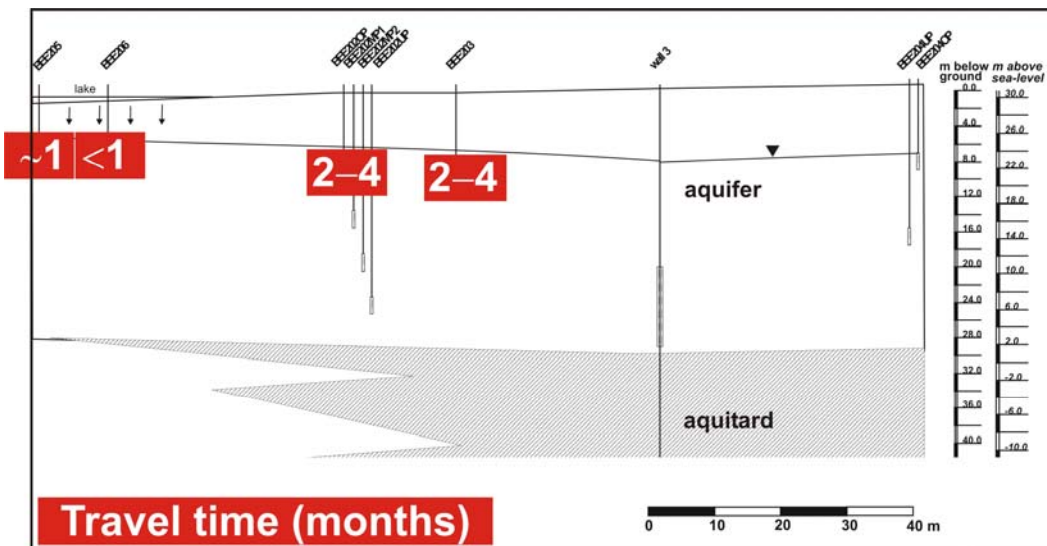
Figure 73: Summary of best estimates for average travel times from tracer breakthrough curves of the lake Wannsee transect 2.

The new deeper observation wells BEE201OP (filter screen 13-15 m below ground) & BEE201UP (18-20 m below ground) at Wannsee 1 and BEE202MP2 (18.3-20.3 m below ground) and BEE202UP (23.1-25.1 m below ground) do not show a seasonal isotopic variation and resemble average surface water values with regard to the isotopes (Figure 74b). The also show no variability in the concentration of any other potential tracer (e.g. B, Cl⁻ , EDTA). The same is true to some extent for the shallower well BEE202MP1 (13.3-15.3 below ground) which already has a strongly damped signal. The succession of the 4 observation wells at BEE202 therefore does not reflect a chronological sequence (with increasing travel times with depth) but a decrease of the proportion of "young" BF (in terms of BF directly from the adjacent shore) and an increase of "old" BF with depth. Even though this does reflect an age/travel time succession, these wells do definitely not lie on a single flow-path. The maximum depth of Lake Wannsee is ~ 9 m. The groundwater flow direction is from SW towards the well gallery. The elevated concentrations of wastewater indicators B (Figure 74) or EDTA in greater depth within the first aquifer and in particular elevated concentrations of substances such as phenazone and AMDOPH (compare chapter 2.5) which presumably have been present in the surface water in higher concentrations in the past, suggests that these wells contain bank filtrate which is at least partly originating from the past decades rather than from the past months, which had already been suspected by the T/He age dating results (Figure 69). The elevated concentrations could also be (at least partly) caused by the location of the catchment area of well 3 in the south of Lake Wannsee, where due to the closer location to the Teltowkanal, concentrations are presently (and have probably been for a long time) higher than in front of the transect (Figure 39, Figure 41).

106

The water abstracted in production well 3 does not show any seasonalities either. Therefore, the proportion of very young BF in the well itself can also not be very high (compare chapter 2.5).
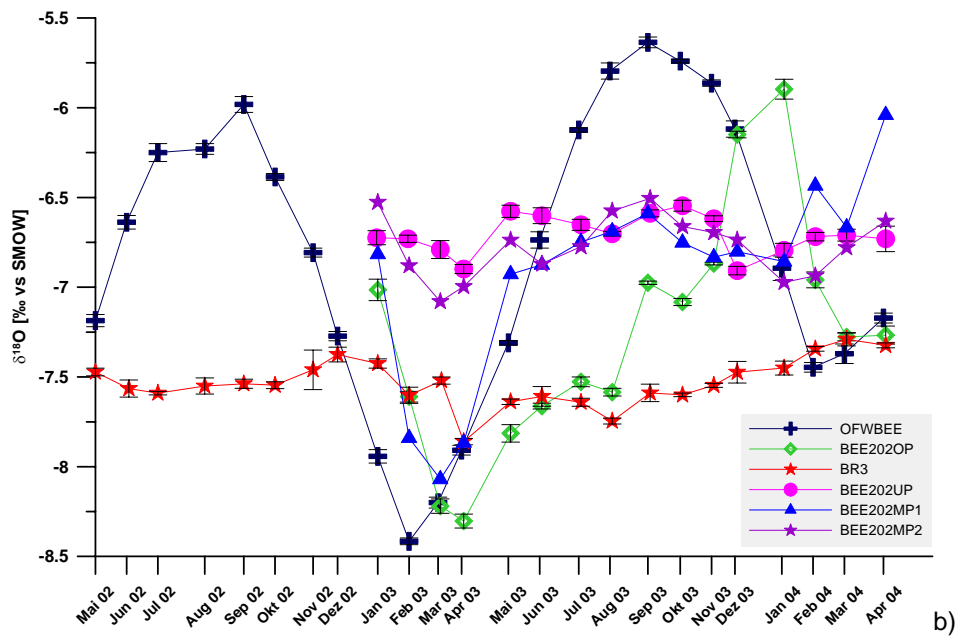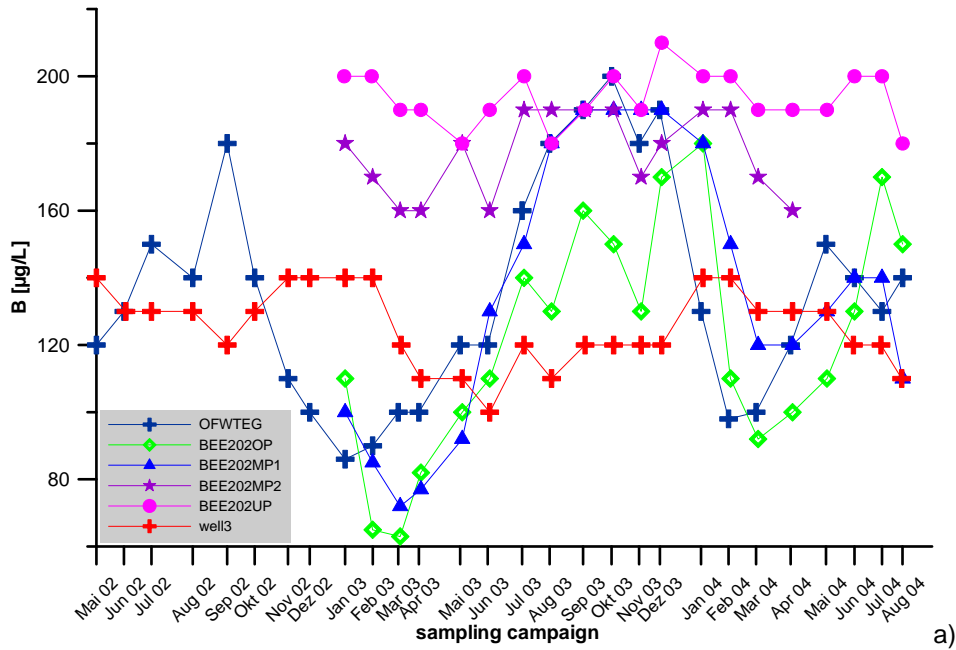
Figure 74: B (a) and δ^{18}O (b) in the lake, observation wells BEE202OP-UP and production well 4 (Data source: BWB & AWI).

2.5 Tracer evaluation: Mixing

The water abstracted at Lake Wannsee is a mixture of water from at least 6 distinctable sources, which makes the calculation of individual proportions in the production wells rather complicated, in particular since they are likely to differ with time too. Figure 75 displays the exemplary concentration of Cl^-, SO_4^{2-} and AMDOPH in the single sampling campaign in March 2004 in order to illustrate the differences between the water types. The ages have already been given in chapter 2.4.

The different water components are:

1. Bank filtrate with an age of a few months, originated from a close shore. The BF is characterised by a T/He age of 0 (i.e. < 6 months), a reflection of the variable (seasonal) input curve of all tracers and therefore a tracer concentration of similar magnitude as presently observed in the lake (encountered in 3335, 3337, 3338, 3339, BEE205, BEE206, BEE202OP, (BEE202MP1), BEE203).

2. Deeper, older bank filtrate with an age of years to decades, originating from a distant shore. The T/He age of this BF is at least a few years; tracer curves display no seasonality and the concentration of a number of minor water constituents differs largely from the present concentration in the lake (i.e. higher EDTA, B, AMDOPH, Phenazone; lower Carbamazepine, Gd-DTPA). Major water components and the stable isotopes tend to be present in the same order of magnitude as today, only with a lack of the seasonal variability (encountered in BEE201OP, BEE201UP, BEE202MP2, BEE202UP).

3. Background groundwater characterised by slightly elevated Cl^- concentrations, very high SO_4^{2-} (above the drinking water limit) and higher Ca^{2+}, a T/He age of 14 years and a general absence of waste-water indicators such as PhAC`s, B or EDTA. However, the occasional presence of some waste-water indicators suggests that the groundwater inland may at least sometimes and in parts be under surface water influence (observation wells inland: BEE200OP, BEE200UP, BEE204OP, BEE202UP).

4. Deeper groundwater from the *Elster* aquifer below the *Holstein* aquitard. The groundwater is of "pre-bombing" age (pre-1950) and shows no anthropogenic influence at all. Substances denoting bank filtration influence are not present. The hydrochemical conditions are sulfate-reducing; the water is almost SO_4^{2-}-free. The isotopic signature is more negative than at present because the formation temperature was much lower (3334).

5. Very deep, slightly more saline groundwater from the *Elster* aquifer below the second (*Elster)* aquitard represented by 3336. Again, the water is (at least) of pre-bombing

age but probably much older, the groundwater displays no anthropogenic influence, the hydrochemical conditions are sulfate-reducing, the water is almost SO_4^{2-}-free and the isotopic signature is also more negative than at present. The main difference to 3332 ad 3334 is that 3336 contains more Cl^- Na^+ and B and appears to be influenced by saline deeper groundwater (Na-Cl-HCO$_3$ water type). When the well was sampled monthly in 2001 (Hinspeter, 2002), the Cl- concentration varied between 268 and 495 mg/L.

6. Very pristine groundwater is encountered in 3332, in the same aquifer as 5 but inland. The concentration of Cl^- is very low (typical for pre-industrial freshwaters). As 4 and 5, the water is very old, sulfate reducing and isotopically more negative than at present.
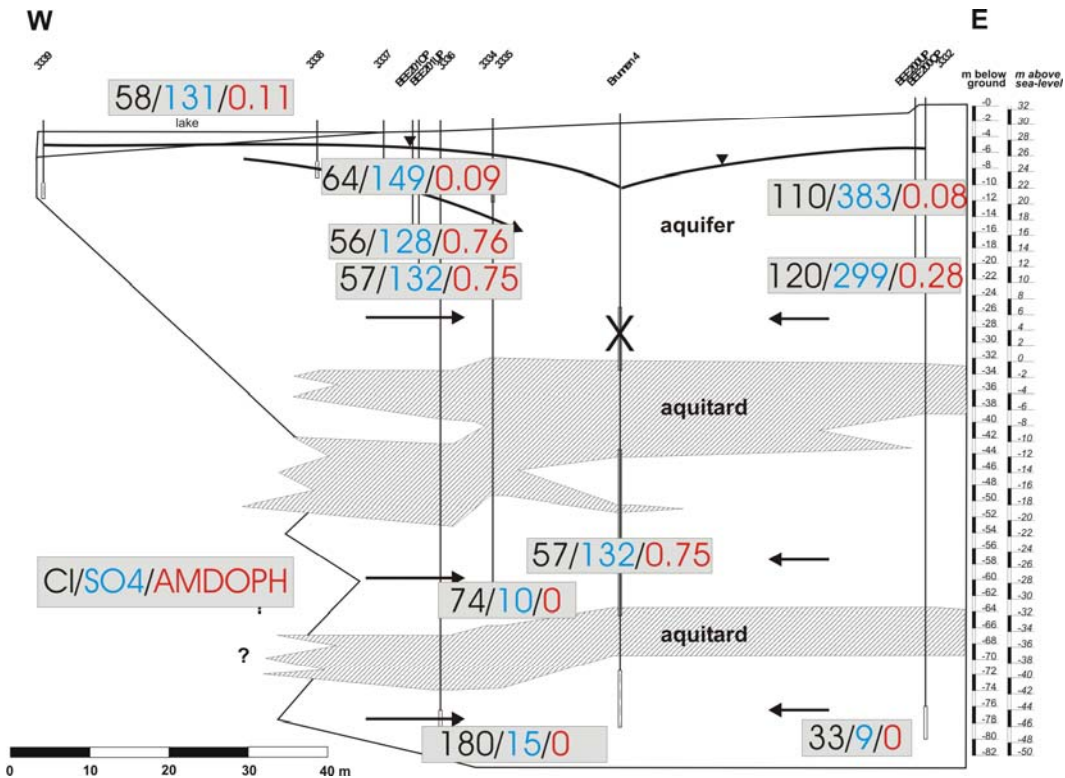
Figure 75: Concentration of Cl⁻ (mg/L), SO₄²⁻ (mg/L) and AMDOPH (µg/L) at transect Wannsee 1 in March 2004 (values plotted at loction of the relevant filter screen (data source: BWB). Values inland are those of BEE204OP & UP at Wannsee 2.

The two deeper aquifers at the site are free of Gd-DTPA (< 5 pmol/L), Carbamazepine, AMDOPH or any other persistent (and likewise less persistent) wastewater indicator, the same is (mostly) true for the groundwater inland of the production wells. Therefore, in order to estimate the proportion of "old/deep" bank filtrate (2) and "young/shallow" bank filtrate (1) in the production well, 3 parameters with clearly differentiable concentrations in 1 and 2 and similar

concentrations in the remaining groundwater (3, 4, 5 and 6) were chosen, namely AMDOPH (Figure 77a), Carbamazepine (Figure 77b) and the value of $\delta^{18}O$ (the slight differences between 3, 4, 5 and 6 were neglected and a value of -8.8 was assumed, Figure 78). The individual proportions can then be calculated by solving a system of equations with the average concentrations of AMDOPH, Carbamazepine and $\delta^{18}O$ in the different water components:

$$c_{br} = c_1 {}^* x + c_2 {}^* y + c_r {}^* z$$

with: c_1 = concentration in young BF (value of BEE203 used)
c_2 = concentration in old BF (value of BEE202MP2 used)
c_r = concentration in groundwater (3, 4, 5 and 6)
c_{br} = concentration in production well 3 or 4
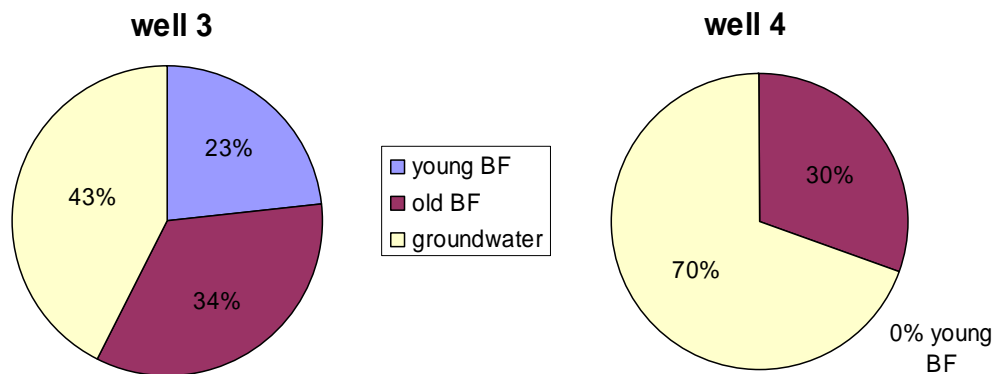
Figure 76: Percentage of young and old bank filtrate and remaining groundwater in well 3 and 4, calculated with average concentrations of AMDOPH, Carbamazepine and $\delta^{18}O$.

The results, shown in Figure 76, are clearly only a very rough estimation, since the proportions are likely to vary, depending on the pumping regime and the data/time-period used. Also, the calculation assumes that both Carbamazepine and AMDOPH are perfectly conservative tracer, which is, even though they are largely persistent, not correct. In order to reduce the effect of degradation, the concentrations of BEE203, close to the production wells, rather than the surface water concentrations were used. EDTA could also be use for calculations but its detection limit of 2 µg/l leads to even bigger uncertainties in the numbers.

According to the calculations, well 3 abstracts a total of 57 % BF, while well 4 only abstracts 30 %. Because Carbamazepine was always below the detection limit in well 4, the calculated percentage of young BF in well 4 is 0, compared to 23 % in well 3. However, this may be a slight underestimation due to the confining detection limit. Using anthropogenic Gd (Figure 77c, data from 2003) instead of Carbamazepine for the calculation of the proportion of young bank filtrate yields a proportion of young BF of 15 % in well 3 (Gd_{anth}= 10 ng/l) and 4.5 % in well 4 (Gd_{anth}= 10 ng/l). Again, this assumes that anthropogenic Gd is a conservative tracer which is not the case. Knappe (in prep.) could show that it is subject to very slow biological

degradation. However, using BEE203 instead of the surface water concentration for the mixing calculation diminishes the error associated to the degradation. Since the exact travel time from BEE203 to the well is unknown, degradation cannot be included in the caclulation. Therefore, the mixing proportion may be underestimated and the real proportion of young BF slightly higher.

Hinspeter (2002) used EDTA and anthropogenic Gd to calculate the monthly proportion of BF in well 4, which resulted in 10.3 $\pm$ 6.6 % and 3.6 $\pm$ 1.1 % respectively. With the new knowledge of the vertical stratification of Gd (Figure 77c), the first value (EDTA) is representative for the proportion of total BF, while the latter (Gd) for the proportion of young BF only, which explains the difference between the values.

The lack of any seasonality in the production wells at Wannsee can therefore be explained with the low proportion of young bank filtrate. However uncertain and approximate, the calculations give an idea on the mixing proportions in the production wells themselves. Using minor water components such as anthropogenic Gd and AMDOPH has the advantage that young (i.e. < 1 year) and old (i.e. <<1 year) proportions of bank filtrate can be differentiated. While well 4 abstracts only a few percent of young BF, it does abstract a considerable proportion of older BF. In general, well 3 has a rather high (> 50%) proportion of BF in total, while well 4 has a rather low percentage of total BF, caused by the (incomplete) sealing of the uppermost filter screen.
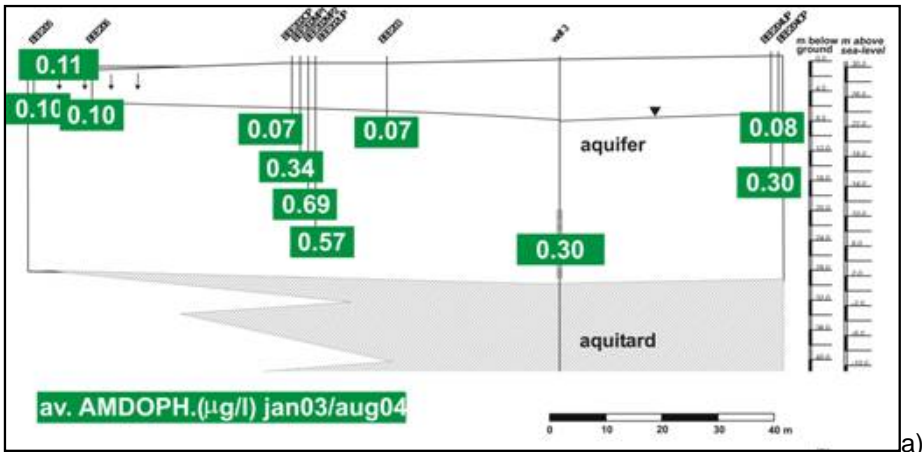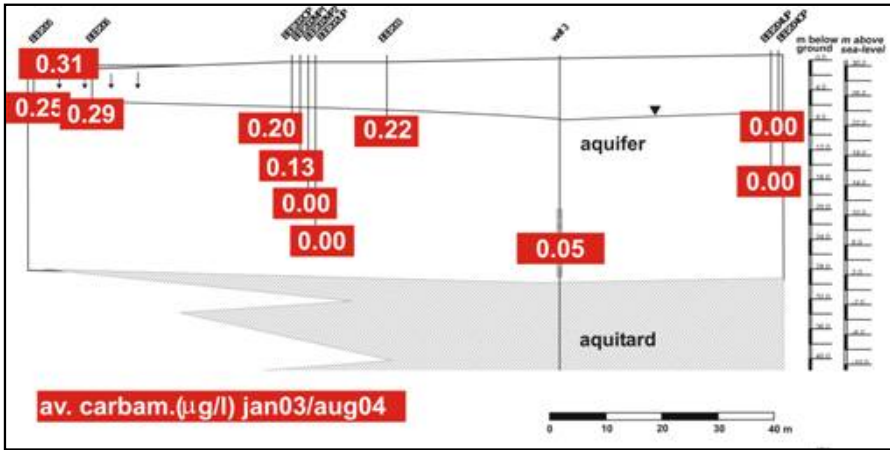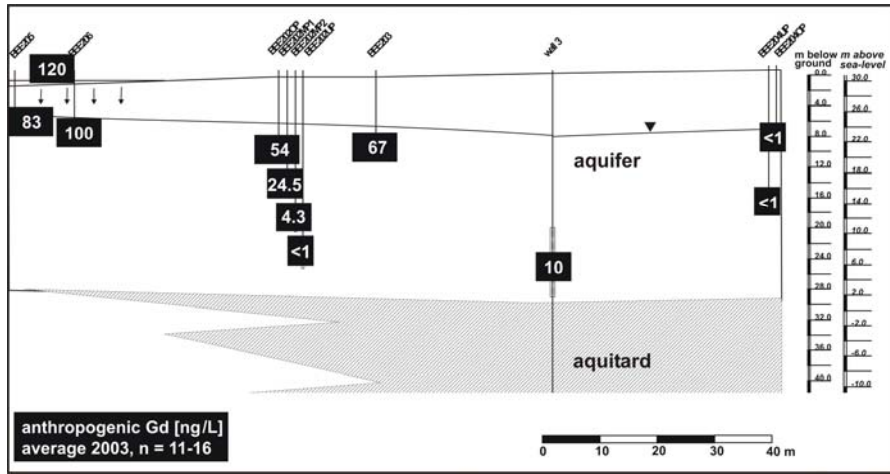
Figure 77: Average AMDOPH (µg/L), Carbamazepine (µg/L) and Gd (pmol/L) concentrations in observation wells of transect Wannsee 2. Production well 3 has filter screens in the deeper aquifers too. AMDOPH and Carbamazepine concentrations from January 2003-August 2004 (Data source: BWB) Anthropogenic Gd concentration from January 2003-December3003 (Knappe, in prep).

The scatter plot of δD versus δ^{18}O in surface water, production wells, deeper groundwater and background groundwater inland of the wells illustrates that well 4 has the lowest and well 3 the highest proportion of bank filtrate. It also shows that the isotopic signature is comparatively similar in the observation wells inland and those in deeper aquifers.
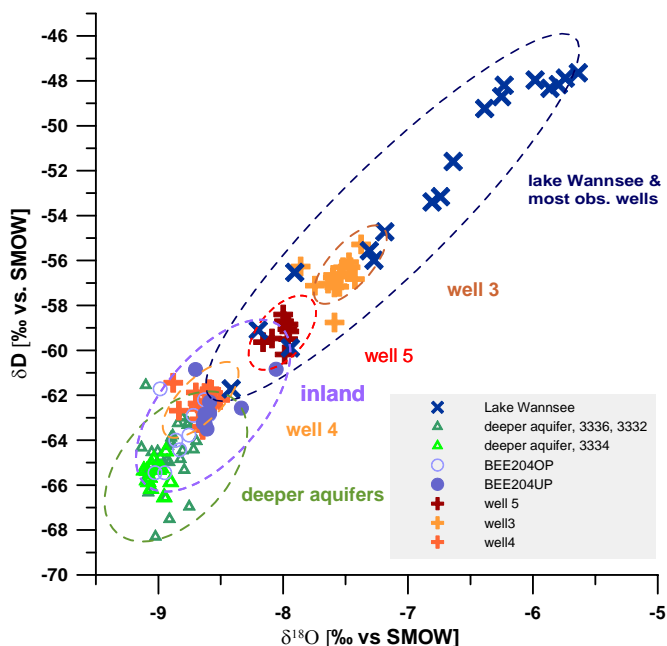
Figure 78: δD versus δ^{18}O in surface water, background and deeper groundwater and abstracted water in Wannsee. Deeper aquifers: Data 10/2000 –11/2001 (Hinspeter, 2002); remaining samples from May 2002-October 2003, data source: AWI.

The elevated concentrations of wastewater indicators and more positive isotopic signatures give evidence that since autumn 2003, the groundwater observation wells inland of the production wells have been under surface water influence (Figure 79). This could be due to the catchment area of well 3 seasonally reaching Lake Schlachtensee as illustrated in the hydraulic model. The model also suggested that due to the low abstraction of well 4 in the upper aquifer and local bulges in the Holstein aquitard, bank filtrate from Lake Wannsee can reach well 3 from inland.
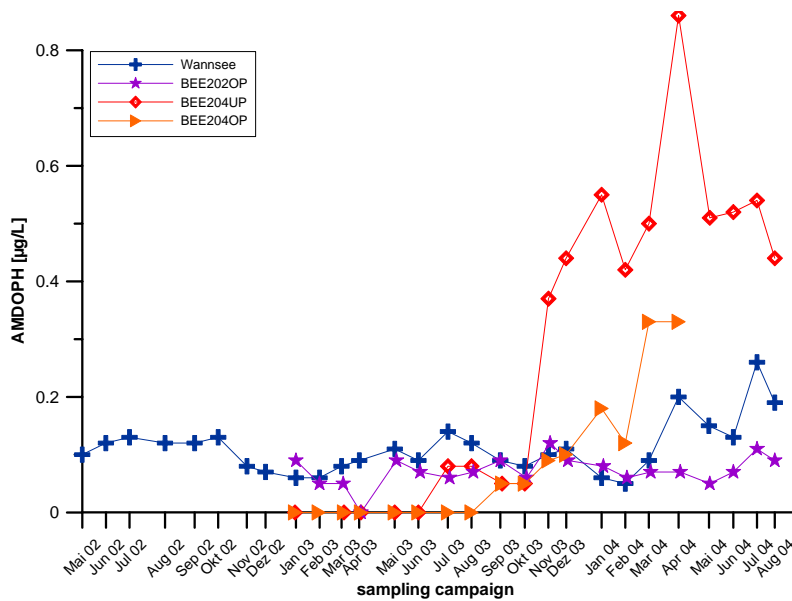
Figure 79: Time-series of AMDOPH in surface water, bank filtrate and groundwater inland (BEE202UP & OP) in Wannsee (Data source: BWB).

2.6 Hydrochemistry at the transect

2.6.1 Redox processes during bank filtration

As at transect Tegel, redox changes during infiltration are of particular importance, since they cause the appearance of the undesired metals Fe^{2+} and Mn^{2+} (Bourg and Bertin, 1993), influence the behavior of a number of organic pollutants such as pharmaceutically active substances (Holm et al., 1995), halogenated organic compounds (Bouwer and McCarthy, 1993; Grünheid et al., 2004) and effect the pH and calcite solution capacity (Richters et al, 2004).

Rather than concentrating on the Eh, redox zones may be characterised by the disappearance of reactants (oxygen, nitrate, sulphate) or the appearance of reactants (iron, manganese) as suggested by Champ et al. (1979). Boxplots of redox indicators in Figure 80 give a first idea on the redox conditions. While the shallower (younger) wells contain oxygen and nitrate throughout most of the year, the deeper observation wells are free of these but contain manganese (Mn^{2+}), iron (Fe^{2+}) and often ammonia (NH_4^+).
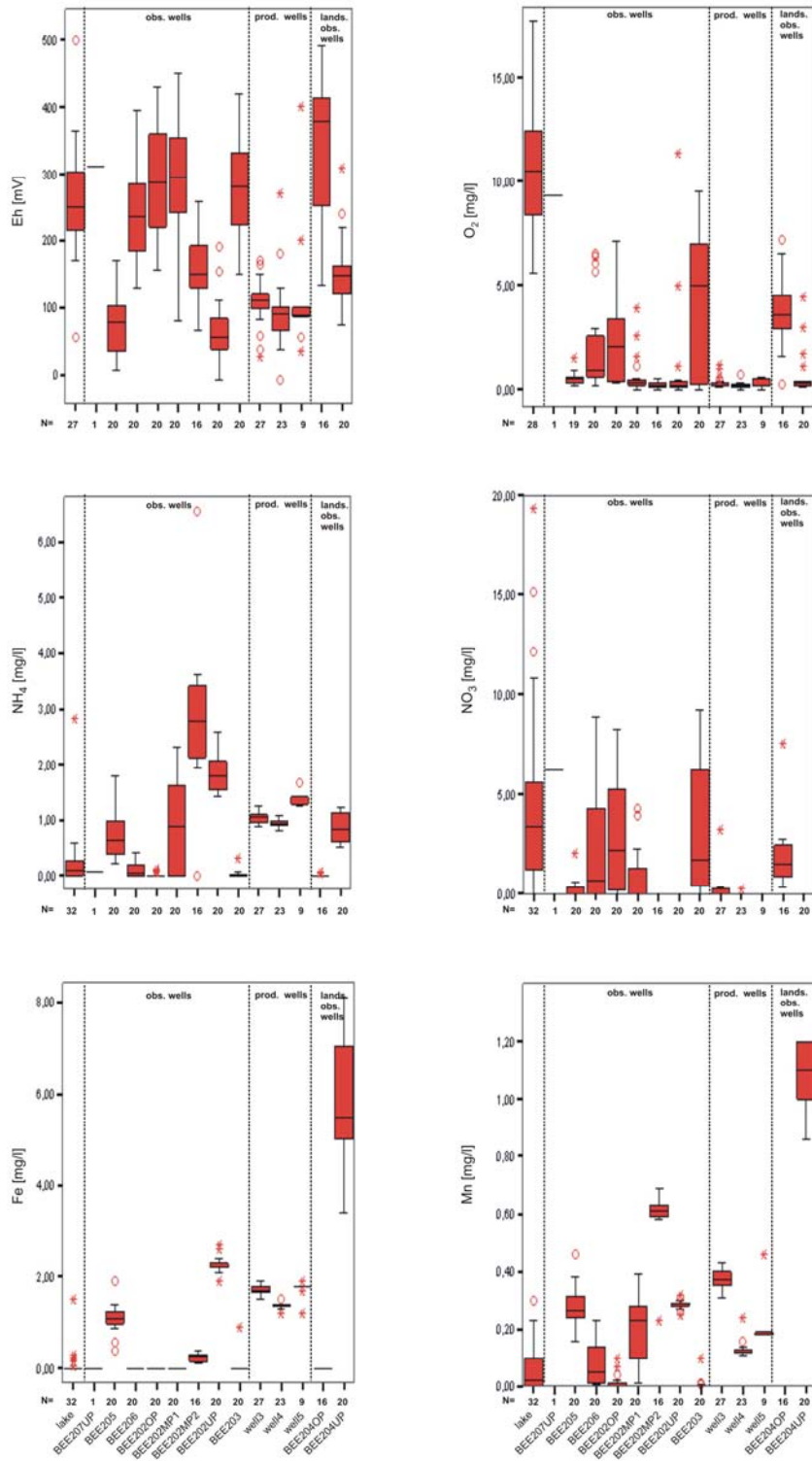
Figure 80: Boxplots of redox indicators at the transect Lake Wannsee 2 (May 2002-August 2004).

The two observation wells below the lake are quite different from each other with respect to their hydrochemistry. While BEE206 closer to the shore is still aerobic, BEE205 is mostly oxygen and nitrate-free which is likely to be due to the higher amount of organic carbon and lower hydraulic conductivities (chapter 2.2) which results in longer travel times and more reducing conditions at BEE205 in comparison to BEE206.

Figure 81 indicates the approximate redox zoning as indicated by the presence (or absence) of redox indicators given in Figure 80. The vertical redox zoning may be a result of the different groundwater ages. However, it may also be caused by re-oxidation of more reducing bank filtrate by oxygen penetrating though the permeable unsaturated zone, possibly enhanced by the water-level fluctuations caused by the irregular pumping regime (compare chapter 2.7). Bourg and Bertin (1993) investigated biogeochemical changes during bank filtration at the Lot River. They observed a similar reduced anaerobic zone close to the river followed by aerobic conditions further along flow direction. They concluded that the observed redox processes were reversible and oxidation caused by aeration through the permeable unsaturated zone close to the river. Similar to our findings, Richters et al. (2004) describe a vertical redox zonation at a bank filtration site near the River Rhein.

The deeper aquifers (not shown in Figure 81) are sulfidic (Figure 75) and do not contain oxygen, nitrate and only little sulfate.
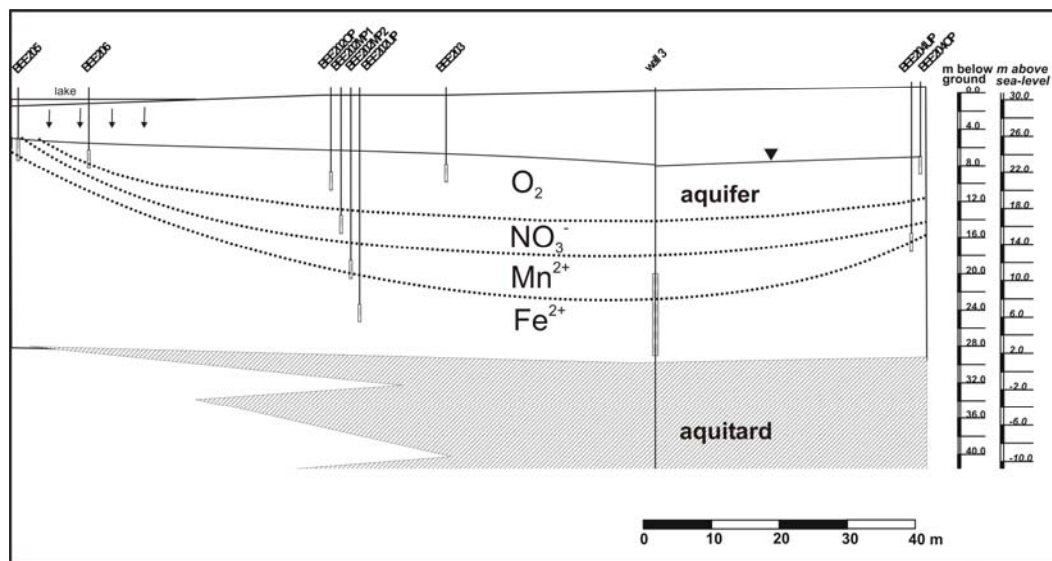
Figure 81: Approximate redox zoning as indicated by O$_2$, NO$_3$, Mn and Fe presence.

However, these zones (Figure 81) are not immobile and redox boundaries move seasonally (Figure 82). The younger bank filtrate undergoes strong seasonal temperature changes of up to 25 °C, depending on the distance from the lake. Because redox processes are microbially catalysed, these changes lead to differences in microbial activity (e.g. David et al., 1997;

Prommer and Stuyfzand, 2005). As a result, oxygen and nitrate disappear at times when temperatures are highest which is in summer or autumn, depending on the respective time lag to the well. It is interesting to note that nitrate concentrations in the lake itself decrease to zero in summer, probably due to consumption by algae. The disappearance of nitrate in the observation wells therefore appears to reflect the input signal rather than a reduction in the aquifer itself (figure 3).
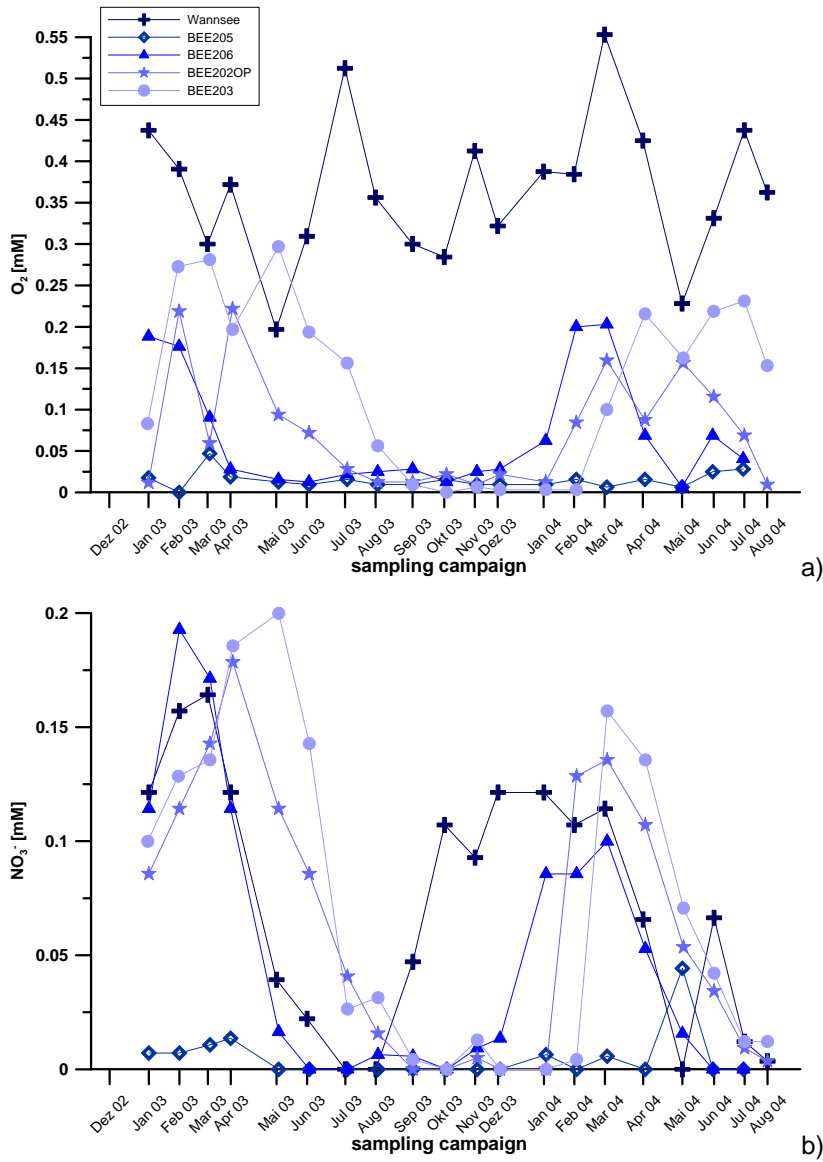
Figure 82: Seasonal variation of oxygen (a) and nitrate (b) in Lake Wannsee the shallow observation wells (data source: BWB).

2.6.2   *Hydrochemical conditions of inland groundwater/origin of sulfate*

As mentioned in chapter 2.5, the groundwater inland of the production wells strongly differs from the bank filtrate between observation wells and lake. In particular sulfate (SO_4^{2-}) but also Calcium (Ca^{2+}), Magnesium (Mg^{2+}), hydrogen carbonate (HCO_3^-) and carbon dioxide (CO_2) concentrations are higher than in the BF while the pH is lower (around 6.9 instead of 7.5). Boxplots of sulfate and calcium are shown in Figure 83.
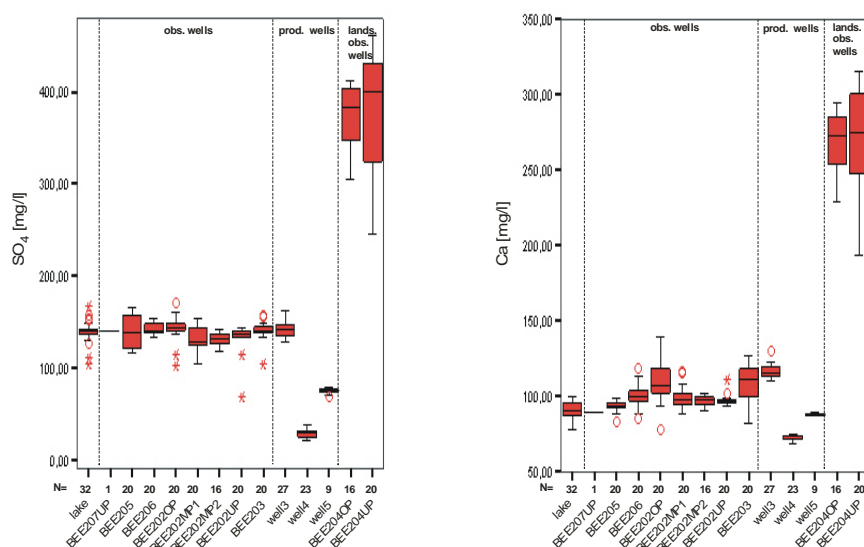
Figure 83: Boxplots for sulfate and calcium in transect 2 at Wannsee (Data source: BWB).

In particular the sulfate concentrations of almost 400 mg/l in average could potentially be problematic, since they exceed the drinking water limits. At present, they are unproblematic, because the groundwater is diluted by bank filtrate with a much lower sulfate concentration (chapter 2.5). The sulfate concentrations (and also Ca and Mg content) are explainable with:

1. gypsum resolution from war debris as often described for the shallow Berlin groundwater (Sommer von Jarmerstedt et al., 1998).

2. oxidation of finely distributed sulphides in the sediment due to the permanent fluctuations and lowering of the groundwater table induced by the pumping regime. Since the oxidation also releases acidity, this may also explain the lowered pH and the elevated calcium and alkalinity in the groundwater, which would be the result of dissolution of the calcite present in low contents in the sediment (Figure 66).

3. the influence of sewage farms formally present upstream of the catchment area of the well gallery.

Isotope analysis of ^{34}S and ^{18}O of sulfate was performed at the Institute of Mineralogy of the Technical University Bergakademie Freiberg. The results for transect 2 are shown in Figure 84 and Figure 85.
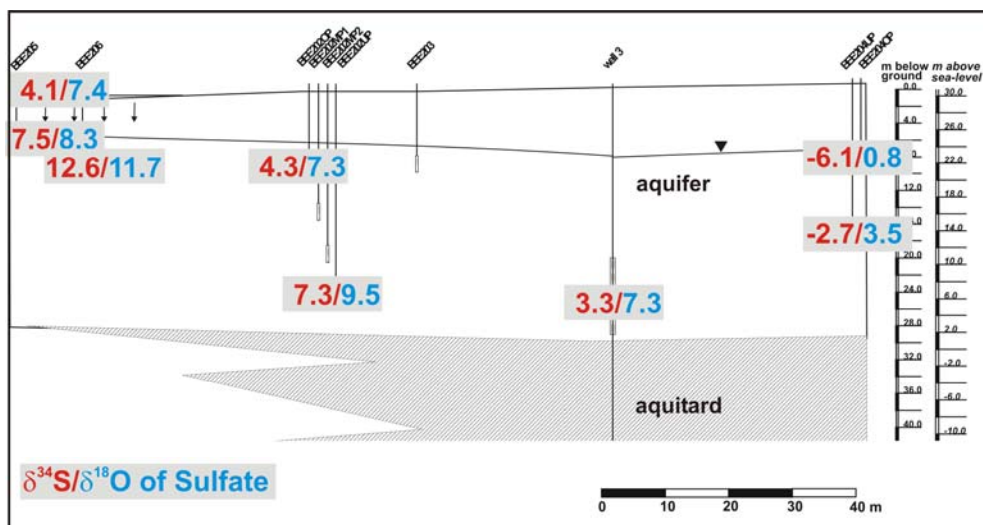
Figure 84: δ^{34}S (‰ vs. CDT) and δ^{18}O (‰ vs. V-SMOW) of sulfate at Wannsee 2 in March 2004, analysed at the Institute of Mineralogy of the Technical University Bergakademie Freiberg.

Because the isotopic signature of the observation wells inland is very low (negative values for δ^{34}S), an origin from gypsum dissolution can be excluded for the Wannsee site. Marine sulfate (which is where gypsum is most likely to originate from), has positive values around +10 - +35 ‰ CDT for δ^{34}S, depending on the geological time of formation (Clark and Fritz, 1997). Negative values like the ones observed are typical for biogenic pyrite or shales (Krouse, 1980). Hence, possibility 1, gypsum dissolution can be excluded. Possibility 2, pyrite oxidation triggered by the regular water-level fluctuations, is a possible explanation. Possibility 3, an influence of the sewage farms south-west of Berlin, can also not be exluded, in particular since the groundwater of the same shallow aquifer in Lankwitz (3756, Figure 85), in south-west Berlin revealed a similar sulfate concentration and isotopic signature, which cannot be explained by water-level fluctuations at the site. It is not possible to solve the question of the sulfate origin with the limited amount of data within this project. If water table oscillations were the cause for the elevated sulfate concentrations, optimisation of the pumping regime could, at least, reduce the sulfate input.

119
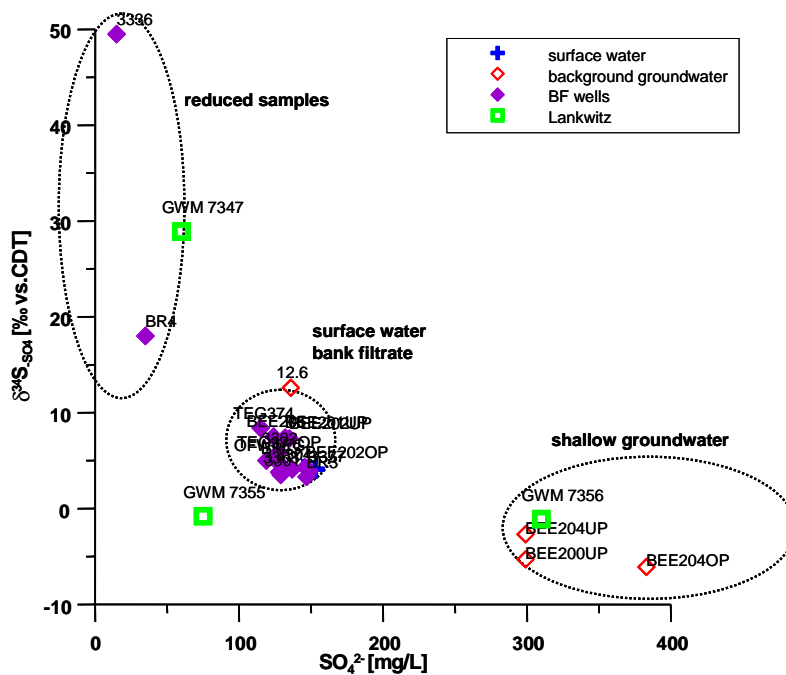
Figure 85: $\delta^{34}S$ (‰ vs. CDT) versus sulfate concentrations (mg/l) at Wannsee and Lankwitz in March 2004, analysed at the Institute of Mineralogy of the Technical University Bergakademie Freiberg.

2.7 Input of oxygen into groundwater during bank filtration

2.7.1 Introduction

As discussed in chapter 2.6.1, the redox conditions, in particular the amount of oxygen in the groundwater used for the drinking water supply is a crucial factor for the drinking water quality as well as for the operating production wells. Microbial degradation of pharmaceuticals may depend strongly on redox conditions. Furthermore the durability of the production wells is decreasing considerably at the presence of oxygen, which leads to precipitation of trivalent iron- oxides and subsequent clogging. And thirdly, the elevated sulfate concentrations may be caused by the continuous input of oxygen (chapter 2.6.2). The different potential pathways of oxygen input into the aquifer are illustrated in Figure 86.
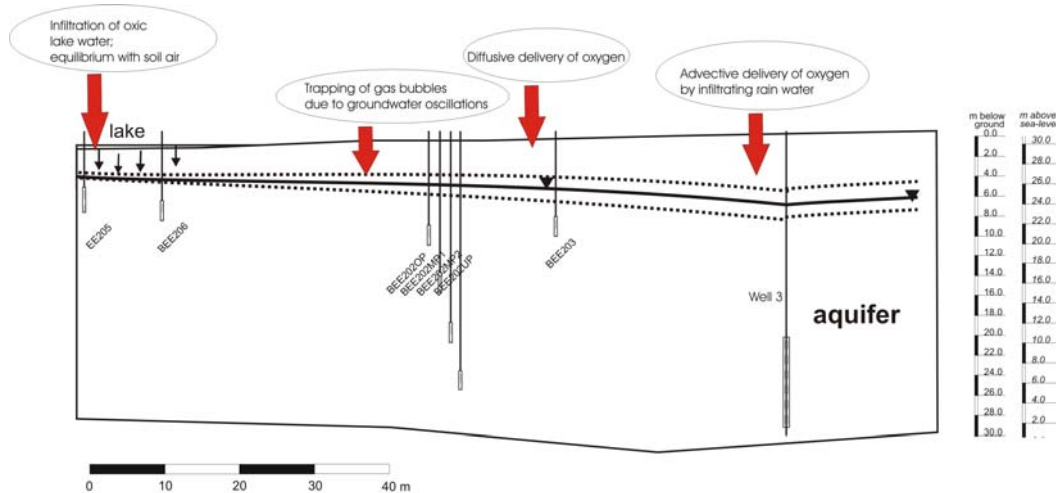
Figure 86: Sketch describing different sources of oxygen input into the groundwater during bank filtration exemplified for the Wannsee Transect 1.

Figure 86 shows four different mechanisms of oxygen input represented by the red arrows which are described in the following from the left to the right:

The first oxygen source is related to the infiltration of oxic lake water and the subsequent equilibration of seepage water with soil air of the unsaturated zone below the lake. According to the measured time series of oxygen at the observation wells (Figure 82) this mechanism works only during the cold period when microbial degradation is inhibited due to the low temperatures. This can be observed for example at BEE206, BEE204 OP and BEE203 (Figure 82). At BEE205, the colmation layer is thicker and shows a higher content of organics (Figure 54) which leads to oxygen consumption all over the year (Figure 81, Figure 82).

The second mechanism of oxygen input is related to the oscillations of the groundwater level due to the pumping regime of the production wells. Rising groundwater tables always lead to entrapped gas bubbles within the newly saturated zone of the sediment. Laboratory experiments with columns have shown that upward saturation of sediments may lead to volumetric entrapped air content up to 10% or more of the sediment bulk volume (Faybishenko, 1986). It was found that entrapped air can be divided in mobile bubbles of air and immobile entrapped air that is captured in pores and can be removed from the sediment only by dissolution leading to rising oxygen contents of the groundwater. Faybishenko (1995) found that with upward saturation the remaining volume of entrapped air was less than 5%, which corresponds to a sixth part of the pore space assuming a porosity of 30%.

The third way of oxygen input is caused by diffusive delivery of oxygen from soil air into the groundwater and the fourth mechanism considers the oxygen delivery by infiltrating rain water.

121

The seasonal character of the oxygen time series in the study area with low concentrations in summer and high concentrations in winter indicates that the oxygen input due to oxic bankfiltrate seems to be a major component in our system. But nevertheless more oxic conditions and vertical broadening of the oxic zone along the pathline of bankfiltrate towards the wells Figure 81) lead to the conclusion that other mechanisms also have to be taken into account. To get a deeper understanding of the processes which lead to elevated amounts of oxygen in the groundwater during bank filtration, rough estimates about the quantitative importance of the different mechanisms are described in the following. The calculations can be adapted easily to hydraulic and hydrogeochemical conditions at other locations.

2.7.2 Methods

Oxygen input by bankfiltrate:

The oxygen input below the lake into the groundwater was derived by measured oxygen concentrations in groundwater at offshore observation wells close to the shoreline. The redox conditions are related to the infiltration of oxic lake water, microbial mediated consumption of oxygen and the subsequent equilibration of seepage water with soil air of the unsaturated zone below the lake. The total mass input of oxygen was calculated by multiplying observed concentrations with the oxic volume according to

$$nO_2 = cO_2 \times L \times A$$

where nO_2 is the total amount of moles of oxygen, cO_2 is the measured oxygen concentration of groundwater below the lake, L is the vertical thickness of the oxic zone below the lake and A is the unit area of 1 m^2.

In the case of the Wannsee 1 the observation well BEE206 shows an oxic zone with an approximate vertical thickness of 2 m. Between 2002 and 2004, oxygen concentrations around 0.8 mg/l were measured in summer and 5 mg/l in winter, which is owing to reduced microbial activity in winter because of the low average temperature of about 4° C.

Diffusive oxygen delivery:

The diffusive delivery of oxygen was calculated using the analytical solution of the advection-diffusion equation from Ogata and Banks (1961) simplified for pure diffusion without advection:

$$c(x,t) = c_0 + \frac{c_{in} - c_0}{2} \, erfc\left(\frac{x}{2\sqrt{Dt}}\right)$$

where $c(x,t)$ is concentration as a function of space and time, c_0 stands for the initial concentration, D represents the effective diffusion coefficient corrected for porosity and tortuosity ($L^2\,t^{-1}$). The equation is valid for the boundary condition

$$c(x = 0, t) = c_0$$

The molecular diffusion coefficient D_0 was corrected according to (Troeh et al., 1982) as follows:

$$D = \frac{D_0 \times \theta}{\tau^2}$$

with D_0 =molecular diffusion coefficient of oxygen in water ($L^2\,t^{-1}$), θ =porosity (-)and τ = tortuosity (-) which means the ratio of the actual path length over the direct path length.

The total amount of diffusive oxygen input into the groundwater during the entire travel time was calculated for a volume with cross-sectional unit area according to:

$$nO_2 = \sum_{i=1}^{m}\left(c_i \times dz\right)$$

where nO_2 is the total amount of moles, i and m are index variables which refer to different depths, dz is the vertical distance, c_i is the calculated oxygen concentration of groundwater at depth l.

Infiltrating rain water:

The calculation of the oxygen delivery by infiltrating rainwater is based on the assumption that 1 litre water contains 10 mg of oxygen considering an average annual groundwater recharge of the corresponding location.

$$nO_2 = cO_2 \times GWR \times t$$

where nO_2 is the total amount of moles entering during travel time in a unit area of 1 m^2, cO_2 is the oxygen concentration of rainwater, GWR is the annual water flux of recharge in litre per m^2 per year and t is the travel time.

Entrapped soil air:

The amount of oxygen in the groundwater related to trapped gas bubbles is calculated according to the ideal gas law:

$$nO_2 = \frac{\theta_{air} \times pO_2}{RT} \times \omega$$

where nO_2 is the number of moles oxygen, θ_{air} is the entrapped air volume within one oscillation, pO_2 means partial pressure of oxygen in soil air, R is the gas constant, T is the temperature in Kelvin and ω is the number of oscillations during travel time. The calculations are based on an average value of the oscillation amplitude which is applied for the entire transsect at the location.

Input data:

The defined input data for all scenarios is given in Table 6.

Table 6: Input data for the simulations and calculations. Unless stated otherwise, the data are based on compilations given in the CRC Handbook of Chemistry and Physics, adjusted as necessary to bank filtrate conditions of Berlin.

Parameter	Units	Value	Comments
D_0:	$cm^2 s^{-1}$	1E-05	Based on the diffusion of oxygen at infinite dilution.
.	(-)	1.57	ratio of the half periphery of an ideal shaped circular particle over its diameter,
c_0:	mg/l	summer: 0.2: winter: 5:	averaged value derived by measured oxygen concentrations at observation wells showing oxic conditions below the lake
c_{in}:	mg/l	10	We assumed oxic concentrations of 10 mg/l at the groundwater surface which is in contact with soil air
θ_{air}	(-)	0.025	entrapped air volume with relation to the bulk sediment volume estimated according to Faybishenko (1995)
θ	(-)	0.2	Porosity estimated based on representative sediment analysis in study area
R:	$J\,K^{-1}$	8.31	gas constant
T	K	285	average annual temperature
pO_2	(-)	0.1	Estimated value for partial pressure of oxygen representative for soil air
GWR	mm/a	100	groundwater recharge

Scenarios:

Calculations have been performed for the conditions documented in Table 7:

Table 7: Scenarios for the calculation of oxygen input into the groundwater from different sources

	scenario A1	scenario A2	scenario A3
oscillation amplitude (m)	0.5	2	5
oscillation frequency	daily	daily	daily
traveltime (month)	3	3	3
	secanario B1	**secanario B2**	**secanario B3**
oscillation amplitude (m)	2	2	2
oscillation frequency	daily	weekly	monthly
traveltime (month)	3	3	3
	secanario C1	**secanario C2**	**secanario C3**
oscillation amplitude (m)	2	2	2
oscillation frequency	daily	daily	daily
traveltime (month)	1	3	6

Limitations and simplifications of the calculations:

The above described methods for the calculations were carried out based on the following simplifications:

- These calculations represent a one dimensional flow path for the upper oxic zone of the aquifer.

- The oscillation amplitude is constant over the entire pathway of the bank filtrate towards the well.

- The observed concentrations of oxygen below the lake are representative for the entire oxic profile below the lake

- The partial pressure of oxygen in soil air is constant in time and does not show seasonal variations.

- Constant temperature of 285 K is used in gas law.

- The different mechanisms are not correlated, i.e. an increasing oscillation frequency does not change the travel time etc.

2.7.3 Results

The contributions of oxygen calculated for the different sources are illustrated in Figure 87.
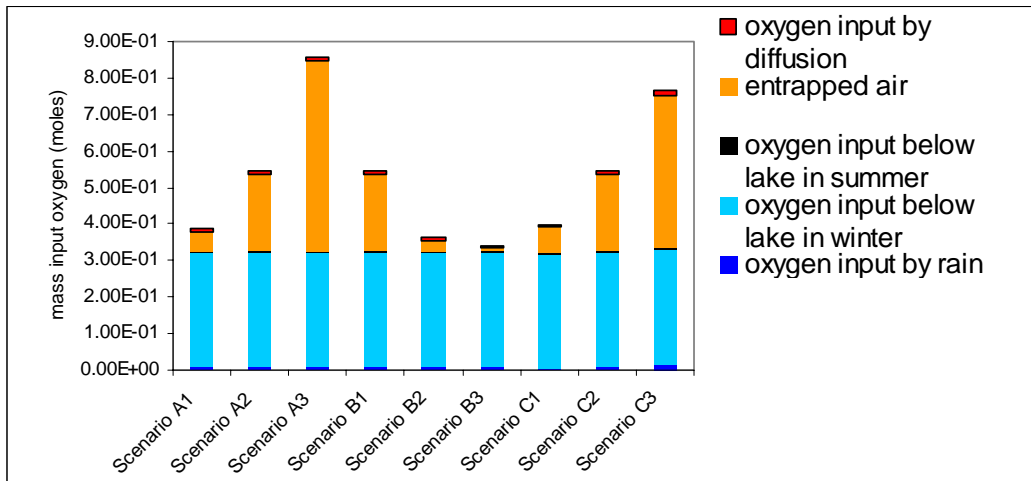
Figure 87: Estimated input of oxygen into the groundwater originated by different mechanisms

Due to the simplifications which have been specified for these rough estimates, the quantitative results obtained from this study can be interpreted in a relative and qualitative sense only. The calculations are representative for a one dimensional flow path only and can not be applied directly to a three-dimensional flow field of a production well. Therefore the results are not feasible for predicting and interpreting concentrations observed at the production wells itself, which shows only a certain amount of water originating from young bank filtrate. However, some important results have emerged from this study, which are enumerated in the following points:

1. Bank filtrate during winter and entrapped soil air due to oscillations constitute the major sources of oxygen in the hydrogeochemical system of the study area. Sources of oxygen input by percolating rain water and by diffusive delivery of oxygen in the gas phase are negligible.

2. Conditions of daily oscillations of 5 m and travel times about 6 month may lead to oxygen input by entrapped soil air comparable with the oxygen source due to bank filtrate in winter.

3. Due to the importance of water oscillations for the oxic conditions in our system the operational mode of the production wells can be used to control oxic conditions in the aquifer in order to optimize drinking water quality and durability of production wells.

2.8 Major conclusions and summary Lake Wannsee site

2.8.1 Surface water

- The surface water quality and conditions varies strongly within Lake Wannsee and also with time, in particular close to the transects. The sample taken each month in front of transect 1 is not sufficient to cover temporal and spatial variations in front of the transect.

2.8.2 Clogging layer / Infiltration zone

- The mapping showed that the geochemical and hydraulic conditions are highly variable over small distances.

- The sediments deposited in 0 to 7 meters water depth consist of fine grained sand with increasing proportions of silt and clay and decreasing proportions of fine grained sand along with the water depth.

- The organic carbon content generally increases with distance from the shore and water depth, reaching levels of > 20 weight-% in the laccustrine sappropel.

- Impermeable laccustrine sappropel dominates in water depths below 7 meters.

- Oxygen is completely consumed in the uppermost few cm of the sediment recovered as an undisturbed column taken in 20 m distance from the shore (at the location of BEE205). The redox conditions reach Mn(IV)/Fe(III) reducing conditions within only a meter of flow, equivalent to the conditions observed in the groundwater well BEE205.

- Oxic bank filtration can therefore only take place at a narrow stripe of less than 20 m width.

2.8.3 Travel times/age

- A realistic travel time evaluation is only possible with the combination of T/He age dating with breakthrough curves of stable isotopes, boron, chloride and temperature.

- Like at Lake Tegel, the bank filtrate is strongly stratified with regard to the age distribution. The shallow young bank filtrate is only a few months old while the deeper bank filtrate (in the upper aquifer) is several years old.

- The travel times of the bank filtrate to the production wells vary between < 3 months in the fastest case to > 10 years in the deeper layers of the uppermost aquifer.

- For observation wells deeper than ~10 m, i.e. those deeper than the lake, the share of young BF (directly from the shore) decreases with depth.

127

- The travel times of the young BF, determinable by the travel breakthrough curves appear to show large differences between summer and winter.

2.8.4 Mixing

- At least 6 distinguishable types of water from 3 different aquifers mix in the production wells including young and old bank filtrate, high sulfate groundwater from inland, deeper groundwater from the *Elster* aquifer below the *Holstein* aquitard and very deep, slightly more saline groundwater from the *Elster* aquifer below the second (*Elster*) aquitard and very pristine groundwater is in the same aquifer but from inland.

- Young and old bank filtrate contain different concentrations of a number of minor water constituents, reflecting the surface water quality changes of the past few years.

- Well 3 abstracts at least 57 % of BF, out of which less than half are young BF, while well 4 abstracts much less BF (~30%), containing hardly any young BF.

2.8.5 Hydrochemistry

- The redox zones are vertically stratified and zones are broadening towards the production well.

- With increasing distance from the shore, the redox zones become narrower, due to higher organic carbon contents in the lake sediments and longer retention times. In 20 m shore distance, the redox conditions are already anoxic.

- In the shallow groundwater, the redox zones are seasonally variable and more reducing in summer, when the microbial activity is higher due to higher temperatures.

- Entrapped soil air due to water-level oscillations and, in winter, bank filtration are the main sources for oxygen input into the shallow aquifer.

- Gypsum dissolution as the cause of elevated sulfate concentrations in the shallow groundwater inland of the production wells can be excluded.

2.9   References

AG Boden,1996. Bodenkundliche Kartieranleitung, 4. Aufl., Nachd., 392 S., Hannover.

Beyerle, U., Aeschberg-Hertig, W., Hofer, M., Imboden, D. M., Baur, H. & Kipfer, R., 1999. Infiltration of river water to a shallow aquifer investigated with 3H/3He, noble gases and CFCs. J. of Hydr. 220, 169-185.

Bourg A.C.M. and Bertin C.,1993. Biogeochemical processes during the infiltration of river water into an alluvial aquifer. Environ. Sci. Technol. 27, 661-666

Bouwer, E. J. and McCarty, P. L. 1983. Transformations of halogenated organic compounds under denitrification conditions. Appl. Environ. Microbiol., 45(4), 1295–1299.

Champ D.R., Gulens J. and Jackson R.E., 1979. Oxidation-reduction sequences in ground water flow systems. Canadian Journal of Earth Sciences, 16, 12-23.

Clark, I.D. and Fritz, P., 1997. Environmental Isotopes in Hydrogeology. Lewis Publishers, Boca Raton, New York.

David M.B., Gentry L. G., Smith K. M. and Kovacic D. A. (1997). Carbon, Plant, and Temperature Control of Nitrate Removal from Wetland Mesocosms. Transactions of the Illinois State Academy of Science, 90(3 and 4), 103-112.

Faybishenko, B.A., 1986. Influence of entrapped air on soil permeability. Vod. Resur., 4: 48-60.

Faybishenko, B.A., 1995. Hydraulic behaviour of quasi saturated soils in the presence of entrapped air: Laboratory experiments. Water Resources Research, 31(10): 2421-2435.

Fritz, B., 2002. Untersuchungen zur Uferfiltration unter verschiedenen wasserwirtschaftlichen, hydrogeologischen und hydraulischen Bedingungen. Dissertation, Freie Universität Berlin, Berlin, 203 pp.

Fritz, B., Sievers, J., Eichhorn, S., Pekdeger, A., 2002. Geochemical and hydraulic investigations of river sediments in a bank filtration system. In: P.J. Dillon (Editor), 4th International symposium on

Hinspeter, S. 2002. Geochemisch – Isotopenhydrogeologische Untersuchungen zur Uferfiltration am Wasserwerk Beelitzhof – Wannsee. Diplomarbeit Freie Universität Berlin

Hiscock, K.M. and Grischek, T.: Attenuation of groundwater pollution by bank filtration. J. Hydrol. 266, 139-144 (2002).

Holm J.V., Rügge K., Bjerg P.L., Christensen T.H.1995. Occurrence and Distribution of Pharmaceutical Organic Compounds in the Groundwater Downgradient of a Landfill (Grindsted, Denmark). Environ. Sci. Technol. 29(5), 1415-1420.

Knappe, A., Hubberten, H.-W., Pekdeger, A., Dulski, P., Möller, P. 2002. A multi-tracer study on bank filtration processes in Berlin. In: Dillon, P. (Ed.): Management of Aquifer Recharge for Sustainability, Balkema, Adelaide, Australia, pp 239-244.

Knappe, A., in prep. Das Verhalten der Seltenerd-Elemente -insbesondere Gadolinium als Abwasserindikation- in Oberflächen- und Grundwässern. Ph.D. diss. Department of Earth Science, Free University of Berlin, Berlin.

Krouse, H.R., 1980. Sulphur isotopes in out environment. In: P.a.F. Fritz, J.CH. (Editor), Handbook of Environmental Isotope Geochemistry. The Terrestrial Environment. A. Elsevier, Amsterdam, pp. 435-471.

Langguth & Voigt, 2004. Hydrogeologische Methoden, Springer Verlag, D-Heidelberg

Massmann, G., Knappe, A., Pekdeger, A., Richter, D., 2004. Investigating the influence of treated sewage in ground- and surface water using wastewater indicators in Berlin, Germany. Acta Hydrochim. et Hydrobiol. 32 (4-5), 336-350.

Nogeitzig, A., 2005. Processes During Infiltration At The Water-Sediment Interface. Diplomarbeit Institut für Geologische Wissenschaften, Freie Universität Berlin (unpublished).

Ogata, A., 1970. Theory of dispersion in granular medium. U.S. Geol. Surv. Prof. Paper, 411(I)

Ogata, A. and Banks, R.B., 1961. A solution of the differential equation of longitudinal dispersion in porous media, US Geological Survey.

Prommer, H., and Stuyfzand, P. J., 2005. Identification of temperature-dependent water quality changes during a deep well injection experiment in a pyritic aquifer, Environ. Sci. and Technol., 39(7): 2200-2209.

Richter, D. 2003. Untersuchung des Gewässersystems von Spree und Havel im Berliner Westen mit Hilfe verschiedener Tracer. Diplomarbeit Freie Universität Berlin.

Richters L., Eckert P., Teermann I., Irmscher R. (2004). Untersuchung zur Entwicklung des pH-Wertes bei der Uferpassage in einem Wasserwerk am Rhein. *Wasser Abwasser* **145**(9), 640-645.

Schumacher, Skripalle, 1999. Arge Uferfiltration Detailbericht 1: Ermittlung der Uferfiltratanteile über die Abflussverhältnisse sowie die Durchflussaufteilung und Abwasseranteile im Berliner Gewässersystem bei Niedrigwasser für verschiedene Ableitungsvarianten der Klärwerke.- Abschlußbericht Uferfiltration Berlin: S 31

Sommer-von Jarmersted, C., Kösters, E. & Pekdeger, A., 1998. Die Sulfat- und Chloridgehalte des Berliner Grundwassers.- Terra nostra 98/3: V341 - V342, Alfred- Wegener-Stiftung, Köln

Stute, M., Deák, J., Révész, K., Böhlke, J. K., Deseö, É., Weppernig, R. & Schlosser, P., 1997. Tritium /3He Dating of River Infiltration: An Example from the Danube in the Szigetköz Area, Hungary. Ground Water 35(5), 905-911.

Sültenfuß, J. & Massmann, G., 2004. Datierung mit der [3]He-Tritium Methode am Beispiel der Uferfiltration im Oderbruch. Grundwasser, 9(4): 221-234.

Tolstikhin, I. N. & Kamenskiy, I. L., 1969. Determination of groundwater ages by the T-[3]He method. Geochemistry International 6, 810-811.

3   RESULTS ARTIFICIAL RECHARGE POND TEGEL

The field site lies within the catchment area of Tegel water works, which belong to the Berlin Water Company (Berliner Wasserbetriebe, BWB). Near Lake Tegel, three ponds surrounded by over 40 production wells are used for groundwater replenishment (Figure 88); pond 3 is the subject of these investigations. The pond bottom is located approximately 3 m below ground (31 masl). A transect of groundwater observation wells screened in various depths was installed between pond 3 and production well 20 of the Saatwinkel production well gallery to study processes occurring during infiltration and passage to the production well (Figure 89). The filter screen of the production well 20 extends from 20-34 m below ground; the length of the observation well screens is restricted to 2 m, allowing a vertical differentiation of the groundwater.
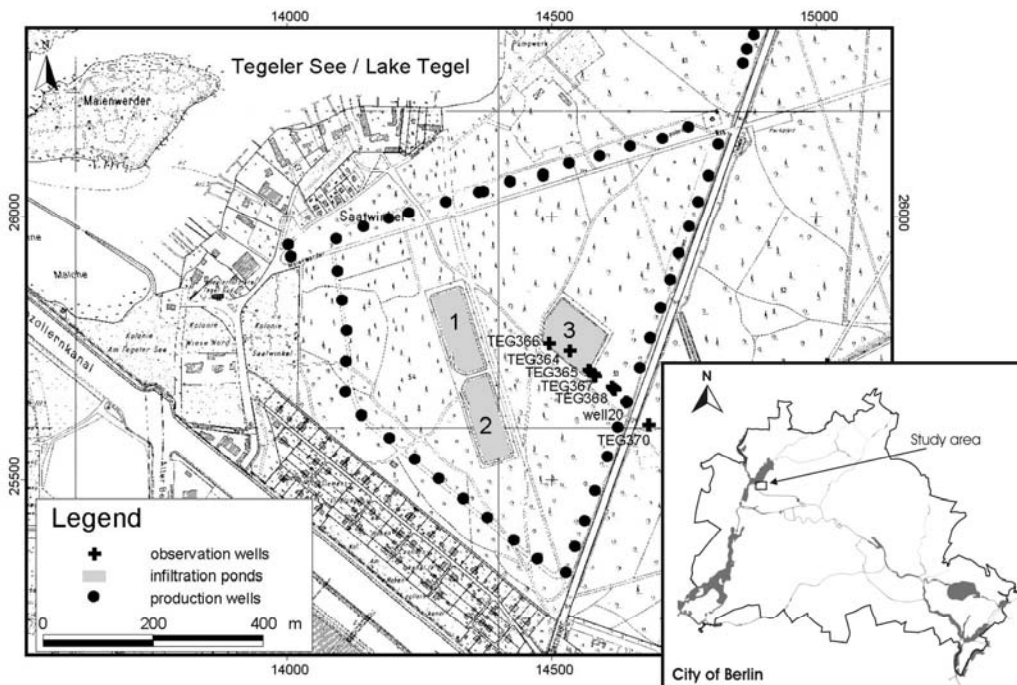
Figure 88: Recharge ponds 1, 2 and 3, production well triangle and transect at the artificial recharge site Tegel (Massmann et al., subm.)).
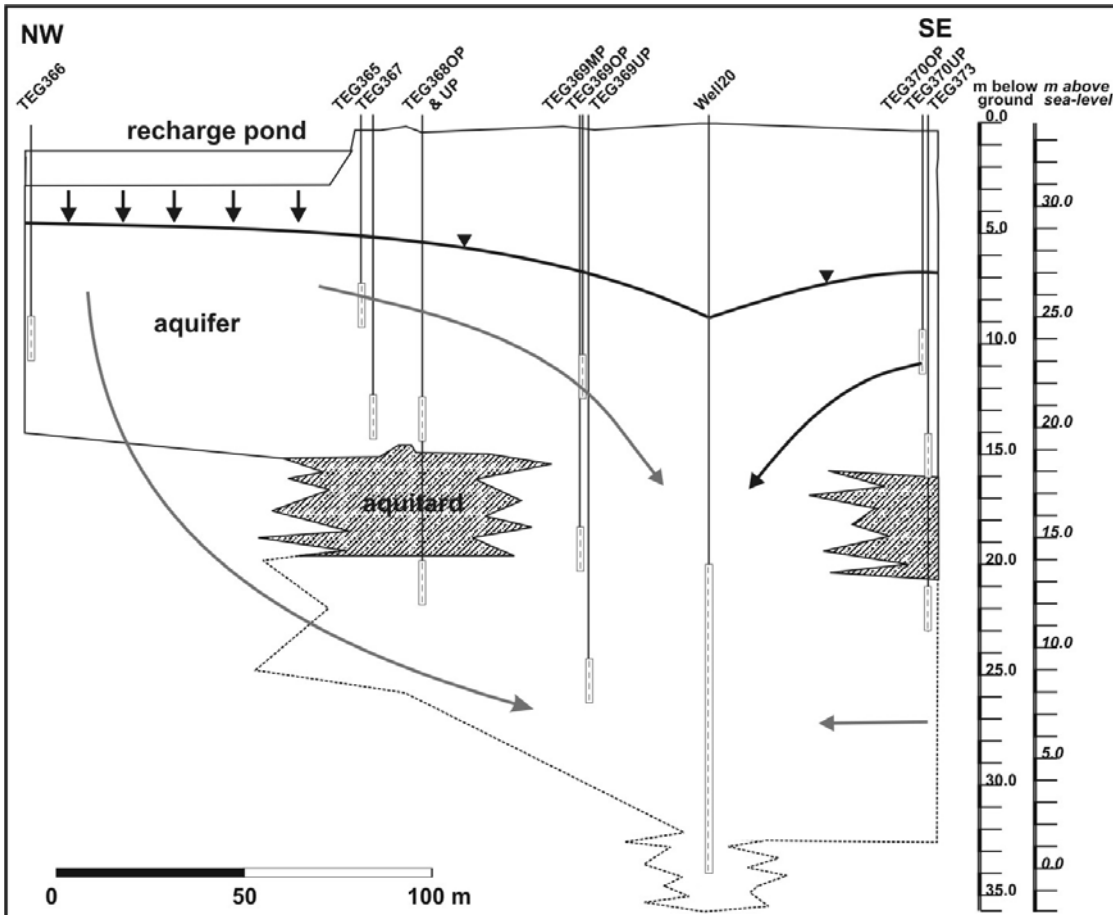
Figure 89: Schematic cross section of the transect between recharge pond 3 and production well 20 (Saatwinkel well gallery). Filter screens shown as dashed bars. The flow direction is indicated. The aquitard (glacial till) is not consistent and was not encountered below (parts of) the pond and at the location of the production well (Massmann et al., subm.)).

3.1 Pond operation/Hydraulic situation

Surface water of the adjacent Lake Tegel is pumped into the pond (pond area: 8700 m²) after passing through a microstrainer for pre-filtration. In 2002 (and 2003), 3.39 (4.79) million m³ of surface water were recharged via pond 3.

Figure 90: illustrates the principal operational cycle at the site, starting after the pond has been emptied and the pond bottom sands (the upper ~0.1 m) have been washed and cleaned of finer grained material and algae. The pond is refilled and the groundwater level below the pond rises owing to the infiltration of water, causing hydraulic conditions below the pond to change from unsaturated to fully saturated (reached when the groundwater-table is ~1 m or less below the pond, Figure 90, No. 1). The infiltration capacity is largest when saturated conditions prevail. With time, the pond bottom becomes increasingly more clogged un-

132

til, at some stage, the infiltration capacity decreases to such an extent that conditions below the pond become unsaturated again owing to decreasing groundwater levels (Figure 90, No. 2). As soon as this happens, the infiltration capacity decreases even more. The pond has to be redeveloped. During redevelopment, the pond bottom is exposed to the atmosphere (Figure 90, No. 3).
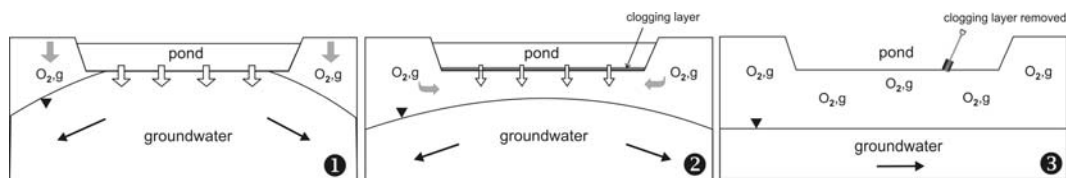
Figure 90: Schematic illustration of the operational cycles of the recharge pond. 1: The pond has been refilled and the conditions below the pond are fully saturated. 2: The infiltration rate decreases due to clogging of the pond base, leading to a drop of the groundwater mount and the development of an unsaturated zone below the pond. Oxygen can penetrate below the pond from the pond margins. 3: The pond is emptied for redevelopment (Massmann et al., subm.)).

Figure 91 shows the water-level of the pond (a) and groundwater well TEG364 below the pond (filter screen depth 5-7 m below pond base, b), the infiltration rate (c, equivalent to amount of water recharged divided by pond area) and oxygen concentration in the groundwater below the pond (d). During operation of the pond, the water level in the pond was kept more or less constant around 32.5 metres above sea-level (masl). The pond bottom level lies around 31 mNN (m above sea-level), but may vary slightly both spatially and temporarily due to the sediment cleaning procedures. The hydraulic conditions below the pond were highly transient; the groundwater-level fluctuated by almost 6 metres (Figure 91, b). The decline of the infiltration capacity with time due to clogging is clearly visible Figure 91, c). Clogging and the associated drop of the water-level and the infiltration capacity occurred more rapidly in summer, probably due to sudden algae growth. The decrease of the hydraulic conductivity of the pond bottom due to clogging has often been described in artificial recharge via ponded infiltration (Okubo and Matsumoto, 1983; Schuh, 1990; Bouwer, 2002).

Altogether, 9 cycles can be defined for the monitoring period (Figure 91). The intervals between redevelopments varied strongly. For example, in October 2002, the pond was in operation for only about a month. By contrast, from November 2002 till the end of March 2003, the pond was in operation for almost 4 months without being redeveloped. In addition, redevelopments were not always similarly efficient. In winter 2001/2002, for example, the infiltration capacities after two redevelopments did not come near those reached later (groundwater-level data does not exist for winter 2001/2002).
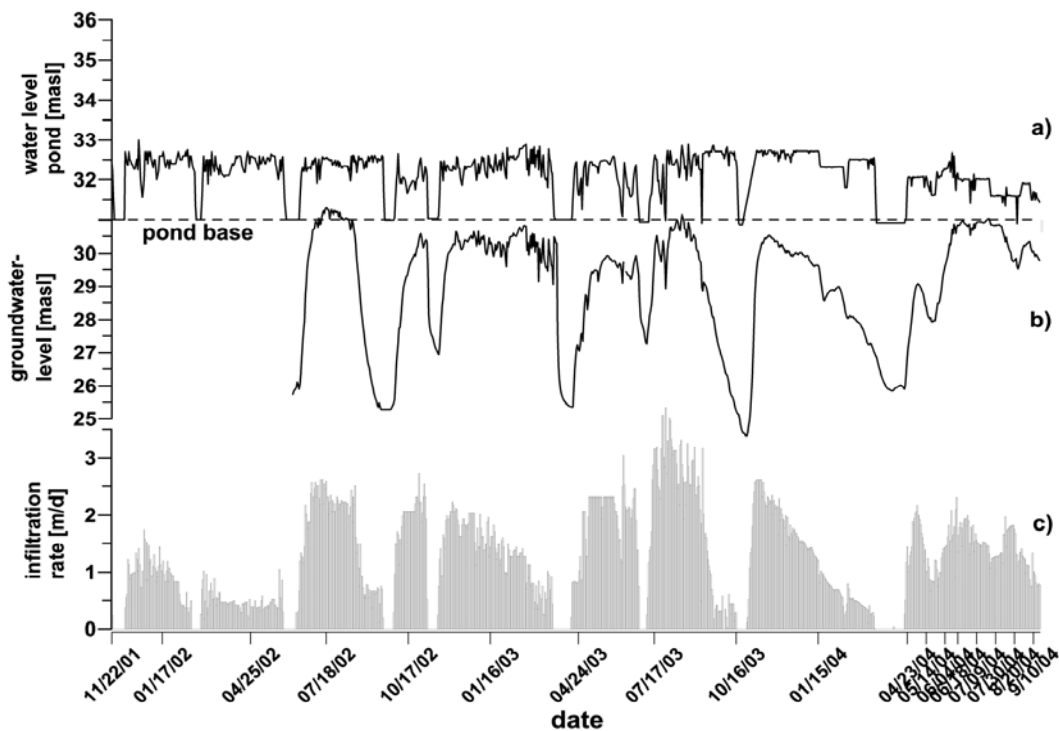
Figure 91: a) Water-level of the pond [masl] and b) groundwater below the pond (TEG364) [masl] and c) recharge rate [m/d]. The infiltration rate was provided by BWB.

Because of the groundwater elevation below the pond and the abstraction of water from production wells in the well triangle around the ponds (Figure 88), the groundwater flows concentrically away from the ponds to the production wells. The monitoring transect (Figure 88) is oriented in flow direction. But because the pumping performance of the wells is irregular, wells are not operating constantly and the 3 ponds are emptied at different times, individual flow paths may deviate slightly from the transect. Average travel times to individual wells of the transect can be estimated with the help of breakthrough curves of conservative tracers and a number of wastewater residues such as B or EDTA (Table 3, part 1 Tegel).

Figure 92 shows the water level of pond 3 and the groundwater in selected observation wells between pond and well 20 as well as of the production well and an inland observation well. The pond water-level was mostly around 32.5 masl, times where the pond was empty display a value of 31.0 masl. Towards the end of the project, around May 2004, the pond water-level was lowered to 32.0 masl. The data shows that like the groundwater-level below the pond (Figure 91b) as discussed above, the groundwater-level of the entire transect is governed by the pond operation and the infiltration and clogging dynamics. Lowest groundwater elevations are encountered when the pond is empty. Close to the pond, the water-level fluctuates up to 6 m. Even at TEG369UP, closest to the production well, the groundwater-level still varies up to 5 m, depending on the infiltration dynamics. Towards the production well, the

134

groundwater-level declines gradually. When the pump is turned of, the groundwater level of the production well is similar to the level of TEG369UP. When turned on, it decreases about 3 m. Whenever the pump is turned of, the surrounding groundwater level responds and increases slightly, but relatively little compared to the changes caused by the pond cycling.
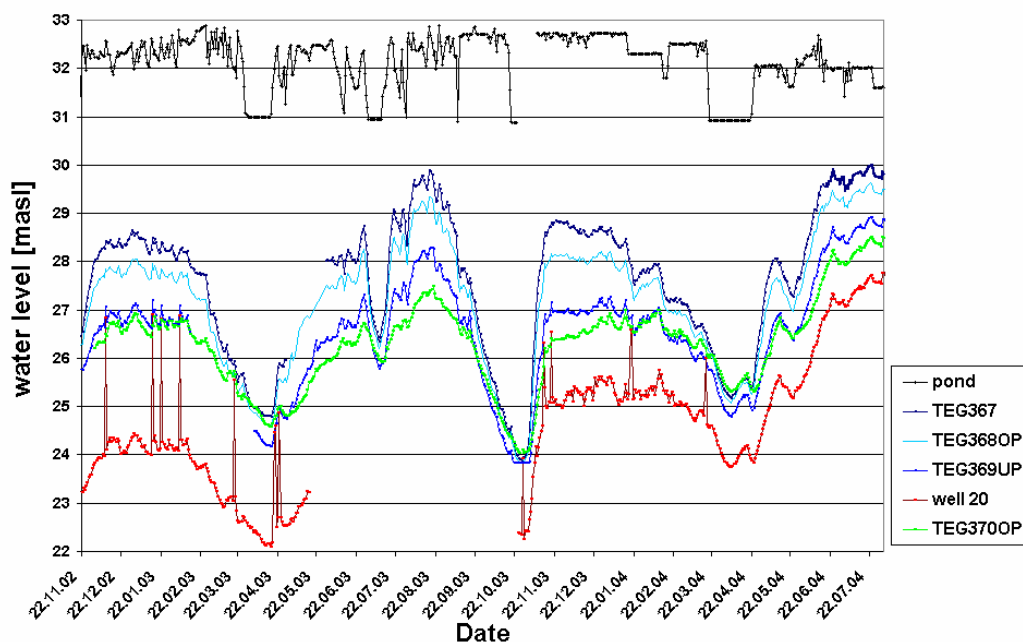
Figure 92: Daily measurements of the pond level and the groundwater-level from data logger in observation wells TEG367, TEG368OP, TEG369UP, production well 20 and TEG370OP (inland).

3.2   Surface water investigations

The surface water in pond 3 is essentially Lake Tegel water which passes through a microstrainer before it enters the pond. The intake of the pond water is in the southern part of Lake Tegel, which itself receives treated WW via the Nordgraben ditch from the WWTP Schönerlinde, in the north of Berlin (*compare chapter 3.1, part 1*). Like Lake Tegel, the pond contains a variable amount of treated WW.

The pH of the pond water varied from 7.5 to 9.1 but was usually around 8. The pond water was always saturated with oxygen, which is why the Eh was high ($\varnothing$ 365 $\pm$ 85 mV). The NO_3^- concentrations in the lake showed a strong seasonality with the highest concentration in winter and lower concentrations in summer, probably due to algae consumption in the pond. Similar changes of total inorganic N have been observed in a recharge pond by Haeffner et al., (1998). A summary of the average surface water composition is given in Table 8. Because the pond water contains a proportion of treated effluent from the WWTP Schönerlinde, a number of WW residues were detectable, such as AOX (Grünheid et al., 2005), B and EDTA a number of PhACs (Massmann et al., 2004). The sulfate concentration was also ele-

vated, because FeSO₄ is added in the surface water treatment plant of Lake Tegel. The concentration of dissolved organic carbon (DOC) was relatively low. The pond water is oversaturated with regard to calcite (Greskowiak et al., 2005).

Table 8: Average pond water composition and standard deviation from November 2001 to September 2005.

Parameter	Average concentration and standard deviation
pH	8.0
Redox potential, Eh	365 ± 85 mV
O_2	0.34 ± 0.09 mmol/L
Electrical conductivity, EC	686 ± 57 µS/cm
Ca^{2+}	2.09 ± 0.19 mmol/L
Na^+	1.71 ± 0.39 mmol/L
Mg^{2+}	0.40 ± 0.06 mmol/L
K^+	0.24 ± 0.06 mmol/L
HCO_3^-	2.85 ± 0.22 mmol/L
Cl^-	1.43 ± 0.28 mmol/L
SO_4^{2-}	1.22 ± 0.20 mmol/L
NO_3^-	0.16 ± 0.05 mmol/L
DOC	0.61 ± 0.06 mmol/L

In general, the concentration of most tracer, including some WW residues in Berlin tends to show some seasonality, with higher concentrations in summer and lower concentrations in winter due to higher natural discharge (and consequent dilution of the treated WW) in winter (Massmann et al. 2004). In Lake Tegel, the situation is somewhat more complicated because a pipeline pumps river Havel water into the northern end of the lake (mainly in summer) to improve the water quality (*compare chapter 3.1, part 1)*. In addition, the total discharge of the WWTP Schönerlinde increased strongly at the end of 2002 (it approximately doubled). Therefore, similar to Lake Tegel itself, a seasonal influence is not visible for any WW residues (Figure 93) and the increase of WW residues including several PhACs in the second sampling half may have been associated to the increase in the proportion of treated WW in the samples due to the increased discharge of treated WW into Lake Tegel. This did, however, not influence the behaviour of the stable isotopes, which display the classic pattern of more negative values in winter and less negative values in summer (Figure 93).
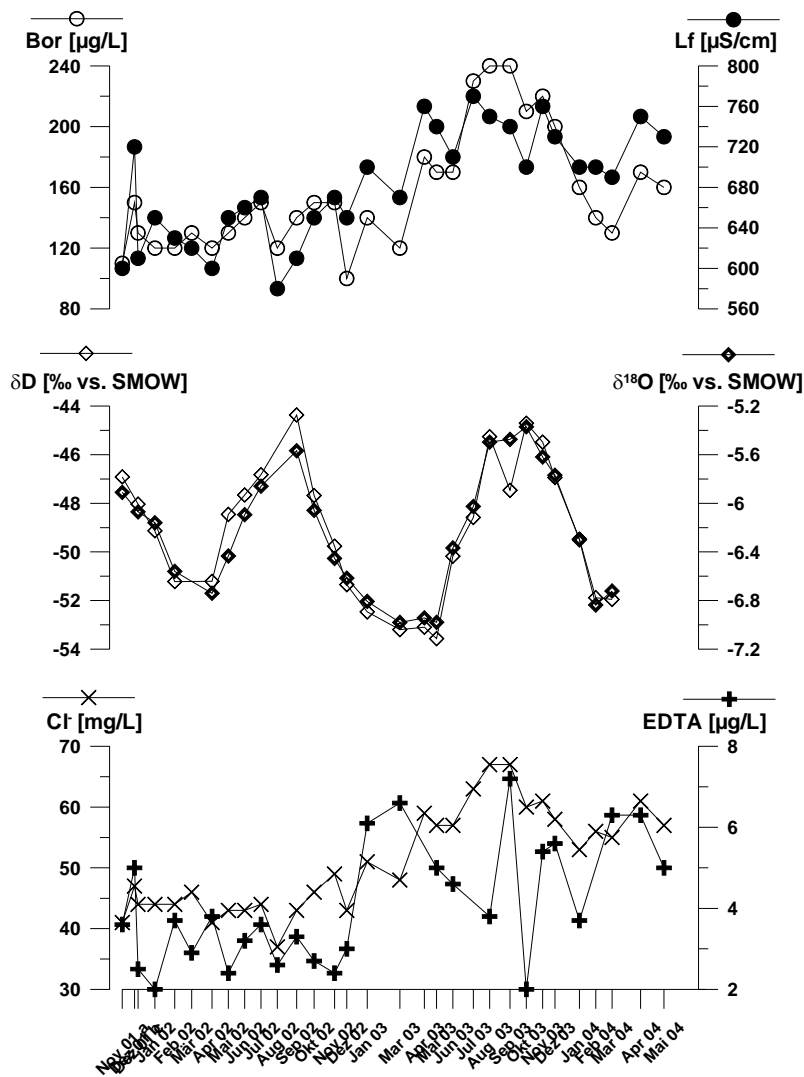
Figure 93: Boron, electric conductivity, $\delta^{18}O$, δD, chloride and EDTA concentration in the pond water (data source: BWB & AWI).

3.3 Clogging layer

Generally, the water infiltrating into the aquifer below the recharge pond has to pass through a sediment zone where, over long periods of time, unsaturated conditions prevail. Because the pond level is kept constant at all times, the amount of water infiltrating into the aquifer is mainly a function of the hydraulic conductivity of the clogging layer at the bottom of the pond. During redevelopments, the pond is emptied and the upper sediment layers are scraped of and cleaned to restore the infiltration capacity. Samples from the upper 0.48 m were taken and sieved before and after washing treatment (3 depths with 2 samples each). The hydraulic conductivities increase considerably (by a factor of ~ 2-10, depending on the individual

137

sample) after washing.
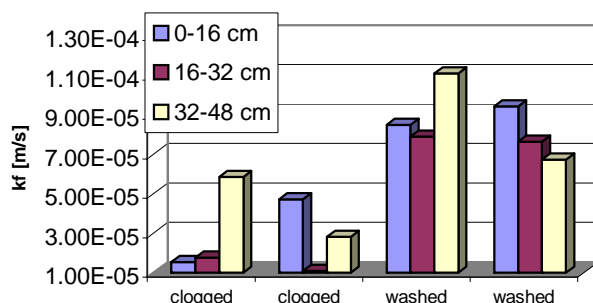
Figure 94: Hydraulic conductivities (k$_f$) of 6 samples (3 depths, 2 parallel samples each) of the clogged sands and of the same sands after cleaning treatment (data source: FU Berlin).

3.4 Aquifer sediments

The porous sediments in the area are of Quaternary age. The lithological cross-section along the transect is shown in Figure 95. The sediments encountered are mainly glacio-fluvial sands with varying proportions of fine, medium and coarse sand. The local aquitard, a glacial till of Saale age (local denotation qsWA), was not always encountered and contains interior holes. While it is present north-west and south-east of well 20 and in the adjacent production wells, it is absent near well 20. According to (Hannappel and Asbrand, 2002), the glacioflu-vial sediments above the till were deposited during the Saale (Warthe, qsWA) glacial period, while those below belong to the Saale (qs) only. The aquifer is underlain by an aquitard of the Holstein interglacial at less than 5 m below sea-level (Hannappel and Asbrand, 2002).
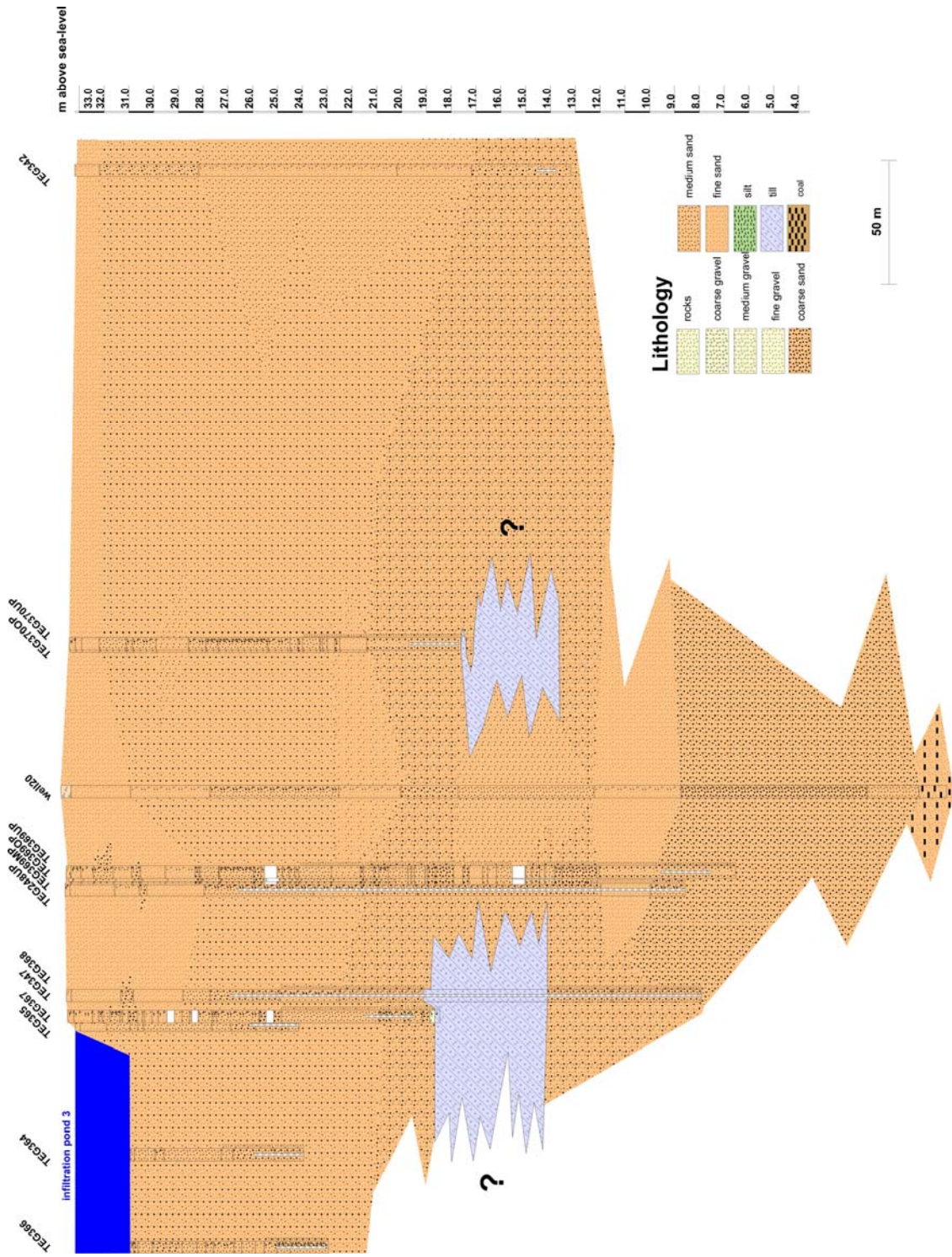
Figure 95: Lithological cross section of the transect at the AR site Tegel.

139

The extent and distribution of the Saale glacial till (qsWA//gm) was evaluated with statistical methods, because cross-sections only existed for the production well galleries and few was known about the presence of the till below the recharge ponds. Additional drilling data was made available by BWB. The till is rarely thinning out, it tends to be either present or not, usually with a thickness of a few meter. Because for the hydraulic and hydrochemical properties of the area, the presence, rather than the extent of the till, is of importance. The data was interpolated with the inverse distance method (5 m grid) using Surfer 7.02 (Golden Software, 2000) with the criteria present (1, green) or not present (0, red) only. The result is shown in Figure 96 and illustrates that the till, which was encountered in most cores in the north-east, is only present in a few patches in the south-west. The till is missing partly below the recharge ponds. Hence, the recharged water can infiltrate into the deeper aquifer parts and reach all production wells of the galleries Hohenzollernkanal and Saatwinkel, which have filter screens below the till.
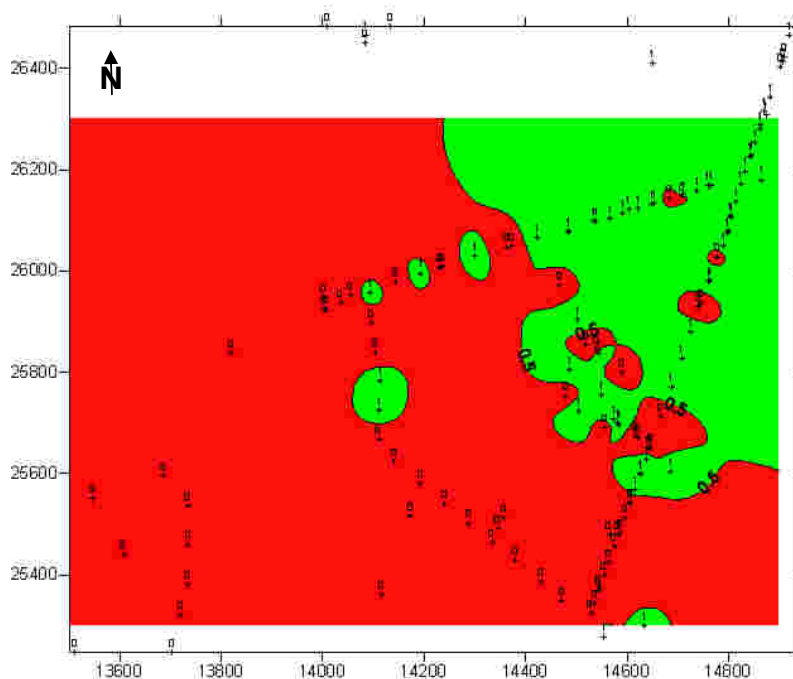
Figure 96: Glacial till distribution, inverse distance method (5 m Grid). 1= till present, 0 = no till. Areas where till is more likely to be present (>0.5) are shown green.

Two cores were taken at the site to get an idea on the major hydraulic and geochemical sediment properties. Results are illustrated for one core only (TEG369UP, Figure 89). The sands are fine to coarse grained with very little silt or clay. The k_f values derived from sieving are fairly similar in both cores and vary over one order of magnitude from 1.5E-04 to 1.1E-03

m/s (Figure 97). In both cores, the most striking differences in terms of the geochemical characteristics of the sediment are found between the unsaturated and saturated sediment zone (water-table depth: 6-9 m, depending on pond level). Carbonate (inorganic carbon) appears from a depth of around 6.4 m onwards (Figure 98). The organic carbon content is low with 0.02-0.16 weight % (Figure 98). With a few exceptions, the total iron content is 1-2 g/kg Fe (Figure 98). The share of reducible iron and manganese (Fe & Mn(hydr)oxides) seems to be getting slightly less with depth. In terms of total ion concentrations (Figure 97), aluminum and iron are the main cations in the unsaturated sands, while calcium dominates within the saturated zone.
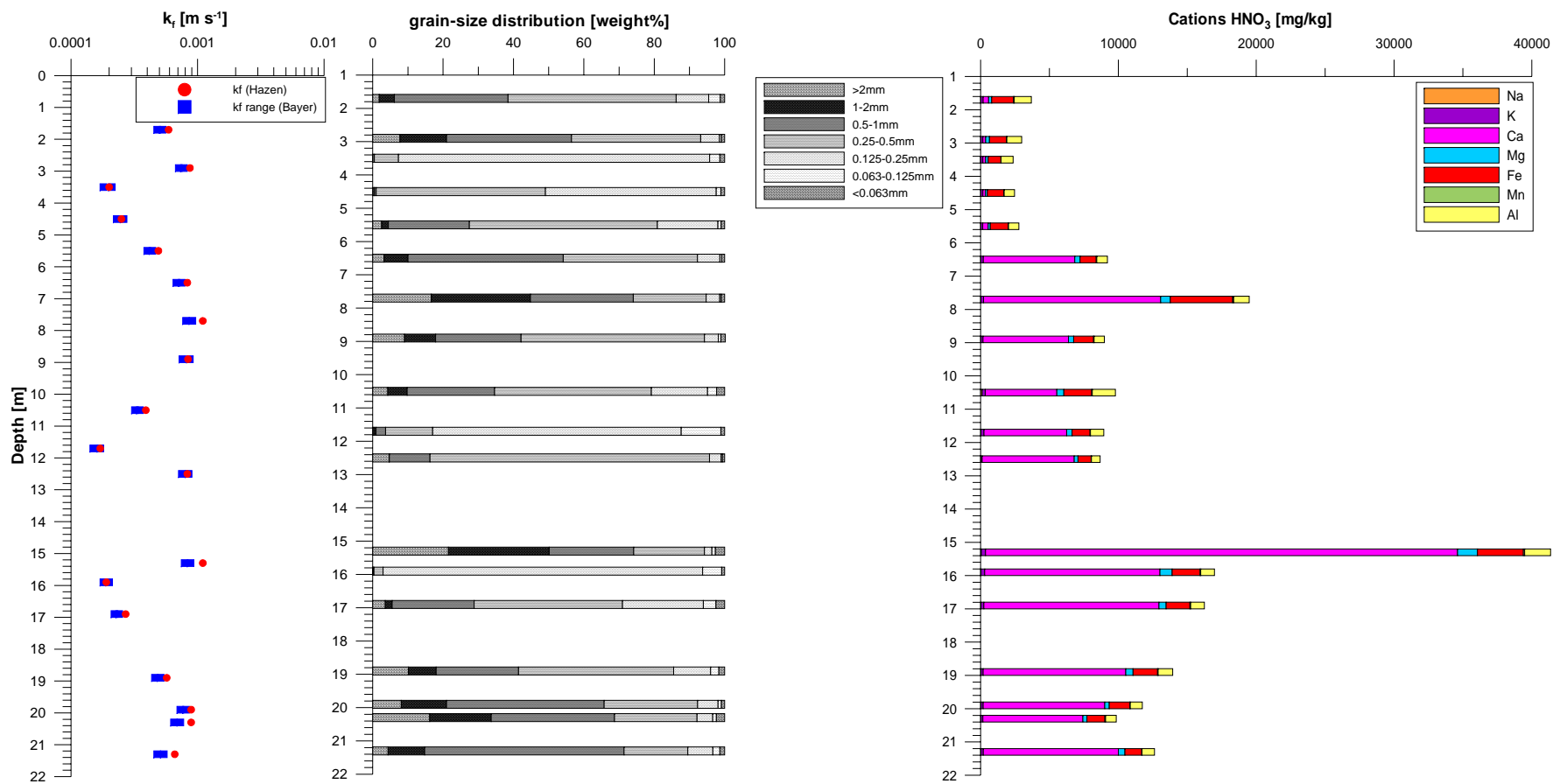
Figure 97: Hydraulic conductivities (k_f), grain-size distribution and cations from HNO3 extraction in core TEG369UP (data source: FU Berlin).
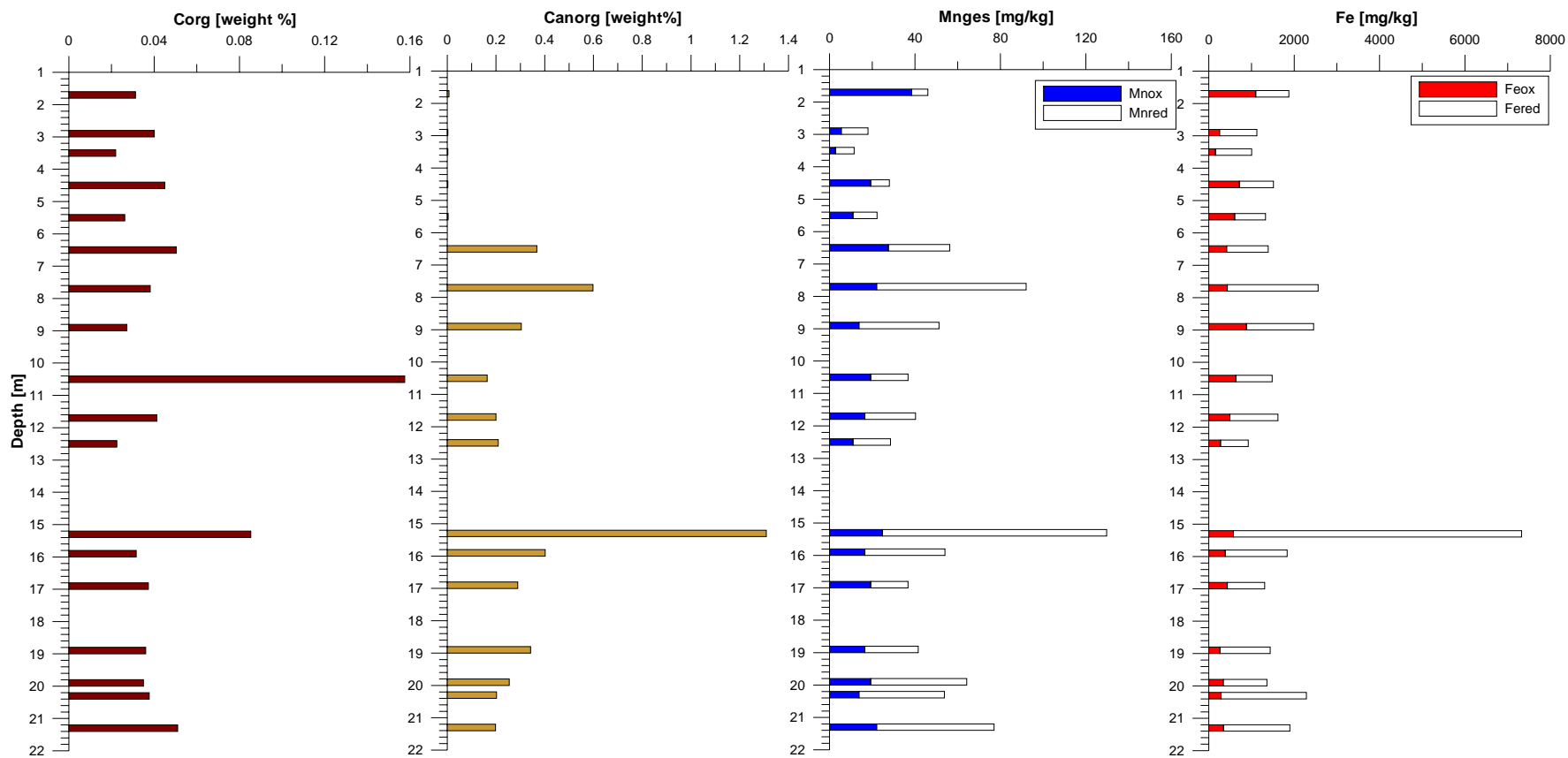
Figure 98: Organic and inorganic carbon content, reducible (Feox) and non-reducible (Fered) iron, reducible (Mnox) and non-reducible Mn(red) manganese content in core TEG369 (data source: FU Berlin).

3.5 Tracer evaluation: Travel times/groundwater age

The travel times at the GWA transect are clearly faster than at the bank filtration sites (at least at the transect at well 20, which is one of the closest to a pond of all wells in the triangle (Figure 88). Other than at the bank filtration sites, the resolution of the time-series with a monthly sampling was therefore too low to gain precise travel times from the tracer data. The tracer chloride, boron and, with little retardation, potassium would principally work, since they showed a clear increase in spring 2003 (at least for this time period). However, the fluctuations are too large and the curves are too close to each other to give nice shifts. The following tracer time-series were divided into curves for the shallow observation wells TEG365, TEG366, TEG368OP and TEG369OP as well as the deeper ones TEG368UP and TEG369UP plus production well 20 for a better overview (compare Figure 89).
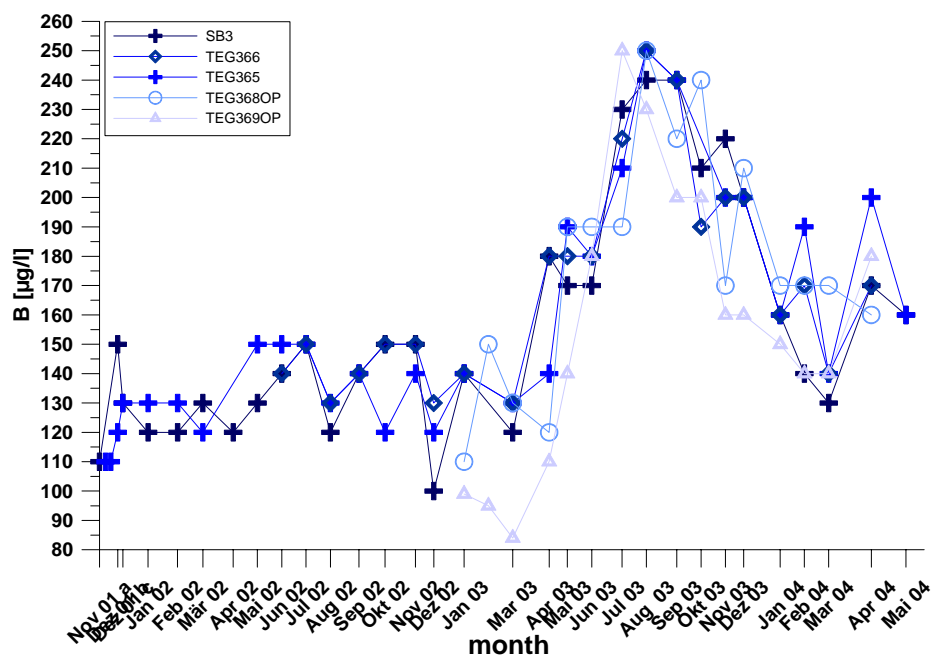
Figure 99: Boron concentrations over time for the shallow observation wells (data source: BWB).

Figure 99 and Figure 100 shows exemplary time-series for B and Cl⁻ for the shallow observation wells. Clearly, the data does not allow a travel time evaluation or only in the sense that it shows that the travel times are below one month to each observation well. Slightly better curves were gained from the stable isotope analysis. The isotopes showed seasonal peaks in both 2002 and 2003. At least for the shallow observation well TEG369OP, furthest away from the pond, an offset of slightly less than a month (~ 25 days) can be seen. Increasing the sampling frequency for TEG366 below the pond did not result in more precise estimates (Figure 102). The curves lie on top of each other, suggesting a very short travel time.

144
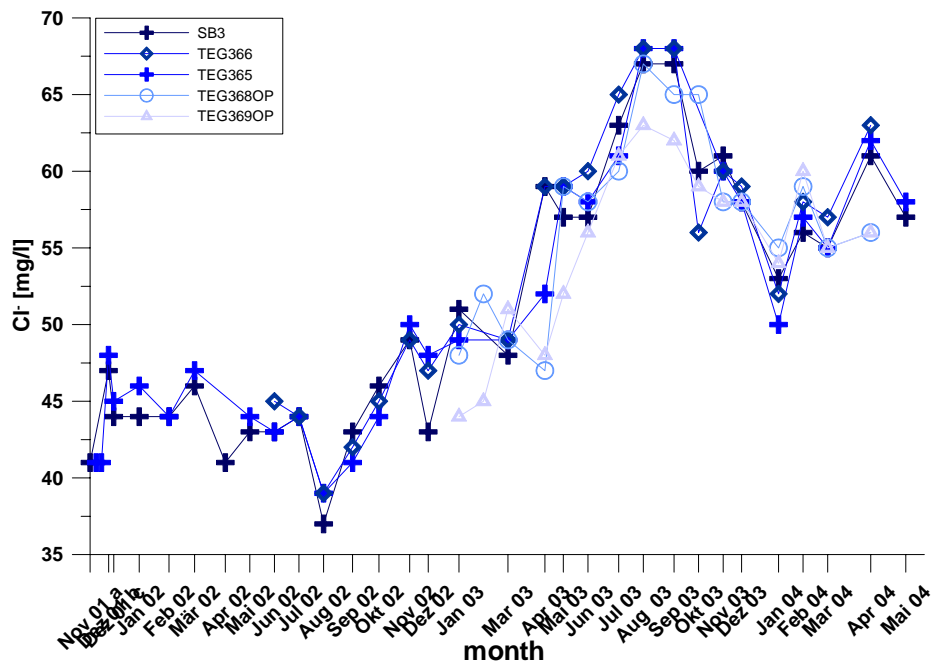
Figure 100: Chloride concentrations over time for the shallow observation wells (data source: BWB).
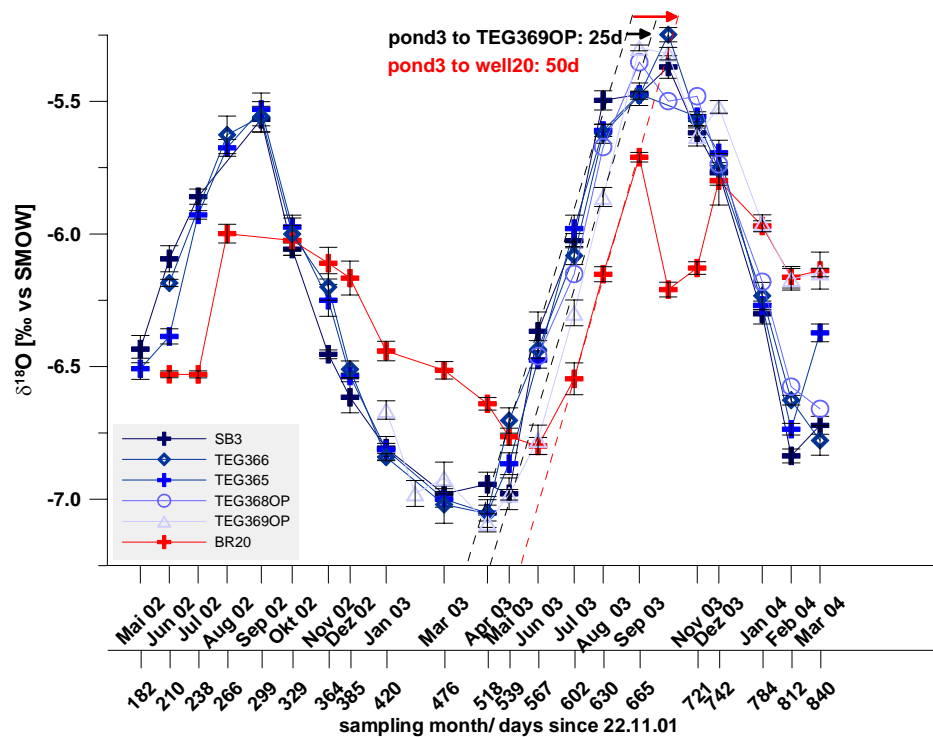
Figure 101: $\delta^{18}O$ values over time for the shallow observation wells and the production well (data source: AWI).
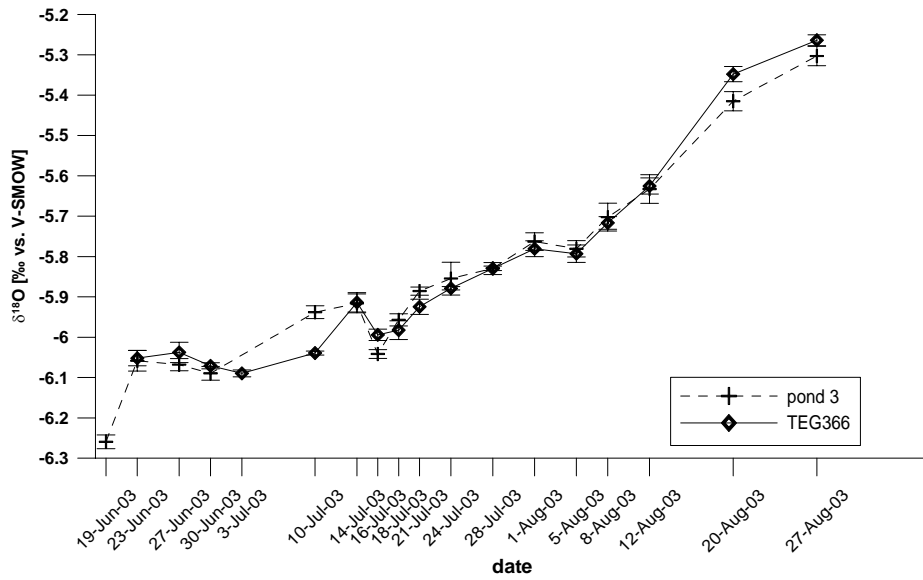
Figure 102: δ^{18}O values over time for TEG366 (data source: AWI).
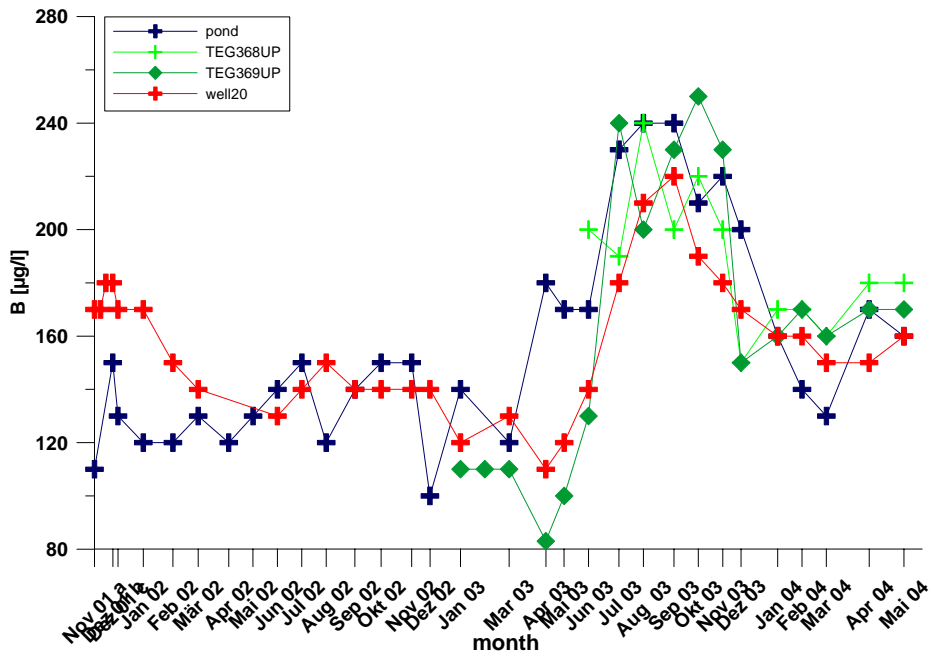
Figure 103: Boron concentrations over time for the deep observation wells (data source: BWB).
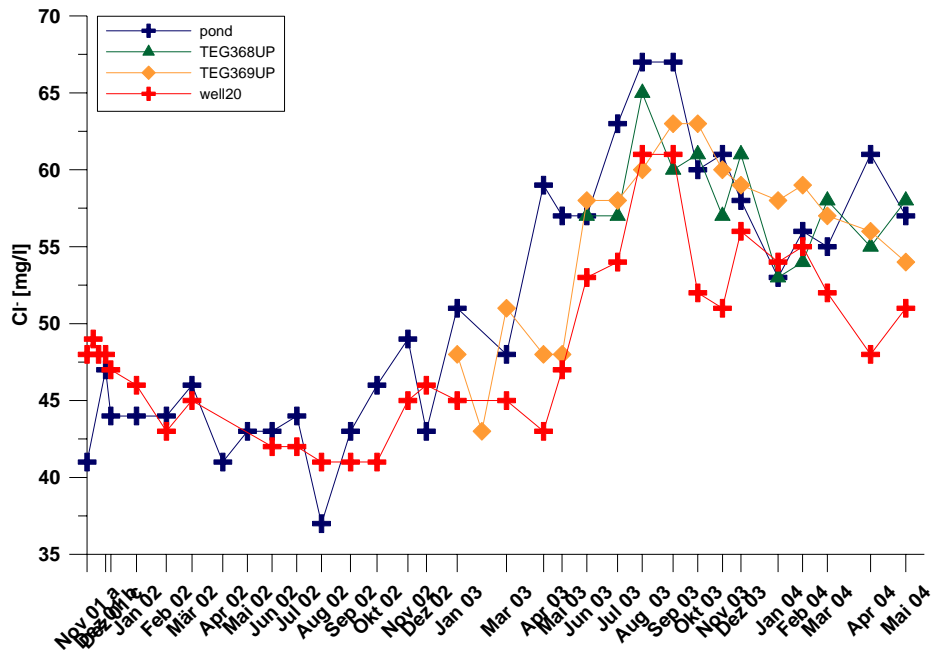
Figure 104: Chloride concentrations over time for the deep observation wells (data source: BWB).
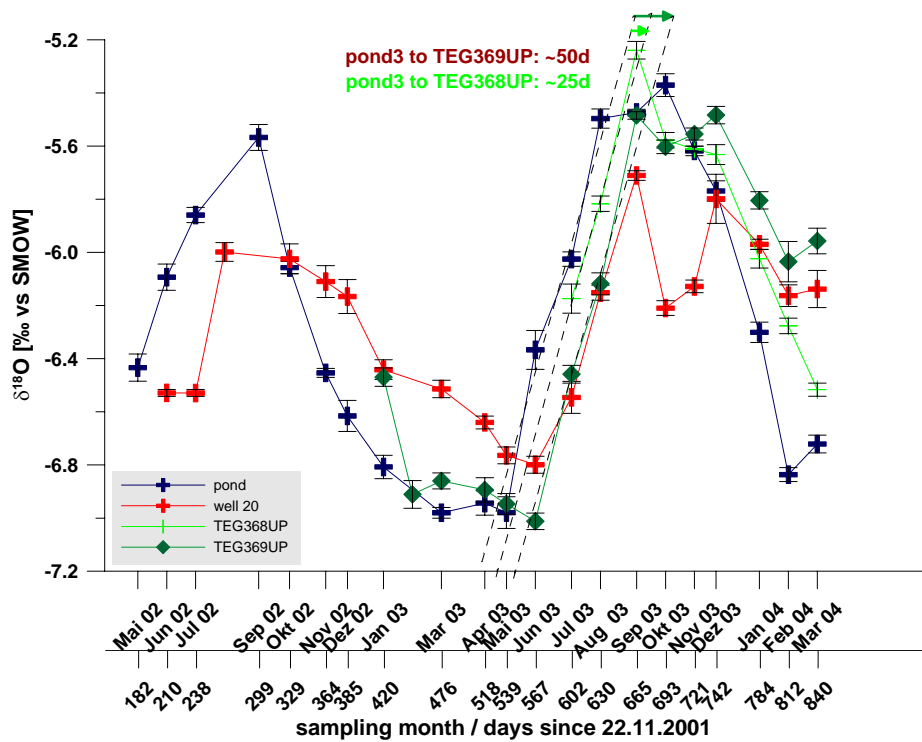
Figure 105: δ^{18}O values over time for the deep observation wells and the production well (data source: AWI).

147

The travel times to the deeper observation well (below the glacial till) are likewise short. Using Cl⁻ and B data, there appears to be a slight offset (Figure 103, Figure 104), however, the fluctuations do not allow a precise determination of the shift. Again, the stable isotopes give clearer signals. Figure 105 indicates that the travel time to TEG368UP is slightly less than a month, whereas the travel time to TEG369UP, closest to the production well, is similar to the travel time to the production well itself (1-2 months or roughly 50 days in spring/summer 2003).
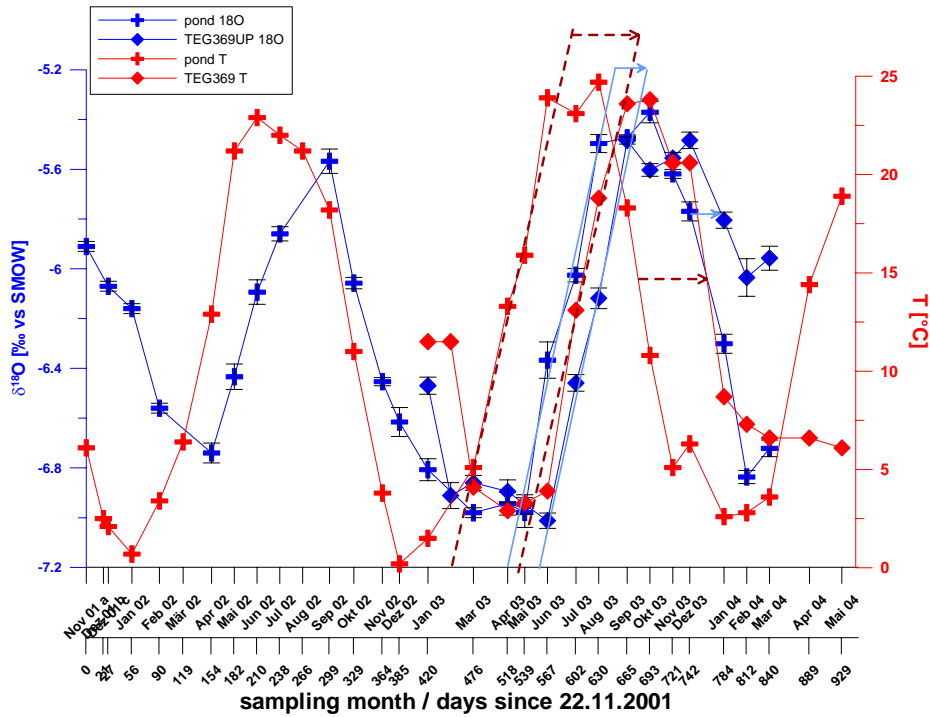
Figure 106: δ^{18}O values (blue) and temperatures (red) over time

The temperature data has a much better time resolution, because daily values exist. The temperature data can be used to estimate travel times below 1 month. However, temperature is not a conservative tracer and the retardation factor has to be estimated from a conservative tracer. Judging from the difference between the temperature and the δ^{18}O shift to TEG369UP (Figure 106), the temperature retardation factor is ~ 2.1.

Figure 107 shows the temperature data of the pond, TEG366, TEG365 and TEG368OP with peak shifts indicated by arrows and dotted lines. The grey rectangle indicated the times when the pond was empty. It becomes clear, as obvious from the variable recharge rate (Figure 92), that the travel times vary, depending on the permeability of the pond bottom. In the most extreme cases, the shifts in Figure 107 fluctuate between 4-8 days (TEG366), 5-15 days (TEG365) and 15-44 days (TEG368OP). Hence, using a retardation factor of 2.1, the effective travel time to the wells are 1.9-3.8 days (TEG366), 2.4-7.1 days (TEG365) and 7.1-21.0

days respectively. However, the slower travel times (and larger residence times) appear around times when the pond was empty, while the faster end of the spectrum is representative for larger time periods during operation. Note that the temperature varies between 0 and 25°C, which may have an effect on the behaviour of water constituents subject to microbial degradation, which may be temperature sensitive.
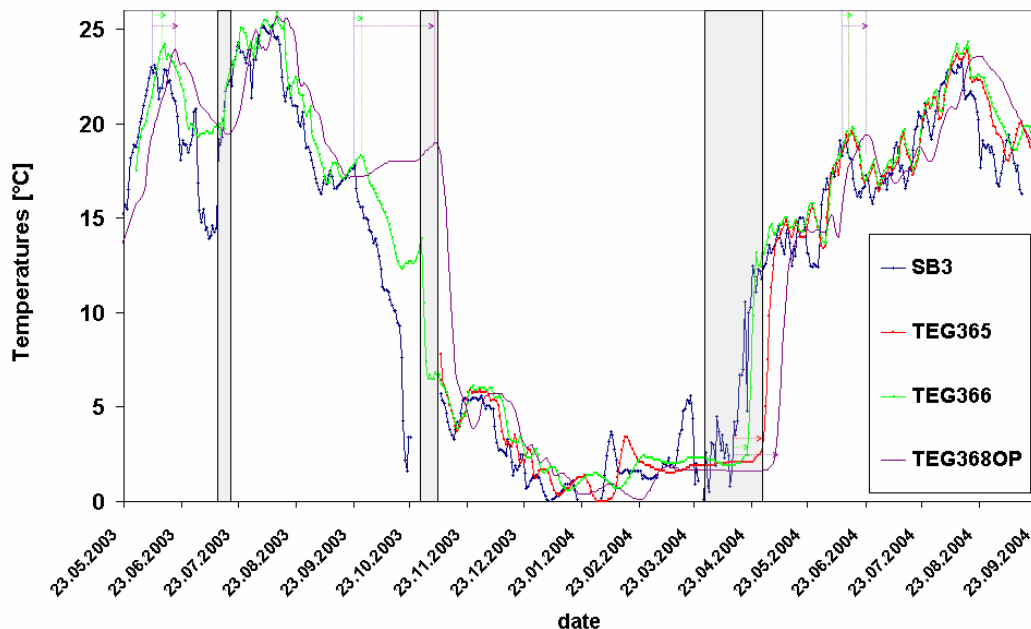
Figure 107: Daily temperature data for the pond (SB3) and 3 observation wells with short travel times. The grey shading indicates times when the pond was empty, the dotted lines and arrows point out the temperature peak shifts.

Figure 108 summarises the results of the travel time investigations and shows effective T/He ages, which are consistent with the travel times. The travel times are only rough estimates for times of pond operation, as discussed above, they vary largely in time. The observation wells TEG369OP and TEG369UP had an effective T/He age of 0. With a resolution of the method of half a year at the side, this could be expected and it proves, that 100% of the sampled water north-west of well 20 are, in fact, originating from the pond only. A vertical age stratification as discovered at the BF sites, with decade old water in greater depth, was not encountered. However, it may still exist at the very bottom of the aquifer. The background water had an effective T/He age of 1.3 (shallow) and 4.3 (deep) and 10.3 (very deep below till) years. The groundwater observation well TEG342 in greater distance from the pond (next to the airport) is screened at 18.4-19.4 m below ground. The T/He age was 27.4 years. It is free of surface water influence and probably recharged by infiltration of seepage water

149

through the soil. The production well, as a mixture of bank filtrate and native background water, lies in between with 2.3 years.
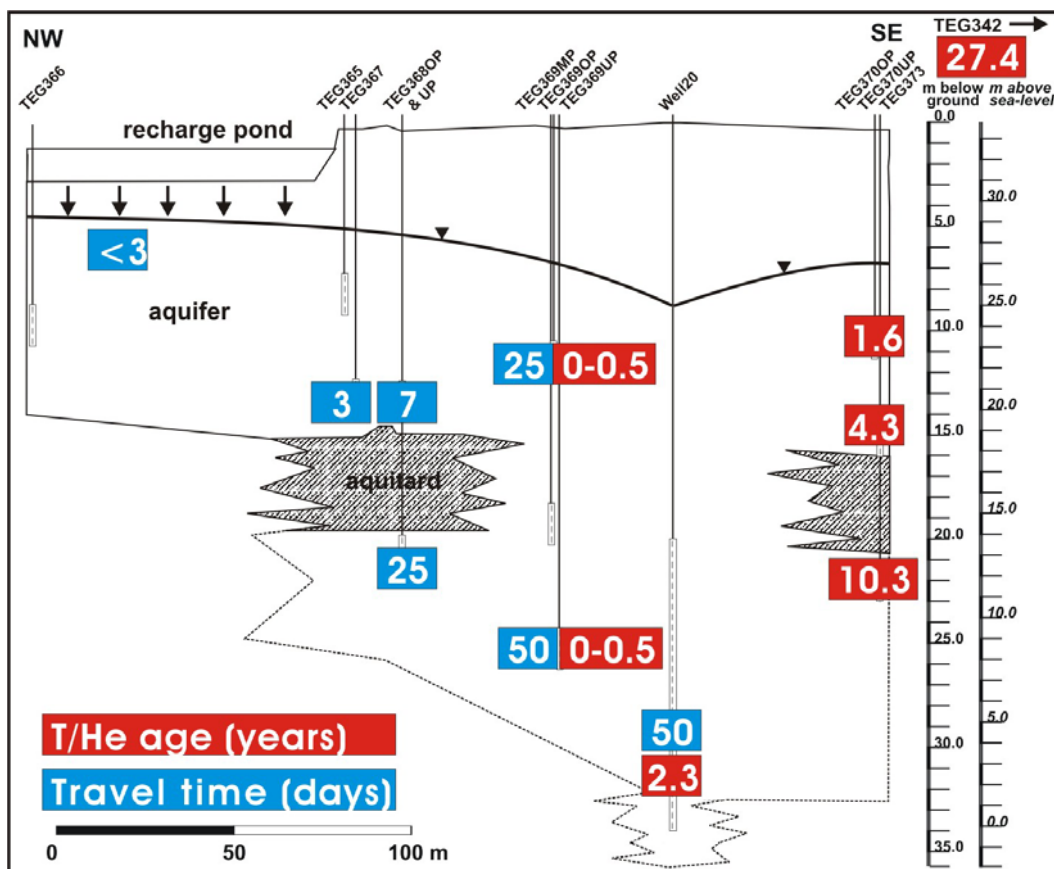
Figure 108: Estimates for approximate travel time for times of pond operation and effective T/He age in observation and production well.

3.6 Tracer evaluation: Mixing

The scatter plot of $\delta^{18}O$ data versus δD of the pond and the deep and shallow wells TEG368 and TEG369 (Figure 109) illustrates that the groundwater flowing between the pond and well 20, both below and above the glacial till, is purely made of "young" recharged water. Unlike at the bank filtration site, there is no "older" bank filtrate (or artificially recharged water) with a different chemical composition mixing with the pond water.
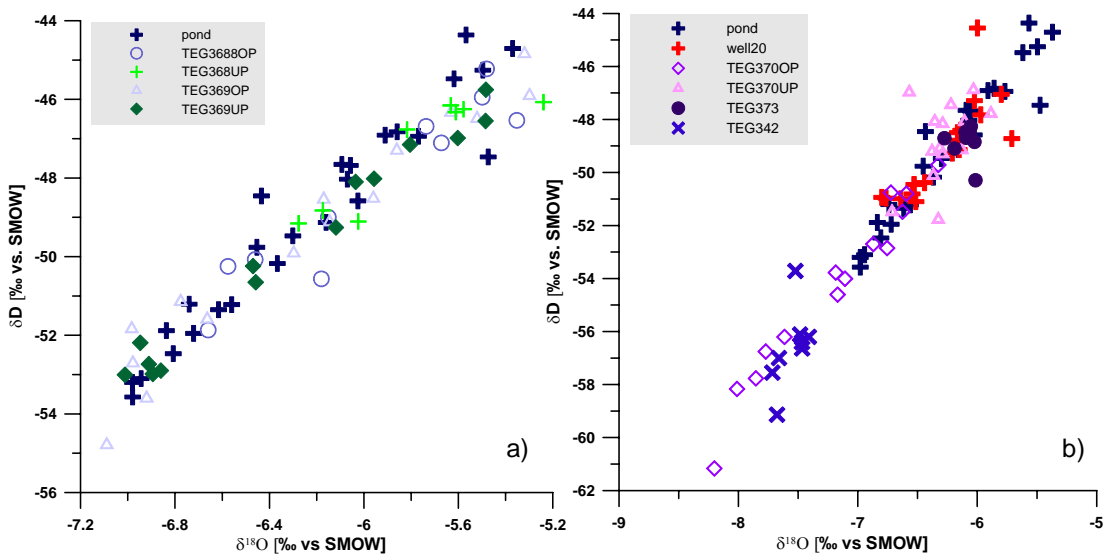
Figure 109: δ^{18}O versus δD [‰ vs. SMOW] of pond water (SB3), production well and background ground-water (Data source: AWI Potsdam).

The amplitude of the fluctuations of the tracer concentrations in the production well, as it can be seen in the time-series in chapter 3.5, is still quite distinct. This is not the case in any of the other production wells at Wannsee or Tegel, where seasonal variations have been largely eliminated by mixing and dispersion processes. The difference is a combination of several facts:

1. The average travel time to well 20 is relatively short (50 days).
2. There is no mixing of recharged water of distinctly different residence times.
3. The proportion of recharge water in the production well is lager than at the BF sites.

Figure 109b shows the isotope scatter plot for pond, production well and the observation wells TEG370OP, TEG370UP and TEG373 directly inland of well 20 (Figure 89) as well as TEG342 in greater distance (Figure 119). It shows that, with regard to the isotopes, the background water does not deviate distinctly from the surface water, as it does at the BF Tegel site. The well plots within the field of the surface water (only with less variability) and so do the two lower inland observation wells. The shallowest (TEG370OP) has a distinctly more negative signal, similar to that of TEG342. Overall, the vertical background groundwater variation is very large as is the spatial variation of the background water (chapter 3.8).
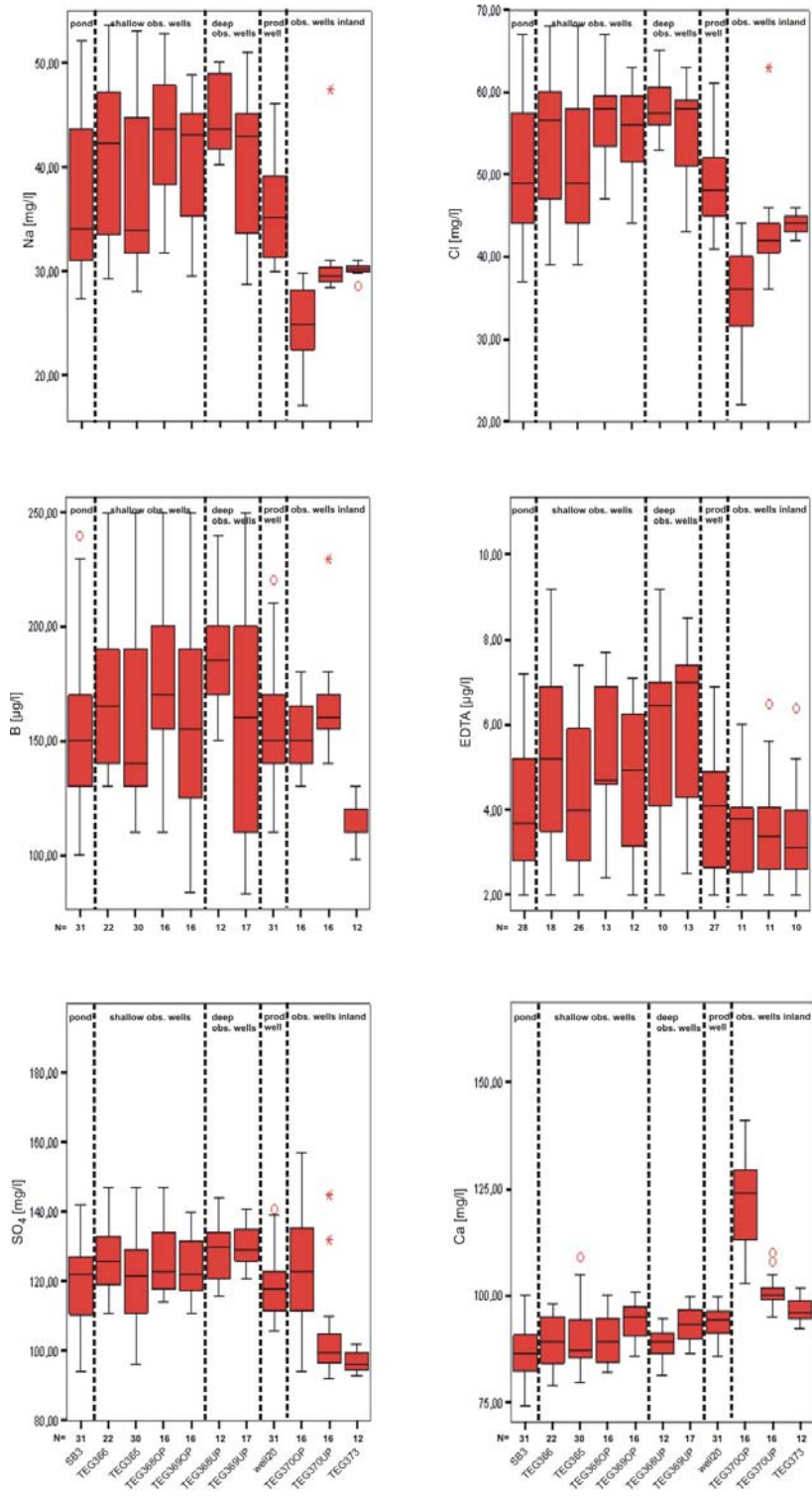
Figure 110: Boxplots for Na⁺, Cl⁻, B, EDTA, K⁺ & SO₄²⁻ at the GWA Tegel (data source: BWB); November 2001-May 2004, N = number of samples (31 at maximum).

Selected box plots of Na, Cl, B, EDTA, K and SO_4 are given in Figure 110. They likewise illustrate, that the pond is the only source of the sampled water north-west of well 20. Differences in the are thought to be due to the difference in samples (some observation wells were constructed later and sampled less often. They also show that it is not possible to calculate proportions of BF in the well with a simple 2 component mixing formula. In most cases, there is no clear difference between the water on both sides of the production well (EDTA or B). If there are clear differences, they are only found in one or two of the inland wells. For example, TEG370OP resembles the surface water in its B, EDTA, and SO_4 content, but contains less Cl and Na and has a more negative isotope signal. TEG370UP differs mainly in the SO_4 content, but resembles the surface water in the remaining water constituents shown. TEG373 contains less B than the transect wells. The vertical differences are even more extreme in some of the pharmaceutical residues, examples for phenazone (analgesic) and AMDOPH (persistent oxidation product of dimethylaminophenazone) are given in Figure 111 , where concentrations increase with sampling depth. These phenomena are currently not fully understood and probably the result of a complicated and transient flow regime. However, it can be concluded that the variations in the background groundwater composition are much larger and far more complicated than expected, both in their vertical and horizontal extent.

From the large scale investigations around the GWA and the existing flow model (compare chapter IGB) it becomes clear that, depending on the pumping regime of the production well gallery, the background groundwater can flow towards the transect from further north or south, which would each result in a very different water quality (chapter 3.8). However, judging from the strong seasonal variations, the proportion of BF in well 20 is likely to be rather large (> 80 %).
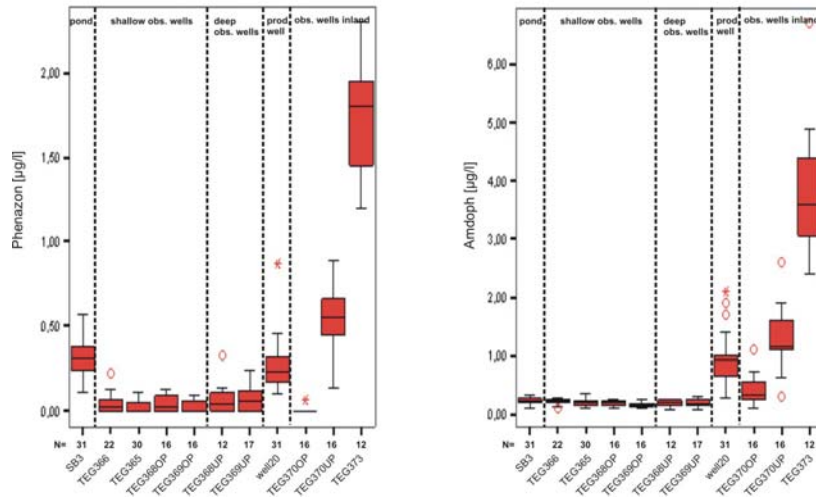
Figure 111: Boxplots for phenazone and AMDOPH at the GWA Tegel (data source: BWB); November 2001-May 2004, N = number of samples (31 at maximum).

3.7 Hydrochemistry at the transect

3.7.1 Hydrochemical conditions of the infiltrate

TEG366 and TEG365 are two shallow observation wells below and very close to the pond with a depth of 6-8 m below the pond (23.0-25.0 masl) and 7-9 m below ground surface (24.7-26.7 masl) respectively (Figure 112). They were used for the description of redox conditions of the infiltrate on the first metres of flow (Massmann et al., subm.). According to the isotope and temperature data, both are generally reached within a travel time of hours to less than 3 days, depending on the recharge rate (Figure 91c). The groundwater wells were fully saturated at all times.

Throughout the year, the DOC concentration (Figure 112b) decreased about 0.15-0.20 mmol/L from the pond to the shallowest wells, which is equivalent to a reduction of ~33-48 % of the total DOC present. The DOC input and the degree of removal fluctuated slightly but did not show any seasonality, nor did it show a clear relation to the hydraulic conditions.

The pond water was saturated with O_2 at all times. Because of the temperature dependency of the O_2 saturation, the actual O_2 concentration was ~0.35-0.55 mmol/L in winter and ~0.20-0.35 mmol/L in summer. The O_2 concentration in the shallow groundwater (Figure 112c) showed a strong seasonality. In mid-summer (at water temperatures above 14°C as indicated by the grey shading in Figure 112), all O_2 (~0.20-0.35 mmol/L) was removed before reaching the first groundwater observation well. In winter, O_2 was not reduced completely, only ~0.05-0.25 mmol/L (at maximum) of O_2 was consumed on the way to the shallowest

154

wells. The temperatures of the infiltrate are given in Figure 112a for comparison. It seems that on top of the seasonal variations, the O_2 concentrations occasionally peaked towards the end of the unsaturated phases, for example in July 2003 (Figure 112c). At all times, but particularly in summer, the decrease in O_2 exceeded the decrease in DOC. If O_2 was the only terminal electron acceptor (TEA), the O_2 decrease should be equivalent to the decrease in DOC (Eq. 1). This indicates that besides dissolved organic carbon, particulate organic matter (POC) present in the aquifer or, more likely, fresh organic matter of the clogging layer may act as an additional electron donator.

$$CH_2O + O_2 \rightarrow CO_2 + H_2O \qquad \text{Eq. 1}$$
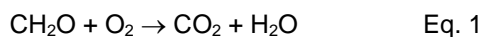
A clear difference between the redox potential of the surface water and the infiltrate could only be seen in summer. When conditions turned anaerobic, the Eh of the infiltrate was about 100 mV less than in the surface water (data not shown).

The seasonally variable input of nitrate is largely reflected in the infiltrate (Figure 112d). When O_2 was the only TEA (mainly in winter), NO_3^- concentrations in the surface water tended to be even lower than in the shallow groundwater, because NO_3^- is a reaction product of the aerobic degradation of particulate organic matter which contains nitrogen (van Cappellen and Wang, 1996). Nitrate reduction was rarely observed. If denitrification did take place, it happened mainly in summer and then towards the end of a saturated phase, for example in July/August 2004, when temperatures were high and conditions had been saturated for a while (Figure 112). Nitrate reduction is bacterially catalysed and leads primarily to the production of nitrogen via several complicated pathways with intermediates such as NO_2^-, NO and N_2O. The process can be described by the overall reaction (Appelo and Postma, 1996):

$$5CH_2O + 4NO_3^- \rightarrow 2N_2 + 4HCO_3^- + CO_2 + 3H_2O \qquad \text{Eq. 2}$$
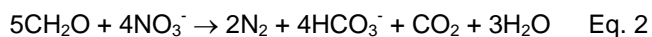
Manganese (Mn^{2+}) appeared only in summer when temperatures exceed 14°C (Figure 112e), at times when O_2 had been fully depleted. During the unsaturated phase in July 2003, when Mn^{2+} had previously been detected, the concentrations dropped to zero again despite the fact that temperatures were high. If observed, Mn(IV) reduction commenced before NO_3^- was fully removed. Iron (Fe^{2+}) was never detected in TEG365 or TEG366 and, likewise, SO_4^{2-} reduction did not occur.

Many authors have described the importance of seasonal temperature variations on redox processes in the groundwater (e.g., Olivie-Lauquet et al., 2001; Carrera et al., 2003; Prommer and Stuyfzand, 2005). Because redox processes are generally microbially catalyzed, the temperature variation influences the microbial activity, reflected in changes in the concentration of redox-sensitive parameters. A temperature dependency of denitrification was reported in various studies and environments (e.g., David et al. 1997; Carrera et al., 2003). A correlation between increased dissolved iron, manganese and trace element con-

155

centrations with increasing temperatures was observed in a wetland in France by (Olivie-Lauquet et al., 2001). The particular importance of the role of large temperature variation in artificial recharge systems on redox-related hydrochemical changes has recently been acknowledged. (Prommer and Stuyfzand, 2005) discovered during deep well injection of aerobic surface water into an anaerobic aquifer in the Netherlands that reaction rates of pyrite oxidation by oxygen depended significantly in spatially and temporally varying groundwater temperatures. They found that oxygen breakthrough from the injection well to the first observation well 8 m away occurred in winter only, while no breakthrough was observed when the injectant temperatures rose above approximately 14 °C, which is very similar to our findings.
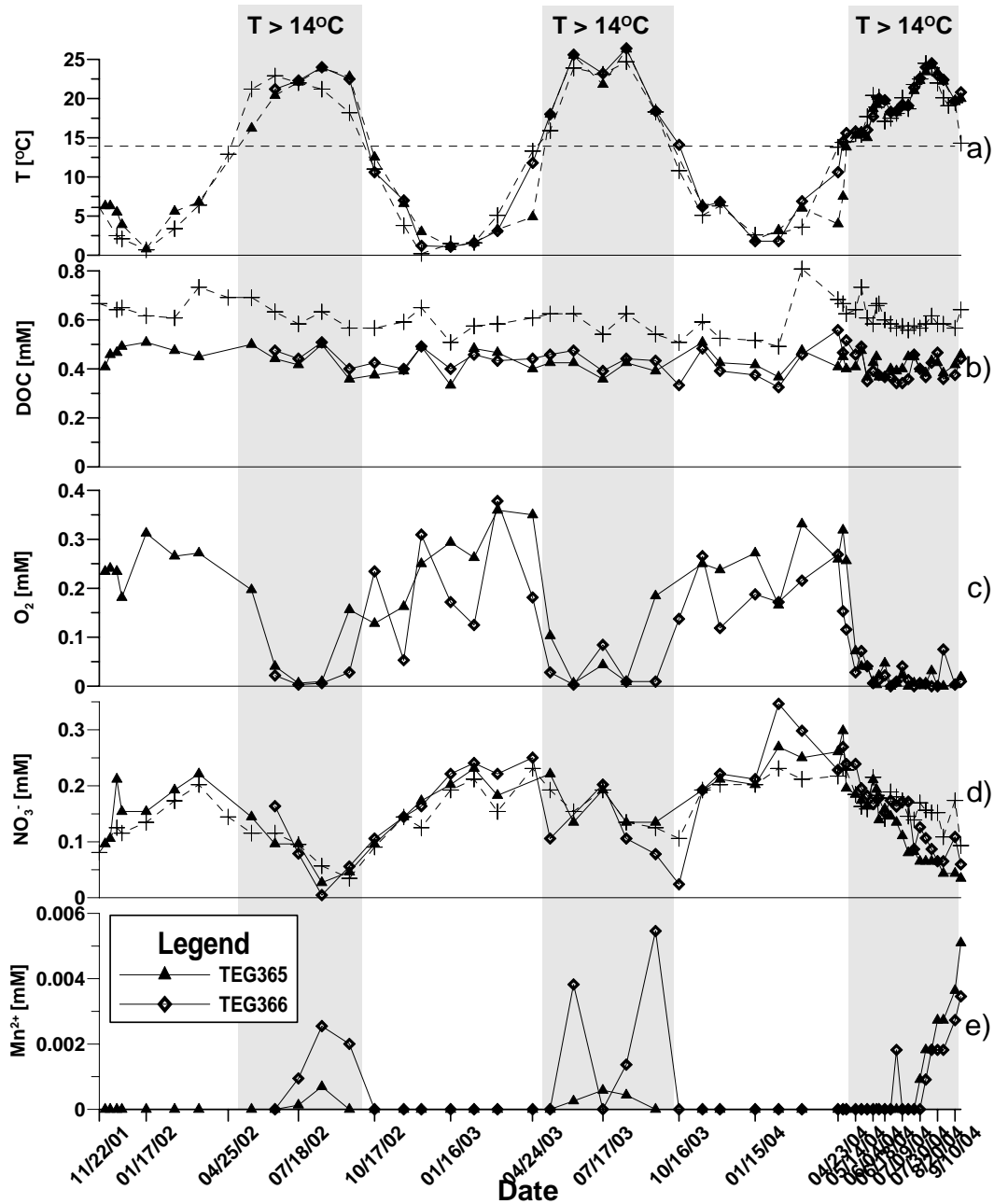
Figure 112: a) Temperatures [⁰C] and b) concentration of dissolved organic carbon (DOC, mM) and redox indicators O₂ (c, mM), NO₃⁻ (d, mM) and Mn²⁺ (e, mM) in pond 3 and groundwater observation wells TEG365 and TEG366 below the pond (compare Figure 89). The times when the temperatures in the surface water and infiltrate were above 14 ⁰C are marked with grey bars. The pond itself was saturated with oxygen at all times (pond concentration, average 0.36 ± 0.1 mmol/L not shown) and largely free of Mn²⁺ (data not shown). The dominating influence of the temperatures on the redox conditions is visible (Massmann et al., subm.).

Figure 113 illustrates the bicarbonate (HCO_3^-, a) calcium (Ca^{2+}, b) concentrations in the infiltrate in relation to the saturated/unsaturated phases (white/grey shading). In general, the pond concentrations were reflected in the groundwater. However, distinct peaks in the groundwater exceeding the input concentration could sometimes be seen towards the end of the unsaturated phases (u, grey bars). Within these peaks HCO_3^- concentrations increased roughly twice as much as the Ca^{2+} concentrations, indicating that calcite dissolution took place. Calcite dissolution is an important process often induced by redox reactions at the presence of calcite (von Gunten and Zobrist, 1993).
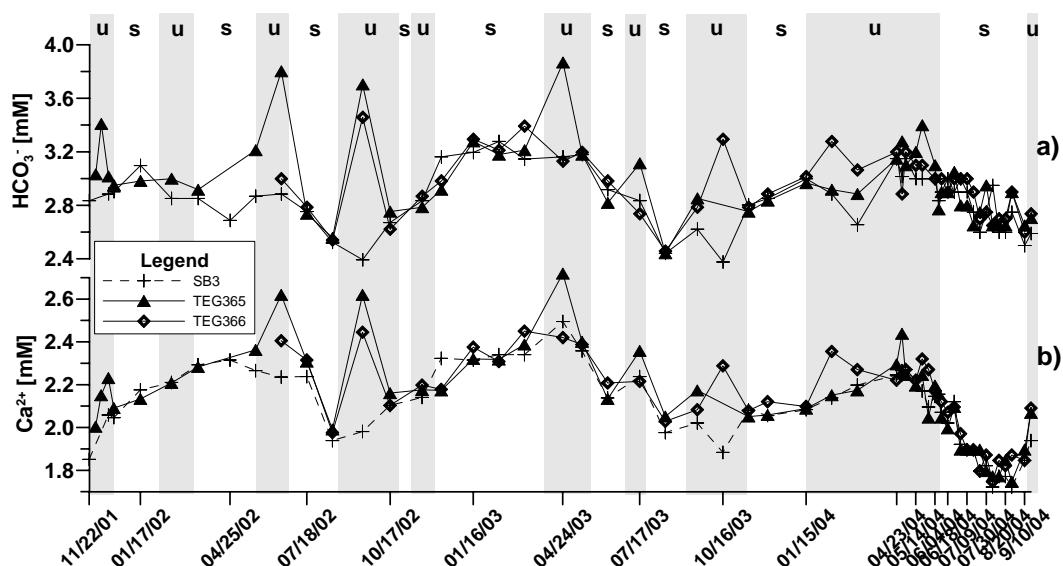
Figure 113: a) Bicarbonate and b) calcium concentrations in the pond and groundwater wells TEG365 and TEG366. Grey shading represents the changes between saturated (annotation s, white bars) and unsaturated (annotation u, grey bars) phases. The groundwater concentrations often clearly exceeded the input concentrations towards the end of the unsaturated phases (Massmann et al., subm.).

Compared to the seasonal temperature variations, the hydraulic changes had only a minor effect on the redox chemistry of the groundwater. An effect was only clearly visible when, as a result of unsaturated conditions, gaseous oxygen intruded into the anoxic environment during summer, leading to a temporary shift from Mn-reducing to aerobic conditions (Figure 112). However, an indirect influence of the cyclic changes in the water saturation was visible in the increased Ca^{2+} and HCO_3^- concentrations in the unsaturated phases (Figure 113). This process could have been enabled by the additional rapid oxidation of filtrated labile organic matter by gaseous O_2 entering the unsaturated zone (Eq. 3). The fact that DOC concentrations did not show an additional decrease when conditions were unsaturated suggests that DOC degradation was outcompeted by the degradation of sedimentary bound organic matter. $CH_2O + CaCO_3 + O_2 \rightarrow Ca^{2+} + 2HCO_3^-$ Eq. 3

It was found that the redox conditions, which are temperature dependant, appear to affect the behaviour of a number of phenazone type PhACs (Massmann et al., subm.). The removal of phenazone, and possibly also FAA and AAA is not complete at the absence of oxygen. Microbial degradation by aerobic bacteria rather than adsorption was suggested to be the removal process. Results indicate that marginal removal of AMDOPH, a very persistent metabolite of dimethylaminophenazone, might also be coupled to the presence of oxygen (Massmann et al., subm.).

3.7.2   Redox conditions along the groundwater transect

In terms of the redox conditions (Figure 114), the evaluation of the box-plots shows that the shallow observation wells towards the pond still contain oxygen and nitrate. The deeper observation wells TEG368UP (below the till) and TEG369UP contain much less O_2. Nitrate is still present, but in lower concentration than in the shallow wells and in the pond. Most observation wells between pond and production well contain some Mn^{2+}, in particular the deeper wells, but Fe^{2+} was never detected.

The observation wells inland are O_2 free. In the shallowest observation well TEG370OP, NO_3^- could still be detected, but Mn^{2+} is also present. TEG370UP above the till is NO_3^- free and Mn^{2+} and even Fe^{2+} could already be analysed. The highest Fe^{2+} concentrations were encountered in TEG373. TEG373 and also TEG370UP may even be slightly sulfate reducing, since SO_4 concentrations are comparatively low (Figure 110) but sulfide was not analysed and the original background SO_4^{2-} concentration is unknown.

The boxplots (Figure 115) demonstrate that the largest drop in DOC (and TOC) concentration occurs between pond and the first observation well, i.e. in the clogging layer, even though it is removed regularly. A slight decrease along the remaining transect is also visible. The DOC concentration drop is smaller than the O_2 reduction, which is why sedimentary bound organic carbon is likely to be an additional electron donator.
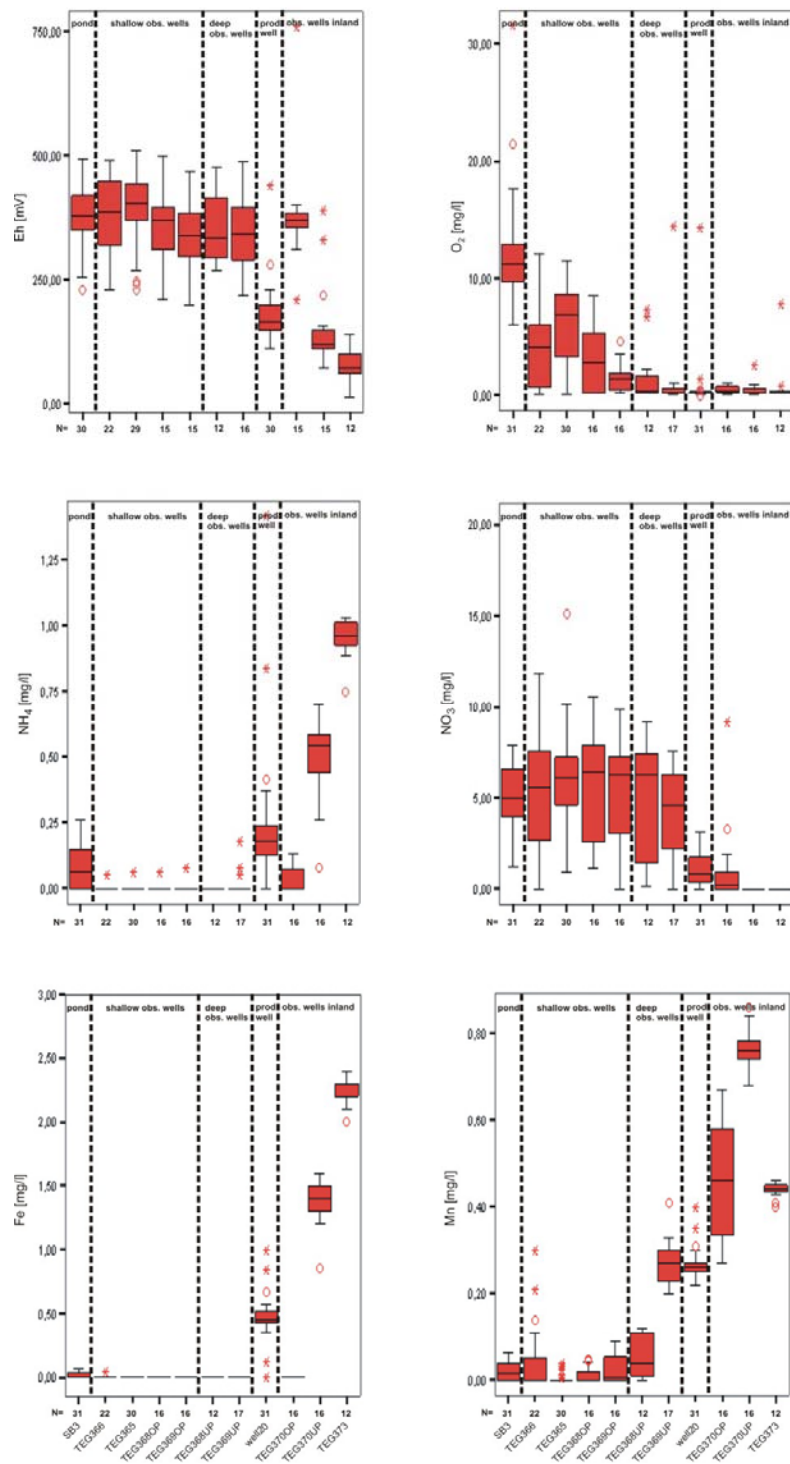
Figure 114: Boxplots for redox indicators Eh, O$_2$, NH$_4^+$, NO$_3^-$, Mn^{2+} and Fe^{2+} at the GWA Tegel transect (data source: BWB); November 2001-May 2004, N = number of samples (31 at maximum).
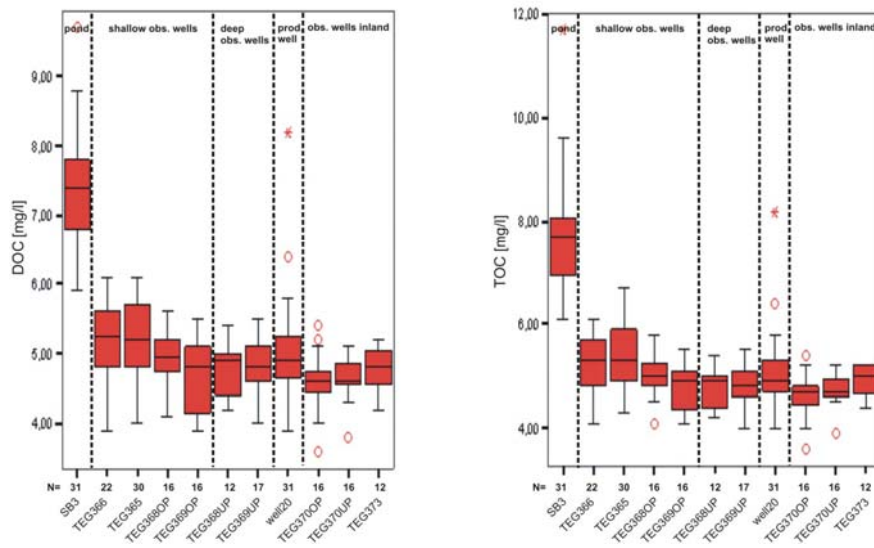
Figure 115: Boxplots for dissolved organic carbon (DOC) and total organic carbon (TOC) at the GWA Tegel transect (data source: BWB); November 2001-May 2004, N = number of samples (31 at maximum).

The seasonal redox changes as described above for the area close to the pond (chapter 3.7.1) print through along the entire transect (Figure 116). The NO_3^- concentration of all observation wells decreases largely in the summer months, while at the same time, Mn^{2+} appears. While TEG368OP still contains traces of NO_3^- even in the summer months, Mn^{2+} was analysed in samples from TEG369UP at all times.
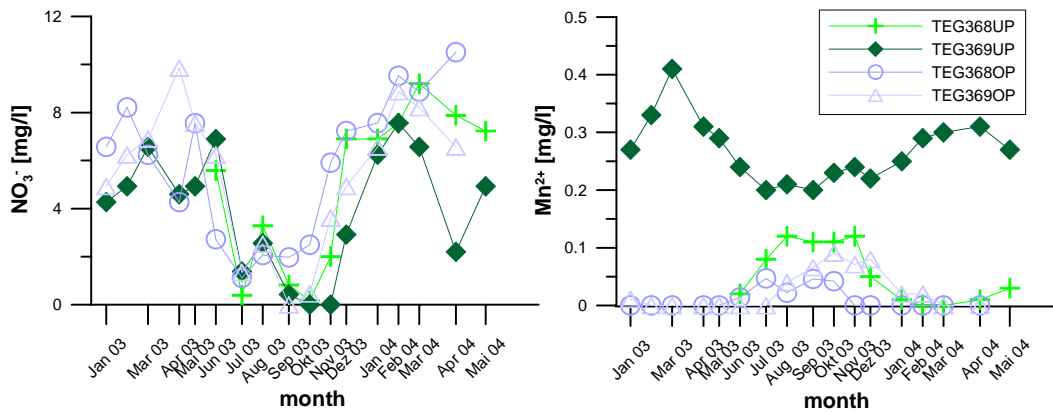
Figure 116: Time series of NO_3^- and Mn^{2+} in deep and shallow screened observation wells TEG368 and TEG369 (data source: BWB).

Figure 117 shows O_2 and NO_3^- concentrations plotted versus travel times along the transect for three summer and winter months in 2003. In summer, O_2 was consumed within the first metres of infiltration as explained above Figure 112c) and oxygen remained absent along the transect. Nitrate reduction, which was rarely observed close to the pond (Figure 112d) continued along the transect, while at the same time Mn^{2+} concentrations increased due to commencing reduction of Mn(IV)hydroxides present in the sediment (not shown). The fit through the plot of NO_3^- versus travel time is shown in Figure 117 (left). Rate constant estimates vary strongly (between 0.01 and 0.043 d^{-1}), probably partly due to the highly variable input concentration and the fact that the time-lag to the observation wells was not considered. The corresponding half-lives of NO_3^- were 16 days to 2 ½ months; hence towards the production well, NO_3^- was largely diminished and Mn^{2+} concentrations were elevated (Figure 114).

In winter, at low temperatures, oxygen was present throughout the entire area between the pond and the production well (Figure 117, right). The O_2 reduction proceeded much more slowly and O_2 was the major TEA along the entire transect (little change in the NO_3^- concentration, Figure 117 right). The fit through the O_2 concentration versus travel time is now exponential with rate constants of 0.049 - 0.061 d^{-1} (Figure 117, right) and corresponding half-lives of 11 to 14 days. Mn^{2+} could only be detected in the observation well TEG369UP, closest to the production well that receives water from above and below the glacial till and also has the longest travel time (Figure 108).
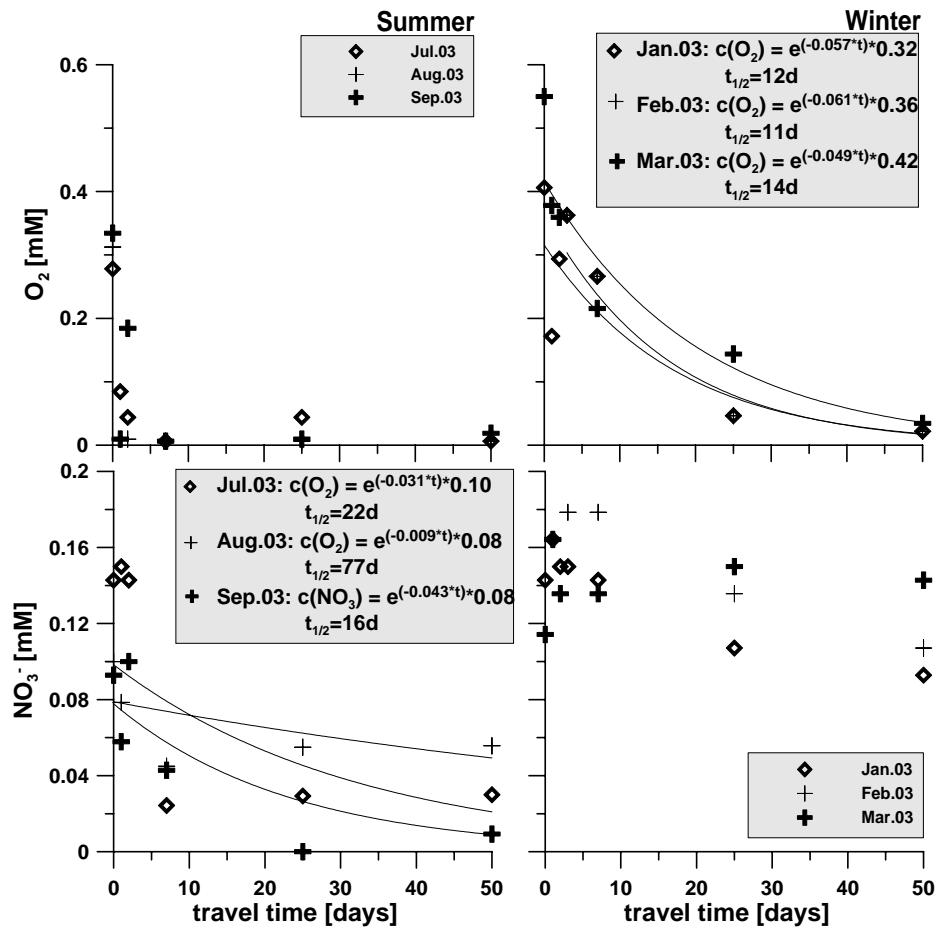
Figure 117: O_2 and NO_3^- concentrations [mM] plotted versus travel times estimated from tracer results for three summer and winter months. The travel times to TEG366 and TEG365, both < 3 days, were assumed to be 1 and 2 days respectively. In summer, O_2 was rapidly consumed in the infiltration zone and NO_3^- reduction observed along the transect, while in winter O_2 reduction continued along the entire transect and little NO_3^- reduction occurred (Massmann et al., subm.).

Figure 118 shows the approximate redox zoning in the groundwater in summer and winter. It exemplifies where O_2 and NO_3^- are still present and where Mn^{2+} and Fe^{2+} appear seasonally. The zoning is different NW and SE of the production wells. Rather than abrupt changes, the transition from one zone to the next is fluent and also moving with time. The redox regime is highly transient and changes seasonally. Hence, the zoning does not primarily depend on the removal of the clogging layer but mainly on the largely variable temperatures (Figure 107).
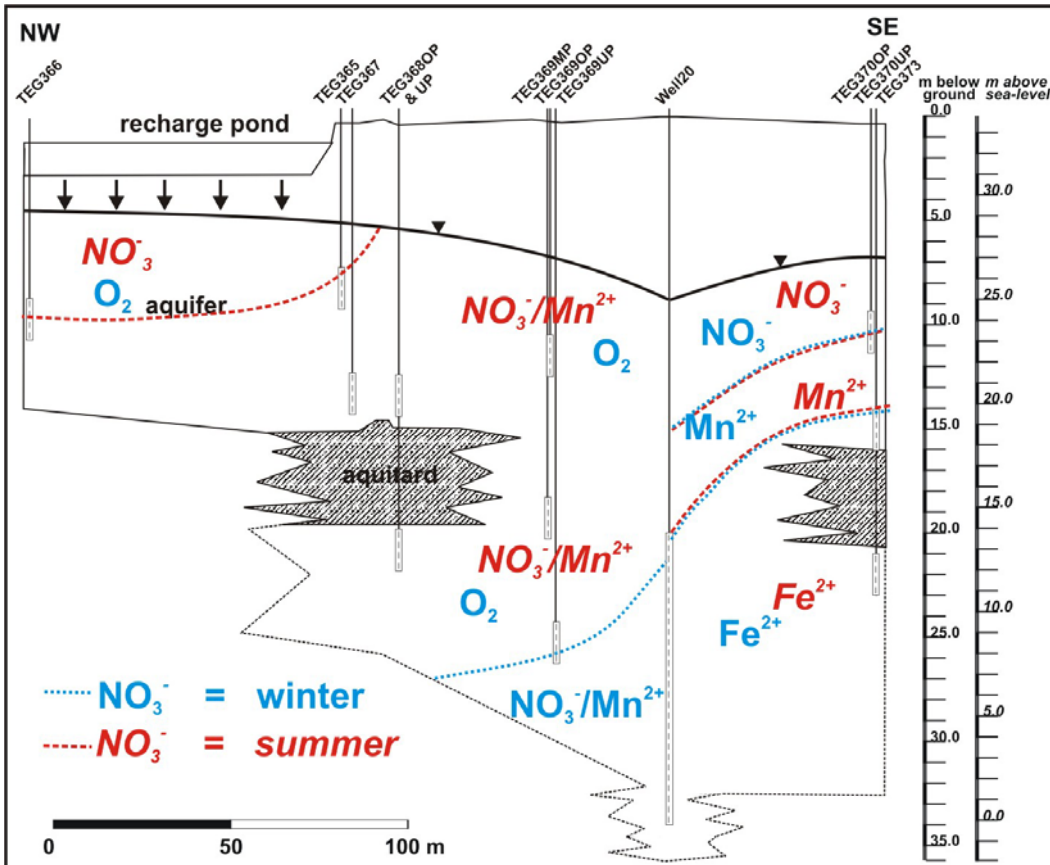
Figure 118: Approximate redox zoning at the GWA transect in summer (red) and winter (blue), defined by the presence of redox indicators.

3.8 Large Scale Hydrochemical Investigations

In order to get an idea of the variations in the groundwater and production well chemistry on a larger scale, a joint sampling campaign of the Free University of Berlin and BWB was conducted together in spring 2003. All production wells operating at the time of the well galleries Hohenzollernkanal and Saatwinkel as well as surface water and available groundwater observation wells in the area were sampled (Figure 119).

The sampling was done in order to evaluate the following questions:

What are the hydrochemical properties and the variability of the background groundwater in the surrounding of the well triangle?

What are the effects of variations on single production wells of the two galleries?

What is the share of artificially recharged groundwater in the individual wells?

Did condition change since the last production well sampling campaign in the area in 1999?

164
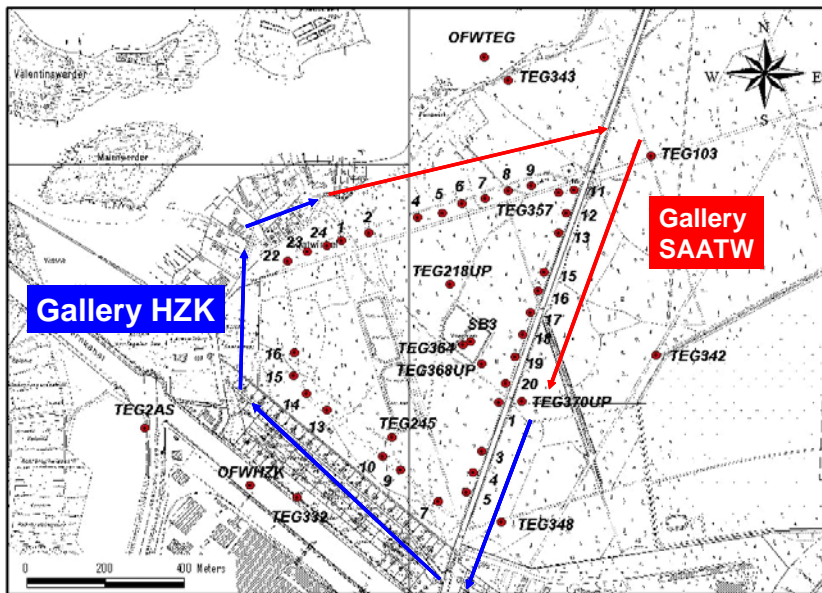
Figure 119: Production wells of the Hohenzollernkanal-Saatwinkel well triangle and surrounding observation wells sampled in spring 2003.

The production wells near the airport (SAAT 11-20; HZK 1-5) are likely to be influenced by background groundwater and artificially recharged groundwater, while the production wells oriented towards lake Tegel (HZK 22-24; SAAT 1-9) should be a mixture of Lake Tegel and pond water, i.e. they should contain approximately 100 % of bank filtrate. The triangle side to the south-east may contain proportions of groundwater flowing below the Hohenzollernkanal which originates from the river Havel located > 1 km west.

Figure 120 shows that the hydrochemistry of the "background" groundwater towards the airport, represented by TEG103, TEG342, TEG370UP & TEG348 is highly variable. While TEG103 and, to an extent, TEG342 represent the "typical" landside groundwater (e.g. low $\delta^{18}O$ & δD, high SO_4 & Ca, low Cl, Na, B), the $\delta^{18}O$ & δD and SO_4 values of TEG348 and TEG370UP lie within the range of those of the surface water (temporal variation of the surface water see previous chapters), indicating that there is a hydraulic connection between surface water (Hohenzollernkanal or even the Spree further south. Because there is hardly a difference between surface water and groundwater in the southern triangle, the proportion of BF can only be calculated for production wells SAAT 11-20 (Figure 120 calculated with TEG103 only) and values are probably only accurate for well 11-13, which receive water from the TEG103 direction and differ strongly from the remaining wells (lower $\delta^{18}O$ & δD, higher SO_4 & Ca, lower Cl, Na, B).

165
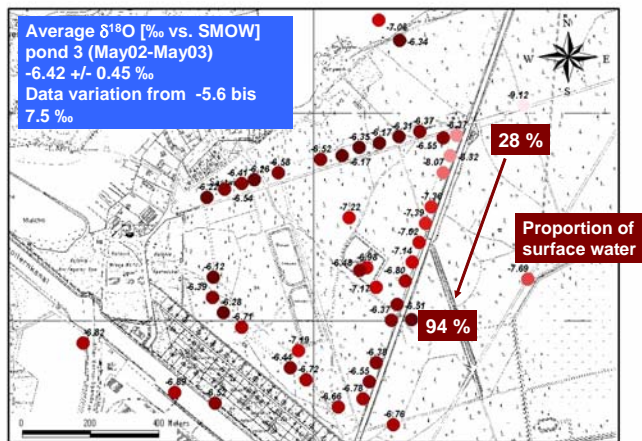
a)
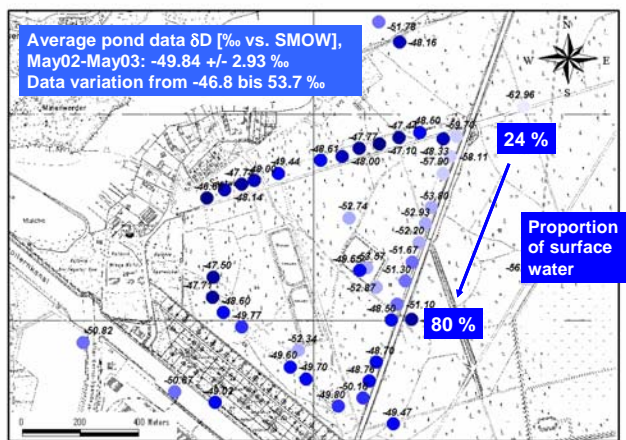
b)
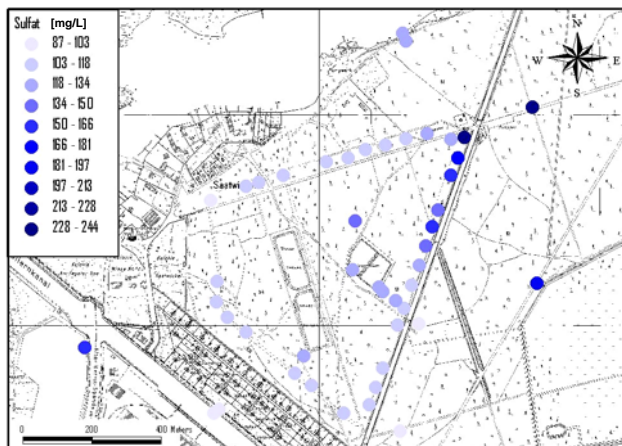
c)

Figure 120: Influence from the NE: δ^{18}O (a) & δD (b) values [‰ vs. SMOW] and sulfate concentrations, March/May 2003.
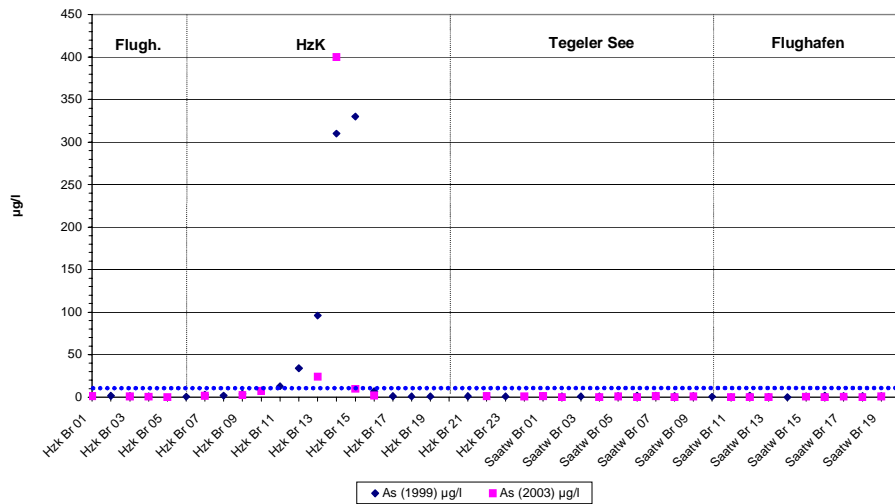
Figure 121: Arsenic concentrations in the production wells in 1999 and 2003. Blue-line: drinking water limit (data source: BWB).
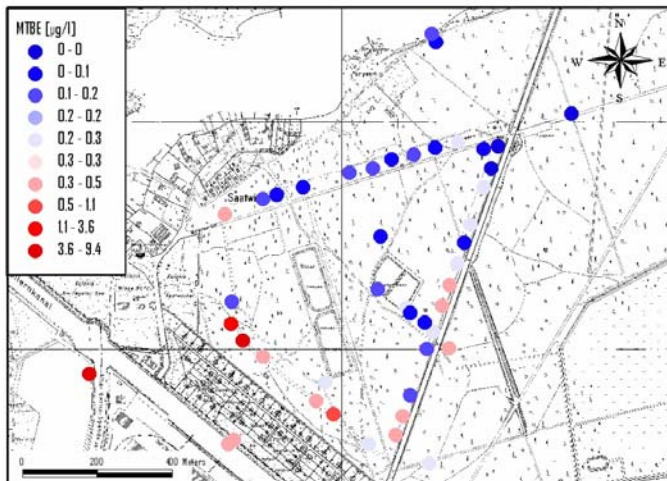
Figure 122: MTBE concentrations in samples wells in 2003 (data source: BWB).

The production wells in the south-west contain elevated concentrations of arsenic (Figure 121, exceeding the drinking water limit), MTBE (Figure 122), phenazone (Figure 123a), AMDOPH (Figure 123b) and EDTA, clearly originating from the south-western side of the Hohenzollernkanal, where highest concentrations are found in TEGAS2. As and MTBE origi-nate from different contaminated industrial sites west of TEGAS2. The As pollution is known by BWB and As is removed during drinking water treatment (personal communication BWB).

While highest phenazone and AMDOPH concentrations are found in the south-west, highest propyphenazone (analgesic/anti-inflammatory) concentrations are found in the south-west and in the north, towards Lake Tegel. The phenazone-type pharmaceuticals and related substances originate from the surface water, where their presence is caused by their discharge from WWTP (Heberer, 2002) or from former production spills of a pharmaceutical plant near Oranienburg on the Upper Havel, which produced phenazone-type pharmaceuticals. Reddersen et al. (2002) suspected that spills of the plant released into the environment in the past, when regulations were less strict, are the cause of some of today's findings of PhAC residues. Because of the pharmaceutical plant, phenazone and dimethylaminophenazone (not detected) concentrations in the surface water of the Upper Havel were probably considerably higher in the past decades than they are today (exact values are not known). In addition, the production of dimethylaminophenazone was stopped in 1978 (Reddersen et al., 2002). Therefore, the high concentrations of phenazone and AMDOPH in the south-west indicate that the groundwater is probably older bank filtrate (similar to findings in greater depth at the bank filtration transects, where high phenazone and AMDOPH concentrations always corresponded to an older age of the bank filtrate). It infiltrated from the Upper Havel 1-2 km further west, passed the industrial contamination sites (thereby accumulating As, MTBE etc.) and is now abstracted by the production wells with a considerable time lag of a few years to a few decades. In addition, it appears that the share of "older" BF containing phenazone and, in particular, AMDOPH is getting larger with depth at all investigated sites (Figure 111 and previous BF chapters)
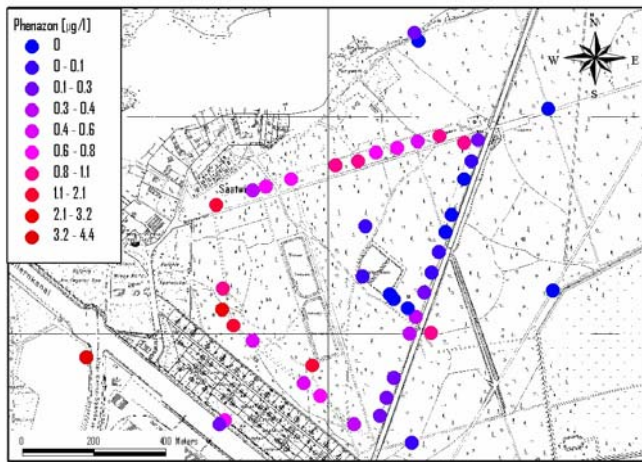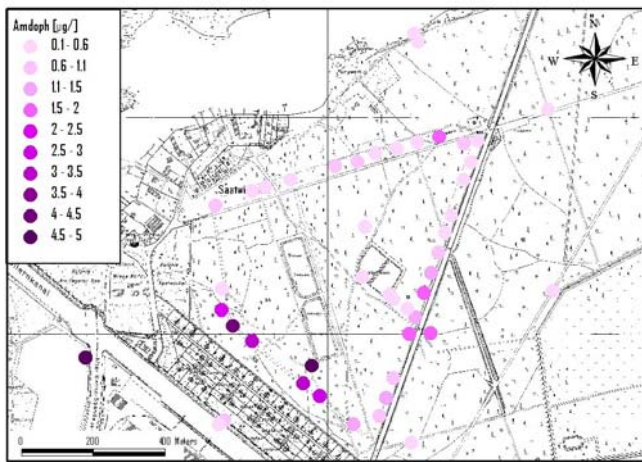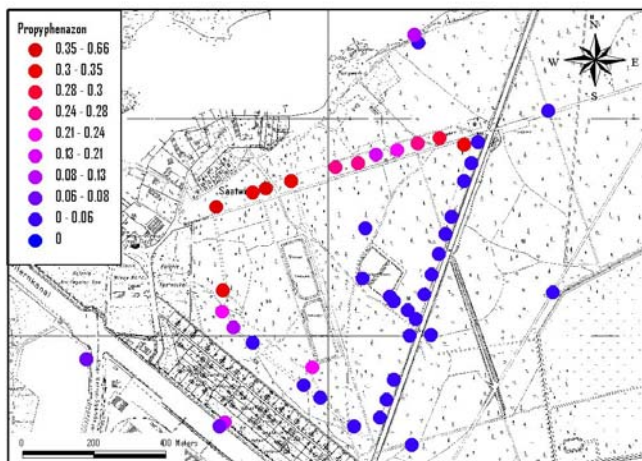
Figure 123: Phenazone-type pharmaceuticals and residues phenazone (a), AMDOPH (b) & propyphena-zone(c). Data source: BWB.

The higher propyphenazone concentrations towards Lake Tegel, where travel times should be in the order of magnitude of a few months suggest that it is presently brought in with the treated WW, thereby representing "younger" bank-filtrate. Approximate input pathways in the area are shown in Figure 124.
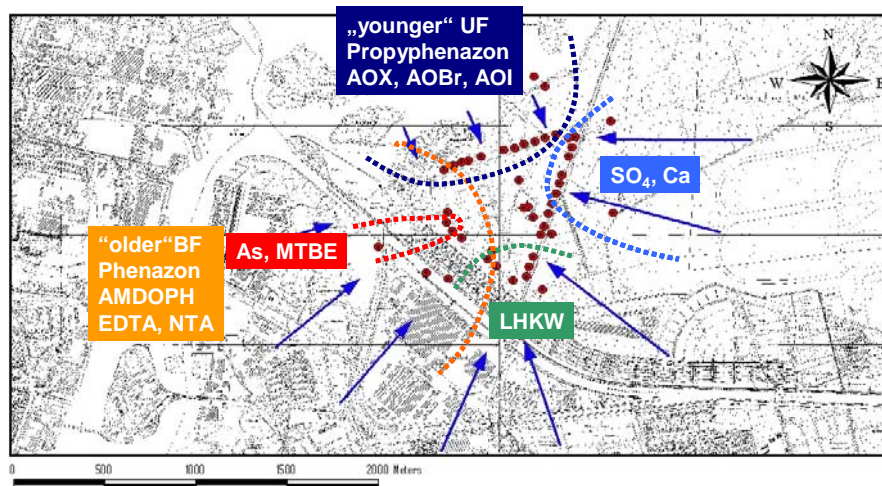
Figure 124: Summarising the major input paths for various water constituents in the area of the recharge ponds.

3.9 Major conclusions & summary of GWA Tegel Site

3.9.1 Operation/Clogging layer

- The hydraulic and hydrochemical conditions during artificial recharge are highly transient.
- The infiltration capacity varies in relation to the changes of the hydraulic conductivity of the pond bottom sediments.
- The pond bottom is covered with sand which are removed regularly and washed in order to restore the infiltration capacity by removal of finer grained material and algae.

3.9.2 Travel times/ age

Travel times from the pond to the observation well at the transect are short and vary between a few days to observation wells below the pond to ~ 50 days to production well 20.

None of the wells between the pond and production well 20 contain a share of "older" bank filtrate.

3.9.3   Mixing

The observation wells within the well triangle contain 100 % of artificially recharged water from the pond with a residence time of less than 50 days.

The production well 20 abstracts > 80 % BF.

Within the entire production well triangle proportions of BF vary largely between 25 % (north-eastern corner of the triangle) and 100 % in the west.

3.9.4   Hydrochemistry

- The redox conditions are influenced by seasonal temperature changes and changes between saturated and unsaturated conditions below the pond.

- The large temperature variations of ~ 25°C of the infiltrate have the greatest effect on the distribution of redox indicators in the groundwater. Above temperatures of approximately 14 °C, the redox conditions turn anoxic within hours to days of travel time, while oxic conditions prevail along the entire transect at temperatures below 14 °C.

- The hydraulic conditions (saturated/unsaturated below the pond) alternate at short time intervals and have a minor additional influence on the redox regime. A secondary effect of the cyclic operational changes is the oxidation of particulate organic matter caused by the presence of gaseous O_2 below the pond during unsaturated phases, which leads to calcite dissolution reflected by elevated concentrations of Ca^{2+} and HCO_3^-.

- The redox conditions, in turn, appear to affect the behaviour of a number of phenazone type PhACs. The removal of phenazone, and possibly also FAA and AAA is not complete at the absence of oxygen.

- The background groundwater variations are large, both in horizontal and in vertical direction.

In the SW, the concentrations of As and MTBE are very high, because of several old contamination sites south-west of the Hohenzollernkanal.

Elevated concentrations of phenazone and AMDOPH in the south–west originate from bank filtration at a time, when surface water concentrations of these substances were considerably higher (typical "old" bank filtrate).

3.10 Major differences between the artificial recharge site and the bank filtration sites

3.10.1 Differences

- At the AR site, the clogging layer is removed regularly; the natural lakes are covered with thick layers of low permeability laccustrine sappropels and clogged sands at the lake shores; unlike at the AR site, these layers are never removed artificially.
- At the BF sites infiltration takes place only at the clogged lake shores while at the AR site, infiltration occurs everywhere.
- At the AR site, the travel times are shorter; However, this may be site specific for our transects (even though the difference in the clogging layer suggests it could be a general trend).
- The most important difference is the lack of the vertical age stratification encountered at both BF sites, suggesting that this is a "real" difference and not only site specific for our transects (the suspected cause is the difference in the pond/lake base)
- Due to this stratification into 2 (or more, compare hydraulic models) BF types of different origin and age, the production wells themselves differ from each other with regard to their hydrochemistry.
- Overall and in average, the BF sites are more reducing, the infiltrate reaches ferrous / postoxic conditions before the production well at all times.
- The different redox conditions affect redox sensitive species, e.g. Phenazone, AOX and others.
- Depending on the substance, its elimination is favored at more anaerobic (AOX, BF site) or aerobic conditions (phenzone, AR site).

3.10.2 Similarities

- The artificial recharge site resembles the bank filtration sites with regard to the sediment characteristics. Production and observation wells are screened in the same Pleistocene glacio-fluvial porous aquifer with a thickness ~40 m (with the exception of the Wannsee site, where the production wells are also screened in deeper aquifers); the aquifer is partly divided by patches of glacial till, but the contact to deeper aquifer parts is never restricted.
- The surface water quality is similar.

- Both sites reveal a distinct and seasonally variable redox zoning, only because of the shorter travel times are conditions towards the production wells more reducing at the BF sites.

3.11   References

Appelo, C.A.J. and Postma, D., 1996. Geochemistry, groundwater and pollution. A.A. Balkema, Rotterdam.

Bouwer, H., 2002. Artificial recharge of groundwater: Hydrology and engineering. Hydrogeol. J., 10(1): 121-142.

Carrera, J., Vicent, T. Lafuente, F.J., 2003. Influence of temperature on denitrification of an industrial high-strength nitrogen wastewater in a two-sludge system. Water SA, 29: 11-16.

David, M.B., Gentry, L. G., Smith, K. M. Kovacic, D. A., 1997. Carbon, Plant, and Temperature Control of Nitrate Removal from Wetland Mesocosms. Transactions of the Illinois State Academy of Science, 90(3 and 4): 103-112.

Greskowiak, J. et al., 2005. The impact of variably saturated conditions on hydrogeochemical changes during artificial recharge of groundwater. Appl. Geochem., 20: 1409-1426.

Grünheid, S., Amy, G., Jekel, M., 2005. Removal of bulk dissolved organic carbon (DOC) and trace organic compounds by bank filtration and artificial recharge. Water Research, 39(14): 3219-3228.

Haeffner, H., Detay, M. and Bersillon, J.L., 1998., 1998. Sustainable groundwater management using artificial re-charge in Paris region. In: J.H. Peters (Editor), Artificial Recharge of Groundwater. A.A. Balkema, Amsterdam, pp. 9-14.

Hannappel, S., Asbrand, M., 2002. Entwicklung eines Hydrogeologischen Modells im unterirdischen Einzugsgebiet eines Wasserwerks im Lockergestein. Schriftenreihe der Deutschen Geologischen Gesellschaft, 24: 55-68.

Heberer, T., 2002. Tracking persistent pharmaceutical residues from municipal sewage to drinking water. Journal of Hydrology, 266(3-4): 175-189.

Massmann, G. et al., subm. The impact of variable temperatures on the redox conditions and the behaviour of pharmaceutical residues during artificial recharge. J. Hydrol.

Okubo, T. and Matsumoto, J., 1983. Biological clogging of sand and changes of organic constituents during artificial recharge. Water Res., 17(7): 813-821.

Olivie-Lauquet, G. et al., 2001. Release Of Trace Elements In Wetlands: Role Of Seasonal Variability. Wat. Res., 35(4): 943-952.

Prommer, H. and Stuyfzand, P., 2005. Identification of Temperature-Dependent Water Quality Changes during a Deep Well Injection Experiment in a Pyritic Aquifer. Environ. Sci. and Technol., 39(7): 2200-2209.

Reddersen, K., Heberer, T. and Dünnbier, U., 2002. Identification and significance of phenazone drugs and their metabolites in ground- and drinking water. Chemosphere, 49: 539-544.

Schuh, W.M., 1990. Seasonal variation of clogging of an artificial recharge basin in a northern climate. J. Hydol., 121: 193-215.

van Cappellen, P. and Wang, Y., 1996. Cycling of iron and manganese in surface sediments: A general theory for the coupled transport and reaction of carbon, oxygen, nitrogen, sulfur, iron, and manganese. American Journal of Science, 296: 197-243.

Table 9: Age dating results from all sites, analysed at the Institute for Environmental Physics, University of Bremen.

Well ID	Site	T [TU]	$^3\text{He}_{tri}$ [TU]	"stable" T [TU]	T/He age [years]
BR20	GWA Tegel	10.69	1.52	12.21	2.39
BR20	GWA Tegel	10.69	1.40	12.09	2.21
TEG342	GWA Tegel	12.12	43.45	55.58	27.30
TEG342	GWA Tegel	12.12	44.10	56.22	27.51
TEG3690P	GWA Tegel	10.54	-0.03	10.51	-0.05
TEG369UP	GWA Tegel	10.91	-0.04	10.87	-0.06
TEG369UP	GWA Tegel	10.91	0.10	11.01	0.17
TEG3700P	GWA Tegel	11.09	0.85	11.94	1.32
TEG3700P	GWA Tegel	11.09	1.25	12.34	1.91
TEG370UP	GWA Tegel	10.00	2.69	12.69	4.28
TEG368	GWA Tegel	8.47	0.16	8.63	0.34
TEG368	GWA Tegel	8.47	0.22	8.69	0.46
TEG373	GWA Tegel	9.29	7.90	17.19	10.93
TEG373	GWA Tegel	9.29	6.65	15.94	9.60
BR13	TS Tegel	12.12	12.49	24.61	12.71
BR13	TS Tegel	12.12	12.52	24.64	12.73
3301	TS Tegel	11.17	1.04	12.21	1.59
3301	TS Tegel	11.17	1.20	12.37	1.83
3303	TS Tegel	10.95	-0.17	10.78	-0.28
3304	TS Tegel	12.64	12.07	24.70	12.02
3304	TS Tegel	12.64	11.81	24.44	11.83
TEG3710P	TS Tegel	10.05	-0.13	9.93	-0.23
TEG3710P	TS Tegel	10.05	0.32	10.37	0.56
TEG374	TS Tegel	10.60	32.51	43.11	24.94
TEG374	TS Tegel	10.60	32.31	42.91	24.85
OFWBEE	TS Wannsee	10.64			0.00
3332	TS Wannsee 1	0.02	0.00	0.02	100.00
3334	TS Wannsee 1	0.03	1.08	1.11	65.53
3335	TS Wannsee 1	11.12	0.00	11.05	0.00
3336	TS Wannsee 1	0.02	4.48	4.49	99.40
3337	TS Wannsee 1	10.75	0.00	10.78	0.00
3338	TS Wannsee 1	10.94			
3339	TS Wannsee 1	11.15	0.00	11.15	0.00
BR4	TS Wannsee 1	2.41	8.01	10.42	26.23
BR4	TS Wannsee 1	2.41	6.65	9.07	23.73
3332	TS Wannsee 1	0.02	0.26	0.28	47.73
BEE202UP	TS Wannsee 2	9.39	8.27	17.66	11.33
BEE202UP	TS Wannsee 2	9.48	8.27	17.75	11.25
BEE202UP	TS Wannsee 2	9.39	7.16	16.55	10.16
BEE202UP	TS Wannsee 2	9.48	7.15	16.64	10.08
BEE203	TS Wannsee 2	9.24	-0.79	8.45	0.00
BEE203	TS Wannsee 2	8.78	-0.78	8.00	0.00
BEE204UP	TS Wannsee 2	13.97	15.76	29.73	13.54
BEE204UP	TS Wannsee 2	13.97	17.36	31.34	14.48
BEE202OP	TS Wannsee 2	8.99	-1.75	7.24	0.00
BEE202OP	TS Wannsee 2	8.80	-1.75	7.06	0.00
BEE202OP	TS Wannsee 2	8.99	-1.98	7.01	0.00
BEE202OP	TS Wannsee 2	8.80	-1.97	6.83	0.00
BEE202MP1	TS Wannsee 2	9.16	2.02	11.18	3.58
BEE202MP1	TS Wannsee 2	9.16	1.34	10.50	2.45
BEE202MP2	TS Wannsee 2	9.18	6.20	15.38	9.25
BEE202MP2	TS Wannsee 2	9.10	6.20	15.30	9.32
BR3	TS Wannsee 2	7.63	9.03	16.66	14.00
BR3	TS Wannsee 2	7.63	8.29	15.93	13.19

Table 10: Data of δ^{34}S (‰ vs. CDT) and δ^{18}O (‰ vs. V-SMOW) of sulfate at all sites, analysed at the Institute of Mineralogy of the Technical University Bergakademie Freiberg.

Well ID	Origin	Date	$\delta^{18}O_{V-SMOW}$ ‰	$\delta^{34}S_{CDT\ DELTA\ PLUS}$ ‰
TEG 365	GWA Tegel	July 2004	8.0	4.9
TEG 366	GWA Tegel	July 2004	8.9	4.9
OFWGWA	pond 3 water	July 2004	8.0	4.8
OFWTEG	surface water Lake Tegel	21.07.04	7.8	5.0
OFW-WS-11	surface water Lake Wannsee	17.03.04	6.6	4.2
OFW-WS 6	surface water Lake Wannsee	17.03.04	8.0	4.1
OFWBEE	surface water Lake Wannsee	15.03.04	7.4	4.1
3304	TS Tegel	20.07.04	7.6	4.1
TEG371OP	TS Tegel	20.07.04	8.6	5.4
3301	TS Tegel	20.07.04	8.9	3.5
3302	TS Tegel	20.07.04	8.5	5.8
3303	TS Tegel	21.07.04	7.8	3.8
TEG374	TS Tegel	21.07.04	12.5	8.4
BR13	TS Tegel	20.07.04	8.8	4.7
3337	TS Wannsee	16.03.04	7.5	3.9
3336	TS Wannsee 1	16.03.04	17.3	49.5
3334	TS Wannsee 1	16.03.04	not enough sulfate	not enough sulfate
3332	TS Wannsee 1	18.03.04	not enough sulfate	not enough sulfate
BR4	TS Wannsee 1	16.03.04	15.0	18.0
BEE200UP	TS Wannsee 2	16.03.04	0.9	-5.3
BEE204UP	TS Wannsee 2	16.03.04	3.5	-2.7
BEE204OP	TS Wannsee 2	16.03.04	0.8	-6.1
BEE201UP	TS Wannsee 2	16.03.04	9.5	7.4
BEE202UP	TS Wannsee 2	18.03.04	9.5	7.3
BEE202OP	TS Wannsee 2	18.03.04	7.3	4.3
BEE205	TS Wannsee 2	21.07.04	8.3	7.5
BEE206	TS Wannsee 2	21.07.04	11.7	12.6
BR3	TS Wannsee 2	18.03.04	7.3	3.3

2

"Integrated modelling concepts for bank filtration processes: coupled ground water transport and biogeochemical reactions"

"model" group: Institute for Ecohydrology and Inland Fisheries

Responsible project leader: Prof. Dr. Gunnar Nützmann

Content

List of Figures

List of Tables

1. Lake Tegel Bank filtration site

1.1. Objectives

The main objective of this part of the NASRI project was the modelling of hydraulic and hydrogeochemical processes during bank filtration at the Lake Tegel test site. Based on hydrogeological, geo- and hydrochemical investigations (see the chapter above) numerical models are used in order to understand the time-dependent and spatial distributed flow and transport regimes in the vicinity of well galleries taking into account the natural conditions and anthropogenic influences, e. g. pumping regimes. These models should be sufficiently correct to allow an integration and interpretation of the measured data including a predictive analysis. On the other hand, they should be simple enough to really be used in order to optimise the operational scheme.

The focus of this study is divided into two parts: (a) modelling of spatially and temporally changing three-dimensional flow structures to identify flow paths and water budgets for transport modelling; (b) development of a conceptual reactive transport model for the Lake Tegel test site in order to identify and verify observed time series of water chemistry and quality depending on transient water flow paths and velocities. Because the infiltration behaviour of the Lake Tegel sediments has shown effects, which can not be explained by the common used description of groundwater flow mechanisms only, some possible physical effects were considered, e. g. the dependence of viscosity and/or leakance on water temperature. Then, integrated flow and reactive transport modelling allows to evaluate the relation between transient groundwater movement and hydrogeochemical processes.

Beside others, the main objective of the project phase was to get a detailed and complex hydraulic model of the test site and based on that, development of a conceptual understanding of the hydro- and geochemical reactions at the Lake Tegel field-test site.

The key questions dealt with were:

What are the flow paths and travel time distributions dependent on continuously changing pumping regimes and bank sediment properties?

What is the proportion of bank-filtrate and landside groundwater in the production wells?

What are the dynamic hydrochemical conditions at the test site, in particular with regard to redox conditions?

Which chemical reaction network can be identified?

The combination of these questions is important because only with the knowledge of the spatialdistribution and dynamics of the processes studied,understanding of the predominant hydraulic mechanisms is possible. Furthermore, it is important to understand and to quantify

the behaviour of specific substances studied by all working groups, relating these to field conditions present at the transect at Lake Tegel.

1.2. Methods

1.1.1. Computational Methods

MODFLOW is a well-known finite difference groundwater flow model. It was developed by the US Geological Survey (USGS) in 1988 (McDonald et. al 1988) as a modular and extensible simulation tool for modeling groundwater. Since 1988 it has been developed continuously, for this study MODFLOW 2000 (Harbaugh et al. 2000) is applied. MT3DMS (Zheng et al. 1998) is based on the MODFLOW suite and is used for conservative tracer and heat transport calculations. Water budgets are calculated with PMWBLF (Harbaugh 1990). PHT3D (see below) also uses the MODFLOW-MT3DMS suite.

PEST (Doherty 2004) is a program for nonlinear parameter estimation. PEST was coupled to MODFLOW which results in more precise calibrations with less effort.

The subprogram to calculate steady-state water balance from MODFLOW was extended to transient water balance. Several tools, either as subprogram/macro or as executable had been developed in order to handle the huge amount of data. The MODFLOW code had been extended to include temporal variable parameters in the reservoir package.

PHREEQC (Parkhurst & Appelo, 1999) is a widespread, well documented geochemical software package originating from the software package PHREEQE (Parkhurst et al., 1980) which consideres aqueous chemical equilibrium and batch reactions as mineral precipitation/dissolution, ion exchange, 1D transport, and kinetics.

During the last years reactive transport packages with interfaces to PHREEQC (Parkhurst & Appelo, 1999) were developed, e. g. PHAST (Parkhurst & al., 2004) which uses HST3D (Kipp, 1997) as flow/transport code, and PHT3D (Prommer, 2002) which uses MT3DMS (Zheng & Wang, 1999) as transport code and is embodied to the latest versions of the GUI Processing Modflow Pro (Chiang 2003).

The actual limitation of this software actually are Isothermal conditions during simulation, and only one reaction framework for the whole model domain.

PHT3D is chosen to model reactive transport, as it is based on the widespread Modflow suite and widespread PHREEQC and the reaction setup is highly adaptable to specific problems.

1.1.2. Measurement of infiltration

In order to obtain leakance values for infiltration, a simple in situ method is applied. Amounts of infiltrated water are measured directly under natural field conditions. A cylinder is used

which is open at the bottom and closed at the top, leaving a small hole at a flange where a hose can be put up (Figure 1).

Figure 1 Barrel used for direct infiltration measurements. The open bottom is pushed into the ground, a hose with the reservoir bag is plugged to the flange at the top.

The bottom of the cylinder is inserted a few cm into the lake bed, to the flange on the top a hose is put up (Figure 2). At the end of the hose is a water filled plastic bag acts as reservoir. The difference in volume of the reservoir bag within a defined time is equal to the amount of infiltrated water. As inside the barrel the pressure is the same as outside the water infiltrates under natural field conditions.
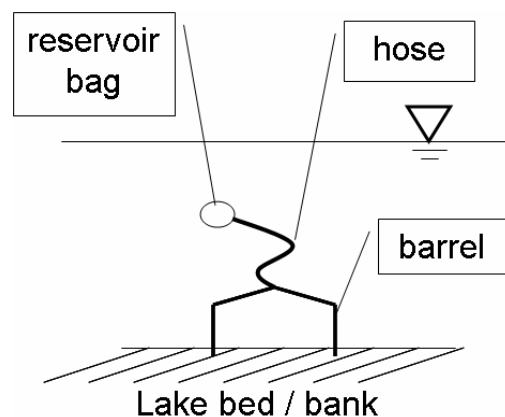
Figure 2 Vertical cross section through an infiltration barrel during infiltration measurement

1.1.3. Previous information

1.2.1.1. Previous Modelling

Models of different model concept, purpose and scale have been set up which include the transect at well 13. Although the model concepts are not adequate for answering the questions of this study, some benefit could be obtained.

(a) A steady state model by Eichhorn (2000) was set up to quantify the bank filtrate ratio, flow paths and travel times at the transect. The model is calibrated to data from June 1999, its extent is shown in Figure 3. The benefit from the model is an estimation of the kf values of the bed of Lake Tegel. Travel time information is neither detailed enough as the model is steady state nor applicable as the study is carried out for the hydraulic situation in 1999. As in this study turned out that the boundary conditions in the north, south and west are not correct and therefore the calculated flow paths are not valid.
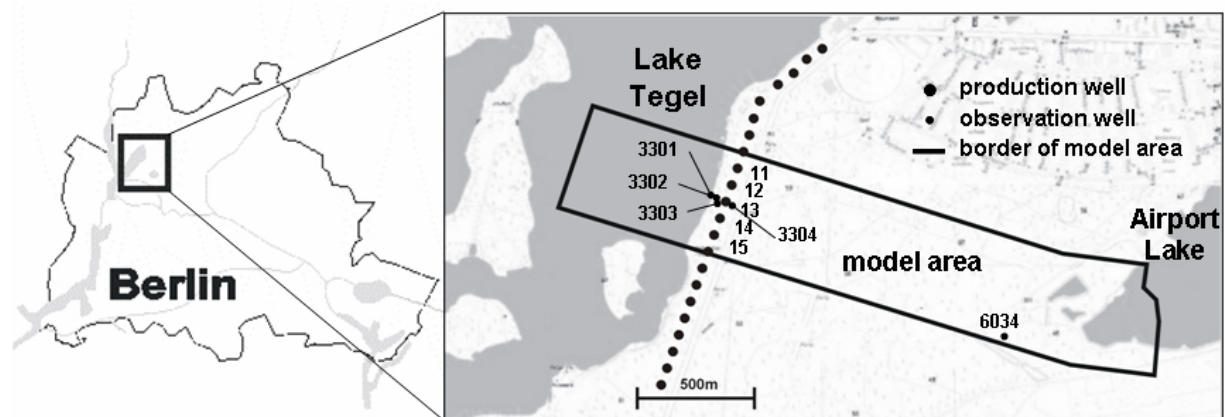
Figure 3 Model area of the steady state hydraulic Model by Eichhorn (2000)

(b) WASY (2004) set up a steady state and as well transient catchment model on behalf of BWB (see Figure 4) to evaluate the impact of different pumping scenarios on the water resources and to give recommendations for future water management. A special issue herein is the behaviour of contaminated sites. The benefit for this study is the specification of the water divides between well field West and the adjacent well fields as the no flow boundary between well field West and well field East. This model also approves the postulation of the existence of old bank filtrate at the bottom of the main aquifer Massmann (personal communication). According to WASY (2004) this water infiltrated at the eastern bank of Scharfenberg (Figure 7) and at the western bank of Lake Tegel at the height of well field North.

The model is calibrated steady state to selected data of 2002, and run transient for 2002 as well. This period is much shorter than the sampling period of the NASRI project (May 2002 - September 2004) and not sufficient to detect long term effects. The temporal and spatial discretisation is too coarse to give a detailed description of the transect, besides the model is too bulky/extensive and hardly manageable for this purpose. The reactive transport potentials of FEFLOW (Diersch 2002) are not as sophisticated as MODFLOW-PHT3D (Prommer 2002).
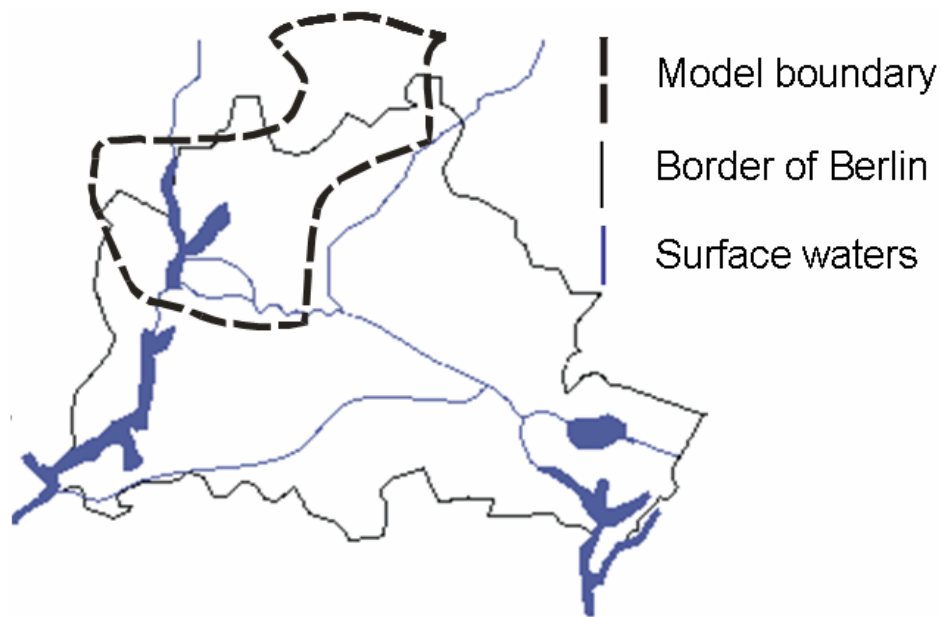
Figure 4 Model area of the model catchment (dashed line) for WW Tegel and Spandau set up by WASY GmbH 2004

(c) Rümmler (2003) and Wiese et al (2004) set up a transient two-dimensional model to assess the effects of oscillating pumping regimes on bank filtrate with approximated field conditions (see Figure 5). With this model the leakance factor could be roughly estimated. Though representing a hypothetical well field operation mode, the pumping rates are within real range and it could be detected that the boundary conditions as shown in Figure 5are not correct, that the model area has to be enlarged towards north, west and south. It is developed to the model presented in this report.
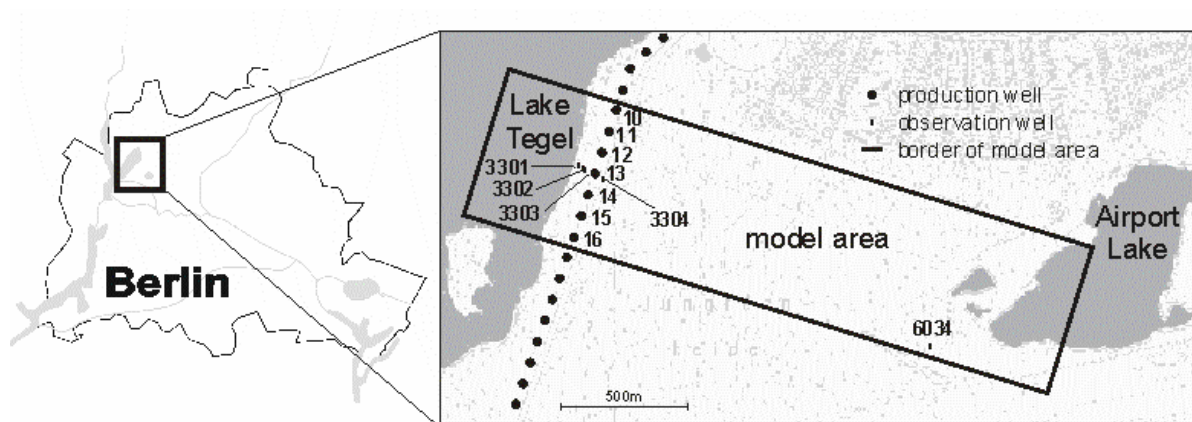
Figure 5 Model area of Rümmler (2003) and Wiese et. al. (2004)

Lake Tegel and the aquifers in the region are sandy formation formed during quarternary Saale ice-age. Lake Tegel (Figure 7) has maximum depth of 17m, with the deeper regions already being filled up with thick sediments and mud, decreasing and vanishing towards the shore (Brühl et al. 1986, Pachur et al. 1977). The two upper aquifers are important for the well field West, sealed to the bottom by thick Pleistocene mud and silt layers. (Pachur et. al. 1977) The main aquifer, where the wells are screened, is about 30 m thick and predominantly covered by glacial till of about 4 m thickness. The upper aquifer is about 10 m thick, half of which is saturated. The aquifers consist of glaciofluviatile fine to coarse sands resulting in a range of k_f values between 10^{-4} to $5*10^{-4}$. (Fugro 2000). At the transect the analysis of sieve curves resulted in mean k_f values of $2.9*10^{-4}$ for the aquifer (Fritz, personal communication). A vertical cross section of the transect was set up by the group Hydrogeo. A tertiary fine sand aquifer with 70 m thickness lies below, although separated by 20 to 30 m thick glaciofluvial silt and clay, piezometric heads and present modelling suggest that connections to the second aquifer exist.

The airport lake (Figure 7) has a depth of 40 m and thus penetrates both upper aquifers. For further information see HSM Tegel (Hydrogeologic Structural Model), Fugro 2000.

The bathimetry of Lake Tegel is available, the origin of the data is not known.

Sieve analyses of the lake bottom in front of the transect (Sievers 2001) result in k_f values of $5.4*10^{-6}$ m/s for the upper 12 cm.

1.3. Modelling

Two ways have been chosen in order to increase our knowledge of the test sites by means of modelling. Hydraulics was modelled separately to geochemistry but unexpected hydraulic results and thus questions remaining unresolved made it impossible to merge the two aspects in a way which makes sense. Nevertheless, interesting results have been worked out which probably are be useful for understanding and operation of test site Tegel and bank filtration in general.

1.1.4. Hydraulic and transport modelling

1.3.1.1. Model input time series

It was intended to include all factors of possible relevance and asses their hydraulic impact. Data were collected from NASRI, BWB and the Berlin authority for urban development and environmental protection (SENSUT) and the "Institut für Geologische Wissenschaften

Fachbereich Geochemie, Hydrogeologie, Mineralogie, FU Berlin". Most of the available data were incorporated in the model:

Water levels

-from 17 observation wells and extraction wells 12 to 14 as for Lake Tegel with intervals from monthly to hourly were provided by the group Hydrogeo

-from 13 observation wells with monthly intervals in the catchment were provided by BWB

-from Lake Tegel, Airport lake and 1 observation well in the catchment with daily intervals (Jan. 1998 – May 2005) was provided by SENSUT.

Physico-chemical parameters of the transect

-Water temperature data with monthly intervals (May 2002 – Aug. 2004) for observation wells, extraction wells and Lake Tegel was provided by the group Hydrogeo. Partially hourly intervals are available

-SENSUT provided the temperature of Lake Tegel for the time before the NASRI project.

Tracer data

-Tracer Data as chloride and boron was provided by the group Hydrogeo for observation wells, extraction wells and Lake Tegel with monthly intervals (May 2002 – Aug. 2004) and by SENSUT for Lake Tegel (Jan. 1998 – May 2005)

-Monthly data (May 2002 – Apr. 2004) of the stable Isotopes 18O and 2H are provided by the group Hydrogeo.

Well data

-Daily operational hours (1999-2005), well switching times (hourly) (1999-2004), pumpage test data (2 to 4 times per year 1998-2005) were provided for well field West, monthly sums of extracted water from each well field and amounts of artificial recharge of waterworks Tegel (1993-2005) was provided by BWB.

Precipitation

Daily data of precipitation for waterworks Tegel was provided by BWB (1998-2005).

1.3.1.2. Investigation area and corresponding model set up

The area of main interest is the transect at well 13 at the well field West (Figure 7) However during the evolution of modelling, the area that has to be regarded is much larger for three reasons:

During the NASRI Project it turned out that part of the water of Well 13 is of an age of at least 10 to 15 years and infiltrated on the other side of Lake Tegel.

The ratios of extracted water, between the well fields and within well field West between the wells, may vary considerably. In order to minimise boundary effects, the model area has to be much larger than the transect.

During some periods groundwater levels at the transect are lower than the elevation where most of the infiltration from Lake Tegel occurs. This means that changes in pumping rates are not be mitigated any more by changes in infiltration and thus drawdown affects much larger regions and the catchment grows larger. The location of the well fields pertaining to waterworks Tegel is shown on

Figure 6.

The model area now includes large parts of Lake Tegel with the islands Reiswerder, Scharfenberg, Lindwerder, the entire well field West, up to the Airport lake (see Figure 7).
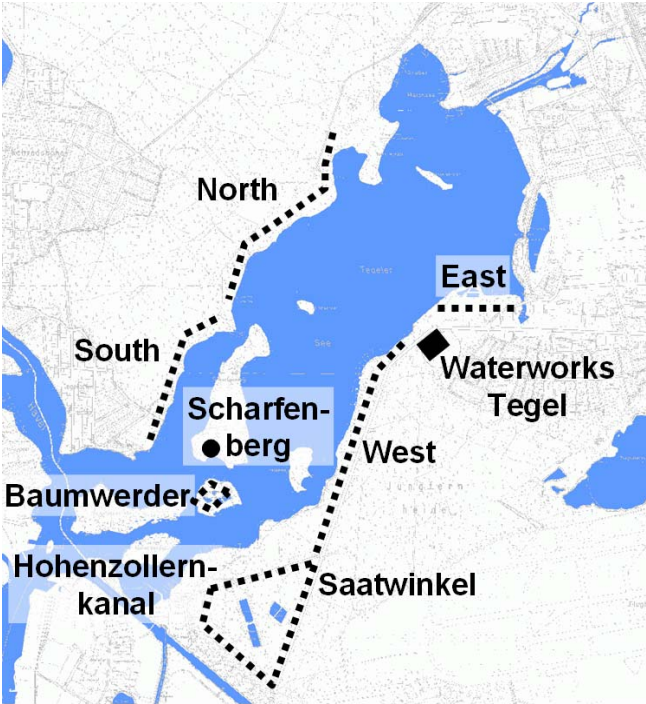
Figure 6 Location of the well fields pertaining to the waterworks Tegel. The dotted lines represent vertical abstraction wells, the black dot represents the horizontal well at Scharfenberg
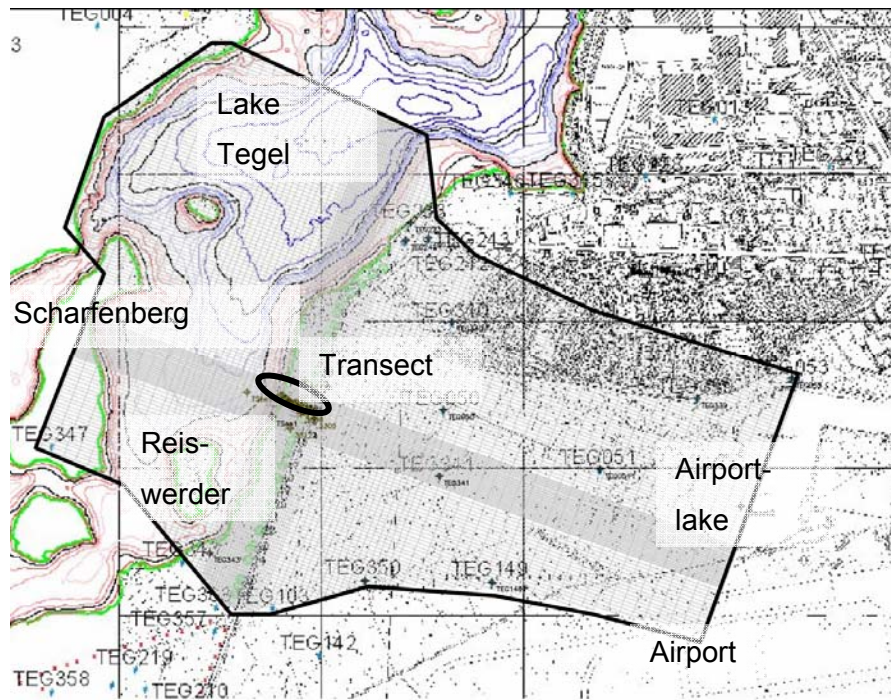
Figure 7 Extent of the hydraulic model, model cells are represented by grey lines the border by a thick black line, the bathymetry of Lake Tegel is represented by Isolines with a colour ramp from red to blue in with black 5 m intervals. Wells of the well field West are dots in green colour.

No Flow boundaries

In the north a no flow boundary is applicable, as the ratio ob abstracted water between the adjacent well field East and well field West (

Figure 6) maintains almost constant. However, modelling also showed that the not flow boundary north of well field west has to be shifted to the north, as well field West extracts water from the extended regions of shallow water next to the waterworks Tegel (Figure 8).

The lower face of the model generally is a no flow boundary, with exception of a region where contact to the underlying aquifer exists.

Specified Head boundaries

Starting from the western boundary at the location of the Airport lake and continuing clockwise the choice of boundary conditions is based of the following situation:

Western boundary: Piezometers in the model area filtered in different aquifers show that at the airport lake upper and lower aquifer have the same head, as groundwater flows mainly horizontally. So to both aquifers the same boundary condition is assigned. As this region still is under influence of the well field the boundary has to be transient. At the southern model boundary the ratio of extraction amounts between the well field West and adjacent

Saatwinkel vary by factor 3, so highly variable flow directions and water levels occur, which is respected with time variant specified head boundaries. Unfortunately it is not possible to move it farer from the well field to have at least one control piezometer in between because from the airport (Figure 8, bottom right) not data is available. On Scharfenberg a piezometer exists at the horizontal well. To avoid setting a time invariant watershed the level of the hydraulic heads is introduced as function of time. The western boundary represents the well field North. It is set to a constant head of 29 m asl. This simplification appears to be correct, as Lake Tegel sediments reach deeply into the aquifer and recharge from Lake Tegel above the boundary is considered. At Scharfenberg the situation is similar, besides modelling shows the head of the boundaries are rather insensitive parameters.
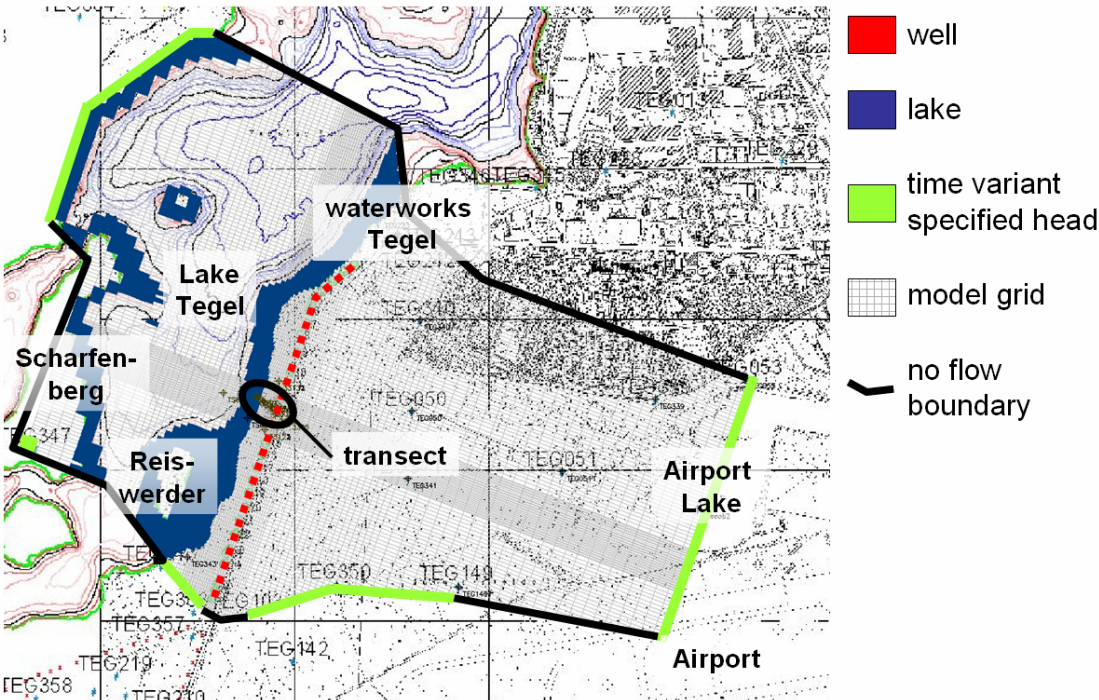
Figure 8 Top view of the boundary conditions of the model area, wells of the well field West are marked red, Lake Tegel introduced as 2nd/3rd type boundary is marked blue, time variant specified head boundaries use a pale green. Please note that boundaries are not assigned to every layer (see Fig. 9). All borders with no value assigned are "no flow" boundaries. Tiny grey lines represent the model grid.

Figure 9 Cross section of the model at well 13, wells are marked with red color, Lake Tegel as 2nd/3rd type with dark blue, leakage from the underlying aquifer by 3rd type as light blue, the eastern bourndary with pale green. All white fields belong to the aquifer, dark green represents rather impermeable material as the mud and sediments of Lake Tegel and the glacial till, respectively. All borders with no value assigned are "no flow" boundaries. Tiny grey lines represent the model grid.

Wells

Using daily well operation time and pumpage, pumping rates are calculated. Amounts are checked using the sums from the water meters and hours of well operation, both registered at the well capacity measurements which take place between 2 and 4 times a year. Wells are only filtered in the second aquifer (exemplary see Figure 9). Different pumping rates for each wells 10 to 16 are split up to the model layers according to the filter depth as, vertical flow might affect the conditions at the transect. For the other wells, due to the distance to the transect, the Dupuit assumption is used the pumping rates are split according to the layer thickness.

Bottom water

Piezometric heads from the 3rd aquifer (below the model, see Figure 9) show hydraulic contact to the second aquifer, expecially pronounced west of the airport lake. Geological profiles and drilling profiles show a glacial trough in this area. Flow direction is from the third to the second aquifer. Though the extent and place of the recharge area can not be located exactly, the amount of intruding water is calibrated.

Lake Tegel

Characteristics of infiltration of lake water to the aquifer are widely unknown. The parametrisation of the boundary condition presented here is result of model calibration. Sievers (2001) showed that sulfate is reduced within the upper cm of mud. As sulfate

concentrations are almost the same in Lake Tegel and the adjacend groundwater, it is a strong indication that mud inhibits infiltration of lake water. Thus infiltration is assigned only to the shallow regions (>25 m above sea level, surface water level is approximately 31.3 m above sea level, as the bathymetry is known). As further simplification regions with the same elevation are assumed to have the same leakance factors. The temporal behaviour of the leakance factor as well as the distribution of the leakance factor by water depth are estimated by inverse modelling using the software PEST. As the temporal behaviour is estimated as well as the distribution of the leakance by depth, different parameter combinations result in an almost equally good model fit. The Figures Figure 10 and Figure 11 show exemplarily such a parameterisation.

In comparison to a k_f value the leakage has the advantage to include the unknown thickness of the clogging layer, so two unknown parameters which have to be estimated are lumped thus only one parameter has to be estimated. The leakance is related to the k_f value according to equation 1:

$$L \ [1/s] = k_f \ [m/s] \ / \ m \ [m] \qquad (1)$$

where L is the leakance, k_f the hydraulic conductivity and m the thickness of the clogging layer.
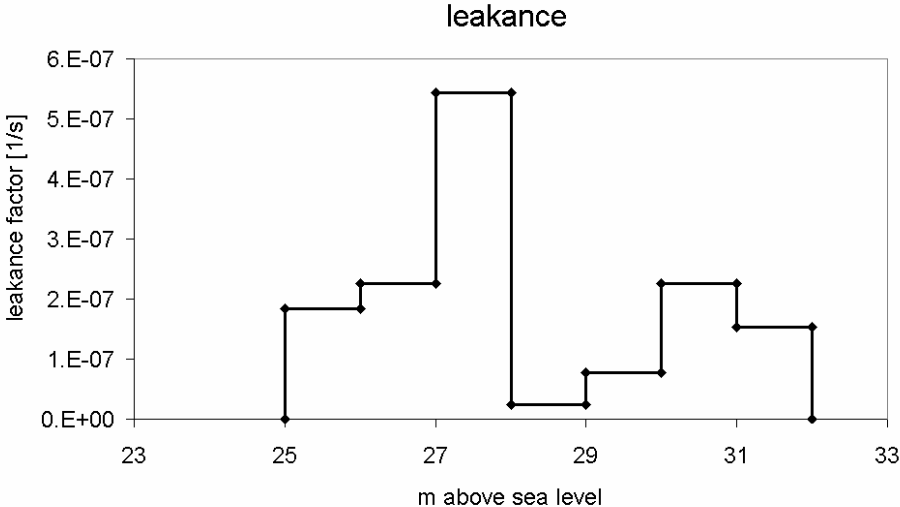
Figure 10 Distribution of the leakance according to the elevation of the bed of Lake Tegel.
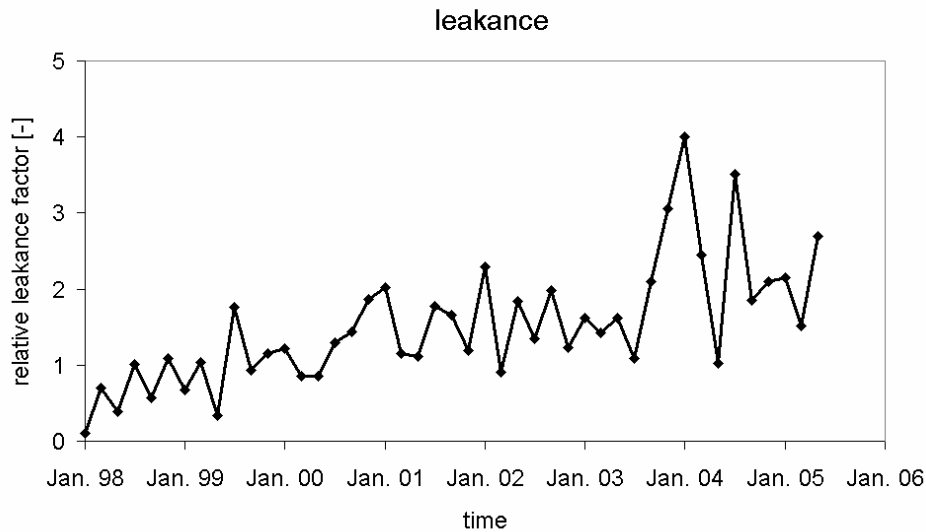
Figure 11 Relative leakance factor. The leakance values in Fig. 8 are multiplied with the relative leakance factor at each stress period.

Aquifer parameters

According to sieve analysis carried out at the transect (Fritz 2002), drilling profiles in the modelarea, and parameter estimation a homogeneous k_f value of $3.5*10^{-4}$ $m*s^{-1}$ is applied to the aquifers in the entire model. The present information does not support a reliable spatial distribution of the k_f value. Specific yield is set to 0.2, obtained by calibration of the velocity of propagation of drawdown events induced by the well field west. These values correspond with the specific yield measured near the artificial groundwater recharge site near Lake Tegel (Greskowiak 2005). The specific storage coefficient is set to $5*10^{-5}$.

Discretisation

Spatially the model is discretised in 174 rows, 117 columns, 6 layers. The rows are either 15 or 5 m wide, the columns have a width between 5 and 50 m. The layer thickness depends on the thickness of geologic formations and land surface elevation. (see Figure 8, Figure 9)

The interval between the 1. Jan. 1998 and 30. Apr. 2005 is modelled, including the entire duration of the NASRI project. Temporally the discretisation varies between the different stages of model evolution. The temporal discretisation is one week, with a 3 month steady state period at the beginning of the simulation period, in total 370 stress periods.

Results of infiltration measurements

Three measurement campaigns to measure the amount of water infiltrating to the aquifer were carried out near sampling well 3311 directly at the transect at the bank of Lake Tegel. The leakance factor is calculated according to equation 2:

$$l = (v * dl) / (h_w + dl) \quad (2)$$

where l is the leakance factor [s^{-1}], v is the infiltration velocity [m/s], dl is the thickness of the inner colmation [m] and h_w is the water depth [m]. It is assumed that the inner colmation has a water content of nealy 100% of the porespace. The thickness of the inner colmation is estimated to be 1 m (Sievers, personal commucation). The ground water level does not affect the infiltration as below the infiltration area it is lower than the lake bed resulting in atmospheric pressure.
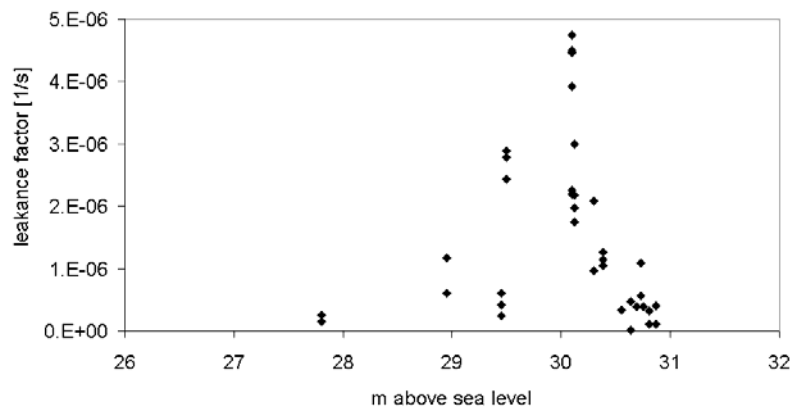
Figure 12 Leakance factor calculated according to measured infiltration rates. The depth of the lake bed is assumed to be 1 m.

The spatial variability of the leakance factor is very high. For the water depth of about 1 m, corresponding to 30.3 m above sea level, the range of infiltration is from 10^{-6} to 4.8*10^{-6} (Figure 12).

1.3.1.3. Results of flow and transport modelling

Temporal variant leakance

The leakance factor shows to vary by time. The reason for this behaviour could not be determined, but several observations suggest it increases with the pumping rate. The trend of temporally increasing leakance factor is the same for different depth distributions of the leakance factor, though some characteristics are different (Figure 13, Figure 15). Two scenarios are presented here.

In Figure 14and Figure 15 the temporal leakance factor and the leakance distribution by elevation of the lake bed are calibrated simulataneously, however the calibrated depth dependent leakance (Figure 14) seems to have too high values for the deeper water (25 to 28 m above sea level) compared with the shallow water (29 to 32 m above sea level).

The depth distribution of infiltration is set as fixed (Figure 16), according to the present assumptions about infiltration characteristics. The temporal leakance factor is calibrated (Figure 13).

As only scarce measurements of the infiltration characteristic exists (compare section 3.1.3) none of these scenarios may be preferred. But the existence a temporal variable leakance factor is confirmed.
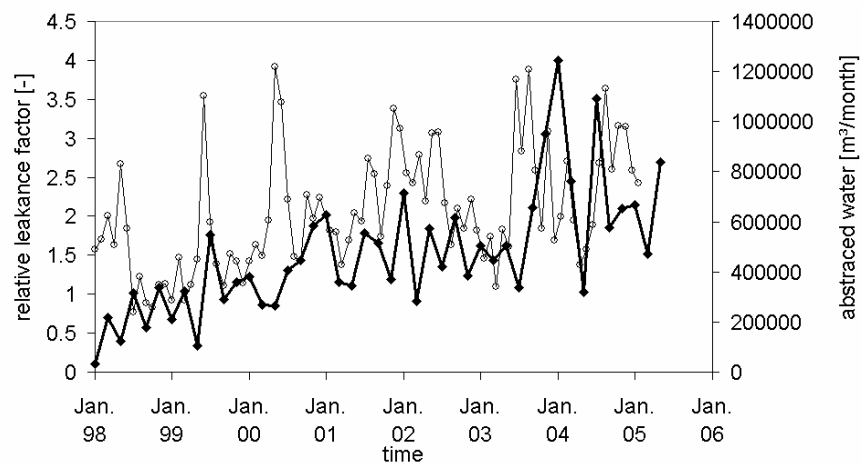
Figure 13 Calibrated relative leakance factor of the lake sediments of Lake Tegel (thick line, diamonds, left y-axis) in comparison with the monthly abstracted water from the well field west (thin line, circles, right y-axis), calibrated simultaneously with the depth dependent leakance distribution shown in Fig. 14.
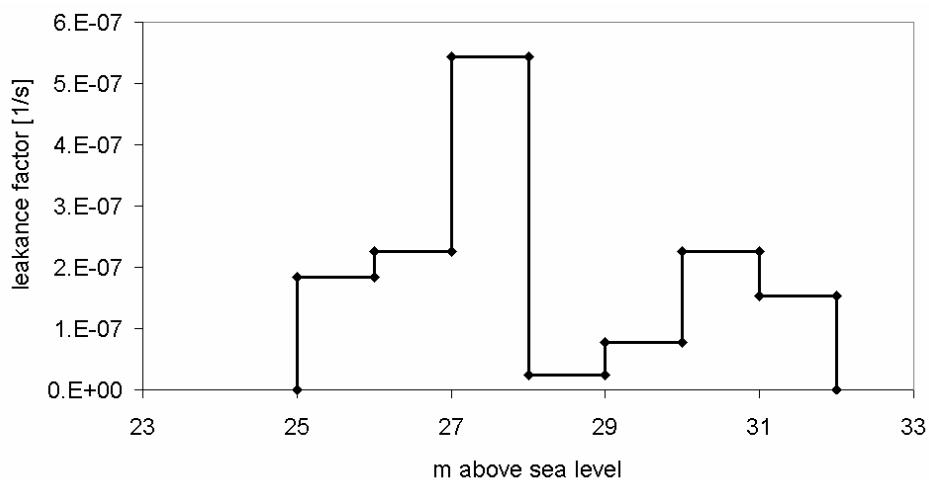
Figure 14 Calibrated distribution of the leakance factor by depth, corresponding with Fig. 13
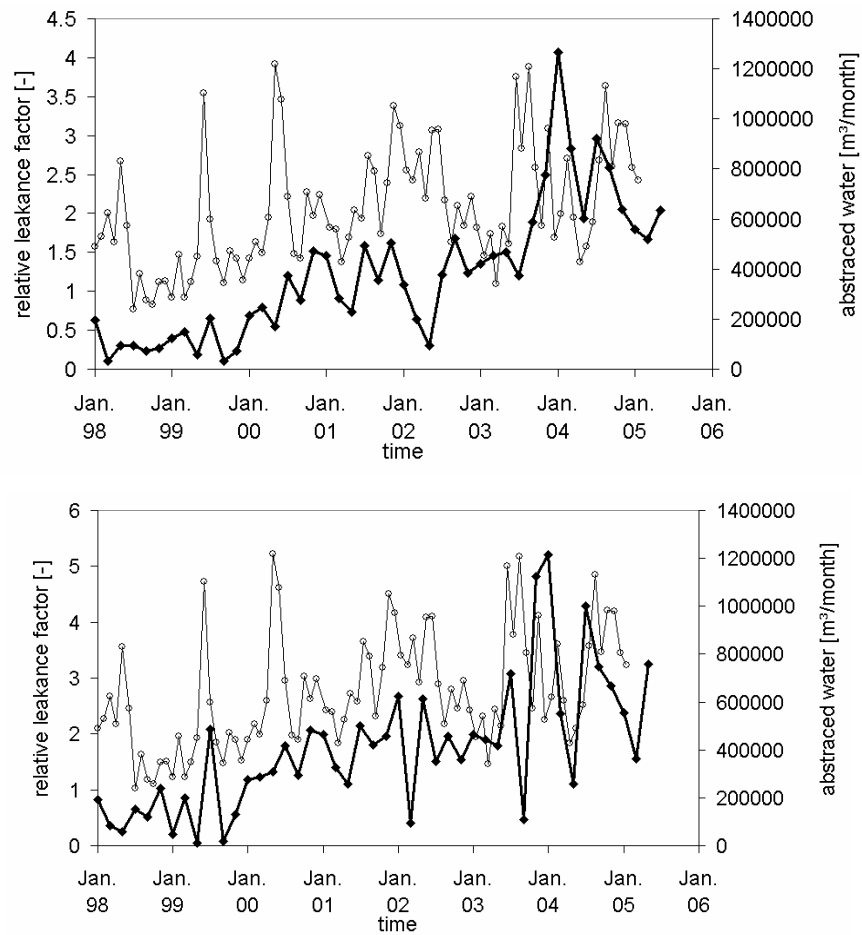
Figure 15   Calibrated relative leakance factor of the lake sediments of Lake Tegel (thick line, diamonds, left y-axis) in comparison with the monthly abstracted water from the well field west (thin line, circles, right y-axis), calibrated using the depth dependent leakance distribution of Fig. 16
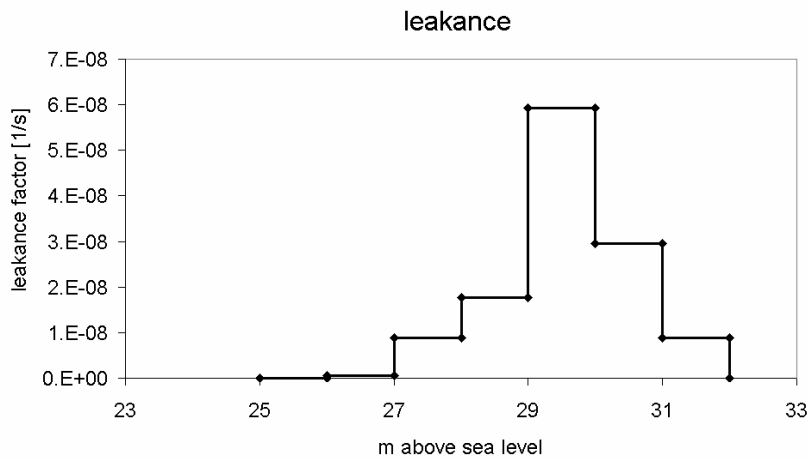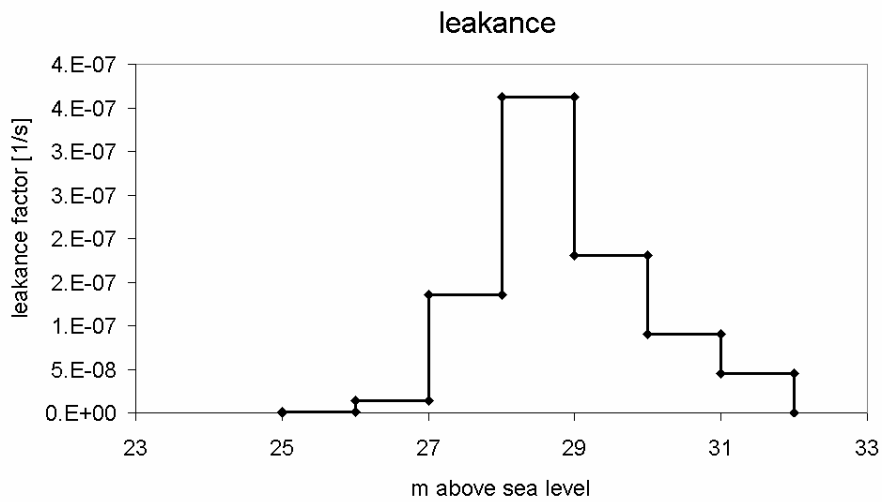
Figure 16 Hypothetical distribution of the leakance factor by depth, corresponding with Fig. 15

Comparing the relative leakance factors of Figure 15, the factor of the lower picture has higher variations than can be seen in the upper. This is a hint, the upper scenario to be closer to the real conditions than the lower. Taking also into account calibration sets the highest leakance factor to 27 to 28 m, which corresponds to a water depth of about 5 m, it seems to be likely that leakance factors tend to be highest in water depth of 4 to 6 m.

Three types of bank filtrate

The bank filtrate extracted by well 13 has 3 different origins: The top of the well gets water which infiltrated directly in front of the transect. The middle region of the well extracts water which infiltrated north of Reiswerder, the bottom extracts water which infiltrated at the shore of Scharfenberg (Figure 17). The flowfield is expressed in this way, as infiltration in the shallow regions of Lake Tegel around Reiswerder is significant.
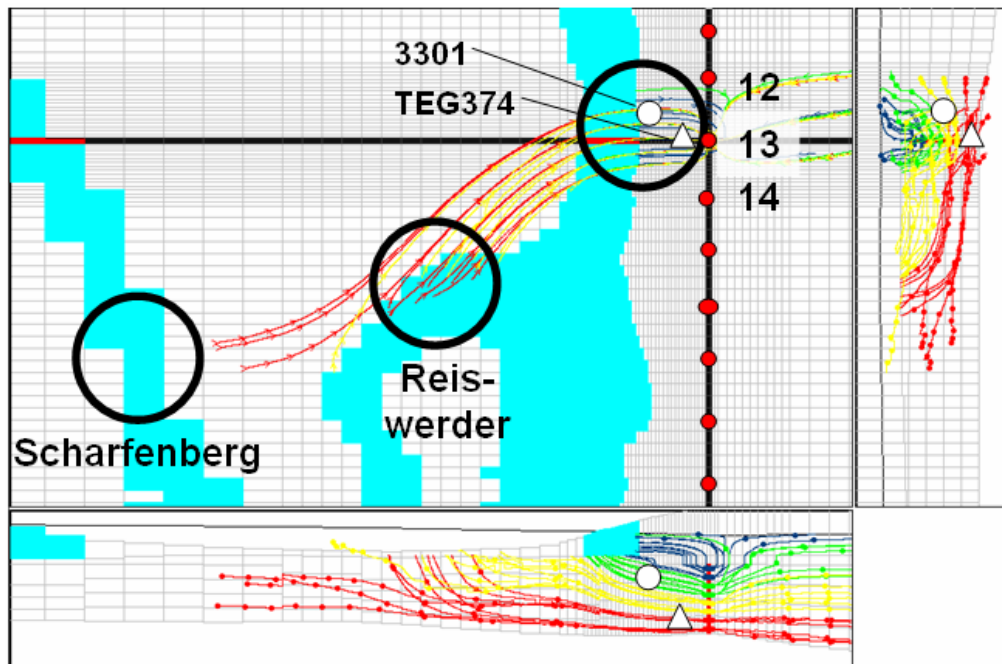
Figure 17 Backward flow lines from well 13, view from top (big image), and two cross sections along the black cross on the top view (right and bottom image). Total simulation length is 10 years, tick labels mark an interval of 1 year. The lower and right cross sections are projections along the axes of the black lines. The stationary flow field between January and March 2001 is extrapolated to the duration of 10 years. A colour ramp from blue to red is used to mark particles arriving in different depths of well 13, big black circles indicate their infiltration area. Small red circles indicate wells, the white circle indicates observation well 3301, the white triangle observation well TEG374. The grey areas indicate areas of leakage from Lake Tegel into the groundwater. The top view is a zoom of Fig. 8, well 13 lies within the transect.

This flowfield explains boron and chloride concentration measurements. Observation well 3301 shows a different water composition than the rest of the transect (NASRI 2005). At the beginning of the study period, namely in summer 2002, the latter can be seen as the concentrations of eg. chloride (Figure 18) and boron (Figure 19) being significantly higher than concentrations in Lake Tegel. Assuming a travel time of a few months, these concentrations cannot be explained. However, assuming a travel time of at least 15 month, the concentrations match the lake concentrations. Temporal variations of physico-chemical parameters in observation well TEG374, situated 2 m above the lower bound of the aquifer, can be assigned to water of about 20 month years age infiltrated north of Reiswerder, mixing

with water showing concentrations of anthropogenic substances higher than surface water concentrations during the last 15 years, which can be assigned to water which infiltrated at the western shore of Scharfenberg. The travel time can not be determined as the model period covers only 4 years, but extrapolation of a three month duration stationary flow field are with 15 years in the same order of magnitude.
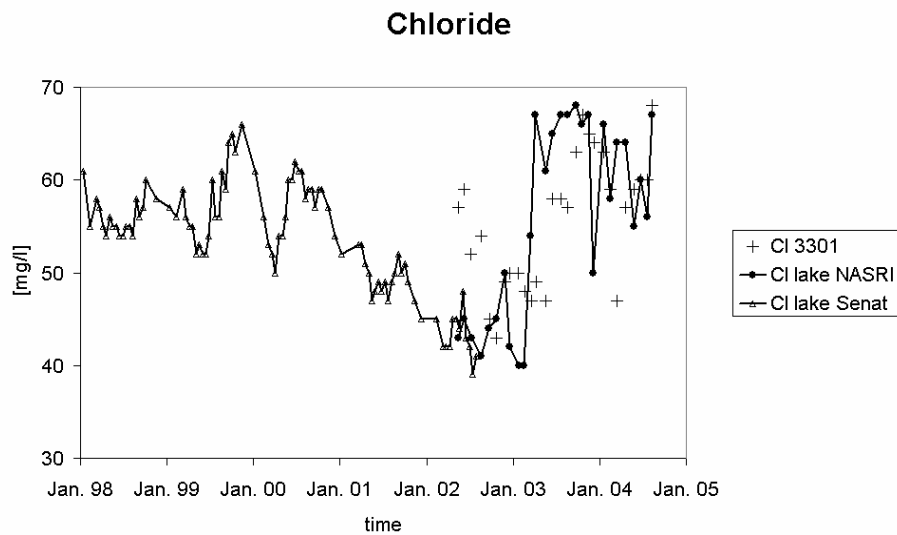
Chloride

Figure 18 Concentration of chloride measured in Lake Tegel by Senat Berlin and NASRI and observation well 3301 measured by Nasri. During 2002 chloride values measured by the Senat are 5 mg/l. Without respecting this discrepance, the travel time to 3301 is at least 8 month, taking it into account the travel time is at least 16 month.
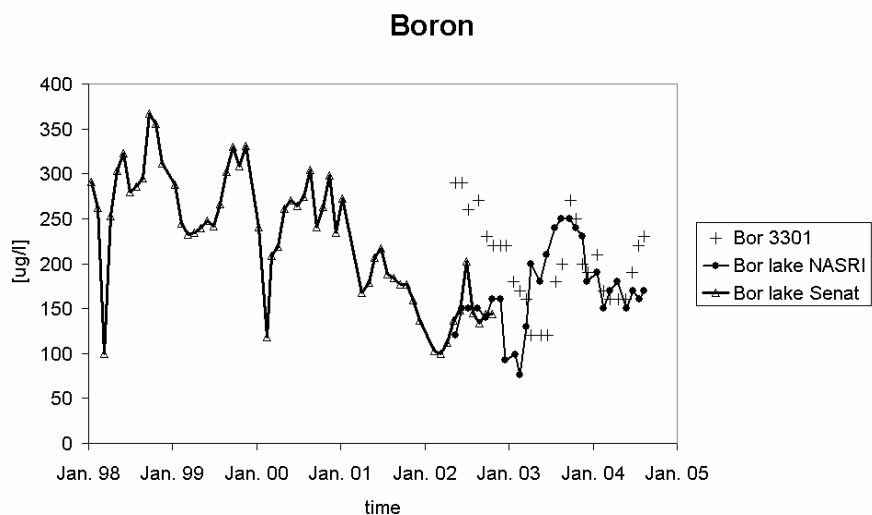
Boron

Figure 19 Concentration of boron measured in Lake Tegel by Senat Berlin and NASRI and observation well 3301 measured by Nasri. It can be seen that concentrations in summer 2002 in 3301 match boron concentrations of Lake Tegel at least 2 years ago. However, as boron may be retarded in the subsurface, travel times can not be assessed from this graphic.

Age dating

Age dating of water extracted from 3301 in spring 2003 showed an age of 20 month. (NASRI 2004) This coincided quite well with the modelled travel times of 15 month and is higher than the minimum age boundary of 15 months obtained by chloride data. The model reveals the age of 20 month is the real age of the water and not an artefact of old and young waters mixing.

Anthropogenic chemical substances

Anthropogenic chemical substances (as ADOPH, MTBE) are detected in observation well TEG374 in high concentrations (NASRI 2004). It was postulated that these substances infiltrated into the subsurface many years ago, when surface water concentrations are much higher than nowadays. As the model starts in 1998, modelling of this infiltration is not directly possible, but extrapolation of the hydraulic conditions to the past result in travel times of 12 to 15 years, which is about the minimum flow time possible, to show the concentrations observed in TEG374.

Glacial till extent

Using a precursor of the model described in section 2.3.1 the extent of the glacial till acting as aquitard can be estimated much more reliable by evaluating the drawdown by pumping experiments rather than conservative geological interpretation of pointwise borehole profiles. The first image of the first line in figure DRAWDOWN shows such an estimation of the glacial tills extent . The advantage is a pumping experiment provides areal information of hydraulic properties and reacts to very tiny confining layers which may be overseen during drilling. However it has to be taken into account the shape of the sill shown in all figures is a best estimation for the real shape, which always remains unknown.

Analysis of grain size distributions of 3301, 3302 and suggest horizontal k values of 1.8 to 3.4 10^{-4}m/s. Statistically the distribution is not significant, but variability of hydraulic conductivity in vertical direction in contrast to the relatively constant horizontal average

conductivity suggests the influence on the hydraulic properties by k_f value variability of the aquifer is less important than of the marl.

A calibration sequence with a constant k_f value of $5*10^{-4}$ is the following is shown in figure DRAWDOWN. The first line shows a till as it was estimated by geologic profiles (Fritz 2002). Data is taken from a pumping test carried out from 13th till 26th June 1999. (Fritz 2002) During this test different wells or combinations of wells was run during 1 day, each combination followed by 1 day without pumping.

The first line of Figure 20shows that observation well 3301 (screened below the elevation of the aquitard) reacts rather confined, with a sudden drop of piezometric head as the wells start pumping. The simulation with the till not covering 3301 does not reproduce this behaviour. In the second line of figure 20, where 3301 is assumed to be under a confining layer, this behaviour is reproduced much better. Observation well 14 (screened above the elevation of the aquitard) however. This can be achieved by assuming the tills extend also around well 14. This calibration (line 3 in Fig. 20) already significantly improves the modelled behaviour of observation well 3312. However, the window in the till directly around Well 14 according to its geological profile is maintained and the reaction of 3312 still is much too strong. When the window is closed the reaction improves.

So it has to be assumed the confining layer at well 14 is so tiny that it could not be recognized during drilling. The same has to be assumed for observation well 3301, whose geological profile does only show a tiny till layer of about 10 cm. This suggest the fluviatile filling around Lake Tegel according to Voigt et. al. 2000, is missing at the transect or has an extend which is very small.
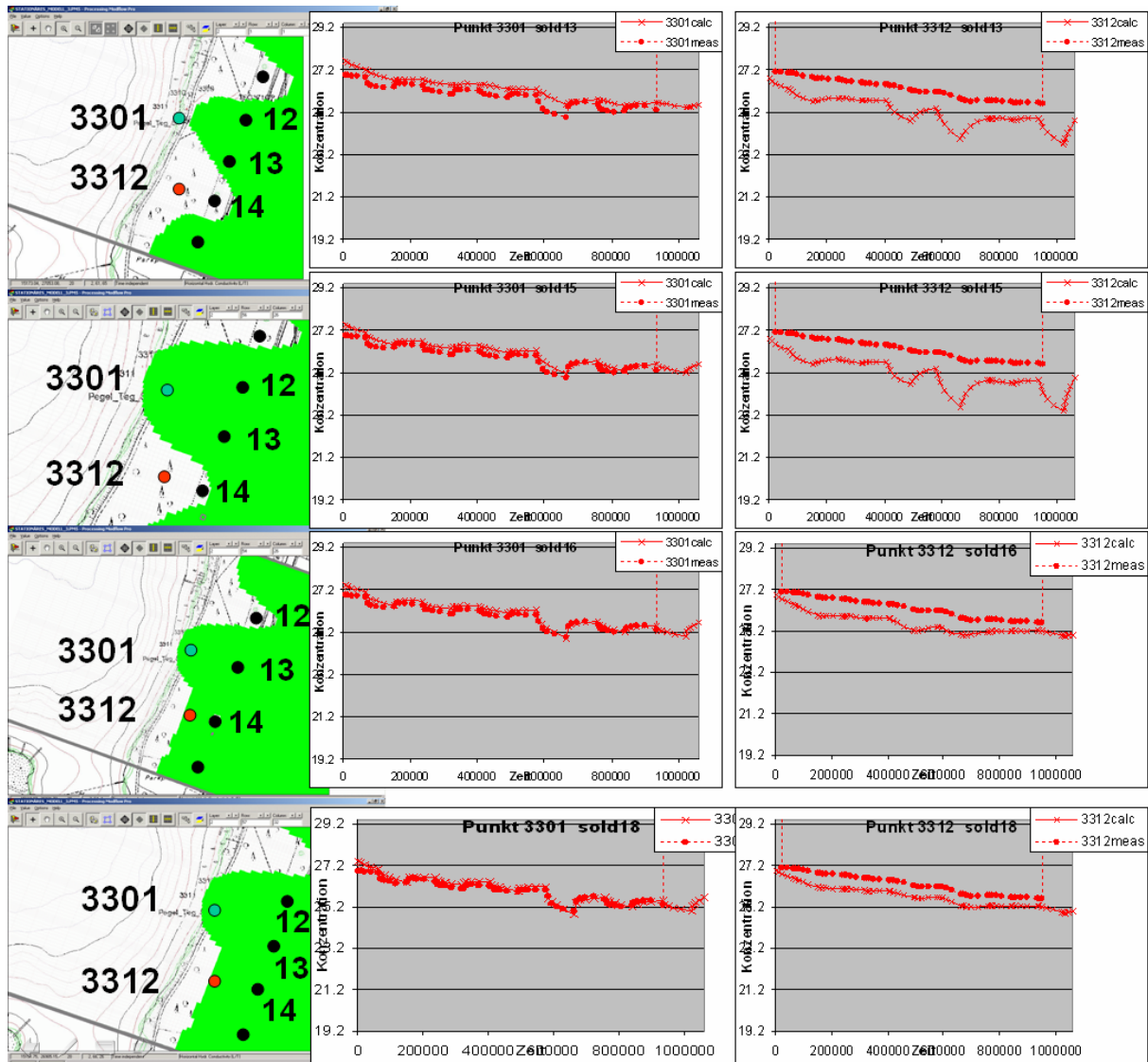
Figure 20 **Variation of the extend of the till (left column) and response of observation wells 3301 (middle column, deep aquifer) and 3312 (right column, shallow aquifer). The graphs show the simulated (crossed line) and measured (dotted line) piezometric head over the time using observations and pumping rates from 13th to 26th June 1999. The numbers 12 to 14 denote abstraction well 12 to 14 of well field west.**

Water balance

The origin of the water extracted by the well field west as average between Jan. 1998 and May 2005 may be seen from Table 1. Total bank filtration ratio is 70%, split up to 54% of relatively young (>3 years) and 16% of old (~15 years). Interesting is the relatively high portion of bottom water from the 3rd aquifer of 11%, as this has not been detected in previous works.

Table 1 Cumulative water balance for the whole model period, identical with the added up waterbalance from figure 21. The water quantitiy of Scharfenberg and western bank of Lake Tegel is calculated as the difference of the well field west to the terms of line 2 to 5.

	m³	% of well field west
abstraction well field West	64751134	100
leakance eastern bank Lake Tegel	35127411	54
eastern boundaries	10404901	16
bottom water	7293932	11
recharge	2574587	4
Scharfenberg and western bank	9350303	14

The transient water balance is presented in Figure 21. The high temporal variation of the pumping rate of well field west shows up mitigated in the flow of the boundary conditions as the storage capacity has a mitigating effect. Nevertheless, the variations in leakance from Lake Tegel e.g. in winter 2004 are considerably and the reason is not obvious (compare section 3.1.4.1).
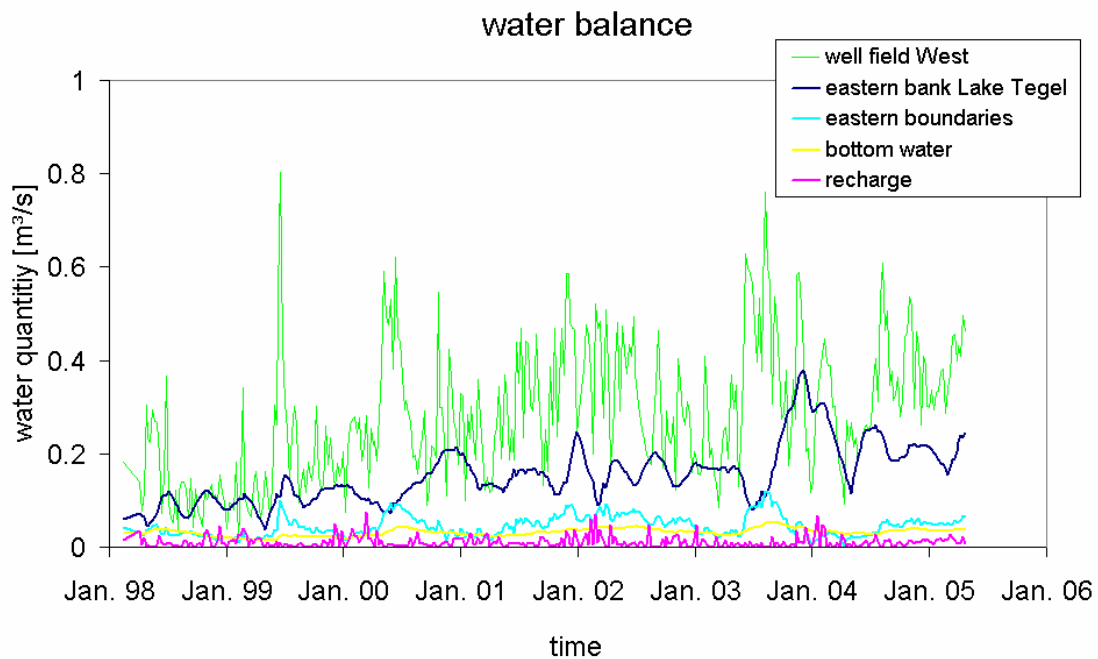
Figure 21 Transient water balance for the model area.

Bottom water

Piezometric heads of Piezometers west of the airport lake show than water from the 3rd aquifer, underlying the main aquifer intrudes into the modelarea (Figure 22, Figure 23). The difference including bottom water or not results in piezometric head differenced of 20-30 cm. This is remarkable, especially considering the small distance to the boundary condition of 300 m and the well documented piezometric head of the boundary by observation well TEG053 which is located in a distance of 330 m from TEG339.
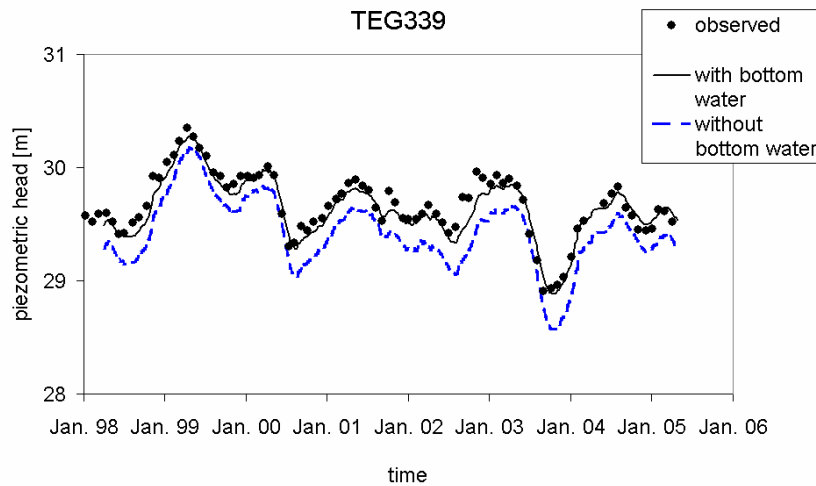
Figure 22 Piezometric head of observation well TEG339: black circles represent the observed piezometric heads, the tiny black continuous line show the model results with bottom leakage incluced, the blue dashed line shows the model results without bottom leakage.
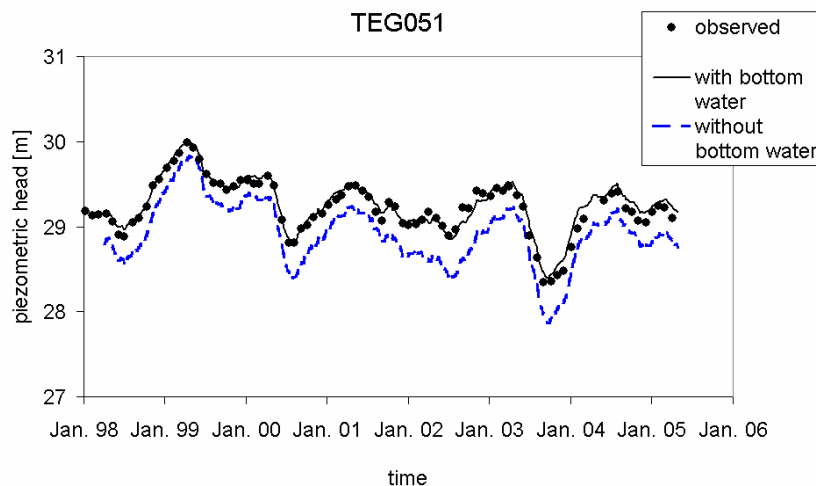
Figure 23 Piezometric head of observation well TEG051: black circles represent the observed piezometric heads, the tiny black continuous line show the model results with bottom leakage incluced, the blue dashed line shows the model results without bottom leakage.

As addtional example the heads of TEG051 (Figure 23) are shown. This coincides with piezometric heads of the 3rd aquifer reacting parallel to piezometric heads of the main aquifer (Figure 24). A large glacial trough exists in the region of the observation wells cited above (Fugro 2000) disturbing the aquitard between the 2nd and the 3rd aquifer. With the present model a hydraulic contact could be detected.
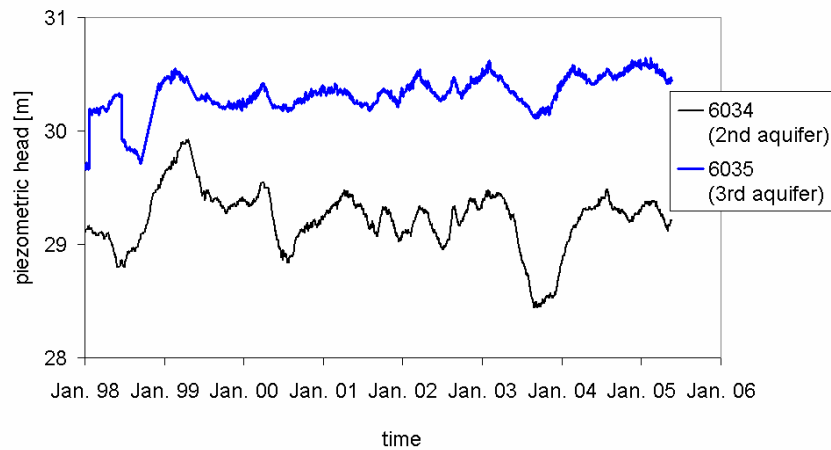
Figure 24 Piezometric heads of the observation wells 6034 and 6035. The two wells are built at the same location.

Open questions

The reasons for the temporal variant leakance could not be identified. Although the leakance factor appears to be proportional to the pumping rate on the scale of some years, and sometimes also on the the scale of a few month (Spring 99, summer 2000 to spring 2002, Figure 13, Figure 15) in Summer-Autumn 2003 the leakance reacts delayed, in winter-spring 1998 and spring 2000 the leakance does not react at all to the increased pumping rate. Infiltration measurements (Beulker et. al 2005) Different Mechanisms which may be the reason for such a conductance were introduced into MODFLOW2000, as k_f of the bank being linear or nonlinear dependent on the pressure gradient, including inertia of the bank in reacting to changes, without satisfying result. It was taken into account the pumping rates may vary considerably with the water level in the wells, but this hypotesis could not explain the present conductance. Changes of the boundary conditions within a reasonable range did not affect considerably the temporal conductance of the bank.

The maximum leakance factor calculated from measured infiltration rates takes place in a water depth of about 1.4 m (section 3.1.3). Simulations however suggest in 4-6 m depth the

the leakance factor has its maximum. As local heterogeneity is high, the model results seem to be more reliable.

Leakance factors calculated for the bank on the scale of the whole model area are about one order of mangnitude lower than values obtained by measurements (section 3.2, Sievers 2001). The discrepance may be have its reason sampling always disturbes the sediments and observed values are too high. Spatial variability may also be an explanation, as all measurements have been carried out in front of the transect.
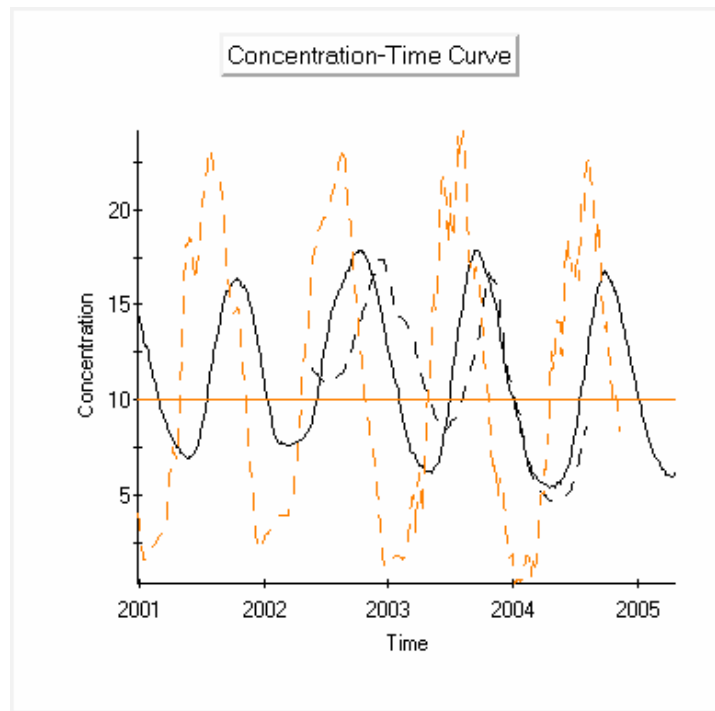
Figure 25: Water temperature of Lake Tegel (orange dashed line) observed water temperature in observation well 3301 (black dashed line) and modelled water temperature in observation well 3301 (plain black line)

Water temperature measured in 3301 during the regular sampling could not be modelled. The minimum temperature in 2002 is 11°C (Figure 25). Temperatures modelled are always considerably lower than the mean annual temperature of 10 °C. This behaviour probably occurs due to water infiltrating in front of Reiswerder affects observation well 3301. Transport simulation of ^{18}O however could reproduce the measured concentrations.

1.1.5. Geochemical modelling

Three steps have to be carried out in order to set up a geochemical model. A simplified or generic flow and transport model was set up, the chemical analyses are verified, and a reaction module is set up, calibrated and verified to the measured data.

1.3.1.4. Setup of the generic flow and transport model

In order to assess the biogeochemical and hydrochemical development and characteristics along the riverbank filtration test site and as preparation to expand the calibrated/verified flow and transport model 'test site Tegel' as reactive transport model, a generic/conceptual flow model was set up which considers

the idealised geological stratification of the Tegel Test site

the Lake Tegel as 3rd kind flow boundary

3 wells from well field West with strongly unsteady pumping regime as typical for the test site 'Lake Tegel'

The model area was specified as a rectangle 1000 m in length, 100 m in width, and 50 m in vertical thickness. The horizontal and vertical model geometries and discretisation are shown by Figure 26and Figure 27.
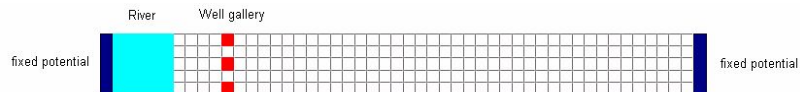
Figure 26: horizontal model geometry
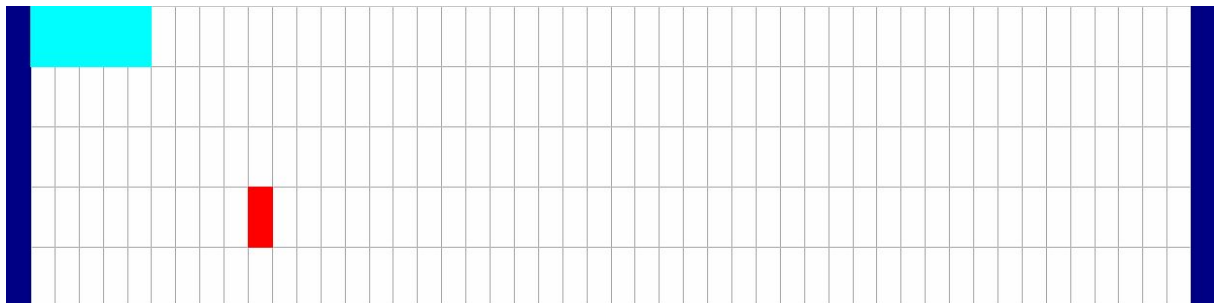
Figure 27 model vertical cross section

The 3D-model is spatially discretised by 50 columns, 5 rows, and 5 layers. As Figure 27shows, the well field is assigned to a depth of 20 m below the model surface as derived from the screen positions of the production wells at the Tegel test site. The model top was assigned at 35 m above sea level, the model bottom at –15.0 m above sea level, according to a geological profile (Fugro 2000).

The hydrogeological model applied to the generic model is based on the information available from the investigations at the Tegel test site (NASRI 2003) and a hydrogeological

structural model (Fugro 2000) which show an about 50 m thick aquifer partially intersected by an aquitard (glacial till) of up to 5 m thickness, see Figure 26. Near the Lake Tegel bank, no aquitard was detected during drilling, so all model layers in this part are homogeneous.

As shown by Figure 28, the aquitard was placed to third model layer (from the model top) by an adequate k_f value parameterization. A k_f value of 43.2 m d^{-1} (or $5*10^{-4}$ m s^{-1}) was assigned to the aquifer, whereas to the aquitard a k_f value of $8.6*10^{-3}$ m d^{-1} (or $1*10^{-7}$ m s^{-1}) was assigned. As a first approach, isotropic conditions were assumed. Additionally, a storage coefficient of $1*10^{-5}$ (as required for transient simulations) and an effective porosity of 0.25 were specified to the whole generic model.
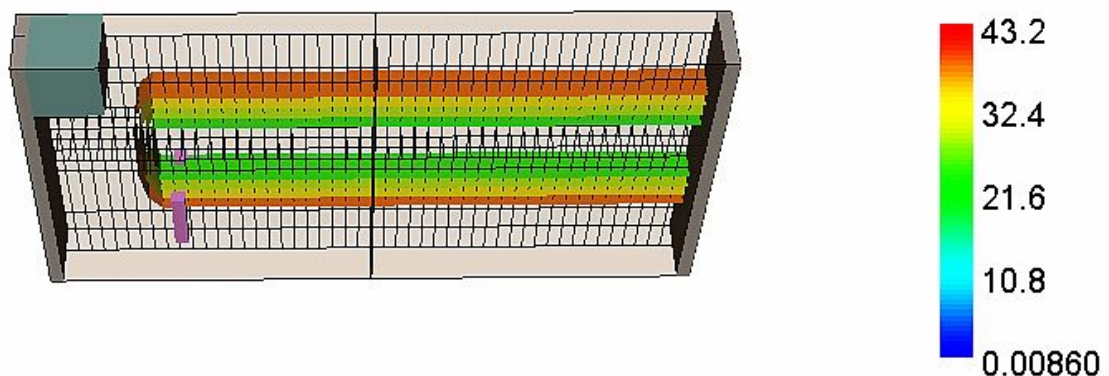
Figure 28 Aquitard within the generic model (bar column shows k_f values in [m d^{-1}])

Reflecting the local conditions at the Tegel test site, an initial hydraulic head of 28.0 m above sea level was specified for all model layers. Below the lake (left) the constant head boundary was set to a hydraulic head of 28.0 m. To the right model constant head boundary (landside) a hydraulic head of 28.5 m above sea level was assigned.

Because at the Tegel test site the screens of the production wells are below the base of the aquitard, the well nodes were placed within the fourth model layer (counted from the model top).

1.3.1.5. Flow field of the generic flow model

The flow model was run transient over 1095 days. In a first period (up to a simulation time of 365 days), no pumping was assigned to the wells in order to achieve a reliable initial flow solution. After 365 days, the wells were switched on applying an oscillating pumping

regime. The central well (900 m^3 d^{-1}) is operated in alternation with the border wells (each 450 m^3 d^{-1}) in periods of 10 days (Figure 29).
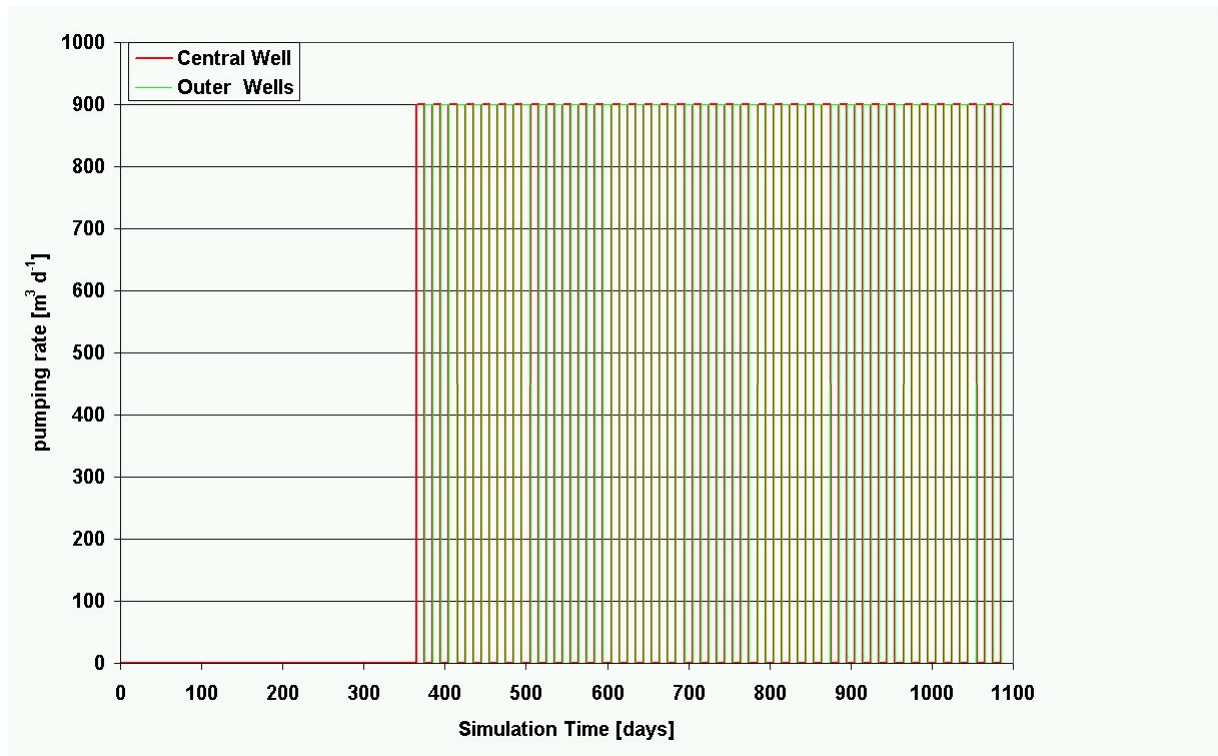
Figure 29 Pumping schedule assigned to the wells during simulation time
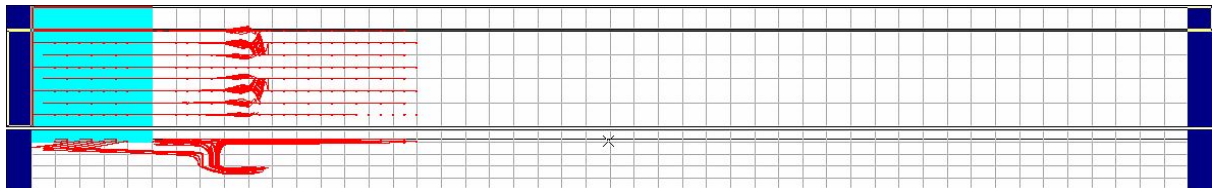
Figure 30 Transient flow paths in the generic model area (upper section base view, lower section vertical cross section along y axis). Light blue represents 3rd type boundary Lake Tegel, dark blue constant head boundaries. Red lines are flowpaths.

As a result of the applied pumping regime the flow paths calculated using transient simulation are shown by Figure 23. Due to the applied pumping regime the calculated flow paths (which are saved at every time step) are smeared as they approach the actually active (and actually switched off) wells. The flow paths were started as well from the river as from

the land side to get an overview about the transient flow field between the river and the well field as well as the impact of the aquitard on the flow field. Vertically, the flow paths started at the land side are expected to flow around the aquitard in order to reach the production wells screened below the aquitard. If the aquitard is modelled using a greater leakage, a significant vertical flow (though retarded) through the aquitard especially above the filter screens is possible. The flow paths started at the river side are also influenced by the extent of the aquitard resulting also in a downwards deviation near the aquifer border followed by a tracking below the aquitard toward the wells.

Reflecting the highly transient flow regime, piezometric head distributions only can be given for the 2 regime situations applied here. By Figure 31and Figure 32 the calculated vertical piezometer head distributions are shown for two situations
Outer wells are pumping
Only the central well is pumping

For both situations, the drawdown cone around the well gallery is expected to occur within the deeper parts of the aquifer also due to the modelled geology, especially the extension of the aquitard, which generates a strong vertical piezometer head gradient. Below the aquitard, flow is horizontal toward the active production wells. By both flow path analysis and piezometer head distribution the most probable pattern of hydrodynamic transport (as basic for the reactive transport) can be evaluated.
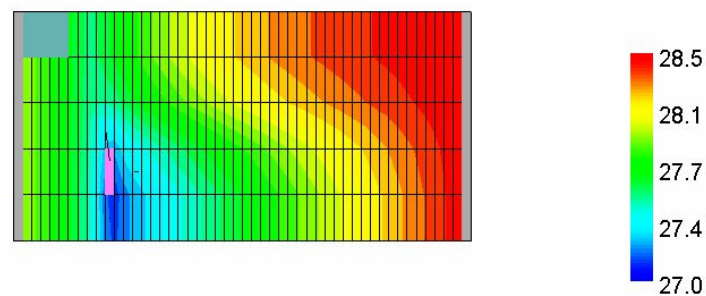
Figure 31 Hydraulic heads after 379 days (outer wells active as indicated by the magenta bar)
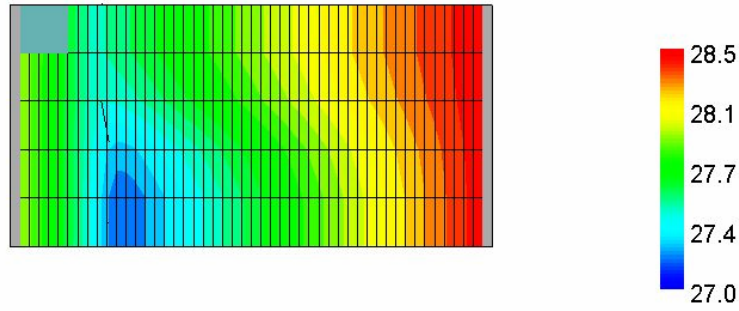
Figure 32 Hydraulic heads after 469 days (central well active)

1.3.1.6. Evaluation of hydrochemical analyses

A verification of groundwater sample analyses as good as possible is a prerequisite for an adequate reactive transport simulation at the riverbank filtration test site. In order to estimate correct initial and boundary hydrochemical conditions all available chemical analyses of sufficient quality (ion charge balance error) were subjected to a verification using PHREEQC (Parkhurst & Appelo 1999).

As data basis, 293 groundwater and 25 surface water analyses sampled at the Tegel transsect are available from January 2002 to September 2004. 4 groundwater analyses were not complete (due to a lack of temperature, pH, E_H, O_2, or relevant cation/anion data). Only analyses with less than 5% ion balance error were processed. The ion balance error was calculated for each analysis dataset based the main cation and anion concentrations (in meq l^{-1}) provided as input for PHREEQC calculation using equation 3.

$$Ion-Balance-error = \frac{\sum cations + \sum anions}{\sum cations - \sum anions} \cdot 100$$

(3)

Applying this criterion, 9 groundwater analyses had to be discarded. Finally 280 groundwater analyses were provided to be processed by PHREEQC. All 25 surface water analyses taken from Lake Tegel fulfilled the required quality criteria and were processed.

Conceptually, the analysed hydrochemistry is regarded as a result of solution equilibration with an adequate mineral assemblage within the aquifer matrix. The selection of typical equilibrium mineral-assemblages relies to the core matrix analyses (NASRI, 2003). Relevant mineral phases to be considered in this context are Calcite ($CaCO_3$), Pyrolusite (MnO_2), Ferrihydrite ($Fe(OH)_3$ (amorphous)), Rhodochrosite ($MnCO_3$), and Siderite ($FeCO_3$).Using MATLAB, an automated processing of the large amount of chemical analyses data by PHREEQC was performed.

An uncertainty exists for the verification of the chemical analyses arises from the scarcely known matrix composition (one drilling core analysed). Especially the content of trace minerals such as Calcite, Fe- and Mn oxides/hydroxides and carbonates affect the equilibrium.

The parameters analysed and used for verification using PHREEQC are listed in Table 2.

Table 2 Analysed chemical parameters (NASRI DATABASE, 2004) and chemical parameters used for verification by PHREEQC. Grey fields denote parameters used for PHREEQC processing.

Analytical Parameter	Unit	Analytical Parameter	Unit
Temperature	°C	El. Conductivity	µS/cm
pH	-	DOC	mg/l
O_2	mg/l	TOC	mg/l
E_H	mvolt	UV 254	1/m
Fe (total)	mg/l	AOX	µg/l
Mn	mg/l	AOCl	µg/l
Acid Capacity pH 4.3	meq/l	AOBr	µg/l
Base Capacity pH 8.2	meq/l	AOI	µg/l
CO_2	mg/l	B	µg/l
HCO_3	mg/l	EDTA	µg/l
Ca	mg/l	NTA	µg/l
Mg	mg/l	AMDOPH	µg/l
Na	mg/l	AMPH	µg/l
K	mg/l	DMAPH	µg/l
NH_4-N	mg/l	Carbazepin	µg/l
NO_3-N	mg/l	Phenazon	µg/l
Cl^-	mg/l	Propyphen	µg/l
SO_4	mg/l	MTBE	µg/l

Parameters affected by PHREEQC equilibration are all components involved in precipitation/dissolution reactions or redox reactions, available from the PREEQC database such as: pH, E_H (pe), Ca, TIC (predominantly HCO_3^-), Fe, Mn, O_2, NO_3-N and NH_4^+-N.

Other parameters (such as Na, K, Mg, Cl) are assumed to be involved only in aqueous chemical equilibria and are therefore expected to be unchanged during PHREEQC calculations. Due to the observed redox conditions, SO_4 is also expected to be practically not involved. Temperature is included as a important parameter for equilibrium constants and therefore chemical speciation.

The parameters CO_2 and HCO_3^- were summed up to the PHREEQC input parameter tetravalent inorganic carbon (C(4)). Because PHREEQC requires pe values instead of E_H as data input, E_H was therefore converted to pe using equation 4

$$pe = -\lg(e^-) = \frac{F}{2.303 \cdot R \cdot T} \cdot E_H$$

(4)

with

F = FARADAY constant 96484 [C/mol or J/(Volt * mol)]

R = 8.315 [J/(°K * mol)]

T in [°K]

E_H in [Volt] (Appelo & Postma, 1996)

The assumed initial mineral concentrations to get equilibrated are given by Table 3, and are in the order of magnitude as detected by the core analysis (NASRI, 2003).

Table 3 Assigned initial Mineral concentrations

Mineral	Initial concentration		
	mol l^{-1}aq $^{1)}$	weight %	mg element/kg dry soil
Calcite	5.9×10^{-2}	0.1	-
Ferrihydrite or Siderite	1.132×10^{-1}	-	1170
Pyrolusite or Rhodochrosite	3.8×10^{-3}	-	29

$^{1)}$ used for PHREEQC calculations

An adequate choice of the mineral phase assemblage is decisive to verify the sampled analysis data set.

Analyses typical for an iron reducing environment could adequately be verified on the basis of a phase assemblage Calcite+Ferrihydrite+Rhodochrosite+Siderite+Pyrolusite. For all analytical datasets showing a pe value less than 3.0, deduced from redox potential measurements, an equilibrium phase assemblage without Pyrolusite was assigned.

The initial mineral concentrations in the surface water samples were set to zero. This way, the minerals potentially (if oversaturated) can be equilibrated. The range of redox conditions was found from oxic conditions in the surface water and in the shallow groundwater samples to anoxic conditions (until iron oxide reduction stage) in the deeper groundwater samples (NASRI, 2003).

Figures Figure 33 to Figure 39 give an overview of the verification of the analytical data by PHREEQC.
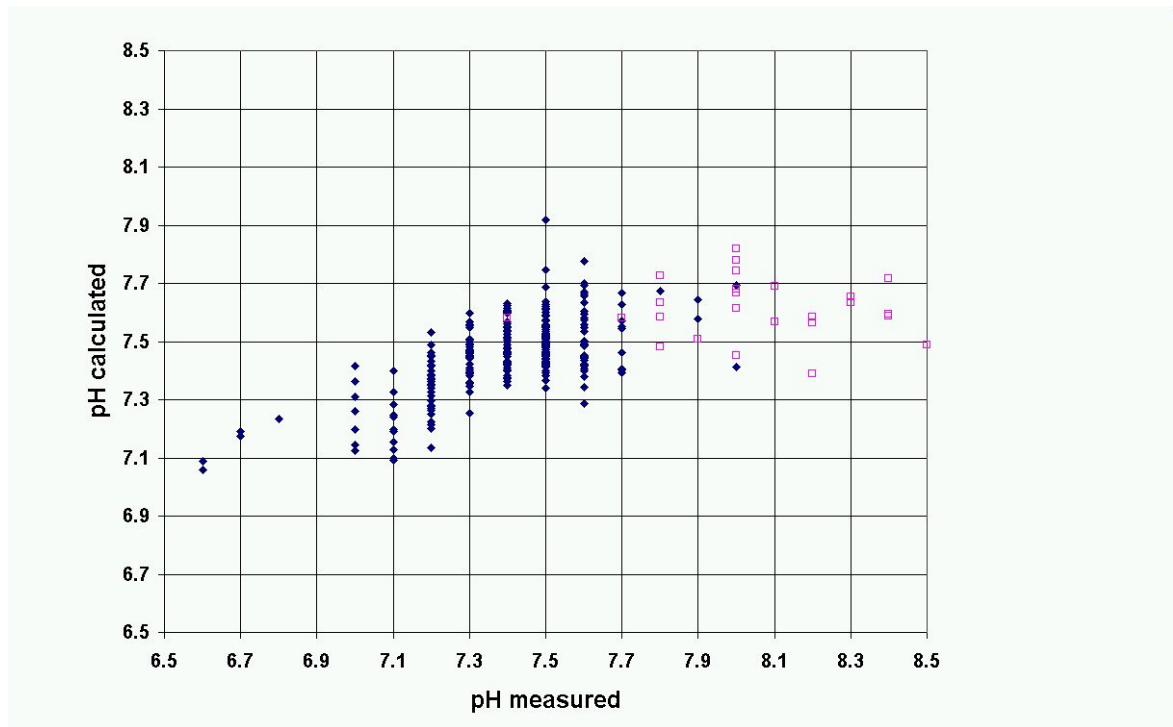
Figure 33 Scatter diagram of all measured and calculated pH values of groundwater samples (blue ♦) and surface water samples (pink ▢) from the Tegel test site
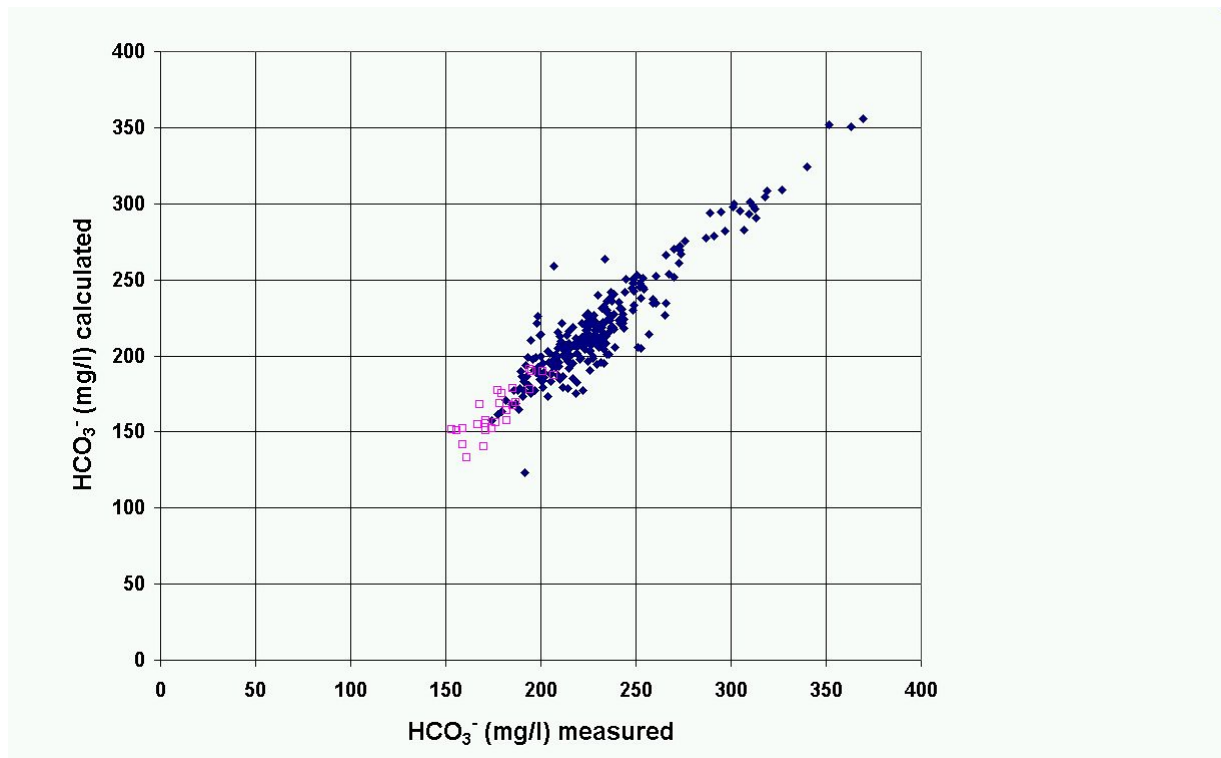
Figure 34 Scatter Diagram of all measured and calculated HCO3- concentrations of groundwater samples (blue ♦) and surface water samples (pink ▢) from the Tegel test site
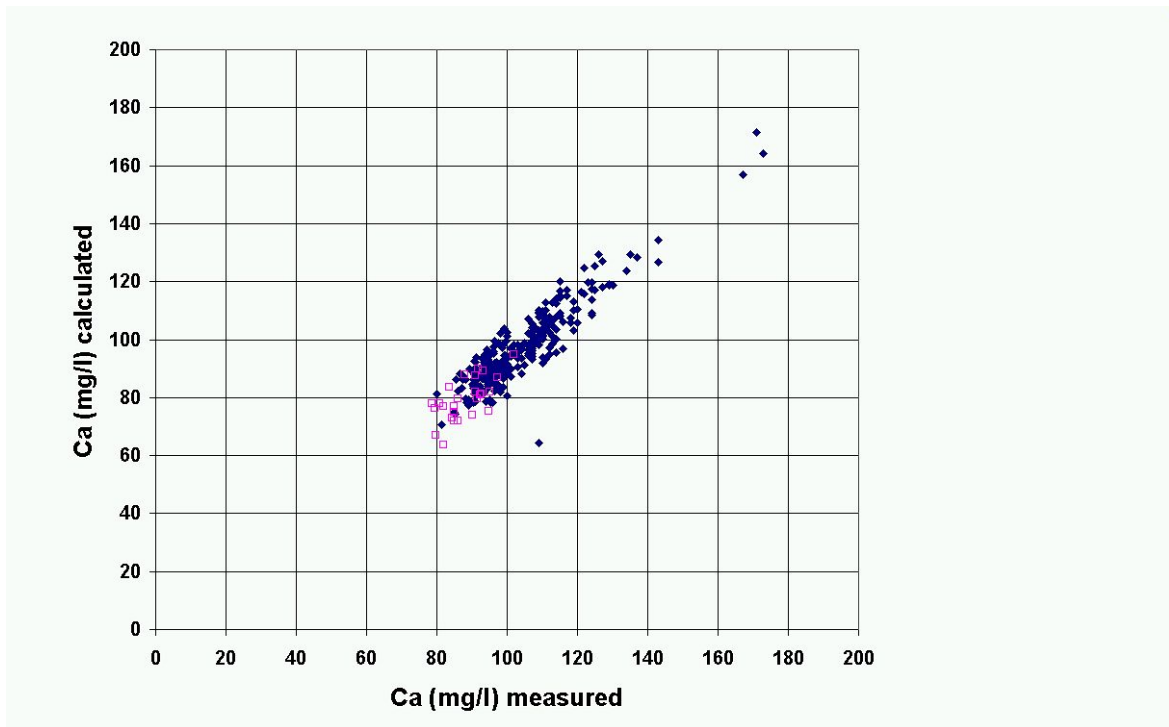
Figure 35 **Scatter Diagram of all measured and calculated Ca concentrations of groundwater samples (blue ◆) and surface water samples (pink □) from the Tegel test site**
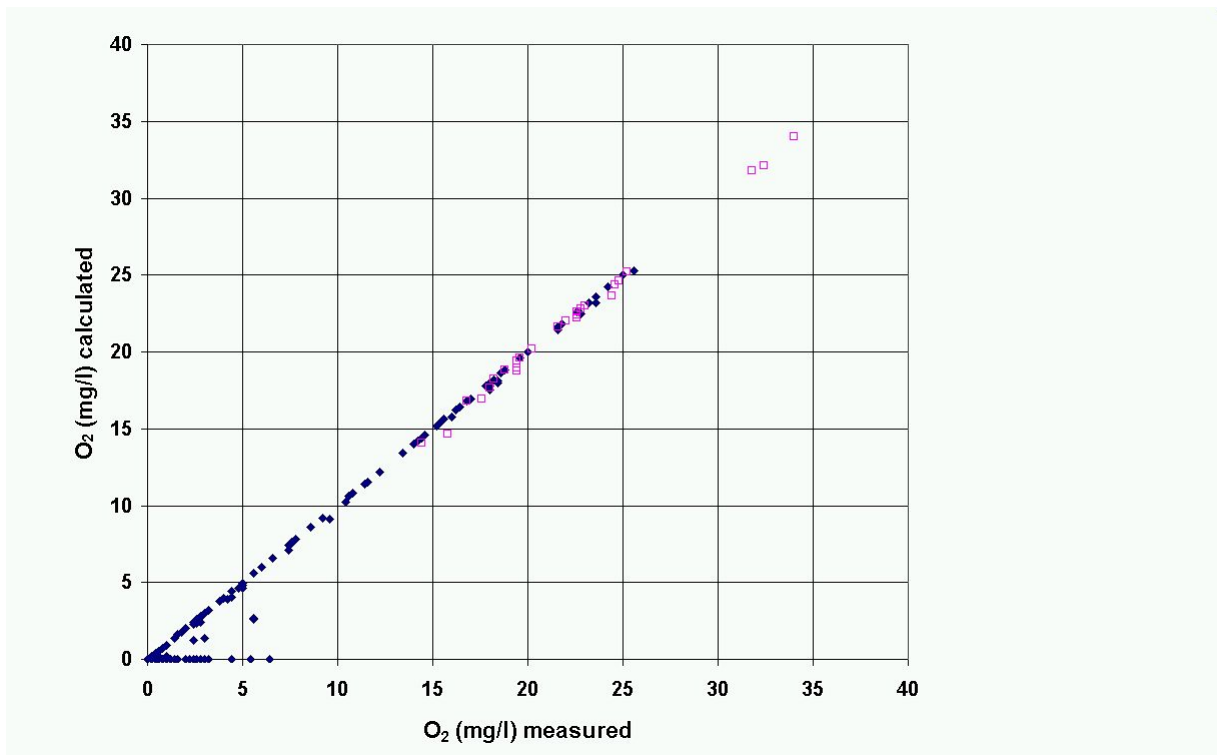
Figure 36 **Scatter Diagram of all measured and calculated O2 concentrations of groundwater samples (blue ◆) and surface water samples (pink □) from the Tegel test site**
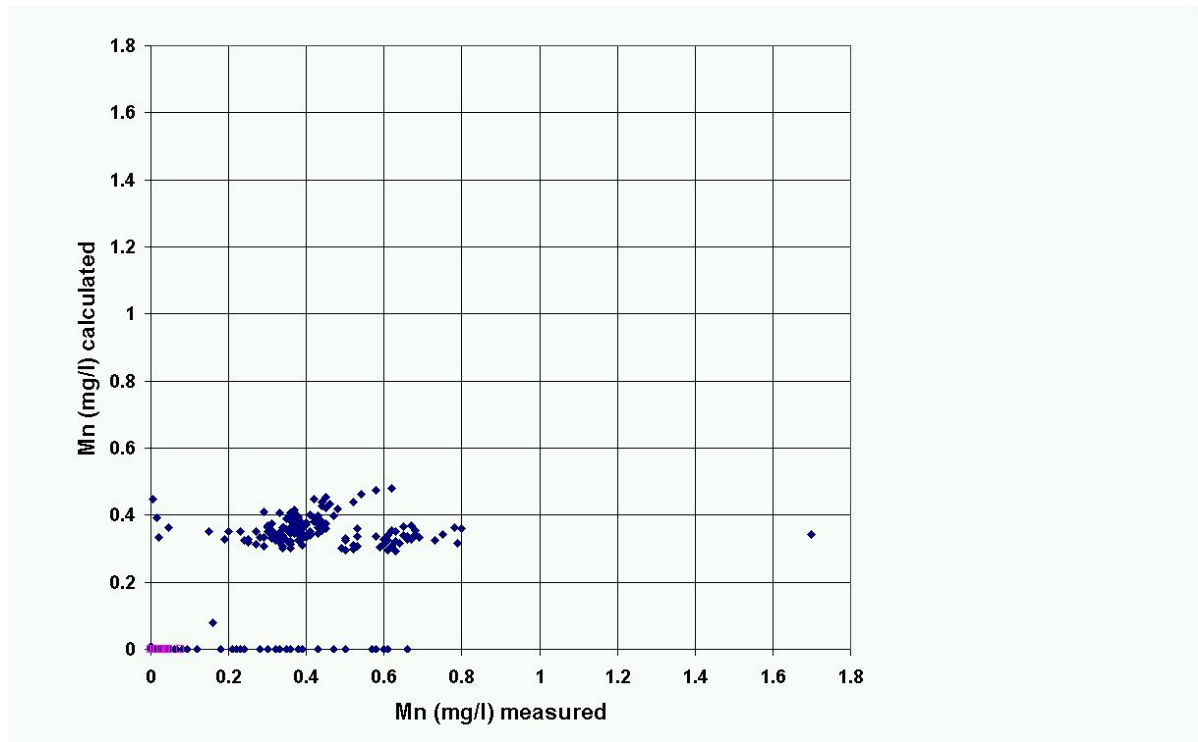
Figure 37: Scatter Diagram of all measured and calculated Mn concentrations of groundwater samples (blue ♦) and surface water samples (pink □) from the Tegel test site
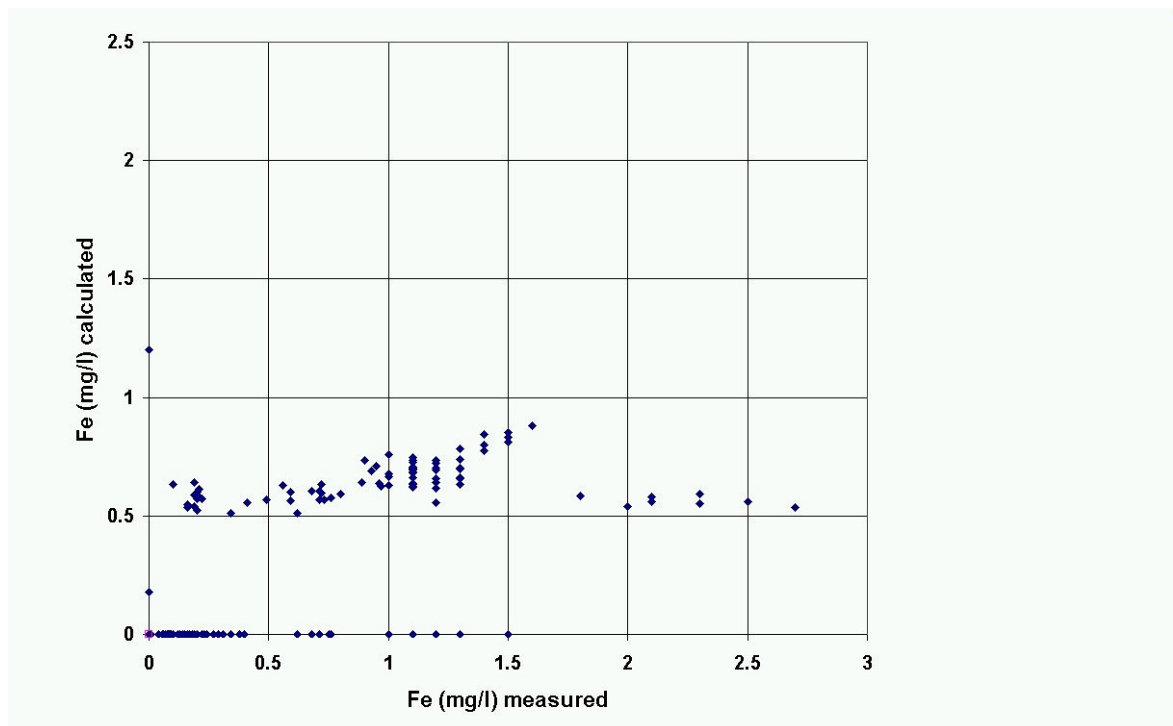
Figure 38Scatter Diagram of all measured and calculated Fe concentrations of groundwater samples (blue ♦) and surface water samples (pink □) from the Tegel test site
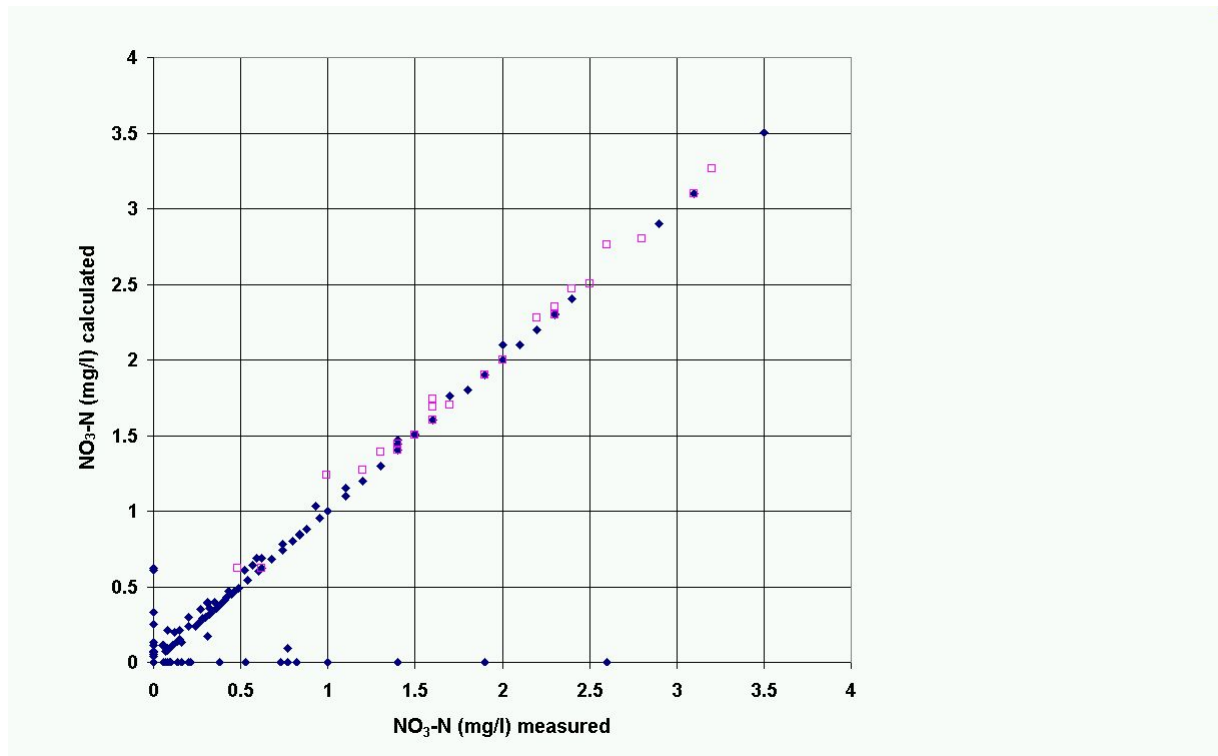
Figure 39Scatter Diagram of measured and calculated NO3-N concentrations of groundwater samples (blue ♦) and surface water samples (pink ▫) from the Tegel test site

Figure Figure 33 to Figure 39 show that the processed chemical analyses are

in a good agreement for HCO_3^- (Figure 34), Ca (Figure 35)

and as long as oxic conditions prevail, for O_2 (Figure 36) and NO_3-N (Figure 39),

only in partial agreement for pH (Figure 33), Mn (Figure 37) and Fe (Figure 38) reflecting charge balance assumption for pH, and specified mineral equilibria for Fe and Mn.

NH_4-N was not found to be stable after PHREEQC processing (and therefore not verified) because inorganic Nitrogen was assumed to be in redox equilibrium. At oxic conditions NO_3^- is the only stable N-species, so that analysed NH_4^+ is added to the analysed NO_3^- concentration.

The discrepancies between calculated and measured pH values (Figure 33) may result from the fact that the pH calculation within PHREEQC is performed based on the charge balance (as performed during the reactive transport simulation using PHT3D, see Prommer 2002). In other cases (such as surface water analyses) the cursory assumption of calcite and other mineral equilibrium, which has applied to all processed analyses, may not be valid.

Due to the fact, that in most cases calcite saturation occurs, the measured Ca and HCO$_3$-concentrations are for most cases satisfactorily verified (Figure 34 and Figure 35). As long as conditions are oxic, measured O$_2$ and NO$_3$-N concentrations could also be well verified. The calculated Fe and Mn concentrations reflect in general the applied mineral equilibria resulting in nearly constant values depending on the actual redox conditions. For anoxic conditions, Mn and Fe concentrations can be reproduced only at the same magnitude order as analysed, if rhodochrosite and/or siderite is stable during PHREEQC processing. Following this approach, Mn and Fe concentrations measured in oxic environment are not verified by PHREEQC processing, which assumes equilibration with Iron and Manganese oxides under these conditions and which results in calculated Fe and Mn concentrations near zero.

As expected the measured redox potentials (not shown) in most cases were not confirmed by the calculation except for analyses reflecting an anoxic iron reducing environment. Reasons may be a possible surface passivation of the electrode in oxic environments, or the fact that no redox equilibrium was reached (Lindberg & Runnels, 1984). For the reactive transport modelling, nevertheless an (equilibrated) pe value is required and had to be calculated in spite of the difficulties described above.

1.3.1.7. Reactive Transport: Conceptual chemical reaction framework

The conceptual chemical reaction framework set up for verification of the groundwater and surface water analyses (see section 2.2.1) at the Tegel test site is applied and extended to the reactive transport modelling presented here.

As given by the PHT3D intrinsic systematics the following has to be specified: aqueous components controlled by chemical equilibrium or by kinetics, minerals and solids controlled by chemical equilibrium or by kinetics, and as a special case, the pH and the pe as immobile components resulting from charge balancing and from the operation valence electron balancing. All components considered by reactive transport modelling are given by Table 4.

Table 4 Summary of components considered in the reactive transport modeling (indicated by a cross)

Component	Aqueous controlled by chemical equilibrium	Aqueous kinetically controlled	Immobile controlled by chemical equilibrium	Immobile kinetically controlled
pH			x	
pe			x	
C(4)	x			
C(-4)	x			
Ca	x			
Mg	x			
Na	x			
K	x			
Cl	x			
Fe(2)	x			
Fe(3)	x			
Mn(2)	x			
Mn(3)	x			
S(6)	x			
S(-2)	x			
N(3)	x			
N(5)	x			
N(0)	x			
N(-3)	x			
O(0)	x			
DOC		x		
Particulate OC				x
Calcite			x	
Pyrolusite			x	
Ferrihydrite			x	
FeS (ppt)			x	
Rhodochrosite			x	
Siderite			x	

All aqueous components controlled by chemical equilibrium or by kinetics are subjected to hydrodynamic transport. pH and pe are treated formally as immobile, but they are calculated using the chemical equilibria of all species, charge balance (derived from mobile species) and operational valence electron balances (using mobile and immobile species). DOC is treated as a mobile component controlled by biogeochemical degradation kinetics (MONOD approach) using terminal electron acceptors here available as O_2, NO_3^-, Pyrolusite (MnO_2),

Ferrihydrite (Fe(OH)$_{3(amorphous)}$) and SO$_4^{2-}$. Particulate OC (organic carbon) is considered as a kinetically controlled immobile component releasing DOC.

The minerals Calcite (CaCO$_3$), Pyrolusite (MnO$_2$), Ferrihydrite (Fe(OH)$_3$ $_{(amorphous)}$), FeS (ppt), Rhodochrosite (MnCO$_3$), and Siderite (FeCO$_3$) are immobile components subjected to chemical equilibrium.

The kinetics of DOC degradation are formulated using a MONOD approach. Here, with DOC, the reactive fraction of DOC (differing from refractory DOC fractions) is denoted. The overall DOC decay rate R$_{DOC}$ is formulated as the sum of individual decay rates with a given terminal electron acceptor:

$$R_{DOC} = R_{O_2} + R_{NO_3^-} + R_{MnO_2} + R_{Fe(OH)_3} + R_{SO_4^{2-}} \tag{5}$$

$$R_{O_2} = \frac{\partial c_{DOC,O_2}}{\partial t} = -k_{O_2} \cdot c_{DOC} \cdot \frac{c_{O_2}}{K_{m,O_2} + c_{O_2}} \tag{6}$$

$$R_{NO_3^-} = \frac{\partial c_{DOC,NO_3^-}}{\partial t} = -k_{NO_3^-} \cdot c_{DOC} \cdot \frac{c_{NO_3^-}}{K_{m,NO_3^-} + c_{NO_3^-}} \cdot \frac{I_{O_2}}{I_{O_2} + c_{O_2}} \tag{7}$$

$$R_{MnO_2} = \frac{\partial c_{DOC,MnO_2}}{\partial t} = -k_{MnO_2} \cdot c_{DOC} \cdot \frac{c_{MnO_2}}{K_{m,MnO_2} + c_{MnO_2}} \cdot \frac{I_{O_2}}{I_{O_2} + c_{O_2}} \cdot \frac{I_{NO_3^-}}{I_{NO_3^-} + c_{NO_3^-}} \tag{8}$$

$$R_{Fe(OH)_3} = \frac{\partial c_{DOC,Fe(OH)3}}{\partial t} = -k_{Fe(OH)_3} \cdot c_{DOC} \cdot \frac{c_{Fe(OH)3}}{K_{m,Fe(OH)_3} + c_{Fe(OH)3}} \cdot \frac{I_{O_2}}{I_{O_2} + c_{O_2}} \cdot \frac{I_{NO_3^-}}{I_{NO_3^-} + c_{NO_3^-}} \cdot \frac{I_{MnO_2}}{I_{MnO_2} + c_{MnO_2}} \tag{9}$$

$$R_{SO_4^{2-}} = \frac{\partial c_{DOC,SO_4^{2-}}}{\partial t} = -k_{SO_4^{2-}} \cdot c_{DOC} \cdot \frac{c_{SO_4^{2-}}}{K_{m,SO_4^{2-}} + c_{SO_4^{2-}}} \cdot \frac{I_{O_2}}{I_{O_2} + c_{O_2}} \cdot \frac{I_{NO_3^-}}{I_{NO_3^-} + c_{NO_3^-}} \cdot \frac{I_{MnO_2}}{I_{MnO_2} + c_{MnO_2}} \cdot \frac{I_{Fe(OH)3}}{I_{Fe(OH)3} + c_{Fe(OH)3}} \tag{10}$$

with k$_i$ as rate constants, K$_{m,i}$ as MONOD constants, and I$_i$ as inhibitor constants for the terminal electron acceptor i.

The solution kinetics of particulate OC is formulated as

$$R_{OC} = \frac{\partial c_{OC}}{\partial t} = -k_{sol} \cdot c_{OC} \cdot \left(c_{DOC,sat} - c_{DOC} \right) \tag{11}$$

using k$_{sol}$ as solubility rate constant, c$_{DOC,sat}$ as OC solubility, and the DOC concentration. Depending on the relation of the DOC concentration to the particulate OC solubility, particulate OC dissolution or precipitation is possible. This term was introduced because along the Tegel test site DOC concentrations were found independent from the terminal electron acceptor consumption.

Basics about coupling of biogeochemical reactions to inorganic hydrogeochemistry are available from Brun & Engesgaard (2002) and Barry et al. (2002).

To perform reactive transport simulations using PHT3D, initial and boundary concentrations must be assigned to each modeled component. From the evaluation of the NASRI chemical database (NASRI Database, 2004), an oxic redox environment for the shallow sample points, and an anoxic redox environment for the deeper sample points can be deduced. As typical analyses for the oxic redox environment a dataset from well 3305 and for the anoxic redox environment a dataset from well 3304 (NASRI Database 2004) were chosen and assigned to the model. As representative analysis for the surface water hydrochemistry related to the river package, a surface water analysis dataset from the NASRI Database (2004) was chosen and assigned as boundary concentrations.

The effective chemical composition of the groundwater recharge was deduced from precipitation water analyses as outlined by Merkel & Planer-Friedrich (2002). Conceptually, the initial precipitation water chemistry is concentrated by subtracting the evaporation and the surface run-off from the precipitation.

The initial and boundary hydrochemistry assigned to the reactive transport model is available from Table 5.

The parameter set 'oxic milieu' (Table 5) was assigned to the entire 1st model layer and to the 2nd model layer except for the lake. The remaining model part was specified with the parameter set 'anoxic milieu' (Table 5). The specified head boundaries (left and right model boundaries) were specified in the same way as the initial conditions of the neighbouring blocks (the left boundary as oxic only in the 1rst model layer, the right boundary as oxic in model layer 1 and 2 from the top).

Table 5: initial and boundary hydrochemistry assigned to the reactive model (units mol l^{-1} for dissolved components except pH and pe, and mol $l(bulk)^{-1}$ for solids)

Component	Oxic milieu	Anoxic milieu	Surface water	Groundwater Recharge
DOC	$1*10^{-7}$	$1*10^{-4}$	$5*10^{-4}$	$1*10^{-20}$
C(4)	$5.668*10^{-3}$	$3.296*10^{-3}$	$1.082*10^{-5}$	$1.082*10^{-5}$
C(-4)	$1*10^{-20}$	$1*10^{-20}$	$1*10^{-20}$	$1*10^{-20}$
Ca	$4.174*10^{-3}$	$2.938*10^{-3}$	$2.122*10^{-3}$	$2.233*10^{-5}$
Cl	$1.242*10^{-3}$	$1.609*10^{-3}$	$1.863*10^{-3}$	$8.295*10^{-5}$
Fe(2)	$3.02*10^{-17}$	$1.320*10^{-5}$	$1*10^{-20}$	$1*10^{-20}$
Fe(3)	$4.437*10^{-8}$	$3.311*10^{-8}$	$1*10^{-20}$	$1*10^{-20}$
Mg	$7.741*10^{-4}$	$3.169*10^{-4}$	$4.527*10^{-4}$	$2.233*10^{-5}$
Mn(2)	$9.99*10^{-15}$	$7.882*10^{-6}$	$1*10^{-20}$	$1*10^{-20}$
Mn(3)	$1*10^{-20}$	$1*10^{-20}$	$1*10^{-20}$	$1*10^{-20}$
N(3)	$1.79*10^{-17}$	$1*10^{-20}$	$1*10^{-20}$	$1*10^{-20}$
N(5)	$1.258*10^{-4}$	$1*10^{-20}$	$1.357*10^{-4}$	$1.934*10^{-4}$
N(0)	$1*10^{-20}$	$1.572*10^{-5}$	$1*10^{-20}$	$1*10^{-20}$
N(-3)	$1*10^{-20}$	$1*10^{-20}$	$1*10^{-20}$	$1*10^{-20}$
Na	$1.302*10^{-3}$	$1.428*10^{-3}$	$2.333*10^{-3}$	$6.189*10^{-5}$
K	$5.146*10^{-5}$	$4.018*10^{-5}$	$3.327*10^{-4}$	$6.366*10^{-5}$
O(0)	$1.134*10^{-3}$	$1*10^{-20}$	$1.376*10^{-3}$	$5.012*10^{-4}$
S(-2)	$1*10^{-20}$	$1*10^{-20}$	$1*10^{-20}$	$1*10^{-20}$
S(6)	$2.636*10^{-3}$	$1.729*10^{-3}$	$1.437*10^{-3}$	$5.462*10^{-5}$
pH	6.918	7.212	8.549	4.056
pe	13.791	1.458	5.715	16.566
Calcite	$1.478*10^{-2}$	$1.479*10^{-2}$	0	0
Ferrihydrite	$2.83*10^{-2}$	$2.83*10^{-2}$	0	0
Pyrolusite	$9.5*10^{-4}$	0	0	0
Rhodochrosite	0	$9.5*10^{-4}$	0	0
Siderite	0	$8.32*10^{-6}$	0	0
FeS (ppt)	0	0	0	0
Particular OC	$1*10^{-5}$	$2*10^{-2}$	0	0

The applied kinetic parameters are summarised in Table 6 for Monod parameters and in Table 7 for the dissolution of particulate OC.

Table 6 Assigned Monod kinetics parameters

Parameter	Dimension	Value
k_{O2}	d^{-1}	$1*10^{-7}$
k_{NO3}	d^{-1}	$1*10^{-8}$
k_{MnO2}	d^{-1}	$1*10^{-8}$
$k_{Fe(OH)3}$	d^{-1}	$5*10^{-10}$
k_{SO4}	d^{-1}	$1*10^{-9}$
$K_{m,O2}$	$mol\ l^{-1}$	$1*10^{-4}$
$K_{m,NO3}$	$mol\ l^{-1}$	$1*10^{-5}$
$K_{m,MnO2}$	$mol\ l^{-1}$	$1*10^{-5}$
$K_{m,Fe(OH)3}$	$mol\ l^{-1}$	$1*10^{-4}$
$K_{m,SO4}$	$mol\ l^{-1}$	$1*10^{-4}$
I_{O2}	$mol\ l^{-1}$	$1*10^{-5}$
I_{NO3}	$mol\ l^{-1}$	$1*10^{-5}$
I_{MnO2}	$mol\ l^{-1}$	$1*10^{-5}$
$I_{Fe(OH)3}$	$mol\ l^{-1}$	$1*10^{-5}$

Table 7 Assigned particulate OC dissolution parameters

Parameter	Dimension	Value
k_{sol}	d^{-1}	$5*10^{-4}$
$C_{DOC,sat}$	$mol\ l^{-1}$	$1*10^{-8}$

All values depicted in Table 6 and Table 7 are first approaches. The MONOD decay constants are specified as not exceeding the minimum value given by Hunter et al. (1998) for the decay of DOC ($3*10^{-5}$ year^{-1}). A first indication for the order of magnitude for the solubility of particulate OC ($C_{DOC,sol}$) is given by the sampled DOC values along the Tegel test site (4-7 mg DOC l^{-1}).

Model runs showed that beside the local availability of particulate OC, the ratio between MONOD decay constants of DOC and the dissolution constant of particulate OC is mainly decisive for the spatial distribution of redox zoning. The supply of DOC is controlled by the solution rate constant for particulate OC (k_{sol}) and the local concentration of particulate OC in the aquifer matrix. The hydrochemical feature along the Tegel transect test site as deduced from the results of the sampling campaign (NASRI DATABASE (2004), especially the spatial distribution of the redox zones) is verified on principle by the conceptual reactive transport model. From the simulation results the great impact of the local flow field and of the geologic pattern, such as variations in the leakance of the river bed or the local aquitard

distribution, on the local hydrochemical groundwater composition is illustrated. Further, simulation results will be strongly influenced by the interplay of hydrodynamic transport, biodegradation kinetics, the extent of supply of reactive DOC by dissolution of particulate OC, and the spatial distribution of particulate OC within the aquifer system. As in most cases, compared to groundwater analyses informations about the aquifer matrix composition are scarce. In the NASRI project, only one drilling core was analysed (NASRI 2003). From all theses perceptions it follows that only a general verification of hydrochemistry has to be aimed in the light of the uncertainties discussed above.

1.3.1.8. Results of reactive transport model simulation

The reactive transport simulation was performed using a time step of 1 day over a total simulation time of 1095 days. The reactive transport simulation results are demonstrated as vertical cross sections showing the initial and final component concentration distributions by Figure 40- Figure 53. The range of calculated concentrations are shown using the colour bars positioned on the right side of the plots
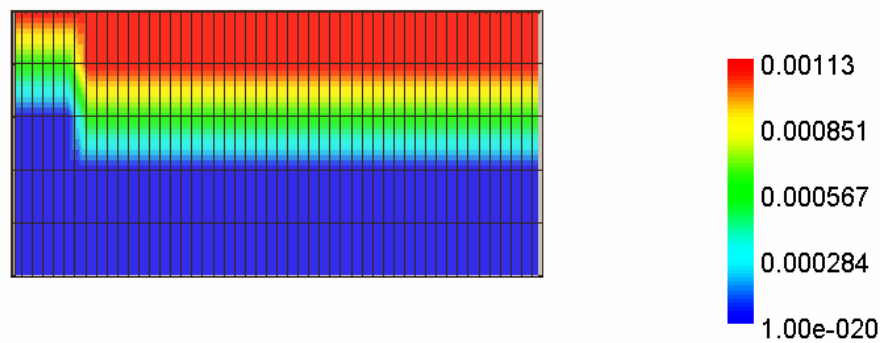
Figure 40 Initial O(0) concentrations (mol l^{-1})
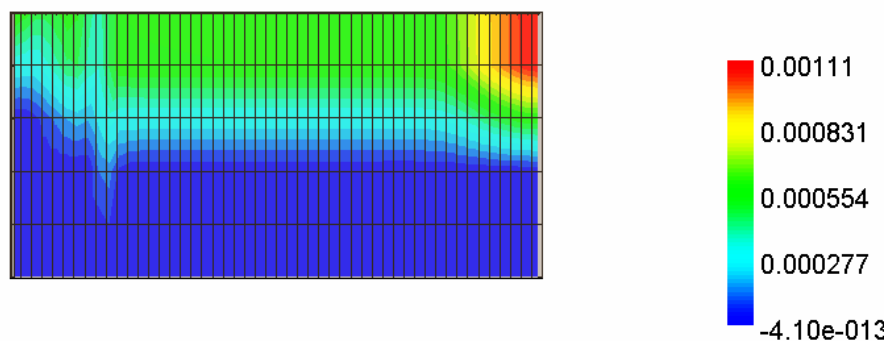
Figure 41 Calculated O(0) concentrations (mol l^{-1}) at the end of the simulation (after 1095 d)
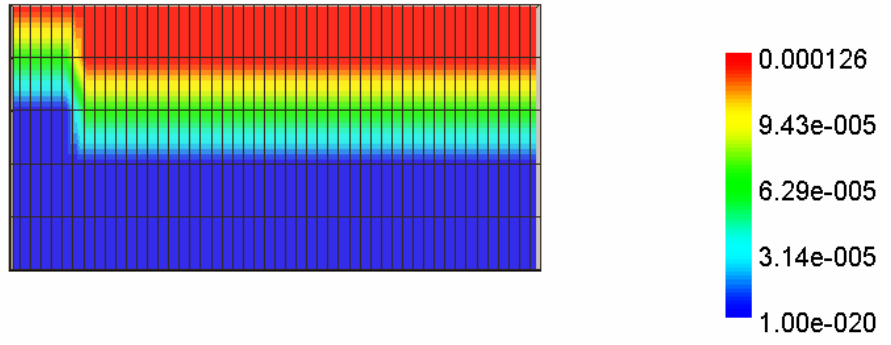
Figure 42: Initial NO$_3$-N concentrations (mol l^{-1})
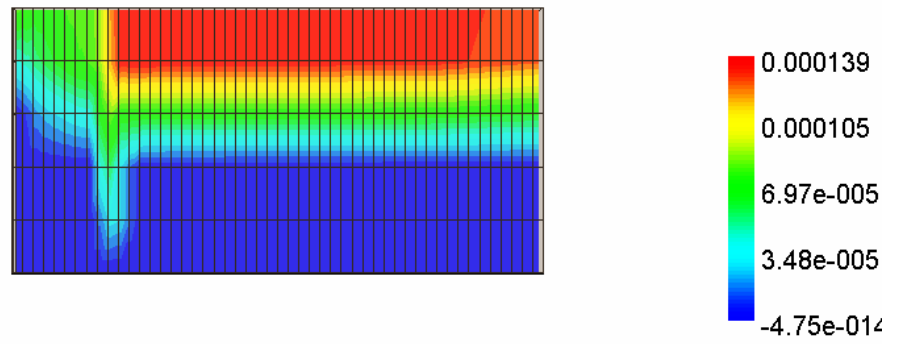
Figure 43 Calculated NO$_3$-N concentrations (mol l^{-1}) at the end of the simulation (after 1095 d)
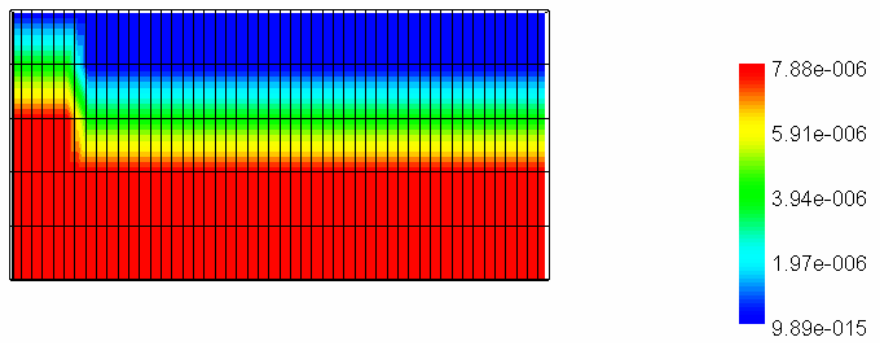
Figure 44 Initial Mn concentrations (mol l^{-1})
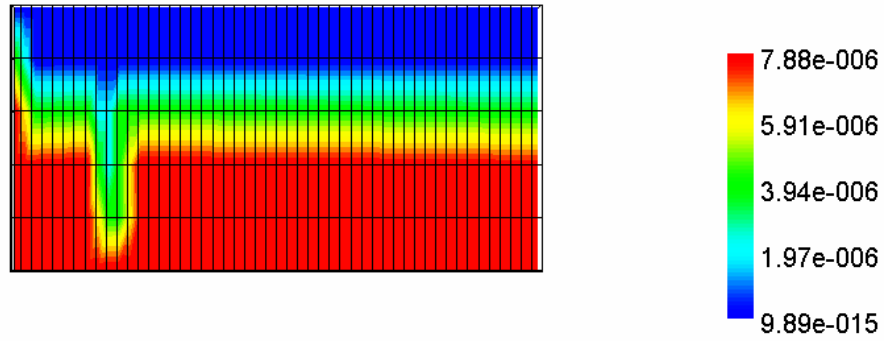
Figure 45 Calculated Mn concentrations (mol l^{-1}) at the end of the simulation (after 1095 d)
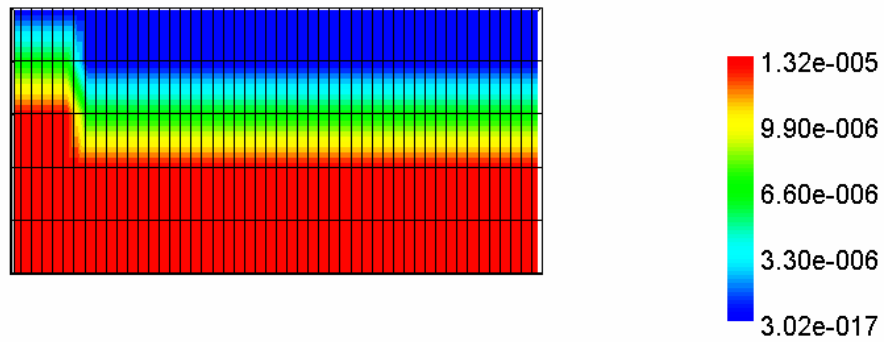
Figure 46 Initial Fe concentrations (mol l^{-1})
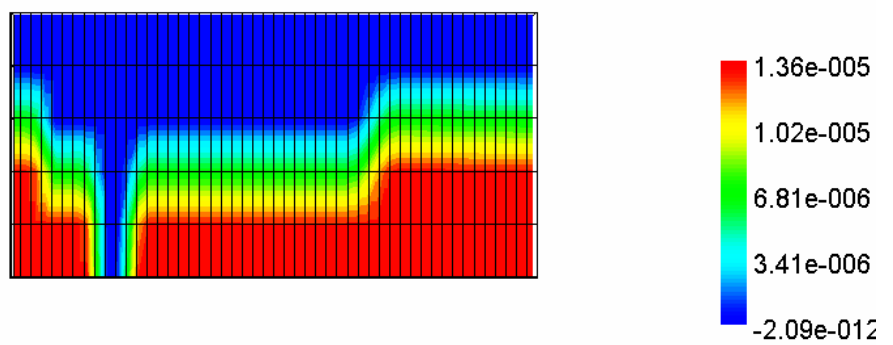
Figure 47 Calculated Fe concentrations (mol l^{-1}) at the end of the simulation (after 1095 d)
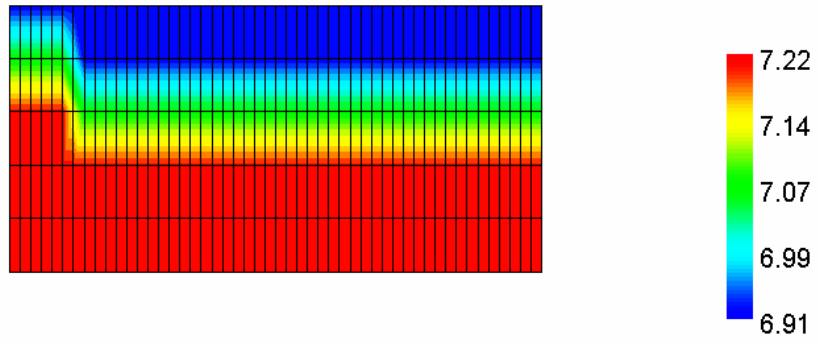
Figure 48 Initial pH values
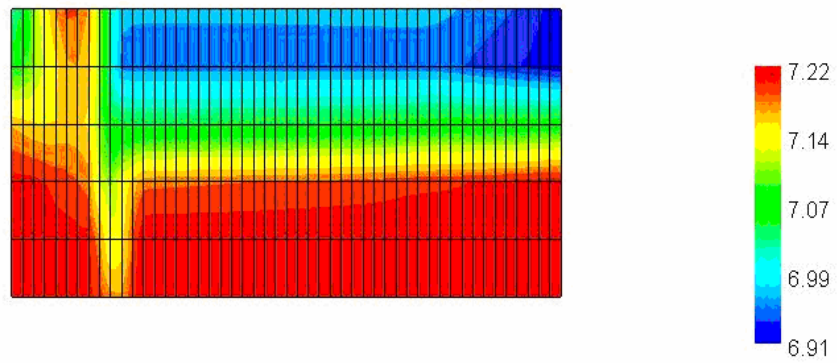
Figure 49 Calculated pH values at the end of the simulation (after 1095 d)
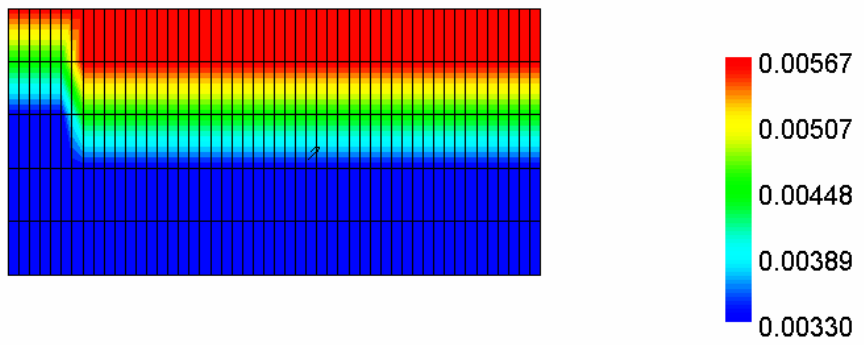
Figure 50 Initial HCO_3^- concentrations (mol l^{-1})
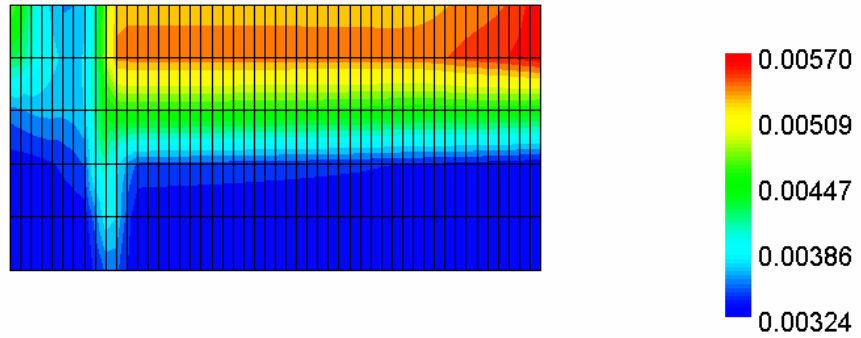
Figure 51 Calculated HCO$_3^-$ concentrations (mol l^{-1}) at the end of the simulation (after 1095 d)
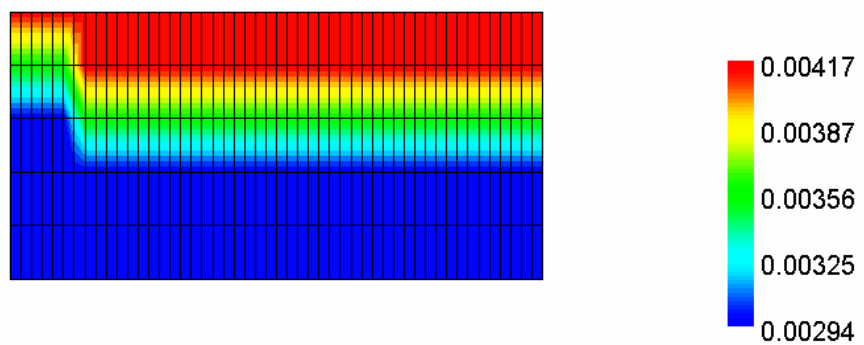
Figure 52: Initial Ca concentrations (mol l^{-1})
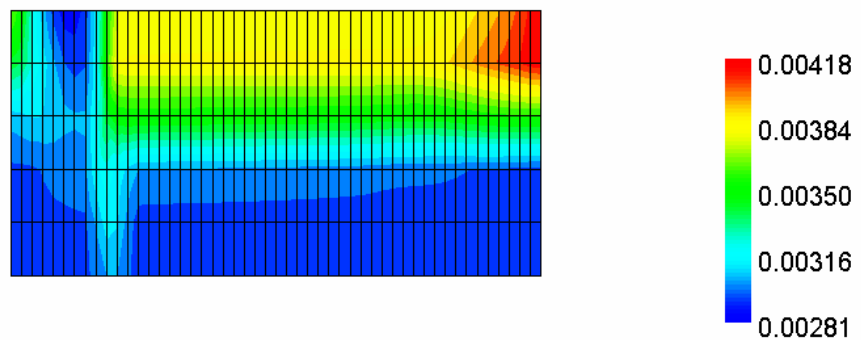
Figure 53 Calculated Ca concentrations (mol l^{-1}) at the end of the simulation (after 1095 d)

The hydrochemical feature along the Tegel transect test site as deduced from the results of the sampling campaign (NASRI DATABASE (2004), especially the spatial distribution of the redox zones) is verified on principle by the conceptual reactive transport model. From the simulation results the great impact of the local flow field and of the geologic pattern, such as variations in the leakance of the river bed or the local aquitard distribution, on the local

hydrochemical groundwater composition is illustrated. Further, simulation results will be strongly influenced by the interplay of hydrodynamic transport, biodegradation kinetics, the extent of supply of reactive DOC by dissolution of particulate OC, and the spatial distribution of particulate OC within the aquifer system. As in most cases, compared to groundwater analyses informations about the aquifer matrix composition are scarce. In the NASRI project, only one drilling core was analysed (NASRI 2003). From all theses perceptions it follows that only a general verification of hydrochemistry has to be aimed in the light of the uncertainties discussed above.

1.4. Major Conclusions and summary

Hydraulic modelling revealed, the leakance factor of the bank is time variant. The reason for this behaviour could not been identified, however it seems to increase with increasing pumping rates of the well field west. This effect stabilizes bank filtration and should be considered for further studies.

Leakance factors show a high spatial variance, factor 4 within a distance of 1.4 m is measured. Merging this with increased leakance by increased pumping rates, infiltration occurs as fingering, with the regions of high infiltration rather stabilizing than being clogged by increased suspended matter in the infiltration water.

The maximum leakance factor calculated from measured infiltration rates takes place in a water depth of about 1.4 m (Section 3.1.3). Simulations however suggest in 4-6 m depth the the leakance factor has its maximum. As local heterogeneity is high, the model results seem to be more reliable.

Water at the transect is demonstrated to be stratified in three fractions of bank filtrate. The existence of the medium aged fraction is detected by the hydraulic model. As the medium aged fraction is more similar to the young than to the old fraction it was considered to be part of the young fraction, thus travel times for the sum of bankfiltrate at well 13 would been underestimated. This may be an explanation why many substances show up in the observation wells just below the glacial till but are not detectable in the abstraction well 13. A point of vulnerability

It was demonstrated, that using a generic hydrogeological model approximated to results of hyrogeological investigations (NASRI, 2003) the redox zoning observed along the Lake Tegel riverbank filtration test site can be verified by reactive modelling. The applied reactive transport modelling software PHT3D (Prommer, 2002) has been proven as a suitable modelling tool, which can also deal complicated hydrochemical conditions.

As a first attempt, the reactive model is based on an simplified pattern of hydrogeological pattern considering the observed hydrogeological situation and a highly transient idealised pumping regime of the well field as performed in principle by the well field pumping management. The reactive transport model set up on the generic flow model is based on schematized concentration parameters such as surface water chemistry, oxic groundwater chemistry within the shallow groundwater and anoxic groundwater chemistry for the deeper groundwater, but the applied conceptual reactive network was shown to be adequate to verify by principle the observed redox zonation along the Lake Tegel test side described by (NASRI, 2003). Both infiltration from Lake Tegel and groundwater flow from Land side were recognized to be important factors of redox zoning formation. As a main factor influencing the reactive transport modelling results the interaction of DOC biodegradation kinetics and supply of DOC by dissolution of particulate organic carbon was recognized. Furthermore, it results that a correct flow modelling also in detail is a precondition to verify the observed redox zoning. Other factors, such as seasonal temperature oscillations affecting the shape of redox zoning (see contribution of J. Greskowiak on the artificial recharge pond) were not considered. In assessing the results of reactive modelling, the scarce data basis about the mineralogical aquifer composition has to be taken into account.

1.5. References

Appelo, C. A. J., & Postma, d. (1996): Geochemistry, Groundwater and Pollution. Balkema, Rotterdam.

Barry, D. A., Prommer, H., Miller, C. T., Engesgaard, P., Brun, A., & Zheng, c. (2002): Modelling the fate of Oxidable Organic Contaminants in Groundwater. Adv. Water Resour., 25., 945-983.

Beulker, C., Gunkel, G., Hoffmann, A., Kosmol, J., (2005) Fluorrescence Markers of POM transport and Biogenic Metabolism in litoral sediments, Limnology and Oceanography Methods, submitted Dec. 2005

Bouwer, H. (2002). Artificial Recharge of Groundwater: Hydrogeology and Engineering. Hydrogeology Journal, 10(1), 121-142.

Bouwer, H; Rice, R. C.; (1989) Effect of Water Depth in Groundwater Reacharge Basins on Infiltration, Journal of Irrigation and Drainage Engineering, Vol. 115, No. 4, p. 556-567

Brühl, H.; Sommer-von Jarmersted, C; (1986) Ergebnisbericht: Baugrunduntersuchung auf der Kabeltrasse im Tegeler See (Wasserwerk Tegel – Trafostation Tegelort); Institut für Angewandte Geologie der Freien Universität Berlin, unpublished work

Brun, a., Engesgaard, p. (2002): Modelling Transport And Biogeochemical Processes In Pollution Plumes: Literature Review and Model Development. J. Hydrol., 256., 211-227.

Chiang, W.-H., (2003) Processing Modflow Pro,V 7.0, Users guide,

Diersch, H. J.-D., (2002), Grundwassersimulationssystem FEFLOW. User-/Reference-Manual. WASY GmbH Berlin, 2002

Doherty, John, (2004) PEST – Model independent Parameter estimation, User Manual 5th Edition, Watermark Numerical Computing

Eichhorn, S.; (2000); Numerische Strömungsmodellierung der Uferfiltration am Tegeler See, Diplomarbeit; Institut für Geologie, Geophysik und Geoinformatik FU Berlin

Fritz, B. (2002) Untersuchungen zur Uferfiltration unter verschiedenen wasserwirtschaftlichen, hydrogeologischen und hydraulischen Bedingungen, Dissertation, Fachbereich für Geowissenschaften, FU Berlin.

FUGRO (2000) Hydrogeologischen Stukturmodell für das Wasserwerk, FUGRO GmbH, im Auftrag BWB, Juni 2000, unpublished work

Greskwiak, J., Prommer, H., Massmann, G., Johnston, C. D., Nützmann, G., Pekdeger, A. (2005); The impact of variably saturated conditions on hydrogeochemical changes during artificial recharge of groundwater, Applied Geochemistry vol. 20, 1409-1426

Harbaugh, AW (1990), A computer program for calculating subregional water budgets using results from the U.S. Geological Survey modular three-dimensional ground-water flow model: U.S. Geological Survey Open-File Report 90-392, 46 p.

Harbaugh AW, Banta ER, Hill MC and McDonald MG (2000), MODFLOW-2000, The U.S. eological Survey modular ground-water model User guide to Modularization concepts and the ground-water flow process, U. S. Geological Survey, Open-file report 00-92.Hunter, k. S., Wang, y. & van Cappellen, p.(1998): Kinetic modelling of Microbially-Driven Redox Chemistry of Subsurface Environments: Coupling Transport, Microbial Metabolism and Geochemistry. J. Hydrol. 209, 53-80.

Kipp, K. L. (1997): Guide to the revised heat and solute transport SIMULATAOT: HST3D, version 2. U.S. Geological Survey, Water Resources Investigation Report 97-4157, Denver, Co., U.S.A.

Lin, Chunye; Greenwald, Dan; Banin, Amos (2003) Temperature Dependence of Infiltration Rate During Large Scale Water Recharge into Soils, Soil Sci. Soc. Am. J. 67 p. 487–493

lindberg, r. b. & runnels, d. d. (1984): Ground water redox reactions: An analysis of equilibrium state applied to Eh measurements and geochemical modeling. Science 225, 925-927.

McDonald MG and Harbaugh AW (1988), MODFLOW, A modular threedimensional finite difference ground-water flow model, U. S. Geological Survey, Open-file report 83-875, Chapter A1

Merkel, B. J. & Planer-Friedrich, B. (2002): Grundwasserchemie, praxisorientierter Leitfaden zur numerischen Modellierung von Beschaffenheit, Kontamination und Sanierung aquatischer Systeme. Springer, Berlin, Heidelberg.

NASRI (2003): Natural and Artificial Systems for Recharge and Infiltration, 1st Report. Kompetenzzentrum Wasser, Berlin.

NASRI database (2004): Natural and Artificial Systems for Recharge and Infiltration, Chemical Analyses Database (Time interval 2002-2004). Kompetenzzentrum Wasser, Berlin. unpublished work

Pachur, Hans-Joachim and Haberland, Wolfram (1977). Untersuchungen zur Morphologischen Entwicklung des Tegeler Sees (Berlin). Die Erde 108[4], 320-341

parkhurst, d. l., thorstenson, d. c., & plummer, l. n. (1980): PHREEQE – a computer program for geochemical calculations. U.S. Geological Survey Water-Resources Investigation Report 80-96, Denver, Co., U. S. A., pp 195.

Parkhurst, D. L., & Appelo, C. A. J. (1999): User's Guide to PHREEQC (Version 2) – a computer program for speciation, batch-reaction, one-dimensional transport, and inverse geochemical calculations. U.S. Geological Survey Water-Resources Investigation Report 99-4259, Denver, Co., U. S. A., pp 312.

Parkhurst, D. L., Kipp, K. L., Engesgaard, P. & Charlton, S.R. (2004): PHAST – a computer program for simulating groundwater-flow, solute transport, and multicomponent geochemical reactions. U.S. Geological Survey Techniques and Methods 6–A8, 154 p.

Prommer, H. (2002): A reactive multicomponent transport model for saturated porous media. Draft of user's manual version 1.0, contaminated land assessment and remediation research centre, the university of Edinburgh (available from http://www.pht3d.org)

Ripl, W., Heller, S., and Linnenweber, C. (1987) Limnologische Untersuchungen an den Sedimenten des Tegeler Sees. Eigenverlag Fachgebiet Limnologie, Technische Universität Berlin.

Rümmler, J. (2003) 2-Dimensional-horizontal-ebene Simulation der Grundwasserströmungsverhältnisse unter Uferfiltrationsbedingungen, Diplomarbeit; Mathematisch-Naturwissenschaftliche Fakultät 2, Geographisches Institut, Humboldt-Universität zu Berlin

Sievers, J., (2001), Geochemische und hydraulische Untersuchungen an Mudde- und Sandkernen aus dem Tegeler See. unveröffentlichte Diplomarbeit, Institut für Geowissenschaften, FU Berlin.

Stuyfzand, P.,. Juhàsz-Holterman, M., de Lange, W. (2004), Riverbank filtration in the Netherlands: well fields, clogging and geochemical reactions, NATO Advanced Research Workshop: Clogging in Riverbank Filtration Bratislava, 7-10 Sept. 2004.

Terzaghi, Karl; Peck, Ralph B., (1948) Soil Mechanics in Engineering Practice, John Wiley & Sons, Inc., New York

Voigt, I., Eichberg, M., (2000) Hydrogeologische Übersichtsprofile Nr.1- Nr.10, erstellt von der Fugro im Auftrag der BWB, 2002.

WASY (2004) Hydrogeologisches Fachgutachten zur Auswirkung grundlegender Änderungen des Betriebs zur Grundwasseranreicherung Wasserwerk Tegel, Unpublished Work, WASY Gesellschaft für wasserwirtschaftliche Planung und Systemforschung mbH, Berlin. unpublished work

Wiese, B., Holzbecher, E., Rümmler, J, and Nützmann, G. (2004) Effects of Oscillating Pumping Regimes of Bank-Filtration Galleries. Proc. International Conference on Finite-Element Models, FEM-MODFLOW, Modflow and more 2004, Carlovy Vary, Czech Republic, 411-414.

Zheng, C., & Wang, P. P. (1998): MTD3MS, A modular three-dimensional transport model. Technical report, US Army Corps of Engineers Watewrways Experiment Station, Vicksburg, Miss., U.S.A.

Abbreviations:

GUI Graphical User Interface

SENSUT Senatsverwaltung für Stadtentwicklung und Umweltschutz, Environmental Authority of Berlin

2. Artificial Recharge site

2.1. Objectives

This part of the NASRI project focussed on the hydraulic and hydraulic processes and their interaction occurring during artifical recharge of groundwater at the field site GWA Tegel. The research conducted for this part of the NASRI project was aimed to meet the following objectives:

(1) Understanding the impact of transient saturated and unsaturated conditions directly below the artificial recharge pond at GWA Tegel on the dynamics of hydrogeochemical changes during infiltration, and verifying the findings by multicomponent reactive transport modelling

(2) Providing a process-based modelling framework to interpret the seasonal degradation behaviour of the pharmaceutical residue phenazone within the aquifer surrounding the artificial recharge pond at GWA Tegel

In order to meet these objectives, the research was carried out by three separate studies in close collaboration with the NASRI group Hydrogeology. For clarity, the studies are described by three chapters, each of them containing a methods and results (and discussion) section. The final chapter summarizes the conclusions of all three studies and gives prospects for future research.

2.2. Hydraulic and hydrogeochemical changes below the pond

1.1.6. Materials and Methods

From July 2003 until December 2003, sampling of (i) the pond water, (ii) groundwater from an observation well (screened at 6-8 m below the pond), and (iii) water extracted from four ceramic suctions cups at 50 cm, 100 cm, 150 cm and 200 cm below the artifical recharge pond was carried out on a weekly base. Water content and pressure heads were continuously recorded at two different depths, i.e., 50 cm and 150 cm below the pond. The locations of all these probes are shown schematically in Figure 54. Alkalinity and pH were measured in the field immediately after sampling. Alkalinity was determined by Gran Titration. All samples were analysed for major ions and dissolved organic carbon (DOC) using standard methods. Data from samples with a charge balance error of more than 5 % were discarded. Dissolved oxygen (DO) concentrations were measured by optical sensor-type oxygen probes (Hecht and Kölling 2001) placed next to the suction cups. All of the installations, including the groundwater monitoring well, are positioned approximately 4 m from the edge of the pond.
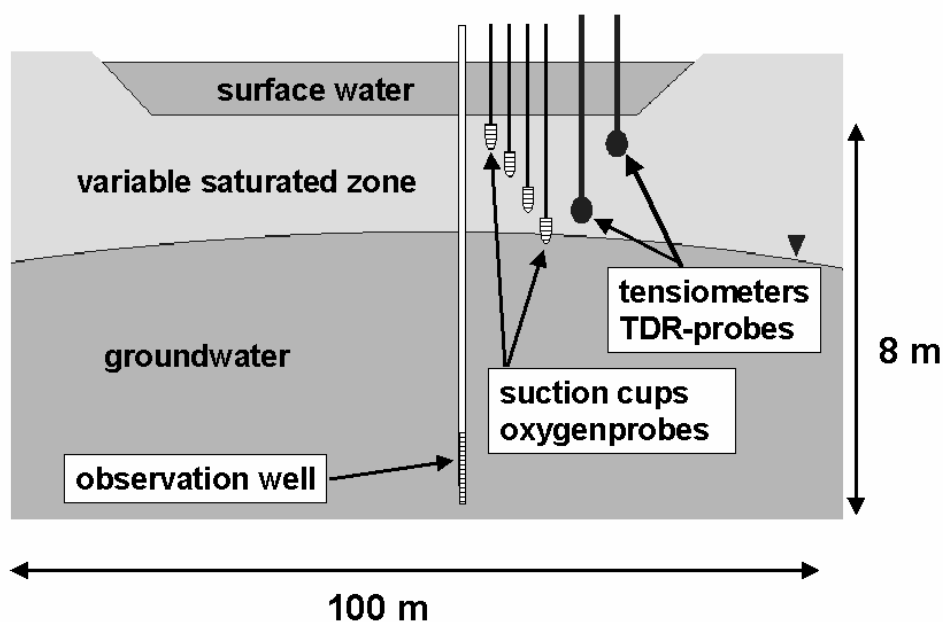
Figure 54 Schematic cross-section of study area and locations of sample collection and measurement devices.

1.1.7. Results and discussion

2.2.1.1. Hydraulic conditions

Measured time-series of water contents (Figure 55) and pressure heads (data not shown) below the pond indicated that the transient hydraulic conditions of each operational cycle could be classified hydraulically into four different major stages. Stage 1 marked the transition from unsaturated to saturated conditions beneath the pond (Figure 55), which occurred soon after the removal of the clogging layer once infiltration was restarted. The saturated conditions prevailed for approximately 50 days (Stage 2) until the of the groundwater table dropped abruptly within a few days. The decline of the water table forced air from the pond margins to the centre beneath the recharge pond and water contents fell from about 40-45 % to 30-35 % (Figure 55). The unsaturated conditions prevailed for 40 days (Stage 3). During the last period of the operational cycle (Stage 4) the pond was empty and the redevelopment of the pond took place. Hence, no recharge occurred. A schematic diagram of the relevant hydraulic stages is given in Figure 56.

2.2.1.2. Dynamics and Distribution of redox environments

During Stage 1, oxygen concentrations declined from about 5 mg/l to zero at all observed depths (Figure 57), i.e., oxygen was consumed within the first 50 cm below the pond. During the entire Stage 2, DO concentrations remained zero at all observed depths. About 20 to 30 days after the beginning of Stage 2, nitrate concentrations at various depths started to drop below the concentrations found in the surface water (Figure 58). At 50 cm and 100 cm depth nitrate was totally depleted within a few days, whereas the concentrations in the groundwater decreased more slowly (Figure 58). In contrast, at 150 cm and 200 cm depth, nitrate was not fully consumed.
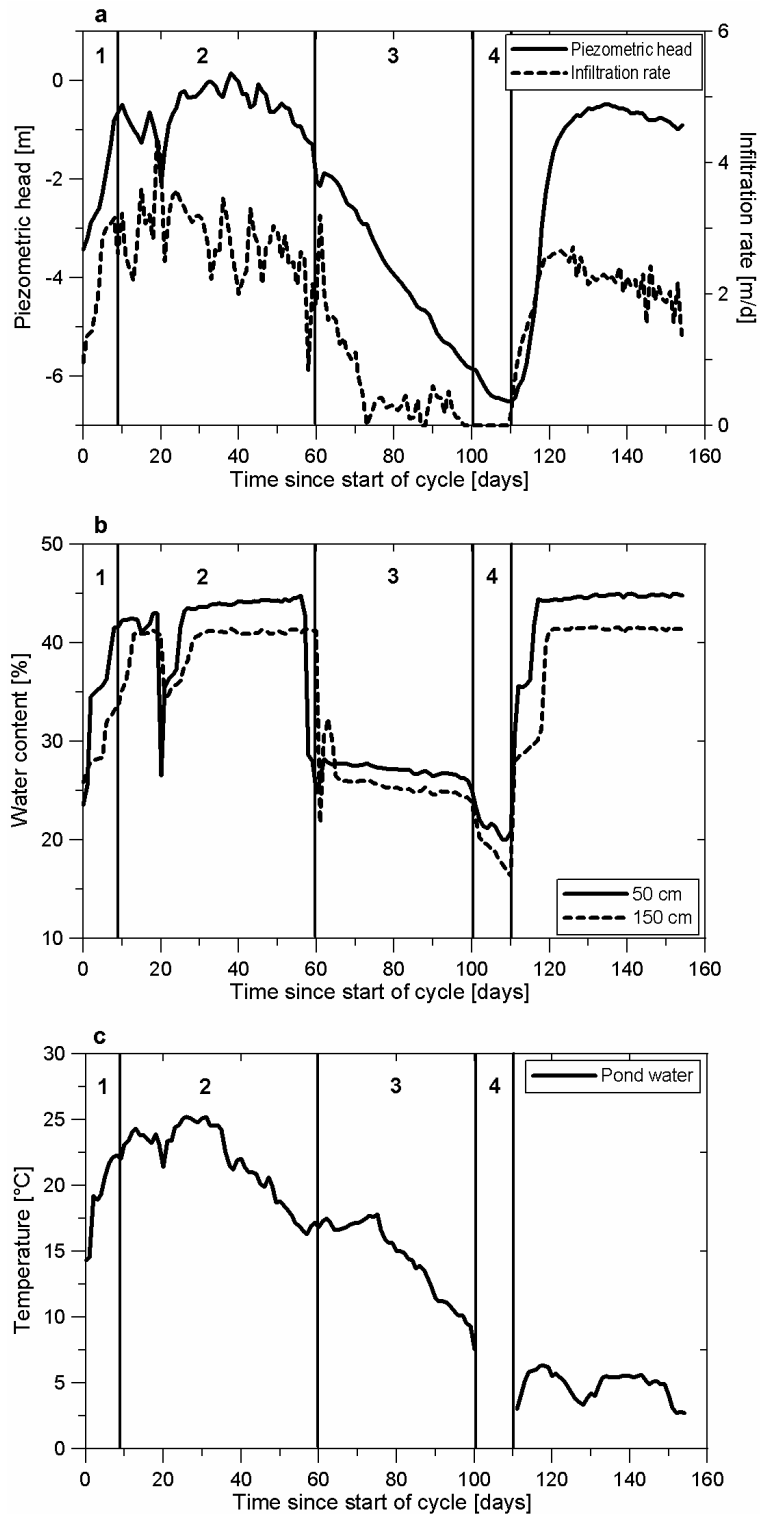
Figure 55 a. **Piezometric head at a depth of 8 m below the pond and infiltration rate. The data for the infiltration rate has been provided by the BWB;** b. **Water contents at depths of 50 cm and 150 cm below the pond;** c. **Temperature of the pond water. The numbers 1-4 refer to the Stages 1-4 of the operational cycle. Note that the pond was dry during Stage 4.**
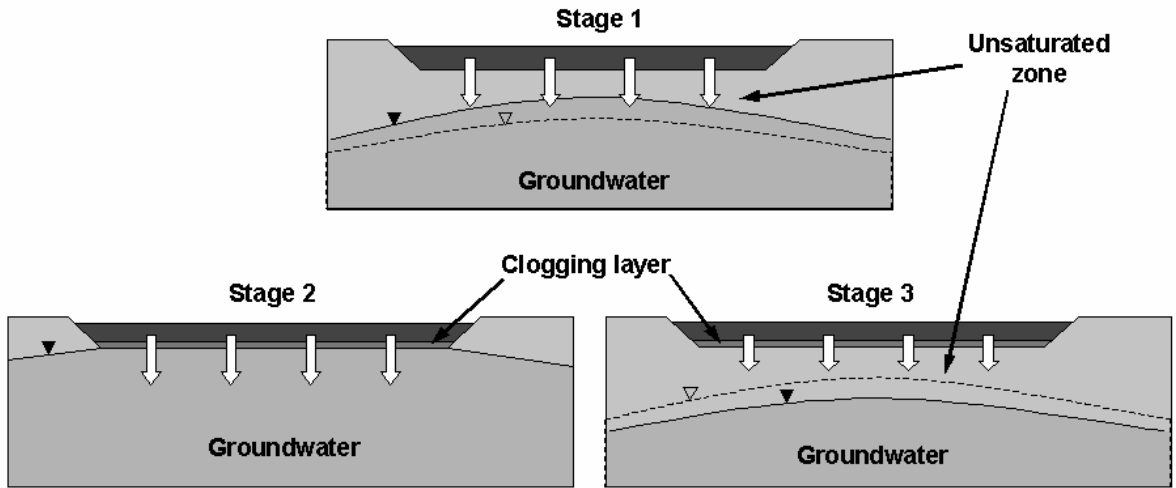
Figure 56 Schematic cross-sectional diagram of the pond for the Stages 1, 2 and 3.
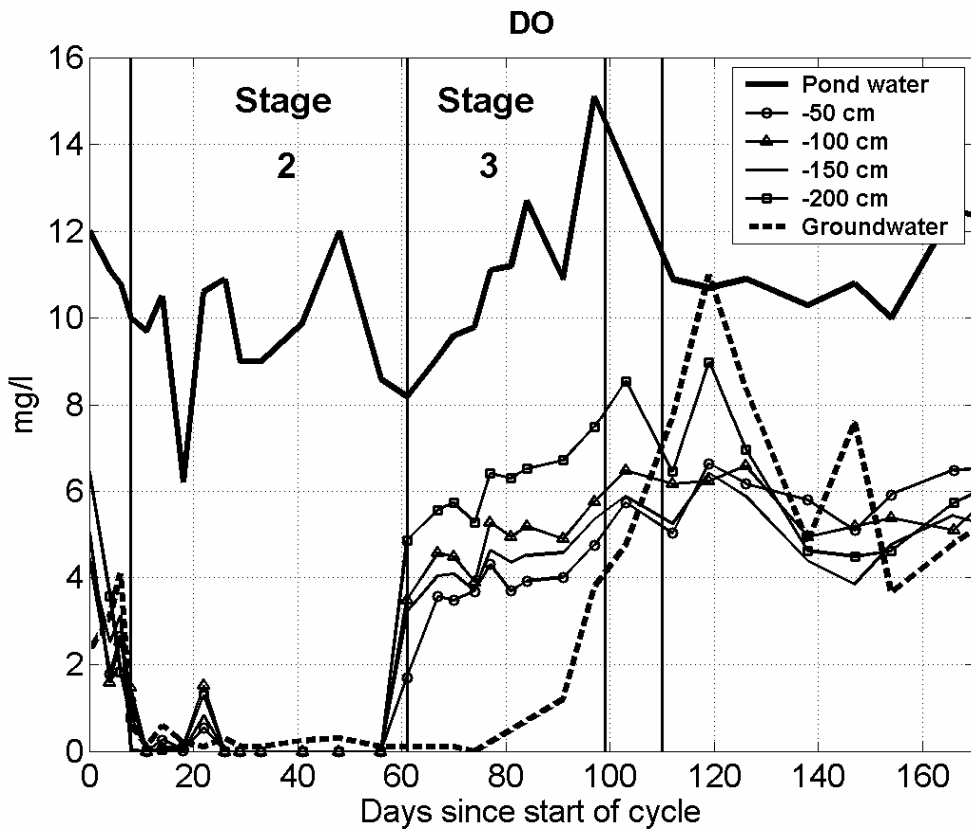
Figure 57 Oxygen concentrations in the pond and groundwater and at depths of 50 cm, 100 cm, 150 cm and 200 cm beneath the pond.
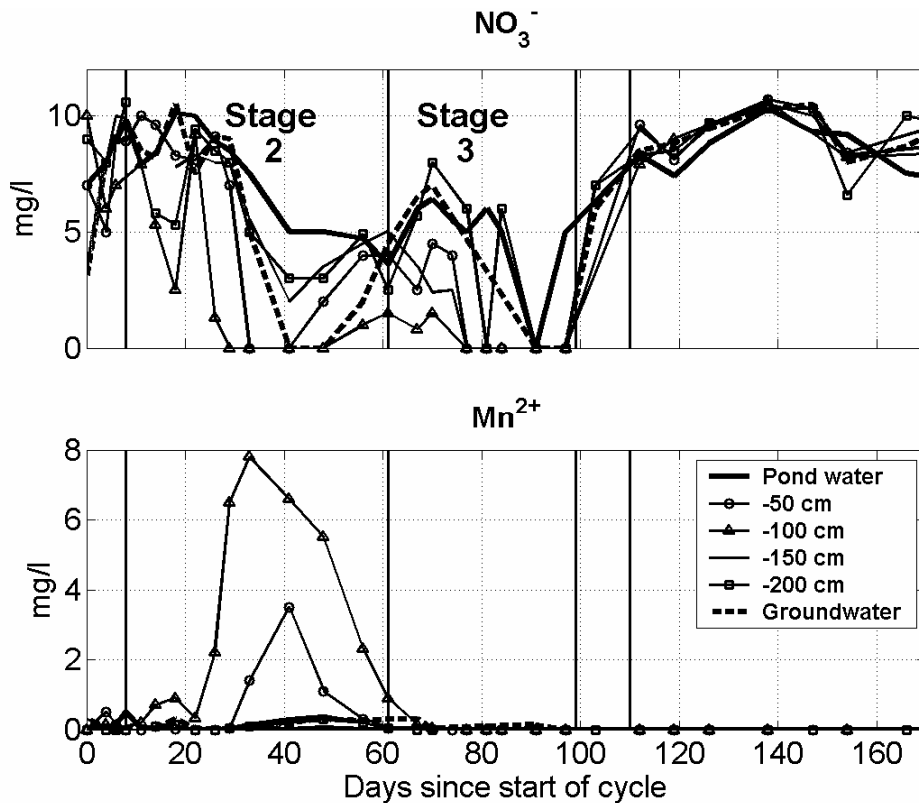
Figure 58 Nitrate (as NO₃⁻) and manganese (Mn²⁺) in the pond and groundwater and at depths of 50 cm, 100 cm, 150 cm and 200 cm beneath the pond.

At locations where nitrate was depleted, the redox-environment shifted to manganese reducing conditions, as indicated by an increase of manganese (Mn^{2+}) concentrations (up to 8 mg/l, see Figure 58). At a depth of 100 cm below the pond, where Mn^{2+} concentrations were highest, iron (Fe^{2+}) concentrations increased to 0.3 mg/l (Figure 59), indicating that iron reduction took place during Stage 2. The heightened Mn^{2+} concentrations at these depths lasted for approximately 10 days before they started to decline again. The decline was most likely the result of a decrease in water temperature (Figure 55), associated with a decrease of microbial activity and coincided with a simultaneous rise of nitrate concentrations beneath the pond (Figure 58). During Stage 1 and Stage 2, sulphate concentrations were generally around 140 mg/l and did not show any significant variations with depth (Figure 59). Although not directly observed, sulphate reduction is assumed to have occurred at non-detectable levels during Stage 2, as it is known to take place in parallel or even before iron reduction, dependent on the local geochemical setting (Postma and Jakobsen 1996).

During the rapid change from water saturated (Stage 2) to water unsaturated conditions (Stage 3), oxygen concentrations increased up to 5 mg/l (Figure 2.4). Although aerobic respiration seems to be the dominant redox reaction during Stage 3, nitrate concentrations at 3 suction cups were still somewhat lower than in the surface water (Figure 58). These patchily distributed zones of more reducing conditions (also observed in Stage 2) are considered to

result from (i) the formation of anaerobic microsites caused by particulate organic carbon contained in the sediment and (ii) non-uniform flow caused by the physical heterogeneity of the sediment, i.e., hydraulic conductivity. Concomitant with the appearance of atmospheric oxygen (during the transition from Stage 2 to Stage 3) extremely high sulphate concentrations of up to 370 mg/l were observed in the water extracted from three suction cups. However, in the following 20 days they declined rapidly and returned to background concentrations (Figure 59). The observed peaks of sulphate concentrations are most likely caused by the rapid oxidation of iron sulphide minerals that had formed previously (during Stage 2) as a result of sulphate reduction. However, rapid oxidation of sulphide minerals due to water table fluctuations has been observed for other, comparable hydrogeochemical systems (e.g., Sinke et al. 1998). Concomitant with the peaks of sulphate concentration, very high concentrations of calcium were observed at the same locations below the pond (Figure 59). As sulphide oxidation produces protons, the heightened calcium concentrations apparently resulted from pH buffering by the dissolution of calcite.

During the next recharge cycle, i.e., approximately after day 100, DO concentrations did not decrease when the sediment below the pond became saturated again, as is was the case in the previous cycle. This is thought to result from lower microbial activity due to lower temperatures during winter. During the entire winter period, the redox status remained aerobic, independently from the hydraulic situation below the pond.
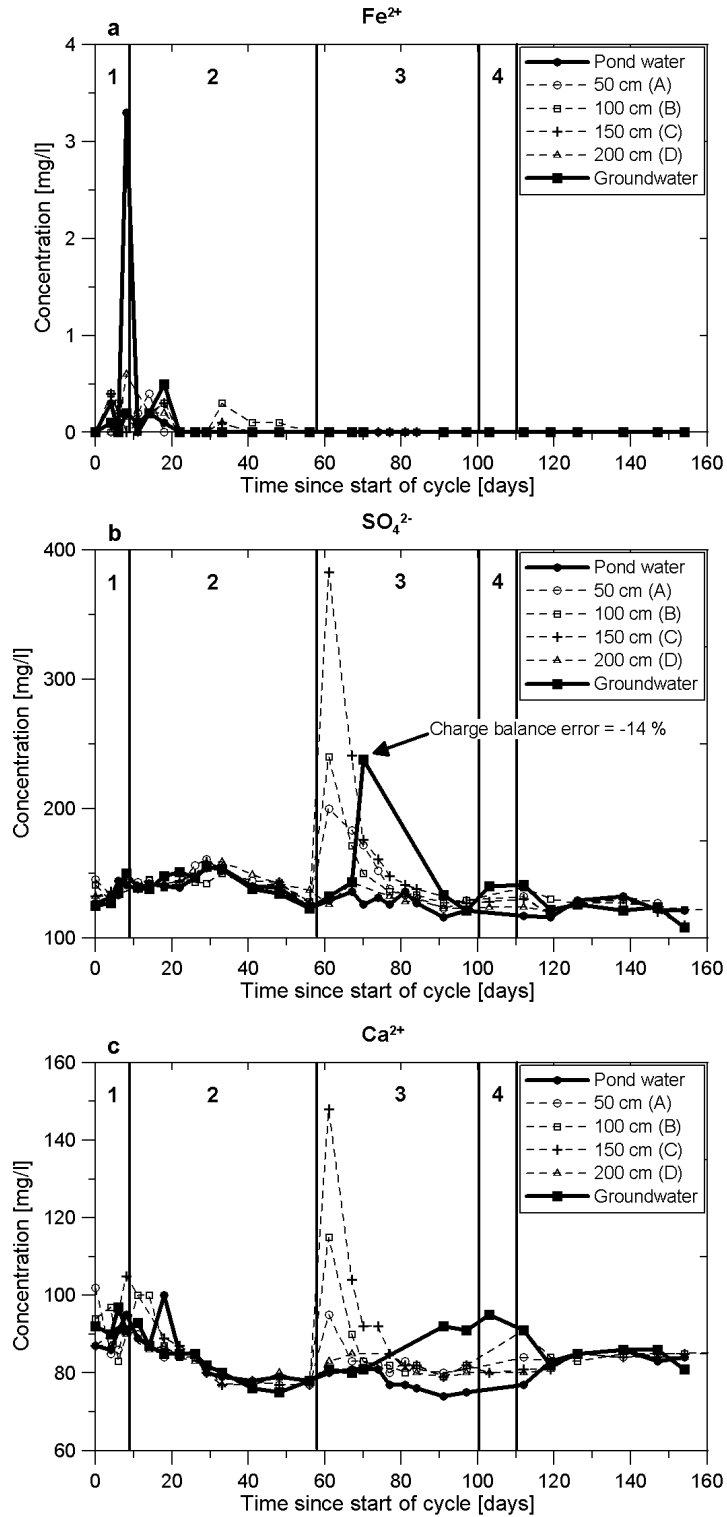
Figure 59 Concentrations of a. dissolved iron (Fe^{2+}), b. sulphate (SO$_4^{2-}$) and c. calcium (Ca^{2+}) in the pond water, groundwater (depth 8 m) and at depths of 50 cm, 100 cm, 150 cm, 200 cm below the pond. The numbers 1-4 refer to the Stages 1-4 of the operational cycle.

2.2.1.3. Carbon system

The effect of organic carbon degradation on the carbonate system below the pond was observed during the entire sampling period and can be seen most clearly when the hydrochemical compositions of the surface water and the groundwater are compared.

During Stage 2, dissolved oxygen and nitrate contained in the infiltration water are fully consumed due to organic carbon degradation as expressed by the reactions 2.1 and 2.2 (Table 2.1). For simplification purposes, organic carbon is represented by CH_2O. According to reaction 2.1, the full depletion of 10 mg/l dissolved oxygen (surface water concentration) accounts for a degradation of about 3.7 mg/l organic carbon. When the system moved to nitrate reducing conditions, the consumption of 10 mg/l dissolved oxygen plus 5 mg/l nitrate according to reactions 2.1 and 2.2 requires about 4.9 mg/l organic carbon. This is more than twice the amount of DOC assumed to be mineralised during transport to the monitoring well (Figure 60). From this, it is evident that there must have been an additional carbon source besides DOC causing the observed consumption of oxidation capacity. Since the total organic carbon (TOC) concentration generally does not exceed the DOC concentration in the surface water of the pond (unpublished data of BWB), the additional carbon source must have been POC within the sediments below the pond. The DIC concentrations of the groundwater were about 4 - 5 mg/l higher than in the surface water (Figure 60) and matched the mineralised organic carbon concentration of 3.7 - 4.9 mg/l that is calculated from the observed TEA consumption. This implies that calcite dissolution due to carbonic acid production (as a result of organic carbon degradation) did not significantly contribute to the DIC production during Stage 2.

Atmospheric oxygen had a profound impact on the organic carbon degradation during the entire Stage 3. The heightened concentrations of calcium and DIC in the groundwater compared to the surface water during Stage 3 (Figure 59 and Figure 60) indicates that calcite dissolution took place as a result of aerobic organic carbon degradation described by reaction 2.3 (Table 8). At the end of Stage 3, the difference between the DIC concentrations (mainly as bicarbonate) of the groundwater and surface water (13 mg/l = 1.1 mmol/l, Figure 60) was twice as high as the difference between the calcium concentrations (20 mg/l = 0.5 mmol/l, Figure 59). This concentration ratio is as expected from reaction 2.3 and indicates that calcite dissolution was taking place and was caused by the degradation of organic carbon. As a result of calcite dissolution, the pH of the groundwater remained stable during this stage (Figure 60). During Stage 3, the DOC concentrations of the groundwater did not differ significantly from the surface water concentrations (Figure 60), suggesting that sedimentary POC was degraded in preference to DOC.
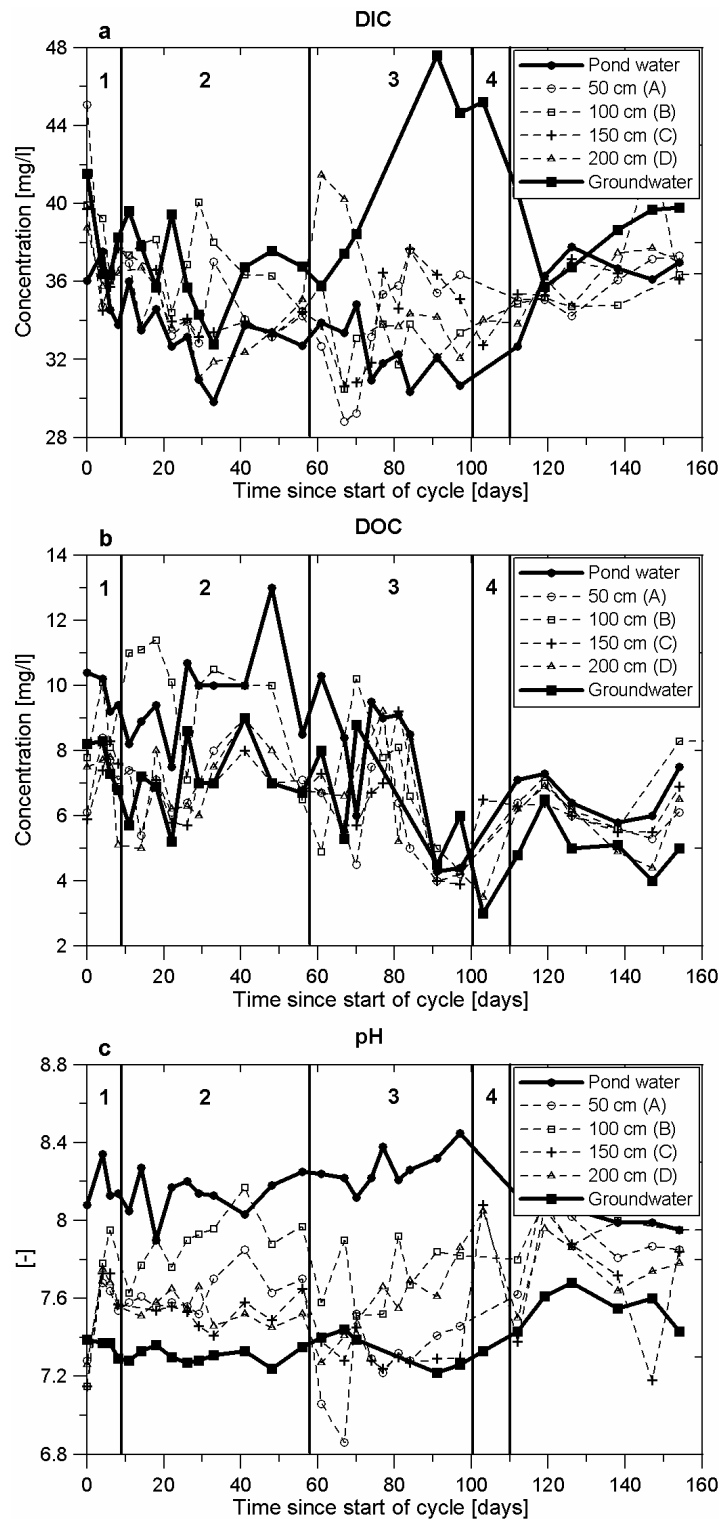
Figure 60 Concentrations of a. **dissolved inorganic carbon (DIC),** b. **dissolved organic carbon (DOC) and** c. **pH in the pond water, groundwater (depth 8 m) and at depths of 50 cm, 100 cm, 150 cm, 200 cm below the pond. The numbers 1-4 refer to the Stages 1-4 of the operational cycle.**

This is possible, as labile (highly degradable) POC is expected to be available for decomposition, which is assumed to originate from seasonal blooms of algae within the pond and transport into the first meters of the profile.

Table 8 Summery of the relevant geochemical reactions occurring below the pond.

$$CH_2O + O_2 \rightarrow H^+ + HCO_3^- \qquad\qquad (2.1)$$

$$5CH_2O + 4NO_3^- \rightarrow H^+ + 5HCO_3^- + 2N_2 + 2H_2O \qquad (2.2)$$

$$CH_2O + CaCO_3 + O_2 \rightarrow Ca^{2+} + 2HCO_3^- \qquad\qquad (2.3)$$
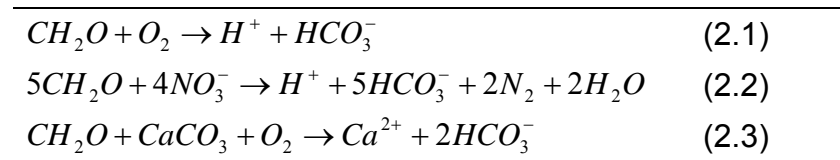
2.3. Reactive transport modelling of the unsaturated zone

It was shown in the previous chapter, that during summer the lateral intrusion of air from the pond margin due to transient unsaturated hydraulic conditions seem to have a considerable impact on the hydrogeochemistry of the seepage water. During this study, a two-dimensional multi-component reactive transport model was developed in order to (i) verify this hypothesis and (ii) find out how far gaseous oxygen migrates from the margins towards the centre below the pond during the unsaturated conditions (Stage 3), since there were no observations available clarifying this. The model included advective and dispersive transport of the relevant major ions in the water phase and O_2 and CO_2 in the gas phase. Thereby, heterogeneous reactions were considered between immobile (e.g., minerals, sediment bound organic matter), water and gas phase. Kinetic reactions were only included when the local equilibrium assumption (LEA) appeared to be violated. All other reactions (e.g., aqueous speciation, dissolution/degassing of gaseous O_2 and CO_2) were assumed to occur instantaneously.

1.1.8.

1.1.9. Conceptual gas transport model

The transient pore velocity field of air within the unsaturated zone below the pond was approximated as radial symmetric, assuming that the pond was a circle. When assuming (i) air to behave incompressible and (ii) a slip boundary for air flow at the groundwater table and at the lower end of the clogging layer, an analytical solution based on the so-called squeezing flow model (James, 2002; Lee and Ladd, 2002) can be used to simulate the pore velocity field $v_{a,r}$ of air in r-direction below the pond. The following relationships hold:

$$v_{a,r}(r,u) = -\frac{1}{2}\frac{v_V}{u}r + \frac{1}{2}\frac{v_V}{u}\frac{R^2}{r} - \frac{R}{r}v_H \text{ , for R > 0 and r ≥ R} \tag{3.1}$$

$$v_{a,r}(r,u) = -\frac{1}{2}\frac{v_V}{u}r \text{ , for R=0} \tag{3.2}$$

The parameters are explained in Figure 61. Thereby, Eqn. 3.1 was developed in order to account for the lateral propagation of the air-front in the early stage of the unsaturated conditions (Figure 61). When the air-front reaches the centre of the pond, the horizontal pore velocity of air can be described by Eqn. 3.2, which is the original squeezing flow model (James, 2002; Lee and Ladd, 2002).
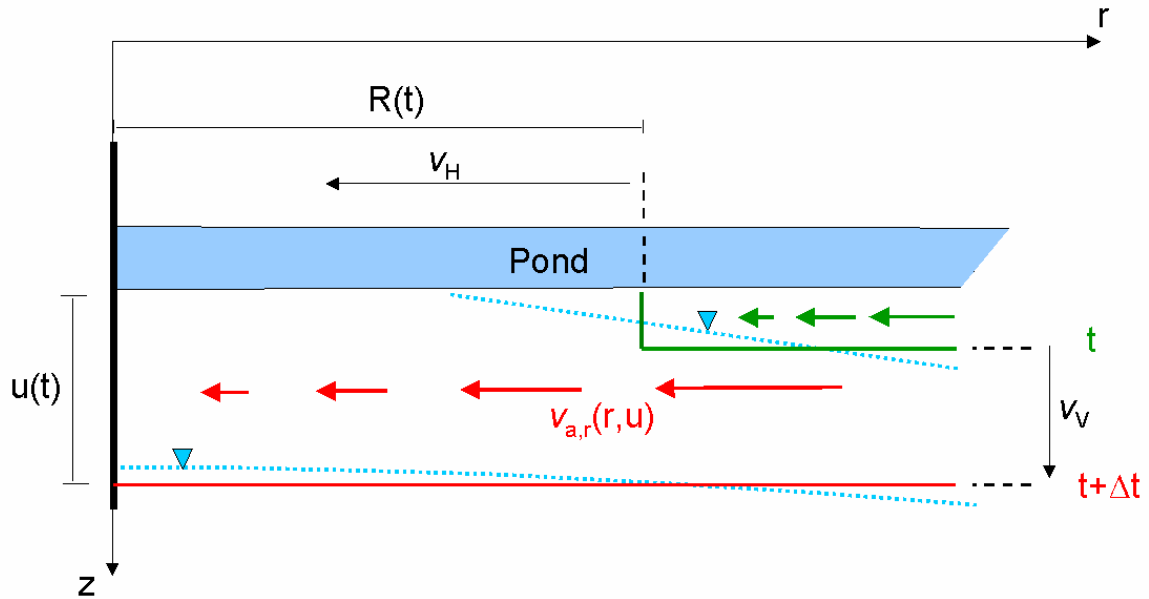
Figure 61 Conceptual radial symmetric model of the air flow in r-direction below the pond. The z-axis represents the symmetry axis at the center of the pond. The blue dotted lines are the groundwater tables at time t and t+Δt, respectively. The red line and green are the corresponding conceptual groundwater tables. Thereby, u is the distance from the pond's bottom to the conceptual groundwater table, v_v is the falling velocity of the groundwater table during the unsaturated stage, v_H is the propagation velocity and R the position of the air-front in the early stage of the unsaturated conditions.

The pore velocity of air in vertical direction can be approximated by:

$$v_{a,z}(z,u) = \frac{z}{u} v_v \text{ , for } 0 \leq z \leq u \tag{3.3}$$

Clearly, this model is a drastic simplification of the real physical system, since in reality the air flow depends on the water saturation changes during the transient unsaturated conditions, which were not explicitly modelled in here. Such a system can only be fully described by complete multi-phase flow models (e.g., Gray and Hassanizadeh, 1998). However, the simplification made here is justifiable, since (i) the aim of this study is the simulation of the principal pattern of air intrusion and its impact on the hydrochemistry of the seepage water and (ii) only few fully coupled two-phase flow and multi-component reactive transport models exist, which might be able to simulate such a hydrogeochemical system, e.g., UTCHEM (Pope et al., 1999) or RETRASO (Saaltink et al., 2004) and are too complex that they could have applied to the here described field site within the predefined time schedule of the project.

1.1.10. Conceptual solute transport model

The transport of the solutes in the water phase through the variably saturated zone to TEG366 is assumed to be purely vertical within the entire pond area. Thus, the pore velocity of water v_w is depends on the recharge rate (Darcy velocity) and the water content of the sediment.

1.1.11.

1.1.12. Conceptual reaction model

2.3.1.1. <u>Redox reactions</u>

The breakdown of organic matter leads to the sequential consumption of terminal electron acceptors (TEA's), such as oxygen, nitrate, manganese- and iron(hydr)oxides, sulfate and carbonate. At the study site, biodegradation of organic matter was only observed under aerobic, denitrifying and manganese reducing conditions:

Aerobic respiration:

$$CH_2O(NH_3)_{0.15} + 1.3O_2 \rightarrow HCO_3^- + 0.15NO_3^- + 1.15H^+ + 0.15H_2O \qquad (3.4)$$

Denitrification:

$$CH_2O(NH_3)_{0.15} + 0.89NO_3^- \rightarrow HCO_3^- + 0.52N_2 + 0.11H^+ + 0.67H_2O \qquad (3.5)$$

Manganese reduction:

$$2[CH_2O(NH_3)_{0.15}] + 4.45 MnO_2(s) + 6.9H^+ \rightarrow 2HCO_3^- + 0.15N_2 + 4.45Mn^{2+} + 4.9H_2O \quad (3.6)$$
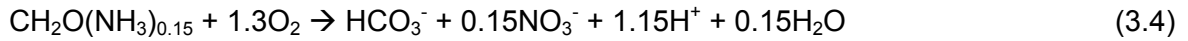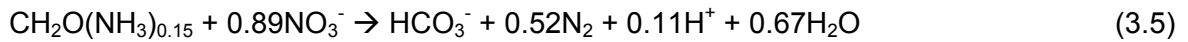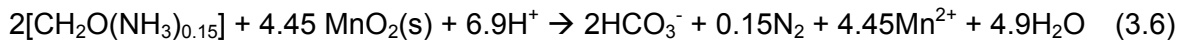
In the above equations $CH_2O(NH_3)_{0.15}$ represents a simplified version of the generalised organic matter composition $(CH_2O)_{106}(NH_3)_{16}(H_3PO_4)$.

Biodegradation was thought to be kinetically controlled and described by standard Monod-type rate expressions. Thus, the following rate expression for the degradation of organic matter was considered:

$$r_{OM} = f_T \left[r_{ox} \left(\frac{C_{ox}}{K_{ox} + C_{ox}} \right) + r_{nitr} \left(\frac{C_{nitr}}{K_{nitr} + C_{nitr}} \right) \left(\frac{K_{ox\_inh}}{K_{ox\_inh} + C_{ox}} \right) + r_{mn} \right] \qquad (3.7)$$

where r_{OM} is the overall degradation rate of organic matter, r_{ox}, r_{nitr} and r_{mn} are the maximum rate constants under aerobic, denitrifying and manganese reducting conditions, respectivly. C_{ox} and C_{nitr} are the concentrations of DO and nitrate, respectively. K_{ox} are K_{nitr} are

halfsaturations concentrations and K_{ox_inh} is an inhibition constant. Monod-terms for organic matter and $MnO_2(s)$ (pyrolusite) were not included, assuming that the concentration of organic matter and pyrolusite were not rate limiting throughout the simulation time. Moreover, f_T describes the dependence of the organic matter mineralisation rate on the temperature T (°C) as propsed by Jenkinson (1990):

$$f_T = \frac{47.9}{1 + \exp\left[\dfrac{109}{T + 18.3}\right]} \tag{3.8}$$

2.3.1.2. Mineral reactions

During subsurface flow, biodegradation reactions, such as Eqn. (3.4)-(3.6) can affect the hydrogeochemical environment considerably and may induce further reactions, for instance dissolution/precipitation of minerals. Based on sediment analyses, calcite ($CaCO_3$) and rhodochrosite ($MnCO_3$) were assumed to dissolve or precipitate during the simulation. Whereas rhodochrosite was set in equilibrium with the aqueous solution, dissolution/precipitation of calcite was assumed to be kinetically controlled based on the formulations found by Plummer et al. (1978).

1.1.13. Numerical model

Both the conceptual gas and solute transport model were implemented into the numerical two-dimensional multi-component reactive transport model PHUNSAT2D, which was newly developed within this study. PHUNSAT2D couples the two-dimensional transport simulator ASM (Chiang et al., 1998) and the geochemical model PHREEQC-2 (Parkhurst and Appelo, 1999) through a sequential split operator technique. The coupling procedure is adopted from PHT3D (Prommer et al., 2003), a multi-component reactive transport model for saturated porous media. For the simulation of the equilibrium reactions, including aqueous speciation, the original PHREEQC-2 standard database was used. Kinetic reactions that were not part of the standard database, were added as BASIC-routines (Parkhurst and Appelo, 1999).

The redox reactions (3.4) – (3.6) are linked to Eqn. 3.7 by applying the so-called partial equilibrium (or two step) approach (PEA). It relies on the assumption that (i) the electron donating step (i.e., oxidation of organic carbon) is the rate-limiting step that controls the reaction kinetics and (ii) that the electron accepting step (i.e., consumption of TEAs) can therefore be simulated as instantaneous reactions (e.g., Postma and Jakobsen, 1996). This means, the TEAs are automatically consumed in the order of their thermodynamic favourability.

1.1.14. Model domain, initial and boundary conditions, and simulation time

The horizontal extent of the model domain was 52.5 m from the centre of the pond to the pond margin, assuming the pond's shape was approximately circular. Vertically the model domain ranged from the bottom of the pond (31 m.a.s.l) to the lower end of the filter screen of TEG366 (23 m.a.s.l).

The (transient) boundary conditions of the gas transport were as follows: The top of the model domain and the approximate location of the groundwater table were set as no-flux-boundaries (2nd type). Below the groundwater table, gas transport was not calculated. Throughout the simulation of the unsaturated Stage 3, the lower boundary (groundwater table) changed its location, as it was measured in the field (see previous chapter). The propagation velocity v_H and the position of the air-front R in the early stage of the unsaturated conditions, was derived from a modelling exercise, in which the variably saturated flow of water below the pond and the adjacent aquifer was simulated with HYDRUS2D (Šimůnek et al., 1999). The right boundary (pond center) was set as flux-boundary (3rd type). The left boundary (pond margin) was set as constant concentration boundary (1st type) for the O_2 and CO_2 concentration, i.e., partial pressure of the soil air. Their values were set as typical for soil air, i.e., $pO_2 = 0.1$ atm and $pCO_2 = 0.01$ atm. For the solute transport in the water phase, the left and the right boundary were set as no-flux-boundary. The top of the model domain was set as constant concentration boundary for the considered aqueous components. Their concentration values were taken from the pond water composition described in the previous chapter. The lower boundary of the model domain was set as flux-boundary.

Fresh and highly degradable organic matter (OM_{high}), which was assumed to originate from seasonally occurring algae blooms (see previous Chapter), was placed within the first 20 cm below the simulated recharge pond representing the clogging zone. A second, less degradable fraction of organic matter (OM_{low}) was placed in the remaining model domain. In contrast to OM_{high}, OM_{low} did not contain organic nitrogen.

The simulation time was from day 40 since the start of the recharge cycle (middle of Stage 2, see previous chapter) to the end of Stage 3 (see previous Chapter). The model accounted for the seasonal temperature variations of the pond water during the simulation time.

1.1.15. Calibration

During model calibration of the model, the kinetic rate parameters of Eqn. 3.7 were adjusted such that the simulation satisfactorily reproduced the concentrations of the relevant components observed at TEG366.

1.1.16.   Results and Discussion

After model calibration, the observed concentration pattern of essentially all relevant components was adequately described by the final simulation (**Figure 62**). The results in particular showed that calcium and total dissolved inorganic carbon (DIC) started to increase compared to the pond water concentration, as soon as unsaturated conditions (Stage 3) developed below the pond. This clearly demonstrates that the intrusion of gaseous oxygen enhanced the mineralisation of organic carbon and subsequently the dissolution of calcite, as it was hypothesised in the previous chapter. Moreover, the simulation agreed with the observed behaviour of dissolved oxygen (DO) and nitrate. The model revealed that during saturated conditions (Stage 2), DO was already completely consumed within the clogging zone. Nitrate, however, passed the clogging zone and depleted before reaching TEG366. As soon as gaseous oxygen penetrated underneath the pond at the beginning of Stage 3, nitrate reduction ceased (as a result of aerobic conditions) and organic nitrogen contained in the clogging zone was oxised to nitrate, leading to an increased nitrate concentration at TEG366 compared to the pond water. Although DO was completely consumed within the saturated part of the aquifer before reaching TEG366, nitrate did not so and thus could break through to the monitoring well. The breakthrough of nitrate ceases when the residence time became to long due to the decreasing recharge rate, leading to a full depletion of nitrate within the saturated part of the aquifer. Towards the end of Stage 3, the DO concentration at TEG366 didn't increase until the water saturated layer between groundwater table and filter screen (**Figure** 62 and Figure 63) became small enough for a breakthrough before DO was entirely consumed. Interestingly, nitrate didn't break through. The model revealed that nitrate was now also completely consumed within the clogging zone due to the longer residence time in this zone at the end of Stage 3.
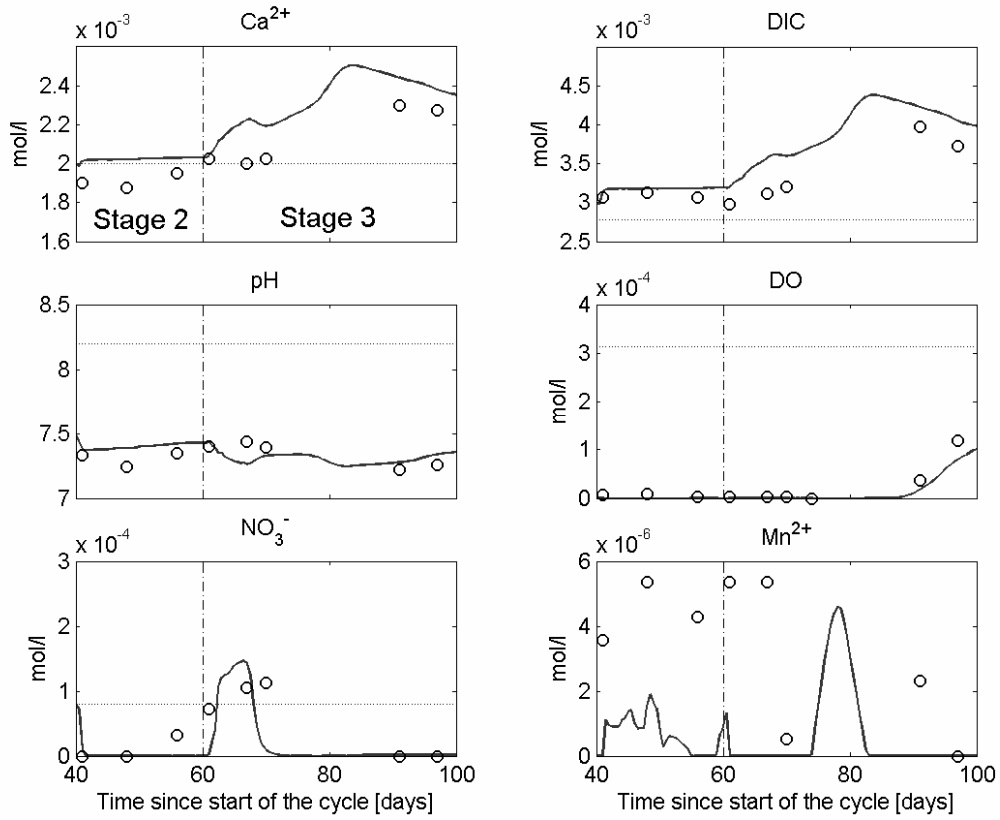
Figure 62 Simulated and observed pH and concentrations of calcium, total dissolved inorganic carbon (DIC), dissolved oxygen (DO), nitrate and dissolved manganese at TEG366. Horizontal lines represent average pond water concentrations.
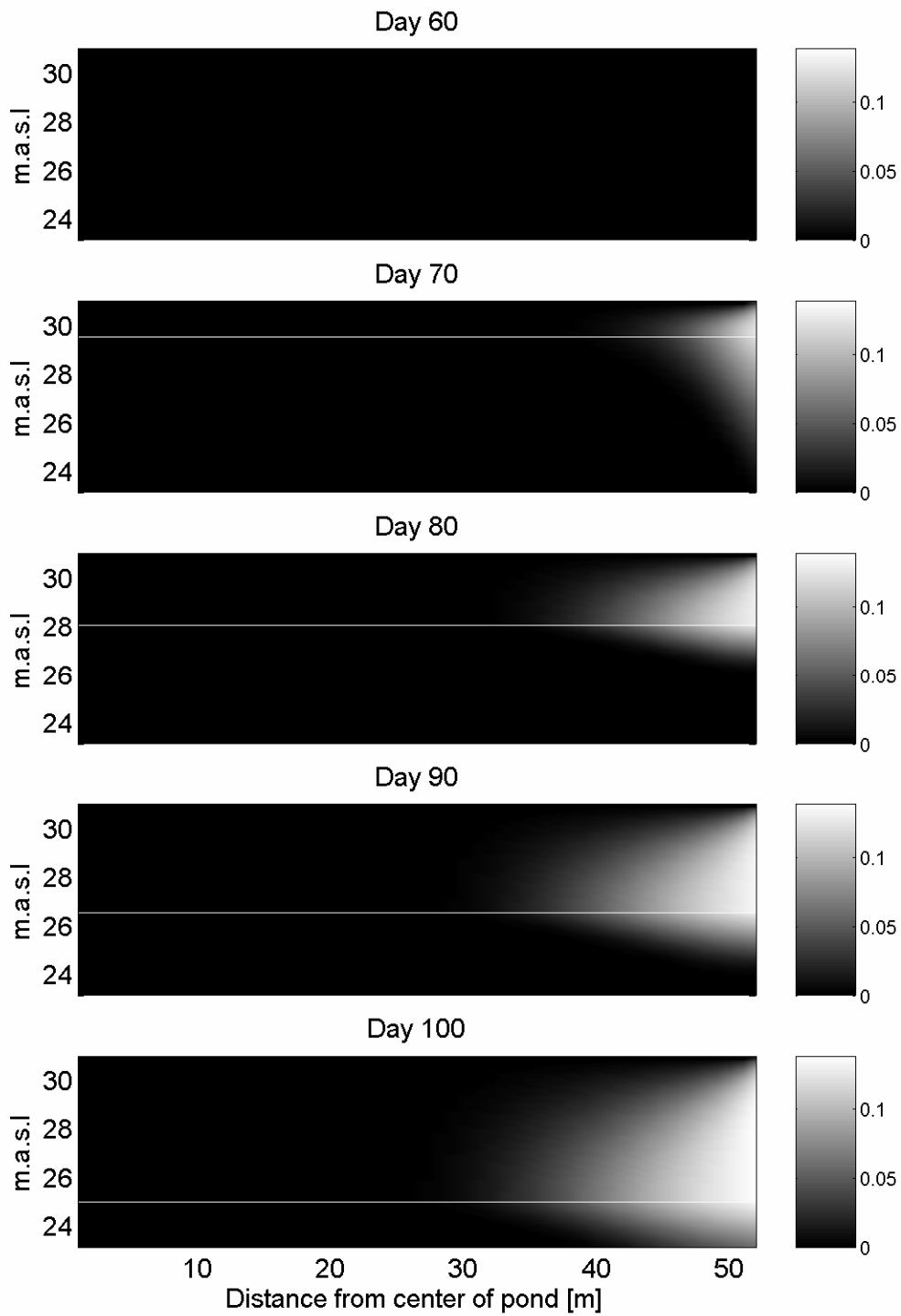
Figure 63 Simulated concentration of dissolved oxygen (DO) within the cross-sectional area below the pond for different times after the start of the cycle (Stage 3). White vertical line indicates approximate position of the groundwater table.

The simulated concentrations of dissolved manganese were in the same order of magnitude of the observed concentrations. However, the model could not reproduce the observed concentration pattern. The discrepancy appears acceptable, as the deviations between simulated and the relatively low measured manganese concentrations are unlikely to have a significant impact on the electron balance.

The cross-sectional view of the simulation showed that during the entire simulation period the gaseous oxygen front did not reach the centre area below pond (Figure 63). Aerobic conditions only developed within the first 20m from the pond margins. Thus, the enhanced mineralisation of organic carbon and dissolution of calcite very likely occur only below the fringe area of the pond rather than below the entire pond.

2.4. Modelling redox dynamics and the fate of phenazone

1.1.17. Observed Redox zonation and travel times

The redox status of the groundwater in the surrounding pond area is generally characterized by aerobic, denitrifying and manganese reducing conditions. Thereby, the position and the extent of these redox zones were found to be strongly dependent on the seasonal temperature changes of the recharge water (see Final report of NASRI group Hydrogeology). During summer, when the microbial activity is higher, dissolved oxygen (DO) and nitrate become depleted in the close vicinity of the pond and manganese reducing conditions were found to be dominating most parts of the studied aquifer section. During winter, however, manganese reducing conditions were only found in the deep monitoring well TEG369UP, which is located at the maximum distance from the pond. Average travel times of the recharged water from the pond to the monitoring wells were estimated from stable isotope data and from observed temperature variations (see Final report of NASRI group Hydrogeology). A clear breakthrough of the seasonal stable isotope signal was only available at TEG396UP (average travel time was about 50 days). This allowed the calculation of a (site-specific) retardation factor for temperature transport, i.e., R = 2.1 (see Final report of NASRI group Hydrogeology). A similar retardation factor has been found by Prommer and Stuyfzand (2005) for an artificial recharge site in the Netherlands. Note, that the travel times were highly variable in time, dependent on the recharge rate (Figure 64).
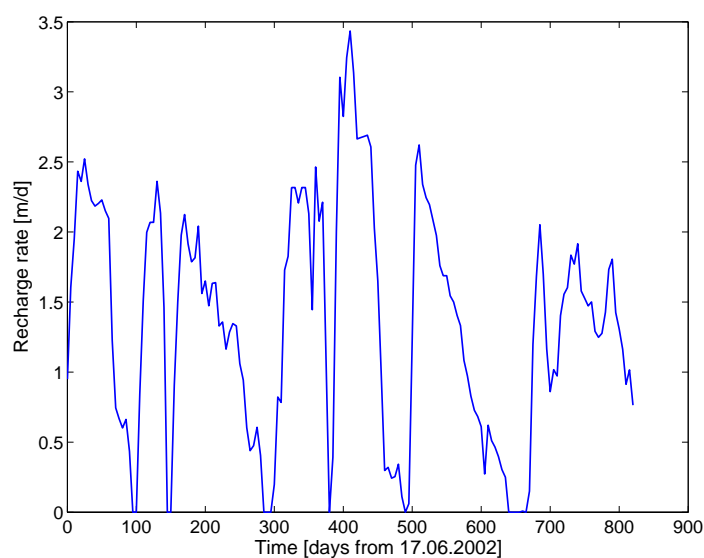
Figure 64 Time series of recharge rate (data was kindly provided by Berliner Wasser Betriebe).

1.1.18. Flow and non-reactive transport model

In a first step a flow and non-reactive transport model was set up for the aquifer surrounding pond 3. The simulations were performed for a radial symmetric vertical two-dimensional profile, assuming that (i) the ponds shape could be approximated as a circle and (ii) the recharged water spreads radially and homogeneously from the pond. The flow simulations were carried out with the USGS flow simulator MODFLOW (McDonald and Harbaugh, 1988). The transport simulator MT3DMS (Zheng and Wang, 1999) was used for the transport of temperature, which, under consideration of the site-specific retardation factor, served for the calibration of the non-reactive transport processes.

The horizontal extent of the model domain was 134 m, i.e., the distance from the centre of the pond to the two most distant monitoring wells TEG369OP/UP. In vertical direction the domain extended from the bottom of the pond, i.e., 31 m below sea level (m.b.s) to -10 m.b.s, where an aquitard of the Holstein interglacial forms the base of the aquifer (Voigt and Eichberg, 2000). A no-flow boundary was set at the symmetry axis (left) representing the center of the pond. The right boundary was set as constant head boundary with an average value of the hydraulic heads as measured at TEG369OP/UP. A time-variant flux boundary represented the recharge pond. An additional no-flow boundary approximated the time-averaged groundwater surface between the pond margin and downstream boundary, neglecting the temporarily unsaturated conditions below the pond. The model discretisation was 2 m in horizontal direction. In vertical direction it ranged from 0.5 m at the upper part to 4 m at the lower part of the model domain. The model aquifer was assumed to be isotropic and homogeneous. Furthermore, the model did not explicitly incorporate the glacial till layer, because its abundance was found to be very patchy in this area (see Final report of NASRI group Hydrogeology).

The total simulation time was 825 days, discretised into 165 stress periods and starting from 17th June 2002. The time-variant fluxes and seasonal temperatures in the pond were defined for each stress period on the base of 5-day-averages that were calculated from daily recharge and temperature values, respectively.

1.1.19. Reaction network

The simulated reaction network was largely taken from Chapter 3. There were the following modifications: (1) the original temperature function was changed to a function propsed by O'Connell (1990) and Kirschbaum (1995, 2000):

$$f_T = \exp\left[\alpha + \beta T\left((1 - 0.5\frac{T}{T_{opt}})\right)\right]$$ (4.1)

where α and β are fitting parameters, and T_{opt} (°C) is the optimal temperature for the decomposition process. (2) Calcite was here simulated as to be in equilibrium with the aqueous solution.

1.1.20. Phenazone degradation

Phenazone is an analgesic PhAC contained in the painkillers Antipyrin® and SpaltN® (Zühlke, 2004). It has been previously detected in surface waters, groundwater and drinking water of Berlin (Reddersen et al., 2002, Zühlke, 2004). Laboratory experiments demonstrated that phenazone is degradable under oxic conditions (Sauber et al., 1977, Zühlke, 2004) by the aerobic bacteria *Phenylobakterium immobile* (Lingens et al, 1985). Sorption of phenazone to filter material, sludge or soil samples was found to be negligible (Reddersen et al, 2002; Zühlke, 2004).

In the model, it was assumed that the degradation rate of phenazone is dependent on the DO concentration, similar to other micropulltants such as pesticides (Vink and van der Zee, 1997, Tuxen et al. 2005). Further it was assumed that the degradation rate is temperature-dependent, as the degradation of phenazone is due to microbial metabolism. Those rate dependencies were incorporated, which leads to the following rate expression for phenazone degradation:

$$r_{phena} = f_T r_{phena\_max}\left(\frac{C_{ox}}{K_{phena\_ox} + C_{ox}}\right)C_{phena}$$ (4.2)

where, r_{phena} is the degradation rate of phenazone, r_{phena_max} is the maximum degradation rate constant, K_{phena_ox} is the halfsaturation concentration and C_{phena} is the concentration of phenazone.

1.1.21. Numerical Model

The multi-component reactive transport model PHT3D was used to set up the conceptual reaction model and simulate the biogeochemical characteristics at the artificial recharge site. PHT3D couples the transport simulator MT3DMS and the geochemical reaction model PHREEQC-2 via sequential split operator technique. The simulation of equilibrium and kinetic reactions was carried out as in Chapter 2.3.

4.5.1 Simulated initial and recharge water composition and aquifer composition

The simulated recharge water comprised only of components that were relevant for this study rather than the complete set of components analysed. To account for the time variant surface water quality, their concentrations were adjusted for each stress period based on monthly measurements by the NASRI group Hydrogeology. The applied concentration ranges are listed in Table 9. Note that total dissolved organic carbon (DOC) was not included in the simulation, since the consumption of TEAs seemed to be mainly driven by the mineralisation of labile OM that was filtrated within the first 1-2 meters below the pond and which appeared to originate from seasonal algae blooms (see Chapter 2.2). Thus, high degradable OM_{high} was emplaced within the first 2 m below the simulated recharge pond. Furthermore, it was assumed that its concentration would never become rate limiting, as in reality there is a continuous input of organic matter from periodic algae blooms. Less degradable OM_{low} was emplaced in the remaining model domain. Thereby, OM_{high}/OM_{low} is the relative reactivity r_{reac}. The initial concentrations of the two types of SOM, as well as the initial concentrations of the simulated minerals can be found in Table 9. As the simulation starts in summer 2002, the initial groundwater composition represented a typical summer situation given in Table 9.

1.1.22. Calibration

The calibration of the reactive transport model occurred in two steps. In the first step, the flow and non-reactive transport model was calibrated in order to reproduce the observed groundwater temperature variations that were recorded daily at the monitoring wells TEG367, TEG368OP, TEG368UP, TEG369OP and TEG369UP. The monitoring wells TEG365 and TEG366 were not used for calibration, since the breakthrough of the seasonal temperature signal at these locations was not distinguishable from the signal in the pond water due to too short travel times. For the locations of the monitoring wells see final report of NASRI group Hydrogeology. The so derived flow field and transport parameters served as the base for the reactive transport model and were not further modified during the reactive simulations. Thus, the calibration of the biogeochemical processes occurred separately in a second step. Therein, mainly rate parameters of the kinetic reactions were adjusted in order to reproduce the observed field data at the monitoring wells TEG365, TEG366, TEG368OP,

TEG368UP, TEG369OP and TEG369UP. The sensitivity of the model behaviour against the rate parameters was recorded during the calibration process and evaluated further below. Note that the equilibrium reaction constants provided by the PHREEQC-2 standard database were not modified und thus not involved in the calibration process.

Table 9 Initial and range of recharge water composition, and initial concentrations of minerals and OM used for the model simulations.

Component	Unit	Initial concentration	Range of concentration in recharge water
DO	[mol L^{-1}]	0	$1.8 \times 10^{-4} - 6.7 \times 10^{-4}$
NO$_3^-$	[mol L^{-1}]	0	$2.6 \times 10^{-5} - 1.7 \times 10^{-4}$
Mn^{2+}	[mol L^{-1}]	6.56×10^{-06}	0
Ca^{2+}	[mol L^{-1}]	2.3×10^{-3}	$1.7 \times 10^{-3} - 2.5 \times 10^{-3}$
TIC	[mol L^{-1}]	3.5×10^{-3}	$2.4 \times 10^{-3} - 3.4 \times 10^{-3}$
pH	[-]	7.2	7.5 – 9.1
pE	[-]	9	11.6 – 13.2
Phenazone	[mol L^{-1}]	0	0.11 – 1.2
Pyrolusite	[mol L$_{bulk}^{-1}$]	3.0×10^{-3}	-
Calcite	[mol L$_{bulk}^{-1}$]	1.7	-
Rodochrosite	[mol L$_{bulk}^{-1}$]	0	-
OM$_{high}$	[mol L^{-1}]	1	-
OM$_{low}$	[mol L^{-1}]	1	-

1.1.23. Results and discussion

2.4.1.1. Non-reactive transport

The solute transport processes determined by the proposed flow and non-reactive transport model were solely dependent on the effective porosity n_e and the longitudinal and transversal dispersivities α_L and α_T, respectively. Thus, these parameters were adjusted during calibration of the non-reactive transport model. The simulation results of the calibrated non-reactive transport model agree very well with the observed data, especially with its dynamics (Figure 65). The good fit clearly supports the simplifying assumptions made for the conceptual flow and non-reactive transport model.
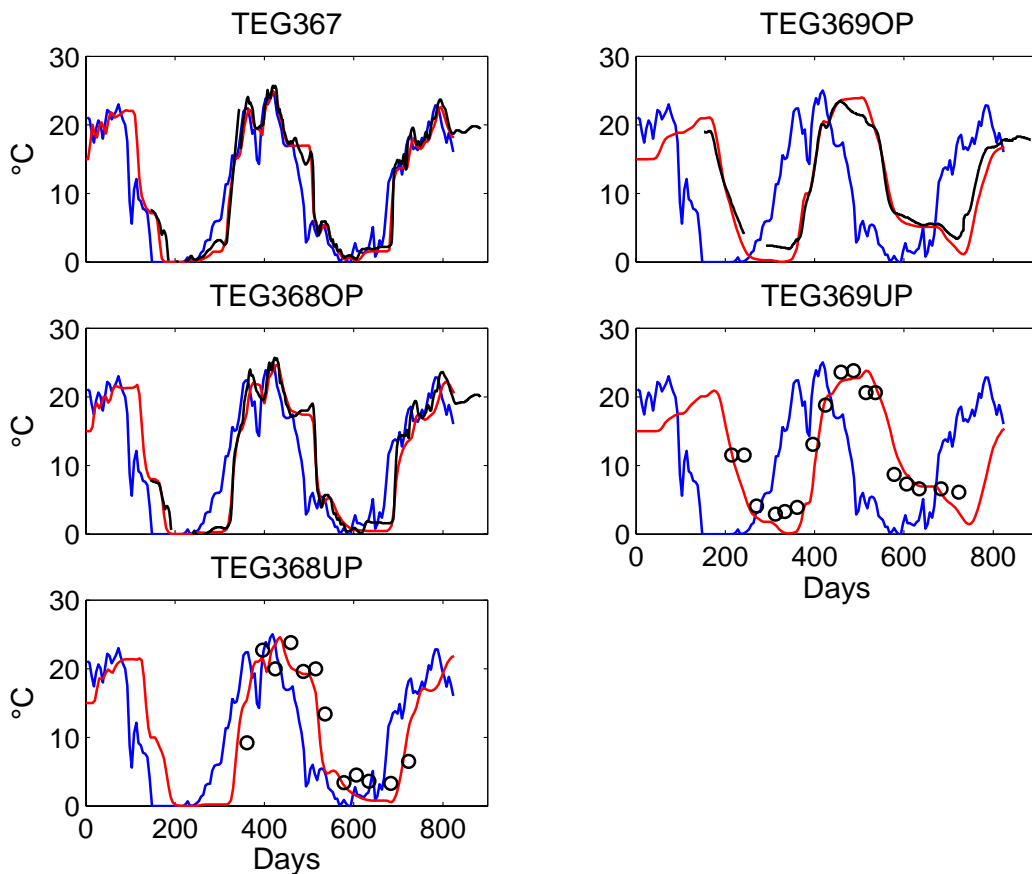
Figure 65 Calibration results of non-reactive transport model for the monitoring wells TEG367, TEG368OP/UP and TEG369OP/UP. Blue lines represent the temperature of the pond water. Black lines and black circles represent the observed temperature with data loggers and (monthly) manual measurements, respectively. Red lines indicate the simulated temperature.

2.4.1.2. Reactive transport

The final calibrated biogeochemical transport model is capable of reproducing almost all biogeochemical characteristics and their seasonal dynamics that were observed in the aquifer surrounding the recharge pond. The simulation results and the influence of the most relevant parameters are discussed below.

Redox system

The simulation results of nearly all components showed a very good agreement with the observed data at all monitoring wells when variably water temperatures were taken into account (Figure 66). Thereby, the fate of DO, nitrate, Mn^{2+} and phenazone was highly affected by the proposed biogeochemical reaction network, as the contrast to the corresponding non-reactive simulations show. During winter, almost no consumption of oxygen occurred and its breakthrough was observed at all monitoring wells except TEG369UP. As long as aerobic conditions prevailed and nitrate reduction has not started yet, nitrification of organic nitrogen is the dominant process causing the elevated nitrate concentrations at all monitoring wells compared to the pond water. These effects could be well reproduced by the simulation. In summer, DO concentrations became depleted before the reaching TEG365 and TEG366 and thus were zero further downstream. However, nitrate did not fully deplete and break through at all of the monitoring wells. These breakthroughs had a very dynamic behaviour, which resulted from the drastic variations in recharge rate and thus travel times. This means, breakthrough occurred when recharge rates were highest and vice versa. The observed behaviour of the nitrate breakthroughs during summer could also be successfully simulated.

Although the simulated Mn^{2+} concentrations in principle reproduced the seasonal pattern they still significantly deviate from the observed data. In the simulation, manganese reduction only started when nitrate was entirely depleted. This contradicted the observations, which rather showed a simultaneous occurrence of manganese and nitrate reduction. During the calibration procedure, a number of manganese (hydr)oxide minerals of different solubility other than pyrolusite were tested in order to reproduce this behaviour. However, none of them could account for the observed overlap of nitrate and manganese reduction. A possibility to overcome this problem would be to adjust the solubility of pyrolusite within the PHREEQC-2 database, since in general the solubility of a mineral reflects its reactivity (Jakobsen and Postma, 1999). However, in order to satisfactorily simulate the observed overlap of nitrate and manganese reduction, a solubility change of about 4 orders of magnitude would have been necessary, which we think is not justifiable. For comparison, Jakobsen and Postma (1999) adjusted the reaction constant of $Fe(OH)_3(s)$ during model calibration only within one order of magnitude. However, as the crude simulation of the

manganese reducing conditions did not affect the fate of phenazone on which this paper was focussed on, we decided to refrain from improve the simulation with respect to manganese reduction.

In order to evaluate the impact of temperature on the proposed biogeochemical reaction network, extra simulations considering different constant temperatures were carried out. They show that with constant temperatures of 5°C, 10°C and 15°C, the seasonal dynamics of the redox components, pH and phenazone cannot be reproduced at all (Figure 67). The dynamic behaviour of breakthroughs only results from the time variant recharge rates. In principle, the same breakthrough pattern is generated for higher temperatures. The only difference, however, is a shift of the redox zones towards the recharge pond due to the higher reaction rates.
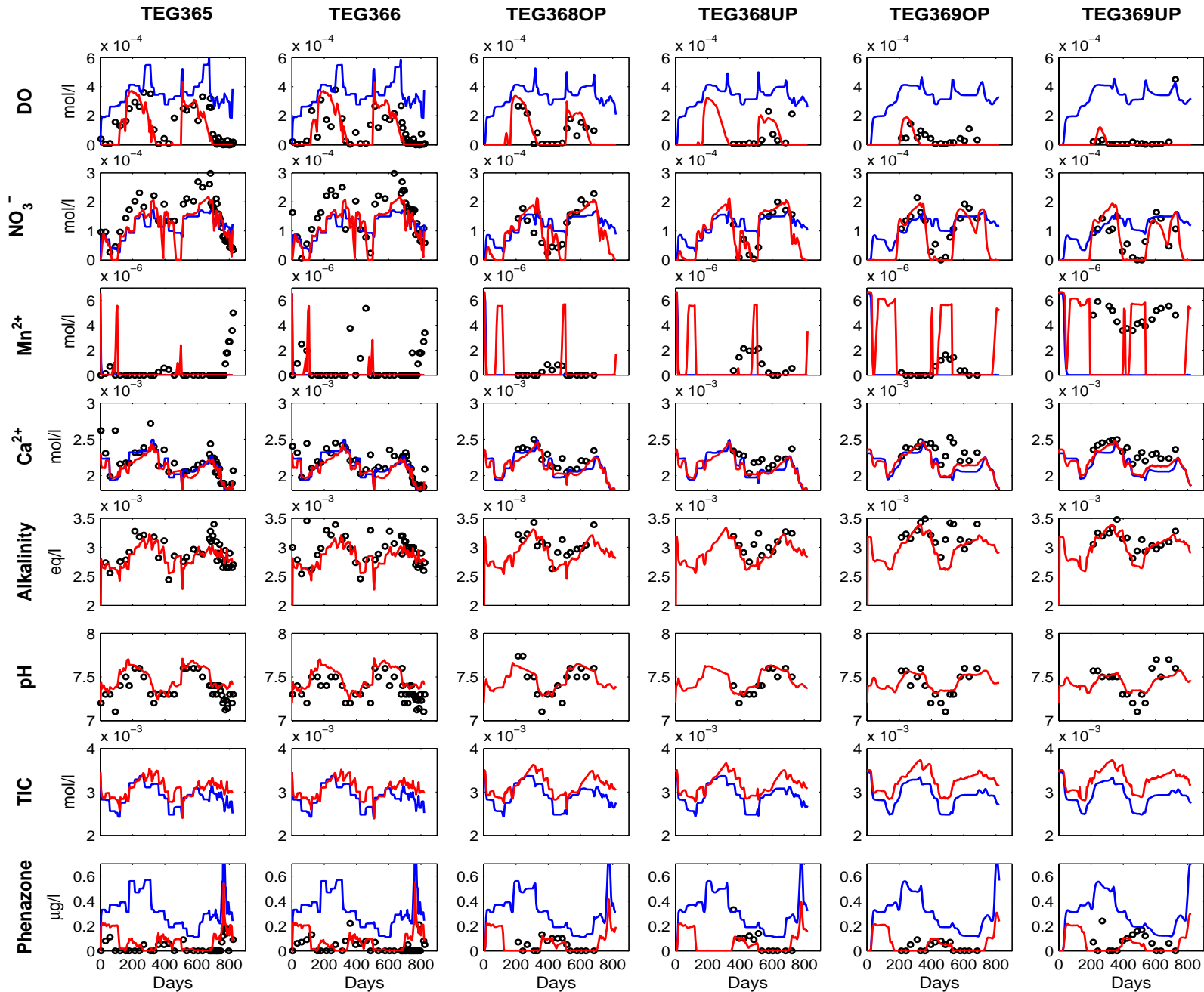
Figure 66 Simulation results for dissolved oxygen (DO), nitrate, Mn^{2+}, calcium, alkalinity, pH, TIC and phenazone at the monitoring wells TEG365, TEG366, TEG368OP/UP and TEG396OP/UP. Black circles represent the observed data and red lines represent the final calibrated reactive transport simulation. The blue lines represent the non-reactive simulation, in which all biogeochemical reactions were excluded.

Figure 67 Temperature dependence of dissolved oxygen (DO), nitrate, Mn^{2+}, calcium, alkalinity, pH, TIC and phenazone at the monitoring wells TEG365, TEG366, TEG 368OP/UP and TEG396OP/UP. The blue, black and green lines represent simulations with constant temperatures of 5°C, 10°C and 15°C, respectively. The red lines represent the final calibrated reactive transport simulation (variable temperature).

Carbonate system

The seasonal dynamics of calcium and carbonate concentrations are generally reflected by the pond water concentrations, as the non-reactive simulation shows (Figure 66). Moreover, the constant temperature simulations reveal that there is no significant dependence on temperature (Figure 4.4). In contrast, pH shows considerable temperature dependence (Figure 4.4). The lower pH at high temperatures is thought to be due to the fact that protons were less buffered, as the solubility of calcite is lower for higher temperatures.

Phenazone degradation

The simulated phenazone concentrations of the final calibrated model agreed very well with the observed concentrations at all monitoring wells (Figure 66). In contrast, the constant temperature simulations clearly failed to reproduce the good fit of the final model simulation (Figure 67). In general, it appears that higher temperatures lead to higher phenazone concentrations. If the degradation rate was dependent on temperature alone, the opposite behaviour would be expected, which suggests that phenazone degradation must also be affected by the redox status. In order to be able to evaluate the impact of the temperature and redox effect separately, the final calibrated model was modified and three different cases were considered.

In <u>*Case 1*</u> the degradation rate has been decoupled from temperature, i.e., the temperature function in Eqn. 4.2 has been set to unity. The simulation results for *Case 1* are shown in Figure 4.5. With the original value of r_{phena_max}, the simulation can satisfactorily account for the observed phenazone concentrations. With lower r_{phena_max}, the breakthrough concentrations increase and diverge from the observations. However, the observed breakthrough times are still well simulated.

In <u>*Case 2*</u>, the degradation rate of phenazone has been decoupled from the DO concentration, i.e., the Monod-term in Eqn. 4.2 has been set to unity. Even for a broad range of r_{phena_max}, the simulation cannot reproduce the observed phenazone concentrations at all (Figure 68). The simulation rather shows an inverted dynamics of phenazone concentrations in comparison to the observed. This is because in *Case 2*, the degradation rate of phenazone is solely dependent on temperature, which leads to higher breakthrough concentrations in winter and vice versa.

<u>*Case 3*</u> was a combination of *Case 1* and *Case 2*. Therein, degradation rate of phenazone has been decoupled from both temperature and DO concentration and thus follows a first-order rate law. This means the breakthrough pattern of phenazone at the monitoring wells is solely dependent on r_{phena_max} and the recharge rate. Again, even for a broad range of r_{phena_max} it was not possible to reproduce the observed concentrations at the monitoring wells

(Figure 68). This analysis showed that the temperature dependency of the degradation rate is not necessary in order to describe the fate of phenazone within the aquifer. On the other hand, the observed breakthrough pattern of phenazone could not be reproduced, if the redox dependence of the degradation rate was neglected. Hence, the unsatisfying simulation of phenazone concentrations in the constant temperature simulations (Figure 67) solely results from the inadequate reproduction of redox conditions.
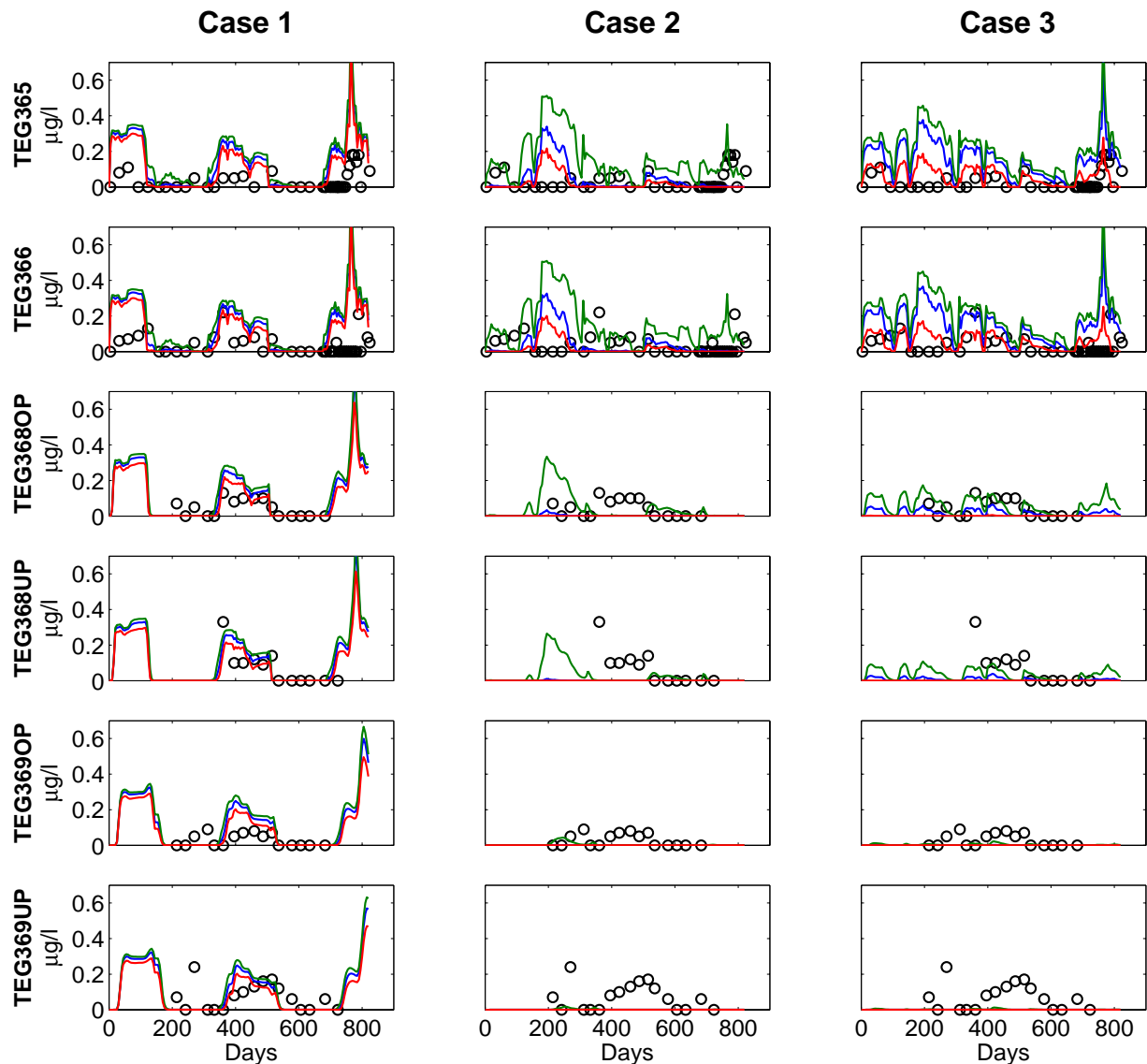
Figure 68: Simulated phenazone concentrations for temperature decoupled (Case 1), redox decoupled (Case 2) and first-order (Case 3) degradation rate. Case 1: red, blue and green lines represent a r_{phena_max} of 12.0 d^{-1}, 6.0 d^{-1} and 3.0 d^{-1}, respectively; Case 2: red, blue and green lines represent a r_{phena_max} of 3.0 d^{-1}, 1.5 d^{-1} and 0.25 d^{-1}, respectively; Case 3: red, blue and green lines represent a r_{phena_max} of 0.75 d^{-1}, 0.25 d^{-1} and 0.125 d^{-1}, respectively;

2.5. Conclusions and prospects

The artificial recharge pond in Berlin was investigated with the aims of (i) identifying the hydraulic regime and its impact on the dynamics of the hydrogeochemical environment immediately below the pond, and (ii) providing a quantitative process-based modelling framework for simulating the fate of the redox-sensitive PhAC phenazone within the surrounding aquifer of the pond.

Directly below the recharge pond, the hydrogeochemical environment is predominantly impacted by transient hydraulic conditions and seasonal temperature variations. Thereby, the entire hydraulic system is controlled by the formation of a clogging layer at the bottom of the pond resulting in alternating saturated/unsaturated conditions below the pond. During summer, when the infiltrated water is relatively warm (about 20-25°C), the spatial and temporal distribution of different redox conditions is strongly determined by the prevailing hydraulic conditions and their dynamics below the pond. When the sediment below the pond is fully water saturated in the earlier part of the operational recharge cycle, nitrate reducing and manganese reducing conditions are dominant. Iron and sulphate reducing conditions develop only in anaerobic micro-sites due to chemical and/or physical heterogeneity. When the hydraulic conditions change from water saturated to water unsaturated conditions, which is approximately in the middle of the recharge period, remarkable changes of the local hydrogeochemistry below the pond can be observed. They result from the temporal re-oxidation of previously formed iron-sulphides due to the lateral intrusion of atmospheric oxygen penetrating from the pond margins into the centre below the pond. During the following unsaturated period, the availability of atmospheric oxygen enhances the mineralisation of particulate organic carbon, which in turn promotes the dissolution of calcite. Reactive transport modelling of the area below the pond supported this hypothesis. However, modelling also revealed that the described processes seem not to occur in the center below the pond. Whereas in summer the dynamics and the character of the hydrochemical system are strongly affected by the hydraulic situation, hydrogeochemical changes are relatively independent from the hydraulic conditions in winter.

The modelling study at larger scale for this site showed that the hydrogeochemical processes, in particular the redox processes, are predominantly controlled by seasonal temperature changes rather than transient groundwater flow due to varying recharge rates. The influence of transient saturated/unsaturated conditions appeared not to be important for the behaviour of the hydrogeochemical system on that scale. It could be clearly demonstrated that solely the redox dependency of the degradation rate of phenazone controls the fate of phenazone in the subsurface of this artificial recharge site rather than variations in recharge rate and the temperature dependence of the phenazone's degradation rate.

With the successful simulation of the redox dynamics and the fate of phenazone at the Berlin site, one can expect that it is also possible to model the fate of other phenazone-type pharmaceuticals such as 1-acetyl-1-methyl-2-dimethyloxamoyl-2-phenylhydrazide (AMDOPH), 1-acetyl-1-methyl-2-phenylhydrazid (AMPH), Acetoaminoantipyrin (AAA), formylaminoantipyrin (FAA), 1,5-dimethyl-1,2-dehydro-3-pyrazolone (DP) and 4-(2-methylethyl)-1,5-dimethyl-1,2-dehydro-3-pyrazole (PDP) that were also detected at the artificial recharge site.

An appealing option for the site operator (BWB) might be the ability to simulate the quality of the water extracted by the surrounding production well field, because the extraction water quality is likely to be altered by operational changes of the pumping regime or recharge rates. The development of a three-dimensional reactive transport model for a larger model domain capturing the production well field is undoubtedly possible, since a calibrated site-specific reaction module for the aquifer now exists.

2.6. References

Chiang, W.-H., Kinzelbach, W., Rausch, R. (1998), Aquifer simulation model for Windows, Gebrüder Borntraeger, Berlin – Stuttgard, 137 p.

Gray, W.G. and Hassanizadeh, S.M. (1998), Macroscale continuum mechanics for multiphase porous-media flow including phases, interfaces, common lines and common points, Advances in Water Resources, 21(4), 261-281.

Hecht, H. and Kölling, M. (2001) A low-cost optode array measuring system based on 1mm plastic optical fibers – new technique for in situ detection and quantification of pyrite weathering processes. Sensors and Actuators B 81, 76-82.

Jakobsen, R., and D. Postma (1999), Redox zoning, rates of sulfate reduction and interactions with Fe-reduction and methanogenesis in a shallow sandy aquifer, Rømø, Denmark, Geochim. Cosmochim. Acta, 63(1), 137-151.

James, T. (2002), Numerical Solution of Advection-Diffusion Equations for Radial Flow, Master thesis, University of Oxford.

Jenkinson, D.S. (1990), The turnover of organic carbon and nitrogen in soil. Philosophical Transactions of the Royal Society of London. Series B, Biological Sciences; 329:p361-368.

Kirschbaum, M.U.F. (1995), The temperature dependence of soil organic matter decomposition, and the effect of global warming on soil organic storage, Soil Biol., Biochem., 27(6), 753-760.

Kirschbaum, M.U.F. (2000), Will changes in soil organic carbon act as a positive or negative feedback on global warming ?, Biogeochemistry, 48, 21-51.

Lee, J., and Ladd, A.J.C. (2002), A computer simulation study of multiphase squeezing flows, Physic of Fluids, 14(5), 1631-1641.

Lingens, F., Blecher, R., Blecher, H., Blobel, H., Eberspächer, J., Fröhner, C., Görisch, H., Görisch, H., Layh, G. (1985), Phenylobacterium immobile gen. nov., sp. Nov., a Gram-Negative Bacterium that degrades the Herbicide Chloridazon, Int. J. Syst. Bact., 35(1), 26-39.

McDonald, J. M., and A. W. Harbaugh, MODFLOW (1988), A Modular 3D Finite Difference Ground-Water Flow Mode, Open-file report 83-875, U.S. Geological Survey.

O'Connel (1990), Microbial decomposition (respiration) of litter in eucalypt forests of south western Australia: An empirical model based on laboratory incubations, Soil Biol. Biochem., 22(2), 153-160.

Parkhurst D. L., and C. A. J. Appelo, (1999), PHREEQC (Version 2) - A computer program for speciation, batch-reaction, one-dimensional transport, and inverse geochemical calculations, Water Resources Investigations report 99-4259, U. S. Geological Survey.

Plummer, L.N., Wigley, T.M.L., Parkhurst, D.L. (1978), The kinetics of calcite dissolution in CO_2 water systems at 5° to 60° and 0.0 to 1.0 atm CO_2, Am. J. Sci. 278, 179-216.

Postma, D., and R. Jakobsen (1996), Redox zonation: equilibrium constraints on the Fe (III)/SO4-reduction interface, *Geochim. Cosmochim. Acta,* 60, 3169-3175.

Pope, G. A., Sepehrnoori, K., Sharma, M.M, McKinney D.C, Peitel, G.E., Jackson, R.E. (1999), The dimensional NAPL fate and transport model, Technical Report, U. S. Environmental Protection Agency, EPA/600/R-99/011, 361 p.

Prommer H., Barry, D.A., Zheng, G.B. (2003), MODFLOW/MT3DMS-based multi-component reactive transport modelling. Groundwater, 42(2), 247-257.

Prommer, H., and P. J. Stuyfzand (2005), Identification of temperature-dependent water quality changes during a deep well injection experiment in a pyritic aquifer, *Environ. Sci. and Technol.*, 39(7), 2200-2209.

Reddersen, K., Heberer, T., Dünnbier, U. (2002), Identification and significance of phenazone drugs and their metabolites in ground- and drinking water, Chemosphere, 539-544.

Saaltink, M.W., Batlle, F., Ayora, C., Carrera, J., Olivella, S. (2004), RETRASO, a code for modeling reactive transport in saturated and unsaturated porous media, Geologica Acta, 2(3), 235-251.

Sauber, K., Müller, R., Keller, E., Eberspächer, J., Lingens, F. (1977), Degradation of Antipyrin by Pyrazon-Degrading Bacteria, Z. Naturforsch, 32c, 557-562 (in german).

Šimůnek, J., Šejna, M., van Genuchten, Th.-M. (1999), The HYDRUS2D Software package for simulating the two-dimensional movement of water, heat and multiple solutes in variably saturated media – Version 2.0, Tech. Rep., U.S. Salinity Laboratory, USDA, ARS, Riverside, CA..

Sinke, A.J.C., Dury, O., Zobrist, J. (1998). Effects of a fluctuating water table: column study on redox dynamics and fate of some organic pollutants. J. Cont. Hydrol. 33, 231-246.

Tuxen, N., Reizel, L.A., Albrechtsen, H-.J., Bjerg, P.L. (2005), Oxygen-enhanced Biogedradation of Phenoxy Acids in Groundwater at Contaminated Sites, Groundwater (in press).

Vink, J.P.M., Van der Zee, S.E.A.T.M. (1997), Pesticide biotransformation in surface waters: Multivariate analyses of environmental factors at field sites. Water Research, 31 (11), 2858-2868.

Zheng, C., and P. P. Wang (1999), MT3DMS: A modular three-dimensional multispecies model for simulation of advection, dispersion and chemical reactions of contaminants in groundwater systems, Documentation and User's Guide, Contract Report SERDP-99-1, U.S. Army Engineer Research and Development Center, Vicksburg, MS.

Voigt, I., and Eichberg, M., (2000), Hydrogeologisches Strukturmodell Wasserwerk Tegel, Fugro Consult GmbH.

Zühlke, S. (2004), Verhalten von Phenazonderivaten, Carbamazepin und estrogenen Steroiden während verschiedener Verfahren der Wasseraufbereitung, PhD Thesis, Technische Universität Berlin (in german).

3. Laboratory experiments: Modelling studies on Column experiments

3.1. Methods

Reactive transport model of the large column

There are many examples of soil column flushing simulation models involving bio-geochemical degradation reactions. Examples are given by Von Gunten & Zobrist (1996), Schäfer et al. (1998a, 1998b), and Amirbahman et al. (2003). These models require a large database including an adequate reaction framework and exact knowledge about soil matrix composition (see Heron et al., 1996), otherwise reaction models can be partially ambiguous (Appelo et al. 1998). Up scaling from micro-columns studies leads to field-site scale models studying riverbank filtration, or contamination of groundwater by reducing leachate plumes originating from landfills or oil spills (Lensing et al. 1994, Van Breukelen et al. 1998, Hunter et a. 1998, Prommer et al. 1999a, 1999b, Brun et al. 2002). Large-scale semi-technical soil columns are of intermediate scale between small laboratory columns and field sites.

In contrast to numerous small laboratory column experiment simulations and field-site scale models there are a few references for large soil column experiments simulating river bank filtration (Drewes & Jekel 1996, NASRI 2003). The experiments performed by Drewes & Jekel (1996) dealt with the elimination of organic trace compounds under different redox conditions by evaluating only mass balances. Simulations of non-reactive tracer transport through large uniform and layered soil columns (column length of about 6 m) are reported by (Porro et al. 1993a, 1993b). Reactive transport simulation within a large column is available from Phanikumar et al. (2002) who studied microbial-mediated degradation of chlorinated hydrocarbons. The goal of all these studies was to verify the observed breakthrough of contaminants using an problem adequate reaction framework.

Semi-technical soil column experiment

The experimental set-up of the large soil column ensemble is shown in PART 6. It consisted of 6 soil columns 5 m in length connected in line. Sampling was possible on 21 sampling points (5 points along the first column, 10 points along the adjacent columns, one point at the inlet, 4 points between the columns and one point on the outlet). Initially the column soil matrix was loaded by interstitial residual air over its whole length, and it took a time interval

of about 10 months until this interstitial air was nearly completely removed from the column sections apart from the inlet (Figure 69). The new experiment started in April 2003 and is still ongoing. A decrease of the DOC concentration resulting from oxygen consumption due to biodegradation was noticeable only near the inlet, while DOC concentrations were found nearly constant and independent of oxygen concentrations in the column sections apart from the inlet. The inorganic hydrochemistry sampled on the sample points along the length of the individual columns reflected the time variable composition of the sampled flushing surface water. A mineralogical analysis of the soil column material was not available, but from core analysis from different waterworks test sites in Berlin, a calcite content of 0.1 weight % was reported. Thus a calcite content in the soil column matrix seems probable (cf. NASRI 2003). Detailed results are presented by Horner et. al. (2004).
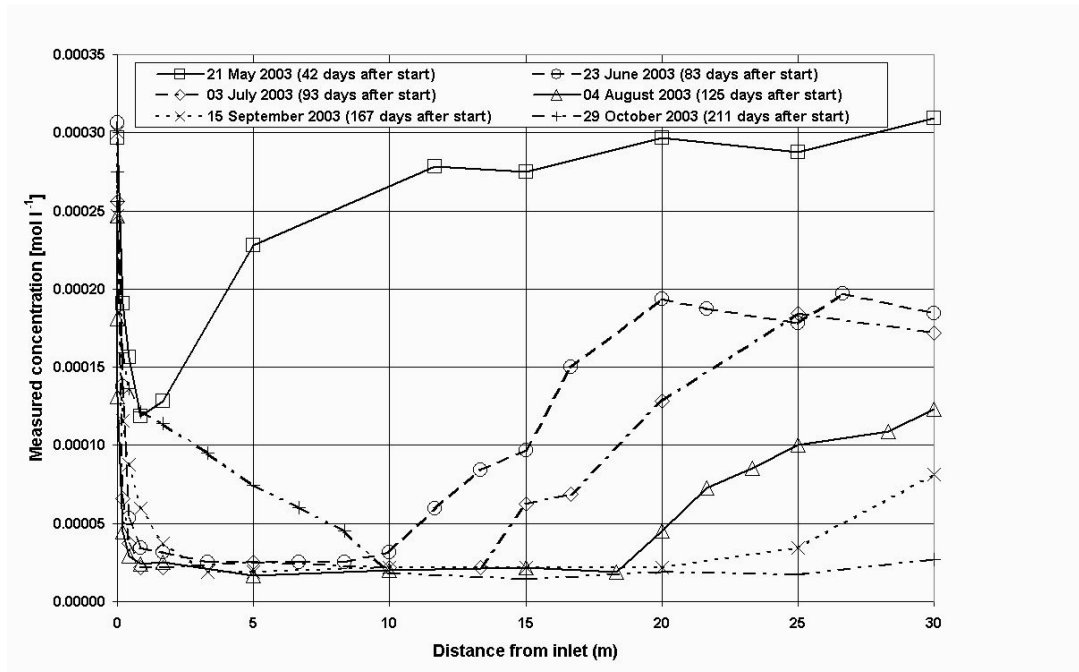
Figure 69 : Oxygen breakthrough during soil column flushing.

Basics of reactive transport

Brun & Engesgaard (2002) presented two approaches for modelling biodegradation: the singe step and the two step process model. The single step process models describe the biodegradation reaction as a geochemical reaction using a definite electron acceptor. Examples for single process models are presented by Kinzelbach et al. (1991), Lensing (1994), Schäfer et al. (1998a, 1998b), Abrams et al. (1998), and Abrams & Loague (2000).

The two-step process models conceptualise the overall biogeochemical degradation as a fermentation process consuming available terminal electron acceptors depending on the actual redox state using a partial equilibrium approach for the redox half reactions. Only organic degradation is the rate-limiting process for two-step process models. Using the latter approach, a close coupling of biodegradation kinetics to inorganic hydrochemistry is straightforward. Jakobsen & Postma (1999), Prommer et al. (1999a, 1999b) and Prommer (2002) used PHREEQE (Parkhurst et al. 1980) or PHREEQC (Parkhurst & Appelo 1999) as the geochemical equilibrator in the second (partial equilibrium) step. The reactive transport model presented here also follows this approach. The reactive multi-species transport is given by equation 1.

$$\frac{du_i}{dt} + v \cdot \nabla u_i - D \cdot \nabla(\nabla u_i) = ss_i \tag{1}$$

and for a solid species pi by equation 2

$$\left(\frac{\rho_b}{\theta}\right) \cdot \frac{dp_i}{dt} = ss_i \tag{2}$$

where v is the pore velocity (L/T), D is the hydrodynamic dispersion coefficient (L^2/T), ρ_b is the bulk density (M/L^3), and θ is the porosity. The source/sink term ss_i subsumes all external and internal sources and sinks, focussing on the chemical reactions (kinetics and/or chemical equilibrium). In general, the chemical reaction term is strongly non-linear. The aqueous total component concentration u_i results from the master species concentration c_i, and Nc concentration of complexed (or secondary) aqueous species and their stochiometric coefficients a_i derived from from the association reactions involving the master species (equation 3)

$$u_i = c_i + \sum_{j}^{N_c}\left(X_j \cdot a_j\right) \tag{3}$$

The complex concentrations Xj are calculated using the mass action relations derived from the master species concentrations and their equilibrium constants available from thermodynamic databases (Appelo & Postma 1996). The numerical solution of the reactive transport equation is made difficult by the different mathematical nature of the advective-dispersive subset (partial differential equation systems) and of the chemical reaction term (ordinary differential equation systems for kinetic terms and non linear algebraic equation systems for equilibrium reaction terms). Thus, an adequate strategy to solve the reactive transport equation results by coupling both subsets sequentially, e. g. by coupling MATLAB (The MathWorks 2003) as a powerful intrinsic solver for partial differential equation systems

with PHREEQC. An external program such as PHREEQC can easily be called from the MATLAB environment so that a coupling of both transport and reaction subsets is simply performed (for details see Horner et al. 2004). Numerical errors inevitably result from the coupling procedure (operator splitting) due to the different time marching for the physical transport step and for the chemical speciation step (Herzer & Kinzelbach 1989, Engesgaard & Kipp 1992, Walter et al. 1994, Barry et al. 2002). The numerical error introduced by the chemical perturbation can be minimized by internal iteration between the physical transport step and chemical speciation step during a time step, or by using small time steps if only one operator split per time step is performed. Based on the assumption of a local equilibrium for a given time step a constant mass balance including dissolved total concetration ui and solids pi (equation 4) will result

$$u_i^{before} + \left(\rho_b / \theta\right) \cdot p_i^{before} \equiv u_i^{after} + \left(\rho_b / \theta\right) \cdot p_i^{after} \tag{4}$$

where „before" and „after" denote the time before and after the reaction step. Computational load will increase dramatically by performing internal iterations. To limit the computational load, here the option of one operator split per time step was chosen.

3.2. Modelling

Conceptual model

From the previous developing of the column experiment difficulties result to provide reliable initial conditions over the whole column. As noted above, it is evident that the decrease in oxygen concentration in the column portions far from inlet does not correlate with the measured changes of DOC concentrations. There are two options to explain this observation Continuous supply of DOC by dissolution of particular organic carbon over the whole column extent so that oxygen is consumed by biodegradation also in the inner portions of the column,

Or, if no particular organic carbon is available over the whole column extent, a continuous dissolution and flushing of oxygen from interstitial air implying a double-porosity approach in the inner column portions.

Close to the inlet, oxygen consumption can be attributed to preferential biodegradation as indicated by the decrease of both oxygen and DOC. In the inner part of the column, physical removal of oxygen bubbles was also chosen for model conceptualisation. The double porosity approach for oxygen was formulated as follows (equations 5a and 5b)

$$\frac{\partial M_{mobile}}{\partial t} = \theta_{mobile} \cdot R_{mobile} \cdot \frac{\partial C_{mobile}}{\partial t} = \alpha \cdot \left(C_{immobile} - C_{mobile} \right) \tag{5a}$$

$$\frac{\partial M_{immobile}}{\partial t} = \theta_{immobile} \cdot R_{immobile} \cdot \frac{\partial C_{immobile}}{\partial t} = \alpha \cdot \left(C_{mobile} - C_{immobile} \right) \tag{5b}$$

using the concentrations Cmobile and Cimmobile, the compartment porosities θmobile and θimmobile, the retardation coefficients Rmobile and Rimmobile, and the mobile-immobile exchange coefficient α, as outlined by (Parkhurst & Appelo 1999). As the first numerical test runs showed, the biodegradation reaction front movement near the inlet wass considerably slowed in relation to the apparent flow velocity determined from tracer experiments performed in the column (NASRI 2003) so that sorption had to be considered as an additional process. Sorption was conceptualised using the Freundlich approach

$$Q_{orgc} = k_f \cdot \left(C_{orc} \right)^{nex} \tag{6}$$

with the concentration of sorbed organic carbon Q_{orgc}, the distribution coefficient k_f, and an empirical exponent n_{ex}.

Two differently reactive fractions of DOC as indicated by chromatographic analysis (NASRI, 2003) were considered using individual rate constants λ_1 and λ_2 (indicated using j in equation 7)

$$\frac{\partial C_{orgc,j}}{\partial t} = -\lambda_j \cdot C_{orgc,j} \tag{7}$$

of the biodegradation kinetics following a simple first-order approach. As a consequence of different rate constants, the refractory or less reactive DOC fraction can be expected to prevail far from the inlet.

Only scarce information was available about the matrix composition of the column aquifer. Because surface water from Lake Tegel (Berlin) used to flush the column is reported to be saturated/over saturated with respect to calcite (cf. NASRI 2003), and aquifer material sampled below the groundwater surface along the Lake Tegel test site has calcite contents within a magnitude order of 0.1 weight % (NASRI 2003), the calcite equilibrium was included in the reaction framework. Iron and manganese oxides/hydroxides also are to be expected in trace amounts. They were included in reactive transport modelling as solids in order to be able to model also anaerobic redox conditions if all oxygen has been consumed during flushing.

Discretisation and parameterization

The soil column was modelled as a 1D finite-difference domain. In detail, the physical parameters of the model domain are listed in Table 10. The pore velocity was specified as confirmed by tracer tests (NASRI 2003). A simulation time of 587 d was set up for the model simulation (i.e. the time interval ranging from April 2003 to November 2004, for which measurements were available). The chemical species considered by the reactive transport model, and their initial and boundary conditions are listed in Table 11.   As a first approximation, the initial and inflow concentrations were specified using the mean values sampled along the column system and for the surface water (NASRI 2003). By assuming oxic conditions at the start of the simulation, nitrogen, ammonium, methane and sulphide concentration were set to zero, but included as species to provide possible redox half reactions if anaerobic or anoxic conditions are achieved during biodegradation. Initial and boundary concentration conditions were equilibrated using PHREEQC (Parkhurst & Appelo 1999). At each simulation time, the reactive transport model requires a local charge balance. Initial solution and inflow solution ion charge balances were achieved by modification of Cl^- or alternatively of Na^+ concentrations (cf. Table 11). Except for oxygen, the inflow was modelled as a fixed time-constant concentration boundary. For oxygen, time-variable inflow concentrations had to be specified that reflected the experimental implications about the real inflow conditions as good as possible in order to verify the observed breakthrough. As the most important solid buffering pore solution hydrochemistry calcite was included. During the simulation, solution charge balance was achieved by adapting the actual pH, in contrast to the speciation of the initial and influx concentrations.

Table 10 Discretisation and physical parameters used for the semi-technical soil column simulation.

Parameter	Unit	Value
Length of column	m	30.0
Spatial discretisation interval	m	0. 50
Time step length	d	0.25
Final solution time	d	211
Pore velocity	$m\ d^{-1}$	1.0
Dispersivity	m	0.1
Effective porosity	-	0.25
Bulk density	$kg\ dm^{-3}$	1.80

Table 11 Initial and boundary conditions: chemical parameters and concentrations (NASRI 2003)

Parameter	Unit	Initial	Boundary inflow
Temperature	°C	20	20
pH	-	7.56	7.89
pe	-	13.5	13.2
O_2 (mobile)	mol l^{-1}	3.0×10^{-4}	See Table 3
O_2(immobile)	mol l^{-1}	3.0×10^{-4}	0.0
Cl^-	mol l^{-1}	1.0×10^{-3}	8.1×10^{-4}
NO_3-N	mol l^{-1}	2.0×10^{-4}	2.0×10^{-4}
N_2-N	mol l^{-1}	1.0×10^{-12}	0.0
NH_4-N	mol l^{-1}	1.0×10^{-12}	0.0
Ca	mol l^{-1}	1.36×10^{-3}	1.99×10^{-3}
Na	mol l^{-1}	4.67×10^{-3}	1.0×10^{-3}
HCO_3^-	mol l^{-1}	3.36×10^{-3}	9.92×10^{-4}
C(-4) , as CH_4	mol l^{-1}	1.0×10^{-12}	0.0
DOC (reactive)	mol l^{-1}	1.0×10^{-8}	See Table 3
DOC (refractory)	mol l^{-1}	1.0×10^{-8}	See Table 3
OC particulary	mol l^{-1}	0.0	0.0
SO_4^{2-}	mol l^{-1}	1.5×10^{-3}	1.5×10^{-3}
HS^-	mol l^{-1}	0.0	0.0
Calcite	mol l^{-1}	9.6×10^{-3}	0.0

Table 12 Specified time variable boundary conditions: chemical parameters and concentrations

Parameter	Unit	Time interval (d)	Boundary inflow
O$_2$ (mobile)	mol l^{-1}	0-50	2.0×10^{-4}
		50.25-146	1.0×10^{-4}
		146.25-220	2.0×10^{-4}
		220.25-350	1.5×10^{-4}
		350.25-400	5.0×10^{-5}
		400.25-587	3.2×10^{-5}
DOC (reactive)	mol l^{-1}	0-50	2.0×10^{-4}
		50.25-146	2.0×10^{-4}
		146.25-220	2.0×10^{-4}
		220.25-350	2.0×10^{-5}
		350.25-400	2.0×10^{-5}
		400.25-587	2.0×10^{-5}
DOC (refractory)	mol l^{-1}	0-50	3.0×10^{-4}
		50.25-146	3.0×10^{-4}
		146.25-220	3.0×10^{-4}
		220.25-350	3.3×10^{-4}
		350.25-400	3.3×10^{-4}
		400.25-587	3.9×10^{-4}

Table 13 most adequate combination of kinetic, sorptive and exchange parameters used to simulate the column experiment.

Parameter	Unit	Value
Retardation coefficient mobile O_2	-	1.0
Retardation coefficient immobile O_2	-	4.2
Exchange coefficient mobil-immobil	-	0.1
Porosity mobile (θ_{mobile})	-	0.3
Porosity immobile ($\theta_{immobile}$)	-	0.1
Sorption coefficient (k_f)	-	4.8
FREUNDLICH exponent (n_{ex})	-	0.99
Decay rate constant λ_1	d^{-1}	1.5×10^{-3}
Decay rate constant λ_2	d^{-1}	1.0×10^{-10}
Decay rate constant λ_3	d^{-1}	1.5×10^{-3}

3.3. Results and discussion

In summary, sensitive parameters influencing model calibration are the kinetic and sorption parameters of the organic carbon fractions and the double porosity exchange parameters for oxygen. Optimization as included as tools within the MATLAB software package was not performed because of the implications of the externally accessed PHREEQC module. By multiple simulation runs the combination of kinetic, sorption and exchange parameters were extrapolated. Table 12 gives the most adequate parameter combination resulting from these multiple runs to verify the sampled breakthrough. The simulation results are shown as breakthrough curves in Figure 70 – Figure 74 providing the simulation results for oxygen in relation to the sampled oxygen breakthrough. They generally illustrate that using the conceptual model set up a quite good match of measured and modelled oxygen breakthrough can be achieved. Figure 74 depicts the flushing stage when oxic conditions were forced to change to anoxic conditions. Here the simulation reacts faster (dropping the oxygen concentration to zero) than available from the measurement.
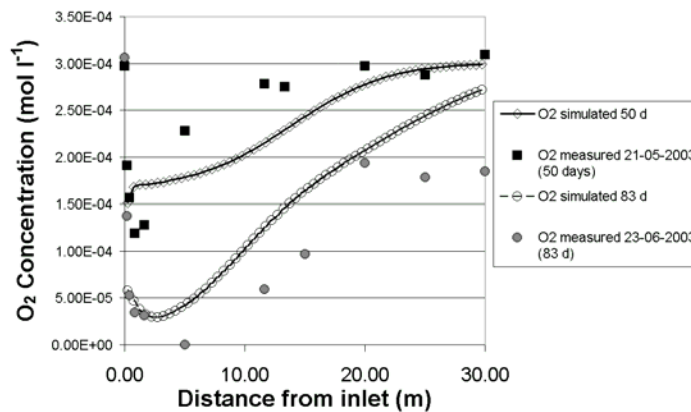
Figure 70 Measured and simulated Oxygen breakthrough during soil column flushing (1)
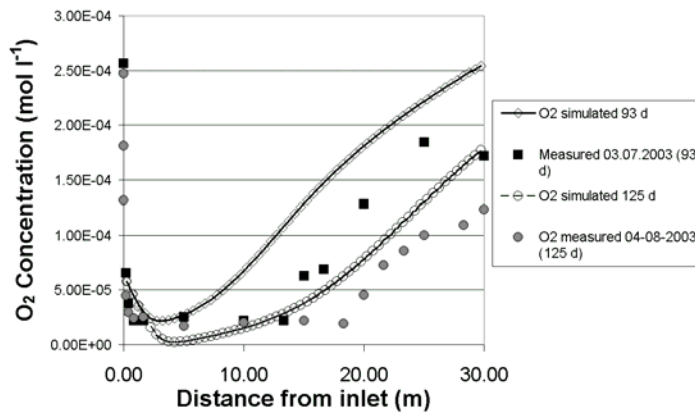
Figure 71 Measured and simulated Oxygen breakthrough during soil column flushing (2)
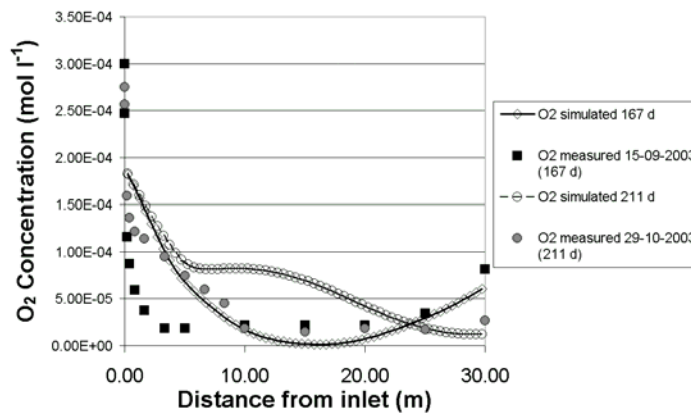
Figure 72 Measured and simulated Oxygen breakthrough during soil column flushing (3)
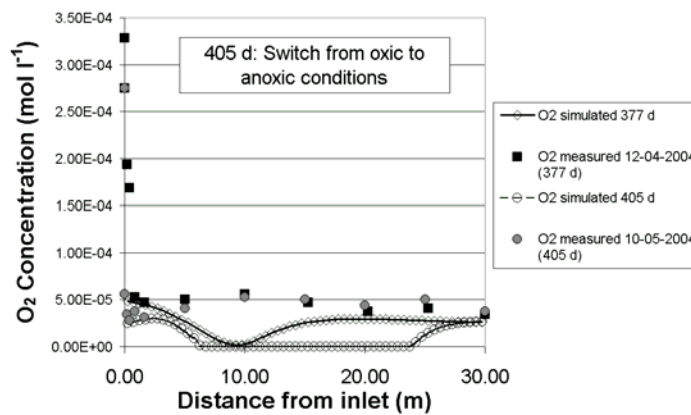
Figure   73   **Oxygen**   **column**   **Measured and simulated**   **breakthrough during soil**   **flushing (4)**
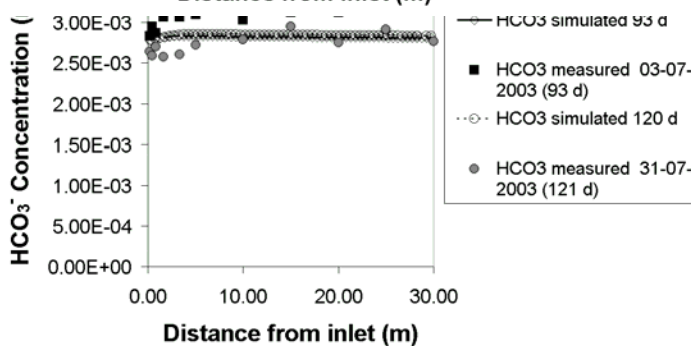
Figure 74 Measured and simulated Oxygen breakthrough during soil column flushing (5)

The verification of the pore water hydrochemistry - here shown in terms of HCO_3^- ,pH and Ca (Figs. Figure 75 -Figure 80) - confirms that mainly the calcite equilibrium is critical for the sampled pore water hydrochemical composition as conceptualised by the reaction framework set up.   Differences between simulation results and measurements may reflect variable hydrochemical composition of the applied surface water as available from the NASRI Database and uncertainty about the initial pore water chemistry. Other minerals able to act as electron acceptors , such as Pyrolusite (MnO_2) and Ferrihydrite ($Fe(OH)_{3, amorphous}$), are confirmed to not by model simulation the be consumed by biodegradation. By measurement, only low Mn concentrations of $1x10^{-7}$ to $3x10^{-6}$ mol l^{-1} were found in the pore solution under anoxic conditions (NASRI Database) indicating some activation of Pyrolusite as terminal electron acceptor during biodegradation.
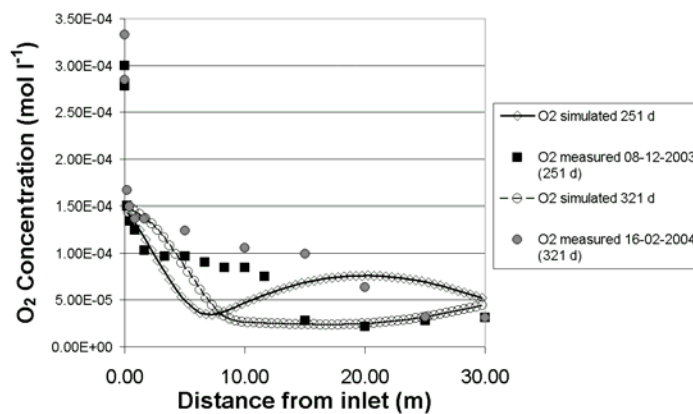
Figure 75 Measured and simulated HCO_3^- breakthrough during soil column flushing (1)
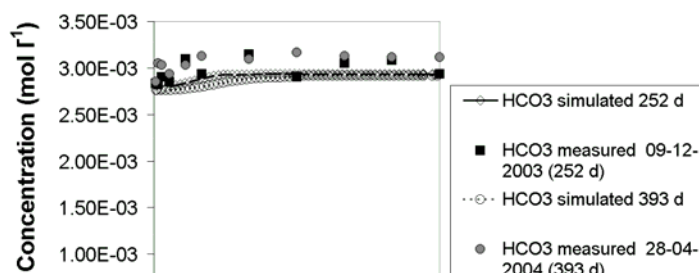
Figure 76 Measured and simulated HCO₃⁻ breakthrough during soil column flushing (2)
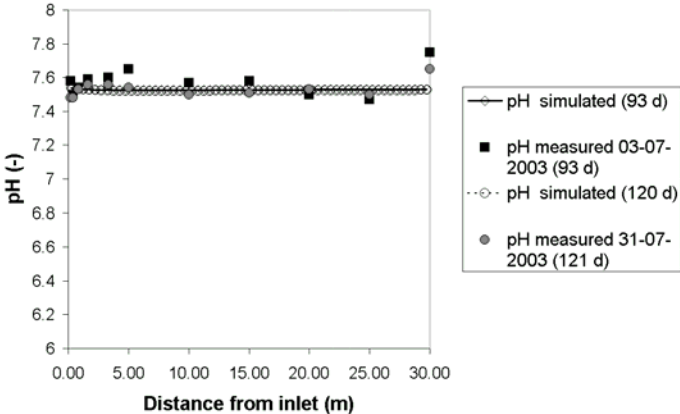
Figure 77 Measured and simulated pH breakthrough during soil column flushing (1)
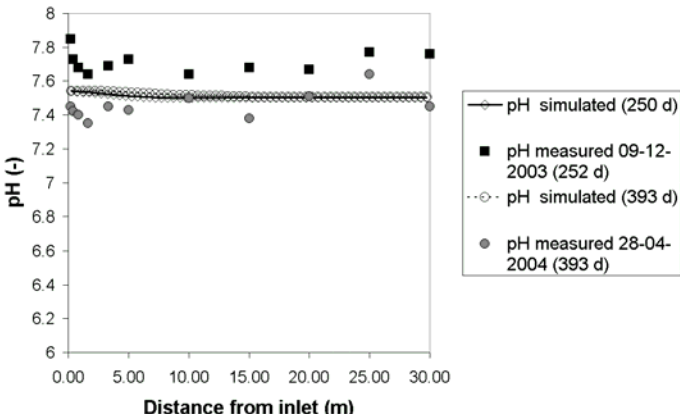
Figure 78 Measured and simulated pH breakthrough during soil column flushing (2)
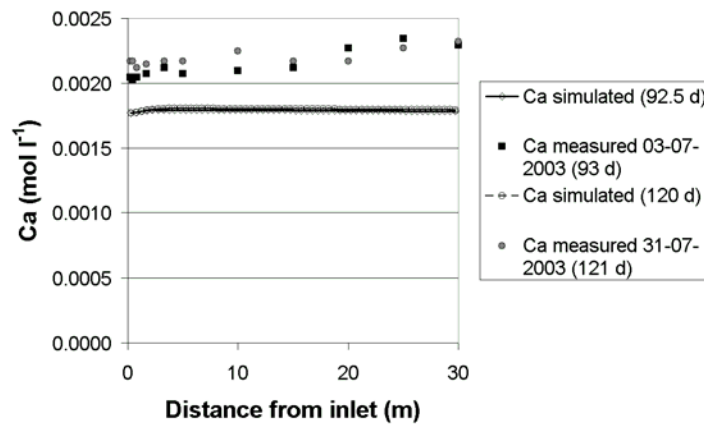
Figure 79 Measured and simulated Ca breakthrough during soil column flushing (1)
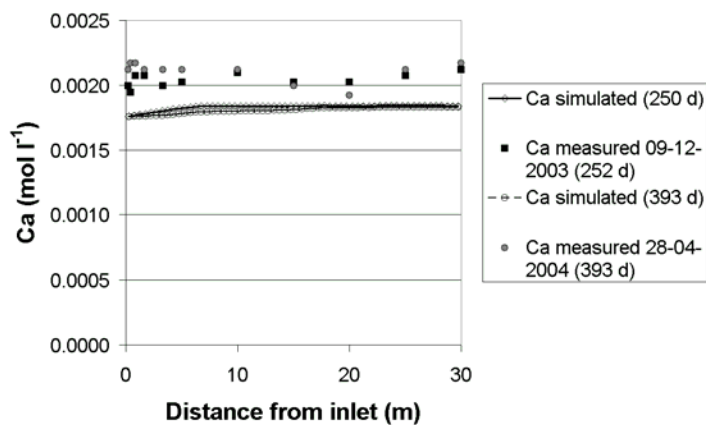
Figure 80 Measured and simulated Ca breakthrough during soil column flushing (2)

3.4. Major conclusions and summary

Based on a conceptual model, which includes biodegradation and sorption of differently reactive organic carbon species, a double porosity approach for residual oxygen and

hydrogeochemical speciation, a large soil column flushing experiment was simulated by reactive transport modelling. The conceptual model accounts for a biodegradation kinetics approach for DOC and a chemical equilibrium approach to model the geochemical response on biodegradation. The applied numerical reactive transport model combines a MATLAB tool (to solve the advection-dispersion PDE, the double porosity exchange term for oxygen and the sorption term for DOC) and a PHREEQC module as solver for chemical equilibrium and biodegradation kinetics and has proven to verify the observed breakthrough of oxygen, DOC and inorganic hydrochemistry. In summary, the assessment of the simulation results must reflect the data uncertainties among the soil matrix composition (trace minerals and biomass resulting from older experiments), variable inflow hydrochemistry (due to technical implications and to seasonal variable composition of the infiltrated surface water), and the fate of the column before starting the actual flushing experiment. The simulation results are applicable to the issue of riverbank filtration waterworks test sites in Berlin characterized by a particular unsteady pumping regime.

3.5. References

AMIRBAHMAN, A., SCHöNENBERGER, R., FURRER, G. & ZOBRIST, J. (2003): Experimental study and steady-state simulation of biogeochemical processes inlaboratory columns with aquifer material. J. Contam. Hydrol., 64., 123-125.

APPELO, C. A. J., V., POSTMA, D. (1996): Geochemistry, groundwater and pollution. Balkema, Rotterdam.

APPELO, C. A.J., VERWEIJ, E., SCHÄFER, H. (1998): A hydrogeochemical transport model for an oxidation experiment with pyrite/calcite/exchangers/organic matter containing sand. Appl. Geochemistry, 13., 257-268.

BARRY, D. A., PROMMER, H., MILLER, C. T., ENGESGAARD, P., BRUN, A., & ZHENG, C. (2002): Modelling the fate of oxidable organic contaminants in groundwater. Adv. Water Resour., 25., 945-983.

VAN BREUKELEN, B. M., APPELO, C. A. J., OOLSTHOORN, T. N. (1998): Hydrogeochemical modelling of 24 years of Rhine water infiltration in the dunes of the Amsterdam water supply. J. Hydrol., 209., 281-296.

BRUN, A., ENGESGAARD, P. (2002): Modelling transport and biogeochemical processes in pollution plumes: literature review and model development. J. Hydrol., 256., 211-227.

BRUN, A., ENGESGAARD, P., & ROSBJERG D. (2002): Modelling transport and biogeochemical processesin pollution plumes: Vejen lanfill, Denmark. J. Hydrol., 256., 228-247.

DREWES, J. E., & JEKEL, M. (1996): Simulation of groundwater recharge with advanced treated wastewater. Wat. Sci. Tech., 33 (10-11), 409-418.

VON GUNTEN, U., & ZOBRIST, J. (1996): Biogeochemical changes in groundwater-infiltrating systems: column studies. Geochim. Cosmochim. Acta, 57., 3895-3906.

HERON, G., CHRISTENSEN, T. H., & TJELL J. C. (1996): Oxidation capacitiy of aquifer sediments. Environ. Sci. Technol., 29., 187-192.

HERZER, H., & KINZELBACH, W. (1989): Coupling of transport and chemical processes in numerical transport models. Geoderma, 44., 115-127.

HOLZBECHER, E., MASSMANN, G., HORNER, CHR., PEKDEGER, A. (2001): Redox processes in the Oderbruch Aquifer. In: GEHRELS, H., PETERS, N. E., HOEHN, E., JENSEN, K., LEIBUNDGUT, C., WEBB, B., & ZAADNOORDLIJK, W. J. (eds.): Impact of Human activity on Groundwater Dynamics), (Sixth Scientific Assembly of the IAHS, Maastricht, the Netherlands, July 2001) , IAHS Publication 269, IAHS Press, Wallington, UK, 229-238.

HOLZBECHER, E., HORNER, CHR. (2003): A reactive transport model for redox components – verification of transport and test of field data. In: SCHULTZ, H. D., & HADELER, A. (eds.): GeoProc 2002 Geochemical Processes in Soil and Groundwater, Wiley–VCH Verlag GmbH Co. KgaA, Weinheim, Germany, 414-433.

HORNER,CHR., HOLZBECHER, E. &NÜTZMANN, G. (2004) : A Coupled Transport and Reaction Model for long Column Experiments simulating Bank Filtration. Hydrological Processes (in print).

HUNTER, K. S., WANG, Y., VAN CAPPELLEN, P. (1998): Kinetic modelling of microbially-driven redox chemistry of subsurface environments: coupling transport, microbial metabolism and geochemistry. J. Hydrol., 209, 53-80.

JAKOBSEN, R., & POSTMA, D. (1999): Redox zoning, rates of sulfate reduction and interaction with Fe-reduction and methanogenesis within a shallow sandy aquifer. Geochim. Cosmochim. Acta, 63, 137-151.

KINZELBACH, W., SCHÄFER, W., & HERZER, J. (2004): Numerical modelling of natural and enhanced denitrification in aquifers. Water Resour. Res. 27 (6)., 1123-1135.

LENSING, H. J., VOGT, M., & HERRLING, B. (1994): Modelling of of biological mediated redox processes in the subsurface. J. Hydrol., 159, 125-43.

MASSMANN, G (2001): Infiltration of river water into the groundwater – investigation and modeling of hydraulic and geochemical processes during bank filtration in the Oderbruch, Germany. Dissertation zur Erlangung des Doktorgrades des Fachbereichs Geowissenschaften der Freien Universität Berlin. Dissertation.de, Verlag im Internet., Berlin.

NASRI, (2003): Natural and Artificial Systems for Recharge and Infiltration, 1st Report. Kompetenzzentrum Wasser, Berlin.

PHANIKUMAR, M. S., HYNDMAN, D. D., WIGGERT, D. C., DYBAS, M. J., WIGG, M. W., & CRIDDLE, C. S. (2002):): Simulation of microbial transport and carbon tetrachloride biodegradation in intermittently-fed aquifer columns. Water Resour. Res., 38 (4)., 1-13.

PARKHURST, D. L., THORSTENSON, D. C., & PLUMMER, L. N. (1980): PHREEQE – a computer program for geochemical calculations. U.S. Geological Survey Water-Resources Investigation Report 80-96, Denver, Co., U. S. A., pp 195.

PARKHURST, D. L., & APPELO, C. A. J. (1999): User's Guide to PHREEQC (Version 2) – a computer program for speciation, batch-reaction, one-dimensional transport, and inverse geochemical calculations. U.S. Geological Survey Water-Resources Investigation Report 99-4259, Denver, Co., U. S. A., pp 312.

PORRO, I., WIERENGA, P. J., HILLS, R. G. (1993a): Solute transport through large uniform and and layered soil columns. Water Resour. Res., 29 (4), 1321-1330.

PORRO, I., WIERENGA, P. J. (1993b): Solute transport through large unsaturated soil column. Groundwater., 31 (2), 193-200.

PROMMER, H., BARRY, D. A. & DAVIS, G. B. (199a): A one-dimensional reactive multi-component transport model for biodegradation petroleum hydrocarbons in groundwater. Environ. Model. Softw., 14, 213-233.

PROMMER, H., DAVIS, G. B. & BARRY, D. A. (199b): Geochemical changes during biodegradation of petroleum hydrocarbons: field investigations and biogeochemical modelling. Org. Geochem., 30, 423-435.

PROMMER, H. (2002): A reactive multicomponent transport model for saturated porous media. Draft of user's manual version 1.0, contaminated land assessment and

remediation research centre, the university of Edinburgh (available from http://www.pht3d.org)

SCHÄFER, D., SCHÄFER, W., & KINZELBACH W. (1998a): Simulation of reactive processes to biodegradation in aquifers, 1 structure of the three-dimensional reactive transport model . J. Contam. Hydrol., 31., 167-186.

SCHÄFER, D., SCHÄFER, W., & KINZELBACH W. (1998b): Simulation of reactive processes to biodegradation in aquifers, 2. model application to a column study on organic carbon degradation. J. Contam. Hydrol., 31., 187-209.

THE MATHWORKS (2003): MATLAB, The language of technical computing (Version 6). The MathWorks Inc. 3 Aple Hill drive, Natick, MA 01760-2098, U.S.A.

WALTER, A. L., FRIND, E. O., BLOWES, D. W., PTACEK, C. J., & MOLSON, J. W. (1994): Modelling of multicomponent reactive transport in groundwater 1. model development and evaluation. Water Resour. Res., 30 (11), 3137-3148.

4. Modelling of enclosure experiments: microcystin and bacteriophages

4.1. Methods: Inversion Modules VisualCXTFIT and MATLAB®

For inverse modelling two different software tools are applied, VisualCXTFIT and MATLAB®, corresponding to the inversion of different parameters in two steps. Modelling is based on the general transport equation, a partial differential equation for the unknown fluid phase concentration c:

$$\theta R \frac{\partial c}{\partial t} = \nabla \mathbf{D} \nabla c - \mathbf{v} \nabla c - \theta R \lambda c \tag{1}$$

with the parameters: porosity θ, retardation R, dispersion tensor $\mathbf{D}$, Darcy-velocity $\mathbf{v}$ and degradation rate λ. For column or enclosure experiments it is common to make the assumption that flow can be treated as one-dimensional. Then the transport equation can be formulated in a simpler form:

$$R \frac{\partial c}{\partial t} = \frac{\partial}{\partial x} \alpha_L u \frac{\partial c}{\partial x} - u \frac{\partial c}{\partial x} - \lambda R c \tag{2}$$

with longitudinal dispersivity α_L and interstitial 'real' flow velocity u. Altogether there are four parameters: α_L, u, R and λ. Instead of u one may use the porosity $\theta = v/u$ as parameter, because the Darcy-velocity v is given implicitly by the applied flow rate. In the literature one often finds the combination $\mu = \lambda R$ used in estimation runs, for example in CXTFIT (1995). The first two of the four parameters are species independent, the latter two are usually species dependent. The first two parameters can be best obtained from tracer experiments, because for tracers the 1D transport equation reduces to:

$$\frac{\partial c}{\partial t} = \frac{\partial}{\partial x} \alpha_L u \frac{\partial c}{\partial x} - u \frac{\partial c}{\partial x} \tag{3}$$

Within the project the inversion procedure was divided into two steps. In the first step species-independent parameters are determined from the tracer experiments, followed by the second step for the remaining parameters for each specie separately:

Determination of velocity u and dispersivity α_L from tracer experiments

Determination of retardation R and degradation rate λ from experiments with non-tracers

Step (1) was performed using VisualCXTFIT, which is a graphical user interface (GUI) for the CXTFIT code for parameter estimation. CXTFIT was developed at the U.S. Salinity Laboratories (Toride *et al.*, 1995) and is based on analytical solutions of the 1D transport equation. Analytical solutions have the advantage that direct solutions of the differential equation have no problems with discretization errors, as they appear in numerical solutions. On the other hand analytical solutions exist only for specific conditions and can not be given for general boundary and initial conditions. However for the given experimental set-up in the enclosures as well as in the columns it was possible to use CXTFIT.

The VisualCXTFIT user interface for CXTFIT was developed within the NASRI project. An EXCEL-Add-in is produced, which allows the input and manipulation of measured data, as well as the specification of the inversion parameters and options. Moreover a graphical representation of the results is produced in the EXCEL sheet. Detailed description as well as application examples are given by Nützmann *et al.* (2005).

Step (2) was performed using a newly developed tool for parameter inversion, written as a m-file module in MATLAB® (2002). The module has been used for inversions of transport processes only, but could be used for other applications as well. The MATLAB® module works also for the inversion of temperature time series. For such an application the module is described in detail by Holzbecher (2005).

Within the MATLAB® module direct simulations of the transport equation are performed. The direct solution is obtained by using the 'pdepe'-solver, which is part of core MATLAB®. The direct solver is called within an inversion procedure, which is based on the MATLAB® optimization module. There various options, concerning the search algorithm and the numerical parameters can be specified.

In the module the user can specify the parameters, which are to be estimated. Within the automatic inversion procedure it is attempted to modify the selected parameters from their start values, in order to obtain a better fit with the remaining time-series in the input-data set. The objective function is sum of the squares of the deviations between measured and modelled values, what is usually known as least squares optimization. Parameters, not selected for the estimation procedure, remain on their starting value.

As input the MATLAB® inversion module requires time series, measured at least at two positions along the flowpath. The first time series, given in the input data-set, is treated as a boundary condition; the other time series are used for the parameter estimation procedure. When several time-series are given there is the additional option to estimate parameters from various possible estimation intervals. For example, in case of three time series, the first can be treated as boundary condition, user either the second, or the second and the third for

the estimation. Moreover, the second time series can be used as boundary condition, in order to use the third for the estimation. In that way it is possible to obtain an impression of the variability of the parameters with the spatial intervals.

Each estimation run MATLAB® finally produces a plot, visualizing the following:

- Measurements used as boundary conditions (one time series)
- Measurements used for parameter estimation
- Modelled concentration curve based on best-fit parameters

In the estimation runs for the enclosures, slow sand filters and column experiments, performed during the NASRI project, it turned out that the automatic inversion procedure did not deliver optimal results. The problem is well-known, as the algorithms find local minima of the objective function, which are not necessarily global minima. When the user suspects that the automatic solver has not found the global minimum yet, the algorithm is usually re-started again with a new starting set, which differs both from the obtained local minimum parameter set and from the previous starting values. Such 'fine-tuning' was required in almost all reported simulations.

Moreover the comparison of parameter values, obtained for different spatial intervals (as described above) mostly revealed substantial differences. It can be concluded that parameters are obviously not constant, but change with space. A more detailed description, concerning phage transport in the enclosures, is presented by Holzbecher *et al.* (2005).

4.2. Results

Microcystin

The following figures show best fit results for enclosure experiments E2 and E3 for different parts of the flow path. Depicted are

- Measured concentrations at 1. position of concerned spatial interval, here denoted as 'inlet' (diamonds with scale on the right); used as boundary condition for inverse modelling
- Measured concentrations at 2. position of concerned spatial interval, here denoted as 'outlet' (crosses with scale on the left); used for objective function in inverse modelling
- Modelled concentrations at 2. position (line with scale on the left); simulated using best-fit parameter values.

Shown in the figure are also: velocities v and longitudinal dispersivities α_L, obtained form inverse modelling using VisualCXTFIT as well as retardation R and degradation rate λ, obtained form MATLAB® inverse modelling.

The intervals along the flowpath are denoted by 1->2, when the concentration in the input reservoir is taken as boundary condition, and the concentration at 20 cm depth for the parameter estimation. In the analogous manner the other spatial intervals are denoted as: 2->3, 3->4, 4->5 and 5->6.

$v = 0.32$ m/h $\alpha_L = 0.0063$ m

$R = 1.97$ $\lambda = 0.74$ 1/h
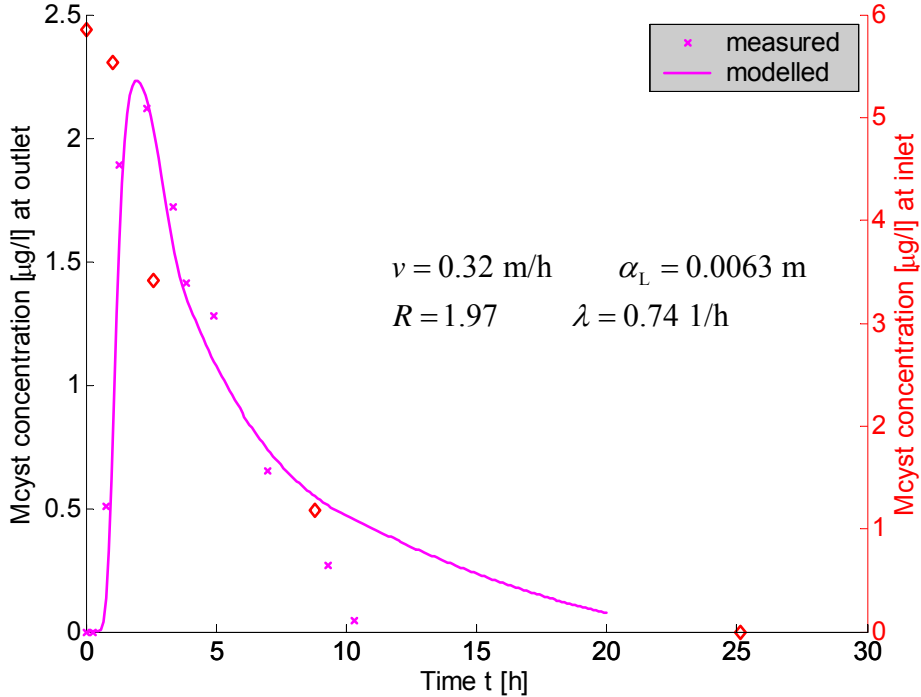
Figure 81 Inverse modelling result for EN2, 1->2

$v = 0.2$ m/h $\alpha_L = 0.005$ m

$R = 1.9$ $\lambda = 0.24$ 1/h
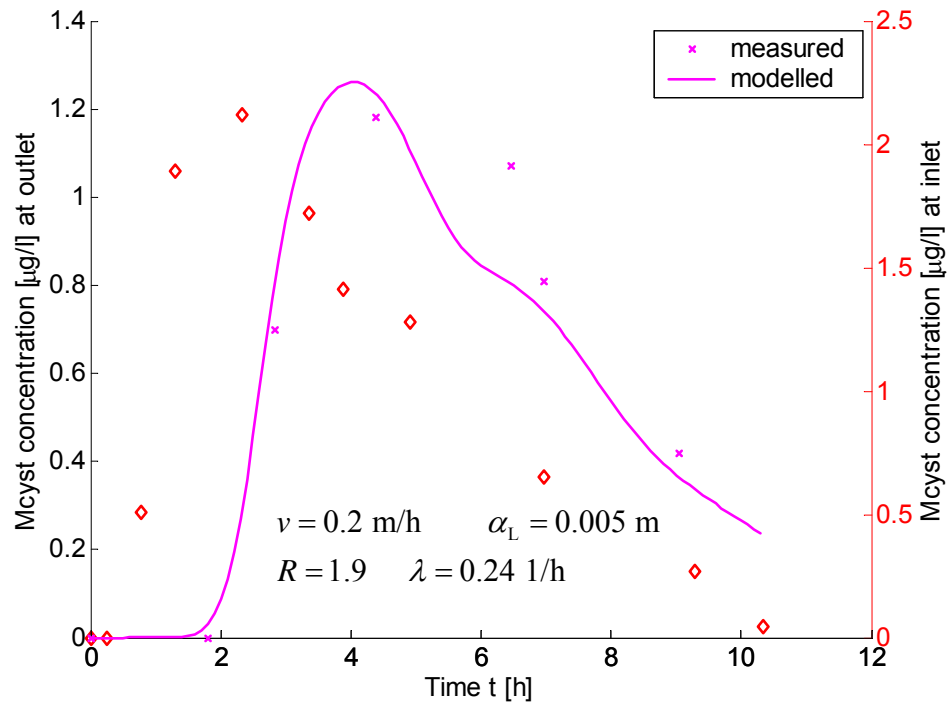
Figure 82 Inverse modelling result for EN2, 2->3

$v = 0.18$ m/h $\alpha_L = 0.0044$ m

$R = 1.0$ $\lambda = 0.75$ 1/h
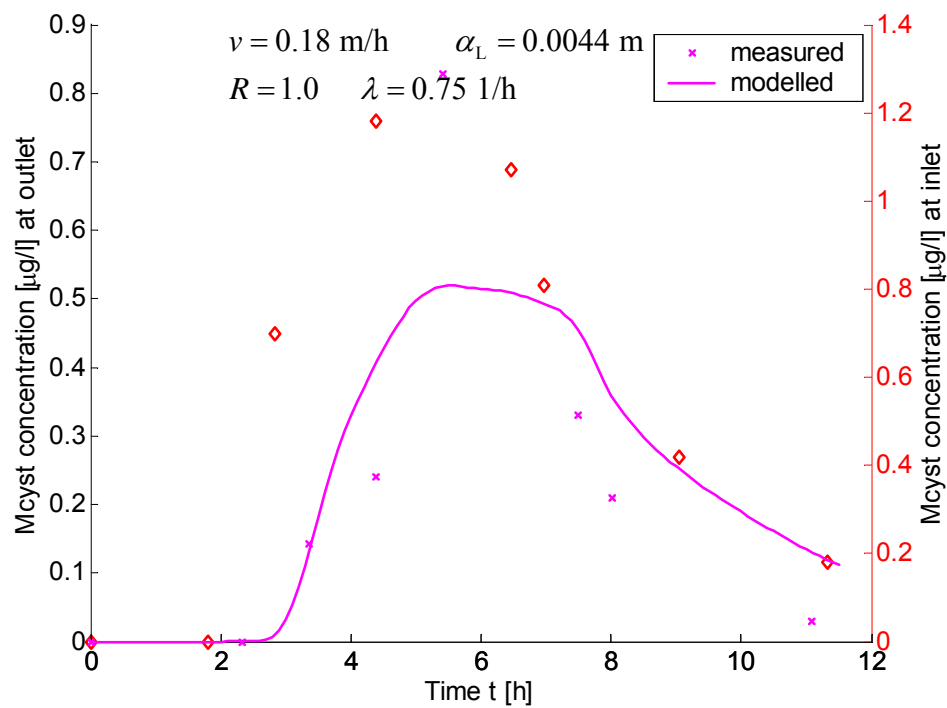
Figure 83: Inverse modelling result for EN2, 3->4
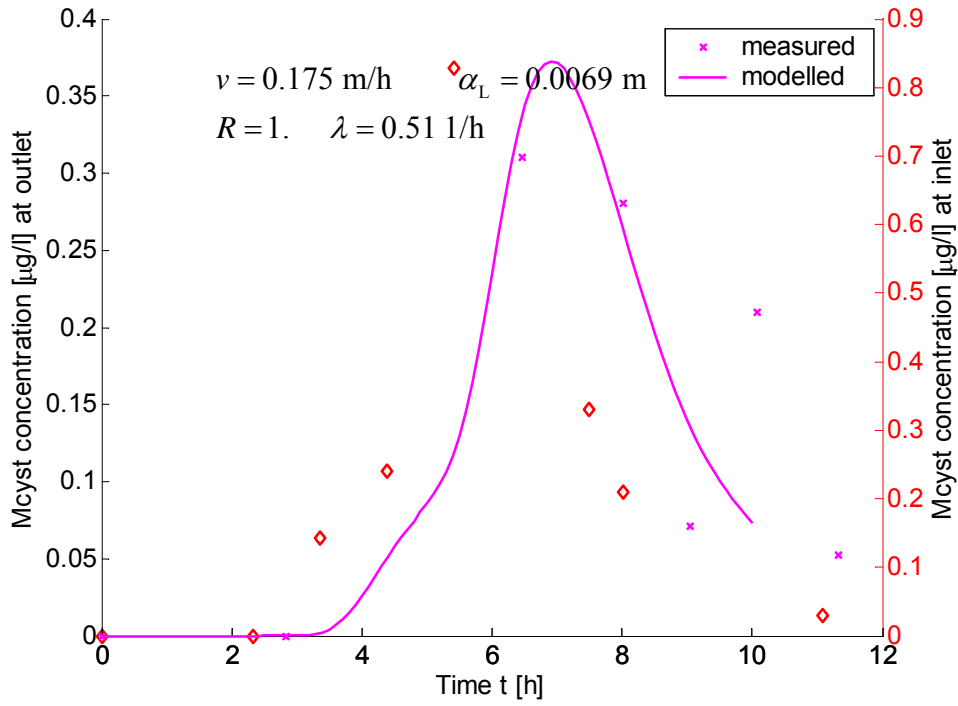
Figure 84 Inverse modelling result for EN2, 4->5
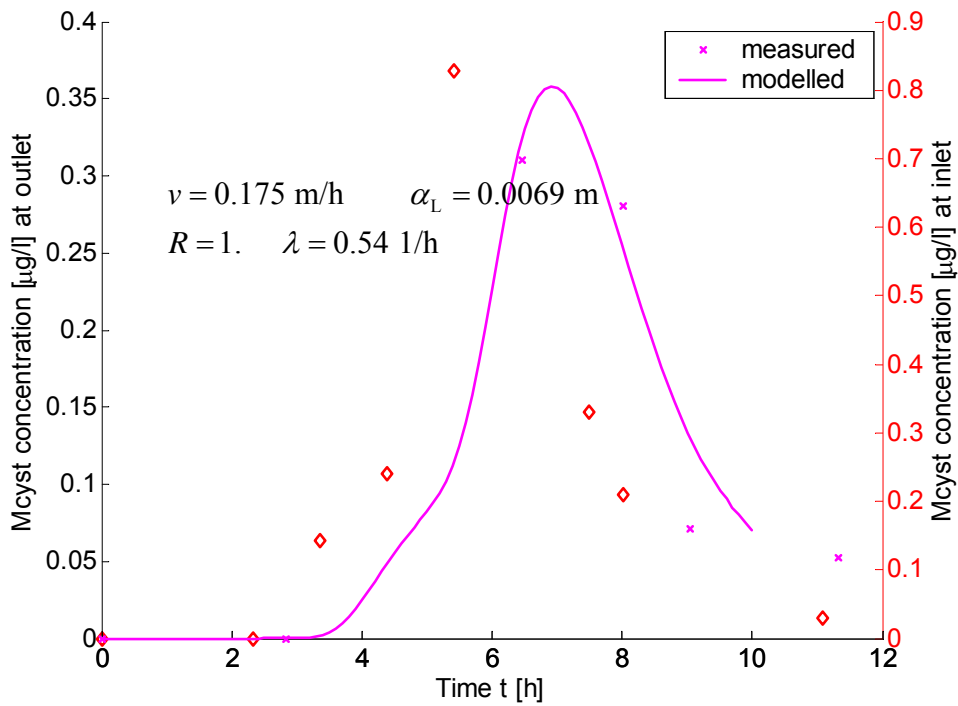
Figure 85 Inverse modelling result for EN2, 4->5; without outlier
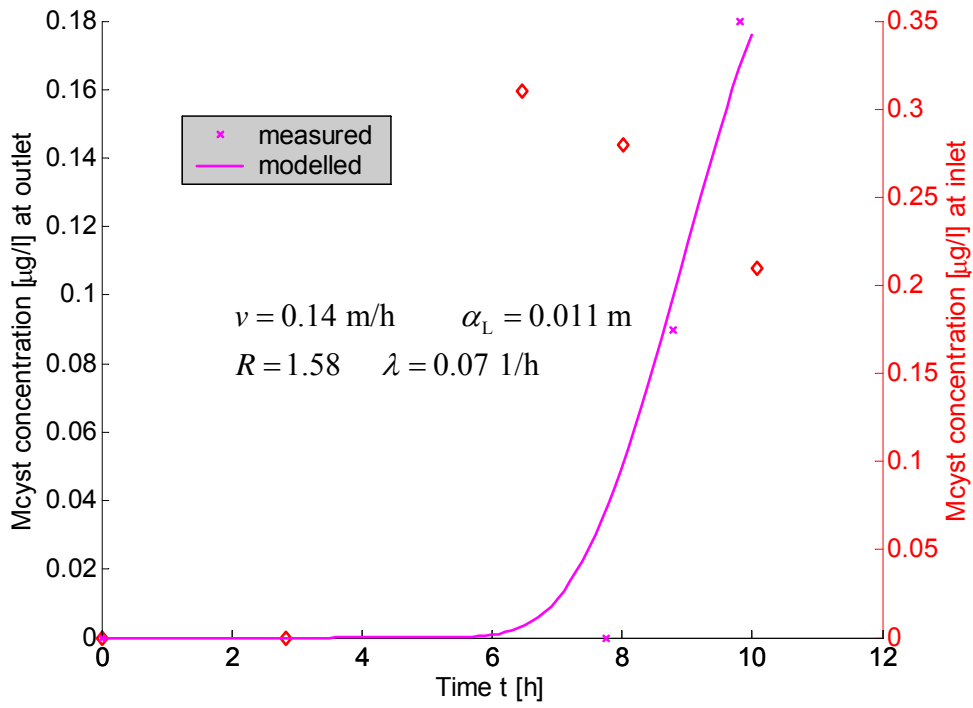
Figure 86 Inverse modelling result for EN2, 5->6
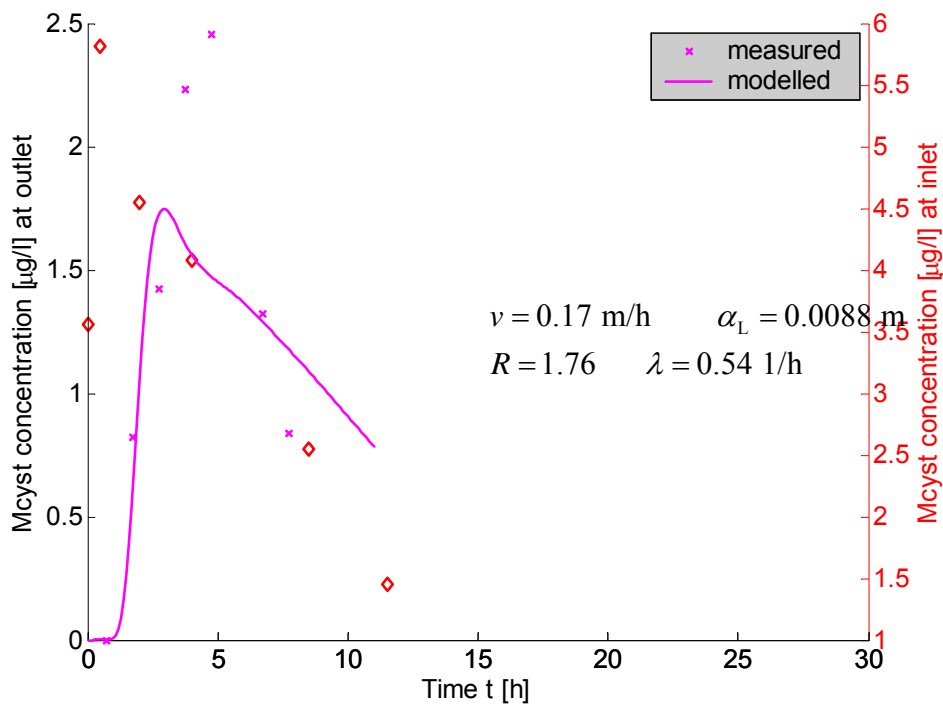
Figure 87: Inverse modelling result for EN3, 1->2

$v = 0.15$ m/h $\alpha_L = 0.0053$ m

$R = 1.0$ $\lambda = 0.74$ 1/h
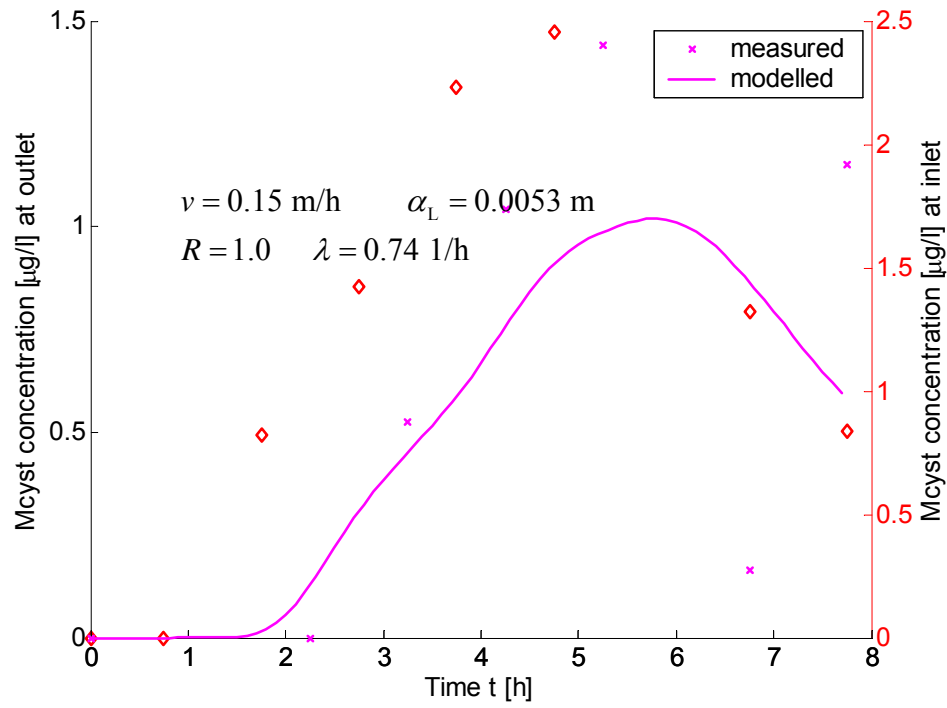
Figure 88 Inverse modelling result for EN3, 2->3

$R = 1.25$ $\lambda = 0.31$ 1/h
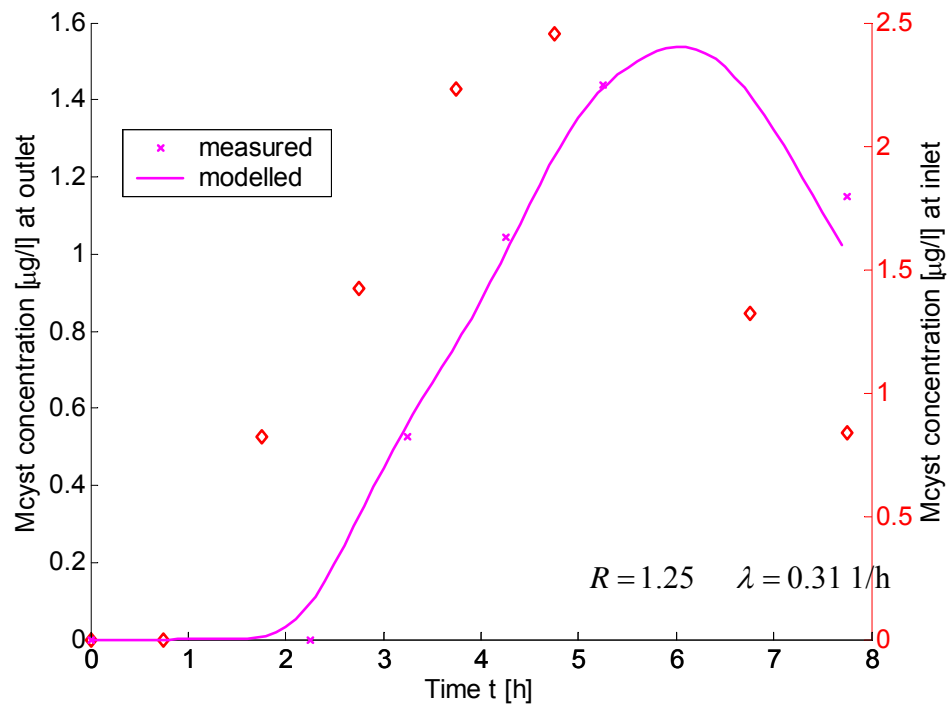
Figure 89 Inverse modelling result for EN3, 2->3, without outlier

$v = 0.15$ m/h $\alpha_{\mathrm{L}} = 0.0053$ m

$R = 1.23$ $\lambda = 0.25$ 1/h
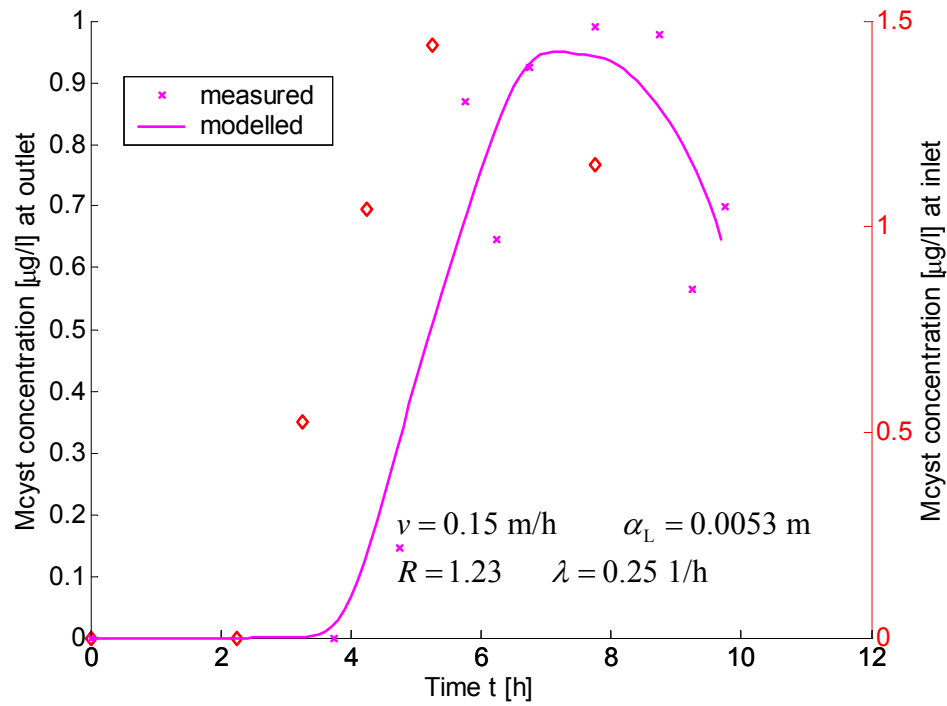
Figure 90 Inverse modelling result for EN3, 3->4

$v = 0.15$ m/h $\alpha_{\mathrm{L}} = 0.0053$ m

$R = 1.36$ $\lambda = 0.19$ 1/h
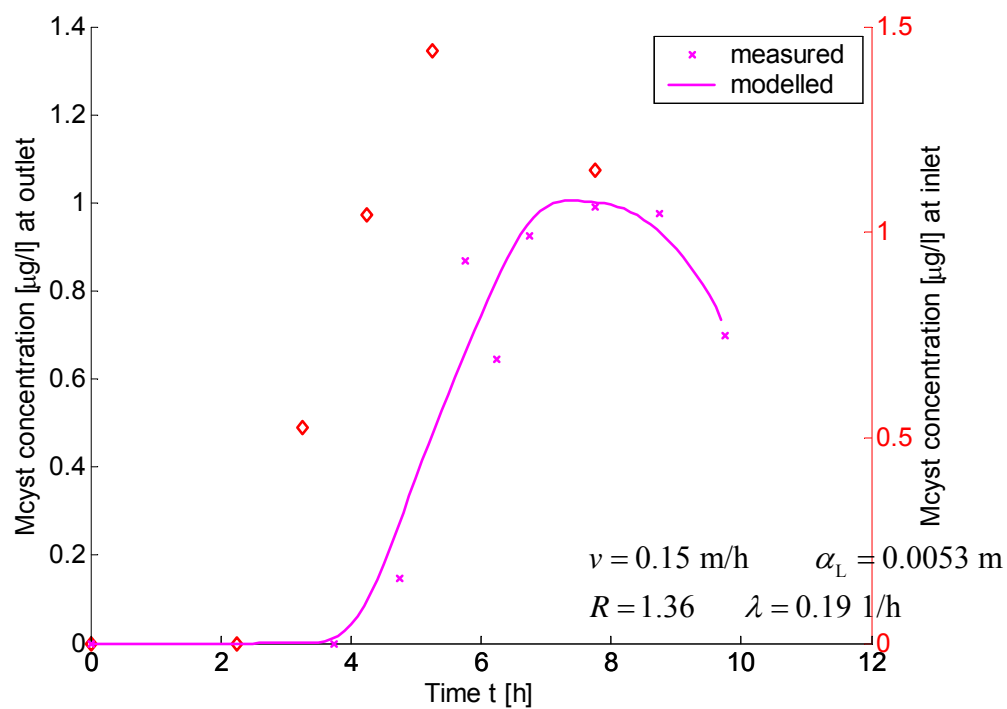
Figure 91 Inverse modelling result for EN3, 3->4, without outlier
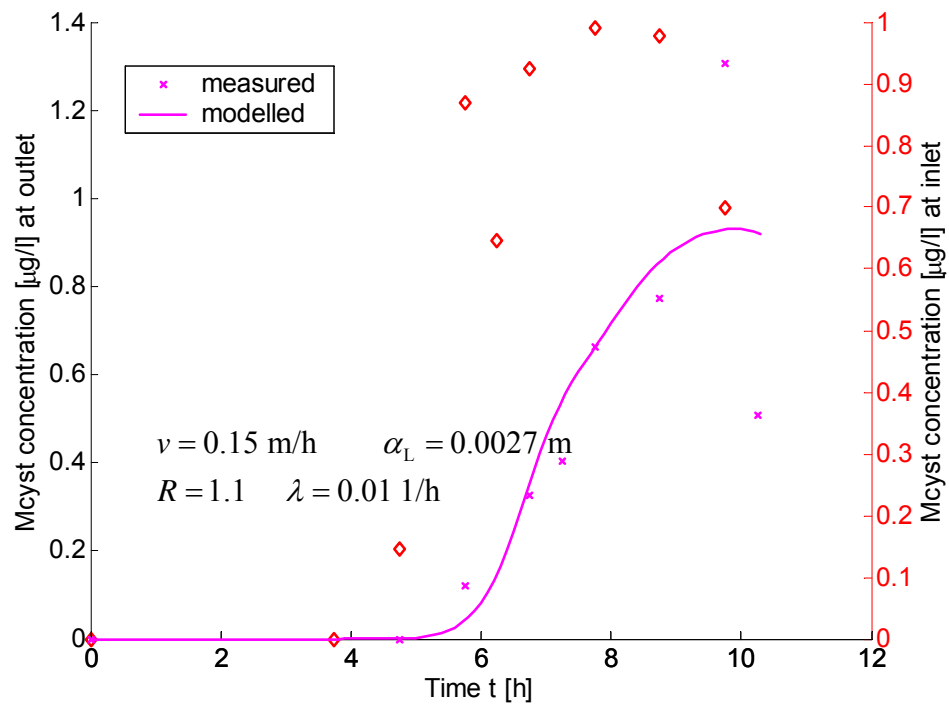
Figure 92 Inverse modelling result for EN3, 4->5
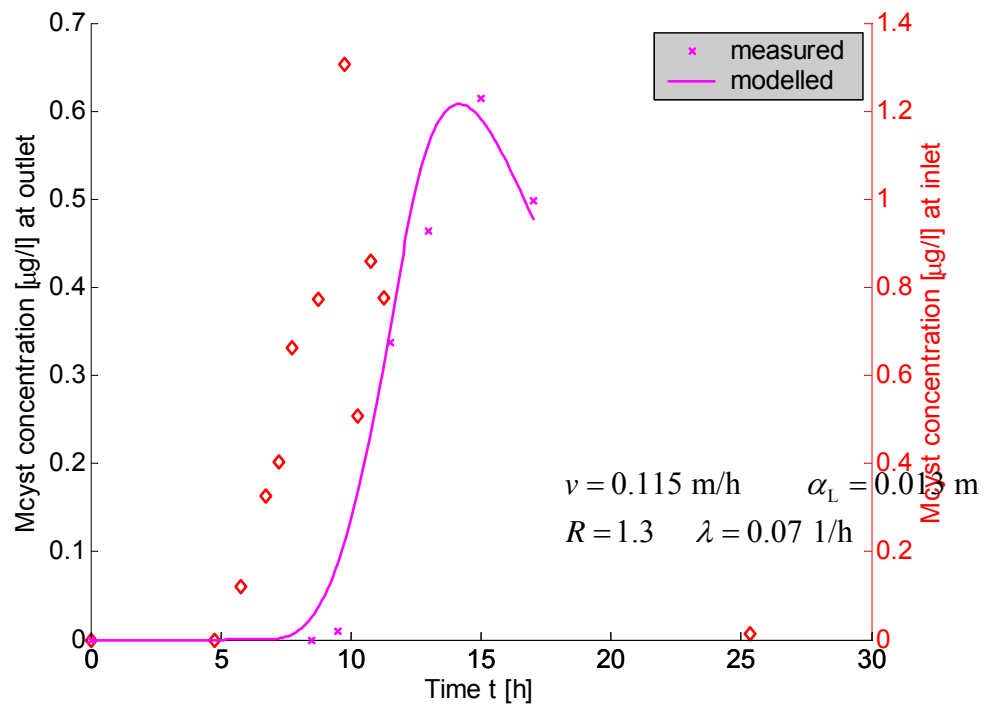
Figure 93 Inverse modelling result for EN3, 5->6, without outlier

The results of the inversion modelling procedure are depicted in Figures 1-13. For some simulations an additional start was performed, in which one or two outliers, observed in the measurements, were not considered in the parameter estimation procedure. In all cases the restart improved the fit substantially. Some parameter values changed significantly also by omission of outliers.

Bacteriophages

Enclosure experiments 2, 3, 9 and 10 were modelled. Modelling techniques were the same, as described in the section about microcystins. There were two steps:

- Velocity and dispersivity were obtained from inverse modelling based on tracer experiment measurements. Both the experiments as well as the inverse modelling was performed at the UBA. For inverse modelling VisualCXTFIT (Nützmann et al., 2005) was applied.
- Retardation and deactivation rate were obtained by inverse modelling, using MATLAB. The inversion module is described by Holzbecher (2005). Velocity and dispersivity values were taken from the first step.

The inversion was performed for different space intervals, as it turned out that 'global' values, valid for the entire column, are hardly to justify. All space intervals are related to the inlet of the enclosures, but have different lengths: 0.2, 0.4, 0.6, 0.8 and 1.2 m, if measurements are available.
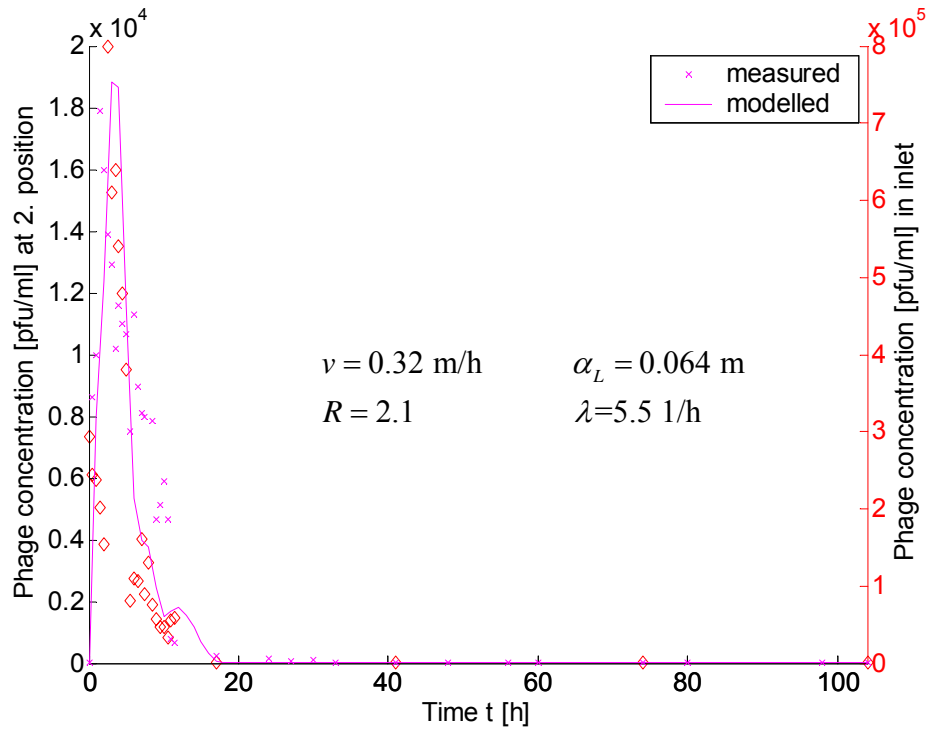
Figure 94 : *Phages 138, Encl 2, Flowpath: 20 cm*
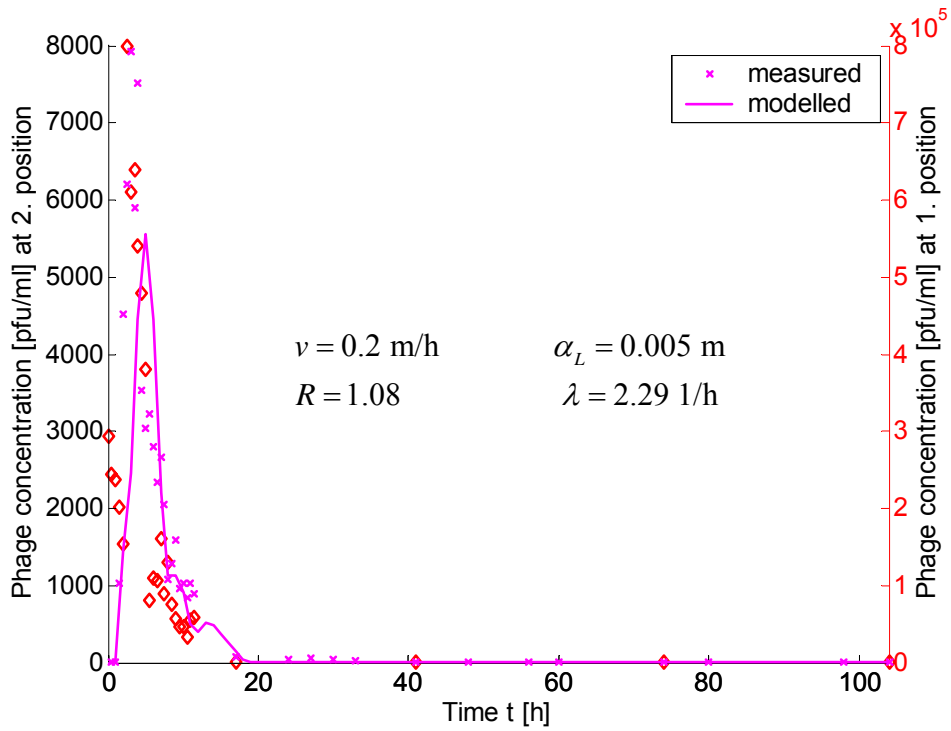
Figure 95 Phages 138, Encl 2, Flowpath: 40 cm
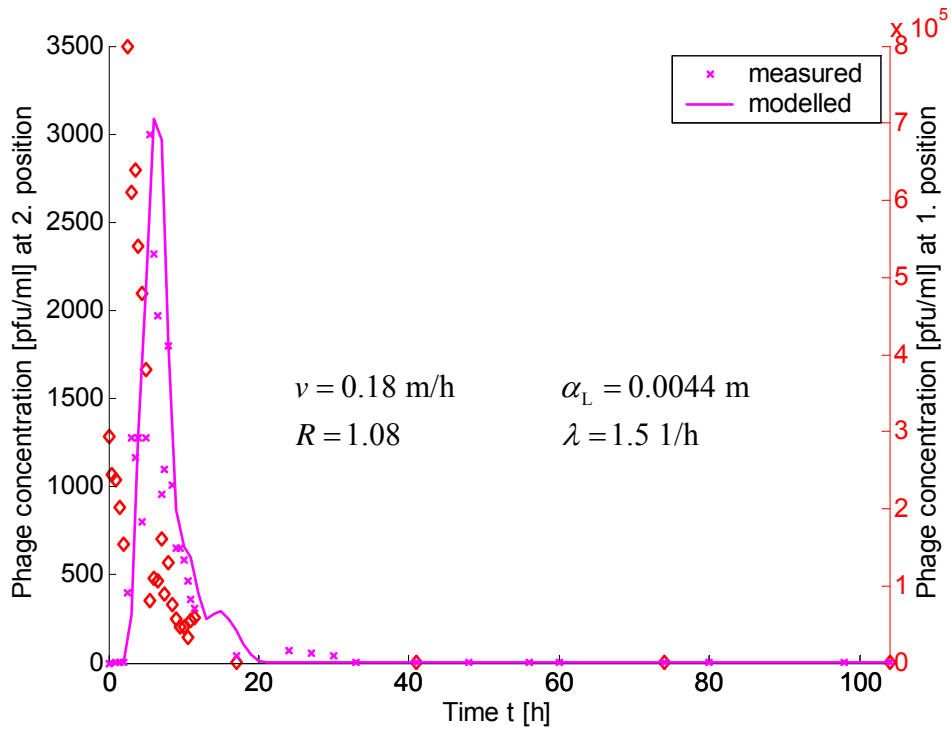
Figure 96 Phages 138, Encl 2, Flowpath: 60 cm
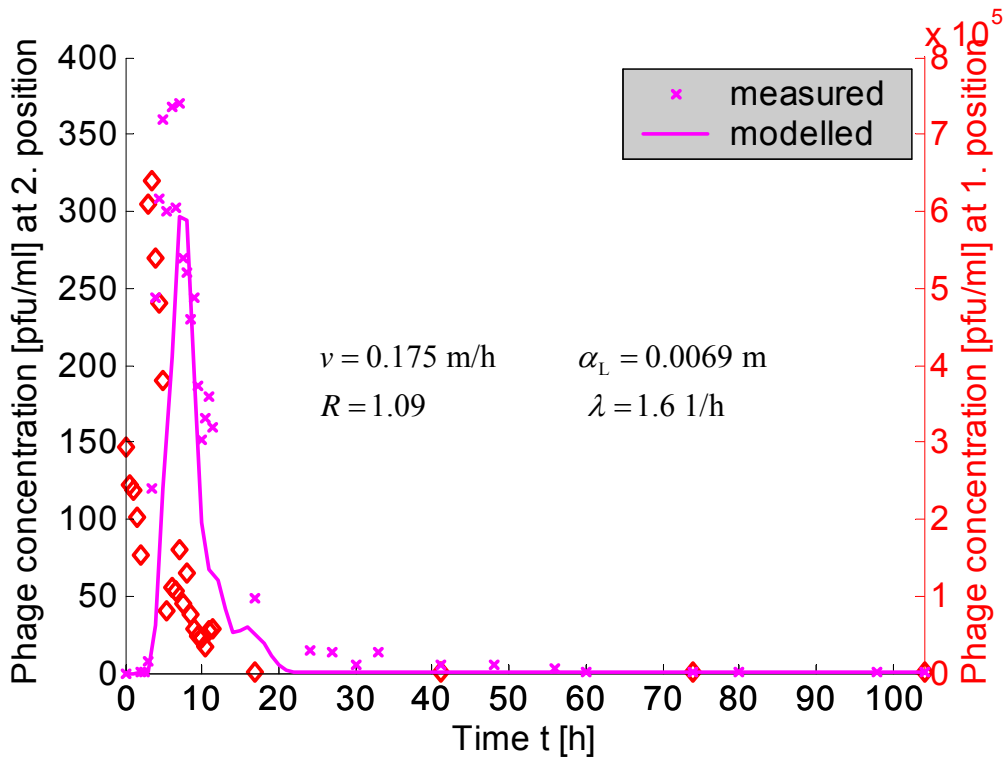
Figure 97 Phages 138, Encl 2, Flowpath: 80 cm
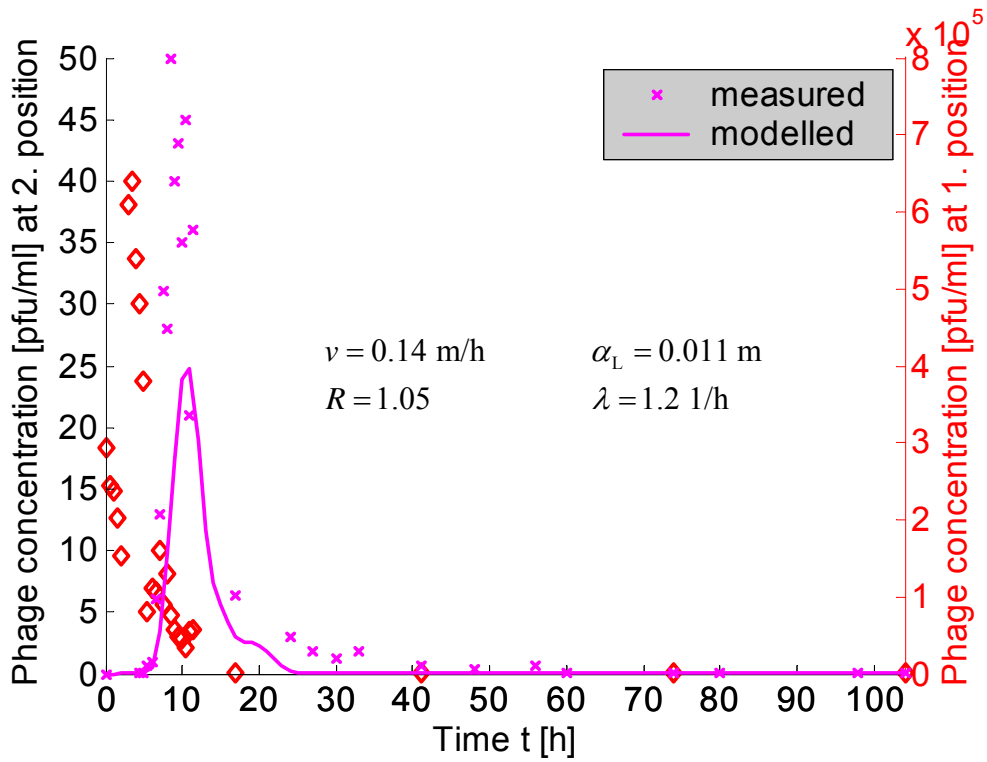
Figure 98 Phages 138, Encl 2, Flowpath: 120 cm
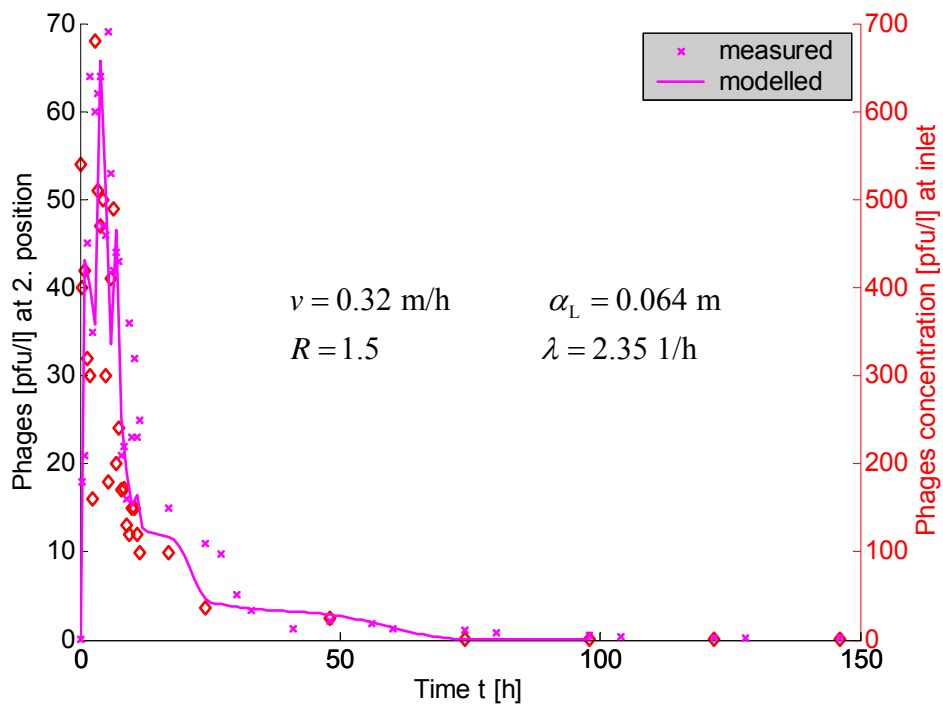
Figure 99 Phages 241, Encl 2, Flowpath: 20 cm
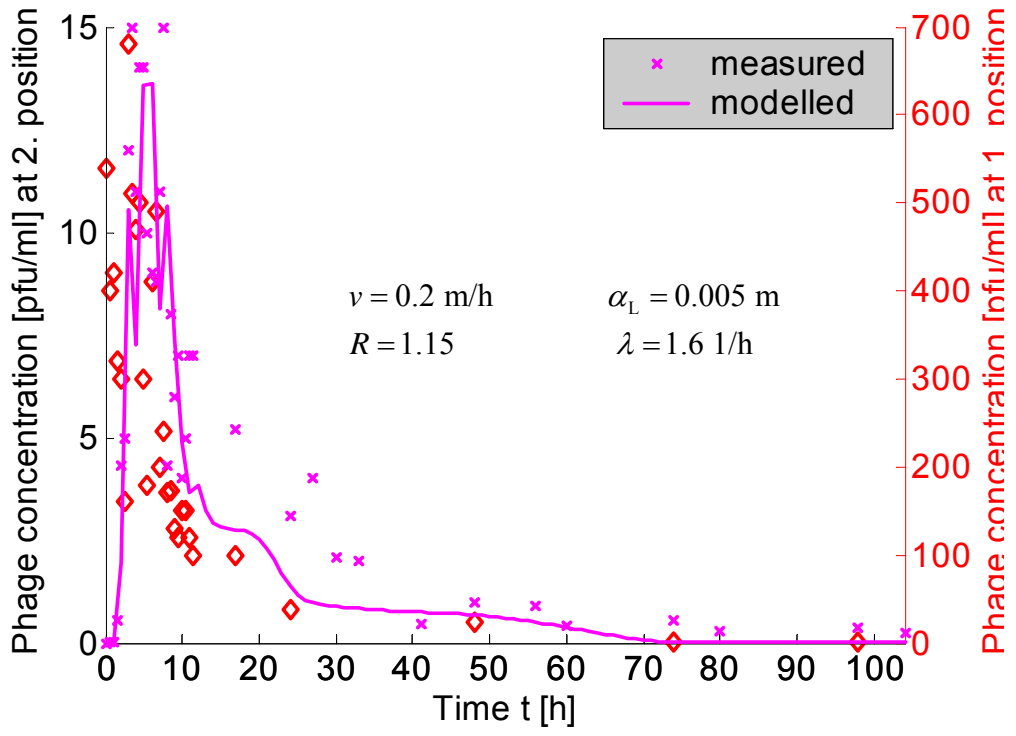
Figure 100 Phages 241, Encl 2, Flowpath: 40 cm
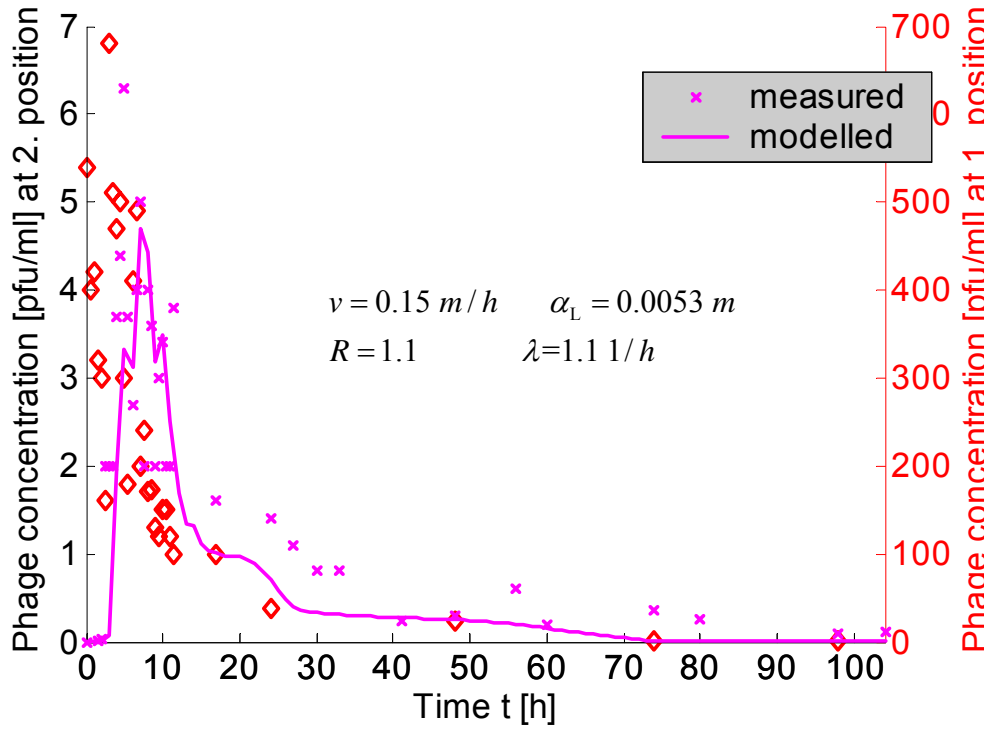
Figure 101 Phages 241, Encl 2, Flowpath: 60 cm
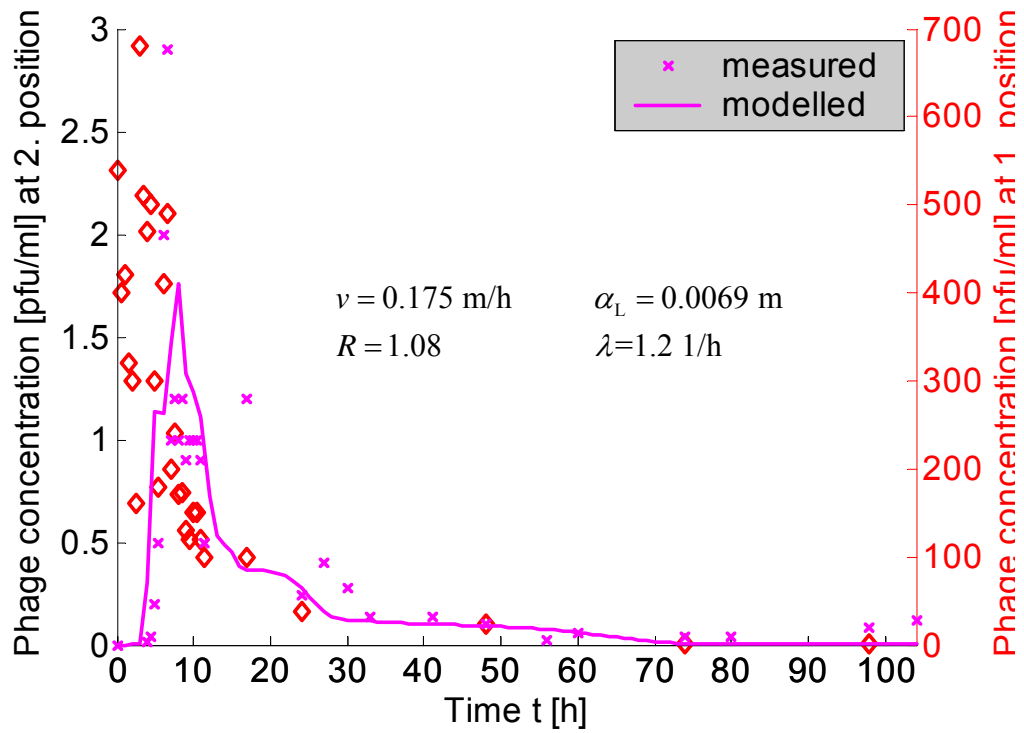
Figure 102 : Phages 241, Encl 2, Flowpath: 80 cm

$v = 0.175$ m/h $\alpha_L = 0.0069$ m
$R = 1.08$ $\lambda = 1.2$ 1/h
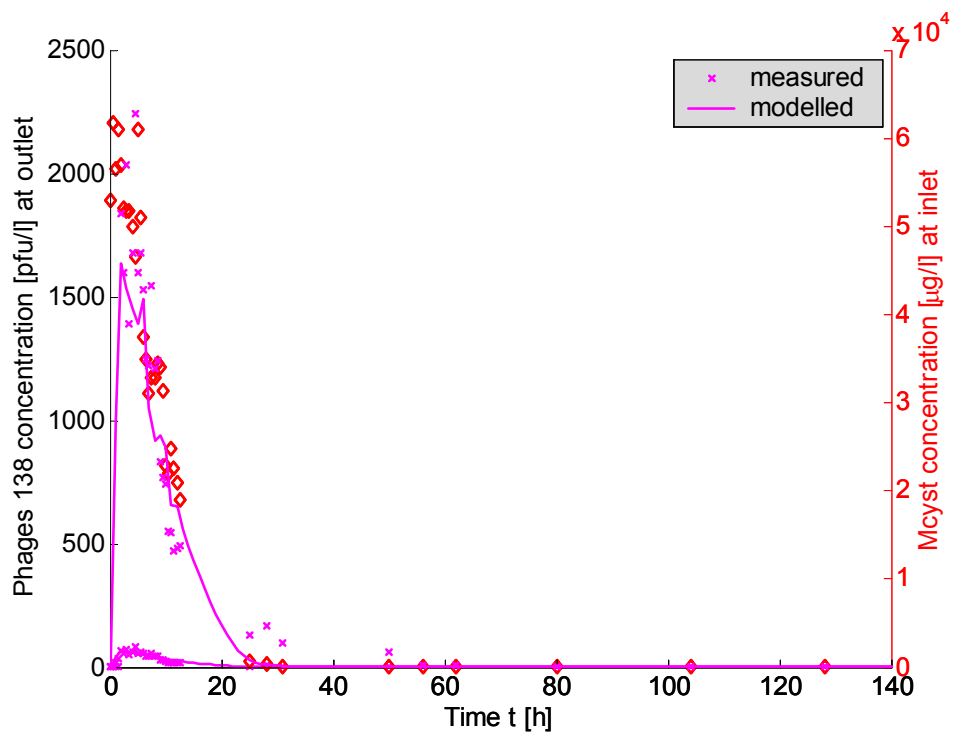
Figure 103 Phages 138, Encl 3, Flowpath: 20 cm
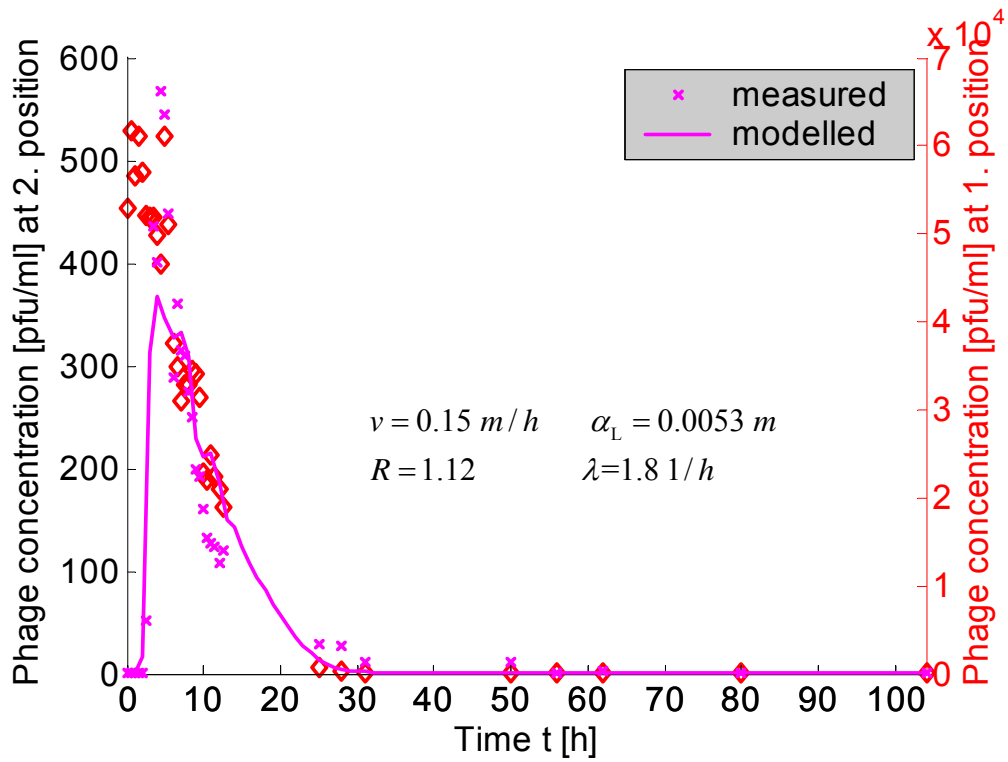
Figure 104 Phages 138, Encl 3, Flowpath: 40 cm

$v = 0.15 \ m/h \qquad \alpha_L = 0.0053 \ m$

$R = 1.12 \qquad \lambda = 1.8 \ 1/h$
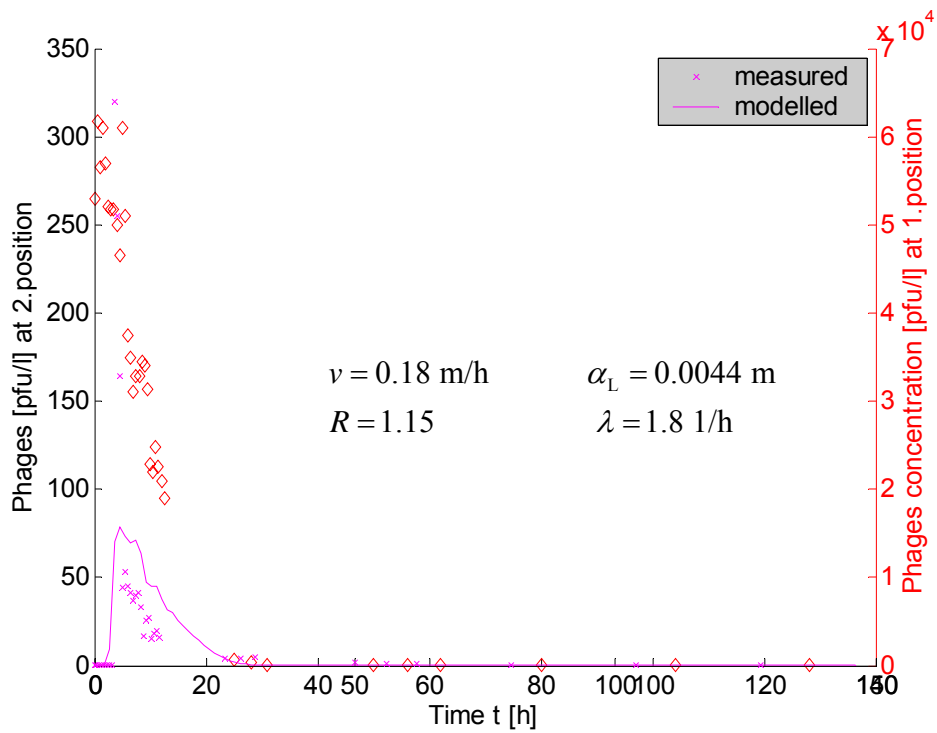
Figure 105 Phages 138, Encl 3, Flowpath: 60 cm

$v = 0.18 \ m/h \qquad \alpha_L = 0.0044 \ m$

$R = 1.15 \qquad \lambda = 1.8 \ 1/h$
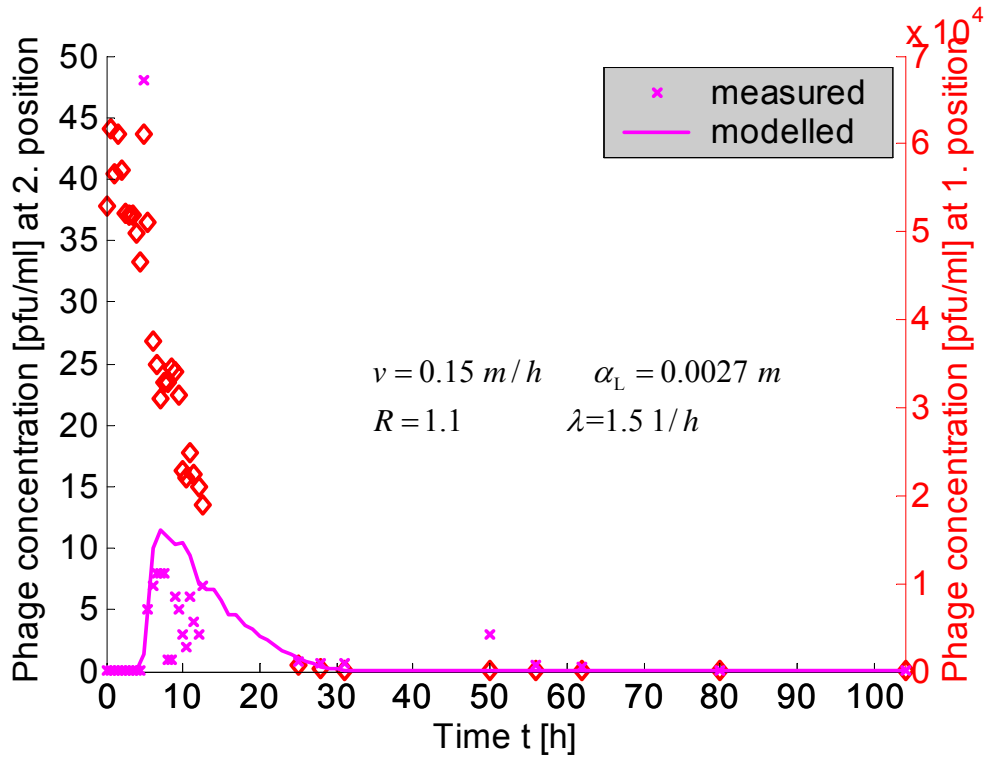
Figure 106 Phages 138, Encl 3, Flowpath: 80 cm

In the figure:

$$v = 0.15 \ m/h \qquad \alpha_L = 0.0027 \ m$$
$$R = 1.1 \qquad \lambda = 1.5 \ 1/h$$
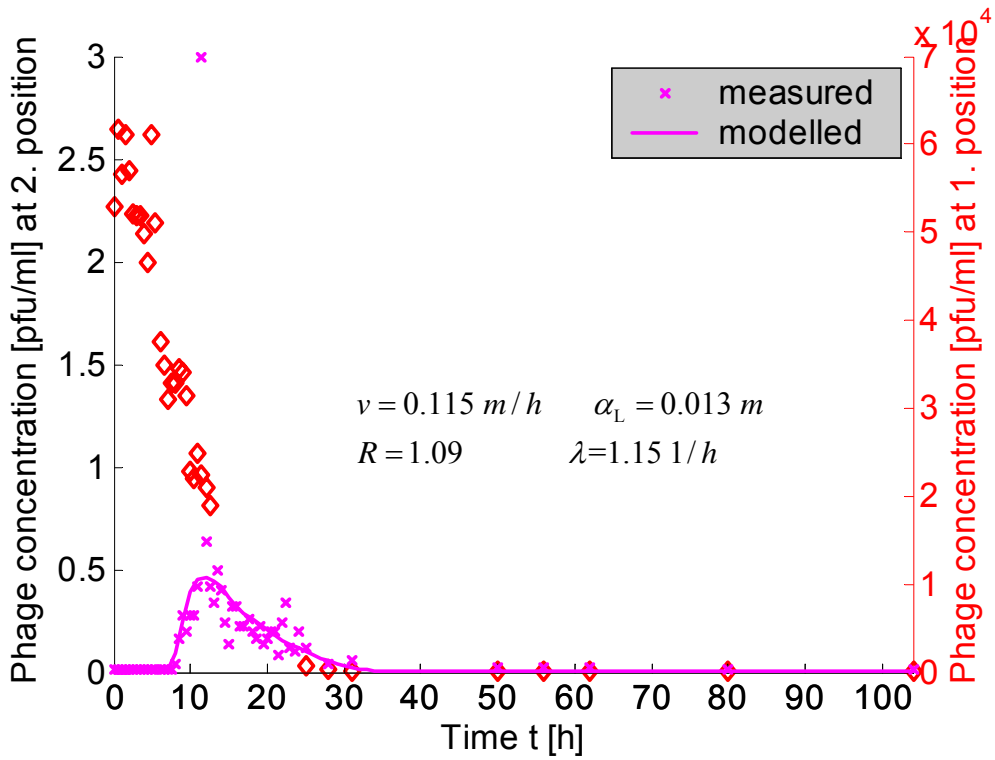
Figure 107 Phages 138, Encl 3, Flowpath: 120 cm

In the figure:

$$v = 0.115 \ m/h \qquad \alpha_L = 0.013 \ m$$
$$R = 1.09 \qquad \lambda = 1.15 \ 1/h$$

$$v = 0.17 \ m/h \qquad \alpha_{\mathrm{L}} = 0.0088 \ m$$
$$R = 2.8 \qquad \lambda = 0.44 \ 1/h$$
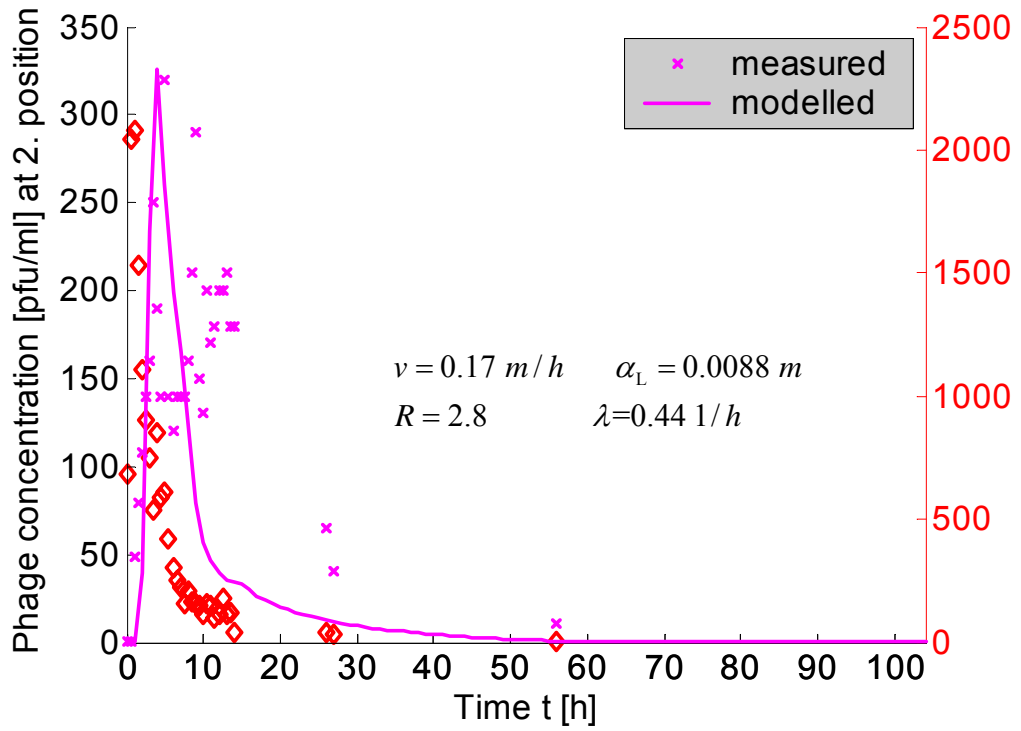
Figure 108 : Phages 241, Encl 3, Flowpath: 20 cm

$$v = 0.15 \ m/h \qquad \alpha_{\mathrm{L}} = 0.0053 \ m$$
$$R = 1.56 \qquad \lambda = 0.67 \ 1/h$$
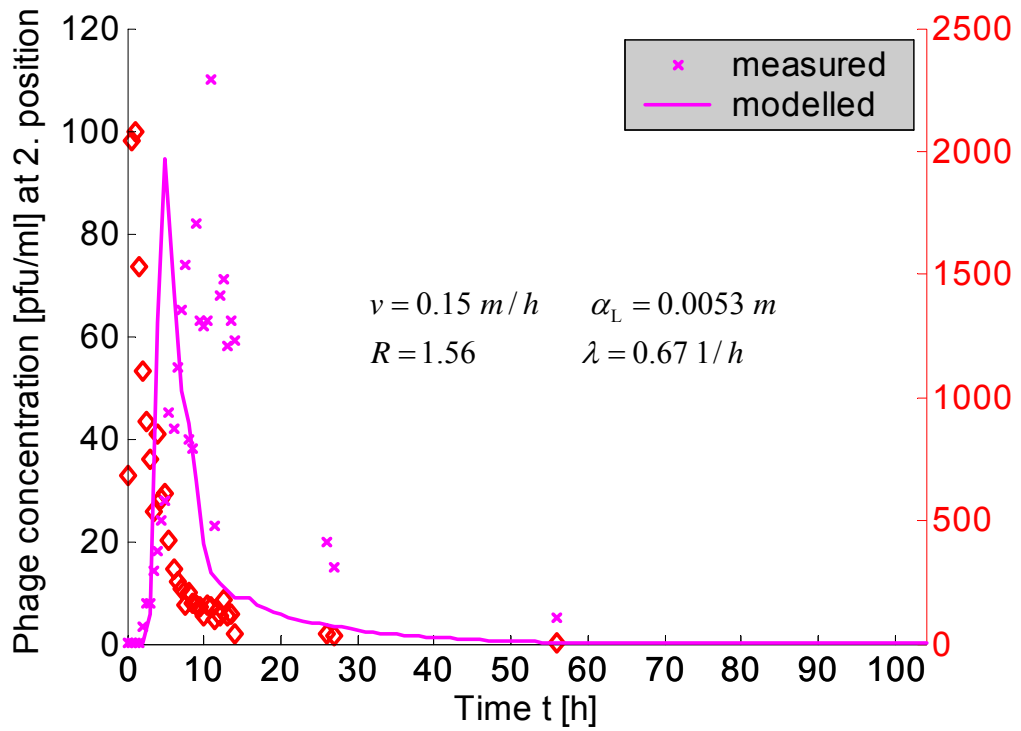
Figure 109 Phages 241, Encl 3, Flowpath: 40 cm
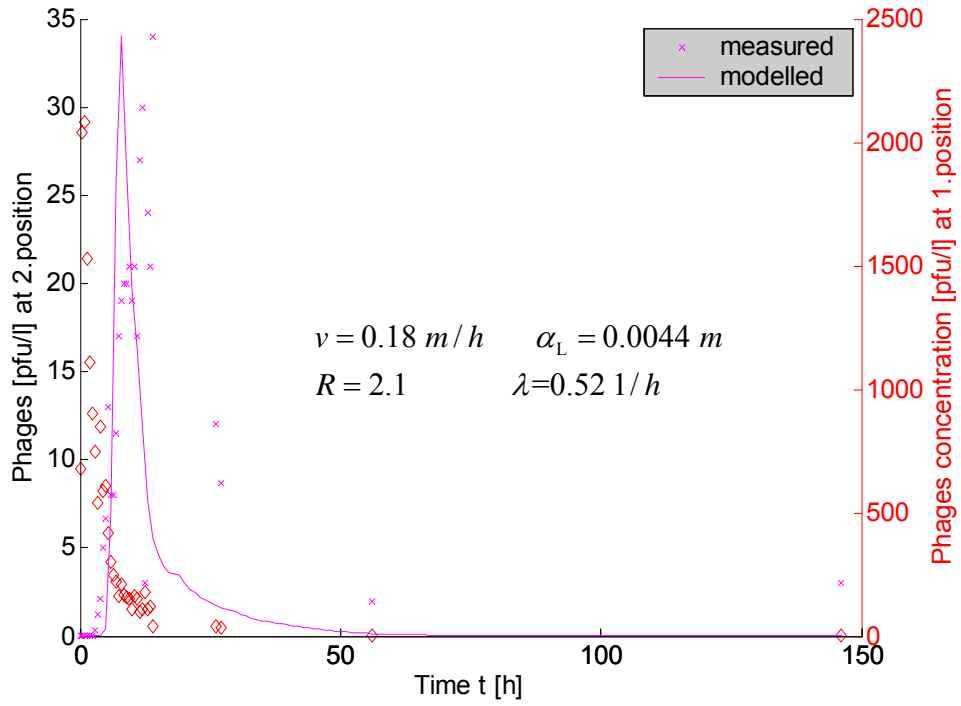
Figure 110 Phages 241, Encl 3, Flowpath: 60 cm
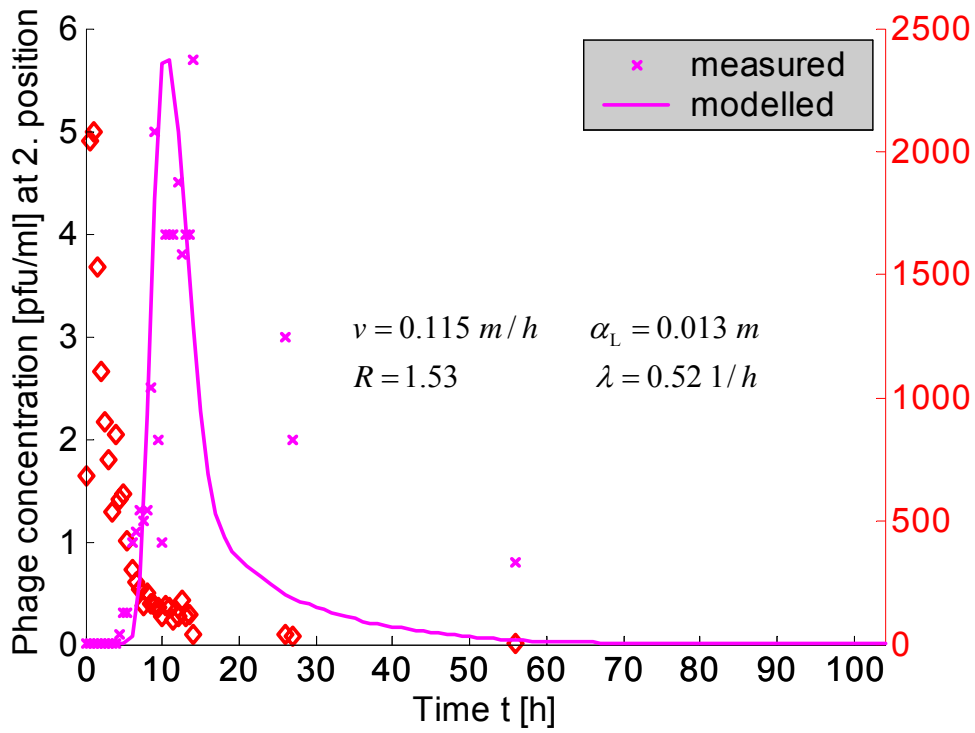
Figure 111 : Phages 241, Encl 3, Flowpath: 80 cm
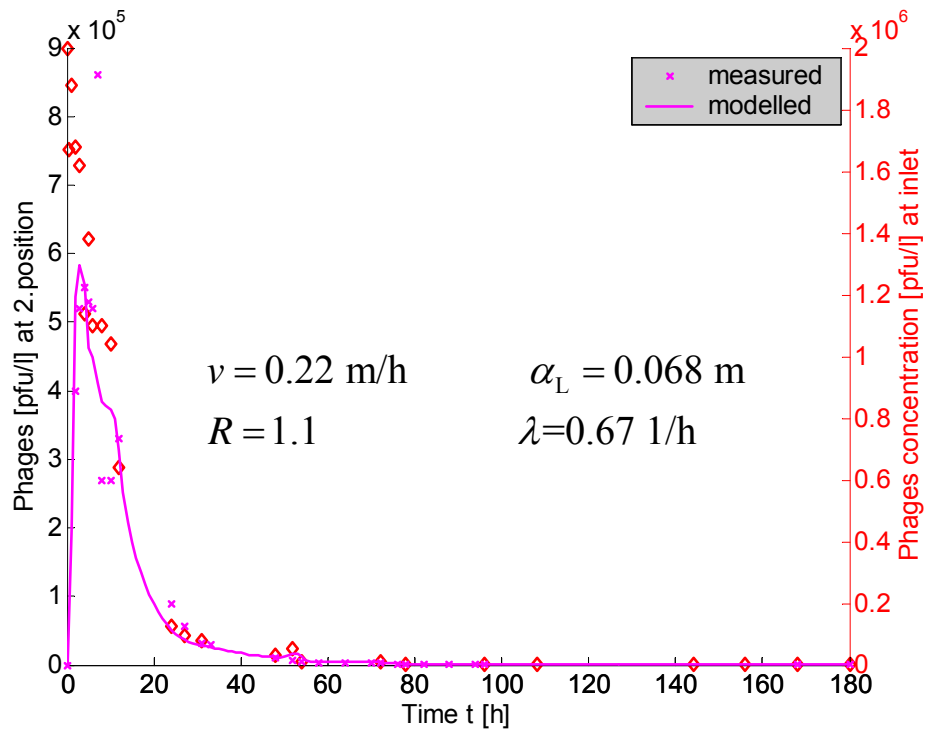
Figure 112 Phages 138, Encl 9, Flowpath: 40 cm

$v = 0.22$ m/h $\alpha_L = 0.068$ m
$R = 1.1$ $\lambda = 0.67$ 1/h
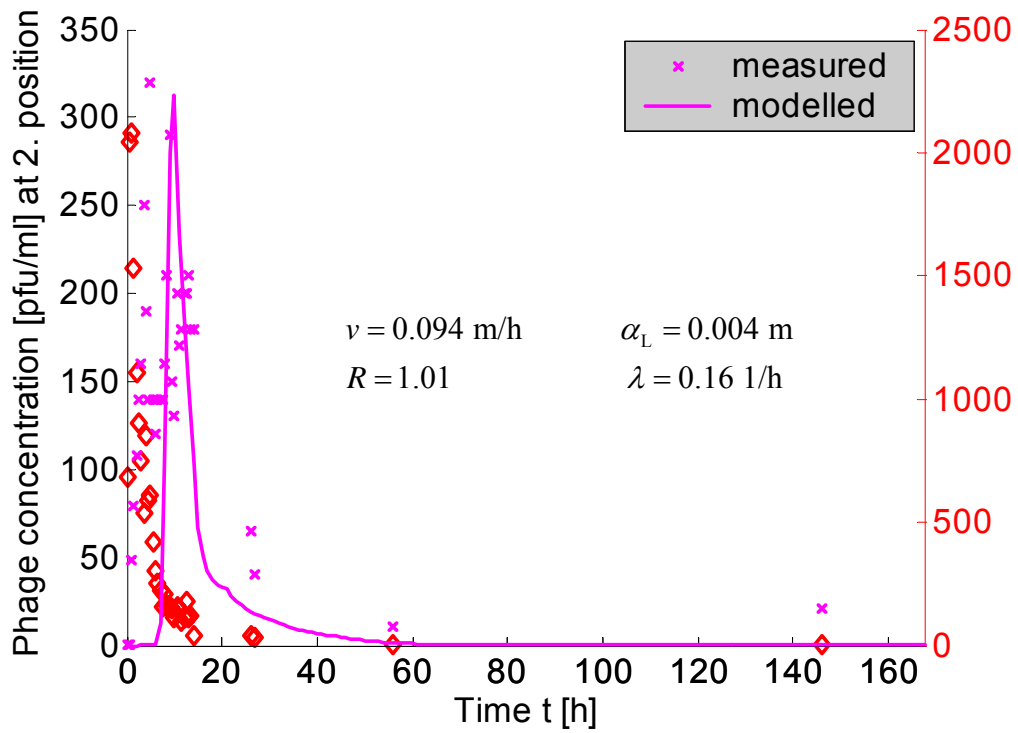
Figure 113 Phages 138, Encl 9, Flowpath: 80 cm

$v = 0.094$ m/h $\alpha_L = 0.004$ m
$R = 1.01$ $\lambda = 0.16$ 1/h
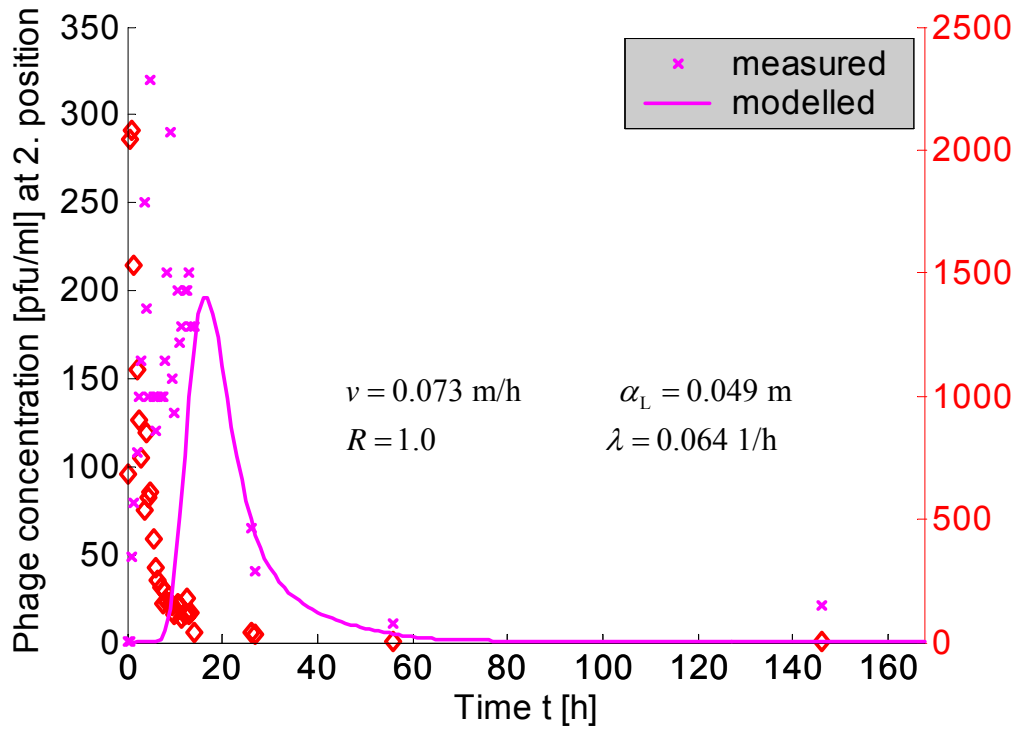
Figure 114 : Phages 138, Encl 9, Flowpath: 120 cm
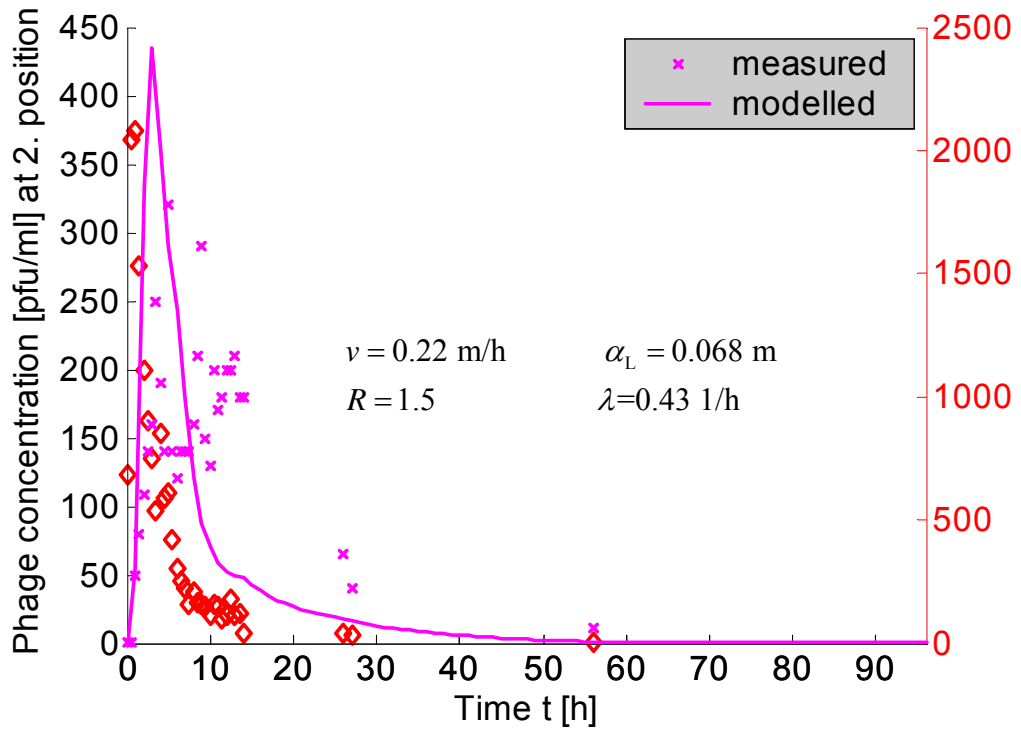
Figure 115 Phages 241, Encl 9, Flowpath: 40 cm
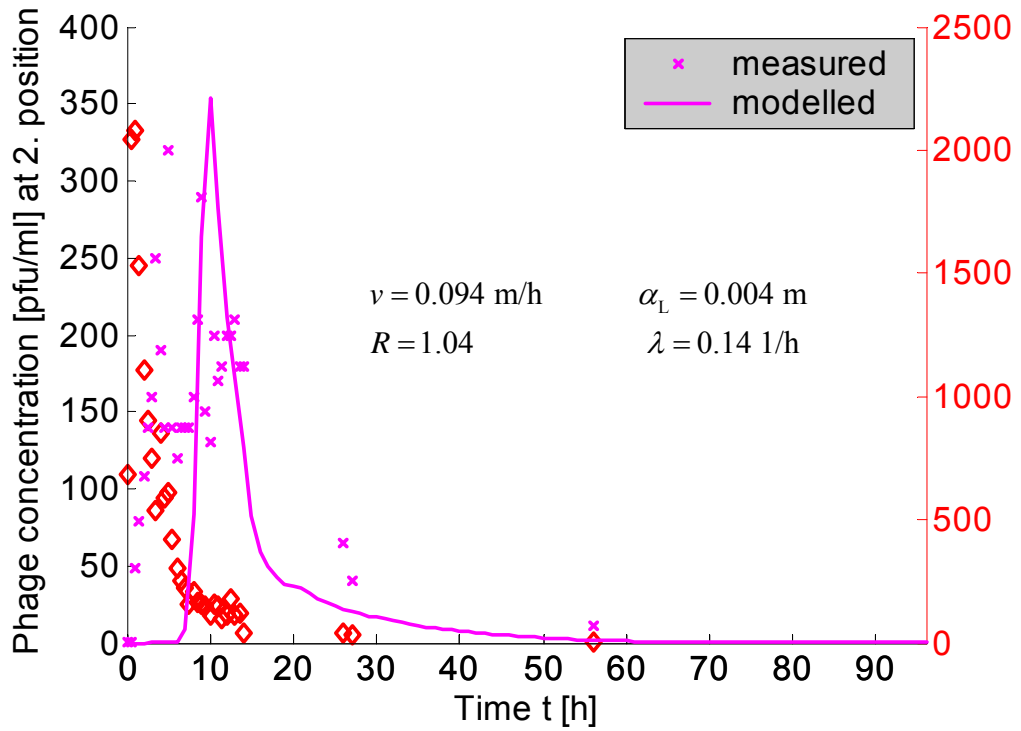
Figure 116 Phages 241, Encl 9, Flowpath: 80 cm
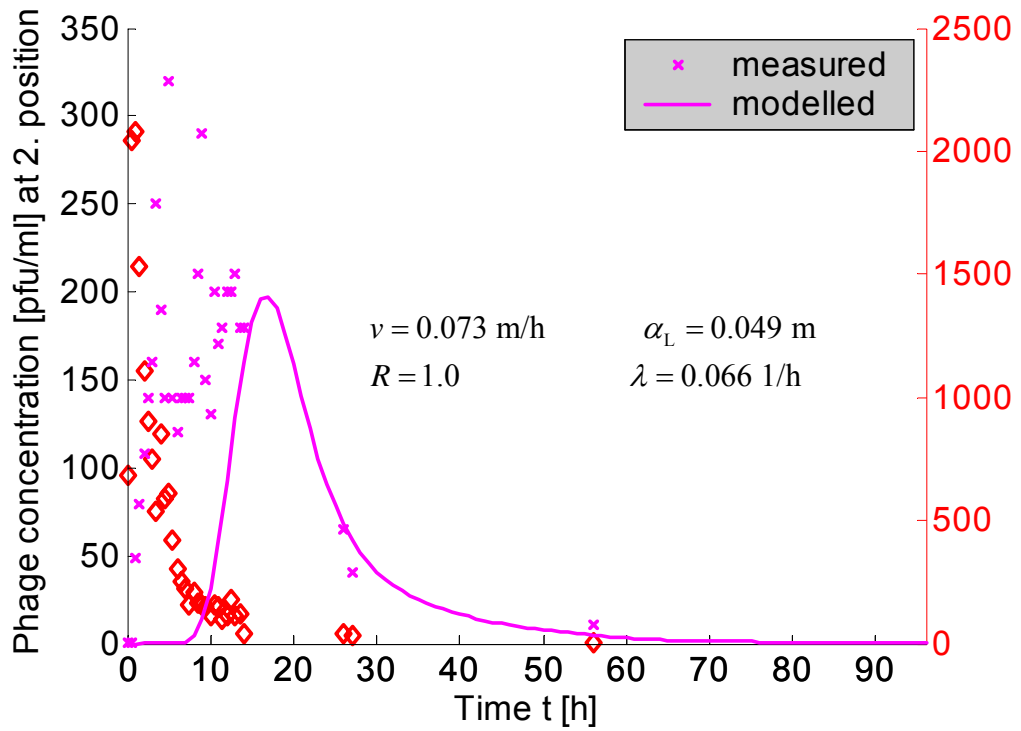
Figure 117 Phages 241, Encl 9, Flowpath: 120 cm
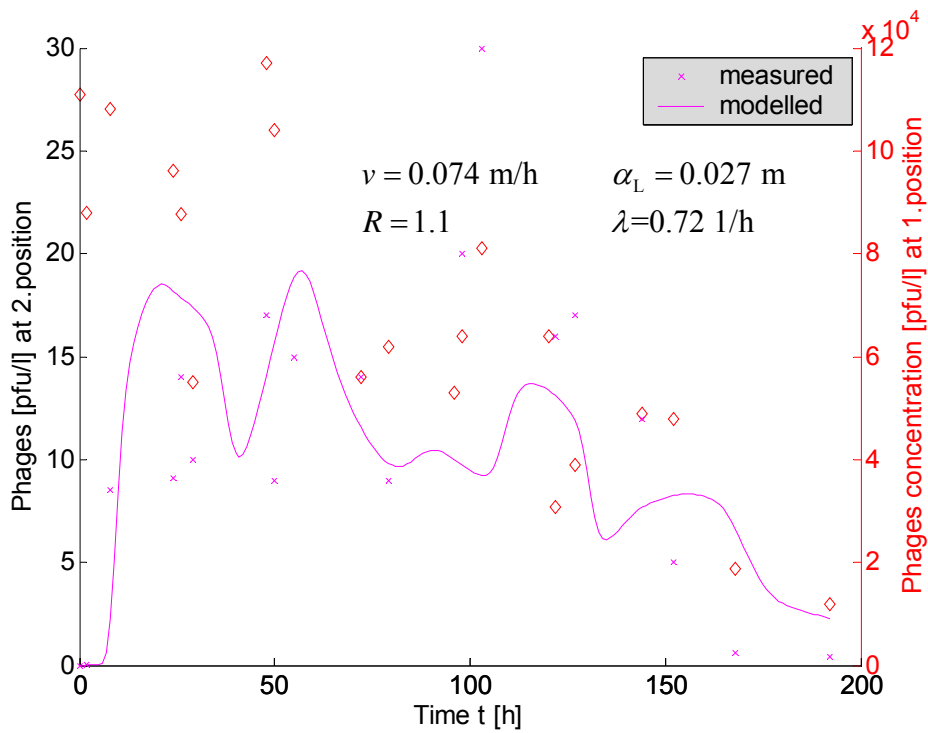
Figure 118 Phages 138, Encl 10, Flowpath: 120 cm
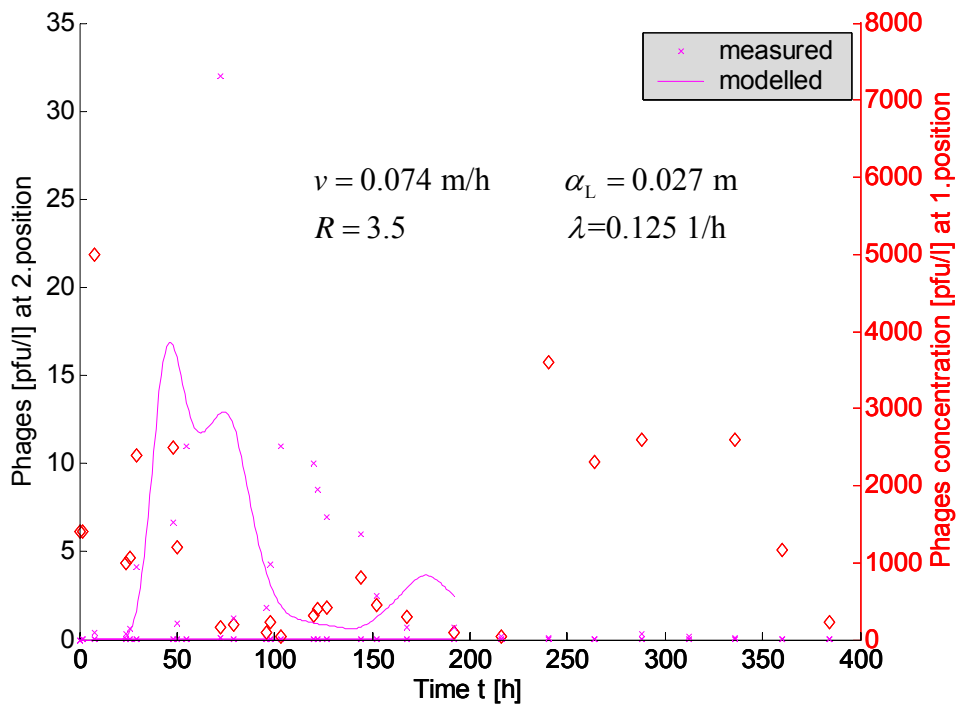
Figure 119 Phages 241, Encl 10, Flowpath: 120 cm

4.3. Summary of Results and Discussion

Results from the enclosure experiments with microcystin are summarized in Table 14. Retardations and degradation rates are listed for the experiments E2 and E3 and for the different spatial intervals along the flow path. Notation for intervals is adopted from the former sub-chapter.Also the last passage shows some peculiarities, maybe due to column-end-effects; note that the final part of the flow path is located in a gravel layer and the measurements were made in the outlet tube. For all experiments highest retardations and degradation rates are observed in the upper 20 cm.

Retardations and degradations show a tendency to decline along the flow paths. However outliers with respect to that rule are present in all columns.

Most peculiar is the flow path between 20 and 40 cm, with either a reduced degradation (E2), or reduced retardation (E3); a possible explanation is variable water saturation, which could be present in that horizon

Also the last passage shows some peculiarities, maybe due to column-end-effects; note that The final part of the flow path is located in a gravel layer and the measurements were made in the outlet tube.

Table 14 Estimated retardation and degradation rates from microcystin experiments

Enclosure	Retardation		Degradation [1/h]	
	E2	E3	E2	E3
1 → 2	1.97	1.76	0.74	0.54
2 → 3	1.9	1.25	0.24	0.31
3 → 4	1.0	1.36	0.75	0.19
4 → 5	1.0	1.14	0.54	0.01
5 → 6	1.58	1.3	0.07	0.07

Results for both phages and all experiments (enclosures E2, E3, E9 and E10 with phages 138 and 241) are gathered in Table 15.

The following conclusions were drawn during the column meetings:

- Retardation and deactivation rates decrease with depth in the enclosure, i.e. along the flowpath (there are few exceptions). In almost all cases the highest values for both parameters are in the uppermost 20 cm of the enclosures.
- Retardation and deactivation rates of phages 138 are smaller in enclosure E3 than in enclosure E2 (despite of beginning colmation, formation of clogging layer).
- In enclosure E3 there is almost no retardation of phages 138, whereas phages 241 are strongly retarded, in particular in the first part of the flowpath.
- In anaerobic enclosure experiment E9 both retardation and deactivation are significantly reduced in comparison to experiments E2 and E3.
- Experiment E10 concerning phages 241 stands out due to high retardation and small deactivation, whereas there are no distinctive features concerning phages 138

The change of retardation and deactivation rates along the flowpath can be explained by the presence of colloids (Holzbecher & Dizer, 2006). Depending on the conditions on the micro-scale effective parameter values, which are measured in experiments, may change along the flowpath. The increased abundance of carriers in the initial part of the flowpath may explain the observed behaviour in the enclosures.

Table 15   a: Estimated retardation and degradation rated for phages 138 experiments

Interval [cm]	Enclosure 2		Enclosure 3		Enclosure 9		Enclosure 10	
	R	λ	**R**	λ	**R**	λ	**R**	λ
0 - 20	2.1	5.5	1.08	3.25				
0 - 40	1.08	2.29	1.12	1.8	1.1	0.67		
0 - 60	1.08	1.5	1.15	1.8				
0 - 80	1.09	1.6	1.1	1.5	1.01	0.16		
0 - 120	1.05	1.2	1.09	1.15	1.0	0.064	1.1	0.72

b: Estimated retardation and degradation rated for phages 241 experiments

Interval [cm]	Enclosure 2		Enclosure 3		Enclosure 9		Enclosure 10	
	R	λ	**R**	λ	**R**	λ	**R**	λ
0 - 20	1.5	2.35	2.8	0.44				
0 - 40	1.15	1.6	1.56	0.67	1.5	0.43		
0 - 60	1.1	1.1	2.1	0.52				
0 - 80	1.08	1.2	1.53	0.52	1.04	0.14		
0 - 120					1.0	0.066	3.5	0.125

In Holzbecher *et al.* (2006) the following summary is given:

The parameter change within one experiment may reach a factor of 10 (for λ in E9). In most experiments, for most parameters a clear tendency is visible, but not always. Velocities decrease with increasing interval with a maximum factor of about 3 (E9). The dispersion parameter is decreasing also, if two measurements for the long intervals (from 0-80 cm for E2 and E9, and 0-120 cm for E2 and E3) are taken as outliers. Retardations mostly exceed 1 only marginally and maximum value is approximately 2 (E2). There is a slight tendency to decreasing sorption with longer spatial interval. Degradation rates are clearly decreasing with increasing interval where λ values are growing.

The results from the model with constant parameters clearly show that parameters are not constant. Otherwise the values, obtained for one experiment, should fluctuate around a mean value. Instead most parameters show a tendency within each experiment, as described. The parameters are surely not constant within the enclosures and the following conclusions are drawn:

An influence of the clogging layer could not be confirmed in the enclosure experiments. Temperature effects could be detected indirectly, as comparable experiments performed under different seasonal conditions showed different results: the deactivation of the phages increases with increasing temperature.

Redox conditions could be expected to play an important role as degradation / deactivation processes as well as sorption processes are often biologically mediated. The presented enclosure experiments show significantly different behaviour of the studied phages under aerobic and anaerobic conditions. It can not be excluded that some other conditions could be

responsible for the observed behaviour, but the redox state seems to be most pronounced difference (E9 in comparison to other experiments). The results confirm the message of Tufenkji et al. (2002) that redox processes are relevant for bank filtration systems. Similarly the migration of heavy metals or other problem substances may also be influenced by redox conditions, if the substance participates in microbial mediated reactions...

Redox dependencies, determined in controlled laboratory or enclosure experiments, can be used for modelling field situations with spatially or temporally changing redox conditions. A transport model, based on differential equations (1) and (2) with variable degradation and retardation factors, has to be complemented by a model of redox zones. Examples for redox zone modeling were presented by Hunter et al. (1998) or Holzbecher and Horner (2003). In that way degradation and sorption of harmful substances can be embedded in biogeochemical cycles, if necessary.

4.4. References

MATLAB® Version 6.5, Release 13 (2002). The MathWorks, Inc., 3 Apple Hill Drive, Natrick, MA 01760-2098, USA

Nützmann G., Holzbecher E., Strahl G., Wiese B., Licht E., Knappe A. (2006) Visual CXTFIT – a user-friendly simulation tool for modelling one-dimensional transport, sorption and degradation processes during bank filtration, Proceedings ISMAR 2005

Holzbecher E., (2005) Inversion of temperature time series from near-surface porous sediments, *Journal of Geophysics and Engineering*, Vol. 2, 343-348

Holzbecher E., Dizer H. (2006) Facilitated and retarded transport and degradation in porous media due to carriers, *Colloids and Surfaces A: Physicochemical and Engeering Aspects* (to appear)

Holzbecher E., Dizer H., Grützmacher G., Lopez-Pila J., Nützmann G., The influence of redox conditions on phage transport – enclosure experiments and modelling, *Environmental Engineering Science* (to appear)

Holzbecher E., Horner Ch. (2003). A reactive transport model for redox components. In: H.D. Schulz and Hadeler A., Eds., *Geochemical Processes in Soil and Groundwater*, Proceedings GeoProc2002, Wiley, Chichester, pp. 414-434.

Hunter K.S., Wang Y., van Cappellen P. (1998). Kinetic modeling of microbially-driven redox chemistry of subsurface environments: coupling transport, microbial metabolism and geochemistry. *J. of Hydrol*., Vol. 209, 53-80

Toride N., Leij F.J., van Genuchten M. Th., The CXTFIT code for estimating transport parameters from laboratory or field tracer experiments, U.S. Salinity Lab., Agric. Res. Service, US Dep. of Agric., Research Report No. 137, Riverside (CA), 1995

Tufenkji N., Ryan J.N., Elimemech M. (2002) Bank Filtration, Environm. Science & Techn., Vol. 36, 423A

5. ELEMENTS OF A MANAGEMENT MODEL

5.1. Overview

The following partial tasks were performed:

1. Implementation of a simulator for the evaluation of the hydraulics of generic bank-filtration situations

2. Partial implementation of a simulator for the evaluation of the hydraulics of specific bank filtration facilities

3. Set-up of a flow and transport model to identify increased concentrations in pumped water

The first two tasks were performed using MATLAB; the model in the third task was set up using FEMLAB. The product of the first task 'The NASRI Bank Filtration Simulator' was presented during the ISMAR 2005 conference, June 2005 in Berlin, Germany. The second task is an extension of the first task, which could not be completed within the NASRI project. The results of the third part were summarized in a manuscript, which is submitted for publication (Holzbecher, 2005).

5.2. The NASRI Bank Filtration Simulator

The product was developed in several steps using MATLAB, starting with version 1.1. The version 1.3 was presented at the ISMAR2005 conference; here the slightly extended version 1.3a is presented.

The purpose of the software is the evaluation of generic situations of bank filtration facilities. The user has to input basic characteristics of the aquifer (thickness, hydraulic conductivity, base flow and reference head value at the bank), of the bank (straight horizontal line or straight lines, meeting at an angle of 90°, clogging parameter), at of the well gallery (position and pumping rates of single wells). The user may also specify the spatial extension of the model region and the grid spacing, used for graphical output. Moreover several options concerning the graphical output can be specified: there are options to visualize head contours, streamlines, flowpaths and/or velocity arrow fields.

The graphical user interface of the NASRI Bank Filtration Simulator is depicted in **Figure 120**. After the specification of input data, computations are initiated by a click on the 'Plot' button. The variables of the flow field are calculated at the grid points and visualized at the graphic

panel. Moreover the share of bank filtrate in pumped water is computed and shown in the corresponding output field. After the plot the user may alter input values in the graphical user interface and perform new computations using the 'Plot' button again. The software is equipped with a help-system, which enables even novices to explore the program.
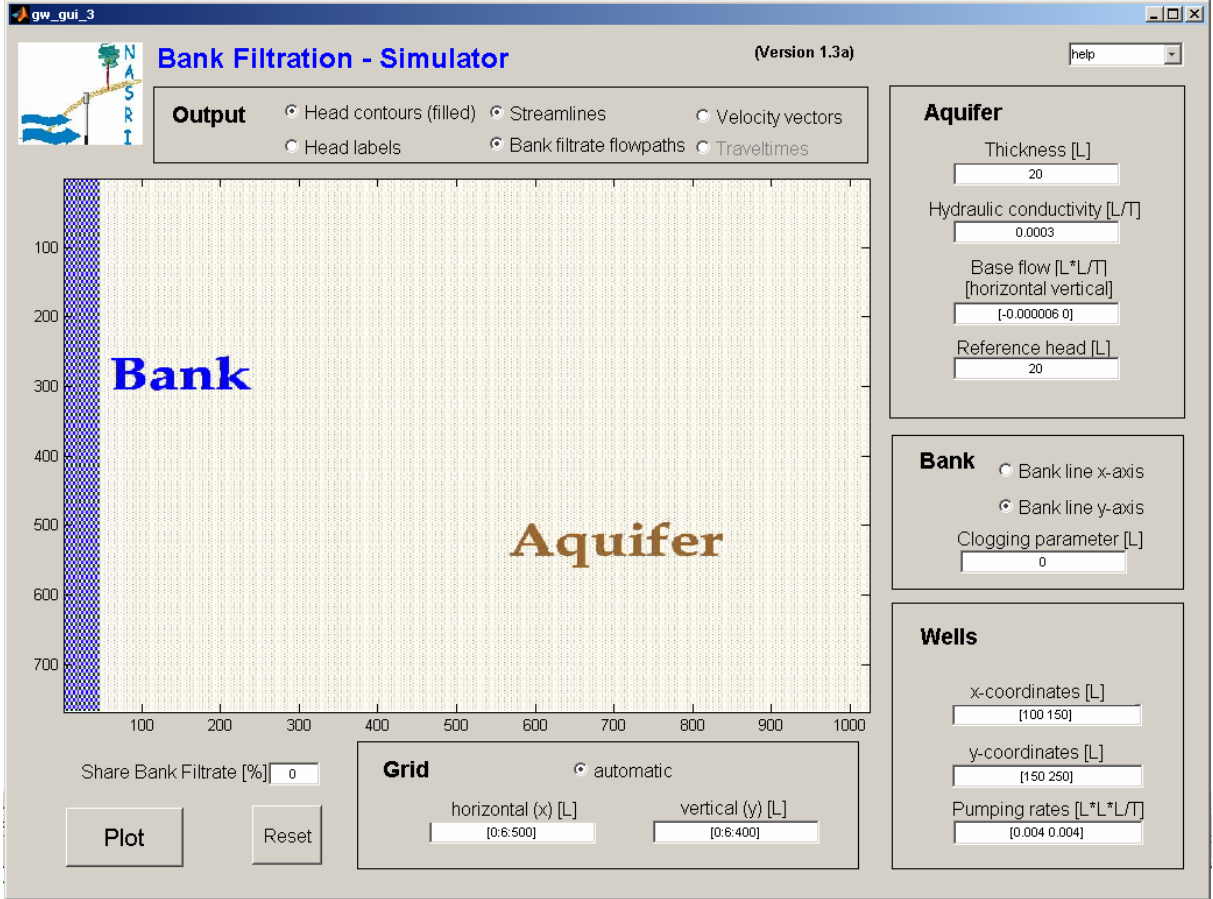
Figure 120 Graphical User Interface for the NASRI Bank Filtration Simulator, initial window
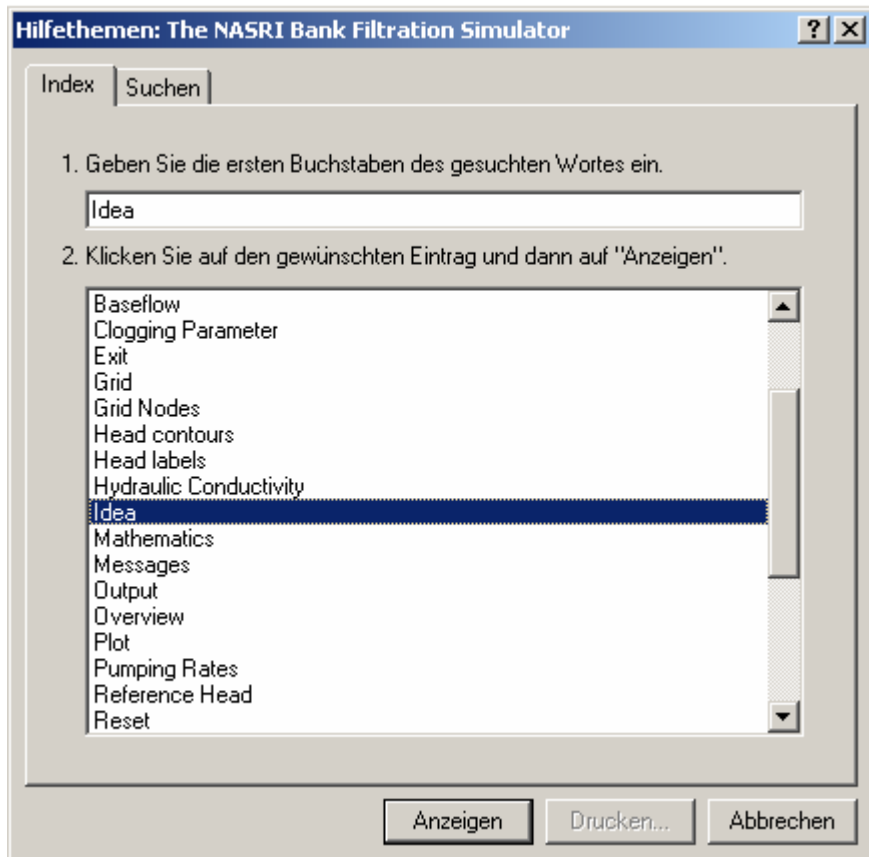
Figure 121 Keyword selection in the Help system of the simulator software

The user may choose from several keywords, for which information are given (Figure 121). In the following some excerpts from the 'Help'-system are given.

The idea of the NASRI Bank Filtration Simulator is described under the 'idea' keyword:

Idea

The idea for the Bank Filtration Simulator is derived from the following task.

Task: Assume you have to design a bank filtration facility at a location, where limited information is available only. Maybe one borehole has been drilled and there are some basic geological data. How to decide about:

· positions of wells

· distance between bank and wells

· distance between wells

· pumping rates

· ...

The program may hopefully provide some useful information in such a situation.
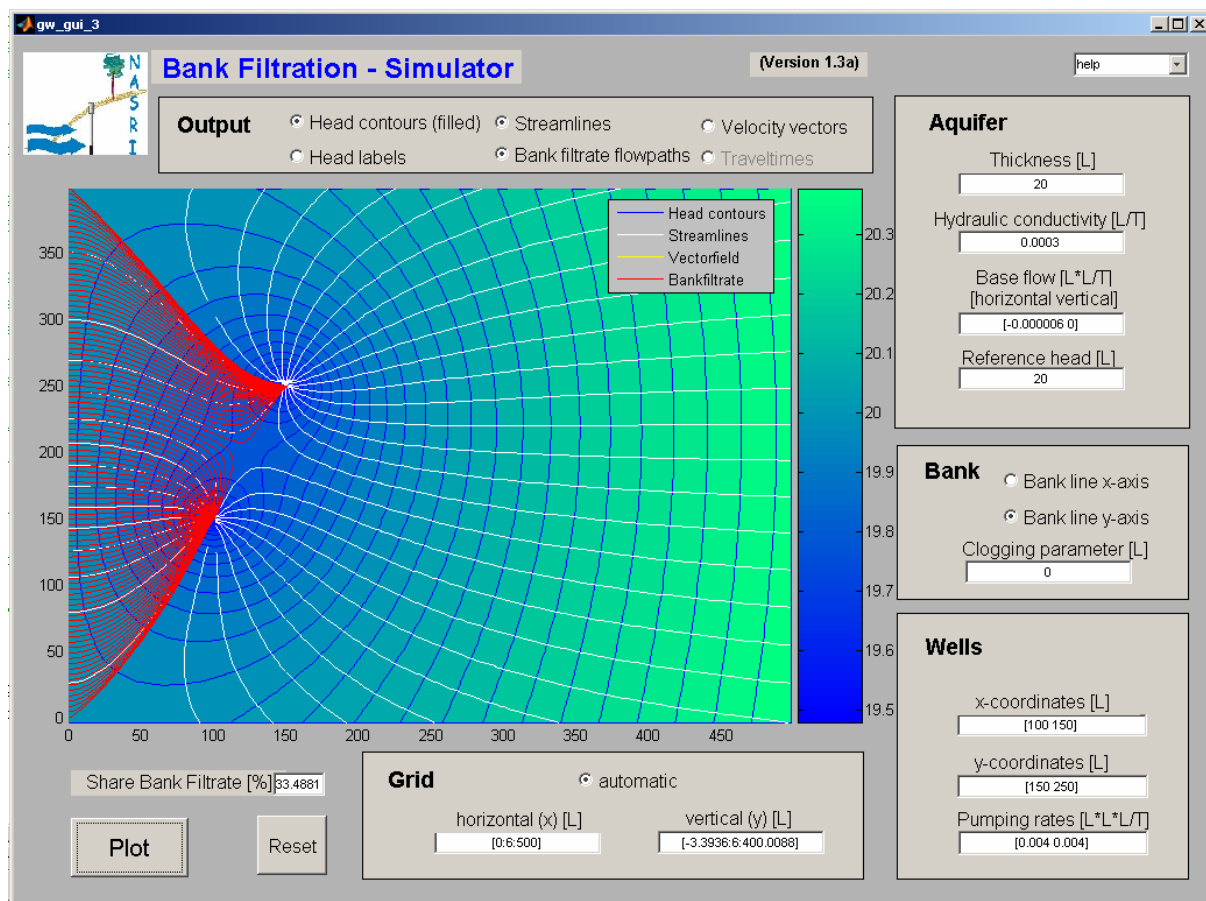
Figure 122   Graphical User Interface for the NASRI Bank Filtration Simulator with output for default settings

The output for the default settings of the program is shown in Figure 122. The distribution of piezometric head in the model region is shown by blue contours and a green-blue fill pattern. Bank filtrate flowpaths, entering from the bank boundary on the left side of the panel are shown in red. A streamline pattern for the entire model region is depicted by white lines.

The vertical extension of the aquifer, represented in the graphic panel, is calculated automatically for the output, shown in Figure 122. The outer-most positions, where surface water enters the aquifer, are computed by the software, which is explained in more detail under the 'automatic gridding' keyword of the help system:

Automatic Gridding

Automatic gridding can be chosen by the user under the grid header. If automatic gridding is active, the grid spacing and extension of the grid along the bank is selected automatically. The region, represented in the graphical output window, is extended to capture the entire region of bank filtration.

Note: Automatic gridding is performed for the coordinate axes only, which are banklines. The scales in vertical and horizontal direction may become quite different. If that is not wished by the user, the coordinate scale can be adjusted manually after the automatic gridding run in the grid block of the graphical user interface.

Note: Automatic gridding is performed only, when there is a change between groundwater outflow and bank filtrate inflow on the bank. In situations, where there is bank filtrate only, either flowing to the wells or migrating further in the aquifer, the automatic gridding is not performed. Then the former limits of the graphics on the display remain unchanged.

The white lines illustrate the flow field not only by streamlines, but by streamtubes, as explained under the 'streamlines' keyword:

Streamlines

Streamlines provide a lot of information concerning the flow field. A pattern of streamlines for the situation, selected by the user, is given in the graphical output, after pressing the 'Plot' button. If the streamline option was selected, a pattern of white lines is shown on the display. The flow of a water particle can be envisaged by following the streamlines. Moreover the strength of the flow at different parts of the figure, can be compared by the fact that between neighboured streamlines there is the same amount of flow everywhere. There are higher velocities, where streamlines are near to each other. Velocities are low, where there is a wide space between streamlines.

Spacing of streamfunction is chosen as the 20s part of the pumping rate of well number 1, if that is non-zero.

Method: Streamlines are calculated as contours of the streamfunction (see mathematics).

Note: The streamline figure depicts straight lines from the well positions to the left towards the y-axis. These are not streamlines, but by-effects of the analytical element method, as the complex logarithm is not a unique function in the complex plane. Details are found under mathematics.

In version 3.a the straight line plotting is circumvented!

Default: on

Aside from graphical output, after plotting one numerical value is presented on the display: that is the part of bank filtration in pumped water for the specified set-up. It is explained in the help system under the 'share of bank filtration' keyword:

Share of Bank Filtration

The share of bank filtration in pumped water is calculated by the Bank Filtration Simulator after pressing the plot button. The ratio of bank filtrate is valid for the pumping of the entire set-up, and does not distinguish between single wells.

Note: If there is no baseflow across a bankline, either on the x-axis or on the y-axis, bank filtrate enters along the entire bank line (theoretically only of course). In that case the share of bank filtrate in pumped water is 100%.

Unit: -

For the default set-up bank filtration contributes to pumped water with a share of 1/3, as shown in Figure 122.

Using the NASRI Bank Filtration Simulator the user has the option to choose between three different options concerning the bank, as described in the help system:

Bank

The bank is assumed to be a straight line or the combination of straight lines. The optional cases are:

·   the bank is identical with the x-axis
·   the bank is identical with the y-axis
·   the bank is located along x- and y-axis

Moreover the effect of a clogging layer can be taken into account, by choosing a clogging parameter.

The point is illustrated under the help topic 'bank line':

Bank Line

In the NASRI Bank Filtration Simulator the bank line can be either along the x-axis, the y-axis or along both:

The user can choose between these alternatives, using two checkboxes under 'bank' header.

An example calculated with the third option, is given in Figure 123. Bank filtration in situations with general angles is described in detail by Holzbecher (1996).
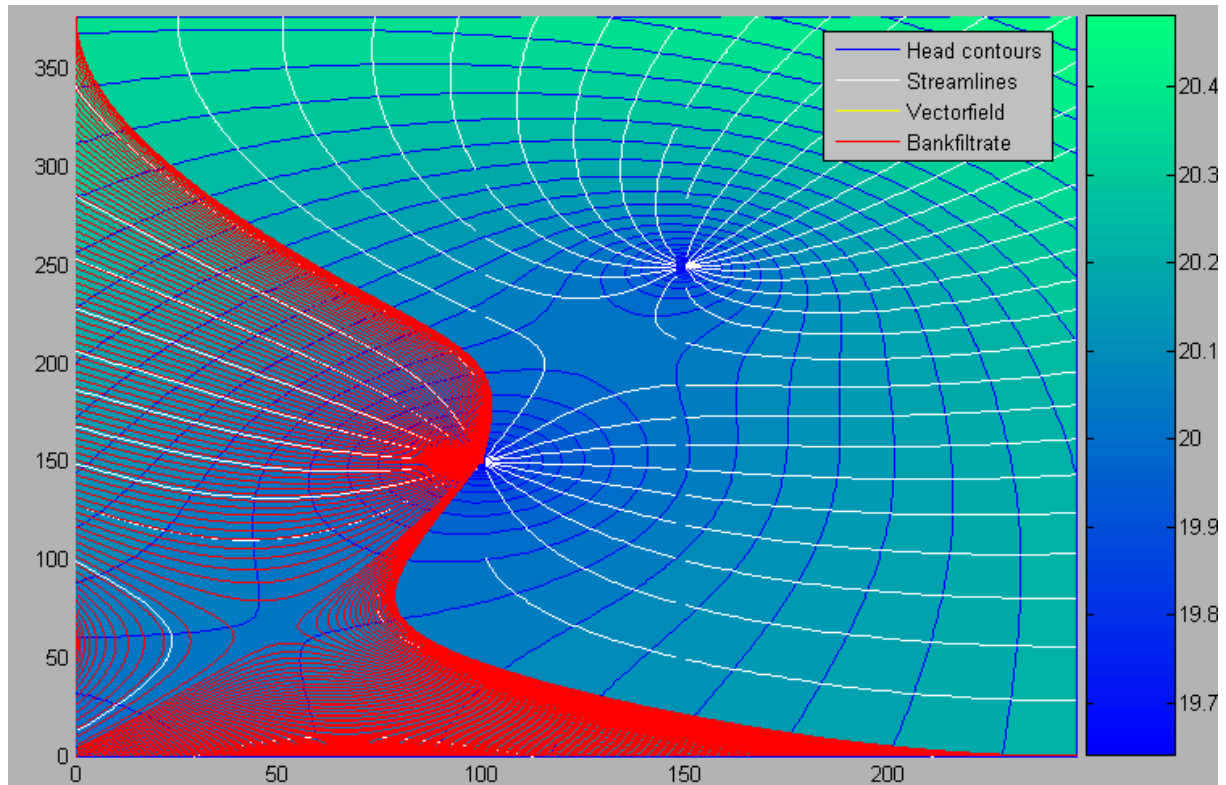
Figure 123   Example output for two wells and two banks, meeting by an angle of 90°

The user can influence bank filtration visualisation by changing the grid nodes manually, as explained in the help system under keywords 'grid nodes' and 'bank filtration flowpaths':

Grid Nodes

A rectangular grid is specified by the two vectors for x- and y-coordinates of the grid nodes. These are input parameters for the user to be specified under the grid header. Concerning the choice of the units see remarks given in aquifer.

Both coordinates have to be given in two edit boxes in [ ]-brackets. It is convenient to use the double-dot option for equidistant grids, as shown by the following example.

Example: [0:6:400] gives 8 pumping wells, of which the two medium wells are pumping at the double rate than the outer wells.

Note 1: The user has to take care that the wells do not coincide with the grid nodes. Otherwise the program may calculate heads near to negative infinity, which may cause severe problems of the program. In any case the color bar scaling is effected and may show

an unrealistic scale. Moreover the warning about the aquifer falling dry, may appear, which may no be true in reality – the program does not consider well diameters!

Note 2: Settings in the grid node edit vectors are ignored in case of automatic gridding .

Unit: L

Default: [0:6:500] for x-coordinates, [0:6:400] for y-coordinates

A revised figure for the same situation, depicted in Figure 123, is shown in Figure 124. The grid has been extended and refined.
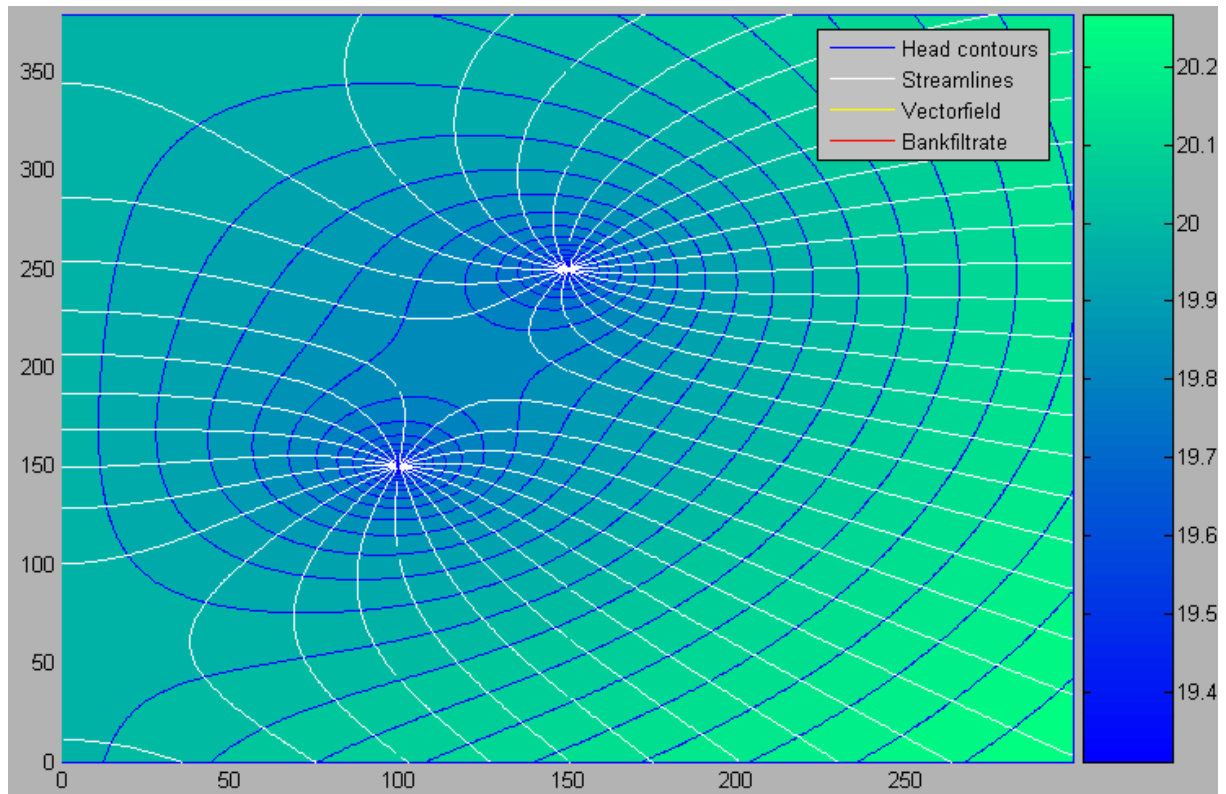
Figure 124Situation from Figure 4 with refined grid, without bank filtrate flowpaths

The bank filtrate flow paths the help system yields the following explanations:

Bank Filtrate Flowpaths

Bank filtrate flowpaths are calculated and drawn in the graphics window, if the corresponding option is set by the user. Bank filtrate flowpaths are drawn in red. Starting positions for the bank filtrate are choosen automatically along the bank lines. The calculation is based on a flowpath tracing algorithm, which works fine, if the grid spacing in x- and y-axis are identical. If spacings in both directions do not coincide, a message box appears on the screen. The user may adjust the grid spacing manually (see Grid).

Note 1: Bank filtrate flowpaths are calculated only for starting positions on the bank within the choosen spatial extension of the graphical output. Thus not the entire region of bank filtrate may be captured, if the minimum or maximum value of the grid is not appropriately selected. If the user selects automatic Gridding, the window is chosen wide enough automatically.

An exception is the situation, in which the bank filtrate infiltrates everywhere on the axes. Such a situation is given, when there is no baseflow across a bank line. In that case the share of bank filtrate in pumped water is 100%.

Note 2: When bank filtrate flowpaths are plotted, there is no distinction between bank filtrate flowing towards the wells or migrating further within the aquifer. Such a situation is given for baseflow from the bank into the aquifer.

Note 3: Flowpaths coincide with streamlines, if the flowpath start position coincides with a streamline passing through the bank.

Default: on

Also the mathematical background of the computations is explained in the help system:

Mathematics

The mathematical calculations are based on the analytical element method. A elaborate description of the method is given by Strack (1989). The (x,y)-plane is identified with the complex z-plane by z=x+i*y. The following formulae are used for the calculation.

Formulae:

The complex potential for baseflow:

$$\Phi(z) = -Q_0 \overline{z}$$

The complex potential for a well:

$$\Phi(z) = \frac{Q_{well}}{2\pi} \ln(z - z_{well})$$

The complex potential for an image well across the x-axis:

$$\Phi(z) = -\frac{Q_{well}}{2\pi} \ln(z - \overline{z}_{well})$$

The complex potential for the clogging layer on the x-axis (van der Veer, 1993):

$$\Phi(z) = -\frac{Q_{well}}{\pi} \exp\left(\frac{i}{kc}(z + \overline{z}_{well})\right) E_1\left(\frac{i}{kc}(z + \overline{z}_{well})\right)$$

Real potential:

$$\varphi(z) = \operatorname{Re}(\Phi(z))$$

Streamfunction:

$$\Psi(z) = \operatorname{Im}(\Phi(z))$$

Hydraulic head:

$$h(z) = \begin{cases} H/2 + \varphi(z)/KH & \text{if confined} \\ \sqrt{2\varphi(z)/K} & \text{if unconfined} \end{cases}$$

Velocities are calculated from the real potential using Darcy's Law.

Clogging can be considered using the approach of van der Veer (1994), where a clogging parameter with the unit of a length is introduced:

Clogging Parameter

The clogging parameter is an input parameter for the user to be specified under the bank header. Concerning the choice of the units see remarks given in aquifer. For the NASRI Bank Filtration Simulator the clogging layer is assumed to be homogeneous and constant.

The clogging parameter is the product of clogging layer thickness and relative impermeability compared with the aquifer. If there is no clogging layer, the value of the clogging parameter is zero.

Example: If the clogging layer is 1 meter thick and 100 times less permeable than the aquifer, the clogging parameter is 100 in the MKS physical unit system.

Unit: L

Default: 0

The clogging layer is thus identified with the semi-permeable layer in the original publication. Another method, which was examined for implementation, was proposed by Anderson (2000). However, finally the approach of van der Veer was given the preference because of the isotropy of the less permeable layer: in Anderson's method the clogging layer has a higher conductivity tangential to the bank. When in the previous examples a clogging layer is considered, the following figure results:
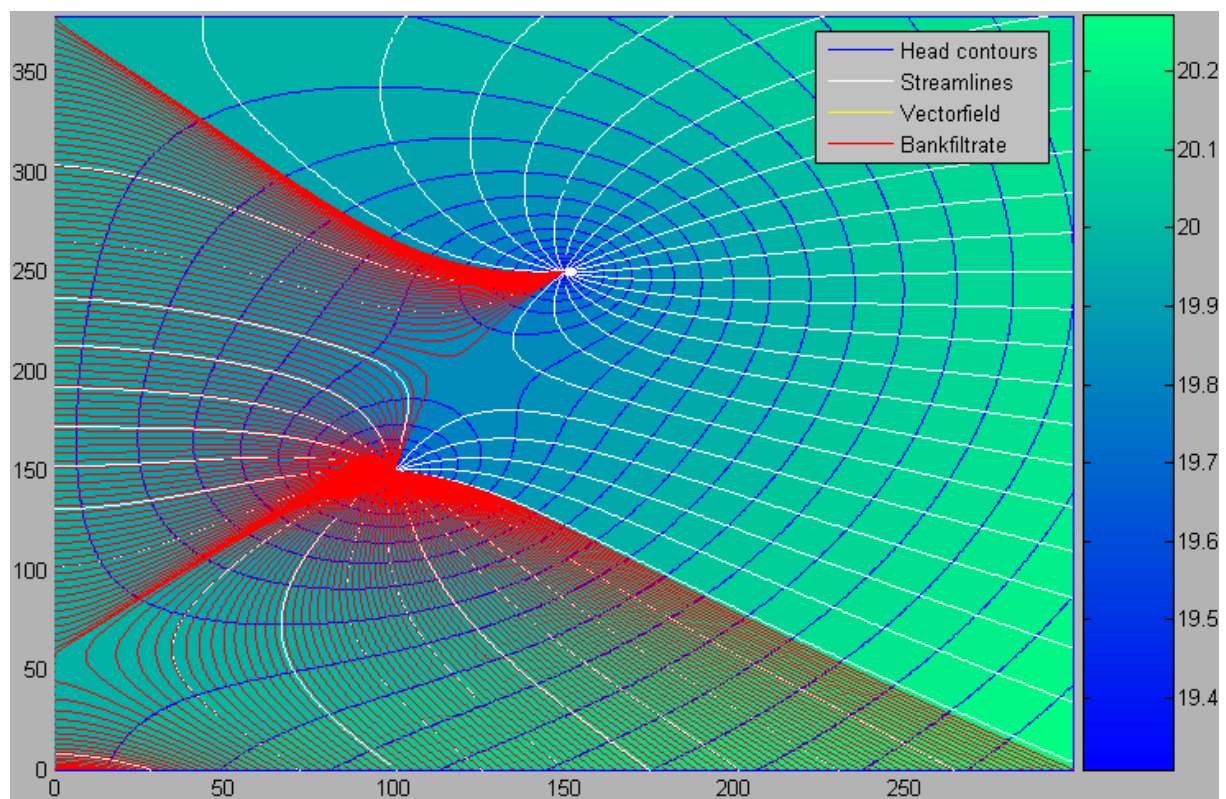
Figure 125 The two-well gallery from the previous figures under a consideration of a clogging layer with a clogging parameter of 10 m.

The menu entry 'traveltimes' is already present in the graphical user interface, but is not yet tested sufficiently, to become enabled.

5.3. *Modified Version of the NASRI Bank Filtration Simulator*

The development of a modified version of the NASRI Bank Filtration Simulator, which is designed for special set-ups, was started. In contrast to the former software specific settings of a given facility can be considered. An example, concerning Lake Wannsee gallery, is given in Figure 126.
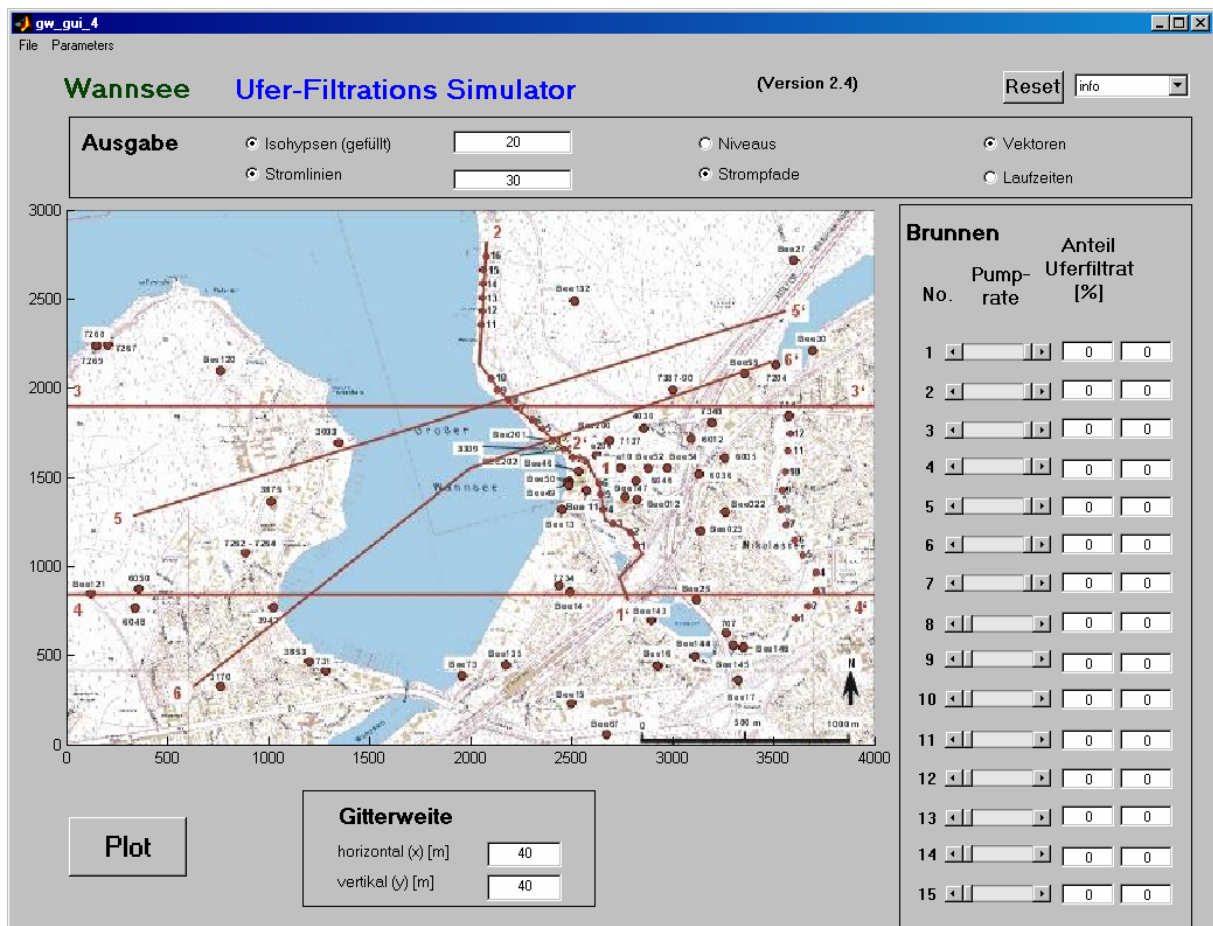
Figure 126   Modified version of the NASRIBank Filtration Simulator, as a blueprint for a management model for a specific facility, here the Lake Wannsee gallery in Berlin

The site-specific settings are specified in an initiation run. Based on a map in the background the user has to follow the bank-line by mouse clicks. In hat way a polygon is specified, which is an approximation of the bank-line and can be used for bank filtration calculations. Also wells are entered into the program by mouse clicks on the graphic panel.

In addition aquifer properties, bank characteristics, well locations and pumping rates are to be entered, as in the NASRI Bank Filtration Simulator. These values are site-specific, but can also be altered in a usual run of the management model by using the menu, as shown in Figure 127

The graphical user interface is designed to switch wells on and off and to explore the effects of various well operation schemes. The user may also change various output options as in the worked out bank filtration simulator, and to change the grid resolution. The corresponding input fields can be recognized in Figure 8. In the shown example, a maximum of 15 operating wells can be modelled.

An output field is added for each well, in which the share of bank filtrate in the well is to be shown. In addition the flow field is to be visualized in the graphic panel, as described in the previous chapter and as implemented already in the simulator software.
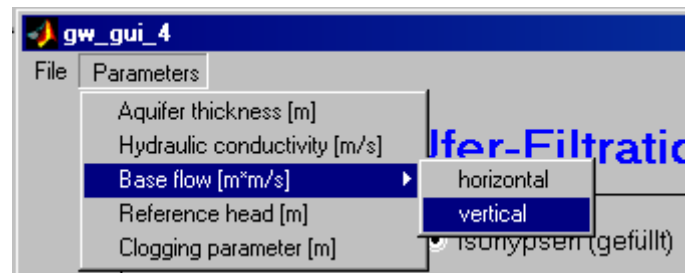
Figure 127 Menu for the site-specific version of the NASRI Bank Filtration Simulator.

The modified version of the simulator is not fully implemented, yet. Visualisation is to be improved, in order to restrict the output to regions landinward from the bank line. The calculation of the bank filtrate share on pumped water has to be implemented, too.

The site-specific version could be used for well gallery management, in order

- to visualize bank filtration flow towards wells

- to explore the effects of certain well operation decisions

The graphical output of the software shows the reach of a well gallery, i.e. the area and the part of the bank line, which is effected by bank filtrate for a specific pumping regime. Such information can be used to select between various pumping alternatives, if some regions are to be excluded from bank filtrate flow, for example.

The share of bank filtrate in each well is an appropriate indicator for optimal pumping regimes. It could be checked, for which operation regimes the share of bank filtrate is highest, in the entire gallery or for specific wells.

5.4. *Flow and Transport Model*

A flow and transport model was set up in order to identify increased concentrations in pumped water. The underlying problem for the model set-up is: what is the minimum degradation rate, for which a certain concentration margin in pumped water is exceeded? The idea is outlined in a submitted manuscript (Holzbecher, submitted), for which the following passages are taken. The figure numbers have been changed from the manuscript.

Along their path from the surface water body to the well, a biogeochemical substance may underlie several degradation processes. The relevant processes can be of biological, chemical, biochemical or physical nature and may depend on various conditions within the aquifer, as for example the redox state, the biogeochemistry within the pore space including the porous medium, the temperature, recharge conditions. Often the first few centimetres of the bank filtration path are crucial, where a clogging layer may have built up. Generally holds: the higher the degradation, the lower the concentration in the well, or vice versa: the lower the degradation, the higher the concentration in pumped water. There are problems with bank filtration, if the degradation of a potentially harmful substance is too low.

For both existing and projected facilities it is important to estimate the effect of natural attenuation on the concentration distribution along the flowpath of bank filtrate and on the concentration of pumped water. Pumping rates should be kept below the threshold above which tolerable concentrations of problem substances in pumped water are exceeded. In the design of a projected well or well gallery the distance between bank and well should be chosen in accordance with requirements concerning the degradation of such possible problem substances.

Currently numerous studies are being undertaken to determine degradation characteristics on the microscale. Very often such studies result in a single value for the degradation parameter of a substance. The next question is, how relevant the obtained value is for a certain bank filtration facility. The aim of this paper is to present an inexpensive method for determining a range of degradation rates that are relevant for a given bank-well constellation in the field. Experimental work should be accompanied by such a method, as otherwise the meaning of determined degradation rates for a field situation remains uncertain.

The approach presented here does not aim at prediction in terms of forecasting but a mathematical-computational method. For that reason comparison with experimental results is not intended. The simplest possible approach for degradation was chosen, as it is intended to propose the method as a supplement within experimentally oriented research. It may prevent too much effort being invested in determining degradation rates that are above the relevant (or critical) range even under most unfavourable conditions for degradation-relevant species.

In this study the simplest degradation approach with a degradation rate in a first-order law is treated throughout. However, the outlined mathematical procedure can easily be applied to more complex degradation characteristics, such as Monod-type terms. This study is based on the fact that the validity of any mathematical degradation characteristics for the entire flowpaths of bank filtrate can hardly be proved. Because of that uncertainty it is important to know which parameter range really counts. The question is about the minimum degradation rate, for which no significant breakthrough in the pumped water can be expected.

Numerical models are an appropriate and necessary tool not only for a quantitative evaluation of the effectiveness of natural attenuation processes. In the following a new approach is presented, which is easy to implement using mathematical tools for partial differential equations. Moreover the method is fast, as it solves for the steady state directly, and has small numerical errors, as it is combined with analytical solutions as far as possible.

The Modelling Concept

For many characteristic situations the flow of bank filtrate and groundwater towards wells can be computed by analytical methods. Using the analytical element method (Strack 1989, 1999) the solution for hydraulic potential φ and streamfunction Ψ is combined by superposition from basic solutions. For the following presentation the solutions for baseflow are relevant

$$\varphi(x, y) = -Q_0 x \qquad \Psi(x, y) = Q_0 y \qquad (1)$$

with baseflow discharge Q_0 ([m^2/s] in MKS units) as product of Darcy velocity and aquifer depth; and for flow towards a well:

$$\varphi(x, y) = \frac{Q_{well}}{2\pi} \text{Re}\left(\log\left(\mathbf{r} - \mathbf{r}_{well}\right)\right) \qquad \Psi(x, y) = \frac{Q_{well}}{2\pi} \text{Im}\left(\log\left(\mathbf{r} - \mathbf{r}_{well}\right)\right) \qquad (2)$$

with pumping rate Q_{well} ([m^3/s] in MKS units). The logarithm in formulae (2) is the complex logarithm, defined in the complex plane with $\mathbf{r} = x + i \cdot y$. $\mathbf{r}_{well}$ denotes the well location in the complex plane. Following the principle of superposition the distributions of baseflow and wells to potential or streamfunction have to be added. The Darcy velocity $\mathbf{v}$ can be obtained from the streamfunction Ψ or from the potential φ, using the formulae:

$$v_x = -\frac{1}{h}\frac{\partial \Psi}{\partial y} \qquad v_y = \frac{1}{h}\frac{\partial \Psi}{\partial x} \qquad \text{or} \qquad \mathbf{v} = -\frac{1}{h}\nabla\varphi \qquad (3)$$

In the vicinity of a straight isopotential boundary the method of images delivers the solution by introducing image wells. A detailed description of these methods is given by Strack (1989).

The presented method can be applied for the confined and for the unconfined aquifer, and also for situations in which the aquifer is partially confined and unconfined. The specific

situation, confined or unconfined, is taken into account when hydraulic head h is calculated from the potential φ to. Details are given in the next sub-section.

Transport, first-order degradation and equilibrium sorption are usually described by the transport equation (for example: Holzbecher, 1996):

$$\theta R \frac{\partial c}{\partial t} = \nabla \mathbf{D} \nabla c - \mathbf{v} \nabla c - \theta R \lambda c \qquad (4)$$

with dispersion tensor $\mathbf{D}$, velocity vector $\mathbf{v}$, porosity θ, retardation coefficient R and decay constant λ. In two space dimensions the dispersion tensor is given by:

$$\mathbf{D} = \begin{pmatrix} D_m + (\alpha_L v_x^2 + \alpha_T v_y^2)/v & (\alpha_L - \alpha_T) v_x v_y / v \\ (\alpha_L - \alpha_T) v_x v_y / v & D_m + (\alpha_T v_x^2 + \alpha_L v_y^2)/v \end{pmatrix} \qquad (5)$$

with diffusivity D_m, longitudinal dispersivity α_L, transversal dispersivity α_T, velocity components v_x and v_y, and $v = \sqrt{v_x^2 + v_y^2}$ (Bear, 1972). For the steady state the differential equation can be simplified to:

$$\nabla \mathbf{D} \nabla c - \mathbf{v} \nabla c - \mu c = 0 \qquad (6)$$

with a modified degradation parameter $\mu = \theta R \lambda$, which depends both on the sorption and the degradation characteristic of the component. Equation (6) is a condition for the steady state concentration distribution, which can be obtained directly for a specified set of boundary conditions (see below).

Most modelling codes are implemented for the unsteady situation, as given in equation (4), and steady state solutions can be obtained by choosing long time periods in the simulation. As the time period necessary to come close to the steady state is not known beforehand, several runs of the transient simulation are usually necessary in order to obtain the steady-state concentration distribution. Moreover, at least one additional run is necessary in order to check whether the solution shows only marginal changes for an extended time period. These complications are avoided when the steady state is sought directly from equation (6). Mathematical tools allow such a direct approach. Here the FEMLAB® code was chosen for implementation.

FEMLAB® Implementation

FEMLAB® (2004) is a multi-purpose code for simulations of multi-physics situations. Various partial differential equations can be used and coupled for various subdomains. It is possible to combine various flow regimes with transport equations with general one-way or two-way couplings. Partial differential equations can be specified explicitly by the user in coefficient or general form, or can be chosen from a list of predefined alternatives. The transport equation (4) is included as a convection-diffusion equation and can be found under the 'diffusion' topic

or under 'classical PDEs'. In FEMLAB® there is an additional alternative between 'steady-state analysis' and 'transient analysis'; only the former is relevant for the aim of this paper.

For flow towards a well, the 'Poisson equation' from the 'classical PDEs' list could be chosen in combination with a weak term under 'point settings'. However, in order to be even more precise, the analytical solution, as described above, was explicitly implemented using the 'subdomain expressions':

$$
\begin{aligned}
r_1 &= (x + x_{well})^2 + y^2 \\
r_2 &= (x - x_{well})^2 + y^2 \\
q_x &= -Q_0 + \frac{Q_{well}}{2\pi}\left(\frac{x + x_{well}}{r_1} - \frac{x - x_{well}}{r_2}\right) \\
q_y &= \frac{Q_{well}}{2\pi}\left(\frac{y}{r_1} - \frac{y}{r_2}\right) \\
\varphi &= -Q_0 x + \frac{Q_{well}}{2\pi}\log\left(\sqrt{\frac{r_1}{r_2}}\right) \\
\Psi &= Q_0 y + \frac{Q_{well}}{2\pi}\left[\tan^{-1}\left(\frac{y}{x - x_{well}}\right) - \tan^{-1}\left(\frac{y}{x + x_{well}}\right)\right]
\end{aligned}
\tag{7}
$$

The vector $\mathbf{q}=(q_x, q_y)^\top$ is the discharge vector (Strack 1989). Thus flow is explicitly given in the presented model and included in the specification of the transport model (convection-diffusion equation). Formulae for analytical solutions, as presented above, are difficult to introduce into the usual groundwater software. But they are easy to specify in general mathematical tools, such as FEMLAB®. However, for a site-specific model, including one extended well gallery or even several galleries in FEMLAB®, it is advisable to use the option for numerical flow solution.

The connection with transport is also implemented by 'subdomain expressions':

$$
\begin{aligned}
v_x &= q_x / h \\
v_y &= q_y / h \\
v &= \sqrt{v_x^2 + v_y^2} \\
D_{xx} &= D_m + (\alpha_l v_x^2 + \alpha_t v_y^2)/v \\
D_{yy} &= D_m + (\alpha_t v_x^2 + \alpha_l v_y^2)/v \\
D_{xy} &= (\alpha_l - \alpha_t)v_x v_y / v
\end{aligned}
\tag{8}
$$

with hydraulic head $h = \begin{cases} h_0 & \text{where the aquifer is confined} \\ \sqrt{h_0^2 + 2\varphi/K} & \text{where the aquifer is unconfined} \end{cases}$.

h_0 denotes the aquifer depth in the confined case, and hydraulic head along the bank for the unconfined case.

The first version of this model used the earlier 2.3 version of FEMLAB®, in which the implementation of a general dispersion tensor, as given in equation (5), was not possible. Thus the 'pde-general form' option was chosen (not the predefined 'convection-diffusion' mode), in which the differential equation has the general form:

$$\nabla \cdot \Gamma = F \tag{9}$$

For the bank filtration problem the subdomain settings in the general form are as follows:

$$\Gamma(c) = \left(-D_{xx}c_x - D_{xy}c_y + v_x c, -D_{xy}c_x - D_{yy}c_y + v_y c \right)$$
$$F(c) = -\mu c \tag{10}$$

The FEMLAB® 3.0 and 3.1 versions allow the introduction of a full dispersion tensor. Thus the 'convection-diffusion' option could be chosen in these versions as alternative mode instead of the 'pde-general form'. If a more general degradation characteristic is to be taken into account, it can easily be specified in the source/sink term $F(c)$. The formulation, given in equation (10), represents first-order decay with degradation rate μ. Note that μ includes both sorption and degradation processes. For a linear sorption isotherm the formula $\mu = R \cdot \lambda$ is valid, with retardation factor R and degradation rate λ for a pure fluid environment.

The boundary conditions for the transport model were chosen as follows:

$$
\begin{aligned}
\text{bank:} \quad & g = 0, \; r(c) = c - c_0 \quad \text{(Dirichlet)} \\
\text{aquifer:} \quad & g(c) = (v_x n_x + v_y n_y)c \quad \text{(Neumann)} \\
\text{well:} \quad & g(c) = (v_x n_x + v_y n_y)c \quad \text{(Neumann)}
\end{aligned}
\tag{11}
$$

where (n_x, n_y) denotes the vector normal to the boundary. There is a concentration c_0 specified at the bank. The problem substance is assumed to have a constant concentration c_0 in the surface water. For a field situation in which the concentration in surface water is not constant in time, a maximum value should be specified for a worst case simulation. All other boundaries have Neumann boundary conditions.

All mentioned parameters are introduced as constants in the related sub-menu of the FEMLAB® graphical user interface. Thus changes of the model are easy for non-expert users... .

As an example for the described concept an example for a single well near a straight boundary was set up as depicted schematically in the corresponding figure. The model region is a square of 200 by 200 m, extending from 0 to 200 m in x-direction and from -100 to 100 m in y-direction, with the well located at the central position r_{well}=(100 m, 0 m) and the bank at the y-axis. The well diameter is 1 m. Parameters were chosen as:

$$\alpha_L = 10 \text{ m}$$
$$\alpha_T = 1 \text{ m}$$
$$Q_0 = 6.25 \cdot 10^{-6} \text{ m}^3/\text{s}$$
$$Q_{well} = 2.5 \cdot 10^{-3} \text{ m}^3/\text{s}$$
$$x_{well} = 100 \text{ m}$$
$$h_0 = 25 \text{ m} \tag{12}$$
$$\mu = 5 \cdot 10^{-10} \text{ 1/s}$$
$$K = 3 \cdot 10^{-4} \text{ m/s}$$
$$D_m = 1 \cdot 10^{-9} \text{ m}^2/\text{s}$$
$$c_0 = 1 \text{ g/m}^3$$

Some parameter values were adopted from a situation which is typical for bank filtration facilities in Germany, e.g. pumping rate Q_{well}, baseflow Q_0, distance between bank and well x_{well}, and aquifer depth h_0. Similarly designed facilities are found at other locations in Europe (Jekel, 2003; Grischek et al., 2003), while in the United States wells are often placed nearer to the bank (Bouwer, 2003). Bank filtration facilities are mostly installed in sand or gravel aquifers: K is typical for gravel with relatively low hydraulic conductivity or coarse sand with relatively high conductivity. In many groundwater studies it has been observed that dispersion length values are correlated to the typical length of the observed phenomenon. They are one or two orders of magnitude smaller (Beims & Mansel, 1990; Luckner & Schestakow 1986). When the characteristic length scale for bank filtration is the distance between bank and well, the chosen value for α_L lies near the upper limit of the expected range. It is also common that the transversal dispersion length α_T lays one order of magnitude below the longitudinal dispersion length. For the given set-up the chosen values are thus in the expected range, but site-specific conditions may lead to substantially different parameters.

A finite element mesh is created by FEMLAB® for the square excluding the disk which represents the well. The initial coarse mesh was refined near the well and along the bank boundary and consists of 6285 nodes, 3055 elements and 175 boundary elements.

The problem for the steady-state solution of the two-dimensional concentration distribution $c(x,y)$ is solved directly following equation (6). The start solution is $c \equiv 0$ in the entire domain. Solutions for the linear equations are obtained by the UMFPACK direct method. For that method all default conditions were kept, a pivot threshold of 0.1 and automatic scaling for example.

5.5. Results and Discussion

Results for the confined case are depicted in Figure 9 as a contour plot and in Figure 10 as a surface plot. The unconfined case and the given parameters results differ only slightly from those presented for the confined situation. Streamlines can be obtained as contours of the streamfunction Ψ or using the FEMLAB® option to calculate streamlines from the velocity vector field. The latter approach has the advantage that cuts of the complex logarithm (see equation (2)) do not disturb the picture. On the other hand, contour plots to equidistant levels have the advantage of indicating flow velocities by contour distances (Holzbecher, 2002). For Figure 9 the FEMLAB® 'streamline' option (from the plot menu) was chosen. Along the bank (left boundary) the region with infiltrating surface water can clearly be recognized by streamlines (white lines) connecting bank and well. By contrast in the outer parts streamlines enter the bank from the aquifer, where flow has a negative *x*-component – these are regions with groundwater discharge into the river or lake.
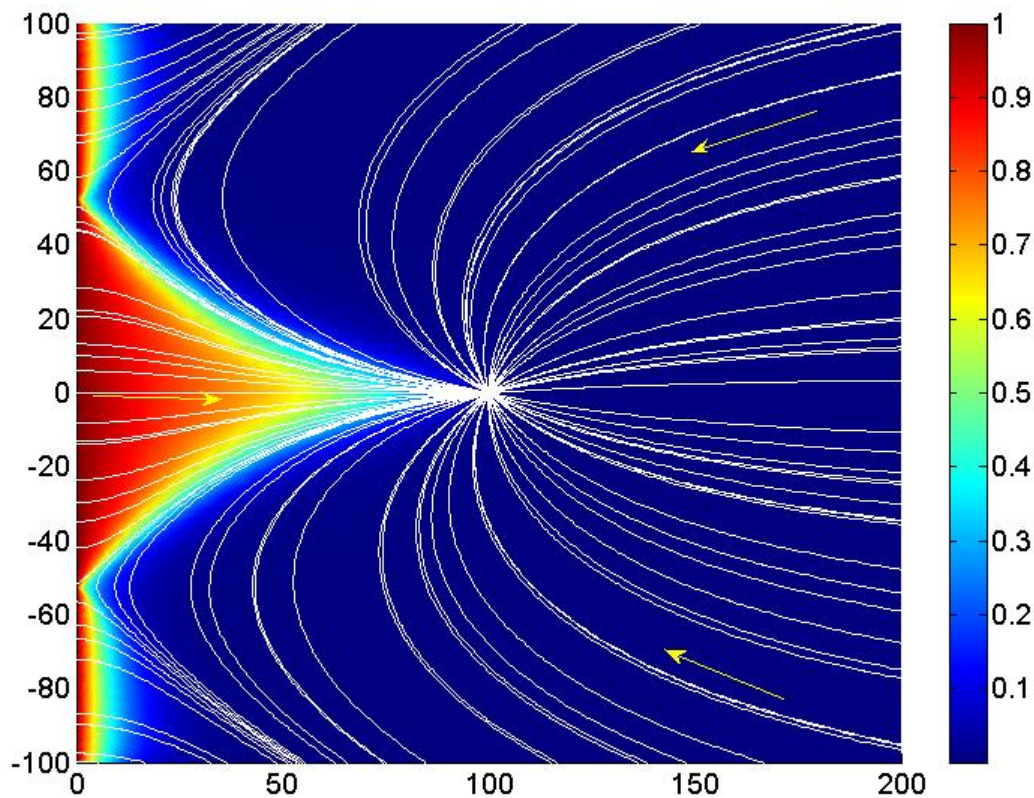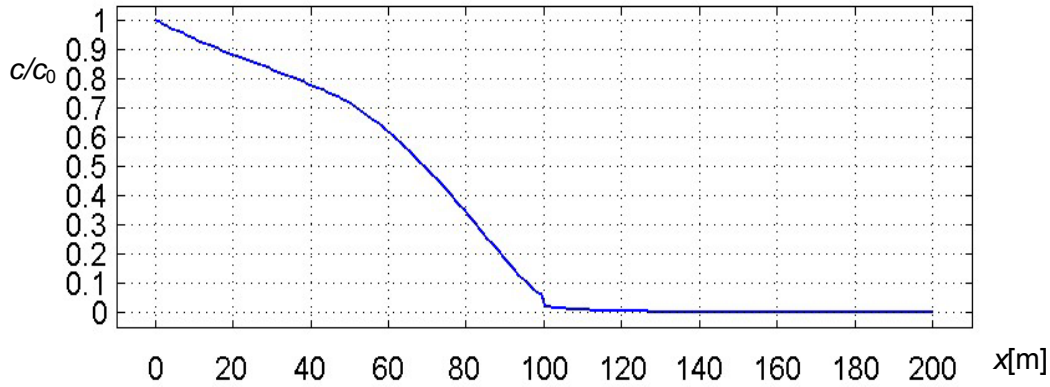
Figure 128 : Bank-filtration for a single well in the vicinity of a straight shoreline; depicted is a window of 200 m in both directions with a single well at the central position and bank line on the left; white lines are streamlines; the colour map depicts the steady state concentration distribution of a chemical component present in surface water, which is degraded during the bank filtration passage: red colour for high concentrations, blue colour for background concentrations; lower part of the figure provides normalized concentrations (c/c_0) along the central axis in horizontal direction through the well

Visualisation of the results shows increased concentrations within the bank filtrate flowing towards the well. The penetration is smallest at both stagnation points on the shore line, increasing again in the part with aquifer discharge. While the further penetration in the bank filtrate region is due to the flow regime, the difference between the stagnation points and the discharge region can be attributed to longitudinal dispersion. At the stagnation points both velocities and dispersion become almost negligible, which is not the case in the region of groundwater discharge.
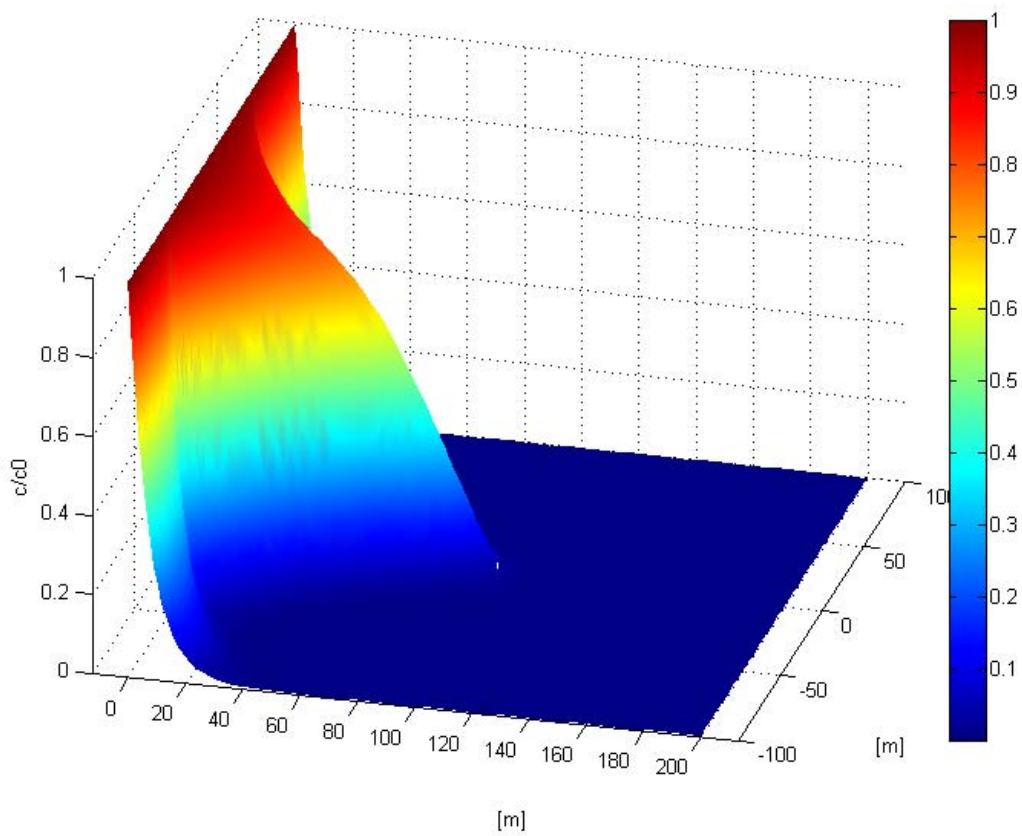
Figure 129 Concentration distribution due to the bank-filtration for the reference case, depicted in a surface plot
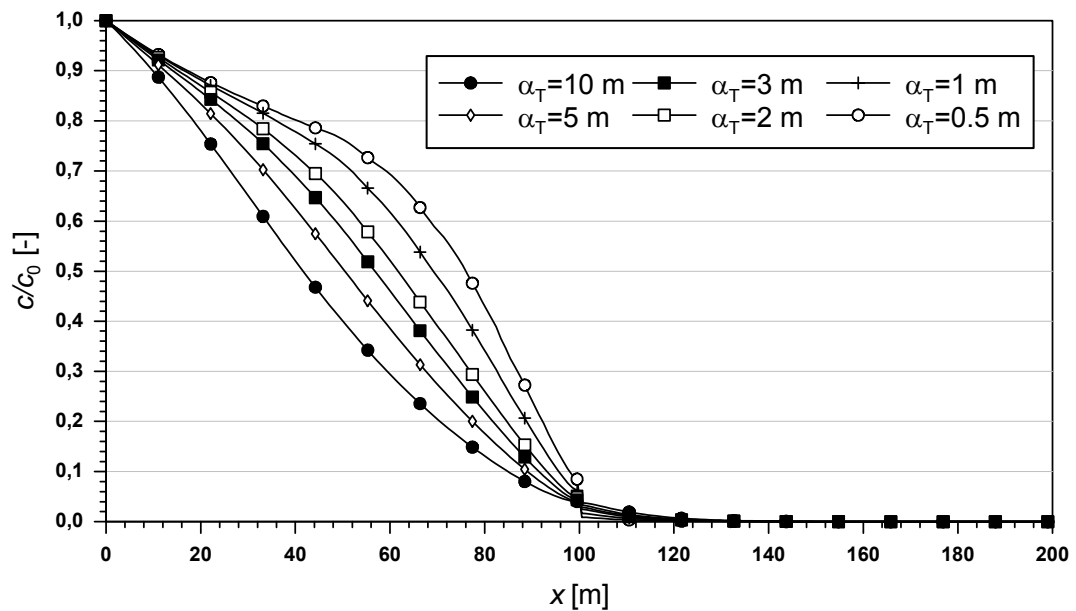
Figure 130 The effect of transversal dispersivity on the steady-state concentration profile along the shortest flowpath between bank and well

Another interesting observation can be made in the profile through the central axis (in x-direction) through the figure. The concentration profile obviously changes its gradient during the path towards the well: from a smoother to a steeper slope. The increase of velocity along the flowpath would lead us to expect the opposite: with higher velocities the effective degradation decreases and lowers the concentration gradients. However, the observed behaviour can be explained by another process:, transversal dispersion.

The sensitivity of the results to transversal dispersivity was examined for the unconfined aquifer, leaving all other parameters unchanged in comparison with the reference case, defined by list (12). The transversal dispersion coefficient α_T was varied between values of 0.5 and 10 m, representing factors between 1 and 20 for the α_L/α_T ratio. Higher values of α_T are unlikely, as transversal dispersivity almost never exceeds longitudinal dispersivity. Results are shown in Figure 130. For $\alpha_T = \alpha_L = 10$ m the steady state concentration profile is smooth, whereas a bend becomes visible with decreasing α_T, showing the transition from a moderate to a steep gradient. It is clear that the effect of transversal dispersion increases when the bank filtration wedge becomes slender in the vicinity of the well (see Figure 128).
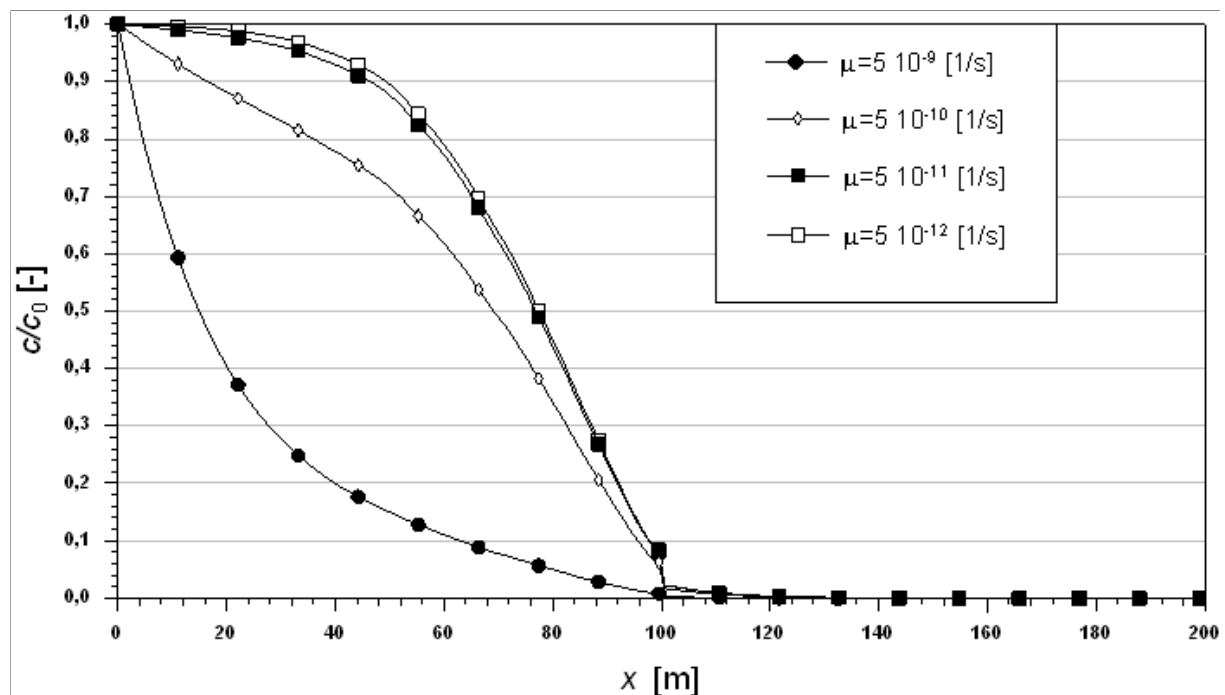
Figure 131 The effect of decay rate on the concentration distribution along the shortest flowpath between bank and well

The effect of the generalized decay rate μ is shown in Figure 131, demonstrating the transition from a concave to a convex shape. With four orders of magnitude between 10^{-9} and 10^{-12} [1/s] a wide parameter range is chosen. In fact degradation rates probably differ

even more, as they depend not only on the specie, but also on climatic, seasonal and redox conditions and on the biogeochemical environment in general. The variability of the parameter motivates the chosen range, as it represents the interval, where the value of the degradation rate becomes important. For values above 10^{-9} 1/s the substance reaches the well in very low concentrations. For values lower than 10^{-12} 1/s the concentration in the well is more likely to be relevant: concentrations in the direct vicinity of the well screen reach 1/10 of the concentration in the surface water, a level which under certain conditions may exceed the tolerable limit. A likely interpretation of Figure 130 is that for degradation rates below 10^{-10} 1/s the concentrations in pumped bank filtrate could reach levels comparable to input concentrations. These findings are valid for the chosen set-up and should not be transferred to other situations.

The total mass of substance per time unit, pumped with the water, can be obtained by the boundary integral:

$$q = \oiint_{\text{well boundary}} h \cdot c \left(v_x n_x + v_y n_y \right) ds \qquad (13)$$

FEMLAB® is able to perform such boundary integrals in the post processing mode. The integrant is specified exactly as given in formula (13). For the reference case the resulting value is $5 \cdot 10^{-7}$ g/s. The concentration in pumped water after mixing is thus $c_{well} = q / Q_{well} = 2 \cdot 10^{-4}$ g/m^3.

5.6. Summary

The described method allows a direct and therefore fast computation of the steady-state solution for the bank filtration flow and transport problem. Concentrations of surface water substances can be expected to be higher in permanently pumping wells than in sporadically pumping wells. With appropriate parameters the steady state represents a worst case scenario and can be applied as such also for transient situations with changing pumping rates of the wells, and/or for changing concentrations of a problem substance in the surface water body. For the latter situation the highest measured concentration should be used in the boundary condition (c_0), see equation (11).

The margin at which degradation rates deliver values comparable to the inlet concentration was found to be around 10^{-10} 1/s: above that margin concentrations in pumped bank filtrate will be significantly lower than c_0. Experimental studies in enclosures under near field conditions, performed with phages within the NASRI project in Berlin (Germany), show values around 3 10^{-8} 1/s (Holzbecher *et al.*, to appear). Even under anaerobic conditions minimum degradation rates reach 2 10^{-9} 1/s, which according to the findings in this paper is a range for which problems with increased concentrations in pumped water cannot be

expected. In the same experiments for microcystins degradation rates above 10^{-7} 1/s were obtained, which is even more unproblematic.

The given estimation of a relevant parameter range is not valid for substances that are a potential hazard at concentrations several orders of magnitude below the concentration in surface water. Such a situation is conceivable in the case of a severe accident upstream in the surface water body. However, in such a case the steady-state assumption for the concentration distribution, as made above, would probably not be justified. However, multi-physics tools like FEMLAB® could handle emergency scenarios with unsteady transport as well.

The multi-physics approach presented here can easily be extended to account for more general degradation characteristics compared to the simple linear approach. However, in most cases it is unknown whether a more complex degradation regime is valid under field conditions for the entire flowpaths of bank filtrate towards a well. In such a situation one may consider adopting a conservative worst case study, as presented here, in which a more complex approach could also be implemented.

The presented approach with an analytical solution for flow calculation allows several extensions. Shorelines meeting at a certain angle can be represented by extending the method of mirror wells (Bear, 1972; Strack, 1989) or conformal mappings (Holzbecher, 2005). In case of a gradient on the bank an appropriate analytical solution is described by Wilson (1993). The approach proposed by van der Veer (1994) allows the consideration of a clogging layer at the bottom of the surface water body.

The presented concept can also be extended for more general situations. Multiple wells can be introduced. Such well galleries may also include recharge wells. As the notation for the explicit flow solution becomes lengthy in the case of multiple wells, it is recommended to let FEMLAB® calculate the flow solution using the 'Poisson' equation with point sink at the well location. Using the FEMLAB® flow solver it is also possible to take into account irregular boundaries, either at the bank or for the aquifer. Material properties are allowed to change, which allows the consideration of inhomogeneities in hydraulic conductivity, and of anisotropies. All such extensions can be performed using the multi-physics approach of FEMLAB®.

5.7. References

Anderson E.I., The method of images for leaky boundaries, *Adv. in Water Res.*, Vol. 23, No. 5, 461-474, 2000

Bear, J., 1972. Flow through Porous Media, Elsevier, New York, 764pp.

Beims, U., Mansel H., 1990. Assessment of groundwater by computer model design and pumping tests, in: Groundwater Monitoring and Management, IAHS Publ., No.173, pp11-22.

Bouwer, E.J., 2003. Riverbank filtration - the American experience. In: Melin, G. (Ed), Riverbank Filtration: the Future is Now, Proc. 2nd Riverbank Filtration Conf., National Water Research Institute, pp 105-110.

FEMLAB®, Version 3.1, 2004. COMSOL AB, Tegnérgatan 23, SE-111 40 Stockholm, Sweden.

Grischek, T., Schoenheinz, D., Worch, E., Hiscock, K., 2003. Bank filtration in Europe - an overview of aquifer conditions and hydraulic controls. In: Dillon P.J. (Ed), Management of Aquifer Recharge for Sustainability, Balkema, Lisse, pp485-488

Holzbecher, E., 1996. Modellierung dynamischer Prozesse in der Hydrologie: Grundwasser und ungesättigte Zone, Springer Publ., Heidelberg

Holzbecher, E., 2002. Groundwater Modelling - Simulation of Groundwater Flow and Pollution, Electronic Book on CD-ROM, FiatLux Publ., Fremont (USA)

Holzbecher E., Analytical solution for 2D groundwater flow in presence of two isopotential lines, *Water Resources Research*, Vol. 41, No. 12, W12502, 2005

Holzbecher E., Calculating the effect of natural attenuation during bankfiltration, to: *Computers & Geosciences,* submitted

Holzbecher, E., Dizer H., Grützmacher G., Lopez-Pila J., Nützmann G., The influence of redox conditions on phage transport – enclosure experiments and modelling, *Enviromental Engineering Science*, to appear

Jekel., M., 2003. Riverbank filtration: the European experience. In: Melin, G. (Ed), Riverbank Filtration: the Future is Now, Proc. 2nd Riverbank Filtration Conf., National Water Research Institute, pp105-110.

Luckner, L., Schestakow W.M., 1986. Migrationsprozesse im Boden- und Grundwasserbereich, Deutscher Verlag für Grundstoffindustrie, Leipzig.

Strack, O.D.L, 1989. Groundwater Mechanics, Prentice Hall, Englewood Cliffs, 732pp.

Strack, O.D.L., 1999. Principles of the analytic element method, *J. of Hydrol.* 226, 128-138.

van der Veer, P., 1994. Exact solutions for two-dimensional groundwater flow in a semiconfined aquifer, *J. of Hydrol.* 156, 91-99.

Wilson, J.L., 1993. Induced infiltration in aquifers with ambient flow, *Water Resources Research.* 29(10), 3503-3512.

3

Occurrence and fate of drug residues and related polar contaminants during bank filtration and artificial recharge

"drugs"-group, Technical University of Berlin, Dept. of Food Chemistry

Responsible project leader: Prof. Dr. Martin Jekel, PD Dr. Thomas Heberer

Content

List of figures

VII

List of tables

List of Abbreviations

2,4-D	2,4-dichlorophenoxy acetic acid
AMDOPH	1-acetyl-1-methyl-2-dimethyl-oxamoyl-2-phenylhydrazide
BEE	Beelitzhof (designation of the water works located at lake Wannsee)
BWB	Berlin Water Company
GWA	ground water replenishment site
LOQ	limit of quantitation
MCPA	4-chloro-2-methylphenoxy acetic acid
MID	multiple ion detection
n.d.	not detected
NPS	N-(phenylsulfonyl)-sarcosine
o,p'-DDA	2-(2-chlorophenyl)-2-(4-chlorophenyl) acetic acid
OWA	surface water purification plant
p,p'-DDA	2,2-bis(4-chlorophenyl)acetic acid
PhaC's	pharmaceutically active compound
SIM	selected ion monitoring
SPE	solid phase extraction
STP	sewage treatment plant
TEG	Tegel (designation of the water works located at lake Tegel)
TS	transect

1 Pharmaceutically active compounds

1.1 Introduction

This part of the NASRI project provided a quantitative data basis for a better understanding and improvement of the removal of pharmaceutically active compounds (PhAC's) and related polar compounds during groundwater recharge by conducting detailed process studies. Residues of drugs (parent compounds or drug metabolites) originating from therapeutical use in human medical care are excreted unchanged or as water-soluble conjugates via faces and/or urine. Conjugates are easily cleaved in the municipal sewers and/or the receiving sewage treatment plants (STPs). Some of these compounds are not or only partially removed in the municipal STPs and have thus been detected in several samples of surface, ground and drinking waters (Heberer et. al., 2004b). For the investigations within the NASRI project, two highly sensitive analytical methods have been applied to water samples collected monthly from the transects at the lakes Tegel and Wannsee. Using these methods, eight drug residues were identified in the surface water of both lakes and were thus recognized as being important for bank filtration at the investigated field sites. The PhAC's occurring at both field sites included the analgesic/anticonvulsant drugs diclofenac, indometacine and propyphenazone, the antiepileptic drugs carbamazepine and primidone, the blood lipid regulating drug bezafibrate and the two drug metabolites AMDOPH (1-acetyl-1-methyl-2-dimethyl-oxamoyl-2-phenylhydrazide) and clofibric acid. Together with these residues, the herbicides bentazone and mecoprop, NPS (N-(phenylsulfonyl)-sarcosine), a metabolite of a corrosion inhibitor, as well as the herbicide metabolites p,p'-DDA (2,2-bis(4-chlorophenyl)acetic acid) and its isomer o,p'-DDA (2-(2-chlorophenyl)-2-(4-chlorophenyl)acetic acid) were also detected in several samples during these investigations. The observed PhAC's were also subject of further detailed studies. The investigations of their behaviour during bank filtration were accompanied by batch experiments, column studies, slow sand filter and enclosure experiments. Additionally, the ground water replenishment site located at lake Tegel and the surface water purification plant (OWA) Tegel were investigated to get more information about the behaviour of the drug residues during aerobic infiltration and during phosphate elimination treatment, respectively. Besides the monthly sampling at the transects, the distributions of the observed compounds within lake Wannsee as well as the occurrence of these substances in further adjacent surface waters (the river Unterhavel, lake Kleiner Wannsee, and the Teltowkanal) were determined. The results of these investigations are described in detail in this report.

1

1.2 Method

The analysis of the collected samples was carried out by solid-phase extraction (SPE), derivatization and detection applying gas chromatography-mass spectrometry (GC-MS) with selected ion monitoring (SIM). As shown in Table 1, a total of twenty pharmaceuticals and seven related polar contaminants, most of them pesticides, were detectable and quantifiable down to the low ng/L range in surface and ground water samples.

Table 1. Detectable compounds, their affiliation and the individual limits of quantification

Compound	Affiliation	LOQ (ng/L)
1-acetyl-1-methyl-2-dimethyl-oxamoyl-2-phenylhydrazide (AMDOPH)	metabolite analgesic	5
2-(2-chlorophenyl)-2-(4-chlorophenyl) acetic acid (o,p'-DDA)	metabolite of an insecticide	10
2,2-bis(4-chlorophenyl)acetic acid (p,p'-DDA)	metabolite of an insecticide	10
2,4-dichlorophenoxyacetic acid (2,4-D)	herbicide	5
4-chloro-2-methylphenoxy acetic acid (MCPA)	herbicide	5
bentazone	herbicide	5
bezafibrate	blood lipid regulator	50
carbamazepine	antiepileptic	5
clofibric acid	metabolite of blood lipid regulator	10
dichlorprop	herbicide	5
diclofenac	analgesic / anticonvulsants	5
fenofibrate	blood lipid regulator	20
fenoprofen	analgesic	5
gemfibrozil	blood lipid regulator	5
ibuprofen	analgesic / anticonvulsants	5
indometacine	analgesic / anticonvulsants	30
ketoprofen	analgesic / anticonvulsants	20
meclofenamic acid	analgesic / anticonvulsants	5
mecoprop	herbicide	5
mefenamic acid	analgesic / anticonvulsants	5
N-(phenylsulfonyl)-sarcosine (NPS)	metabolite of a corrosion inhibitor	30
naproxen	analgesic / anticonvulsants	5
oxazepam	vasodilator	20
pentoxifylline	vasodilator	30
phenacetin	analgesic / anticonvulsants	40
primidone	analgesic / anticonvulsants	5
propyphenazone	analgesic / anticonvulsants	10
tolfenamic acid	analgesic / anticonvulsants	5

1.2.1 Sample preparation procedure

During the sampling 2 liters of water were collected for PhAC analysis. The samples were acidified (<pH 2) with hydrochloric acid and then stored in brown flask at a temperature below 4°C. For each method 500 to 1000 mL of the sample were spiked with 100 ng of the surrogate standards (dehydrocarbamazepine, 4-chlorophenoxybutyric acid) and then directed to SPE (Figure 1). SPE cartridges were dried over night (~ 12 hours) under a gentle stream of nitrogen and then eluated with methanol.

Figure 1. Picture shows the build up of a solid phase extraction

After adding 100 ng of an internal standard (2-(m-chlorophenoxy)propionic acid) to control the derivatization process, the sample was dried again using a gentle stream of nitrogen and derivatized with pentafluorobenzylbromide (PFBBr) or N-(tert.-butyldimethylsilyl)-N-methyl-trifluoroacetamide (MTBSTFA), respectively. Both methods have been elaborated, validated and published. More information on sample preparation, conditions for derivatization, MS conditions, reproducibility and limits of detection and quantitation are also available from Reddersen and Heberer (2003).

1.3 Laboratory & semi technical investigations

1.3.1 Batch experiments

1.3.1.1 Introduction

During the investigations at the transects lake Tegel and lake Wannsee, clofibric acid, metabolite of three different blood lipid regulators, and the antiepileptic drug carbamazepine occurred among other drug residues in surface water and groundwater monitoring wells. At the investigated field sites clofibric acid concentrations were observed with attenuation rates between 43% and 89% during the first meters of infiltration induced by bank filtration (chapter 1.4.4 & chapter 1.4.6) or by artificial groundwater replenishment (chapter 1.4.3). Opposite to this, carbamazepine concentrations at the shallow monitoring wells near the bank were observed to be stable within the measurement accuracy of 20 %. Both substances and ibuprofen which is known to be easily biodegradable [Buser et al., 1999; Stumpf et al., 1998; Winkler et al., 2001] were investigated in two batch experiments with mixtures dissolved in de-ionized water and surface water from lake Wannsee using two different types of Wannsee sediment. Experiments were accomplished in cooperation with the hydrogeology group of the Free University of Berlin. Three different experiments were conducted. In the first approach, only the solvent was spiked. In the second experiment, the spiked solvents were mixed with Wannsee sediment type 2 (WS2, soil from different parts of the aquifer at transect Wannsee) and in the third experiment, spiked solvents were mixed with Wannsee sediment type 3 (WS3, from the colmation layer, first 10 cm the bottom of lake Wannsee) and sampled over a period of 26 days.

1.3.1.2 Carbamazepine

In the experiments with de-ionized water as solvent (Figure 2, left), carbamazepine concentrations were stable with around 100 % recovery after a period of 26 days.
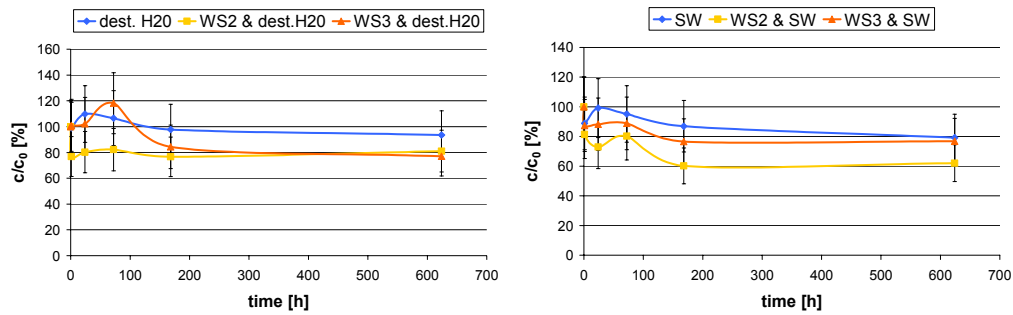
Figure 2. Concentrations of carbamazepine during the batch experiments and a sampling period of 26 days (left: de-ionized water; right: surface water from lake Wannsee)

In the experiments with de-ionized water and Wannsee sediments no.2 or no. 3, the carbamazepine concentrations show a slight decrease down to 80 % of the initial concentration. However, this concentration change is within the measurement accuracy of the analytical method of 20 %. Thus, this obvious decrease is no final proof for the occurrence of effects of sorption or even degradation. As presented in Figure 2 (right), the experiments with surface water showed only one difference, in the mixture with WS2 carbamazepine concentrations decreased to a recovery of 60 % after a contact time of 7 days.

1.3.1.3   Clofibric acid

As illustrated in Figure 3, the observed concentrations of clofibric acid in the batch experiments varied between 85 % and 130 % in de-ionized water and in the mixture with WS2 . The experiments with surface water in a mixture with WS2 showed recoveries between 85 % and 110 %. Thus, no significantly attenuation could be recognized for these experiments. In contrary to this, during the experiments with sediment WS3 added to the mixture, a decrease down below the LOD was noticed.
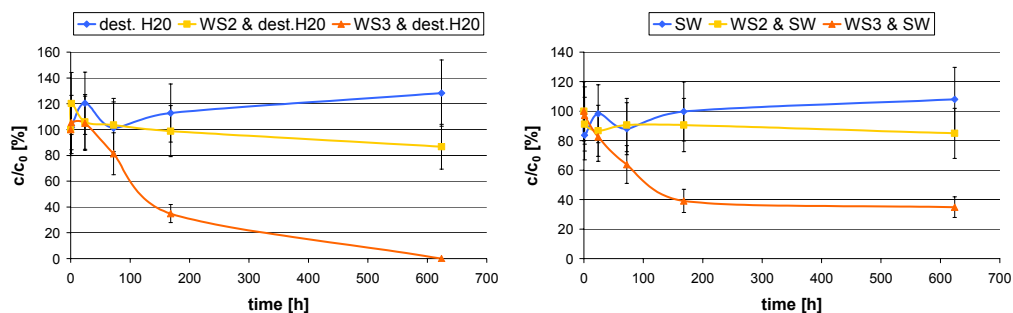
Figure 3. Concentrations of clofibric acid during the batch experiments and a sampling period of 26 days (left: de-ionized water; right: surface water from lake Wannsee)

1.3.1.4   Ibuprofen

After a period of 7 days, ibuprofen concentrations in spiked de-ionized water decreased by 34 % and in spiked surface water by 79 %, as Figure 4 shows. The experiments with added sediments lead to a complete attenuation of ibuprofen. Comparing the different sediment types, the approach with surface water showed a faster attenuation of ibuprofen down to concentrations below the LOD after 7 days.
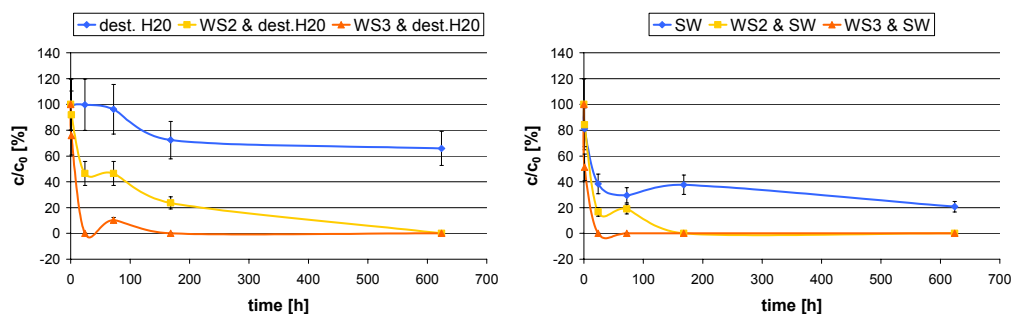
Figure 4. Concentrations of ibuprofen during the batch experiments and a sampling period of 26 days (left: de-ionized water; right: surface water from lake Wannsee)

1.3.1.5   Conclusions

During these experiments it was noticed that carbamazepine showed no (within the analytical measurement accuracy of 20%) attenuation when dissolved in de-ionized water or additionally mixed with WS2 and WS3. However, when using surface water and surface water with added Wannsee sediments a slightly attenuation between 20% and 40 % was recognized. No tendencies for decrease were observed for dissolved clofibric acid or with the added soil material from the aquifer (WS2) at transect Wannsee. Opposite to this behaviour, added sediments from the colmation layer (WS3) lead to attenuations within a range of

concentrations below the LOD up to 40 % of initial concentrations. As expected from other studies [Buser et al. 1999; Stumpf et al. Winkler, 2001, Zwiener et al., 2000], ibuprofen only dissolved in de-ionized water was easily removed with an attenuation rate of 35 % and rapidly when using surface water instead of de-ionized water. Dissolved in both kinds of water and in contact with Wannsee sediments WS2 and WS3, a complete degradation was observed after period of 26 days.

1.3.2   Sand filtration experiments

1.3.2.1   Introduction

In this part of the NASRI project, the fate of four selected pharmaceuticals during sand filtration was investigated. Four experiments were carried out at the test-field site of the *Umweltbundesamt* (UBA, German Federal Environmental Agency) in Berlin-Marienfelde. Enclosure No. 3, which was used in the experiments presented here. Additional informations are available.

Contaminant-free groundwater from the area underneath this filed-site was used to fill the storage pond and to carry out the experiments at the sand filtration facility. Some parameters measured for this water are shown in Table 2.
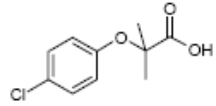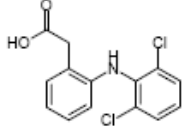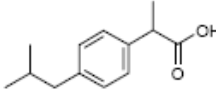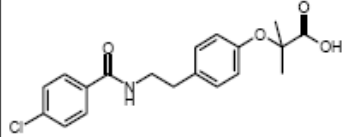
Table 2. Physical-chemical parameters measured of the groundwater used for the experiments

Cations			
Na^+	K^+	Ca^{2+}	Mg^{2+}
46,4	4,3	125	17,7
Anions			
SO_4^{2-}	NO_3^-	PO_4^{3-}	SO_4^{2-}
236	0,3	<0,1	236
Other parameters			
DOC^2		pH	conductivity
5,5 mg/L		7,8	963 µS/cm

Four pharmaceuticals, namely clofibric acid, diclofenac, ibuprofen, and bezafibrate were chosen for this study. All four substances have already been found in the aquatic environment and have been selected as model-substances due to their different physical-

chemical properties and their expected or reported different behaviour during groundwater recharge.

Table 3. Selected pharmaceuticals

Name	Structure	Molecular weight totals formula	Group of prescription/use
Clofibric acid		296,2 $C_{14}H_{11}Cl_2NO_2$	blood lipid lowering agent (metabolite)
Diclofenac		214,7 $C_{10}H_{11}ClO_3$	non-steroidal antiphlogistic
Ibuprofen		203,3 $C_{13}H_{18}O_2$	non-steroidal antiphlogistic
Bezafibrate		361,8 $C_{19}H_{20}ClNO_4$	blood lipid lowering agent

1.3.2.2 Slow sand filter experiment no. SSF3

A first experiment (slow sand filter experiment SSF3) with clofibric acid and diclofenac was carried out with one of the slow sand filters, where only samples from surface water and outlet could be taken. Results are shown in Figure 5

Tabelle 1. Experimental conditions of enclosure experiment #1

Slow sand filter experiment #1 (SSF3)		
Date	23.– 25.04.2003	
Flow rate	6.4 m^3/h	
Filtration velocity	2.1 m/d	
Initial concentration of pharmaceuticals	clofibric acid	diclofenac
	1µg/L	1µg/l
Condition of the sediment surface	large algae growth	

In addition, sodium chloride was added as a tracer and conductivity was measured by the working group of Dr. Chorus from the Federal Environmental Agency (UBA). The results from this experiment are shown in Figure 5.
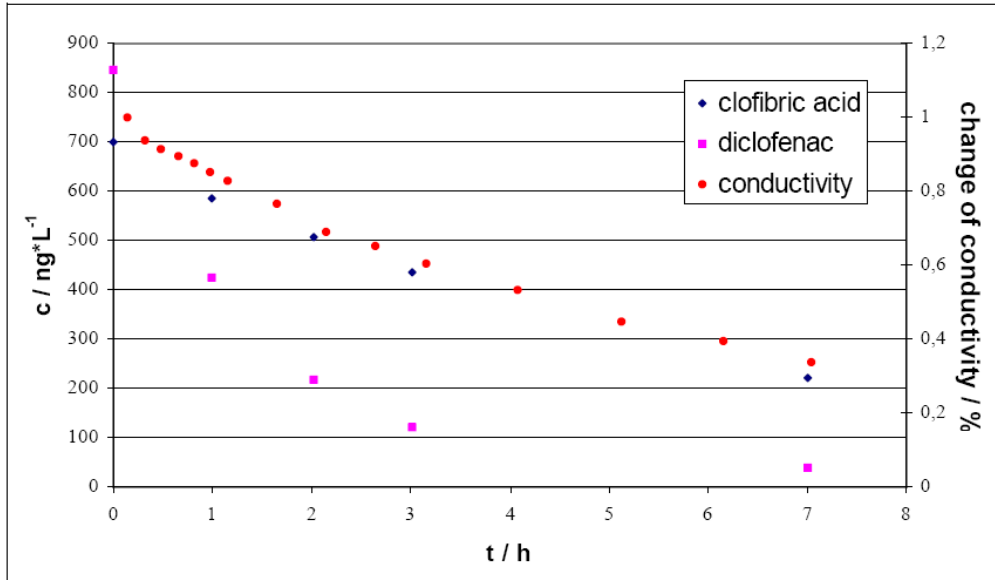
Figure 5. Concentrations of pharmaceuticals and temporal change of conductivity measured in spiked surface water during slow sand filter experiment #1 (23.-25.04.2003).

As can be seen from the results of this experiment presented in Figure 6, the concentration of clofibric acid changed similar to the concentration of sodium chloride that was observed by measuring the conductivity. Thus, clofibric acid showed the tracer-like behavior that has already been described for this substance in various references for this substance (e.g. Mersmann et al., 2002; Verstraeten et al., 2002). In contrast to that, there is a distinct decrease of the diclofenac concentration was observed in the surface water and it was assumed that this was caused by photolytical degradation, which has previously been reported for diclofenac in the literature (Buser et al., 1998, Tixier et. al., 2003).
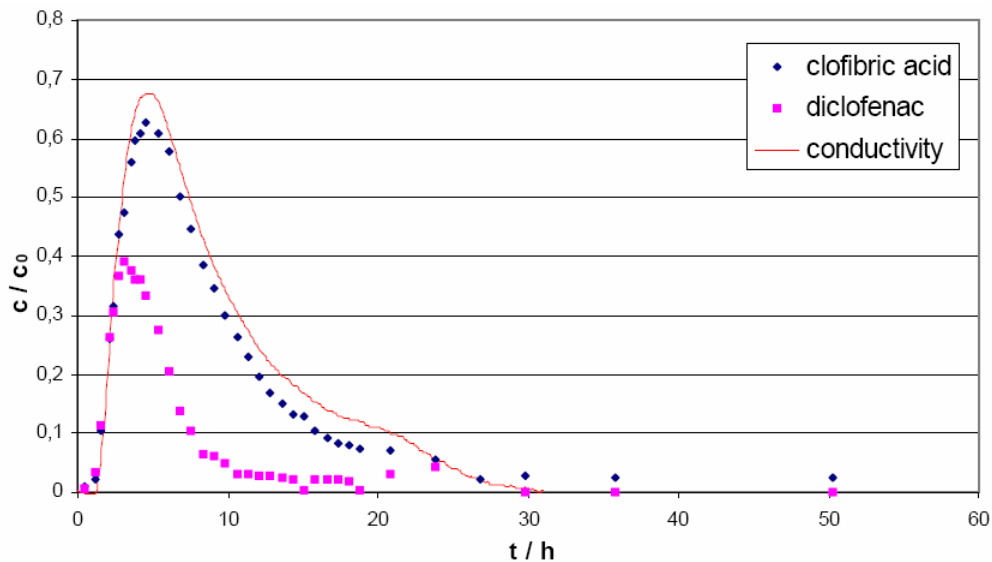
Figure 6. Proportions (c/c₀) of pharmaceuticals and temporal change of conductivity measured at the outlet of slow sand filter during slow sand filter experiment #1 (23.-25.04.2003).

A mass balance was calculated which showed that 70% of the infiltrated amount of clofibric acid was detected at the outlet, while only 30% of the spiked amount of diclofenac was recovered (for diclofenac photolytical degradation has to be taken into account resulting in an unknown amount of diclofenac that was removed from the surface water without being infiltrated into the sand filter).

1.3.2.3   Slow sand filter experiment no. SSF5

The experiment was repeated two month later (slow sand filter experiment #2) under different conditions and with all four substances to a test mixture (clofibric acid, diclofenac, ibuprofen, bezafibrate) applied to the slow sand filters. Again sodium chloride was used as a tracer. Additionally, microcystines (algae toxins) and bacteriophages (viruses) were added by the two working groups from the UBA (Chorus/Lopez-Pila).
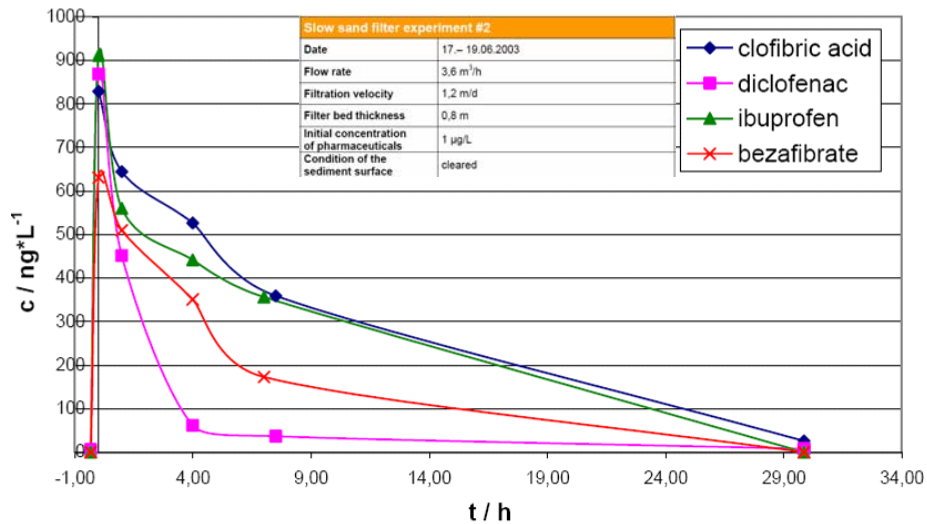
Figure 7. Concentrations of pharmaceuticals and temporal change of conductivity measured in the spiked surface water during slow sand filter experiment #2 (17.-19.06.2003). Additionally experiment parameters are shown.

The results for clofibric acid and diclofenac shown in Figure 7 were comparable to those of slow sand filter experiment #1. The calculated mass balance showed that in this experiment 85% (70% SSF3) of the infiltrated amount of clofibric acid and 30% (30% SSF3) of the initial amount of diclofenac could be recovered in the outlet as presented in Figure 8.
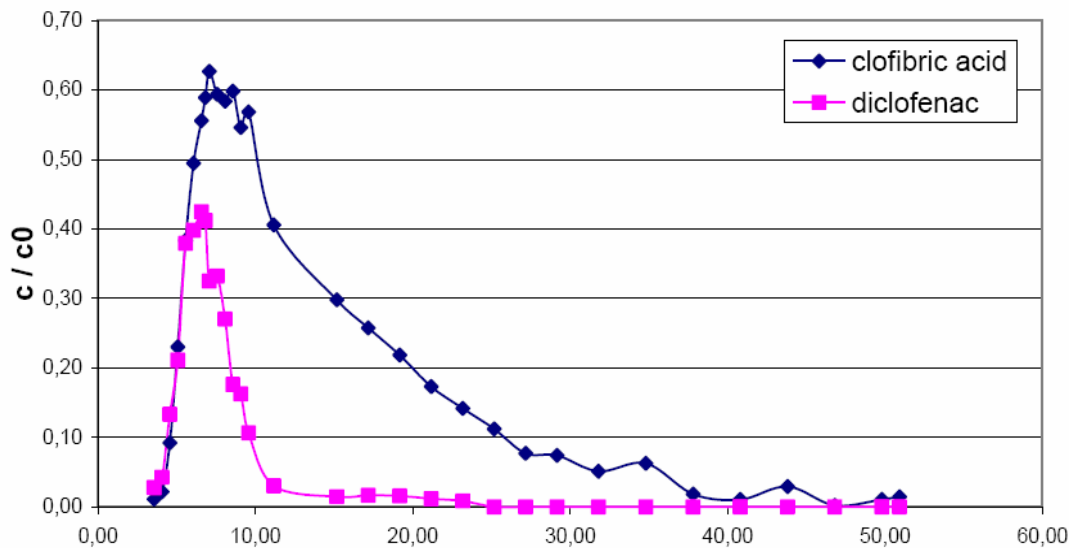
Figure 8. Proportions (c/c0) of pharmaceuticals and temporal change of conductivity measured at the outlet of slow sand filter during slow sand filter experiment #2 (17.-19.06.2003).

11

The two additional substances ibuprofen and bezafibrate were fully attenuated during slow sand filtration and could not be detected in the outlet.

1.3.2.4   Enclosure experiments E2o, E3d, E4d & E5d

Behavior of clofibric acid, diclofenac, bezafibrate and ibuprofen during experiment no. E2o

The first enclosure experiment (E2o) was carried out in August 2003. The joined experiments were carried out together with several other groups of the NASRI project. Besides PhAC's some other compounds (microcystines, viruses, Gadolinium and again sodium chloride as a tracer) were also spiked to the feed water of the enclosures. Therefore, and a minor sample-volume of only 25ml/min could be collected at the four sampling-points the initial concentrations of our pharmaceuticals had to be increased. The enclosure was covered to protect the UV-sensitive bacteriophages and to avoid photochemical reactions. Table 4 shows the experimental parameters during enclosure experiment no. 1.

Table 4. Experimental conditions of enclosure experiment #1

Enclosure experiment #1 (E2o)		
Date	05.– 06.08.2003	
Flow rate	0,05 m^3/h	
Filtration velocity	1,3 m/d	
Initial concentration of pharmaceuticals	clofibric acid diclofenac	ibuprofen bezafibrate
	2µg/L	5µg/l
Condition of the sediment surface	cleared	

Figure 9 shows the temporal changes of concentrations for the four spiked pharmaceuticals in the supernatant water layer. Apart from their different initial concentrations, the change of concentration was quite similar for all four substances. The rapid decrease of the diclofenac concentration that was observed in the first slow sand filter experiments did not occur because the enclosure was covered. This result also confirmed the assumption of a photolytical degradation of diclofenac in the supernatant water layer in both experiments with slow sand filtration. Therefore, adsorption at the top of the sand filtration facilities can be excluded being an important cause for the decrease of the diclofenac concentration. The results measured for all four pharmaceuticals in the column of the enclosure at a depth of 20cm are presented in Figure 9.
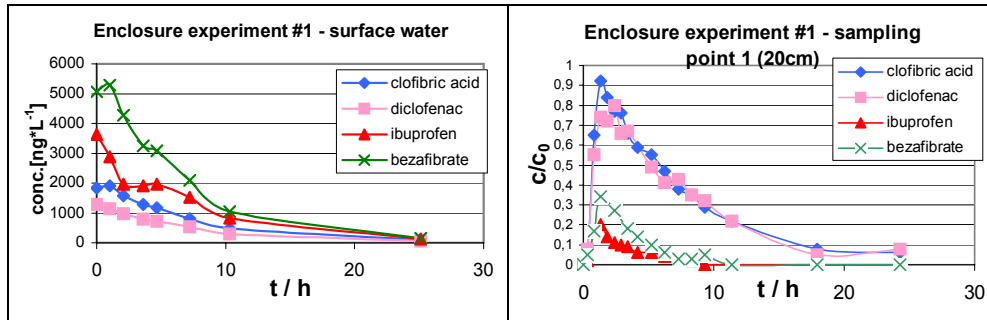
Figure 9. Concentrations of pharmaceuticals measured in the spiked surface water and breakthrough curves at a depth of 20cm during enclosure experiment #1 (E2o)

Ibuprofen and bezafibrate were already strongly attenuated resulting in rather low maximum c/c_0 values of <0.4 and <0.2 respectively. From the mass balance it was calculated that only 10% and 20% of the infiltrated amount of ibuprofen and bezafibrate were found at sampling-point #1, respectively. In contrast to that clofibric acid was found at about 80% and diclofenac at about 85% of the initial amount.
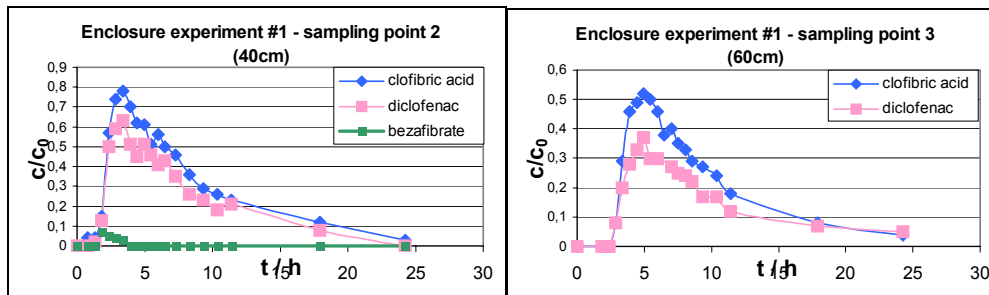
Figure 10. Breakthrough curves of pharmaceuticals measured at a depth of 40cm and 60cm in the enclosure during enclosure experiment #1 (E2o)

As shown in Figure 10 ibuprofen was not detected any longer after a passage of 40cm. Only about 2% of the initial quantity of bezafibrate was recovered at sampling-point #2, while the mass balance resulted in 70% and 65% of the initial amount for clofibric acid and diclofenac, respectively. The decrease of the recovered quantities continued at sampling-point #3 (60cm). 50% and 40% of the initial amounts of clofibric acid and diclofenac were found here, respectively. Bezafibrate was not detected in any sample from this sampling-point.
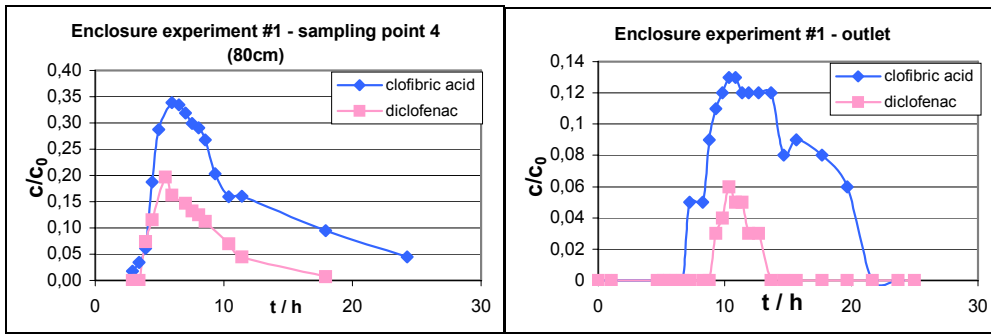
Figure 11. Breakthrough curves of pharmaceuticals measured at a depth of 80cm and enclosure outlet during enclosure experiment #1 (E2o)

Figure 11 shows the breakthrough curves for clofibric acid and diclofenac after 80cm (sampling-point #4), which is comparable to the thickness of the filter bed of the slow sand filtration units, described before. In contrast to both experiments at the slow sand filter, a significant decrease of the clofibric acid concentration was observed in enclosure experiment #1. After 80cm only 35% of the initial amount was detected. Finally in the outlet (Figure 11) there were only 15% and 5% of clofibric acid and diclofenac found, respectively.

Results for clofibric acid and diclofenac are summarised in Figure 12. Similarly, the amount of diclofenac recovered at enclosure outlet were also much lower (15%) than in the slow sand filtration experiments (~30%), although photolytic degradation was inhibited by covering the enclosures.
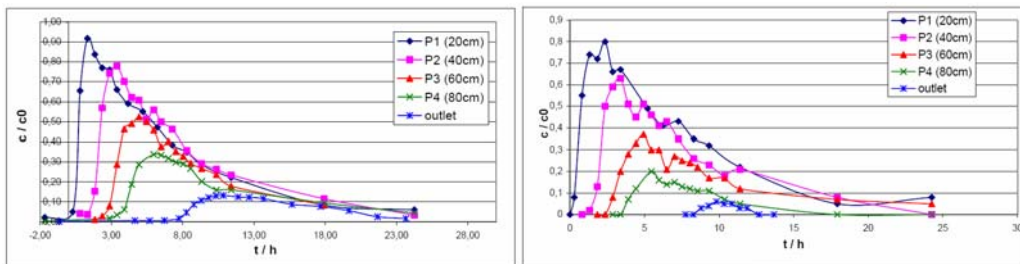
Figure 12. Breakthrough curves of clofibric acid and diclofenac measured during enclosure experiment #1 (E2o)

In contrast to that, the data of the conductivity measurement was nearly identical to those of the first two slow sand filtration experiments resulting in the breakthrough curves shown in Figure 13.

14
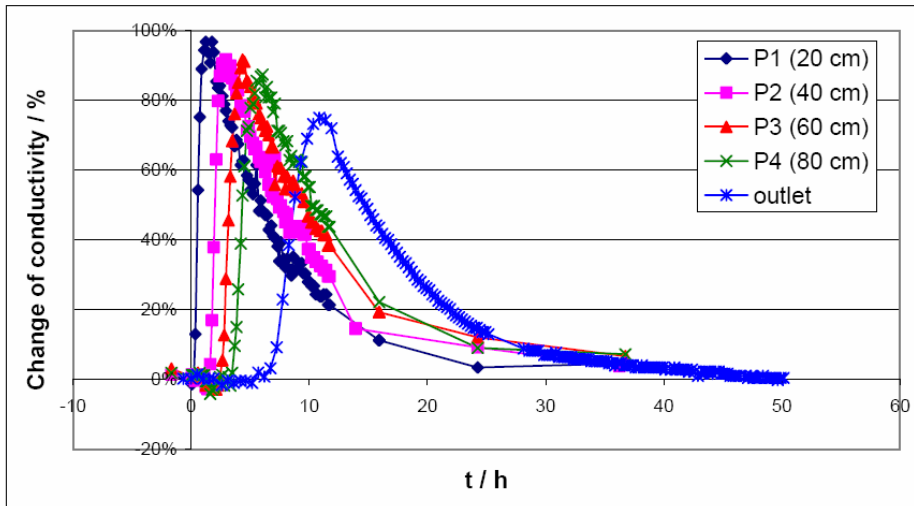
Figure 13. Temporal change of conductivity measured during enclosure experiment #1 (E2o)

These curves showed only the typical decrease of the maximum conductivity after breakthrough caused by dispersion. Thus, a distinct difference between the conductivity data and the results for clofibric acid was observed in this experiment.

Behavior of clofibric acid, diclofenac, bezafibrate and ibuprofen during experiment no. E3d

The second experiment (E3d) at the enclosures was carried out one month later. Table 5 shows the experimental parameters during enclosure experiment no. 1.

Table 5. Experimental conditions of enclosure experiment #2

Enclosure experiment #2 (E3d)		
Date	09.– 10.09.2003	
Flow rate	0,05 m^3/h	
Filtration velocity	1,1 m/d	
Initial concentration of pharmaceuticals	clofibric acid diclofenac	ibuprofen bezafibrate
	2µg/L	5µg/l
Condition of the sediment surface	slightly developed clogging layer	

15

For ibuprofen and bezafibrate the results of the first enclosure experiment were also confirmed in this experiment. However, both substances appeared to be removed even more efficiently in this experiment with a slightly developed clogging layer. After 20cm (Figure 14) only about 3% of bezafibrate and 1% of ibuprofen were recovered, respectively. However, about 85 % of the infiltrated amount of Clofibric acid could be recovered. For diclofenac the calculated mass balance resulted 115%, obviously caused by unavoidable mistakes of the used analytical and mathematical methods.
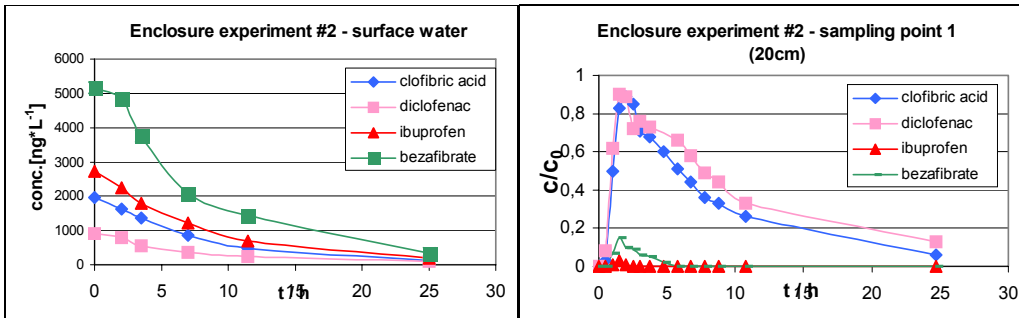
Figure 14. Concentrations of pharmaceuticals measured in the spiked surface water during enclosure experiment #2 (E3d)

As shown in Figure 15, ibuprofen could not be observed after 40 cm (sampling point 2). Bezafibrate is recovered at about 1 %, while clofibric acid and diclofenac were found at levels of 80 % and 110 % of the initial amounts, respectively.
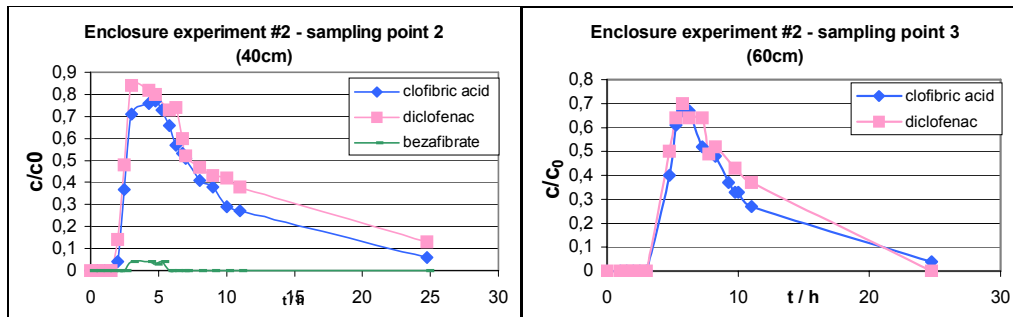
Figure 15. Breakthrough curves of pharmaceuticals measured at a depth of 40cm and 60cm in the enclosure during enclosure experiment #2 (E3d)

Clofibric acid and diclofenac were found at 65 % and 80 % of the infiltrated quantity after 60 cm (sampling point 3), respectively.

At sampling-point #4 (80cm depth) shown in Figure 16, the mass balance resulted in a recovery of 60% of the initial amount of diclofenac. For clofibric acid the results of enclosure experiment #2 did not confirm those of experiment #1. 55% of the initial quantity of clofibric acid was detected at sampling-point 4.
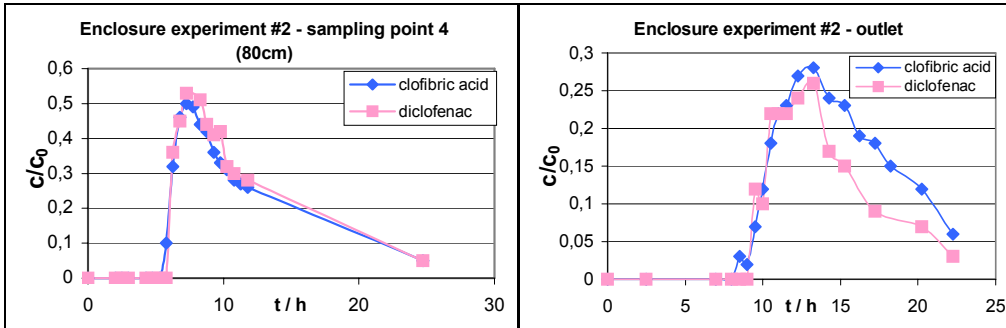
Figure 16. Breakthrough curves of pharmaceuticals measured at a depth of 80cm and enclosure outlet during enclosure experiment #2 (E3d)

This is still less than the amount that was recovered in the first two slow sand filtration experiments, but the dramatic decrease of the total amount of clofibric acid that was observed in the first enclosure experiment (35%) was not observed again.

Behavior of carbamazepine, clofibric acid, diclofenac, ibuprofen and primidone during experiment no. E4d

The third and fourth enclosure experiments were carried out during November 11th - November 12th and during November 25th - 26th. Opposite to enclosure experiment no. E2o and E3d, added target compounds were varied. Additionally to clofibric acid, diclofenac and ibuprofen, the antiepileptic drugs carbamazepine and primidone were spiked to the feed water of the enclosure. The parameters of the enclosure experiment E4d are shown in Table 6.

Table 6. Experimental conditions of enclosure experiment #3

Enclosure experiment #3 (E4d)		
Date	11.– 12.11.2003	
Flow rate	0,05 m^3/h	
Filtration velocity	1,2 m/d	
Initial concentration of pharmaceuticals	carbamazepine diclofenac ibuprofen	clofibric acid primidone
	2 - 3 µg/L	4 µg/L
Condition of the sediment surface	cleared	

Over a period of 50 hours during experiment no. 3, samples were collected at two different depths of 40 cm and 80 cm. After 2.6 hours all compounds excluding ibuprofen could be observed at maximum relative concentrations between 74 % and 96 % at the first sampling point (40 cm) as shown in Figure 17. Ibuprofen was only detected at a maximum relative concentration of 20 %.
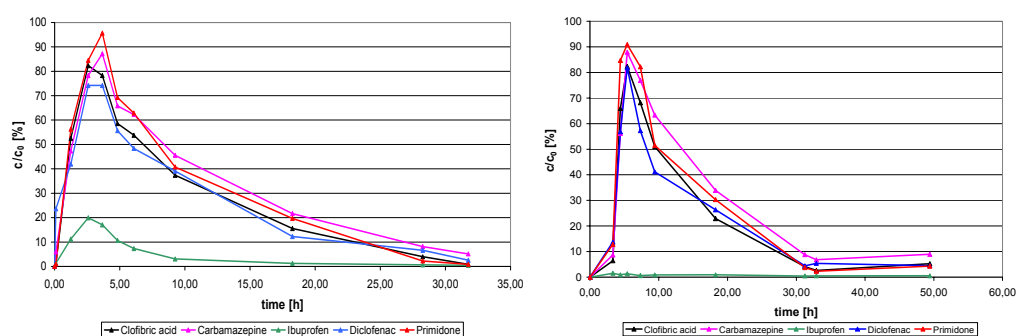
Figure 17. Breakthrough curves of pharmaceuticals measured at two different depths (40cm & 80cm) during enclosure experiment #3 (E4d).

At the second sampling point (80cm), ibuprofen concentrations were below the limit of quantification. The other compounds show maximum recoveries between 80 and 90 %.

Behavior of carbamazepine, clofibric acid, diclofenac, ibuprofen and primidone during experiment no. E5d

The fourth enclosure experiment was carried out during the 25. & 26.11.2003 and was a repeat of experiment E4d. The spectrum of spiked compounds and other experiment

parameters like flow rate etc. were unchanged and are shown in Table 7. Only the initial concentration of ibuprofen was increased to 4 - 5 µg/L to obtain concentrations above limit of quantification at the second sampling point (80 cm). Sediment surface was not cleared before the experiment.

Table 7. Experimental conditions of enclosure experiment #4

Enclosure experiment E5d		
Date	25.– 26.11.2003	
Flow rate	0,05 m^3/h	
Filtration velocity	1,2 m/d	
Initial concentration of pharmaceuticals	carbamazepine diclofenac	clofibric acid ibuprofen primidone
	2 - 3 µg/L	4 - 5 µg/L
Condition of the sediment surface	slightly developed clogging layer	

The results for the fourth enclosure experiment (E5d) were absolutely comparable to the former experiment E4d and are shown in Figure 18 . Carbamazepine, clofibric acid, diclofenac and primidone were observed with recoveries between 84 % and 96 % of initial concentrations after a passage of 40 cm at sampling point 1. In spite of the increased initial concentration, ibuprofen was again observed with a recovery around 20 %. That is very similar to the result of the former experiment. After a passage of 80 cm (sampling point 2) ibuprofen was below limit of quantification. The other substances show recoveries from 74 % to 84 %.
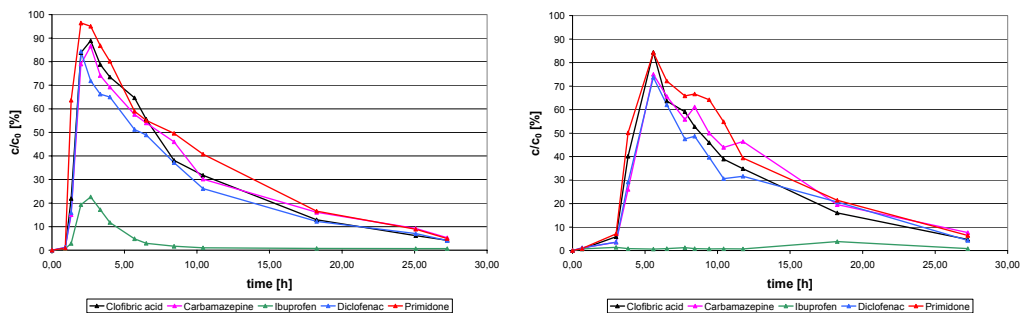
Figure 18. Breakthrough curves of pharmaceuticals measured at two different depths (40cm & 80cm) during enclosure experiment #4 (E5d).

Using the added tracer (sodium chloride) the experiment parameters like filtration and distance velocity etc. were determined by using Visual CXTFIT and are shown in Table 8.

Table 8. Calculated experiment parameters using Visual CXTFIT

experiment no.	E4d		E5d	
sampling point	40 cm	80 cm	40 cm	80 cm
condition of sediment surface	cleared	cleared	not cleared	not cleared
filtration velocity vf [m/h]	0.051	0.051	0.045	0.045
distance velocity va [m/h]	0.38	0.32	0.5	0.35
dispersion coefficient D [-]	0.008	0.02	0.04	0.08
dispersion length αL [cm]	2.11	6.3	8.00	22. 9
effective pore volume nf [%]	13.4	15.9	9.00	12. 9

The retardation coefficients and the attenuation coefficients of the investigated substances were calculated using the experiment parameters in Table 8. Results of Visual CXTFIT for the spiked drug residues are presented in Table 9.

All compounds showed retardation during the soil passage. Only minor attenuation coefficients ($\mu < 0.1$ h^{-1}) caused by adsorption or metabolism were observed for all tested compounds excluding ibuprofen. For ibuprofen a higher attenuation coefficient of 1.6 up to 2.0 was calculated. The condition of sediments surface did not have any significantly effect on the attenuation and the retardation coefficients of the compounds carbamazepine, clofibric acid, diclofenac and primidone. In contrast, for ibuprofen the retardation coefficient increased from 1.5 up to 2.9 after 80 cm of soil passage.

Table 9. Calculated attenuation and retardation coefficients using Virtual CXTFIT

Compound	Parameter	40 cm [cleared]	80 cm [cleared]	40 cm [not cleared]	80 cm [not cleared]
Clofibric acid	retardation coefficient R	1.4	1.5	1.2	1.5
	attenuation coefficient μ [h^{-1}]	0.00	0.05	0.00	0.00
Carbamazepine	retardation coefficient R	1.5	1.7	1.3	1.5
	attenuation coefficient μ [h^{-1}]	0.00	0.04	0.00	0.00
Diclofenac	retardation coefficient R	1.4	1.6	1.6	1.5
	attenuation coefficient μ [h^{-1}]	0.09	0.10	0.00	0.03
Ibuprofen	retardation coefficient R	1.6	1.5	2.0	2.9
	attenuation coefficient μ [h^{-1}]	1.6	2.0	2.0	2.0
Primidone	retardation coefficient R	1.0	1.5	1.0	1.3
	attenuation coefficient μ [h^{-1}]	0.00	0.00	0.00	0.00

1.3.2.5 Conclusions for the slow sand filter experiments and enclosure experiments

The results from the experiments at the UBA facilities show that sand filtration is an efficient method to remove several selected residues of pharmaceuticals such as ibuprofen and bezafibrate. This was confirmed by the slow sand filter experiments where both substances were not detected in the outlet. This result was also confirmed in enclosure experiments E2o & E3d where the calculated mass balance showed that both substances are already significantly attenuated in the first cm of the sand passage. Additionally, in enclosure experiments E4d (just cleared surface) and E5d (slightly developed colmation layer) ibuprofen has also been removed about 80 % after 40 cm soil passage. In enclosure experiment E3d, with a slightly developed clogging layer, the removal seemed to be even more efficient. This may indicate that ibuprofen and bezafibrate are subject to a microbial degradation and that their removal is not only a result of an adsorption to the sediment. This is also in line with results from other studies investigating these substances, which describe

bezafibrate as a substance with sorption properties (Ternes et al., 2002) and ibuprofen to be well degradable by microorganisms under aerobic conditions (Zwiener et al., 2000). For diclofenac the enclosure experiments approved the assumption of a photolytic degradation reported by Buser et al. (1998) . Thus, the rapid decrease of the diclofenac concentration that was observed in the first two experiments with slow sand filtration did not occur in the covered enclosure experiments carried out in the dark. Enclosure experiments E2o and E3d show that diclofenac can be significantly attenuated but not completely removed by sand filtration. Contrary to this attenuation rates of diclofenac observed during the enclosure experiments E4d and E5d were negligible. Clofibric acid showed a different and varying attenuation behavior in these experiments. Especially, the results of enclosure experiment E2o and enclosure experiments E4d and E5d as well as the first two experiments with slow sand filtration (SSF3 & SSF5) are contradictory. A recovered amount of only 35 % of the initial quantity after 80 cm sand passage in enclosure experiment (E2o) was not expected for this substance, which has been described as being rather persistent (Zwiener et al., 2000; Ternes et al., 2002, Andreozzi et al., 2003) and mobile (Mersmann et al., 2002) during groundwater recharge. As described above the first two experiments SSF3 & SSF5 seemed to confirm this behavior during sand filtration, too. Nevertheless, it was also reported that sand filtration has a certain ability to remove clofibric acid (Sacher et al., 2000; Preuß et al., 2001). Several suggestions were considered about the differences between the experiments that could possibly give an explanation for the observed differences. For example, it was suggested that there was an increased microbial activity caused by the high temperatures during enclosure experiment E2o in August 2003. On the other hand, results of the first two experiments were comparable, although data showed that at least air temperatures varied stronger between these experiments than for example between slow sand filter experiment SSF5 and enclosure experiment E2o. Other considerations were made concerning a possible adaption of microorganisms at the filtration facility after the first two experiments or experimental errors like the usage of methanol helping to dissolve the pharmaceuticals for the experiments at the slow sand filter. But finally the observed differences could not be explained satisfactorily. For the antiepileptic drugs carbamazepine and primidone no significant removals were observable during enclosure experiments E4d & E5d.

1.3.3 Column experiments

1.3.3.1 Long column experiments

Behavior of AMDOPH, bezafibrate, clofibric acid, diclofenac, and ibuprofen during long column experiments

The study investigating the mobility of pharmaceutical residues in the long column studies was divided into two experiments. At first, the selected compounds shown in Table 10 were added for two weeks (May 12th – May 26th) at a concentration of around 1.5 µg/l. Samples were only taken at the end of the soil column using an auto sampler for 13 weeks (until August 11th).

Table 10. Selected pharmaceuticals and some chemical properties

Compound	Structure	Mol. weight and formula	Log K_{ow}	solubility	Indication group
Diclofenac		296.2 $C_{14}H_{11}Cl_2NO_2$	4.51	2.37 mg/l	Antiphlogistic/ Antirheumatic
Clofibric Acid		214.7 $C_{10}H_{11}ClO_3$	2.57	582.5 mg/l	Blood lipid regulator (Metabolite)
Ibuprofen		203.3 $C_{13}H_{18}O_2$	3.97	21.0 mg/l	Antiphlogistic/ Antirheumatic
Bezafibrate		361.8 $C_{19}H_{20}ClNO_4$	4.25	k.A.	Blood lipid regulator
AMDOPH		263.2 $C_{13}H_{17}N_3O_3$	k.A.	k.A.	Metabolite of the antiphlogistic Dimethylamino-phenazone (no longer produced since 1978)

In addition, samples from sampling point 1-0 were taken twice to measure the actual influent/feed concentration of the pharmaceuticals. In the second experiment, the inflow/feed water was spiked at the same concentration for one week (June 23rd – June 30th) to investigate the behavior of the added compounds within the first few decimeters of the

23

column. Assuming that degradation and adsorption take place especially in the first meter of the column, samples have been taken manually once a day at sampling points 1-1 (21 cm), 1-3 (84 cm) and 1-4 (166 cm). A list of all collected samples is shown in table 11.

Table 11 Overview of all samples collected during this study.

Description	Volume*	Dates of Sampling	Details
Lake Tegel	100 ml	May: 12., 23.; June: 3., 12., 24. July: 7., 21.; August: 4.	Taken from the storage tank after each filling
Col 1-0 (ColIn)	50 ml	May: 12., 23.; June: 26., 30.	
Col 1-1 (21 cm)	50 ml	June: 20., 23.-30. July: 1.-5., 7., 8.	No samples on 21./22. 6. and 6.7. (weekend)
Col 1-3 (84 cm)	50 ml	June: 20., 23.-30. July: 1.-5., 7., 8.	No samples on 21./22. 6. and 6.7. (weekend)
Col 1-4 (166 cm)	50 ml	June: 20., 23.-30. July: 1.-5., 7., 8.	No samples on 21./22. 6. and 6.7. (weekend)
Col6Out (column outlet)	100 ml	May: 16.-26. June: 3.-30. July: 1.-31. August: 1.-11.	

* volume used for one analysis

Influent concentrations of added pharmaceuticals

The target influent concentrations of all four added compounds were 2 µg/l, respectively. To achieve this concentration, a stock solution (10 mg/l) was prepared using S0-solutions (1 mg/ml in ethyl acetate). The stock solution was used for both experiments. The determined concentration at the influent are shown in Table 12

Table 12. Measured concentrations of the pharmaceuticals at sample point 1-0 (influent)

Sample name	Diclofenac [µg/l]	Clofibric acid [µg/l]	Ibuprofen [µg/l]	Bezafibrate [µg/l]
Col 1-0 13.5.	1.4	1.2	1.3	2.1
Col 1-0 23.5.	1.3	1.6	1.0	1.9

To avoid an increase of the natural DOC in the influent water, organic solvents had to be evaporated and compounds were then re-dissolved in purified water. Analysis of the influent/feed water from Lake Tegel revealed the presence of AMDOPH at concentrations between 430 and 530 ng/l (median value: 500 ng/l – see also box plot in Figure 19).

24

Background concentrations of the four added compounds have usually been below limits of determination.
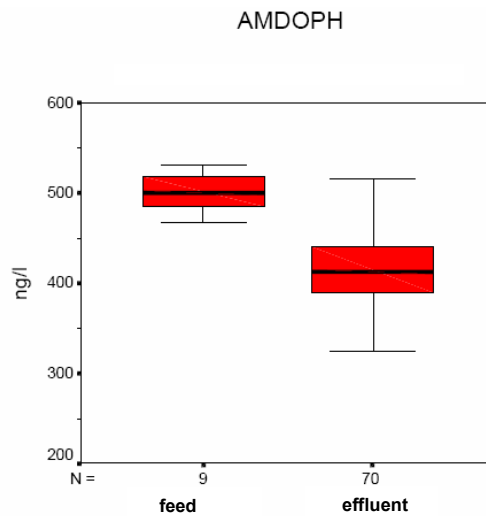
Figure 19. Distribution of AMDOPH concentrations before (feed water) and after soil passage (column effluent).

First experiment

During the first experiment (influent spiked from 5/12/03 to 5/26/03), only the effluent concentrations of the pharmaceutical residues have been measured (Col 6.21). It has been expected that at least clofibric acid (that has been characterized in the literature as hardly degradable and very mobile) can be measured at the end of the column. Instead, the effluent concentrations of all four added compounds (clofibric acid, diclofenac, ibuprofen and bezafibrate) were below limit of detection. Only AMDOPH which was already detected in the surface water from Lake Tegel was also detected in the effluent of the column. Statistical calculations show a little decrease – median concentrations were decreased from 500 ng/l to 420 ng/l (16 %) (see box plot in Figure 19).

Second experiment

During the second experiment (pharmaceuticals added from 23rd to 30th of June), samples were taken only from the first few sampling points to investigate if the elimination process

taking place within the first decimeters of the soil column. Samples were taken daily (see Table) from sample points Col 1.1 (21 cm), Col 1.3 (84 cm), and Col 1.4 (166 cm). The breakthrough curves are compared with a modeled tracer breakthrough curve that was generated using the parameters gained from a Gd-tracer experiment (Table 13). The modeled curve simulates the behavior of the Gd-tracer added together with the pharmaceuticals over the same time period.

Table 13. Parameters of the soil column derived from a Gd-tracer experiment

Mean velocity	0.91 m/d
Porosity	31.9 %
Dispersion	0.04 m
Dispersion coefficient	0.036 m²/d
Average residence time	33 days

Breakthrough curves of the four added pharmaceutical residues at the three analyzed sampling points are shown in Figure 20 - Figure 22.
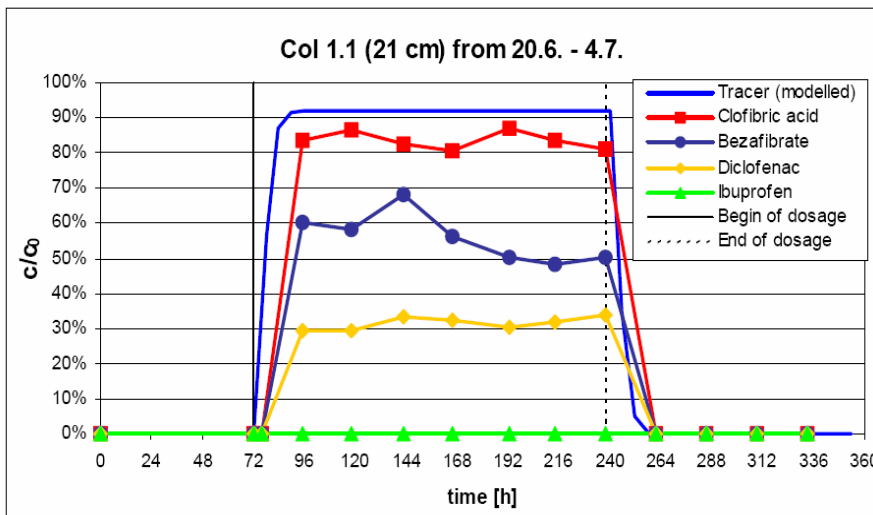
Figure 20. Breakthrough curves for the spiked pharmaceuticals at Col 1.1 (21 cm)

As shown in Figure 20, the concentrations of the four added pharmaceuticals considerably changed already after a soil passage of only 21 cm. The concentration of ibuprofen was already below the detection limit of 20 ng/l.

26
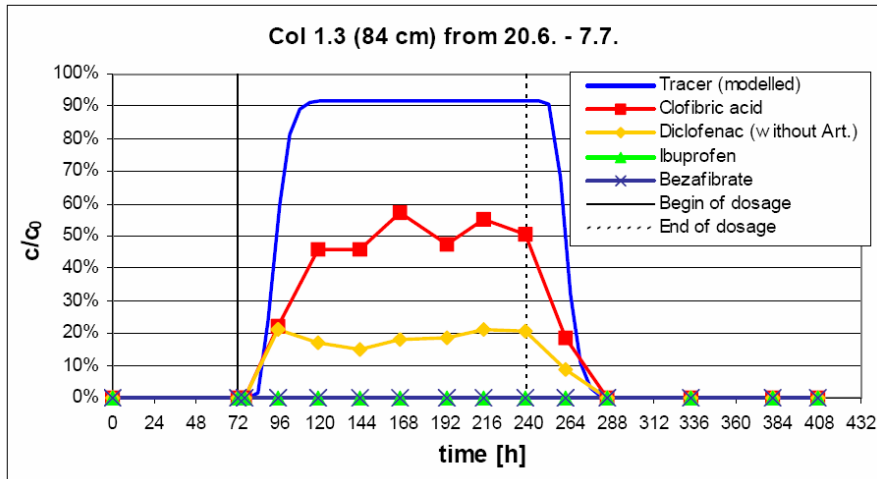
Figure 21. Breakthrough curves for the spiked pharmaceuticals at Col 1.3 (84 cm)

After 84 cm (Col 1.3) presented in Figure 21, bezafibrate was also not detectable any longer. The concentration of clofibric acid had also decreased to approximately 50% of the initial concentration.
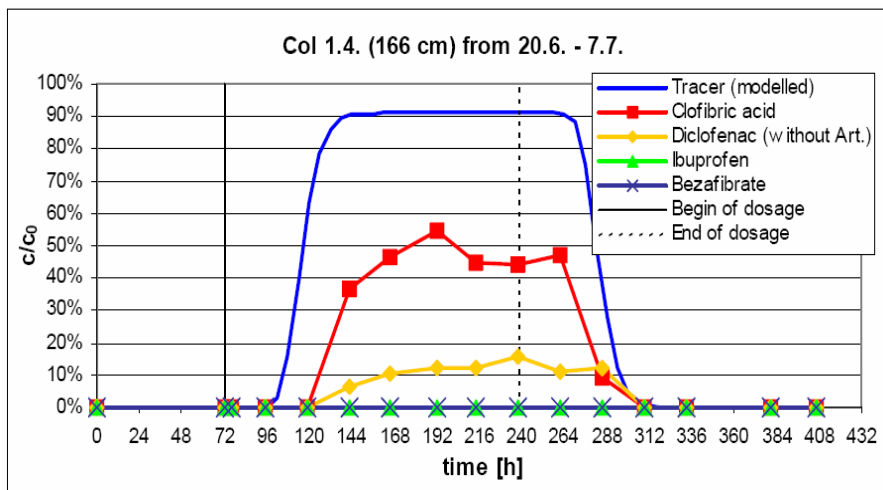
Figure 22. Breakthrough curves for the spiked pharmaceuticals at Col 1.4 (166 cm)

As shown in Figure 12 the concentrations of the remaining two compounds (clofibric acid and diclofenac) only decreased slightly at 166 cm (Col 1.4), compared to sample point Col 1.3. It has to be considered that due to the low resolution in time (one sample per day), the real start or ending of a peak may differ by several hours.

27

1.3.3.2   Summary of the results

Comparing the results of the sample points Col 1.0 (influent), Col 1.1, Col 1.3, Col 1.4 und Col 6.21 (effluent), the following points can be summarized:

- all four compounds (clofibric acid, diclofenac, ibuprofen, bezafibrate) added to the feed water were removed within the soil column system,

- the concentration of AMDOPH was reduced by 15-20%,

- ibuprofen was eliminated within the first 21 cm of the soil column,

- bezafibrate was eliminated within the first 84 cm of the soil column

- the concentration of diclofenac was reduced by around 70% within the first 21 cm, and thereafter it continued to decrease slowly,

- the concentration of clofibric acid was reduced by approximately 50% within the first 84 cm, and thereafter it continued to decrease slowly.

It can be seen that the largest decrease in concentrations takes place within the first decimeters of the soil column. This zone is also characterized by an extended microbial degradation, as confirmed by the elimination of the DOC.

1.3.3.3   Conclusions

The experiments at the soil column system in Marienfelde revealed some unexpected results. A complete removal of clofibric acid has not been reported in the literature until now. In fact, some studies even described clofibric acid as an almost persistent and tracer-like compound (Heberer, 2002; Mersmann, 2002,Ternes et al., 2002;Winkler et al., 2001, Zwiener et al. , 2001;Zwiener et al., 2002). Only Preuß et al., 2001 reported a decrease of clofibric acid concentrations by 40-60% in a soil column experiment. The concentration of diclofenac was reduced comparably quickly. Already at the first sampling point (after 21 cm), only 30% of the initial concentration could be measured. Reported degradation of diclofenac in batch experiments ranged from only a few percent, to a maximum of 50% (Möhle et. al, 1999; Zwiener et al., 2002). In a soil column experiment conducted by Mersmann et al.,

2002), no removal of diclofenac could be observed after passage through a 35 cm long column. On the contrary, Preuß et al., 2001 reported a reduction of diclofenac concentrations by 60-80% after 80 cm. The easy degradability of ibuprofen, as described in the literature (Buser et al., 1999; Stumpf et al., 1998; Winkler et al., 2001; Zwiener et al., 2000) completely removed (concentration below limit of detection).

1.3.3.4   Small columns

The aim of these investigations was to examine the behavior of selected drug residues in short retention columns at different redox conditions. Altogether the behavior of nine pharmaceutically active compounds including AMDOPH, bezafibrate, carbamazepine, clofibric acid, diclofenac, indometacine, primidone and propyphenazone was examined. The influences and efficiency of attenuation during the infiltration process should be clearifieed and assigned to definite parameters which are hardly to be precisely recognized at the field sites. The experiments were carried out in cooperation with the organics group of the Technical University Berlin.

Three experiments were carried out using eight columns with various conditions. Apart of columns no. 7 & 8 which were filled with real bank material and aquifer material, all other columns were filled with technical sand. The columns had a length of 1 m with a diameter of 0.14 m. Each column was charged daily with 800 mL of lake Tegel surface water and spiked during the three experiments with different concentrations of selected drug residues. The flow of 0.8 L/d leads to a retention time around 6 days. Columns no. 4, 5 and 6 were charged with anoxic water and should be used for a comparisons with oxic water charged columns. The effluent of column no. 2 charged column no. 5, so that means apllied compounds passaging 2 meters of technical sand under anoxic conditions. The influent of column no. 0 was additionally spiked with sodiumazide to achieve abiotic conditions. At columns no. 3 & 6, starch, an easily degradable substance, was added to the influent to get anaerobic conditions during column passage. The influent of column no. 4 was spiked with nitrate to promote denitrification. Table 14 shows parameters and conditions of the investigated columns.

Table 14. Column conditions including filling material, lenght, type of charging water, added compounds and the individual redox condition trend.

column no.	0	1	3	4	5	6	7	8
Material	tech. sand	tech. sand	tech. sand	tech. sand	tech. sand	tech. sand	bank	aquifer
length [m]	1	1	1	1	2	1	1	1
type of charging water	oxic	oxic	oxic	anoxic	anoxic	anoxic	oxic	oxic
added substances	10 g/L NaN3	-	3 mg/L starch	5 mg/L NO3-N		3 mg/L starch		
redox condition trend	oxic (abiotic)	oxic	oxic anoxic anaerobic	anoxic (denitri-fication)	anoxic	anoxic anaerobic	oxic anoxic anaerob	oxic

Each experiment was carried out within four weeks and was started with an equilibration time of three weeks. The initial concentrations of the investigated compounds were selected at concentrations of 10 µg/L, 5 µg/L and 1.3 µg/L, during the experiments A, B and C. The oxic and anoxic influents were sampled during week three and four and the individual effluents were sampled three times during the fourth week. Caused by a power failure during the first experiment, the pump that mixed surface water with investigated compounds was out of order and the gained data of the column effluents were unusable. Additionally, some unexplainable effects (like higher effluent concentrations than influent ones etc.) lead to data that were hard to interpret and so the results could only be considered as tendencies for the behavior of the investigated compounds.

1.3.3.5   Results

Generally higher attenuation rates were observed at the columns fed with oxic surface water as shown in Table 15. Surprisingly, almost all applied drug residues showed removal rates between 23 % and more than 95 % at the abiotic column no. 0 where only sorption effects should take affect. Using the individual logP$_{OW}$ the behaviour of bezafibrate (log P$_{OW}$ 4.2) and indometacine (log P$_{OW}$ 4.27) could be explained by their high sorption potential. However, diclofenac was also attenuated about 61 %, despite of the reported low log P$_{OW}$ of 1.13. The low observed sorption between 0 % and 50 % of AMDOPH (log P$_{OW}$ unknown), carbamazepine (log P$_{OW}$ 2.45), clofibric acid (log P$_{OW}$ 3.1), ibuprofen (log P$_{OW}$ 3,97) and primidone (log P$_{OW}$ 0.91) seem to be relatively independent from the individual log P$_{OW}$. Propyphenazone (log P$_{OW}$ 3.1) did not show any significant sorption rate at the abiotic column no.0.

Table 15. Attenuation tendencies of the investigated drug residues

	Effluent column no. 0	Effluent column no. 1	Effluent column no. 3	Effluent column no. 7	Effluent column no. 8	Effluent column no. 4	Effluent column no. 5	Effluent column no. 6
AMDOPH	-	-	-	-	-	-	-	-
Bezafibrate	+	++	++	++	++	++	++	-
Carbamazepine	-	-	-	-	-	-	-	-
Clofibric acid	-	+	+	-	-	+	+	-
Diclofenac	+	-	+	-	++	-	+	-
Ibuprofen	+	++	++	++	++	++	++	++
Indometacine	++	-	++	++	++	-	++	-
Primidone	-	-	-	-	-	-	-	-
Propyphenazone	-	+	+	+	+	-	+	-

-     low attenuation < 45 %
+   medium attenuation between 46 % and 95 %
++   high attenuation between >95 %

At column no. 1 (aerobic) AMDOPH, carbamazepine, diclofenac and primidone showed low attenuation rates up to 45 %. Despite of the behaviour at column no. 0 indometacine observed attenuation rates were lower than 30 %. Bezafibrate and ibuprofen were observed with high attenuation rates over 95 %. Medium removal rates (46 - 95 %) were recognized for propyphenazone and for clofibric acid that has previously been reported as a highly persistent compound and tracer like compound (Mersmann et al. Heberer, Ternes et al. 2002, Winkler et al. 2001, Zwiener 2000a&b).

The fate of the applied compounds at column no. 3 with successive conditions inside (aerobic, anoxic, anaerobic) was comparable to their behaviour at column no. 1. However, diclofenac and propyphenazone were observed with a medium attenuation rate. The determined removal of clofibric acid was lower (63 %) than at column no. 1.

The column no. 4 fed with anoxic water and added nitrate to increase denitrification was sustainable (> 95 %) for the removal of bezafibrate and ibuprofen. AMDOPH, carbamazepine, indometacine and primidone only show insignificant attenuation rates around 20 %. Clofibric acid, diclofenac and propyphenazone were observed with a medium attenuation rate 34 % and 49 %.

At column no. 5 with anoxic conditions and a length of 2 meters equal attenuation tendencies to column no. 3 (suksessive conditions) were recognized. AMDOPH, carbamazepine and primidone showed low attenuation. Clofibric acid and diclofenac were observed with a medium attenuation rate of 52 % at the effluent. Highest attenuations (more than 95 % %) were determined for bezafibrate, ibuprofen, indometacine and propyphenazone.

Column no. 6 shows only for diclofenac low attenuation rates of 30 % and complete removal of ibuprofen. The concentrations of the other compounds were not obviously decreased during soil passage under anaerobic conditions.

At column no. 7 filled with real bank material, high attenuation rates (> 95 %) were observed for bezafibrate, ibuprofen and indometacine. Propyphenazone was removed about 83 % and clofibric acid was only slightly attenuated around 37 % %. No significant attenuations were observed for AMDOPH, carbamazepine and primidone.

During the passage of real aquifer material at column no. 8 with oxic conditions, only AMDOPH, carbamazepine, clofibric acid and primidone showed no significant attenuation rates. The remained compounds were efficiently attenuated (> 95 %).

1.3.3.6   Conclusions

AMDOPH (log POW unknown), carbamazepine (log POW 2.45) and primidone (log POW 0.91)

- showed only low sorption under abiotic conditions (column no. 0)
- concentrations were only partly decreased (up to 40 %) in almost all of the oxic charged columns (column no. 1 & 3)
- under anoxic or anaerobic conditions no significant removal was observed (column no. 4, 5 & 6)
- similar behaviour at the columns filled with real field site material and with successive redox conditions (columns no. 7) or exclusive oxic conditions (column 8)
- transport is comparable to results at the field sites GWA & TS Tegel and TS Wannsee (chapters 1.4.3, 1.4.4 & 1.4.6).

Bezafibrate (log POW 4.2)

- a sorption of 69 % under abiotic conditions (column no. 0) was observed
- passing technical sand under oxic or successive redox conditions (columns no. 1 & 3) initial concentration were also reduced by more than 97 %
- high attenuation rates (>97 %) were noticed under anoxic - denitrifying and exclusively anoxic conditions (columns no. 4 & 5)

33

- real bank and aquifer materials (columns no. 7 & 8) lead to high removal (>97 %). This behaviour is comparable to the fate of bezafibrate at field sites lake Tegel and lake Wannsee (chapters 1.4.3, 1.4.4 & 1.4.6).

Clofibric acid (log POW 3.1)

- under abiotic conditions (column no. 0) low attenuation (43 %) was found
- observed low and medium attenuations were between no obvious removal and 63 % removal in almost all other columns
- under oxic conditions (column no. 1), a decrease of 87 % was noticed and during the passage of column no. 5 (filled with technical sand and anoxic conditions), an attenuation of 52 % was observed
- low attenuation rates of 37 % and 42 % were determined in the columns filled with real field site materials. This result is similar to the observations at transects Tegel and Wannsee (chapters 1.4.3, 1.4.4 & 1.4.6).

Diclofenac (log POW 1.13)

- abiotic conditions (column no. 0) lead to a medium removal rate of 61 %
- medium attenuation rate of 52 % and of 57 % were observed under long anoxic passage (column no. 5) and during passage oxic - anoxic conditions (column no. 3), respectively
- low attenuation (45 %) were observed under exclusive oxic (column no. 1) or (in column no. 6) exclusive anoxic conditions (decrease of about 30 %)
- the noticed medium attenuation rate of 39 % in column no. 7 filled with bank material is comparable to the field sites investigations but in column no. 8 filled with aquifer material a high removal (> 95 %) was observed.

Ibuprofen (log POW 2.45)

- a sorption of 49 % was noticed under abiotic conditions (column no.0)
- high removal rates (> 95 %) were determined in the oxic and anoxic charged columns
- passage of bank material (column no. 7) and aquifer material (column no. 8) under oxic anoxic conditions leads to a high removal (> 95 %)

Indometacine (log POW 4.27)

- under abiotic conditions (column no. 0) a sorption rate of > 95 % was determined
- surprisingly only low removal / sorption was observed under oxic (column no. 1) conditions
- In columns under oxic - anoxic (column no. 3) and anoxic - anaerobic (column no. 6) conditions high attenuation rates (> 95 %) were observed
- passing bank or aquifer material (columns no. 7 & 8) leads to high attenuation rates (> 95 %) comparable to the behaviour at the field sites (chapters 1.4.3, 1.4.4 & 1.4.6).

Propyphenazone (log POW 3.1)

- showed low sorption (23 %) under abiotic conditions (column no. 0)
- low attenuation of about 39 % were observed under anoxic – denitrifying conditions (column no. 4)
- medium removal rates between 66 % and 86 %) could be noticed under oxic conditions (column no. 1), successive redox conditions (column no. 3) and in column no. 5 with a 2 meter soil passage under anoxic conditions
- passing real bank / aquifer material leads to medium removal rates of 83 % (columns no. 7) and 89 % (column no. 8), respectively. This behavior was comparable to the fate at the investigated field sites (chapters 1.4.3, 1.4.4 & 1.4.6).

Generally, aquifer material with a oxic redox regime seems to have the highest potential for the removal of the investigated compounds. Oxic charged column with successive redox conditions (column no. 3) and anoxic conditions and greater passage time at column no. 5 leads to comparable attenuations for all investigated drug residues. Easily degradable dissolved organic carbon (e.g. starch) under anoxic conditions (column no. 6) seems to reduce the removal potential for the applied compounds. In opposite to this, added starch under successive redox conditions (column no.3) did not show this inhibiting effect. Surprising results in the abiotic column no. 0 may be explainable by high sodium azide concentration (10 g/L) of the charging surface water. This properly lead to a displacement of balance of applied compounds between charging water and soil.

1.4 Field site investigations

1.4.1 Surface water preparation plant Tegel

The OWA Tegel located north of lake Tegel is used for mechanical purification and phosphate elimination of surface water influxing lake Tegel (influxes from the Nordgraben receiving the effluents from the STP Schönerlinde and from the Tegeler Fließ). Additionally, water can be pumped bidirectionally through a six kilometres long pipeline between river Havel and lake Tegel. Corresponding to the influxes and depending on the amounts of rain in summer or winter it is necessary to guarantee a relative constant discharge of 3 m^3/s *phosphate reduced water* to be discharged into lake Tegel. Table 16 shows the amount from the influxes and the amounts pumped through the lake pipeline into lake Tegel or respectively the river Havel.

The OWA Tegel was sampled monthly starting in January 2004 and was accomplished in July 2004. Additionally, two weeks with daily sampling were included. The first one during winter from January, 27th until February, 1st and the second one from July, 25th till July to 31st in 2004. The lake pipeline was sampled monthly at the same days of the influent and effluent sampling.

Table 16. Total discharge into Lake Tegel from the influxes Nordgraben & Tegeler Fließ. The direction and amounts of water pumped through the lake pipeline.

	Amounts of water [m3]			
Sampling date	**Nordgraben**	**Tegeler Fließ**	**Lake pipeline to the OWA Tegel**	**Lake pipeline to Havel**
19.01.2004	121.000	64.000	0	27.500
16.02.2004	104.500	60.500	0	26.500
15.03.2004	115.000	31.000	101.000	0
19.04.2004	113.500	26.000	153.000	0
24.05.2004	99.000	23.500	70.000	0
21.06.2004	84.500	24.000	106.000	0
26.07.2004	124.000	23.500	155.000	0

During this investigation eight drug residues were observed and quantified up to the µg/L range, as reported in Table 17.

Table 17. Drug residues with positive findings and their minimum, median and maximum concentrations [ng/L]

	Influent			Effluent			Lake pipeline		
	n=20			n=20			n=7		
	min	median	max	min	median	max	min	median	max
AMDOPH	126	307	419	146	323	475	133	362	930
Bezafibrate	35	159	453	< LOQ*	173	277	< LOQ*	< LOQ*	< LOQ*
Carbamazepine	675	1359	3452	866	1410	3023	171	344	651
Clofibric acid	52	85	141	40	83	123	< LOQ	19	28
Diclofenac	438	976	1522	478	1033	1583	35	68	263
Primidone	172	474	770	167	492	730	30	74	170
Propyphenazone	49	90	137	10	57	122	42	117	172
Indometacine	< LOQ*	97	514	21	110	417	< LOQ*	< LOQ*	189

*LOQ   limit of quantification

1.4.1.1   AMDOPH

As shown in Figure 23, AMDOPH was detected at concentrations of 120 ng/L up to 460 ng/L in influent and effluent samples. Concentrations in the lake pipeline vary between 130 ng/L and 930 ng/L. The high concentrations of AMDOPH in the lake pipeline between March and July 2004 are from the sampling location of the lake pipeline near the river Oberhavel. Comparing the median concentrations of 307 ng/L in influent water and 323 ng/L in effluent water, the values are within the analytical measurement accuracy for AMDOPH.
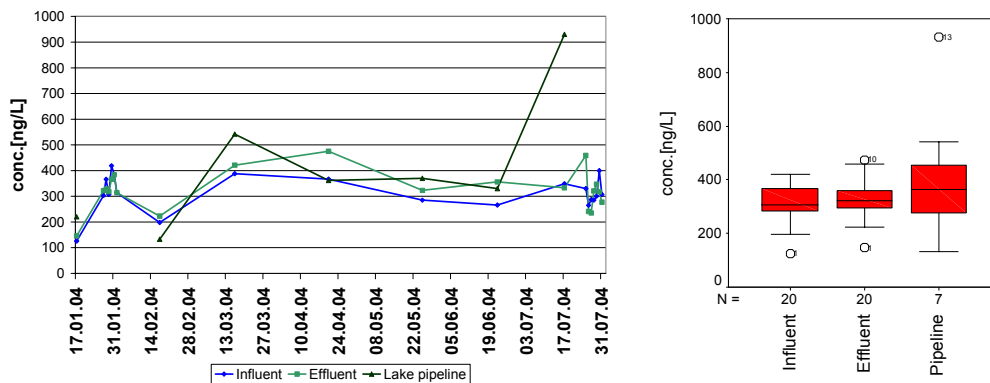
Figure 23. Fate of AMDOPH during the passage of the OWA Tegel.
(a: time series, b: box plots)

1.4.1.2   Bezafibrate

As illustrated in Figure 24, bezafibrate concentrations between the limit of quantification of 50 ng/L for bezafibrate in surface water and 453 ng/L were detected in the three compartments of the OWA Tegel. Similar to AMDOPH, the median concentrations of the influent (159 ng/L) and the effluent (173 ng/L) showed no great difference. The observed concentrations in the lake pipeline were below the limit of quantification.
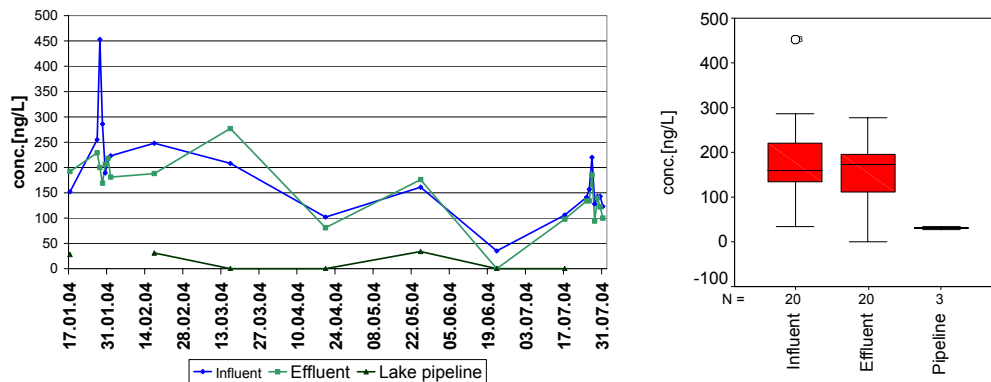
Figure 24. Fate of bezafibrate during the passage of the OWA Tegel.
(a: time series, b: box plots)

1.4.1.3   Carbamazepine

Carbamazepine was detected in influent and effluent water at concentrations between 675 ng/L and 3450 ng/L, as shown in Figure 25. No significant discrepancy of the median concentrations of 1359 ng/L (influent) and 1410 ng/L (effluent) were recognized. At the lake pipeline minor concentrations around a median of 344 ng/L were measured.
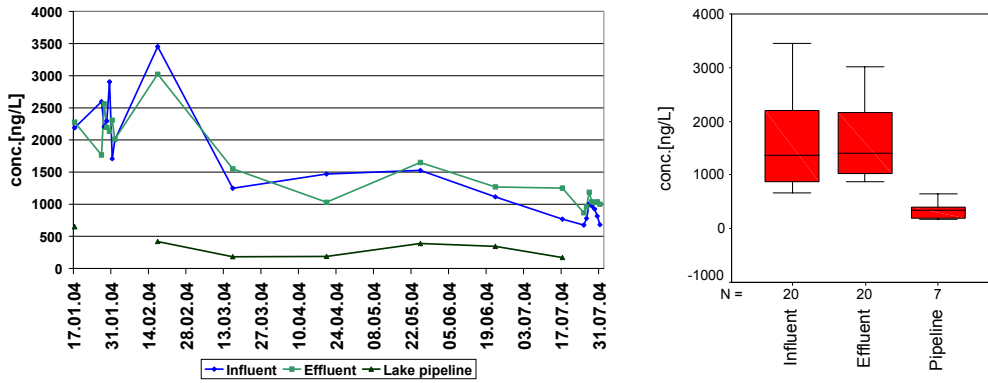
Figure 25. Fate of carbamazepine during the passage of the OWA Tegel.
(a: time series, b: box plots)

1.4.1.4 Clofibric acid

As shown in Figure 26, clofibric acid was observed at concentrations between 40 ng/L and 141 ng/L at the influent and effluent sampling locations. The median concentrations of 85 ng/L (influent) and 83 ng/L (effluent) were similar. In the lake pipeline, clofibric acid concentrations lower than the limit of quantification and up to 28 ng/L were found.
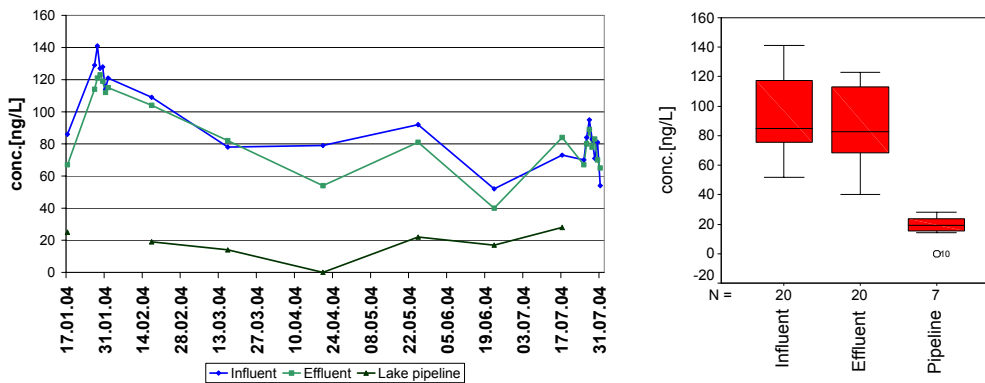
Figure 26. Fate of clofibric acid during the passage of the OWA Tegel.
(a: time series, b: box plots)

39

1.4.1.5   Diclofenac

The antiphlogistic / antirheumatic drug diclofenac was detected in influent water and effluent water in a concentration range starting at 438 ng/L up to 1583 ng/L as presented in Figure 27. Similar to the previous described compounds, the comparison between the median concentrations of 976 ng/L in influent and 1033 ng/L effluent water showed no clear difference. Concentrations in the pipeline varied between 35 ng/L and 263 ng/L with a median value of 68 ng/L.
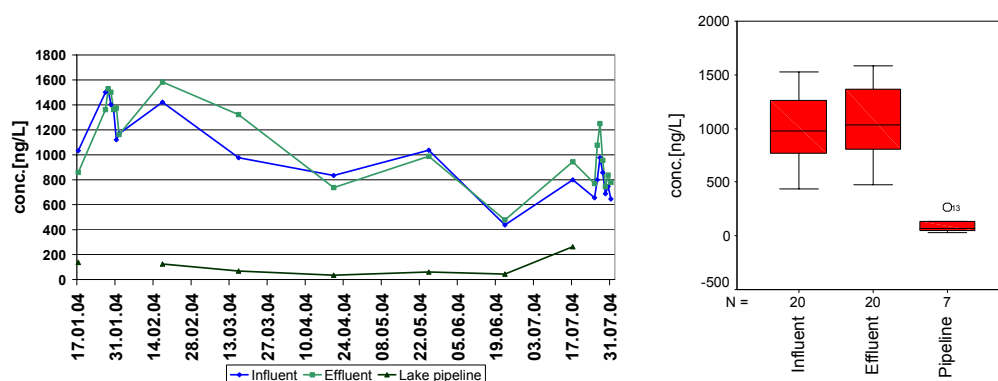
Figure 27. Fate of diclofenac during the passage of the OWA Tegel.
(a: time series, b: box plots)

1.4.1.6   Indometacine

Indometacine, a pharmaceutical with antiphlogistic / antirheumatic features, was observed with concentrations (displayed in Figure 28) between the limit of quantification and 137 ng/L in influent and effluent water. During the investigation, detected concentrations unexpectedly started to increase in March 2004 from around 90 ng/L to a maximum of 514 ng/L at July 27th. The median concentrations at both compartments were very comparable with amounts of 97 ng/L and 110 ng/L. At lake pipeline a minimum below the limit of quantification and 189 ng/L were recognized.
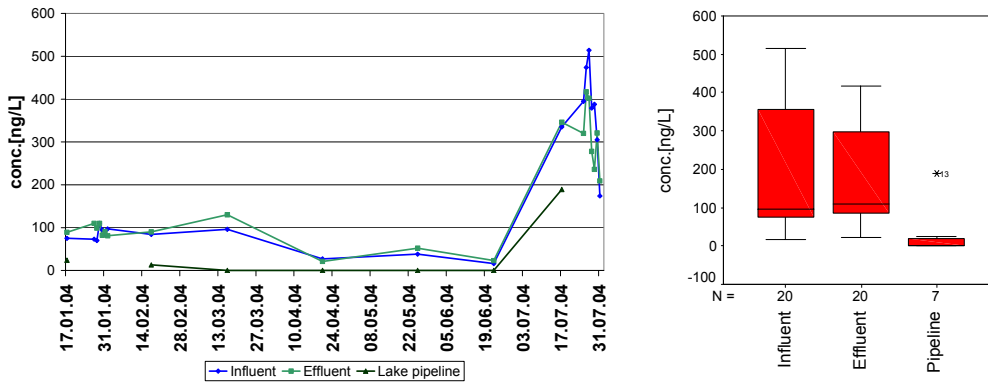
Figure 28. Fate of indometacine during the passage of the OWA Tegel.
(a: time series, b: box plots)

1.4.1.7   Primidone

As presented in Figure 29, primidone concentrations between 167 ng/L and 770 ng/L were found in the influent and the effluent water. The antiepileptic drug was observed with median concentrations of 474 ng/L (influent) and 492 ng/L (effluent). Thus, a significant removal during passage the treatment processes of the facility was not noticed. Concentrations of 35 ng/L up to 263 ng/L and a median value of 68 ng/L were detected.
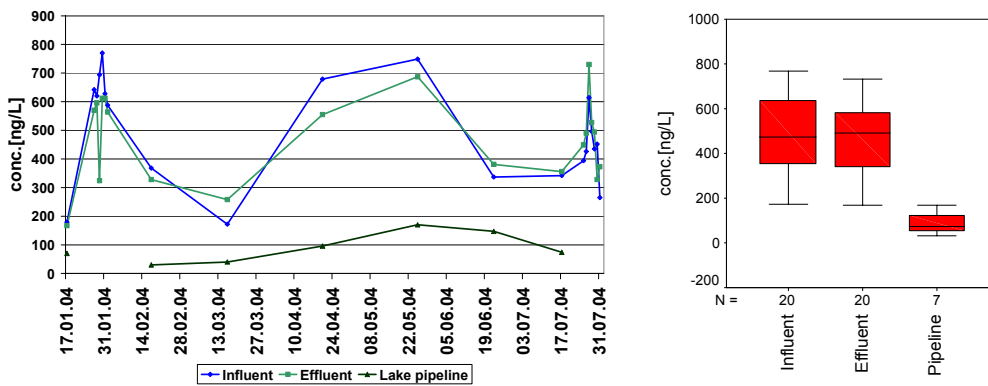
Figure 29. Fate of primidone during the passage of the OWA Tegel.
(a: time series, b: box plots)

1.4.1.8   Propyphenazone

Propyphenazone concentrations between 10 ng/L and 137 ng/L were detected in influent and effluent water, as also shown in Figure 30. The median concentrations of 90 ng/L (influent) and 57 ng/L (effluent) reveal an attenuation rate of 36 % during the passage. The observed concentrations in pipeline water range from 42 ng/L up to 172 ng/L and a median value of 117 ng/L, are comparable to the concentrations found in the influent water. This effect can be explained because propyphenazone is discharging from the same superfund site as AMDOPH and is additionally in steady use as an antiphlogistic / antirheumatic drug.
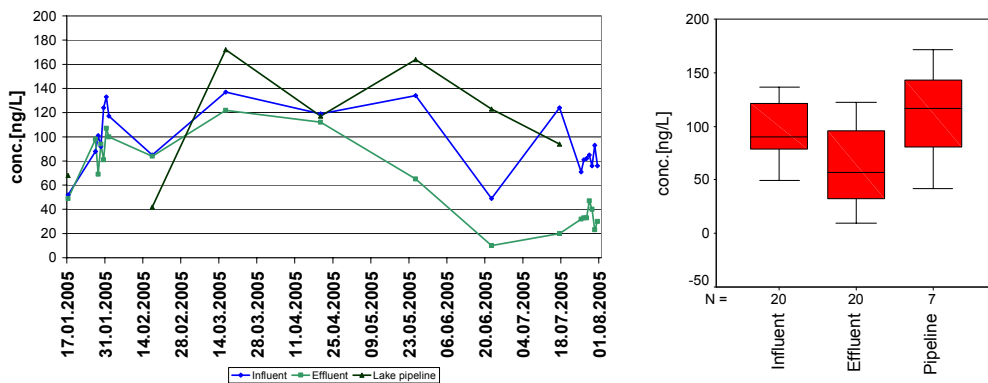
Figure 30. Fate of propyphenazone during the passage of the OWA Tegel.
(a: time series, b: box plots)

1.4.2 Conclusions

During the investigation at the OWA Tegel, eight different PhAC's were observed. As expected these compounds are the same as those detected in surface water of transect Tegel, namely AMDOPH, bezafibrate, carbamazepine, clofibric acid, diclofenac, primidone, propyphenazone, and indometacine. Comparing the detected influent and effluent median concentrations, no significant attenuation rates were observed. The individual case of propyphenazone showed an attenuation rate of 36 % during April and July 2004. Maybe this could be interpreted by a better removal behavior during warmer parts of the year. Detected concentrations at sampling location of the pipeline water were negligible for all compounds except for AMDOPH and propyphenazone. These two phenazone-type derivatives were discharged into the environment by spills from a pharmaceutical plant located north-west of Berlin and are transported to the city via the river Oberhavel. Because of the short sampling period of only six month a seasonal effects or variations of the concentrations of the drug residues could not be observed.

1.4.3 Groundwater replenishment site Tegel (GWA)

The measurements at the GWA Tegel started in July 2002 and were carried out over a 12 months period. Sampling points TEG366 and TEG365 and the water supply well 20 were sampled for 12 months, whereas sampling points TEG247, TEG248 and TEG342 were monitored for 8 months (July 2002 to February 2003) and sampling points TEG368, TEG369OP, TEG369UP, TEG370OP und TEG370 UP for 6 months (January 2003 to June 2003).

1.4.3.1 Results from the GWA investigations (July 2002 to June 2003)

In the monthly measurements at the transect GWA-Tegel 8 PhAC's and 5 other contaminants were detected. The drug residues were bezafibrate, carbamazepine, diclofenac, indometacine, primidone, propyphenazone and the drug metabolites clofibric acid and AMDOPH. Furthermore, the pesticides 2,4-D, dichlorprop, MCPA and mecoprop as well as NPS (metabolite of a corrosion inhibitor) were also found in these samples. Figure 31 shows a MID-chromatogramm of the PFBBr-derivatized extract of sample RP 3 collected in November 2002. The antiepileptic drugs carbamazepine and primidone were only analyzed with the MTBSTFA method and do therefore not appear in this chromatogramm.
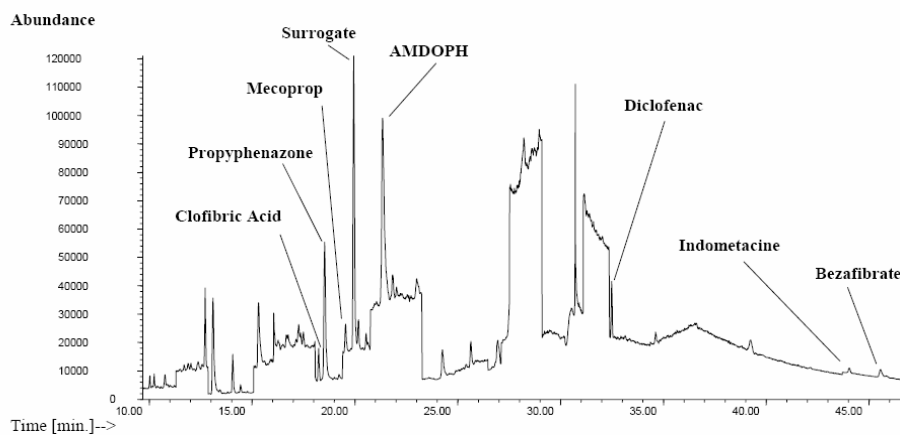
Figure 31. MID-chromatogram of the derivatized extract of sample RP 3 collected in November 2002

A summary of all results is shown in Table 18. It compiles the mean concentrations (n=12/8/6) of drugs and drug metabolites detected at the individual sampling points

throughout the entire sampling period. The individual PhAC's show a very different removal behaviour on their way on the soil passage to water-supply well 20.

Table 18. Mean concentrations [ng/l] of observed PhAC's throughout July 2002 to June 2003

	RP 3	TEG366	TEG365	TEG247	TEG368	TEG248	TEG369 OP	TEG369 UP	Well 20	TEG370OP	TEG370 UP	TEG342
	n=12	n=12	n=12	n=8	n=6	n=8	n=6	n=6	n=11	n=6	n=6	n=8
Flowdirection:												
AMDOPH	455	440	395	425	390	315	300	330	1570	1085	3915	160
Bezafibrate	30	n.d.	n.d.	n.d.	n.d.	n.d.	n.d.	n.d.	n.d.	n.d.	n.d.	n.d.
Carbamazepine	470	545	430	385	460	430	220	230	210	20	20	15
Clofibric Acid	20	5	5	10	10	5	5	5	5	15	n.d.	10
Diclofenac	135	15	45	5	15	10	< LOQ	< LOQ	10	n.d.	n.d.	n.d.
Indometacine	< LOQ	< LOQ	< LOQ	n.d.	n.d.	n.d.	n.d.	n.d.	n.d.	n.d.	n.d.	n.d.
Primidone	135	140	125	115	170	95	80	90	100	30	70	15
Propyphenazone	120	20	20	30	15	20	10	10	40	10	55	20

n.d. not detected

<LOQ. < limit of quantitation

1.4.3.2 Annual variations of the concentrations of the target PhAC's

AMDOPH

As illustrated in Figure 32, AMDOPH was detected at relatively constant concentrations in the surface water and in all wells that were only influenced by recharge with recent surface water. In contrast to well 20 and the landward sampling wells, they are not affected by contaminated landward groundwater as they are containing AMDOPH only at concentrations "lower" concentrations of between 225 and 570 ng/l. On the other hand, concentrations between 350 and 5845 ng/l of AMDOPH were found in the landward wells. The strong fluctuations of the concentrations in the monitoring wells TEG370OP and TEG370UP have to be attributed to not yet completely clarified hydraulic conditions in the deeper groundwater aquifer.
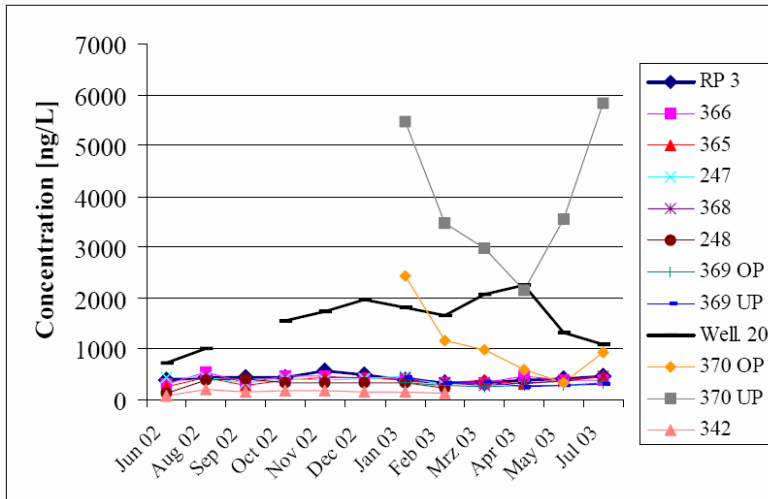
Figure 32. Concentration profiles of AMDOPH at the sampling points/wells (July 02 - June 03)
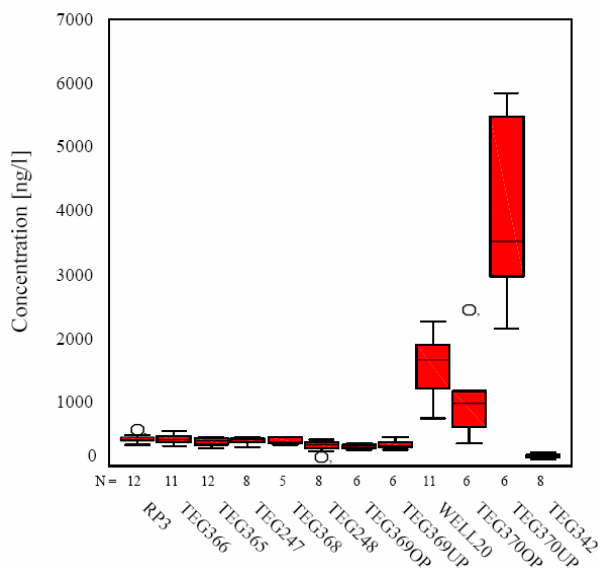
Figure 33. Box plots of AMDOPH concentrations [ng/l] at the individual monitoring wells and the receiving water-supply well 20

For the complete clarification of the hydraulic conditions in the deeper groundwater aquifers further hydro geological investigations will be required. During the soil passage a mean removal rate for AMDOPH of 28 % (compared to the surface water concentration) was observed. This implies that under the prevailing recharge conditions, the majority of the AMDOPH residues (approx. 70%) was not adsorbed at soil particles or biodegraded by the microbial soil flora and reached almost unaffected the groundwater aquifer. Thus, the GWA

46

is less suitable for the removal of AMDOPH from surface water. Figure 33 shows a statistical evaluation of the AMDOPH concentrations at the individual sampling points as box plot graphs. This figure also demonstrates the high mobility of AMDOPH as well as the low removal during the infiltration process. In addition, it shows the high load of AMDOPH in the landward monitoring wells TEG370OP and TEG370UP and in water-supply well 20.

Carbamazepine

Carbamazepine was found with very variable concentrations in the surface water (RP 3) and in all wells except for the landward monitoring wells (Figure 34).
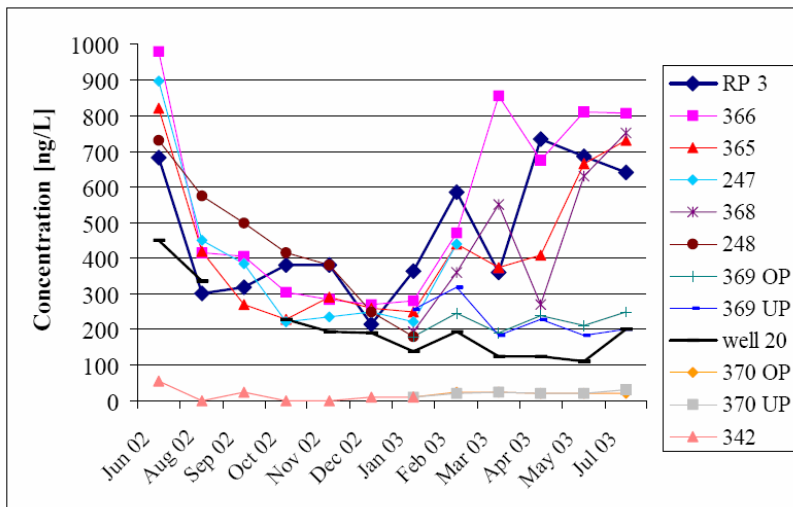
Figure 34. Concentration profiles of carbamazepine at the sampling points/wells (July 02 - June 03)

It was detected in the surface water at concentrations up to 1 µg/l. The strong increase of the concentrations of carbamazepine starting in March 2003 might be explained by the phasing out of the sewage water treatment plant in Falkenberg located in the east districts of Berlin. Since March 27, 2003 its waste water was directed to the sewage water treatment plant in Waßmannsdorf (2/3) located in the south of Berlin and to the sewage water treatment plant in Schönerlinde (1/3) north of Berlin.
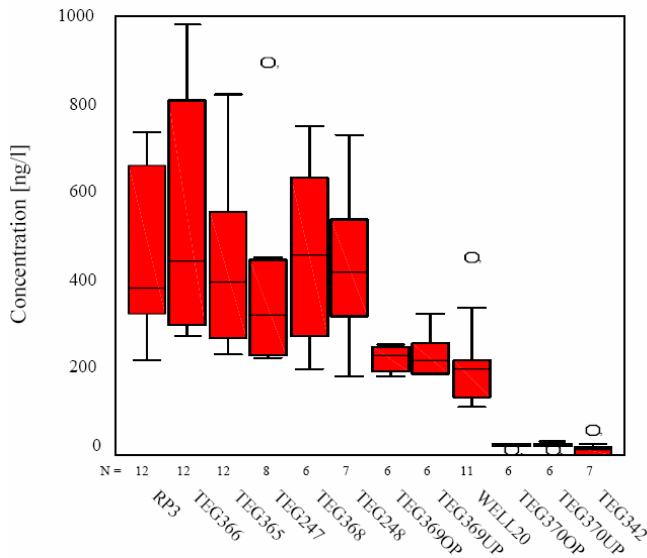
Figure 35. Box plots for the carbamazepine concentrations [ng/l] measured at the individual sampling wells

The treated waste water from the STP in Schönerlinde is discharged into the Nordgraben, which flows into Lake Tegel and causes an increase of the drug concentrations in the surface water. In tendency, the concentration profiles at the monitoring wells up to the water-supply well 20 follow the temporal changes of the concentration measured in the surface water. There is no significant removal of carbamazepine along the transect. Thus, up to monitoring well TEG248, a mean removal rate of only 9 % was observed for carbamazepine. Similar to AMDOPH, carbamazepine represents a very mobile drug residue, only attenuated to a small degree under the prevailing recharge conditions. Thus, the GWA is less suitable for the removal of carbamazepine from surface water. Figure 35 shows a statistical evaluation of the carbamazepine concentrations detected in the individual monitoring wells and in water-supply well 20. It shows the high mobility of carbamazepine as well as the small removal during the infiltration process.

Primidone

Exactly as carbamazepine, primidone was detected with variable concentrations in the surface water and in all monitoring wells, as shown in Figure 36. Starting in March 2003, the increase of the concentrations, due to the enhanced discharges from the STP Schönerlinde caused by the phasing out of the STP in Falkenberg, could been recognized. In tendency, the concentration profiles of the monitoring wells up to the water-supply well 20 follow the temporal changes of the concentrations measured in the surface water. There is no significant removal of primidone along the transect. Thus, up to monitoring well TEG248, a

48

mean removal rate of 30 % was observed for primidone. The removal rate of primidone up to well 20 is not substantially improved (26 %), because primidone was also detected in the landward sampling points at average concentrations of 70 ng/l.
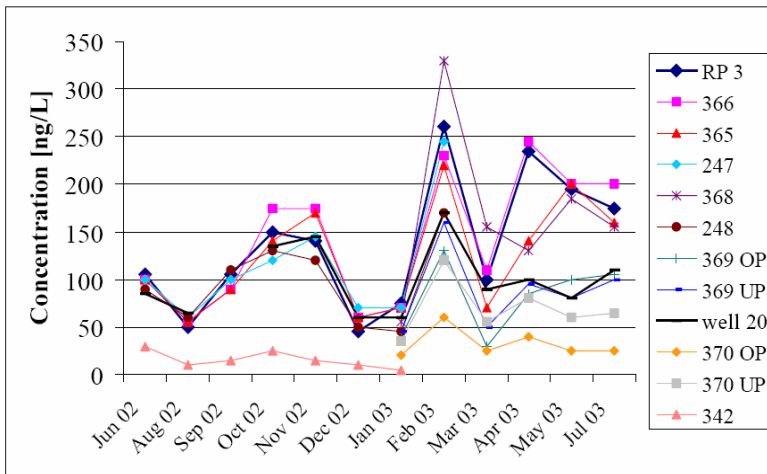
Figure 36. Concentration profiles of primidone at the sampling points/wells (July 02 - June 03)

Primidone, similar to AMDOPH and carbamazepine, is characterized by its very high mobility, and is only attenuated to small degree under the prevailing recharge conditions. Figure 37 shows a statistical evaluation of the primidone concentrations at the individual sampling points as box plots graph. This figure also demonstrates the high mobility of primidone as well as the low removal during the infiltration process.
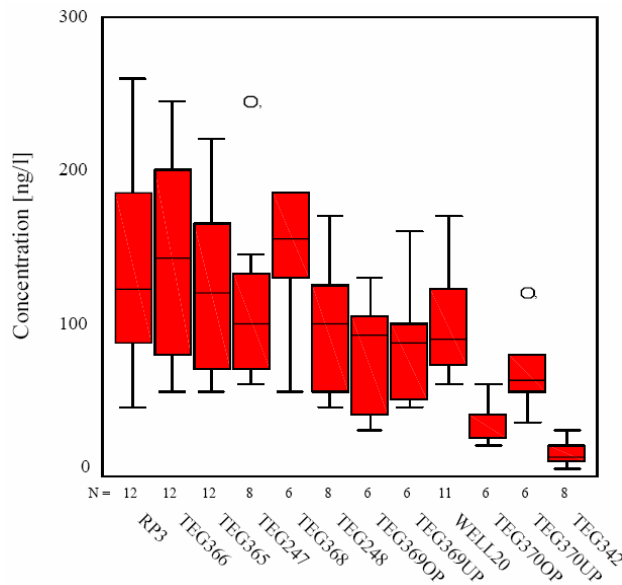
Figure 37. Box plots for the primidone concentrations [ng/l] measured at the individual sampling wells

Propyphenazone

Propyphenazone was detected with relatively constant concentrations in the surface water (Figure 38). The enhanced discharges from the STP Schönerlinde starting in March 2003 did not cause a significant increase of propyphenazone concentration in the surface water of Lake Tegel. The main source for propyphenazone in the surface water of Lake Tegel are residues from the Havel river, which is contaminated by production spills of a former pharmaceutical production plant [Reddersen et al., 2002]. In contrast to the group 1 PhAC's, a much higher removal rate is observed for propyphenazone.
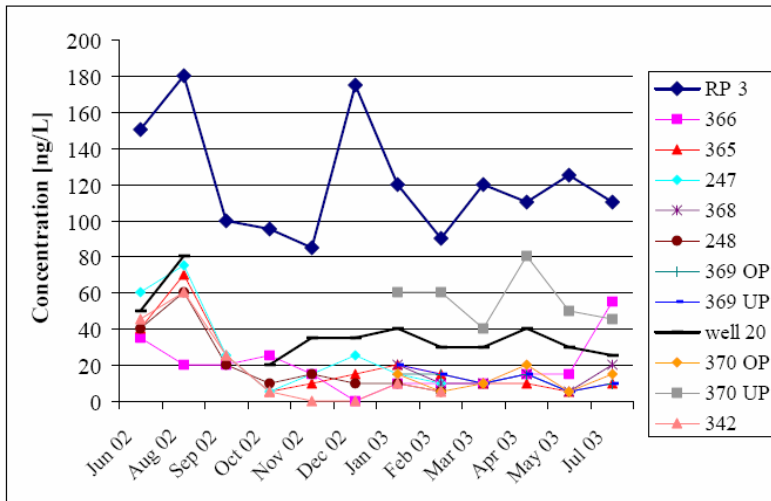
Figure 38. Concentration profiles of propyphenazone at the sampling points/wells
(July 02 - June 03)

A removal rate of 83 % was observed up to the monitoring well TEG248. Propyphenazone loaded landward groundwater (TEG370UP) caused an alleged lowering of the removal rate to 67 % at well 20. In general, the GWA is suitable for the pre-treatment of propyphenazone loaded surface water lowering its concentrations. Figure 39 shows a statistical evaluation of the propyphenazone concentrations at the individual sampling points as box plots graph. This figure also demonstrates the attenuation of propyphenazone during the soil passage.

50
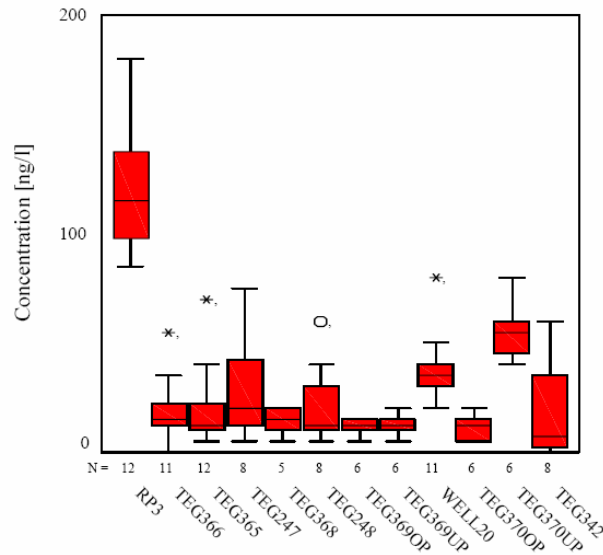
Figure 39. Box plots for the propyphenazone concentrations [ng/l] measured at the individual sampling wells

Diclofenac

The concentration profile of diclofenac in surface water shows pronounced temporal variations (Figure 40). Higher concentrations between 65 and 435 ng/l during the winter and spring months decreased to values below 50 ng/l in the summer months. This is most likely caused by the photochemical degradation of diclofenac, as already described by Buser et al. (1998) and Tixier et al. (2003).
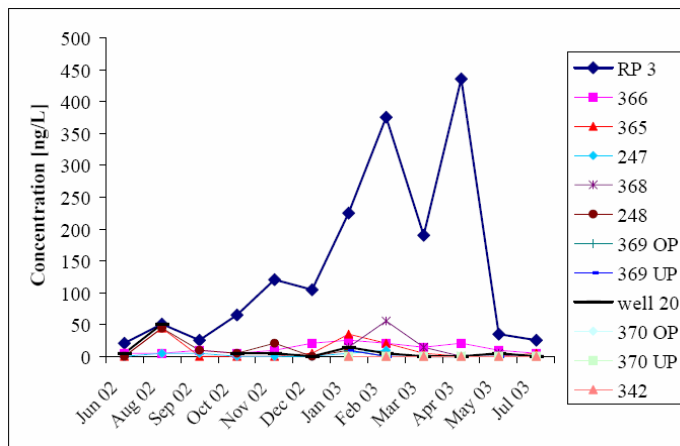
Figure 40. Concentration profiles of diclofenac at the sampling points/wells
(July 02 - June 03)

Diclofenac was measured at relatively constant concentrations clearly below 50 ng/l in all monitoring wells up to water-supply well 20. This also demonstrates the ability of the GWA for the attenuation of diclofenac even with high concentrations in the winter months. At monitoring well TEG248 and at water-supply well 20 a mean removal rate of 93% was determined.
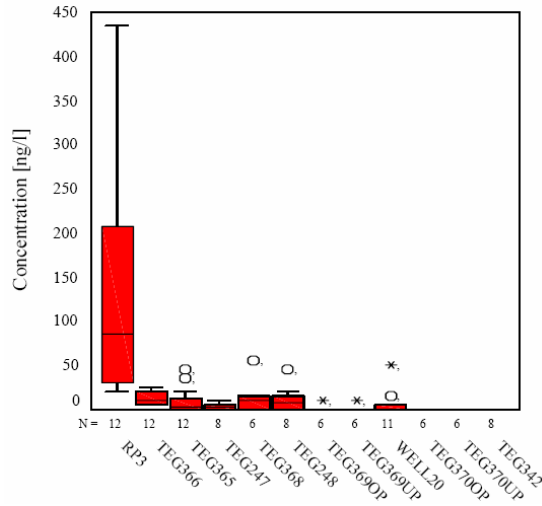
Figure 41. Box plots for the diclofenac concentrations [ng/l] measured at the individual sampling wells

Thus, the GWA was found as being suitable for the pre-treatment of diclofenac loaded surface water. Nevertheless, the removal is not complete and still small loads of diclofenac infiltrate into the groundwater aquifer and reach water supply well 20. Figure 41 shows a statistical evaluation of diclofenac concentrations at the individual sampling points as box plots graph. This figure also demonstrates the attenuation of diclofenac during the soil passage.

Clofibric acid

The drug metabolite clofibric acid was found with relatively constant concentrations in the surface water and in all monitoring wells as shown in Figure 42. It was detected in the surface water at concentrations between 10 and 30 ng/l. Up to both sampling points TEG248 and water supply well 20 an average removal rate of 75 % was observed. The clofibric acid based active substances were used more frequently in the past decades, thus, this persistent metabolite could infiltrate into and adsorb to the soil particles of the groundwater aquifer.
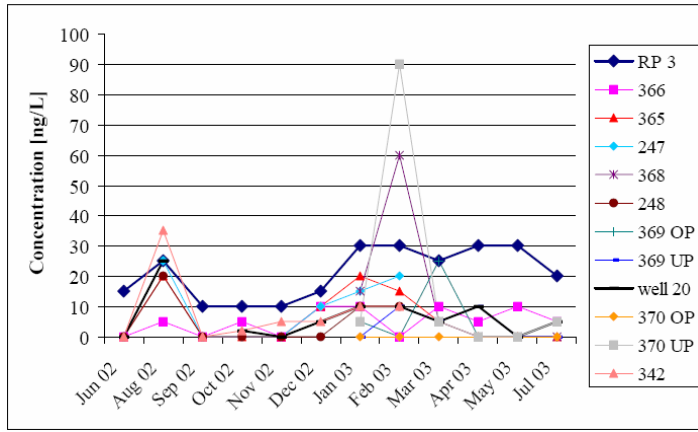
**Figure 42. Concentration profiles of clofibric acid at the sampling points/wells
(July 02 - June 03)**

The decreasing administration trend of medication containing the precursor derivatives of clofibric acid is illustrated by the small concentrations in the surface water. However, thereby the high persistence of the clofibric acid is also demonstrated. Nevertheless, a significant decrease of the concentrations wasobserved. Thus, the GWA was found as being suitable for the pre-treatment of clofibric acid loaded surface water.
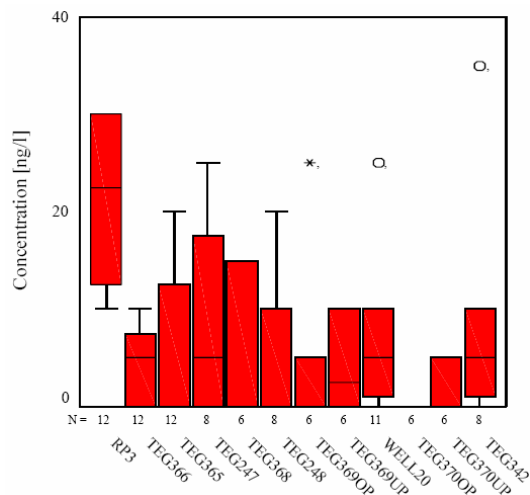
Figure 43. Box plots for the clofibric acid concentrations [ng/l] measured at the individual sampling wells

Figure 43 shows a statistical evaluation of clofibric acid concentrations at the individual sampling points as boxplots graph. This figure also demonstrates the attenuation of clofibric acid during the soil passage.

Bezafibrate and indometacine

Bezafibrate and indometacine only occur at very small concentrations close to the limit of determination in the surface water. The remaining residues of both compounds were completely attenuated during ground water recharge, which was also observed and described by Brauch et al. (2000) and Heberer et al. (2002).

1.4.3.3 Conclusions

On the basis of PhAC's removal rates calculated between RP 3 and shallow monitoring well TEG248, the drug residues could been classified into three groups as described in Table 19 and also reported earlier by Heberer and Adam (2004).

Table 19. Classification of target PhAC's according to their removal rates

Group	Compound	Median rate of attenuation of at TEG248	Median rate of attenuation at WSW 20	
1 low removal rates 0-50 %	AMDOPH	31%	-245%	(exceptional case)
	Carbamazepine	9%	55%	
	Primidone	30%	26%	
2 medium removal rates 51-95 %	Clofibric acid	75%	75%	(exceptional case)
	Diclofenac	93%	93%	
	Propyphenazone	85%	67%	(exceptional case)
3 high removal rates > 95 %	Bezafibrate	> 97 %	> 97 %	
	Indometacine	> 95 %	> 95 %	

• Group 1 includes AMDOPH, carbamazepine and primidone and is characterized by modest removal rates of ≤ 30 % up to well 20. The higher removal rate (55%) for carbamazepine observed in well 20 is mainly caused by dilution with landward groundwater (TEG370OP to TEG342), which shows only very low concentrations of carbamazepine. This assumption is also supported by the results obtained for sampling point TEG248, which almost exclusively consists of water recharged from RP 3. In this case only a minor removal rate of 9 % was observed for carbamazepine. The drug metabolite AMDOPH represents an

exceptional case. AMDOPH was detected in ground water samples from well 20 at average concentrations 240 % higher, than those in RP 3. This observation can be explained by the production spills of a former pharmaceutical production plant north of Berlin, which led to high concentrations of AMDOPH and the original drug dimethylaminophenazone in the Havel river and in the groundwater of north-western districts of Berlin (Reddersen et al., 2002). For sampling point TEG248, only influenced by the surface water of RP 3, a mean removal rate of 28 % was observed for AMDOPH.

• Group 2 includes clofibric acid, diclofenac and propyphenazone. These drugs are characterized by high removal rates of more than 70%. The elevated concentrations of propyphenazone in well 20 can be explained by the shares of contaminated landward groundwater (TEG370UP). Despite their good removal rates, portions of all three drugs arrived in the water of well 20.

• Group 3 includes bezafibrate and indometacine. These drugs were removed completely during the soil passage and could not even be quantified at sampling point TEG366 (underneath RP 3) and near the bank at sampling point TEG365.

The results of this investigations show that there is a breakthrough of six of the eight detected drug residues during the artificial groundwater recharge into the water supply well 20. The behaviour of the observed compounds could be classified into three groups with different removal rates. Thus, the GWA may serve at best for the pre-treatment of contaminated surface water but is not sufficient for the complete removal of these residues.

1.4.4 Transect Tegel

Starting in May 2002, the surface water, the shallow monitoring wells (3311, 3310, 3308 and 3305), the deep monitoring wells (3301, 3302, 3303, 3304), and water supply well no. 13 of the transect located at lake Tegel were sampled monthly until August 2004. Due to a low ground water levels in summer the shallow wells 3311, 3310 and 3308 could not be sampled during June and September. The multi-level well TEG371OP/UP and the shallow monitoring well TEG372 have been included in the investigations since January 2003. Additionally, the deep monitoring well TEG374 was drilled and sampled since January 2004. Table 20 shows that altogether eight pharmaceutical residues were quantified up to the µg/L level in the surface water from lake Tegel. These compounds are: AMDOPH (1-acetyl-1-methyl-2-dimethyl-oxamoyl-2-phenyl-hydrazide), bezafibrate, carbamazepine, clofibric acid, diclofenac, indometacine, primidone and propyphenazone. Furthermore, two herbicides namely bentazone and mecoprop, a metabolite of an insecticide (p,p'-DDA), and N-Phenylsulfonylsarcosin (NPS) another metabolite of a corrosion inhibitor were detected in the surface water.

The analgesic drug diclofenac, the antiepileptic drugs carbamazepine and primidone, the two drug metabolites AMDOPH and clofibric acid and the analgesic propyphenazone were detectable in the shallow monitoring wells (3311, 3310, 3308), the multi level well (TEG371UP/OP) and the deep monitoring wells (3301, 3302, 3303). Except for AMDOPH and propyphenazone, the other PhACs occur in low concentrations at the water supply well 13. AMDOPH and clofibric acid were observed in obliviously higher concentrations in the deepest monitoring well TEG374 (e.g., up to 8,3 µg/L for AMDOPH) Up to 1,8 µg/L of AMDOPH were found in the receiving water supply well 13. Bezafibrate (a blood lipid regulator) and indometacine (an antiphlogistic drug) were detectable up to 100 ng/L in the surface water, but they are efficiently removed during the infiltration process and were not detectable behind the first two monitoring wells as shown in Table 20 and Table 21.

Table 20. Compounds with positive findings and their concentration range [ng/L] at the shallow monitoring wells and the multi level well of transect lake Tegel

ng/L	Surface water (n=26)		3311 (n=16)		3310 (n=12)		3308 (n=16)		TEG371OP (n=18)		TEG371UP (n=18)		TEG372 (n=18)		well 13 (n=22)		3305 (n=6)	
	min	max	min	max	min	max	min	max	min	max	min	max	min	max	min	max	min	max
AMDOPH	175	605	145	605	120	545	55	345	165	510	160	1215	80	525	260	1755	65	90
carbamazepine	180	1170	210	1240	210	1100	255	1100	90	620	50	310	140	745	30	185	n.d.	20
clofibric acid	<LOQ	125	<LOQ	55	<LOQ	70	<LOQ	65	<LOQ	75	<LOQ	55	<LOQ	35	10	65	n.d.	<LOQ
diclofenac	5	375	5	130	5	165	5	65	5	100	5	95	5	105	5	60	n.d.	<LOQ
primidone	30	480	30	370	25	440	20	270	45	475	65	365	25	265	30	190	5	10
Propyphena-zone	35	385	5	195	15	60	5	175	10	220	15	1075	5	70	60	280	n.d.	50
indometacine	<LOQ	55	<LOQ	40	<LOQ	45	n.d.	n.d.	n.d.	n.d.	n.d.	n.d.	n.d.	n.d.	n.d.	n.d.	n.d.	n.d.
bezafibrate	<LOQ	140	<LOQ	<LOQ	<LOQ	35	n.d.	n.d.	n.d.	n.d.	n.d.	n.d.	n.d.	n.d.	n.d.	n.d.	n.d.	n.d.
bentazone	n.d.	30	n.d.	25	n.d.	35	n.d.	30	n.d.	20	n.d.	25	n.d.	30	n.d.	15	n.d.	n.d.
mecoprop	n.d.	45	n.d.	40	n.d.	45	n.d.	45	n.d.	60	n.d.	40	n.d.	50	n.d.	35	n.d.	n.d.
NPS	n.d.	55	n.d.	30	n.d.	30	n.d.	30	n.d.	95	n.d.	60	n.d.	215	15	145	n.d.	n.d.
p,p'-DDA	n.d.	20	n.d.	5	n.d.	n.d.	n.d.	5	n.d.	5	n.d.	15	n.d.	5	n.d.	10	n.d.	n.d.
o,p'-DDA	n.d.	5	n.d.	n.d.	n.d.	n.d.	n.d.	n.d.	n.d.	n.d.	n.d.	5	n.d.	n.d.	n.d.	5	n.d.	n.d.

n.d. not detected

<LOQ. < limit of quantitation

Table 21. Compounds with positive findings and their concentration range [ng/L] at the deeper monitoring wells of transect Tegel

ng/L	Surface water (n=26)		3301 (n=26)		3302 (n=26)		3303 (n=21)		TEG374 (n=8)		Well 13 (n=22)		3304 (n=26)	
	min	max	min	max	min	max	min	max	min	max	min	max	min	max
AMDOPH	175	605	165	915	160	935	150	770	4150	8320	260	1755	85	835
carbamazepine	180	1170	100	360	100	480	165	545	n.d.	10	30	185	n.d.	145
clofibric acid	<LOQ	125	<LOQ	80	<LOQ	35	<LOQ	20	115	235	10	65	<LOQ	45
diclofenac	<LOQ	375	5	100	5	75	5	95	n.d.	n.d.	n.d.	60	n.d.	55
primidone	30	480	40	385	35	365	30	315	45	185	30	190	5	55
propyphenazone	n.d.	385	40	875	5	1020	5	215	15	115	60	280	n.d.	160
indometacine	<LOQ	<LOQ	35	35	n.d.	n.d.	n.d.	n.d.	n.d.	n.d.	n.d.	n.d.	n.d.	n.d.
bezafibrate	<LOQ	140	<LOQ	50	<LOQ	<LOQ	n.d.	n.d.	n.d.	n.d.	n.d.	n.d.	n.d.	n.d.
bentazone	n.d.	30	n.d.	25	n.d.	25	n.d.	10	n.d.	n.d.	n.d.	15	n.d.	5
mecoprop	5	45	n.d.	40	n.d.	25	n.d.	10	n.d.	15	n.d.	35	n.d.	30
NPS	n.d.	55	n.d.	310	n.d.	105	5	30	n.d.	95	15	145	25	610
p,p'-DDA	10	20	n.d.	30	n.d.	10	n.d.	10	n.d.	5	n.d.	10	n.d.	5
o,p'-DDA	5	10	n.d.	10	n.d.	5	n.d.	5	n.d.	n.d.	n.d.	n.d.	n.d.	n.d.

n.d.   not detected

<LOQ.   < limit of quantitation

1.4.4.1 AMDOPH and propyphenazone at transect Tegel

AMDOPH was observed in surface water of lake Tegel at concentrations between 175 ng/L and 605 ng/L. Propyphenazone concentrations varies from not detectable up to 385 ng/L in lake Tegel.
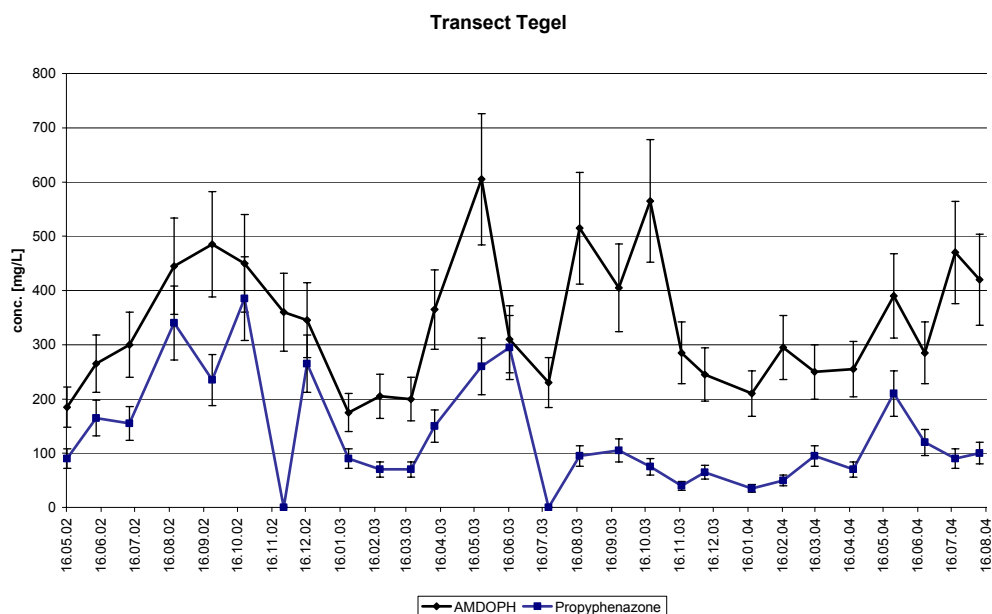
Figure 44. AMDOPH and propyphenazone concentrations at lake Tegel surface water

As shown in Figure 44, concentration trends for AMDOPH and propyphenazone were very similar and seemed to depend on the proportion of Havel water discharged into lake Tegel via the OWA Tegel as illustrated in Figure 45. The visuability of this dependence is explainable by an old environmental damage caused by a leakage at a pharmaceutical plant located in Oranienburg, where different phenazone derivates were produced (Reddersen et. al, 2002).
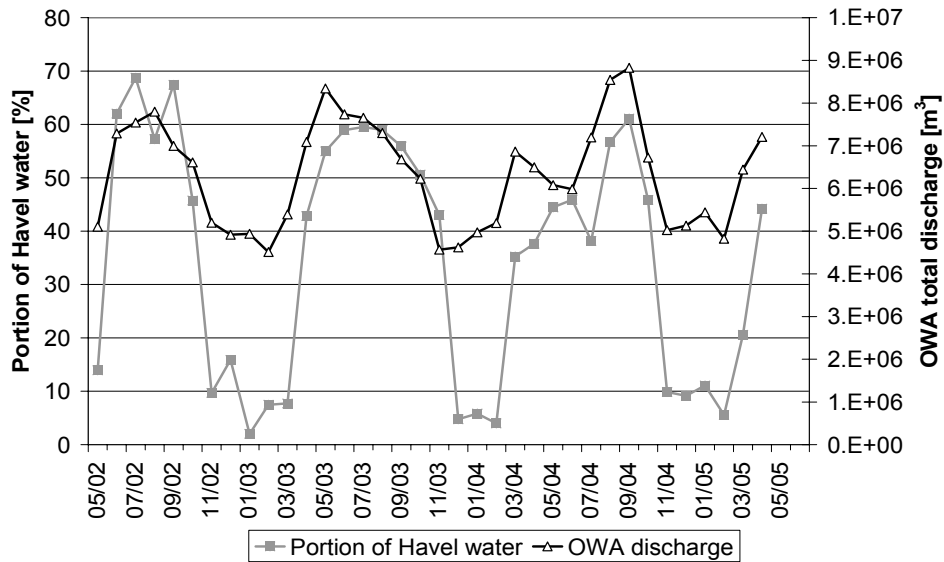
Figure 45. Total discharge into Lake Tegel and the portion of water from the Havel lake pipeline (data BWB)

1.4.4.2   AMDOPH

Median concentrations of 328 ng/L down to 170 ng/L were observed in surface water and in ground water from the shallow monitoring wells 3311, 3310, 3308 and TEG372. As presented in Figure 46 the median concentrations of AMDOPH are decreasing slightly with distance and depth from the infiltration area.

With regard to the analytical measurement accuracy, no significant removal was noticed at the first monitoring wells 3310 & 3311. The attenuation rate between surface water and the bank filtrate at sampling point 3308 was about 44 %. At monitoring well TEG371UP the concentrations are slightly increased in comparison to TEG371OP which can be explained by a mixture of young bank filtrate with formerly infiltrated water at times when AMDOPH surface water concentrations were much higher. The deeper monitoring wells and the water supply well no.13 show much higher concentrations of AMDOPH. The median concentrations at the monitoring wells are increasing by depth and at the deepest monitoring well TEG374, a maximum around 6 µg/L was observed. At the landsite monitoring wells, the detected median concentrations are increasing by depth from 78 ng/L up to 220 ng/L. The

water supply well no.13 represents a mixing of older bank filtrate / groundwater from deeper layers (TEG374), landsite groundwater (3304) and young bank filtrate from the lake Tegel.

Figure 46. Transect Tegel - median concentrations of AMDOPH at the different monitoring wells and the water supply well 13. Values in brackets show the calculated attenuation rates in percent.
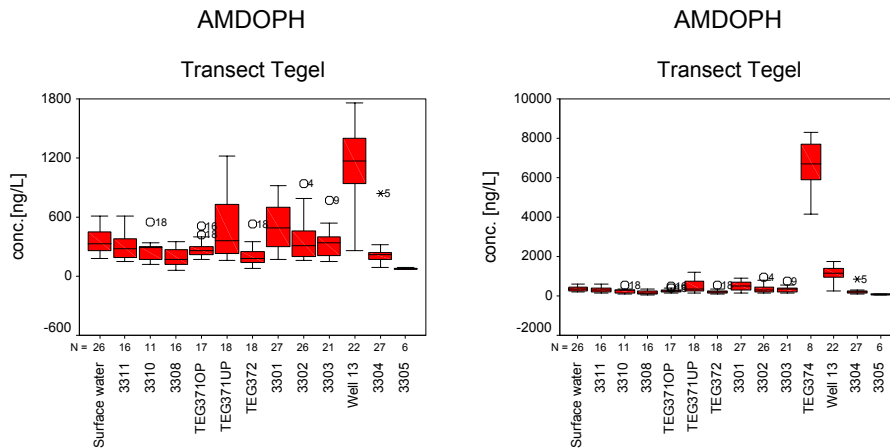
Figure 47. Distribution of AMDOPH concentrations at transect lake Tegel. In the first box plot monitoring well TEG374 is excluded for better resolution. Second box plot show the concentrations at TEG374 in comparison with the other monitoring wells.

The distribution of AMDOPH concentrations shown in Figure 47 are comparable with the distribution of ammonium concentrations (Figure 48) determined by the BWB. Like AMDOPH, the ammonium concentrations at the shallow monitoring wells are decreasing from surface water to TEG372, but show higher values at TEG371UP than in surface water and the other deeper monitoring wells (3301-3304). At monitoring well TEG374 AMDOPH and ammonium concentrations show their maximum.
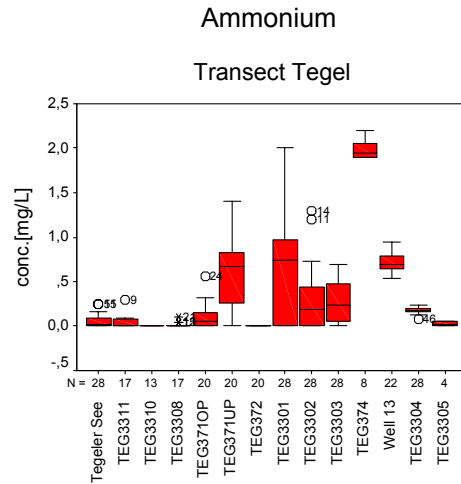
Figure 48. Distribution of ammonium concentrations at the transect Tegel

1.4.4.3 Propyphenazone

The median concentrations of propyphenazone from surface water to the first shallow monitoring wells 3308, 3310 and 3311 are significantly decreased and an attenuation rate around 85 % was observed at 3308 as shown in Figure 49 . At the deep monitoring well 3301 a higher median concentrations (300 ng/L) than in surface water (98 ng/L) was measured. Additionally, at the deeper screens of the multi-level well TEG371 an increased median concentration of 190 ng/L was detected and support the assumption that during the infiltration older bank filtrate formerly higher amounts of phenazone-type compounds from the before mentioned superfund site are mixed with younger bank filtrate. At TEG374, the deepest monitoring well, a median concentration of 60 ng/L was observed. The water supply well with a median concentration of 135 ng/L represents a mixture of younger and older bank filtrate. The monitoring wells behind water supply well no.13 in the south east only showed traces of propyphenazone below the limit of quantification (10 ng/L).

Figure 49. Transect Tegel - median concentrations of propyphenazone at the different monitoring wells and the water supply well 13. Values in brackets show the calculated attenuation rates in percent.

As illustrated in Figure 50 , the distribution of propyphenazone concentrations at TEG371UP and monitoring well 3301 show concentration tendencies with higher values than in surface water and e.g. TEG372. This seems to be similar to the distributions observed for AMDOPH (Figure 47) and ammonium (Figure 48).
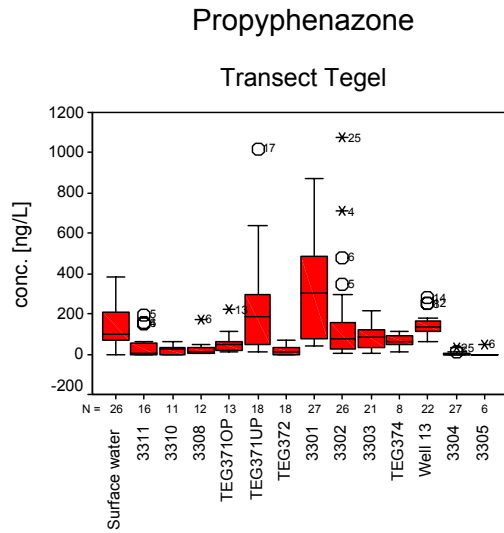
Propyphenazone

Figure 50. Distribution of propyphenazone concentrations at transect Tegel

1.4.4.4   Clofibric acid

The median concentrations at almost all sampling locations were detected in a concentration range from the limit of quantification up to 35 ng/L, as presented in Figure 51.
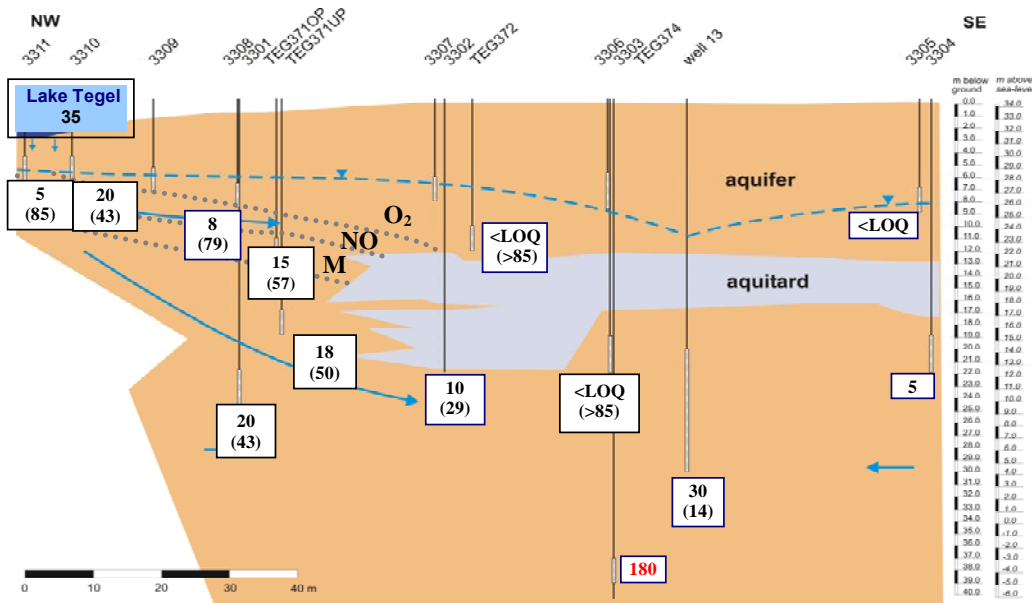
Figure 51. Transect Tegel - median concentrations of clofibric acid at the different monitoring wells and the water supply well 13. Values in brackets show the calculated attenuation rates in percent.

Depending on the low observed concentrations clofibric acid showed no significantly attenuation during infiltration. In opposite to the others, the deepest monitoring well TEG374 show a median concentration of 180 ng/L as illustrated in Figure 52. This median concentration of clofibric acid is probably caused by formerly infiltrated water when the precursor pharmaceutical compounds clofibrate ethyl, etofibrate and etofyllinclofibrate were applicated at higher amounts. The persistence of clofibric acid was already reported in literature [Zwiener, 2000; Winkler, 2001; Preuß, 2001 and Scheytt, 2001].

Clofibric acid
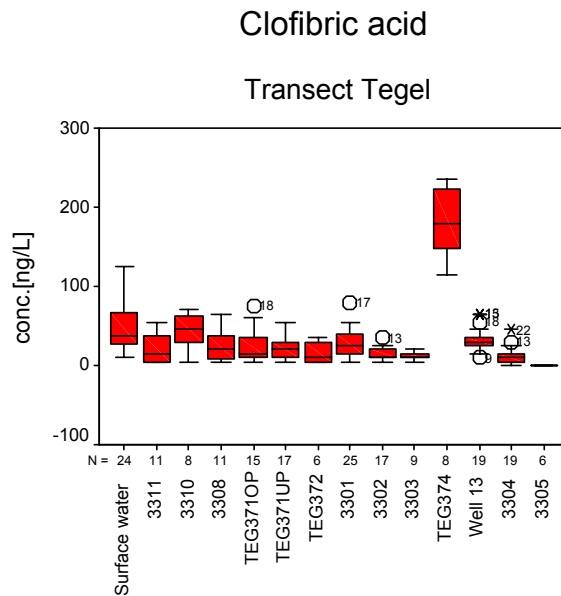
Transect Tegel

Figure 52. Distribution of clofibric acid concentrations at transect Tegel

At the deeper landsite monitoring well 3304 only traces of clofibric acid were observed.

1.4.4.5   Diclofenac

As Figure 53 shows, a median concentration of 103 ng/L was detected in surface water. Attenuation rates between 74 % and 85 % were observed at the shallow monitoring wells 3311, 3308, TEG371OP and TEG372 and in the deep monitoring well 3303 in front of water supply well no.13. However, the shallow monitoring well 3310 located close to the bank only shows an attenuation rate of 41 %. In deeper monitoring wells 3301 and TEG371UP an attenuation rate of about 64 % was observed. At the shallow landsite monitoring well 3305 no diclofenac was found. In the deeper landsite monitoring well 3304 a median concentration of 13 ng/L was observed.
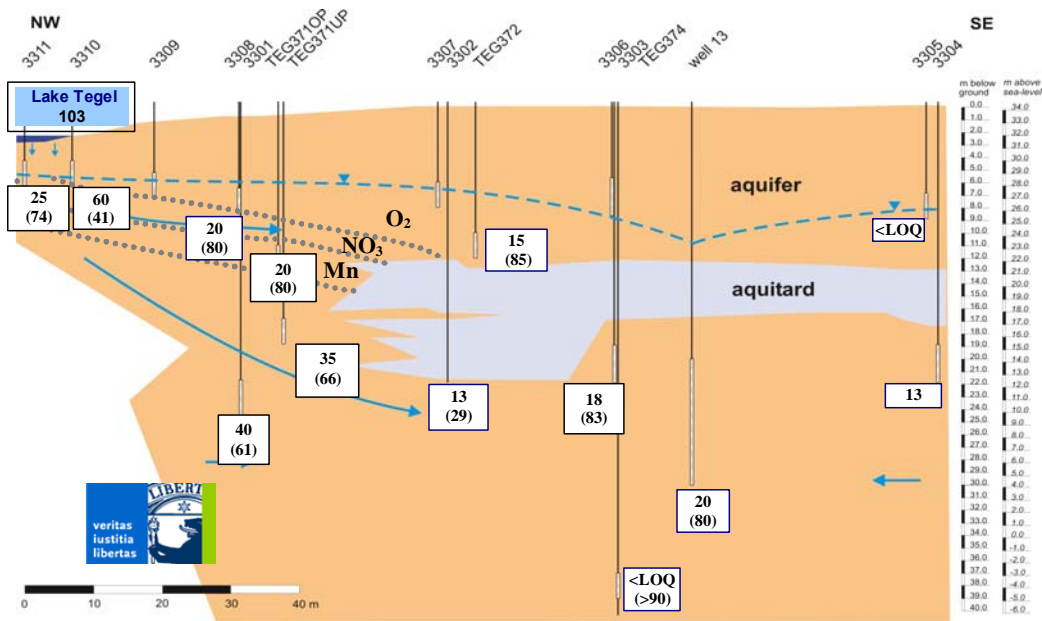
Figure 53. Transect Tegel - median concentrations of diclofenac at the different monitoring wells and the water supply well 13. Values in brackets show the calculated attenuation rates in percent.

In contrast to the results for AMDOPH, propyphenazone and clofibric acid, no diclofenac was found in the deep monitoring well TEG374. The Figure 54 shows a statistical evaluation of the observed concentrations.
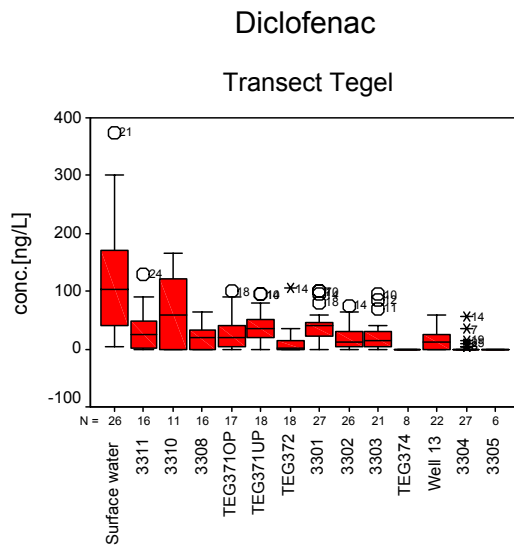
Figure 54. Distribution of diclofenac concentrations at transect Tegel

1.4.4.6   Primidone

Concentrations around 140 ng/L were detected at the surface water and the shallow monitoring well 3310. At monitoring well 3311 a minor attenuation rate of 26 % was noticed.
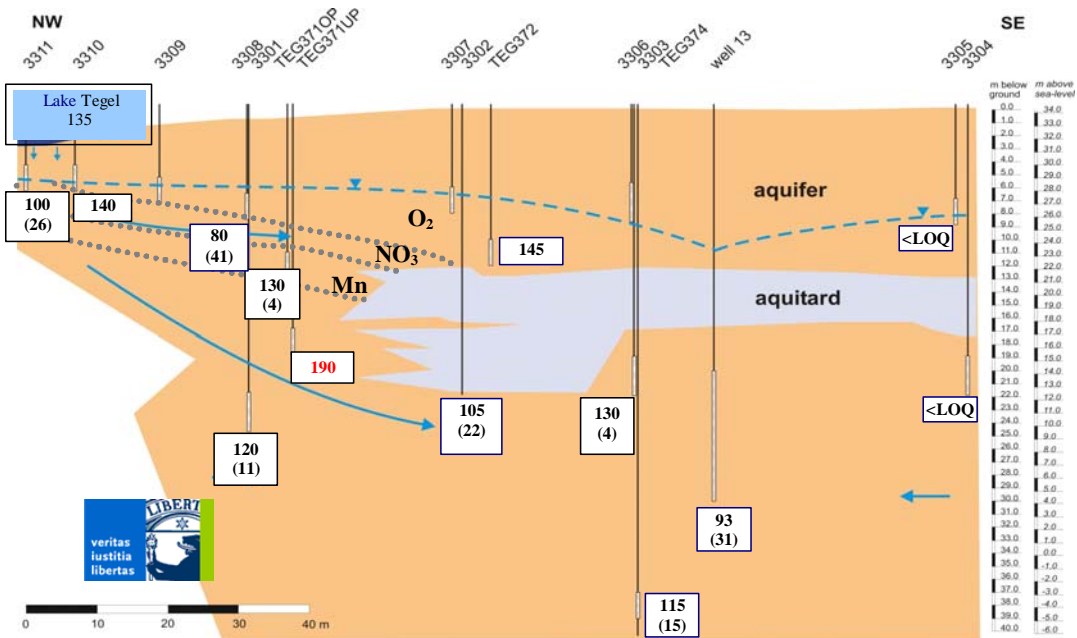
Figure 55. Transect Tegel - median concentrations of primidone at the different monitoring wells and the water supply well 13. Values in brackets show the calculated attenuation rates in percent.

Maximum attenuation rate of 41 % was observed at the shallow well 3308. Similar to the previously described compounds attenuation rates of primidone at the monitoring wells 3301, 3302 were slightly decreased or respectively higher median concentrations than in surface water were noticed. At the deep monitoring wells 3303 and TEG374 equal median concentrations as observed in surface water were observed. The landsite monitoring wells behind the water supply well only showed traces of primidone below the limit of quantification.

Primidone
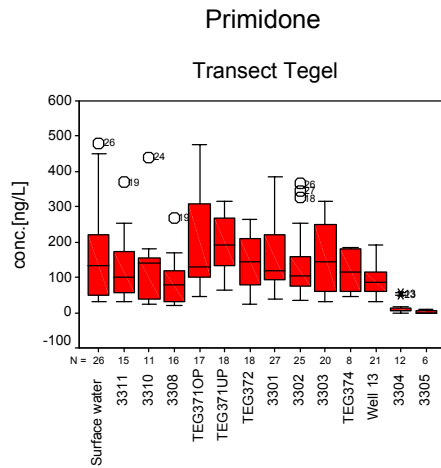
Transect Tegel

Figure 56. Distribution of primidone concentrations at transect Tegel.

As Figure 56 illustrates, the values of detected primidone concentrations are decreasing during infiltration starting from surface water along the shallow monitoring wells 3311 to 3308.

Boron   Chloride

Transect Tegel   Transect Tegel
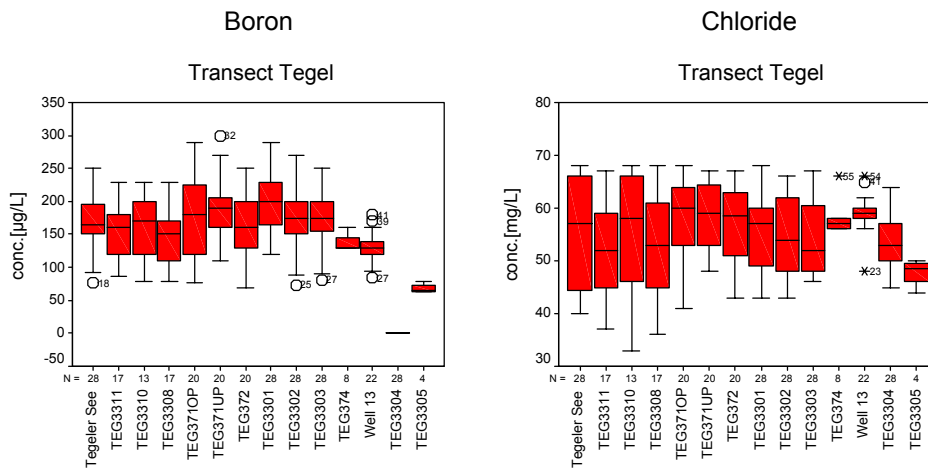
Figure 57. Distribution of boron and chloride concentrations at transect Tegel (data by BWB)

Contrary to these investigations, median concentrations of primidone were increased in the multi-level well TEG371 up to 190 ng/L at its deeper screens. Along the track to the water supply well no.13, no significant attenuation was observed within the analytical measurement accuracy of 20 %. The distribution of primidone concentrations at the monitoring wells in front of water supply well no. 13 were comparable to the distributions of the conservative tracer

boron and chloride which were analysed by the BWB as displayed in Figure 57. A median concentration of 93 ng/L was detected at the supply well no. 13.

1.4.4.7   Carbamazepine

During infiltration from surface water along the shallow monitoring wells 3311, 3310 and 3308, carbamazepine median concentrations around 527 ng/L were detected as Figure 58 shows.

Figure 58. Transect Tegel - median concentrations of carbamazepine at the different monitoring wells and the water supply well 13. Values in brackets show the calculated attenuation rates in percent.

However, these concentrations were within the measurement accuracy of 20 % and thus no significant attenuation was recognized. At monitoring well TEG371OP a slight attenuation of 24 % was noticed. In the deeper screened monitoring wells TEG371UP and 3301 attenuation rates around 65 % were observed. Surprisingly, minor attenuation rates between 49 and 57% were obtained at the monitoring wells 3302 and 3303. The deepest monitoring well TEG374 only show traces of carbamazepine at a median concentration below the limit of quantification. At the water supply well 80 ng/L (median concentration) of carbamazepine was detected that corresponds to an attenuation rate of 86 %. As Figure 59 shows carbamazepine concentrations of the surface water increased since march 2003 up to a maximum of 1170 ng/L. This increase could be explained by the higher amounts of purified

effluents of the STP Schönerlinde reaching lake Tegel and also leads to higher concentrations of indicators of sewage prone waters like boron, chloride and sodium.
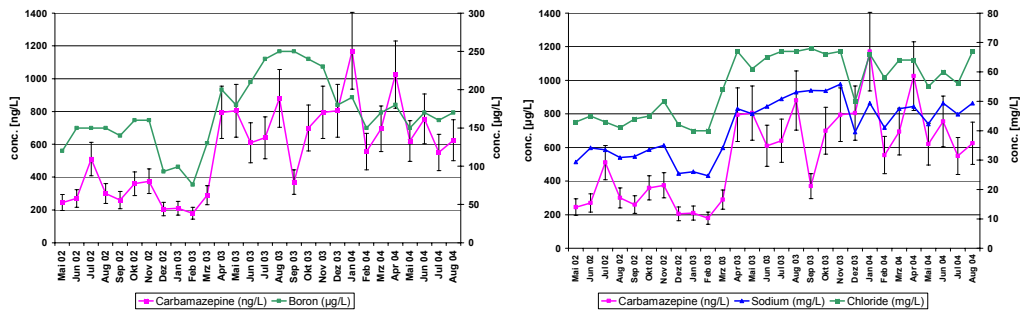
Figure 59. Comparison of concentration trends of carbamazepine and other sewage prone ions (data BWB)

Comparing surface water concentrations of carbamazepine with observed concentrations in monitoring wells 3301, 3302, 3303 and in water supply well 13 (Figure 60), observed concentrations in the bank filtrate / groundwater did not show any significant changes within the analytical measurement accuracy. Due to this no time shift was recognizable.
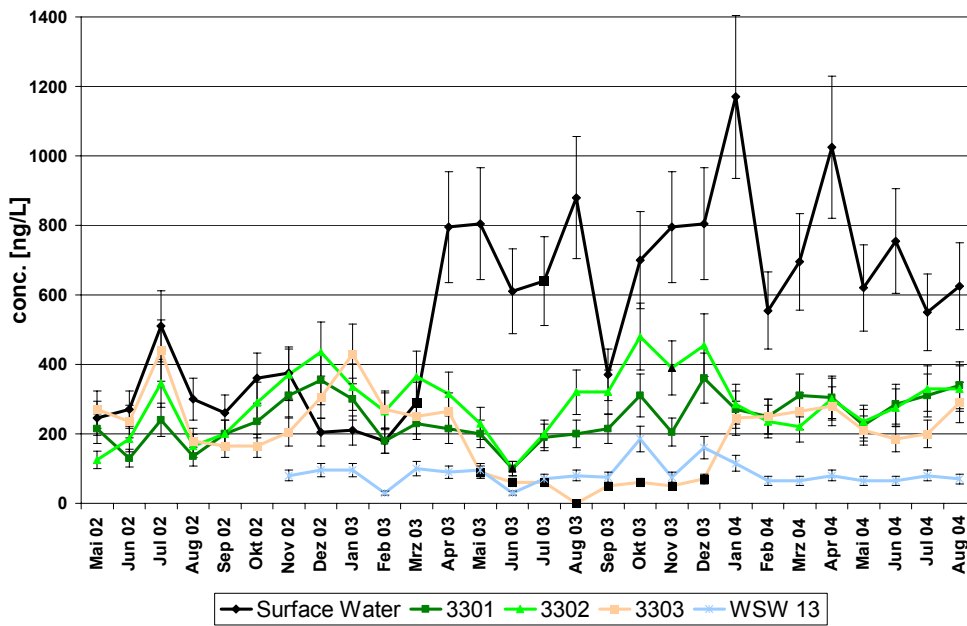
Figure 60. Transect Tegel - Concentrations of carbamazepine in lake Tegel and at the deep monitoring wells and the water supply well 13. (Black marked concentrations data by BWB)

As Figure 63 illustrates, distribution of carbamazepine concentrations seem to have a relation with the determined redox potential. Distributions of carbamazepine concentrations

70

at surface water and the shallow monitoring wells 3311, 3310 and 3308 were observed at a similar level like the distribution of the redox potential at these monitoring wells.
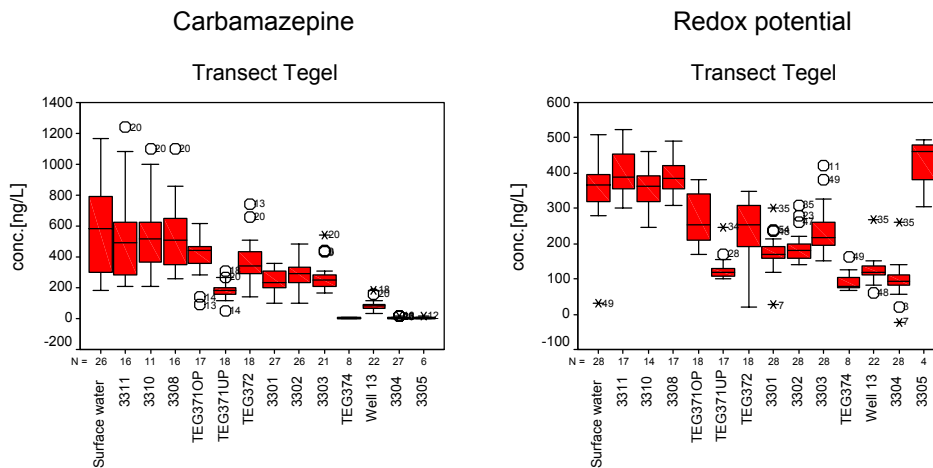
Figure 61. Distribution of carbamazepine concentrations and the determined redox potential (data by BWB) at transect Tegel

1.4.4.8 Other observed polar residues

Additional to the investigated drug residues two pesticides namely bentazone and mecoprop, 2,2-bis(4-chlorophenyl)acetic acid (p,p'-DDA) and its isomer 2-(2-chlorophenyl)-2-(4-chlorophenyl)-acetic acid could be detected in traces just around limit of quantification along the infiltration path at all monitoring wells and the water supply well no. 13. N-(phenylsulfonyl)-sarcosine (NPS) a metabolite of a corrosion inhibitor also was observed with low concentrations (< 20 ng/L) in surface water and at the shallow monitoring wells. Similar to AMDOPH, clofibric acid and propyphenazone increasing median concentrations of 55 ng/L at monitoring well TEG374 and about 85 ng/L at 3304 a deep land site monitoring well were noticed. Due to this a median concentration around 65 ng/L at the receiving water supply well 13 was detected.

1.4.4.9 Conclusions

Eight drug residues were detected in the surface water of lake Tegel. Six of them were identified as being relevant for drinking water production because they were transported along the infiltration path and found in water supply well 13. The analgesic drug indometacine and the blood regulating pharmaceutical bezafibrate were determined in very low concentrations in the surface water of lake Tegel and were sustainably removed with attenuation rates higher than 95 % during first meters of infiltration at TEG372, a shallow

monitoring well in front of the water supply well 13. Clofibric acid, the pharmacologically active metabolite of three blood regulating drugs, and the analgesics diclofenac and propyphenazone showed medium removal rates up to the shallow monitoring well TEG372. Only low attenuations were observed for AMDOPH the metabolite of dimethylaminophenazone (analgesic) and the antiepileptic drugs carbamazepine and primidone.

Table 22. Classification of target compounds according to their rates of attenuation

Group	Compound	Median rate of attenuation at TEG372	Median rate of attenuation at WSW 13	
1 low removal rates 0-45 %	AMDOPH	45 %	- 256 %	(exceptional case)
	Carbamazepine	41 %	86 %	
	Primidone	0 %	31 %	
2 medium removal rates 46-95 %	Clofibric acid	90 %	14 %	(exceptional case)
	Diclofenac	85 %	80 %	
	Propyphenazone	90 %	- 38 %	(exceptional case)
3 high removal rates > 95 %	Bezafibrate	> 95 %	> 95 %	
	Indometacine	> 97 %	> 97 %	

At water supply well 13, where infiltrated surface water is mixed with land sited groundwater and old groundwater from the deep aquifer, carbamazepine and diclofenac were attenuated by 80 % and 86 %, respectively. A low attenuation rate of around 14 % was observed for clofibric acid at the water supply well 13 resulting from mixture of young bank filtrate and older bank filtrate / groundwater with higher amounts of this compound. The observed clofibric acid median concentration of 180 ng/L at TEG374 also were higher than the concentrations noticed at surface water and could be explained by a formerly higher application of the precursor compounds clofibrate ethyl, etofibrate and etofyllinclofibrate. AMDOPH and propyphenazone represent exceptional cases with detected concentrations that were partly higher (up to 200 %) in water supply well 13 than those observed in the surface water. The explanation of this behavior for AMDOPH and propyphenazone is a formerly production spill of a pharmaceutical plant in the city Oranienburg located upstream from the north-western districts of Berlin (Reddersen, 2002). Additionally, very high AMDOPH concentrations (around a median of 6.2 µg/L) were detected at TEG374. T/He effective age dating yielded an age of 25 years for the groundwater at TEG374 [B.Fritz: Bitte Verweis auf Hydrogeologen Teil age dating Tegel] which supported the hypothesis of the mixing with older groundwater contaminated with higher concentrations of phenazone-type residues..

72

1.4.5   Wannsee surface water

Former investigations by the hydro geologic group reported the distribution of anthropogenic tracer compounds in lake Wannseesuch as boron and EDTA [B. Fritz: Bitte Verweis auf Hydrogelogenteil Wannsee]. To get an idea of the distribution of the drug residues across lake Wannsee in front of transect Wannsee I and Wannsee II, the lake was sampled two times in March 2004 and July 2004. As Figure 62 shows, nineteen different locations were chosen and sampled in cooperation with the algae group [Birgit: Bitte Verweis auf Chourus Teil Wannsee]. Additionally sampling point 9 was sampled during both campaigns at the surface and at the different depths of 2, 4, 6 and 7 meters.
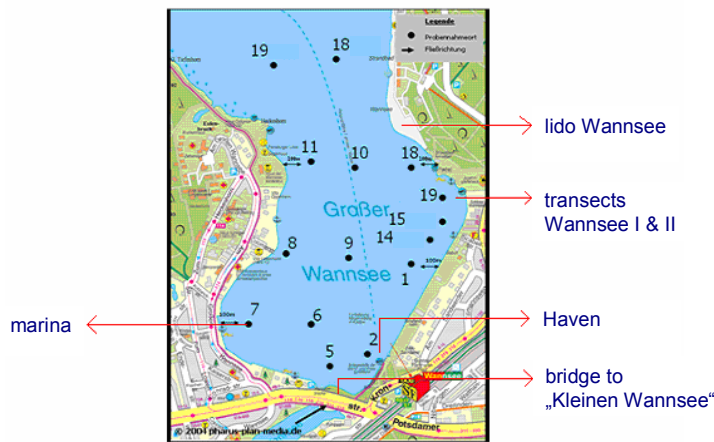
Figure 62. Sampling locations across lake Wannsee

Because the Teltowkanal is seasonally loaded with the effluents from up to three STP and partially flows into the south of lake Wannsee, the channel affects the concentrations of drug residues within this lake. Therefore, four different locations along the channel, one near the influx to lake Wannsee and another one in front of transect Wannsee were sampled in September 2004, as shown in Figure 63.
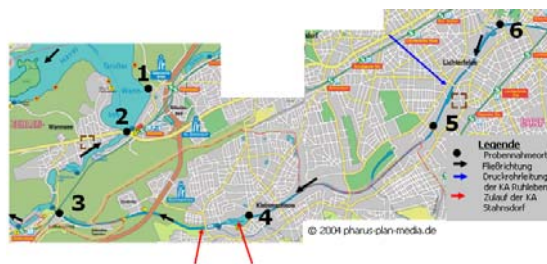
Figure 63. Sampling locations along the Teltowkanal

Table 23 gives an overview of the six sampling locations of the third sampling event.

Table 23. Investigated locations along Teltow channel at lake Wannsee.

Nr.	Location
1	Steg beim Jugendgästehaus (in front of transect Wannsee)
2	Wannsee bridge (connection between kleiner Wannsee and lake Wannsee)
3	Nathanbrücke (end of Teltowkanal)
4	Friedensbrücke; Zehlendorfer Damm
5	Eugen-Kleine-Brücke; Wismarer Straße
6	Prinzregent-Ludwig-Brücke;Birkbuschstr.

During this investigation seven pharmaceutical residues were detected, namely AMDOPH, bezafibrate, carbamazepine, clofibric acid, naproxen, primidone and propyphenazone. Table 24 shows concentration range and mean concentrations of the observed compounds.

Table 24. Concentration (ng/L) range of pharmaceutically active compounds with positive findings in lake Wannsee.

	March 2004 (n=15)			July 2004 (n=15)		
	min [ng/L]	max [ng/L]	mean concentration [ng/L]	min [ng/L]	max [ng/L]	Mean concentration [ng/L]
AMDOPH	110	170	129	200	250	228
Bezafibrate	50	220	93	10	40	25
Carbamazepine	440	1050	611	200	470	367
Clofibric acid	30	100	53	20	40	31
Diclofenac	150	830	298	60	170	83
Naproxen	20	70	29	30	30	30
Primidone	190	560	294	190	320	241
Prophyphenazone	50	70	60	120	140	129

Results of the sampling at different depths are presented in Table 25 and show no significant distribution between different layers in the surface water within the analytical measurement inaccuracy. Only in July 2004, surface water concentrations for diclofenac show a clear decrease of 100 ng/L by depth. This behaviour is unexpected because diclofenac is known to be eliminated by photo chemical reactions (Buser, 1998) and if a depth distribution would be presumed then a concentration increase with the depth would be expected.

Table 25. Results of different depth sampling in March and July 2004

Date	March 2004						July 2004				
Sampling point	FU 9						FU 9				
Depth	Surface	2m	4m	6m	7m		Surface	2m	4m	6m	7m
	[ng/L]						[ng/L]				
AMDOPH	150	140	130	120	130		250	270	240	230	230
Bezafibrate	50	70	70	50	60		10	20	20	20	30
Carbamazepine	470	430	440	480	560		410	380	460	470	370
Clofibric acid	40	40	40	40	40		30	30	30	30	30
Diclofenac	210	210	260	230	200		170	100	70	70	80
Naproxen	20	20	20	20	20		30	30	30	30	30
Primidone	350	230	290	280	330		240	170	220	240	250
Prophyphenazone	60	50	50	50	50		130	130	130	130	130

The results for the third sampling campaign at Teltowkanal and two sampling points in September 2004 are presented in Figure 64.
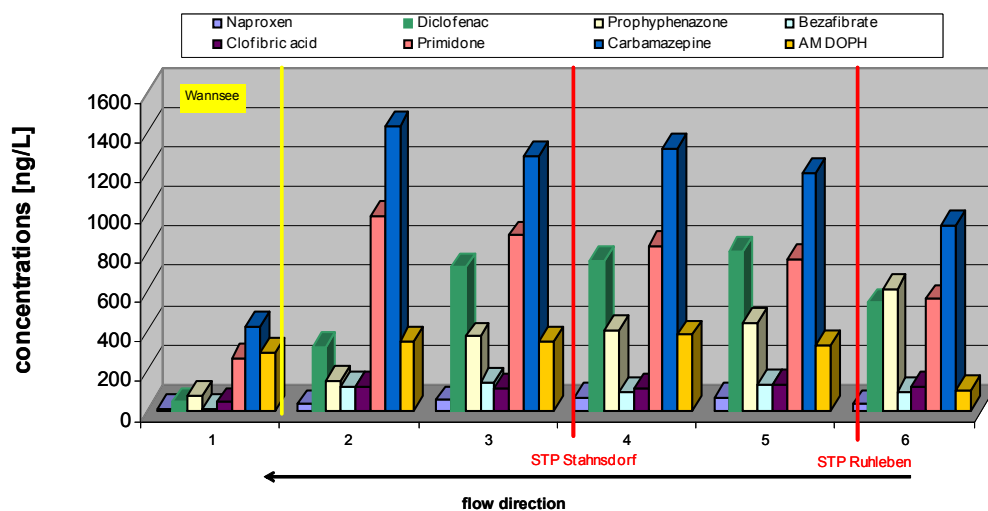
Figure 64. Concentrations of the observed compounds at the Teltowkanal

1.4.5.1 AMDOPH

The observed concentrations of AMDOPH were very similar across lake Wannsee in March 2004. Concentrations between 110 ng/L - 170 ng/L with a mean concentration of 129 ng/L were found during the first sampling. Opposite to this, the concentrations during the second sampling event are higher and vary between 200 ng/L - 250 ng/L with a mean concentration of 228 ng/L.
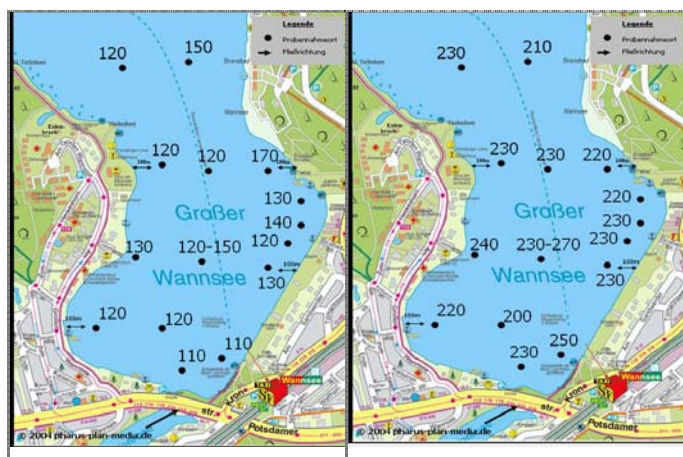
Figure 65. AMDOPH concentrations [ng/L] across lake Wannsee in March (left) and July (right) 2004

During third sampling event in September 2004 at the Teltowkanal and the two other sampling locations, AMDOPH concentrations between 100 ng/L and 380 ng/L were observed as Figure 67 presents. A concentration of 100 ng/L was detected at sampling point upstream the pipeline from the sewage water treatment plant Ruhleben. After the passage of the pipeline effluent from STP Ruhleben, concentration increased up to 380 ng/L. At the location in front of transect Wannsee 290 ng/L of AMDOPH were detected.
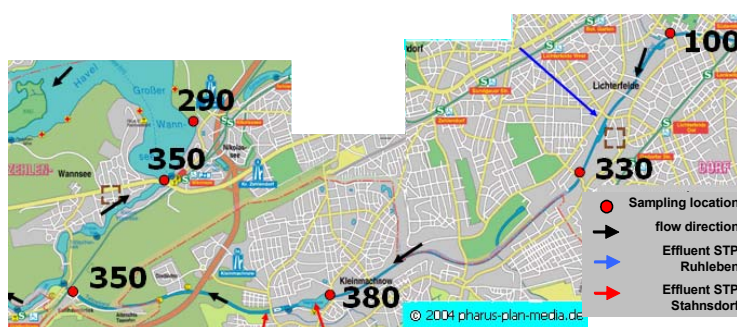
Figure 66. AMDOPH concentrations [ng/L] along the Teltowkanal and lake Wannsee in September 2004

1.4.5.2 Propyphenazone

In March 2004 the concentrations of propyphenazone across lake Wannsee were between the measurement inaccuracy of 20 %, concentrations around 60 ng/L were detected. Samples in July 2004 were increased in comparison to first sampling event around a concentration of 130 ng/L. Similar to results of AMDOPH no significant distribution differences could be observed in lake Wannsee during both campaigns.

Figure 67. Propyphenazone concentrations [ng/L] across lake Wannsee in March (left) and July (right) 2004

Figure 68 shows detected concentrations at Teltowkanal that are slightly decreasing with a maximum of 610 ng/L at upstream sampling point no. 6 (see Figure 63) in the east a minimum of 70 ng/L in surface water in front of transect Wannsee. The effluents of the sewage water treatment plants Ruhleben and Stahnsdorf show no obvious effect on the concentration of Propyphenazone along the Teltowkanal.
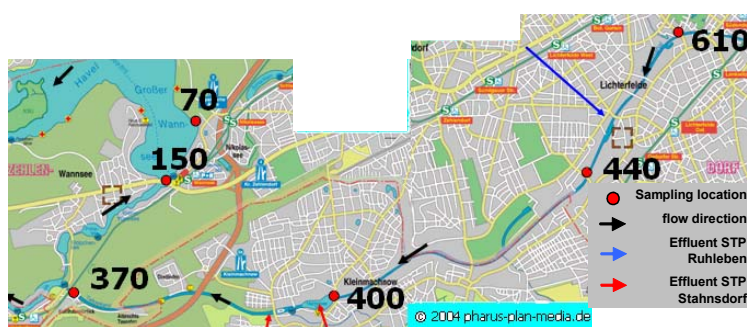
Figure 68. Propyphenazone concentrations [ng/L] along Teltowkanal and lake Wannsee in September 2004

77

1.4.5.3   Bezafibrate

In Figure 69 bezafibrate concentrations in March 2004 are presented for the different sampling points in lake Wannsee. They were between a minimum of 60 ng/L and increasing up to 220 ng/L in the south near bridge Wannsee. During investigations in July 2004 very low concentrations under the limit of quantification of this compound (LOQ < 50 ng/L) were observed.
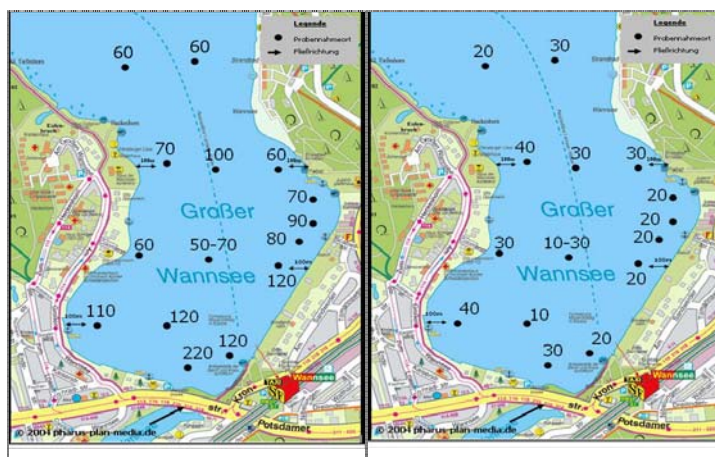
Figure 69. Bezafibrate concentrations [ng/L] across lake Wannsee in March (left) and July (right) 2004

Teltow channel sampling in September 2004 show bezafibrate concentrations between 90 ng/L and 130 ng/L, as represented in Figure 69. The sampling points before the effluents of STP Ruhleben and Stahnsdorf reaching the channel, show concentrations of 90 ng/L. Behind them concentrations are increased up to 130 ng/L respective 140 ng/L. At the sampling location in front of transect Wannsee only a trace (10ng/L) of bezafibrate could be identified in September 2004.
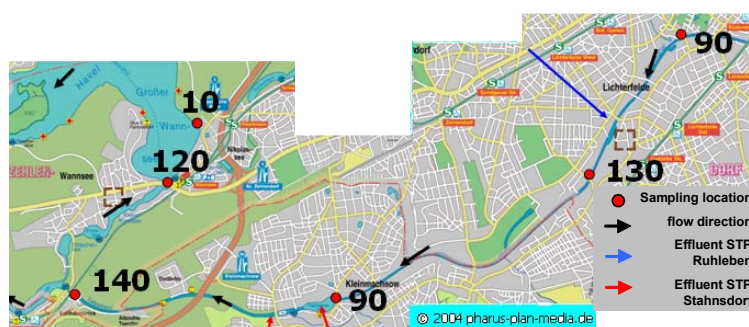
Figure 70. Bezafibrate concentrations [ng/L] along the Teltowkanal and lake Wannsee in September 2004

1.4.5.4   Carbamazepine

As shown in Figure 71, carbamazepine concentrations in March 2004 were detected with a maximum of 1050 ng/L at sampling point near the Wannsee bridge in the south of the lake. Minimum concentrations of 440 ng/L were measured at sampling point 10 (see Figure 62) in the north of the lake. High concentrations between 720 ng/L and 800 ng/L were observed at the eastern bank of lake Wannsee. In summer the concentrations of carbamazepine were significantly lower than during the first sampling event.

Figure 71. Carbamazepine concentrations [ng/L] across lake Wannsee in March (left) and July (right) 2004

During investigations at the Teltowkanal, carbamazepine concentrations of 930 ng/L were observed upstream the effluent of STP Ruhleben as illustrated in Figure 72. Behind that effluent increased concentrations from 1200 ng/L to 1430 ng/L were founded. The effluent of STP Stahnsdorf has no clear effect on carbamazepine concentrations, this is very similar to the behaviour of AMDOPH concentrations. In front of transect Wannsee only 420 ng/L were detected.
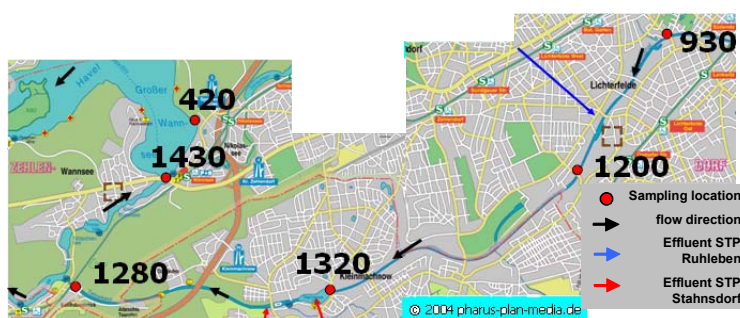
Figure 72. Carbamazepine concentrations [ng/L] along the Teltowkanal and lake Wannsee in September 2004

1.4.5.5   Clofibric acid

In March 2004, clofibric acid concentrations around a mean concentration of 53 ng/L were observed and no obviously distribution could be concluded as displayed in Figure 73. In spite of this sampling point no.5 (see Figure 62) that is nearly the connection of the Teltow channel and lake Wannsee, showed a concentration of 100 ng/L. During second sampling period a little lower mean concentration of 31 ng/L was determined across the lake. In contrast to March sampling, concentration near the Wannsee bridge show an amount like the other sampling locations.
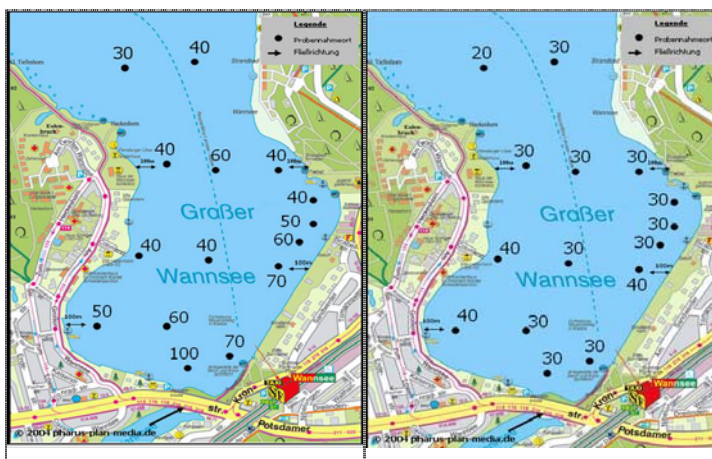
Figure 73. Clofibric acid concentrations [ng/L] across lake Wannsee in March (left) and July (right) 2004

The investigations at Teltowkanal show constant concentrations around a mean of 120 ng/L, as presented in Figure 74. The effluents of the two sewage water treatment plants have no obvious effect on clofibric acid concentrations. At the sampling location in front of transect Wannsee a significantly decreased concentration of 40 ng/L was detected.

Figure 74. Clofibric acid concentrations [ng/L] along the Teltowkanal and lake Wannsee in September 2004

1.4.5.6   Diclofenac

Diclofenac concentrations with a minimum of 150 ng/L in the north of the lake and a maximum of 830 ng/L in the south near Wannsee bridge were observed during sampling in March 2004. A mean concentration of 298 ng/L was detected. Like the distribution of carbamazepine, the concentrations at the south-eastern bank were higher than at the

western bank as Figure 75 shows. In July 2004, the mean concentration of only 83 ng/L was determined. A clear distribution as shown during the first sampling, was not observed.
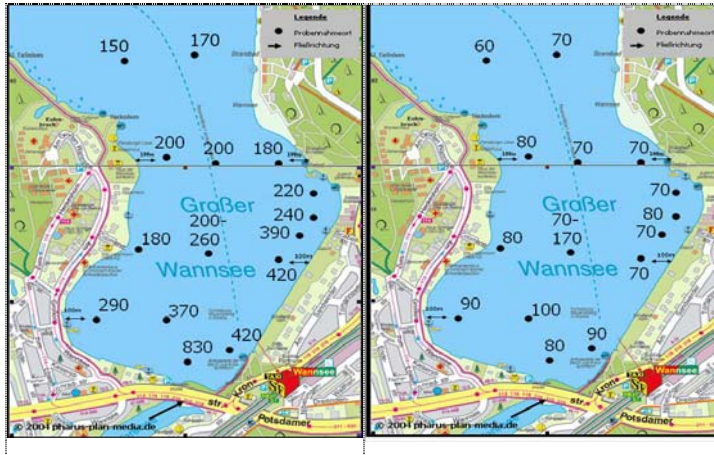
Figure 75. Diclofenac concentrations [ng/L] across lake Wannsee in March (left) and July (right) 20042004

The diclofenac concentrations investigated at Teltowkanal were detected between 540 ng/L and 720 ng/L as shown in Figure 76. At the additional sampling locations at the Wannsee bridge and in front of transect Wannsee concentrations of 320 ng/L respective only 40 ng/L were observed. Concentrations along the channel are increased behind the effluent of STP Ruhleben but were not affected behind effluent of STP Stahnsdorf. This effect is very similar to the behaviour of AMDOPH and carbamazepine.
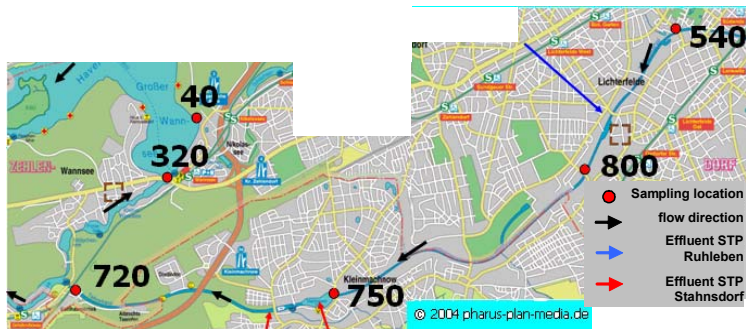
Figure 76. Diclofenac concentrations [ng/L] along the Teltowkanal and lake Wannsee in September 2004

1.4.5.7 Primidone

Concentrations of primidone in March 2004 were detected between 190 ng/L up to 560 ng/L with a mean of 294 ng/L, as illustrated in Figure 77. The concentrations show a distribution with minor concentrations in the north and higher concentrations in the south. A significant

distribution among the western and eastern bank were not observed. In July 2004, a mean concentration of 241 ng/L was detected within a range of 190 ng/L to 320 ng/L. A clear distribution between north and south respectively west and east was not observed.

Figure 77. Primidone concentrations [ng/L] across lake Wannsee in March (left) and July (right) 2004

As shown in Figure 78, primidone concentrations from 560 ng/L up to 880 ng/L along the Teltowkanal were detected. Behind the effluents of the STP Ruhleben a concentration increase of 200 ng/L was observed. Effluent of Stahnsdorf leads to no significantly increase within the measurement inaccuracy of around 20 % at the sampling locations behind it. At the sampling location near Wannsee bridge a maximum concentration of 980 ng/L was observed. In front of transect Wannsee a significant concentration decrease around 500 ng/L was recognizable.
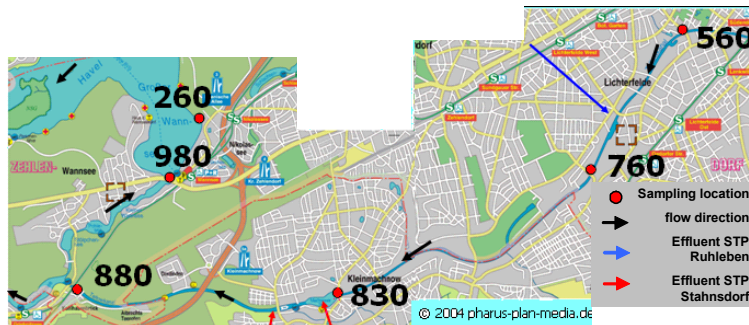
Figure 78. Primidone concentrations [ng/L] along the Teltowkanal and lake Wannsee in September 2004

1.4.5.8   Naproxen

Naproxen concentrations across lake Wannsee in sampling campaigns March and July 2004 presented in Figure 79 show an approximate similar concentration level around a mean concentration around 30 ng/L. A distribution of the naproxen concentrations in lake Wannsee was not observable.
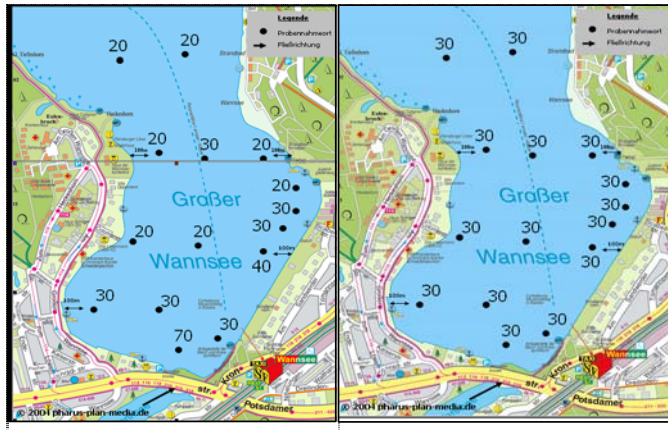
Figure 79. Naproxen concentrations [ng/L] across lake Wannsee in March (left) and July (right) 2004

Concentrations of naproxen along the Teltowkanal were detected at a mean of 50 ng/L. At sampling location no.6 (see Figure 63) before the effluent of STP Ruhleben reached the channel, a naproxen concentration of 30 ng/L was detected. Behind the effluent the measured concentrations were increased up to 60 ng/L. Near Wannsee bridge only 30 ng/L were observed and in front of transect Wannsee only a trace (4 ng/L) of naproxen was identified.
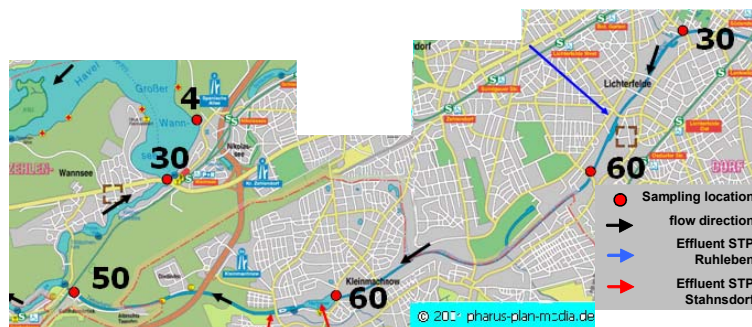
Figure 80. Naproxen concentrations [ng/L] along the Teltowkanal and lake Wannsee in September 2004

1.4.5.9 Conclusions about the occurrence of PhAC's in surface water

Up to eight PhAC's were observed in surface water of lake Wannsee. The metabolite of dimethylaminophenazone AMDOPH, the antiepileptic drugs carbamazepine and primidone, the antirheumatic / antiphlogistic drugs indomethacine, naproxen and propyphenazone, the blood lipid regulator bezafibrate and the metabolite of different blood lipid regulators clofibric acid were identified and quantified in the lake water. In March 2004 a tendency of distribution of higher concentrations at the eastern bank was observed for carbamazepine, clofibric acid, diclofenac and bezafibrate at lake Wannsee. In July 2004, the distribution tendency for bezafibrate, carbamazepine and primidone was observed in the reverse direction. This may be explainable with the western located marina that is especially used in summer and where toilette reservoirs partly excreted untreated in the lake. The other compounds did not show any western / eastern distribution. A north / south distribution was established for all compounds (except for AMDOPH and propyphenazone) with higher concentrations in the south most likely caused by influents from the Teltowkanal which is loaded during summer with effluents of three sewage water treatment plants. AMDOPH and propyphenazone did not show the behaviour caused by the main origin of these two compounds from a superfund site at a pharmaceutical plant located in the city of Oranienburg north-west of Berlin.

1.4.6   Transects Wannsee 1 & Wannsee 2

From the beginning of the NASRI project in May 2002 the surface water, the shallow wells (3338, 3337, 3335) and the water supply well no. 4 at transect Wannsee 1 were sampled monthly until April 2004. The multi-level well BEE201UP/OP was sampled since January 2003. The monitoring well 3338 could only be sampled in 2002 and three times in 2003 and 2004 because the ground water level was beyond the screen of the well. The deep monitoring wells 3332, 3334 and 3336 have only been sampled one time in March 2003. Since the completion in January 2004 the transect Wannsee 2 was sampled monthly until August 2004. Differences in the sample numbers (n) shown in the Table 26 and Table 27 depend on an intensive sampling period during September and October 2003 and an effort to reduce the number of samples at monitoring wells delivering unnecessary data.

The results show that similar to the transect Tegel the already named compounds have been detected in the surface water in front of transects Wannsee 1 and 2. The pharmaceuticals carbamazepine, diclofenac and primidone could be observed in the shallow monitoring wells and the multi-level wells at the transect Wannsee 1 and Wannsee 2 as shown in Table 26. They also occur in low concentrations at the water supply wells 3 and 4.

The metabolites AMDOPH, clofibric acid and the analgesic drug propyphenazone could be detected in the shallow wells and appeared in significantly higher concentrations in the multi-level wells in front of the water supply wells at both transects at lake Wannsee.

Table 26. Compounds with positive findings and their concentration range [ng/L] at transect Wannsee 1

ng/L	Surface Water (n=28)		3338 (n=11)		3337 (n=27)		BEE201OP (n=18)		BEE201UP (n=14)		3335 (n=12)		Well 4 (n=23)	
	min	max	min	max	min	max	min	max	min	max	min	max	min	max
Diclofenac	10	265	15	80	n.d.	85	n.d.	65	5	85	n.d.	50	n.d.	55
Clofibric acid	<LOQ	120	n.d.	70	n.d.	60	15	270	n.d.	240	n.d.	15	40	245
Propyphenazone	20	350	45	180	n.d.	280	105	565	55	505	n.d.	125	n.d.	90
AMDOPH	45	365	55	295	70	425	130	1790	425	1770	65	430	100	615
Carbamazepine	185	760	180	620	185	610	30	275	15	105	205	565	n.d.	60
Primidone	20	245	20	190	n.d.	280	95	235	90	220	20	305	n.d.	100
Indometacine	n.d.	85	n.d.	<LOQ	n.d.	<LOQ	n.d.	n.d.	n.d.	n.d.	n.d.	n.d.	n.d.	n.d.
Bezafibrate	n.d.	105	n.d.	<LOQ	n.d.	<LOQ	n.d.	n.d.	n.d.	n.d.	n.d.	n.d.	n.d.	n.d.
Bentazone	n.d.	50	n.d.	65	n.d.	55	n.d.	30	n.d.	30	n.d.	45	n.d.	40
Mecoprop	n.d.	50	n.d.	60	n.d.	30	n.d.	45	n.d.	55	n.d.	60	n.d.	40
NPS	n.d.	55	n.d.	60	n.d.	75	20	925	30	600	n.d.	25	25	130
p,p'-DDA	n.d.	50	5	55	n.d.	50	10	60	n.d.	55	n.d.	45	n.d.	35
o,p'-DDA	n.d.	15	n.d.	20	n.d.	15	5	20	n.d.	20	n.d.	15	n.d.	10

n.d.   not detected

<LOQ.   < limit of quantitation

Table 27. Compounds with positive findings and their concentration range [ng/L] at transect Wannsee 2

ng/L	Surface water (n=24)		BEE 205 (n=22)		BEE 206 (n=23)		BEE 202OP (n=23)		BEE 202MP1 (n=18)		BEE 202MP2 (n=16)		BEE 202UP (n=20)		BEE 203 (n=24)		well 3 (n=20)		BEE 204UP (n=17)		BEE 204OP (n=14)	
	min	max	min	max	min	max	min	max	min	max	min	max	min	max	min	max	min	max	min	max	min	max
Diclofenac	n.d.	175	n.d.	150	n.d.	70	n.d.	65	n.d.	80	5	75	n.d.	90	n.d.	40	n.d.	65	n.d.	40	n.d.	45
Clofibric acid	10	120	n.d.	45	n.d.	40	n.d.	55	n.d.	70	n.d.	385	10	340	n.d.	40	25	160	n.d.	100	n.d.	35
Propy-phenazone	20	215	10	175	n.d.	85	n.d.	55	5	565	235	635	150	650	n.d.	370	25	200	n.d.	60	n.d.	40
AMDOPH	45	365	75	305	80	270	45	220	85	1725	270	1845	385	1660	60	1120	245	905	25	895	5	345
Carbamazepine	185	760	145	775	135	875	150	470	65	265	n.d.	110	n.d.	65	80	620	n.d.	110	n.d.	50	n.d.	30
Primidone	20	270	40	285	45	305	n.d.	200	30	215	n.d.	190	40	245	25	275	35	140	n.d.	25	n.d.	20
Indometacine	n.d.	85	n.d.	25	n.d.	25	n.d.	n.d.	n.d.	n.d.	n.d.	n.d.	n.d.	n.d.	n.d.	n.d.	n.d.	25	n.d.	n.d.	n.d.	n.d.
Bezafibrate	n.d.	105	n.d.	25	n.d.	25	n.d.	n.d.	n.d.	n.d.	n.d.	n.d.	n.d.	n.d.	n.d.	n.d.	n.d.	n.d.	n.d.	n.d.	n.d.	n.d.
Bentazone	n.d.	45	n.d.	25	n.d.	30	n.d.	20	n.d.	n.d.	n.d.	n.d.	n.d.	n.d.	n.d.	n.d.	n.d.	n.d.	n.d.	n.d.	n.d.	n.d.
Mecoprop	n.d.	50	n.d.	65	n.d.	25	n.d.	10	n.d.	30	n.d.	35	n.d.	35	n.d.	15	n.d.	25	n.d.	20	n.d.	15

n.d.   not detected

<LOQ.   < limit of quantitation

Bezafibrate and indometacine could not be detected behind the shallow wells 3338 and 3337 at transect Wannsee 1 and at BEE205 and BEE206 of transect Wannsee 2. At the deeper wells 3332, 3334 and 3336 only traces (< 20 ng/L) of AMDOPH, clofibric acid and primidone were observable.

1.4.6.1   AMDOPH

As presented in Figure 81, the median concentration of AMDOPH detected in the surface water in front of the transects Wannsee was around 185 ng/L. The attenuation rates at the shallow monitoring wells BEE205 and BEE206 were between 20 % and 28 % and show only a slightly removal of AMDOPH still within or slightly higher than the analytical measurement accuracy of 20 %. At BEE202OP and BEE203 attenuation of around 47 % were obtained. However, as it was noticed in the deeper screens of the multi-level well BEE202, AMDOPH concentrations are increasing by depth and showed a maximum median concentration of 870 ng/L in BEE202MP2. This behaviour is caused by the origin of AMDOPH and is confirmed by age dating investigations that show in the share of young bank filtrate decreases by depth of the multi-level well BEE202. [B.Fritz: Bitte Verweis auf Hydrogelogen Teil]. Same behaviour was recognized at the landsite multi-level monitoring well with concentrations of 15 ng/L at BEE204OP and 220 ng/L at BEE204UP. Water supply well no. 3 with 375 ng/L is a mixture of older and landward groundwater and recently infiltrated surface water.
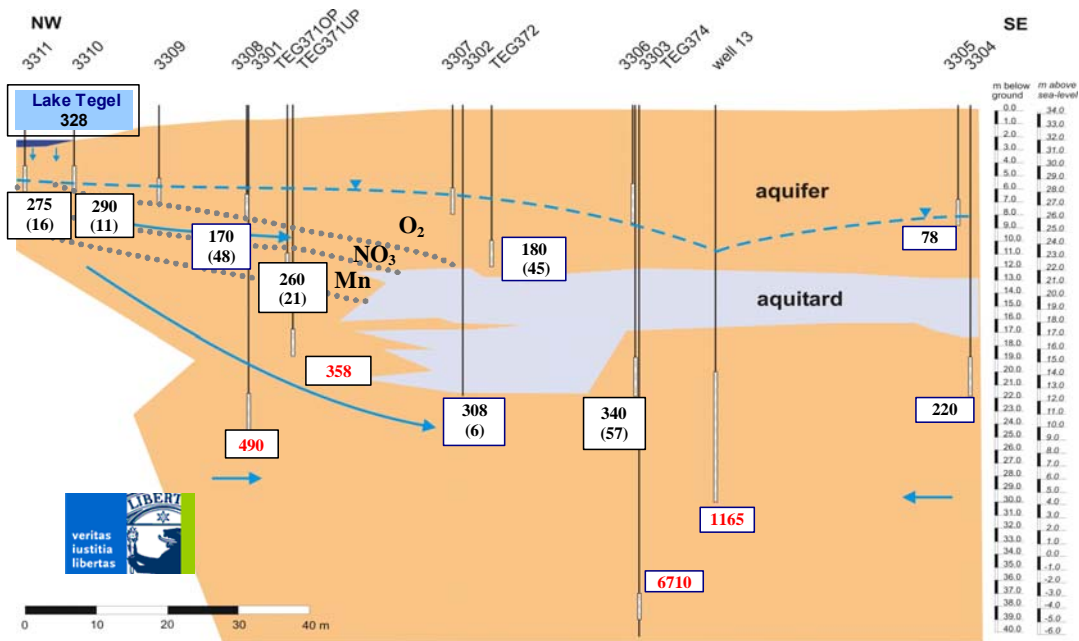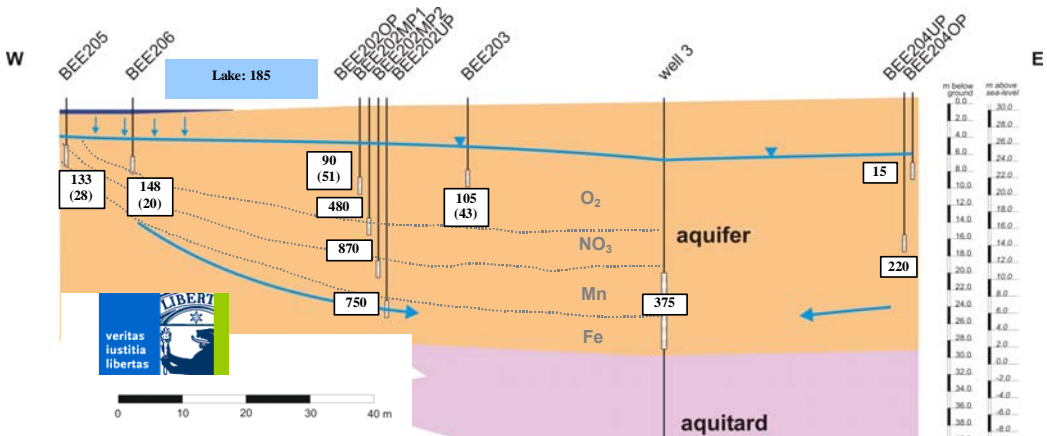

Figure 81. Transect Wannsee 2 - median concentrations of AMDOPH at the different monitoring wells and the water supply well 3. Attenuation rates in percent are given in brackets.

Similar to the observations at lake Tegel, the distribution of AMDOPH concentrations was comparable to the distribution of ammonium concentrations as illustrated in Figure 82.
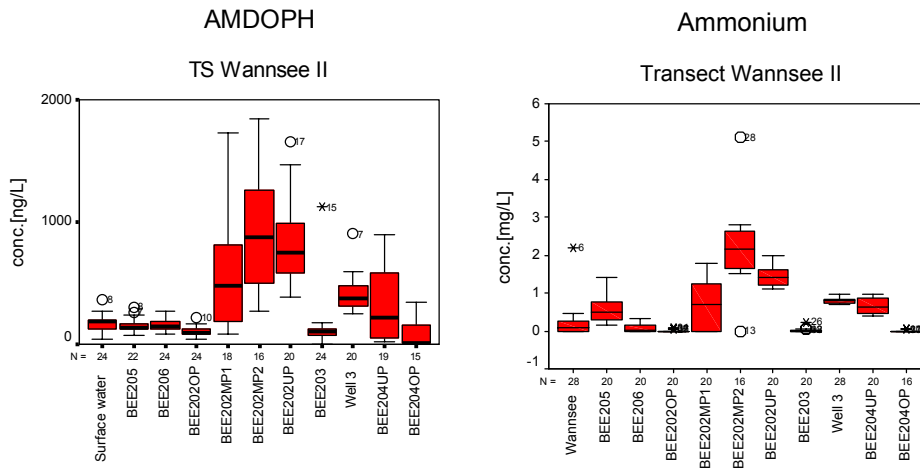
Figure 82. Distribution of AMDOPH (left) and ammonium (right, data by BWB) concentrations at transect Wannsee 2.

1.4.6.2 Propyphenazone

In the surface water propyphenazone was detected with a median concentration of 80 ng/L. It was attenuated below the limit of quantification at BEE203 as shown in Figure 83. Similar to AMDOPH concentrations of propyphenazone at the multi-level well BEE202 are increasing from 15 ng/L up to 350 ng/L. In the landward multi-level well only in the deeper part (BEE204UP) 20 ng/L of propyphenazone were detected. In the upper part only traces were identified.
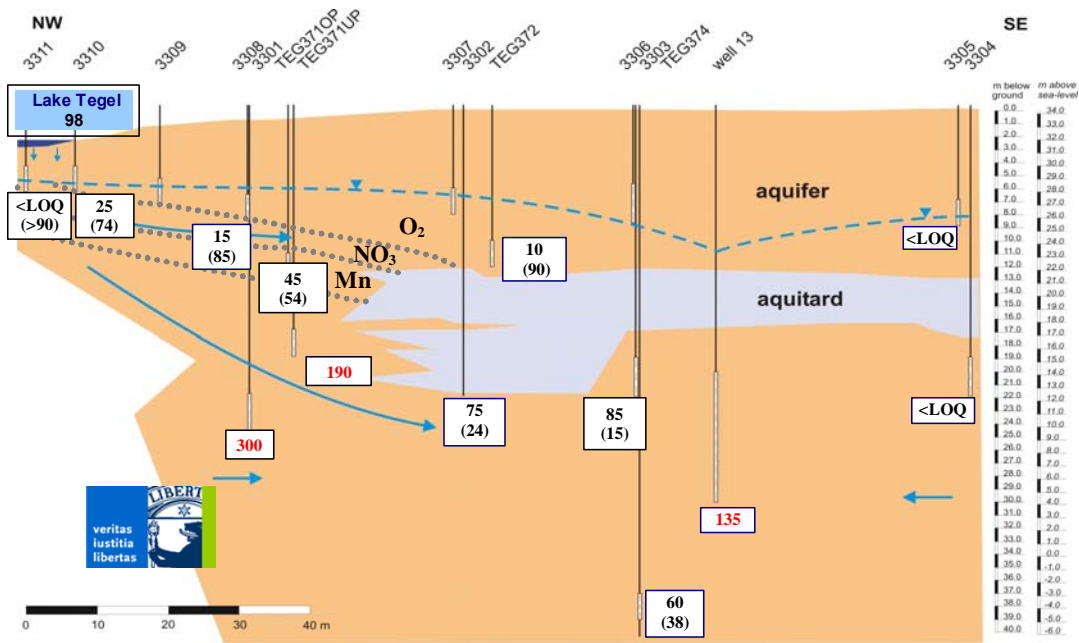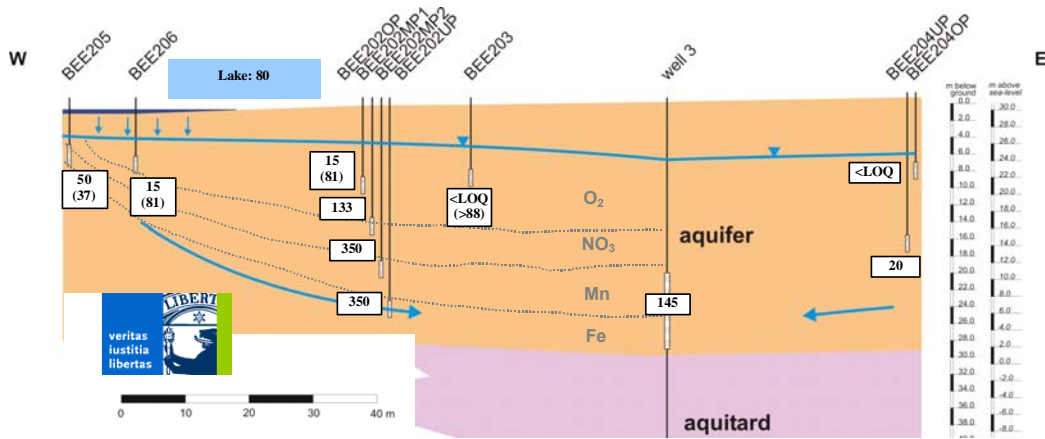
Figure 83. Transect Wannsee 2 - median concentrations of propyphenazone at the different monitoring wells and the water supply well 3. Attenuation rates in percent are given in brackets.

The distributions of detected propyphenazone concentrations at the different sampling locations shown in Figure 84 were comparable to previously described distributions of AMDOPH.
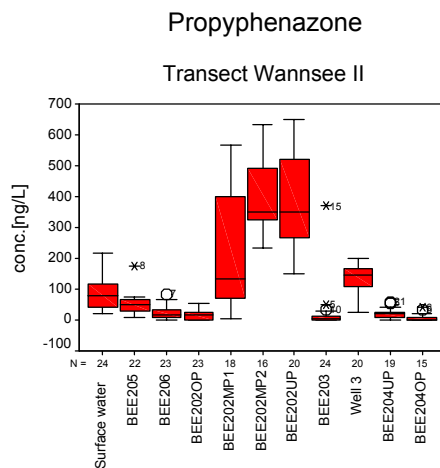
Figure 84. Distributions of propyphenazone concentrations at transect Wannsee 2.

1.4.6.3   Carbamazepine

Within the analytical measurement accuracy the observed median concentration of 380 ng/L found in surface water of lake Wannsee was not significantly decreased up to BEE206 as

shown in Figure 85. The monitoring well under the lake BEE206 only shows a minor attenuation rate of 24 %. During further infiltration along BEE202OP and BEE203 concentrations between 218 ng/L and 260 ng/L were detected and represent a removal rate of carbamazepine of around 38 %.
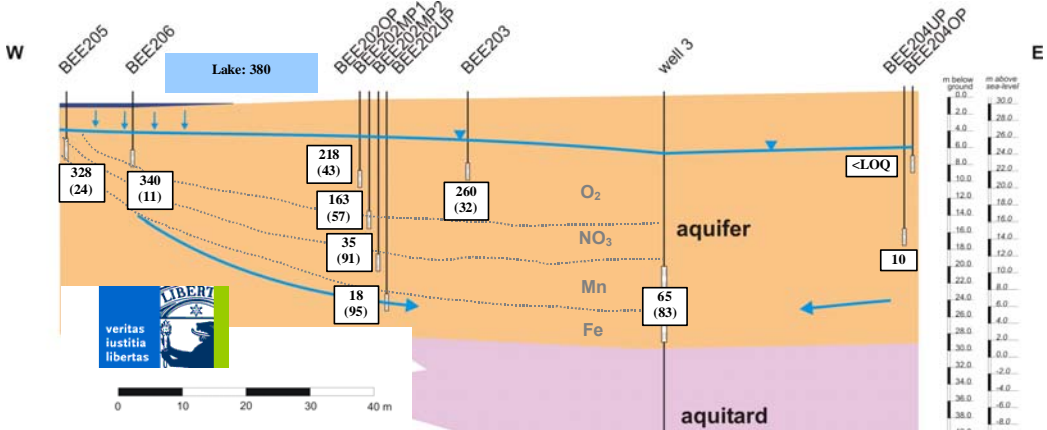
Figure 85. Transect Wannsee 2 - median concentrations of carbamazepine at the different monitoring wells and the water supply well 3. Attenuation rates in percent are given in brackets.

As can be seen in Figure 86, surface water concentrations of carbamazepine are increasing during the third quartile of 2004 up to maximum of around 750 ng/L in September 2003. Concentrations were also temporaily shifted at monitoring wells BEE203 and BEE202OP in December 2003. This is in accordance with the determined travel times between the surface water and the monitoring wells BEE203 or BEE202 of 2-4 months (please referee to [B.Fritz: Bitte Verweis auf Hydrogelogenteil: Wannsee 2, travel times]). Thus, the behaviour of carbamazepine is in line with this assumption. Looking at the surface water concentrations during the intensive sampling period (Sep. 03 - Oct. 03) a high variability of detected concentrations was noticed. That means a monthly sampling deliver only a minor resolution and is only a compromise between analytical costs and good and better reproducible data.
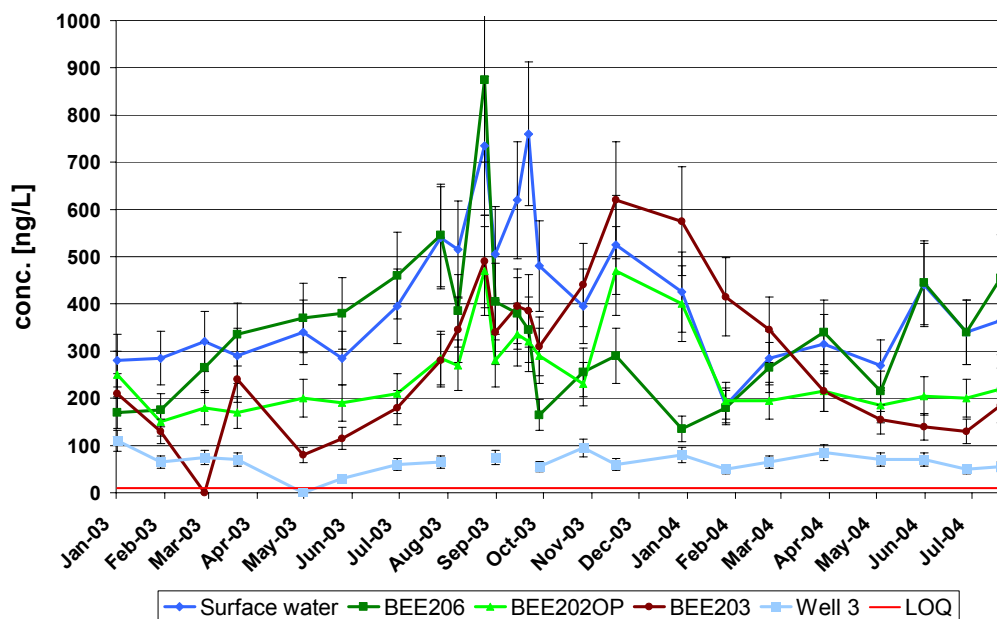
Figure 86. Concentrations of carbamazepine at the different sampling locations inclusive the intensive sampling period from September the 15th until October 20th in 2003.

In contrast to AMDOPH and propyphenazone, median concentrations for carbamazepinewere decreased at multi level well BEE202 by depth to a minimum of 18 ng/L that means an attenuation rate of 95 %.
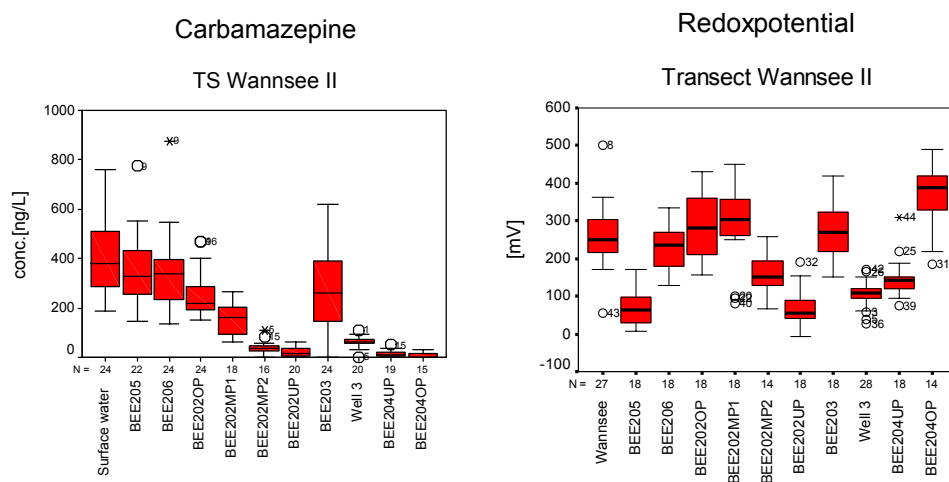
Figure 87. Distribution of carbamazepine (left) and the redox potential (right, data by BWB) concentrations at transect Wannsee 2.

Observed median concentrations in landward groundwater were around the limit of quantification of 10 ng/L. At water supply well no. 3 a median concentration of 65 ng/L was detected and that correspond an attenuation of 83 %. As illustrated distributions of carbamazepine and the redox potential didn't show a similarity like it was observed at transect lake Tegel.

1.4.6.4   Clofibric acid

The median concentration of 48 ng/L obtained at surface water of lake Wannsee was decreased to 5 ng/L and 15 ng/L at the shallow monitoring wells BEE205 and BEE206, respectively as shown in Figure 88. During soil passage to monitoring well BEE202OP a removal greater than 90 % was recognized.
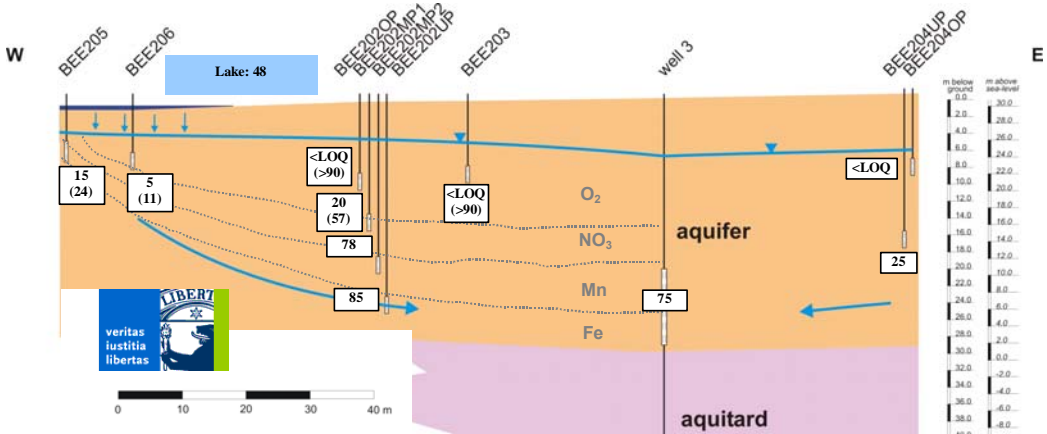
Figure 88. Transect Wannsee 2 - median concentrations of clofibric acid at the different monitoring wells and the water supply well 3. Attenuation rates in percent are given in brackets.

The presented distributions of concentrations in Figure 89 are comparable to the behaviour of AMDOPH and propyphenazone. Similar to AMDOPH and propyphenazone, the detected median concentrations at multi-level well BEE202 are increasing by depth up to a maximum of 85 ng/L. At the deeper land sided monitoring well BEE204UP a median concentration of 25 ng/L was observed and at the upper part of this multi-level well only traces of clofibric acid were identified. The supply well no. 3 showed a median concentration of 75 ng/L, caused by mix of just infiltrated water and older bank filtrate / groundwater.

Clofibric acid
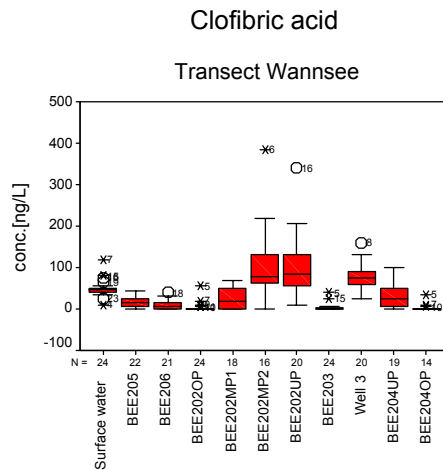
Transect Wannsee

Figure 89. Distribution of clofibric acid concentrations at transect Wannsee 2.

1.4.6.5   Diclofenac

As presented in Figure 90, the median concentration of 65 ng/L was detected at surface water. After infiltration at BEE205 an attenuation of 48 % was observed. Diclofenac was removed by 85 % at BEE206 and was not quantifyable in BEE203. Surprisingly, diclofenac was detected in median concentrations between 15 ng/L and 33 ng/L in the multi-level well BEE202 and the water supply well no.3. In the landward monitoring wells BEE204UP and BEE204OP only traces were identified.
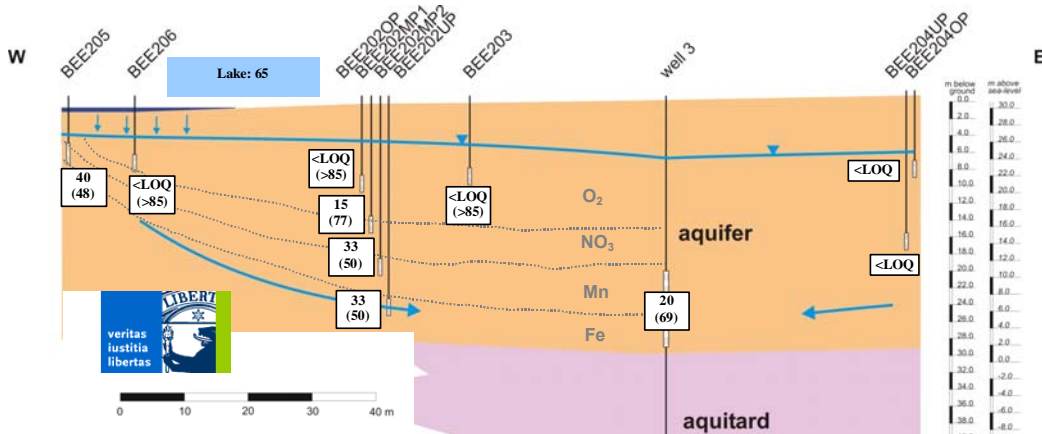
Figure 90. Transect Wannsee 2 - median concentrations of AMDOPH at the different monitoring wells and the water supply well 3. Attenuation rates in percent are given in brackets.

As shown in Figure 91, the distribution of diclofenac concentrations are decreasing quickly after infiltration as it was also observed for bezafibrate and indometacine (not illustrated). However, in monitoring wells drilled in deeper layers of the aquifer minor concentrations were sporadically quantified.

Diclofenac

Transect Wannsee II
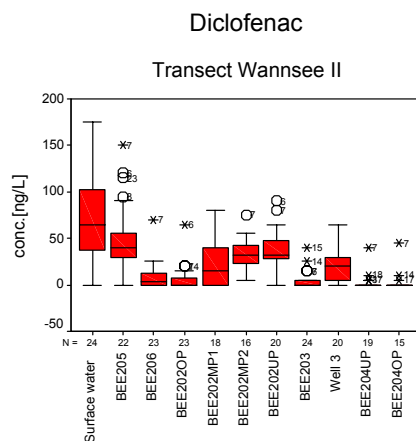
Figure 91. Distribution of diclofenac concentrations at transect Wannsee 2.

1.4.6.6   Primidone

Primidone was detected with a median concentration of 130 ng/L at surface water of lake Wannsee as presented in Figure 92. The observed attenuation rates at the first monitoring wells BEE205 and BEE206 were lower than the analytical measurement accuracy of 20 %. Similar to this, the attenuation at BEE202MP1, BEE202MP2 and BEE202UP were negligible.
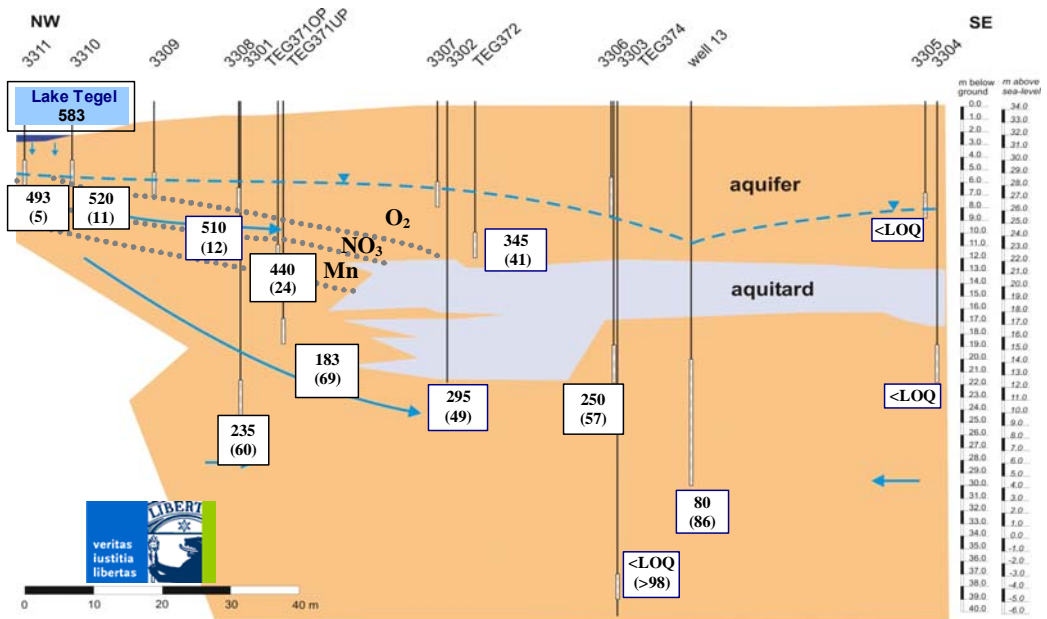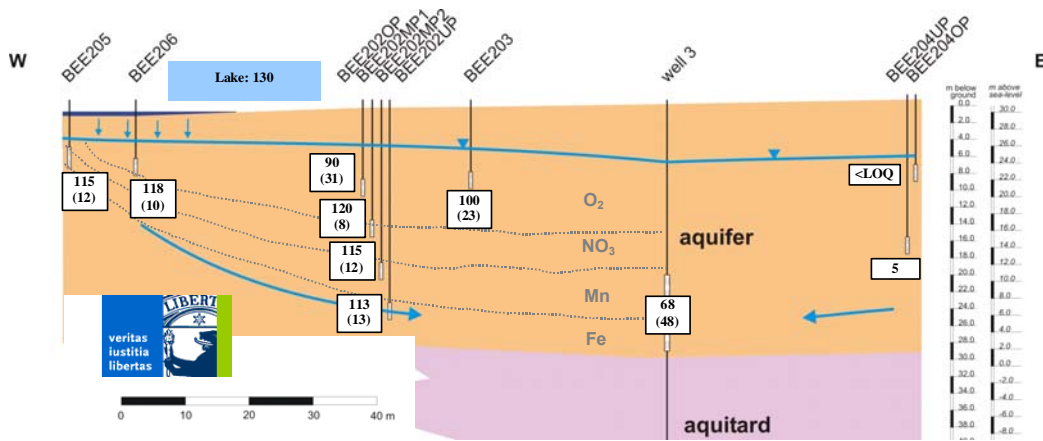
Figure 92. Transect Wannsee 2 - median concentrations of primidone at the different monitoring wells and the water supply well 3. Attenuation rates in percent are given in brackets.

However, at BEE202OP and BEE203 a slightly removal between 23 % - 31 % was noticed. In the landward monitoring wells only traces of primidone were detectable and in the receiving water supply well no. 3 a median concentration of 68 ng/L was detected. Looking at the distributions of primidone concentrations in Figure 93 no significant decreasing effect during bank filtration were observed. Comparing primidone with boron, the antiepileptic drug behaves similar with the exception of higher boron concentrations found at BEE202MP2 and BEE202UP. These are most likely caused by the mixture of recently infiltrated surface water with older bank filtrate and deeper groundwater with higher amounts of boron from geogenic sources.
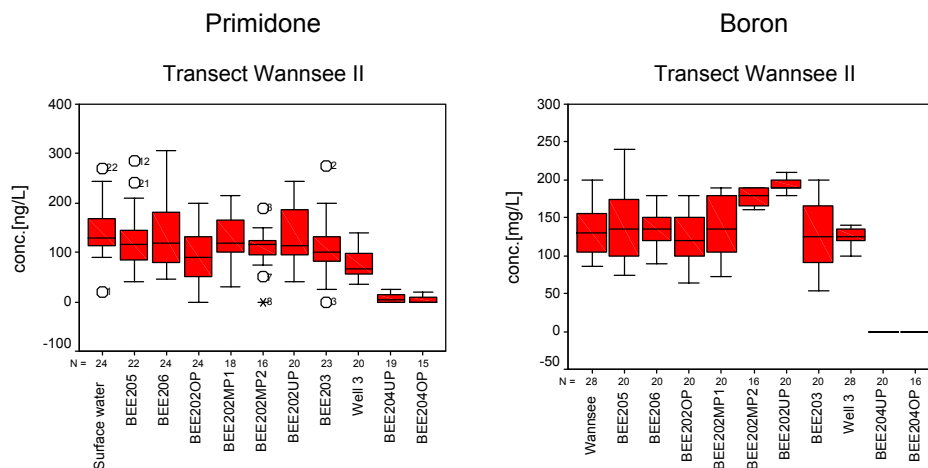
Figure 93. Distribution of primidone (left) and boron (right) concentrations at transect Wannsee 2.

1.4.6.7   Other observed polar residues

Similar to the investigations at transect Tegel, bentazone and mecoprop (pesticides) and 2,2-bis(4-chlorophenyl)acetic acid (p,p'-DDA) metabolite of a pesticide and its isomer 2-(2-chlorophenyl)-2-(4-chlorophenyl)-acetic acid were detectable at trace concentrations around the limit of quantification along all monitoring wells and water supply well no. 3. NPS, metabolite of a corrosion inhibitor, was observed in surface water of lake Wannsee with a median concentration about 25 ng/L. Like AMDOPH, clofibric acid and propyphenazone, NPS concentrations at multi-level well BEE202 are increasing with a maximum median concentration of 260 ng/L at BEE202MP2. At the landward monitoring well BEE204 only 25 ng/L were found and result in a median concentration of 95 ng/L in the receiving water of supply well no. 3.

1.4.7   Conclusions

In conclusion the previously presented results for the field sites at lake Wannsee showed that eight of the investigated drug residues occurred in the surface water. Six of them were observable in the monitoring wells along the infiltration path. Their behavior during bank filtration at both transects were comparable and could be divided into three groups with different attenuation rates as shown in Table 28 & Table 29.

Table 28. Classification of target compounds according to their rates of attenuation at transect lake Wannsee 2

Group	Compound	Median rate of attenuation at BEE203	Median rate of attenuation at WSW 3	
1 low removal rates 0-45 %	AMDOPH	43 %	-103 %	(exceptional case)
	Carbamazepine	32 %	83 %	
	Primidone	23 %	48 %	
2 medium removal rates 46-95 %	Clofibric acid	> 90 %	- 58 %	(exceptional case)
	Diclofenac	> 86 %	69 %	
	Propyphenazone	> 88 %	- 81 %	(exceptional case)
3 high removal rates > 95 %	Bezafibrate	> 97 %	> 97 %	
	Indometacine	> 95 %	> 95 %	

Bezafibrate and indometacine were observed in surface water close to their limit of quantification and they were completely removed during the infiltration process. Diclofenac, clofibric acid and propyphenazone show medium attenuation rates between 62 % and 90 % at the shallow monitoring wells in front of the receiving water supply wells. AMDOPH, carbamazepine and primidone were not significantly removed during bank filtration and the obtained attenuation rates at the monitoring wells in front of the water supply wells were between 23 % and 43 %. In the receiving water supply well no. 3 where the generated raw water is a mixture of bank filtrate and groundwater the determined attenuation rates for carbamazepine and diclofenac were greater than 69 % For primidone only a minor attenuation rate of 48 % was observed. Carbamazepine concentrations shows a temporary shift between the surface water and wells BEE202 or BEE203 which is similar to the travel times determined in age dating experiments conducted by the hydrogeology group. AMDOPH, propyphenazone and clofibric acid are exceptional cases because their detected concentrations in the deeper wells were significantly higher than surface water concentrations. The explanation of this behavior of AMDOPH and propyphenazone is a formerly production spill from a pharmaceutical plant in the city Oranienburg located north-west of Berlin [Reddersen et al., 2002].

Table 29. Classification of target compounds according to their rates of attenuation at transect lake Wannsee 1

Group	Compound	Median rate of attenuation at 3335	Median rate of attenuation at WSW 4	
1 low removal rates 0-45 %	AMDOPH	13 %	- 88 %	(exceptional case)
	Carbamazepine	14 %	94 %	
	Primidone	17 %	91 %	
2 medium removal rates 46-95 %	Clofibric acid	89 %	- 133 %	(exceptional case)
	Diclofenac	62 %	> 99 %	
	Propyphenazone	49 %	74 %	(exceptional case)
3 high removal rates > 95 %	Bezafibrate	> 97 %	> 97 %	
	Indometacine	> 95 %	> 95 %	

The exceptional case of the metabolite clofibric acid could be explained by formerly higher application rates for the precursor compounds clofibrate ethyl, etofyllinfibrate and etofibrate. At transect Wannsee the upper screen of water supply well no. 4 is almost blocked and pumped raw water is only slightly influenced by bank filtration. Due to this only traces of PhAC's were detectable.

1.5 Overall conclusions

As reported in previous investigations (Reddersen, K., 2004) pharmaceutical residues are discharged by municipal STPs and are present at considerable concentrations in Berlin's surface waters. These contaminants are also reaching the surface water in lake Tegel and lake Wannsee which are used as resources for bank filtration or groundwater recharge. During the investigations eight PhACs, the metabolites AMDOPH and clofibric acid, the blood lipid regulating drug bezafibrate, the antiepileptics carbamazepine and primidone, as well as the analgesic / antiphlogistic drugs diclofenac, indometacine, propyphenazone, were detected at the groundwater replenishment site Tegel (GWA), the surface water preparation plant Tegel (OWA) and the bank filtration sites at lake Tegel and lake Wannsee. The observed behaviour for the investigated compounds during the infiltration process at the GWA Tegel and transects Tegel and Wannsee were comparable. According to their attenuation behavior, the detected compounds were assigned to three groups as shown in Table 30.

Table 30. Classsification of the observed drug residues according to their rates of attenuation

Group	Compound	GWA		TS Tegel		TS Wannsee 1		TS Wannsee 2	
		TEG248	WSW 20	TEG372	WSW 13	3335	WSW 4	BEE203	WSW 3
1 low removal rates 0-45 %	AMDOPH*	31%	-245%	45%	-256%	13%	-88%	43%	-103%
	Carbamazepine	9%	55%	41%	86%	14%	94%	32%	83%
	Primidone	30%	26%	0%	31%	17%	91%	23%	48%
2 medium removal rates 46-95 %	Clofibric acid*	83%	75%	90%	14%	89%	-133%	> 90 %	-58%
	Diclofenac	75%	93%	85%	80%	62%	> 99 %	> 86 %	69%
	Propyphenazone*	93%	67%	90%	-38%	49%	74%	> 88 %	-81%
3 high removal rates > 95 %	Bezafibrate	> 97%	> 97%	> 97 %	> 95 %	> 97 %	> 97 %	> 97 %	> 97 %
	Indometacine	> 95%	> 95%	> 95 %	> 97 %	> 95 %	> 95 %	> 95 %	> 95 %

* exceptional cases

When passing the OWA Tegel, only propyphenazone showed a attenuation around 37 %. All other detectable compounds were not affected by the treatment process. AMDOPH and propyphenazone are exceptional cases because their main loads entered the aquatic environment of Berlin during a production spill in the late 1970s when high amounts of these

compounds infiltrated into the groundwater aquifers under influent conditions (Reddersen et. al. 2002). The drug metabolite clofibric acid also represents an exceptional case because ground water concentrations are partly higher than surface water concentrations. This is most likely caused by higher amounts of the precursor drugs (clofibrate ethyl, etofibrate and etofyllinclofibrate) administrated in the past. In laboratory and semi-technical investigations the behaviour observed at the field sites could partly be confirmed. The mobility and persistence of AMODOPH (classified as group 1 compound), the metabolite of dimethylaminophenazone, was confirmed in long column and small column experiments where attenuation rates up to 45 % were observed as also presented in Table 31. The antiepileptic drug carbamazepine (classified as group 1 compound) also proved its mobility and high persistence during the batch, enclosure and small column experiments with only low attenuation rates of up to 45 %. Additionally, attenuation rates for primidone (classified as group 1 compound) an antiepileptic pharmaceutical were determent up to 45 % during enclosure and small column experiments.

Table 31. Comparison of labratory and semi technical experiments. Additionnally results of two reported column studies are shown

	Voigt SSF3b	Voigt SSF5d	Voigt E2o	Voigt E3d	Licht E4d & E5d	Wicke	Hagemann	Hagemann	Ternes column	Mersmann column
Distance [cm]	80	80	80	80	80	84	1 m	1 m	80	35
k [m/s]	2 *10⁻³	2 *10⁻³	2 *10⁻³	2 *10⁻³	2 *10⁻³	1 *10⁻⁴	Bank	Aquifer	2,9 *10⁻³	5 *10⁻⁴
Temperature [°C]	9	20	21	16	7	15	15	15	k.A.*	22
Filtration velocity [m/d]	2,1	1,2	1,2	1,2	1,1 – 1,2	0,3	0,17	0,17	1,25	0,33
AMDOPH (rec. [%])	n.a.*	n.a.*	n.a.*	n.a.*	n.a.*	80 - 100	~ 80 - 100	~ 80 - 100	n.a.*	n.a.*
Bezafibrate (rec. [%])	n.d.***	n.d.***	n.d.***	n.d.***	n.a.**	n.d.***	n.d.***	n.d.***	n.a.**	n.a.**
Carbamazepine (rec. [%])	n.a.**	n.a.**	n.a.**	n.a.**	90 - 100	n.a.**	~ 80 -100	~ 80 - 100	60 - 80	85 - 97
Clofibric acid (rec. [%])	70	85	35	55	90 - 100	45 - 60	~ 60	~ 60	40 - 60	100
Diclofenac (rec. [%])	30	30	15	60	90 - 100	15 - 20	~ 60	~ n.d.***	20 - 40	90 - 100
Ibuprofen (rec. [%])	n.d.***	n.d.***	n.d.***	n.d.***	20 - 30	n.d.***	~ n.d.***	~ n.d.***	20 - 40	45
Primidone (rec. [%])	n.a.**	n.a.**	n.a.**	n.a.**	~ 80 -100	n.a.**	~ 80 -100	~80 - 100	n.a.**	n.a.**

k.A * no information n.a. ** not analyzed n.d.*** not detected available

The behaviour of clofibric acid (classified as group 2 compound) during the different laboratory and semi technical experiments shows a high variability starting from no observed attenuation (E4d & E5d) up to a maximum attenuation of 65 % (E2o)(please also refer Kapitel enclosure experiments). Diclofenac (classified as group 2 compound) was observed with attenuation rates between 40 % and 85 % during the investigations at slow sand filters,

enclosures (with the exception of E4d & E5d) and small columns. Photochemical degradation reported by Buser et. al. (1998) and Tixer et al. (2003) was confirmed during slow sand filter experiments. Attenuation tendencies of propyphenazone (classified as group 2 compound) during small column experiments yielded medium removal rates between 46 % and 95 %. Behaviour of bezafibrate and indometacine (classified as group 3 compounds) was also observed during small column investigation with real bank / aquifer material where these compounds were completely removed. Summarizing these conclusions, bank filtration and artificial ground water recharge were identified as efficient tools for a sustainable removal of several pharmaceutical residues including bezafibrate and indometacine. Other compounds such as clofibric acid, diclofenac and propyphenazone are also significantly attenuated. Concentrations of highly persistence and mobile substances like AMDOPH, carbamazepine and primidone are decreased up to the receiving water supply wells by dilution with non contaminated groundwater. Thus, both recharge techniques are useful tools for the pre-treatment of contaminated surface water but will be not sufficient for the complete removal of all kinds of pharmaceutically active compounds occurring in surface water under the influence of non-purified or purified municipal sewage effluents.

1.6 References

Andreozzi, R., Marotta, R., Paxéus, N., 2003. Pharmaceuticals in STP effluents and their solar photodegradation in aquatic environment, *Chemosphere, Vol. 50, Iss. 10, pp. 1319-1330.*

Brauch, H.-J., Sacher, F., Denecke, E., Tacke, T., 2000. Wirksamkeit der Uferfiltration für die Entfernung von polaren organischen Spurenstoffen, *Wasser Abwasser, Vol. 141 Iss. 4, pp 226-234.*

Buser, H.-R.; Poiger, T.; Müller, M.D., 1998. Occurrence and Fate of the Pharmaceutical Drug Diclofenac in Surface Waters: Rapid Photodegradation in a Lake, *Environmental Science & Technology, Vol. 32, Iss. 22, pp. 3449-3456.*

Buser, H.-R.; Poiger, T.; Müller, M.D.: Occurrence and Environmental Behavior of the Chiral Pharmaceutical Drug Ibuprofen in Surface Waters and in Wastewater, *Environmental Science & Technology, 1999, Vol. 33, Iss. 15, pp. 3529-2535.*

Heberer, T., 2002: Tracking persistent pharmaceutical residues from municipal sewage to drinking water, *Journal of hydrology, Vol. 266, pp. 175-189.*

Heberer, Th., Adam, M., 2004a. Transport and Attenuation pf Pharmaceutical Residues During Artificial Groundwater Replenishment, *Rapid Communication, Environmental Chemistry Vol. 1, pp. 22-25*

Heberer, Th., Adam, M., 2004b. Occurrence, fate, and removal of pharmaceutical residues in the aquatic environment: An extended review of recent research data.

Mersmann, P.; Scheytt, T.; Heberer, T., 2002. Säulenversuche zum Transportverhalten von Arzneimittelwirkstoffen in der wassergesättigten Zone. *Acta hydrochim. Hydrobiol., Vol. 30, pp. 275–284.*

Möhle, E.; Kempter, C.; Kern, A.; Metzger, J.W.: Untersuchungen zum Abbau von Pharmaka in kommunalen Kläranlagen mit HPLC – Electrospray –Massenspektrometrie, *Acta hydrochim hydrobiol, 1999, Vol. 27, Iss. 6, pp. 430-436.*

Preuß, G.; Willme, U.; Zullei-Seibert, N., 2001. Verhalten ausgewählter Arzneimittel bei der künstlichen Grundwasseranreicherung - Eliminierung und Effekte auf die mikrobielle Besiedlung. *Acta hydrochim hydrobiol, Vol. 29, Iss. 5, pp. 269-277.*

Reddersen, K.; Heberer, Th., Dünnbier, U., 2002. Identification and significance of phenazone drugs and their metabolites in ground- and drinking water. *Chemosphere Vol. 49 pp. 539–544.*

Reddersen, K.; Heberer, Th., 2003. Multi-compound methods for the detection of pharmaceutical residues in various waters applying solid phase extraction (SPE) and gas chromatography with mass spectrometric (GC-MS) detection. *Journal of Separation Science, Vol. 26, pp. 10-16.*

Reddersen, K., Dissertation, (2004). Das Verhalten von Arzneimittelrückständen im Wasserkreislauf Berlins. Technical University of Berlin.

Sacher, F., Haist-Gulde, B., Brauch, H.-J., Preuß, G., Wilme, U., Zullei-Seibert, N., Meisenheimer, M., Welsch, H. & Ternes, T.A., 2000. Behaviour of selected pharmaceuticals during drinking water treatment. *Symposia Papers, Preprints of extended abstracts, 40/1:, pp. 116-118.*

Scheytt, .T, Grams, S, Fell, H, 1998. Vorkommen und Verhalten eines Arzneimittels (Clofibrinsäure) im Grundwasser. *Grundwasser - Zeitschrift der Fachsektion Hydrogeologie, Vol. 2 pp. 67-77.*

Stumpf, M.; Ternes, T.A.; Haberer, K.; Baumann, W., 1998. Isolierung von Ibuprofen-Metaboliten und deren Bedeutung als Kontaminanten der aquatischen Umwelt, *Vom Wasser, Vol. 91, pp. 291-303.*

Stumpf, M.; Ternes, T.A.; Haberer, K.; Baumann, W: Isolierung von Ibuprofen-Metaboliten und deren Bedeutung als Kontaminanten der aquatischen Umwelt, *Vom Wasser, 1998, Vol. 91, pp. 291-303.*

Ternes, T.A.; Meisenheimer, M.; Mcdowell, D.; Sacher, F., 2002. Removal of Pharmaceuticals during drinking water treatment. *Environmental Science & Technology, Vol. 36, pp. 3855- 3863.*

Tixier, C., Singer, H.P., Oellers, S., Müller, S.R. Müller, 2003. Occurence and Fate of Carbamazepine, Clofibric Acid, Ibuprofen, Ketoprofen, and Naproxen in Surface Waters. *Environ. Sci. & Technol., Vol. 37 Iss.. 6, pp. 1061 - 1068.*

Verstraeten, I.M., Heberer, Th., Scheytt, T., 2002. Occurrence, Characteristics, and Transport and Fate of Pesticides, Pharmaceutical Active Compounds, and Industrial and Personal Care Products at Bank-Filtration Sites. *Chapter 9, In: (Ray, C., Melin, G., Linsky, R.B. (eds.): Riverbank Filtration: Improving Source- Water Quality. Dordrecht: Kluwer Academic Publishers, pp. 175-227.*

Winkler, M., Lawrence, J.R., Neu, T.R., 2001. Selective degradation of ibuprofen and clofibric acid in two model river biofilm systems. *Water Research 35 (13); pp. 3197-3205.*

Zwiener, C., Glauner, T., Frimmel, F.H., 2000. Biodegradation of pharmaceutical residues investigated by SPE-GC/ITD-MS and on-line derivatisation. *HRC-J. High res. Chromatogr., Vol. 23, pp. 474-478.*

Zwiener, C.; Frimmel, F. H., 2002. Oxidative treatment of pharmaceuticals in water. *Water Research, Vol. 34, Iss. 6, pp. 1881-1885.*

2 Antibiotics

2.1 Introduction

The objective of the sub-project "Bank Filtration: Drug Residues" was the investigation of the occurrence of antibiotic residues in surface waters under the influence of municipal sewage effluents and their behavior and fate during bank filtration.

An analytical method has been developed for the trace analysis of 21 compounds from important human-use antibiotic classes (penicillins, sulfonamides, macrolide groups, fluoroquinolones, and tetracyclines) to identify antibiotics which are environmentally relevant. A screening of surface water samples collected from lake Wannsee and lake Tegel showed that only five antibiotic compounds and two metabolites are important for bank filtration in Berlin, Germany. The antibiotics occurring in the surface water include the macrolides clarithromycin, roxithomycin and erythromycin (measured as metabolite dehydro-erythromycin), the sulfonamide sulfamethoxazole, its main human metabolite acetyl-sulfamethoxazole, the sulfonamide synergist trimethoprim and the lincosamide clindamycin. Except for acetyl-sulfamethoxazole, these substances were subject for detail studies. Batch sorption studies and small column experiments were carried out, to get more information about the behavior of these antibiotic residues during soil passage. Additionally, the distributions of these antibiotic compounds in lake Wannsee as well as the occurrence of these substances in further adjacent surface waters (the river Unterhavel, lake Kleiner Wannsee, and the Teltowkanal, a sewage-prone canal) were determined. Investigations at the phosphate elimination plant OWA Tegel provided further information about the antibiotic loads in lake Tegel. From May 2003 to August 2004, the occurrence and fate of all environmentally relevant antibiotics was investigated monthly at three transects located at lakes Wannsee and Tegel. The following report describes the results of the investigations in detail.

2.2 Method

A highly selective and sensitive multi-residue method was developed for the trace-level analysis of antibiotics in environmental water samples (see also Figure 94). The method allows the determination of 21 antibiotics belonging to various prescriptions classes including macrolide antibiotics, sulfonamides, fluoroquinolones, penicillins and tetracyclines. The antibiotic residues are measured using high-performance liquid chromatography with positive electrospray ionization and tandem mass spectrometric detection (LC/ESI-MS/MS). After

solid phase extraction (cartridges: OASIS HLB (Waters, Milford, MC, USA)) at pH 4 and consecutive two step elution (1. acetonitrile, 2. acetonitrile/water/triethylamine), samples are dried and dissolved in acetonitrile 10 vol% in water. The analysis of the resulting sample extracts was performed in multiple reaction monitoring mode (MRM) using a Quadro-LC tandem-mass spectrometer from Micromass, Manchester, UK. Standard addition method was used for the quantification of the antibiotic residues. The method is described in detail by Fanck and Heberer [1].
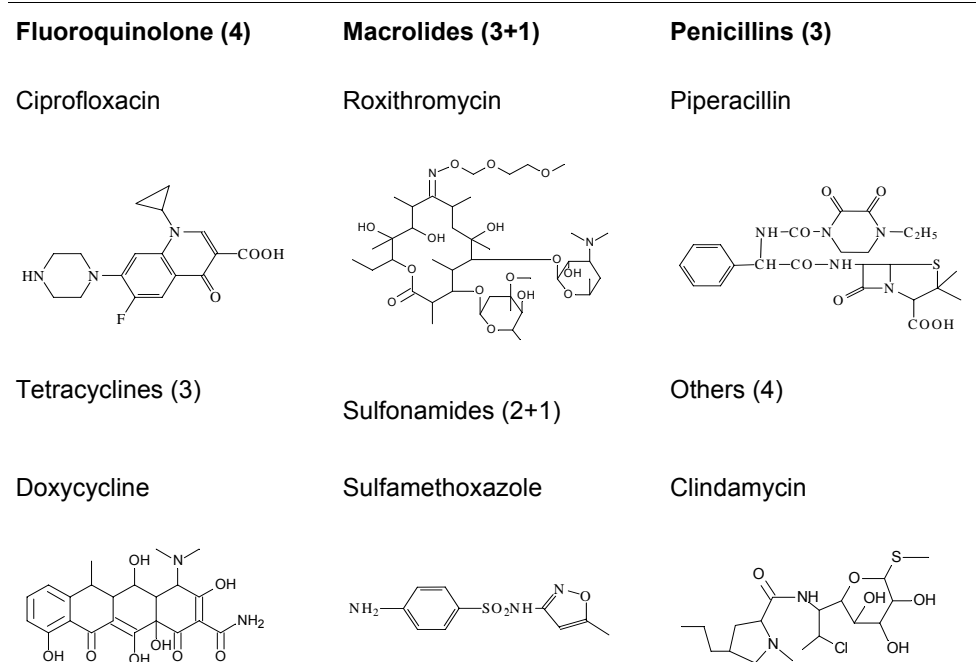
Figure 94: Chemical structures of selected compounds for each of the investigated classes.

In brackets: investigated number of compounds from each class

2.3 Surface water investigations

Only five out of the 19 investigated compounds, the macrolides clarithromycin and roxithromycin, the sulfonamide sulfamethoxazole, the sulfonamide synergist Trimethoprim, and the lincosamide clindamycin were detected in the surface water of the transects. Additionally, dehydro-erythromycin, the metabolite of the macrolide erythromycin and acetyl-sulfamethoxazole, the main human metabolite of sulfamethoxazole, were found.

Tetracyclines and penicillines were not detected in any sample. This is in line with the results from other studies [2-8]. Tetracyclines have shown to be strong chelators and can sorb strongly to soil organic matter and mineral particles and are therefore rarely found as free molecules in surface waters [3-6]. Penicillines are not expected to occur in surface water because the ß-lactam ring, a common moiety in their structures, is unstable. It can easily be cleaved by ß-lactamase, a widespread enzyme in bacteria, or by chemical hydrolysis. Thus, intact penicillins do not frequently occur in the environment [2]. Fluoroquinolone antibiotics were also not found in surface or ground water because they are substantially removed during wastewater treatment (65-100%) mainly by sorption to sewage sludge [1,9-11].

2.3.1 Lake Wannsee

Trimethoprim, clarithromycin, and roxithromycin were detected in Lake Wannsee with concentrations between two and 69 ng/L. These three analytes showed a very similar, time-dependent concentration trend (see Figure 95). In winter, they were found at higher concentrations than during summer. The opposite might be expected regarding the low surface water flows measured during summer. From a medical health care position, elevated concentrations and loads in winter might be assigned to higher seasonal consumption of antibiotics which are mainly prescribed against respiratory infections. These observations are also in line with investigations at the sewage treatment plant (STP) in Berlin-Ruhleben which have also shown seasonal variations. In winter, residues from these compounds were found at increased concentrations both in samples collected from the influents and the effluents [1]. In the same study, better removal of residues of macrolide antibiotics was observed during summer.
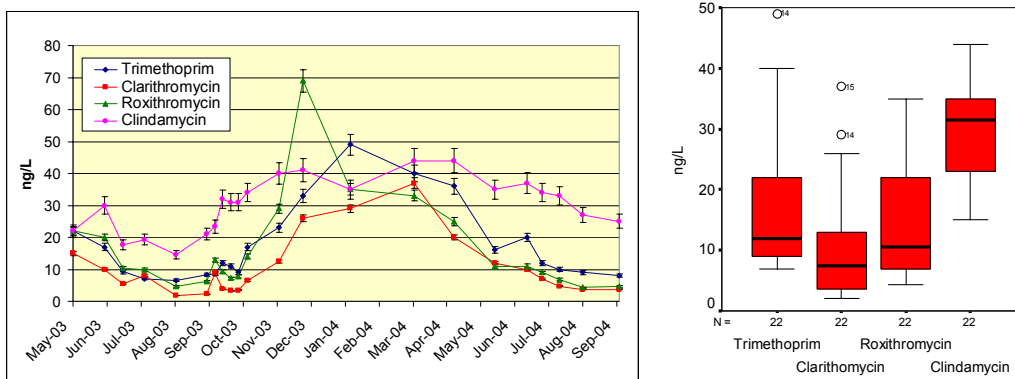
Figure 95: *Lake Wannsee – Concentrations for Trimethoprim, Clarithromycin, Roxithromycin and Clindamycin*

Clindamycin was detected in the lake with a median concentration of 31ng/L. Its concentration profile did not show such a strong time-dependent trend as the substances mentioned before (see Figure 95). This result is also consistent with those obtained from the study at the STP in Ruhleben where the influent and effluent concentrations of clindamycin were similar during summer and winter [1]. The prescription of clindamycin does apparently not vary with the season. This might be explained by its use pattern in dentistry and against abdomen and pelvis infections, which all are independent from the season.

The highest concentrations in lake Wannsee were determined for the drug metabolite dehydro-erythromycin and the bacteriostatic sulfonamide drug sulfamethoxazole (see Figure 96). Dehydro-erythromycin, formed by hydrolysis from the macrolide erythromycin, was detected in lake Wannsee at concentrations between 33 and 94 ng/L. Sulfamethoxazole occurred in the lake at concentrations between 100 and 326 ng/L. Beside the penicillins, both compounds belong to those antibiotics with the highest consumption volume in Germany [1]. The individual concentrations measured for both compounds varied significantly and a seasonal variation was not observed. Additional investigations at the STP Ruhleben have shown similar effluent concentrations for sulfamethoxazole in winter and summer. The higher consumption of sulfamethoxazole in winter was balanced by higher removal rates observed for this compound during winter [1]. Acetyl-sulfamethoxazole, the main human metabolite of sulfamethoxazole, was detected in lake Wannsee at very low concentrations between 4 and 14ng/L. For acetyl-sulfamethoxazole, a removal rate of more than 99% was found in the sewage treatment plant of Ruhleben [1]. This metabolite exhibits no more bacteriostatic effect.

A weekly sampling in September/ October 2003 showed that in contrary to the other antibiotics, the concentration of sulfamethoxazole in front of the transect varies considerably. For this substance a monthly sampling of the surface water was not sufficient to derive a

reliable input concentration. Additional investigations of the lake Wannsee also showed a large variability of the surface water quality in front of the transects (e.g. by variations of the electrical conductivity and the $\delta^{18}O$ values). Thus, a monthly sampling of the lake may not be sufficient to obtain representative samples characterizing the surface water used as a resource to feed the bank-filtration field sites.
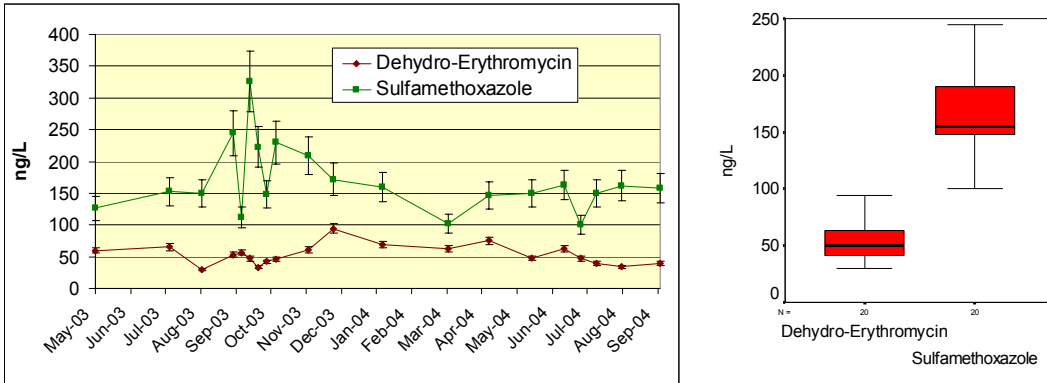
Figure 96: *Lake Wannsee – Concentrations for Dehydro-Erythromycin and Sulfamethoxazole*

In terms of a diploma thesis additional investigations have been carried out at lake Wannsee. The distributions of the antibiotic residues in the lake as well as the occurrence of these compounds in further adjacent surface waters (river Unterhavel, lake Kleiner Wannsee and Teltowkanal) were determined.

The distributions of the antibiotic residues in the lake Wannsee were investigated in March and July in 2004. The concentration profiles measured for all detected antibiotics show a similar distribution in the lake. For the comparison of the two sampling series, the measured total concentrations at the respective sampling points are shown in Figure 97.
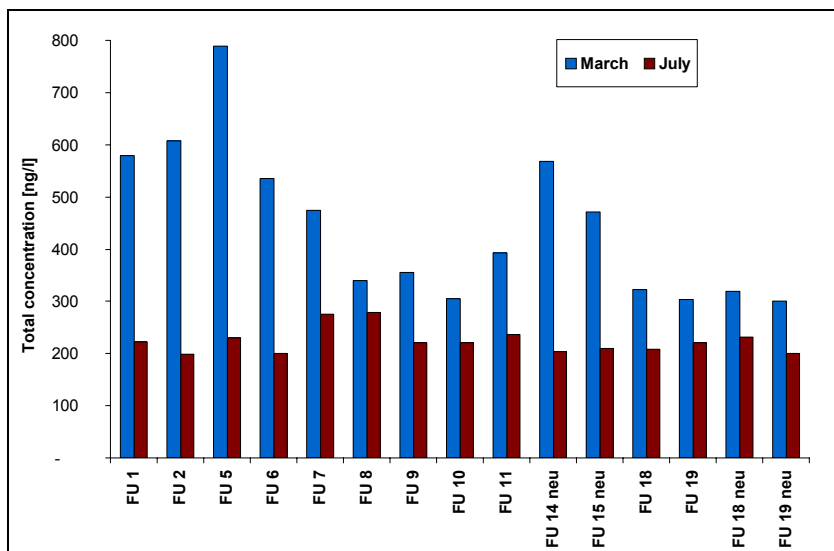
Figure 97: *Lake Wannsee - Comparison of the total concentrations of antibiotics at different sampling locations in March and July 2004.*

In March, total concentrations of antibiotics between 300 and 800 ng/L were detected at different sampling locations in lake Wannsee. The large variations between the different sampling points are indicating a poor mixing of the sewage-prone waters that are entering the lake via the river Havel and the lake "kleiner Wannsee". The highest concentrations of the antibiotics were determined at sampling point FU 5 which is located close to the merger of both lakes. The high concentration measured at this point can be explained by the waste water loads originating from the Teltowkanal with approximately one third of its surface water flowing into and through lake "kleiner Wannsee". In former investigations, concentrations of pharmaceutical residues determined in lake kleiner Wannsee were identical to those measured in the surface water of the Teltowkanal before it is leaving this highly sewage-prone canal. In March, the lowest concentrations of antibiotics were measured in the northern part of the lake. This shows that the river (Unter-)Havel contributes only to a small extent to the total degree of antibiotics found in this lake.

In July, antibiotics were only detected at much lower total concentrations in the lake ranging between 200 and 300 ng/L. The differences in the concentrations between March and July can be attributed to higher consumption of antibiotics during winter (see chapter 2.3.2). Additionally, the concentrations show a rather even distribution. It was assumed that in the summer an intensified shipping traffic might be responsible for a better mixing and a more evenly distribution. This becomes also clear in Figure 98, where the distributions of the concentrations of clarithromycin in March and in July are compared. In March, the decrease of the concentration on the eastern bank proceeded more slowly than on the western bank. Consequently, in March sewage-prone surface from lake kleiner Wannsee flows

predominantly along the eastern bank of lake Wannsee where the transects and the wells from the water works in Berlin-Beelitzhof are located.
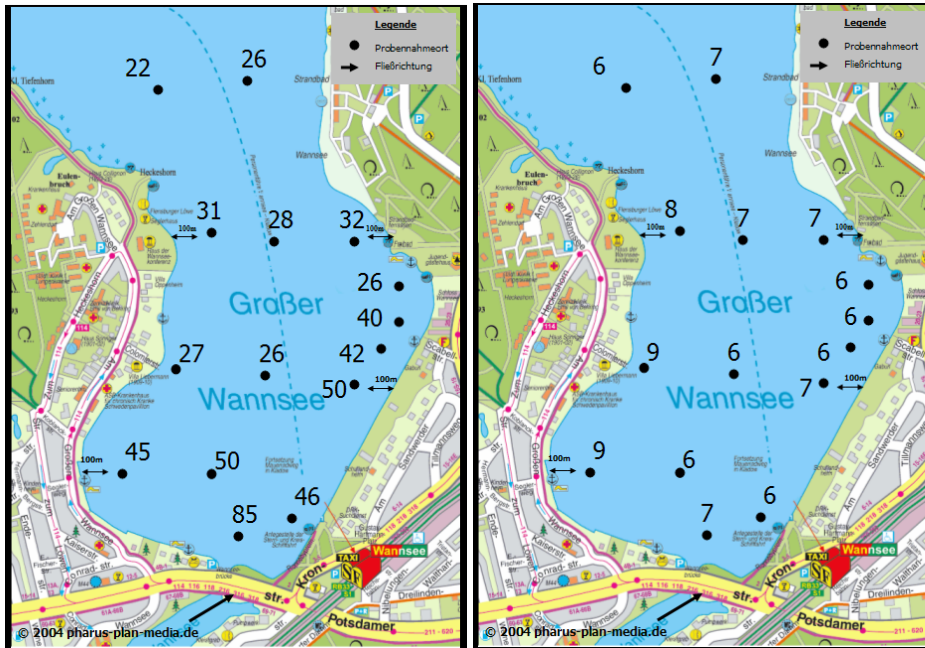
Figure 98: *Lake Wannsee - Comparison of the concentrations of Clarithromycin in March and July 2004.*

Figure 99 shows this by the example of trimethoprim and its concentrations measured in September 2004 in lakes Wannsee and kleiner Wannsee and upstream in the Teltowkanal. Depending on the season, up to three STPs discharge their purified effluents into the Teltowkanal.
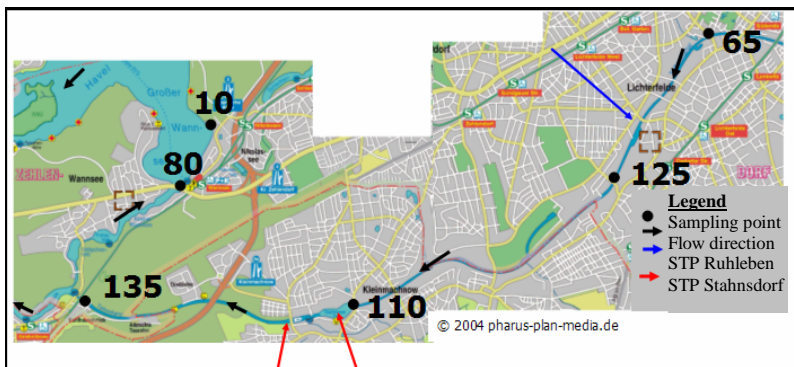
Figure 99: *Concentrations for Trimethoprim [ng/L] along the Teltow channel and in Lake Wannsee in September 2004.*

Figure 100 shows that slightly increased concentrations of antibiotic residues were also detected in the river Havel. However, these concentrations were evidently diluted in before

the lower part of the river (Unterhavel) reaches lake Wannsee. This means that the loads from the Unterhavel are not crucial for the high concentrations of antibiotics determined in lake Wannsee although they also add to the total loads found in this lake.
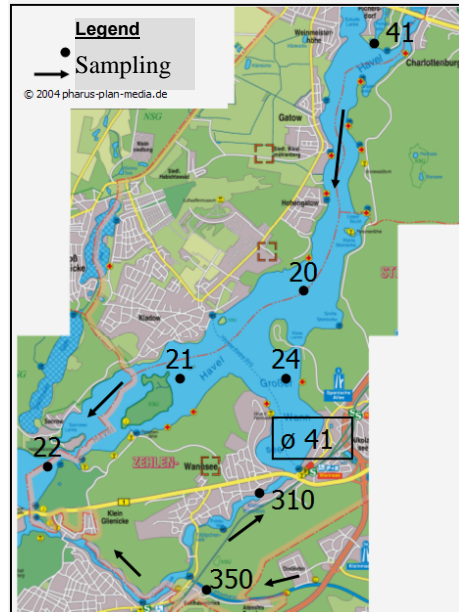
Figure 100: *Concentrations for Dehydro-Erythromycin [ng/L] determined in the surrounding area of Lake Wannsee in July 2004.*

The anthropogenic impact of sewage-prone surface water on the water quality of lake Wannsee was also confirmed by other waste water indicators such as boron (see Figure 101) showing a similar distribution pattern in the surface water of the lake.
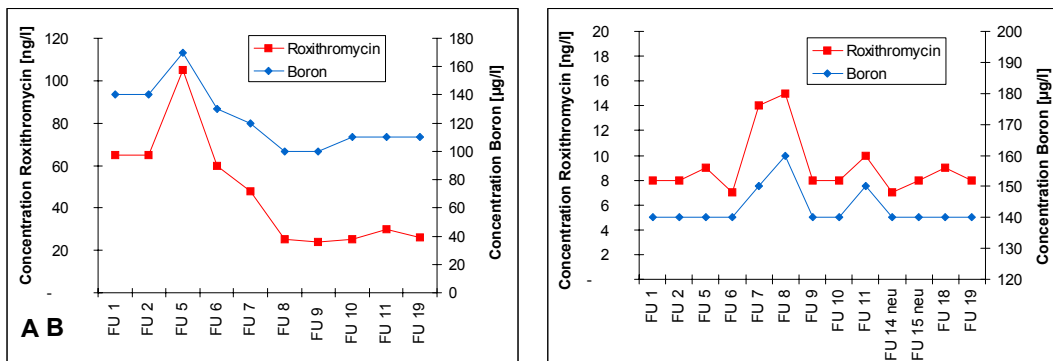
Figure 101: *Lake Wannsee - Comparison of the concentrations of Roxithromycin and Boron (BWB data) in A) March and B) July 2004.*

In another sampling series, samples were collected at different depths in the center of lake Wannsee. No significant differences in the concentrations of the measured antibiotics was observed (data not shown). Thus, no distinct formation of layers was found in the lake.

2.3.2   Lake Tegel

In general, antibiotic residues were found at higher concentrations in Lake Tegel than in Lake Wannsee. Trimethoprim, clarithromycin, and roxithromycin were found in the lake Tegel at concentrations between nine and 85ng/L (see Figure 102). As already reported for lake Wannsee, a seasonal variation was observed for these compounds. However, in lake Wannsee this trend is more distinct.
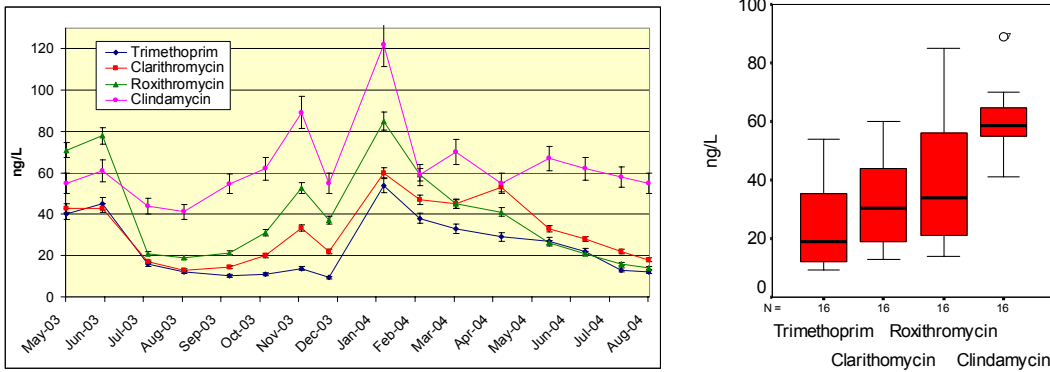
Figure 102: *Lake Tegel – Concentrations for Trimethoprim, Clarithromycin, Roxithromycin and Clindamycin*

The lincosamide clindamycin was found in the lake at concentrations between 41 and 122 ng/L. Again, it did not show such a strong time-dependent trend as the substances mentioned before (see Figure 102). For more explanations also refer to chapter 2.3.1. Figure 102 shows a decrease of all concentrations in December 2003. A comparison with other waste-water indicators such as sulfate and chloride (see Figure 103) also shows lower concentration values in December 2003. The reason for this could not to be clarified (e.g. sampling error).
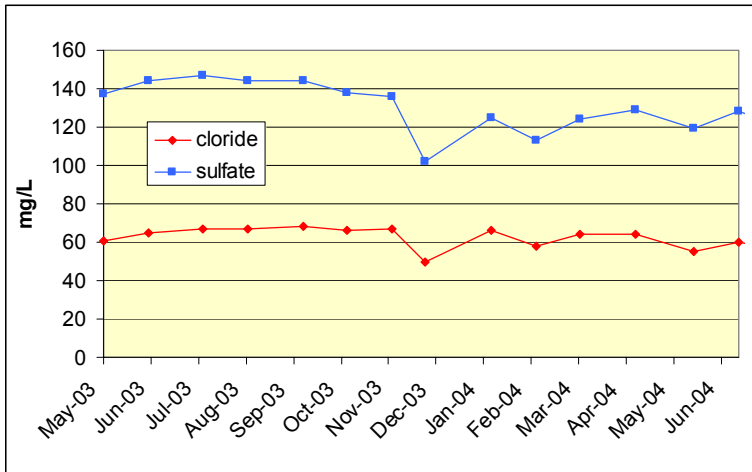
Figure 103: *Lake Tegel – Concentrations for Chloride and Sulfate (BWB data)*

Figure 104 presents the concentrations measured for dehydro-erythromycin and sulfamethoxazole in lake Tegel. Again, they were found at higher concentrations than all the other antibiotic substances. They were detected with median concentrations of 118 and 286 ng/L, respectively. Both compounds did not show any seasonal variations (see also chapter 2.3.1). The results for sulfamethoxazole are comparable to screening results (n=5) reported earlier by Hartig et al. [14].
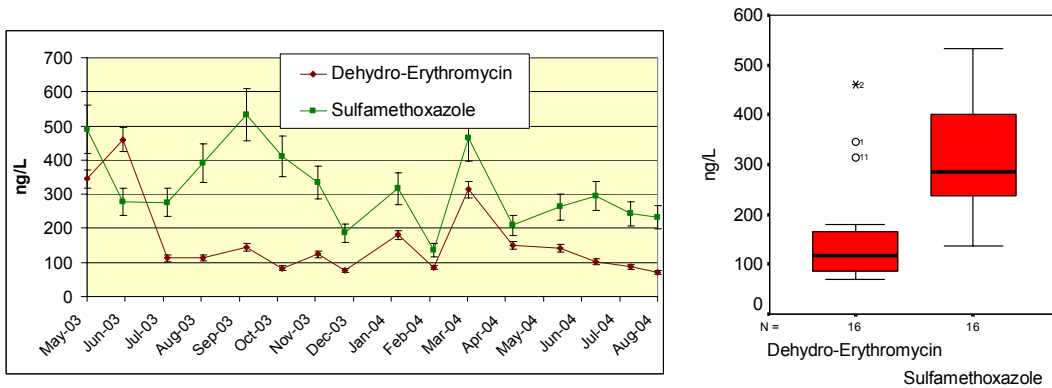
Figure 104: *Lake Tegel – Concentrations for Dehydro-Erythromycin and Sulfamethoxazole*

The pharmacologically inactive human metabolite of sulfamethoxazole, acetyl-sulfamethoxazole, occurred in lake Tegel at very low concentrations between eight and 30 ng/L. For acetyl-sulfamethoxazole, a removal rate of more than 99% was reported for the STP in Ruhleben [1].

Primary source of antibiotic residues in the lake Tegel are the effluents from the phosphate elimination plant (OWA) in Berlin-Tegel. The OWA Tegel receives its water from the Tegler Fließ and the Nordgraben, which is almost exclusively fed by effluents from the STP in Schönerlinde. The STP Schönerlinde is located north of Berlin. It purifies municipal sewage from Berlin's northern districts and from several other municipalities located north of Berlin. In terms of a diploma thesis influents and effluents of the OWA Tegel were analyzed for the occurrence of various drug residues. These investigations also provided some information about the behavior of the antibiotic residues during the passage through the OWA Tegel and about the loads of antibiotics entering lake Tegel. From January to July 2004 composite samples collected monthly from the influents and the effluents of the OWA. Additionally, water samples from the river Havel (Oberhavel) were investigated. These samples were collected directly in front of a pipeline feeding the OWA with additional surface water during low flow conditions. Eight antibiotic compounds were detected in the influents and the effluents collected from the OWA Tegel. In Table 32, the results of the OWA Tegel effluent samples are compared with the results obtained for the surface water samples collected from lake Tegel in front of the bank filtration transect. Generally, antibiotic residues were detected at higher concentrations in the OWA Tegel than in the lake. As already mentioned for the investigation of Berlin's surface waters, the highest concentrations of antibiotic residues in the OWA Tegel were determined for dehydro-erythromycin (322ng/L), the main degradation product of erythromycin, and for the bacteriostatic sulfamethoxazole (420ng/L). Beside the penicillins, both compounds belong to the antibiotics with the highest consumption in Germany but are not eliminated completely in the STP's [1]. The macrolide antibiotics roxithromycin and clarithromycin were determined with similar concentrations of 165ng/L and 146ng/L, respectively, in the OWA effluent. This might be due to their similar structures, a similar behavior in the STP and due to similar quantities of prescription. The lincosamide clindamycin was detected with a median concentration of 148ng/L. It is prescribed in quantities similar to those of roxithromycin and clarithromycin. In medical therapy, trimethoprim is usually used in combination with sulfamethoxazole in a ratio of 5:1 ("Cotrimoxazol"). However, trimethoprim is to a lower degree also used alone or in combination with other sulfonamides. With regard to its primary use in the combinatory formulation "Cotrimazol", trimethoprim is expected occur in smaller quantities in the aquatic environment compared to those of sulfamethoxazole. Thus, it was detected in the OWA effluent at a median concentration of only 124ng/L. Acetyl-sulfamethoxazole also occurred in the OWA effluent but only in minor concentrations of 25 ng/L. As mentioned before, this compound is eliminated almost completely in STPs [1]. Additional to the antibiotic compounds occurring in the lake, the cephalosporine ceftazidime was also found in the influents and effluents of the OWA Tegel with concentrations between 26 and 264ng/L.

Table 32: *Median concentration for antibiotic residues in the OWA effluent and the Lake Tegel and calculated median antibiotic loads from the OWA effluent in the Lake Tegel (n≤7).*

Substances	Median concentration [ng/L]		Median loads	
	OWA effluent (n≤7)	**Lake Tegel (n=16)**	**[g/d]**	**[kg/year]**
Acetyl-Sulfamethoxazole	25	12	8	3
Trimethoprim	124	19	134	49
Clarithromycin	146	31	23	9
Roxithromycin	165	34	36	13
Clindamycin	148	59	30	11
Dehydro-Erythromycin	322	118	34	12
Sulfamethoxazole	420	286	69	25
Ceftazidime	112	n.d.	23	8

On the basis of these investigations, average annual loads of antibiotic residues were determined that flow via the OWA effluents into lake Tegel. The calculation was carried out by multiplying the monthly OWA effluent discharge volumes with the corresponding average effluent concentrations of each individual compound. As shown in Table 32, the average annual loads of antibiotics discharged via the OWA into lake Tegel was 130kg in 2004. Sulfamethoxazole (49kg/year) was the compound with the highest annual load of all detected antibiotics. Dehydro-erythromycin (25kg/year) was in second place. For none of the antibiotics a decrease in concentration during OWA passage was observed. To a lesser degree, antibiotic residues may also reach lake Tegel via the river Havel. However, the quantities that were detected in water samples collected from the river Havel were clearly below those discharge by the OWA. The concentrations of antibiotics detected upstream the Havel river were in general also lower than those detected in front of the bank filtration transect in lake Tegel. This is also demonstrated by the example of clarithromycin in Figure 105.
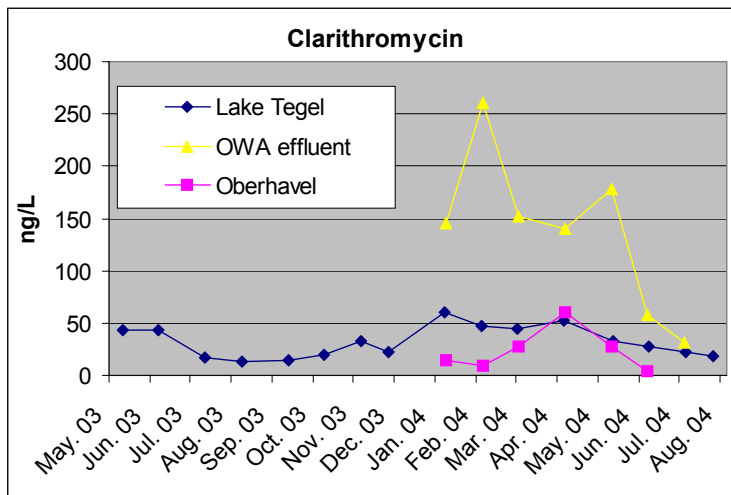
Figure 105: Concentrations for clarithromycin in Lake Tegel in front of the transect Tegel, in the OWA effluent, and in the surface water of the Oberhavel.

2.3.2.1 Conclusions

Purified effluents discharged by the municipal STPs were identified as the main sources for the occurrence of antibiotic residues in Berlin's surface waters. These residues discharged into the receiving waters such as the Teltowkanal or the Nordgraben are also reaching areas such as lake Wannsee or lake Tegel which are used as resources for groundwater recharge. Five compounds, the sulfonamide sulfamethoxazole, the sulfonamide synergist trimethoprim, the macrolides clarithromycin and roxithromycin, and the lincosamide clindamycin were detected in surface water samples collected from these lakes. Additionally, dehydro-erythromycin, the metabolite of the macrolide erythromycin and acetyl-sulfamethoxazole, the main human metabolite of sulfamethoxazole, were found.

In general, antibiotic residues were detected at higher concentrations in lake Tegel than in lake Wannsee. Trimethoprim, clarithromycin, and roxithromycin were detected in the lakes at concentrations between two and 85ng/L. The seasonal variation of the concentrations of these substances in the lakes reflects the consumption pattern of these antibiotics. The highest concentrations of all antibiotic compounds were determined for dehydro-erythromycin and sulfamethoxazole. Dehydro-erythromycin, formed by hydrolysis from the macrolide erythromycin, was detected in lake Tegel and lake Wannsee with median concentrations of 118ng/L and 52ng/L, respectively. Sulfamethoxazole occurred with median concentrations of 286ng/L and 155ng/L and in lake Tegel and lake Wannsee, respectively. In investigations of effluents discharged by the OWA Tegel an average annual total load of antibiotics of 130kg was calculated for lake Tegel.

116

2.4 Bank Filtration Field Sites

Since May 2003, the occurrence and fate of 19 environmentally relevant antibiotics and two of their metabolites (see also Figure 94) was investigated at three transects located at lakes Wannsee (Wannsee 1 and Wannsee 2) and Tegel. A comparison of the three field sites revealed a similar behavior of the detected compounds during the riverbank filtration.

2.4.1   Transect Wannsee 1 and 2

Table 33 and 3 present ranges of concentrations measured in the water samples collected from both transects located at lake Wannsee. At transect "Wannsee 1" well 3335 was only sampled during an "intensive" sampling series in September/ October 2003 and the deep wells 3332, 3334 and 3336 were only investigated in March 2004. Well 3338 could not be sampled in these investigations because the groundwater level was always beyond the screen of the wells. In the monitoring wells 204OP and 204UP, used to investigate background groundwater, no antibiotic residues were found.

Table 33: Positive findings of antibiotic residues and their concentration range [ng/L] at transect "Wannsee 1"

ng/L	surface water (n=21)	3337 (n=16)	BEE 201OP (n=15)	BEE 201UP (n=12)	3335 (n=5)	well 4 (n=11)
Acetyl-Sulfa-methoxazole	4-14	n.d	n.d	n.d	n.d	n.d
Trimethoprim	7-49	n.d	n.d	n.d	n.d	n.d
Clarithromycin	2-43	n.d	n.d	n.d	n.d	n.d
Roxithromycin	4-69	n.d	n.d	n.d	n.d	n.d
Clindamycin	15-48	1-9	0.4-2	n.d.-2	n.d.-2	n.d
Dehydro-Erythromycin	33-94	0.7-5	1-8	n.d.-3	n.d.-1	n.d
Sulfamethoxazole	100-326	1-136	<LOQ-2	n.d.-6	18-26	n.d
Sulfadimidine	n.d.	n.d.-4	<LOQ-5	3-8	n.d.-<LOQ	n.d
Not detected (n.d.): Benzylpenicillin, Ceftazidim, Ciprofloxacin, Doxycycline, Metronidazole, Moxifloxacin, Norfloxacin, Ofloxacin, Oxytetracycline, Phenoxymethylpenicillin, Piperacillin, Tetracycline, Tylosin; >LOQ: > limits of quantification; n: number of samples						

No antibiotic residues were found in samples collected from water-supply well 4. Unfortunately, the upper screen of well 4 was blocked. Since this is the only screen which is directly influenced by bank filtration, transect "Wannsee 1" was not found to be suitable for the investigation of the behavior of sewage-borne residues during bank filtration.

Table 34: Positive findings of antibiotic residues and their concentration range [ng/L] at transect "Wannsee 2"

ng/L	surface water (n=21)	BEE 205 (n=19)	BEE 206 (n=20)	BEE 202OP (n=19)	BEE 202MP1 (n=17)	BEE 202MP2 (n=11)	BEE 202UP (n=14)	BEE 203 (n=19)	well 3 (n=15)	BEE 204UP (n=15)	BEE 204OP (n=11)
Acetyl-Sulfa-methoxazole	4-14	n.d.	n.d.	n.d.	n.d.	n.d.	n.d.	n.d.	n.d.	n.d.	n.d.
Trimethoprim	7-49	n.d.	n.d.	n.d.	n.d.	n.d.	n.d.	n.d.	n.d.	n.d.	n.d.
Clarithromycin	2-43	n.d.-3	n.d.	n.d.	n.d.	n.d.	n.d.	n.d.	n.d.	n.d.	n.d.
Roxithromycin	4-69	n.d.-7	n.d.	n.d.	n.d.	n.d.	n.d.	n.d.	n.d.	n.d.	n.d.
Clindamycin	15-48	16-34	0.4-5	n.d.-<LOQ	n.d.	n.d.	n.d.-<LOQ	n.d.-<LOQ	n.d.-<LOQ	n.d.	n.d.
Dehydro-Erythromycin	33-94	n.d.-8	n.d.-10	n.d.-<LOQ	n.d.	n.d.- 4	<LOQ-2	n.d.-<LOQ	n.d.-<LOQ	n.d.	n.d.
Sulfa-methoxazole	100-326	n.d.-22	34-251	16-138	5-73	n.d.	n.d.	21-121	1-4	n.d.	n.d.
Sulfadimidine	n.d.	n.d.-6	n.d.-<LOQ	n.d.-<LOQ	<LOQ - 5	3-9	3-8	n.d.-<LOQ	<LOQ	n.d.	n.d.

Not detected (n.d.): Benzylpenicillin, Ceftazidim, Ciprofloxacin, Doxycycline, Metronidazole, Moxifloxacin, Norfloxacin, Ofloxacin, Oxytetracycline, Phenoxymethylpenicillin, Piperacillin, Tetracycline, Tylosin;
>LOQ: > limits of quantification; n: number of samples

In the field site investigations the antibiotic residues showed a different attenuation behavior during infiltration. Trimethoprim, clarithromycin, and roxithromycin were efficiently removed by the bank filtration. They were detected in the lakes and sometimes also in the first wells but mostly at concentrations below their limits of quantification (LOQs). **Photodegradation does not play a significant role for these substances. Trimethoprim** absorbs light with a

wave length greater than 290 nm. However, it was found to be stable in seawater for up to 20 weeks when exposed to UV light [15]. Further investigations such as column and batch experiments (link to Batch- and column experiments) showed a very fast and complete decrease of the concentrations for these three compounds. Both sorption and biodegradation may play an important role for their attenuation. In these studies, roxithromycin and clarithromycin showed a very similar behavior as might also be expected with regard to their similar chemical structures. In the batch experiments, clindamycin and dehydro–erythromycin have shown a weaker sorption behavior than other antibiotics such as trimethoprim, clarithromycin, and roxithromycin.

Figure 106 presents the results from the investigation of clindamycin at transect "Wannsee 2". Based on solubility data (link to batch experiments), this compound is expected to be relatively mobile. However, the residues of clindamycin were completely attenuated during the soil passage. Clindamycin only occurred at trace levels in the wells close to the bank.
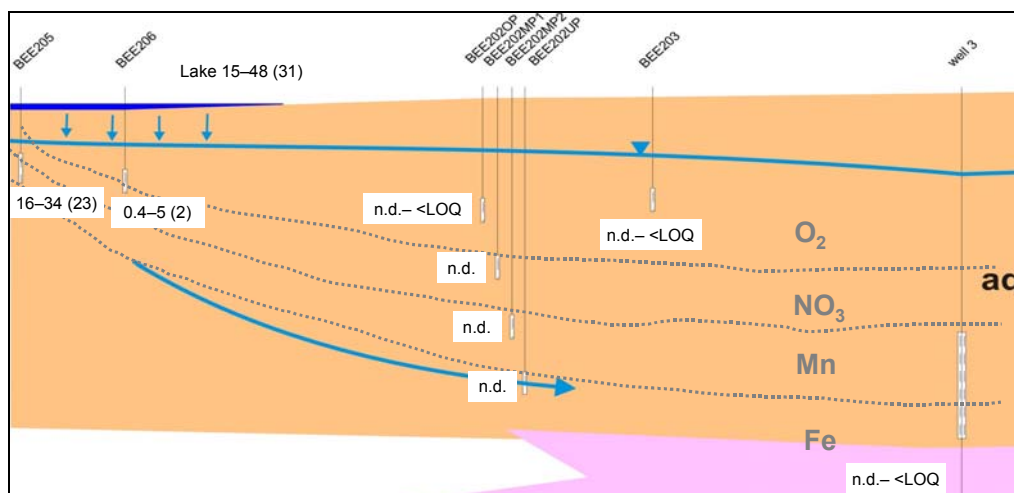
Figure 106: Transect "Wannsee 2" – Results for Clindamycin [ng/L]

(Median values are given in parentheses; n.d.: not detected; >LOQ: > limits of quantification = 0,1ng/L)

In well BEE205, it was detected with an average concentration of 23ng/L. Whereas in well BEE206, it was only found with less than 7% of the average concentration measured in the lake (15-48ng/L) (see Figure 108).

The concentrations of the macrolide metabolite dehydro-erythromycin are also significantly decreased during the soil passage (see Figure 107). In the lake it was found with concentrations between 33 and 94 ng/L. Compared to clindamycin, dehydro-erythromycin shows, however, a better attenuation rate (~98%) in monitoring well BEE205 (see Figure 108).
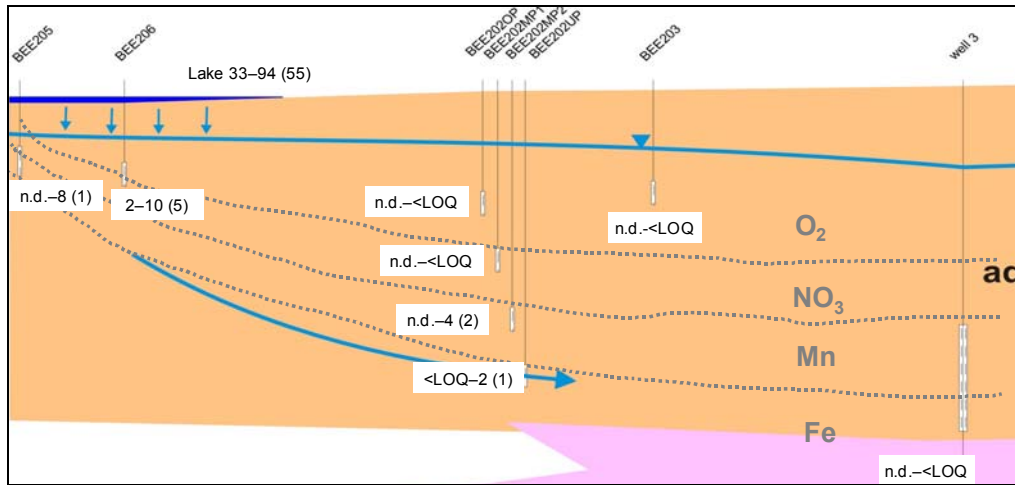
Figure 107: Transect "Wannsee 2" – Results for Dehydro-Erythromycin [ng/L]

(Median values are given in parentheses; n.d.: not detected; >LOQ: > limits of quantification = 0,5ng/L)

Wells BEE205 and BEE206 have different redox–conditions. The water in well BEE205 tends to be more reducing than that in well BEE206 (B.Fritz: Bitte Querverweis auf Hydrogeologenteil einfügen). This indicates that under reduced conditions dehydro–erythromycin might be better degradable than clindamycin. Further investigations could not conclusively confirm this observation: In the small column experiments, anaerobic conditions comparable to those observed in well BEE205 were not achieved. The column experiments have shown that both substances are most efficiently degraded under oxic conditions with dehydro-erythromycin being slightly better removed. However, clindamycin and dehydro-erythromycin were also readily degraded under strongly denitrifying conditions.
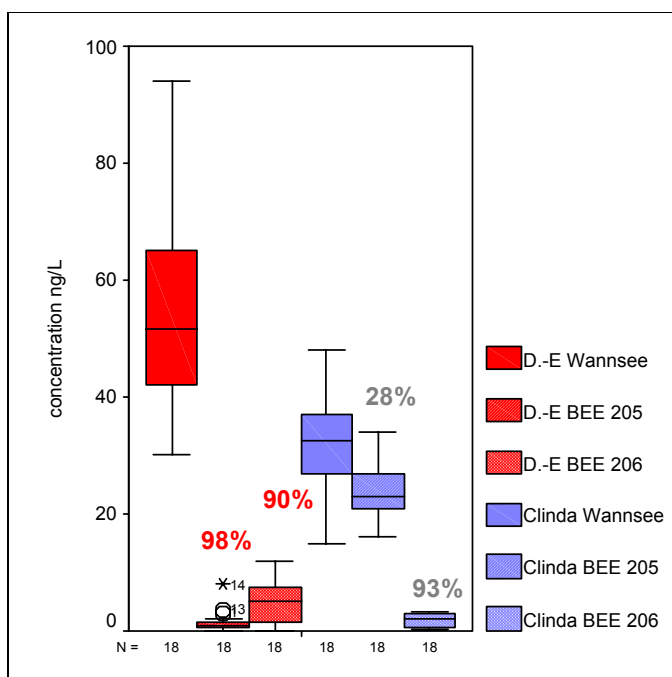
Figure 108: *Boxplots and attenuation rates of dehydro-erythromycin (D.-E) and clindamycin (Clinda) at transect " Wannsee 2".* (Data reported between May 2003 and August 2004, N = number of samples for respective well.)

In general, the sulfonamide sulfamethoxazole was found at higher concentrations than the other antibiotic compounds and it also clearly showed the highest mobility of all six antibiotics. For sulfamethoxazole, a significant but not a complete removal was observed during bank filtration. It is the only antibiotic residue that was also detected in water-supply well 3. However, the median concentration in well 3 corresponds only to about 1% of the median surface water concentration. This might be caused both by sorption and/or degradation processes and by dilution with non-polluted groundwater. The results obtained from the investigations of transect "Wannsee 2" are shown in Figure 109.
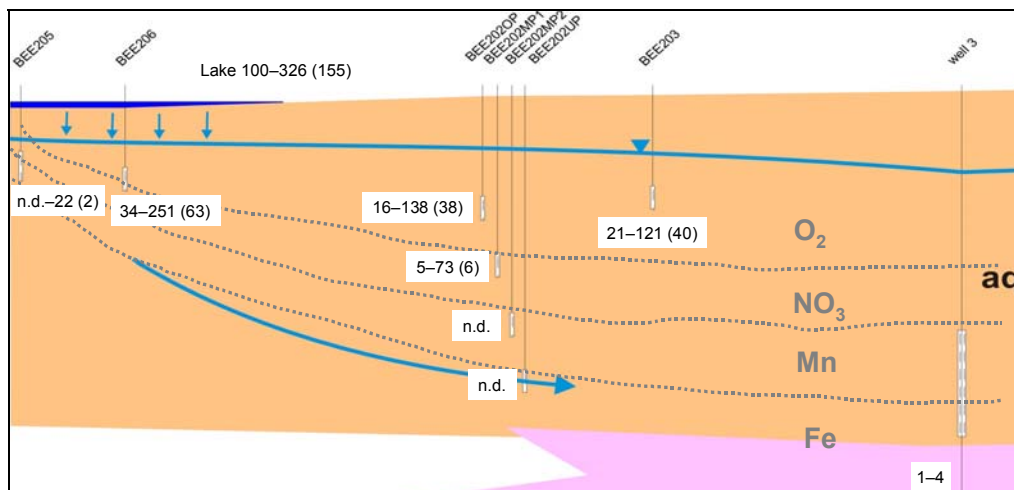
Figure 109: Transect "Wannsee 2" – Results for Sulfamethoxazole [ng/L]

(Median values are given in parentheses; n.d.: not detected; >LOQ: > limits of quantification = 1ng/L)

In Figure 110, the concentrations measured for sulfamethoxazole in monitoring well BEE206 are compared with the corresponding values measured in the same samples for manganese, nitrate, and oxygen and with decrease of the temperature given as a 10 divided by the value of the temperature. As already proposed for dehydro–erythromycin, a better degradation under reduced conditions can be assumed for residues of sulfamethoxazole (also see Figure 111).
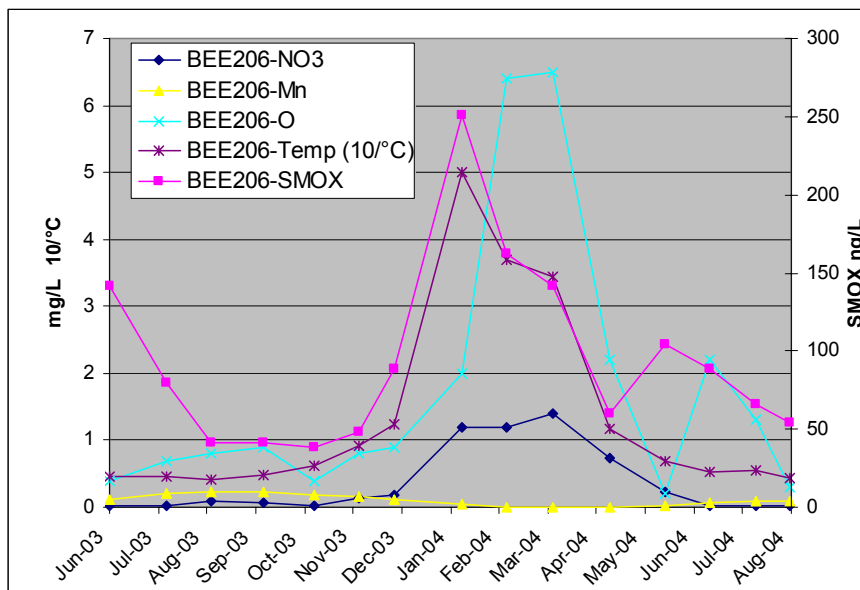
Figure 110: *BEE206 – Concentrations of nitrate (NO3), manganese (Mn), oxygen (O) [BWB data] and sulfamethoxazole (SMOX) and the temperature given as a 10 divided by the value of the temperature.*

122
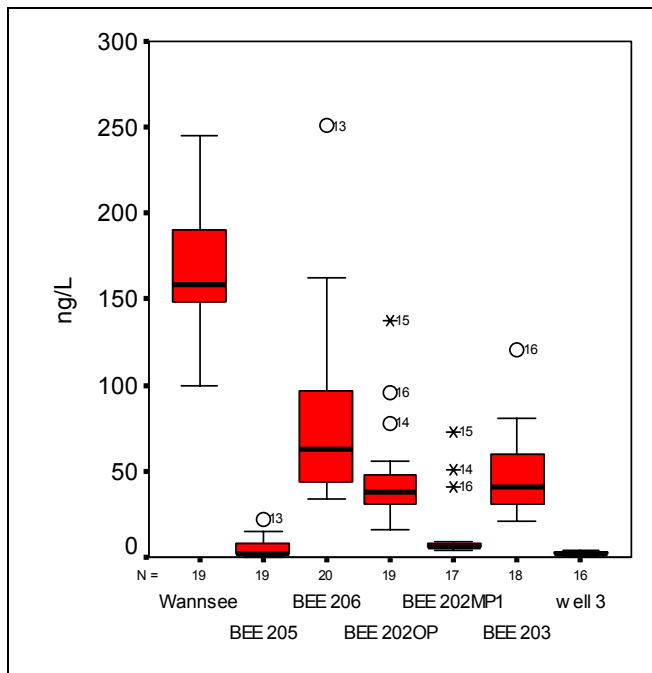
Figure 111: *Boxplots and attenuation rates of Sulfamethoxazole at the transect "Wannsee 2".* (Data from May 2003-August 2004, N = number of samples for respective well.)

Figure 112 shows that in the first half of the year 2004 the concentrations of sulfamethoxazole were increasing in some of the monitoring wells. This increase is temporarily shifted between the different monitoring wells according to the travel times of the groundwater in the aquifer (B.Fritz: Bitte Querverweis auf Hydrogeologenteil einfügen). In wells BEE206 and BEE205 the maximum concentrations were measured in January, whereas the water in wells BEE202OP and BEE202MP1 was detected with maximum values in March and BEE203 in April 2004. In monitoring well BEE206, the peak concentration of sulfamethoxazole was equal to the values measured in the surface water and about five times higher than those concentrations measured before and after this incident. Besides all variability, a similar increase of the concentrations was not observed in the lake.
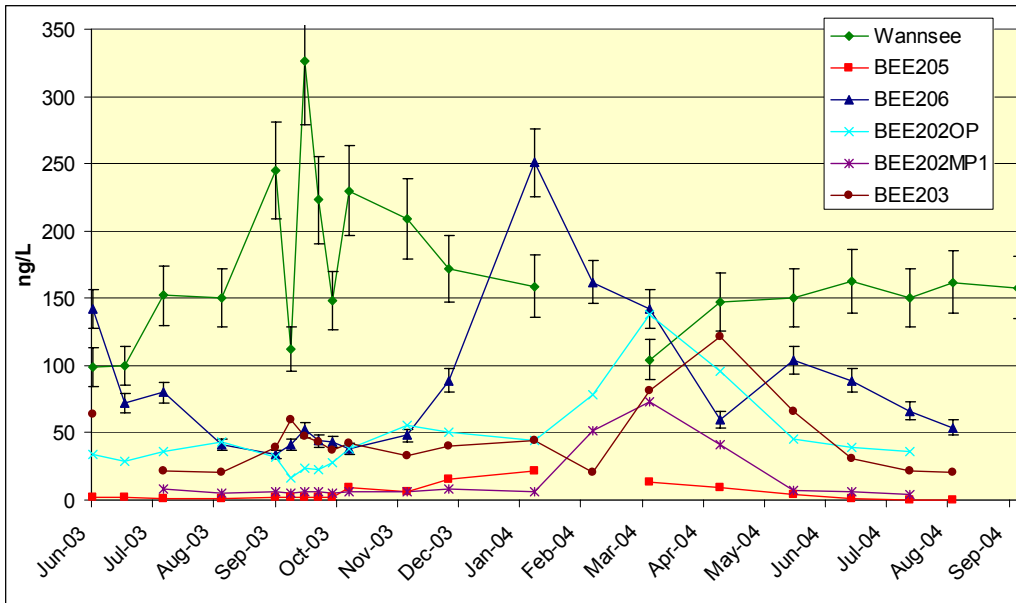
Figure 112: *Transect "Wannsee 2" – Temporal changes of the concentrations of Sulfamethoxazole*

Surprisingly, the sulfonamide drug sulfadimidine was detected at low concentrations (between 3 and 9 ng/L) in some of the deeper wells (BEE202MP2, BEE202UP) (see Figure 113) but not in the surface water samples.
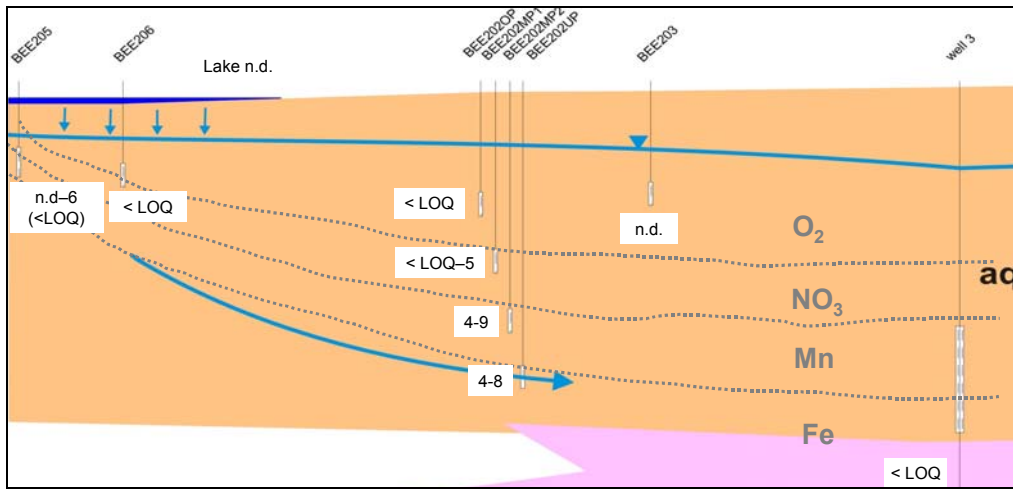
Figure 113: "Wannsee 2" – Results for Sulfadimidine [ng/L]

(Median values are given in parentheses; n.d.: not detected; >LOQ: > limits of quantification = 3ng/L)

Age dating investigations shown that in the multi-level wells BEE202 the share of young bank filtrate decreases by depth (B.Fritz: Bitte Querverweis auf Hydrogeologenteil einfügen). Sulfadimidine has only been used for veterinary purposes in Germany. Thus, the occurrence of sulfadimidine might be explained by the use of large quantities of this compound in the past, when it was used as a growth promotor in livestock farms north of Berlin.

2.4.2 Transect Tegel

Table 35 gives an overview of the found concentration ranges determined in samples collected at transect "Lake Tegel". At transect "Lake Tegel" the shallow wells 3311, 3310 and 3308 could not be sampled during June and September because the groundwater level was beyond the screen of the wells. Since January 2004 the deep well TEG374 was included in the investigation. However, in this well and in well 3304 (representing background groundwater) no antibiotic residues were found.

Table 35: Compounds with positive findings and their concentration range [ng/L] at transect "lake Tegel"

ng/L	surface water (n=16)	3311 (n=7)	3310 (n=7)	3301 (n=15)	3308 (n=7)	TEG 371OP (n=16)	TEG 371UP (n=15)	3302 (n=16)	TEG 372 (n=16)	3303 (n=10)	TEG 374 (n=8)	well 13 (n=16)	3304 (n=16)
Acetyl-Sulfa-methoxazole	8-30	n.d.	5-13	n.d.	n.d.	n.d.	n.d.	n.d.	n.d.	n.d.	n.d.	n.d.	n.d.
Trimethoprim	9-54	N.D.	N.D.-<LOQ	n.d.	n.d.	n.d.	n.d.	n.d.	n.d.	n.d.	n.d.	n.d.	n.d.
Clarithromycin	13-60	n.d.-<LOQ	n.d.-<LOQ	n.d.	n.d.	n.d.	n.d.	n.d.	n.d.	n.d.	n.d.	n.d.	n.d.
Roxithromycin	18-85	n.d.-<LOQ	N.D.-4	n.d.	n.d.	n.d.	n.d.	n.d.	n.d.	n.d.	n.d.	n.d.	n.d.
Clindamycin	41-122	3-8	12-40	1-3	n.d.-0.3	0.2-7	0.3-3	n.d.-0.8	n.d.-<LOQ	n.d.	n.d.	n.d.-<LOQ	n.d.
Dehydro-Erythromycin	70-460	3-6	5-75	n.d.-3	n.d.-<LOQ	n.d.-8	n.d.-3	n.d.-3	n.d.-<LOQ	n.d.-<LOQ	n.d.	n.d.	n.d.
Sulfa-methoxazole	136-533	57-254	146-662	n.d.-200	69-407	24-316	n.d.-77	20-233	26-197	34-151	n.d.-<LOQ	3-22	n.d.
Sulfadimidine	n.d.	n.d.	n.d.	n.d.-4	n.d.	n.d.-<LOQ	n.d.-7	n.d.-<LOQ	n.d.-<LOQ	n.d.-<LOQ	n.d.-<LOQ	n.d.-<LOQ	n.d.

Not detected (n.d.): Benzylpenicillin, Ceftazidim, Ciprofloxacin, Doxycycline, Metronidazole, Moxifloxacin, Norfloxacin, Ofloxacin, Oxytetracycline, Phenoxymethylpenicillin, Piperacillin, Tetracycline, Tylosin;

>LOQ: > limits of quantification; n: number of samples

Again, clarithromycin, roxithromycin (macrolide), trimethoprim (synergist for sulfonamides) and acetyl-sulfamethoxazole (metabolite) were efficiently removed by bank filtration. Residues of clindamycin (lincosamide) and dehydro-erythromycin (metabolite) were completely attenuated during the soil passage. For sulfamethoxazole (sulfonamide), a significant but not complete removal during bank filtration was observed. It was the only compound that was also detected at trace levels in samples collected from water-supply well 13. In general, the data obtained from the investigation conducted at transect "lake Tegel" confirmed the results from the field study at transect "Wannsee 2". The results are also in line with results from a preliminary study on sulfamethoxazole conducted by Hartig [14]. In 1999, Hartig [14] investigated water samples from transect "lake Tegel" collected at six sampling dates. A comparison of the mean concentrations measured in this and the current study (NASRI 2003-04) are shown in Table 5. Especially, the concentrations measured for sulfamethoxazole in the surface water and in water-supply well 13 are very similar in both studies. Thus, the above mentioned proposal of an almost but not complete removal of sulfamethoxazole during bank filtration was confirmed by both studies.

Table 36: Comparison of mean concentrations for sulfamethoxazole at transect "lake Tegel" reported by Hartig [14]] and the NASRI project.

[ng/L]	Hartig 1999 (n≤6)	Nasri 2003-04 (n≤16)
Lake Tegel	223	286
3311	22	165
3310	85	328
3308	34	219
3301	21	65
3302	24	73
3303	17	66
Well 13	2	9

2.5 Laboratory experiments

2.5.1 Sorption and degradation of selected antibiotics in soil-water systems (batch-experiments)

2.5.1.1   Introduction

The occurrence of some investigated antibiotics in surface water (like Lake Wannsee) but their absence in well waters along the transect for the most part leaded to the necessity to get some general information about the behaviour of the detected compounds concerning soils. In order to support the results of the transect investigation and possibly explain their environmental fate respectively laboratory investigations in cooperation with the NASRI project partners FU/Hydrogeology were performed to determine the sorption and (bio)degradation behaviour.

A mixture of six antibiotics were batched to different soil-water systems of three sediments from lake Wannsee mixed with either lake water (Wannsee) or distilled water. Some soil suspensions were put together with the very toxic substance sodium azide to inhibit microbial activity.

The goal of the experiment was to estimate the adsorption and degradation behaviour of the substances on sediments from the investigated transects. Different adsorption and degradation processes could not been distinguished by using this method. Adsorptions occurring on colloids generated by the soils are not taken into account 0.

2.5.1.2   Materials and methods

*T*est antibiotics

In surface waters of Berlin observations in context of the NASRI- project showed five relevant antibiotics: trimethoprim, clindamycin, sulfamethoxazole, clarithromycin and roxithromycin and two antibiotic derivates: acetyl- sulfamethoxazole (a human metabolite of sulfamethoxazole) and dehydro-erythromycin (a degradation product of erythromycin), see

Table 37. Except acetyl-sulfamethoxazole all of them are selected for these investigations.

128

Table 37: Investigated antibiotics and their properties 0.

Substance	Molecular Weight [g/mol]	Water Solubility [mg/l]	pK$_a$	log K$_{ow}$
Trimethoprim	290	hardly soluble	6.6-7.2	0.91
Clindamycin	425	hardly soluble	7.6	1.02
Sulfamethoxazole	253	unsolvable	5.6-5.99	0.89 / 0.74
Dehydro-Erythromycin	716	hardly soluble		
Clarithromycin	748	hardly soluble	8.76	2.6
Roxithromycin	837	hardly soluble	7.1-9.2	2.5

Test sediments and water

- Two sediments of the Wannsee transect from October 2003 were used: "W2" is a mixture of different aquifer parts; "W3" comes from the bottom of the lake Wannsee (the first 10 cm) near the bank. A third sediment used for the experiments was W3 glowed at 800°C for about 12 hours. In November 2004 when experiments started W2 was already dried (at 40°C) and sieved (2 mm) whereas most part of W3 was in moist condition, both stored cool. W3 was then treated the same as W2 und mixed with some already dried sediment of W3.W2 was obvious more coarse-grained than W3 but contained more very fine sediment which was visible during sampling because in both cases some fine material was hardly deposited. See also the results of the sieving analysis by FU/Hydrogeology [1]. Both sediments are mostly free of silt and clay (< 1%).W3 contained an easy visible amount of shell fragments and organic material (< 2mm), the organic carbon content was 0.573 %. W2 contained 0.162 % of organic carbon 0.More geochemical properties of the sediments W3 and W2 are described elsewhere (see 0).Glowed W3 changed colour from beige-green of W3 to light red. Organic material was obviously gone and shell fragments appeared to be clean white. The colour of W2 was red brown.

- Lake water comes from Lake Wannsee in November 2004.

Preliminaries

- Soil to solution ratio: An appropriate ratio guarantees that the percentage adsorbed is above a minimum and concentration of test substances in the aqueous phase are kept high enough to get accurate results. A generally recommended soil/solution ratio of 1:5 was used 0, 0.

- Equilibration time: To determine the amount of test substance adsorbed to a soil it should be measured when the system has reached a plateau. Since experiments were performed to get results during a long period (four weeks) to better observe biodegradation it was necessary to take several samples at the beginning until plateau was possibly reached (three days) and only few samples were necessary for the rest of the period (see "sorption experiments").

- *Stability of test substances:* To check general stability of the test substances stock solutions with distilled water of same concentration as in containers used for experiments were prepared in duplicate with and without sodium azide. Samples were taken and analyzed immediately, after eight days and after four weeks. Following conditions were kept: Temperature of 20°C, darkness, glass bottles, no agitation.

- *Starting concentration and stock solution:* Solution of the antibiotic mix was prepared in pure water without any solubilizing agent such as methanol or acetonitrile (concentration: 100 mg/l). Only Clindamycin was easy soluble but six hours of ultrasound stirring produced a clear solution of the substance mix. The stock solution was stored at 10°C. An appropriate amount of this solution was added to the testing systems. Detection limits of all substances are close to 1ng/l. Starting concentration in containers were chosen three orders of magnitude higher (1 µg/l) 0. This ensures accurate measurements concerning the methodology used. Unfortunately occurrence in the environment means concentrations which are one to two orders of magnitude lower than 1 µg/l.

- *Filter materials:* Available filters were tested to make sure that no losses of substances occur during filtering. No significant losses were detected.

- *Controls:* In order to check the starting concentration, the stability of the test substances in agitation and its possible adsorption on the surface of the test vessels respectively controls with only water but no sediment were also started 0.

- *Sodium azide concentration:* In addition to sorption biodegradation can play a role. A toxic system to inhibit microbial activity was found to be economical and easy workable in comparison to sterilization. However, sodium azide has the following

disadvantage: Changing the kind of electrolytic solution means possibly changes in sorption properties of the test substances dependent on concentration of the additional electrolyte. However, with low concentration of the toxin it is difficult to preserve effective inhibition of microorganism important for degradation during a long period. Quite the reverse it is presumed that for batch experiments a rather larger amount of toxic substance is needed than usually used in column studies where continuous addition of toxin means permanent revival of toxic effects.

A sodium azide concentration as low as possible but high enough to inhibit microorganism effectively during four weeks was needed. In practice concentrations of 5 – 10 g/l with continuous addition are usual but there are no standardized recommendations because it depends on the soil/solution system.

Therefore different amounts of sodium azide (0.5/5/10/20 g/l) were added to mixtures of W3 and lake water (ratio of 1:5) and agitated for four weeks under almost same conditions as in batch experiments. A fluid culture medium for testing water/soil samples of being sterile ("R2A", TU/Environmental Microbiology) was used to check each aqueous phase of inhibition effect every week.

The culture medium went little cloudy only with water from the soil/solution system with sodium azide concentration of 0.5 g/l while with larger amounts of sodium azide no visible growth was discovered for four weeks. A sodium azide concentration of 5 g/l was then expected to inhibit sufficiently in batch experiments.

Sorption experiment

For each of 11 sediment/solution systems (control samples inclusive) a duplicate sample was prepared and pre-equilibrated 84 hours by shaking overhead. Partly systems were prepared in triplicate but samples of the third container could not been analyzed. After antibiotic batching and further agitation an aliquot of the aqueous phase was taken and frozen immediately at six defined time intervals. Experiment continued always with the original mixture until the next aliquot was taken (serial method). The amount of test substances remaining in the aqueous phase was analyzed directly after quick thawing and filtering for comparison to the amount of substances which were initially batched (indirect method). A direct determination of the amount of the adsorbed substances by analyzing the soil was not carried out 0.

The necessary concentration of the test substances and the kind of analyzing method has to be used required a rather large sample volume of 150 ml at each sampling. To provide an appropriate starting volume 5 l petrol containers were filled with 900 g sediment and 4.5 l water and were agitated overhead while packed firmly in concrete mixers (Fig. 1) 0. In some

cases 22.5 g sodium azide per canister were added. By batching the antibiotic mix 45 µl of the stock solution with a concentration of 100 ng/µl was added to every container.

Figure 114: Concrete mixer with firmly packed petrol containers. For agitating it was additionally covered.

After batching the antibiotic-mix and short shaking first sampling was carried out during at most fifteen minutes (time point t_1). Following samplings took place after agitation time in concrete mixers of one (t_2), 24 (t_3), 72 (t_4), 168 (t_5) hours and four weeks (t_6) 0. Sodium azide activity was checked with culture medium at the time point's t_1, t_5 and t_6. Four controls without sediment but only 4.5 l water were run the same way: 1. Lake water (Wannsee), 2. Distilled water, 3. Lake water with sodium azide, 4. Distilled water with sodium azide. Room temperature was nearly constant over the whole testing period of about 20°C. Figure 3 show all tested soil-water combinations and the controls.
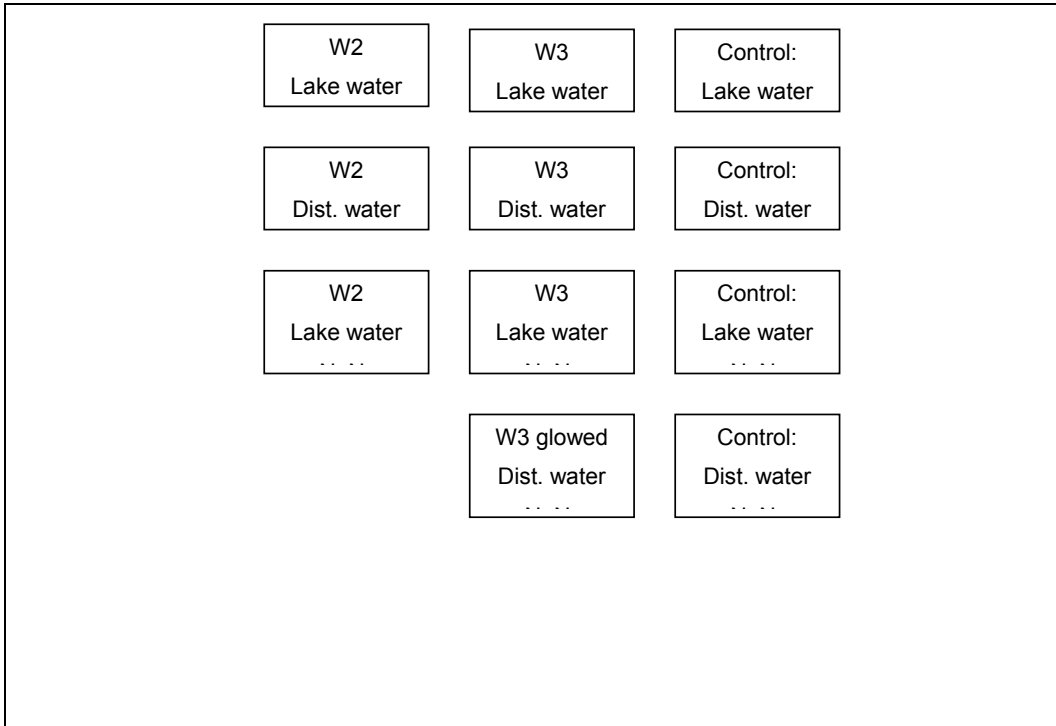
Figure 115: Testing scheme

Analysis method

Two volumes of 50 ml of each filtered sample were thinned with 250 ml water and then preconcentrated via solid phase extraction (SPE) and quantified using HPLC- electrospray- tandem- mass spectrometry [Bitte Verweis auf Brittas Teil einfügen].

Chemical and physical properties of aqueous phases

After antibiotic analyzing rest of thawed samples were stored at 10 °C. Chemical and physical properties (see appendix) were investigated later with photometric tests ("Dr. Lange Küvetten Test"). First and last sample of each container was analyzed once.

2.5.1.3   Results and discussion

Intensity of reaction

The substance concentrations in the aqueous phase were always high enough to be measured accurately although clarithromycin and roxithromycin were partly measured near their limit of quantification of 0.5 ng/l.

On the other hand a minimum of 20% adsorption of substance, preferably more than 50% is useful for further evaluation like calculating distribution coefficients 0. **Table 38** shows that in most cases of this experiment the loss of substances after 72 hours of agitating is sufficient to give an opinion of the processes.

Table 38: Percentage of loss of substance in the aqueous phase after 72 h (* after 168 h) on the basis of the nominal initial concentration.

Substance	W3/lake	W3/dist	W3/NaN3/lake	W2/lake	W2/dist	W2/NaN3/lake	W3gl/NaN3/dist
Trimethoprim	76	70	33	81	71	72	7*
Clindamycin	62	59	26	67	68	52	57
Sulfamethoxazole	88	83	14*	43	26	4*	7*
Dehydro-Erythromycin	45	55	31	70	83	56	71
Clarithromycin	97	98	91	99	99	96	88
Roxithromycin	96	97	89	99	99	96	89

Only some sodium azide samples, e.g. sulfamethoxazole, shown too little reaction, it seems that no or only little sorption took place (4 –14% loss after 168 hours). To determine distribution coefficient, batch experiment must have been repeated with more soil but same water amount (for example with soil/solution ratio of 1:1). Possibly adsorbed amount must directly be determined in addition 0. The other extreme is the very fast and nearly complete attenuation of roxithromycin and clarithromycin on W2 (99%) and W3 (96 –98%). Soil/solution ratio of 1:50 to 1:100 would produce favorable measurement results.

Figure 3 shows a typical sorption reaction (equilibration reaction) from the experiments (Trimethoprim with W3/lake water) in comparison to a very weak reaction (Sulfamethoxazole with W2/lake water and sodium azide) and to a very strong reaction (Clarithromycin with W2/lake water).
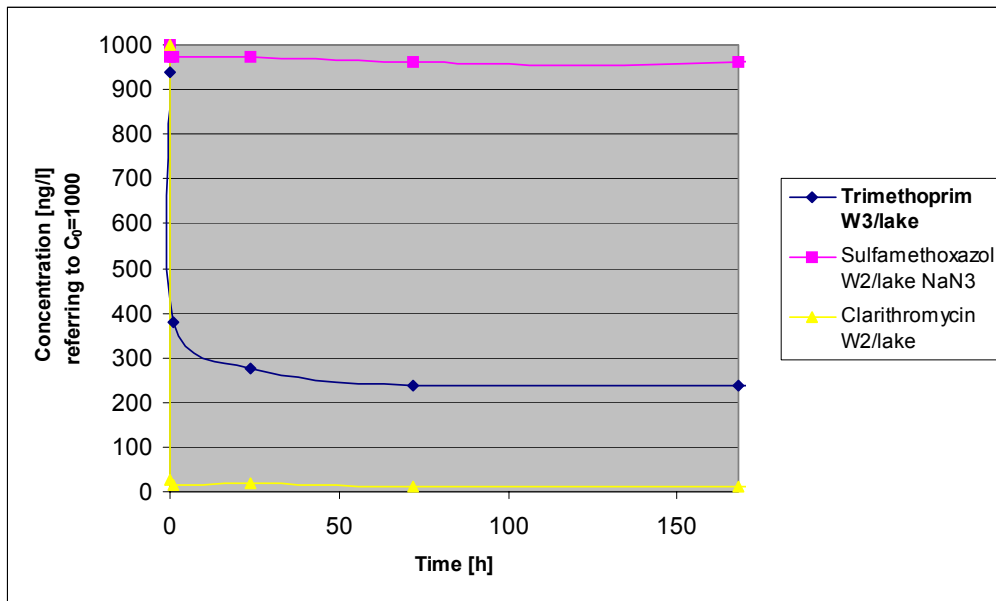
Figure 116: Mean concentration of duplicate samples of three example substances in the aqueous phase versus time referring all to an initial concentration of 1 µg/l. Here an equilibrium reaction is only observed with trimethoprim. (W3 = lake bottom, W2 = aquifer mix)

Adsorption and degradation processes

A sorption reaction is found when achievement of an equilibrium plateau can be observed 0. Distribution coefficients can be calculated by determining the time after which sorption equilibrium is attained (equilibration time). If no plateau after 24 to 72 hours is achieved but a steady increase of supposed adsorption is found, there are also other processes like slow diffusion or biodegradation (which is in the following always expressed as "degradation") in dissociation from adsorption as an equilibration reaction 0. Figure 5 shows an example from the experiments (Clindamycin with W3/distilled water): The degradation process(es) start before equilibrium of sorption reaction can be attained and continue four weeks. In case of biodegradation plateau should be achieved with sterilized/poisoned sample of the soil/water system which can be checked only for the lake water systems within these experiments. Here the process could be rather put down to slow diffusion or other processes because of decreased conductivity of aqueous phase of the W3/distilled water system in comparison to the W3/lake water system. Trimethoprim shows same reaction phenomena with W3 and W2.

135
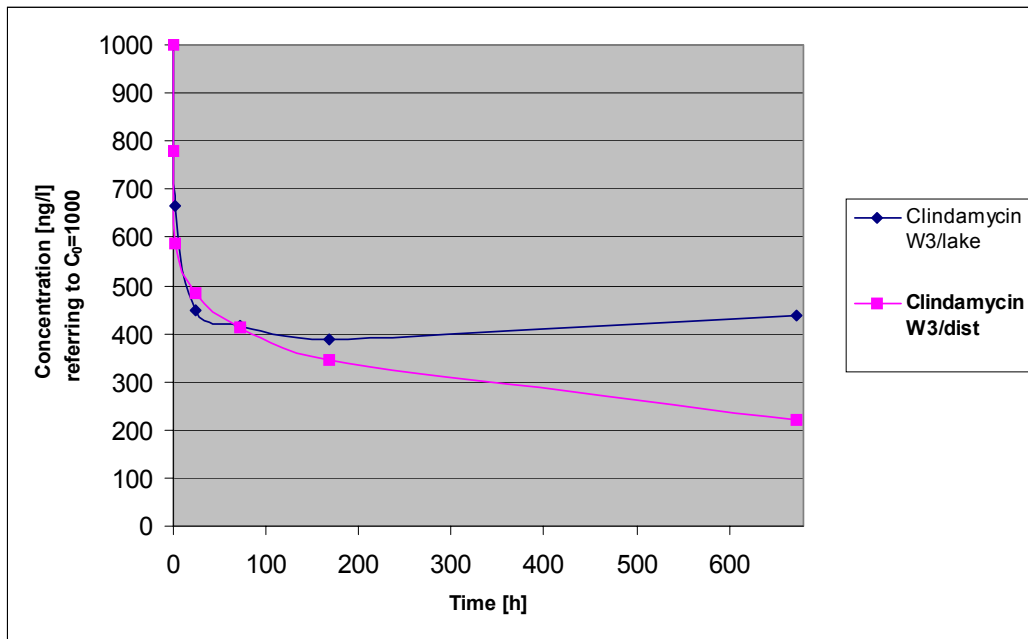
Figure 117: Mean concentration of duplicate samples of clindamycin in the aqueous phase versus time referring to an initial concentration of 1 µg/l. With W3/lake water an equilibration plateau is achieved after about 48 hours whereas with W3/distilled water a more steady decrease is observed. (W3 = lake bottom, W2 = aquifer mix)

A degradation reaction of substance from the more beginning of the test period like the example of Clindamycin showed above was observed with 33 % of the batch samples. 17 % showed degradation from later time points than t_3 (72 hours). There equilibration time was detectable.

Only seven of the samples with reaction intensity from 26 to 81 % loss of substance (17 % of all batch samples) showed purely a sorption reaction.

Test substance stability test and controls

Within the test, which was carried out with the substances in glass bottles without agitation, no significant losses could be detected over the four week period. This means that the substances showed chemical stability at room temperature.

Agitated controls in petrol containers (material: high density polyethylene) partly showed high losses (see Table 39). The highest losses are of sulfamethoxazole from 35 to 41% and roxithromycin of about 33% from the beginning on whereas in other cases losses were detected at later time points or only at the end of the testing period. After four weeks up to

66% loss were detected. Adsorptions on the surface of the containers or biodegradation or both have to be considered.

Table 39: Percentage of loss of substance in the controls after 0.25 / 72 / 672 hours on the basis of the nominal initial concentration as far as 10% loss was exceeded.

Substance	lake water	lake w./NaN$_3$	distilled water	dist. w./NaN$_3$
Trimethoprim	stable/stable/49	stable/stable/17	stable/stable/17	stable/stable/stable
Clindamycin	stable/stable/29	stable/19/17	stable/26/46	stable/49/stable
Sulfamethoxazole	41/58/58	stable/stable/stable	35/29/43	stable/stable/24
Dehydro-Erythromycin	stable/stable/20	stable/stable/17	23/24/57	stable/stable/stable
Clarithromycin	19/32/35	17/31/29	21/20/60	stable/stable/stable
Roxithromycin	33/45/39	stable/stable/33	32/17/66	stable/stable/stable

Controls should show stability of the substance up to the time plateau was reached in soil/solution samples to calculate distribution coefficient. If losses are detected in controls soil should be investigated directly to correct adsorption amount determined with the indirect method. The direct method was not carried out within these experiments.

Controls are also useful to possibly help understanding the observed courses from the soil/solution experiment but data cannot be directly extrapolated to those. The presence of soil will affect adsorption on the surface of the test vessels 0. According to the goals of the experiments and because soils could not be investigated directly data of controls was nevertheless quite used for estimating coefficients.

Sodium azide samples

Sodium azide activity (checked with test culture medium) was stable for four weeks. All sodium azide samples show less removal of investigated substances in comparison to the samples without sodium azide independent on whether degradation in the normal samples was observed or not (data not shown). This observation lets assume at first that for all substances also biodegradation play a role. Relating to the following points it is improbable that always only biodegradation alone is responsible for the lower concentration decrease. Like mentioned above it seems that sodium azide disturbs also the sorption reactions of the substances:

1. Even the very strong reactions of roxithromycin and clarithromycin with W2 are reduced. Triple amount of these substances in the toxic aqueous phase could be detected. The

reaction is very quick (within 15 minutes) which means that reduced reaction in the presence of sodium azide can hardly be due to an inhibition of biodegradation alone.

2. In four cases of non toxic samples no degradation over the whole period can be observed but only a typical equilibration reaction. With sodium azide equal reaction is expected but in the aqueous phase of the appropriate toxic samples double up to triple amount of test substances are detected.

3. From **Table 39** appears that some non-toxic controls show immediately (time point t_1) a loss of some substances, e.g. sulfamethoxazole. In contrast substances are stable (clarithromycin with lake water is the only exception) with sodium azide. This suggests besides biodegradation also an adsorption on the surface on the test container which is prevented with sodium azide.

Since there are disturbing factors data from sodium azide samples could not be used for calculating coefficients.

Some substances of the sodium azide samples nevertheless show degradation mainly relating to time point t_6. Other processes than biodegradation could be considered.

Sorption

Mean concentrations in the aqueous phase were plotted versus time. Each case was checked carefully if sorption could be observed and equilibration time could be determined. If a plateau was reached within 24 to 72 hours equilibration time and related concentration in the aqueous phase was determined to calculate distribution coefficient.

The adsorption distribution is defined as the ratio of the pharmaceutical concentration in the soil (C_s [ng/g]) to the antibiotic concentration in the aqueous phase (C_{aq} [ng/ml]) after equilibration has been achieved 0. The distribution coefficient, K_d, and the adsorption percentage were calculated according to the following equations and are presented in **Table 40**:

$$K_d = C_s\,(eq)/C_{aq}\,(eq) \ \ [ml/g] \qquad A\,(\%) = (C_s/C_0) \times 100$$

C_{aq} was determined directly whereas C_s was measured indirectly as the difference between the initial (C_0 [ng/l]) and the final (mostly after 72 h) concentration in the solution (C_{aq} [ng/l]). C_{aq} refers to the freely dissolved molecules in the soil solution 0.

$$C_s = (C_0 - C_{aq}) \ast 4.5l/900g \ [ng/g]$$

138

Accurate determining of C_0 and C_{aq} are of great importance to get precise distribution coefficient. In comparison of those little changes (less than 1%) on the calculated amount of the adsorbed substances on the soil are the results when taking reduced volume at each time point into account 0 includes instructions on calculating corrected adsorption. For trimethoprim and the W3/lake water system an increase of adsorbed amount from 76 (uncorrected) to 77% (corrected) adsorption on the soil was calculated at time point t_4. Volume corrections then were not carried out because of high time requirements and larger dependency of K_d from test conditions and determining of equilibration time. The kind of K_d dependency on C_{aq} (linear/nonlinear) 0,0 is not taken into account here because several initial concentrations had to be investigated (Freundlich isotherm).

Anyway precise K_d could only be calculated in four cases where no additional degradation in the soil/solution system and stability of test substances in the control system could be observed (grey coloured rows at **Table 40**). For other cases K_d is estimated.

C_0 was the nominal initial concentration which was 1µg/l for distilled water systems and 1µg/l plus Lake Wannsee water content of each substance for the lake water systems.

If equilibration time hardly could be determined because of simultaneous degradation, K_d was estimated by using C_{aq} at a time point which was sufficient for most other cases (72 hours). Given value for K_d and sorption percentage then are always too high (marked with "<").

Equilibrium time could be determined from twelve samples as 24 to 72 hours with at most 72 hours. For comparative purposes within these experiment results all the calculated values for K_d are related then to 72 hours as sufficient equilibration time. Only for a few samples with very weak reaction 168 hours was a sufficient time because of varying values in between the duplicate sample at the beginning of the testing period.

Partly equilibration time could not be determined because of very quick sorption and only few sampling time points during the first 24 hours. Little more losses were observed from 24 hours until 72 hours time point and equilibration time of 72 hours for the calculating was also established.

Last case to look at was instability of test substance in the control. Those cases indicate a direct investigation of soil which could not been carried out here. If loss of substance in the control was observed from the first time point on (not observed with clindamycin and trimethoprim) adsorption on the test container was assumed. The initial concentration C_0 was corrected then by using the controls C_{aq} of the substance at time point t_1 to estimate K_d and the sorption percentage. For the other cases with instability of test substance in control at time point t_4 C_0 was not corrected. Loss of substance in control at time point t_4 compared to initial concentration was taken for calculating is given for both cases.

Table 40: Distribution coefficient and adsorption percentage at equilibration time (t4=teq) of 72 h.

Substance	Soil/ water	C_0 (t0) [ng/l]	C_{aq} (teq) [ng/l]	loss in control (teq) [%]	K_d (teq) [ml/g]	Sorption A (teq) [%]
Trimethoprim	W3/lake	1015	239	stable	16.2	76
	W3/dist	1000	305	stable	<11.4	<70
	W2/lake	1015	209	stable	22.0	81
	W2/dist	1000	291	stable	<12	<71
Clindamycin	W3/lake	1039	392	stable	8.2	62
	W3/dist	1000	412	26	<7.1	<59
	W2/lake	1039	342	stable	<10.2	<67
	W2/dist	1000	321	26	<10.6	<68
Sulfamethoxazole	W3/lake	676*	142	17	<18.7	<79
	W3/dist	647*	174	stable	<13.6	<73
	W2/lake	676*	657	17	0.1	3
	W2/dist	647*	761	stable	0	0
Dehydro-Erythromycin	W3/lake	1065	581	stable	4.2	45
	W3/dist	768*	455	stable	<3.4	<41
	W2/lake	1065	316	stable	<11.9	<70
	W2/dist	768*	174	stable	<17.0	<77
Clarithromycin	W3/lake	817*	31	13	128	96
	W3/dist	795*	24	stable	161	97
	W2/lake	817*	11	13	354	99
	W2/dist	795*	6	stable	666	99
Roxithromycin	W3/lake	688*	40	12	88	95
	W3/dist	676*	29	15	111	96
	W2/lake	688*	12	12	288	98
	W2/dist	676*	9	15	388	99

*: Partly C0 is corrected to Caq of control at time point t1.

Loss in control: difference between C0 and Caq in control at time point t4.

Results of grey colored fields are from experiments with stability of test substances in control and no other observed processes than an equilibration reaction (sorption).

Results marked with "<" indicate other processes than sorption in addition until time point t4.

Instability in controls at teq indicates possibly additional adsorption at the test containers surface.

W3 = lake bottom, W2 = aquifer mix; t4=teq=72 h

Substances with $K_d < 1$ are supposed to be very mobile concerning the tested soil because hardly any adsorption could be determined. Increasing values for K_d means increasing adsorption and decreasing mobility respectively. From Table 40 it is shown that in most cases a removal of at least <59% up to 81% on the investigated sediments could be determined. Dehydro-erythromycin was less adsorbed than the other antibiotics onto sediment W3 ("lake bottom"). Clarithromycin and roxithromycin were very strongly sorbed on both sediments (A = 95 to 99%) which is expressed with high K_d values of 88 up to 666 whereas the K_d values of the other antibiotics are most at 22.

The distribution coefficients for lake water systems compared to the distilled water systems show partly great differences but values are always of the same magnitude. The distilled water system of roxithromycin and clarithromycin show always a higher K_d value compared to the lake water system which means a higher adsorption percentage. For the other antibiotics in most cases the contrary is observed.

The adsorption of the compounds was generally higher in sediment W2 (aquifer mix) than in sediment W3 since the adsorption don't correlates positively with organic carbon content. The exception in sorption properties shows sulfamethoxazole with little or no adsorption on W2 but high sorption reaction to W3. It should be taken into account that controls show high losses for sulfamethoxazole from the very beginning and values for sulfamethoxazole of the controls are extrapolated to the values of the samples. Samples with no or little sorption should be repeated in further investigations with a sediment to solution ratio of 1:1 to determine distribution coefficient more exactly.

Table 41 shows all six tested antibiotics in the sequence of strength of reaction to the two sediments after 72h beginning with the weakest test substance.

Table 41: Sequence of sorption reaction strength to W3 = lake bottom, W2 = aquifer mix, soil/solution ratio 1:5, time point t4 = 72 h.

W3			W2		
Test Substance	Sorption A [%]	K_d [ml/g]	Test Substance	Sorption A [%]	Kd [ml/g]
Dehydro-Erythromycin	<41 - 45	<3.4 - 4.2	Sulfamethoxazole	0 - 3	0 - 0.1
Clindamycin	<59 - 62	<7.1 - 8.2	Clindamycin	<67 - 68	<10.2 - 10.6
Trimethoprim	<70 - 76	<11.4 - 16.2	Dehydro-Erythromycin	<70 - 77	<11.9 - 17.0
Sulfamethoxazole	<73 - 79	<13.6 - 18.7	Trimethoprim	<71 - 81	<12.0 - 22.0
Roxithromycin	95 - 96	88 - 111	Roxithromycin	98 - 99	288 - 388
Clarithromycin	96 - 97	128 - 161	Clarithromycin	99	354 - 666

For roxithromycin and clarithromycin the values for the distribution coefficient and the adsorption percentage could be accurately determined. Since the K_d is related to sediment/lake water systems it can not be directly compared to results from external investigations which in most cases use 0.01 M $CaCl_2$ solution 0 but it is assumed that values are of the same magnitude. For other cases further investigations on the additional processes and possibly adsorption on the surface of the test containers are recommended.

Data of sodium azide samples are present in a separate table only to show reduced reaction but not to characterize sorption of substances to the soils (see **Table 42**)!

Table 42: Distribution coefficient and adsorption percentage for sodium azide samples. See notice for Table 40. "+" equilibration time of 168 hours, Kd and sorption percentage of appropriate samples without sodium azide for comparison purposes. (W3 = lake bottom, W2 = aquifer mix)

Substance	Soil/ water	C_0 (t_0) [ng/l]	loss in control (t_{eq}) [%]	K_d (t_{eq}) [ml/g]	Sorption A (t_{eq}) [%]	K_d of approp. sample (t_{eq}) [ml/g]	Sorption of approp. sample (t_{eq}) [%]
Trimethoprim	W3/lake/NaN3	1015	stable	2.5	33	16.2	76
	W2/lake/NaN3	1015	stable	13.1	72	22.0	81
	W3glowed/dist/NaN3	1000	stable[+]	0.4[+]	7[+]		
Clindamycin	W3/lake/NaN3	1039	19	1.8	26	8.2	62
	W2/lake/NaN3	1039	stable	5.5	52	<10.2	<67
	W3glowed/dist/NaN3	1000	49	<6.5	<57		
Sulfa-methoxazole	W3/lake/NaN3	1152	stable[+]	0.8[+]	14[+]	<18.7	<79
	W2/lake/NaN3	1152	stable	0.2	4	0.1	3
	W3glowed/dist/NaN3	1000	stable[+]	0.4[+]	7[+]		
Dehydro-Erythromycin	W3/lake/NaN3	1065	stable	2.2	31	4.2	45
	W2/lake/NaN3	1065	stable	<6.4	<56	<11.9	<70
	W3glowed/dist/NaN3	1000	stable	12.1	71		
Clarithromycin	W3/lake/NaN3	838*	14	41	89	128	96
	W2/lake/NaN3	838*	14	108	96	354	99
	W3glowed/dist/NaN3	1000	stable	<37	<88		
Roxithromycin	W3/lake/NaN3	1020	stable	41	89	88	95
	W2/lake/NaN3	1020	stable	122	96	288	98
	W3glowed/dist/NaN3	1000	stable	42	89		

Sodium azide samples of trimethoprim and clindamycin show half adsorption with W3 and little lower adsorption with W2 than normal samples. Sulfamethoxazole shows no sorption reaction in the presence of sodium azide whereas high percentage is adsorbed to W3 without sodium azide. Also for dehydro-erythromycin, clarithromycin and roxithromycin little reduced sorption is observed.

With the glowed sediment of "lake bottom" no sorption could be observed with trimethoprim and sulfamethoxazole but high adsorption percentage with the four other tested antibiotics.

The organic carbon normalized adsorption coefficient K_{OC} which is a favored measure of sorption in environmental risk assessment 0 is not given here because the main purpose of K_{OC} is to reduce variability between K_d data of one compound in different soils. That requires dependency of the sorption from the organic carbon content of the soil which has been found for non-polar organic chemicals. For the existing test substances reduction of variability could not been found out.

Degradation

Partly other processes than a sorption equilibration reaction was observed with trimethoprim, clindamycin, sulfamethoxazole and dehydro-erythromycin. It is always a steady decrease and always starts before equilibration plateau could be observed and keep on going until experiment was stopped. There is only one exception with sulfamethoxazole and the "aquifer mix" W2 (see Table 43) and some sodium azide samples (see Table 44) where degradation starts at a time point later than 72 hours. In four cases the other process at time point $t_4 = 72$ hours could be only observed with the distilled water system but not with the lake water system. It is not assumed that here is biodegradation the main process resulting in a steady decrease with distilled water but a slow sorption process.

Some sodium azide samples show also additional degradation processes though there was inhibition of microbial activity proved. The sodium azide samples were not suitable to prove biodegradation of the normal samples (see also above).

Data of the controls does not help to interpret the degradation behaviour of the samples here and can not be directly extrapolated to the samples. All the controls show losses at the end of the experiment which means that biodegradation is probable concerning all six tested substances. The exceptions are sulfamethoxazole, clarithromycin and roxithromycin in lake water controls where no difference was observed to the loss at time point $t_4 = 72$ hours. With distilled water great difference could be determined which is again not due to biodegradation because distilled water is supposed to be rather less microbial active.

143

Further investigations are essential to get an opinion about the processes.

Table 43: **Percentage of degradation and sorption processes at time point t4=72 h in comparison to the loss in the controls on the basis of the nominal initial concentration.**

Substance	Soil/ water	loss in control (t_1) [%]	loss in control ($t_{eq}=t_4=72h$) [%]	Degrad. + Sorpt. ($t_{eq}=t_4=72h$) [%]	Degrad. + Sorpt. ($t_6=672$ h) [%]	loss in control ($t_6=672$ h) [%]
Trimethoprim	W3/lake	stable	stable	no degrad.	no degrad.	49
	W3/dest	stable	stable	70	93	17
	W2/lake	stable	stable	no degrad.	no degrad.	49
	W2/dest	stable	stable	71	84	17
Clindamycin	W3/lake	stable	stable	no degrad.	no degrad.	29
	W3/dest	stable	26	59	78	46
	W2/lake	stable	stable	67	74	29
	W2/dest	stable	26	68	92	46
Sulfa-methoxazole	W3/lake	41	58	88	87	58
	W3/dest	35	29	83	90	43
	W2/lake	41	58	no degrad.	90	58
	W2/dest	35	29	no degrad.	62	43
Dehydro-Erythromycin	W3/lake	stable	stable	no degrad.	no degrad.	20
	W3/dest	23	24	55	68	57
	W2/lake	stable	stable	70	84	20
	W2/dest	23	24	83	95	57
Clarithromycin	W3/lake	19	32	no degrad.	no degrad.	35
	W3/dest	21	20	no degrad.	no degrad.	60
	W2/lake	19	32	no degrad.	no degrad.	35
	W2/dest	21	20	no degrad.	no degrad.	60
Roxithromycin	W3/lake	33	45	no degrad.	no degrad.	39
	W3/dest	32	17	no degrad.	no degrad.	66
	W2/lake	33	45	no degrad.	no degrad.	39
	W2/dest	32	17	no degrad.	no degrad.	66

Table 44: Percentage of degradation and sorption processes at time point t4=72 hours in comparison to the loss in the controls on the basis of the nominal initial concentration.

Substance	Soil/ water	loss in control (t_1) [%]	loss in control (t_{eq}) [%]	Degrad. + Sorpt. (t_{eq}) [%]	Degrad. + Sorpt. $(t_6=672\ h)$ [%]	loss in control $(t_6=672\ h)$ [%]
Trimethoprim	W3/lake/NaN3	stable	stable	no degrad.	52	17
	W2/lake/NaN3	stable	stable	no degrad.	no degrad.	17
	W3glowed/NaN$_3$	stable	stable	no degrad.	no degrad.	stable
Clindamycin	W3/lake/NaN3	stable	19	no degrad.	48	17
	W2/lake/NaN3	stable	stable	no degrad.	72	17
	W3glowed/NaN$_3$	stable	49	57	76	stable
Sulfa- methoxazole	W3/lake/NaN3	stable	stable	no degrad.	no degrad.	stable
	W2/lake/NaN3	stable	stable	no degrad.	no degrad.	stable
	W3glowed/NaN$_3$	stable	stable	no degrad.	no degrad.	24
Dehydro- Erythromycin	W3/lake/NaN3	stable	stable	no degrad.	38	17
	W2/lake/NaN3	stable	stable	56	84	17
	W3glowed/NaN$_3$	stable	stable	no degrad.	no degrad.	stable
Clarithromycin	W3/lake/NaN3	17	31	no degrad.	95	29
	W2/lake/NaN3	17	31	no degrad.	no degrad.	29
	W3glowed/NaN$_3$	stable	stable	88	99	stable
Roxithromycin	W3/lake/NaN3	stable	stable	89	95	33
	W2/lake/NaN3	stable	stable	no degrad.	no degrad.	33
	W3glowed/NaN$_3$	stable	stable	no degrad.	98	stable

Conclusions

Six antibiotic substances, including the macrolides clarithromycin, roxithromycin and erythromycin (measured as metabolite dehydro-erythromycin), the sulfonamide sulfamethoxazole, the sulfonamide synergist trimethoprim and the lincosamide clindamycin, were batched to different soil-water systems of three sediments from Lake Wannsee ("aquifer mix" (W2) , "lake bottom" (W3) and "lake bottom" glowed) mixed with either lake water (Lake Wannsee) or distilled water.

With this investigation it is possible to get a general idea of the sorption behavior of the tested antibiotics on the Wannsee sediments. As far as possible, the distribution coefficient K_d was calculated. However, partly further investigations are recommended to confirm the results. The values of K_d decreased in the following order: clarithromycin > roxithromycin > trimethoprim > clindamycin > dehydro-erythromycin > sulfamethoxazole.

For roxithromycin and clarithromycin no mobility could be found out. The investigation showed a fast removal (> 97%) of the concentration of these two substances. They are strongly sorbed to both sediments, which is expressed with high K_d values (K_d 88 – 161 for W3, 288 – 666 for W2).

Trimethoprim and clindamycin showed a similar concentration decrease in both kinds of sediment, whereby the concentration of trimethoprim (<70-81%) was reduced somewhat better than of clindamycin (<59-68%). Their values of K_d range from <7.1 to 22.0 which means weak mobility relating to the aquifer mix and the lake bottom.

Dehydro-erythromycin was less adsorbed than the other antibiotics onto sediment W3 ("lake bottom") (K_d <3.4 – 4.2) and the difference in adsorption strength between the two sediments is higher as it is of trimethoprim and clindamycin (K_d <11.9 – 17.0 for W2).

Generally, the adsorption of all compounds, except from sulfamethoxazole, was faster and higher at the sediment W2 „aquifer mix".

Sulfamethoxazole shows great difference and opposite reaction than the rest of the tested substances relating to the two sediments. It was found to be strong mobile concerning the sediment "aquifer mix" of the Wannsee transect (K_d max. 0.1) whereas it is only weakly mobile in sediment from Wannsee lake bottom (K_d < 13.6 – 18.7). Since sorption behaviour is far more complex in comparison to the other tested antibiotics sulfamethoxazole should be first if further investigations are possible.

For the differences in reaction strength of the two sediments organic carbon content of the two sediments is not the decisive factor because "aquifer mix" contents less organic carbon but reacts stronger. Variability of K_d concerning different soils could not be reduced by relating K_d to the organic carbon content which could be caused by the lack of dependency of the sorption from the organic carbon content of the soil.

Whether the higher content of very fine grained material (<0.063 mm) within the aquifer mix (W2) is due to stronger adsorption reactions is hard to decide because both sediment contain less than 1% 0.

For trimethoprim, clindamycin, sulfamethoxazole and dehydro-erythromycin other processes than sorption were observed in addition but there is no opinion about the reason. Further investigations are essential. Biodegradation can not be excluded and can not be proved either. For some cases slow sorption processes seem to be predominant.

References

OECD: Adsorption/Desorption Using a Batch Equilibrium Method. - Paris: Organisation for Economic Cooperation and Development (OECD), 2000. (OECD Guidelines for the Testing of Chemicals, Test No. 106)

Fanck, B.: Untersuchungen von Antibiotikarückständen im aquatischen System mittels Flüssigkeits-Chromatographie-Elektrospray-Tandem-Massenspektrometrie (HPLC-ESI-MS/MS). – PhD work TU Berlin, in prep.

Massmann, G., Taute, Th., Bartels, A., Ohm, B.: Characteristics of sediments used for batch-, enclosure- and column studies. Draft by Free University of Berlin, working group Hydrogeology (2004)

Tolls, J.: Sorption of veterinary pharmaceuticals in soils: A review. – Environmental Science & Technology 35 (2001), No. 17, p. 3397-3406.

Rabolle, M., Spliid, N.H.: Sorption and mobility of metronidazole, olaquindox, oxyteracycline and tylosin in soil. – Chemosphere 40 (2000), p. 715 – 722.

Boxall, A.B.A., Blackwell, P., Cavallo, R., Kay, P., Tolls, J.: The sorption and transport of a sulphonamide antibiotic in soil systems. – Toxicology Letters 131 (2002), p. 29-37.#

Scheffer, F.: Lehrbuch der Bodenkunde/Scheffer/Schachtschabel. – 15. Aufl., Heidelberg: Spektrum Akademischer Verlag, 2002.

2.5.2   Attenuation behavior of selected antibiotics in laboratory experiments at small retention columns

Several investigations described the occurrence of antibiotics in the aquatic environment and are comprehensively reported in an extended review (Heberer and Adam, 2005, [1]). In surface waters of Berlin observations in context of the NASRI- project showed five relevant antibiotics and two antibiotic derivates; trimethoprim, clindamycin, sulfamethoxazole, acetyl-sulfamethoxazole (a human metabolite of sulfamethoxazole), dehydro-erythromycin (a degradation product of erythromycin), clarithromycin and roxithromycin [2]. Except acetyl-sulfamethoxazole all of them are selected for further investigations. Under influent conditions induced by bank filtration or artificial groundwater recharge antibiotics infiltrate into the subsoil while undergoing a natural attenuation. But little is known about attenuation behavior of the selected antibiotics. Possible ecotoxic effects of such pharmaceutically active compounds (PhACs) or a possible link between the occurrence of antibiotics at subinhibitory concentrations and bacterial resistance in the environment supply additional motivation for investigations to understand and optimize attenuation by artificially induced infiltration processes. Laboratory experiments in small retention columns should supply more detailed information about attenuation behavior. Samples were preconcentrated via solid phase extraction (SPE) and quantified using HPLC- electrospray- tandem- mass spectrometry. Experiments were conducted in co- operation with working group Prof. Jekel ("organics", Department of water quality control, TU- Berlin) and working group Prof. Pekdeger (hydrogeology, FU- Berlin) as part of the NASRI project.

2.5.2.1   Short columns (TU- columns)

Setup / carrying out

Setup and carrying out were generally set in advance by Steffen Grünheid (working group organics).

Three experiments (A, B & C) were conducted, each of them over a time period of 4 weeks. Effluent sampling took place within every fourth week. Influent samples were taken approximately one week before and directly after effluent sampling at the end of each experiment, respectively. Following illustration shows target influent concentrations of target compounds in experiments A, B and C. Three effluent sample collections were conducted for experiment A and two effluent sample collections for experiments B and C.
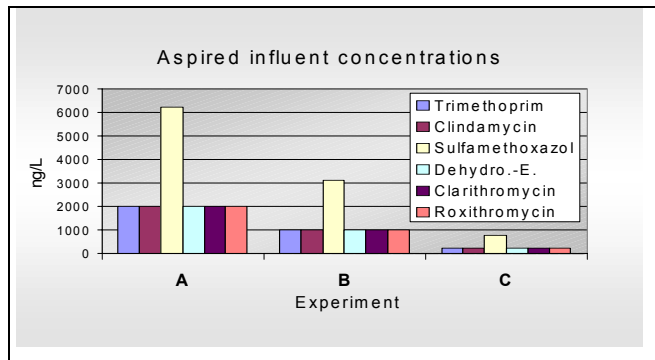
Figure 118: target influent concentration.

Aims

Influent concentrations of experiment A should guarantee measurable effluent concentrations. So in experiment concentrations were chosen ten to twenty times higher values than those which could be found in surface water (Bitte Verweis auf Brittas Teil einfügen). Furthermore influent concentrations in experiments B and C were reduced (factors 0.5 and 0.125 of stock solution from experiment A). All antibiotics were dissolved in purest water to avoid additional DOC. Evaluation should supply statements according to attenuation behavior of the selected antibiotics, for example about:

- Influence of free oxygen (oxic vs. anoxic conditions)
- Influence of denitrification (column No. 4, forced denitrification by NO3- addition in absence of free oxygen,)
- Effects of additional, easily degradable DOC (consequences of complete decrease of free oxygen and lack of other terminal electron acceptors with chemically bound oxygen like NO3- and so caused anaerobe conditions, see columns No.3 & No.6 and influence of the relatively short oxic redox zone at the beginning of column No.3)
- Influence of column length and column material (See column No.5 and comparison of columns No. 1 vs. No.7 vs. No.8)
- Effects of influent concentration level C0, (Comparison of experiments A, B & C)
- Differences and common features between attenuation behaviors of the selected antibiotics etc.

Results and discussion

Laboratory experiments with antibiotics started in September 2004 and operated until December 2004. Discovered influent and effluent concentrations with statistical deviation maximum are presented in appendix (Table 1-3). The data basis with mean concentrations is presented in the table below.

149

Table 45: Mean concentrations at sampling period

Experiment A (mean values for time period [ng/L])									
Date (time period)	18.09.-21.10.04	11.-15.10.04			18.09.-21.10.04	11.-15.10.04				
Measuring point	Anoxic influent	Effluent col. No.			Oxic influent	Effluent col. No.				
		5	4	6		3	1	7	8	0
Trimethoprim	2890	170	2030	680	2700*	250	30	1	1	830
Clindamycin	1810	1	110	1340	2300*	120	14	65	1	310
Sulfamethoxazole	6530	360	6180	2320	7100*	1610	90	55	376	2840
Dehydro-erythromycin	2030	3	110	2040	2800*	4	4	23	1	510
Clarithromycin	2120	40	70	1280	2400*	70	100	13	6	1040
Roxithromycin	1940	40	500	1410	2200*	20	40	12	2	220
Experiment B (mean values for time period [ng/L])										
Date (time period)	21.10.-22.11.04	15.-21.11.04			21.10.-22.11.04	15.-21.11.04				
Measuring point	Anoxic influent	Effluent col. No.			Oxic influent	Effluent col. No.				
		5	4	6		3	1	7	8	0
Trimethoprim	1320	670	780	400	1650	340	13	0	1	460
Clindamycin	840	23	90	860	1280	140	20	61	2	300
Sulfamethoxazole	3300	194	2500	900	4200	850	390	70	210	1040
Dehydro-erythromycin	1020	7	100	1020	1530	8	3	15	5	380
Clarithromycin	1000	14	1050	870	1380	5	5	8	1	270
Roxithromycin	900	33	940	860	1150	130	13	8	3	270
Experiment C (mean values for time period [ng/L])										
Date (time period)	22.11.-20.12.04	13.-19.12.04			22.11.-20.12.04	13.-19.12.04				
Measuring point	Anoxic influent	Effluent col. No.			Oxic influent	Effluent col. No.				
		5	4	6		3	1	7	8	0
Trimethoprim	280	470	260	260	260	130	1100	0	50	340
Clindamycin	240	13	28	450	250	50	180	60	12	180
Sulfamethoxazole	850	100	290	320	710	120	50	50	180	960
Dehydro-erythromycin	300	6	22	400	320	6	14	14	8	310
Clarithromycin	220	8	770	610	240	6	4	6	3	230
Roxithromycin	240	30	760	560	260	250	9	7	3	200

*calculated

$$c(A_{oxic}) = \frac{\{2 \times c(\exp erimentB) + 8 \times c(\exp erimentC)\}}{2}$$

In experiment C, where the influent concentrations were reduced in relation to experiment B again by the factor 0.25, some antibiotics showed higher effluent concentrations than the

influent concentrations of experiment C at the columns No. 5, 4, 6, 1 and 0 (see Table 45) now. That can be explained by a desorption that occurs now from the earlier experiments A and B with higher influent concentrations. So sorption of trimethoprim, dehydro-, clarithro- and roxithromycin could be recognized as a reversible process. With hindsight it would have been more favorable to begin with the smallest influent concentration (experiment C) followed from B and A.

Observed antibiotic concentrations in effluent samples showed partly a time dependent concentration course (see appendix) which makes interpretation surprisingly more difficult and reduces the meaning of data. Effluent concentrations of some antibiotics increased at several columns from the first sampling collection until the third sampling collection within experiment A. Affected substances and columns are listed in Table 46. The other measured concentrations showed constant values.

Table 46: Substances without constant effluent concentrations (exp. A)

Substance	Effluent column No.
Trimethoprim	5, 6, 3, 0
Dehydro-erythromycin	4, 0
Clarithromycin	4, 3, 0
Roxithromycin	4, 0

Possible reasons:

Increasing effluent concentrations indicate larger retention times and extended dispersions. So maximum concentration levels were not achieved for the cases mentioned above at sampling time. Therefore it could be concluded that the three weeks before effluent sampling were not sufficient and did not yielded equilibrium. But this explanation is assumed as not very likely, because of tracer experiment of the project partner showed a 6d (12d column No.5) retention time for the mobile phase [Bitte Querverweis Steffen einfügen]. According to this, after 21 days antibiotics should be appeared in effluent with concentration maximum and other reasons like desorption processes could be possible explanations for increasing values.

 On the other site variations could be caused by antibiotic and column dependent lack of adsorption capacity with the consequence that several antibiotics (which are added continuously) reached the column effluents attenuated within the three weeks before effluent sampling, but already covered adsorption places disabled an equal adsorption of new infiltrating antibiotics and could cause the increasing concentrations. So equilibrium was not achieved for the cases mentioned above.

Antibiotics with strong sorption properties are concerned. Observations in batch experiments showed strong sorption for clarithromycin and roxithromycin (B.Fritz: Bitte Querverweis auf Batchteil einfügen).

Nevertheless to compare and evaluate the attenuation behavior of selected antibiotics during sampling period, the ratio C(mean)/C0 of experiment A and B were calculated, to show the attenuation behavior as a trend of attenuation at several redox conditions. Figure 119 demonstrated this exemplary for sulfamethoxazole. Data of experiment C could not analyzed this way, because concentrations of experiment C interfered with desorption of antibiotics which were immobilized in previous experiments A and B at higher C0 levels.
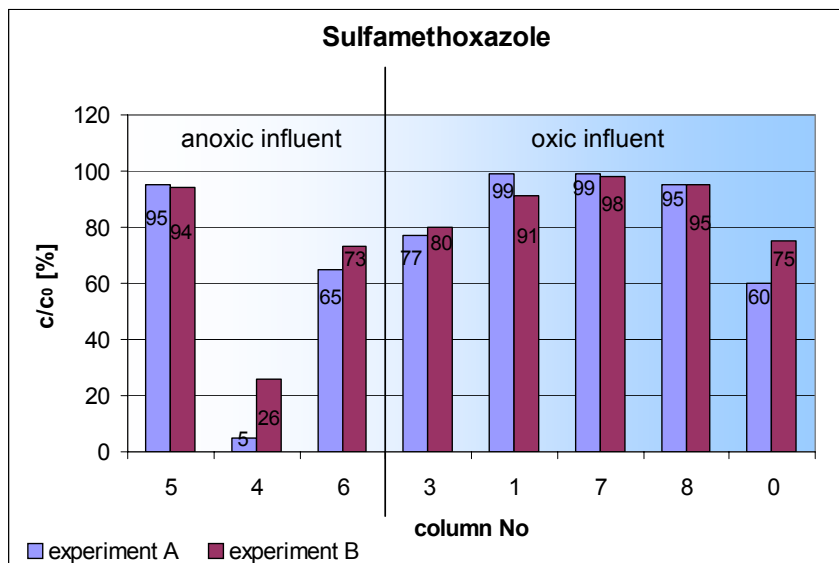
Figure 119: Sulfamethoxazole experiment A and B.

Sulfamethoxazole showed most effective attenuation under oxic conditions (see Figure 119). In this connection different column materials (technical sand [column No. 1] vs. bank material [column No. 7] vs. aquifer [column No. 8]) did not yield different attenuation performances. Column No. 5 showed with double soil passage under anoxic conditions comparably good attenuation like the columns with oxic influent and an oxic zoning.

In experiment A the effluent of column No. 4 shows a nearly complete break-through (c/c0≈95% → approx. 6200ng/L)) for sulfamethoxazole. In experiment B (influent concentration 1/2 of A) and in experiment C (influent concentration 1/8 of A, data here not shown) the attenuation capacity improves from a break-through of c/c0≈74% (approx. 2500ng/L) up to c/c0≈35% (approx. 300ng/L), respectively. Thus under denitrificated conditions a dependence on the influent concentration (within this range) of sulfamethoxazole becomes clearly. The relative decrease capacity improves with smaller becoming inlet concentration.

Detailed explanations for the other investigated antibiotics are given elsewhere [3]. Conclusions are listed in table 4 and in the summary.

Results overview

Table 47 shows a result overview. All investigated antibiotics showed most effective attenuation under oxic conditions. Different column materials (technical sand vs. bank material vs. aquifer) did not yield different attenuation performances under oxic conditions after 1m soil passage. The double soil passage under anoxic conditions resulted in a comparably good attenuation, trimethoprim excluded.

During observed removal by sorption always a reversible adsorption and not an irreversible absorption was assumed. That could be concluded, if in the subsequent experiments B and C (with halved and/or eight-divided inlet concentrations) in relation to experiment A worse depletion capacity were obtained and/or effluent concentration in experiment C were larger than the influent concentration of the experiment C. Due to the smaller inlet concentration here a desorption could occurred from in the preceding experiments with higher influent concentrations by adsorption immobilized antibiotics, which not became depleted yet by other mechanisms like e.g. biodegradation at the solid surface.

For sulfamethoxazole an improvement of the relative depletion capacity could be determined under anoxic conditions (column Nr.4, nitrate respiration) as only of the examined substances, if the inlet concentration is reduced. That applies to the investigated concentration range of approx. 7000-800ng/L. Clindamycin and dehydro-erythromycin were under these conditions almost completely attenuated.

Since with trimethoprim and sulfamethoxazole the depletion capacity under anoxic/anaerobic conditions was reduced and/or with starch addition in relation to oxic soil passages only weakly, it was further concluded that oxygen does not possess the prior role as terminal electron acceptor for the portion, which became biodegraded. Fermentation and anaerobic respiration as well as cometabolic degradation are considered equally by biodegradation.

In contrast to it oxygen has with the three examined macrolides (Dehydro -, clarithro and roxithromycin) as well as with the lincosamide, clindamycin, a greater importance for biodegradation than anaerobic respiration or fermentation. The anaerobic soil passage in column No.6 don't effect a good decrease capacity particularly for these substances. However, an addition of starch with oxic influent leads only to an insignificant until no decrease of the depletion achievement with the macrolides.

Table 47: Results / conclusions over view (TU- column experiments)

TU- column, L = 1m bzw. 2m Ø=14cm, Q≈0,8L/d T=(15± 4)°C	Relative attenuation performance			Contribution to attenuation		Other influence factors to relative attenuation behavior	
	oxic	anoxic	anaerob	microbial	sorption	negative effects	C_0
	++		+	+	++	e. d. surplus DOC,	No effect

Weak or no sorption contribution was concluded, if in any column effluent of experiment (A) a nearly complete breakthrough could be observed. That could be observed with dehydro-erythromycin and sulfamethoxazole.

2.5.2.2   Clogging column

Setup / carrying out

Following graphic illustrates the column system. Extended descriptions are given by the project partner (working group hydrogeology) (B.Fritz: Bitte Querverweis auf Hydrogeologenteil einfügen) and elsewhere [3]. Influent concentration level were similar to those values, which could be found in surface water (150ng/L to 400ng/L).Three sampling collections were conducted.

Results and discussion

Laboratory experiments with antibiotics started in February 2005 and were carried out until March 2005. Discovered influent and effluent concentrations with statistical deviation maximum are presented in appendix (Table 4).

To achieve a better comparison of attenuation performances for the individual antibiotics with given redox conditions, measuring point concentrations of the three experiments A, B and C were standardized and averaged. These values are illustrated in the following Table 48 and Figure 120.

Table 48: standardized and averaged data

Results: mean values C/C0 of the 3 experiments A,B,C

measuring point	remark	Trimetho.	Clinda.	Sulfa.	Dehydro-E.	Clarithro.	Roxithro.	depth [cm]
WS 2C1	influent	1	1	1	1	1	1	0
WS 2C2	tap1	0,27	0,88	0,79	0,88	0,88	0,83	2
WS 2C3	tap2	0,12	0,86	0,94	0,77	0,79	0,81	8
WS 2C4	tap3	0,11	0,80	1,01	0,73	0,17	0,39	12
WS 2C5	tap4	0,08	0,47	0,89	0,19	0,01	0,02	25
WS 2C6	tap5	0,01	0,26	0,86	0,10	0,01	0,01	50
WS 2C7	tap6	0,00	0,08	0,78	0,06	0,01	0,01	80
WS 2C8	tap7	0,01	0,08	0,92	0,06	0,01	0,01	90
WS 2C9	effluent	0,00	0,06	0,64	0,04	0,00	0,02	100

remark.: C/C0;

C:= concentration at measuring point

C0:= influent concentration (mean of both values, before and after sample collection for each experiment)
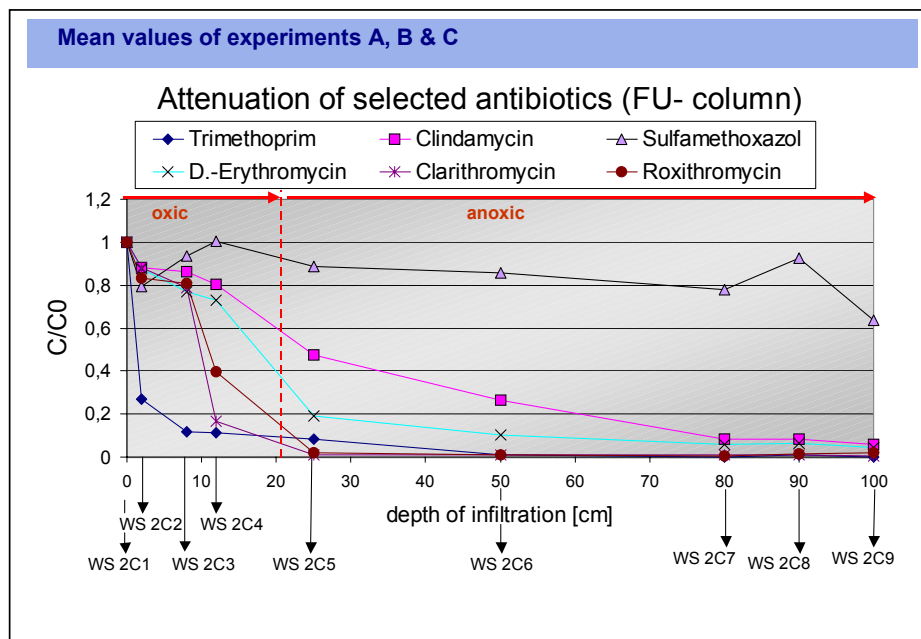
Figure 120: Results C/C0, FU- column

Trimethoprim, dehydro-erythro -, clarithro -, roxithro- and clindamycin were almost completely attenuated after 80cm soil passage. Alone sulfamethoxazole was not effectively held back or attenuated in contrast to the other examined antibiotics during the passage through the 1m sediment column, and the weak concentration reduction after column passage in experiment A could not be confirmed as significant reduction in the two repetition measurements (experiment B and C).

A complete reduction of free oxygen within the first 21cm of sediment could be observed, caused by oxidation of background DOC. Similarly to it strongest reduction of antibiotic concentrations was measured there, sulfamethoxazole excluded. This both is a sign of a biodegradation beside sorption. However, sorption can be made mainly responsible for the attenuation of trimethoprim. The observations showed also a good attenuation of clindamycin under anoxic conditions, which runs off somewhat faster under oxic conditions.

Detailed explanations for the other investigated antibiotics are given elsewhere [3]. Conclusions are listed in Table 49 and in the summary..

Table 49: Results / conclusions over view (FU- column experiments)

FU- column, L = 1m Ø=7cm, Q≈0,8L/d T=(20±3)°C	Relative attenuation performance		Contribution to attenuation	
	oxic	anoxic	microbial	sorption
trimethoprim	++	?	-	++
clindamycin	+	+	+	-
sulfamethoxazole	-	-	? / -	-
dehydroerythromycin	+	-	+	-
clarithromycin	+	?	+	? / -
roxithromycin	+	?	+	? / -

? not differentiable	oxic: free dissolved O_2 present
- no remarkable contribution	anoxic: no free dissolved O_2, but only
+ good / great	chemical bound oxygen
++ very good / very great	(for example NO_3^-)

A general difference of the two column systems exists in the quadruple higher flow rate per unit cross section of the FU- column opposite to the TU- columns with otherwise comparable column conditions such as pH value, temperature, length of the soil passage, the sediment as well as infiltrating surface water. Thus the ineffective attenuation of sulfamethoxazole at the FU- column in relation to the good attenuation at the TU- columns after one meter soil passage can be explained. These observations showed also as trend, that like already assumed, those oxic and anoxic attenuation performances with larger flow rates become smaller, because less time remains at the disposal for sorption processes and other reduction mechanisms.

Beyond that, the conclusions of both column experiments agree well and are confirmed mutually and supplementing.

Sulfamethoxazole

showed (with distance) highest mobility of all investigated antibiotics

sorption supplied no remarkable contribution to attenuation (also confirmed in batch experiments for aquifer material (B.Fritz: Bitte Querverweis auf Batchteil einfügen))

157

no significant attenuation after 1m soil passage with a flow rate of approx. 20(mL/d cm2)

nearly complete attenuation after 1m soil passage with a flow rate of approx. 5(mL/d cm2), microbial processes could effect attenuation under several conditions (under oxic and double anoxic soil passage without additional DOC)

nearly complete breakthrough under anoxic conditions with forced denitrification (TU- column No.4) but attenuation dependent on influent concentration (C0); relative attenuation performance became larger with smaller becoming influent concentration: from approx. 5% in experiment A to approx. 65% in experiment C (investigated concentration range: C0: 7000-800ng/L)

negative effects: easily degradable, surplus DOC (simulated with 3mg/L starch, 20-30% breakthrough, TU- columns No.3 & 6) and monotonous, strong denitrification conditions reduced attenuation performance and yielded no complete retardation

Trimethoprim

Complete attenuation under oxic conditions (at both flow rates)

Largest concentration reduction took place within the first 2cm (FU- column) with an relative attenuation of approx. 70%

Thus sorption could be found as main attenuation mechanism, which could be recognized as a reversible process in TU- experiments

Worse attenuation under anoxic / anaerobe conditions, especially under monotonous, strong denitrification conditions (breakthrough up to 70%, TU- column No.4)

lower attenuation in presence of easily degradable DOC (3mg/L starch),(approx. 10-30% breakthrough after 1m, TU- column No.3 & No.6)

Dehydro-erythro-, Clarithro-, Roxithro- und Clindamycin

- nearly complete attenuation under oxic and double anoxic soil passage
- there are serious indications for a microbial degradation as main attenuation mechanism (beside sorption for roxithromycin and clarithromycin)
- sorption could be recognized as a reversible process
- clarithromycin und roxithromycin showed analogous patterns of behavior, explainable by the similar chemical structure and attenuation mechanisms (sorption + biodegradation) were relatively stronger than those of dehydro- and clindamycin, because attenuation became slower with increasing depth of infiltration than for clarithro- and roxithromycin, see FU- column (batch- experiments confirming these conclusions, which showed stronger sorption for clarithro- and roxithromycin (B.Fritz: Bitte Querverweis auf Batchteil einfügen))

158

under oxic conditions intensity of relative attenuation performances of these four antibiotics can be reported in following sequence: clindamycin < dehydroerythromycin < roxithromycin ≤ clarithromycin, (see FU- experiment)

dehydro-erythromycin and clindamycin were also good attenuated under denitrification conditions, but observations for roxithromycin and clarithromycin are not allowing this statement; both antibiotics were almost effective aerobe attenuated, before nitrate respiration could begin (FU- column), and in TU- column No. 4 (experiment B & C) relative attenuation performances were interfered by desorption or data were invalid because of larger retention times and early sampling collections

negative effects to attenuation performances: easily degradable DOC (3mg/L starch) in combination with anoxic influent, so no satisfactory attenuation could be observed at TU- column No.6. (but in combination with oxic influent attenuation was good and was not significantly influenced)

aerobe microbial oxidation of back ground DOC included these four antibiotics (metabolic and / or co- metabolic) and yielded most effective attenuation within the first 21cm of sediment (oxygen reduction zone, FU- column) (behavior of the three macrolides and clindamycin at the TU- columns No.3 & 6 confirming these conclusions)

so the three macrolides; dehydro-erythro-, clarithro- and roxithromycin as well as the lincosamide, clindamycin, showed attenuation patterns which situated between the both „extreme" patterns of sulfamethoxazole and trimethoprim (sulfamethoxazole with no remarkable sorption and no significant attenuation by microbial processes within FU- column passage and trimethoprim with strongest sorption, (70% attenuation within the first 2cm FU- column passage)

2.5.2.3   References

[1] Heberer T. and Adam M. (2005): Occurrence, Fate, and Removal of Pharmaceutical residues in the Aquatic Environment: An Extended Review of Recent Research Data

[2] S. Rögler, K. Prausa, B. Fanck, A. Mechlinski, T. Heberer, Berlin: Untersuchungen zu Vorkommen und Verhalten von Antibiotika- und Arzneimittelrückständen im Berliner Wannsee. GDCh, 71. Jahrestagung 2005, Bad Mergentheim, P61

[3] Wollenhaupt T. diploma thesis (2005): Untersuchung des Abreicherungsverhaltens ausgewählter Antibiotika in Laborsäulenversuchen an kurzen Retentionssäulen

Table 1: TU- columns, experiment A

date	meas. point	Trimethoprim conc. ng/L	Δx ng/L	%	Clindamycin conc. ng/L	Δx ng/L	%	Sulfamethoxazole conc. ng/L	Δx ng/L	%	Dehydroerythromycin conc. ng/L	Δx ng/L	%	Clarithromycin conc. ng/L	Δx ng/L	%	Roxithromycin conc. ng/L	Δx ng/L	%	%int.deviation. Sulfame-thizol	Fenuron-D6	remark
2004	column nr.																					
18.-19.10.	influent (oxic)	51	6	12	167	28	17	351	80	23	155	26	17	163	32	20	127	20	16	3	4	without spiking
11.-12.10.	8	n.n.	-	-	1	0	0	326	53	16	n.n.	-	-	n.n.	-	-	1	0	0	1	0	
14.-15.10.	8	2	0	0	1	0	0	425	108	25	1	0	0	11	1	9	3	0	0	1	2	
11.-12.10.	7	n.n.	-	-	74	16	22	57	8	14	25	1	4	9	1	11	13	1	8	4	1	
12.-13.10.	7	n.n.	-	-	58	7	12	54	6	11	23	3	13	7	1	14	10	1	10	2	2	
14.-15.10.	7	3	0	0	62	13	21	53	9	17	20	1	5	24	2	8	12	1	8	2	1	
11.-12.10.	1	6	0	0	11	2	18	93	14	15	n.n.	-	-	6	1	17	15	1	7	3	0	
12.-13.10.	1	11	1	9	14	2	14	75	8	11	8	1	13	11	2	18	22	2	9	1	1	
14.-15.10.	1	74	4	5	16	3	19	114	20	18	3	0	0	288	33	11	81	7	9	7	2	
11.-12.10.	3	166	10	6	110	9	8	1606	171	11	n.n.	-	-	8	1	13	10	1	10	7	8	
12.-13.10.	3	212	21	10	118	15	13	995	169	17	6	1	17	9	1	11	13	1	8	4	6	
14.-15.10.	3	372	23	6	132	30	23	2228	703	32	7	0	0	180	19	11	30	2	7	4	1	
11.-12.10.	0	380	24	6	258	23	9	3046	371	12	377	35	9	4	1	25	6	0	0	7	3	
14.-15.10.	0	1286	95	7	366	33	9	2634	309	12	651	65	10	2072	361	17	439	39	9	10	9	
18.-19.10	influent(anox)	2	1	50	46	17	37	237	122	51	83	10	12	35	7	20	26	5	19	1	1	without spiking
18.-19.10	influent(anox)	9	2	22	53	19	36	284	162	57	93	11	12	51	10	20	40	7	18	19	2	without spiking
18.-19.10	influent(anox)	9	2	22	55	20	36	322	198	61	101	12	12	52	10	19	45	8	18	7	4	repetiton
05.-06.10.	influent(anox)	2866	267	9	1814	231	13	6527	1037	16	2034	276	14	2116	372	18	1940	239	12	4	2	
11.-12.10.	5	n.n.	-	-	n.n.	-	-	373	49	13	1	1	100	7	1	14	31	3	10	3	0	
12.-13.10.	5	45	4	9	n.n.	-	-	361	47	13	3	1	33	8	1	13	32	3	9	5	1	
14.-15.10.	5	458	37	8	4	1	25	333	42	13	4	1	25	96	12	13	49	5	10	7	1	
11.-12.10.	4	1993	165	8	101	9	9	6328	992	16	77	7	9	23	3	13	239	20	8	4	0	
12.-13.10.	4	1974	163	8	106	9	8	5847	887	15	103	9	9	23	3	13	436	39	9	3	3	
14.-15.10.	4	2131	180	8	123	11	9	6365	1001	16	144	13	9	167	18	11	819	80	10	7	1	
11.-12.10.	6	474	31	7	1115	123	11	2620	348	13	1920	253	13	1096	154	14	1201	128	11	6	4	
					1231	139	11	2105	262	12	1957	260	13	1218	176	14	1466	165	11	13	3	
12.-13.10.	6	822	41	7	1279	146	11	2219	281	13	2170	299	14	1203	174	14	1490	169	11	6	0	repetiton
14.-15.10.	6	939	66	7	1630	201	12	2111	263	12	2019	271	13	1551	243	16	1545	177	11	7	0	

Δ x := statistical deviation maximum

160

Table 2: TU- columns, experiment B, discovered concentrations

date	meas. point	Trimethoprim			Clindamycin			Sulfamethoxazole			Dehydroerythromycin			Clarithromycin			Roxithromycin			%int.deviation		remark
date	point	conc.	$\triangle$x		conc.	$\triangle$x		conc.	$\triangle$x		conc.	$\triangle$x		conc.	$\triangle$x		conc.	$\triangle$x		Sulfame-	Fenuron-	
2004	column nr.	ng/L	ng/L	%	ng/L	ng/L	%	ng/L	ng/L	%	ng/L	ng/L	%	ng/L	ng/L	%	ng/L	ng/L	%	thizol	D6	
07.-08.12.	influent (oxic)	241	33	14	243	43	18	662	109	16	295	57	19	223	47	21	259	45	17	1	2	
19.-20.12.	influent (oxic)	282	39	14	259	47	18	761	131	17	344	69	20	260	57	22	266	47	18	5	3	
13.-16.12.	3	122	34	28	49	15	31	125	28	22	8	2	25	5	2	40	220	81	37	3	2	
16.-19.12	3	129	36	28	45	13	29	113	25	22	4	1	25	6	2	33	272	107	39	4	2	
13.-16.12.	1	1094	572	52	207	78	38	43	14	33	16	4	25	4	1	25	9	2	22	4	2	
13.-16.12.	1	1241	377	30	170	36	21	59	12	20	13	2	15	4	1	25	8	1	13	2	1	RP
16.-19.12	1	1008	162	16	170	24	14	37	5	14	13	2	15	4	1	25	9	1	11	3	0	
16.-19.12	1	1058	297		167	36		36	7		12	2		4	1		10	2		4	3	RP
13.-16.12.	7	n.n.	-	-	64	20	31	48	15	31	18	5	28	5	1	20	6	2	33	3	0	
16.-19.12	7	n.n.	-	-	56	17	30	47	15	32	10	3	30	6	2	33	8	2	25	4	1	
13.-16.12.	8	98	27	28	23	6	26	173	68	39	12	3	25	2	1	50	2	1	50	3	3	
16.-19.12	8	3	1	33	0	-	-	180	72	40	3	1	33	3	1	33	3	1	33	4	2	
13.-16.12.	0	342	49	14	202	35	17	1022	197	19	346	68	20	263	58	22	210	35	17	2	2	
16.-19.12	0	333	47		152	25		894	163		279	52		200	41		191	31		2	1	
07.-08.12.	influent(anox)	264	36	14	228	40	18	839	149	18	292	56	19	193	39	20	235	40	17	1	1	
19.-20.12.	influent(anox)	289	40	14	244	44	18	859	154	18	298	57	19	236	51	22	247	43	17	4	2	
13.-16.12.	5	466	170	36	12	3	25	106	38	36	11	3	27	8	2	25	34	10	29	5	2	
13.-16.12.	5	443	90	20	14	2	14	109	24	22	4	1	25	7	1	14	28	5	18	2	2	RP
16.-19.12	5	468	96	21	13	2	15	84	18	21	5	1	20	9	2	22	38	7	18	7	3	
16.-19.12	5	489	63	13	12	2	17	91	14	15	4	1	25	8	1	13	26	3	12	9	3	RP
13.-16.12.	4	289	27	9	30	3	10	288	39	14	24	3	13	733	154	21	774	125	16	7	0	
16.-19.12	4	220	20	9	25	3	12	308	42	14	16	2	13	800	174	22	749	120	16	4	1	
13.-16.12.	6	278	38	14	460	99	22	307	47	15	425	90	21	716	233	33	612	141	23	5	0	
13.-16.12.	6	294	27	9	472	68	14	353	49	14	431	61	14	572	110	19	602	89	15	2	2	RP
16.-19.12	6	217	19	9	415	58	14	297	40	13	347	47	14	533	100	19	474	66	14	2	1	

Δ x := statistical deviation maximum

Table 4: FU- column, discovered concentrations

date	meas. point	Trimethoprim			Clindamycin			Sulfamethoxazole			Dehydroerythromycin			Clarithromycin			Roxithromycin			%int.deviation.		remark
date	point	conc.	Δx		conc.	Δ x		conc.	Δ x		conc.	Δ x		conc.	Δx		conc.	Δx		Sulfame-	Fenuron-	
2004	column nr.	ng/L	ng/L	%	ng/L	ng/L	%	ng/L	ng/L	%	ng/L	ng/L	%	ng/L	ng/L	%	ng/L	ng/L	%	thizol	D6	
09.-10.11.	influent (oxic)	1955	228	12	1581	271	17	5292	1088	21	1753	323	18	1682	386	23	1358	206	15	0	2	
09.-10.11.	influent (oxic)	1800	204	11	1397	226	16	4433	830	19	1712	310	18	1488	324	22	1260	185	15	1	0	RP
21.-22.11.	influent (oxic)	1183	115	10	862	117	14	2924	453	15	1135	175	15	982	177	18	845	108	13	1	1	
15.-18.11.	1	14	1	7	20	4	20	77	16	21	3	0	0	3	1	33	15	2	13	7	0	
18.-21.11.	1	11	1	9	20	5	25	704	358	51	2	0	0	6	1	17	11	2	18	4	1	
15.-18.11.	3	375	35	9	149	45	30	1381	503	36	6	1	17	2	1	50	128	16	13	2	0	
18.-21.11.	3	310	28	9	132	38	29	327	64	20	9	1	11	8	2	25	134	19	14	5	2	
15.-18.11.	7	n.n.	-	-	65	16	25	70	14	20	16	1	6	8	1	13	16	2	13	6	3	
18.-21.11.	7	n.n.	-	-	56	14	25	69	14	20	14	1	7	7	1	14	n.n.	-	-	3	2	
15.-18.11.	8	n.n.	-	-	2	0	0	213	58	27	8	1	13	n.n.	0	-	5	1	20	1	1	
18.-21.11.	8	2	0	0	1	0	0	203	55	27	1	0	0	1	1	100	n.n.	-	-	3	0	
15.-18.11.	0	476	38	8	326	35	11	1066	123	12	390	46	12	278	38	14	289	30	10	0	1	
18.-21.11.	0	437	34	8	278	30	11	1003	114	11	374	42	11	254	35	14	248	28	11	2	2	
09.-10.11.	influent(anox)	1392	142	10	837	112	13	3562	601	17	1074	162	15	1111	210	19	952	126	13	1	1	
21.-22.11.	influent(anox)	1248	123	10	849	114	13	3109	494	16	963	139	14	872	151	17	842	107	13	0	1	
15.-18.11.	5	650	73	11	23	5	22	193	51	26	5	1	20	12	2	17	35	4	11	1	3	
18.-21.11.	5	680	77	11	23	5	22	195	52	27	8	0	0	16	2	13	30	4	13	1	2	
15.-18.11.	4	641	54	8	67	6	9	2304	327	14	66	8	12	1149	223	19	1048	144	14	3	2	
18.-21.11.	4	927	84	9	113	11	10	2666	399	15	131	13	10	944	171	18	827	109	13	8	2	
15.-1…					…8	109	13	858	106	12	1015	149	15	904	161	18	970	130	13	5	5	
18.-2…					…93	122	14	950	120	13	1028	149	14	832	144	17	750	96	13	3	2	

Δ x := statistical deviation maximum

162

2.6 Overall conclusions

Purified effluents discharged by the municipal STPs were identified as the main sources for the occurrence of antibiotic residues in Berlin's surface waters. These residues discharged into the receiving waters such as the Teltowkanal or the Nordgraben are also reaching areas such as lake Wannsee or lake Tegel which are used as resources for groundwater recharge. Five compounds, the sulfonamide sulfamethoxazole, the sulfonamide synergist trimethoprim, the macrolides clarithromycin and roxithromycin, and the lincosamide clindamycin were detected in surface water from these lakes and in several cases also in the monitoring wells from the transects. Additionally, dehydro-erythromycin, the metabolite of the macrolide erythromycin and acetyl-sulfamethoxazole, the main human metabolite of sulfamethoxazole, were found. Surprisingly, the sulfonamide sulfadimidine was observed at low concentrations in some of the deeper wells. This observation was explained by the use of large quantities of sulfadimidine in the past, when it was used as a growth promotor in livestock farms north of Berlin.

With one exception, antibiotic residues are not found in the water-supply wells. Sulfamethoxazole was the only compound that could be detected at trace-levels in samples collected from monitoring and water-supply wells. Most of the other compounds are readily **attenuated** close to the bank where the surface water is infiltrated. Thus, most of the compounds are not or only found at trace levels in the first two monitoring wells located close to the bank. For sulfamethoxazole and dehydro-erythromycin it was assumed that an improved degradation occurs under reduced conditions, whereas compounds such as clindamycin are preferably degraded under oxic conditions.

The low quantities of sulfamethoxazole that have been detected in the raw water used for drinking water purification are, however, way too low to cause any toxic effects in humans. In general, bank filtration has proven as being an efficient method for the removal of antibiotic residues by **natural attenuation** and as a useful tool for the pre-treatment of surface water under the influence of sewage effluents for drinking-water supply.

2.7 References

1] **Fanck, B.; Heberer, T.:** Multi method for the detection of antibiotic residues in various waters using Solid-Phase Extraction and Liquid Chromatography/Mass Spectrometry. Journal of Separation Science, in prep.

2] **Hirsch, R.; Ternes, T.; Haberer, K.; Kratz, K.-L.:** Occurrence of antibiotics in the aquatic environment. The Science of the Total Environment, 1999, Vol 225, pp 109-118

3] **Christian, T.; Schneider, R.J.; Färber, H.A.; Skutlarek,D.; Meyer, M.T.; Goldbach, H.E.:** Determination of Antibiotic Residues in Manure, Soil, and Surface Waters. Acta hydrochim hydrobiol, 2003, Vol 31, pp 36-44

4] **Lindsey, M.E.; Meyer, M.; Thurman, E.M.:** Analysis of Trace Levels of Sulfonamide and Tetracycline Antimicrobials in Groundwater and Surface Water Using Solid-Phase Extraction and Liquid Chromatography/Mass Spectrometry. Analytical Chemistry, 2001, Vol 73, Iss 1, pp 4640-4646

5] **Kolpin, D.W.; Furlong, E.T.; Meyer, M.T.; Thurman; E.M.; Zaugg, S.D.; Barber, L.B.; Buxton, H.T.:** Pharmaceuticals, Hormones, and Other Organic Wastewater Contaminates in U.S. Streams, 1999-2000: A National Reconnaissance. Environmental Science & Technology, 2002, Vol 36, Iss 6, pp 1202-1211

6] **Tolls, J.:** Sorption of Veterinary Pharmaceuticals in Soils: A Review. Environmental Science & Technology, 2001, Vol 35, Iss 17, pp 3397-3406

7] **Sacher, F.; Lange, F.T.; Brauch, H.-J.; Blankenhorn, I.:** Pharmaceuticals in groundwaters- Analytical methods and results of a monitoring program in Baden-Württemberg, Germany. Journal of Chromatography A, 2001, Vol 938, Iss 1, pp 199-210

8] **Hirsch, R.; Ternes, T.; Haberer, K.; Mehlich, A.; Ballwanz, F.; Kratz, K.-L.:** Determination of antibiotics in different water compartments via liquid chromatography- electrospray tandem mass spectrometry. Journal of Chromatography A, 1998, Vol 815, Iss 2, pp 213-223

9] **Golet, E.M.; Strehler, A.; Alder, A.C.; Giger, W.:** Determination of Fluoroquinolone Antibacterial Agents in Sewage Sludge and Sludge-Treated Soil Using Accelerated Solvent Extraction Followed by Solid-Phase Extraction Analytical Chemistry, 2002, Vol 74, Iss 21, pp 5455-5462

10] **Giger, W.; Alder, A.C.; Golet, E.M.; Kohler, H.-P.E.; McArdell, C.S.; Molnar, E.; Siegrist, H.; Suter, M.J.-F.:** Occurrence and Fate of Antibiotics as Trace Contaminants in Wastewaters, Sewage Sludges, and Surface Waters. Chimia, 2003, Vol 57, Iss 9, pp 485-491

11] **Lindberg, R.H.; Wennberg, P.; Johansson, M.I.; Tysklind, M.; Andersson, B.A.V.:** Screening of Human Antibiotic Substances and Determination of Weekly Mass Flows in Five Sewage Treatment Plants in Sweden. Environmental Science & Technology, 2005, Vol 39, Iss 10, pp 3421-3429

12] **Al-Almad, A., Daschner, F.D.; Kümmerer, K.:** Biodegradability of Cefotiam, Ciprofloxacin, Meropenem, Penicillin G, and Sulfamethoxazole and Inhibition of Wastewater Bacteria. Archives of Environmental Contamination and Toxicology, 1999, Vol 37, pp 158-163

13] **Schmidt, C.K.; Lange, F.T.; Brauch, H.-J.:** Assessing the impact of different redox conditions and residence times on the fate of organic micropollutants during riverbank filtration. Proceedings "4th International Conference on Pharmaceuticals and Endocrine Disrupting Chemicals in Water", 13.-15.10.2004, Minneapolis, Minnesota

14] **Hartig, C.**: Analytik, Vorkommen und Verhalten aromatischer Sulfonamide in der aquatischen Umwelt. PhD work TU Berlin, 2000

15] **HSDB Database** (http://toxnet.nlm.nih.gov/cgi-bin/sis/htmlgen?HSDB) 2004

4

Organic Substances in Bank filtration and Groundwater Recharge-
Process Studies

"organics" group: Technische Universität Berlin

Responsible project leader: Prof. Dr. Martin Jekel

Contents

I List of Abbreviations

AOBr	Adsorbable Organic Bromine
AOC	Assimilable organic carbon
AOI	Adsorbable Organic Iodine
AOX	Adsorbable Organic Halogens
BDOC	Biodegradable dissolved organic carbon
BTS	Benzene- and Toluene sulfonamides
COD	Chemical oxygen demand
D	Dalton
d	Dispersion [m^2/d]
DC	Direct Current
DOC	Dissolved Organic Carbon
DWQC	Department of Water Quality Control
ELGA	Ultra Pure Deionized Water
FIA	Flow injection analysis
FLD	Fluorescence detection
HPLC	High Pressure (Performance) Liquid Chromatography
IC	Ion chromatography
LC-OCD	Liquid Chromatography – Organic Carbon Detection
LOD	Limit of detection
LOQ	Limit of quantification
MS	Mass spectroscopy, Mass spectrometer
MON	Mean Oxidation Number
NASRI	Natural and Artificial Systems for Recharge and Infiltration
NBDOC	Non-biodegradable DOC
NDSA	Naphthalenedisulfonic Acid
NSA	Naphthalenesulfonic Acid
OC	Organic Carbon
POC	Particulate Organic Carbon
POP	Persistent Organic Pollutants
R	Factor of retardation
SPE	Solid Phase Extraction
TIC	Total Inorganic Carbon
TOC	Total Organic Carbon
TrBA	Tributylamine
UPW	Ultra Pure Water
UVA	UV-Absorption (254 nm)

II   List of Figures

III   List of Tables

1 Results

1.1 Lake Tegel bank filtration site

The monitoring of the bank filtration field site Berlin-Tegel by the „Organics"-subproject within NASRI started in May 2002. Previous research projects of the Department for Water Quality Control (DWQS) conducted research at this transect and several uncontinuous datasets are available. The monitoring of abstraction and monitoring wells ended in August 2004, but the sampling of surface water was continued until June 2005.

The monthly analytical program for all samples was comprised of DOC, UVA_{254}, UVA_{436}, LC-OCD, and differentiated AOX (adsorbable organic halogens e.g. AOI, AOBr)-analysis. Additionally, trace organic compounds were analyzed for a time period of 16 months. Trace compound analysis focused on three groups of target compounds. These groups were X-ray contrast media (Iopromide); bacteriostatica (Sulfamethoxazole), and Naphthalenedisulfonates (1,5-NDSA; 1,7-NDSA; 2,7-NDSA). Results of the field monitoring are reported in the following chapters.

1.1.1 Lake Tegel - Results bulk organics

1.1.1.1 Surface water Lake Tegel

In Lake Tegel the amount and character of bulk organics were characterized by measurements of dissolved organic carbon (DOC), UV-absorption at 254 nm, and color at 436 nm. The SUVA, a measure of aromaticity of the water, was calculated as a quotient of UVA_{254} and DOC. Table 1 provides the arithmetic mean, median and standard deviation of 36 monthly measurements.

Over these three years of monitoring, the DOC-concentration in Lake Tegel remained in a range between 6.5 mg/l and 8 mg/l. A variation between winter and summer of 0.5-1 mg/l was observed. Slightly higher DOC concentrations were found in the summer months March to September. Figure 1 confirms these results. A comparison of the recent concentrations with data obtained from 06/1998 – 06/2000 (Ziegler; 2001) shows that the DOC-level in Lake Tegel decreased by 1-1.5 mg/l. Ziegler (2001) reported a median DOC-concentration of 8.6 mg/l.

Table 1 Results bulk organic parameters in surface water Tegel 2002-2005 (n=36)

	DOC	UVA$_{254}$	UVA$_{436}$	SUVA
	[mg/l]	[1/m]	[1/m]	[l/m*mg]
Arithmetic mean	7.17	15.08	0.52	2.11
Median	7.10	15.02	0.48	2.09
Standard deviation	0.48	1.11	0.11	0.17
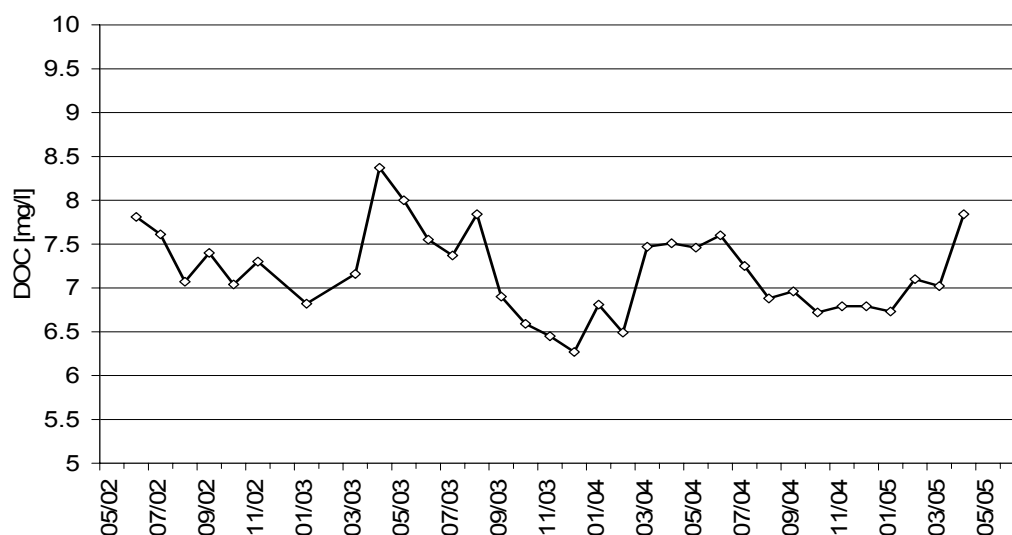
Figure 1 Time series of DOC concentration in Lake Tegel

UVA$_{254}$ of the surface water was measured between 13 and 17 m^{-1}. A clear seasonal variation was revealed (Figure 2), which did not correspond with changes in DOC concentration. Generally, higher UVA$_{254}$ were found in winter months November to May. This variation is a stable long term effect since it was already observed in the years 1998-2000 by Ziegler (2001).

The calculated SUVA ranged between 1.7 to 2.4 l/m*mg. Changes in aromaticity (SUVA) of the surface water resulted from the described changes of DOC and UVA$_{254}$. The share of aromatic structures on total DOC (expressed by SUVA) was high in periods of low DOC and high UVA$_{254}$ (e.g. winter). With beginning of spring rising DOC concentrations generated a decrease of SUVA. It can be concluded that additional DOC during summer is mostly of aliphatic nature.

The UV absorption at 436 nm of water from Lake Tegel was relatively stable during the observation period at 0.5 m^{-1}. The water was not visibly colored and no seasonal or other changes were observed.
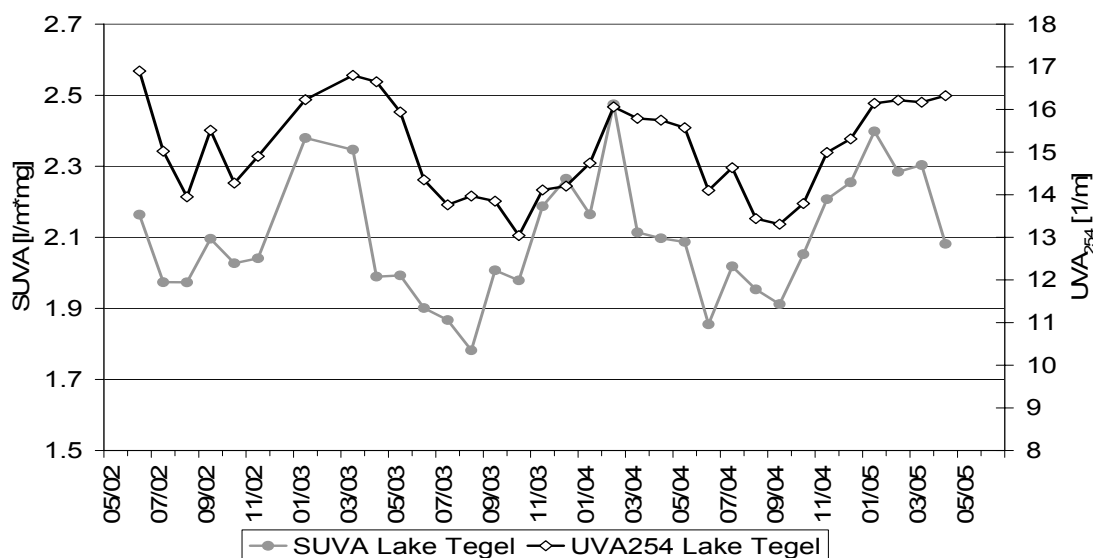
Figure 2 UVA$_{254}$ and SUVA of Lake Tegel surface water

In three years of monitoring different potential factors of influence for bulk organic concentration and character in Lake Tegel were revealed.

- algae blooms in spring and summer
- seasonal variation of the discharge of the Lake Pipeline (water from upper Havel)
- changes in the discharge of sewage treatment plant (STP) Schoenerlinde
- seasonal differences in natural precipitation

The observed seasonal variations of bulk organic parameters in the lake are the sum of these different influences. By comparison of time frames a weighting of importance of the factors for the observed changes was possible.

- Algae blooms can occur in Lake Tegel between March and October because of preferential light and temperature conditions.
- The proportion of water from upper Havel, which is pumped through the lake pipeline, treated in the surface water treatment plant (OWA) and then discharged into the lake, varies highly with the seasons. During winter less than 10% of the total discharge of the OWA originates from the Havel-River. Between May and October the proportion rises to more than 60% (Figure 3).
- Natural precipitation might also affect the DOC concentration in Lake Tegel. A lack of precipitation could result in a reduced dilution of the effluents of the sewage treatment plant Schoenerlinde which discharges over the Nordgraben and the OWA into Lake Tegel. The sum of monthly precipitation since 2002 is presented in Figure 4.

- The discharge of the waste water treatment plant Schoenerlinde increased during the observation period. But the singular event did not significantly affect the character of the surface water DOC in Lake Tegel. Commonly, the effluent quality (regarding bulk organics) and quantity of STP`s are relatively constant over the seasons. Therefore, it is unlikely that seasonal variations in Lake Tegel originate from the STP Schoenerlinde.
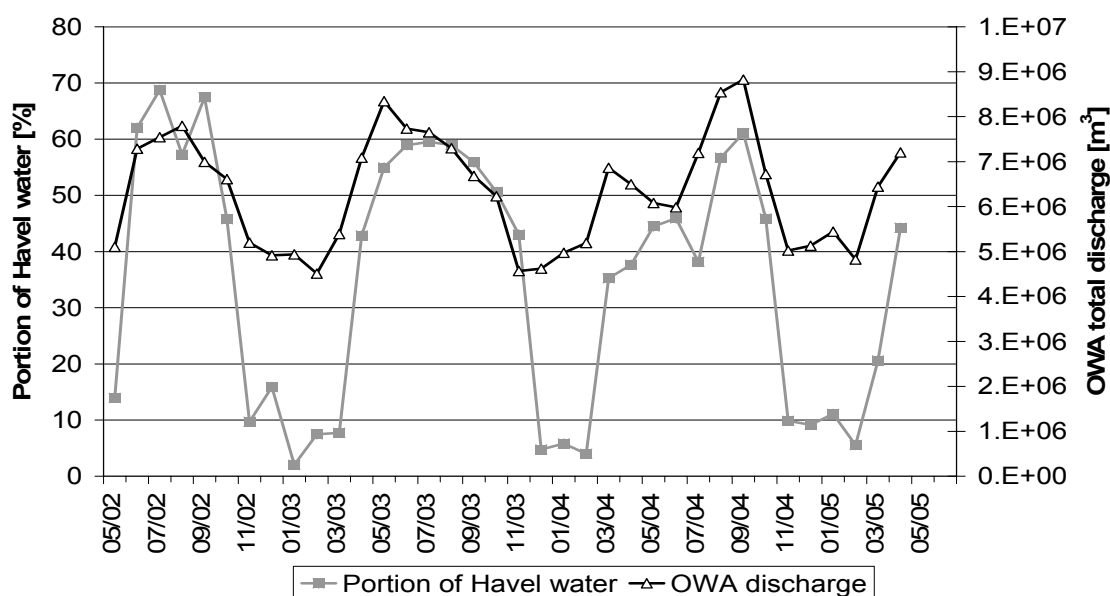
Figure 3 Total discharge into Lake Tegel and the portion of water from the Havel (lake pipeline)
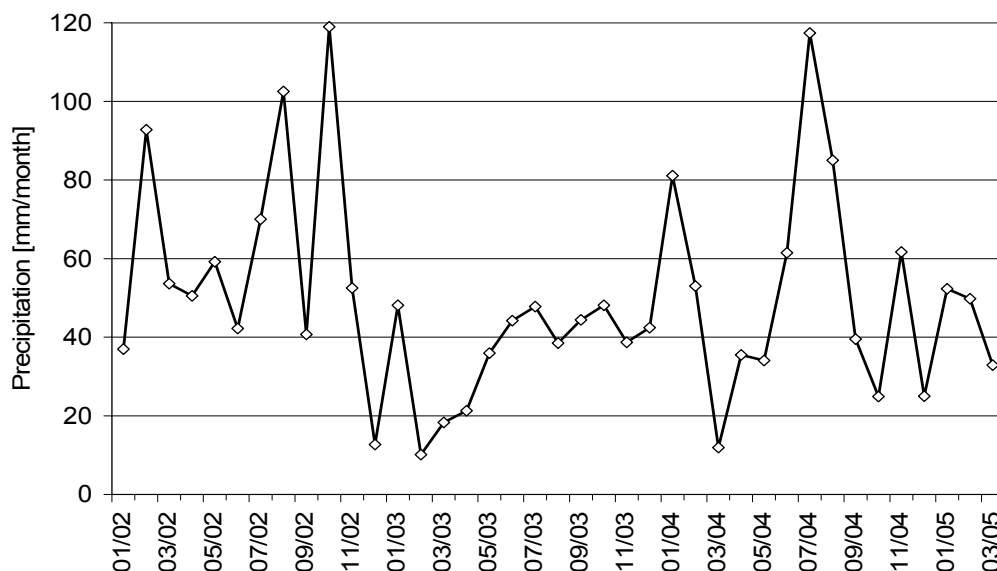
Figure 4 Natural precipitation in the area of Lake Tegel (data from BWB, WW Tegel)

An evaluation of the four different factors of influence was conducted by taking into account all available data. It was found, that seasonal variation of DOC in Lake Tegel

seems to originate mostly from annual algae blooms. The time frame of elevated DOC concentration fits to the observed time for algae blooms. Furthermore, the additional DOC was found to be of aliphatic nature (SUVA results) what is characteristic for algae associated DOC.

The reversed seasonal variation of UVA_{254} in Lake Tegel can be explained by changing dilution of the effluent of the treatment plant Schoenerlinde by water from the upper Havel. Highest UVA_{254} results are observed in time periods of very few dilution of the treated effluent in winter. A minimal time shift between the peaks can be explained by the retention time of the lake. The transect is located approximately 2 km south of the point where the OWA effluent enters the lake.

Distribution of natural precipitation in the observation period is very irregular (Figure 4). Strong differences in total precipitation (2002: 733 mm; 2003: 438 mm; 2004: 630 mm) and distribution of the annual precipitation were recorded in the three years of the observation period for the region of Berlin. Therefore, it is unlikely, that any regular changes of bulk organic parameters in the lake originate primarily from changes in dilution by precipitation. But heavy or missing precipitation can be an additional effect which adds to other factors of influence. For instance, the highest DOC concentration in the lake (04/04: 8.4 mg/l) was measured after three subsequent months of very few precipitation.

However, concentration and character of bulk organics in Lake Tegel is relatively stable with some seasonal variations, which are mainly due to algae blooms and changing operation of the lake pipeline. Natural precipitation and the effluent of sewage treatment plants are only of minor importance.

Furthermore, the seasonal change in character of DOC can be accessed by LC-OCD. Chapter 1.1.2 provides more information on general composition of the DOC and changes during the observation period.

1.1.1.2 Bank filtration-DOC

The fate of bulk organics during infiltration was monitored for 2¼ years with a monthly sampling of monitoring wells which were located along the infiltration path of the surface water. The change in concentration and character of bulk organics during infiltration depended on various factors, like retention time, redox conditions, soil properties, and hydrogeological conditions. The minor seasonal changes that were described for the surface water could not be found in the time series of the monitoring wells, since they were superposed by an effective mineralization of organic material.

Results are presented in form of time series and box plots (Figure 5, Figure 6). Box plots are defined by the median (horizontal centre line), the 25%- and 75%-quartiles (box), and the minimum and maximum values (vertical lines). Extreme values and outliers are shown but not considered for quartile calculation. Removal rates are calculated from the medians, because for some wells the data pool is relatively small

and the median is a more stable indication in the case of small data sets (Zöfel, 2002). The results are actual measured concentrations and were not adjusted for potential dilution.

Data illustration was simplified by a separation of the infiltration process in two stages. The more shallow monitoring wells located close to the bank area in the top aquifer represent mostly short term infiltration (retention time <3 months) under oxic conditions. Monitoring wells in the second aquifer have longer retention times and showed for most of the observation period anoxic and anaerobic redox conditions. However, the two groups are regarded as two different flow paths but have to be considered as two subsequent stages. Most of the lake water is initially infiltrating under oxic conditions at the water/sediment interface. The major flow path runs through 3310, 371OP, 371UP, 3302 towards 3303, and the production well 13. During infiltration oxygen is used up quickly because of mineralization of DOC and sedimentary bound particulate organic carbon (POC) (~0.5 % w/w) and most of the 4-5 months long infiltration (100 m) to the production well is usually taking place under anoxic and anaerobic conditions (iron and manganese reduction). The extension and position of the redox zones varies seasonally and is horizontally stratified. For a more detailed description of the hydrogeological setup of the field site read chapter X (hydrogeological group).

An evaluation of the data pool 2002-2004 showed that the DOC concentration of the lake water is reduced considerably along the transect to a residual of around 4.7 mg/l, based on the last monitoring well (3303) in front of the production well 13. It was found that the initial infiltration under oxic conditions is very important for an efficient DOC removal. Figure 5 shows that a DOC removal of 25-30 % can be achieved under oxic conditions with retention times of some days or a few weeks. During summer the shallow monitoring wells (3310, 3311) could not be sampled because of lower surface water level, but the recorded data exhibit some indications that the efficiency of DOC degradation during initial oxic infiltration is temperature dependent. Higher DOC concentrations during colder months were found in monitoring well 3311, 3310 and 3308.

The low DOC levels in 372 might be explained by longer retention time under permanently oxic conditions. In the upper aquifer oxygen is continuously introduced into the ground water by variations of the water level, which is caused by the pumping schedule of BWB.
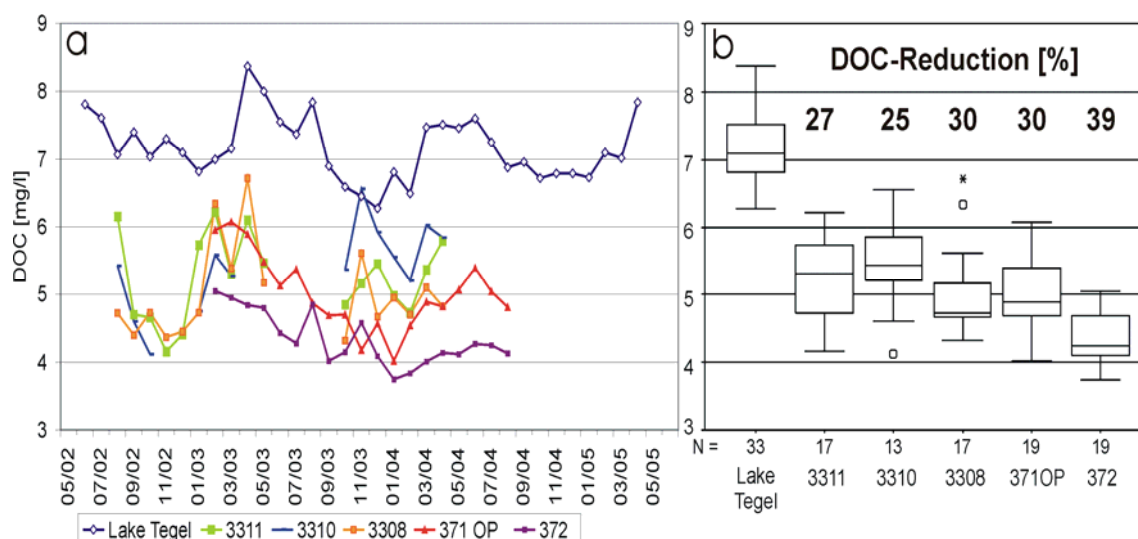
Figure 5a/b Fate of DOC during infiltration to the shallow monitoring wells (a: time series; b: box plots)

Bank filtrate in the second aquifer originates mainly from surface water that infiltrated under oxic conditions from the lake through the first aquifer. Besides by infiltration through the upper aquifer, minor portions of bank filtrate of different ages enter the transect from under the lake. Water composition of this fraction is not exactly clear, since no monitoring well is located under the lake. Without much doubt monitoring well 374 (only sampled eight times towards the end of the project) contains water that is representative for this fraction. The DOC of 374 was 4.6 mg/l (δ=0.3 mg/l). The results for 374 show that the water composition is similar to the actual young bank filtrate, but because of the higher age it does not directly depend on surface water quality. It is believed that the water in 374 represents a very old bank filtrate (~25 years).

Furthermore, a hydraulic model of the "Model" group (see Chapter IGB) proposed that the influence of the older bank filtrate changed during the observation period. Therefore, it is difficult to access initial parameters for the infiltration path in the second aquifer. To provide results, the bulk organic data evaluation of the "Organic" group uses surface water concentration as reference instead, because for most monitoring wells the majority of water is young bank filtrate (retention time < 4.5 months) and the influence of older water is negligible. However, in some datasets slightly different characteristics of the samples, predominantly from 3301, are visible.

Reduction of DOC concentration during infiltration in the second aquifer is displayed in Figure 6. The average DOC mineralization ranges from 30-35% and is increasing with higher retention times. As mentioned, monitoring well 3301 is somehow influenced by older bank filtrate from under the lake and exhibits slightly elevated DOC levels. Presumably, well 3301 receives also portions of young bank filtrate that infiltrated with a short oxic zone under mostly anaerobic conditions. A slower DOC removal under anaerobic conditions explains higher average DOC concentration in well 3301.

Monitoring well 371UP, 3302 and 3303 are dominated by water infiltrating through the top aquifer with retention times of 2.8 to 4 months. During this time 32-34% of the initial surface water DOC is degraded. Water from production well 13 is a mixture of infiltrated water of different age and approximately 25-30% of background groundwater. The background well 3304 shows a relatively low DOC of 2-3 mg/l and dilution reduces the DOC concentration of the abstracted raw water to ~4 mg/l.
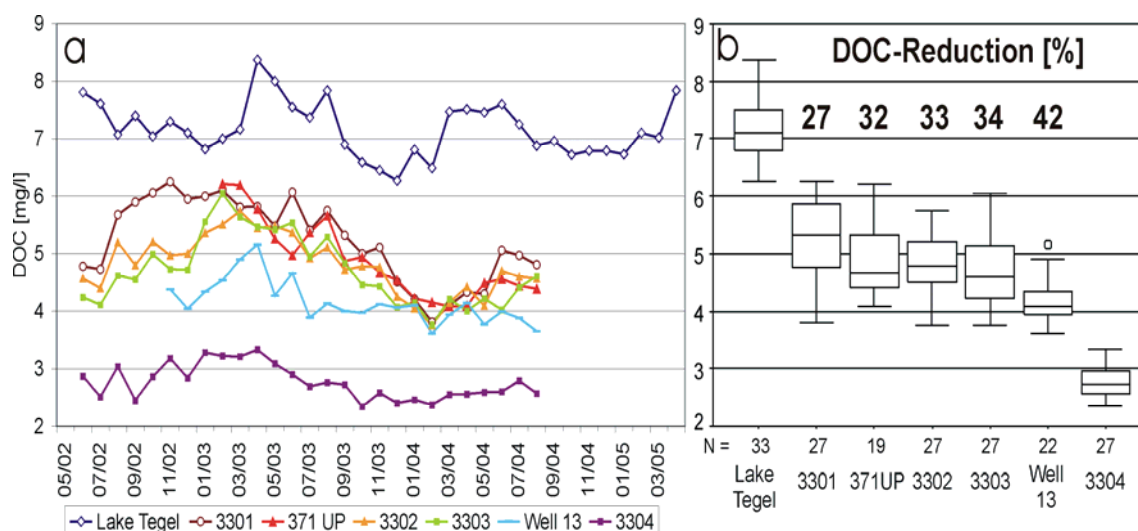
Figure 6a/b Fate of DOC during infiltration to the deep monitoring wells (a: time series; b: box plots)

However, DOC concentrations in the deep monitoring wells showed heavy variations over the observation period (more than 2 mg/l fluctuation). The changing DOC concentrations can not be ascribed to different DOC levels in the surface water. A factor of influence for DOC removal which was confirmed in pilot scale experiments are the dominant redox conditions. It is assumed that the variation in DOC levels in the second aquifer is motivated by changing redox conditions.

During the first sixteen months (05/02 – 09/03) of the observation period the redox conditions in the deeper aquifer were strongly anaerobic with occurring iron and manganese reduction. Nitrate levels were significantly reduced during infiltration (Average NO_3-N: 3302: 0.07 mg/l and 3303: <LOQ). The average nitrate concentration in the surface water was 1.83 mg/l NO_3-N. After summer 2003 the redox status of the transect changed. Summer 2003 was very dry in Berlin and the combination of low water level in Lake Tegel and heavy pumping of the production well pumps led to an expanded zone of unsaturated infiltration under the lake. After passaging the biologically very active water-sediment interface the bank filtrate was aerated again during an unsaturated infiltration. Beginning in October 2003 until June 2004, elevated oxygen and nitrate concentrations were observed in the deeper monitoring wells and the production well ($\varnothing$-NO_3-N: 3302: 1.16 mg/l and 3303: 0.47 mg/l). During these nine

months the dominant redox conditions at the field site changed from anoxic/anaerobic with Fe/Mn-reduction to oxic. The time series of Figure 6 gives insight to the effect of changed redox conditions. The differences in fate of bulk organics between the two redox conditions are discussed below.

Comparing mineralization of DOC during the oxic and anoxic/anaerobic infiltration period reveals that under both conditions similarly ~3.0 mg/l DOC were removed between surface water and production well. Dilution in the production well is assumed to be constant (~30% background groundwater) and the background monitoring well 3304 shows low DOC-

concentrations during the entire observation period (oxic: 2.5 mg/l; anoxic/anaerobic: 2.9 mg/l). Figure 7 proves that the degradation kinetics of DOC, which can be assessed by the monitoring wells between surface water and production well, is different under oxic or anoxic/anaerobic conditions. A more rapid removal of DOC under oxic conditions was observed, whereas anoxic/anaerobic conditions cause a slower but continuing removal. Under oxic conditions, 35% of DOC is degraded from surface water to the first deep monitoring well 3301.

Figure 7 Fate of DOC during infiltration under different redox conditions

During further infiltration the fraction of degraded DOC is increasing by only 5 % (3303) or 8% (Well 13, includes some dilution). Under anoxic/anaerobic conditions only 24% of the initial DOC is degraded in monitoring well 3301. The continuing removal of DOC leads to reduction rates of 32% (3303) and 41% in the production well (Figure 7). In the extracted raw water, the residual DOC-concentrations are comparable.

However, under anoxic/anaerobic conditions the slower process of DOC-mineralization demands the entire retention time, whereas under oxic conditions the efficient removal during initial infiltration is followed by a plateauing of DOC levels and a slower removal. Under both conditions, a similar residual DOC concentration can be achieved, if sufficient retention time is allowed under anoxic/anaerobic conditions. Results demonstrate that regardless of dominant redox state a fraction of 4-4.5 mg/l of residual DOC is not degradable under Lake Tegel field conditions. This is consistent with DOC concentration of the very old bank filtrate in 374.

Based on all results, it is assumed that (sustainable) biodegradation controls the DOC removal and that (non-sustainable) adsorption of DOC to the sediment is minimal.

Evidence is given by the consistency of DOC removal for ~100 years of operation and the higher SUVA of the infiltrated water (see chapter 1.1.1.4). Additionally, Davis (1982) found that DOC is not adsorbed to quartz at neutral pH.

The biological stability of the residual DOC of 4-4.5 mg/l shows that the portion of BDOC in this residual is very small. This is advantageous for the drinking water supply. Despite of the relative high DOC concentration, the organic carbon is not available for biological growth in the public water supply. Furthermore, the results underline the necessity to control and monitor the system of bank filtration regularly, to avoid drastic changes in the subsoil conditions that affect DOC-removal efficiency.

1.1.1.3 Bank filtration-UVA$_{254}$

UV absorption at 254 nm decreases during infiltration along the transect because aromatic and double-bonded organic structures are degraded. Removal rates are slightly lower but comparable to DOC removal rates (Figure 8). In the shallow monitoring wells the UVA$_{254}$ reaches to 60-80% of the surface water. Monitoring well 3310 exhibits a considerably higher UVA$_{254}$ than well 3311, showing a stronger influence of surface water. The very low UVA$_{254}$ of 372 is consistent with low DOC concentrations of this well, which are assumed to be caused by long retention time for this well (Figure 8a).

The UVA$_{254}$ in the deeper wells is in a similar range. The mentioned change in redox conditions also affected the UVA$_{254}$-results. During the oxic period the UV-absorption was slightly lower. But for some wells this effect was superposed by a strong fluctuation of UVA$_{254}$. Particularly, well 3301 and 371UP showed strong seasonal variations of UV-absorption. From summer to late fall, a higher UVA$_{254}$ was measured than during the rest of the year. Contrary to Ziegler (2001), who hypothesized the variations as a time shifted response to the seasonal UVA-changes in the surface water, it is now believed that two different effects might be responsible for the variations.

First, monitoring well 374 (UVA$_{254}$=12.9 1/m; δ=0.3 1/m) proves that older bank filtrate from under the lake has a higher average UVA$_{254}$ than young bank filtrate. Due to heavier pumping of the abstraction well during summer the influence of older bank filtrate on the wells 3301 and 371 UP might be increased, leading to higher UV-absorptions in these samples during summer.

Secondly, due to higher water temperature during summer and fall, the transformation of particulate organic matter (POC) from sediment and the release of fractions of humic like material from the POC could be elevated. Or parts of the minimal fraction of hydrophobic DOC that adsorbed during infiltration to the sediments are released because of the smaller adsorption capacity of the sediments at higher temperatures. However, the small amounts are not detected by DOC-analysis but by UVA, because of the high UV activity of the released material. Schoenheinz et al. 2004 showed on

examples from the Elbe river that during periods of elevated water temperatures sediments can release DOC fractions.
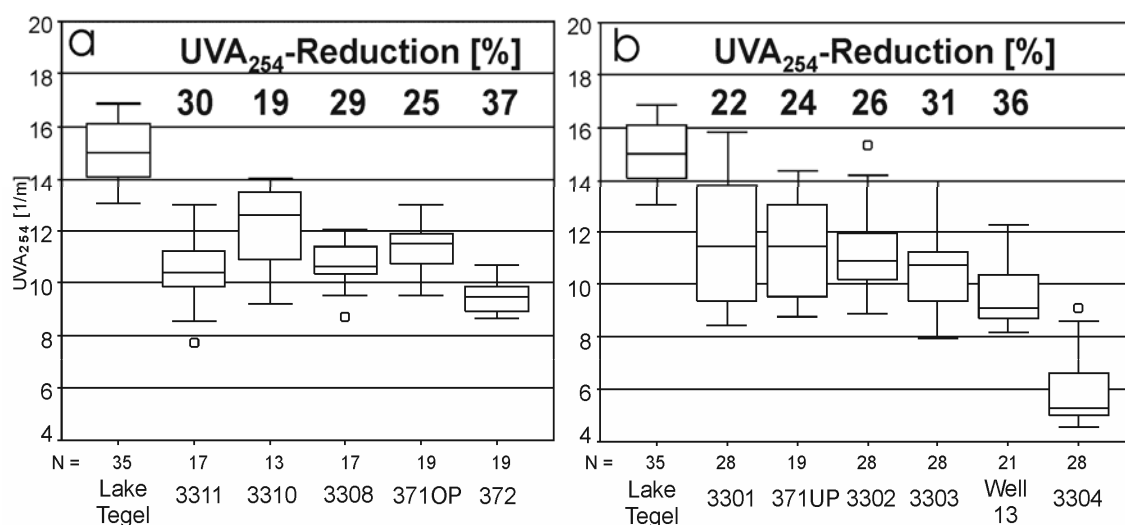
Figure 8 Change of UVA$_{254}$ during infiltration to the monitoring wells (a: shallow wells; b: deep wells)

It remains unclear which effect is responsible for the seasonal variations of UV$_{254}$ in the deeper monitoring wells, but because of results of the hydrogeology group the second explanation seems more likely. The hydrogeology group found out that the influence of older bank filtrate on the deep monitoring wells to be relatively small. The assumption of Ziegler (2002) that seasonal fluctuations in the second aquifer are shifted responses of the surface water quality is unlikely, because the time shift is 8 months (too long) and the variation in the deeper monitoring wells have higher amplitudes than the surface water variations. Therefore, it is assumed that the seasonal change in UVA in the deep wells is caused by temperature effects. Figure 8b displays the heavy variations and the relative low UVA$_{254}$ reduction in 3301 and 371UP. The background groundwater has, consistently with DOC-results, a lower UVA$_{254}$, leading to some dilution effects in the production well.

The color measured at 436 nm decreased during infiltration from 0.5 1/m (surface water) to average values of 0.3-0.4 1/m in the individual monitoring wells. No seasonal changes or effects were observed.

1.1.1.4 Bank filtration-SUVA

DOC-results and UVA$_{254}$-measurements can be used to calculate the specific UV-absorbance (SUVA), which reveals more details about the mechanisms of DOC-mineralization because a change in SUVA during treatment or infiltration indicates a preferred removal of aliphatic (SUVA-increase) or aromatic (SUVA-decrease) carbon sources.

SUVA of surface water in Lake Tegel is around 2.1 l/m*mg. During infiltration at the bank filtration site an averaged increase of 5-10% was observed in the shallow monitoring wells. Unfortunately, the shallow monitoring wells fell dry during summer so that recorded SUVA results were mostly measured during winter. The results are often unstable and show high standard deviations. However, existing results indicate that during short aerobic soil passage aliphatic carbon sources are preferentially used. As an exception, well 3311 showed a slightly lower SUVA than the surface water. Monitoring well 3311 is located close to the lake but shows the lowest nitrate levels of all shallow wells. Potentially, more aromatic and double-bond structures are degraded during a partly anoxic infiltration to well 3311. The seasonal variation of SUVA which was reported for the surface water could not be found in the shallow monitoring wells.

The deep monitoring wells also exhibited an increase in SUVA (5-10%) (Figure 9). Very clearly, a seasonal variation of SUVA was found. But the variation did not originate from the time shifted variation in the surface water because in the lake the highest SUVA results were measured during January-March, whereas in the deep wells SUVA peaked during August-December. This time shift of 8 months can not be explained by 3-5 months retention time.

In fact, since SUVA is calculated from UVA_{254} (and DOC) the seasonal variation of SUVA in the deep wells most likely derives from the same effect that is responsible for the variation of the UVA_{254}. Similarly to the discussion of UVA_{254} for 3301 and 371UP, the deep monitoring wells could be influenced by small portions of organic material with a high aromaticity which were released from the sediments because of the higher temperature of the infiltrating water. This would explain the observed effects in SUVA. The assumption that heavier pumping during summer increased the influence of older bank filtrate from under the lake in the deep wells is unlikely for the already mentioned reasons (Chapter 1.1.1.3). However, SUVA of the older bank filtrate was found to be 25% higher than the actual SUVA of the surface water (374: SUVA=2.6 l/m*mg; δ=0.1 l/m*mg).

Because of these uncertainties it is difficult to discuss the SUVA results in the deep aquifer. But in column experiments (see soil column chapter1.4) it was found that the SUVA decreases during longer anoxic/anaerobic infiltration pointing towards a better removal of aromatic compounds under low redox conditions.
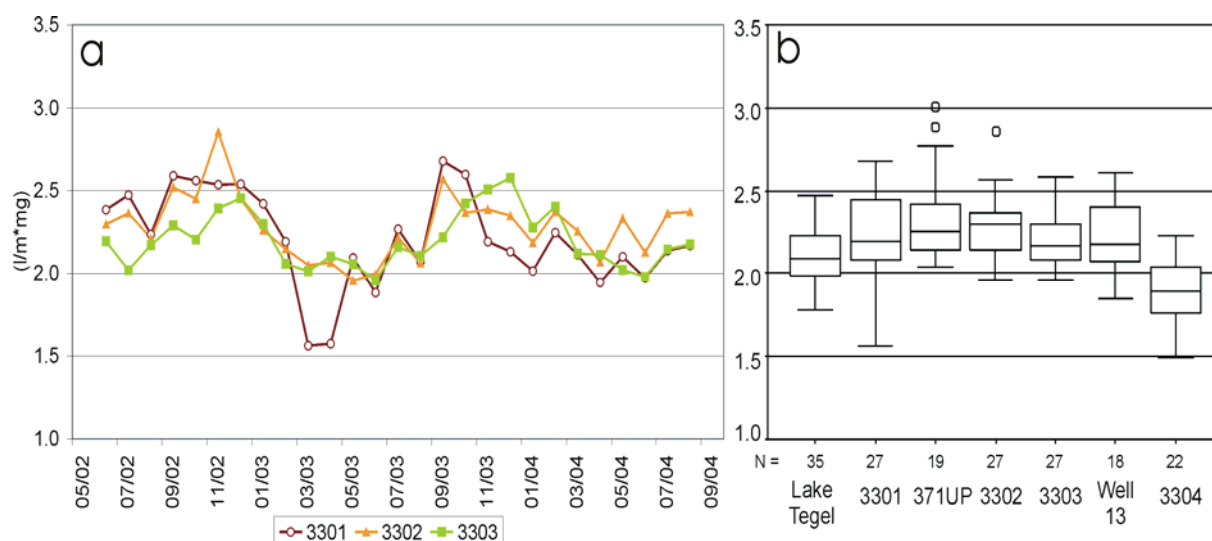
Figure 9 Fate of SUVA during infiltration to the deep monitoring wells (a: time series; b: box plots)

The SUVA of the extracted raw water from well 13 (median: 2.2 l/m*mg) is similar to the surface water. In background groundwater, SUVA was calculated to be 1.9 l/m*mg. Results also indicate that permanent adsorption of DOC onto clay or particulate organic matter in the sediment is not important. In such a case, lower SUVA results could be expected because aromatic organic compounds tend to be more hydrophobic and prone to adsorption. Therefore, it is not likely that permanent adsorption of DOC to the subsoil occurs.

However, results also show that aliphatic carbon sources are preferentially used during initial aerobic soil passage. Aliphatic compounds are rapidly degraded under oxic conditions. Furthermore, some results point towards a better mineralization of aromatics under anaerobic conditions.

LC-OCD measurements revealed that the changes in SUVA result from the fast removal of the PS-fraction and from a change of aromaticity in the HS-fraction (see soil column chapter1.4). In the online measurement the HS-fraction showed major changes in SUVA, while HS-building blocks and LMA were constant. It is assumed that in the HS-fraction aliphatic side-chains are mineralized quickly, but aromatic and double-bond structures remain for a longer period unchanged. During further infiltration more aromatic structures in the HS-fraction are degraded and the SUVA decreases. In anoxic infiltration, the increase in SUVA is slower. LC-OCD measurements proved that under anoxic conditions the slower removal of PS is responsible for the slower rise of SUVA. In the HS-fraction no initial preferential removal of aliphatic-side chains was observed and the SUVA remained stable during the first 1.6 m of infiltration. Afterwards, the mineralization of aromatics from the HS-fraction leads to a decreasing SUVA.

Generally, it can be summarized that under oxic conditions the degradation of DOC follows more strictly a sequence, where aliphatic compounds are initially degraded and

subsequently aromatics. Under anoxic/anaerobic conditions the fate of aromatics and aliphatics seems to be more balanced.

1.1.2 Lake Tegel - LC-OCD

1.1.2.1 Surface water-LC-OCD

Surface water of Lake Tegel was also analyzed regarding the character of dissolved organic carbon using the technique of liquid chromatography with online carbon detection (LC-OCD), also known as SEC-OC (size exclusion chromatography). This analysis allows differentiating between different fractions of DOC, which are mostly defined by size and hydrophobicity. More detailed information on LC-OCD analysis and on interpretation of the obtained chromatograms are included in the methodology section.

Chromatograms (e.g. Figure 10) are interpreted as follows: The first peak in the chromatogram corresponds to the largest molecular weight fraction, interpreted as polysaccharides (PS; elution time at 35-45 min), the second peak corresponds to humic substances (HS; elution time 52 min) and HS-building blocks (secondary peak; 57 min), and the third to low molecular weight acids (LMA; 62 min). Neutrals and hydrophobic compounds elute after 65 minutes.

Figure 10 displays a characteristic chromatogram of Lake Tegel surface water. Over the time of the project more than 20 monthly measurements of Tegel surface water were conducted. After exclusion of failed and unreliable analysis 16 high quality measurements were selected. To avoid a presentation of all chromatograms, the obtained data was adjusted for retention time and baseline and afterwards mediated.
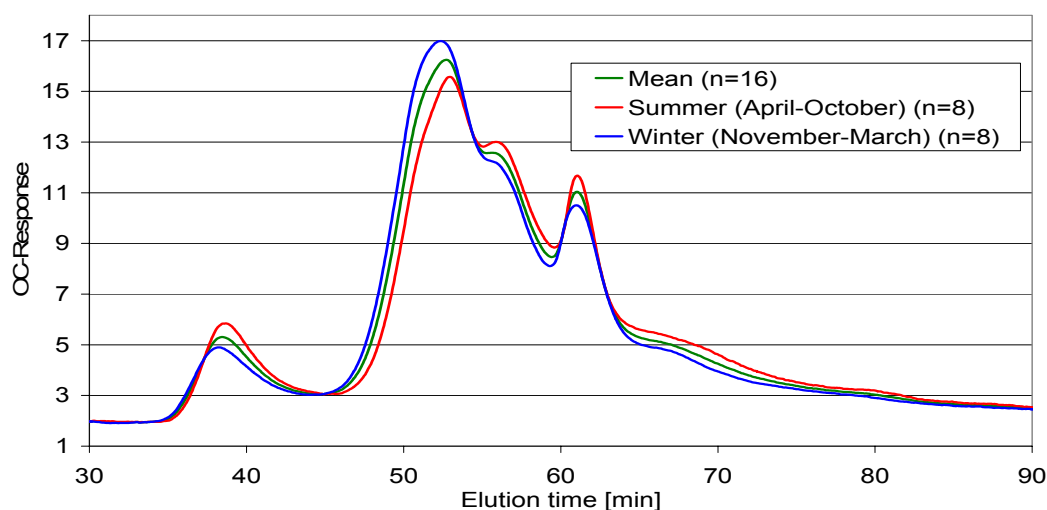
Figure 10 LC-OCD chromatogram of Lake Tegel surface water (seasonal changes)

The mean chromatogram in Figure 10 is the result of pooling all surface water chromatograms from Lake Tegel.

Table 2 gives results on portions of single DOC fractions averaged over the year. Humic substances are the most important fraction in surface water, accounting for ~46% (~3.3 mg/l) of surface water DOC. Other important fractions are humic substances-building blocks and neutrals and hydrophobics accounting for approximately 20-25% of total surface water DOC. Polysaccharides (9%) and low molecular acids (4%) are fractions of minor importance. All portions and equivalent concentrations are given in

Table 2 as a mean from sixteen measurements.

Table 2 Portions and concentrations of different fractions of DOC in Lake Tegel surface water – Differences between the seasons (Summer=April-October; Winter= November-March)

Share of	Poly-saccharides	Humic substances	Humic substances-Building blocks	Low molecular acids	Neutrals and Hydrophobics
Summer (n=8)	9.5 %	41.1 %	24.1 %	3.5 %	21.8 %
	0.70 mg/l	3.04 mg/l	1.78 mg/l	0.26 mg/l	1.61 mg/l
Winter (n=8)	7.8 %	50.1 %	20.1 %	4.2 %	17.8 %
	0.53 mg/l	3.41 mg/l	1.37 mg/l	0.29 mg/l	1.21 mg/l
Mean (n=16)	8.7 %	46 %	22.1%	3.7 %	19.7%
	0.62 mg/l	3.27 mg/l	1.57 mg/l	0.26 mg/l	1.40 mg/l

During evaluation of the chromatograms it became obvious that the proportions of DOC-fractions change slightly with the seasons. To capture the seasonal change, datasets were clustered into two groups; summer and winter. All chromatograms from April to October were pooled and characterized as summer state and data from November to March formed the winter state. The time periods were defined according to the data.

It was found that during summer, the fractions of polysaccharides, HS-building blocks and neutrals accounted for a higher percentage of the DOC, whereas the importance of humic substances decreased. The fraction of low molecular acids remained relatively stable during seasons at ~4%.

Table 2 and Figure 10 give more insight into seasonal effects on the DOC composition. It remains unclear, whether the decreased share of humic substances during summer derived from a more active biomass and more transformation into smaller molecules or from a higher portion of water from upper Havel in Lake Tegel (enforced operation of the lake pipeline during summer). Additionally, slightly higher DOC concentration

during summer shifted the portions. Most probable the three effects (temperature, introduction of more algae associated DOC and a higher influence of Havel water) added up during summer and lead to a shift from humic like material to building blocks and neutrals. Unfortunately, it was not possible to isolate the influences of these effects on DOC composition.

However, there is a high probability that the higher portion of polysaccharides during summer was due to algae blooms. Different literature already described polysaccharide production during algae blooms and formation of extracellular polymer matter (EPM), which falls into the fraction of polysaccharides (Hoyer et al., 1985).

1.1.2.2 Bank filtration-LC-OCD

Figure 11 shows LC-OCD chromatograms of samples from the bank filtration site, and indicates that the character of DOC partly changed during infiltration. The final chromatogram derived from more than 12 measurements over one year by mediation. Under all conditions the fraction of polysaccharides (~0.6 mg/l, ~8.7% of surface water DOC) was most efficiently removed, whereas other fractions (HS, HS-building blocks, LMA and Neutrals) exhibited only partial removal. A seasonal effect (not shown) was observed for the PS concentration in 3310 and 3311. During warmer months a higher percentage of PS was removed. An annual mean of approximately 30% of PS of the infiltrating surface water was found in 3310 and only ~15% in 3311. The more distant monitoring wells did not contain measurable amounts of polysaccharides. LC-OCD results indicate that monitoring well 3310 is dominated by surface water, since the character of DOC corresponds highly to the surface water DOC. Monitoring well 3311 is located under the lake and differs already significantly from surface water regarding DOC-character. This indicates a more bioactive infiltration path or a longer retention time for 3311.
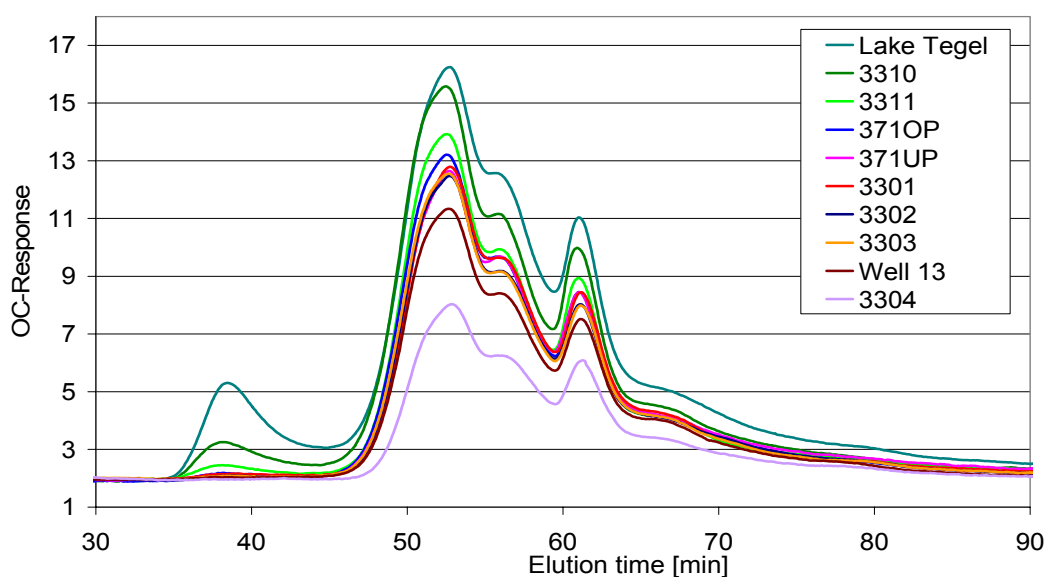
Figure 11 LC-OCD of transect at Lake Tegel (mean, n=12)

For all other fractions, which could be assessed by LC-OCD, decreasing concentrations, but no complete removal was observed during infiltration. The fractions of HS, HS-building blocks, LMA, and Neutrals showed removal rates ranging from 25% to 35% between surface water and monitoring well 3303. The similar removal lead to relatively constant proportions of the fractions regarding total DOC in the monitoring wells. The fraction of humic substances accounted for 46-51% of total DOC (HS-building blocks 22-26%; LMA 4-5%; Neutrals 17-22%). Table 3 gives proportions and concentrations of separate DOC-fractions for different wells. During the observation period, the proportions of DOC-fractions in the monitoring wells remained relatively stable. Potential effects of temporal changes in redox chemistry were not detected by the LC-OCD method because of lacking sensitivity. The fate of single fractions during infiltration is evaluated by comparison of concentrations in the monitoring wells along the infiltration path. Figure 12 displays the changing concentrations.

Plotting concentrations over retention time or infiltration distance did not lead to a clear presentation of the results and was rejected. The reasons for this decision will be discussed shortly. Retention time was not used, because for some wells it could not be determined (e.g. 3310, 3311). For some other wells retention time was strongly changing and was only specified with high standard deviations. The infiltration distance is no significant parameter since the flow velocity of the infiltrating water changes strongly along the transect. Furthermore, several monitoring wells are located on slightly different flow paths (e.g. 3301) which are influenced by small portions of other water types.

Table 3 Portions and concentrations of different fractions of DOC at transect Lake Tegel (n=12)

Share of	Poly-saccharides	Humic substances	HS - Building blocks	Low molecular acids	Neutrals and Hydrophobics
Lake Tegel	8.7 %	46 %	22.1 %	3.7 %	19.7 %
	0.6 mg/l	3.3 mg/l	1.6 mg/l	0.3 mg/l	1.4 mg/l
3310	4.2 %	50.5 %	23.4 %	4.8 %	17.2 %
	0.2 mg/l	2.7 mg/l	1.2 mg/l	0.3 mg/l	0.9 mg/l
3311	1.8 %	50.4 %	25.2 %	5 %	17.6 %
	0.1 mg/l	2.7 mg/l	1.4 mg/l	0.3 mg/l	1.0 mg/l
371OP	0.6 %	51.1 %	26.3 %	4.6 %	17.5 %
	0.0 mg/l	2.5 mg/l	1.3 mg/l	0.2 mg/l	0.9 mg/l
371UP	0.5 %	47.2 %	26.4 %	4.3 %	21.7 %
	0.0 mg/l	2.2 mg/l	1.2 mg/l	0.2 mg/l	1.0 mg/l
3301	0.8 %	49 %	26.7 %	4.6 %	18.9 %
	0.0 mg/l	2.6 mg/l	1.4 mg/l	0.2 mg/l	1.0 mg/l
3302	0.2 %	50.2 %	26.7 %	4.4 %	18.5 %
	0.0 mg/l	2.4 mg/l	1.3 mg/l	0.2 mg/l	0.9 mg/l
3303	0.4 %	49.9 %	25.2 %	4.4 %	20.1 %
	0.0 mg/l	2.3 mg/l	1.2 mg/l	0.2 mg/l	0.9 mg/l
Well 13	0 %	51.2 %	26.5 %	4.9 %	17.4 %
	0.0 mg/l	2.1 mg/l	1.1 mg/l	0.2 mg/l	0.7 mg/l
3304	0 %	45.6 %	29.6 %	5.8 %	19 %
	0.0 mg/l	1.2 mg/l	0.8 mg/l	0.2 mg/l	0.5 mg/l

However, Figure 12 shows that the decrease of total DOC is mostly due to a different behavior of separate DOC-fractions. 0.6 mg/l polysaccharides are removed very fast by instant mineralization in the oxic infiltration zone. The results of soil column experiments support the assumption of a rapid biodegradation for this DOC-fraction, because in an abiotic column only minor filtration effects were observed (see soil column chapter 1.4).

The fraction of humic substances is commonly regarded as mostly non-biodegradable, but results for the bank filtration transect Tegel show that 30% of this fraction was removed. Already during short term infiltration (3310) significant amounts of humic substances (0.6 mg/l) are attenuated. In the deeper aquifer the removal continues, but some portions of humic substances-rich water were introduced to the flow path from under the lake. This was obvious for monitoring well 3301, which shows considerably higher amounts of humic substances. Finally, 2.1 mg/l humic substances were found in abstraction well 13. The background groundwater concentration for humic substances was low with 1.2 mg/l.

The fraction of HS-building blocks remains relatively stable during infiltration after some removal close to the bank. Concentration level remained between 1.2 mg/l and 1.4 mg/l. A slight influence of older bank filtrate from under Lake Tegel may be indicated by a concentration increase in 3301. It is possible that fragments of partly

mineralized humic substances add to this fraction. This would explain the constant concentration during further infiltration. Generally, all smaller DOC- fractions might be replenished by products of humic substances degradation. The background concentration of HS-building blocks is 0.8 mg/l. This means that HS-building blocks account for a slightly higher proportion of background DOC (~30%) compared to 22-26% in surface water and bank filtrate.

Low molecular acids are a very small fraction in Lake Tegel surface water, since only 4-5% of the DOC belongs to this fraction. LC-OCD results indicate that the importance of this fraction is not changing during infiltration. The concentrations remain at 0.2-0.3 mg/l. Despite of an apparent stability of this fraction the turn over might be high since LMA are classical mineralization intermediates and not known to be extremely persistent.

The fraction of neutrals and hydrophobics contains different organic molecules that migrate for different reasons slowly through the size exclusion chromatography column. Small sized molecules, hydrophobic and amphoteric organic compounds show up in this portion of total DOC. Therefore, this fraction is not very well defined. However, during infiltration a considerable amount of neutrals is removed instantly (0.5 mg/l). Afterwards the concentration remains stable at around 0.9 mg/l. Background concentration is low with 0.5 mg/l.
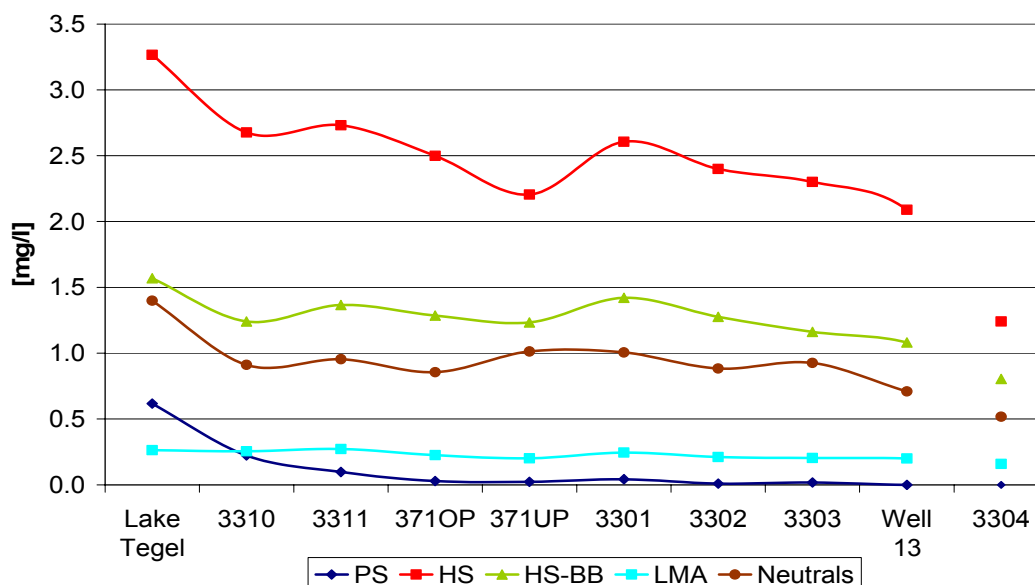
Figure 12 Concentrations of the different fractions of DOC at transect Lake Tegel

However, the LC-OCD analysis reveals that the changes in DOC-character during infiltration have not been dramatic but present. The most important difference between surface water and bank filtrate is the removal of the PS-fraction. For other portions of DOC more quantitative effects than qualitative changes were observed. Results are consistent with total DOC measurements. Furthermore, LC-OCD chromatograms of

bank filtration site Tegel were comparable to the chromatograms obtained from other studied field sites and from soil column experiments. An evaluation of removal kinetics for DOC-fractions will be included in the soil column section (chapter 1.4), where exterior influences are minimized and retention times are definite.

1.1.3 Lake Tegel - AOI results

1.1.3.1 Surface water-AOI

Long term AOI-monitoring confirmed seasonal changes of AOI-concentration in Lake Tegel. Since 1998, the AOI in Lake Tegel surface water is measured in the Department for Water Quality Control of the TU Berlin. Figure 13 shows all measured data of the last seven years. Surface water AOI concentration was found to be highly variable over the year. During six of seven years, higher AOI concentrations were measured during late summer and fall. It is assumed that these seasonal changes derive from variations in dilution of sewage treatment plant effluents that are discharged into Lake Tegel.
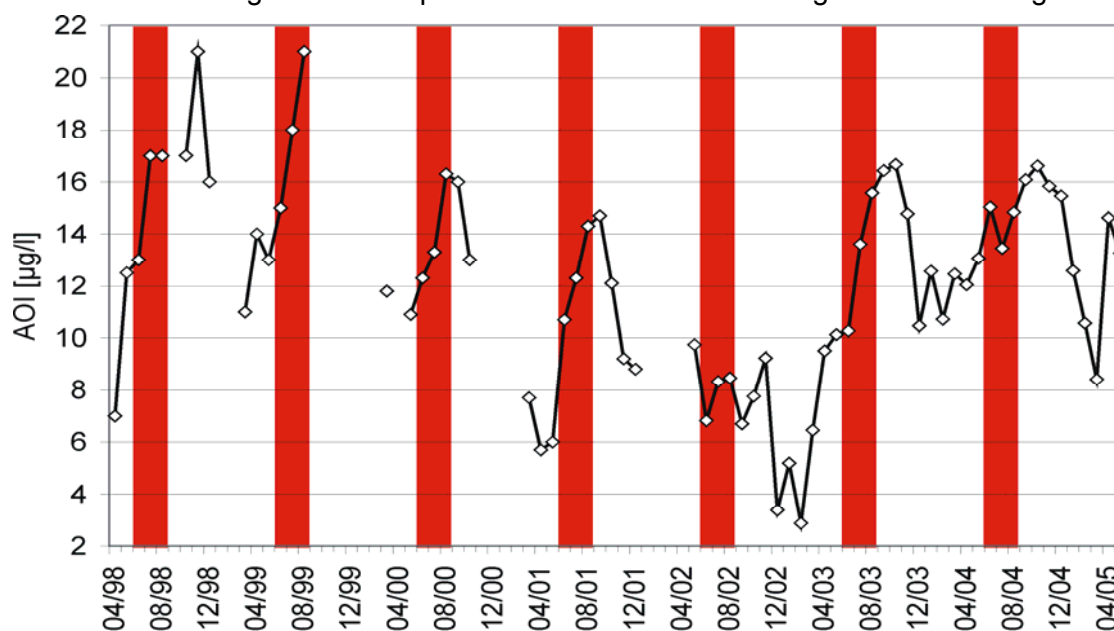
Figure 13 AOI concentration in Lake Tegel (1998-2005, summer months June, July, August marked)

From 1998 to 2001 the time series is incomplete, but available datasets show seasonal trends. During these four years, the average lake AOI concentration decreases and the peaks during summer show lower concentrations. In October 2001, the lake pipeline was reactivated and during the following year very low AOI concentrations were monitored. The dilution effect of the lake pipeline was enhanced by a very cold and wet summer in 2002. Here, no increased AOI levels during late summer and fall were found. With start of 2003 the AOI concentrations started to rise in Lake Tegel surface water. This increase corresponded well with higher concentrations of other waste-water borne contaminants (=> hydrogeology section) and was caused by the extension of the

sewage treatment plant (STP) Schoenerlinde. The effluent amount of STP Schoenerlinde increased considerably to more than 80.000 m^3/d. In 2003 and 2004, the known seasonal variations were observed despite of strong dilutions by the lake pipeline. Seven measurements in the upper Havel (01/2004-08/2004) confirmed that the AOI concentration of the diluting water is considerably lower than in Lake Tegel (Median=6.8 µg/l, δ=2.1 µg/l). Therefore, it can be concluded that the AOI-peaks are reduced by heavier dilution during summer. Without operation of the lake pipeline much higher concentrations during summer can be expected.

1.1.3.2 Bank filtration-AOI

Within the NASRI-project, AOI concentrations of samples from monitoring wells of transect Tegel were measured over 27 months. For a better presentation the transect was divided into shallow monitoring wells with mostly oxic conditions and deep monitoring wells with primarily lower redox potentials. Figure 14 presents AOI concentrations of the shallow wells, where fewer data is available because of dry periods during summer (3311; 3310) or late installation of the well (371OP). Therefore, this data needs to be interpreted carefully if no complete seasonal cycle was recorded.

For two of the shallow wells with retention times of less than a month (3310 and 3308) it was found that AOI concentrations corresponded closely to the surface water concentration. During some periods, the concentrations in the wells exceeded surface water AOI-concentrations. Overall, the available data for well 3310 and 3308 show, that AOI-levels were only reduced by 12% and 20%, respectively. Monitoring well 3311 displayed a relatively strong influence of surface water with comparable AOI levels during 2002 and early 2003. After the summer of 2003 AOI levels in 3311 were noticeably lower than in surface water. Monitoring well 3311 exhibited an AOI elimination of ~51%. This high elimination rate is caused by the predominant redox conditions in 3311. Contrary to 3310 and 3308, clear denitrification occurred in 3311. Despite of a short retention time and the presence of oxygen, nitrate concentrations in 3311 are significantly lower than in the other two wells and the surface water. Denitrification and AOI-mineralization probably occur in micro-anoxic compartments of the soil matrix in absence of oxygen.
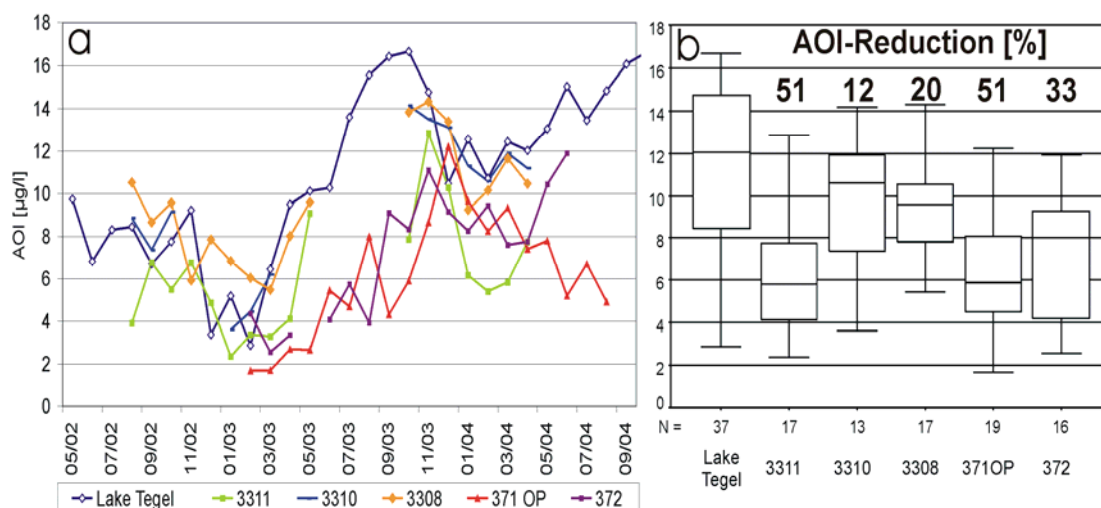
Figure 14 Fate of AOI during infiltration to the shallow monitoring wells (a: time series; b: box plots)

For shallow monitoring wells with longer retention times (371OP=> 1.1 months, 372=> 3.3 months), AOI-reduction rates of 51% and 33% were found (Figure 14). AOI-concentrations were highly variable, but did not follow necessarily the surface water concentration. It is unlikely that the increase of AOI-concentration in late summer 2003 was only caused by higher AOI-levels of Lake Tegel since spring 2003. In this case, retention times would propose an earlier peak. But the peak-period of AOI in 371OP and 372 occurs simultaneously with the already mentioned breakthrough of higher oxygen and nitrate levels to deeper and more distant wells from October 2003 - May 2004 (=> hydrogeology section). Monitoring wells 371OP and 372 showed strong indications of occurring denitrification before and after this breakthrough. Until October 2003, no nitrate was found in 371OP and only low nitrate levels in 372 were observed. From October 2003, nitrate levels increased in both wells to surface water concentration before returning to the former low levels in June 2004. Fate of AOI in both wells indicates an association between these two parameters. During periods of high nitrate levels (missing denitrification), more AOI breaks through. The data also show that occurring denitrification seems to be more important for an effective AOI removal than longer retention times. Unfortunately, the effect of increased surface water concentration could not be quantified for the wells because it was superposed by the stronger effect of changing redox conditions.
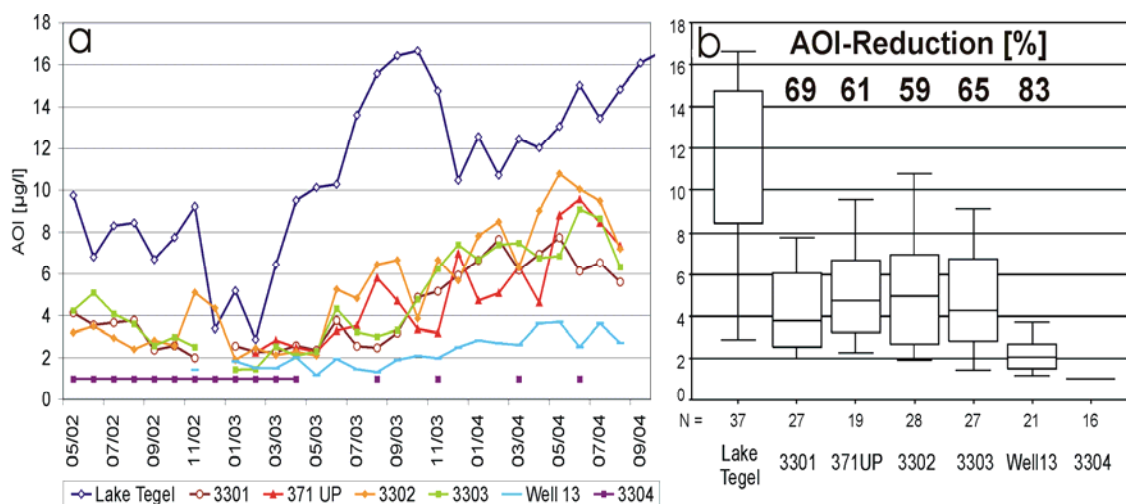
Figure 15 Fate of AOI during infiltration to the deep monitoring wells (a: time series; b: box plots)

Results for the deeper monitoring wells are depicted in Figure 15. In the deep aquifer at the bank filtration site Tegel, a relatively efficient degradation of AOI takes place under mostly anoxic/anaerobic conditions. Figure 15 shows that at low redox potentials, an AOI degradation of 60-70% is possible. AOI concentration of the background groundwater at the bank filtration site is very low (<1 µg/l) and the mixture leads to an AOI-concentration in the extracted raw water of 1-4 µg/l.

The time series of AOI measurements showed an increase in concentrations in the deep monitoring wells starting in June 2003. It is assumed that higher AOI levels are partly caused by changes of the surface water concentration. The deep wells (3301, 3302, and 3303) react approximately three months later with an increase in AOI-concentration. This retention time is similar to the one that was proposed by the hydrogeology group from FU Berlin (=> hydrogeology section). Furthermore, changed redox conditions allowed an easier break through of AOI. Hydrogeological effects which were explained earlier caused elevated nitrate levels in the deep wells (3301=>02/04-05/04; 3302=>11/03-06/04; 3303=>01/04-06/04). The two effects of rising surface water concentration and higher redox potentials could not be quantified separately, but it is believed that both effects add to the observed increase of AOI in the second aquifer. Measurements in abstraction well 13 confirm that changes also affect the raw water. A comparison of AOI levels in well 13 reveals an increase of 200-300% between the years 2002 and 2004. It is difficult to predict future AOI levels in the transect and abstracted water, but it can be summarized that degradation of AOI is more effective in soil passages with low redox potential. A general inverse correlation between AOI removal and redox potential seems to be valid. This inverse correlation most probably originates from the initial step of AOI-mineralization - reductive dehalogenation. It is known that degradation of halogen substituted organics is more effective in soil passages with low redox potential (Mohn&Tiedje, 1992). Therefore, low

water level in Lake Tegel and heavy pumping over longer periods should be avoided to guarantee low AOI concentrations in the bank filtrate.

1.1.4 Lake Tegel - AOBr results

1.1.4.1 Surface water-AOBr

AOBr concentration in Lake Tegel showed seasonal variations during the observation period (Figure 17). Higher concentration of AOBr during late summer and fall were observed and confirmed findings of earlier monitoring events (1998-2000). Contrary to AOI it is believed that the origin of AOBr in Lake Tegel is not mainly discharged waste water, but AOBr is also produced during algae blooms in the lake. Within the project, it was found that AOBr in Lake Tegel probably originates from three sources:

First, the AOBr load of the effluent of STP Schoenerlinde, which is relatively constant. Seven measurements (01/2004-08/2004) proved that the AOBr concentration of treated effluent, that is discharged via Nordgraben and Tegler Fließ into Lake Tegel, is relatively constant (Median=7.6 µg/l, δ=0.9 µg/l). The Nordgraben contains to a high percentage (65-90%) effluent of STP Schoenerlinde and is not prone to algae blooms (body of flowing water). It can be assumed that the share of AOBr which is introduced into Lake Tegel by the Nordgraben is constant and mainly of anthropogenic origin (disinfectants, flame retardants etc.).

During the same period (01/2004-08/2004) an increase of AOBr in the upper Havel was monitored (Median=9.4 µg/l, δ=1.7 µg/l, n=7). Water from the upper Havel is pumped to the northern end of Lake Tegel by the lake pipeline and represents more than 50% of the influent to Lake Tegel in the summer months. The upper Havel is a strongly eutrophic, slow flowing water body with algae blooms during summer. Therefore, it can be expected that the AOBr content of the upper Havel follows a seasonal pattern and that a share of AOBr is introduced by the lake pipeline to Lake Tegel. The origin of AOBr from the upper Havel is probably anthropogenic and algae associated with seasonally changing portions.

The third source for AOBr in Lake Tegel is production in the lake by algae. The build up of this fraction is strongly dependent on diverse factors that affect algae blooms (temperature, light, nutrients). It occurs predominantly during late summer.
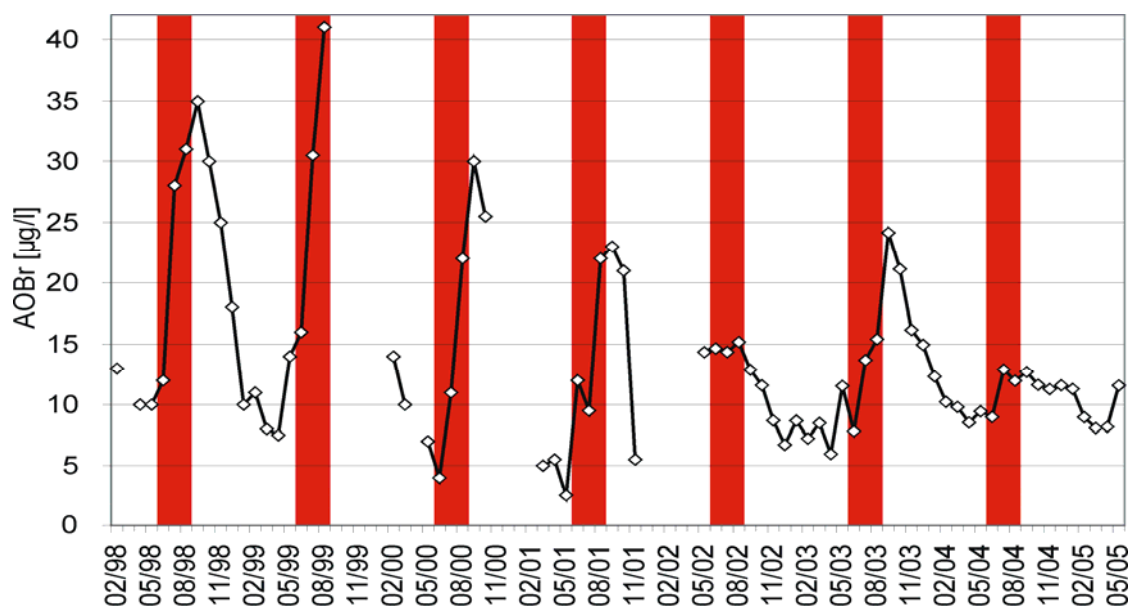
Figure 16 AOBr concentration in Lake Tegel (1998-2005, summer months June, July, August marked)

Figure 16 displays AOBr-concentrations of Lake Tegel which have been measured at the DWQC at TU Berlin since 1998. A clear seasonal variation can be recognized. Overall the peak concentrations measured in earlier projects (1998-2001) were not found during the NASRI-project. The highest concentrations in the observation period were measured during summer 2003. It is assumed that the measured peaks consisted to a high percentage of algae associated AOBr. During summer 2002 and 2004 no strong AOBr peaks in the surface water were observed, but the concentration increased slightly by 5-8 µg/l. During winter the AOBr concentration in the lake drops to 5-8 µg/l. This level is consistent with the AOBr concentration of the treated effluent. Therefore, the AOBr load of the lake during winter is probably of anthropogenic origin.

1.1.4.2 Bank filtration-AOBr

The fate of AOBr in the bank filtration process shows similarities to the behavior of AOI. Averaged for all monitoring wells removal rates were slightly lower. The observations revealed that AOBr concentrations in monitoring and abstraction wells are mainly dependent on surface water concentration and dominant redox conditions along the infiltration path. Overall, the AOBr-data set is difficult to interpret because some peaks in bank filtrate could not be linked to certain factors of influence. Furthermore, it is presently not clear whether anthropogenic and algae associated AOBr behave similar during infiltration.

Shallow monitoring wells with low retention times (<1 month) and oxic conditions showed very low removal rates (3310=> 9%, 3308=> 14%). For both wells, the data point towards a break through of the very high concentrations of the summer peak in

fall 2003 (Figure 17). Unfortunately, data points for most summer months are missing. In well 3311, which has similar retention times but lower oxygen and nitrate levels, only 48% of surface water AOBr was found. This indicates a redox sensitivity of AOBr removal, similar to the process described for AOI.

For the more distant shallow monitoring wells 371UP and 372 removals of 45% and 24% were observed, respectively. The better reduction in 371UP is caused by a lower average redox potential of this well. In both wells no real break through of the surface water AOBr peak of 2003 was observed and the higher AOBr-concentrations during fall and winter of 2003/04 are assumed to be connected with the described change in redox conditions during this period.
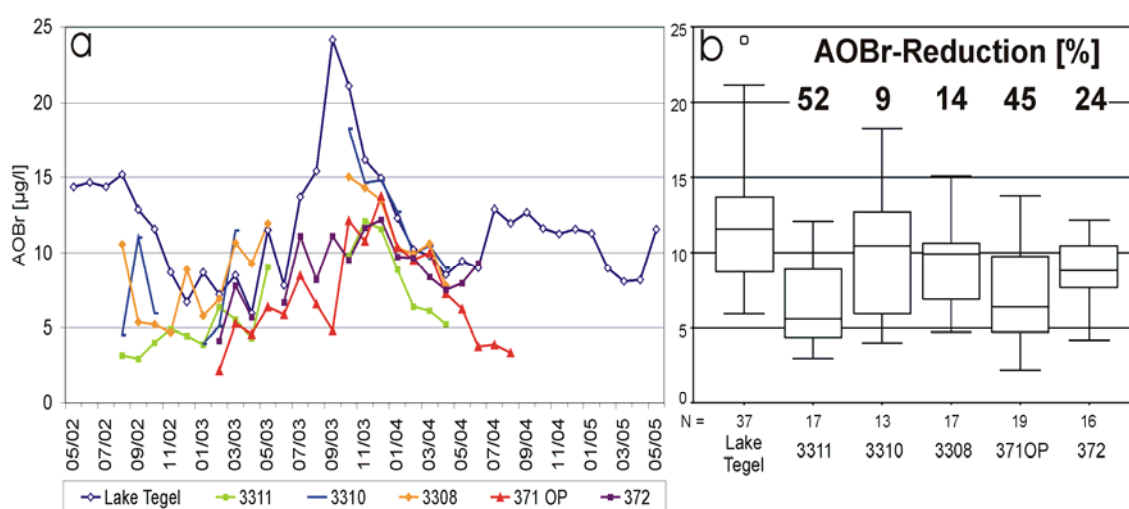
Figure 17 Fate of AOBr during infiltration to the shallow monitoring wells (a: time series; b: box plots)

Deeper monitoring well with mostly lower redox potentials showed reduction rates ranging from 50-70% (Figure 18). The abstracted raw water contained only 21% of surface water AOBr. Despite of an averaged high removal rate some of the deep wells exhibited a very low removal during certain periods. Particularly, during summer 2003 and summer 2004 the wells 3302 and 3303 showed AOBr concentrations that were comparable to surface water concentrations measured 3-4 months earlier. During these periods a considerably lower AOBr-removal took place. AOBr concentrations in monitoring well 3301 and 371UP increased only during the period of oxygen and nitrate break trough (09/03-06/04). This underlines the redox sensitivity of AOBr mineralization.
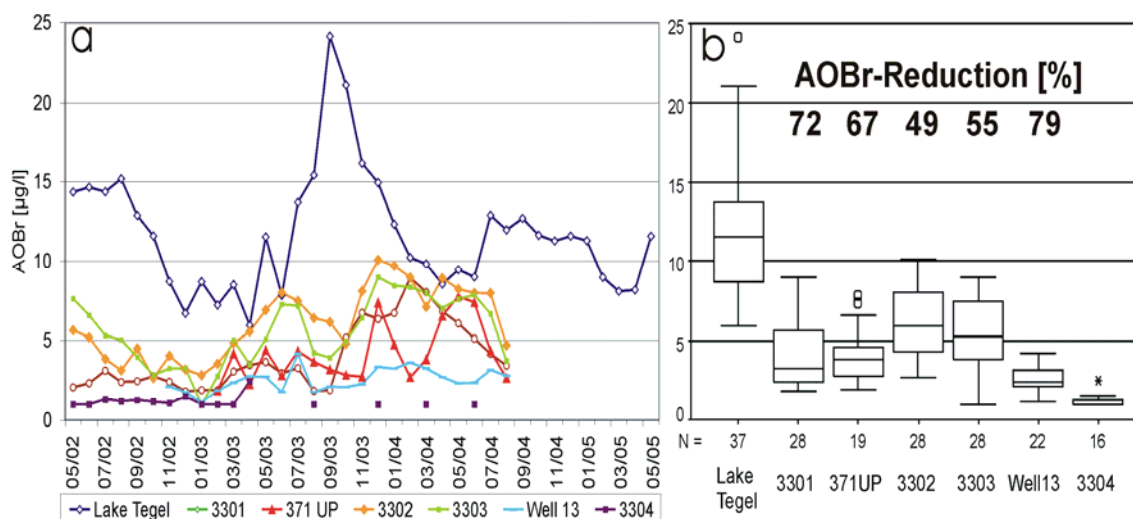
Figure 18 Fate of AOBr during infiltration to the deep monitoring wells (a: time series; b: box plots)

Data of the transect Tegel does not allow strong statements about the degradability of the two fractions of AOBr. But the strong summer peak of 2003 was only found in the shallow oxic monitoring wells. AOBr-concentrations in the deeper wells did not exceed the winter level of AOBr in Lake Tegel. In combination with data from other field sites the conclusion arises that the seasonal fraction of AOBr seems to be easier degradable than the anthropogenic fraction. Clearer results supporting this assumption were measured at transect Wannsee and the artificial groundwater recharge facility in Tegel (chapter Wannsee =>1.2, GWA =>1.3).

1.1.5   Lake Tegel – Trace pollutants results

1.1.5.1 *Surface water-Trace organic compounds*

Five different trace organic compounds were monitored in the surface water of Lake Tegel from May 2003 to June 2005. Iopromide, Sulfamethoxazole and three isomers of NDSA were selected. Origin and relevance for the Berlin area of these five trace compounds is explained in the methodology section (=> Chapter Methodology). All five compounds are of anthropogenic origin and indicate an influence of treated waste water or a different type of contamination. Therefore, the pollutant level depends on the water quality of the discharging water bodies. The concentration in Lake Tegel is a function of the load discharged by Nordgraben (and Tegeler Fließ) and upper Havel (lake pipeline) since other sources for these compounds to Lake Tegel are not known. For the five compounds it is assumed that attenuation in surface water is of minor importance. All compounds are persistent and were not efficiently removed in sewage treatment plants. A photosensitivity is not described for one of the compounds.

Consistently, earlier studies found that the X-ray contrast agent Iopromide and the bacteriostatic Sulfamethoxazole originate mostly from the effluent of treatment plant

Schönerlinde and enters the lake via Nordgraben and Tegler Fließ (Wischnack, 2000; Hartig, 2000). Measured concentrations in the upper Havel were considerably below the contamination level of the Nordgraben. Isomers of the naphthalenedisulfonic acid were reported with highly variable concentrations in the effluent of STP Schönerlinde and in river Havel (Storm, 2002). The compounds are widely used and often found in the aqueous environment. However, Nordgraben and Tegeler Fließ showed generally higher concentrations than the Havel, pointing toward a higher pollutant load originating from the sewage treatment plant.

Figure 19 presents the concentrations of the target compounds in Lake Tegel during the observation period. All selected compounds were continuously detected in changing concentrations in surface water samples in front of the transect. Concentrations ranged from 50 ng/l to nearly 2000 ng/l for the different trace substances. A strong seasonal variation could not be determined, neither was a clear trend observed for one of the compounds. The results have to be interpreted with the knowledge that the concentration in Lake Tegel depend strongly on the quality of the effluent of the treatment plant Schönerlinde. Earlier studies demonstrated that the concentration of pollutants in the effluent varies highly, even on a daily basis (Storm, 2002; Hartig 2000). The level of pollution is smoothed during retention times in the receiving waters and in the surface water treatment plant Tegel. But nevertheless, it is possible that the pollution in front of the transect varies with a high frequency which can not be reproduced with monthly sampling events. The spatial variation of the substances in Lake Tegel was not determined in this study.
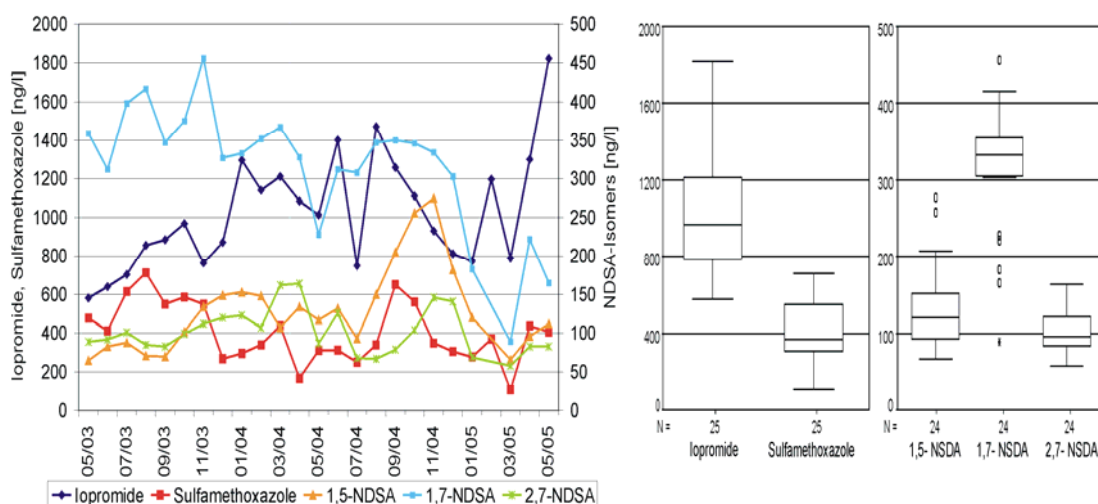
Figure 19 Trace pollutant concentration in Lake Tegel

The X-ray contrast agent Iopromide was detected in Lake Tegel with a median concentration of 969 ng/l (δ=297 ng/l, n=25). This is consistent with concentrations reported by Schittko (2004). Overall, concentrations were highly erratic with a slight trend to higher levels towards the end of the monitoring period.

The antibiotic drug Sulfamethoxazole showed median contamination levels of 371 ng/l (δ=153 ng/l, n=25). For this compound, slightly higher concentrations during the summers of 2003 and 2004 pointed toward a possible seasonality. The general contamination level in Lake Tegel did not change during the observation period.

Isomers of naphthalenedisulfonic acid were monitored for 26 months in surface water. Median concentrations were 96 ng/l (δ=30 ng/l, n=24) for 2,7-NDSA, 119 ng/l (δ=55 ng/l, n=24) for the 1,5-Isomer, and 334 ng/l (δ=83 ng/l, n=24) for 1,7-NDSA. These results differ considerably from monitoring results (n=7) obtained in 1999 and 2000 by Storm (2002). Compared with these results the concentrations of the 1,5- and the 2,7-Isomer were reduced by 40-50%, whereas concentrations of the 1,7-Isomer increased significantly to 150%. Time series of 2002-2005 demonstrated a decrease in contamination levels for the 1,7-Isomer toward the end of the monitoring, but it remains unclear whether this trend is going to continue. The 1,5-Isomer concentration peaks during summer and fall 2004 but returns to base level in winter.

Unfortunately, attempts to correlate trace compound concentrations in front of the transect to other waste-water indicators like Boron, Chloride, or electric conductivity failed on monthly basis. Presumably, the concentrations of the compounds in waste-water varies highly, so that the waste-water portion in front of the transect is no appropriate measure for trace pollutant concentration. But, on a more general long term basis the waste water portion and the pollution level for some single compounds behave similar. For instance, the NDSA-isomers concentrations increased in the surface water with the enlargement of STP Schoenerlinde in spring 2003.

1.1.5.2 Bank filtration-Trace organic compounds

Monitoring of infiltration behavior of the single compounds Iopromide, Sulfamethoxazole and different naphthalenedisulfonic acids had been started in spring 2003, providing data for the time period May 2003 to August 2004. The monitoring showed that these trace organic compounds which stand for different groups of persistent pollutants behave differently during infiltration. For some compounds, an influence of the redox conditions on the degradability could be revealed.

Iopromide occurred in the highest concentrations in surface water. Due to the fact that Iopromide as a triiodinated benzene derivate is part of the bulk parameter AOI (share in surface water ~5%), it was expected that the removal mechanisms for both parameters are similar. This was not confirmed. Contrary to the fate of AOI (see chapter AOI=>1.1.3) Iopromide showed a very good removal (99%) along the infiltration pass to the production well independently from redox conditions. At the bank filtration site Tegel Iopromide concentrations were reduced from the lake (969 ng/l, n=25, σ=297 ng/l) to the first observation well 3310 (80 ng/l, n=4, σ=75 ng/l) by 91%. In the last monitoring well in front of the production well (3303) sixteen measurements resulted in one measurement above limit of quantification (LOQ) and two detections

under the limit of quantification. In the other 13 samples no Iopromide was detected. The limit of quantification for Iopromide was 20 ng/l. Detected traces below LOQ were entered into the data base with a concentration of half the LOQ (10 ng/l). Summarizing, more than 99% of surface water Iopromide was attenuated during soil passage at Tegel bank filtration site. Figure 20 displays the measured concentrations in the different monitoring wells. Only surface water results were included, that correspond to the measurements in the wells. These results did not point towards a difference in attenuation efficiency at different redox conditions. The break through of oxygen and nitrate in fall and winter 2003 did not affect removal performance. However, Iopromide is effectively removed during initial infiltration at the water- soil interface.

From the field data it remains unclear whether the attenuation of Iopromide is based on degradation or metabolization. Results from soil-column experiments (soil column chapter => 1.4) where the removal of Iopromide was compared with the reduction of AOI during infiltration showed that Iopromide and AOI behave different of during soil passage. It was found that a high percentage of the Iopromide molecule is altered (partially transformed) but not mineralized during the first part of soil passage. A complete mineralization is probably more efficient under anoxic/anaerobic conditions, as showed in the AOI-section (see chapter on AOI=>1.1.3). Iopromide was not detected in background groundwater.

Figure 20 Fate of Iopromide during infiltration at the bank filtration site Tegel

The effluent concentration of the bactriostatic Sulfamethoxazole in Berlin treatment plants varies between 370-1200 ng/l. Because of its high stability it is also found in the surface waters at bank filtration sites. Sulfamethoxazole displayed an efficient removal during infiltration at bank filtration site Tegel, where it is degraded to approximately 25% of the initial concentration (monitoring well 3303). The concentration in the drinking water well is only 7% of the surface water concentration due to attenuation and dilution with non-polluted background groundwater (Figure 21). The compound was not found in background ground water. The degradation of Sulfamethoxazole seems to be redox dependent. Unfortunately, only 4 measurements of the oxic monitoring well 3310 (retention time <1 month) were conducted, because this well fell dry during summer. Higher concentrations of Sulfamethoxazole in 3310 compared to the surface water are most probably due to short term variations in surface water, which were not captured by monthly sampling events. However, data indicates no efficient removal during initial oxic infiltration. Consistently, with other field sites and column experiments, a removal
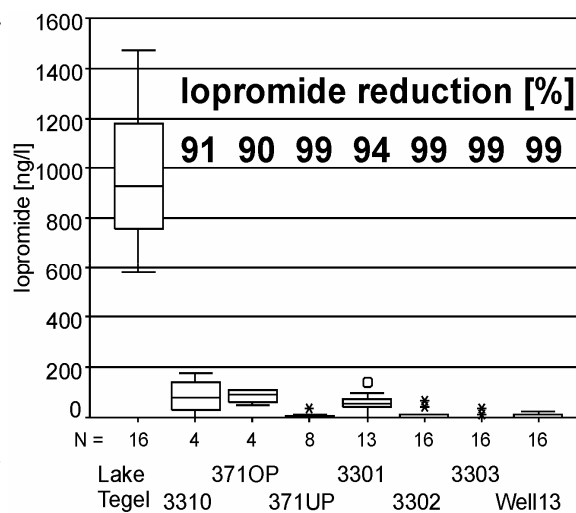
is more efficient under anoxic/anaerobic conditions in the deeper monitoring wells (chapter Wannsee => 1.2 and soil columns =>1.4). The low concentrations in 371UP and 3301 are probably due to a cumulative effect, since these wells are characterized by very low redox potentials and some influence of older bank filtrate (chapter hydrogeology). Figure 21a also shows higher Sulfamethoxazole concentrations in the monitoring well 3301, 3302 and 3303 from fall 2003 to spring 2004. It is assumed that the change in redox conditions (indicated by the break through of nitrate) during this period is responsible for the restricted attenuation and the higher concentrations. But it can not be ruled out that higher concentrations in surface water from 07/2003 to 11/2003 also play a role for the observed higher concentrations in the subsoil. Therefore, the consequences of a changed redox system for Sulfamethoxazole reduction can not be isolated. But the conducted research points towards a better removal of Sulfamethoxazole under anoxic/anaerobic conditions. This is furthermore consistent with findings of Schmidt et al. (2004) at other bank filtration sites in Germany.
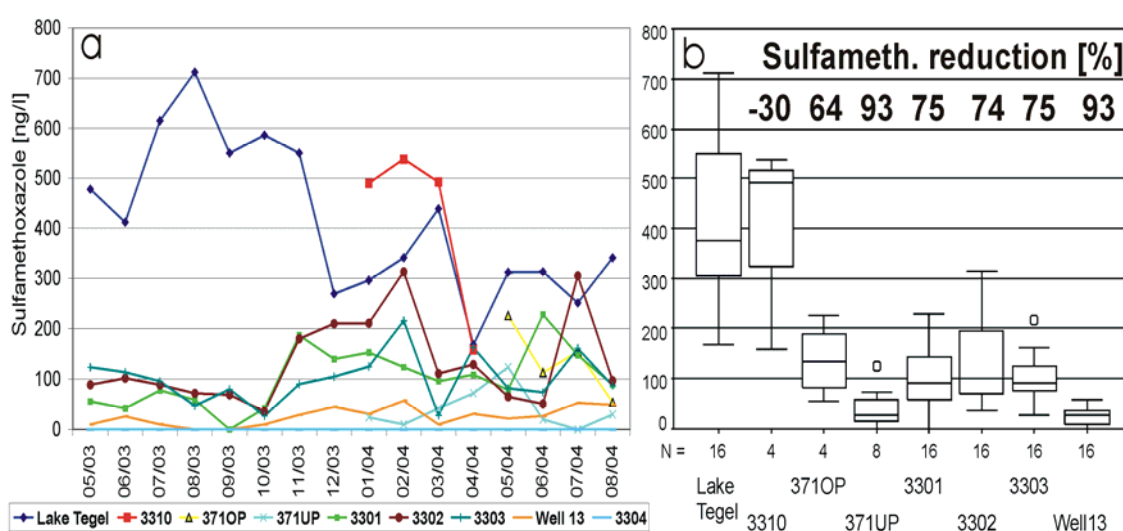
Figure 21 Fate of Sulfamethoxazole during infiltration at the bank filtration site Tegel (a: time series; b: box plots)

Naphthalenedisulfonates (NDSA) are well known polar contaminants of treated waste water and surface water. The different isomers have nearly similar chemical properties, but show a different degradation behavior. Within this study, the 1,5-, 1,7-, and the 2,7-NDSA isomers were monitored during infiltration process. It needs to be mentioned that all three isomers were present in the background groundwater in concentrations that were slightly lower or similar to the concentrations on the surface water influenced side of the well gallery. These pollutions most likely originate from Lake Flughafensee. Since the behavior of the isomers during infiltration differs, the results are presented subsequently.

In contrast to Iopromide and Sulfamethoxazole, the 1,5-naphthalenedisulfonic acid was not efficiently degraded at the bank filtration site Tegel. Concentrations of the very stable 1,5-naphthalenedisulfonic acid remained nearly constant throughout the infiltration process. The initial concentration only decreased by 15-20% during ~4 months of infiltration to the production well. One exception is the monitoring well 3301 which shows slightly lower concentrations of 1,5-NDSA. It is believed that this is partly due to some dilution with older bank filtrate. Furthermore, the data pool for this well is missing data sets for 02/2004-03/2004 which would probably increase the median concentration for this monitoring well. The time series show that during the observation period the concentration of 1,5-NDSA increased in surface water (Figure 22a). All monitoring wells reacted on the higher surface water concentration in order of their retention times. The time frames were consistent with the proposed retention times of the hydrogeological group (compare hydrogeological section). This indicates that the retardation of NDSA is insignificant compared to an ideal tracer. The inefficient removal of 1,5-NDSA is consistent with findings of Stüber et al. (2002) who reported 1.5 NDSA as very stable and persistent in waste water treatment plants. These results proof that 1,5-NDSA is very poorly biodegradable and it can not be expected to eliminate high proportions of this compound during bank filtration.
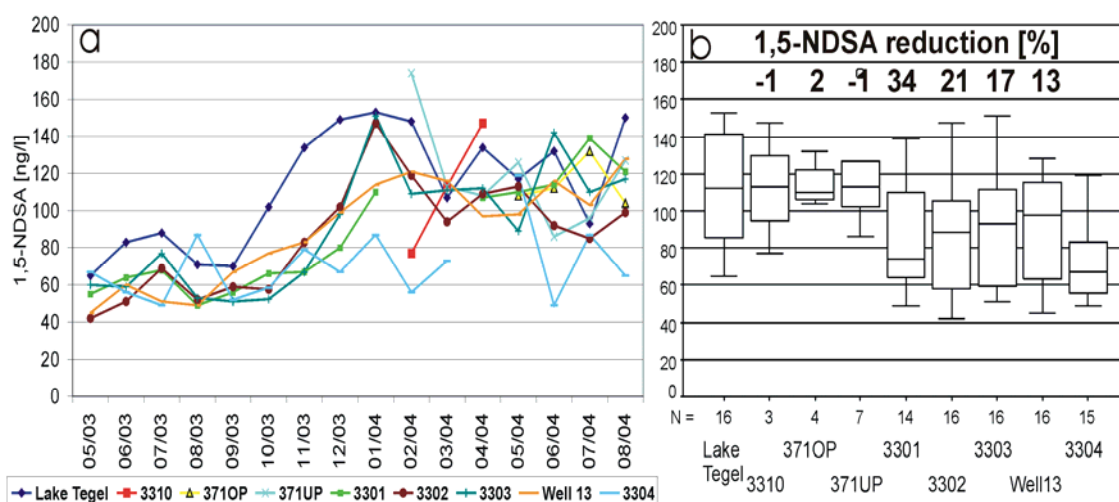
Figure 22 Fate of 1,5 - NDSA during infiltration at the bank filtration site Tegel (a: time series; b: box plots)

1,7-NDSA was present in the surface water of Lake Tegel in higher concentrations (334 ng/l; δ=83 ng/l; n=24) than the 1,5-isomer. Figure 23 displays results of monitoring wells and the corresponding surface water concentrations. Generally, a better removal was observed than for the 1,5-isomer, but the compound was also not attenuated easily in the first meters of infiltration. In the shallow monitoring wells 3310 and 371OP only 15% and 1% of the compound were removed, respectively. The abstracted raw water in production well 13 contained averaged 43% of the measured surface water

concentration. The time series in Figure 23a is strongly dominated by an increase in concentration in the monitoring wells 3301, 3302, and 3303 during fall and winter 2003/04. This corresponds to the already mentioned temporary change in dominant redox conditions. However, at other field sites and in soil column experiments it was found that this isomer of NDSA is more efficiently degradable under oxic conditions. That is the reason why it was surprising to detect higher concentrations during a period of nitrate break through to the monitoring wells. The concentration increase might be explained by a die-off of a great portion of adapted biomass, which did not tolerate elevated nitrate and oxygen levels. A quick growth of an oxygen tolerant biomass, which was able to degrade this compound, might have been limited by low assimilable carbon concentrations in deeper parts of the aquifer. But in January/February 2004, the concentrations of 1,7-NDSA in the deeper monitoring wells decreased, despite of a presence of nitrate in both wells (3302 and 3303) until June 2004. It can be assumed that in the time period 11/2003 to 01/2004 the biomass slowly adapted to elevated nitrate levels. From 02/04 to 06/04 the adapted biomass provided an above average removal of 1,7-NDSA in the deep monitoring wells 3302 and 3303, which showed the highest nitrate concentrations. In Figure 23a, the very low 1,7-NDSA concentrations from 02/2004-06/2004 are visible, which are even below the pollution level in the production well and background groundwater during this period. These results are consistent with findings at other field sites that infiltration under more oxic conditions leads to a better removal of Naphthalenedisulfonates. After July 2004 the 1,7-NDSA concentration increased again in the deeper aquifer because of a return to anaerobic conditions after the depletion of the nitrate break through. The results show impressively that a change in redox chemistry at an infiltration site can cause dramatic changes in removal efficiency for trace compounds. The removal mechanisms in the system of bank filtration are usually robust, but can not be taken for granted since sometimes short term disturbances result in significant changes in pollutant removal.
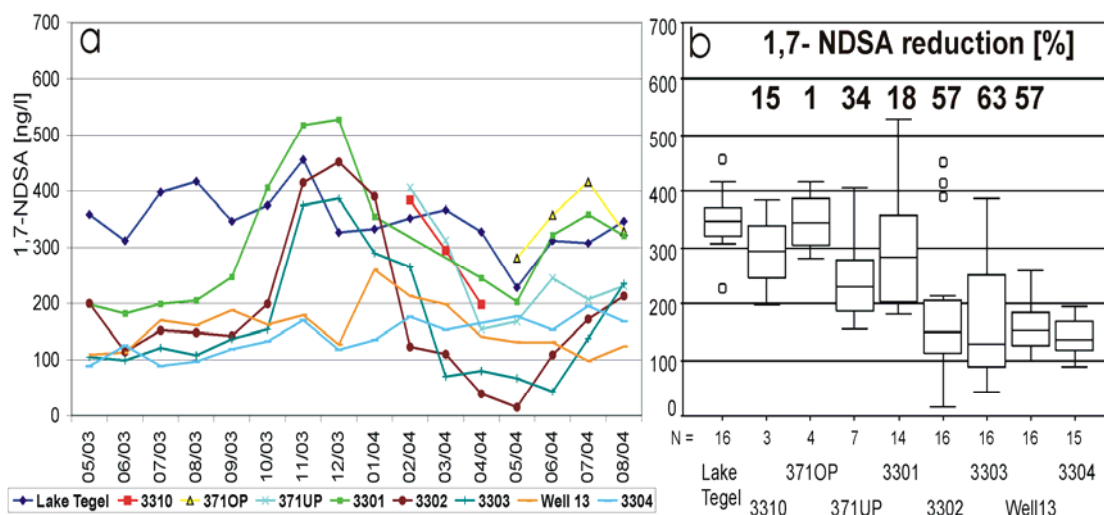
Figure 23 Fate of 1,7-NDSA during infiltration at the bank filtration site Tegel (a: time series; b: box plots)

Results for the 2,7-NDSA show the same trends that were observed for the 1,7-isomer. Generally, a partial removal took place during infiltration at the bank filtration site, and approximately 57% of surface water concentration was found in raw water. Because concentration levels for this compound were close to the limit of quantification in some monitoring wells, it has to be mentioned that detected traces below LOQ (30 ng/l) were set to ½ LOQ (15 ng/l). Figure 24 shows that the degradation performance in the deeper monitoring wells was dominated by redox conditions and kinetics of biomass adaptation. The shallow oxic wells did not exhibit an efficient removal. In the deep monitoring wells an increase in 2,7- NDSA was observed during fall 2003-winter 2003/04, which was followed by a period of very low concentrations in 3302 and 3303. Only traces below limit of quantification were detected in spring 2004 in these monitoring wells. The reasons for these concentration changes are assumed to be similar to the ones discussed for 1,7-NDSA (see above). In observation well 3301 a very low attenuation of the compound was found. In summer (06-08/2004) concentrations in 3301 rose to levels that were observed three months earlier in surface water (Figure 24). The weak attenuation of this partly degradable NDSA and the break through of temporarily higher surface water concentration into 3301 might be due to a higher portion of bank filtrate that infiltrated more distant from the bank under more anoxic/anaerobic conditions where an efficient removal is not feasible.
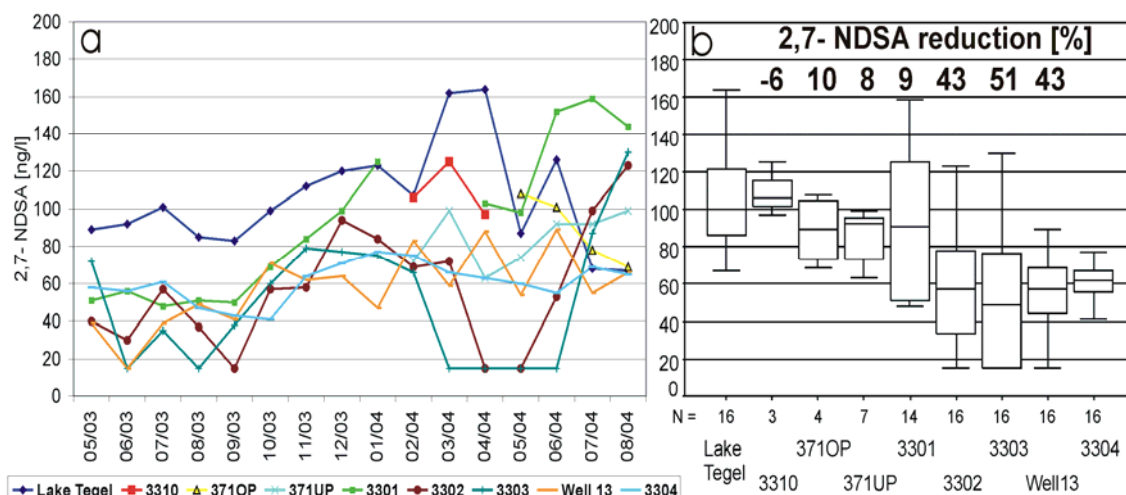
Figure 24 Fate of 2,7-NDSA during infiltration at the bank filtration site Tegel (a: time series; b: box plots)

Summarizing it was found that the X-ray contrast agent Iopromide was efficiently removed during bank filtration in Tegel. The other selected compounds, Sulfamethoxazole and the isomers of NDSA, were found in measurable concentrations in the production well. Concentrations ranged from 60-150 ng/l. Since raw water undergoes further treatment (aeration and rapid sand filtration for Iron and Manganese removal) and blending it is to be expected that the precaution value for anthropogenic organic contaminations in drinking water of the German Drinking Water Ordinance (100 ng/l) is not reached. Nevertheless, a further monitoring of the bank filtration field sites and the concentration in drinking water is advisable.

1.2　Lake Wannsee bank filtration site

The bank filtration field site Berlin-Wannsee was included in the monitoring program of the „Organics"-subproject within NASRI in May 2002. In the first part of monitoring the bank filtration transect Wannsee I at production well 4 was sampled. In February 2003 the drilling of transect Wannsee II was completed and the new transect provided a better insight into the processes at this field site because the distribution of monitoring wells allowed a better resolution of processes in the subsoil. From February 2005, the DWQC focused on the new transect at production well 3 and cancelled all measurements at the old transect. Therefore, the presented results refer mostly to the new transect Wannsee II as longer time series were measured here.

Investigations on the flow scheme of the bank filtrate at this field sites proved that only the upper part of the top aquifer is dominated by young bank filtrate. Monitoring wells with depth higher than ~15 m showed older bank filtrate with several years age which originates from distant infiltration areas. More detailed information on the flow scheme at transect Wannsee II is available in the hydrogeological section. After a screening of the field site of half a year it became clear that all deeper monitoring wells do not show any response to the changes in surface water and all parameter were mostly stable over this period. Short measurement series of the deep monitoring wells characterized the water in this part of the aquifer and data were used for dilution calculation in the abstraction well. Afterwards, the samples of the deep wells were not analyzed for AOX and trace compounds since these methods were too time-consuming, and results were stable and predictable. Investigations of the DWQC focused instead on the shallow monitoring wells (205, 206, 202OP, 203, and abstraction well 3) which were influenced by recent surface water and which showed the fate of bulk and trace organics during infiltration with subsequent retention times. The monitoring of abstraction and monitoring wells ended in August 2004, but sampling of surface water was continued until June 2005. Additionally, spatial variation of surface water in front of the transect was investigated in two sampling campaigns (March and July 2004). The DWQC analyzed these samples for bulk organic parameters.

Generally, the monthly analytical program was comprised, as at the Tegel field site, of DOC, UVA_{254}, UVA_{436}, LC-OCD, and differentiated AOX (adsorbable organic halogens e.g. AOI, AOBr)-analysis. Additionally, trace organic compounds were analyzed for a time period of 16 months. Trace compound analysis focused on X-ray contrast media (Iopromide); bacteriostatica (Sulfamethoxazole), and Naphthalenedisulfonates (1,5-NDSA; 1,7-NDSA; 2,7-NDSA). Results of the field monitoring are reported in the following chapters.

1.2.1 Lake Wannsee - Results bulk organics

1.2.1.1 Surface water Lake Wannsee

The amount and character of bulk organics in Lake Wannsee was monitored over the period May 2002 to June 2005 using the described analytical methods (DOC, UVA_{254}, UVA_{436} and SUVA (calculated)). Table 4 provides the arithmetic mean, median and standard deviation of 36 measurements which were conducted monthly.

Table 4 Results bulk organic parameters in surface water Lake Wannsee 2002-2005 (n=36)

	DOC	UVA_{254}	UVA_{436}	SUVA
	[mg/l]	$[m^{-1}]$	$[m^{-1}]$	[l/m*mg]
Arithmetic mean	7.1	16.0	0.46	2.25
Median	7.2	16.1	0.52	2.27
Standard deviation	0.8 (11.2%)	1.3 (8.1%)	0.10 (20.4%)	0.14 (6.2%)

Average DOC levels of Lake Wannsee are similar to the ones observed at Lake Tegel, but the variation with seasons was found to be more pronounced. At Lake Tegel, the standard deviation of a similar DOC-data pool was only half as high as at Lake Wannsee. The observed range of DOC-concentrations was 5.5 – 9 mg/l with a maximum variation of 3.5 mg/l. Considerably higher DOC concentrations were found in the summer months April to September. The average difference between summer and winter DOC–levels can be quantified with ~2 mg/l, which is twice as high as the average variance in Lake Tegel. Figure 25 confirms these results.
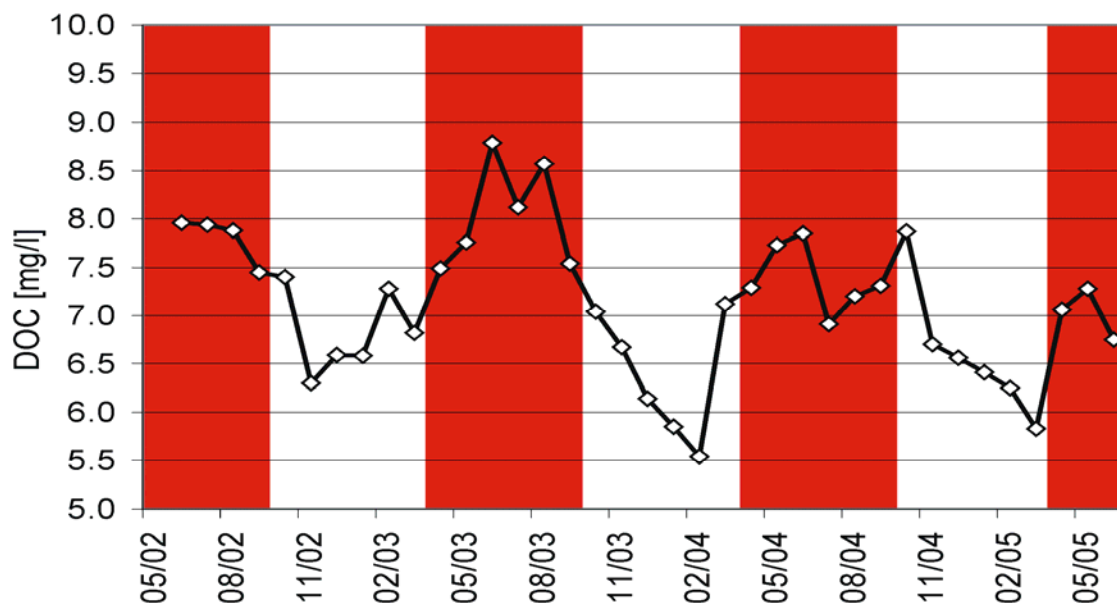
Figure 25 Time series of DOC concentration in Lake Wannsee

In Figure 25 the periods from April to September are marked, since during these times the WWTP Ruhleben discharges into the Teltow-Canal. During winter season, the treatment plant discharges into the Spree-River. Therefore, the waste water portion of the Havel water entering the lake from north is lower during summer. Earlier studies of the FU Berlin proposed that during summer water with a high portion of treated wastewater from the Teltow-Canal is entering Lake Wannsee from south through a chain of small lakes, influencing the water quality of Lake Wannsee. Until now it is unclear to which extend amount and character of organic water constituents in the lake change with this seasonal relocation of the point of discharge of WWTP Ruhleben. Of special importance is the changing waste water portion in front of the transect Wannsee. In order to quantify this effect and provide more insight into the seasonal distribution of the effluent organic matter in the lake, the DWQC took part twice in a surface water sampling campaign. The results of winter and summer campaign are shown in Figure 26 and Figure 27.
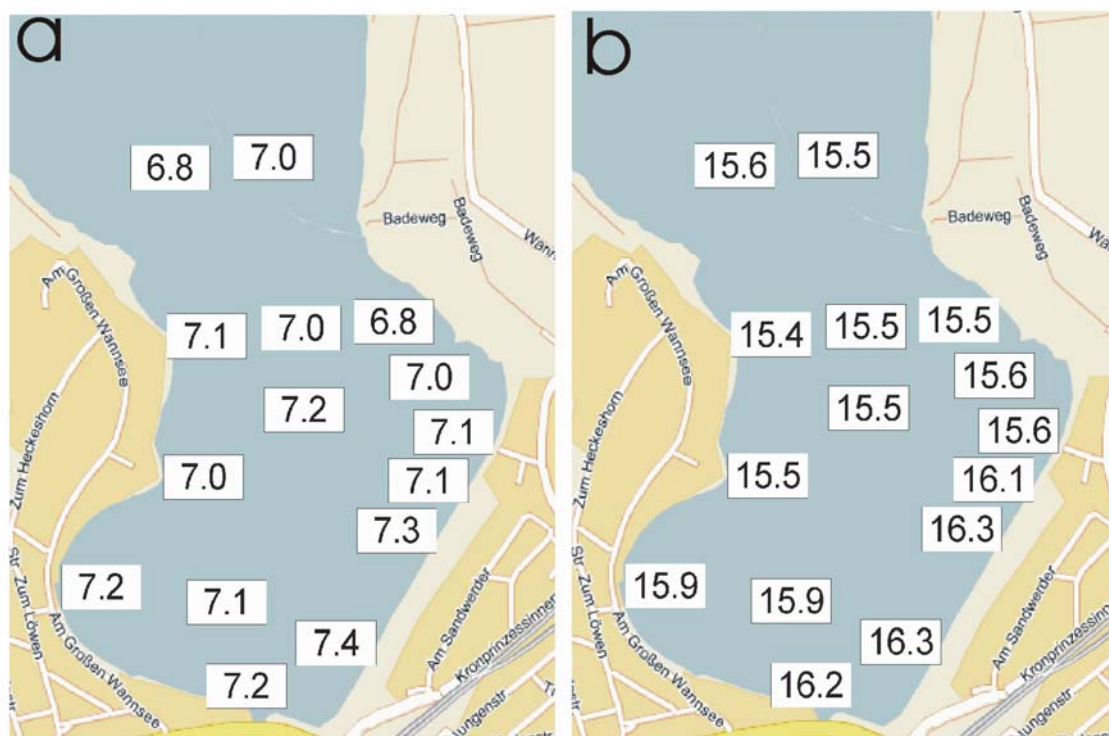
Figure 26 Distribution of DOC (a; mg/l) and UVA254 (b; m^{-1}) in Lake Wannsee in March 2004

Figure 26 provides results of the winter sampling. The DOC and UVA_{254} results show higher concentrations of organics in the south east of the lake in agreement with results of the hydrogeology group (electrical conductivity, MTBE concentration). The elevated concentrations are probably due to an influence of treated wastewater from the Teltow-canal. Concentrations are only slightly higher (~0.3 mg/l DOC and ~0.5 m^{-1} UVA_{254}) in this area, but in combination with the inorganic parameters the results confirm the theory of an influence of Teltow-canal water on Lake Wannsee. In this case the bulk organics are not really an appropriate tracer for WW influence since the concentration difference between treated waste water and unaffected water is low. Unfortunately, trace organic analysis of this samples were not conducted at the DWQC. But the differentiated AOX-results (chapter 1.2.3.1) and the Chapter XX (drug section) will give more insight into spatial distribution of trace organic substances in Lake Wannsee.

Figure 27 shows results of the summer sampling. During this campaign, the elevated concentration of treated wastewater on the south east bank of the lake could not be confirmed. Apart from one sampling point on the west bank of the lake (slightly elevated DOC and UVA_{254}) all sampling points showed comparable bulk organic results. Additionally, in both sampling campaigns a depth-profile (0; 2; 4; 6; and 7 m) in the middle of the lake was analyzed for bulk organic parameters. It was found that at this time no considerable variations occurred and that no pronounced depth-profile existed.
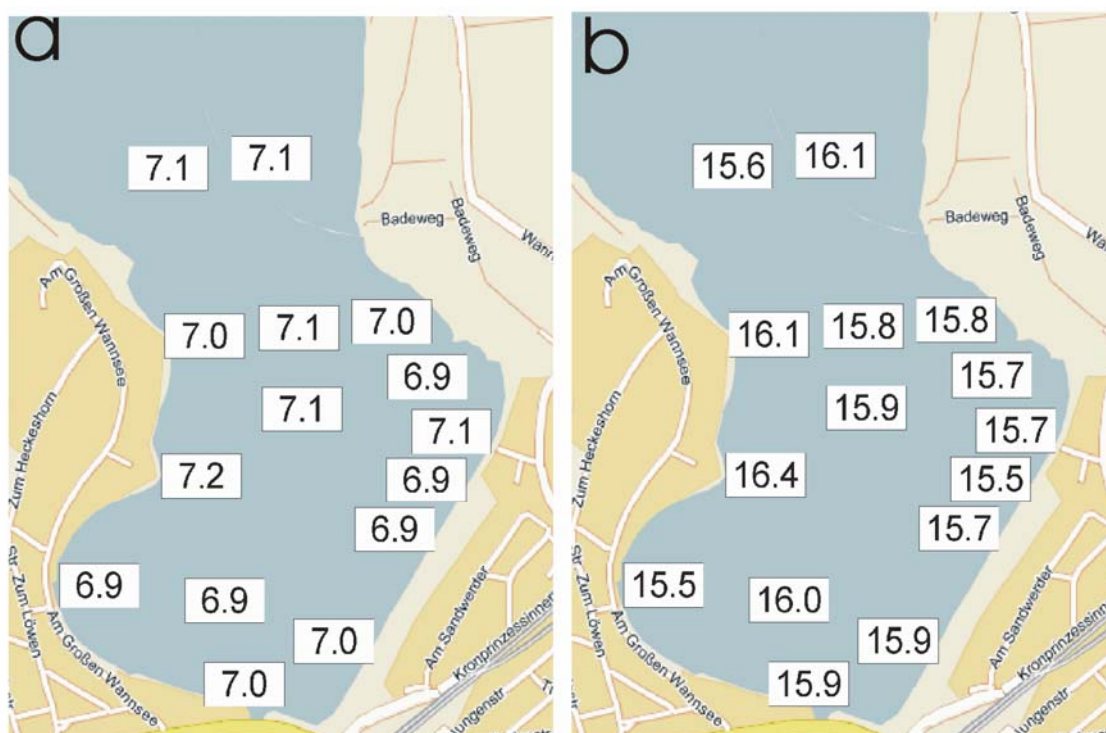
Figure 27 Distribution of DOC (a; mg/l) and UVA$_{254}$ (b; m^{-1}) in Lake Wannsee in July 2004

The limited output of the surface water sampling regarding the bulk organics is also reasoned by the fact that neither March 2004 nor July 2004 were characteristic months (based on bulk organics time series) for the winter or summer situation in the lake. This is evident after comparing the measured DOC concentrations of both sampling events, which are approximately the same. Figure 25 shows that a comparison of the situations in February 2004 and June 2004 would have resulted in more information output, since the characteristic seasonal changes of the bulk organics were more pronounced at this time. More details of this investigation on the spatial distribution of waste water influence are presented in the hydrogeological section. Summarizing, the hydrogeology group assumes a higher wastewater portion in front of the transect during summer because of a lower water flow in the main rivers entering Berlin (Spree, Havel). This leads to less dilution of the discharged treated effluent. Consistently, the DWQC observed higher DOC concentrations during summer (Figure 25).

However, the strong variations in DOC can not only be ascribed to the changing influence of the treated wastewater. It is unlikely that the seasonal variable point of discharge of WWTP Ruhleben cause a variation within surface water DOC concentration in front of the transect of 2 mg/l. It can be assumed that the major part of additional DOC during summer is associated with annual algae blooms. Since the phosphate concentration in Lake Wannsee is considerably higher than in Lake Tegel (phosphate elimination plant in operation), annual algae blooms are much stronger.

Another difference between Lake Wannsee and Lake Tegel is that the enforced operation of the lake pipeline during summer leads to an inverted situation in Lake Tegel. There, the proportion of treated wastewater is, directly opposed to Lake Wannsee, higher during winter.
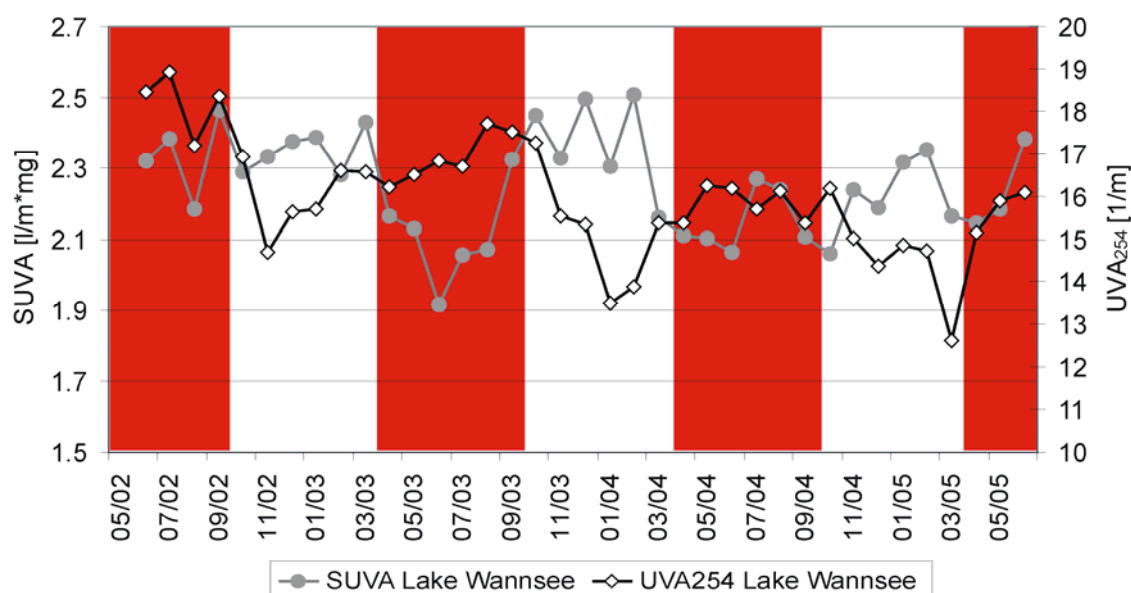
Figure 28 UVA$_{254}$ and SUVA of Lake Wannsee surface water

UV-absorption at 254 nm of Lake Wannsee samples was only slightly higher than the UVA of Lake Tegel samples, with a similar range of variation (13 to 19 m^{-1}) (Figure 28). In Lake Wannsee, higher UV-absorption was observed during the summer months indicating a reversed schedule for seasonal changes of UVA$_{254}$ compared to Lake Tegel. This is explained by the mentioned higher wastewater portion during summer and the artificially reversed situation at Lake Tegel. In Lake Wannsee, seasonal changes of UVA$_{254}$ correspond to the DOC variations, whereas DOC variations are more pronounced. This is due to aliphatic DOC fractions which are produced during strong algae blooms which do not affect the UVA$_{254}$. This effect is visible by calculating the SUVA, a measure for aromaticity of DOC. Figure 28 shows that the SUVA is lower during summer, confirming a higher share of aliphatic carbon's during summer. Therefore, it can be assumed that a great share of additional DOC during summer is associated with algae organic matter.

Generally, the average SUVA in Lake Wannsee (2.27 l/m*mg) is slightly higher than in Lake Tegel (2.09 l/m*mg) proposing that aromatic DOC fractions are more important. It is unclear whether this is a sign of a higher average portion of treated wastewater in front of the transect or whether this is due to other unknown effects. Generally, treated wastewater in Berlin has an average SUVA of 2.4 l/m*mg (Bahr, 2005).

However, it can be summarized that the concentration and character of bulk organic matter in Lake Wannsee is more variable than in Lake Tegel with strong seasonal

trends. This is mostly due to summery algae blooms and higher waste water portions during summer. The influence of seasonal relocation of the point of discharge of WWTP Ruhleben was not clearly visible in organic bulk parameter time series. Furthermore, the surface water sampling events gave no clear insight into spatial variation of organic water constituents. Due to the unclear spatial distribution of water quality in Lake Wannsee it needs to be clarified that all presented time series only reflect the conditions in front of the investigated bank filtration transect Wannsee II.

1.2.1.2 Bank filtration - DOC

Results from February 2003 to June 2004 are presented for the bulk organics at transect Wannsee II. The data is illustrated as time series and box plots, similar to the presentation in chapter 1.1 (Tegel bank filtration). It is essential to understand that only the top part of the aquifer is influenced by recent bank filtrate. The data evaluation will focus on this part of the aquifer, but will also include an overview of the concentration and character of bulk organics in deeper parts of the aquifer and the background groundwater. The most important flow path of actual bank filtrate considered at Wannsee II runs from surface water subsequently along the monitoring wells 205, 206, 202OP, and 203 towards the production well 3. Along this infiltration path it is assumed that nearly no dilution with deeper groundwater takes place. The proportion of older groundwater increases with depth in the deeper monitoring wells 202MP1, 202MP2, and 202UP. In 202MP1, a partial influence of actual surface water was observed, whereas 202MP2 and 202UP are exclusively dominated by older water (bank filtrate) that infiltrated years ago. Two monitoring wells on the landside of the production well, 204OP and UP, were also included within the monitoring. The production well 3 is a multilevel well which pumps only 20-25% young bank filtrate (retention time 3-4 months) because it abstracts water from different aquifers. Therefore, all information about amount and composition of organics in these aquifers will be included. More information of the hydrogeological situation at this field site is provided in the hydrogeological section.

An interesting feature of the field site Wannsee II is the comparison of the two monitoring wells 205 and 206. These wells are comparable regarding position and retention time (0.5-1 month) but belong to different redox zones. The dominant redox conditions depend on various factors of influence and affect the microbial activity. At the water-sediment interface of the bank region of Lake Wannsee water infiltrates under oxic conditions. Depending on the position in the lake, the infiltration takes place under more saturated conditions (monitoring well 205) or under unsaturated conditions (206). Under more saturated conditions, the mineralization of aqueous DOC and sedimentary bound POC during infiltration leads to a depletion of oxygen and nitrate (205) and a decreasing redox potential. Higher temperatures during summer intensify this process. Under unsaturated conditions, no depletion of O_2 and NO_3 occurs

because of the close contact of the water to the interstitial air and the redox potential remains high. Therefore, a comparison of the two wells gives insight into the different effects of an oxic or anoxic/anaerobic infiltration. During further infiltration along the top of the upper aquifer oxygen is delivered to the bank filtrate continuously from the water - soil air interface since the water level varies depending on the pumping schedule of BWB. The infiltration along 202OP and 203 to production well 3 (70 m, 3-4 months) can be regarded as an oxic infiltration.

Contrary to the field site Tegel, strong seasonal surface water variations of organics influence the conditions in the subsoil. Especially, in the monitoring wells near the bank the seasonal variations of the surface water are visible. Figure 29 shows that monitoring well 205 and 206 follow the trend of surface water and show similar variations of DOC-concentration of more than 2 mg/l. In monitoring well 202OP and 203 the variations are observable as well, but with smaller amplitudes. DOC concentration in production well 3 is stable around 3.5 - 4 mg/l proving that only a small percentage originates from the flow path of the recent bank filtrate.
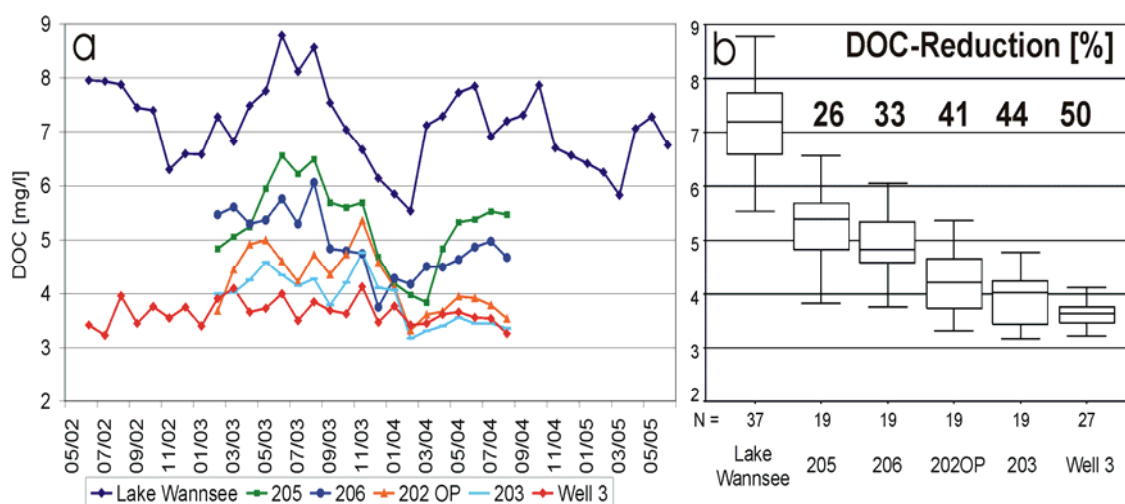
Figure 29 Fate of DOC during infiltration along transect Wannsee II (a: time series; b: box plots)

Figure 29 proves that along the infiltration path the concentration of organic compounds decreases considerably. Consistently with results from other field sites, the initial infiltration zone is very important and accounts for the largest step in DOC mineralization. Between 26 and 33 percent of the surface water DOC are removed within two to four weeks of infiltration to monitoring well 205 and 206. During the more oxic infiltration to well 205 seven percent more DOC are mineralized, supporting the theory of a faster DOC removal under oxic conditions. The further infiltration path constitutes a very long oxic infiltration of nearly 3-4 months. Such a long oxic infiltration was unique in the field sites selected by NASRI. At the bank filtration site in Tegel, the main infiltration path guides the water in the anoxic/anaerobic second aquifer and at the artificial groundwater recharge facility in Tegel retention times are only ~50 days.

Therefore, the long oxic infiltration provided interesting results on the long time behavior of organics under oxic conditions. It was found that after 2 - 4 months of infiltration (202OP and 203), 41 and 44 percent of the surface water DOC was degraded (Figure 29). The corresponding infiltration path was 23 m or 38 m long. Therefore, the infiltration velocity within the subsoil is relatively slow with 0.32-0.45 m/d (Tegel: ~0.75 m/d; GWR: ~2.2 m/d). The observed mineralization rate of 41-44% is higher than mineralization rates at the other field sites. In Tegel, it was found that 34-39% of the DOC was removed and ~40% at the groundwater recharge facility. The increased DOC removal might be due to two effects: first a different composition of the surface water DOC and secondly the long oxic soil passage. LC-OCD analysis and the high seasonal variance in the DOC time series showed that in Lake Wannsee algae associated organic compounds account for a higher percentage of total DOC than in Lake Tegel. It is known that these so called polysaccharides are easy degradable. Therefore, this could add to an increased mineralization rate and result in a difficult comparison of mineralization rates with the Tegel field sites. The effect of a very long oxic infiltration path is not investigated sufficiently. Results from the groundwater recharge facility and long term soil column experiments proposed that under oxic conditions a fast removal of degradable organic carbon is followed by stable conditions, where the non-degradable fraction of DOC remains in the water. But these results where obtained from field sites and experiments with retention times of 30-50 days. It might be possible that very slow transformation processes of this operationally-defined non-degradable DOC-fraction lead to a further mineralization under oxic conditions, which is only recognized during very long time frames.

In production well 3, the DOC concentration remained relatively stable between 3.5-4 mg/l during the monitoring period. This was expected because actual bank filtrate accounts only for a small portion of the abstracted water. Most of the water originates from the lower part of the top aquifer, from the second and third aquifer and from background groundwater. As part of the monitoring program, the organic composition of water from the lower part of the second aquifer (202MP2 and 202 UP) and background groundwater (204OP and 204 UP) were analyzed. Groundwaters from the second and third aquifer (second: 3334; third: 3332 and 3336) were sampled only once in March 2004 to obtain information which are necessary for calculation of the mixing proportions in the production well.
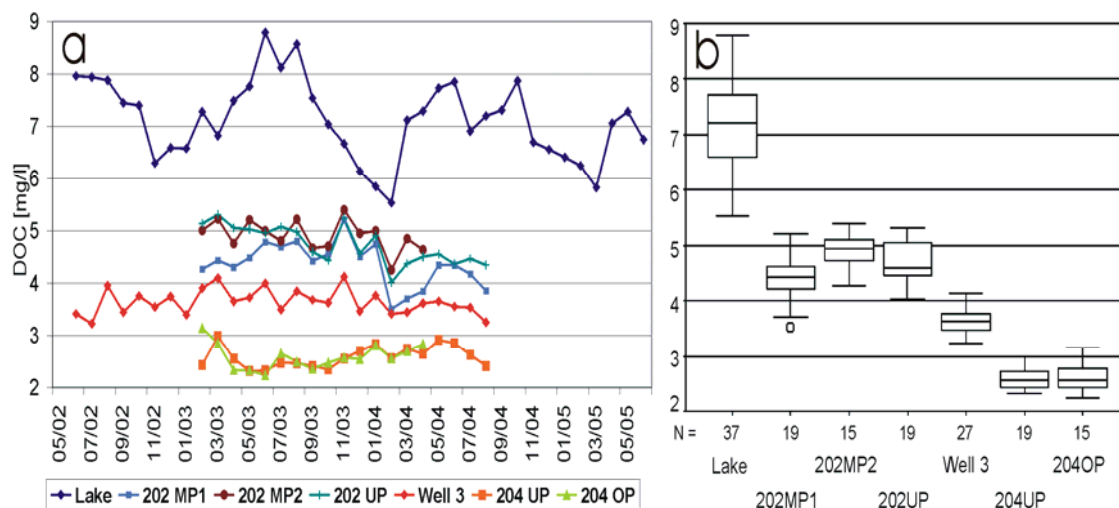
Figure 30 DOC concentration in deeper monitoring wells and background wells at transect Wannsee II (a: time series; b: box plots)

Figure 30 shows that in the deeper part of the top aquifer the influence of surface water declines with depth. No removal rates are given because for all water types the corresponding surface water concentration is not known. Monitoring well 202MP1 shows some of the variations of surface water. Furthermore, some other organic parameters indicated that this well is under certain circumstances under the influence of the surface water. The deeper wells 202MP2 and 202UP show relatively stable DOC concentrations of around 4.5-5.5 mg/l. These wells are representative for a stream of older bank filtrate with an age of ten years to some decades (hydrogeological section). The fact that the DOC concentration in these wells is relatively high, compared with young bank filtrate after 3 months retention time, might indicate that the portion of non-degradable DOC in the surface water was higher at time of infiltration.

Stable DOC-concentrations of 2.3-3 mg/l were observed in the background groundwater. The more shallow well 204OP (8 m deep) behaved similarly to well 204UP (18 m). Therefore, the average concentration in background water can be quantified with ~2.6 mg/l.

Groundwater from deeper aquifers was only analyzed once by the DWQC. Table 5 gives results of the DOC quantification and proves that the concentration of organic water constituents is very low in the second and third aquifer. Since it can be assumed that the DOC concentration in the deep aquifer is stable and not prone to any variations, this screening can be included into the mixing calculations for the production well.

Table 5 Results DOC quantification in aquifer 2 and 3 at field site Wannsee

	3332	3334	3336
	[mg/l]	[mg/l]	[mg/l]
Aquifer	3	2	3
DOC	1.9	1.9	1.8

Altogether, the mixing calculations for production well 4 are based on four different fractions of water. These are young bank filtrate (203, Ø-DOC: 4.0 mg/l), older bank filtrate (202MP2, Ø-DOC: 4.9 mg/l), background groundwater (204UP, Ø-DOC: 2.6 mg/l), and very deep groundwater (3332, Ø-DOC: 1.9 mg/l). The ratio proposed by the hydrogeological group (23% young BF, 34% old BF and 43% deep and background groundwater) would lead to a theoretical DOC concentration in production well 3 of 3.55 mg/l, which is very close to the measured average DOC level of 3.6 mg/l. Therefore, the conducted DOC measurements support the results calculated by the hydrogeological group.

Compared with the bank filtration at Lake Tegel, DOC concentration within the raw water (3.6 mg/l) is slightly lower (Tegel: 4.2 mg/l). This derives mainly from the higher portion of deep groundwater, which is poor in organics. As in Tegel it is assumed that the portion of BDOC in the abstracted water is very small and regrowth potential is expected to be negligible.

1.2.1.3 Bank filtration - UVA$_{254}$

UV-absorption at 254 nm of the water samples was monitored during the same time period. It was found that during the infiltration of 3-4 months approximately 40-45% of UV-absorbing aromatic and double bond structures are removed. This is comparable to DOC removal rates but for certain monitoring wells strong differences between the removal of DOC and UVA have been observed.

Figure 31 shows that the different redox conditions in monitoring well 205 and 206 influence the removal efficiency for aromatic organic compounds. For the more oxic well 206, UVA$_{254}$ follows the trend in surface water and the removal is constant at three to five absorption units throughout the year. Overall, the average UV-absorption in 206 is 29% lower than in surface water. In monitoring well 205, the UVA$_{254}$ shows a very strong seasonal variation which might be connected to the redox system of this monitoring well. During summer, 205 is completely anaerobic with no oxygen and nitrate detectable. Figure 29 proves that during these periods still 2 mg/l DOC are removed during two to four weeks of infiltration to 205. Results of the UVA monitoring show that during summer nearly no removal of aromatic compounds in 205 takes place. This proposes that the 2 mg/l of removed DOC are of aliphatic nature. Since a preferred removal of aliphatic compounds under anaerobic conditions is not consistent with results from other field sites and literature, it is more likely that this strong

seasonality in monitoring well 205 is due to an already mentioned temperature effect. Monitoring well 205 is located inside the lake, approximately 10 m farer from the bank as well 206. Investigations of the hydrogeological group on the character of the lake sediments revealed an irregular distribution of sediments with high organic contents (up to 10%) and sediments with lower organic matter content (chapter XX Hydrogeo Wannsee). With increasing depth of the lake, a thicker organic layer developed. Therefore, it can be assumed, that the weak UVA removal during summer in 205 is due to desorption of organic material from lake sediment material. It is described in literature (Schoenheinz, 2004) that increased temperature leads to desorption of aromatic material which was part of sediment before or was sorbed to the inorganic material during periods of low temperature. Schoenheinz (2005) observed this effect at bank filtration sites at river Elbe. Monitoring well 205 is probably more effected than well 206 because the organic content of the sediments is higher in greater distances from the bank.

The decrease in UV-absorption potential in monitoring well 202OP and 203 complies with the observed DOC removal rates. A comparison of UVA and DOC removal rates for the production well (UVA: 42%; DOC: 50%) proposed an increased aromaticity of other water fractions that are abstracted by well 3.
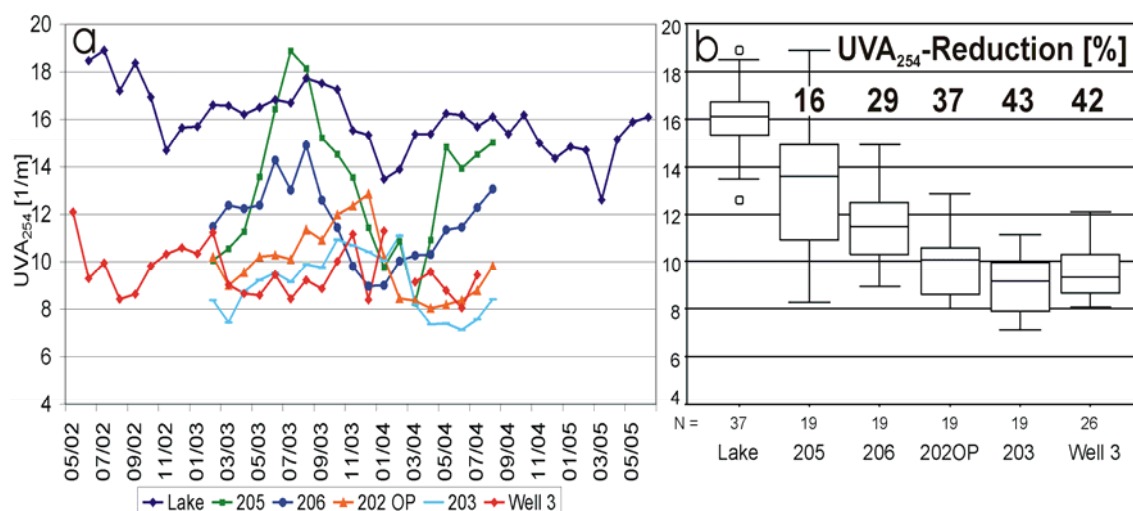
Figure 31 UVA$_{254}$ during infiltration along transect Wannsee II (a: time series; b: box plots)

UV-absorption results for the monitoring well cluster 202 (MP2, MP2 and UP) reveal consistent with the DOC results a decreasing seasonality with increasing depth (Figure 32). Only well 202MP1 shows a seasonal variance that can be compared with the trends in the shallow monitoring wells. Overall, the UV absorption of old bank filtrate is slightly higher than the UVA$_{254}$ of the young bank filtrate after infiltration. These results confirm the findings of DOC analysis. The increase of UVA$_{254}$ in monitoring well 202MP2 in winter 2003/04 could not be explained.

The background groundwater exhibits a very low UV-absorption with an average absorption of four to six absorption units (Figure 32). Some of the extremely high values of monitoring well 204UP might be due to analytical problems, which occur for strongly anaerobic iron containing samples. No seasonality was observed.
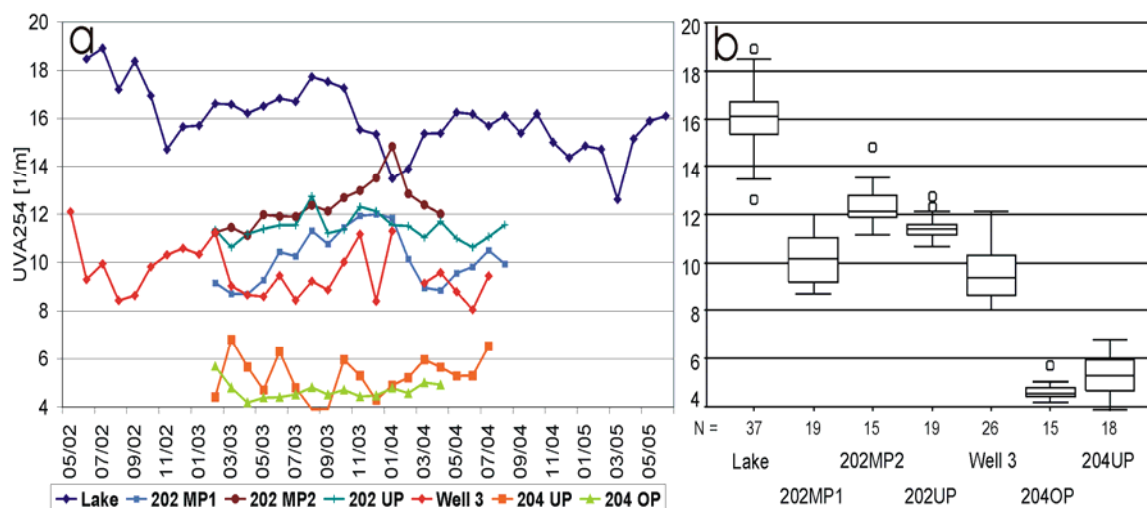
Figure 32 UVA$_{254}$ in deeper monitoring wells and background wells at transect Wannsee II (a: time series; b: box plots)

UVA$_{254}$ in the second and third aquifer was assessed with 4.5 to 6.5 absorption units. The calculation of UVA$_{254}$ of the production well based on the fractionation of the hydrogeological group would result in an absorption of 8.6 m^{-1}. This is similar to the measured average absorption of 9.4 m^{-1}.

Measurements of color at 436 nm were conducted. The low color of surface water (0.6 m^{-1}) was diminished during infiltration to values of 0.3-0.4 m^{-1}. Since these results are close to the detection limit no interpretation and conclusion arose from the conducted measurements.

1.2.1.4 Bank filtration - SUVA

The SUVA as a measure of aromaticity of organic carbon was calculated from the monitored DOC and UVA$_{254}$. It was found that, similarly to the effects observed in Tegel, the aromaticity increases shortly after infiltration and reduces during further infiltration. The average SUVA of the surface water of Lake Wannsee is ~2.3 l/m*mg (Figure 33). In the monitoring wells near the bank (205 and 206) the share of aromatic organic material on the total DOC rises and the average SUVA increases to 2.5 or 2.4, respectively. In 205, some of the high SUVA results were measured in summer when UVA results indicated a temperature driven desorption of aromatic carbon. However, after an initial increase the SUVA reduces along the flow path in monitoring well 202OP and 203. In well 203 the SUVA drops to 2.2 l/m*mg and is lower than in surface water.

This sequence is probably due to a preferred initial degradation of aliphatic compounds and a subsequent mineralization of degradable organics. It was similarly observed at bank filtration site Tegel.

The higher SUVA in the production well exhibits again that the abstracted water is a mixture of different fractions. Judging from the product water, the majority of source fractions is characterized by a higher aromaticity than the surface water. Since the SUVA of the source fractions is assumed to be relatively constant, the high variation of SUVA in the production well indicates variations in the composition of raw water (changing proportions of source fractions).
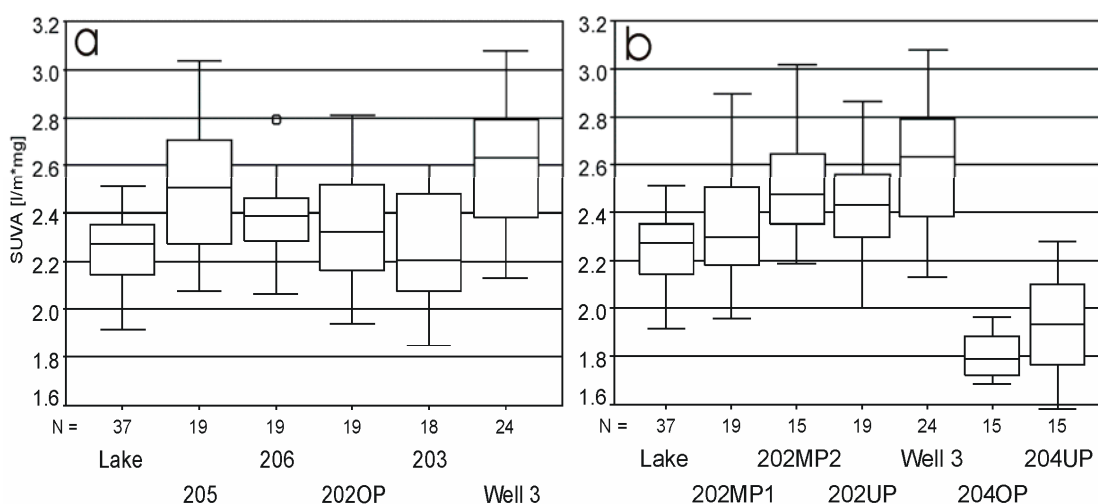
Figure 33 SUVA during infiltration to production well 3 (a: young bank filtrate; b: deeper wells and background groundwater)

Figure 33b shows that the fraction of older bank filtrate in the deeper part of the top aquifer is characterized by a high aromaticity and a SUVA of 2.4 to 2.5. Only for 202MP1, a lower SUVA was calculated because of an increased influence of young bank filtrate. However, observed results prove that the important fraction of long term bank filtrate from under the lake adds to the higher SUVA of the production water. The background groundwater is represented by monitoring well 204OP and UP, which exhibit a reduced importance of aromatic organics and a very low SUVA of 1.8 - 1.9 l/m*mg.

Investigations of the water from deeper aquifers resulted in SUVA calculations of 2.5 to 3.5 l/m*mg for the monitoring wells 3332, 3334, and 3336. Therefore, the aromatic character of carbon in the product water is mainly derived from the influence of old bank filtrate and very deep groundwater.

1.2.2   Lake Wannsee - LC-OCD

1.2.2.1 Surface water - LC-OCD

During the observation period, samples from Lake Wannsee were analyzed by the LC-OCD technique which was explained more detailed in chapter 1.1.2 and the methodology section. The chromatograms give an insight into the composition of dissolved organic carbon. For evaluation purposes, the chromatograms were adjusted for retention time and baseline. The surface water was characterized by more than 20 monthly measurements of water samples from the lake in front of transect Wannsee II and two large scale surface water sampling events in March 04 and June 04. Monthly measurements give insight into any seasonal changes of the DOC-fractions and the surface water screening was conducted to reveal spatial differences across the lake.

Results of the monthly surface water sampling are presented in Figure 34. Unfortunately, some unreliable results had to be excluded from the evaluation process. Overall, thirteen measurements were mediated and pooled into groups that represent summer stage of Lake Wannsee or winter stage. The new results explain the findings of the DOC quantification and show consistently which seasonal changes of bulk organic composition occur in the lake.
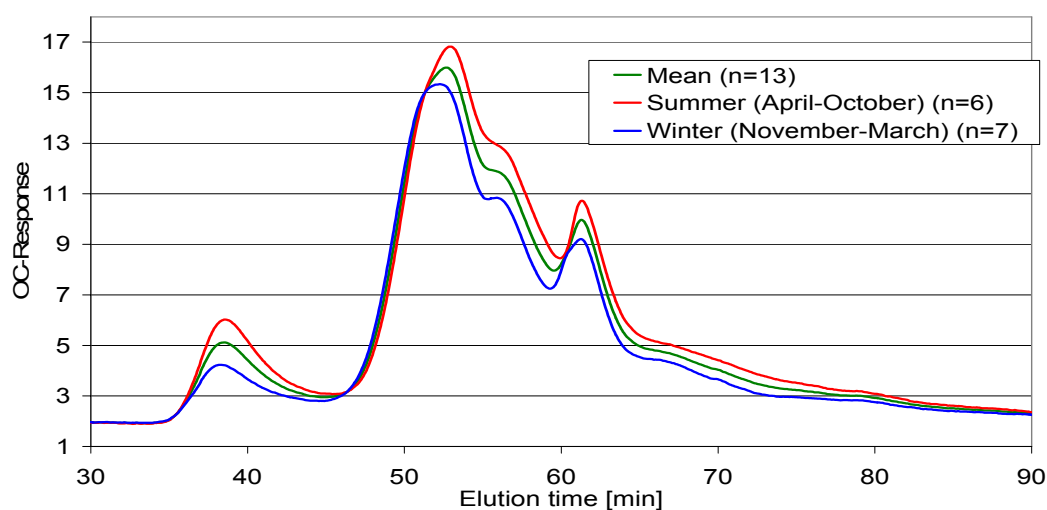
Figure 34 LC-OCD chromatogram of Lake Wannsee surface water (seasonal changes)

The general DOC composition, which is represented by the graph "Mean" in Figure 34, is similar to the bulk organics composition in Lake Tegel. The fractions were quantified by integration of the chromatograms and account for comparable proportions and absolute concentrations (Table 6). A slightly higher concentration of humic substances occurred in Lake Wannsee, whereas the fraction of neutrals and hydrophobics was less important. These variations are very close to the limits of the method and are therefore not interpreted. However, the most important fractions in Lake Wannsee

surface water are humic substances (~48%), humic substances-building blocks (~22%) and neutrals (~18%).

The seasonal variations followed partly a different scheme as at Lake Tegel. Consistently with Lake Tegel surface water, the importance of polysaccharides increased during summer. In Lake Wannsee, the differences between summer and winter were even more pronounced. This can be explained by stronger algae blooms during summer that are not nutrient-limited as in Lake Tegel.

Regarding the other fractions, an increase in concentration of all fractions was observed. This is consistent with the strong seasonal variation of total DOC and proofs that not algae blooms alone are responsible for the changing DOC. Another very important factor of influence is the already mentioned dilution effect. During winter, precipitation and higher water levels lead to lower concentrations of all DOC-fractions. This was evidently shown by the presented results for Lake Wannsee. In Lake Tegel, this effect was not clearly visible because heavy pumping of the lake pipeline during summer leads to an artificial situation, which is not representative for Berlin surface water.

However, the evaluation of the changing proportions of DOC-fractions reveals similarities between the field sites Tegel and Wannsee. Although the concentration of humic substances increased slightly during summer (Table 6) the proportional share decreases from ~51% to ~44%, because of a considerably higher total DOC during summer. During summer the proportional share of polysaccharides, HS-building blocks, and neutrals are increased, which is most probably due to a more active biomass. A transformation of humic material into smaller molecules is boosted by higher temperatures.

A minor influence that could not be quantified could result from the seasonal change of the point of discharge of treatment plant Ruhleben. But a major influence is unlikely since these effects of changing proportional shares were similarly observed at field site Tegel.

Table 6 Portions and concentrations of different fractions of DOC in Lake Wannsee – Seasonal Differences (Summer= April-October; Winter= November-March)

Share of	Poly-saccharides	Humic substances	Humic substances-Building blocks	Low-molecular acids	Neutrals and Hydrophobics
Summer (n=6)	10.7 %	43.8 %	23.2 %	3.2 %	19.1 %
	0.82 mg/l	3.33 mg/l	1.76 mg/l	0.24 mg/l	1.45 mg/l
Winter (n=7)	7.2 %	50.5 %	22.0 %	4.3 %	15.9 %
	0.47 mg/l	3.25 mg/l	1.41 mg/l	0.28 mg/l	1.03 mg/l
Mean (n=13)	8.8 %	48.3 %	21.9%	3.5 %	17.6%
	0.63 mg/l	3.44 mg/l	1.56 mg/l	0.25 mg/l	1.26 mg/l

Investigations of the spatial variation of the DOC composition in Lake Wannsee at two different times in summer and winter exhibited that no measurable variation at a time was present. More than 20 LC-OCD chromatograms that were recorded in March 2004 and June 2004 showed exactly the same DOC composition which complied with the monthly measured sample in front of the transect. This would point towards a well mixed surface water and is consistent with the low variation of the total DOC-concentrations. However, in reality it shows that the LC-OCD technique is not qualified for tracing the influence of treated wastewater in Berlin surface water. Drewes and Fox (2000) showed that the DOC composition of a treated wastewater can be traced back to the DOC composition of the associated drinking water. Since in Berlin the drinking water source is mainly surface water with the intermediate step of bank filtration, no considerable differences between surface water and well treated waste water can be expected. Therefore, the LC-OCD technique is not appropriate to solve the quest of the spatial variation of wastewater influence. Nevertheless, the results confirmed the monthly measurements and show a spatial uniform organic composition in Lake Wannsee surface water.

1.2.2.2 Bank filtration - LC-OCD

Concentration and character of DOC changed during the process of bank filtration. LC-OCD analysis reveals the fate of different bulk organic fractions. At field site Wannsee, two problems influence the final organic composition of the abstracted water: First, the fate of organics during actual bank filtration along the upper part of the top aquifer and secondly, the mixing of different water types in the production well. Both issues were addressed during the observation period by characterizing organics on the flow path of young bank filtrate and determining the organic composition of the different sources of the final raw water.

Figure 35 presents the different LC-OCD chromatograms for the monitoring wells on the flow path of the recent bank filtrate. The results are comparable with the findings of the evaluations at field site Tegel. Similarly, the fraction of polysaccharides was removed most efficiently. The polysaccharides account in Lake Wannsee for ~9% of the surface water DOC, with higher portions during summer. At transect Wannsee II, a breakthrough of measurable amounts of polysaccharides was only found once (January 2004) in monitoring well 206. All other chromatograms indicated a complete removal of this fraction in all monitoring wells and no seasonal effects could be observed. In Tegel, the polysaccharides occurred during winter in the shallow wells close to the bank because the microbial activity was minimal due to low temperatures. At Transect Wannsee II, the infiltration path to monitoring well 205 and 206 is longer (5-6 m, Tegel 3310 and 3311: 2-3 m) and even at low temperatures nearly no polysaccharides break through to the monitoring wells.
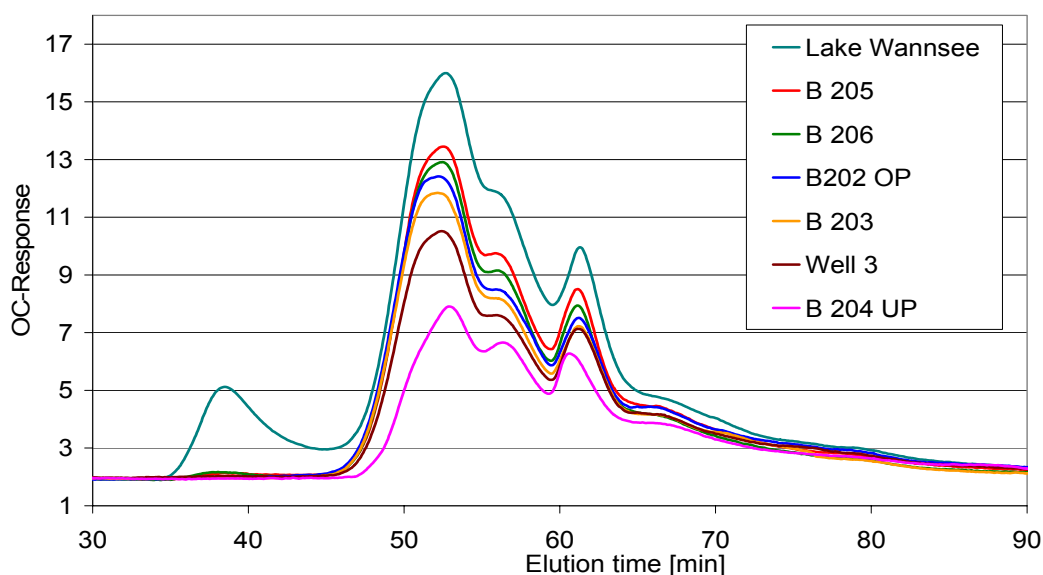
Figure 35 LC-OCD chromatograms of transect Wannsee II (mean, n=10)

All other fractions exhibited a partial removal similar to the observations at transect Tegel. Removal rates of humic substances, HS-building blocks, low molecular acids, and neutrals were found to range from 33-40%, which is slightly higher than in Tegel. This is consistent with results of the DOC analysis and most probably caused by the long oxic infiltration path. The calculation of removal rates is based on the comparison of the surface water and monitoring well 203 (Table 7). The proportions of the different fractions changed slightly because of the complete removal of the polysaccharide fraction. Table 7 shows that during mineralization of polysaccharides the importance of the fractions of HS-building blocks and neutrals increased considerably, whereas the proportion of the humic substances remained nearly stable. But the absolute concentration of all DOC-fractions declined along the infiltration path (Figure 36). However, a comparison of the monitoring wells 3303 in Tegel and 203 in Wannsee reveals that the DOC composition after soil passage is very similar and that only the absolute DOC concentration is slightly lower in monitoring well 203. Therefore, it can be concluded that the processes in the subsoil in Tegel and Wannsee are comparable. The difference in redox chemistry seems to influence mostly the quantity of DOC mineralized. Since all bank filtration processes that influence the DOC-composition and which can be assessed by LC-OCD were included in the discussion of the field site Tegel (Chapter 1.1.2.2. Tegel bank filtration) the following evaluation will focus on the effects of mixing in the production well.

Table 7 Portions and concentrations of different fractions of DOC at transect Lake Wannsee (n=10)

Share of	Poly-saccharides	Humic substances	Humic substances-Building blocks	Low molecular acids	Neutrals and Hydrophobics
Lake Wannsee	8.8 %	48.3 %	21.9%	3.5 %	17.6%
	0.6 mg/l	3.5 mg/l	1.6 mg/l	0.3 mg/l	1.3 mg/l
205	0.3 %	49.4 %	26.1 %	4.3 %	19.9 %
	0.0 mg/l	2.7 mg/l	1.4 mg/l	0.2 mg/l	1.1 mg/l
206	0.1 %	52.9 %	24.8 %	4.3 %	17.8 %
	0.0 mg/l	2.6 mg/l	1.2 mg/l	0.2 mg/l	0.9 mg/l
202OP	0.0 %	48.2 %	24.5 %	3.7 %	23.6 %
	0.0 mg/l	2.0 mg/l	1.0 mg/l	0.2 mg/l	1.0 mg/l
203	0.0 %	51.0 %	25.2 %	4.0 %	20.2 %
	0.0 mg/l	2.1 mg/l	1.0 mg/l	0.2 mg/l	0.8 mg/l
Well 3	0.0 %	45.8 %	24.7 %	4.5 %	24.9 %
	0.0 mg/l	1.7 mg/l	0.9 mg/l	0.2 mg/l	0.9 mg/l
204UP	0.0 %	39.5 %	28.4 %	4.4 %	28.6 %
	0.0 mg/l	1.0 mg/l	0.7 mg/l	0.1 mg/l	0.7 mg/l

Figure 37 gives an insight into the differences in DOC composition of the different source waters of production well 3. The previously discussed portion of young bank filtrate is comparable to the fraction of old bank filtrate in the deeper part of the top aquifer (202MP2 and 202UP). Both source waters are characterized by high DOC concentrations and a similar proportion of humic material (~50%). These similarities support the findings of the hydrogeology group that both water types are derived from Lake Wannsee surface water.

The background groundwater contains lower concentrations of DOC. In comparison with the surface water influenced bank filtrate, the proportions are shifted from the fraction of HS to HS-building blocks and neutrals. This effect is more dominant than in Tegel and is interesting since commonly the fraction of humic substances is regarded as mostly non-biodegradable and stable.
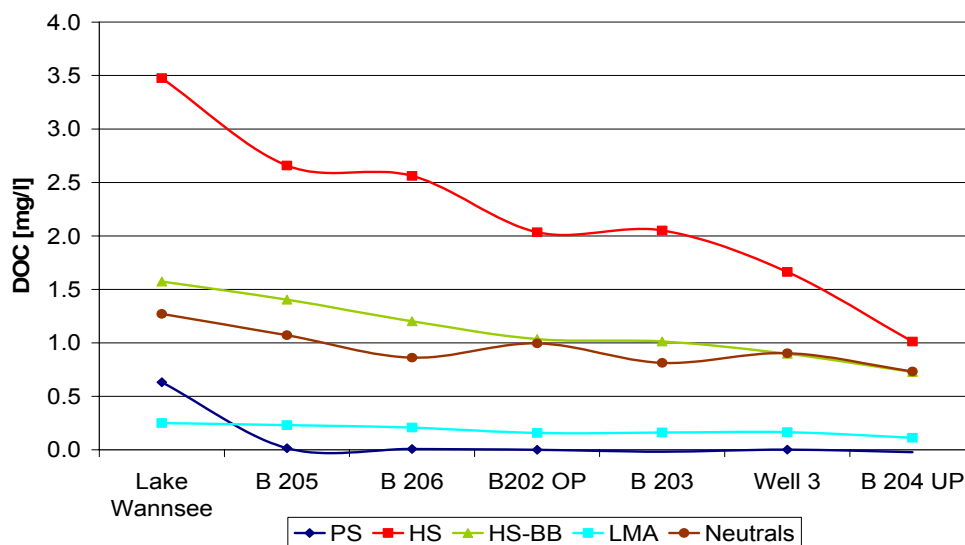
Figure 36 Concentration of different fractions of DOC along the infiltration path at transect Wannsee II

Unfortunately, sources and origin of the background groundwater were not investigated in this study. The deep groundwater from second and third aquifer was also characterized by low DOC concentrations and comparable low proportions of humic substances. Overall, the mixing of the different water types in the production well leads to a final organic composition of the raw water. The LC-OCD technique is not appropriate to discuss the relevant mixing proportions, but the proposed percentages (chapter xxx hydrogeology chapter) fit to the presented results.

All results of the bulk organic characterization can be summarized as follows. During bank filtration, a fast removal of polysaccharides and only partial removal of all other DOC fractions was observed. None of the DOC fractions was persistent. The organics in the raw water of well 3 are a mixture of the bulk organics in the different abstracted water types.
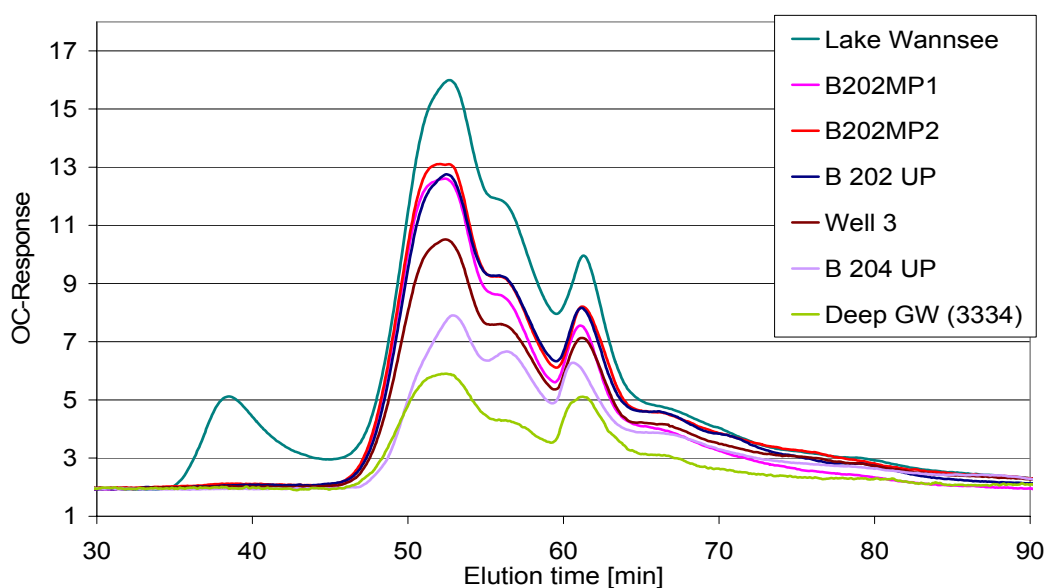
Figure 37 LC-OCD chromatograms of raw water sources at transect Wannsee II

1.2.3 Lake Wannsee - AOI Results

1.2.3.1 Surface water - AOI Results

The concentration of AOX (AOI and AOBr were measured) in the surface water followed a seasonal cycle with higher concentrations during summer. Throughout the observation period it was possible to monitor the influence of the climatic conditions on the AOI concentration in the surface water. Figure 38 shows that during the cold and wet year of 2002 the increase in AOI concentration during late summer and early fall is small compared to the years 2003 and 2004. Similar effects were observed in Lake Tegel. Furthermore, the lowest AOI concentration was measured in winter 2002/03 in both investigated surface waters. Since this was a high-precipitation period it can be assumed that the low concentrations are due to heavy dilution and that the seasonality is mostly derived from changes in dilution. The results indicate that the changing point of discharge of treatment plant Berlin Ruhleben has only a minor influence on the seasonality of AOI in Lake Wannsee.

However, the average AOI concentration in Lake Wannsee is 13.3 µg/l (δ=5.6 µg/l) which is slightly higher than in Lake Tegel (Average: 11.4 µg/l; δ=5.6 µg/l). The difference originates from more dominant summery peaks in front of transect Wannsee II. Here, concentrations of more than 24 µg/l were measured whereas in Tegel the maximum concentration in the years 2002-2005 was 17 µg/l. Since most of the AOI can be assigned to waste-water born contaminants it can be concluded that because of the operation of the lake pipeline in Tegel the influence of wastewater during summer is

higher in Lake Wannsee. The AOI concentrations during winter are similar in both surface waters (6-12 µg/l) with some exceptions.
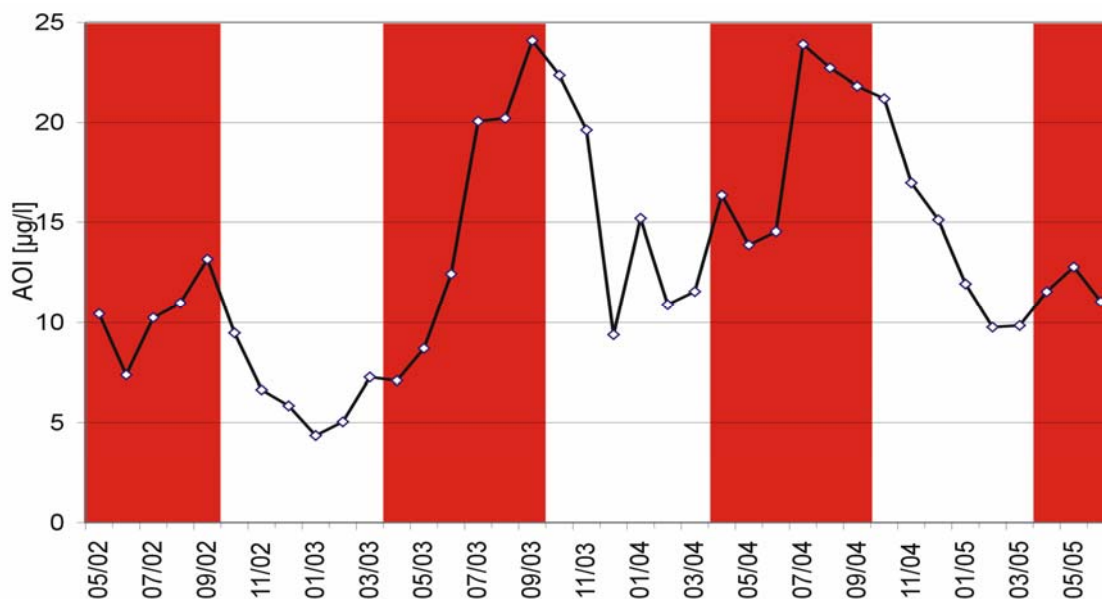
Figure 38 AOI concentration in Lake Wannsee (2002-2005, April-September marked)

Another point of interest was the influence of the treatment plant Ruhleben on the water quality in Lake Wannsee. Two already mentioned sampling campaigns were conducted to assess the spatial distribution of waste-water born contaminants in the surface water. AOI measurements were included into the analytical protocol. Results are presented in Figure 39. No statistically significant differences in the distribution of AOI in Lake Wannsee were found in the winter measurements in March 2004. In the southeast of Lake Wannsee the lowest concentrations were measured. This would implement a lower AOI concentration of the water entering Lake Wannsee from Teltow-canal through the small chain of lakes south of Wannsee. Water incoming from the north (containing WWTP Ruhleben effluent) has a higher AOI level. But the differences are very low and the circumstances of the sampling event (e.g. preceding precipitation) are unclear. Therefore, the results would point towards a nearly even distribution of the AOI concentration during winter in Lake Wannsee. The concentrations measured in the surface water campaign are approximately 4 µg/l lower than in the monthly scheduled sampling in front of the transect in March. This is probably due to a time difference between both sampling events.

The sampling campaign in July 2004 showed slightly higher concentrations of AOI on the east side of the lake compared with the west bank. During summer WWTP Ruhleben discharges into the Teltow-canal and could be responsible for increased AOI levels on the east bank of the lake. Electrical conductivity measurements of FU Berlin propose a preferential flow of the Teltow-canal water northwards along the east bank of Lake Wannsee. This would be consistent with the AOI results of the surface water

sampling campaign. But the differences in concentration are again very low and close to the detection limit. Therefore, the results indicate that the changing point of discharge of treatment plant Berlin-Ruhleben has only minor influence on the seasonality of the AOI in the surface water. The spatial variation of AOI concentrations in the lake was found to be slightly influenced by Teltow-canal water. Unfortunately, the sampling campaigns did not capture peak concentrations of more than 20 µg/l. It remains unclear whether such high AOI concentrations occur only locally or in the whole lake. The depth profiles which were recorded in the middle of the lake as part of the surface water sampling showed AOI concentration similar to surface water in 2 m, 4 m, 6 m, and 7 m depth.
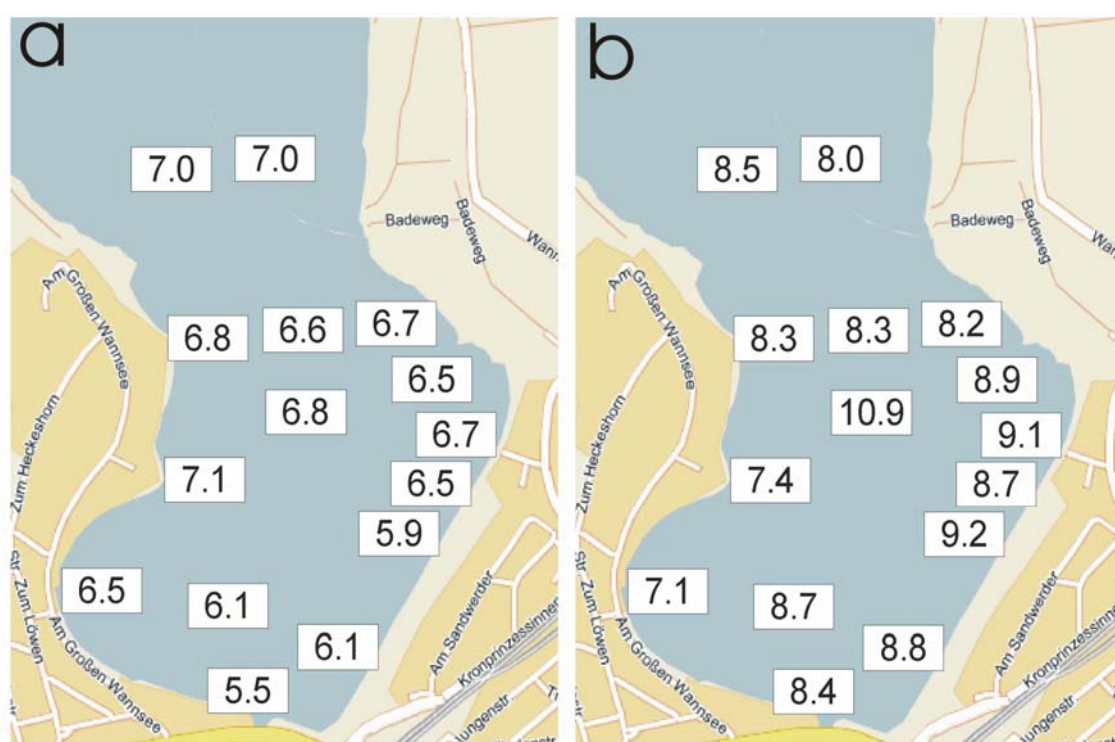
Figure 39 Distribution of AOI (µg/l) in Lake Wannsee in March 2004 (a) and July 2004 (b)

1.2.3.2 Bank filtration - AOI results

Besides the surface water investigations adsorbable organic iodine (AOI) of most of the samples from transect Wannsee II was measured as part of the monthly monitoring schedule. Since AOI is mostly of anthropogenic origin the removal rates were of special interest for the evaluation of the organic composition of the bank filtrate. All findings for the monitoring wells are based on 18 months measurements, whereas surface water and production well were sampled for a longer period.

Results show that the fate of AOI during infiltration is different under more aerobic (206, 202OP and 203) and anoxic/anaerobic (205) conditions. Any surface water variation of

AOI has a stronger effect on the aerobic monitoring wells, where the average AOI-reduction is only 20-35%. This seems not to be strongly dependent on retention times because the monitoring well with retention times of less than a month (206; 34%) shows better results than the monitoring well with retention times of more than 2 months (203; 22%). But all wells exhibited best removal efficiencies during summer season, which is probably due to temperature effects and the coupled changes in redox chemistry. In the shallow wells 206, 202OP, and 203 a shifted seasonal change in oxygen and nitrate concentration was observed. During winter, real oxic conditions dominated and during summer a depletion of oxygen and nitrate was observed. The combination of higher temperatures and lower redox potentials lead to a higher removal efficiency for AOI during summer months. Therefore, the summery surface water AOI-peaks did not occur in the monitoring wells. Highest concentrations in the wells were found during winter when the AOI mineralization was comparable low.

Monitoring well 205 has a slightly different redox chemistry. Due to saturated infiltration the bank filtrate remains anaerobic for nearly the whole year. The redox potential is considerably lower and nitrate reduction was observed in all seasons (NO$_3$-N: surface water: 1.0 mg/l; 205: 0.03 mg/l). The lower redox potential causes a more efficient reduction of AOI during the recharge process (63% during approximately one month retention time).
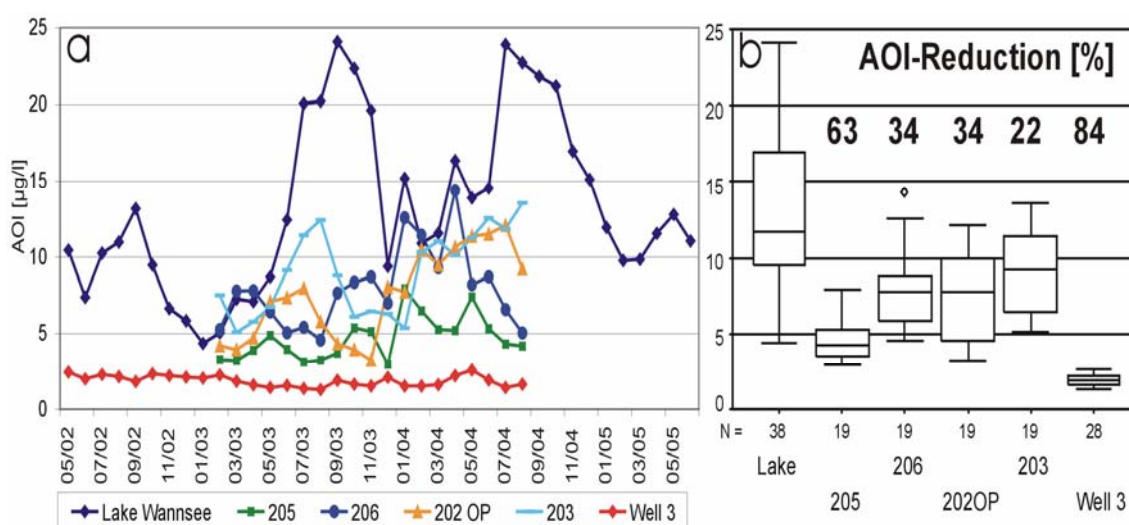
Figure 40 Fate of AOI during infiltration at transect Wannsee II (a: time series; b: box plots)

These results are consistent with findings at other field sites in Berlin. At the predominantly anoxic/anaerobic bank filtration site at Lake Tegel AOI reduction rates of app. 60-70% were observed during a 4-5 months infiltration (100 m infiltration distance). At the more oxic artificial recharge facility in Berlin-Tegel the measured average reduction rate was 30%. This inverse correlation between AOI-removal and redox potential is believed to originate from the initial step of AOI-mineralization -

reductive dehalogenation. The degradation of halogen substituted organics is more effective in soil passages with low redox potential (Mohn & Tiedje; 1992). Results from field site Wannsee evidently show that low redox potentials are essential for an efficient degradation of AOI and that even a duplication or triplication of retention times and infiltration distances can not compensate the absence of reducing conditions.

In Berlin-Wannsee the AOI of the other abstracted water fractions is very low (~2 µg/l) and the mixing in the production well (Well 3) leads to an AOI-concentration in the extracted raw water of 2-2.5 µg/l. The old bank filtrate is represented by the monitoring wells 202MP1, 202MP2 and 202UP. Figure 41 shows that this water fraction contains AOI concentrations of around 2 µg/l. Monitoring well 202MP1 is dominated by the old bank filtrate for most of the observation period but during winter and spring 2004 an influence of the young bank filtrate is visible. The AOI concentrations in 202MP1 increased considerably during this period. A comparison with the shallow wells (Figure 40) reveals that the increase of AOI level was also found in the young bank filtrate.
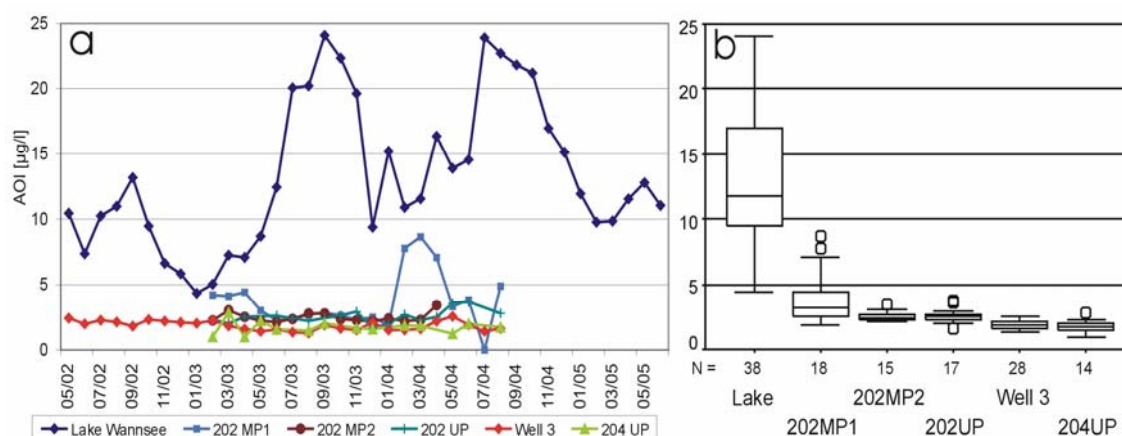
Figure 41 AOI in the multiple raw water sources at transect Wannsee II (a: time series; b: box plots)

Background groundwater (represented by 204UP) contains very low amounts of AOI. The average concentration was found to be 1.7 µg/l (δ=0.5 µg/l). For the deeper aquifers at field site Wannsee only one sampling was conducted. But taking in consideration the depth, it can be assumed that the water composition is very stable and no temporal variations occur. The sampling resulted in AOI levels below the limit of detection of 1 µg/l for the monitoring wells 3332, 3334, and 3336.

These findings explain the very low AOI concentration in the abstracted raw water. A calculation based on the mixing ratios proposed by the Free University Berlin would result in a AOI concentration of 3.3 µg/l in the abstracted raw water. Because of the low share of young bank filtrate, increasing AOI concentration are not expected to influence the product water quality at transect Wannsee II strongly.

1.2.4 Lake Wannsee - AOBr Results

1.2.4.1 Surface water - AOBr Results

The monitoring of adsorbable organic bromine (AOBr) concentration in Lake Wannsee for more than three years revealed a seasonal trend which is more dominant than in Lake Tegel (Figure 42). During winter and spring, AOBr concentration remains on a low level of about 6-8 µg/l. This fraction is believed to contain AOBr from anthropogenic sources (disinfectants, etc.). The concentration level is very similar to the one observed in Lake Tegel during winter. In summer and fall, AOBr concentration strongly increases (e.g. 2003: up to 500%; 2004: up to 400%) for a duration of 4-5 months. Putschew et al. (2003) found that the high AOBr concentrations are associated to algae blooms for two other Berlin lakes. Therefore, it seems consequential that the summery peaks in AOBr concentration are more dominant in Lake Wannsee than in Lake Tegel. Maximum concentration for Tegel were 25 µg/l during the observation period from 2002-2005. In Lake Wannsee, the AOBr level rose to more than 43 µg/l in summer 2003. Wannsee is more prone to algae blooms because of higher phosphorus concentrations (2004/2005: $\varnothing$=173 µg/l; δ=147 ng/l; n=10). Organobromines are formed by special types of algae, which bloom during late summer.

Altogether, the observed seasonality is known from literature and earlier studies of the DWQC. All results strongly support the theory of algae associated AOBr and the findings of Putschew et al. (2003).
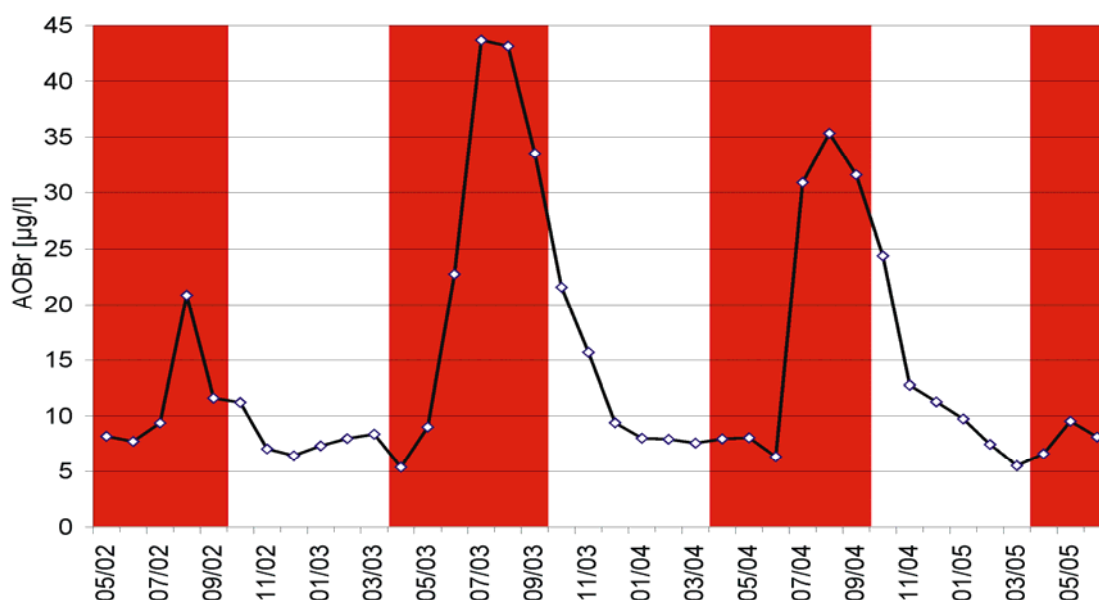
Figure 42 AOBr concentration in Lake Wannsee (2002-2005, April-September marked)

The spatial variation of AOBr concentration was investigated in the mentioned surface water sampling campaigns which is presented in Figure 43. In March 2004, slightly

higher concentrations of AOBr in the north of Lake Wannsee were found. During winter, all AOBr is assumed to originate from anthropogenic sources. Therefore, higher concentrations in the north part of the lake indicate an influence of the treatment plant Ruhleben. No depth variation was found in winter.

At the time of the July campaign, the distribution of anthropogenic AOBr was superposed by algae associated organobromine. Areas with high AOBr concentrations would not specify waste water influence but regions of elevated algae activity. But in summer, AOBr concentrations seem to be evenly distributed in Lake Wannsee. The general concentration is considerably higher in summer compared to the winter sampling. A comparison with the time series (Figure 42) reveals some differences, which might be due to different sampling times (time of day) or sun activity. However, the results show that in July 2004, the activity of algae species which are responsible for the AOBr formation was evenly distributed over Lake Wannsee. It can be assumed that this is valid for all algae species. During summer, a slight depth variation was found in the middle of Lake Wannsee. On the surface, the AOBr concentration was approximately 2 µg/l higher than in the depths of 2, 4, 6, and 7 m. The observed -10% variation appears small since algae need light for growing. But Hütteroth et al. (2004) found that algae release AOBr during stress situations and during die-off. Therefore, higher AOBr levels in deeper waters could originate from descending dying algae.
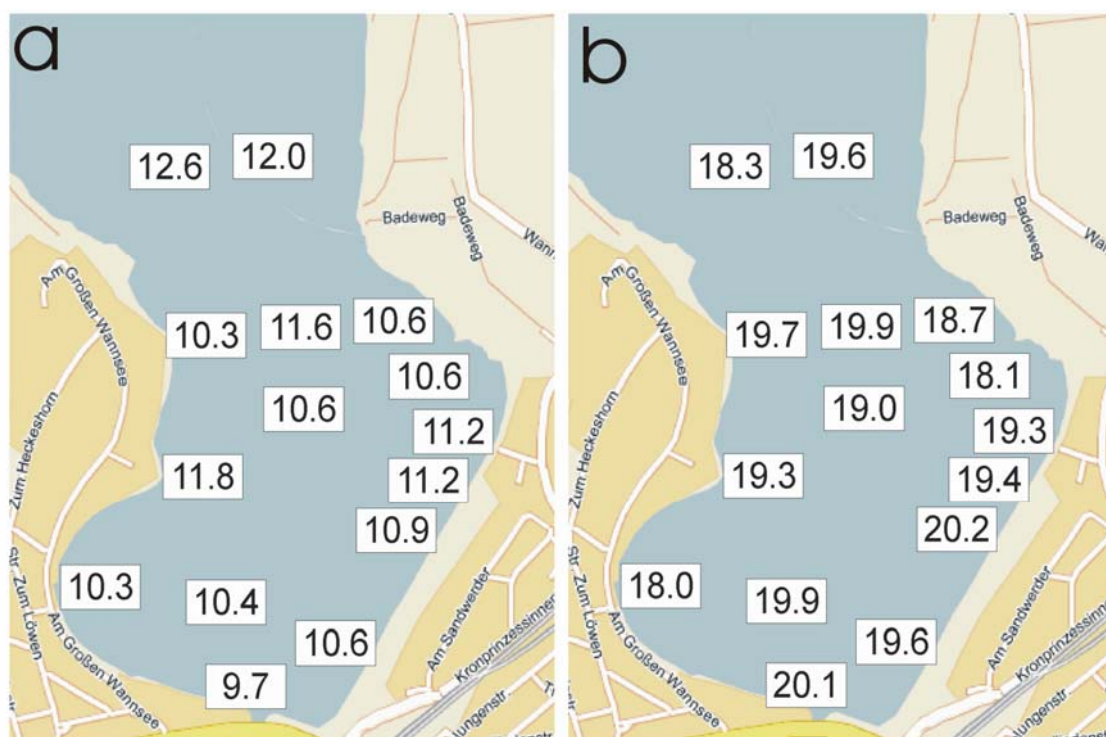
Figure 43 Distribution of AOBr (µg/l) in Lake Wannsee in March 2004 (a) and July 2004 (b)

1.2.4.2 Bank filtration - AOBr results

The fate of AOBr along the infiltration path at Wannsee II was investigated for 18 months. Observations pointed toward a similar removal mechanism for AOI and AOBr. Another important finding was that the strong surface water peaks during late summer did not influence the AOBr concentration in the subsoil.

Figure 44 shows that the monitoring well with the lowest redox potential (205) achieved a reduction of 68%. Under oxic conditions, average removal rates were clearly lower (206: 19%; 202OP: 30%; 203: 26%). These removal rates are based on median concentrations. In the median calculation, the summery surface water peaks are statistically regarded as extreme values and have less influence as in the calculation of the mean. A calculation on the basis of mean concentrations would result in higher removal rates. However, water of the production well contained only 22% of the surface water AOBr. Furthermore, it was proved that the anoxic/anaerobic well 205 is most efficient in removing AOBr, mineralizing more than 60% of the surface water AOBr. The more oxic monitoring wells 206, 202OP, and 203 exhibited only removal rates of 20-30%. It is believed that AOBr removal is influenced by redox potential and temperature, similar to the pattern observed for AOI.
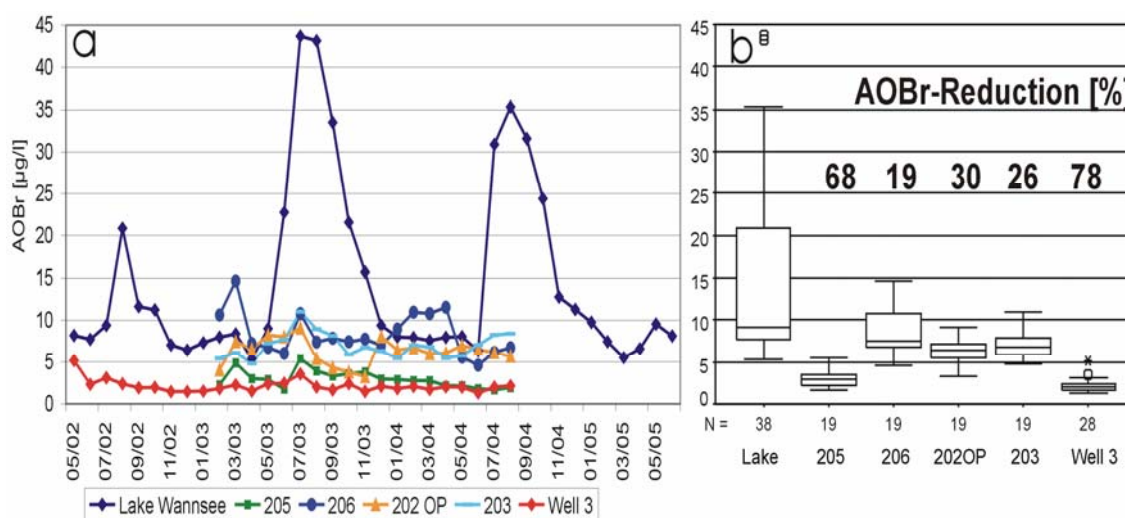
Figure 44 Fate of AOBr during infiltration at transect Wannsee II (a: time series; b: box plots)

For a complete evaluation of the AOBr results, a differentiation between the two fractions of AOBr seems to be necessary. Figure 44 shows that the summery peaks of AOBr in surface water are more dominant than the AOI peaks (Figure 40). It is unlikely that higher temperature and more reducing conditions during soil passage in summer increase the removal efficiency to an extend that a nearly 500% concentration increase is not visible in the monitoring wells. Therefore, the results can only be explained by a higher biodegradability of the algae associated AOBr fraction. Surface water investigations demonstrated that besides the algae associated AOBr fraction a fraction of adsorbable organic bromine exists which is present the year-round in surface water.

This fraction accounts for approximately 8 µg/l in the surface water. With respect to the monitored results, it can be assumed that this fraction behaves similar to AOI. An efficient removal under anaerobic conditions (205) and less mineralization under oxic conditions (206, 202OP etc.) was observed. On the contrary, a better biodegradability of algae associated AOBr was found. This seasonal occurring AOBr seems to be easily degradable under oxic and anoxic/anaerobic conditions, because the 500%-increase of AOBr-concentration during summer was not observed in any of the monitoring wells. A complete adsorption of this fraction onto soil matrix is unlikely, since the substances are very polar. Further research on the character and the behavior of algae associated AOBr are conducted by the DWQC (Hütteroth, 2004).

All other groundwater samples from monitoring wells that were not influenced by recent bank filtrate at Wannsee II contained very low concentrations of AOBr. Older bank filtrate in the lower part of the top aquifer was measured 38 times with concentrations between 1 µg/l and 3 µg/l (202MP2: 2.1 µg/l; δ=0.6 µg/l; 202UP: 1.8 µg/l; δ=0.3 µg/l). The background groundwater contained 1.3 µg/l (204UP; δ=0.3 µg/l) and no AOBr was found in the second and third aquifer (3332, 3334, and 3336).

Summarized, only the AOBr fraction which is present all year in the surface water shows the preferential removal under anoxic/anaerobic conditions that was observed for AOI. The heavy peak loads during summer seem to have no effect on the drinking water production and are therefore regarded as unproblematic.

1.2.5 Lake Wannsee - Trace pollutants results

1.2.5.1 Surface water - Trace organic compounds

It was explained earlier, that the surface water of Lake Wannsee is influenced by the discharge of river Havel entering the lake from north and water from Teltow-canal (through small Wannsee) incoming from south. The discharged volumes and the content of treated wastewater change over the seasons because of natural precipitation and the changing outlet of WWTP Ruhleben. Overall, the system was found to be very complicated. The electrical conductivity, chloride, and boron data indicate a higher waste water portion in front of the transect Wannsee II during summer (Hydrogeological section). This is consistent with the findings of DOC and AOI monitoring. Therefore, it was assumed that the monitoring of trace pollutants would show a similar seasonality. The investigated trace organic compounds were selected because they are present in surface water in detectable concentrations. Furthermore, the compounds can be easily assigned to treated wastewater because they are completely of anthropogenic origin.

Figure 45 presents the results of the surface water monitoring in front of Wannsee II from May 2003 to June 2005. Temporal changes of the concentrations of Iopromide (X-ray contrast agent), Sulfamethoxazole (Bacteriostatic), and three isomers of

naphthalenedisulfonic acid (NDSA) were investigated. The results can not be compared with findings of earlier studies since no older data are available for this transect. However, Figure 45 shows that the concentration of most of the trace compounds varies highly in front of the transect. A comparison with surface water concentrations in Lake Tegel reveals that the average Iopromide concentration is very similar in both water bodies (Tegel: median= 969 ng/l; Wannsee: median= 936 ng/l). Sulfamethoxazole was found in considerably higher concentrations in Lake Tegel, where a median concentration level of 371 ng/l was found (Wannsee: median=195 ng/l). For the isomers of naphthalenedisulfonic acid Wannsee surface water concentrations were 50-100 ng/l higher than in Lake Tegel.
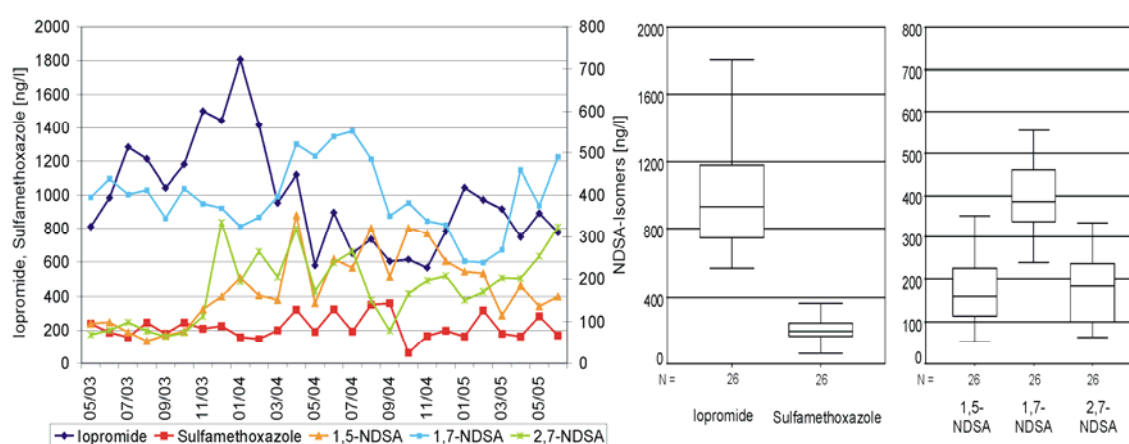
Figure 45 Trace pollutant concentration in Lake Wannsee (2003 - 2005, a: time series; b: box plots)

The selected trace compounds were found in all surface water samples of the monitoring period with concentrations above the limit of quantification. Because of the long time series it was of interest to detect eventual seasonal changes for the trace compounds. Figure 45 shows that the concentrations of the trace organics were highly variable but did not necessarily follow a seasonal scheme. This might be due to the fact that seasonal changes are superposed by strong short-term variations.

The X-ray contrast agent Iopromide was detected in the surface water with a median concentration of 936 ng/l (δ=318 ng/l, n=26). The concentrations were highly erratic with no general trend over the observation period. During summer of 2003, the concentration remained in a range between 800-1200 ng/l. In the following winter, an increase up to 1800 ng/l followed. Afterwards a decrease during spring and constant concentrations of about 700 ng/l during summer 2004 were observed. Another concentration increase during winter 2004/05 supports the trend of slightly higher concentrations during winter in front of the transect. This is contrary to the concentration of other waste water indicators. An explanation may arise from the different concentrations of X-Ray contrast agents in the effluent of the WWTP´s of Berlin. Studies of the DWQC showed that WWTP Schoenerlinde discharge contains

incomparable high concentrations of X-Ray contrast agent because of the health complex Berlin-Buch, which discharges to treatment plant Schoenerlinde. Wischnack and Jekel (2000) found average Iopromide concentrations of more than 20 µg/l in 24h-mixed samples. Bahr et al. (2005) found concentrations of ~5 µg/l Iopromide in ten random samples of the effluent of WW treatment plant Ruhleben. Therefore, higher concentrations during winter could result from a higher portion of treated waste water from Schoenerlinde ending up in front of Wannsee II during winter. However, a comparison with the general waste water indicators like chloride and boron did not lead to satisfying results.

The antibiotic drug Sulfamethoxazole was found in Lake Wannsee with a median concentration of 195 ng/l (δ=72 ng/l, n=26). Figure 45 shows that no seasonality was observed for this pollutant and that the concentration level remained relatively constant. The fact that the average Sulfamethoxazole concentration is only half as high as in Lake Tegel points towards a different origin of the waste water share in Wannsee since all other waste water indicators show similar concentrations. Attenuation in the surface water is unlikely since Sulfamethoxazole is very stable and not photosensitive.

Results for the different NDSA-isomers show consistently with other field sites that the 1,7-NDSA is the most important isomer in Berlin surface waters. The median concentration of this compound was found to be 388 ng/l (δ=85 ng/l, n=26) in Lake Wannsee. The 26 months of monitoring resulted in median concentrations of 162 ng/l for 1,5-NDSA (δ=96 ng/l, n=84) and 183 ng/l for the 2,7-isomer (δ=96 ng/l, n=83). The time series for 1,7-NDSA shows that the pollution level for this compound remains relative stable over the monitoring period. A slight trend towards higher concentrations during summer can be recognized among the erratic concentration changes. This would be consistent with the proposed seasonal change in waste water influence. The time series of 1,7- and 2,7-NDSA show similarly low and stable concentration during summer 2003. With begin of winter 2003/04 the concentration of both isomers increases and shows irregular behavior. No seasonal dependency stands out for both compounds. The most characteristic indication of both time series is the strong increase in pollution level in November/December 2003 which remains high until the end of the observation period. Overall, the concentrations of NDSA are higher than at the other investigated field sites.

Because of strongly variable results for the trace compounds in Lake Wannsee any correlation attempts with other waste water indicators failed.

1.2.5.2 Bank filtration - Trace organic compounds

The single compound analysis for the trace pollutants Iopromide, Sulfamethoxazole, and different naphthalenedisulfonic acids was started in spring 2003, providing data for the time period May 2003 to August 2004. The monitoring was of special interest because transect Wannsee II provided the opportunity to observe very detailed the

difference between oxic and anoxic/anaerobic infiltration. The monitoring wells 205 and 206 receive the same surface water. Both have similar retention times, but differ in the dominant redox conditions. Furthermore, the more distant shallow monitoring wells represent a comparable long oxic infiltration path. Therefore, the long time behavior of the analyzed trace compounds under oxic conditions could be studied.

The older bank filtrate in the deeper part of the top aquifer was sampled to obtain more information about the behavior of these compounds during decades of soil passage. It can be assumed that the trace compounds were present in the surface waters for at least 20 years. Naphthalenedisulfonic acids were used in industry since the second half of the 19th century. Sulfamethoxazole is widely used in medicine since World War II and Iopromide was introduced to the European medicine in 1985 under the product name Ultravist. Since the determination of age for the older bank filtrate proposed a time span of approximately ten years (202UP: 10.7 years) from infiltration to abstraction it is most probable that the analyzed trace compounds were present in the surface water at this time. No information exists about the average concentration ten to twenty years ago. Furthermore, the screening of the background groundwater and the deep groundwater revealed eventual anthropogenic influences on this groundwater streams.

Generally, it was found that these trace organic compounds which stand for different groups of persistent pollutants behave differently during infiltration. For most of the analyzed compounds, an influence of redox conditions on the degradability could be revealed. Furthermore, some temperature effects were observed.

Figure 46 presents data on the fate of Iopromide during infiltration. Surface water pollution level for Iopromide (~1000 ng/l) was considerably higher than for the other compounds. As mentioned, Iopromide is a triiodinated benzene derivate and part of the bulk parameter AOI. The results at Wannsee II confirm that the removal mechanisms under oxic conditions are completely different from the removal under anoxic/anaerobic conditions. This conclusion originates from a comparison of the AOI mineralization with the Iopromide removal. Of special interest was a comparison of the monitoring wells 205 and 206 which revealed more details on the degradation characteristics of Iopromide. Both monitoring wells are located under the lake and differ primarily in dominant redox conditions. During anoxic/anaerobic infiltration Iopromide concentration was reduced from the lake (1081 ng/l, n=16, σ=336 ng/l) to observation well 205 (363 ng/l, n=12, σ=118 ng/l) by 66%. This is consistent with the observed AOI reduction (205: 63%). Therefore, it could be assumed that a high portion of the removal of Iopromide was based on dehalogenation and mineralization. But during oxic infiltration Iopromide showed a clearly better removal of 96% (206: 41 ng/l, n=16, σ=35 ng/l) than AOI (206: 34%). This confirms that Iopromide and AOI behave differently during oxic infiltration. One assumption that arose from results of other field sites and soil column studies is that the Iopromide molecule is rapidly metabolized under oxic

conditions, but not mineralized. The metabolite is not efficiently dehalogenated and remains detectable as AOI.
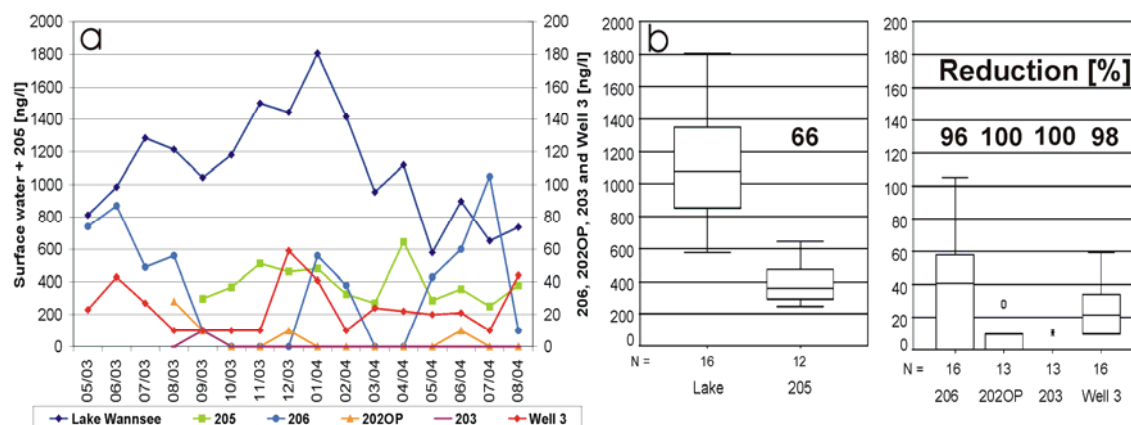
Figure 46 Fate of Iopromide during infiltration at transect Wannsee II (a: time series; b: box plots)

The time series of Iopromide measurements reveal more influences on the Iopromide removal. The contamination level in the anaerobic well 205 remains in the range of 300-500 ng/l over 12 months. For 206, the time series shows seasonal differences between concentrations under the limit of detection (5 ng/l) and concentrations of 60-100 ng/l. These effects can be explained by the influence of temperature and changing redox conditions. During summer, the redox potential in 206 decreases and a complete denitrification leads to anaerobic conditions. This was observed during the summer of 2003 and 2004. In this time, 206 resembles the conditions in 205 and a less efficient metabolization of Iopromide occurs. The higher concentrations during winter are due to reduced bioactivity because of low temperature. Overall, the most efficient Iopromide removal in 206 was observed during spring and fall.

However, along the further infiltration path towards the production well very low Iopromide concentrations were monitored. Contrary to the fate of AOI, Iopromide showed a very good removal along the oxic infiltration path to the production well. Only once a concentration above the limit of quantification (20 ng/l) was found in the monitoring wells 202OP and 203. Curiously, the concentration levels in the production well 3 are higher than in 203. The reason is unclear since all other abstracted water fractions (old bank filtrate, background groundwater, and deep groundwater) did not contain any measurable amounts of Iopromide. The time series of the production well also indicates higher concentrations during summer and winter months and lower concentrations during spring and winter. It must be assumed that these influences originate from a flow path which is not directly sampled by one of the monitoring wells and which also shows the shifted seasonal influences that were observed in 206. Overall, it can be summarized that the X-ray contrast agent Iopromide is efficiently attenuated at Wannsee II, but there were strong indications that one part of removal was based on an aerobic metabolization and not on dehalogenation and mineralization.

The bactriostatic Sulfamethoxazole was present in the surface water with concentrations of 150-350 ng/l. A comparison of monitoring well 205 and 206 showed clearly that the degradation of Sulfamethoxazole seems to be redox dependent as well. In Berlin-Wannsee, Sulfamethoxazole shows a better removal under anoxic/anaerobic conditions. Within approximately one month of infiltration to monitoring well 205 the surface water concentration (204 ng/l, n=16, σ=62 ng/l) was efficiently degraded (205: 3 measurements > LOQ; median: 0 ng/l, n=12, σ=12 ng/l). The oxic infiltration path along 206, 202OP, and 203 displayed smaller degradation rates ranging from 43% to 62%. A slight influence of a longer retention time was observed because the monitoring wells 202OP and 203 (retention times 2-4 months) showed higher removal rates than 206 (0.5 month). But even these very long aerobic soil passages did not eliminate the bacteriostatic compound completely. During the observation period, a trend towards higher concentrations in the shallow oxic monitoring wells was observed. Starting in winter 2003, the contamination levels of 202OP and 203 increased from less than 50 ng/l to more than 100 ng/l. The higher concentrations did not show influence on the abstracted water in well 3. However, the better removal of Sulfamethoxazole under anoxic/anaerobic conditions is consistent with the observations in Tegel and findings of Schmidt et al. (2004) at other bank filtration sites in Germany.

Background groundwater, old bank filtrate, and deep groundwater were found to be free of Sulfamethoxazole residues. Although Sulfamethoxazole was relative stable during oxic soil passage, the mixing with other groundwater fractions in production well 3 lead to very low concentrations, which are far below the precaution value for anthropogenic organic contaminants.
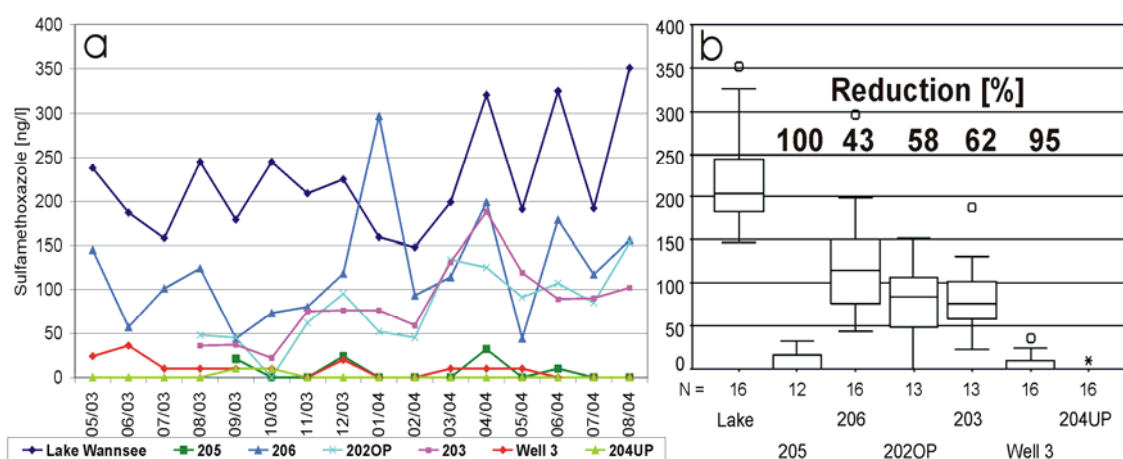
Figure 47 Fate of Sulfamethoxazole during infiltration at transect Wannsee II (a: time series; b: box plots)

The group of naphthalenedisulfonates was present in Lake Wannsee surface water with higher pollution levels than in Lake Tegel. Two of three monitored isomers showed

a strong concentration increase during the observation period. Therefore, it was of interest to investigate the influence of the increased surface water concentration on the monitoring wells and the production well.

At other field sites and in soil column experiments, it was found that 1,5-NDSA is the most stable isomer from the group of the naphthalenedisulfonic acids. Figure 48 shows that surface water concentration increased during the period May 2003 – August 2005 from ~100 ng/l to a maximum concentration of ~300 ng/l. It was observed that the higher concentration in surface water leads to increasing 1,5-NDSA levels in the monitoring wells. Well 205 and 206 very closely follow the surface water concentration, supporting the findings of short retention times for these wells (0.5-1 month). The concentration of 1,5-naphthalenedisulfonic acid remained nearly constant during oxic (206) and anoxic/anaerobic (205) infiltration. The slightly higher median concentration in well 205 is due to short-term variations of the surface water which were not captured by monthly sampling. However, the compound did not show any removal within one month under either redox conditions. Along the further infiltration path only a time shift in the time series was observed. This time shift is consistent with results of tracer evaluations that were conducted by the workgroup from the Free University Berlin. The concentrations in 202OP and 203 increased to a similar pollution level approximately 4 months after the surface water rise. Therefore, it can be followed that no efficient removal of 1,5-NDSA takes place at Wannsee II. The removal rates stated in Figure 48 are strongly influenced by the time shift in the more distant monitoring wells and are therefore mostly too high. For consistency reasons they were calculated similarly to all other mentioned removal rates.
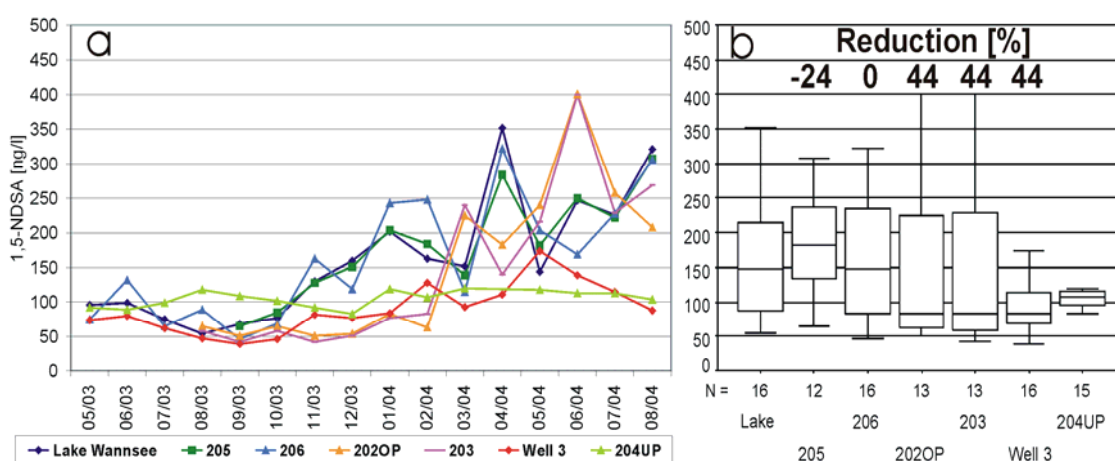
Figure 48 Fate of 1,5-NDSA during infiltration at transect Wannsee II (a: time series; b: box plots)

Figure 48 also shows that the contamination level in the background groundwater was stable over the monitoring period. The concentration of 1,5-NDSA in monitoring well 204UP was found to be 105 ng/l (n=15, σ=12 ng/l). This is similar to the concentrations found in 202MP2 and 202UP (Ø=106 ng/l, n=8, σ=25 ng/l). The sampling event in

March 2004 for the deep monitoring wells 3332, 3334, and 3336 resulted in NDSA concentrations below the limit of detection for the second and third aquifer. Therefore, the deep aquifers are most probable not influenced by anthropogenic substances.

These results show that 1,5-NDSA is very poorly biodegradable and elimination of this compound can not be expected during bank filtration. No influence of the redox conditions on the degradation was found. The final concentration of well 3 product water results from a mixture of non-polluted deep groundwater, 1,5-NDSA-containing old bank filtrate and background groundwater, and young bank filtrate. The calculated mixing proportions are consistent with the observed concentrations. A 300%-increase in 1,5-NDSA concentration in well 3 between fall 2003 and spring 2004 shows that young bank filtrate has a considerable influence on the product water composition. Overall, these results are consistent with findings of Stueber et al. (2002) who reported 1.5-NDSA as very stable in wastewater treatment plants.

1,7-Naphthalenedisulfonic acid was present in surface water of Lake Wannsee (Ø=381 ng/l, n=26, σ=96 ng/l) in slightly higher concentrations than observed at Lake Tegel (Ø=333 ng/l, n=25, σ=84 ng/l). It was found that the compound is partially degraded during oxic infiltration. This is consistent with findings at Tegel field sites and soil column experiments. In these studies it was proved that the degradable isomers of NDSA are more efficiently removed under oxic conditions. This is proved by a comparison of monitoring well 205 and 206. Both wells are receiving the same surface water but show different removal efficiencies in comparable time frames. In well 205, only 11% of the surface water concentration is removed during ~30 days of anoxic/anaerobic infiltration, whereas the oxic soil passage to well 206 removes 41% in less than a month. During further infiltration along the top part of the first aquifer, the concentrations of 1,7-NDSA decrease continuously and in monitoring well 203 75% of the substance is degraded. The time series in Figure 49 show that the measured concentration in monitoring well 205 follows closely the surface water concentration. For the other shallow monitoring wells a temperature effect was observed. The concentrations increased during winter 2003/2004 because of a temperature induced lower bioactivity. In 206, the 1,7-NDSA concentration in January and February 2004 were close to the surface water pollution level. This peak also occurred time shifted in the wells 202OP and 203.
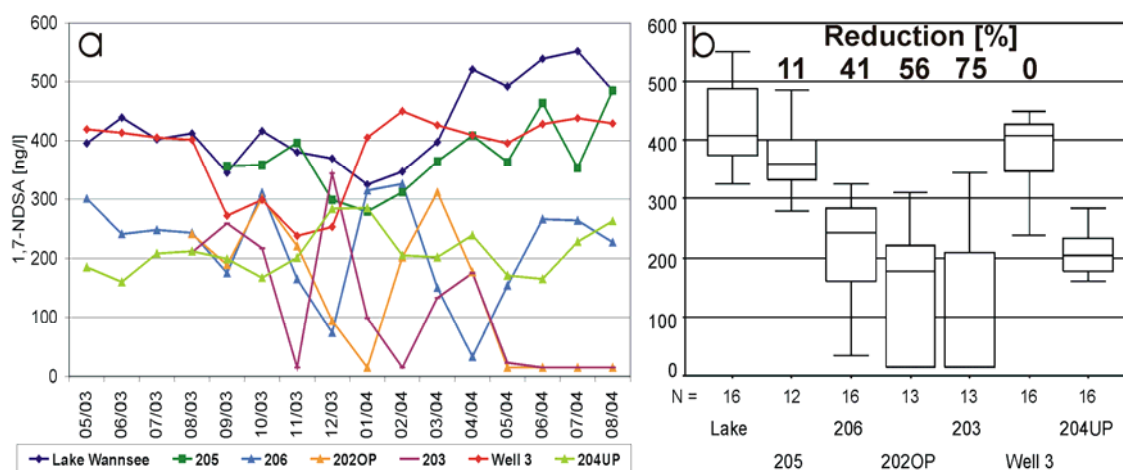
Figure 49 Fate of 1,7-NDSA during infiltration at transect Wannsee II (a: time series; b: box plots)

In production well 3, the 1,7-isomer concentration was measured to be similar to the surface water concentration. This is explained by a strong influence of old bank filtrate from deeper parts of the top aquifer. A screening of the monitoring wells 202MP2 and 202UP, which represent the old bank filtrate, confirmed median concentrations of 461 ng/l (n=8, σ=37 ng/l) for this groundwater stream. Background groundwater contains 1,7-NDSA at a level of 204 ng/l and the water from the second and third aquifer does not contain any measurable amounts of NDSA. This confirms the strong influence of the old bank filtrate on the product water. It can be assumed that the surface water concentration of NDSA was considerably higher during the times of infiltration of the old bank filtrate, or infiltration took place under more reducing conditions which inhibited a efficient removal of 1,7-NDSA (compare 205). The time series of production well 3 exhibits decreasing concentrations during summer and fall of 2003 and more or less stable concentrations during the rest of the observation period. It remains unclear whether an adapted pumping schedule during this hot and dry summer increased the influence of recent bank filtrate on the product water or whether higher temperatures lead to a more efficient degradation of 1,7-NDSA.

The 2,7-NDSA isomer monitoring showed results that were similar to the findings for 1,7-NDSA. Degradation of this compound is also more efficient under oxic conditions. The removal rates along the infiltration path of the recent bank filtrate were slightly higher than for the 1,7-isomer. Unlike 1,7-NDSA, the surface water concentration of 2,7-NDSA increased substantially during the observation period. The concentration increase occurred simultaneously with the already described rise of 1,5-NDSA pollution level during fall 2003. It remains unclear which effect was responsible for this significant change in concentration. The relocation of the discharge point for the WWTP Ruhleben seems to be no adequate explanation, since the contamination level did not drop in April 2004 back to former concentrations. The concentration in monitoring well 205 follows closely the surface water concentration and no efficient removal was found under anoxic/anaerobic conditions (Figure 50). In well 206, the temperature induced

concentration increase in winter 2003/04 resembles the fate of 1,7-NDSA. This peak also occurs in the more distant shallow monitoring wells 202OP and 203 were the overall removal rate is 75% and 91%, respectively.

The average concentration in the production well increases during the observation period from ~50 ng/l to ~100 ng/l. This is most probably due to a cumulative effect, since the background water concentration also increases. The old bank filtrate (202MP2 and 202UP) was found to contain reproducible median concentrations of 80 ng/l (n=8, σ=18 ng/l). Therefore, it can be assumed that the 2,7-NDSA concentration increase in the product water is partly due to the strong concentration build up in surface water. Some uncertainties regarding the nearly simultaneous increase in the surface water and in the product water remain.
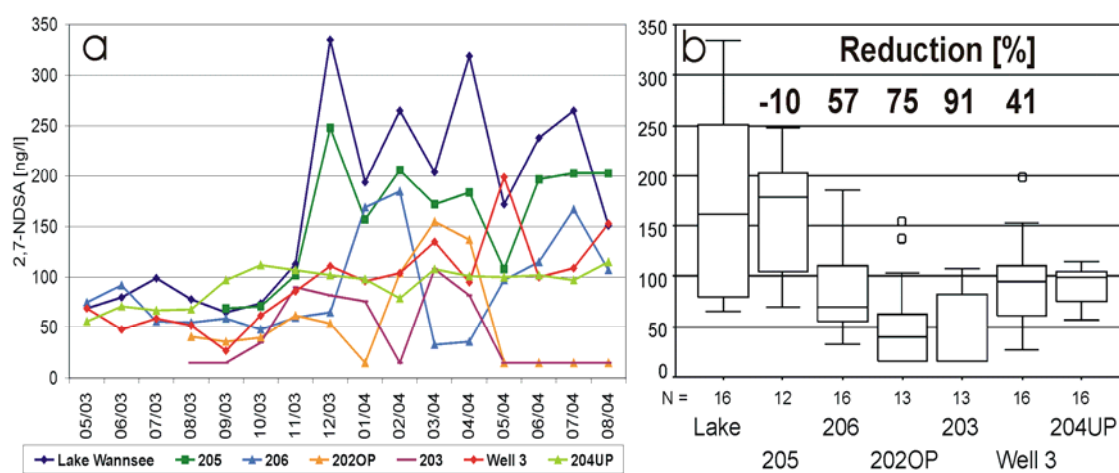
Figure 50 Fate of 2,7-NDSA during infiltration at transect Wannsee II (a: time series; b: box plots)

Summarizing, the results from the field monitoring at the bank filtration site Berlin-Wannsee provided insight into the degradation characteristics of the observed trace organic pollutants under field conditions. It was found that for most compounds the dominating redox conditions are an important parameter for the achievable reduction rates. In comparison with the field site Tegel the product water quality in Wannsee was less dependent from the surface water quality, since a larger portion of the product water derives from old bank filtrate or deep and background groundwater. Nevertheless, the concentrations of most of the investigated waste water born trace contaminants (Iopromide and the NDSA-isomers) were higher in Wannsee product water than in Tegel raw water. Sulfamethoxazole showed lower concentrations. This is reasoned by the strong influence of old bank filtrate at the Wannsee field sites which contains some of the pollutants in higher concentrations. The NDSA-isomers appear to be most problematic, since the mixing in well 3 leads partially to comparably high concentrations. E. g. the 1,7-NDSA isomer is present in well 3 raw water in average concentrations of ~400 ng/l, which is high above the precaution value of the German Drinking water Ordinance (100 ng/l). It appears to be necessary to investigate the

effects of degradation and dilution during further treatment in the water works for these compounds. However, besides the strong influence of old bank filtrate the results for some compounds also display the influence of actual surface water quality on the abstracted raw water (e.g. 2,7-NDSA). Therefore, the protection of surface water and the monitoring of bank filtration processes remain necessary for high quality source water at the field site Wannsee.

1.3   Artificial groundwater recharge facility Tegel (GWR)

Surface water of Lake Tegel is used for groundwater augmentation at the artificial groundwater recharge site Tegel, which is located close to the bank filtration field site Berlin-Tegel. In three infiltration ponds with a total area of ~30.000 m^2 the Berlin Water works infiltrate 15 million cubic meter surface water annually. Since 2004 the amount of infiltrated water is decreasing due to restrictions of the Berlin government.

During summer months the surface water is micro-filtrated to remove suspended algae, which would minimize infiltration rates. The micro-filtration is not affecting any dissolved water constituents. Series of abstraction wells are located around the three infiltration ponds. The artificial groundwater recharge facility was selected as one of the field sites for the NASRI-project, because the conditions for infiltrating water differ considerably from conditions at the two selected bank filtration sites.

Despite of the fact that the distance between infiltration pond and abstraction well (107 m) is similar to the distance at bank filtration site Tegel, the infiltration velocity is higher. This leads to significantly shorter retention times of the filtrate in the subsoil. The average retention time of the in NASRI sampled production well 20 is ~50 days. Furthermore, the character of the sediments at the GWR differs from the naturally grown lake bank sediments. Generally, the sandy sediments are poorer in particulate organic matter than the sediments close to the bank of Lake Tegel and additionally, organic debris on the floor of the infiltration ponds is regularly scraped off to restore permeability. Due to these differences the conditions during infiltration vary from the conditions observed at Tegel bank filtration site.

The redox potential of the infiltrating water shows more often oxic conditions than the bank filtrate in Tegel. Only during summer months July to September measurable amounts of nitrate are removed by denitrification during the infiltration process. Mostly oxic conditions dominate the infiltration path at the GWR throughout the rest of the year. Beside the temperature dependency of the redox conditions an influence of the infiltration cycle was observed. The infiltration conditions at the GWR change significantly with the time schedule for the removal of the filtration cake layer on the bottom of the infiltration ponds. But the changes induced by this maintenance schedule occur in time frames of days or weeks and are not reproducible by a series of monthly measurements. Therefore, the discussion in this chapter will focus on the general situation at the groundwater recharge facility and will ignore short term variations. The twenty monthly measurements of bulk and trace organics capture a close summary of the important processes at the recharge facility. More detailed information on changes due to scheduled maintenance of the infiltration ponds are available in chapter X (hydrogeological section).

Another important factor at the GWR is the short retention time, which is responsible for a very pronounced temperature profile in the abstracted water. Seasonal

temperature variations of surface water of more than 20 K occur only slightly time shifted and nearly not attenuated in the production well. Therefore, the biomass which is responsible for degradation of bulk and trace organic compounds is more exposed to extreme temperatures at the GWR than at the bank filtration sites. This might lead to reduced removal and mineralization rates during long and cold winters.

However, the monitoring period of DWQC for the GWR started in October 2002 and ended in May 2004. A transect of monitoring wells and one production well at infiltration basin 3 was selected. The monthly analytical program consisted of DOC, UVA_{254}, UVA_{436}, LC-OCD, and differentiated AOX analysis. Over a time period of 13 months (May 2003-May 2004) the monitoring was extended by trace compound analysis. The behavior of five earlier mentioned trace compounds during infiltration at the GWR was investigated. Although the infiltrated water is pumped directly from Lake Tegel, samples from the infiltration pond were analyzed. A comparison of Lake Tegel samples and infiltration pond samples will identify eventual differences in organic composition, which might be derived from the micro-filtration process or photocatalytic effects. All results of field monitoring are reported in the following chapters.

1.3.1 Groundwater Recharge - Results bulk organics

Amount and character of bulk organics in the infiltration pond was monitored monthly over the period October 2002 to May 2004 using the described analytical methods (DOC, UVA_{254}, UVA_{436} and SUVA (calculated)). Table 4 provides the arithmetic mean, median and standard deviation of all measurements and the corresponding data from Lake Tegel surface water.

Table 8 Results bulk organic parameters in GWR infiltration pond 3 and Lake Tegel surface water 2002-2004 (n=20)

		DOC	UVA_{254}	UVA_{436}	SUVA
		[mg/l]	[1/m]	[1/m]	[l/m*mg]
GWR Tegel	Arithmetic mean	7.4	15.3	0.47	2.08
	Median	7.5	15.3	0.47	2.05
	Standard deviation	0.8 (10.6%)	1.2 (8.0%)	0.14 (30.5%)	0.16 (7.7%)
Bank filtration Tegel	Arithmetic mean	7.2	15.1	0.52	2.11
	Median	7.1	15.2	0.48	2.09
	Standard deviation	0.5 (7.6%)	1.1 (7.3%)	0.11 (22.9%)	0.18 (8.8%)

It was found, that the average DOC level in infiltration pond 3 is similar to DOC concentrations observed in Lake Tegel. The median of 20 DOC measurements was 7.5 mg/l. Furthermore, a comparison of the parameters UVA_{254}, UVA_{436} and SUVA

pointed towards a very similar composition of bulk organic water constituents in both surface waters. This proves that the treatment by micro-filtration does not affect the dissolved organics. Additionally, it shows that the water composition at the pumping station (~1 km south of the bank filtration transect) is similar to the water quality in front of the transect.

Figure 51 proves that the observed changes over time for all three parameters (DOC, SAK_{254}, and SUVA) occur similarly in lake water and infiltration pond. This similarity confirms the results of the monitoring of the surface water in front of the bank filtration site. Any observed small differences are due to measurement mistakes and variations of time of sampling. During four months in winter 2002/03 the DOC level in the recharge pond is higher than in Lake Tegel. The reasons for this remain unclear, since DOC production by algae blooms in calm water bodies (recharge pond) was expected to occur during summer. Additionally, the comparison proves that no strong seasonal effects, which were not observed in Lake Tegel, influence the water quality in the recharge ponds. Judging from the heavy algae growth in the ponds during summer, an influence on the DOC-concentration and DOC-character could have been expected. This assumption was disproved by the presented results. More detailed information on the DOC-character of the recharge pond water will be provided with the LC-OCD analysis in chapter 1.3.3.
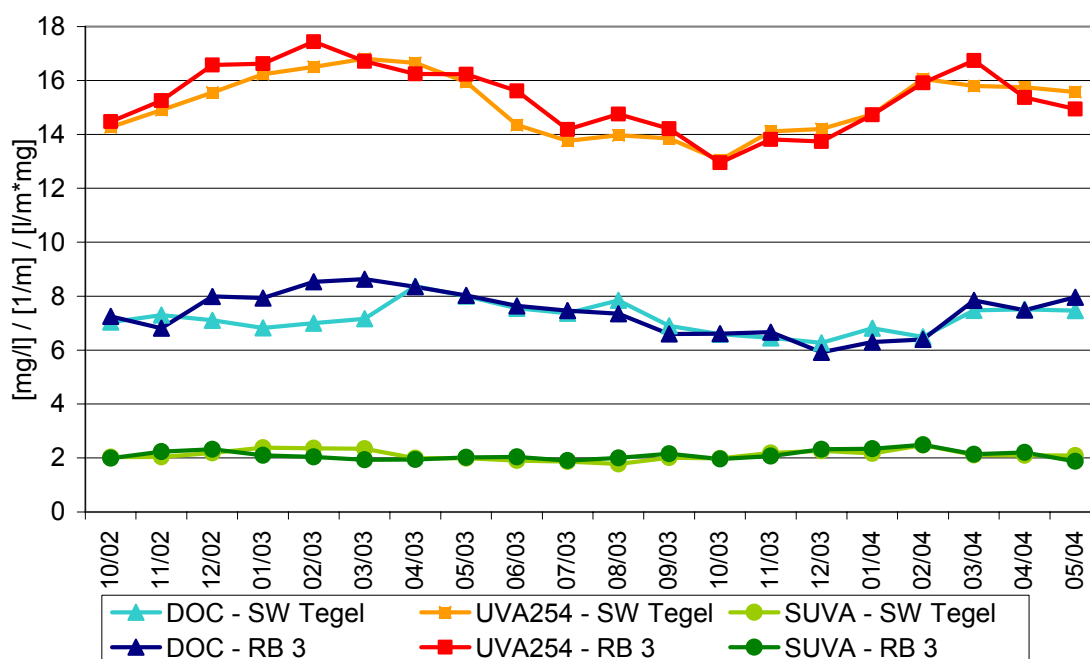
Figure 51 Comparison of bulk organics results for recharge pond 3 and Lake Tegel

Altogether, the study showed that the water quality of infiltrated water at the artificial groundwater recharge facility is similar to Lake Tegel surface water. Therefore, the

discussion on seasonal influences on the organic water composition of the infiltrated water was included in the discussion of the bank filtration field site Tegel (Chapter 1.1).

1.3.1.1 Groundwater Recharge - DOC

During the time period from October 2002 to May 2004 20 monthly samples from the pond, eight monitoring wells and one production well were taken to describe the fate of bulk organics at the artificial ground water recharge facility Tegel. The monitoring wells were located in different distances and depths between recharge pond 3 and the production well 20. Additionally, the background ground water was monitored by separate monitoring wells. The hydrogeological setup of the field site and the exact positions of the monitoring wells were investigated by the hydrogeological group and are included in chapter XX. Data evaluation of the Free University Berlin (Chapter XX) proposed that at this field site no dilution of infiltrating water on its way towards the production well occurs. The proposed mixing rations between infiltrating water and background groundwater in the production well are 80% recent infiltrate and 20% background water.

The two main effects that might influence the removal of bulk organic water constituents are the strong seasonal variations of temperature, which is nearly not attenuated during infiltration, and the changes in redox system. During winter the lowest measured water temperature in monitoring well 369UP (last monitoring well in front of production well) was 2.9°C. In next summer temperature in the same well reached 23.8°C. These temperature differences affect the whole infiltration path. As a consequence the redox system along the transect is dependent from seasons. During spring, fall, and winter oxygen and nitrate are present during infiltration. But during the extreme hot summer of 2003 oxygen and nitrate depleted from the system. It remains unclear, whether this effect occurs regularly or whether it was due to the extreme circumstances. However, compared to bank filtration at Lake Tegel the character of artificial infiltration is more oxic.

Figure 52 shows the fate of dissolved organic carbon during infiltration at the recharge facility. It stands out that after very short retention times of a few days and infiltration distances of 6-7 m (monitoring well 366 and 365) high shares of surface water DOC are mineralized. Compared to results of the mostly anoxic bank filtration site Tegel or monitoring well 205 in Wannsee the mineralization rates in the immediate infiltration zone of the GWR are high. This is most probably due to usually oxic conditions during infiltration. It is consistent with results from soil column experiments that under oxic conditions the mineralization of infiltrated BDOC takes place more rapidly. At GWR 70-80% of the overall DOC removal occurs before the infiltrate reaches the first observation well. During further infiltration the remainder of degradable organics is removed quickly and for most of the infiltration path stable DOC-concentrations were observed. Overall, approximately 40% of surface water DOC is removed during

artificial recharge and the infiltrate DOC-concentration in front of the production well was assessed with 4-5.5 mg/l. Background groundwater was found to contain 4-5 mg/l DOC, similar to the final raw water.
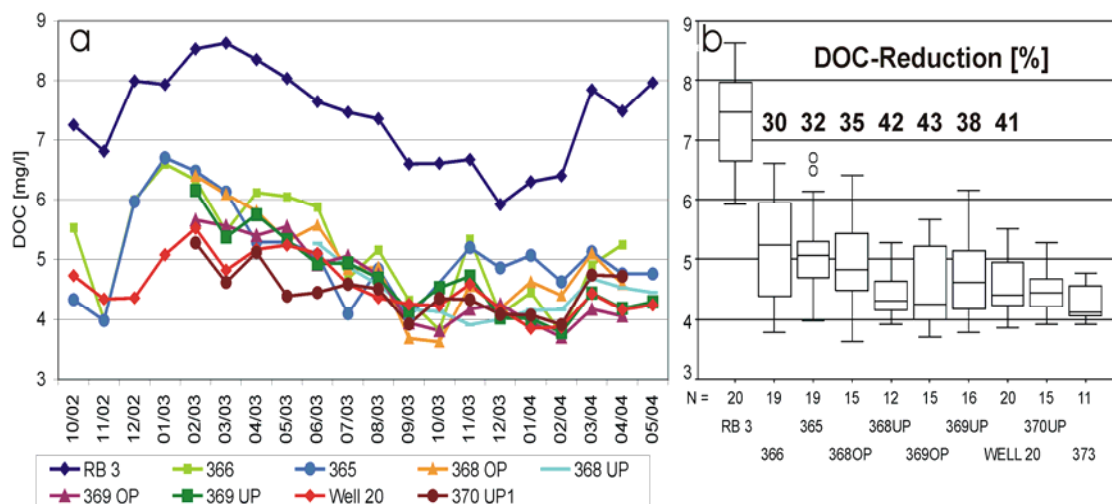
Figure 52 Fate of DOC during infiltration at GWR (a: time series; b: box plots)

The time series in Figure 52a shows that the DOC-concentration in the monitoring wells strongly depended on surface water DOC. Generally, the monitoring well-DOC followed the surface water concentration without a recognizable time shift. A slight seasonal variance of the degraded DOC in the wells near the pond was observed. During winter the efficiency of DOC mineralization in monitoring well 365 is slightly reduced because of the low temperatures. During these cold periods the concentration difference between pond water and well 365 is decreasing to 1 mg/l, whereas during rest of the year 2-3 mg/l are removed in this section of the infiltration path.

The change of redox conditions in summer 2003, which was proved by depletion of oxygen and nitrate from the system, did not affect the DOC removal efficiency. In this time period the temperature-effect which enhances the biodegradation balanced the slower DOC-removal under anoxic/anaerobic conditions.

However, DOC concentration in the abstracted water was found to be variable in a range between 4 mg/l and 5.5 mg/l. The most important factor of influence at the GWR was the surface water quality. A slight influence of the temperature was measurable in the pond-near monitoring wells. Changing redox potentials during warm summers were observed to have no measurable effect on DOC removal. Overall, it can be assumed that abstracted water contains only non-degradable DOC. The achieved DOC-residual is equal to the non-degradable fraction observed during bank filtration at Lake Tegel. Therefore, these results support the findings of the monitoring at the bank filtration site Tegel.

1.3.1.2 Groundwater Recharge - UVA$_{254}$

UV-absorption at 254 nm of the pond water samples was found to follow the seasonal variations of Lake Tegel surface water. Higher UV-absorptions were measured during winter, because the portion of treated waste water in Lake Tegel is higher in winter months. UVA$_{254}$ in pond water was measured between 13 and 17m^{-1}. Figure 53b proves that UVA$_{254}$ is reduced by ~25% in the immediate infiltration zone (monitoring well 366 and 365). During further infiltration the overall removal rates increase to 30-35%.
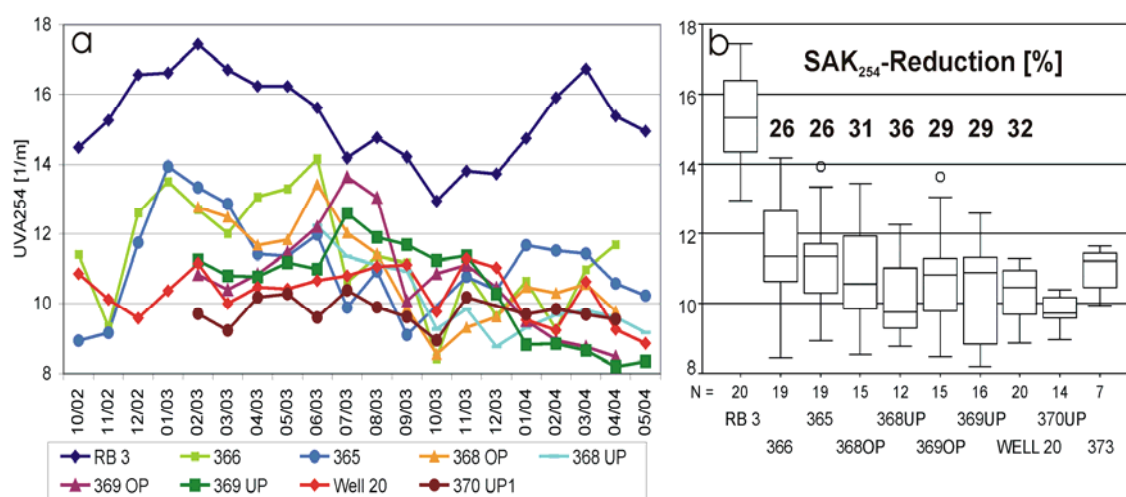
Figure 53 Fate of UVA$_{254}$ during infiltration at GWR (a: time series; b: box plots)

These results are comparable to the decrease of UV-absorption at the bank filtration site Tegel. At Wannsee field site more than 40% of the UVA$_{254}$ were removed during an infiltration of 2-4 months. But a plateauing of UV-absorption in the more distant monitoring wells at the GWR proposes that no additional removal of UVA$_{254}$ would be possible even with longer retention times. The land sided groundwater showed different UVA$_{254}$ in different depths. Average UV-absorption was ~10 m^{-1} in 370UP above the aquitard. Despite of a lower DOC-concentration in monitoring well 373 the UVA$_{254}$ was slightly higher. This indicates a different organic composition of groundwater above and under the aquitard.

The time series of UVA$_{254}$ of the monitoring wells samples at the GWR is difficult to interpret. For monitoring wells in the infiltration zone (366 and 365) a strong dependency of UV-absorption from pond water-UVA$_{254}$ was confirmed. More distant monitoring wells (368OP/UP and 369OP/UP) show a high variation and erratic changes in UV-absorption. Reasons for these changes in UV-absorption (range 8 to 12 m^{-1}) remain unclear. Figure 53 shows that during early summer 2003 water with a higher UV-Absorption dominated the infiltration path. Afterwards, UV-absorption in the mentioned monitoring wells decreased until spring 2004. No reference for this effect

was visible in the pond water quality. Background groundwater and the raw water of the production well exhibited comparably stable UV-absorptions with no seasonal influences.

Overall, the observed UVA_{254} removal rates during artificial recharge are slightly lower than the measured DOC mineralization. This indicates an increased aromaticity in the final raw water compared to the infiltrated surface water.

The results for the color measurements at 436 nm were found to be close to the detection limit. Therefore, no interpretation and conclusion arose from these measurements.

1.3.1.3 Groundwater Recharge - SUVA

A better characterization of the organic carbon in the groundwater recharge system provided the parameter SUVA. SUVA is a measure of aromaticity of organic carbon and is calculated from DOC and UVA_{254}. Figure 54 proves that similarly to the bank filtration sites in Tegel and Wannsee the aromaticity of organic carbon increases shortly after infiltration. For the pond water median SUVA was calculated with 2.05 l/m*mg which is comparable to Lake Tegel SUVA. After infiltration aromaticity increases to a SUVA of ~2.2 l/m*mg in the infiltration zone (366 and 365) and up to 2.4 l/m*mg in more distant monitoring wells. Additionally, the variance and standard deviation of the measurements in the monitoring wells increases with distance from pond. Usually, longer infiltration stabilizes extreme values and smaller amplitudes of SUVA changes could have been expected.

However, Figure 54a provides explanation for the observed fate of SUVA. The time series points out two factors of influence for the SUVA:

First, during summer 2003 the SUVA of infiltrated water increases independently from surface water. It is assumed that the increased SUVA is due to a temperature effect that was similarly observed in the deep wells of bank filtration site Tegel. Organic material with a highly aromatic character is released from the sediment in times of warmer temperatures. It remains unclear whether this material is derived from POC degradation or adsorption processes. Despite of the sandy sediment structure a small percentage of hydrophobic and aromatic organics could adsorb to the material during cold season. If the material is released by higher temperatures, it would increase aromaticity of the infiltrate significantly. The fractions are very small and were not detected by DOC or UVA_{254} analysis. The peak during June to October 2003 can most probably be ascribed to this effect. Furthermore, this finding explains the higher variances of SUVA in more distant monitoring wells.
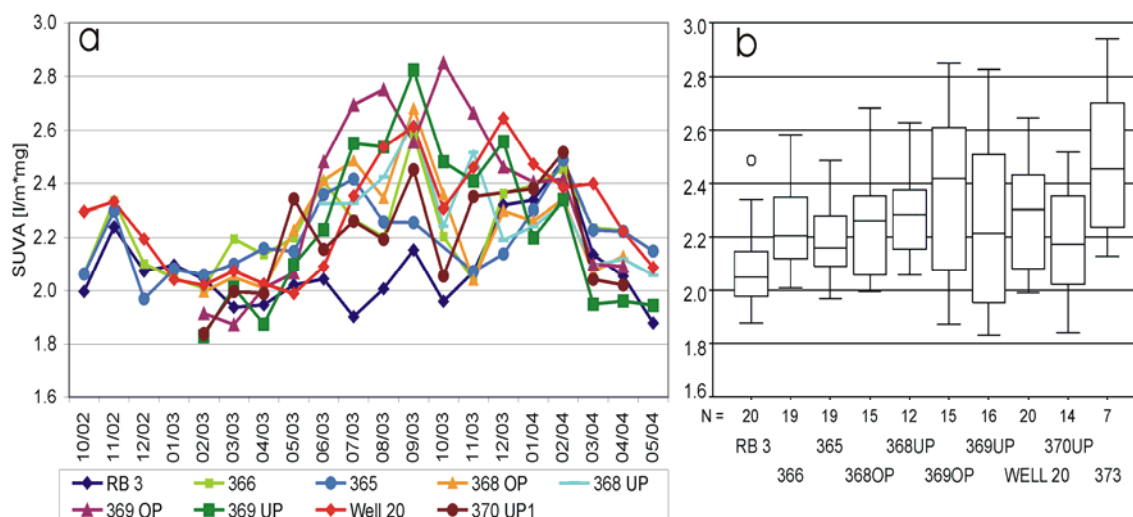
Figure 54 Fate of SUVA during infiltration at GWR (a: time series; b: box plots)

Second factor of influence on the SUVA of organic water constituents during infiltration is surface water quality. Starting in November 2003 until February 2004 the SUVA of the pond water increased to 2.4 l/m*mg. This change in water quality affected all monitoring wells nearly immediately. Because of short retention times the monthly sampling did not reproduce the time shift of the peak in the subsequent monitoring wells.

The background groundwater showed different aromaticities in the sampled depths. As signalized by the UVA results, the water in the deeper aquifer was characterized by a higher aromaticity of organics.

1.3.2 Groundwater Recharge - LC-OCD

The organic water constituents of the recharge pond water were characterized by 10 monthly measurements using LC-OCD technique. One point of interest was a comparison of the DOC character of Lake Tegel surface water and the water of the recharge pond. Table 3 shows that the integration of the LC-OCD chromatograms leads to similar results for both water types.

Table 9 Portions and concentrations of different fractions of DOC (Recharge pond 3, Lake Tegel)

	Poly-saccharides	Humic substances	Humic substances-Building blocks	Low molecular acids	Neutrals and Hydrophobics
Recharge pond	9.1 %	46.6 %	23.8 %	3.2 %	17.4 %
	0.7 mg/l	3.5 mg/l	1.8 mg/l	0.2 mg/l	1.3 mg/l
Lake Tegel (n=12)	8.7 %	46.0 %	22.1 %	3.7 %	19.7 %
	0.6 mg/l	3.3 mg/l	1.6 mg/l	0.3 mg/l	1.4 mg/l

It was found that the amounts and percentages for the five different DOC fractions corresponded closely within the limits of the method. Small variations occurred only in fractions, which were hard to quantify (HS-building blocks and Neutrals). Therefore, it is assumed that no strong influences on the character of organics in the recharge pond existed and that the water quality of the artificially infiltrated water complies with surface water quality of Lake Tegel. Seasonal changes observed for the polysaccharide fraction were found to be of the similar nature as in Lake Wannsee. Since these changes were not as pronounced, they were not evaluated more closely.

During infiltration the character of bulk organic compounds changed. Similar results were obtained at the two monitored bank filtration site. As quantitative DOC analysis indicated, most of the biodegradation of DOC and the changes within DOC-fractions occurred shortly after infiltration. Under mostly oxic conditions at the artificial recharge site BDOC removal was found to be a fast process. After the removal of BDOC the non-degradable DOC remained in the infiltrate and the DOC level plateaued at ~4.5 mg/l. However, Figure 55 shows that the LC-OCD chromatograms of pond water and the first monitoring well (366) are substantially different. Chromatograms of more distant monitoring wells have a similar shape as the 366. This is consistent with the mentioned results of DOC-quantification and proves that at the artificial recharge facility the qualitative and quantitative effects on the bulk organic composition occur concentrated near the water sediment interface close to the recharge pond. It can be assumed that biological activity in these sediment layers is considerably higher than in more distant layers.
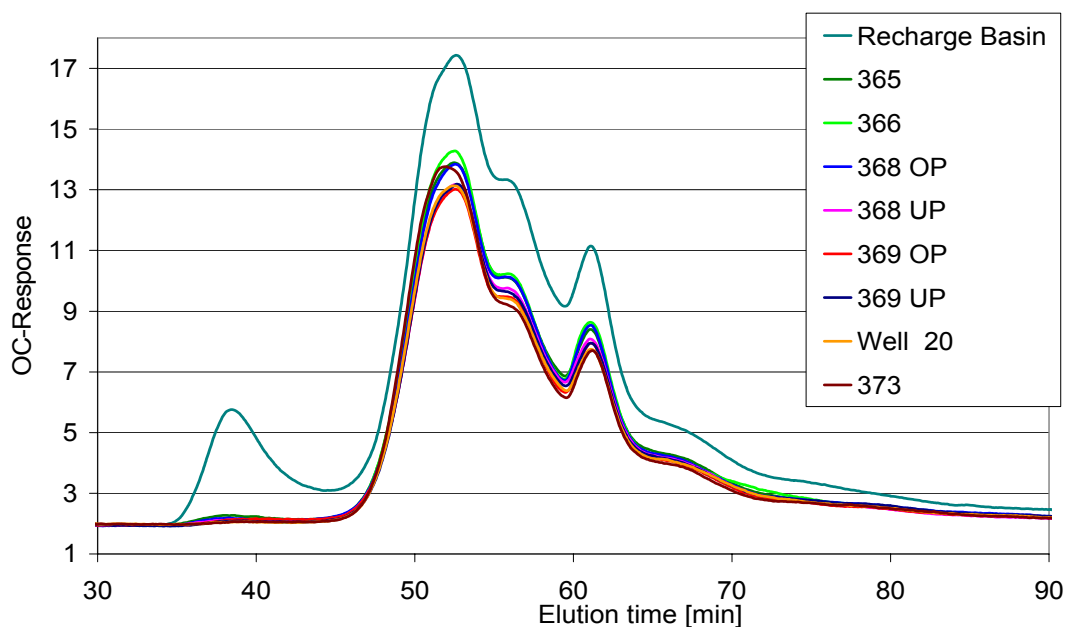
Figure 55 LC-OCD chromatogram of transect at the artificial recharge facility (mean, n=10)

Most important changes were observed within the fraction of polysaccharides, which were degraded very efficiently in the first infiltration step. Nearly no traces of polysaccharides were detected in all monitoring wells and the removal rate was close to 100%. All other fractions were only partially removed during infiltration. Figure 56 depicts in a summary of all ten LC-OCD measurements the monitored changes of DOC composition along the infiltration path. The highest change in concentration was found for the fraction of humic substances, which loose 1.1 mg/l from an initial concentration of 3.5 mg/l (30%). For all other fractions removal rates ranged from 30% to 40%. Together they resulted in an overall DOC mineralization of 38%. The character of bulk organics in background groundwater was found to be very close to the character of the organics in the infiltrated water.
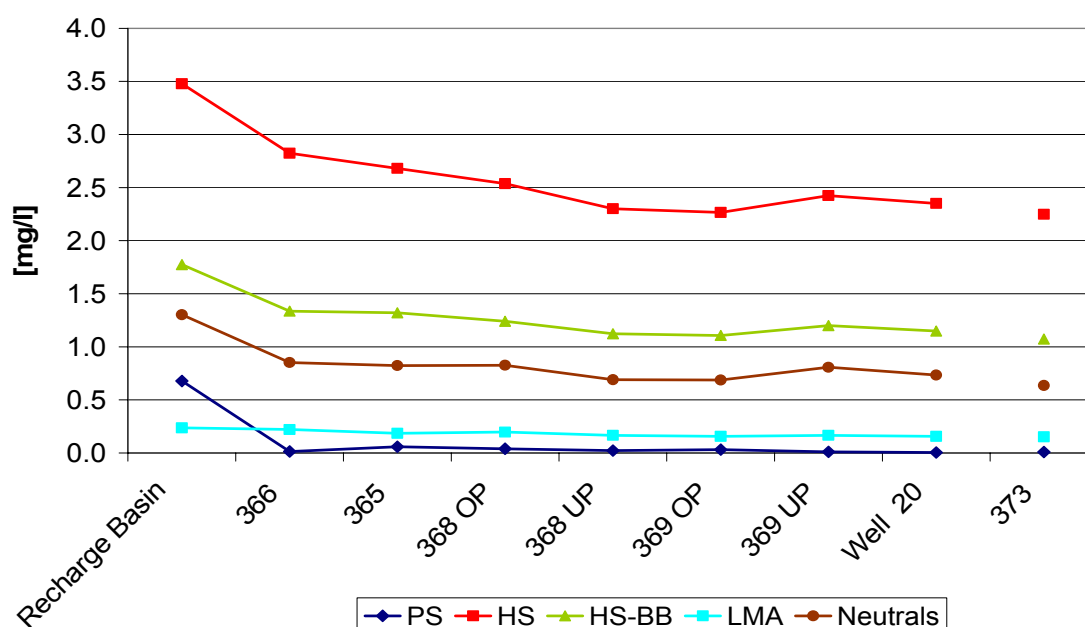
Figure 56 Concentrations of the different fractions of DOC at transect GWR

Table 10 provides the observed changes on concentration basis and the percentage variations. Since at the GWR no dilution with other groundwater within the circle of production wells occurs, all observed effects can be ascribed to biodegradation and transformation. Only in the production wells some dilution with background groundwater was present.

Table 10 Portions and concentrations of different fractions of DOC at transect GWR (n=10)

	Poly-saccharides	Humic substances	Humic substances-Building blocks	Low molecular acids	Neutrals and Hydrophobics
Recharge pond 3	9.1 %	46.6 %	23.8 %	3.2 %	17.4 %
	0.7 mg/l	3.5 mg/l	1.8 mg/l	0.2 mg/l	1.3 mg/l
366	0.3 %	53.8 %	25.5 %	4.2 %	16.2 %
	0.0 mg/l	2.8 mg/l	1.3 mg/l	0.2 mg/l	0.9 mg/l
365	1.2 %	52.9 %	26.0 %	3.7 %	16.2 %
	0.1 mg/l	2.7 mg/l	1.3 mg/l	0.2 mg/l	0.8 mg/l
368OP	0.8 %	52.4 %	25.6 %	4.1 %	17.1 %
	0.0 mg/l	2.5 mg/l	1.2 mg/l	0.2 mg/l	0.8 mg/l
368UP	0.5 %	53.5 %	26.1 %	3.9 %	16.0 %
	0.0 mg/l	2.3 mg/l	1.1 mg/l	0.2 mg/l	0.7 mg/l
369OP	0.7 %	53.3 %	26.1 %	3.7 %	16.2 %
	0.0 mg/l	2.3 mg/l	1.1 mg/l	0.2 mg/l	0.7 mg/l
369UP	0.2 %	52.6 %	26.0 %	3.6 %	17.5 %
	0.0 mg/l	2.4 mg/l	1.2 mg/l	0.2 mg/l	0.8 mg/l
Well 20	0.1 %	53.5 %	26.1 %	3.6 %	16.7 %
	0.0 mg/l	2.4 mg/l	1.1 mg/l	0.2 mg/l	0.7 mg/l
373	0.2 %	54.6 %	26.1 %	3.7 %	15.4 %
	0.0 mg/l	2.2 mg/l	1.1 mg/l	0.2 mg/l	0.6 mg/l

Overall, LC-OCD analysis proved that the same fractions of DOC are responsible for the depletion of total DOC during bank filtration and artificial recharge. In both systems the BDOC is part of all fractions of DOC, whereas the polysaccharide fraction contains only BDOC. It can be assumed that the biological effects in bank filtration and groundwater recharge are of the same nature. The described changes occurred within a maximum infiltration time of 50 days under the mostly oxic conditions of the groundwater recharge facility. Results from bank filtration site Tegel showed that under anoxic or anaerobic conditions this time frame would not be sufficient for a complete mineralization of BDOC.

1.3.3 Groundwater Recharge - AOI Results

The concentration of adsorbable organic Iodine in recharge pond 3 is comparable to concentrations in the surface water of Lake Tegel. Figure 57 compares the time series of both sampling points. The concentration in recharge pond 3 follows the surface water concentration with a slight time shift which is most probably due to the location of the pumping station farer south in Lake Tegel. The results are consistent with the assumption that a high portion of AOI is introduced to Lake Tegel with treated effluent which enters Lake Tegel at the north end. Therefore, it can be assumed that AOI

concentration was neither depleted nor increased by additional retention time in Lake Tegel, micro-filtration treatment or additional retention time in the recharge pond.

Figure 57 Comparison of AOI concentrations measured in recharge pond 3 and Lake Tegel

Fate of AOI during infiltration at the artificial groundwater recharge facility was monitored over a time period of 20 months from October 2002 to May 2004. Within the observation period a strong increase of AOI-levels from concentrations around 6-8 µg/l to more than 14 µg/l was found. The changes in the monitoring wells and the abstracted water after the strong surface water concentration increase revealed interesting details about the fate of halogenated organic compounds during artificial recharge.

Along the infiltration path towards the production well only very few remediation of the AOI occurred. Figure 58 shows that the monitoring wells close to the production well were found to contain most of the time nearly as much AOI as the surface water. Temporarily higher concentrations are due to short term variations of surface water. In well 365, 366 and 368OP removal was less than 10% and observed differences were often close to the limit of detection. Along the further infiltration path some remediation was present, but compared to the bank filtration field site in Tegel the removal rates of maximum 25% were very low. This is explained by very low retention times at the artificial recharge facility and mostly oxic conditions during infiltration. Only during hot summers redox conditions in the infiltration area switch to anoxic and slightly anaerobic. The effect of the changing redox system on the fate of AOI can be observed best in monitoring well 369OP and the production well. At both sampling points AOI concentrations start to rise in spring 2003 with the surface water. But in September 2003 the AOI-concentrations in 369UP and the production well drop although the surface water concentrations remain on a high level. From measurements of redox

potential and nitrate concentration it was known that during summer the system switched to anoxic/anaerobic conditions for approximately 3 months. During this time a better remediation of AOI was found. Reductive dehalogenation was proved at other field sites to be the most effective removal mechanism for adsorbable halogenated compounds. This effect influenced the AOI removal rates during summer 2003 and lead for a limited time period to lower AOI concentrations in the production well.
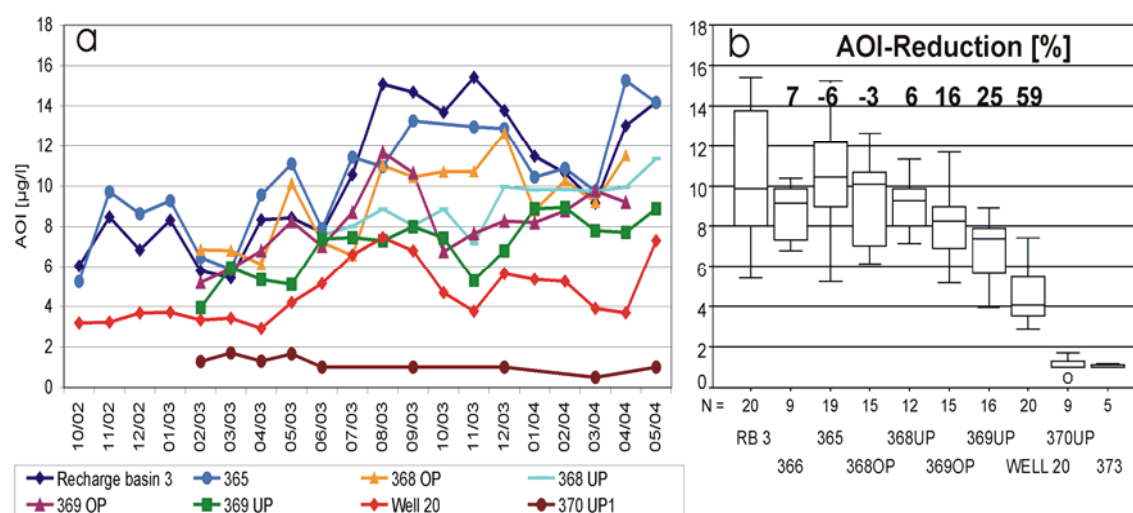
Figure 58 Fate of AOI during infiltration at GWR (a: time series; b: box plots)

However, Figure 58 exhibits clearly that the AOI concentration of the abstracted water is strongly dependent from surface water quality. Because of short retention times increased surface water AOI-concentrations break through nearly immediately to the production well. A 100% increase of AOI concentration in the surface water lead to more than 100% increase in the abstracted water, where AOI-levels rose from ~3 μg/l to more than 7 μg/l. Because of some dilution with background groundwater the overall removal rates for the production well add up to nearly 60%. Background groundwater was found to be very low in AOI with concentrations around the limit of detection (1 μg/l). However, the average AOI concentration of the abstracted water at the artificial recharge site is ~4 μg/l. This is approximately double as high as the AOI concentration of the product water at the bank filtration site (~2 μg/l). Furthermore, the AOI level of the product water at GWR was found to be highly variable. This finding was proved by the last measurement in May 2004.

Overall, it can be summarized that the conditions at the artificial recharge site Tegel are not favorable for an effective dehalogenation of AOI. Short retention times and mostly oxic conditions during infiltration allow high concentrations of AOI to pass through the soil to the production well.

1.3.4 Groundwater Recharge - AOBr Results

Adsorbable organic Bromine at the artificial recharge site was monitored in the same time period as the AOI. Figure 59 shows that for most of the monitoring time AOBr concentration in the recharge pond was equal to the AOBr levels in Lake Tegel. Only during summer of 2003 the recharge basin contained higher concentrations than the surface water of Lake Tegel. This can be explained by additional sun exposure and low water movement in the recharge ponds, which consequentially induced stronger algae blooms. Parts of the AOBr are known to be associated with algae and occur in surface waters in times of strong algae blooms or during die off times of these blooms. The strong AOBr peak in the recharge basin is most probably due to perfect conditions for algaes in the ponds. Contrary to the AOI peak no time shift was observed for the AOBr peak in summer 2003, indicating the origin of the increased AOBr level in the lake and not in discharged treated effluent. This is consistent with all results from the field sites Wannsee and Tegel. The AOBr levels of Lake Tegel and the recharge basin are identical during winter, when most of the AOBr is of anthropogenic origin and enters Lake Tegel with the treated effluent.
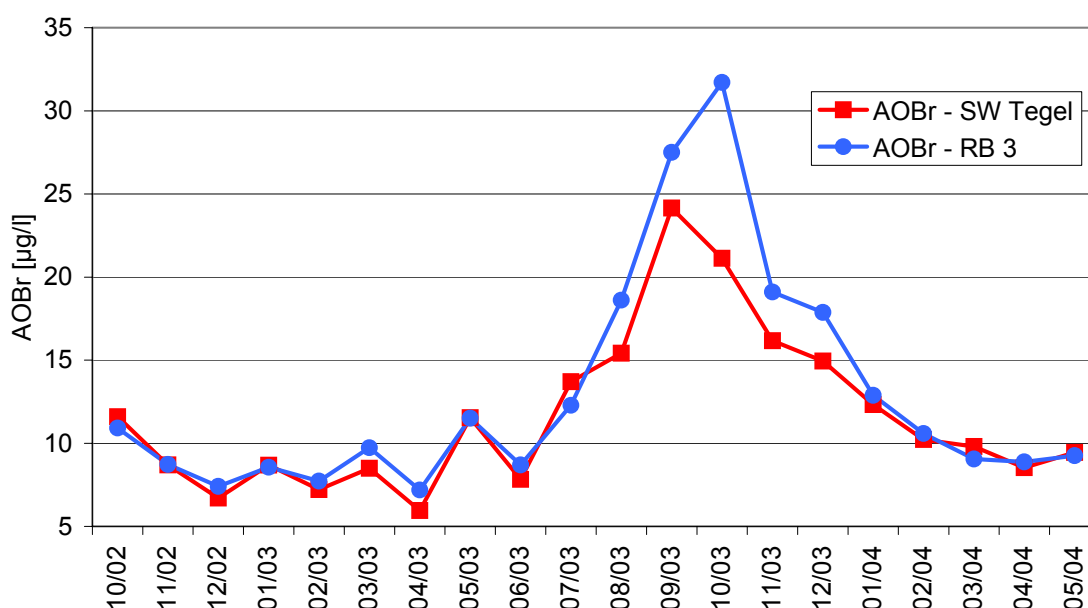
Figure 59 Comparison of AOBr concentrations measured in recharge pond 3 and Lake Tegel

During infiltration towards the production well the two different fractions of AOBr showed a completely different behavior. Anthropogenic AOBr which is present all year in surface water in concentrations between 6 µg/l and 10 µg/l was not removed during the 50 day infiltration time. The observed removals during these times were very often in the range of the accuracy of the method and the average removal rates for all monitoring wells were under 10%. Only in the production well, where dilution with the low AOBr-background groundwater occurs, a removal of 38% of AOBr was observed.

Contrary to this, the algae associated AOBr was removed completely in the first monitoring well 365. The peak in the surface water is statistically regarded as an extreme value (Figure 60b), but the time series in Figure 60a proves that no higher concentrations were measured in pond near monitoring wells during the period of elevated AOBr. Therefore, it can be concluded that algae associated AOBr is easy degradable under oxic conditions, whereas the other anthropogenic AOBr-fraction is not degradable under the conditions of the GWR. A slight indication of a better removal during the anoxic/anaerobic period in late summer 2003 is visible in monitoring well 369UP and the production well. In this time period the AOBr-levels in the mentioned wells decrease despite of high surface water concentrations. Consistently with results from all other field sites a dehalogenation of anthropogenic AOBr occurs only under anaerobic conditions.
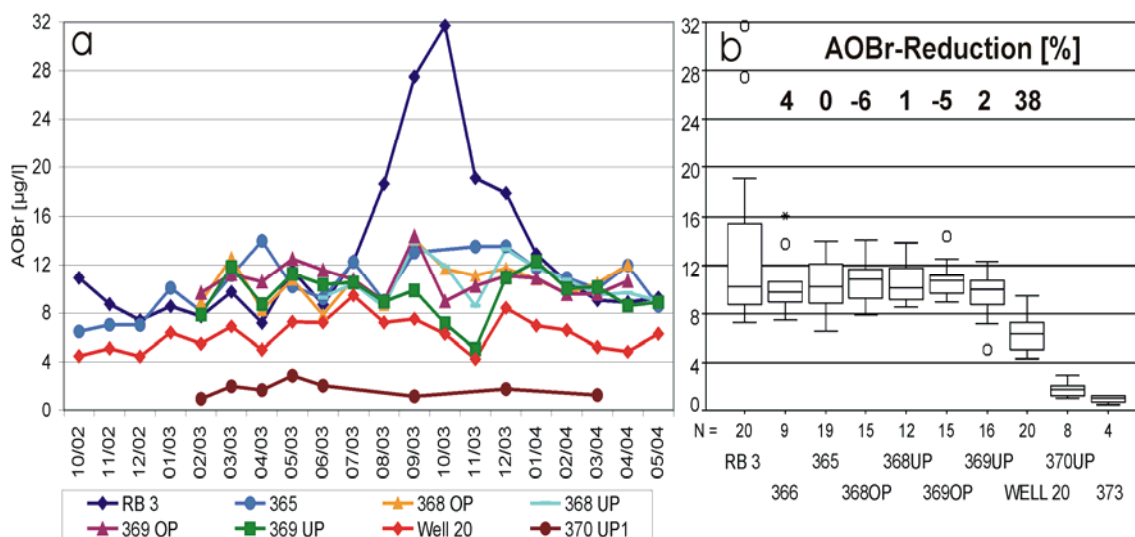
Figure 60 Fate of AOBr during infiltration at GWR (a: time series; b: box plots)

Overall, the results from the artificial recharge site confirm the findings of the two bank filtration field sites. No efficient dehalogenation was expected at the recharge site. A comparison of AOI and AOBr reveals that at all field sites the removal rates for anthropogenic AOBr are lower than for AOI. The summery peaks of AOI, which are due to less dilution of the treated effluent occur most probably also for anthropogenic AOBr. But in the surface waters these peaks are superposed by high algae associated AOBr concentrations that occur only during summer. These very high AOBr levels were found to be unproblematic for the drinking water production since they are easily mineralized during bank filtration and groundwater recharge.

1.3.5   Groundwater Recharge - Trace pollutant results

For a period of thirteen months the fate of trace pollutants along the infiltration path from the recharge pond to the production well 20 was investigated. Not all monitoring wells were included in this analytical program. The following chapter describes the behavior of the selected trace compounds (Iopromide, Sulfamethoxazole and three isomers of naphthalenedisulfonic acid) using datasets of the monitoring wells 365, 368UP, 369UP, 373 and the production well 20.

Infiltration at the artificial groundwater recharge facility is characterized by a high hydraulic loading rate of 1-2 m/d, short retention times and mostly oxic conditions. The fate of the trace compounds under these conditions is different from the behavior at the bank filtration field sites. Additionally, it was of interest to compare the concentration of trace pollutants in the recharge pond and in Lake Tegel. Since the water is pumped from Lake Tegel and seasonally (Summer) micro-filtrated, before it enters the recharge pond, a comparison of the measured concentrations would reveal any effects of this treatment on trace pollutants. Figure 61 shows the time series of Iopromide and Sulfamethoxazole concentrations in the recharge pond and Lake Tegel. It was found that the Iopromide concentration in the recharge pond was most of the time lower than in the lake. The average difference was ~ 100 ng/l. It is assumed that the difference is due to some bioremediation of Iopromide in surface water or in the biofilms of pumps and piping of the GWR facility. Iopromide was found at all field sites and in soil column experiments to be easily metabolized. The triiodinated benzene structure of the molecule remains most likely unaffected under oxic conditions. AOI results proved that no deiodination occurred on the way from the lake to the recharge pond.
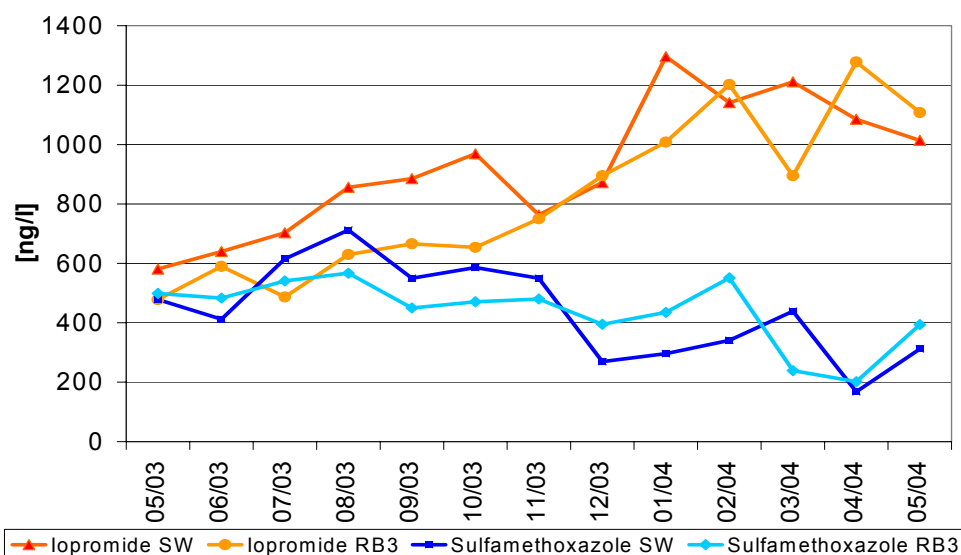
Figure 61 Comparison of Iopromide/Sulfamethoxazole concentration in recharge pond and surface water of Lake Tegel

For all other monitored compounds time series and mean concentrations in the recharge pond and the lake pointed towards no removal in surface water (Figure 62). Temporal variations of surface water concentration were responsible for slight variations. But a statistical evaluation of the datasets revealed no significant differences between lake concentration and recharge pond pollution level. Table 11 provides arithmetic mean, median concentration and standard deviation of all monitored trace compounds in recharge pond 3. All compounds were measured thirteen times during the time period May 2003 to May 2004.

Table 11 Monitoring results for trace pollutants in recharge pond

	Iopromide	Sulfameth.	1.5-NDSA	1.7-NDSA	2.7-NDSA
	[ng/l]	[ng/l]	[ng/l]	[ng/l]	[ng/l]
Arithmetic mean	819	439	104	327	105
Median	750	471	105	348	97
Standard deviation	267	111	30	59	38

The trends of the time series were present in both data sets. Figure 61 and Figure 62 indicated increasing surface water concentrations for Iopromid, 1,5-NDSA and 2,7-NDSA. For 1,7-NDSA the concentrations remained nearly stable during the observation period and for Sulfamethoxazole the pollution level decreased slightly.
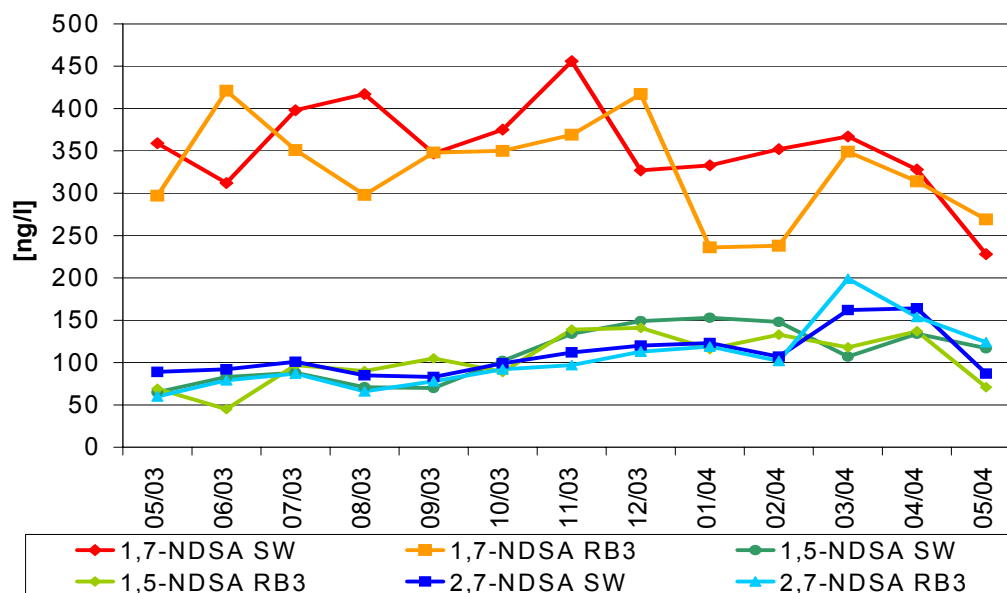
Figure 62 Comparison of NDSA concentrations in recharge pond and surface water of Lake Tegel

Figure 63 provides insight into the behavior of the X-ray contrast agent Iopromide at the artificial recharge facility. It was found that Iopromide is efficiently removed during recharge. Measurable concentrations were only found in monitoring wells close to the recharge pond. In the first monitoring well 365, Iopromide concentration was already depleted to an average of 6% of surface water concentration (removal rate: 94%). In more distant monitoring wells only traces of the Iopromide molecule were detected and removal rates were calculated with 100%. A similar efficient depletion of Iopromide was observed at all field sites and in soil column experiments.
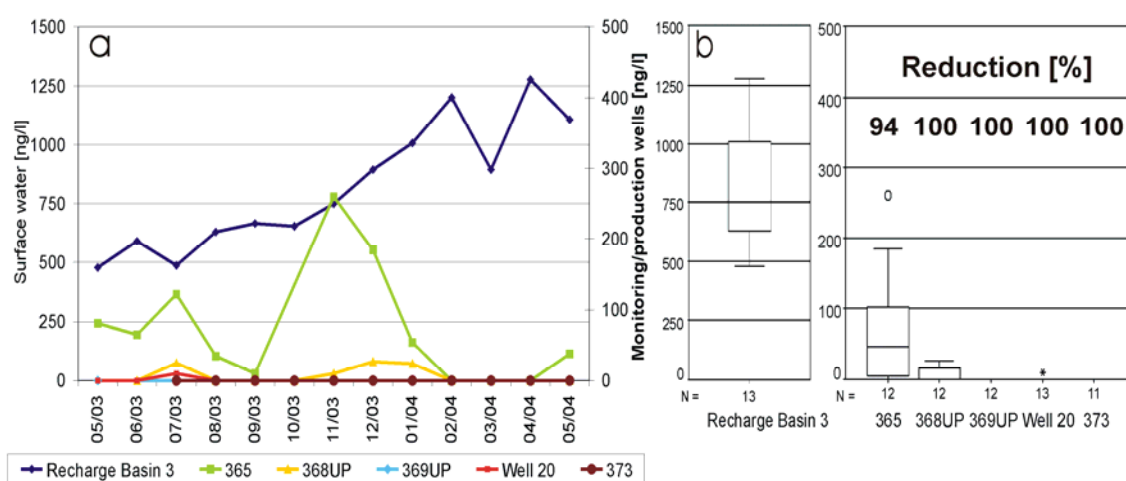
Figure 63 Fate of Iopromide during infiltration at GWR (a: time series; b: box plots)

But it was proved that no efficient mineralization of Iopromide is possible under oxic conditions. Therefore, it is concluded that the low concentrations of Iopromide, which were measured in the monitoring wells at the GWR, are due to a metabolization of the molecule. It was observed that metabolization occurred fastest under oxic conditions. A dehalogenation and mineralization of the Iopromide molecule can only be expected under strongly reducing conditions. Since redox potentials at the GWR are high for most of the year the dominating removal mechanism for this x-ray contrast agent is assumed to be metabolization. The time series of Iopromide in Figure 63a shows an increase of Iopromide concentration in monitoring wells during winter 2003. The significantly higher concentrations in monitoring well 365 and the slightly increased levels in 368UP were most probable due to temperature effects. Low water temperatures and lower biological activity in the infiltration area seem to inhibit the metabolization of Iopromide partly.

The antibiotic drug Sulfamethoxazole was present in recharge pond water in concentrations of 200 – 550 ng/l with a slight trend towards lower concentrations at the end of the monitoring period. From literature data (Schmidt et al. 2004), results of field monitorings and soil column experiments it was known that Sulfamethoxazole is preferably degraded under anaerobic conditions. Since redox conditions at the GWR

are mostly oxic and retention times are short compared to the other field sites, no efficient removal of Sulfamethoxazole could be expected.

Figure 64 shows that the observed removal rates (40-55%) were lower than at the bank filtration site Tegel. There, a reduction of 75% of the antibiotic was achieved within 3-4 months of infiltration (monitoring well 3303) under mostly anoxic/anaerobic conditions. The average raw water concentration at the bank filtration site was 26 ng/l because of some dilution with background groundwater. At the artificial recharge site raw water concentration of Sulfamethoxazole in the production well is four times higher (110 ng/l). This is consistent with the mentioned literature data and indicates a preferred removal of Sulfamethoxazole under anaerobic conditions. Results of the field site Wannsee showed that under oxic conditions even a retention time of 3 months is not improving the removal rates for Sulfamethoxazole significantly. Therefore, it is clear that the less efficient removal of Sulfamethoxazole at the GWR is due to the dominant oxic redox conditions and not necessarily to short retention times.
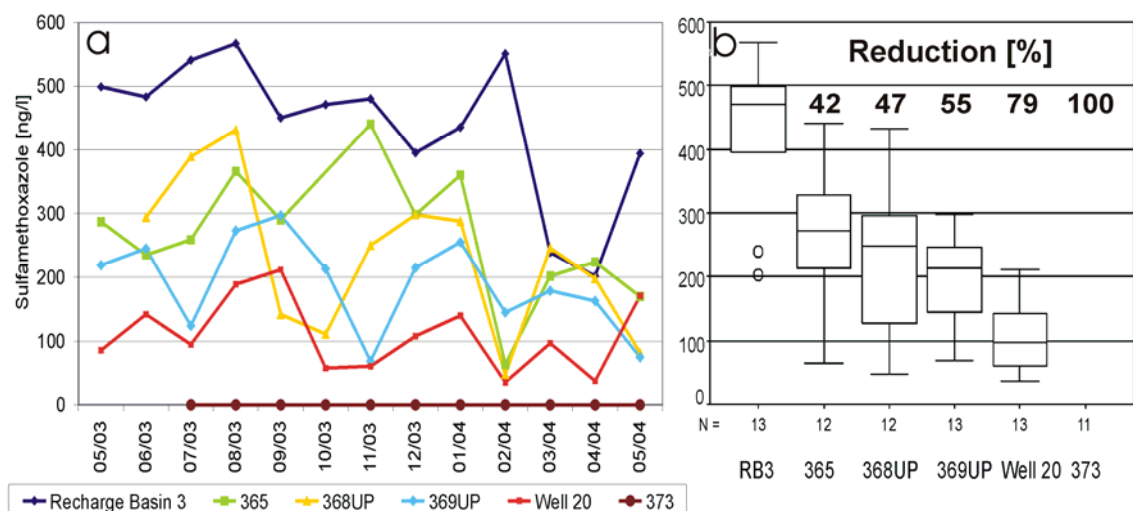
Figure 64 Fate of Sulfamethoxazole during infiltration at GWR (a: time series; b: box plots)

In Figure 64a, the time series of Sulfamethoxazole concentrations in the monitoring wells is presented. It was found that Sulfamethoxazole concentration in the monitoring wells is highly variable and not necessarily dependent on surface water concentration. Erratic changes in concentration indicate several factors of influence. Besides temperature the changing states of the recharge cycle might influence the removal efficiency. Unfortunately, a comparison of the results with recharge schedule (provided by modeling group) did not lead to clarification. A detailed analysis was not possible with monthly measurements. However, Sulfamethoxazole concentration in the raw water was found to be relative stable in the range 50-200 ng/l. No Sulfamethoxazole was present in the background groundwater.

The monitored isomers of the naphthalenedisulfonic acid were found to be present in pond water at the artificial recharge facility. Despite of their nearly similar chemical

structure, the observed removal rates differed substantially. 1,5-NDSA was found to be mostly persistent, whereas 1,7- and 2,7-NDSA showed removal rates of 60-80%. This discrepancy was also observed at two bank filtration field sites. Therefore, the results of the monitoring of the artificial recharge facility confirm the general findings on the biological removal of naphthalenedisulfonates.

1,5-NDSA isomer is the most persistent single compound in the monitoring program of the DWQC. Soil column experiments proved that oxic conditions are favorable for the mineralization of naphthalenesulfonates. Therefore, the infiltration path towards the monitoring well provided good conditions for the mineralization of naphthalenesulfonates. Figure 65 shows that even under these favorable conditions the 1,5-NDSA isomer is not efficiently mineralized and the pollution level decreases only by 10% during 50 days of infiltration towards monitoring well 369UP. The production well was found to contain slightly lower concentrations because of some dilution with background groundwater. All NDSA-isomers were found in the background groundwater in measurable concentrations.
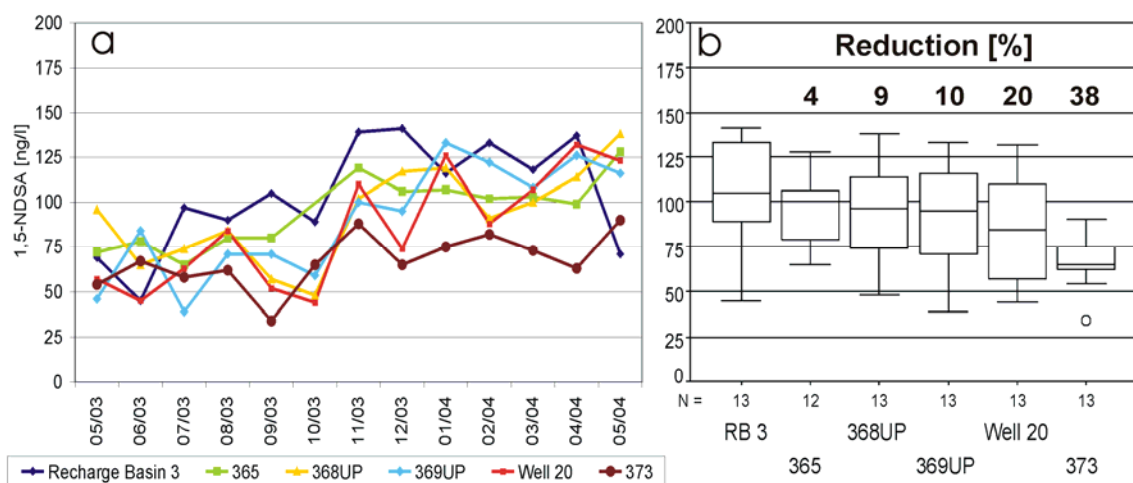
Figure 65 Fate of 1,5-Naphthalenedisulfonic acid during infiltration at GWR (a: time series; b: box plots)

The time series in Figure 65a shows that the slight trend towards higher concentrations during the monitoring period originates from surface water. A comparison with results of the monitoring of Lake Tegel proves that the surface water concentration of 1,5-NDSA increased. Since the retention times are short and the compound is not mineralized during infiltration, higher concentrations reach the more distant monitoring wells in short time. The stability of the compound would allow an interpretation of the results as a tracer, but the monthly sampling does not provide enough data. However, in all monitoring wells 1,5-NDSA concentration was found to be in the range 50-150 ng/l. The background ground water contained 60-80 ng/l. Because of the stability of the compound a high share of the surface water load enters the raw water. Fate of

1,5-NDSA during drinking water treatment was not investigated but considering the stability of the compound it is likely to find 1,5-NDSA in lower concentrations (dilution) in drinking water.

The other two monitored NDSA-isomers were removed more efficiently during soil passage. Figure 66 shows that the observed removal rates for 1,7-NDSA were ~60% and for 2,7-NDSA up to 85% (Figure 67). These removals were higher than mineralization rates observed at the bank filtration site Tegel. The oxic infiltration path at field site Wannsee provided a similar efficient removal of these two isomers. Contrary to the results for the 1,5-isomer, which was not degradable under either redox conditions, the 1,7- an 2,7-isomer were more efficient degraded under oxic conditions. Results of the GWR show that even oxic soil passages with short retention times of only 50 days can act as a barrier against these degradable pollutants.

Figure 66 shows that the surface water pollution level for 1,7-NDSA was high with concentrations between 250-450 ng/l. Despite of a removal of ~60% of the compound the median concentration in the produced raw water was 148 ng/l. Most of the removal was found to occur within the first meter of infiltration. Along the further infiltration path the concentrations were found to remain nearly stable. The time series in Figure 66a proves that a seasonal influence on the removal efficiency for 1,7-NDSA is given. During colder winter months in 2003/04 the concentrations in the monitoring wells increased considerably, indicating a strong influence of temperature on biodegradation. This seasonal influence is leading to a high variability of 1,7-NDSA concentration in the monitoring wells. Background groundwater pollution level was relatively stable between 100-150 ng/l.
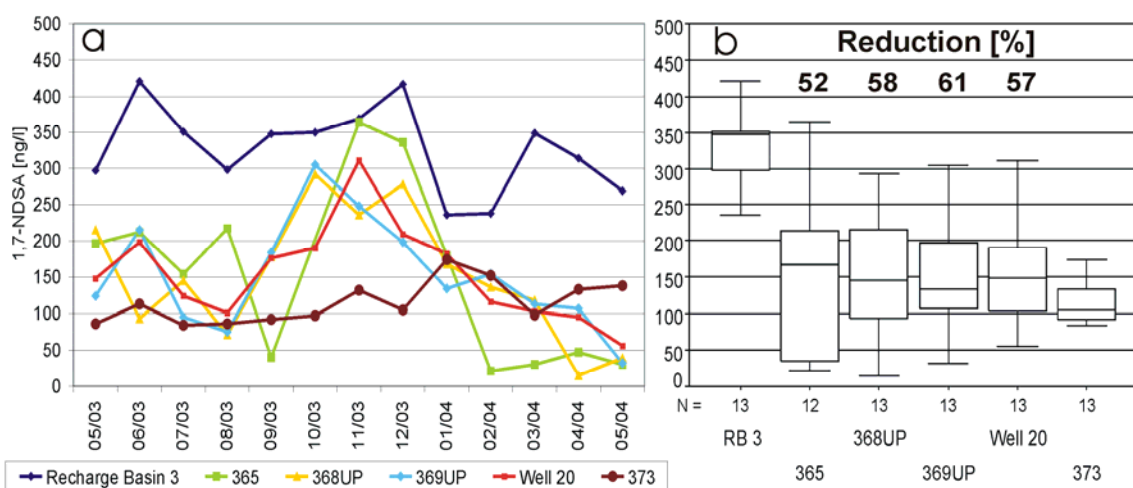
Figure 66 Fate of 1,7-Naphthalenedisulfonic acid during infiltration at GWR (a: time series; b: box plots)

Figure 67 provides results for the 2,7-NDSA isomer. For this compound the surface water concentrations were low in the range of 60-200 ng/l and the observed removal

rates were high. Therefore, measured concentration in the monitoring wells were partly under the limit of quantification of 30 ng/l. Detected traces under the limit of quantification were entered into the database with half the limit of quantification (for 2,7-NDSA =>15 ng/l).

Figure 67 shows that 2,7-NDSA is efficiently removed during oxic soil passage. Most of the time only traces below the limit of quantification were found in the last monitoring well in front of the production well (369UP). During winter concentrations increased slightly because of the mentioned temperature effect, which is more apparent for the 1,7-NDSA. Because of some influence of polluted background groundwater the median concentration in the production well increased again to 42 ng/l. Overall, 2,7-NDSA was found to be the best degradable NDSA-isomer under the conditions of the groundwater recharge facility. Because of low surface water concentrations and the good degradability the raw water concentration is very low.
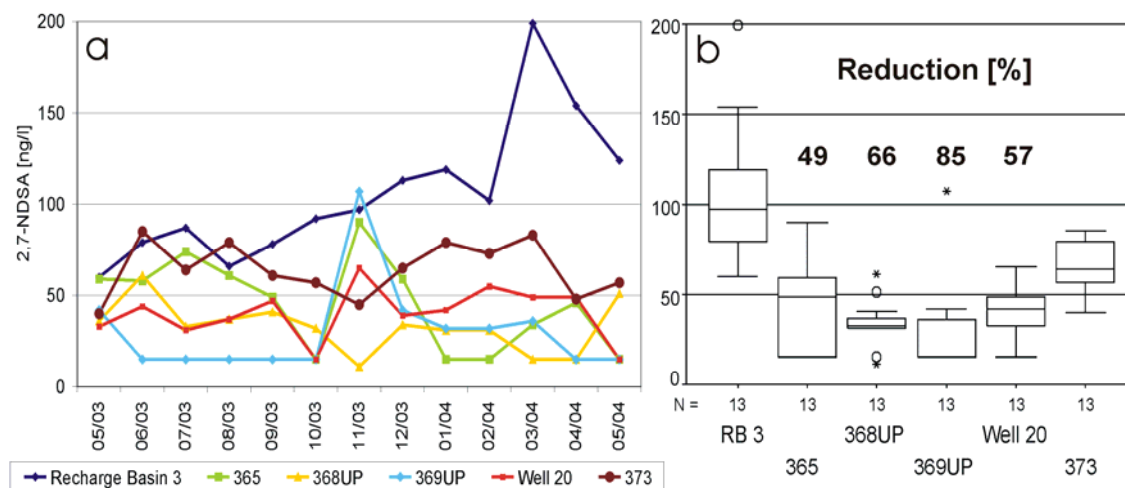
Figure 67 Fate of 2,7-Naphthalenedisulfonic acid during infiltration at GWR (a: time series; b: box plots)

Summarizing, all results of the monitoring of the artificial groundwater recharge facility support the findings of the other investigated field sites. Because of different conditions (retention time, redox potential) the behavior of trace compounds is not equal at all field sites. At the GWR the produced raw water contains the highest concentrations of Sulfamethoxazole. Similar to the other field sites Iopromide was metabolized quickly during infiltration and the 1,5-NDSA isomer remained persistent.

1.4   Soil column experiments

To complete the data basis obtained from the field monitoring, it was necessary to conduct soil column experiments. The experiments on soil columns were launched with the project start in 2002. Different soil column systems were installed, as simulations of one dimensional aquifers, to eliminate outside influences and to provide a closer insight into the kinetics of the degradation processes. The soil column experiments were used to isolate important factors of influence for the removal of the organic compounds (retention time, temperature, DOC-concentration, soil properties and hydrogeological conditions). The experiments without any disturbing outside influences produced results that helped to understand the degradation processes and kinetics of organics in the field.

Overall, four different soil column systems were utilized by the work group of the Department for Water Quality Control of the TU Berlin. The columns and the objectives of the research conducted on the systems are described more detailed in the following chapters.

1.4.1   Long retention soil column system (UBA Marienfelde)

The long retention soil column system was supervised by the work group of the Department of Water Quality Control at TU Berlin. The UBA Marienfelde provided work space and material for this unique opportunity to design a 30 m artificial infiltration path.

1.4.1.1 Set-up

The set-up of the long retention column system was one emphasis of the first phase of the project. The columns were operated in the drinking water treatment facility of the experimental field site at the UBA-Marienfelde. To start experiments it was necessary to combine the single columns to a soil column system and to install all piping and all peripheral equipment.

The columns were filled with natural middle/fine sand from the Berlin area for a preceding project. Precisely, the sand was derived from the sand pit "Horstfeld" near Zossen south of Berlin. Figure 68 shows the grading curve of the material, when it was analyzed for the first time during installation of the columns. The sand was filled to the columns as a disturbed sample and slightly compressed.

The following characteristics of the sand were measured at the time of column filling:

Water content:	2.3%
Loss on ignition:	0.3%
Carbonate-content:	0.3%
Uniformity coefficient:	2.87
k_f-value (from grain size distribution)	1.5-2.6 * 10-4 m/s
k_f-value (from lab experiments):	1.5-4.4 * 10-4 m/s

(in-stationary infiltration through 4 undisturbed samples)

Density:	1.6 g/cm^3
Porosity (from grain size distribution):	31-40%
Porosity (from lab experiments):	40-44%

(calculated from the density of the soil in 4 undisturbed samples)
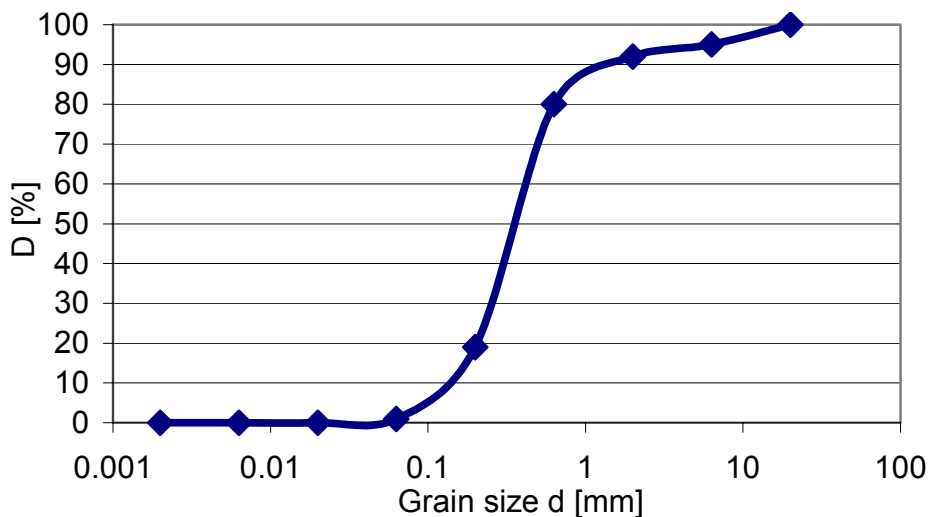
Figure 68 Grading curve of the used filling material

Previously, the columns were operated with a free water level without covers. Therefore, anoxic/anaerobic operating conditions and a reliable oxygen mass balance would have not been possible. To improve the design, covers for all columns were designed and manufactured by the machine shop of the TU Berlin. The covers had to fulfill the functions of keeping air (oxygen) out, to stabilize the redox system, and sealing the columns against leaking in case of a pressure build-up.

For all experiments the six single 5 m columns were connected in series to a 30 m soil column system. The system had a diameter of 0.4 m. The columns were made from 2 mm-stainless steel. At the bottom of each column was a 10 cm layer of coarser sand/gravel and at the top was a 15-20 cm water layer, before the water entered the tubing towards the next column. The columns were operated against gravity. The water entered the column at the bottom and flowed to the top. All six columns were connected with stainless steel tubing, because it was found that measurable amounts

of oxygen diffuse through Teflon tubing (each connection is app. 6 m). For a real simulation of the flow path at the transects the system was operated under saturated conditions. A flow of 36 l/d accounted for a retention time of 30 days. Flow and hydraulic loading rate were selected to fit the conditions at the field site (Table 12).

Table 12 Characteristics of long retention soil column experiment

Total Length	Retention time	Effective Porosity	Total Flow	Hydraulic loading rate	Field-/Pore velocity
30 m	30 d	32 %	36 l/d	0.32 m/d	1.0 m/d

The columns were sampled at different depths to investigate the kinetics of bulk and trace organic degradation. Along the column system 21 sampling ports were sampled on a biweekly basis, to assure a regular monitoring of the fate of the target compounds. The sampling ports were made of stainless steel pipes, which were perforated at the middle of the column. The connection to the column wall was made of PVC. The water temperature in the columns and of the storage tanks was dependent from the temperature in the water work building in Marienfelde. The average temperature was 15°C, whereas during summer the temperature rose to 18-19°C and during winter water temperature dropped to 12°C. Therefore, the average temperature is specified as 15°C ± 4°C.

The water from Lake Tegel was spiked with the five target compounds. The spiking concentrations were selected to be approximately ten times higher than the background concentration in Lake Tegel. This assured stable concentrations in the column feed even when the concentration in the lake varied. An online dosage system for the five trace compounds was installed to assure a constant concentration of these five compounds in the influent. Table 13 gives an overview of the dosages of trace compounds to the lake water.

Table 13 Spiking concentrations for the long retention columns in Marienfelde

Trace compound	Iopromide	Sulfamethoxazole	1,5-NDSA	1,7-NDSA	2,7-NDSA
Spiking concentration	10 µg/l	2.5 µg/l	2.5 µg/l	2.5 µg/l	2.5 µg/l

Disturbances because of sampling were not problematic during experiments. Samples were taken starting at the end of the column system and a maximum of 8 x1 l samples on a sampling day. The sample amount was therefore 8 liter and significantly smaller than the daily flow through the columns (36 l). Sampling days had an interval of 2

weeks. On sampling days a pressure drop along the columns could be realized, but after 2-3 hours the conditions were back to normal. Figure 69 shows the soil column design schematic.
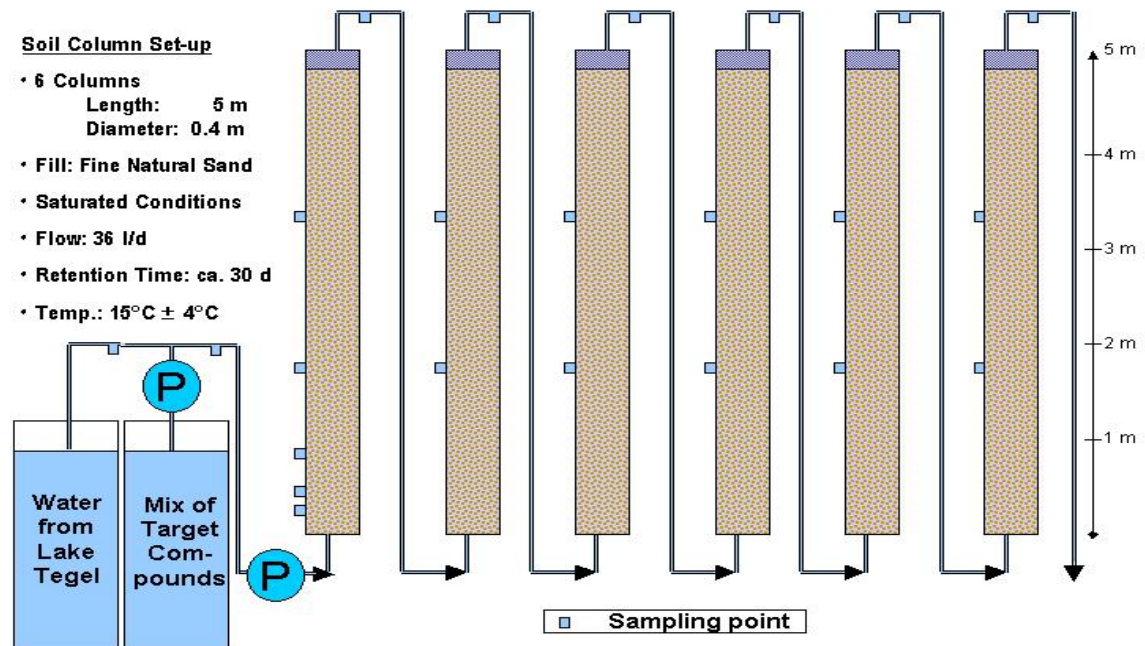
Figure 69 Experimental set-up of the long retention columns

By the end of August 2002 the final set-up of the six columns in series was completed and the operation started. First a rinsing cycle for each column was performed to remove any previous contaminants from the six aquifer columns. Over a time period of 6 weeks local drinking water was used for the rinsing process. The influent and the effluent were analyzed regarding UVA, DOC, Fe-Ions and Mn-Ions. Since the local drinking water is low in DOC (~2 mg/l) a leaching of organic compounds from the filling material would have been recognized. After 6 weeks of rinsing, the characteristics of the effluent were similar to the influent characteristics. However, towards the end of the rinsing the DOC-concentrations in the last sampling ports were approximately 20% lower than in the influent. This can be explained by an established microbial community, which degrades portions of the infiltrated DOC. The thorough rinsing and the detailed monitoring of the water quality during rinsing eliminated every doubt about the qualification of the soil column system (particularly the sand filling) for simulation experiments. The system was found to be free of contamination and perfectly suited for the planned experiments. The findings on the status of the long retention column system were consistent with the expertise of Schulz, 1998, who investigated the conditions of the soil columns in 1998.

Figure 70 Long retention soil columns Marienfelde (top part)

The adaptation period of the columns to the water supply from Lake Tegel was started middle of December 2002. After draining the drinking water, water from Lake Tegel was provided and fed to the columns. The water was pumped with 2 l/h (48 l/d) for nearly three weeks to fill the columns. Afterwards the flow was reduced to approximately 0.5 l/h (12 l/d) for 3 months to allow long term undisturbed development of biomass and an adaptation to the water quality of Lake Tegel. A monitoring of DOC and redox-conditions confirmed stable conditions at the end of the adaptation period. The spiking of the feed with the trace organic target compounds was started within the adaptation period.

In April 2003 the conditions of the columns were stable and the first part of the long term experiments with a flow rate of 36 l/d was started. During the first part of the experiment (04/2003 - 04/2004) oxic conditions were established in the soil columns to simulate the infiltration at the groundwater recharge facility. To assure oxic conditions the storage tank was mixed twice a day by a submergible pump and the infiltrating water was oxygen saturated. During this period oxygen was present in the whole column and no denitrification was observed. From May 2004 to May 2005 the redox status of the column system was switched to anoxic conditions (NO_3-reducing) by sparging the influent with nitrogen in a separate counter current column (O_2 in influent: ~1mg/l). Denitrification was observed but nitrate was not completely depleted from the system. No oxygen was detectable in the sampling ports. Monitoring of the DOC, UVA

and redox-conditions ensured stable conditions over the time of these two experiments. Results from both phases will be presented in the following chapters.

As a service to other work groups in the project the soil column system was available at special times for other experiments. It was a good opportunity for all participants to check results of the monitoring at the transects in a nearly full-scale facility that eliminates all outside influences. The workgroups of Prof. Dr. Lopez-Pila, Dr. Heberer and Prof. Dr. Pekdeger used this possibility of the column system for separate experiments. The results of these studies are included in the respective reports (chapter XXXX).

1.4.1.2 Results

Tracer study

The tracer study was conducted to define the actual porosity, dispersivity and the affiliated characteristics (retention time etc.) of the soil column system. The tracer study was conducted from October 2002 until November 2002. A double tracer (Chloride/Bromide) was used in a pulse application and the flow rate was increased (60 – 80 l/d) to limit the duration of the study to 30-40 days. Drinking water was used as influent until the end of the experiment. During the study a daily sampling was used to describe the tracer movements through the columns as accurate as possible. The samples were analyzed at the TU Berlin for Chloride and Bromide using IC-technology. The background concentration of Chloride and Bromide in the used drinking water were determined in advance of the study with 100 mg/l Chloride und 1.2 mg/l Bromide.

The tracer study was completed by the end of November and determined the actual porosity, the individual travel time for each sampling point and the dispersion. This new knowledge reduced the analysis program, produced rapid results and improved the data basis for the aquifer simulation. The results were adapted to the lower flow during the aquifer simulation. The evaluation of the results was done in cooperation with the work group of Prof. Nützmann, who provided the program CXT FIT and a brief introduction into the program. The analysis of the data resulted in a model which is presented in Figure 71.
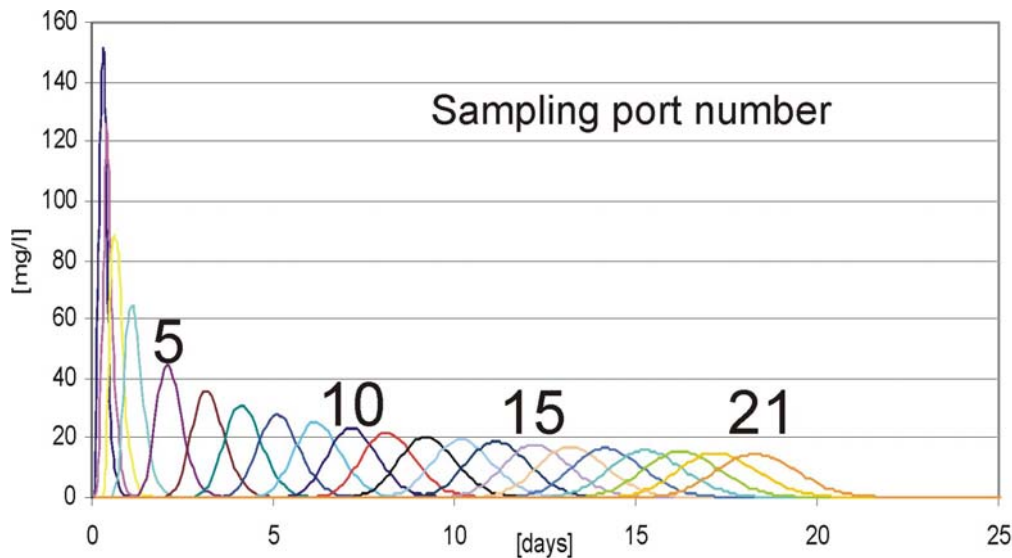
Figure 71 Model of Bromide-concentration at the 21 different sampling ports

The model was done in CXT FIT by calculating the average pore velocity and the dispersion from all bromide data. Afterwards, the findings where used to calculate the theoretical distribution of bromide in samples from the 21 sampling ports. The background concentration of bromide was below 0.15 mg/l in the used drinking water. The chloride background concentration was around 60 to 80 mg/l. Both data sets (chloride and bromide) showed the same results. But the bromide data could be analyzed more accurate because of the lower background concentration. At the last sampling point the results of the ion chromatography were checked by measurements of electrical conductivity, which confirmed the results by showing the same trends (data not presented). As a result of the tracer study it was found that the porosity of the filling sand is about 29% - 34% and the dispersion was approximately 0.1 m/d. The comparison of the model predicted and the measured bromide concentrations was difficult for the first sampling ports. Problems were:

- Short peak length (few hours to 1-2 days) combined with the unsuitable sampling rhythm (each port was sampled once a day except on the weekends).
- Unstable flow in the first five days of the experiment (pump was changed on day 6).

Nevertheless, the results for the sampling ports 9 to 21 were satisfying and fit into the predicted model. Figure 72 compares the measured and predicted concentration of bromide in port 16 and 21.
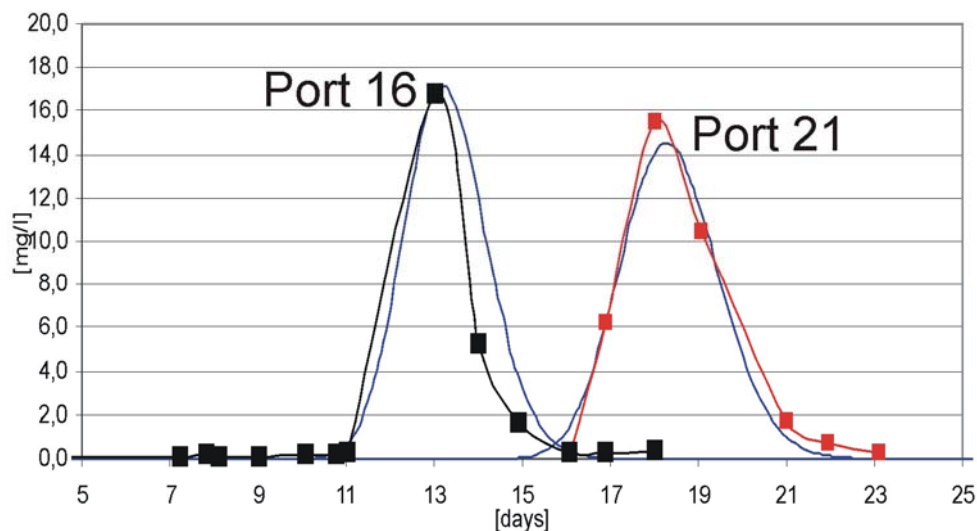
Figure 72 Predicted and measured bromide concentrations (port 16 and 21)

Inorganics - Results

During the experiments, the soil column system was also monitored for changes of inorganic parameters. Most important were the different electron acceptors, which controlled the redox potential (O_2, NO^{3-}, Fe-species). The redox potential itself and the oxygen saturation were measured biweekly. On a monthly basis the different redox sensitive water constituents (e.g. Nitrate, Fe^{2+}) were analyzed. Additionally, the FU Berlin measured monthly the major cations, anions and pH.

Figure 73 and Figure 74 provide the measured oxygen and nitrate content of the column system during both experiments. The following paragraphs describe the actual redox situation during both experiment parts more detailed:

Oxic phase: It was found that during the oxic stage oxygen was present along the whole column in decreasing concentrations. The water entered the column system oxygen saturated with O_2-levels between 8.5 mg/l - 11 mg/l depending on temperature. During the first 50 cm of infiltration or within 12 hours the oxygen concentration was cut by half. Afterwards a slower continuous depletion of oxygen was observed. The average O_2-concentration at the end of the column system was found to be ~1 mg/l. Along the column no reduction of the redox potential was measured. The redox potentials in the different sampling ports were found to range from 280-340 mV with no trend towards lower potentials at the end of the columns. Nitrate was present in all sampling ports in a comparable concentration. During the period May 2003-May 2004 the average surface water concentration of nitrate in Lake Tegel was 1.4 - 1.5 mg/l. Figure 74 does not provide error bars because most of the variation of the nitrate concentration is due to changes in the surface water that was used as influent. However, during the oxic stage the nitrate concentration remained stable along the infiltration path. The slight increase shortly after infiltration was most probably due to a

nitrogen release from organic carbon structures. Overall, no denitrification was present in the oxic phase. This was consistent with the measured oxygen concentrations.
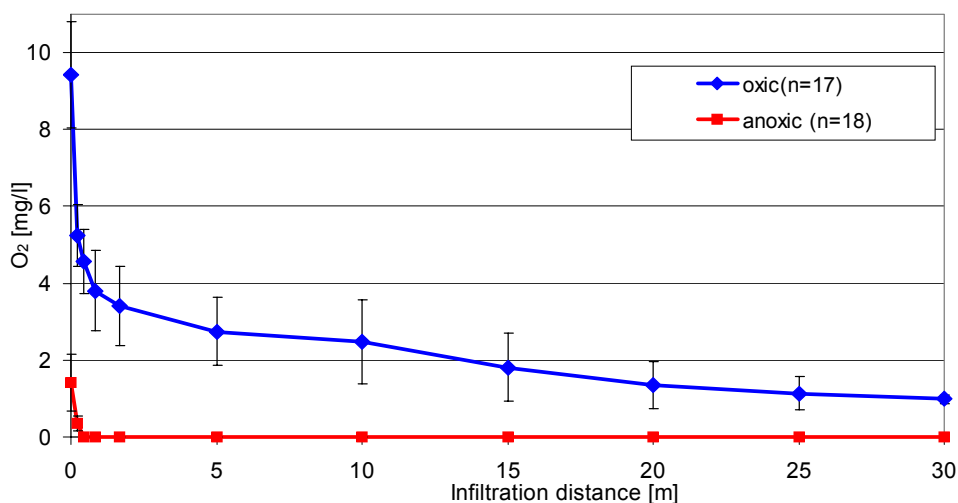
Figure 73 Oxygen concentrations during the both stages of the long retention soil column experiment

Anoxic phase: During the anoxic stage the water from Lake Tegel was sparged with Nitrogen before it was introduced to the column system. Furthermore, the submergible pump was removed to avoid high oxygen levels in the storage tank. Despite of all measures it was not possible to reduce the influent oxygen concentration under the level of 1.0 mg/l. Figure 73 shows that oxygen concentration of the infiltrating water was found to be in the range of 1 – 2 mg/l. But these small amounts of oxygen were rapidly used up by DOC-mineralization in the first centimeters of the column system. In the first sampling port after 0.2 m only traces of oxygen were found and after 0.4 m no oxygen was present in the infiltrate. All biweekly measurements during the anoxic phase confirmed no dissolved oxygen in the soil column system. Since oxygen was not present during this stage the biomass used nitrate as electron acceptor. The nitrate levels of the surface water rose to an average of 1.9 - 2.0 mg/l during the period May 2004 – May 2005. This slightly higher concentration guaranteed that nitrate was not completely depleted from the system. Figure 74 shows that along the column system the nitrate concentration was reduced but at no time of the anoxic stage nitrate was removed. Therefore, the second stage can be characterized as anoxic. The redox potential was not measured regularly during this stage since the monitoring of oxygen and nitrate delivered all necessary information on the redox status of the columns. However, the conducted measurements showed that the redox potential of the infiltrated water was in the range of 250 – 300 mV. Shortly after infiltration the redox potential decreased to 100 - 160 mV and remained nearly stable for the rest of the

infiltration distance. The average redox potential of the soil column effluent was found to be 120 mV.
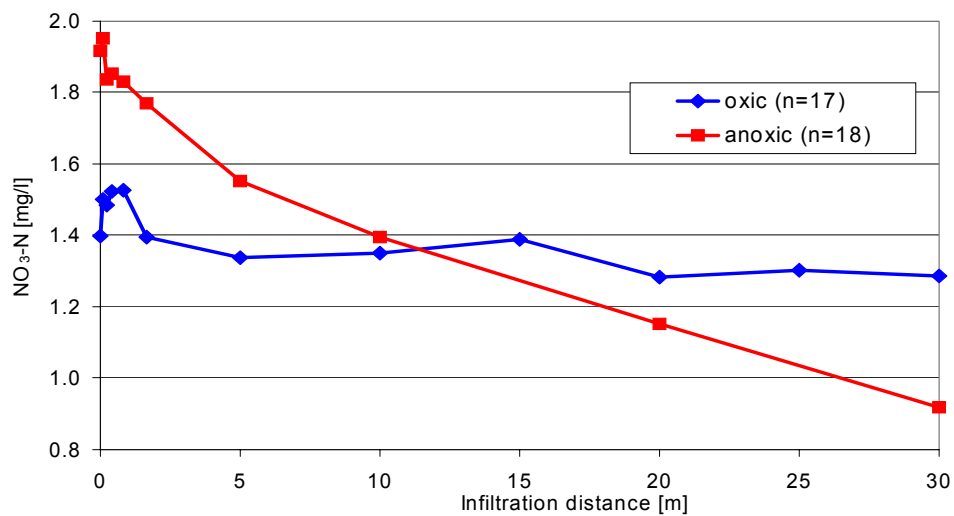
Figure 74 Nitrate concentrations during the both stages of the long retention soil column experiment

Additionally to the monitoring of the redox relevant parameters, the FU Berlin conducted a detailed analysis of the major cations/anions and the development of the pH-factor. It was found that during both stages the average pH decreased during infiltration. Figure 75 shows that during oxic infiltration the pH drops immediately after infiltration by 0.5 pH-units. This drop is explained by the release of CO_2 during mineralization of dissolved carbon, which forms carbonic acid. Furthermore, the oxic degradation pathway contains the formation of organic acids by introduction of oxygen into the molecule. Therefore, the pH-decrease is most probable due to the very fast degradation and mineralization of DOC during oxic conditions.
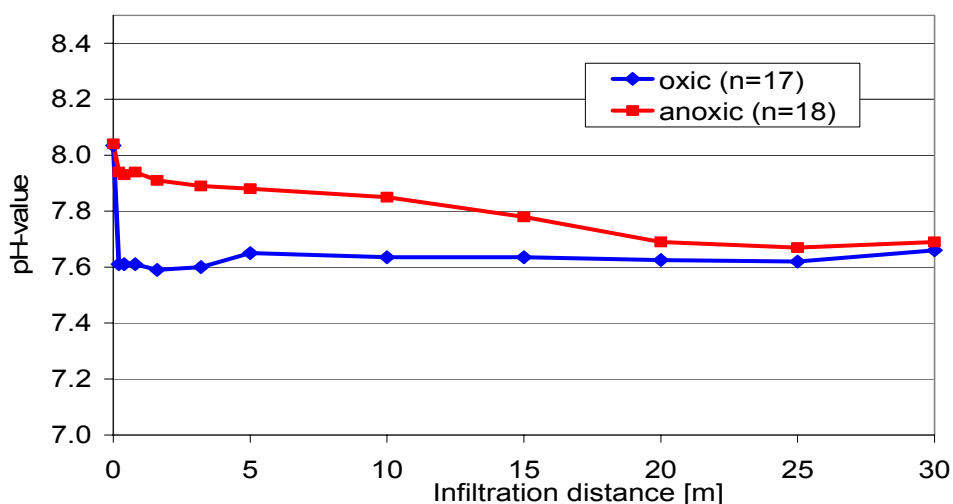
Figure 75 Development of pH during infiltration at both stages of the soil column experiment

During anoxic conditions the development of pH is a slower process. Corresponding to the slower DOC mineralization the pH decrease stretched over the entire infiltration distance. At the end the average pH of the effluent is similar in both phases.

The major cations were monitored to detect eventual changes in the ionic composition of the infiltrate.

Table 14 provides the average concentration of sodium, potassium, calcium and magnesium along the columns during the oxic and the anoxic phase. The table proves that no significant changes in the concentrations of the cations occurred during infiltration. From sediment properties it was known that the cationic exchange capacity of the filling material and the calcium carbonate content are very low. As a result no strong depletion of potassium (high CEC-selectivity) and no dissolution of calcium carbonate (caused by pH-decrease) were observed in the columns.

Table 14 Fate of major cations in soil columns (oxic and anoxic stage)

Sampling port	Infiltration distance [m]	Na+ [mg/l] oxic/anoxic	K+ [mg/l] oxic/anoxic	Ca+ [mg/l] oxic/anoxic	Mg+ [mg/l] oxic/anoxic
Surface water	0.0	46.0 / 43.4	12.0 / 10.8	86.0 / 78.0	11.0 / 9.2
1	0.2	44.5 / 41.0	11.0 / 10.3	83.0 / 75.0	10.3 / 9.1
2	0.4	44.1 / 41.8	11.2 / 10.3	83.0 / 76.0	10.5 / 9.4
3	0.8	45.5 / 42.0	11.0 / 10.4	82.0 / 78.0	10.3 / 9.2
4	1.6	44.0 / 42.0	11.0 / 10.0	83.0 / 77.0	10.3 / 9.1
5	3.2	44.0 / 41.3	11.0 / 10.2	82.0 / 78.0	10.2 / 9.4
6	5	43.2 / 42.3	10.8 / 10.2	83.5 / 75.0	10.2 / 9.0
9	10	43.4 / 42.1	11.1 / 10.2	82.5 / 75.0	10.0 / 8.8

12	15	43.2 / 43.0	10.6 / 9.7	82.5 / 75.0	10.0 / 8.9
15	20	43.2 / 42.5	10.8 / 9.9	84.5 / 79.0	10.0 / 8.7
18	25	43.5 / 42.0	10.4 / 10.0	84.0 / 77.0	9.8 / 8.6
21	30	42.8 / 42.7	10.3 / 9.8	86.0 / 77.0	9.8 / 8.5

Additionally, the analytical program of the FU Berlin revealed that the electric conductivity (620 µS/cm $\pm$ 20 µS/cm) did not change during infiltration. Similarly, the anionic composition (Cl^- and SO_4^{2+}) remained constant. A slight increase in HCO_3^-, which was caused by CO_2 production during DOC mineralization, was observed for the oxic phase.

Bulk Organics - Results

During the two years of experiments on the columns a detailed monitoring of the fate of the bulk organics was conducted. The monitoring program consisted of DOC, UVA_{254}, UVA_{436}, adsorbable organic iodine and LC-OCD analysis. One focus of the investigations was the immediate infiltration zone. In the soil column system it was possible to achieve a high data resolution in this important stage of infiltration. The obtained data can supplement the field data, since no investigated field site provided a sufficient resolution of the bank area near the soil/water- interface. Along further infiltration samples were take every 5 m (equivalent to 5 days retention time).

DOC:

The DOC-results of the soil columns experiments are presented in Figure 76. It was found that in the oxic soil columns 47% of the DOC was removed during 30 days of infiltration. Most of the DOC-mineralization was observed within the first meter of the infiltration path. Overall, DOC-mineralization was a stable process and most of the variations of DOC-levels are due to changing surface water quality and analytical inaccuracies. The oxic stage of the experiment was planned as a simulation of the infiltration process at the artificial groundwater recharge facility. The results point out that the simulation was successful. Very similar to the fate of DOC at the artificial groundwater recharge facility a high portion of DOC was mineralized in the immediate infiltration zone. After 20 days of infiltration (20 m) the DOC-concentration remains constant at a level of 3.8 mg/l and no further reduction was observed. This concentration was found to be a very good estimation of the amount of non-degradable organic carbon in Lake Tegel surface water.

However, these results underline the importance of the soil layer close to the water/soil interface. It can be assumed that the biological activity in this area is significantly higher than in the deeper soil layers. At the GWR only 38% of DOC was removed in 50 days compared to 47% in the solid columns in 30 days. These differences are explained by the following factors of influence. At the GWR the redox system changes during summer to anoxic/anaerobic and the lower mineralization rates of this period are

included in the average DOC-removal. Furthermore, the infiltration path at GWR is exposed to heavy temperature variations (±12°C) that forces the biomass to adaptation processes. The temperature of the soil column experiment changed in a considerably smaller range (±4°C).
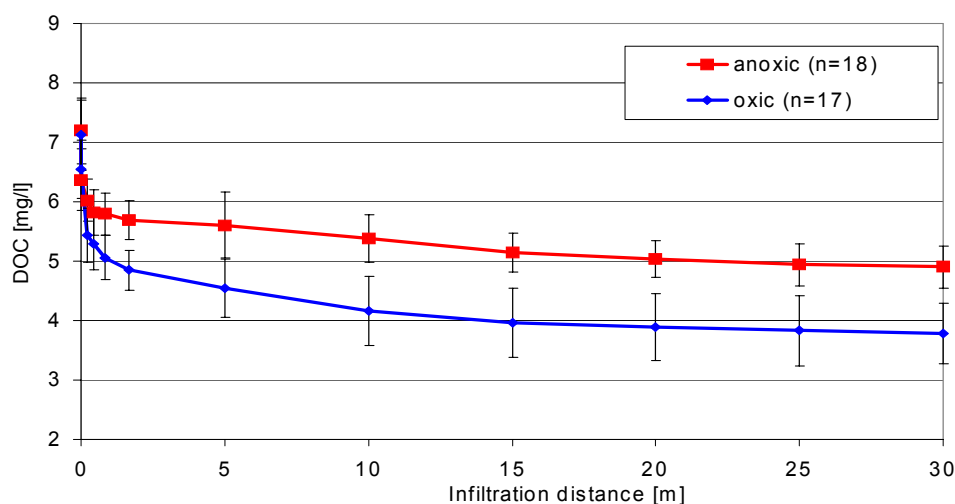
Figure 76 Fate of DOC during the two stages of the soil column experiment

For the simulation of anoxic conditions, the initial oxic phase, which occurs invariably in the field because of oxygen saturated surface water, was reduced to the lowest practicable dimensions (<0.21m). Under these conditions only 31% of the source water DOC was removed during 30 days of infiltration (Figure 76). Similar to the removal under oxic conditions a large portion of DOC is removed in the first infiltration layer. But compared to the oxic conditions the amount of mineralized DOC within the first 1.6 m is 1 mg/l smaller. After this rapid removal of easy degradable organic carbon a slower mineralization process starts. The results confirm that under anoxic conditions a smaller portion of DOC can be considered as easy degradable. The mineralization process in the anoxic column continues until the end of the column. After 30 days the average DOC-level was found to be 4.9 mg/l. Because of their limited retention time the column experiments could not clarify whether the residual non-degradable DOC-concentration is similar under oxic and anoxic/anaerobic conditions. The comparison of the final DOC residuals after infiltration at the bank filtration site Tegel and the GWR raised the explanation that an anoxic infiltration can reach after long retention times the same DOC-residual concentrations as a oxic infiltration.

However, the results supported the field results that the DOC removal under oxic conditions is considerably faster than under anoxic or anaerobic conditions. The simulation experiments allowed a more precise investigation of the fate of DOC during the first month of infiltration depending on the dominant redox conditions and showed that under both conditions the infiltration phase is of eminent importance. The overall

removal rates are within the range of mineralization rates observed in the field. A slightly higher removal can be explained by a higher average water temperature in the soil columns (~15°C, field: ~12°C).

Since the data on DOC-mineralization were obtained in a closed system that rules out every outside influence, it was of special interest to model the fate of DOC. Different approaches on biodegradation of organic carbon are known. The most scientific model is based on a fractionation of DOC in groups of different degradability and a mineralization of the single groups after the rules of MONOD. This approach was originally introduced to water chemistry by Gimbel et al. (1992) and later used for similar modeling by Drewes, 1997 and Schoenheinz, 2004. The model used for the simulation of the soil column DOC-data was based on three different groups of DOC: an easy degradable fraction, a medium- and hardly-degradable fraction and the non-degradable fraction of organic carbon. The non-degradable fraction remained constant during infiltration, whereas the easy and medium-degradable fraction where depleted following the rules of exponential decay postulated by MONOD. Figure 77 shows the theory, which was the basis of the model.
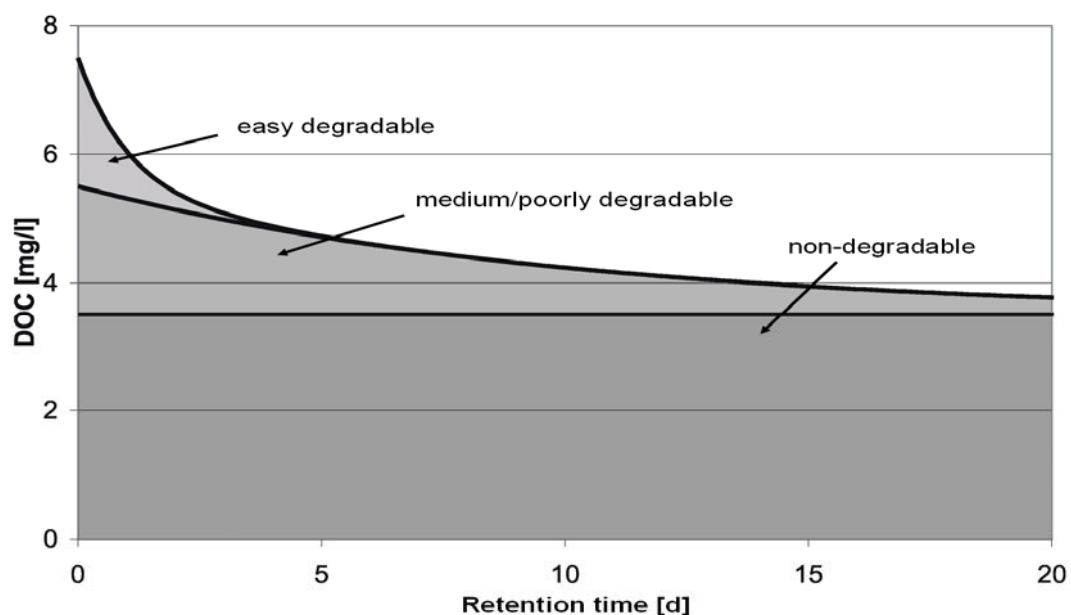
Figure 77 Theoretical basis of the DOC-degradation (adapted from Gimbel et al., 1992)

Based on the literature the DOC-mineralization in the long retention columns was modeled using Equation 1. The concentration of DOC at a certain time after infiltration (c_t) is dependent from the concentration of the three different fractions: easy degradable fraction (c_1), a medium- and hardly-degradable fraction (c_2) and the non-degradable fraction (c_3) and time (t). λ_1 and λ_2 are the degradation constants for the removal of the degradable fractions.

$$c_t = c_1 * e^{-\lambda_1 * t} + c_2 * e^{-\lambda_2 * t} + c_3$$

Equation 1 Model for the mineralization of DOC during infiltration (according to Gimbel et al., 1992)

Some postulations were necessary to receive good results from the model. First, the concentration of the non-degradable fraction was set to 53% of the surface water DOC, because under oxic conditions 47% of the source water DOC was degradable within 30 days. The plateauing of the DOC-concentration towards the end (Figure 76) indicated that all degradable DOC was mineralized. Therefore, under oxic conditions 3.8 mg/l were assigned to the non-degradable fraction. Under anoxic conditions the total DOC-concentration was slightly lower, resulting in 3.7 mg/l non-degradable DOC. Furthermore, the easy degradable fraction was quantified by DOC removal after ~20 h (0.8 m), following the example of Drewes, 1997. Herewith, a higher portion of the total DOC (2 mg/l) was regarded as easy degradable under oxic conditions (anoxic conditions 1.4 mg/l). The medium degradable fraction was calculated from the total DOC and the other two fractions. Table 15 provides the concentrations used in the model.

Table 15 Summary of modeling data for long retention soil column system

	C_1 [mg/l]	C_2 [mg/l]	C_3 [mg/l]	λ_1 [1/d]	λ_2 [1/d]
oxic	2	1.3	3.8	7.97	0.117
anoxic	1.4	1.8	3.7	7.31	0.019

The model used non-linear regression to fit the modeled decay curve to the observed DOC-concentrations. The calculation was conducted for the oxic and the anoxic stage and the results are presented in Figure 78. Overall, the model was able to depict the DOC decay under both conditions very detailed and the resulting R^2 ($R^2 > 0.99$) indicated a successful adaptation. Table 15 shows that despite of the different concentration of easy degradable carbon (c_1) the degradation constant (λ_1) was similar during both stages of the experiment. λ_2 as the degradation constant of the medium degradable DOC fraction pointed toward a faster degradation of this fraction under oxic conditions (factor~6). The calculation of the model showed that the concentration of the medium degradable fraction, which determines the fate of total DOC in the deeper filtration layers, fells under 0.1 mg/l (accuracy of the DOC measurement) after 23 days under oxic conditions. Contrary to this, it takes 155 days under anoxic conditions for the medium degradable fraction to remain under 0.1 mg/l. A comparison of these results with the experiences from the field exposes interesting similarities. At the GWR the DOC degradation process was completed after approximately 30 days and at the

bank filtration site Tegel the DOC mineralization under anoxic/anaerobic conditions continued for 4.5 – 5.5 months (135 – 165 days).
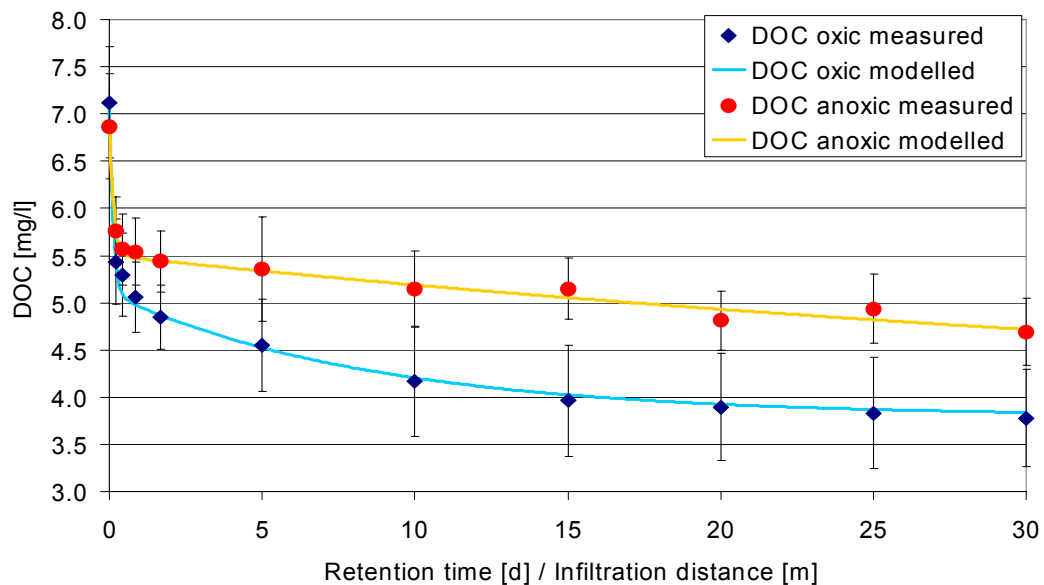
Figure 78 Results of the modeling of the DOC-degradation in the soil column system

To compare the results of the soil column experiments with the findings of the field monitoring Figure 79 depicts all results in one graph. Since most of the investigated field sites have no fine resolution near the bank, only a few data points, describing the fate of DOC during the first 30 days, were found for each transect. Most problematic was field site Wannsee, where only two data sets (monitoring well 205 and 206) are available for this time frame. Well 206 is representative for an oxic infiltration and well 205 has a more anaerobic character. The data sets of the GWR can be regarded as examples of an oxic infiltration and bank filtration site Tegel is a case of anoxic/anaerobic infiltration. Figure 79 shows that the model predicted DOC concentrations and the real DOC levels show similar trends. However, a comparison of the GWR data sets with the oxic model and the bank filtration Tegel data sets with the anoxic model proposes some methodical mistakes. The DOC levels in the reality are higher than the predicted DOC concentrations. This is most probably due to a large range of effects that influence the DOC degradation in the field, that were excluded in the soil columns (heavy temperature variations etc.).
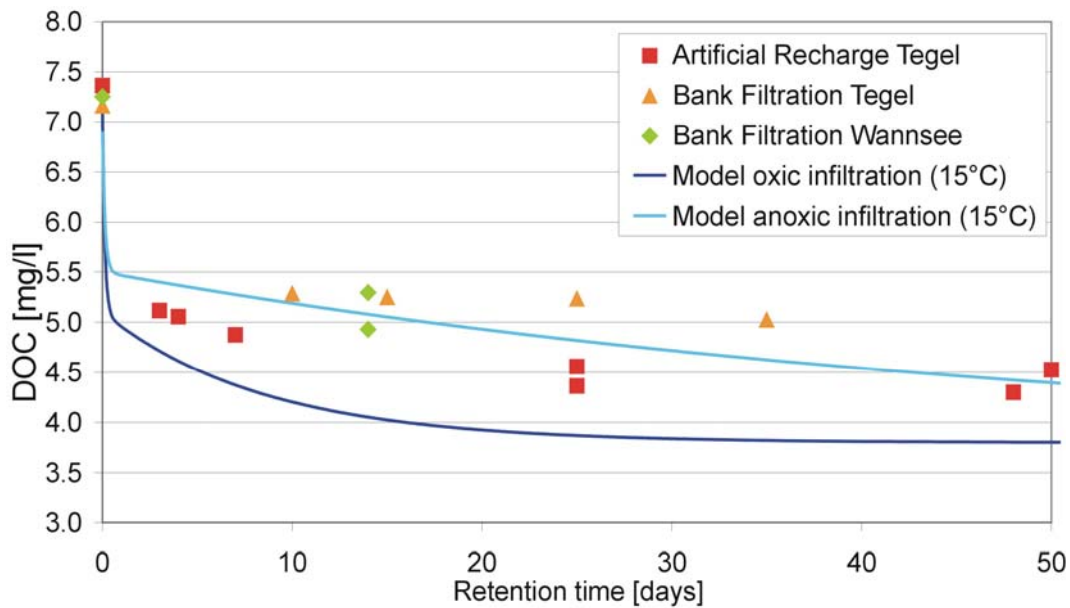
Figure 79 Comparison of model predicted DOC-concentrations with field-measured DOC levels

UVA:

The DOC-analysis was accompanied by a regular monitoring of the UV-absorption at 254 nm. It was found that UV-active organic carbons were removed during the infiltration process. The removal rates pointed towards a similar efficient mineralization of the aromatic and double bond structures and the total DOC. Under oxic conditions the UV-absorption at 254 nm decreased by 50%. A comparison of the actual UVA_{254}-removal with the removal of total DOC (47%) shows that the UV-active compounds were diminished slightly more efficient than DOC on the entire infiltration path. Under anoxic conditions the removal rates for UVA_{254} were 32% and therefore very similar to the rate for total DOC-mineralization (31%). Figure 80 shows the dynamic of UVA_{254}-removal. Most of the UV-active compounds were removed in the first part of the column system. Towards the end of infiltration a stabilization of the UVA_{254} was achieved under both conditions. More information on the behavior of aliphatic and aromatic carbons during infiltration is revealed by the combination of DOC and UVA_{254} results in the SUVA (following chapter).
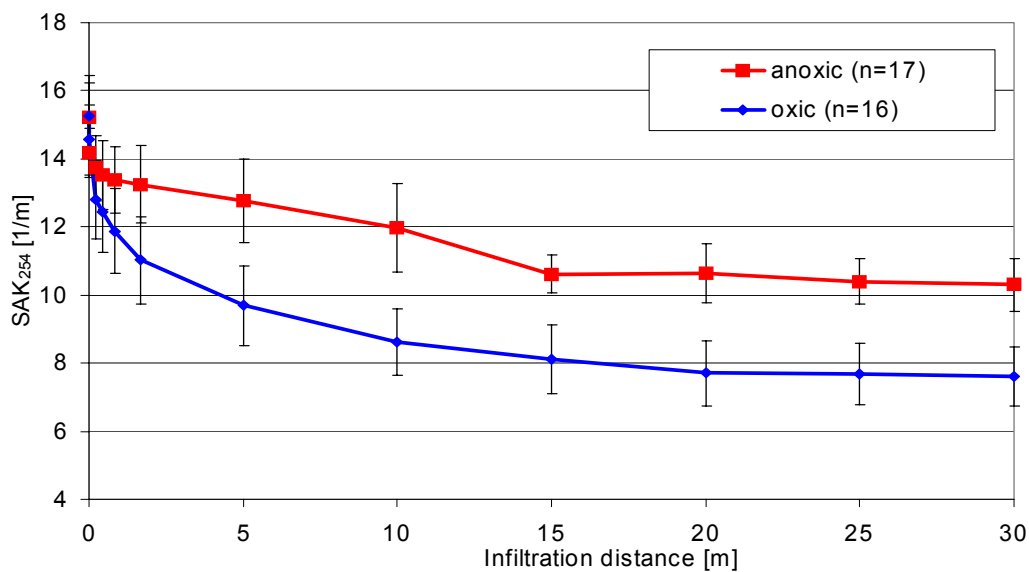
Figure 80 Fate of UVA$_{254}$ during the two stages of the experiment

Measurements of the UVA$_{436}$ (color) provided no additional results since the UVA$_{436}$ level of the infiltrating water was very close to the detection limit. Therefore, no closer description of the parameter is provided.

SUVA:

The SUVA is the quotient of UVA$_{254}$ and DOC-concentration and describes the character of the dissolved organic carbon more detailed. A high share of aromatic organic carbon on the total DOC leads to high SUVA-values. Therefore, the SUVA is a parameter, which is only dependent of the character of DOC but not of the amounts of organic carbon. The SUVA is very reliable in detecting changes in the aromaticity of DOC during infiltration.

The average SUVA of Lake Tegel surface water was 2.1 l/m*mg. During the oxic soil column experiment the SUVA increased very rapidly to 2.36 l/m*mg after 0.21 m infiltration (Figure 81). The results indicate that during initial aerobic soil passage aliphatic carbon sources are preferentially used. During further infiltration more aromatic structures are degraded and the SUVA decreases. After 5 days (5 m) of infiltration the SUVA of the infiltrate is equal to the SUVA of the surface water, which was used as feed water. Towards the end of infiltration the SUVA decreases under the initial SUVA, indicating a more efficient mineralization of aromatics.
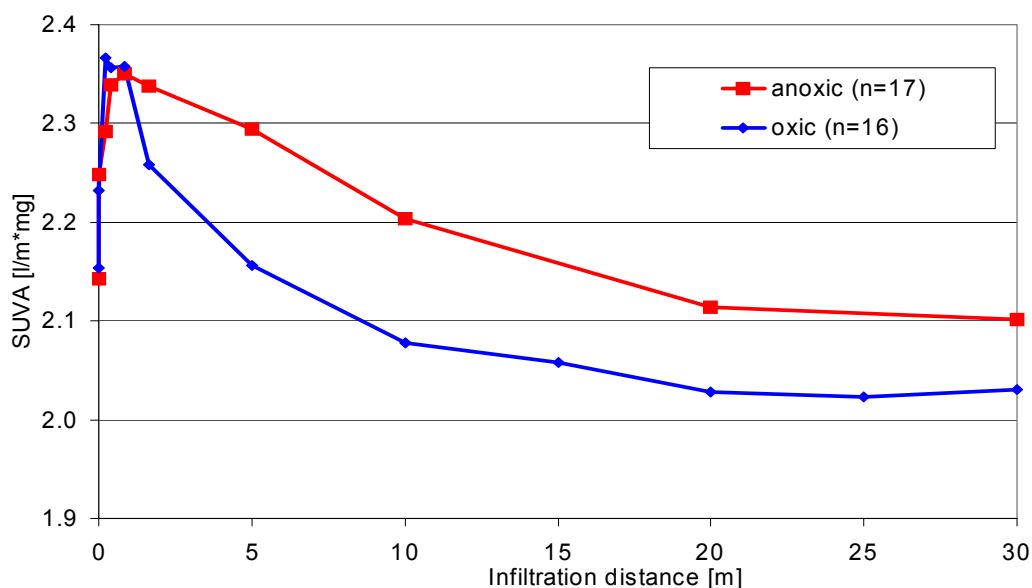
Figure 81 Fate of SUVA during the two stages of the soil column experiment

During anoxic infiltration the increase in SUVA is slightly slower reaching the maximum after 0.8 – 1.6 m of infiltration. Afterwards the SUVA is decreasing, but the aromatic part of the total DOC is mineralized considerably slower. Therefore, the decrease of SUVA continues slowly along the entire column. At the end of the infiltration the SUVA is similar to the initial SUVA.

However, the results indicate that under both redox conditions aliphatic compounds are initially degraded and subsequently aromatic structures. Under oxic conditions aliphatic carbon sources are preferentially degraded within the first 0.2 m. Under anoxic conditions the sequence of the degradation process is similar but significantly slower. Aliphatic carbon sources are preferentially degraded within the first 0.8 m. Therefore, the degradation process under anoxic conditions is slower by the factor of four. This is underlined by the fact that the final SUVA of the anoxic infiltration (2.1 l/m*mg after 30 days) is reached under oxic conditions after 8 days (8 m) of infiltration. Finally, the results indicate that the degradation processes are similar under both redox conditions and that the different SUVA results under oxic and anoxic conditions are mostly due to a stretched time frame.

LC-OCD:

A more detailed analysis of the changing character of the dissolved organic carbon was provided by LC-OCD. The LC-OCD technique allowed a fractionation of the organic water constituents in five fractions. The fate of the different DOC fractions was monitored by biweekly sampling. One important point of interest was the comparison of the DOC character of Lake Tegel surface water and the water infiltrated to the columns. It was necessary to detect potential differences in DOC-character, which

were caused by the storage (maximum two weeks) of the surface water. Table 3 shows that the integration of the LC-OCD chromatograms leads to similar results for both water types. Therefore, it can be concluded that the storage did not influence the organic water composition and the results can be compared to the field results.

Table 16 Portions and concentrations of different fractions of DOC (Columns influent, Lake Tegel)

	Poly-saccharides	Humic substances	Humic substances-Building blocks	Low molecular acids	Neutrals and Hydrophobics
Column in-fluent (n=12)	8.7 %	44.1 %	24.6 %	3.7 %	18.9 %
	0.6 mg/l	3.1 mg/l	1.7 mg/l	0.3 mg/l	1.3 mg/l
Lake Tegel (n=12)	8.7 %	46.0 %	22.1 %	3.7 %	19.7 %
	0.6 mg/l	3.3 mg/l	1.6 mg/l	0.3 mg/l	1.4 mg/l

Generally, LC-OCD chromatograms of the oxic period of the long retention columns (Figure 82) were comparable to the chromatograms of the GWR field site. Both, in the field and in the columns the most fundamental change during infiltration was observed for the fraction of the polysaccharides. PS were efficiently removed in the first 0.21 m of oxic infiltration in the soil columns (Figure 82a). Furthermore, the fractions of HS, HS building blocks and LMA were only partially degraded. It is noteworthy that even a part of the HS peak was removed, generally assumed to be mostly non-degradable.

During the anoxic period of the column system (May 2004 - May 2005) the LC-OCD analysis proved a change in water quality of the surface water. The share of HS-building blocks and LMA on the total DOC of the source water decreased and the peak intensity of the corresponding peaks was reduced (Figure 82b). However, despite of this, a slower degradation of the polysaccharide fraction was observed under anoxic conditions. PS were still detectable after 30 days of anoxic infiltration (Figure 82b). The fractions of HS, HS building blocks and LMA showed a similar partial removal as under oxic conditions. Because of the generally slower DOC degradation kinetic, the chromatograms are more pooled together in the anoxic period. Despite of the PS-fraction, a difference in the general degradability of the single fractions under oxic or anoxic/anaerobic conditions was not observed.
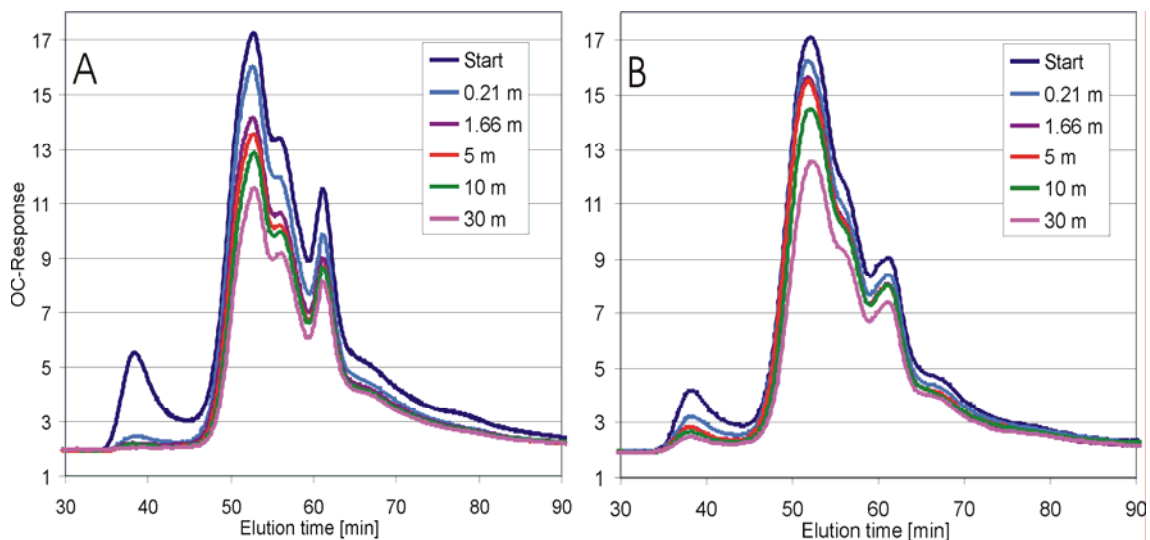
Figure 82 LC-OCD chromatogram of soil column experiment - oxic (A) / anoxic (B)

Furthermore, LC-OCD measurements revealed that the changes in SUVA result from the fast removal of the PS-fraction (elution time 35-45 min) and from a change of aromaticity in the HS-fraction (elution time 48-52 min). In the online measurement of the samples from the oxic stage the HS-fraction showed major changes in SUVA, while the SUVA of HS-building blocks and LMA were constant (Figure 83a). It is assumed that in the HS-fraction aliphatic side-chains are very fast mineralized, but aromatic and double-bond structures remain longer unchanged. LC-OCD measurements proved that under anoxic conditions the slower removal of PS is responsible for the slower rise of SUVA. In the HS-fraction no initial preferential removal of aliphatics was observed and the SUVA remained stable during the first 1.6 m of infiltration (Figure 83b). Afterwards, the mineralization of aromatics from the HS-fraction leads to a decreasing SUVA.
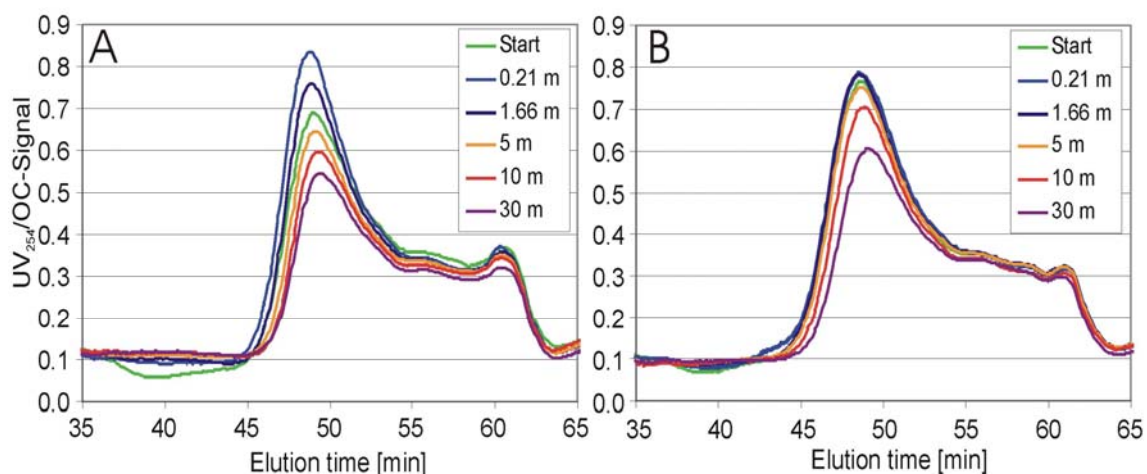
Figure 83 LC-OCD SUVA - chromatogram of soil column experiment - oxic (A) / anoxic (B)

Figure 84 provides more information on the behavior of the five different DOC-fractions along the oxic infiltration path. Most degradation processes in the single DOC fractions were completed after 2 days (2 m). Only, the concentration of the fraction of humic substances was found to change until day 10 after entering the column system. It was found that no significant changes in DOC composition occurred after ~10 days (10 m) of infiltration. The fraction of polysaccharides was completely removed within the first few centimeters. The most important fractions of DOC were the humic substances, followed by the HS-building blocks and the neutral fraction. The concentration of low molecular acids (LMA) remained constant along the infiltration path. It is assumed that this fraction is formed from biodegradation products of the other DOC-constituents. Therefore, no concentration changes were observed.
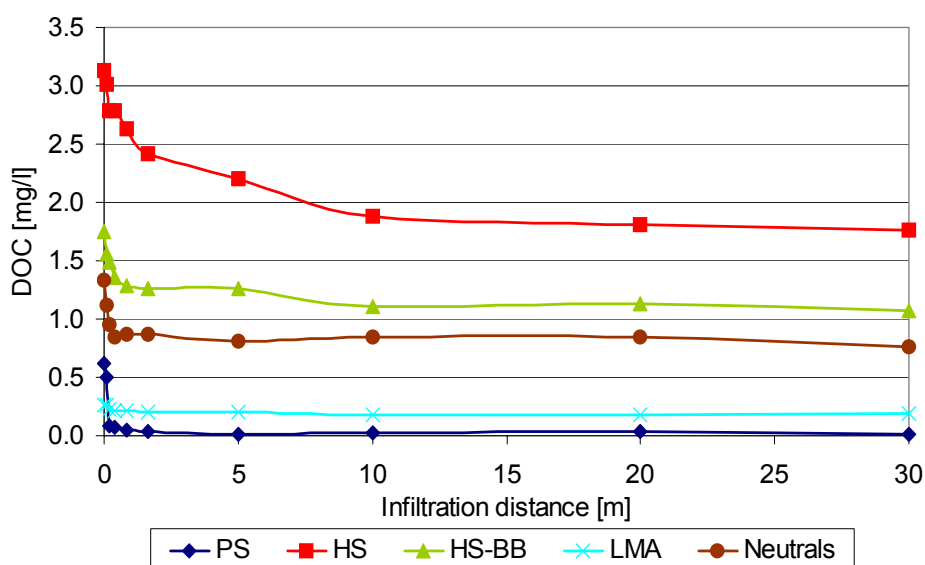
Figure 84 Fate of different DOC fractions along the infiltration path during the oxic stage

Figure 85 provides comparable results for the anoxic stage. It is obvious, that the degradation processes in the single DOC fractions are similar but considerably slower. The concentration of humic substances changes over the entire column. Furthermore, the concentration of neutrals is increasing slightly after 5 m of infiltration. Most probably the increase is due to mineralization fragments, which end up in this DOC-fraction. Figure 85 shows clearly that the fraction of polysaccharides is not completely mineralized.
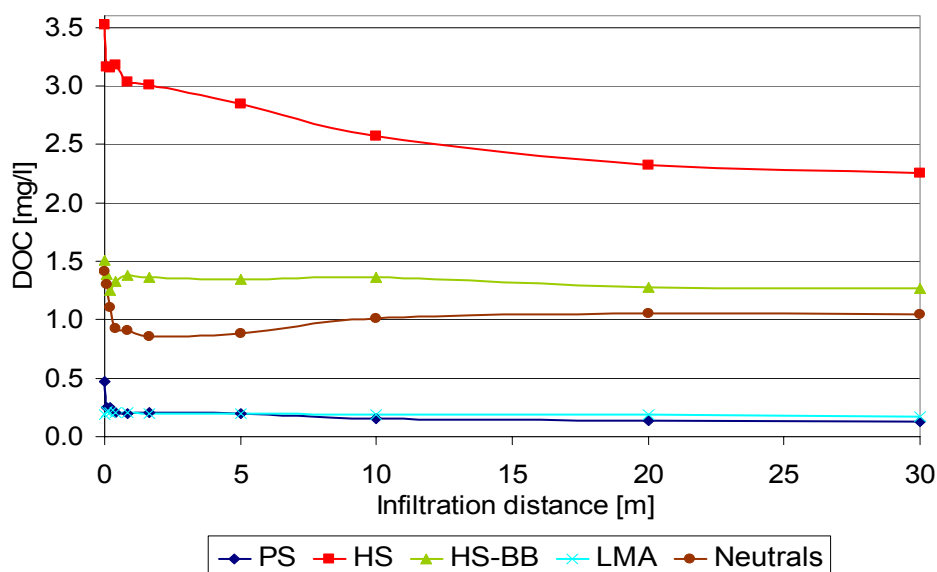
Figure 85 Fate of different DOC fractions along the infiltration path during the anoxic stage

Mass balances:

During infiltration the fate of oxygen or nitrate and organic carbon depend from each other. During mineralization of organic carbon oxygen and nitrate are used as electron acceptors. With the help of mass balances it is possible to assure that changes in oxygen or nitrate concentration are caused by DOC-mineralization. In special cases other factors (like mineralization of POC) influence the electron acceptor level. A mass balance reveals these hidden factors. Figure 86 shows the oxygen mass balance of the long retention column system under oxic conditions. The comparison of the measured oxygen concentration (red graph) with the oxygen concentration calculated on the basis of DOC mineralization (blue graph) proves that no important factors, which were not considered, influence the fate of oxygen.
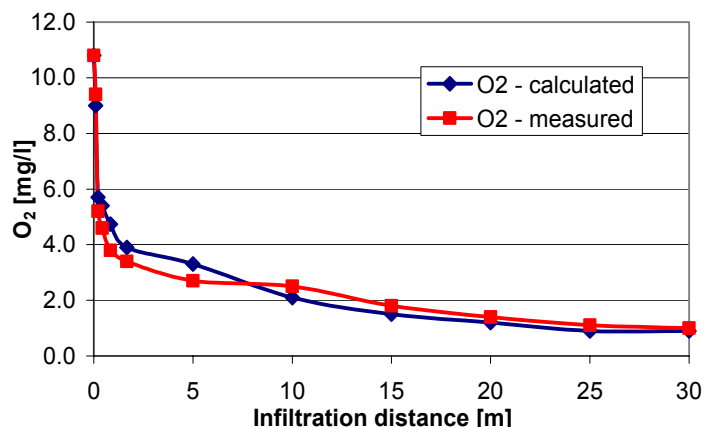
Figure 86 Oxygen mass balance of the long retention columns (oxic stage)

The so called mean oxidation number (MON) is necessary to set up an oxygen mass balance. The MON stands for the amount of oxygen (in mg) which is necessary to mineralize one milligram of organic carbon. The MON for natural surface waters is in the range of 2.5 – 3. In the calculation a MON of 3 was used. The mass balance showed that no significant mineralization of POC from the column sediment material took place. The measured and the calculated fate of oxygen correlate very well.

Figure 87 shows the nitrate balance of the anoxic stage of the long retention column experiment. The very low oxygen levels present in the influent were considered in the calculation. From the observed fate of DOC it was possible to calculate the nitrate consumption by the use of the MON and the oxygen content of NO_3^-. It was found that the calculated and the measured nitrate levels are similar at the different stages of infiltration. These results demonstrate that the objectives of the soil column experiments, to isolate biodegradation as an effect that controls the DOC-level, was successful.
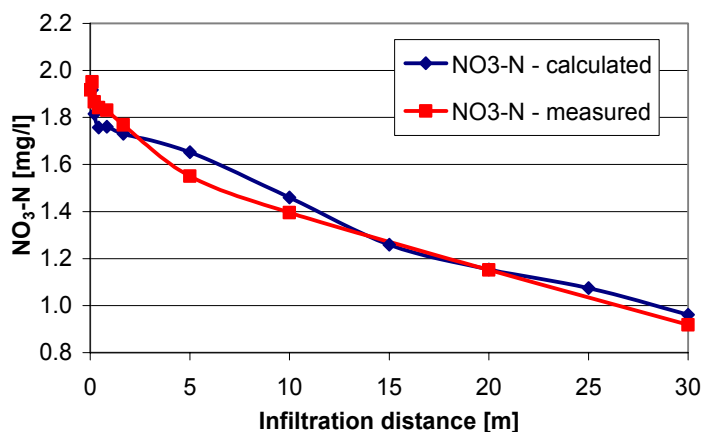
Figure 87 Nitrate mass balance of the long retention columns (anoxic stage)

The production of inorganic carbon is a parameter that could have been used for mass balancing. Unfortunately, the results of the TIC-measurements in the long retention columns are not satisfying and are therefore not used in the mass balance.

Figure 88 shows an overall picture of the bank filtration field site Berlin-Tegel with the most important processes. To simplify the approach a cube of one meter edge length was assumed and all important processes and in- and outputs were stated. The results from the experiment at the long retention column on the MON were transferred to the field. It was found that besides the mineralization of DOC a degradation of POC occurs, which is responsible for the anoxic/anaerobic conditions at the Tegel bank filtration site. A comparison of the effects in the field and at the soil columns showed that most effects that are important at the soil water interface in the field were not relevant in the column studies. The processes in the sediment were similar, whereas the degradation of POC and the dissolution of $CaCO_3$ were in the columns not as pronounced.

Furthermore, the influence of temperature on biodegradation was reduced since the columns were stored in conditions with lower temperature variations as in the field.
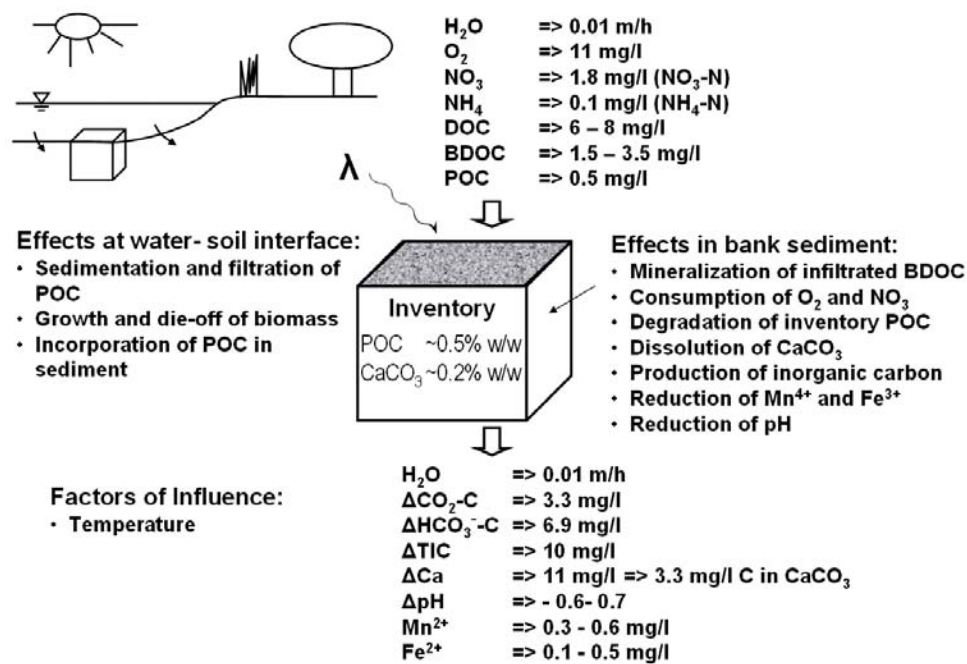
Figure 88 Simplified scheme of most important processes at the bank filtration site Berlin-Tegel

Figure 89 describes the mass balance complementing Figure 88. On the left side the oxygen mass balance is presented and on the right side the carbon balance. Input into the oxygen balance of the filtration process is provided by dissolved oxygen and nitrate. The processes consuming oxygen are BDOC- and POC mineralization and nitrification. Both balances work out nearly even, if the amounts of organic carbon used for oxygen consumption (marked red) are used as input values for the carbon balance.

Oxygen balance

Input

O_2 in infiltrating water	~ 11.0 mg/l
O_2 equivalent in infiltrating NO_3	~ 6.1 mg/l
Sum	**~ 17.1 mg/l**

Consumption

O_2 for BDOC mineralization	~ 6.8 mg/l
= 2.5 * 2.7 (mean oxidation number (MON))	
O_2 for water POC mineralization	~ 1.3 mg/l
= 0.5 * 2.7 (MON)	
O_2 for nitrification	~ 0.35 mg/l
= 0.1 * 3.5	
O_2 for POC mineralization	~ 8.7 mg/l
= 3.2 * 2.7 (MON)	
Sum	**~ 17.15 mg/l**

Carbon balance

Input

BDOC in infiltrating water	~ 2.5 mg/l
POC in infiltrating water	~ 0.5 mg/l
POC in sediment inventory	~ 3.2 mg/l
Carbon from $CaCO_3$ dissolution	~ 3.3 mg/l
Sum	**~ 9.5 mg/l**

Output

Carbon in ΔCO_2	~ 3.3 mg/l
Carbon in ΔHCO_3^-	~ 6.9 mg/l
Sum	**~ 10.2 mg/l**

Figure 89 Oxygen and carbon mass balance complementing Figure 88

The carbon mass balance compares the input concentration of organic carbon and calcium bound carbon with the inorganic species CO_2 and HCO_3^- standing at the end of the infiltration process. Overall, mass balances depict the most important processes during bank filtration and reveal eventual factors of influence, which were not considered earlier. The oxygen and carbon mass balances of the long retention columns confirmed the results presented in the bulk organics chapter.

AOI:

The AOI in the soil column system was composed of surface water AOI, which is present in Lake Tegel, and spiked AOI that was dosed into the influent. The X-ray contrast agent Iopromide was added to the influent at a concentration of 10 µg/l. Since Iopromide consist of nearly 50% iodine, this accounts for ~4.8 µg/l AOI. Therefore, the AOI measurements in the soil columns are ~5 µg/l higher than average surface water samples.

The AOI measurements at the long retention columns proved the assumption that there is nearly no AOI dehalogenation under aerobic conditions. Figure 90 shows that after an initial drop the AOI level remains constant along the column system during 30 days of oxic infiltration. Overall, only 9.1% of the initial AOI were mineralized under oxic conditions. This is consistent with the results of the GWR, where 6-16% of the AOI were removed during 25 days of infiltration (monitoring well 368 UP and 369OP). But at the GWR the redox conditions turned during summer months to anoxic/anaerobic.
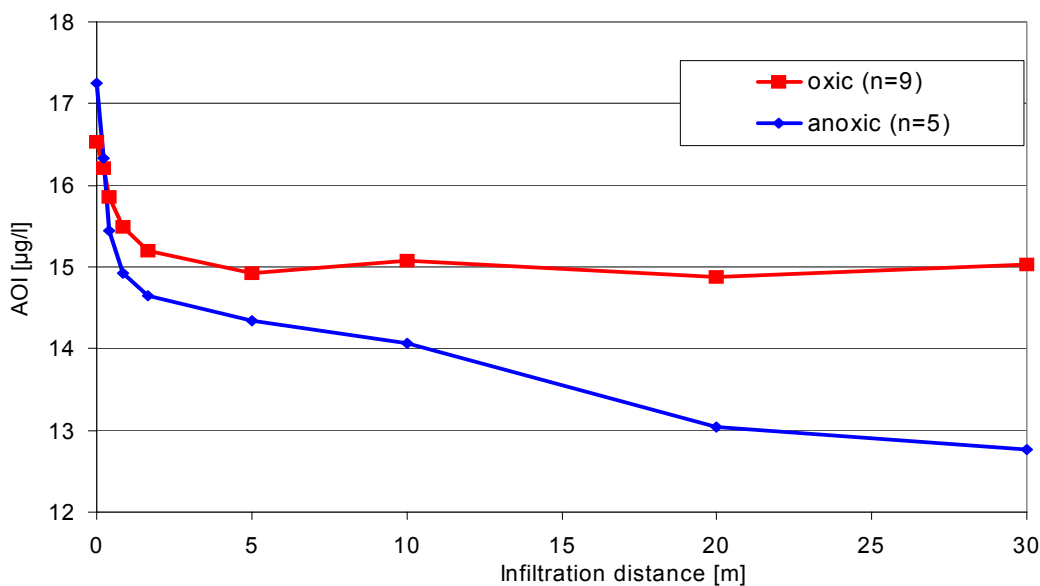
Figure 90 Fate of adsorbable organic iodine (AOI) during the two stages of the experiment

During a complete anoxic infiltration of 30 days 27% of the initial AOI were mineralized. The initial drop in AOI-concentration shortly after infiltration was more pronounced than under oxic conditions and during further infiltration the AOI-mineralization continues. A comparison with the monitoring well 205 (anaerobic, 63% AOI- removal within ~30 days) at the field site Wannsee demonstrates that under more reducing conditions the mineralization of AOI is even more enhanced. The soil column results support the hypothesis that an efficient AOI removal is only possible under reducing conditions by reductive dehalogenation. During the anoxic soil passage anaerobic micro-environments made the more efficient removal of AOI possible.

Trace Organics:

In the experiments on the long retention columns the same trace compounds were analyzed as in the field. Overall, five to six complete sets of samples were analyzed for each tested redox state. Therefore, all presented results are median concentrations of these measurements. A comparison of the results of the different sampling events of one redox state showed that general trend of all measurements was comparable and only small variations in the single sampling points occurred. This proves that over one year of operation in one redox state no significant variations of the removal efficiency for the investigated trace compound took place. Consequently, it can be assumed that the adaptation phase prior the experiments was sufficient and that the removal processes are sustainable over longer time periods.

A comparison of the results of both tested redox conditions showed that under oxic conditions the majority of the trace compounds showed significantly better removal rates. Only one isomer of the naphthalenedisulfonic acid was not degradable under both conditions. Figure 91 proves on a logarithmic scale that for most of the tested

compounds an aerobic degradation was more efficient. But Figure 91 only shows the measured concentrations and does not consider whether the compound was removed by mineralization or metabolization. More information is given in the following pages.
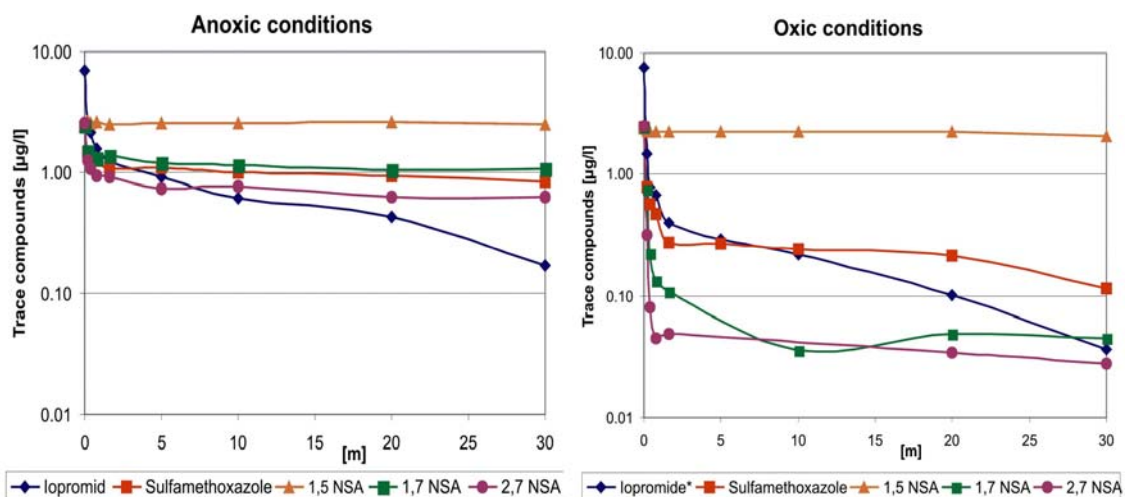
Figure 91 Fate of trace compounds under oxic and anoxic conditions in the long retention columns

Table 17 and Table 18 provide the average concentration of the trace compounds along the soil columns. Since water from Lake Tegel was used as influent, a certain amount of all trace compounds was present in the water before spiking. This concentration varied with the surface water concentration of Lake Tegel. The initial concentration is included in Table 17 and Table 18 under the heading "Lake Tegel". The second heading "Influent" characterizes the water shortly before (20 cm tubing ID 4 mm) it enters the soil column and ~1.2 m tubing after the spiking. The spiking concentrations are included in Table 13. A detailed description of the setup is necessary, since even the short pathways of the water before entering the column system lead to some removal of trace compounds. Most affected was the X-ray contrast agent Iopromide, which was dosed to the influent water in a concentration of 10 µg/l. The measurements right in front of the soil columns showed a concentration increase of only 6-7 µg/l. Since this single compound was found to be easy removed it can be assumed that a mineralization/metabolization of ~30% of this compound took place in the biofilms of the inlet pipe. The real inlet concentrations of the other spiked compounds complied approximately with the calculated concentrations. Because of this fast depletion of Iopromide the spiking concentration of this compound was used instead of the measured inlet concentration for the calculation of the removal rates. All other removal rates were calculated with the measured concentrations.

The other columns of Table 17 and Table 18 show the fate of the trace compounds along the infiltration path in the column system. It is obvious that also for the removal of trace compounds the infiltration zone is of eminent importance. Particularly, under

anoxic conditions the removal trace compounds was limited to the first meter infiltration path.

Table 17 Concentrations of target compounds in long retention columns / oxic conditions (n=6)

Means, n=6		Lake Tegel	LT + TC	BSM 1	BSM 2	BSM 3	BSM 4	BSM 6	BSM 9	BSM 15	BSM 21
Iopromide	[µg/l]	1.08	7.65	1.47	0.79	0.67	0.40	0.29	0.22	0.10	0.04
Sulfamethoxazole	[µg/l]	0.35	2.44	0.78	0.57	0.47	0.28	0.27	0.24	0.21	0.11
1,5-NDSA	[µg/l]	0.10	2.35	2.28	2.24	2.23	2.23	2.21	2.22	2.23	2.05
1,7-NDSA	[µg/l]	0.33	2.40	0.75	0.22	0.13	0.11	0.03	0.04	0.05	0.04
2,7-NDSA	[µg/l]	0.06	2.47	0.32	0.08	0.05	0.05	0.03	0.02	0.03	0.03

Table 18 Concentrations of target compounds in long retention columns / anoxic conditions (n=5)

Means, n=6		Lake Tegel	LT + TC	BSM 1	BSM 2	BSM 3	BSM 4	BSM 6	BSM 9	BSM 15	BSM 21
Iopromide	[µg/l]	0.65	7.02	2.61	2.11	1.56	1.22	0.92	0.61	0.44	0.17
Sulfamethoxazole	[µg/l]	0.39	2.39	1.47	1.31	1.26	1.07	1.10	1.00	0.93	0.83
1,5-NDSA	[µg/l]	0.13	2.56	2.64	2.53	2.61	2.50	2.55	2.52	2.59	2.46
1,7-NDSA	[µg/l]	0.23	2.42	1.49	1.33	1.30	1.35	1.20	1.14	1.05	1.07
2,7-NDSA	[µg/l]	0.08	2.51	1.25	1.07	0.94	0.92	0.74	0.77	0.63	0.63

Iopromide, the X-ray contrast agent was found at all field sites to be easy degradable. In the soil column experiment the concentration of Iopromide was found to decrease quickly under both redox conditions. A slightly faster removal was observed under oxic conditions. After 0.2 m of oxic infiltration the Iopromide concentration was 15% of the spiking concentration (10 µg/l). Under anoxic conditions 26% of the initial concentration was present after 0.2 m. At the end of the column system only traces of Iopromide were found under both redox conditions. (Figure 92)
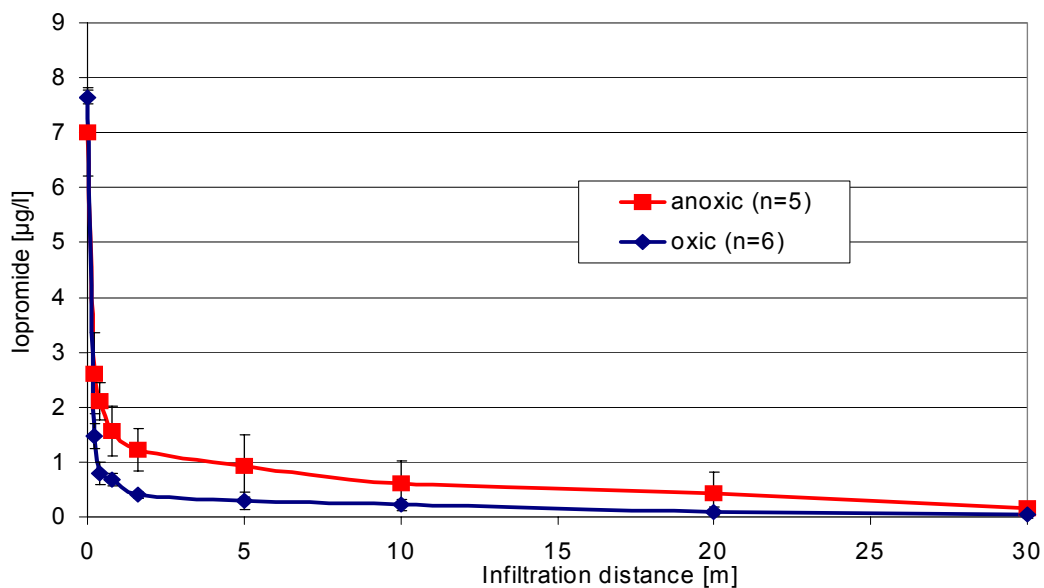
Figure 92 Fate of Iopromide under oxic and anoxic conditions in the long retention column system

A comparison with field results showed that the soil column experiment provides insight into the part of the infiltration path close to the bank. All of the investigated transects did not provide a sufficient resolution of this area. The removal rates of the soil column experiment were in the same order of magnitude as the field results. Most of the field sites were oxic near the bank area. Therefore, a comparison of the removal rates under oxic conditions with the removal rates of monitoring well 365 (GWR) and 3310 (Tegel) was conducted. The Iopromide removal in the GWR-well 365 was 96% after three days of infiltration (7 m infiltration path. The experiments at the soil columns showed exactly the same removal rates in a comparable time frame. At the field site Tegel Iopromide removal in well 3310 was 91% on an infiltration path of 3 m and a not really determinable retention time of less than 14 days. Altogether, the simulation of the Iopromide removal with the long retention soil columns was successful. The column simulations depicted the field results very closely.

To clarify the fate of the Iopromide molecule, it needs to be stressed that for the trace compound analysis a MS/MS-detector was used. This detector identifies the Iopromide molecule only if it is unaltered. A slight modification on the molecule would prevent detection by MS/MS since the exact mass of the molecule is essential for detection. The large molecule of Iopromide with several side chains is prone to metabolization. Therefore, another interesting aspect was to analyze Iopromide as a single compound and as a part of the general AOI. The spiking of 10 µg/l Iopromide increased the AOI concentration in the feed by 4.81 µg/l. The removal of the single compound Iopromide in the soil columns was as efficient as at the field sites. The measurement of AOI parallel to the single compound analysis revealed that Iopromide is not mineralized but

only metabolized during infiltration. This was suspected at the field sites but was confirmed with the soil columns.
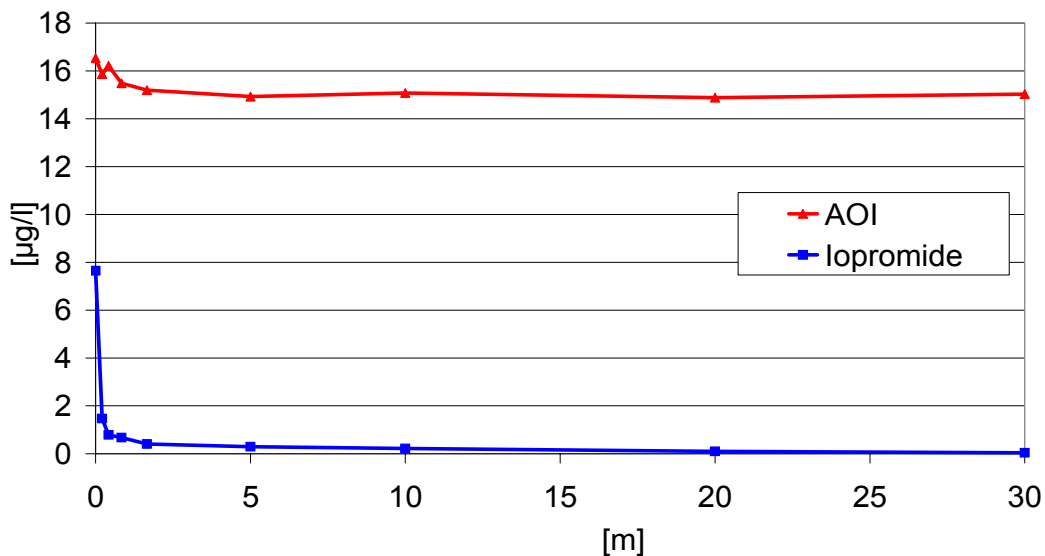
Figure 93 Concentrations of AOI and Iopromide in the columns under oxic conditions (means, n=6)

Figure 93 shows that the Iopromide concentration decreases very rapidly after infiltration. The AOI concentration remains relatively constant. This proves the assumption that the Iopromide molecule is aerobically metabolized during infiltration. But it still remains an iodinated organic molecule and is measurable as AOI. The chemical structure of the products of the metabolization is unclear.

Under anoxic conditions 27% of the AOI were removed during infiltration. A calculation reveals that a total mineralization of the Iopromide would reduce the AOI by 28%. The conformity is no proof of a total mineralization of Iopromide under anoxic conditions. It is believed that under anoxic conditions parts of the lake AOI and parts of the Iopromide derived AOI are mineralized.
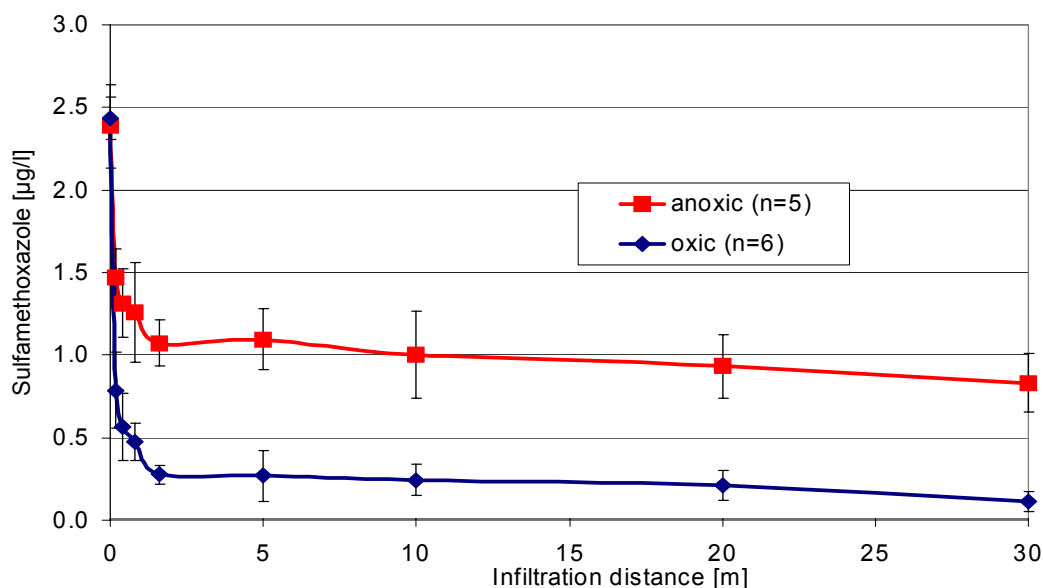
Figure 94 Fate of Sulfamethoxazole under oxic and anoxic conditions in the long retention columns

The bacteriostatic Sulfamethoxazole was spiked to the influent of the soil columns in a concentration of 2.5 µg/l. Figure 94 shows that degradation rates of 95% were reached under oxic conditions and approximately 60% under anoxic conditions. Most of the degradation took place in the infiltration zone. A comparison with other results reveals that in the field Sulfamethoxazole is more efficient degraded under anaerobic conditions. The example of the monitoring wells 205 and 206 at field site Wannsee showed very clear that Sulfamethoxazole is better degradable under anaerobic conditions. A summary of the field results shows, that under oxic conditions removal rates of 50-60 percent were observed within 30 days and 75-90% under anoxic/anaerobic conditions. Similar findings were reported by Schmidt et al. (2004).

Therefore, the results of the soil columns raised different questions. Why is the reduction of Sulfamethoxazole in the soil columns significantly better than at the field sites? An explanation could be derived from the higher spiking concentration and the higher temperature. In the soil columns a much higher (10x) influent concentration was used. It appears possible that higher concentrations of the pollutant are removed by another microbiological degradation step, which shows different redox dependencies. Another possibility could be an improved degradation of higher concentrations of the target compound and no biological effect on concentrations below a certain threshold concentration. Furthermore, the higher degradation rates in the soil columns might be due to the constant and often higher temperature (15°C±4°C).

However, there are different possibilities to explain the results of the soil column system, but the simulation of the Sulfamethoxazole degradation was not successful. Investigations on smaller soil column systems were set up to investigate the reasons for these misleading results.
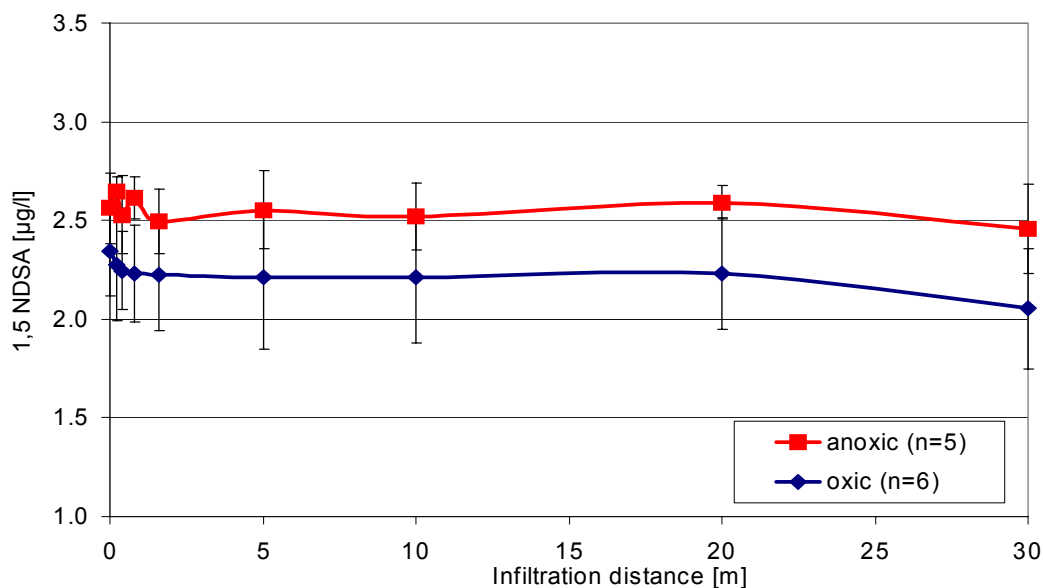
Figure 95 Fate of 1,5-NDSA under oxic and anoxic conditions in the long retention columns

The fate of the different isomers of the naphthalenedisulfonic acids were monitored in the soil column system. Field results showed that the very stable 1,5 –NDSA achieved degradation rates of ~10%. In the soil column system it could be confirmed that this isomer is nearly non-degradable. Under oxic conditions 12% of the initial concentration was degraded, whereas under anoxic conditions only 4% were removed.
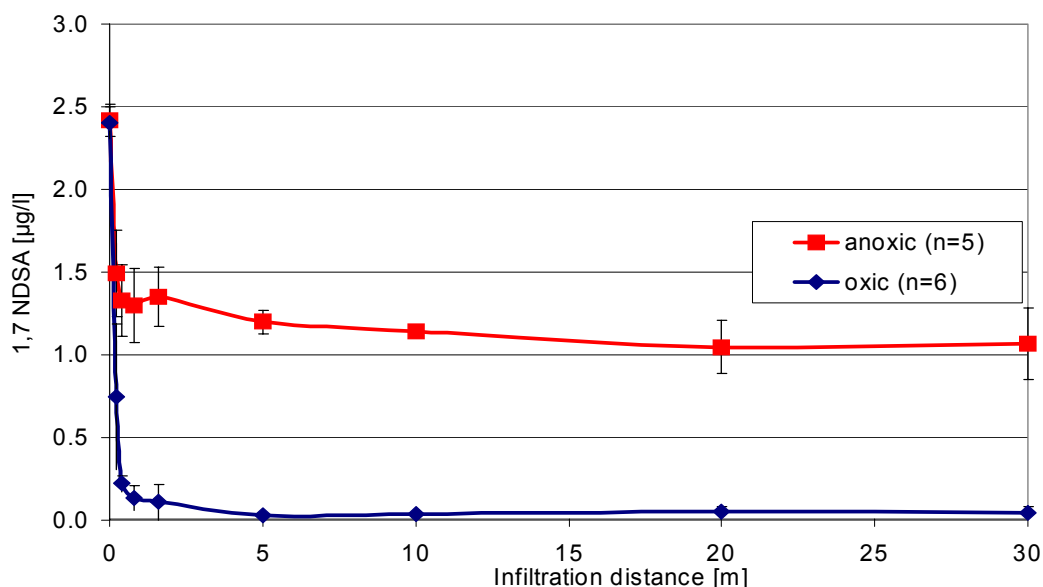
Figure 96 Fate of 1,7-NDSA under oxic and anoxic conditions in the long retention columns

All field results reported the 1,5-NDSA as very biostable and literature on NDSA removal in waste water treatment plants selected 1,5-NDSA as most persistent. The persistence of the 1,5-NDSA demonstrated clearly that the removal of the trace

compounds is due to biodegradation and not adsorption. All monitored compounds are very polar and therefore not adsorbable to quartz sand.

The other two naphthalenedisulfonic acids were better degraded under oxic conditions. This is consistent with observations in the field. But the removal rates were considerably higher in the soil column experiment. For the 1,7- and the 2,7-NDSA, which are known as partly degradable, the calculation resulted in degradation rates of 99% or 100%, respectively. In the recharge facility only rates around 60% were measured. The reasons for the better degradation in the soil column system were most probably answered in the discussion on the behavior of Sulfamethoxazole. It is believed that the higher influent concentration and the elevated temperature are responsible for the better removal rates.
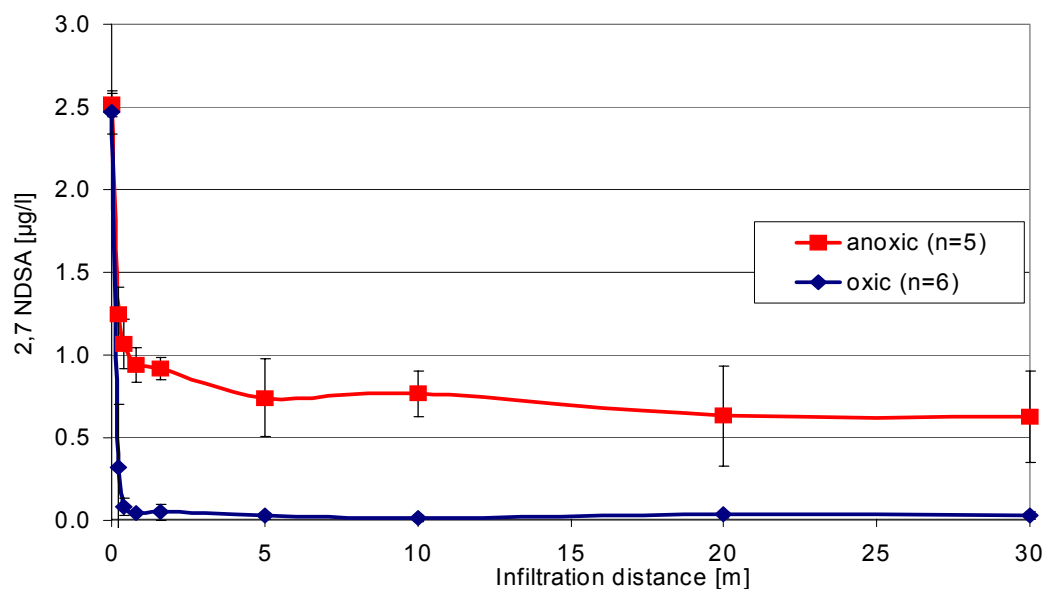
Figure 97 Fate of 2,7-NDSA under oxic and anoxic conditions in the long retention columns

However, the simulation of the fate of NDSA in the field by soil column experiments produced reliable results. The qualitative information on the influence of redox conditions agreed with the field observations. Only in the quantification of the removal rates the soil column experiments lead to an overestimation.

Sediment – Results: (mostly provided by FU Berlin)

Additionally to the characterization of the sediment material at the beginning of the experiments, the FU Berlin conducted sediment analysis of six sediment samples from the soil column system at oxic stage and six samples under anoxic conditions. The samples were taken from the top sediment layer of each column and represented sediment material after 5 m, 10 m, 15 m, 20 m, 25 m and 30 m infiltration. The samples were analyzed for grain size distribution and geochemical properties like C_{org}-content

etc.. Furthermore, the distribution of biomass was assessed by a quantification of phospholipids in the different infiltration depths.

Table 19 Grain size distribution and hydraulic conductivities of sediments in the columns.

Parameter	5 m	10 m	15 m	20 m	25 m	30 m
Grain size [mm]	fraction [%]					
> 2	8.49	10.58	9.3	6.85	5.91	10.21
1-2	5.89	8.01	5.43	3.97	3.71	3.67
0.5-1	19.47	18.88	19.86	21.81	19.37	19.20
0.25-0.5	39.91	36.81	39.79	40.41	41.90	39.45
0.125-0.25	22.08	20.50	20.60	21.39	23.08	21.28
0.063-0.125	3.37	3.60	3.12	3.97	4.49	4.56
<0.063	1.78	1.63	1.89	1.61	1.54	1.63
k_f **Hazen [m/s]**	2.9E-04	3.0E-04	3.1E-04	2.8E-04	2.7E-04	2.7E-04
k_f **Beyer [m/s]**	2.4-2.6E-04	2.4-2.7E-04	2.5-2.8E-04	2.3-2.6E-04	2.2-2.4E-04	2.2-2.4E-04
U	2.8	3.0	2.8	2.8	2.7	2.9

As expected, the grading curves (Figure 98) of the column filling are remarkably similar and consistent with the grading curve recorded at time of the column filling (Figure 68). All 6 samples are medium sized sands with some fine and coarse grained sand and a minor fraction (< 5 %) of fine gravel. Hydraulic conductivities vary between 2.1 and $3.1*10^{-4}$ m/s. These values are similar to those obtained by core samples from the aquifers at the investigated field sites. Details are given in Table 19.
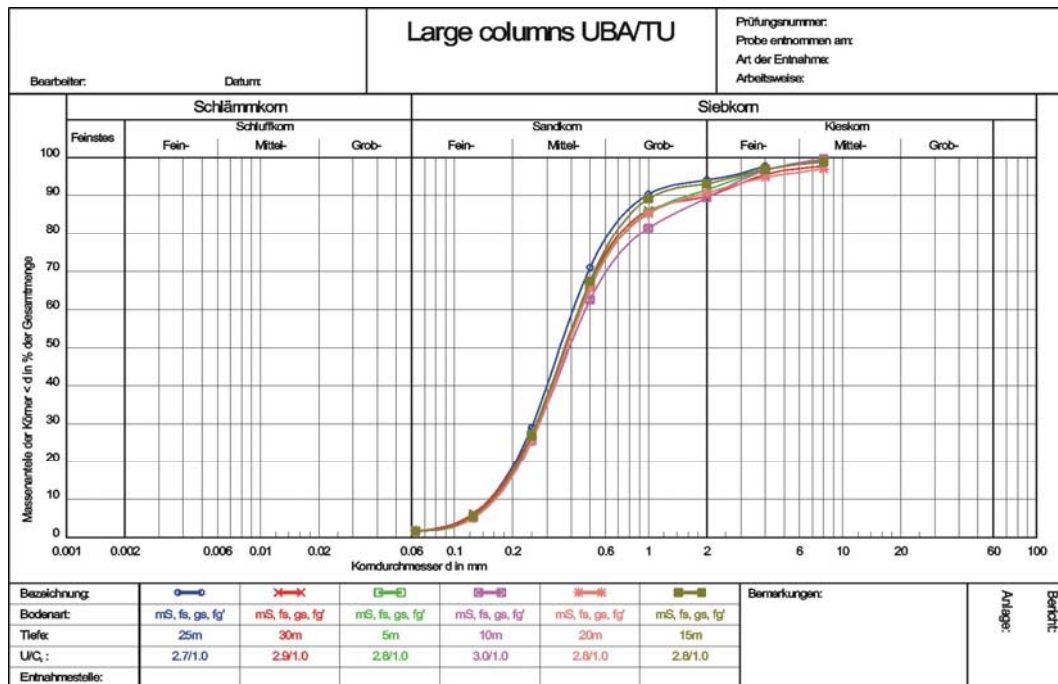
Figure 98 Sum curves of the column sediments.

The geochemical properties of the sediment are summarized in Table 20 and Table 21. The sands contain approximately 1.1-2.6 g/kg total iron, which is well within the range of iron contents encountered in the aquifer sediments from the field sites. Under oxic conditions the average iron content was 1.4 g/kg total iron and under anoxic conditions 1.9 g/kg total iron. At the first sampling (oxic conditions) roughly 46% of the iron is present as crystalline or amorphous Fe(III)Hydroxides- or Oxides, which is more Fe(III) than most field site aquifer samples contain. At the second sampling (representative for anoxic conditions) the share of oxidized iron species is reduced to ~37%.

Table 20 Geochemical properties of the column sediments (sampling after the oxic stage)

Parameter	5 m	10 m	15 m	20 m	25 m	30 m
Fe-ox [mg/kg]	605	660	715	715	550	660
Fe-red [mg/kg]	675	675	1150	725	575	700
Fe-total [mg/kg]	1280	1335	1865	1440	1125	1360
Mn-ox [mg/kg]	56.7	20.4	34.7	20.9	24.8	14.9
Mn-red [mg/kg]	18.3	17.0	16.3	9.8	9.5	10.3
Mn-total [mg/kg]	74.9	37.4	50.9	30.7	34.3	25.1
C-org [weight %]	0.047	0.035	0.034	0.040	0.043	0.027
C-inorg [weight %]	0.032	0.061	0.064	0.032	0.060	0.081
S-total [weight %]	0.001	0.002	0.003	0.003	0.003	0.003
CEC_{eff} [mmol(eq)/100g]	0.406	0.343	0.302	0.374	0.324	0.337

The total manganese content of 25 to 75 mg/kg is similar to that of the aquifer. Under oxic conditions the total manganese content was slightly higher than under anoxic conditions (the difference is mostly due to changes in the first part of the column). Whereas the reduced Mn-species are relatively constant at both samplings, the amount of oxidized Mn-species is reduced under anoxic conditions. This is probably due to redox induced Mn-dissolution.

Table 21 Geochemical properties of the column sediments (sampling after the anoxic stage)

Parameter	5 m	10 m	15 m	20 m	25 m	30 m
Fe-ox [mg/kg]	472	629	532	544	841	1320
Fe-red [mg/kg]	1018	1265	2146	1173	775	991
Fe-total [mg/kg]	1490	1865	2678	1717	1616	2311
Mn-ox [mg/kg]	18.6	24.9	19.1	16.1	11.6	12.0
Mn-red [mg/kg]	13.7	11.2	30.8	21.8	15.4	17.2
Mn-total [mg/kg]	32.3	36.1	49.9	37.9	27.0	29.2
C-org [weight %]	0.032	0.048	0.039	0.032	0.036	0.032
C-inorg [weight %]	0.054	0.092	0.068	0.106	0.040	0.052
S-total [weight %]	0.000	0.001	0.000	0.000	0.000	0.000
CEC_{eff} [mmol(eq)/100g]						

The sands contain between 0.03-0.08 weight % inorganic carbon, most likely to be calcite (Figure 99). The amount is equivalent to 2.5-6.7 g/kg Calcite and in good agreement with the 2-3 g/kg Ca^{2+} dissolved during pressure elution. No significant differences were observed under oxic or anoxic conditions. The inorganic carbon content is lower than in aquifer samples from the field sites which contain, with very few exceptions, >0.2 weight % C-inorg. The organic carbon content ranges under both conditions from 0.027 to 0.048 weight % organic C (0.27-0.48 g/kg). These values are well within the range of those encountered in the field. The Sulphur content (0.000-0.003 weight %) is rather low.
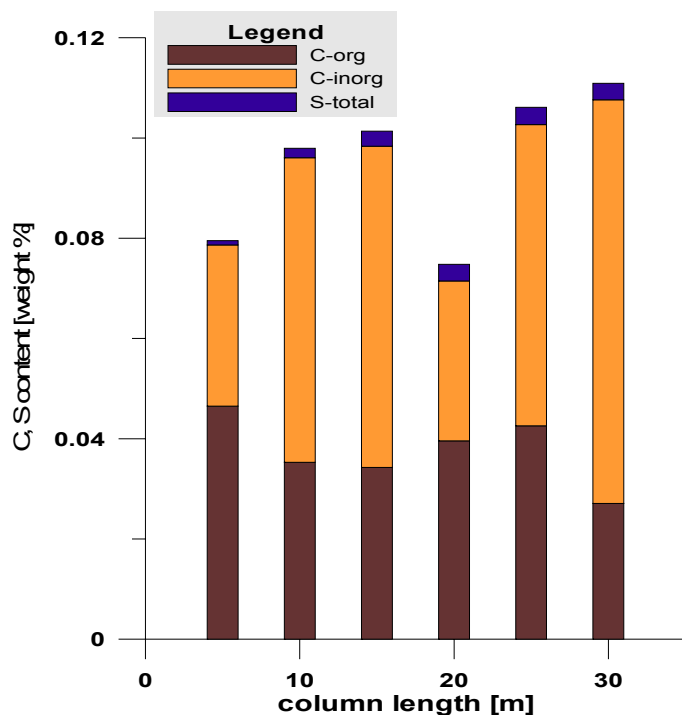
Figure 99 Carbon and sulphur contents of the column sediments under oxic conditions

At both sampling events the acid soluble cations were mainly Ca, Fe and Al with some Mg and K (with decreasing contents). Ca was less dominant than in the aquifer samples from the field sites. The total sum of acid soluble cations was roughly two times as high in the field, mainly due to the higher Ca (and Mg) contents. With 0.6-0.8 mmol (eq)/100g, the sum of the exchangeable cations was larger than the CEC_{eff} derived from the re-exchange with Ba (black crosses in Figure 100, right, 0.3-0.4 mmol (eq)/100g). Again, this may be explained with the dissolution of calcite (Kretschmar, 1991).
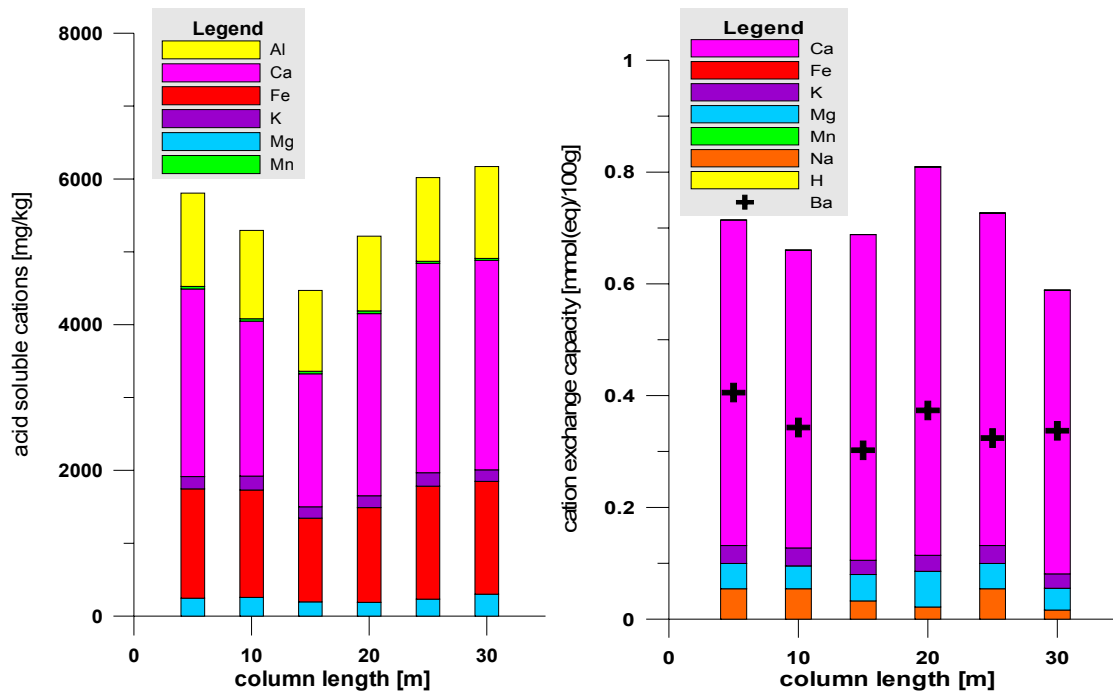
Figure 100 Acid soluble cations (left) and exchangeable cations (right) of the column sediments under oxic conditions

Additionally, the extractable amount of lipid bound phosphates was measured along the column after the oxic and the anoxic stage. The samples were sent to the University of New Hampshire/USA, where the work group of Prof. Collins conducted the phospholipid analysis. The quantification of lipid bound phosphates is a sensitive method for determining microbial biomass in sediments. The used method is described by detail in Findlay et al. (1989).

Since the content of lipid bound phosphates is a good estimate of active microbial biomass, the results give an overview on the distribution of microorganisms along the columns. Because of the laborious method and the expensive shipping only two sets of samples (each containing 6 samples) was sent to New Hampshire. The quantification of phospholipids in these sediments was performed as duplicates. In the analysis of the samples of the oxic stage the samples from 15 m, 20 m, 25 m and 30 m were found to be under the limit of quantification. Therefore, these samples were set to half the limit of quantification. For the quantification of the anoxic samples the sample volume was adapted and the limit of quantification was lower. Figure 101 shows the results of the phospholipid analysis.

The results indicate a considerably higher active biomass accumulation during oxic conditions at the first two sampling points. Unfortunately, no samples from the initial infiltration zone (at the bottom of column 1) and the first 5 m of the infiltration path could be analyzed. This is due to a lack of sediment sampling possibilities along the first column. The stainless steel cylinder only permitted a sampling after 5 m. Assuming an

exponential decline of the biomass density with depth, the biomass profile of the first 5 m of infiltration could be modeled using the data points provided.
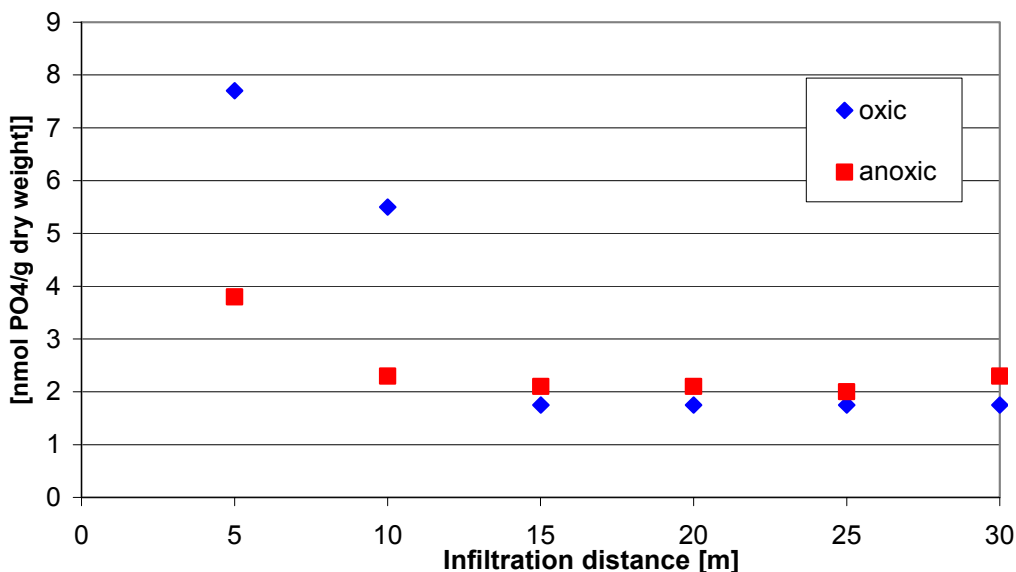
Figure 101 Results of phospholipid quantification along the columns after the oxic and anoxic stage

However, the results are consistent with the findings of the DOC- analysis. Under oxic conditions a larger amounts of DOC are mineralized in the first part of the column system (Figure 76). The phospholipid results show that the enhanced mineralization of DOC led to (is caused by) a higher biomass density in the first 10 m of infiltration. Furthermore, the results indicate that under oxic conditions the biomass density is lower and relatively stable between 15-30 m of infiltration. Under anoxic a higher biomass density at the sampling points at 5 m and 10 m was observed, which was considerably lower than under oxic conditions. Towards the end of the column system the biomass density under anoxic conditions was similar to the results under oxic conditions.

1.4.2 Short retention soil column system (TU Berlin)

Additionally to the soil column system in Marienfelde, soil column studies were conducted to study the fate of bulk and trace organic compounds under different redox conditions. Therefore, a set of short columns was installed at the department of water quality control at the TU Berlin. Furthermore, the column system was used to investigate the influence of the spiking concentration of the trace compounds on the elimination efficiency. A second experiment was designed to assess the importance of the initial amount of BDOC for the trace compound mineralization. These objectives were examined within the diploma project of Cornelia Mundt at the DWQC at TU Berlin.

1.4.2.1 Set-up

Altogether, 9 columns (length 1 m, retention time 6 days) were used to simulate the most important redox conditions and different successions of redox zones. The short retention columns were filled with silica sand and operated under controlled redox conditions with spiked Lake Tegel water. The columns had a retention time of 6 days and a flow of 0.8 l/d. Figure 102 shows a picture of the columns.

Figure 102 Short retention columns at the DWQC at the TU Berlin

Five different combinations of redox conditions were represented in the column system. More short soil columns were utilized to quantify the role of adsorption and the differences between silica sand and original sediment material from a field site. Therefore, two additional columns were filled with sediment material from Lake Tegel; one should be representative for the instant bank region and another for the aquifer conditions. In contrast to the bank material, the aquifer material contains a smaller

fraction of particulate organic carbon. The original material was taken as a disturbed sample and immediately after sampling introduced into the columns.

Additionally, one column was operated as an abiotic control to distinguish between biotic and abiotic processes. For this reason, the influent was spiked with sodium azide. Table 22 contains an overview of the materials used, the conditions of the columns and the concentrations of the spiked substances.

Table 22 Characteristics of the short retention soil columns

Column	Material	Influent (Lake Tegel water)	Concentrations of trace organics in the influent
0	technical sand	oxic + NaN$_3$ [8 g/l]	Iopromide [25 µg/l] Sulfamethoxazole [6.25 µg/L] 1,5-NDSA [6.25 µg/l] 1,7-NDSA [6.25 µg/l] 2,7-NDSA [6.25 µg/l]
1	technical sand	oxic	
2	technical sand	anoxic	
3	technical sand	oxic + DOC [4.5 mg/l]	
4	technical sand	anoxic + NO$_3$-N [5 mg/l]	
5	technical sand	effluent of *column* 2	
6	technical sand	anoxic + DOC [3 mg/l]	
7	bank material	oxic	
8	aquifer material	oxic	

The tank for the oxic columns was permanently aerated with air and had an average oxygen concentration of ~10 mg/l. For the elimination of oxygen, the anoxic tank was aerated with nitrogen gas. Figure 103 presents a schematic of the set-up of the short retention columns. The columns were operated in the basement of the DWQC at 19°C ±3°C.
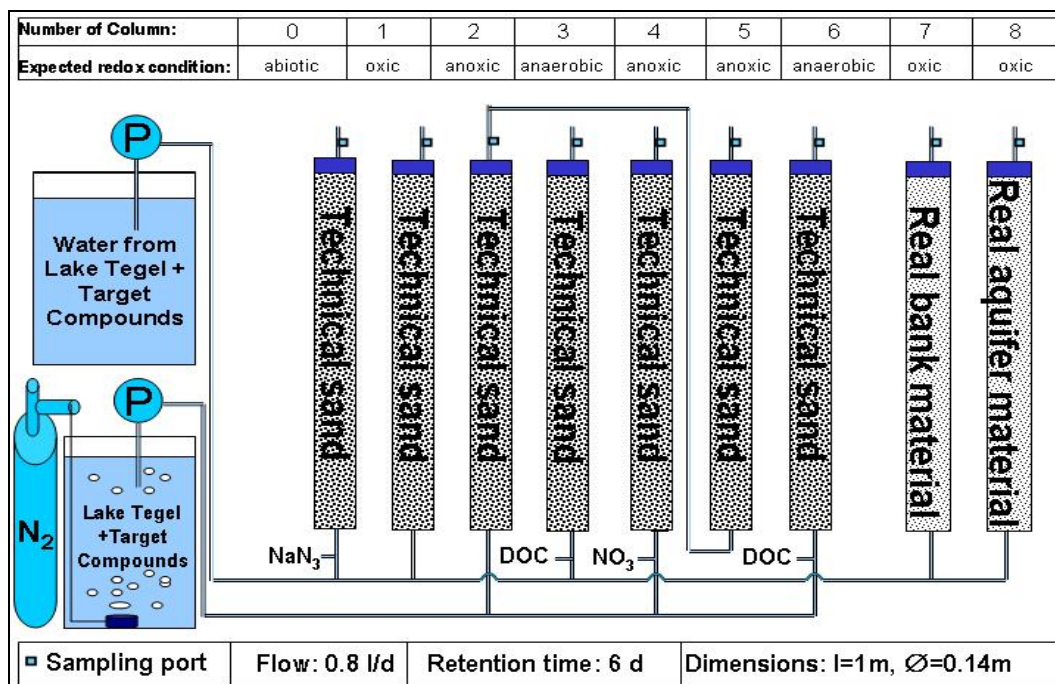
Figure 103 Experimental set-up of the short retention columns

The short columns were made of plexiglas and the tubing was PU (Polyurethane). Because of the considerably shorter distances compared to the long retention columns, oxygen diffusion through the tubing was not a problem. Adsorption tests with the investigated compounds and the used tubing proved no relevant loss due to adsorption onto the tube walls (compounds are very polar).

Columns 0 to *6* were filled with technical sand (Ø = 0.7-1.2 mm) and at the bottom and the top layers of 8 cm coarser gravel (Ø = 5 mm) provided stability and uniform flow conditions. The column system offered sampling ports only at the end of the column. A maximum of 800 ml of sample could be collected each day from one column. By adding organic carbon (starch) and nitrate to the influent different redox conditions were adjusted.

The adaptation period was selected to cover 6 months, to assure stable conditions in the columns and an adapted biomass for each of the enforced redox conditions.

In the first year of operation the main focus was to clarify the redox sensitivity of the bulk and trace compound degradation and the effects of different filling material. This time is referred in the following chapter as *operation period 1 (OP1)*. Within the work of Cornelia Mundt on the column system two additional objectives were included into the work. The project focused on the influence of trace compound concentration and BDOC-concentration, two variable parameters that most probably influence the overall removal efficiency for trace pollutants. Both topics were addressed in separately designed experiments which are referred to as *operation period 2* (influence of trace compound concentration) and *operation period 3* (influence of BDOC-concentration).

Each of the additional experiments (**OP1** and **OP2**) was designed to investigate the trace- (and bulk-) organic removal under three artificially induced conditions, which were set up by variation of the investigated parameter. Thereby, the results of *operational period 1* were used as starting point and one of the three conditions.

However, in *operation period 2* the influence of the trace compound concentration on the removal efficiency (percentage) of the pollutants was investigated. In addition to the results of *operational period 1* two experiments with reduced spiking concentration were performed. The spiking concentration was reduced to one half of the initial concentration (LT 1/2) and one eighth of the initial spiking concentration (LT 1/8). The removal efficiencies on a percentage basis were compared to reveal differences. Eventual differences could have been caused by high threshold-concentrations or different removal mechanisms for diverse concentration levels.

In *operational period 3* the importance of the initial BDOC-concentration was investigated. It was of interest to assess eventual differences in trace compound removal under conditions of high BDOC levels and very low BDOC levels. Variations in the BDOC level affect the overall density of the biomass in the infiltration area. Furthermore, an effect on the variety of the microbial community is likely. Therefore, variations of BDOC are most likely to affect the efficiency of cometabolic mineralization processes. Specialized microorganisms that feed on the investigated trace pollutants are most likely not affected, since the trace compound spiking was not varied in this experiment. The different BDOC concentrations were realized by mixing Lake Tegel surface water with water from production well 13 at BF transect Tegel. It was assumed that well 13-water does not contain any BDOC after 4-5 months infiltration. Experiments were conducted with maximum BDOC (LT 1/2), 50% of the BDOC-concentration by a mixing of 50:50 (50-50 1/2) and 25% of the BDOC level (mixing 25:75=>25-75 1/2). The trace compound spiking was held constant during the experiments at half of the concentration of *operational period 1*.

Table 23 Overview of conducted experiments on short retention columns

Operational period	Variation of	Time frame	Name of experiments
1	Redox conditions	07/03 – 09/04	LT 1/1
2	Trace compound concentration and redox conditions	10/04 – 12/04	LT 1/1 LT 1/2 LT 1/8
3	BDOC- concentration and redox conditions	12/04 – 02/05	LT 1/2 50-50 1/2 25-75 1/2

Each of the new experiments was commenced by a sufficient period of adaptation to the new conditions. Table 23 provides an overview of the different operational periods and time frames. The table also assigns the single experiments and their names to the operational periods. The actual concentrations of BDOC and spiked compounds are described in Table 24. The quantification of the BDOC resulted from the difference of measured DOC- concentration and share of non-degradable DOC.

Table 24 Names and characteristics of the conducted experiments

Experiment	Varied parameter	Spiking-concentration [µg/l]			Portions of Lake Tegel water [%]	Portions of well 13-water [%]	BDOC [mg/l]
		NDSA	Iopro-mide	Sulfame-thoxazole			
Lake Tegel 1/1	Spiking concentration	6.25	25.0	6.250	100	0	2.3
Lake Tegel 1/2		3.125	12.5	3.125	100	0	2.3
Lake Tegel 1/8		0.781	3.12	0.781	100	0	2.3
Lake Tegel 1/2	BDOC-concentration	3.125	12.5	3.125	100	0	2.3
50-50 1/2		3.125	12.5	3.125	50	50	1.3
25-75 1/2		3.125	12.5	3.125	25	75	0.6

1.4.2.2 Results

After the adaptation period of the column system it was of importance to characterize the redox conditions in all columns separately. The redox zone analysis was based on measurements of oxygen and nitrate in the effluent of the columns. The state after 6 months of equilibration is pictured in Figure 104. The conditions remained constant during the time of the experiments.

- **Column 0** is the abiotic control, which is poisoned by NaN_3. The biological activity is very low and the oxygen is not depleted during infiltration.
- In **column 1** the water infiltrates under oxic conditions. In the effluent the oxygen concentration is low, but nitrate is not reduced.
- **Column 2 and 5** describe an anoxic infiltration in a connected system. **Column 2** receives oxygen free water with the nitrate level of Lake Tegel. The effluent of **column 2** is fed to **column 5** to allow longer retention times for the slower denitrifying biomass. Nitrate is still present in the effluent of **column 5**.
- **Column 3** obtains oxic Lake Tegel water spiked with starch. The starch is converted rapidly, leading to short oxic and the anoxic redox zone. It is most likely that most of the filtration in **column 3** takes place under anaerobic conditions.
- **Column 4** is comparable to **column 2**, but to enhance denitrification, nitrate is spiked overstoichiometricly.
- **Column 6** receives oxygen free water with starch, which promotes the fast reduction of nitrate.

It needs to be clear that the dimensions of the different redox zones are not measured, but the redox conditions in influent and effluent prove that these zones have developed during several months of equilibration time.
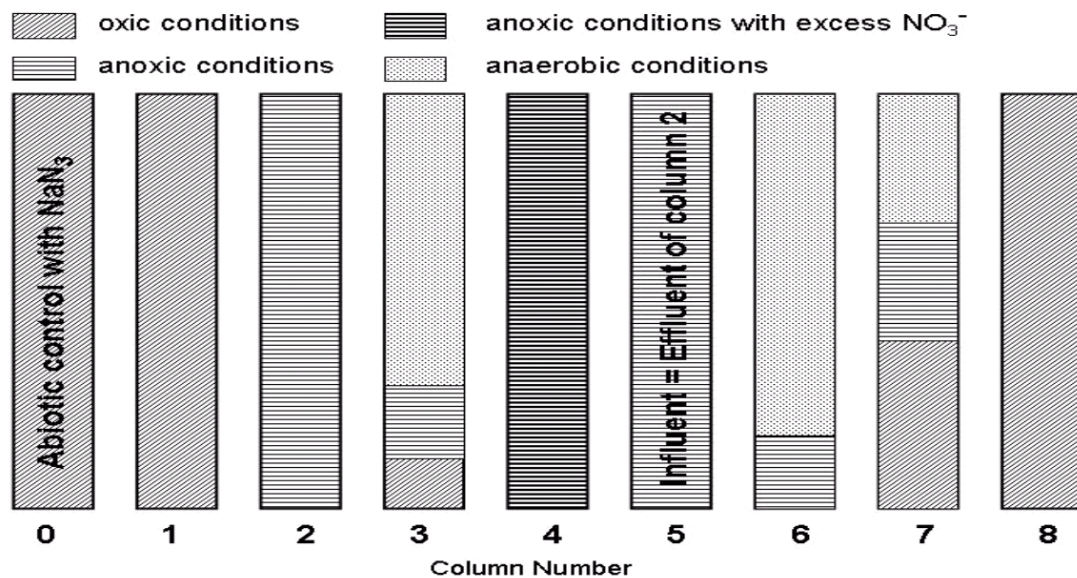
Figure 104 Developed redox zones in short retention columns (dimensions estimated)

In addition to these seven columns two columns with original material from the field site Tegel were operated. Because of high portions of POC in *column 7* organic carbon is still leaching from the soil because of the disturbance of the natural soil structure. Most leaching of DOC was observed in summer in periods of higher temperatures. The result was a high biological activity in the column due to the high amount of available dissolved carbon. Therefore, an oxic, an anoxic and an anaerobic zone are present in *column 7. Column 8* was filled with aquifer material and did not contain high portions of POC. Therefore, the redox conditions remained oxic along the infiltration path, comparable to *column 1*.

Table 25 provides the average oxygen and nitrate concentrations, measured during the entire operation of the short retention column system.

Table 25 Oxygen and nitrate levels in the column system

Column	Oxygen (n=34) [mg/l]	Nitrate (n=19) [mg/l]
Oxic influent	**10.0**	**1.6**
Effluent column 0	8.3	1.5
Effluent column 1	2.6	1.5
Effluent column 3	0.0	0.0
Effluent column 7	0.0	0.1

Effluent column 8	3.4	1.6
Anoxic influent	**0.0**	**1.5**
Effluent column 2	0.0	1.1
Effluent column 4	0.0	7.2 (spiked)
Effluent column 5	0.0	1.0
Effluent column 6	0.0	0.0

Operational period 1 (Influence of redox conditions):

The first operational phase focused on the quantification of the influence of the redox conditions on the bulk and trace organic compound removal. During the experiment conditions were held constant and an extensive monitoring program was conducted on the soil columns.

DOC: Regarding the behavior of the bulk organics it was found that the removal rates of the different columns varied. Figure 105 shows the results of the DOC monitoring. Please refer to Figure 104 to assign the actual redox conditions of the single column to the number of the column used in the description and the graphs. The analysis proved no efficient removal of bulk organics in the poisoned *column 0*. The average DOC effluent concentration of *column 0* is similar to the DOC level of the influent. The most efficient DOC removal was found during complete oxic infiltration in *column 1*. During six days of infiltration along a one meter infiltration path a removal of 18% of the initial DOC was achieved. Under anoxic conditions the DOC removal was not as efficient as under oxic conditions and much slower. *Column 2*, representing anoxic conditions only removed 2% of the DOC after 6 days of infiltration. After a prolonged infiltration period (*column 5*) the removal rate was increased to 17%. The results show evidently that bulk organic mineralization is considerably slower under anoxic conditions. The dosage of excessive nitrate (*column 4*) increased the removal rate of DOC within 6 days from 2% to 9%.
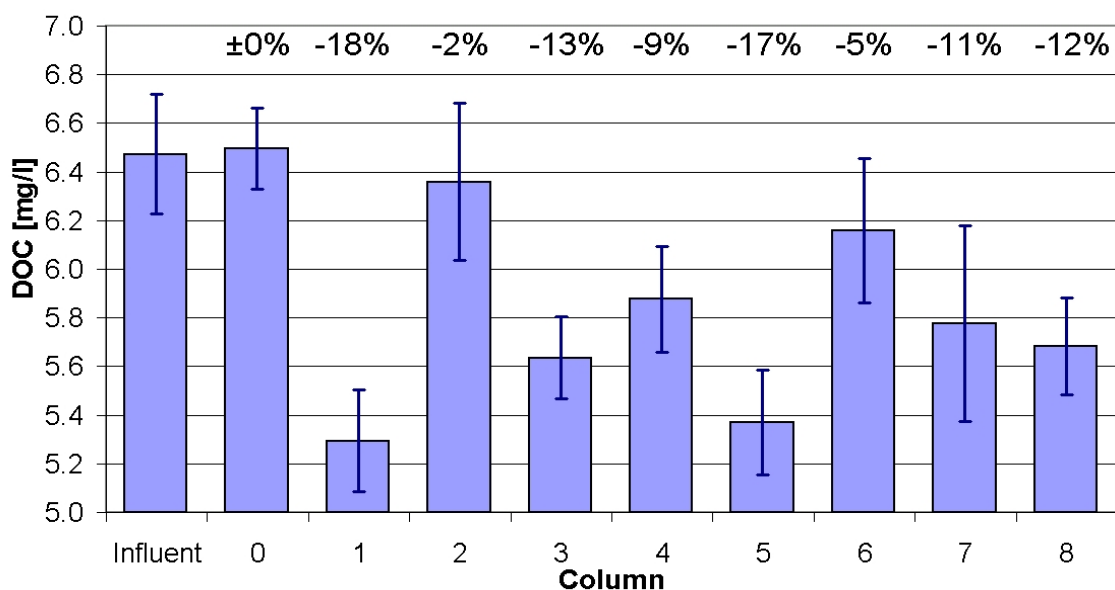
Figure 105 Fate of DOC under different redox conditions including standard deviation (n=25)

Two columns were operated under partly anaerobic conditions (*column 3* and *column 6*). The results of these columns have to be evaluated with care, since starch was added to the influent to achieve anaerobic conditions. It was found that starch dosage resulted in a sort of monoculture in the inlet pipe and in the immediate start of the column. This monoculture mineralized the starch efficiently and adjusted the redox conditions to the desired level, but it is unclear which amount of natural DOC was mineralized by this biomass. However, a comparison of both columns with anaerobic conditions (*column 3* and *column 6*) showed that the mineralization process was more complete in *column 3* which was fed with oxygen saturated water. The dosing of starch in *column 3* resulted in a high amount of available organic carbon for the microorganisms and increased the consumption of oxygen. Anoxic conditions were achieved rapidly, because about 2.7 mg oxygen is necessary for the mineralization of 1 mg DOC. Due to subsequent consumption of nitrate, which was confirmed by the analysis of nitrate, the conditions in *column 3* turned anaerobic. Thus, most of the degradation of BDOC took place under anaerobic conditions. Altogether, *column 3* provided a complete sequence of redox zones (oxic, anoxic and anaerobic) and achieved a mineralization rate of 13%. This is a higher removal than in *column 6*, where the redox situation consisted of anoxic and subsequently anaerobic conditions. In this column a removal rate of 5% was achieved (Figure 105).

Both columns with natural sediment fillings performed similar. Removal rates of 11% and 12% were achieved, respectively. Some influence on the removal rates was observed during summer, when parts of the POC leached from the sediment. This effect resulted in increased DOC levels in the effluent. *Column 7* was mostly affected by this process. Without the leaching the removal rates would have been considerably

higher. *Column 7* showed a similar change of the redox conditions from oxic in the influent to anaerobic in the effluent. The reason was mineralization of POC from sediment filling. Contrary to the fast availability of starch, the mineralized POC is more complex. Therefore, it was assumed, that the anoxic and anaerobic zones begin more distant from the immediate infiltration zone. The oxic zone in *column 7* and the larger surface area available for the biomass (caused by smaller particle size) led to better degradation rates of DOC. The advantage of a larger surface area caused a higher biomass density. Altogether, *column 7* provided good conditions for DOC mineralization but the efficient mineralization is partly compensated by leaching POC. *Column 8* was filled with aquifer material containing less easily degradable POC. But the average particle size in the aquifer is larger than in the bank region. The average surface area combined with oxic conditions throughout the column provided above average removal potential for DOC.
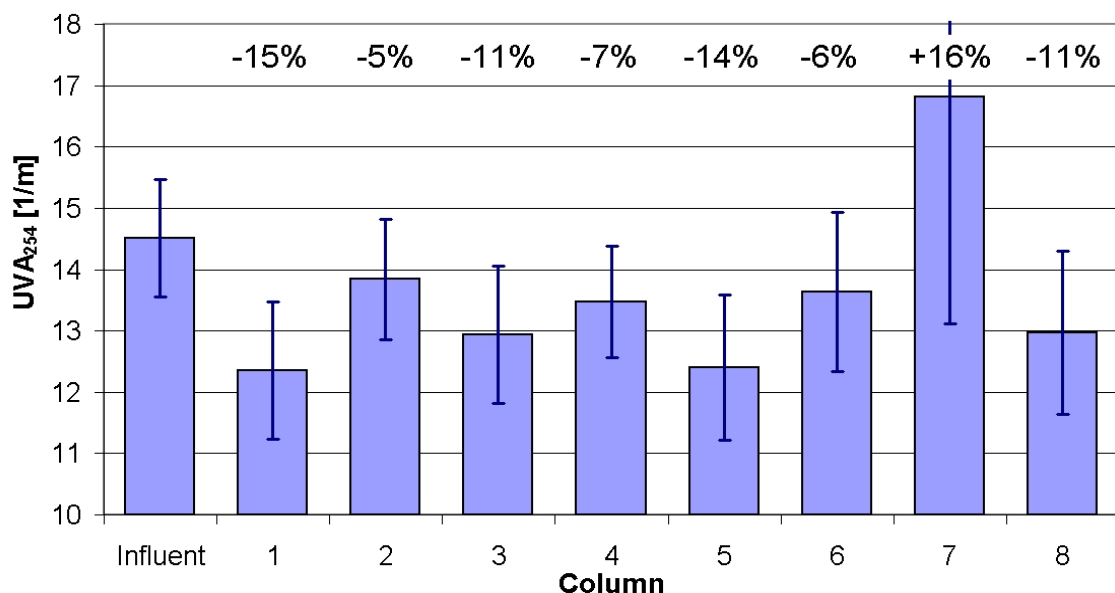
Figure 106 Fate of UVA$_{254}$ under different redox conditions including standard deviation (n=25)

UVA$_{254}$: Figure 106 shows that the UVA measurements were consistent with the DOC results. Because of the UV-absorption of sodium azide at the respective UV-wave length no measurements of the effluent of *column 0* were performed. Leaching of DOC from *column 7* during periods of elevated temperature resulted in an increase of the average UVA-absorption in *column 7* by 16%. The high standard deviation proves that leaching was limited to a few months in summer. Since this effect was not that strong for the parameter DOC, it can be concluded that the DOC that was leaching from the sediment has a very high aromaticity. All other results confirm the findings of the DOC analysis.

LC-OCD: The technique of LC-OCD was used to verify the fractions that were responsible for the decrease of the DOC-concentration during infiltration through the columns. It was of interest, whether different fractions of DOC were mineralized under certain redox conditions. A comparison of the pooled chromatograms of the experiment is presented in Figure 107 and Figure 108.

Because of a high salt content in the samples from *column 0*, the analysis of these samples with LC-OCD was difficult. The salt content lead to high ghost peaks towards the end of the elution time. Therefore, an evaluation of the fractions eluting lately was not possible. In spite of these problems, the measured chromatograms of *column 0* effluent proved, that the fraction of polysaccharides left the column without changes. Thus filtration effects, as a dominant factor influencing the fast removal of PS during infiltration, can be excluded. Because removal of this easily degradable fraction occurred only during passage through bioactive columns, the reduction of polysaccharides can be traced back to a biological degradation.
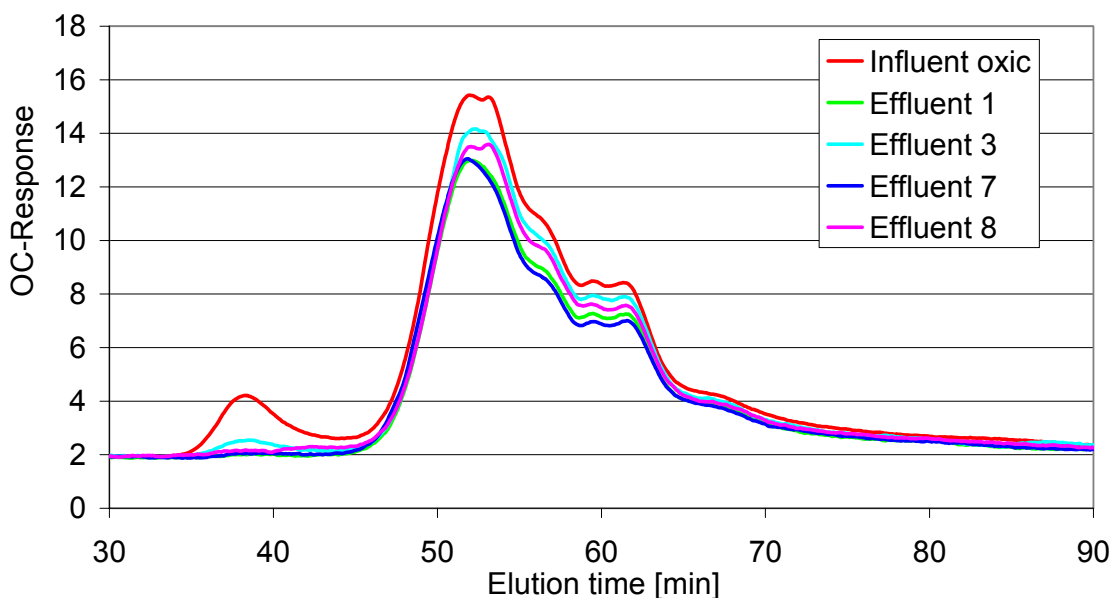
Figure 107 LC-OCD diagrams of the columns with oxic influent

Evaluation of the LC-OCD diagrams shows that the most affected DOC fractions in the columns are the polysaccharides and the humic acids. Low molecular weight acids are also reduced during soil passage.
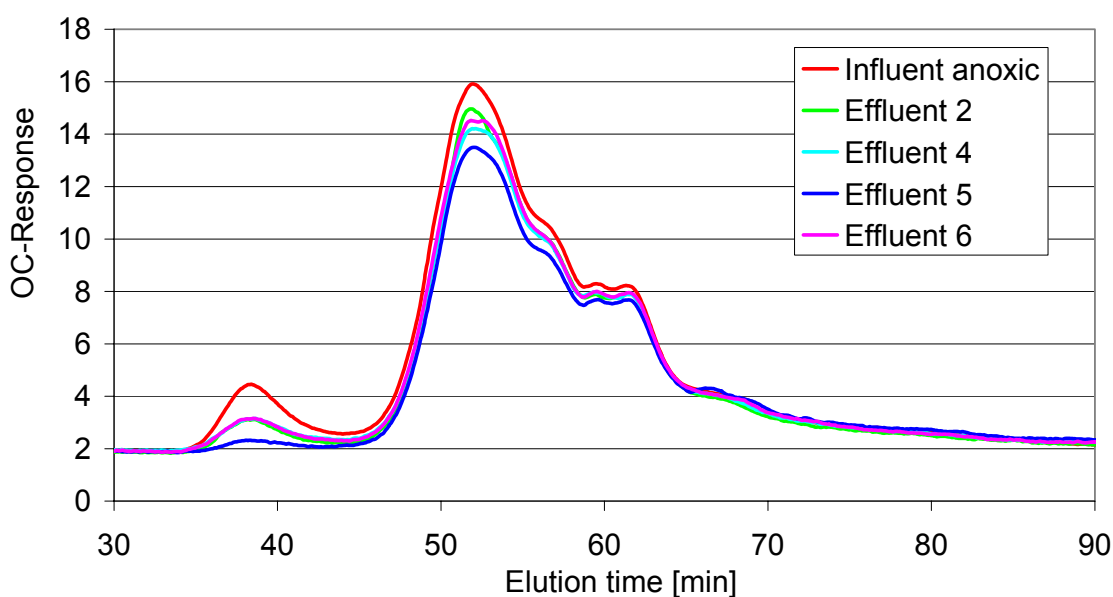
Figure 108 LC-OCD diagrams of the columns with anoxic influent

Figure 107 and Figure 108 show that the PS-fraction is removed completely under oxic conditions (*column 1, 7* and *8*). Columns operated under anoxic conditions show only ineffective degradation of PS (*column 2* and *4*). As an exception, polysaccharides are degraded almost completely in *column 5*, whereas in the other anoxic columns only half of the polysaccharide concentration was degraded. The redox conditions in *column 3* and *column 6*, which become anaerobic after a short distance, did not lead to a complete removal of polysaccharides. Overall, the anaerobic PS-elimination was comparable to the results of the anoxic columns. As polysaccharides are part of the BDOC and only ~50 % of the BDOC is mineralized in these columns, it can be concluded, that polysaccharides belong to the easily degradable fractions within the BDOC. Furthermore, the results in Figure 107 and Figure 108 show that the removal of the other assessable DOC-fractions complies with the results of the DOC-quantification. The investigation proved a comparable stability of the DOC fractions under the different tested redox conditions. The PS-fraction was found to be under all conditions easy degradable. Under anoxic/anaerobic conditions no complete removal of PS was observed but these redox conditions also lead to a minimized removal of the other DOC-fractions.

Summarizing the results of LC-OCD analysis it was found, that polysaccharides can be biodegraded completely during a period of 5 to 6 days under optimal conditions. Humic substances show a maximum degradation rate of 18 %. Only small parts of the humic building blocks and low molecular weight acids were degradable during soil passage under the tested conditions. The fraction of neutrals remained nearly constant under all conditions. This might indicate a balanced equilibrium between degradation and formation of these substances.

AOI: Additionally, the fate of AOI was investigated in the short retention column system. Figure 109 shows the results. Because of slightly different spiking concentrations in the oxic and anoxic influent the results are classified into columns with oxic influent and columns with anoxic influent.
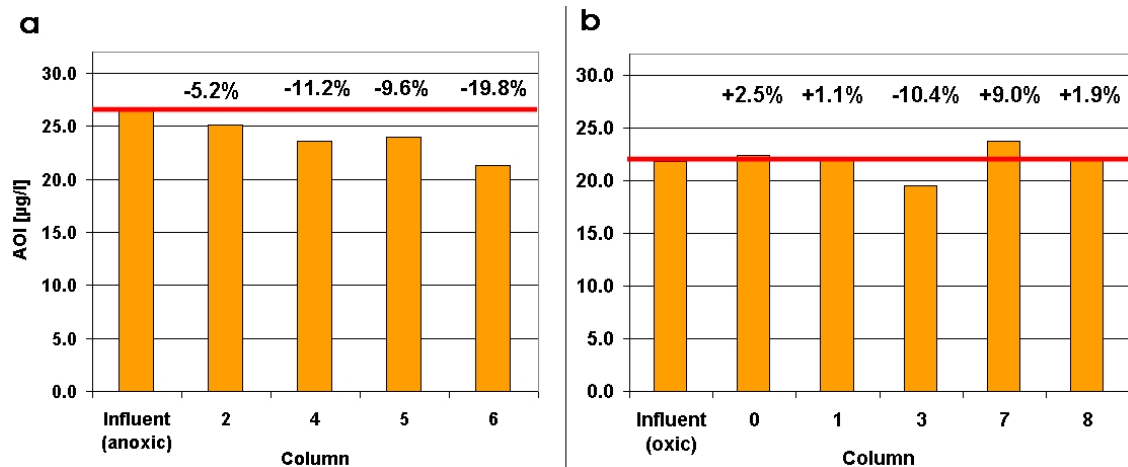
Figure 109 Fate of AOI under different redox conditions (a. anoxic influent/ b. oxic influent; n=6)

It was evident that the mineralization of AOI is more efficient under reducing conditions. Columns with oxic infiltration did not achieve considerable removal rates (*column 0, 1, 8*). Under anoxic conditions (*column 2, 4, 5*) between 5% and 11% of the AOI was mineralized. The highest removal rates were found for anaerobic columns. *Column 3* with an oxic influent but dominant anaerobic conditions achieved a removal rate of 10.4% and was only outperformed by *column 6*, which mineralized 20% of the initial AOI within 6 days of infiltration.

Table 26 Removal rates of AOI in short retention columns (sorted by dominant redox condition)

Oxic removal [%]	
Effluent 1	-1.06
Effluent 8	-1.90
Average oxic degradation	**-1.48**
Anoxic removal [%]	
Effluent 2	5.17
Effluent 4	11.23
Effluent 5	9.64
Average anoxic degradation	**8.68**
Anaerobic removal [%]	
Effluent 3	10.41
Effluent 6	19.78
Average anaerobic degradation	**15.10**

These results confirm the field results and the findings of the long retention column system. The reasons for the increase of AOI-concentration in *column 7* remained unclear. Since additional AOI might derive from AOI formation or AOI leaching from the sediment, the results are not included in the overall evaluation. Table 26 provides a summary of the removal rates and a calculation of the average removal rates. It is evident that the AOI-mineralization increases with decreasing redox potentials.

Trace compounds: The spiked trace organic compounds behave differently in the columns. Figure 110 illustrates the degradation performance of the individual columns. The spiking concentrations were 25 µg/l for Iopromide and 6.25 µg/l for Sulfamethoxazole and the NDSA-isomers. Figure 110 shows the measured concentration in the influent to the columns and the effluent concentrations.

In the abiotic *column 0* a slight decrease in the Iopromide concentration was observed, but the concentrations of the other trace compounds are nearly unchanged. Therefore, it can be concluded that adsorption does not play an important role in the short retention columns. Towards the end of the long term experiment some removal of 1,7- and 2,7-NDSA was observed. Together with the observed oxygen consumption in this column the results point toward a slowly growing azide-resistant biomass in *column 0*.
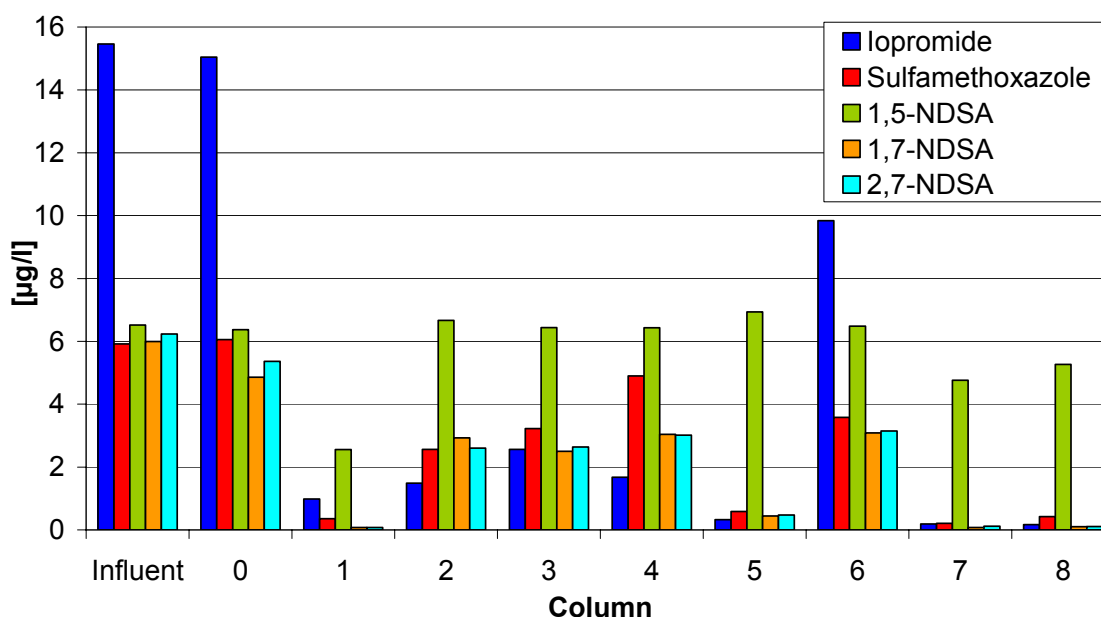
Figure 110 Trace organic compound concentrations in the effluent of the short columns (n=7)

In all technical sand columns (0-6) the 1,5-NDSA-isomer was observed to be very persistent. Only in *column 1* a removal of ~50% of the compound was observed. This removal was above average, since in the long retention columns and at the field sites the removal was considerably lower. The high removal might be ascribed to the higher temperature. The short retention columns were stored in the basement of the DWQC at 19°C ±3°C.

The other trace compounds are most efficiently removed during oxic infiltration in *column 1*. Similar results can be observed after anoxic infiltration with the double retention time. After 6 days retention time (*column 2*) the removal is not as efficient as in *column 1*, but after additional six days of infiltration under anoxic conditions (*column 5*) the results are comparable to those of *column 1*. For the X-ray contrast agent Iopromide the final concentration is even lower than in *column 1*.

An inefficient removal of all compounds could be monitored in the columns, where most of the infiltration took place under anaerobic conditions (*column 3* and *6*). Furthermore, it was found that enhanced denitrification by adding nitrate is not necessarily beneficial for the removal of these trace compounds (*column 4*).

The best results were achieved with the original sediment in *column 7* and *8*. These results were probably due to the strong microbial activity in these columns. Adsorption onto the organic part of the soil matrix is not very likely because of the high polarity of the compounds.

Overall, the results confirmed the findings of the other experiments that oxic conditions are preferable for trace compound removal. The AOI results show that Iopromide is only metabolized under oxic conditions. AOI mineralization can only be achieved under

anoxic/anaerobic conditions, whereas the efficiency increases with lower redox potentials. Similar to the results of the long retention columns the preferential removal of Sulfamethoxazole under anaerobic conditions, which is reported in literature, could not be reproduced. But since this anaerobic removal of Sulfamethoxazole was observed at the field site Wannsee, it is believed that the processes in the soil columns differ from the degradation pathways in the field. The reasons are most probably the different temperature and different concentration levels. This question is addressed more detailed in the discussion of the results of the long retention columns.

Operational period 2 (Influence of trace compound concentration):
Operational period 2 was conducted to test the influence of the trace pollutant concentration on the removal efficiency. The spiking concentration was varied, whereas all other conditions remained constant. The test simulated groundwater recharge or bank filtration at field sites with a different trace pollutant load or at one field site with a surface water of changing quality. It was of interest to confirm the achievable removal rates of the investigated trace compounds for different initial concentrations. To obtain relevant information the trace pollutant spiking was reduced first to ½ and afterwards to ⅛ of the initial spiking concentration.

Since all bulk organic parameters were held constant and the changing trace pollutant concentration did not affect the removal of the bulk organics, an evaluation of the bulk parameters was not included in the final report. The fate of the bulk organics complied with the evaluation of the data in operational period 1.

AOI: Effluent concentrations of AOI of the different experiments were hard to interpret. Since the measured AOI consisted of surface water AOI and spiked Iopromide, the changed spiking level only reduced one fraction of the overall AOI. Furthermore, the inaccuracies of the method constricted a detailed data evaluation because the changes in AOI concentration during soil passage were very small. To assess the information, the effluents of oxic, anoxic and anaerobic columns were pooled. Afterwards, mean values of the effluent concentration of each experiment were calculated, in order to give a general statement. Table 27 shows the calculated degradation rates. The results reveal that there is no significant influence of the spiking concentration on the degradation of AOI. Under all redox conditions no general trend towards lower or higher removal rates was observed. Considering the error of measurement even the variations in the oxic removal rates are not very clear. The results only confirm the redox dependency of AOI mineralization.

Table 27 Influence of spiking concentration on AOI-mineralization

Variation of the spiking concentration	100% [1/1]	50% [1/2]	12.25% [1/8]
Average oxic degradation [%]	-1.5	4.3	-5.8
Average anoxic degradation [%]	8.7	6.6	8.6
Average anaerobic degradation [%]	15.1	14.0	16.5

The limited results were also due to fluctuations of the AOI-level in Lake Tegel surface water. A comparison with degradation rates from field experiments show that the field results (60 - 65% for anoxic infiltration and 30 - 35% for oxic infiltration) deviate clearly from the results of these column experiments. This can be attributed to longer retention times in the field experiments. Altogether, the spiking concentration of the trace organics does not seem to have an influence on the decrease of the AOI-concentration.

Trace organics: During variation of the spiking concentration the efficiency of the trace compound removal was quantified for each of the adjusted pollution levels. Each data point is the median of at least two sampling events (LT 1/1 => n=7) and each sample was run as duplicate.

Figure 111 presents the results of the Iopromide monitoring. It was found that the Iopromide removal was not dependent from the initial concentration of Iopromide. In all columns, with the exception of *column 6*, the removal rates ranged between 80% and 100%. In *column 6* the results of the last trace compound level could not be quantified. Although the removal rates of *column 6* were considerably lower (~40%), in general no influence of the varied spiking concentration was observed. These results on the redox dependency of the metabolization of Iopromide were already confirmed in the experiments during operational period 1.

Focusing on the varied spiking concentration, the results of operational period 2 strengthened the theory that Iopromide is metabolized cometabolically. In this case the unspecified biomass responsible for Iopromide metabolization depends not exclusively on Iopromide as organic carbon source, but mineralizes also other carbon from the BDOC pool. Since the BDOC concentration remained stable, the resources for the respective biomass did not change. This fact resulted in stable removal rates for Iopromide independent from the spiking concentrations. A threshold-concentration, which would point towards a metabolic mineralization of Iopromide, was not found.
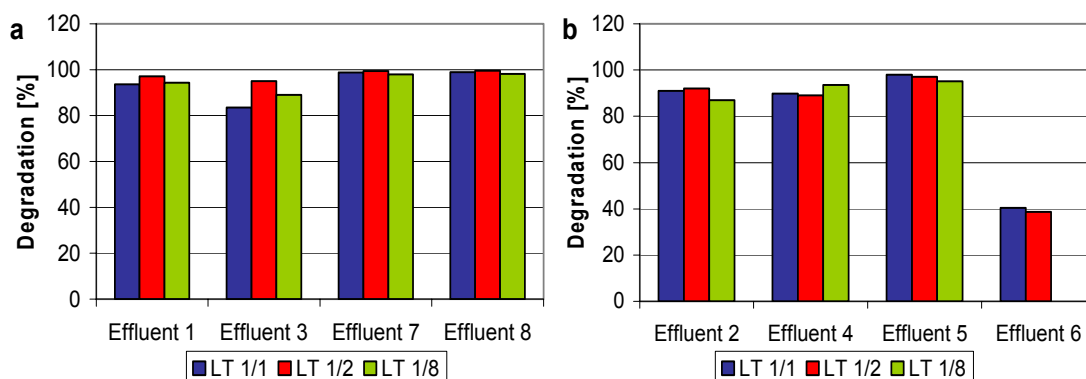
Figure 111 Iopromide degradation in the columns with oxic influent (a) and anoxic influent (b)

The results for the antibiotic Sulfamethoxazole are presented in Figure 112. It was found that the Sulfamethoxazole removal was dependent from the spiking concentration. In most columns the removal efficiency decreased when the initial concentration level was reduced (*Column 1, 2, 5, 7* and *8*). In *column 3, 4* and *6* the trend was not clear. However, the reduction of the removal efficiency at lower spiking concentrations points towards a metabolic mineralization process for Sulfamethoxazole. With decreasing concentration the specialized biomass, responsible for the removal of the antibiotic, does not receive sufficient organic carbon as electron donor. Therefore, the specialized biomass is reduced. If the initial concentration under-runs a so called threshold concentration, the enzymes necessary for Sulfamethoxazole mineralization are not induced any more and the Sulfamethoxazole removal stops. This leads in experiments with decreasing influent concentration to reduced removal efficiencies since these are calculated on percentage basis incorporating the influent and the effluent concentration. In *columns 2, 5, 7* and *8* the decrease in removal efficiency between LT 1/2 and LT 1/8 is above average, which could be interpreted as an approach to an eventual threshold concentration.
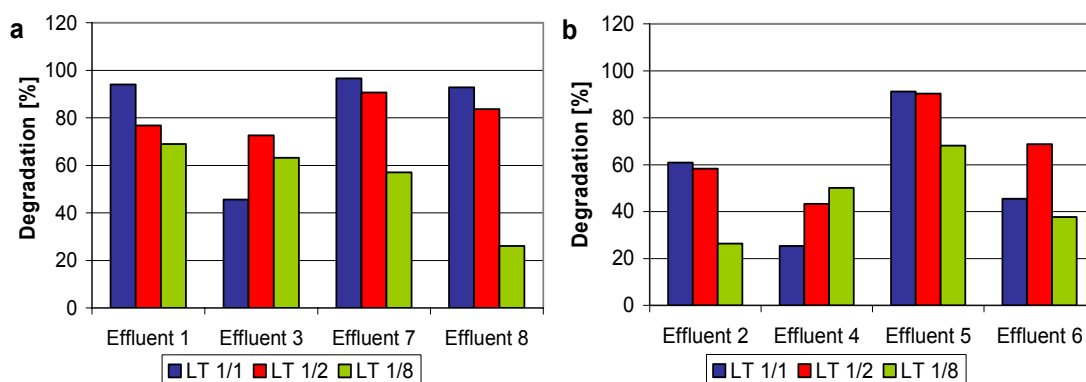
Figure 112 Sulfamethoxazole removal in the columns with oxic influent (a) and anoxic influent (b)

However, the spiking concentration at the lowest level (~780 ng/l) was approximately twice as high as the average concentration in Lake Tegel. This probably explains the overall higher removal rates in the short retention columns. At the artificial recharge site in Tegel the Sulfamethoxazole removal within 50 days of infiltration was 55%.

The monitoring of the NDSA-isomers indicated in some columns higher removal rates in experiments with low initial concentrations. All columns, except the columns with natural sediment filling, showed these tendencies for the degradable NDSA-isomers. In *columns 2, 3, 4* and *6* an increase of 10% to 30% of the degradation rate was observed in "low-spiking"-experiments. In *column 4* the NDSA-removal did not increase until the spiking concentration was reduced to 1/8.

However, this observed improved removal with decreasing initial concentration is contradictory to the expected behavior and the theory of threshold-concentrations. An explanation would be the adaptation of the biomass of the columns to NDSA removal. In case of a decrease of the NDSA concentration, the potential for NDSA removal would remain constant, if the biomass does not exclusively feed on NDSA. A constant removal potential combined with lower initial concentration would lead to increased proportional removal rate. The results might indicate, that the enzymes necessary for NDSA mineralization are present in average biomass (constitutive enzyme) and do not need to be induced.
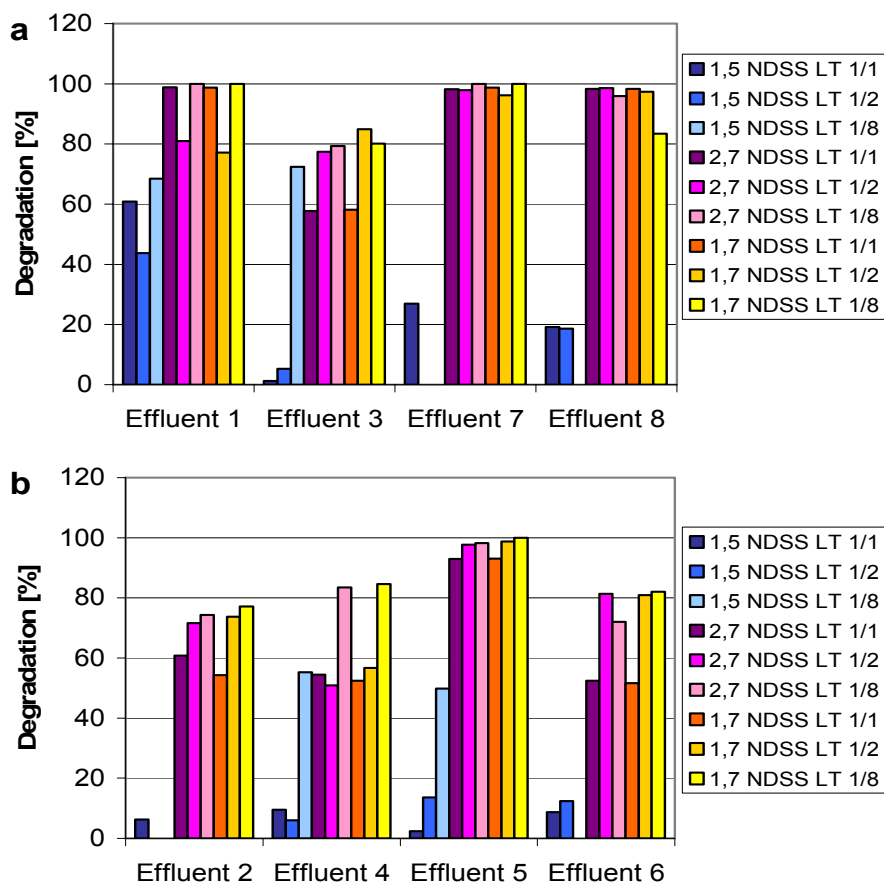
Figure 113 NDSA-removal in the columns with oxic influent (a) and anoxic influent (b)

However, the results of operational period 2 supplement the results of operational period 1. But the results are difficult to generalize, because of the special conditions in the columns. Altogether, these findings are a first approach to the topic. More detailed experiments towards the objectives of identifying the influencing parameters of trace compound removal are necessary.

Operational period 3 (Influence of BDOC-concentration):

Operational period 3 was designed to assess the influence of the initial BDOC concentration on the removal efficiencies for bulk and trace organic compounds. To obtain relevant information the BDOC content of the influent was varied, whereas the trace compound spiking remained stable. Water from Lake Tegel and production well 13 was used to mix the different influents. The DOC-concentration of Lake Tegel water was relatively constant during the experiments. Therefore, the different experiments were comparable. The average DOC-concentration was 6.8 mg/l with a standard deviation of 0.2 mg/l. Influent concentrations were about 6.0 mg/l. The difference between these two values can be explained with BDOC degradation during the storage of the water. Infiltration under optimal aerobic conditions over 30 days in the long retention columns proved that the residual DOC fraction was 3.8 mg/l in Lake Tegel

water. This was defined as non-biodegradable DOC (NBDOC) and used for the calculations of the BDOC-fractions and the BDOC degradation rates. Moreover, it was assumed, that water from production well 13, which was used for the dilution of Lake Tegel water, did not contain any BDOC.

Bulk organics: Figure 114 shows the percentages of degraded BDOC during infiltration classified into columns with oxic and anoxic influent. Unfortunately, the last part of the experiment, using a 25:75 (Lake Tegel : Well 13) mixture could not be evaluated, because the BDOC-concentrations were too low. The differences between influent and effluent and among the effluents were within the accuracy of the DOC-quantification method.
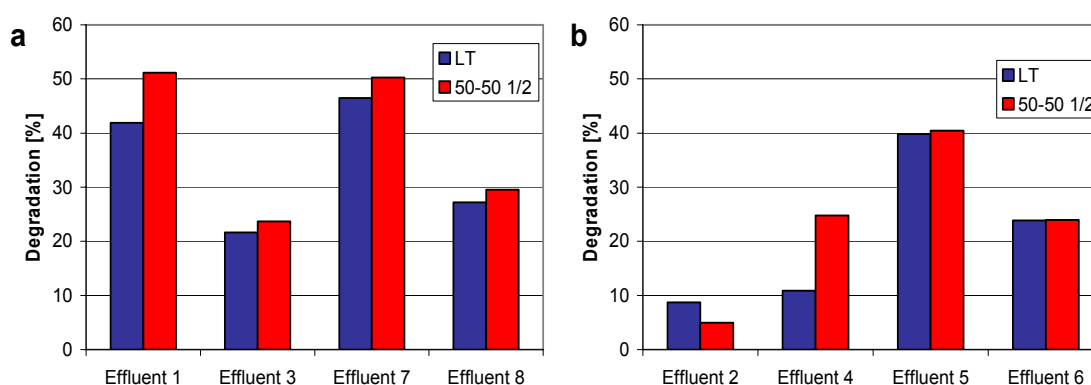
Figure 114 BDOC-degradation in the columns with oxic influent (a) and anoxic influent (b)

The results presented in Figure 114 confirm the results of operational period 1 (Figure 105). It was proved that the average BDOC degradation was higher under oxic conditions. A comparison of *column 1* and *column 2* shows, that the rate of degradation was also faster under oxic conditions. BDOC degradation under different redox conditions showed no significant dependency from the varying influent BDOC-concentrations. Despite of the reduction of available BDOC to one half, the same percentage of the initial BDOC was mineralized. It was concluded, that different BDOC concentrations do not have a fundamental influence on the conversion of BDOC.

LC-OCD: The influence of the reduction of BDOC was monitored via LC-OCD. Thereby, it was found that the decrease of the BDOC of the influent affected all fractions of DOC. The fraction of the polysaccharides showed the most significant decrease. It was concluded, that a relevant part of the polysaccharides can be characterized as BDOC. A comparison of the evaluation of the LC-OCD diagrams and the results of the BDOC-removal proved the already mentioned findings concerning the efficiency of the columns under the tested redox conditions.

AOI: To evaluate the influence of varying BDOC on the AOI-removal, the columns were classified by the dominant redox condition. *Column 1* and *8* were selected as oxic columns, *column 2* and *4* as anoxic column and *column 3* and *6* as anaerobic column. *Column 7* was not considered, because of AOI-formation in the column (discussed earlier). *Column 5* was not included because of the doubled retention time.

Table 28 shows the average AOI removal. The removal rates for the influent with the highest BDOC-concentration (Lake Tegel surface water) were comparable to the mineralization rates assessed during operational period one. During minimization of BDOC by adding water from production well 13 to the influent, the removal rates for AOI partly changed. Under oxic conditions the AOI removal was under all conditions very low and the variations are within the accuracy of the method. In the anoxic columns 8-10% of the initial AOI was mineralized, independently from the BDOC concentration. Only under anaerobic conditions the mineralization rate decreased considerably from 21% to 11% when the BDOC-concentration was cut by 75%.

Table 28 Influence of BDOC-variation on AOI mineralization

Variation of the BDOC-concentration	Lake Tegel	50-50	25-75
Average oxic degradation [%]	-2.5	0.8	3.8
Average anoxic degradation [%]	7.9	9.8	9.7
Average anaerobic degradation [%]	20.7	14.0	11.3

It can be followed that the amount of available BDOC does not directly influence the AOI mineralization under oxic and anoxic conditions. Under anaerobic conditions an influence was found and quantified. A decrease of AOI mineralization was observed when less BDOC was available.

Overall, the BDOC additionally affects the AOI removal, because of its importance for the development of the dominant redox conditions. High BDOC levels are favorable for AOI removal, because mineralization of BDOC leads to more reducing conditions. This effect was not investigated in this study.

Trace organics: The analytical program of the BDOC-variation test was completed by a monitoring of the trace compounds. The efficiency of the trace compound removal was quantified for each of the BDOC-levels. Since the columns represent different redox conditions, it was possible to assess the BDOC-dependency for each of the represented conditions. For some compounds the BDOC-concentration of the influent had an impact on the removal. Prior to the data evaluation the following theoretical considerations were summarized.

Scenarios:

1. If the trace organic removal remains constant during BDOC-reduction this would indicate an independent biomass, responsible for the pollutant removal. The specialized microorganisms are not influenced by the BDOC level, since the concentration of the pollutant (main energy source) does not change. This scenario would indicate a metabolic mineralization by specialized bacteria strains.

2. A decrease of the trace organic removal with BDOC-reduction would point toward a cometabolic mineralization of the trace compounds. In this case it can be assumed that the trace compounds are mineralized within the course of general BDOC-removal. In case of lower BDOC-concentrations the density of unspecialized biomass would decrease, reducing the amount of exo-enzymes and therewith the trace organic removal.

3. An increase of trace organic removal with BDOC-reduction could be explained by a modification of the present biomass. Since the BDOC-concentration decreases, parts of the biomass could induce enzymes that are necessary for the trace compound removal. When the easier degradable BDOC is not available, the focus shifts to more complex carbon structures. This could result in an increasing pollutant removal.

However, the evaluation of the data was found to be very complicated. The trace compound removal was tested for each BDOC-influent concentration and then compared. Figure 115 shows the behavior of Iopromide under different conditions. An evaluation of the sample •Column 6 / 25:75• was not possible and the missing column in the diagram does not indicate a removal of 0%. The removal rates of all samples are between 90% and 100%, with the exception of *column 3* and *6*. The lower removal rates in these columns are most probably caused by the anaerobic conditions in parts of the columns. It is known that mineralization of organic carbon is considerably slower under anaerobic conditions, but on the other side anaerobic conditions are favorable for dehalogenation. All experiments pointed clearly towards a metabolization as the dominant removal process for Iopromide. A comparison of AOI and Iopromide behavior proved this in all soil column experiments. The lower removal rate under anaerobic conditions proposes that the metabolization is an oxic process. Under anaerobic conditions this process was not as efficient. Furthermore, parts of the Iopromide are possibly dehalogenated during the short retention time.
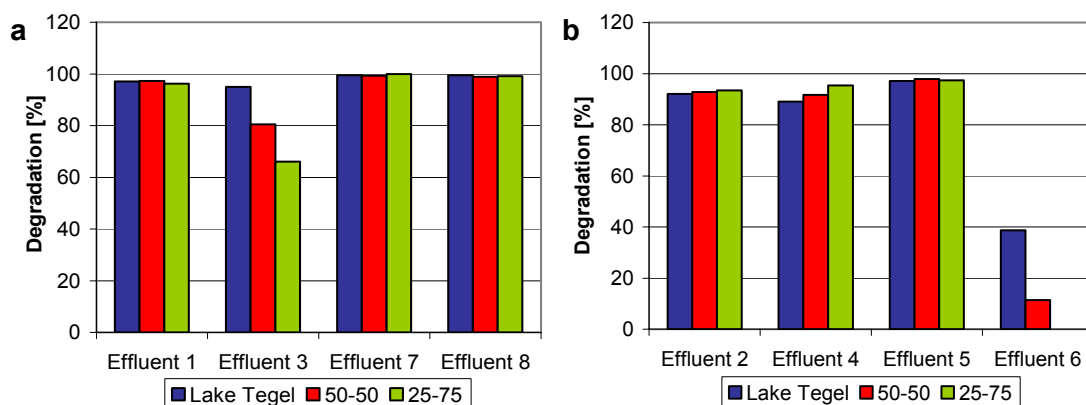
Figure 115 Iopromide degradation in the columns with oxic influent (a) and anoxic influent (b)

The decreasing BDOC-concentration has no influence on the Iopromide metabolization rates under oxic and anoxic conditions. Only in *column 3* and *6*, under anaerobic conditions, the Iopromide removal decreases with lower BDOC-concentrations. This indicates a cometabolic removal mechanism for Iopromide under anaerobic conditions. In oxic or anoxic conditions the decreasing BDOC did not show any effect. This might be explained by the fact that the reduction of BDOC from 2.2 mg/l to 0.6 mg/l did not affect the BDOC degrading biomass strong enough to reduce the metabolization of Iopromide. Since Iopromide is a huge molecule with several aliphatic side chains, a metabolization is a simple process. The biomass is obviously able to metabolize Iopromide under these conditions.

Overall, the Iopromide removal rates are consistent with field data and prove that Iopromide is not persistent during soil passage. But the persistence of the unknown metabolites formed from the Iopromide molecule is indefinite and was not investigated in detail in this project. The results of the AOI measurements propose a high stability of the Iopromide metabolites under oxic conditions.

The results of the comparison of the NDSA are presented in Figure 116. Since the 1,5-NDSA is very persistent, in some cases the effluent concentration was higher than the influent concentration. These negative removal rates, caused by measurement mistakes, were set to zero. Because of the completely different degradation characteristics of the 1,5-isomer and 1,7-and 2,7-NDSA, the isomers are evaluated separately.

The 1,7-and 2,7-NDSA isomer were found to be biodegradable in preceding experiments. In the experiments with varying BDOC-concentrations the removal rates were found to be in a range of 50-100% (Figure 116).

The highest removal rates (90-100%) were achieved in the columns with natural sediments from the field sites. In these columns no dependency of the NDSA-removal from the initial BDOC-level was found. Furthermore, the oxic *column 1* and *column 5* provided an efficient elimination of the 1,7- and 2,7-NDSA.

In the *columns 1, 2* and *4* the removal rates increased with lower BDOC-levels. This would point towards a situation as described in scenario 3. The decreasing BDOC-concentrations could force the active biomass to use alternative organic carbon sources. Within this process the biomass induces enzymes that are necessary for the NDSA-removal. This could explain the more efficient 1,7- and 2,7-NDSA removal under low BDOC conditions.

The anaerobic *columns 3* and *6* did not show a significant trend with changing BDOC concentrations. The removal rates were below average, most probably due to unfavorable redox conditions.
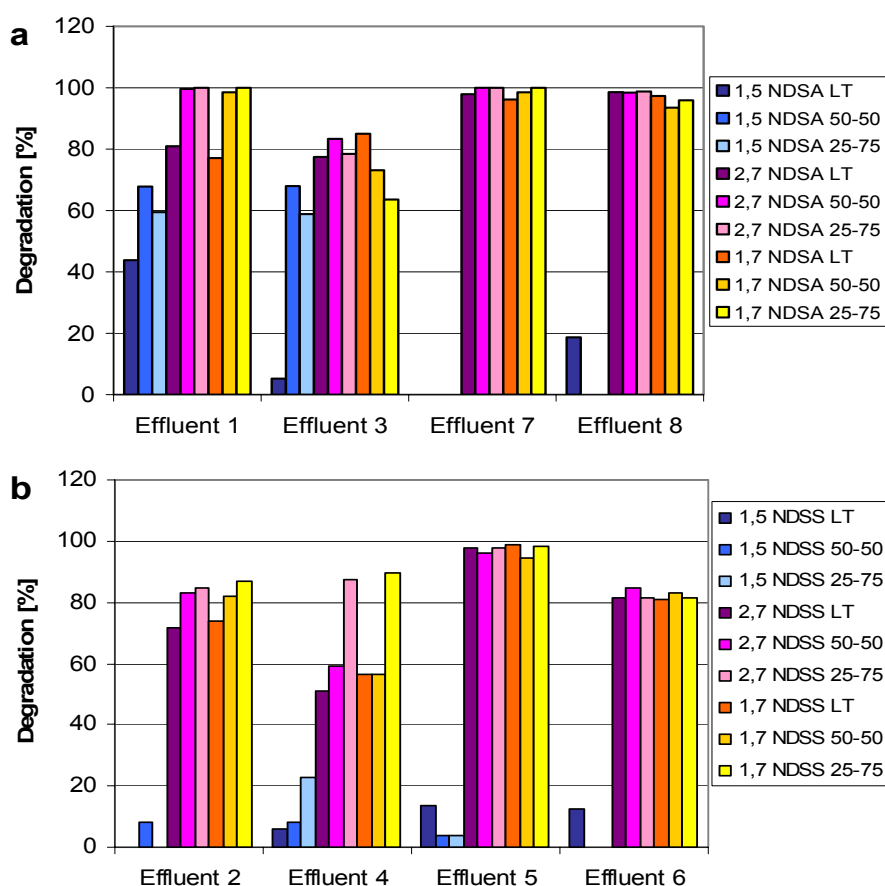
Figure 116 NDSA-degradation in the columns with oxic influent (a) and anoxic influent (b)

The 1,5-NDSA isomer was found to be considerably more persistent than the other investigated isomers. In most columns no removal of this compound was observed. A maximum of 20% mineralization was found in *column 2, 4, 5, 6, 7* and *8.* The results of *column 1* and *3* are contrary to the results of the field monitoring and the long retention columns. These experiments showed that the 1,5-NDSA is slightly better degradable under oxic conditions, but removal rates did not exceed 20% of the initial concentration. The only explanation might be the higher water temperature in the short retention columns.

However, in comparison to all other results of the project the NDSA-removal rates were found to be very high in the short retention columns. Under some redox conditions an influence of the BDOC concentration on the NDSA removal was found.

Unfortunately, an evaluation of the results of the Sulfamethoxazole screening was not possible, because a dilution mistake during the preparation of the stock solution lead to concentrations below the limit of quantification.

1.4.3 Temperature controlled soil column system (TU Berlin)

To assess the influence of different temperature on the degradation properties and kinetics of bulk and trace organic compounds an additional soil column system was installed at TU Berlin. The results of the investigations are mainly based on the project work of Uwe Huebner at the DWQC at TU Berlin.

The results of the field monitoring, especially the long term temperature monitoring by automatic probes revealed strong temperature variations along the flow path at bank filtration sites. Of even greater importance was the temperature variation at the artificial groundwater recharge site in Tegel. The measured temperature differences between summer and winter state in the last monitoring well in front of the production well were more than 20 K. At bank filtration field sites the temperature variation was lower due to longer retention times.

Figure 117 Picture of the set-up used for the investigations of temperature influence

However, since it is known for long that biological degradation processes are temperature dependent it was of interest to quantify this effect. For the objective of the project it was of special interest because the temperature variations occur naturally every year and have significant influence on the raw water quality of the abstracted water. This is most important for the GWR facility.

The objective of this part of the project work was investigating the temperature effect qualitatively and quantitatively. Furthermore, the degradation of the organic compounds

at different temperatures was modeled using different approaches for bulk and trace organic compounds.

1.4.3.1 Set-up

The temperature controlled soil column system was installed to simulate conditions of artificial recharge facility in Berlin-Tegel at different times of the year using a soil column system. The set-up of the system is depicted in Figure 118. Three plexiglas columns with a length of 0.5 m and a diameter of 14 cm were operated with surface water from Lake Tegel at different temperatures. Two columns were cooled in standard fridges at 5°C and 15°C. The third column was stored in a small incubator at constant 25°C. The columns were operated against gravity. To achieve constant concentrations of the investigated trace compounds an online-spiking system was installed. The spiking concentrations were selected to be similar to the spiking of the long retention soil column system (Table 13). Additionally to the sampling ports for column influent and effluent, three sampling opportunities along the columns at 5 cm, 18 cm and 30 cm were included. Each sampling point was combined with an optical oxygen probe.
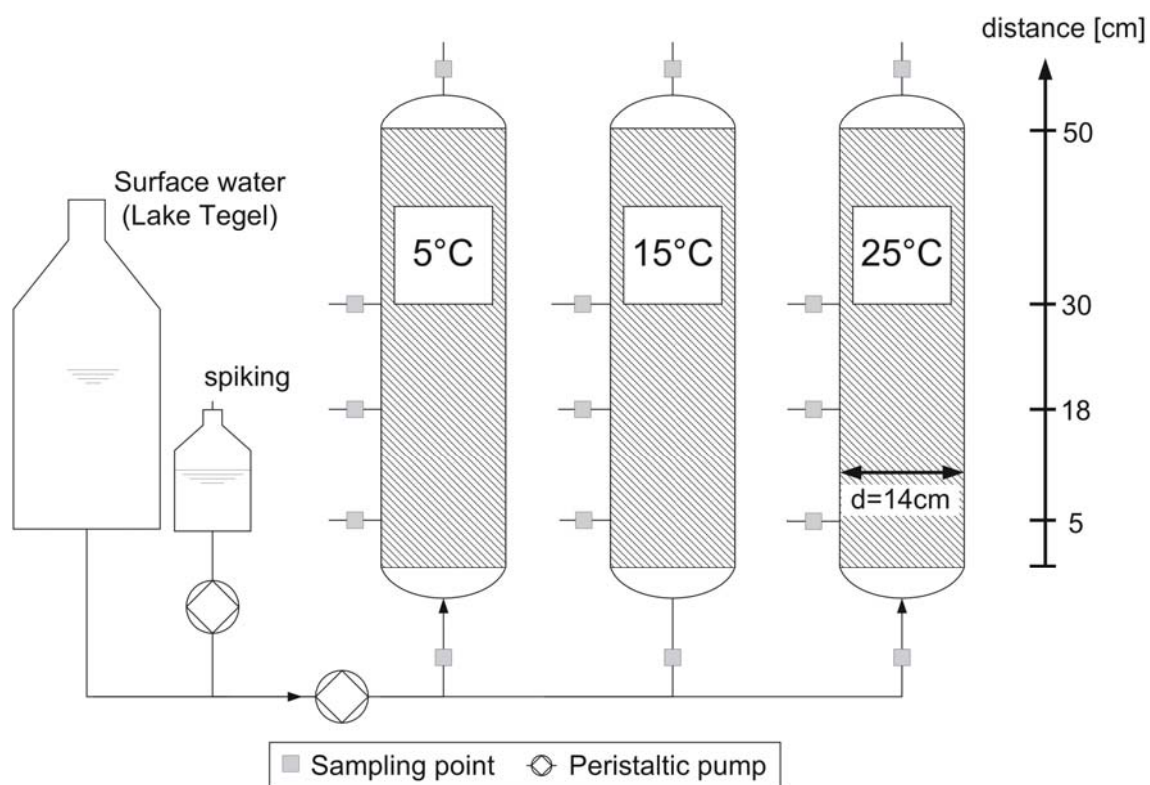
Figure 118 Schematic set-up of the temperature controlled soil column system

The time period which was assigned for adaptation was two months under room temperature and subsequently three months under operating conditions. Afterwards the monitoring proved an intact biomass in all columns and the experiments started.

To guarantee stable conditions the temperature was measured regularly and adjusted if necessary. All characteristics of soil columns are presented in Table 29.

Table 29 Operating conditions for the temperature controlled soil column system

	5°C	15°C	25°C	n
Temperature [°C]	5.9 +/-0.8	15.0 +/-0.7	25.0 +/-0.5	37
Flow [ml/column*d]	439 +/-18	452 +/-25	458 +/-24	14
Retention time [d]	6.3			
Pore velocity [cm/d]	8.3			

The columns were filled with industrial sand (0.7-1.2 mm) which was used already for the short retention soil columns. The characteristics of the sand are described more detailed in chapter 1.4.2.1. Because no fine sand fractions were used for the column filling and the surface of silica sand is particularly negative charged no significant sorption affects were expected.

As mentioned, the column system was operated with water from Lake Tegel, which was filtered with a micro filter to avoid an entry of coarse POC. Before the water entered the columns trace compounds were spiked by a peristaltic pump system. The concentration levels were: X-ray contrast media Iopromide (10 µg/l), antibiotic Sulfamethoxazole (2.5 µg/l) and each isomer of naphthalenedisulfonic acid (2.5 µg/l). Table 30 shows medians and standard deviations of characteristic parameters measured in column influent. Investigations were conducted in winter/spring with high oxygen concentrations in Lake Tegel.

Table 30 Characterization of the surface water used as influent

	Unit	Median	Standard deviation	n
pH-value	-	7.96	0.25	8
Oxygen	[mg/l]	11.12	0.49	29
Nitrate	[mg/l]	2.5	0.31	9
DOC	[mg/l]	7.32	0.43	10
UVA$_{254}$	[m^{-1}]	15.74	0.34	10
SUVA	[l/mg*m]	2.15	0.16	10

To achieve a better picture of the redox situation, the electron acceptors oxygen and nitrate were measured. A direct measurement of redox potentials was not conducted because the columns were completely oxic and the redox potential was similar at the start and the end of the columns.

Results of oxygen measurement are presented in Figure 119. High standard deviation of oxygen results at 25°C is related to comparably high values in the beginning of analysis. In all columns a significant oxygen demand was observed, whereas at higher temperatures more oxygen was consumed. This is consistent with the results of the DOC analysis. A removal of nitrate during infiltration was not observed.

Figure 119 Oxygen concentration in the influent and the three different effluents

Table 31 shows the monitoring schedule of the first part of the experiment, where the pore velocity was adjusted to 8.3 cm/d and the retention time was 6.3 days. To analyze bulk organics and trace organics ten samples were taken on a weekly basis from the influent and the effluent of each column. At the sampling ports along the column the trace compounds were only analyzed three times.

Table 31 Monitoring schedule of the first part of the experiments at the column system (01-04.2005)

		17.1.	24.1.	31.1.	7.2.	21.2.	28.2.	14.3.	28.3.	11.4.	27.4.
Influent and Effluent	pH	x				x	x	x	x	x	x
	DOC	x	x	x	x	x	x	x	x	x	x
	UVA	x	x	x	x	x	x	x	x	x	x
	LC-OCD	x	x	x	x	x	x	x	x	x	x
	AOI	x	x	x	x	x	x	x	x	x	x
	HPLC-MS/MS	x	x	x	x	x	x	x	x	x	x
	HPLC-FLD	x	x	x	x	x	x	x	x	x	x
	FIA		x	x	x	x	x	x	x	x	x
Sampling ports at 5, 18 and 30 cm	pH	x				x	x	x	x	x	x
	DOC	x	x	x	x	x	x	x	x	x	x
	UVA	x	x	x	x	x	x	x	x	x	x
	LC-OCD	x	x	x	x	x	x	x	x	x	x
	HPLC-MS/MS							x		x	x
	HPLC-FLD						x		x		x
	FIA		x	x	x	x	x	x	x	x	x

Some trace compounds were removed that efficient that the data pool for the description of the degradation kinetics was not sufficient. Therefore, in an additional operating period with shorter retention times was started after the first part of the investigations was finished. The second experiment consisted of four weeks adaptation period and subsequently three sampling events in a time interval of two weeks. The experiments at the temperature controlled soil columns ended in July 2005.

1.4.3.2 Results

DOC and SAK$_{254}$

After an adaptation period of 4 months the column system was operated under a close monitoring schedule for the time period of six months. A sampling of the reservoir and the column effluents was performed on a weekly basis. The results of DOC and SAK$_{254}$–measurements are shown in Figure 120 and Figure 121 as medians from ten different measurements. Additionally, the standard deviations, which are mainly due to variations of the surface water quality, are depicted in the diagrams and provide a good impression on the stability of the results. Table 32 explains the dependency between distance and retention time in the columns.
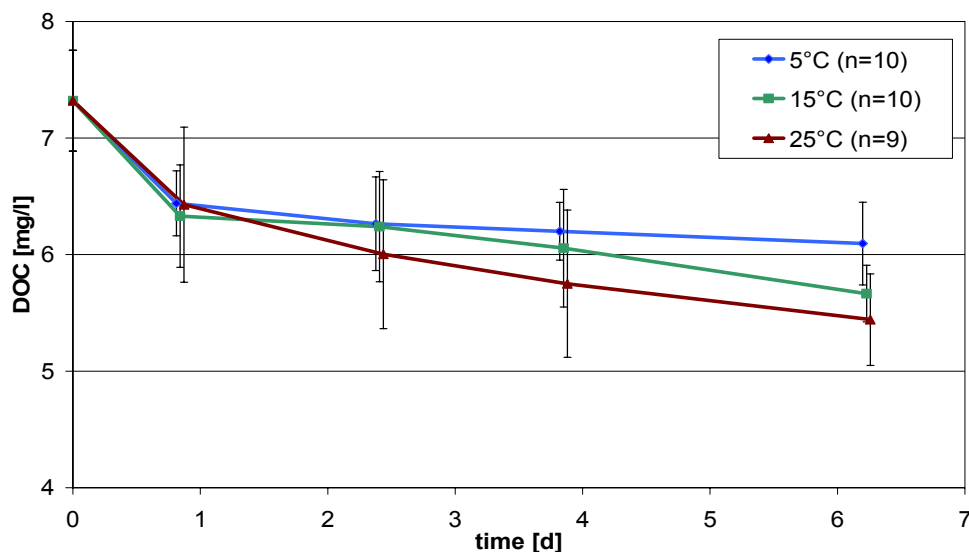
Figure 120 Degradation of DOC along the columns

The DOC-measurements show a fast mineralization of organic carbon in the first few centimeters of the columns, which does not seem to be dependent from temperature. All columns were found to perform similar efficient during the initial infiltration phase. The removal of UV-active organic compounds was also most efficient in the first part of the infiltration. Similar to the results of the DOC analysis no dependencies from temperature were observed. The fast removal can be explained by a mineralization of

easy degradable portions of DOC, which are instantly available for biological degradation. The results indicate that the temperature has no significant influence on the DOC-mineralization in the instant infiltration zone.
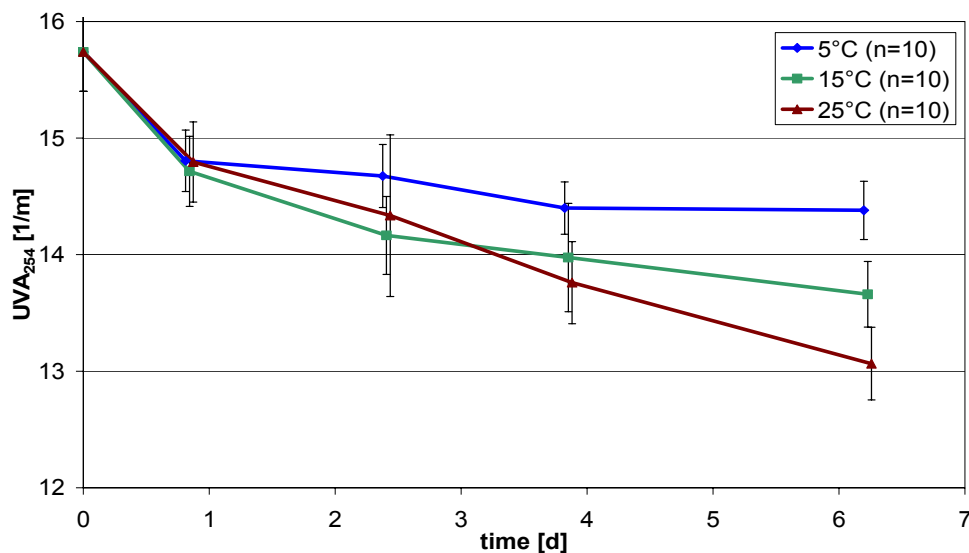
Figure 121 Fate of UVA$_{254}$ along the columns

Along the further infiltration path an influence of the different temperature on the bioactivity was clearly visible. The results of the DOC-analysis and UVA$_{254}$ show consistently that the removal of organic substances is more efficient at higher temperatures. Further degradation of organics in deeper parts of the filter beds is enhanced in the columns with higher temperatures, leading to higher removal rates for DOC and UVA$_{254}$.

Despite of similar trends for DOC and UVA, the more precise analytical method for UVA$_{254}$-measurements provide a clearer picture of the temperature dependency of the bulk organic degradation (Figure 121). The standard deviations of the UVA data pool is lower than for the DOC data pool, showing that differences in the fate of DOC under different temperatures is statistically relevant. The DOC measurements were problematic, since the concentration differences were low and sometime in the range of the accuracy of the quantification method. However, a significant increase of mineralization potential of bulk organic compounds with increasing temperature could be shown. But the temperature effect was of greater importance in the deeper parts of the infiltration path. During initial infiltration no significant effect of temperature was observed.

Table 32 Retention time at the different sampling points along the columns

Distance [cm]	5	18	30	50
Retention time [d]	0.8	2.4	3.9	6.3

A summary of the bulk organic results is provided by Table 33, which shows all removal rates of the different columns. The BDOC removal was calculated assuming a non-degradable DOC-portion of Lake Tegel surface water of 3.8 mg/l. This was a result of a long term infiltration experiment at ~15°C in the long retention column system. Since the amount of BDOC might vary with the temperature, this calculation simplifies the problem and should be regarded as a trend.

At the end of the columns (after 50 cm / retention time: 6.3 d) 26% of the initial DOC and 53% of BDOC were removed at 25°C. In the same infiltration time and distance only 17% of DOC (35% BDOC) could be removed at 5°C. In all columns only a partly removal of BDOC was observed, so that longer retention times would most probably lead to higher removal rates.

Table 33 Degradation rates after 6.3 d (effluent)

	5°C	15°C	25°C
DOC	17%	23%	26%
BDOC	35%	47%	53%
SAK_{254}	9%	13%	17%

The fate of SUVA (ratio of medians from SAK_{254} and DOC) during infiltration along the different columns is shown in Figure 122. A strong increase of SUVA in the beginning of infiltration can be seen in all columns, which is due to the mineralization of aliphatic polysaccharides. In deeper infiltration beds no significant changes were measured. There microorganisms have to mineralize aromatic structures as well, leading to a balance in the ratio aromatic/aliphatic organic compounds. No significant temperature dependency of SUVA could be shown.
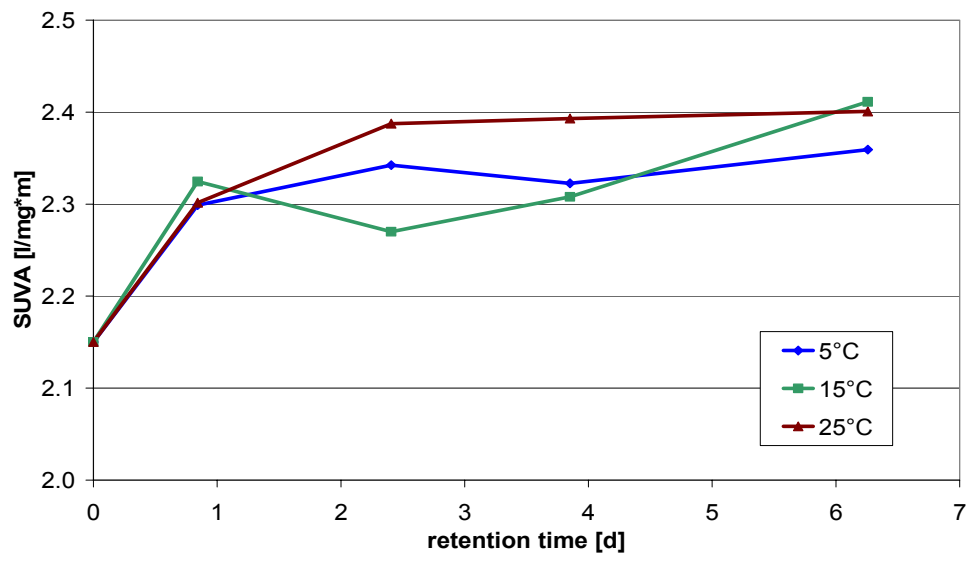
Figure 122 SUVA along the columns (median/ calculation from ten DOC and SAK measurements)

LC-OCD

To assess the fractions that were responsible for the observed changes in the bulk organic composition the LC-OCD technique was used to fractionate the DOC in five fractions. LC-OCD analysis was performed of every sample used for DOC measurement and the results are presented as averages from ten different chromatograms (Figure 123). The mediation of the chromatograms summarizes the obtained results into a presentable amount of data and allows to focus on the most important changes. Therefore, minor changes and single measurement mistakes are not misinterpreted.

Figure 123 shows the results of OC-detection after the fractionation by size exclusion chromatography. Comparing column effluents (Figure 123a) a good removal of polysaccharides at all temperatures was found. A nearly complete degradation of the PS-peak occurs at 15°C and 25°C. At 5°C about 75% of the polysaccharide-fraction was removed. At 25°C the polysaccharide removal accounts for ~16% of the total DOC removal.
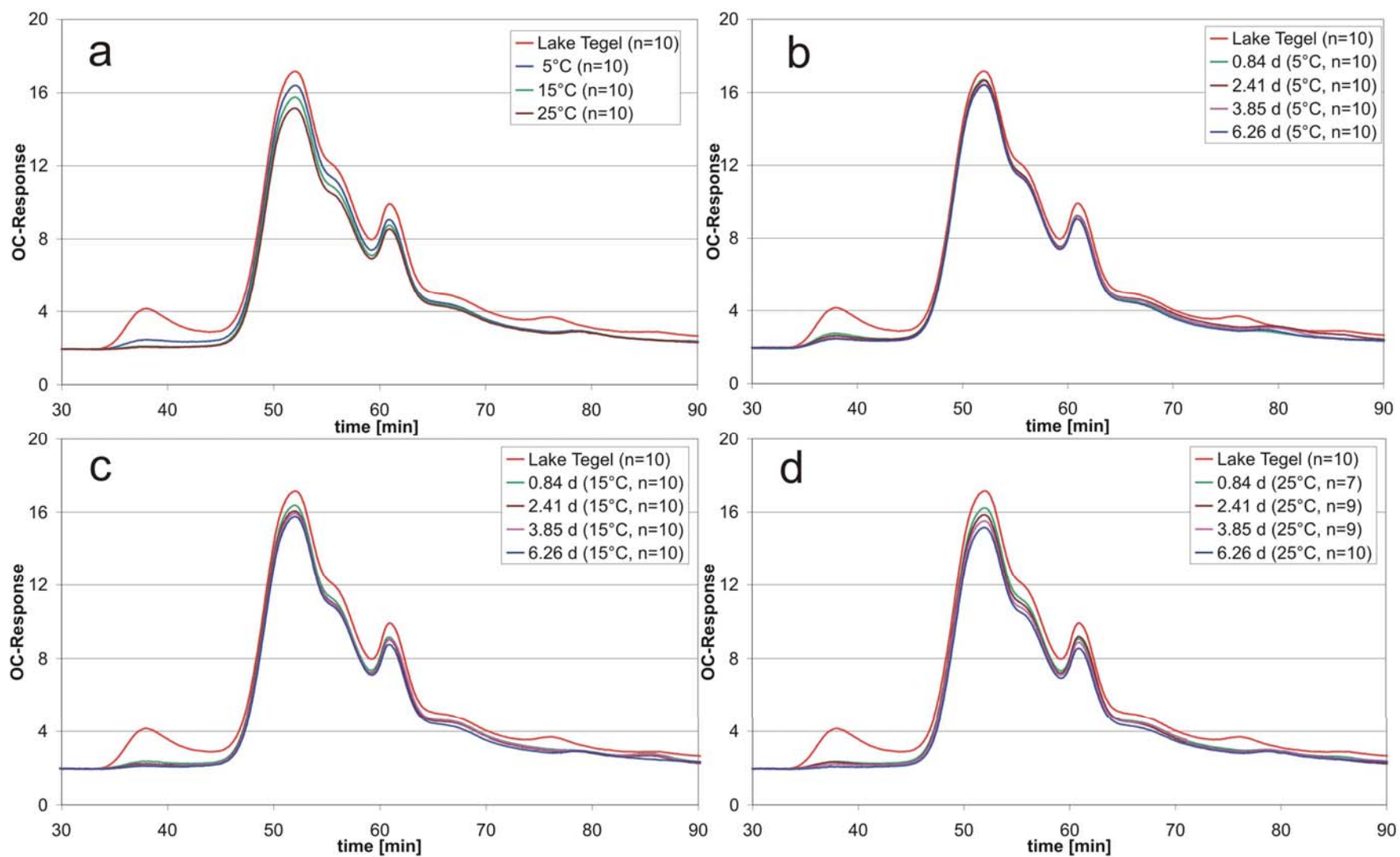
Figure 123 LC-OCD-chromatograms: a) column effluents; b) column at 5°C; c) column at 15°C; d) column at 25°C

For humics the degradation follows a definite temperature dependency. The degradation rates increase with higher temperatures. Whereas at 5°C only in the initial infiltration phase some removal of humic compounds was observed, the degradation of humics continues along the entire infiltration path at 25°C (Figure 123d). Overall, the maximum removal rate for humic substances during 6.3 d of infiltration is ~22% (in the 25°C column) accounting for 28% of the total DOC mineralization (Table 34).

No temperature dependency could be proved for the removal of humic building blocks, low molecular acids and neutrals. For buildings blocks and LMA no significant changes were observed, probably due to reformation during humic degradation. However, these fractions are not discussed more detailed, but Figure 123 shows that most changes in these fractions occurred during initial infiltration.

The measurements along the columns (Figure 123(b-d)) are consistent with the DOC results, showing the highest degradation rates at the beginning of infiltration. Especially degradation of aliphatic polysaccharides was very fast and mostly completed at the first sampling point at 5 cm. Humics were removed continuously at 25°C whereas at 5°C the removal rates decrease considerably after the first sampling point.

More detailed data provide the results presented in Table 34. The quantitative results are derived from an integration procedure for LC-OCD chromatograms, which was developed on the basis of the work of Huber (2001). The OC-response was used for quantification. Table 34 shows the results of integration.

Table 34 Results of LC-OCD integration

		Poly-saccharides		Humics		Building Blocks		Low molecular acids		Neutrals		DOC
		mg/l	%	mg/l	%	mg/l	%	mg/l	%	mg/l	%	mg/l
feed		0.45	6.1	3.57	48.7	1.55	21.2	0.24	3.2	1.52	20.7	7.32
5°C	0.84 d	0.17	2.8	3.28	52.4	1.51	24.1	0.21	3.4	1.08	17.3	6.44
	2.41 d	0.15	2.4	3.25	50.6	1.53	23.7	0.21	3.2	1.29	20.0	6.27
	3.85 d	0.12	1.9	3.19	51.6	1.51	24.5	0.21	3.4	1.15	18.6	6.2
	6.26 d	0.11	1.9	3.18	52.7	1.48	24.5	0.20	3.3	1.06	17.6	6.1
15°C	0.84 d	0.08	1.4	3.14	51.3	1.51	24.6	0.22	3.5	1.17	19.2	6.33
	2.41 d	0.05	0.8	3.07	52.1	1.47	25.0	0.21	3.6	1.09	18.4	6.24
	3.85 d	0.04	0.6	3.02	51.0	1.49	25.1	0.22	3.8	1.15	19.5	6.06
	6.26 d	0.02	0.3	2.95	52.2	1.46	25.9	0.20	3.5	1.02	18.1	5.67
25°C	0.84 d	0.09	1.4	3.08	51.0	1.53	25.3	0.21	3.5	1.13	18.8	6.43
	2.41 d	0.07	1.1	3.00	51.4	1.49	25.5	0.24	4.1	1.05	17.9	6.00
	3.85 d	0.05	0.8	2.92	50.9	1.45	25.3	0.21	3.6	1.11	19.4	5.75
	6.26 d	0.01	0.1	2.77	51.4	1.43	26.5	0.19	3.6	0.99	18.4	5.44

Figure 124 shows the SUVA which was calculated as the quotient of UV-response and OC-response during LC-OCD fractionation. The maximum at 48 min is not identical with maximum of humics (52 min). This proves that the high molecular humics, eluting at 48 min, have the highest share of aromatic structures. This is consistent with the findings at the field sites and the long retention column experiments. The measured increase of SUVA (Figure 122) can primarily be ascribed to the degradation of aliphatic polysaccharides (36-44 min). For the SUVA of humics only little differences without any temperature dependency were detected.
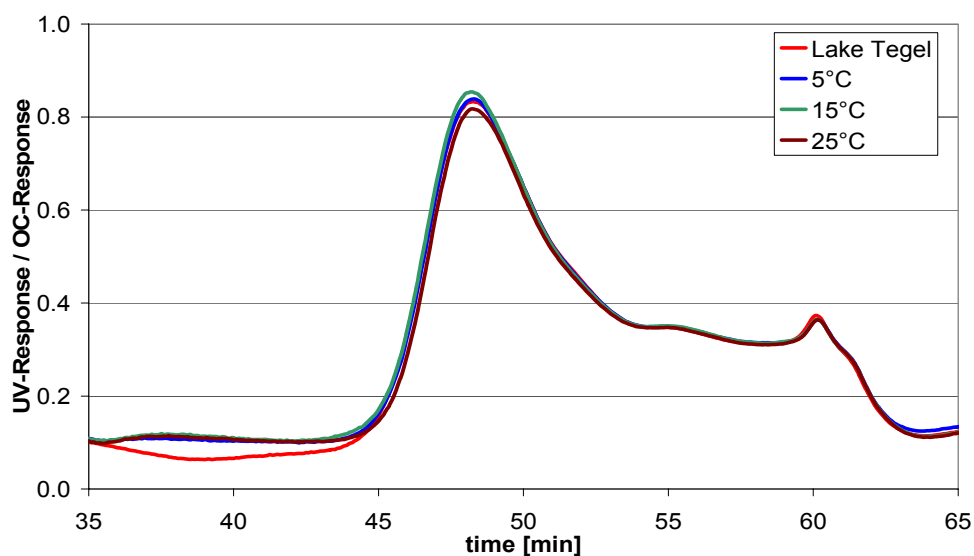

Figure 124 SUVA of column effluents at 5°C, 15°C and 25°C

Figure 125 provides more detailed information by describing the changes of SUVA along the column at 25°C. The graph proves that besides the strong influence of the polysaccharides on the SUVA, the humic substances also show some influence on the overall SUVA.
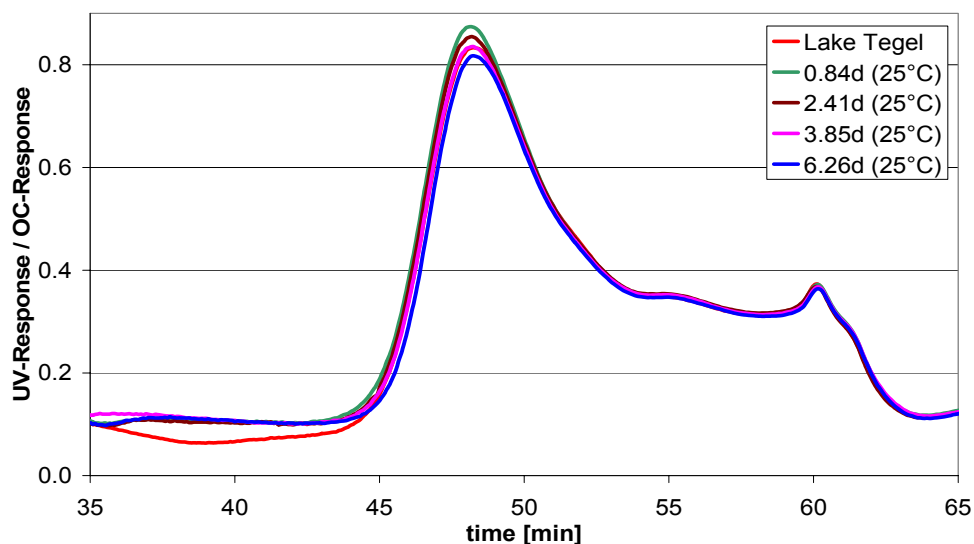
Figure 125 SUVA along the column with 25°C

In the beginning of the infiltration the SUVA of humic substances increases (peak at 48 min). It can be assumed that microorganisms start to crack aliphatic side chains of

the humic molecules, causing an overall increase of the share of aromatic structures in this fraction. In the deeper layers of the filter bed the portion of aromatic carbons is decreasing, most probably because easy degradable aliphatic structures are exhausted and microorganisms have to use aromatics as well. Towards the end of infiltration the ratio of aromatic to aliphatic structures is again similar to the ratio in the feed water.

Adsorbable organic iodide (AOI)

Since the question of the temperature dependency of AOI-mineralization remained unclear, AOI was included into the monitoring program of the temperature regulated column system. Because of the oxic conditions in the column system, no significant mineralization of AOI was expected. However, AOI was measured as additional parameter to characterize the degradation process of Iopromide.

Table 35 shows the AOI results as medians.

The average AOI concentration in Lake Tegel during the operation of the column system was measured with 11.6 +/- 2.7 µg/l (n=4). Feed samples were taken after spiking so that the spiked Iopromide is included in the feed results. Knowing that 10 µg/l Iopromide-spiking would result in an AOI increase of 4.8 µg/l, the estimated feed concentration is about 16.4 µg/l. This corresponds well with the measured concentrations. However, the results implicate a slight increase of AOI-concentration of 1.5-2.9 µg/l at all temperatures during infiltration. This is most probable due to measurements mistakes, since these slight increases do not correspond with other results of the project. An unlikely explanation could be the formation of iodinated organic compounds from inorganic iodine species.

Table 35 AOI results of temperature regulated soil column system, n=9

	Feed	5°C	15°C	25°C
AOI [µg/l]	15.8 +/- 2.4	18.7 +/- 2.6	17.4 +/- 2.3	17.7 +/- 1.4

Modeling

Because a mathematical description of the biological degradation of heterogeneous bulk organics with a model using only one degradation constant is not possible, the three parametric description proposed by Gimbel et al. (1992) is used. This model was used earlier for the modeling of DOC mineralization in the long retention column.

To achieve representative results that describe the biodegradation sufficiently, a fractionation of the total DOC into three fractions (easy, medium/poorly and non-degradable) is necessary. The amount of non-degradable DOC needs to be quantified for the used feed water. For the modeling of the temperature regulated soil column system the amount of non-degradable DOC in Lake Tegel water was derived from results of the long retention soil column system. The fraction removed during infiltration to the first sampling point (after 0.84 d) was defined as easy-degradable DOC. The DOC-results were modeled two times using the software SPSS. Because of the fact that the removal of the easy degradable fraction seemed to be not temperature dependent, the degradation constant of the easy-degradable fraction was fixed as an average from all columns for second modeling (Table 36).
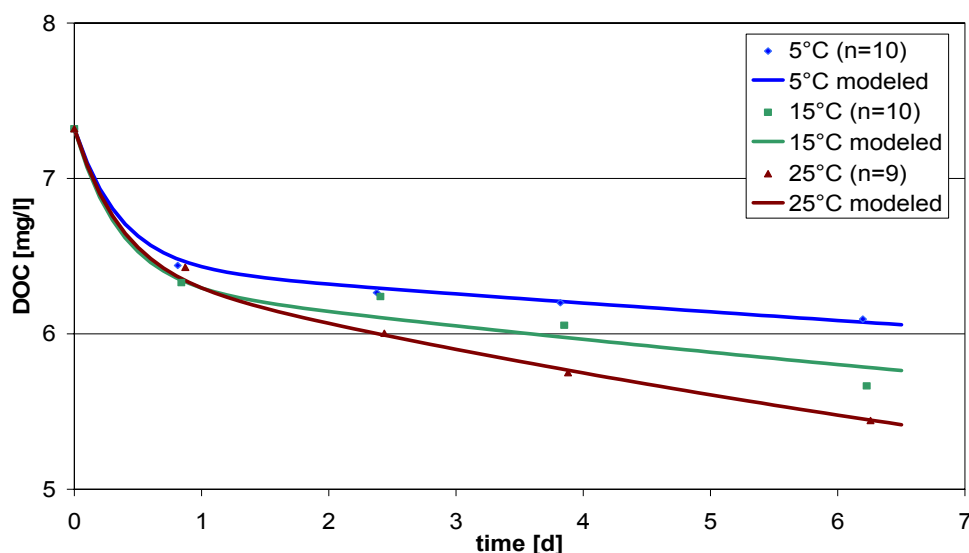

Figure 126 Models for the DOC degradation with the used soil column data

The results of the modeling of total DOC degradation using three fractions of different degradability are shown in Figure 126 and Table 36. It is evident that the kinetic of DOC degradation in the columns was described very well. The correlation coefficients

of the models at all temperatures are sufficiently high with R^2 of more than 0.97 (Table 36).

Furthermore, Table 36 shows that the modeled degradation constant of the medium/poorly degradable fraction (λ_2) increases considerably with higher temperatures. The results indicate that a 10 K temperature rise caused an increase of the degradation constant by the average factor of ~1.8. Thereby the factor of λ_2 was slightly higher between 15°C and 25°C than between 5°C and 15°C.

Table 36 Model constants of the DOC-modeling using Equation 1

	C_1 [mg/l]	λ_1 [d^{-1}]	C_2 [mg/l]	λ_2 [d^{-1}]	C_3 [mg/l]	R^2
5°C	0.88		2.64	0.024		0.997
15°C	0.99	2.77	2.53	0.039	3.8	0.975
25°C	0.89		2.63	0.075		0.997

The description of the fate of DOC, using three fractions and different degradation constants, was tested earlier (e.g. in Drewes (1997) and Schoenheinz (2004)). Because of the use of many variable parameters for the model, time-consuming tests are necessary to assess the concentrations of the fractions. Furthermore, the model must be adapted for each water type separately.

Therefore, one objective of the work at the temperature controlled soil columns was to test the possibility to fractionate the DOC before modeling using LC-OCD and model the mineralization of some of the fractions with one degradation constant. Of special interest was the fraction of polysaccharides, which showed a behavior during infiltration that can be compared with a single compound. The fraction of humic substances was tested, but believed to be too heterogeneous to fit to a model for a single compound decay.
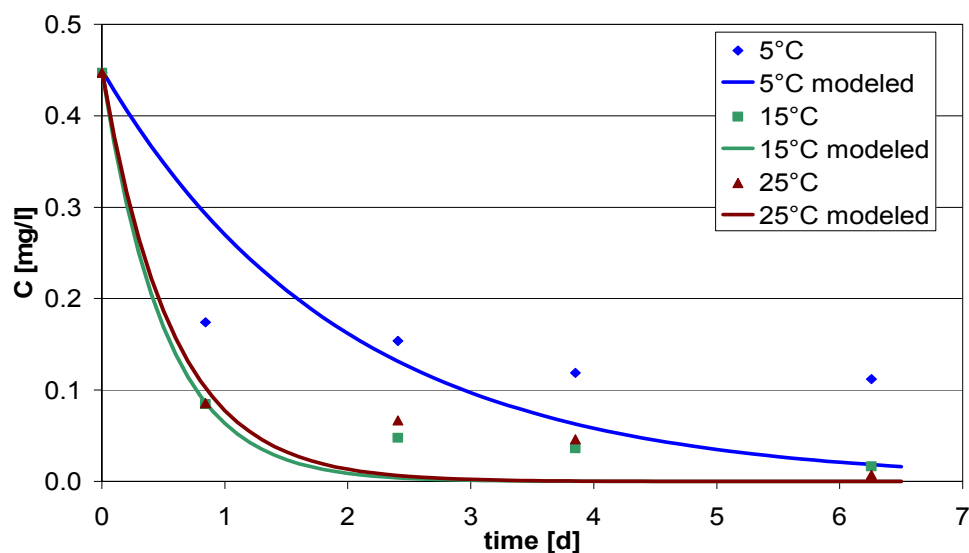
Figure 127 Modeling of polysaccharide removal with a one degradation constant model

Figure 127 and Figure 128 show the results of HS- and PS-modeling with one degradation constant. Analog to the total DOC modeling a non-degradable fraction, which is calculated from results of the long retention column system, was included into the model for humic substances. In Figure 128 the model for the decay of the humic fraction shows an insufficient correlation, proving the humics as a very heterogeneous fraction with easy degradable, poorly and non-degradable substances. Regarding the modeling of polysaccharides a higher correlation factor was achieved, but the description of this fraction is also not sufficient with only one degradation constant.
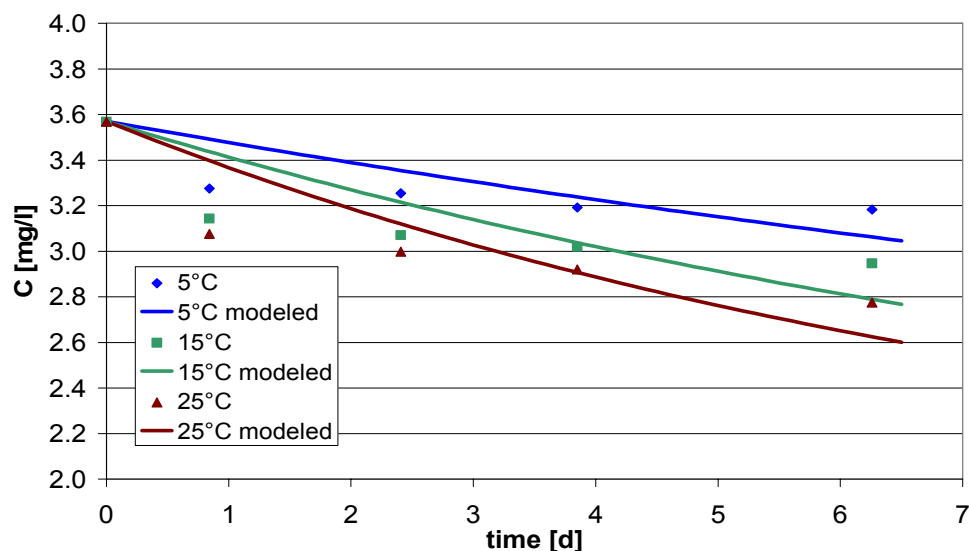
Figure 128 Modeling of the fraction of humic substances with a one degradation constant model

Table 37 proves that the DOC-fractions assessed by LC-OCD are still to heterogeneous to be modeled with a single compound decay model. The models include the temperature variation of the humics and polysaccharide decay but do not predict the kinetics of the real degradation process.

Table 37 Modeling constants of PS- and HS-removal with a one degradation constant model

|		C_1 [mg/l]	λ_1 [d^{-1}]	C_2 [mg/l]	R^2
Polysaccharides	5°C	0.45	0.511		0,663
	15°C	0.45	1.96	-	0,968
	25°C	0.45	1.759		0,947
Humics	5°C	1.77	0.054		0.298
	15°C	1.77	0.093	1.8	0.435
	25°C	1.77	0.122		0.629

Results of HS- and PS-modeling with two degradation constants are presented in Figure 129, Figure 130 and Table 38. Modeling was conducted with a similar approach as the one used for DOC. It was found that the removal of humics as well as polysaccharides can be better described as a degradation process including at least two fractions.

An increase of the degradation constant λ_2 by the factor of 2.7 was observed for the medium degradable fraction of polysaccharides between 5°C and 15°C. Between 15°C and 25°C no differences in removal rates were measured. The polysaccharides are a well defined group of organic compounds, which do not contain a non-degradable portion. But since the ratio of easy degradable to medium degradable PS shifts with temperature, the prediction of the behavior of PS in a given situation remains

complicated. The results provide some insight, but do not eliminate the need of degradation tests before modeling.
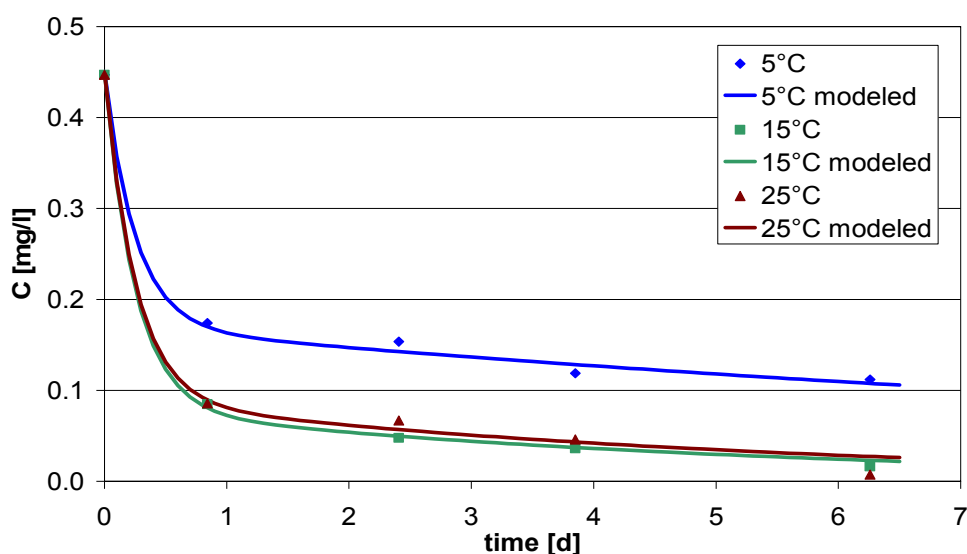

Figure 129 Modeling of polysaccharide mineralization with two degradation constants

The results for the even more heterogeneous humic fraction are presented in Figure 130. It was found that the degradation of the easy degradable fraction of humics was nearly temperature constant. Therefore, a uniform degradation constant for this fraction was used. A significant temperature dependency was measured for medium-degradable humic substances. Consistent with the total DOC results a temperature-rise of 10 K caused an increase of the degradation constant λ_2 by the factor 1.8. In contrast to the influence of temperature on DOC degradation, the effect of temperature rise on HS-degradation was little higher between 5°C and 15°C than between 15°C and 25°C.
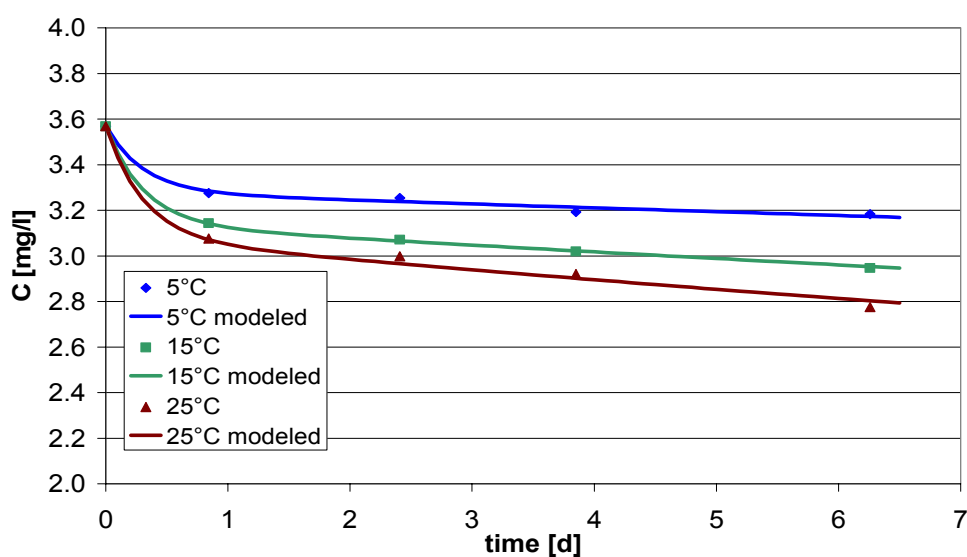
Figure 130 Modeling of HS-removal with two degradation constants

However, the results show that a prediction of the behavior of the LC-OCD assessed DOC fractions in soil columns is possible. The fractions can definitely not be modeled as single compounds. The temperature dependency that was found for the total DOC mineralization was also valid for the degradation of the single DOC-fractions. Overall, it can be summarized that the mineralization of easy degradable fractions of DOC is not significantly dependent from temperature (in the range 5°C –25°C). For medium-/poorly degradable fractions an increase of degradation efficiency by the factor of 1.8 was observed during a temperature increase of 10 K. This proves the often mentioned rule of the thumb, that biological processes are twice as efficient after a temperature increase of 10 K.

Table 38 Results of the HS- and PS-modeling with two degradation constants

		C_1 [mg/l]	λ_1 [d^{-1}]	C_2 [mg/l]	λ_2 [d^{-1}]	C_3 [mg/l]	R^2
Polysaccharides	5°C	0.28		0.17	0.073		0.998
	15°C	0.37	3.973	0.08	0.199	-	0.999
	25°C	0.36		0.09	0.191		0.996
Humics	5°C	0.29		1.48	0.012		0.993
	15°C	0.43	3.234	1.34	0.024	1.8	0.999
	25°C	0.49		1.28	0.039		0.993

Trace organic pollutants

Additionally to the bulk organic parameters, the behavior of selected trace organic compounds was investigated in the temperature controlled column system. The set-up of the columns allowed sampling along the infiltration path, which was beneficial for the assessment of the degradation kinetics of the trace compounds. The monitoring schedule is included in the set-up chapter. Because of the required higher sample volumes for trace compound analysis the influent and the effluent of the columns were sampled more often (10x), whereas the sampling ports along the columns were only used for three sampling events during the operation period. Therefore, the data pool for the sampling ports along the column is smaller than the data pool for the influent and effluent of the column.

The same selection of trace compounds that were used for the field monitoring and the other soil column experiments was used for the investigations at the temperature controlled soil columns. From the group of naphthalenedisulfonic acids the 1,5-, 1,7- and 2,7-isomer were analyzed. Figure 131 shows the concentration of 1,5-NDSA along the columns. Confirming other results no biodegradation was observed even in the column operated at 25°C. In all columns the concentration remained at the level of the influent concentration during the 6.3 d of infiltration. The results of 1,5-NDSA prove that no significant influence of sorption processes is present in the soil columns and that

polar substances (as the tested trace compounds) do not tend to adsorb to the sand surface. Therefore, the removal of other substances must be mostly related to biodegradation. Results of additional experiments with shorter retention time confirm these conclusions.
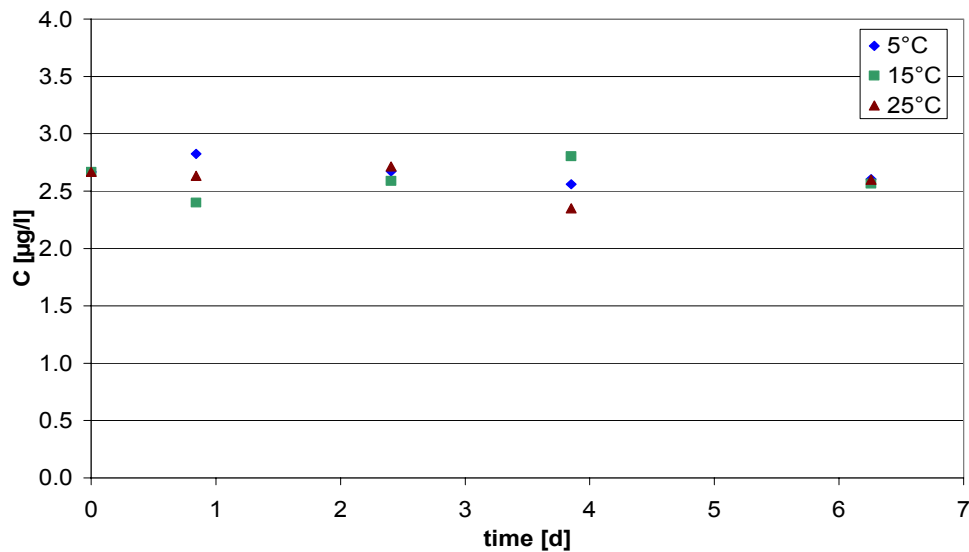
Figure 131 Behavior of 1,5-NDSA (v=8.31cm/d) along the different columns

The other isomers of NDSA were found to be degradable under favorable conditions. After the first test of the degradability with a pore velocity of 8.3 cm/d some of the trace compounds were already degraded in the first sampling port and differences between the efficiency at 15°C and 25°C were not clearly visible. Therefore, a second test with higher flow velocities was performed to emphasize the initial infiltration zone. The second set of experiments was conducted at a pore velocity 15.9 cm/d reducing the retention time of the columns from 6.3 days to 3.2 days. The results confirmed the findings of the first set of experiments and provided a better insight into the processes in the immediate infiltration zone. A better differentiation of the performance of the 15°C column and the 25°C column was possible.
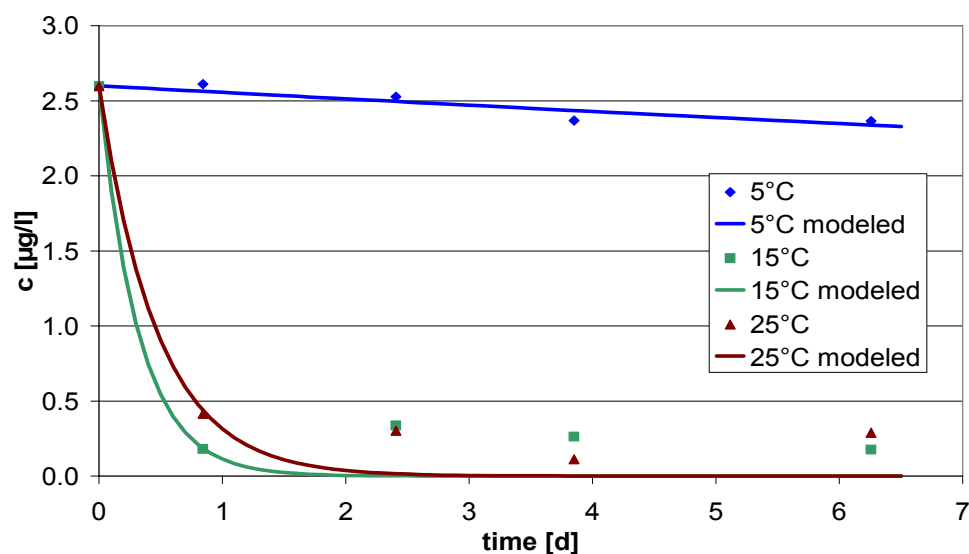

Figure 132 Degradation of 1,7-NDSA at different temperatures (v = 8.31 cm/d; n=3-10)

The behavior of 1,7- and 2,7-NDSA at different temperatures and retention times is presented in Figure 132, Figure 133, Figure 134 and Figure 135.

The data points represent the measured concentrations, whereas the drawn through lines show the results of modeling. Differences of measured start concentrations are related to variations in spiking.
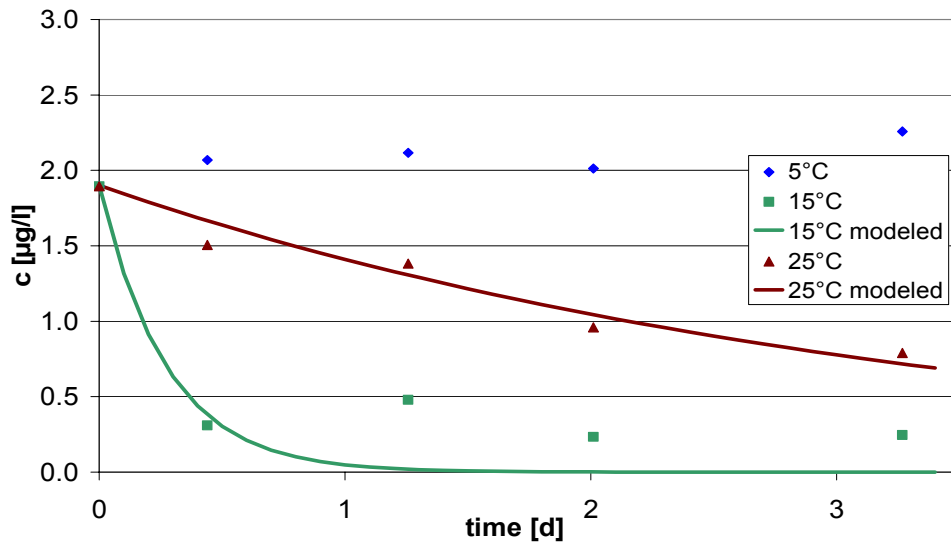

Figure 133 Degradation of 1,7-NDSA at different temperatures (v = 15.92 cm/d; n=3)

Figure 132 shows that at 5°C a very slow removal of 1,7-NDSA was observed and even after more than 6 days of infiltration the removal rate was only around 10%. Under more favorable conditions, at 15°C and 25°C, a considerably higher removal of 1,7-NDSA was found. After one day of infiltration approximately 90% of the initial concentration was removed (Figure 132). Unfortunately, no significant difference between the efficiency at 15°C and 25°C was observed at a pore velocity of 8.3 cm/d. Figure 133 confirms the stability of 1,7-NDSA at 5°C, but clarifies that 1,7-NDSA

biodegradation at 15°C was considerably faster than at 25°C. The degradation constant at 15°C is similar during both experiments, but λ for the decay at 25°C is smaller during the experiment with the higher pore velocity.

The complete stability of 1,7-NDSA at 5°C might be explained by a threshold temperature between 5°C and 15°C under which a not-achievable activation energy limits biodegradation. The fact that such processes are of importance is confirmed by the rising fraction of non-degradable DOC with decreasing temperature that were found by Schoenheinz (2004). Similar to the results of the for 1,7-NDSA, Wesnigk et al. (2001) found a significant decrease of Nitrilotriacetat- mineralization under 7°C.

Table 39 Modeling results for 1,7-NDSA

	v = 8.31 cm/d			v = 15.92 cm/d		
	C_0 [mg/l]	λ [d^{-1}]	R^2	C_0 [mg/l]	λ [d^{-1}]	R^2
5°C		0.017	0.848		-	-
15°C	2.6	3.132	0.952	1.9	3.665	0.837
25°C		2.114	0.959		0.298	0.946

In both experiments the 1,7-NDSA was not mineralized completely, even under the most favorable conditions at 15°C. Therefore, the mathematical modeling of the 1,7-NDSA decay includes a systematic error. The degradation of 1,7-NDSA ceases after a concentration of about 0.3 µg/l is reached. This is maybe due to a threshold concentration. The existence of a threshold concentration would propose a metabolic degradation of 1,7-NDSA, since cometabolic degradations would not be affected by a threshold concentrations.
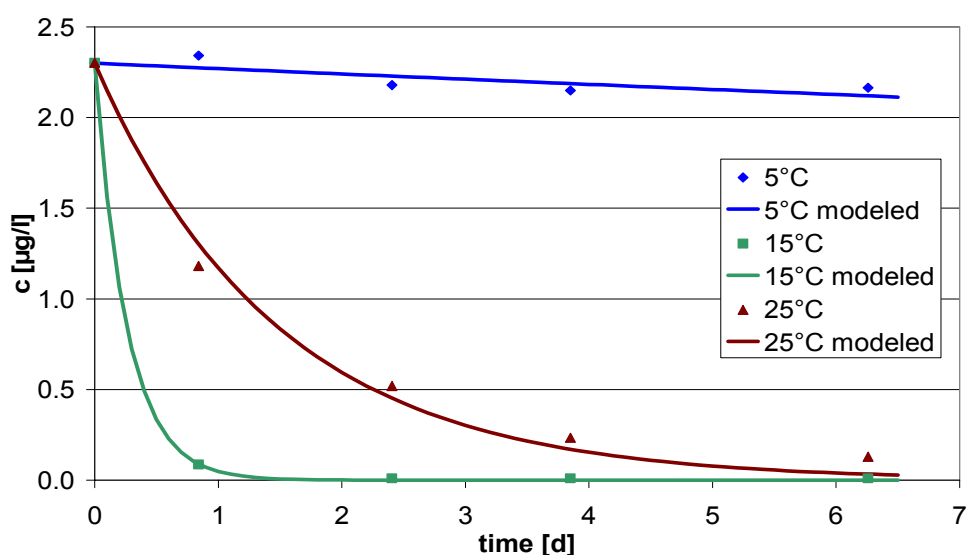
Figure 134 Degradation of 2,7-NDSA at different temperatures (v = 8.31 cm/d; n=3-10)

The results of the degradation experiments for 2,7-NDSA show a similar behavior of this NDSA-isomer. Nearly no removal of 2,7-NDSA was observed in the column at 5°C. At both pore velocities the removal at 15°C is more efficient than at 25°C. Furthermore, no or a much lower threshold concentration was observed during the mineralization of 2,7-NDSA.
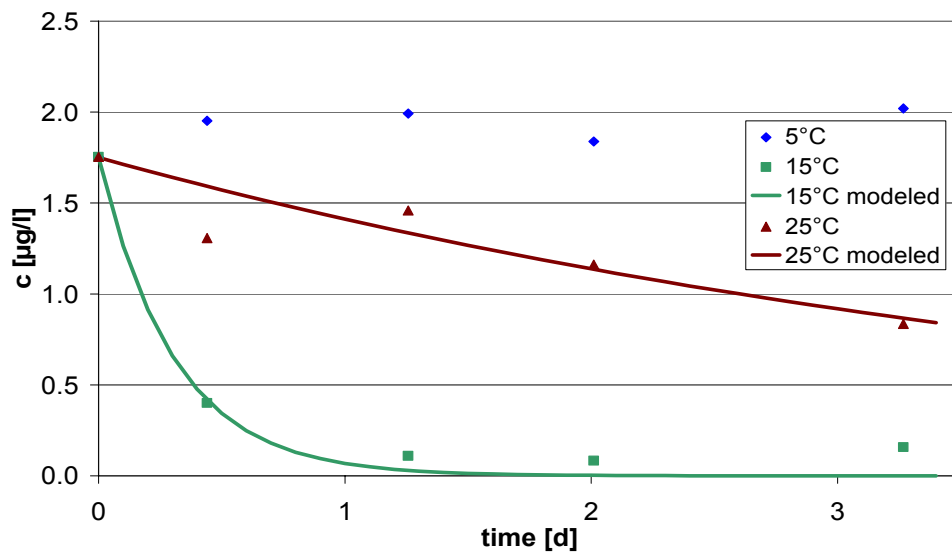
Figure 135 Degradation of 2,7-NDSA at different temperatures (v = 15.92 cm/d; n=3)

Between 15°C and 25°C a decreasing removal of both degradable NDSA-isomers with temperature was observed. This effect was actually clearer in the results of the experiment with shorter retention times. The temperature optimum for NDSA-degrading microorganisms is apparently around 15°C. Maybe this can be related to the adaptation processes. The population in the soil columns is comparable and adapted to conditions at the Lake Tegel bank filtration site. The mean annual water temperature of Lake Tegel is between 10°C and 15°C. Therefore, a more efficient NDSA-removal at 15°C might be due to the adaptation onto the conditions at Lake Tegel. Garing (2005) investigated at the same columns the removal of microcystin under different temperatures and found no improvement of mineralization rates between 15°C and 25°C.

Table 40 Modeling results for 2,7-NDSA

	v = 8.31 cm/d			v = 15.92 cm/d		
	C_0 [mg/l]	λ [d^{-1}]	R^2	C_0 [mg/l]	λ [d^{-1}]	R^2
5°C		0.013	0.687		-	-
15°C	2.3	3.857	0.999	1.75	3.252	0.98
25°C		0.676	0.999		0.215	0.79

Actually, for the experiment with higher pore velocity better degradation rates in a comparable time frame were expected due to a faster transport of nutrients to microorganisms. These expectations were not confirmed by the measurements. At 5°C and 25°C even a negative influence of increasing velocity was observed. However, most of the degradation took part in the first centimeters of the infiltration path.

 Due to the higher pore velocity in the second experiment the contact time in the bioactive layer at the start of the columns was shorter and maybe not sufficient for an effective degradation. A longer adaptation period at higher velocities could have resulted in an extension of the bioactive layer in deeper parts of the filter bed. Eventually, this would lead to higher degradation rates in a similar time frame.

Additionally to the fate of NDSA in the soil column system the behavior of Iopromide and Sulfamethoxazole was investigated. The results of all measurements and the modeling of the fate of the X-ray contrast media Iopromide are presented in Figure 136 and Table 41. A good removal of Iopromide in soil passage was observed in all temperature controlled columns. Consistently, relatively high degradation constants of λ ~2 were found at all temperatures, proposing only very few influence of temperature onto the degradation efficiency of Iopromide. Comparing the Iopromide results with AOI findings it is proved that no dehalogenation of Iopromide occurred, because AOI was not degraded at all. It was already evident in other investigations that Iopromide is only metabolized by microorganisms.
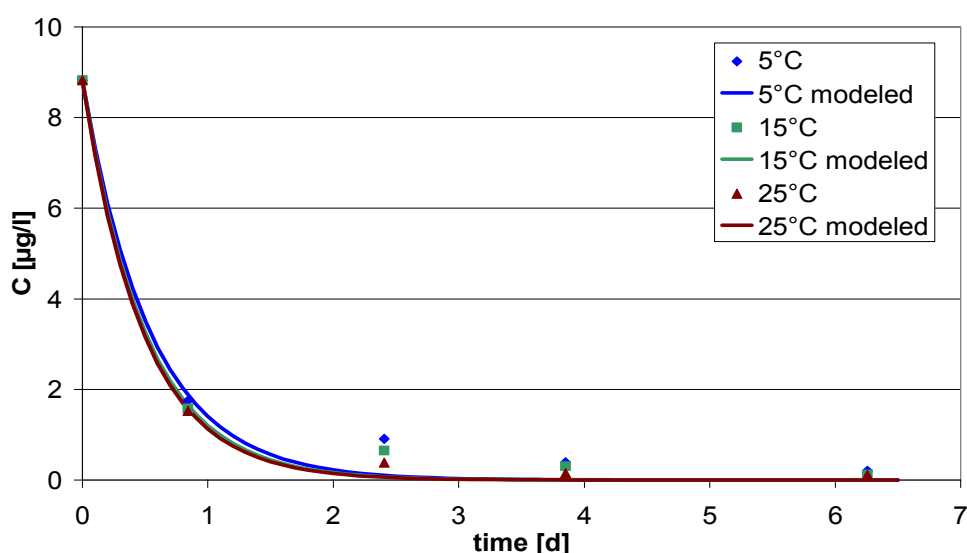

Figure 136 Degradation of Iopromide along the different columns (v=8.31 cm/d, n=3-10)

However, despite of the fact that Iopromid is only metabolized, it was found that Iopromide is apparently easy available for microorganism attack under all investigated temperature conditions. This implies a wide temperature optimum for the responsible microorganisms or a large variety of different microorganisms that are able to metabolize Iopromide. The results for Iopromide show no threshold concentration, which would point toward a metabolic biodegradation. This confirms results of short retention columns, which described a cometabolic degradation of Iopromide under anoxic conditions.

Table 41 Modeling results for Iopromide (v = 8.31 cm/d)

	C_0 [mg/l]	λ [d^{-1}]	R^2
5°C		1.836	0.984
15°C	8.82	1.991	0.992
25°C		2.056	0.997

Degradation of the antibiotic Sulfamethoxazole in the soil column system was monitored closely using the described sampling schedule. The results and the modeling are shown in Figure 137 and

Table 42. It was found that the removal significantly depends on temperature. At 5°C degradation of Sulfamethoxazole was considerably slower than in the 15°C and 25°C column. The degradation rate increased by the factor of 10 when the temperature rises to 15°C, whereas only little differences in λ were observed between 15°C and 25°C. Similar to 1,7-NDSA a threshold concentration of ~0.3 µg/l was found.
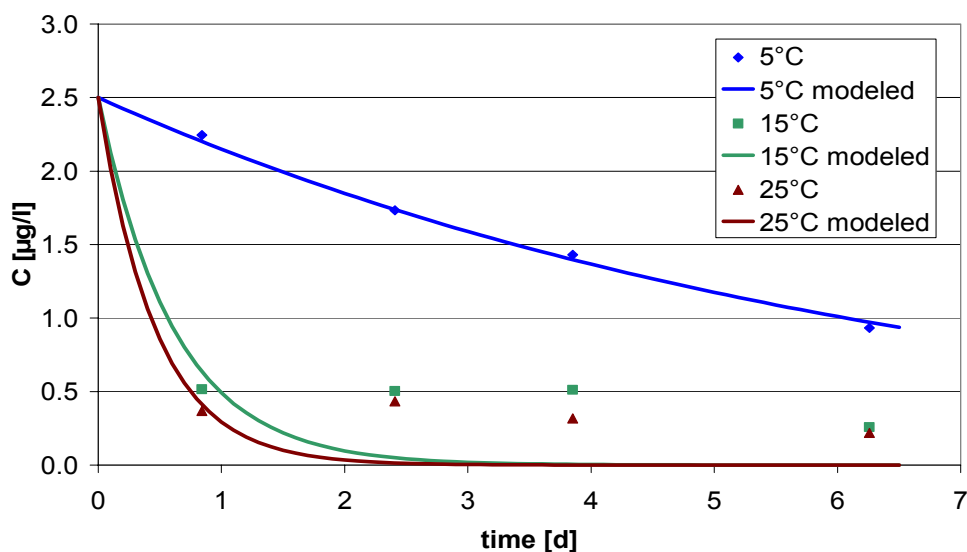

Figure 137 Degradation of Sulfamethoxazole along the different columns (8.31 cm/d, n=3-10)

Temperature optimum and spectrum of Sulfamethoxazole degradation differ from the results for the NDSA-degradation. Apparently, Sulfamethoxazole degrading organisms are more tolerant to temperature variations, because an efficient removal was observed at 15°C and 25°C. It might be possible that the optimal temperature for Sulfamethoxazole-decaying microorganisms is around 20°C and both experiments are similarly suboptimal. The threshold concentration points towards a metabolic process of specialized biomass, but it is also possible that several microbial strains with different temperature optima are able to utilize Sulfamethoxazole.

Table 42 Modeling results for Sulfamethoxazole (v = 8.31 cm/d)

	C_0 [mg/l]	λ [d^{-1}]	R^2
5°C		0.151	0.997
15°C	2.5	1.625	0.842
25°C		2.142	0.914

Results for Iopromide and Sulfamethoxazole behavior in the experiments with shorter retention times are not presented because the results were not representative. In the same period investigations with high spiking concentrations of microcystin were started, which possibly influenced the adapted biomass.

Overall, the degradation of Iopromide is more temperature tolerant than the degradation of the other investigated trace pollutants. This might be due to the fact that Iopromide is metabolized in a cometabolic process whereas the other trace organics are apparently removed by metabolic processes. Thus the temperature dependency can be explained as follows. Nonselective cometabolic enzymes are produced by many microbial strains with different temperature optima whereas metabolic degradation occurs by only few specialized strains with fixed temperature requirements.

1.4.4   Column experiments to assess the retardation coefficients

The column system for the determination of the retardation factor was installed at the TU Berlin. For the evaluation of the field data and the planning of the soil column experiments the retardation factor was of eminent importance. Low retardation factors were expected, because the investigated trace compounds were very polar. Since the particulate organic compound content of the sediment might influence the absorption processes of the organics during soil passage, the retardation tests were conducted with different sediments. Three different POC-contents were tested.

1.4.4.1 Set-up

The used column system consisted of three plexiglas-columns (Figure 138). Each column was 0.451 m long and had a diameter of 0.064 m (Volume: 1.45 l). Column I was filled with Lake Tegel bank material. The filling of column III was the industrial sand used for all column experiments (Ø = 0.7 – 1.2 mm). Column II was packed with a 50:50-mix (weight-based) of both materials. The columns were fed with drinking water (flow = 0.11 l/d), exchanging six pore volumes per day.

Figure 138 Soil columns for the determination of the retardation factor

To determine the retardation of Iopromide, Sulfamethoxazole and the NDSA-isomers 5 ml of a cocktail, containing the trace compounds and sodium chloride, was fed to the column in a pulse application. The cocktail consisted of a mixture of 40 g/l NaCl, 40 mg/l Iopromide and 40 mg/l 1,7-NDSA and 10 mg/l Sulfamethoxazole. The trace compound concentrations were selected in this range because very small sample volumes were taken from the columns and no concentration step was possible before analysis. Sodium chloride was used as an ideal tracer and a retardation factor of 1.0 was assumed. The behavior of the trace compounds was compared to the fate of electrical conductivity measured with a flow through-cell. The conductivity was logged in 5 minutes intervals. Sampling for the trace compound determination was conducted

every 18 minutes. Therefore, the given concentrations are mean concentrations of this interval.

1.4.4.2 Results

Loss on ignition: Before the start of the experiments the loss on ignition was determined. The calculated values for the loss on ignition are shown in Table 43. As expected, bank material of Lake Tegel showed the highest loss on ignition (0.56 %), whereas the technical sand has the lowest loss on ignition (0.13 %). The value of the loss on ignition of the technical sand was above expectations, because it should not contain any organic material. As expected, the ignition lost of the mixture of both materials was near the mean of both materials, proofing the determination method.

Table 43 Loss on ignition of the different filter materials

Number of column	Loss on ignition [%]
I	0.56
II	0.34
III	0.13

Trace compounds: Results of the determination of the retardation coefficients are shown in Figure 139. The Iopromide as well as the Sulfamethoxazole peak reached the end of the columns in all experiments with no significant time differences (compared to the sodium chloride peak). Thus, it appears that neither Iopromide nor Sulfamethoxazole are retarded by the sediment. A difference between the materials with different POC-content was not observed. The results of the 1,7-NDSS were not shown because they were comparable to those of Iopromide and Sulfamethoxazole.

Conclusions concerning the dispersion can be drawn from the different shapes of the peaks. Column II generated a more expanded peak (decreased amplitude) in comparison with the other columns. This indicates a higher dispersion and is consistent with the mixing of the two sediment types. Furthermore, column II was found to have the lowest porosity of the tested columns.
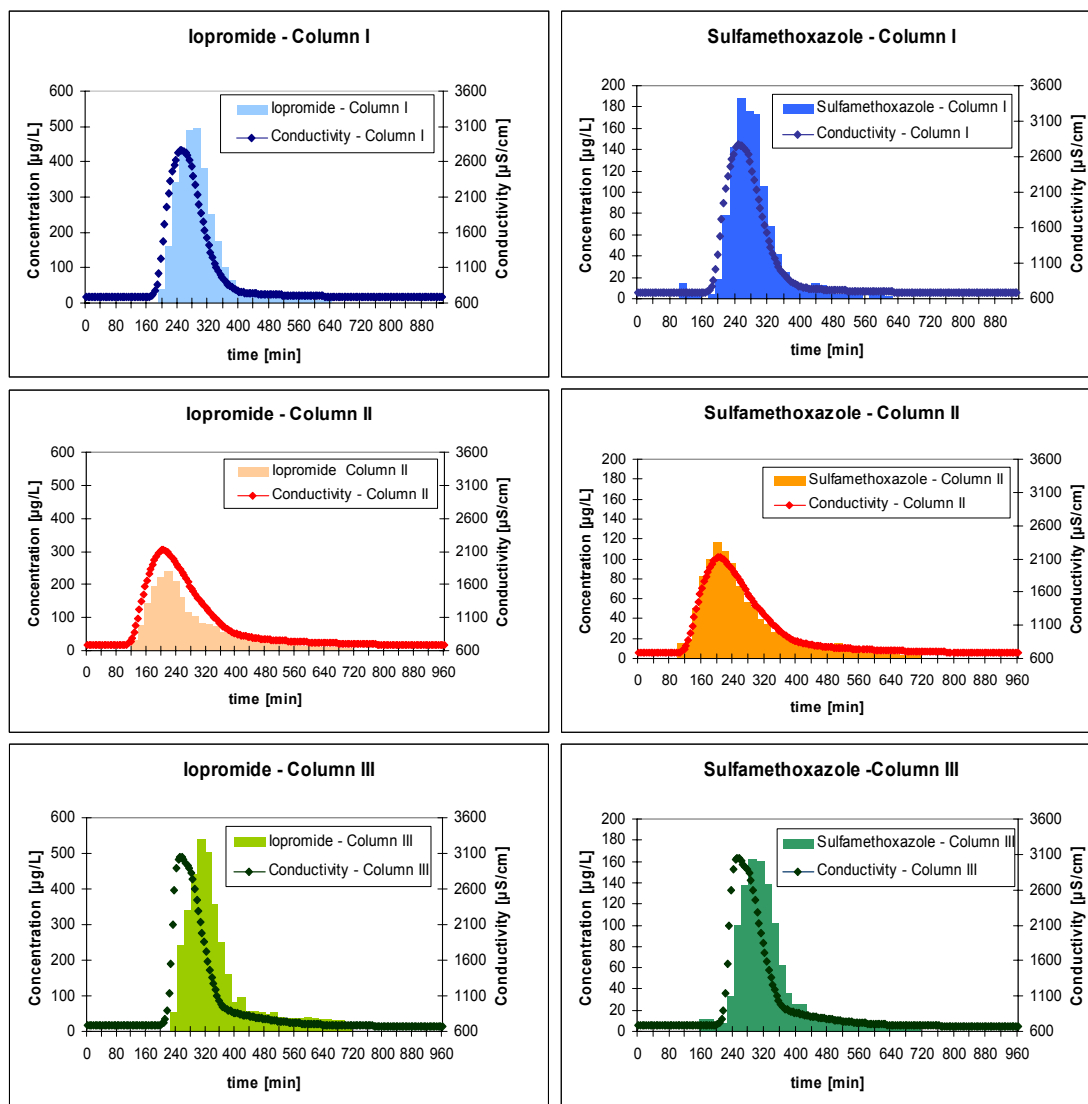
Figure 139 Retardation of Iopromide and Sulfamethoxazole in comparison with the electrical conductivity at different column materials

Calculation of the pore velocity (V), the dispersion (D) and the retardation coefficient (R) were carried out with the program CXT fit (Version 2, Free Software Foundation, Inc. Boston, USA). Determination of V and D was conducted by inverse modeling with the help of the measured conductivity and the assumption R=1 for sodium chloride. The next step was the inverse calculation of R and µ of the different trace organics for each column. Generated values are listed in

Table 44. Additionally, the porosity was determined by the ratio of Darcy- and pore velocity.

Table 44 Retardation coefficients of the trace organics for different filter materials

	Porosity	V	D	R		
	[%]	[m/d]	[m^2/d]	Iopromide	Sulfamethoxazole	1,7-NDSS
Column I	33.4	2.503	0.014700	1.076	1.029	1.004
Column II	29.5	2.833	0.050000	1.064	1.000	1.000
Column III	35.1	2.377	0.009513	1.136	1.092	1.094

The results of the CXT-fit modeling, shown in

Table 44, confirm the conclusions. The results are shown in Figure 140. A mass balance proved that a partial degradation of all three trace organic substances took place in the columns. During modeling, this was taken into account by adjusting the parameter µ. The data showed that degradation of the compounds was comparable in column I and column III, whereas column II showed a slightly elevated degradation. The dispersion in column II was determined with 0.05 m^2/d, which is five times higher than the dispersion of the other columns (dispersion 0.01 – 0.015 m^2/d). The mixing of both materials with different grain sizes leads to differences in the lengths of the infiltration paths and thus to a higher dispersion. The porosity of column II was 29.5 %, whereas values for column I and column III show higher values of 33.4 % and 35.1 %. The pore velocity, which is linked to the porosity, was calculated for column II with 2.8 m/d. In contrast column I and column III show smaller pore velocities of only 2.5 m/d and 2.4 m/d.
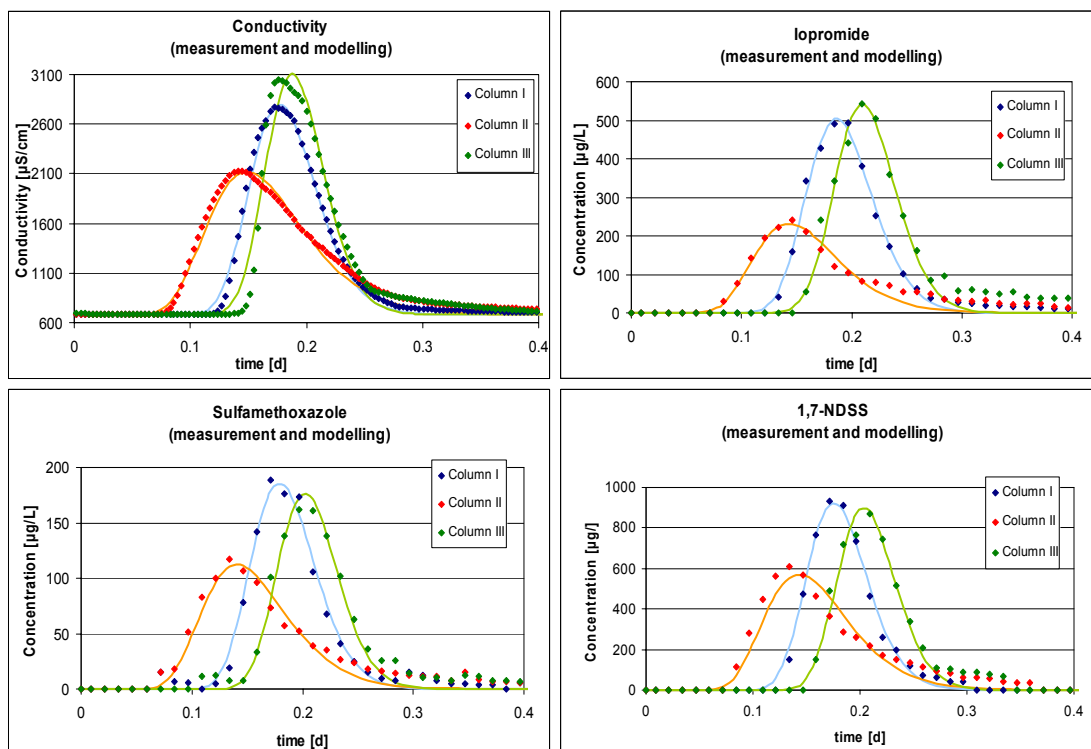
Figure 140 Conductivity and concentration of the trace organics (measured and modeled)

Independently from the material (POC-content) used for the column filling, the retardation coefficient reached values of 1.0-1.1. This proves that retardation does not play an important role for the behavior of the investigated compounds in the subsoil. Contrary to the expectations, different fractions of organic matter (see Table 43) showed no impact on the retardation. In Figure 140 color-coordinated graphs show the measured values (dots) and the modeled breakthrough (line). It is obvious, that the characteristic of the measured data comply with the results of the modeling.

Summarizing, it was confirmed that the polar and hydrophilic character of the investigated trace substances prevents an adsorption onto organic or inorganic parts of the sediment. Retardation was found of no importance for the tested trace compounds. It is assumed that the results can be transferred to the field to understand the behavior of these substances in the field better.

2   References

Bahr, C. (2002) Untersuchungen zur katalytischen Ozonung refraktärer Organik in Abwasser (Catalytic Ozonation of Refractory Organic Compounds in Waste Water) Diploma thesis at Department of Water Quality Control, Technical University of Berlin (in German)

Bahr and M. Jekel (2005) Final Report of "Pilotuntersuchungen zur kombinierten oxidativ-biologischen Behandlung von Klärwerksabläufen für die Entfernung von organischen Spuren- und Wirkstoffen und zur Desinfektion (PILOTOX)", Research Project of the Berlin Center for Competence for Water.

Berliner Wasser Betriebe (Berlin Water Works - BWB) (2003) http://www.bwb.de.

Cosovic B., D. Hrsak, V. Vojvodic and D. Krznaric (1996) Transformation of organic matter and bank filtration from a polluted stream. Water Res., 30(12), 2921-2928.

Davis J. A. (1982) Adsorption of natural dissolved organic matter at the oxide/ water interface. Geochim. Cosmochim. Acta 46 (1982), p. 2381-2393

Drewes J. and P. Fox (1999) Behaviour and Characterization of Residual Organic Compounds in Wastewater Used for Indirect Potable Reuse. Water Science and Technology, 40 (4-5) 391–398

Drewes J. E. (1997) Untersuchungen zum Verhalten organischer Abwasserinhaltsstoffe bei der Wiederverwendung kommunaler Kläranlagenabläufe zur künstlichen Grundwasseranreicherung. (Behavior of organic compounds in domestic effluents used for groundwater recharge). Fortschritt-Berichte VDI-Verlag No 174, Umwelttechnik, Düsseldorf (in German)

Findlay R. H., G.M. King, L. Watling (1989) Efficacy of Phospholipid Analysis in Determining Microbial Biomass in Sediments. Applied and Environmental Microbiology, 11/1989, 2888-2893

Fritz B., J. Sievers, S. Eichhorn and A. Pekdeger (2002) Geochemical and hydraulic investigations of river sediments in a bank filtration system. In: Dillon, P. (ed.): Management of Aquifer Recharge for Sustainability, Balkema, Adelaide, Australia 95-100.

Gimbel R., M. Gerlach, H.-J. Mälzer (1992) Die Testfiltermethode als Simulationsgrundlage des Störstoffverhaltens bei Untergrundpassagen. (A method using test filters as an approach to simulate underground passage of undesired compounds) Sechstes Mülheimer Wassertechnisches Seminar. Berichte aus dem

Rheinisch-Westfälischen Institut für Wasserchemie und Wassertechnologie. Bd. 6, 126-163, Mülheim

Hartig C. (2000) Analytik, Vorkommen und Verhalten aromatischer Sulfonamide in der aquatischen Umwelt. (Analysis and behavior of aromatic sulfonamides in the aquatic environment). Doctoral Dissertation accepted by: Technical University of Berlin, School of Process Sciences and Engineering, 2000-08-29, http://edocs.tu-berlin.de/diss/2000/hartig_claudia.htm

Heberer T., I.M. Verstraeten, M.T. Meyer, A. Mechlinski, and K. Reddersen (2001) Occurrence and fate of pharmaceuticals during bank filtration—Preliminary results from investigations in Germany and the United States. Water Resour. update, 120, 4–17

Hiemstra P., R. J. Kolpa, J. M. van Eekhout, A. L. van Kessel, E. D. Adamse and J. A. M. van Paassen. Natural recharge of groundwater: Bank filtration in the Netherlands. J. Water Supply: Res. T., 52(1), 37-47.

Hoyer O., B. Lüsse, H. Bernhard (1985): Isolation and characterization of extracellular organic matter from algae. Zeitschrift Wasser-Abwasser-Forschung (Journal of water and waste water research) 18, 76-90

Huber S. and A. Balz (2005) DOC-Labor Dr. Huber, What is LCOCD about, 07.01.2006, <http://www.doc-labor.de>

Huber S. and F. Frimmel (1996) Gelchromatographie mit Kohlenstoffdetektion (LC-OCD): Ein rasches und aussagekräftiges Verfahren zur Charakterisierung hydrophiler organischer Wasserinhaltsstoffe (Gelchromatography coupled with carbon detection: A fast and powerful method to characterize hydrophilic organic water constituents). Vom Wasser, Vol. 86,277-290.

Hütteroth A., A. Putschew, M. Mania and M. Jekel (2004) Cyanobakterien: Die Quelle für bromorganische substanzen in Oberflächenwässern? Proceedings of the annual Meeting of the Water Chemical Society Germany, 17.-19.05.2004, Bad Saarow, Germany.

Jekel M. and S. Wischnack (2000) Herkunft und Verhalten iodorganischer Verbindungen im Wasserkreislauf. (Origin and behavior of organic iodine compounds in water cycles). Chemische Streßfaktoren in aquatischen Systemen. Schriftenreihe Wasserforschung, Vol 6, B. Weigert, C. Steinberg and R. Brüggemann (eds.), Wasserforschung e.V., Berlin, 61-69.

Kretschmar, R.,1991. Kulturtechnisch-Bodenkundliches Praktikum, ausgewählte Laboratoriumsmethoden, eine Anleitung zum selbständigen Arbeiten an Böden. Christian-Albrechts-Universität Kiel, 7. Auflage.

Kuehn, W. (2003) Development of drinking water treatment along the Rhine River with special emphasis on riverbank filtration. 6th International Symposium on Water Supply Technology. Kobe, March 18 - 19, 399 - 412.

Miettinen I. T., P. J. Martikainen and T. Vartiainen (1994) Humus Transformation at the bank filtration water plant. Water Sci. Technol., 30(10), 179-187.

NASRI. 2003. http://www.kompetenz-wasser.de.

Oleksy-Frenzel J., S. Wischnack and M. Jekel (2000) Application of ion-chromatography for the determination of the organic-group parameters AOCl, AOBr and AOI in water. Fresen. J. Anal. Chem., 366, 89-94.

Pekdeger A., G. Massmann, B. Ohm. 2nd Periodic Report: Hydrogeological-hydrogeochemical processes during bank filtration and groundwater recharge using a multitracer tracer approach. NASRI-Projekt, (2004) 80 pages.

PreSens (2005) Precision Sensing GmbH, Support, How does a oxygen microsensor work?, 01.12.2005 <http://www.presens.de/html/start.html>

Putschew A., M. Mania and M. Jekel (2003) Occurrence and source of brominated organic compounds in surface waters. Chemosphere, 52, 399-407.

Putschew A., S. Schittko and M. Jekel (2001) Quantification of triiodinated benzene derivatives and X-ray contrast media in water samples by liquid chromatography-electrospray tandem mass spectrometry. J. Chromatogr. A, 930, 127-134.

Ray C., T. Grischek, J. Schubert, J. Wang and T. Speth (2002) A perspective of riverbank filtration. J. Am. Wat. Wks. Assoc., 94(4), 149-160.

Rittmann B.E. and V.L. Snoeyink (1984) Achieving biologically stable drinking water. J. Am. Wat. Wks. Assoc., 76(10), 106-114.

Schittko S., A. Putschew and M. Jekel (2004) Bank Filtration: a suitable process for the removal of iodinated X-ray contrast media? Wat. Sci. Tech., 50 (5), 261-268

Schmidt C.K., F.T. Lange; H.-J. Brauch. (2004) Assessing the impact of different redox conditions and residence times on the fate of organic micropollutants during riverbank filtration. Proceedings "4th International Conference on Pharmaceuticals and Endocrine Disrupting Chemicals in Water", 13.-15.10.2004, Minneapolis, Minnesota.

Schoenheinz D. (2004) DOC als Leitparameter zur Bewertung und Bewirtschaftung von Grundwasserleitern mit anthropogen beeinflusster Infiltration, Doctoral Dissertation accepted by: Technical University Dresden, School of Geohydrological Sciences, 2004-03-15.

Schoenheinz D., T. Grischek, E. Worch (2003) Investigations into Temperature effects on DOC degradation during riverbank filtration. Paper presented at the 11th Biennial Symposium on Groundwater Recharge, Phoenix, AZ, June 5-7.

Schulz H. J. (1998) Gutachten über die Nutzbarkeit einer Säulenanlage zur Durchführung von Simulationen des Abbauverhaltens von Schadstoffen in der Grundwasserpassage (Certificate on the usability of a soil column system for simulation experiments on the fate of pollutants during infiltration). Report of the German Federal Environmental Agency (8 pages).

Stan H. J. and M. Linkerhäger (1994) Vorkommen von Clofibrinsäure im aquatischen System – Führt die therapeutische Anwendung zu einer Belastung von Oberflächen-, Grund- und Trinkwasser? (Occurrence of clofibric acid in aquatic systems – Pollution of surface-, ground and drinking water by therapeutical use?). Vom Wasser, 83, 57 – 68.

Storm T. (2001) Aromatische Sulfonate - Untersuchungen zum Stoffverhalten in Industrieabwasser und aquatischer Umwelt mit HPLC-MS. (Aromatic sulfonates - Investigations into the behaviour in industrial wastewater and the aquatic environment with HPLC-MS), Doctoral Dissertation accepted by: Technical University of Berlin, School of Process Sciences and Engineering, 2002-05-27. http://edocs.tu-berlin.de/diss/2002/storm_ thomas.htm.

Storm T., T. Reemtsma, M. Jekel (1999) Use of volatile amines as ion-pairing agents for the high-performance liquid chromatographic-tandem mass spectrometric determination of aromatic sulfonates in industrial wastewater. J. Chromatogr. A, 854, 175-185.

Stüber, M., T. Reemtsma, M. Jekel (2002) Determination of naphthalene sulfonates in tannery wastewater and their behaviour in a membrane bioreactor. Vom Wasser, 98, 133-144.

Ternes T. A. and R. Hirsch (2000) Occurrence and behaviour of x-ray contrast media in sewage facilities and the aquatic environment. Environ. Sci. Technol., 34(13), 2741-2748.

Ternes T. A., M. Meisenheimer, D. McDowell, F. Sacher, H. Brauch, B. Haist-Gulde, G. Preuss, U. Wilme and N. Zulei-Seibert (2002) Removal of Pharmaceuticals during Drinking Water Treatment. Environ. Sci. Technol., 36(17), 3855-3863.

Tufenkji N., J. N. Ryan and M. Elimelech (2002) The promise of bank filtration. Environ. Sci. Technol. A-Pages, 36(21), 422A-428A.

Van der Kooij D. (2003) Managing regrowth in drinking water distribution systems, in WHO-Heterotrophic plate count and drinking water safety. eds. by J. Bartram, J. Cotruvo, M. Exner, C. Fricker and A. Glasmacher, IWA Publishing, London, UK.

Verstraeten I.M., Th. Heberer, and T. Scheytt (2002) Occurrence, characteristics, and transport and fate of pesticides, pharmaceutical active compounds, and industrial and personal care products at bank-filtration sites. In Riverbank Filtration—Improving Source-Water Quality, chapter 9, eds. C. Ray, G. Melin, and R.B. Linsky. Dordrecht, Netherlands: Kluwer Academic Publishers.

Weiss W. J., E. J. Bouwer, W. P. Ball, C. R. O´Melia, R. Aboyetes and T. F. Speth (2004) Riverbank filtration : Effect of ground passage on NOM character. J. Water Supply: Res. T., 53(2), 61-83.

Wesnigk, J.B., M. Keskin, W. Jonas, K. Figge, G. Rheinheimer (2001) Predictability of Biodegradation in the Environment: Limits of Prediction from Experimental Data. in Biodegradation and Persistence. ed. B. Beek, Springer-Publishing, Berlin-Heidelberg, Germany.

Wischnack S. and M. Jekel (2000) Untersuchungen zu iodierten organischen Stoffen im Tegeler See und im Wasserwerk Tegel. Final report of a research project founded by the Berlin Water Works, TU Berlin, Department of Water Quality Control, February 2000

Ziegler D. (2001) Untersuchungen zur Nachhaltigkeit der Uferfiltration und künstlichen Grundwasseranreicherung in Berlin. (Investigations on the sustainability of bank filtration in Berlin's water cycle), Doctoral Dissertation accepted by: Technical University of Berlin, School of Process Sciences and Engineering, 2001-04-24. http://edocs.tu-berlin.de/diss/2001/ziegler_doerte.htm

Ziegler D., C. Hartig, S. Wischnack and M. Jekel. 2002. Organic substances in partly closed water cycles. In Management of Aquifer Recharge for Sustainability. ed. P. Dillon. Sweets & Zeitlinger, Lisse.

Zöfel P. (2002) Statistik verstehen. (Comprehensive statistics), Addison-Wesley, Munich, Germany

3 Appendix

5

Retention and elimination of cyanobacterial toxins (microcystins) through artificial recharge and bank filtration.

"algae" group: Federal Environmental Agency of Germany (UBA)

Responsible project leader: Dr. Ingrid Chorus, Dr. Hartmut Bartel

Content

List of Figures

5

8

9

List of Tables

1 Analytical Methods for Microcystin Analysis

1.1 Introduction

Among the known cyanotoxins (cyanobacterial toxins or toxins produced by blue-green-algae), the hepatotoxic cyclic peptides called microcystins are considered to occur most commonly (Sivonen & Jones 1999). Their general structure reads as follows: Cyclo-(D-anlanine[1]-X²-C-MeAsp³-Z⁴-Adda⁵-D-glutamate⁶-Mdha⁷) with X and Z being variable L-amino-acids (Figure 1). So far 70 structural variants have been identified from natural samples (Sivonen & Jones 1999) with microcystin-LR and microcystin-YR being the most toxic so far (LD_{50} i.p. mouse (µg/kg) = 50, Botes et al. 1985).
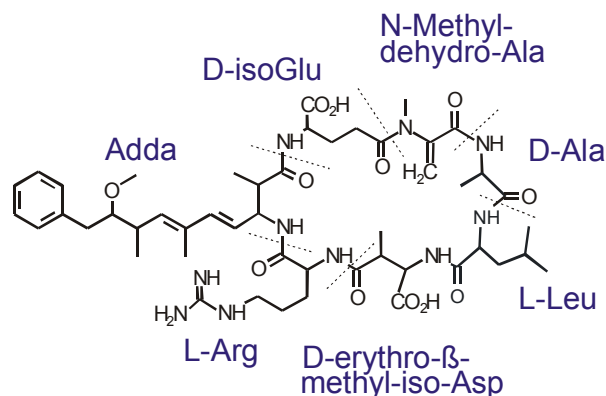
Figure 1: **Structure of MCYST-LR.**

In the NASRI project, different methods of analysis were used to determine microcystin (MCYST) concentrations in water from the field sites and from the experiments (see final report working group algae, part I to VII). These will be described below (chapter 1.2). Some results were, however, surprising and not always unambiguous. This and possible reasons will be discussed in chapter 3.

1.2 Analytical Methods for MCYST Analysis

In most cases microcystin analyses were carried out by ELISA (Enzyme-Linked ImmunoSorbent Assay) and HPLC (High Performance Liquid Chromatography) with a photodiode array (PDA) detector. In the field experiments samples were first tested for their microcystin content using the ELISA and selected ones subsequently analyzed by HPLC to verify the results and distinguish the different MCYST variants. Structural identification of MCYST variants was carried out by MALDI-TOF MS (Matrix Assisted Laser Desorption Ionization Time-of-Flight Mass Spectrometry).

1.2.1 Sample preparation

The water samples for analysis of **total microcystins** (i.e. extra-cellular plus cell-bound) were deep frozen and thawed in order to release cell-bound microcystins, filtered by membrane filters (RC 55, pore size 0.45 µm) and either analyzed directly (ELISA) or enriched by solid phase extraction (SPE) over C_{18}-cartriges according to Harada et al. (1999). If analysis or SPE was not possible within 24 h the samples were stored deep frozen (-18 °C).

For analyzing the **extra-cellular microcystins** samples were filtered (RC 55, pore size 0.45 µm) directly after sampling and then stored deep frozen for subsequent analysis by ELISA or HPLC. In most cases (all samples with exception of those obtained in the microbiological degradation experiments - see part VII) samples for HPLC analysis were filtered again after thawing (RC 55, 0.45 µm pore size) and then enriched via C_{18}-SPE (see above).

Samples for determination of **cell-bound microcystins** were filtered (membrane filter, RC 55, pore size 0.45 µm) immediately after sampling and the filter stored deep frozen until further treatment. The extraction procedure of the filters is described in Fastner et al. (1998).

1.2.2 ELISA (Enzyme-Linked-ImmunoSorbent Assay)

Two different ELISAs were used in the course of the project:

1. MCYST-ELISA, responding to a structural element typical only for MCYST as a cyclic peptide.
2. Adda-ELISA, responding to the adda-group typical for MCYST, but possibly also present in degradation products.

Usually the samples were first analyzed by Adda-ELISA and those with positive results subsequently analyzed by MCYST-ELISA. As the MCYST-ELISA and the HPLC analysis showed comparable results for the sum of different MCYST variants (with exception of some false negative ELISA results due to technical problems, see chapter 1.3.2) and an HPLC analysis gives further information on the different MCYST variants present, the MCYST ELISA was omitted from the analytical program after the first series of experiments.

1.2.2.1 MCYST-ELISA

The method applied was developed by the Technical University of Munich and is described in Zeck et al. (2001). It is based on an immunological reaction with a [4-arginine]MCYST-specific antibody. This antibody has a strong binding (cross reactivity, see Zeck et al. 2001) only with intact microcystin molecules containing an arginine at the 4th position in the cyclic peptide. It therefore does not react with degradation products.

Standard solutions with known concentrations of MCYST-LR as well as solutions without MCYST (blanks, deionized water) were applied to each plate and each calibration point of the calibration curve as well as each sample value was determined by calculation of the

12

arithmetic mean of the data (n = 2 to 4). Standard curves were obtained by fitting the calculated averages to a four parameter function according to Zeck et al. (2001).

The range of determination lies between about 0.1 µg/L and 1.0 µg/L (for details see chapter 3)and was determined for each plate separately. In case of concentrations exceeding 1.0 µg/L the sample was diluted with deionized water for repeated analysis.

1.2.2.2 Adda-ELISA

The Adda-ELISA used was a generic microcystin immunoassay based on monoclonal antibodies against the unusual adda group characteristic for microcystins, nodularins and certain peptide fragments (Zeck et al. 2002). The concentrations measured therefore comprise MCYST as well as possible degradation products. Calibration and determination of blind values was done following the method described for the MCYST-ELISA.

The range of determination also lies between about 0.1 µg/L and 1.0 µg/L (for details see chapter 3). As for the MCYST ELISA each value was determined as the average of two or three parallels taken from the same sample.

1.2.3 HPLC

After C_{18}-SPE (see above) the microcystin variants were analyzed by HPLC - photodiode array detection (PDA) and identified by means of their characteristic UV-spectra (Lawton et al. 1994). A Waters 616 solvent delivery system with 717 WISP autosampler and a 991 photo diode array detector by Waters (Eschborn) was used. The separation was carried out on a LiCrospher® 100, ODS, 5 µm, LiChroCART® 250 – 4 column system at a flow rate of 1 mL/min. The detection limit amounted to 0.1 µg/L.

1.2.4 MALDI-TOF (Matrix Assisted Laser Desorption Ionization Time-of-Flight Mass Spectrometry)

For structural identification a MALDI-TOF MS analysis was carried out in selected samples subsequently to the separation by HPLC according to am method by Fastner et al. (1999).

1.3 Analytical Problems / Open Questions

1.3.1 Values below detection limit and limit of quantification (ELISA)

The detection limits for the ELISA were calculated for each plate separately according to the 3s definition using the mean value of the blanks measured in parallel (n = 11) and setting the detection limit as the 3-fold standard deviation. Depending on various factors like water matrix, temperature or age of reagents, the detection limits varied between 0.04 µg/L and 3.59 µg/L for the Adda-ELISA and 0.02 µg/L and 0.42 µg/L for the MCYST-ELISA. The

median values were 0.2 µg/L and 0.09 µg/L, respectively. The limits of quantification were calculated as the 3-fold detection limit, thus ranging from 0.12 µg/L to 10.77 µg/L (Adda-ELISA) and from 0.06 µg/L to 1.26 µg/L (MCYST-ELISA) In cases of unusually high detection limits (> 1 µg/L) analyses were repeated.

In the field samples from the transects at Lake Tegel and Lake Wannsee, the majority of the values measured were below the limit of quantification. In agreement with the other NASRI working groups, the results for these samples were set to half the limit of quantification and those below detection limit were set zero for the statistical calculations. For the diagrams showing median values and 90th percentile (see final report "algae", part I) values below detection limit were labeled "n.d." (not detected) and values below quantification limit were labeled "T" (for traces). In cases of only one value below quantification limit (and the others not detectable), the exact quantification limit was given (e.g. < 0.22 µg/L).

1.3.2 Comparability of ELISA and HPLC Results

The MCYST-ELISA was performed in parallel to HPLC analysis only during the first field scale experiments (SSF 2, SSF 5, SSF 6 and E 1). Figure 2 shows the results of both methods in relation to each other. Two groups of data points can be distinguished: one group showing a good correlation between ELISA and HPLC-results and a second one with only very little MCYST detected by ELISA and values of up to nearly 2 µg/L by HPLC.

For the first group the regression coefficient amounts to 0.93995. The gradient of the linear regression curve is, however, only 0.18, showing that ELISA results exceed those measured by HPLC by a factor of about five. This is only secondarily due to losses during C_{18} solid phase extraction, as this account for losses only between 10 and 20 %. The main reason for the distinctively higher values by ELISA is probably the varying response of the ELISA to the different MCYST variants and the fact that the ELISA responds to the sum of all MCYST variants present, while the HPLC gives only results for variants present in concentrations above 0.1 µg/L.
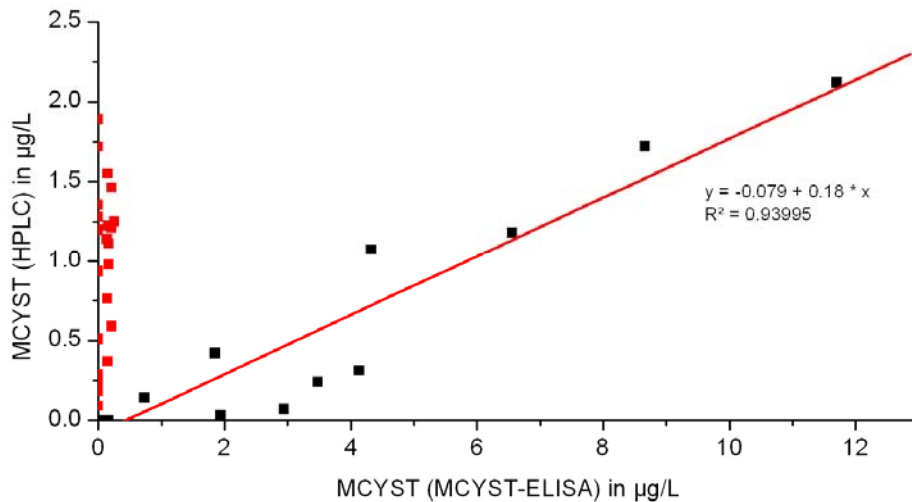
Figure 2: ELISA and HPLC analysis in relation

The second group of data points in Figure 2 was due to analytical problems with the ELISA in summer 2003, during which the temperature in the laboratory exceeded the optimal range of 20° to 25°. This problem was solved in the following summer by using a laboratory with air conditioning.The regression coefficient between results obtained by Adda-ELISA and those acquired by HPLC amounted to 0.24 - showing only very little agreement of both methods. This is due to the fact that the Adda-ELISA responds to all substances with the Adda-group, i.e. also to possible degradation products of MCYST (Zeck et al. 2002).

For this reason the field samples from the transsects Wannsee and Tegel were analyzed first by Adda-ELISA and in case of positive signals, also by MCYST ELISA, thus yielding first all substances containing the Adda-group (i.d. MCYST and possible degradation products) and in a second step MCYST only. As only very low concentrations were expected to occur in the groundwater samples, HPLC-analysis was restricted to an intensive sampling campaign at Lake Wannsee in autumn 2004 (see final report "algae" part I).

In order to allow analysis with HPLC, higher input levels of MCYST were aimed at in the field scale experiments on the enclosures and SSF of the UBA's experimental field (final report "algae", parts IV and V). Thus, the ELISA (in most cases the Adda-ELISA) gave a first impression on the distribution of MCYST in the samples over time (up to 250 samples were taken during one field scale experiment). Subsequently selected samples were analyzed by HPLC yielding further information on the concentrations of the different MCYST variants and higher precision than the ELISA (see above). In most cases the results of the HPLC analysis were used for the modelling and elimination calculations.

In the laboratory experiments (final report "algae", parts VI and VII) the small sampling volume was the restricting parameter. For the clogging column and temperature column

15

experiment this allowed for ELISA analysis only, as realistic MCYST concentrations (< 1 µg/L) were targeted in the effluent. For the batch degradation experiments the input concentrations (about 50 mg/L) were sufficient to conduct HPLC analysis without further concentration by solid phase extraction.

1.3.3   Appearance of new peaks in the HPLC Chromatogram

During the experiments the HPLC analyses yielded surprising results concerning the different MCYST variants: While the input solution showed a dominance of demethylated MCYST-RR (dem. [Asp³] MCYST RR) which is the main variant produced by the cultured *Planktothrix agardhii* HUB 76, a large number of new peaks appeared in the HPLC chromatogram of the effluent samples with UV spectra characteristic for MCYST (Figure 3).

This phenomenon was observed in all experiments in which an HPLC analysis of the effluent samples was carried out (enclosure and SSF experiments as well as the batch degradation experiments). The number of variants and the exact retention time varied, however, from experiment to experiment as well as between different series of measurements. Therefore, experiments were carried out to clarify whether the filtration process actually leads to shifts in MCYST variants or whether this observation is based on an artefact caused by the analytical method.
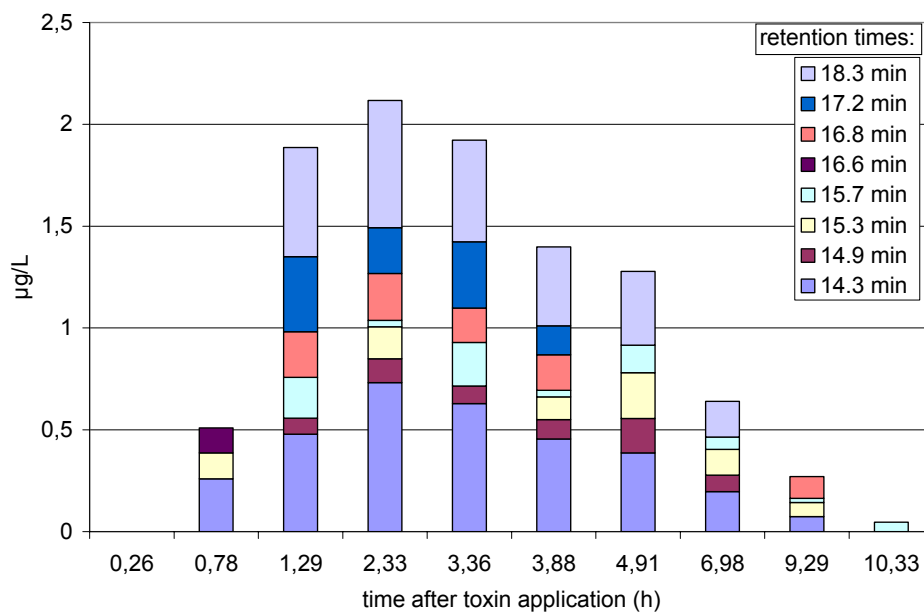
Figure 3:   **Peaks in the HPLC chromatogram with UV spectra characteristic for MCYST in samples from experiment E2 (sampling port in 20 cm depth). The input solution showed only one peak at 13.6 minutes retention time (corresponding to dem. [Asp³] MCYST-RR) which was no longer detected in the effluent.**

An explanation could be that due to the dominance of dem. MCYST-RR in the input solution other MCYST variants (or substances with similar UV-spectra) were not well separated in the HPLC and thus not detectable (or "hidden"), though present in low concentrations. For this reason, a MALDI-TOF analysis were carried out with the extract from the *Planktothrix agardhii* mass culture, first with the total sample and in a second step with previous separation by HPLC PDA. Then the same analyses were carried out with effluent samples after HPLC-PDA separation. The input solution showed the same molecular masses in the total sample and in the previously separated peaks. These were, however, different from the molecular masses detected in the effluent samples, indeed indicating that the substances present in the effluent samples had not been present in the input samples and that they represent (potentially intermediate) degradation products.

An identification of the substances present in the effluent samples was not possible, as the molecular masses did not correspond to known MCYST variants. Clarification of the mechanisms causing this result is important for understanding MCYST degradation and will have to be subject of further research.

In the field experiments all new HPLC peaks showed similar degradation rates to MCYST so that persistence of these degradation products does not seem likely under the conditions simulated. During the anoxic batch degradation experiments, however, the new substance persisted over a period of more than 20 days (see final report "algae", part VII). Here further degradation experiments as well as toxicological tests will be needed in order to assess whether or not this degradation product is of any relevance to human health in bank filtrated drinking water, if it should occur in sufficiently high concentrations.

1.4   References

Botes, D.P., Wessels, P.L., Kruger, H., Runnegar, M.T.C., Santikarn, S., Smith, R.J., Barna, J.C.J. & Williams, D.H. (1985): Structural studies on cyanoginosins-LR, -YR, -YA and YM, peptide toxins from Microcystis aeruginosa, J.Chem. Soc, Perkin Transactions, I: 2747 – 2748.

Fastner J., Erhard M., Carmichael W.W., Sun F., Rinehart K.L., Rönicke H. & Chorus I. (1999): Patterns of different microcystins in field samples dominated by different species of cyanobacteria., Arch Hydrobiol 145 (2): 147 – 163.

Fastner, J., Flieger, I. & Neumann, U. (1998): Optimised extraction of microcystins from field samples - a comparison of different solvents and procedures. Wat. Res. **32**: 3177 - 3181.

Harada, K., Kondo, F. & Lawton, L. (1999): Laboratory analysis of cyanotoxins. – in: Chorus, I. & Bartram, J. (eds): Toxic cyanobacteria in water – a guide to their public health consequences, monitoring and management: 369 – 405. E & FN Spon.

Lawton, L.A., C. Edwards, G.A. Codd (1994): Extraction and high-performance liquid chromatographic method for the determination of microcystins in raw and treated waters, Analyst, 119: 1525 – 1530.

Sivonen, K. & Jones, G. (1999) Cyanobacterial Toxins, Toxic Cyanobacteria in Water, A Guide to their public health consequences, monitoring and management, I. Chorus & J. Bartram (eds.) The World Health Organization, E &FN Spon, London, p. 41-112.

Zeck, A., Eikenberg, A., Weller, M.G., & Niessner, R. (2001): Highly sensitive immunoassay based on a monoclonal antibody specific for [4arginine]microcystins. - Analytica Chimica Acta, **441**: 1 - 13, Elsevier.

Zeck, A., Weller, M.G., Bursill, D. & Niessner, R. (2002): Generic microcystin immunoassay based on monoclonal antibodies against Adda. - The Analyst, **126**: 2002 - 2007.

2 Field Investigations on Transsect Lake Tegel

2.1 Introduction

Monitoring of Lake Tegel's surface water with respect to cyanobacterial toxins was conducted with the aim of triggering bank filtrate monitoring in case of toxic cyanobacterial blooms. Previous investigations had shown that during the last few years (unpublished data of our own working group) cyanobacterial blooms have no longer been occurring in Lake Tegel (though minor populations have been present every summer, and temporarily increased concentrations of total P in 2000 and 2001 provided a carrying capacity sufficient to sustain major populations).

2.2 Results and Interpretation

Figure 4 shows the total and extracellular MCYST-concentrations measured by Adda-ELISA as well as measurements with MCYST-ELISA of total MCYST in 2002. These samples were taken during the monthly sampling campaign of the NASRI project and originate from the lake shore in front of the transsect.
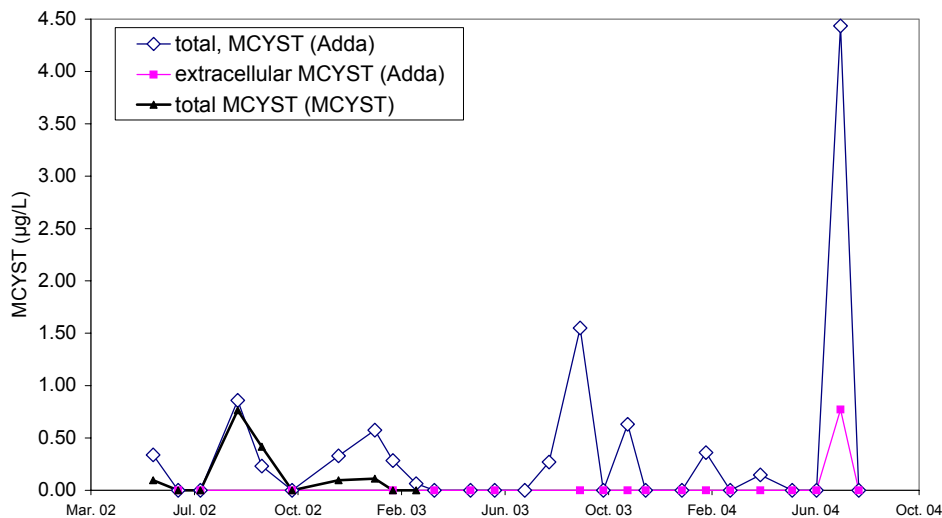
Figure 4 : Total and extracellular Microcystin (MCYST) concentrations determined with different ELISAs (specifically for ADDA and for the MCYST molecule) in Lake Tegel's surface water 2002 - 2004.

These results show

- concentrations measured by MCYST-ELISA are usually lower than those determined by Adda-ELISA. This in accordance with the theory that MCYST degradation products still containing the Adda-group are detected by this ELISA additionally to microcystins themselves. For 2003 and 2004 the analyses therefore were carried out by Adda-ELISA only, giving the worst-case concentration.

- Maximum concentrations were usually measured during July (2004), August (2002) or September (2003), although in winter 2002/2003 traces were also observed in November through January. Measurements carried out by our working group in the context of a different programme in the lake centre (analyses done by HPLC) show a similar pattern although with distinctively lower values (Figure 5). Maximum concentrations measured by HPLC lie around 0.1 µg/L whereas those measured by ELISA reach 1.5 µg/L (2003) and 4.5 µg/L (2004).
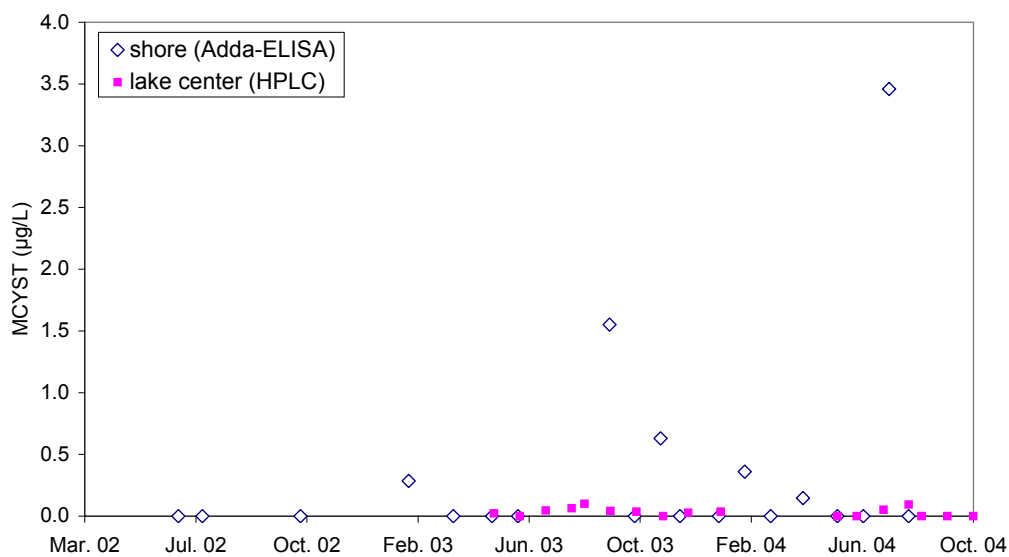
Figure 5 : Cell-bound MCYST for samples taken from the shore, analysed with ADDA-ELISA, and the lake centre, analysed with HPLC.

This is most likely to be due to two factors: i) some portion of the MCYST identified by the Adda-ELISA might result from degradation products and ii) due to wind and currents cyanobacteria tend to accumulate near the eastern shore of Lake Tegel, thus leading to higher toxin concentrations.

The reason for elevated MCYST concentrations during the summer months is shown in Figure 6. Usually high densities of toxic cyanobacteria (in Lake Tegel the only toxic species of relevant population density is Microcystis spp.) coincide with elevated

20

microcystin concentrations. This is true for August 2002, August/September 2003 and July 2004. On other occasions however high densities of cyanobacteria did not lead to elevated MCYST concentrations (July 2003). This is true for samples taken from the lake centre as well as from the shore, so regional variability might not be the primary cause. The main reason therefore seems to be that different toxin concentrations per cell or dominance of subspecies with different toxin content can occur throughout the season.
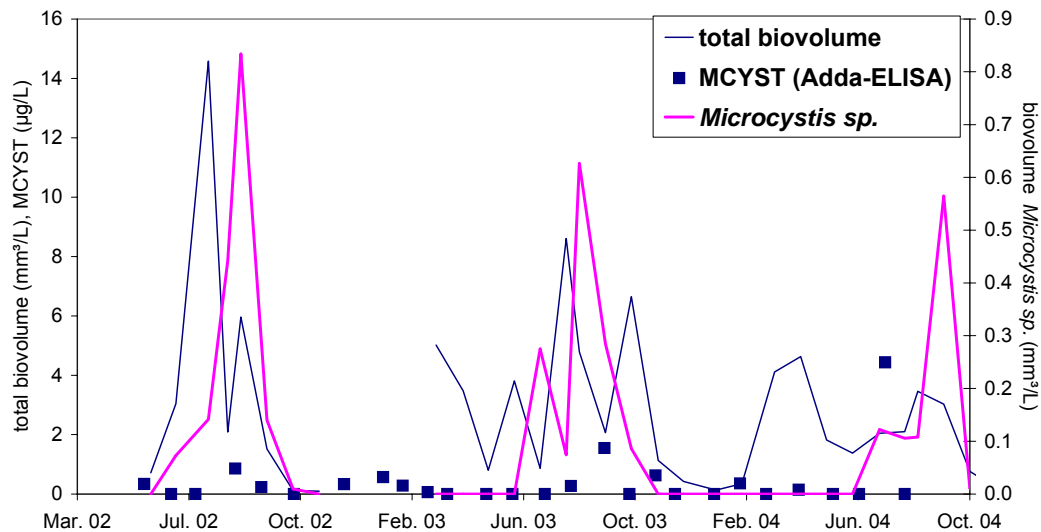
Figure 6 Total phytoplankton biovolume, total MCYST determined by Adda-ELISA (left axis) and biovolume of toxic cyanobacteria Microcystis sp. (right axis) in Lake Tegel.

- extracellular MCYST was usually not detected in the surface water samples. The only occasion with detectable extracellular MCYST was in July 2004, when total MCYST reached 4.5 µg/L and extracellular MCYST amounted to 0.77 µg/L (22 %). Although this inverse ratio is unusual (according to Sivonen & Jones, 1999, the share of extracellular MCYST usually amounts to less than 10 %), it is not unlikely that unfavourable conditions (low temperatures, aging population) can trigger some cell lysis and MCYST release from the cells. On the other hand degradation products that are possibly included by Adda-ELISA measurement are likely to occur outside the cyanobacterial cells thus leading to higher extracellular concentrations.

2.3   Conclusions

Although toxic cyanobacteria occur in Lake Tegel, their share of total biovolume in the years 2002 to 2004 seldom exceeded 10 %. Maximum shares of 20 % to 30 % usually occurred during July, August or September and led to microcystin concentrations measured by Adda-ELISA of less than 1.5 µg/L in 2002 and 2003 on the eastern shore next to the transect. As previous investigations (Chorus et al. 2004) had shown that these concentrations are not high enough to be recovered in the observations wells, groundwater samples from transect Tegel were not analysed during the project.

We recommend, however, to continue surface water sampling in order to ascertain that the input MCYST concentrations for the Lake Tegel bank filtration as well as the artificial recharge site remain on this level.

2.4   References

Chorus, I., Grützmacher, G., Wessel, G. & Pawlitzky, E. (2004): BMBF-Forschungsvorhaben: Strategien zur Vermeidung des Vorkommens ausgewählter Algen- und Cyanobakterienmetabolite im Rohwasser – Abschlußbericht - . BMBF-Förderkennzeichen 02 WT9852/7.

Sivonen K. & Jones G. (1999): Cyanobacterial Toxins, in: Toxic Cyanobacteria in Water, A Guide to their public health consequences, monitoring and management, I. Chorus & J. Bartram (eds.) The World Health Organization, E &FN Spon, London, p. 41-112.

3 Field Investigations on the Transects at Lake Wannsee

3.1   Introduction

Investigations of cyanobacterial toxin removal at the Lake Wannsee Transects required a detailed monitoring of cyanobacterial biovolume in the surface water because of their high temporal variation. For this reason weekly to fortnightly sampling of surface water was carried out during the summer months in addition to the monthly sampling of ground- and surface water by BWB. The aim was not only to obtain detailed information on cyanobacteria and microcystin concentrations in Lake Wannsee, but also to trigger a weekly sampling campaign for one month during autumn 2003 subsequent to a cyanobacterial bloom with high toxin concentrations.

3.2   Results and Interpretation

3.2.1   Surface water

The results of the weekly to fortnightly surface water monitoring conducted by our working group are presented in Figure 7. The data for the biovolume of cyanobacteria show distinct cyanobacterial blooms during summer in all three years. During July and August Microcystis sp. prevailed (in 2003 also Aphanizomenon sp.), in September and October Planktothrix agardhii dominated the cyanobacterial population. Maximum biovolumes ranged from 18 mm³/L to nearly 50 mm³/L total cyanobacteria which correspond to similar values in the years 1999 - 2002 observed by our own working group (pers. communication Kurmayer). The unusually warm and dry summer of 2003 resulted in a bloom of Aphanizomenon, which was not present in the other years. As this species does not produce microcystin (MCYST), concentrations of this toxin during July and August were lower in 2003 than in the other years.

Highest MCYST concentrations were usually found during the Planktothrix bloom in September and October, reaching maximum values of 10 µg/L to 14 µg/L of intracellular MCYST (determined by HPLC) in the water body of the lake. Samples taken from scums accumulating near the shore during a bloom on Sept. 15th 2003 showed significantly higher concentrations, i.e. up to 29 µg/L intracellular MCYST (determined by HPLC). At this occasion also extremely high values of extracellular MCYST concentrations were determined (12 µg/L). One week later intracellular concentrations at this spot had decreased to 19 µg/L and extracellular values reached only 1.5 µg/L (see appendix).

The concentrations measured by ADDA-ELISA also showed peaks during summer. Their time patterns correspond to those determined by HPLC, although generally they tended to be somewhat higher (maximum values reached more than 20 µg/L in 2004). As the ELISA cannot distinguish between pure ADDA and MCYST-breakdown products containing the ADDA-moiety, in the following the signal of this ELISA is interpreted as reflecting concentrations of "ADDA-containing substances" (see also methods). Extracellular ADDA-containing substances occurred in unusually high shares (more than 80% of the total concentrations in September 2003). Although artefacts in sample preparation (see below) cannot totally be excluded, this may be explained by the fact that the ADDA-ELISA responds to MCYST degradation products that are not expected to occur inside the cells.
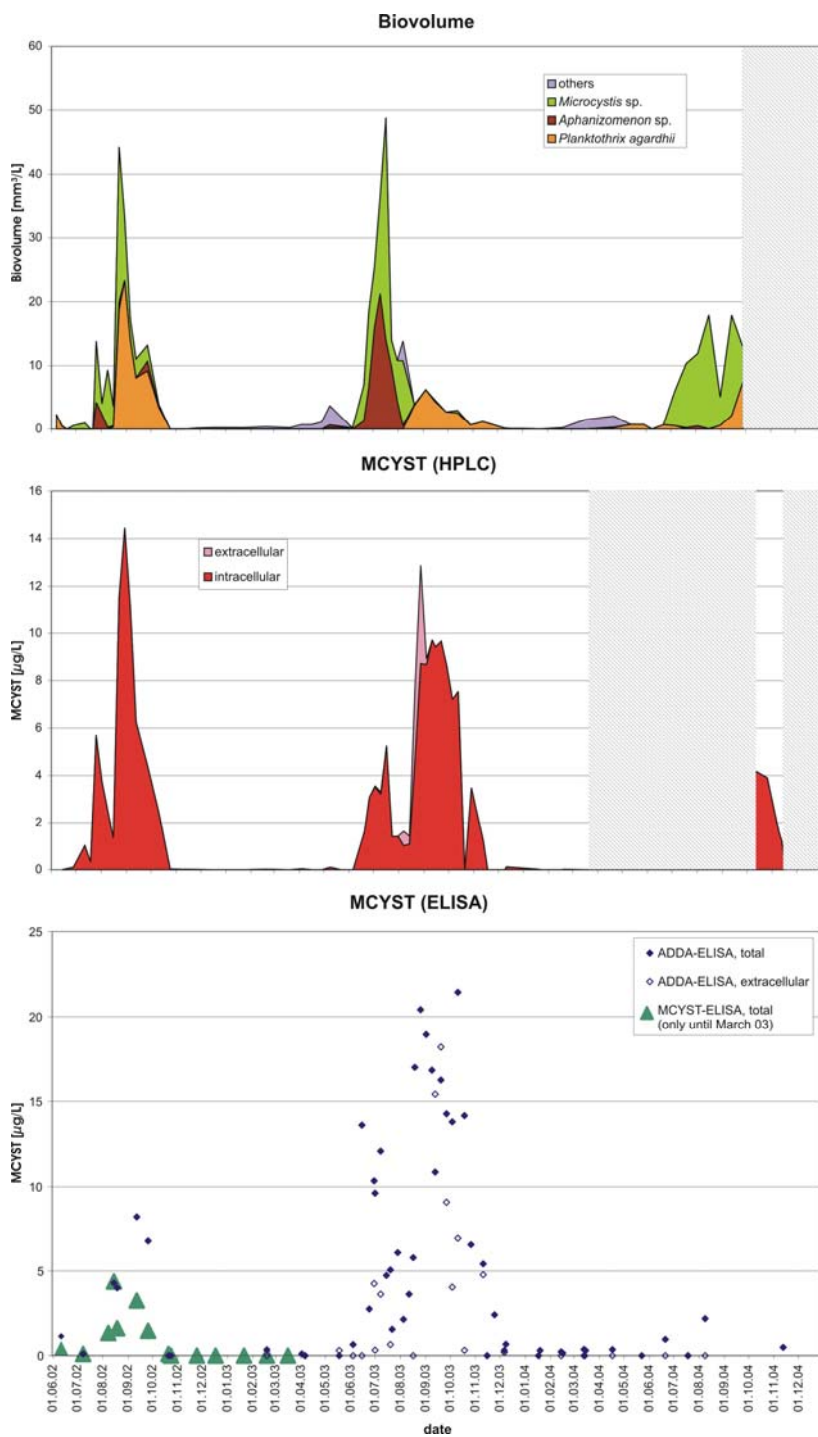
Figure 7: Results of the surface water monitoring at Lake Wannsee: Biovolume of cyanobacteria and MCYST analysed by HPLC and ELISA. (Mean values of up to 4 samples from different places on one occasion. Shaded areas: no data.)

For summer (May through October) of all three years, the median input value for MCYST determined by HPLC into the bank filtration system at Lake Wannsee amounted to 3.4 µg/L and < 0.1 µg/L for intra- and extracellular MCYST, respectively (see Table 1). High values for the 90th percentile of 9.6 µg/L for intracellular and 0.6 µg/L for extracellular MCYST reflect the substantial temporal variability. During winter (November through April) the median concentration of intra- and extracellular MCYST amounted to less than 0.1 µg/L.

Table 1 Median values and 90th percentile for summer and winter concentrations of MCYST in Lake Wannsee's surface water determined by HPLC, MCYST-ELISA and ADDA-ELISA.

MCYST in µg/L	summer		winter	
	intracellular	extracellular	intracellular	extracellular
HPLC				
median	3.4	< 0.1	< 0.1	< 0.1
90th percentile	9.6	0.6	0.1	< 0.1
number of analyses	42	21	16	10
	total	extracellular	total	extracellular
MCYST-ELISA				
median	0.51		< 0.21	
90th percentile	3.26		< 0.21	
number of analyses	11	0	5	0
ADDA-ELISA				
median	5.1	0.3	0.2	< 0.5
90th percentile	16.9	11.6	0.7	2.5
number of analyses	39	17	21	6

3.2.1.1   Groundwater

Figures Figure 8 to Figure 10 give a summary of the results obtained by determination of total and extracellular MCYST with the MCYST-ELISA (Figure 8) and the ADDA-ELISA (Figure 9 and Figure 10).

In transect 1, MCYST determined by MCYST-ELISA was only detected in observation well 3339 which is the well with the shortest travel time (figure 2). Detectable traces (< 0.1 µg/L) were observed in samples taken in September and October 2002, simultaneously to the Planktothrix bloom in the surface water (Figure 7. MCYST and ADDA-containing substances determined by ADDA-ELISA were also detected in the adjacent observation wells 3338 and 3337 with slightly longer travel times (Figure 9). The 90th percentile values of 0.22 µg/L and 0.04 µg/L of extracellular ADDA-containing substances show that there is some migration of MCYST degradation products into the aquifer (Figure 10). These are however retained in the

subsurface as no more values above detection limit were found in the other observation wells nearer to the drinking water production well.

In transect 2, MCYST determined by MCYST-ELISA was found in the one-time samples taken from BEE207OP and BEE207MP1 in January 2003 that are situated in the usually unsaturated zone beneath the lake (Figure 8). In both cases the values cannot be quantified (< 0.58 µg/L and < 0.06 µg/L), but there are, however, clear positive signals above detection limit. The only other observation well on the western side of the drinking water production well with detectable MCYST was BEE202MP2 with a value slightly above detection limit (0.02 µg/L) in January 2003. This value was not confirmed with the ADDA-ELISA, however, this might be due to its higher detection limits. A single positive value > 0.2 µg/L (detection limit) in BEE204OP on the eastern side of the drinking water production well was not confirmed by the ADDA-ELISA. This might have been due to interferences with the groundwater matrix leading to a false positive signal, as usually the trend was towards higher values with the ADDA-ELISA as compared to the MCYST-ELISA.

ADDA-containing substances were detected in the observation wells BEE205, BEE206, BEE207OP, MP1 and UP as well as in BEE202MP1 and MP2 (Figure 9). With exception of a value of 1.38 µg/L measured in BEE207UP in December 2003, no concentrations could be quantified (< limit of quantification). The number of observation wells with detectable traces is clearly higher than for the MCYST-ELISA. This shows that this ELISA responds to a higher number of substances which are probably MCYST degradation products.

Extracellular ADDA-containing substances could not be detected in the groundwater of transect 2, with exception of one value of < 0.6 µg/L on the eastern side of the drinking water well. This is most likely a false positive, as it is unlikely that i) degradation products remain inside cyanobacterial cells and ii) cyanobacterial cells can travel this far in the subsurface. The conspicuous absence of concentrations detectable with the ADDA-ELISA may be a methodological artefact. Potentially the ADDA-containing substances are retained on the membrane filter material used for pre-treatment. This could be due to either adsorption on the membrane filter or adsorption on suspended particles. These results show a need for specifically targeted investigations of behaviour of trace concentrations of extracellular MCYST in the laboratory system, which are intended in the context of future research. This uncertainty of the results in these minimal concentration ranges need to be taken into account for data interpretation.
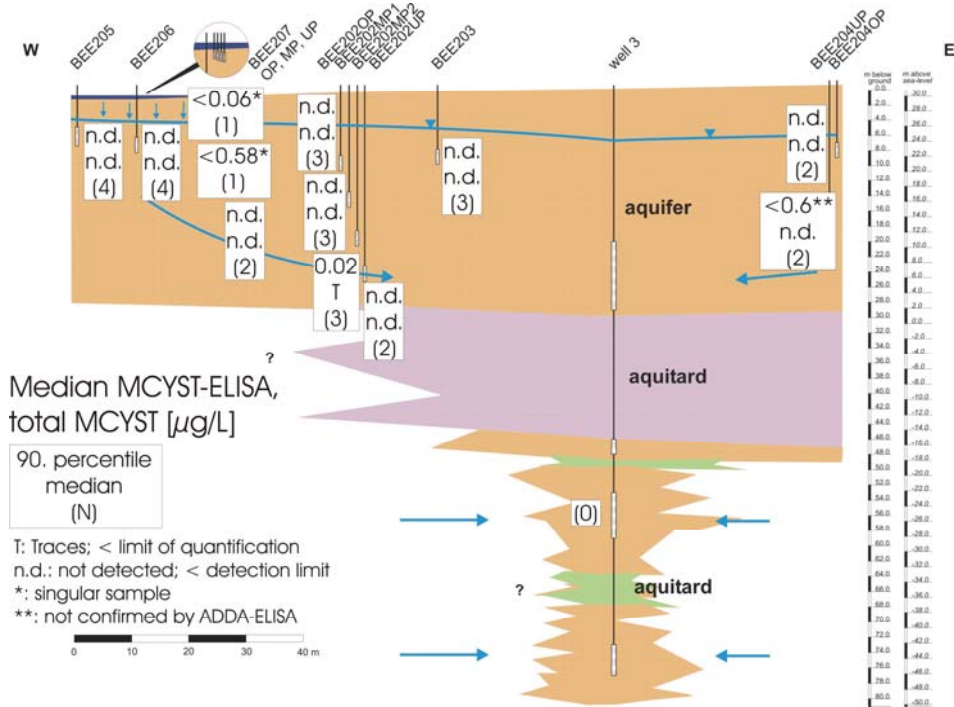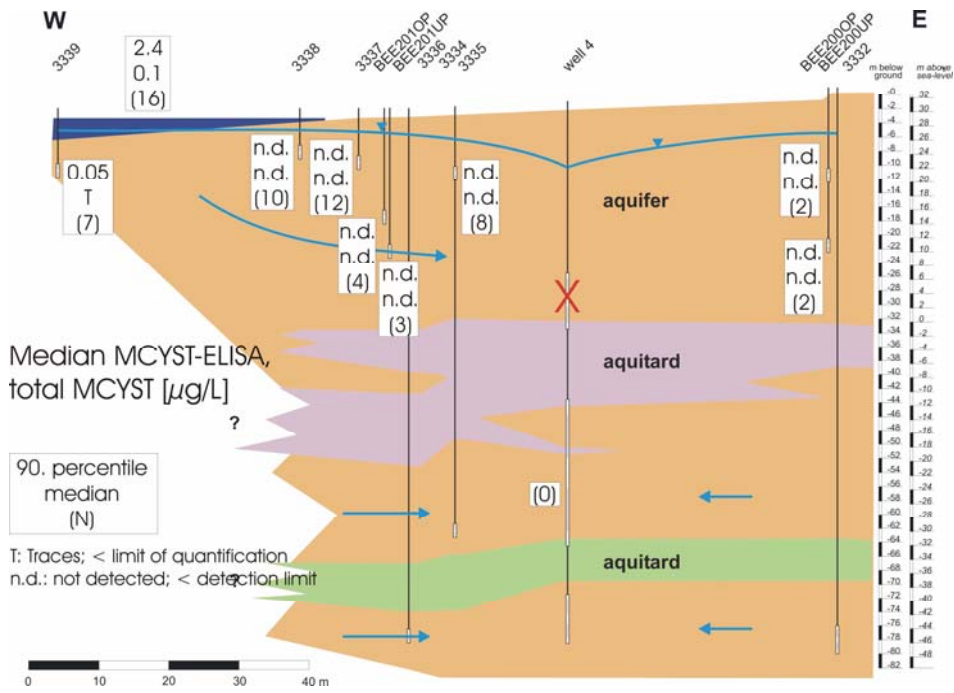
Figure 8: Results of total MCYST at transect 1 and 2, analysed by MCYST-ELISA (May 2002 to August 2004).
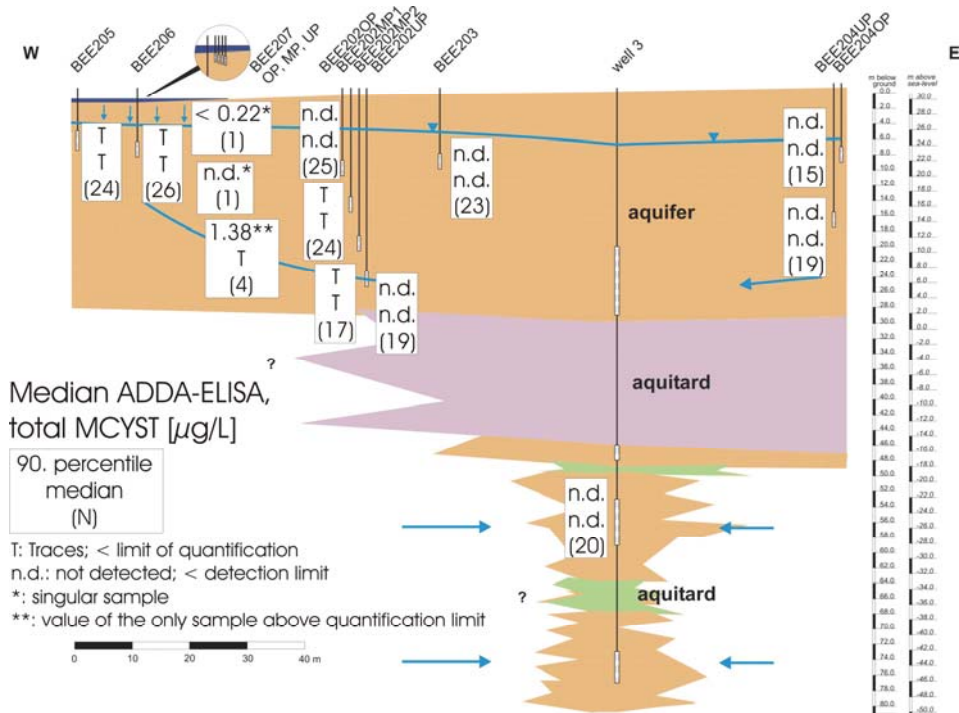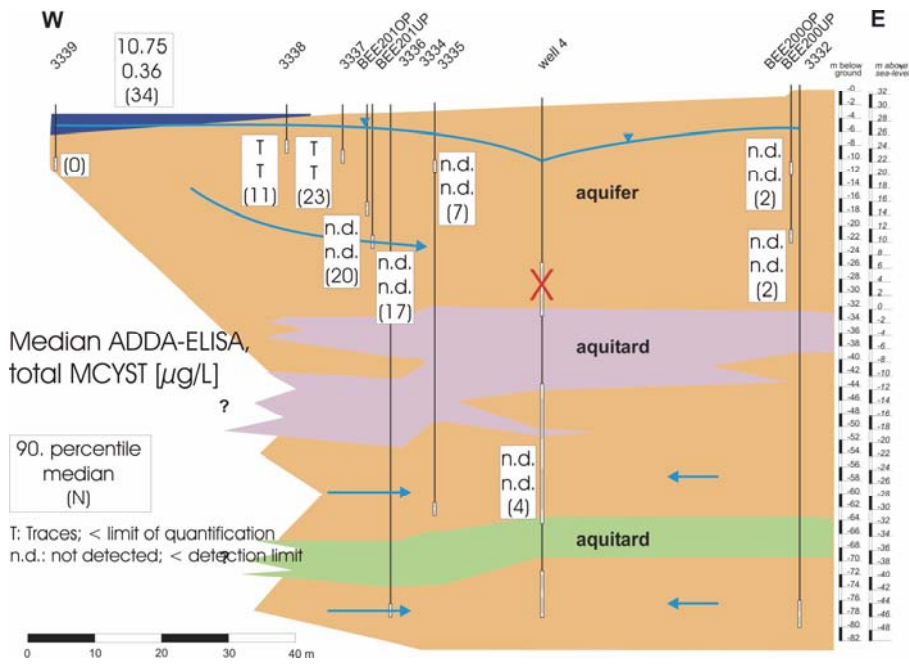
Figure 9: Results of total MCYST at transect 1 and 2, analysed by ADDA-ELISA (May 2002 to August 2004).
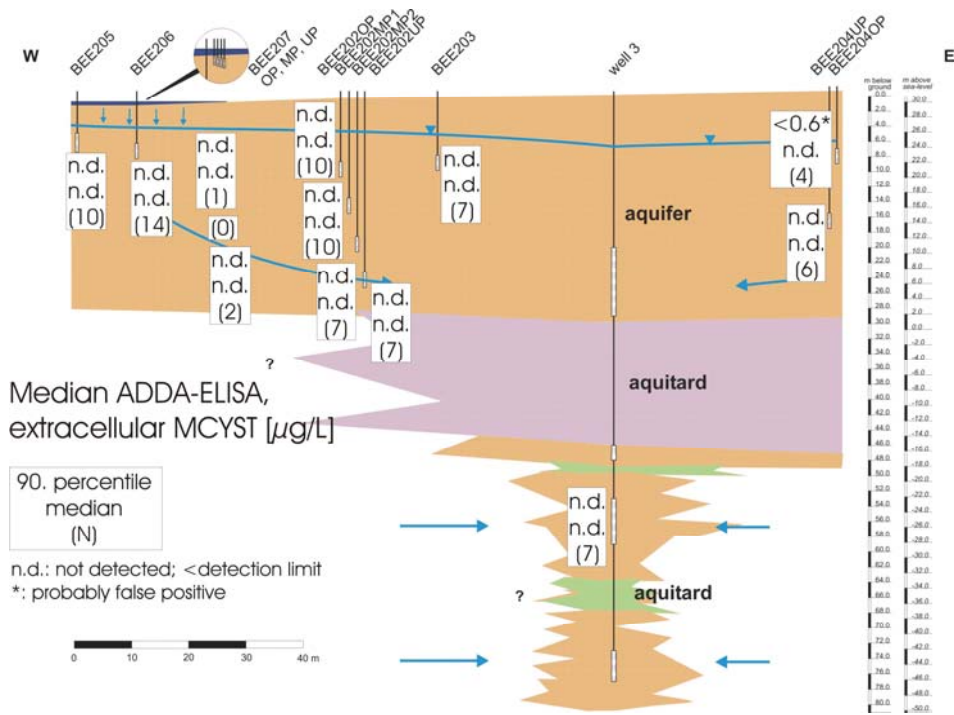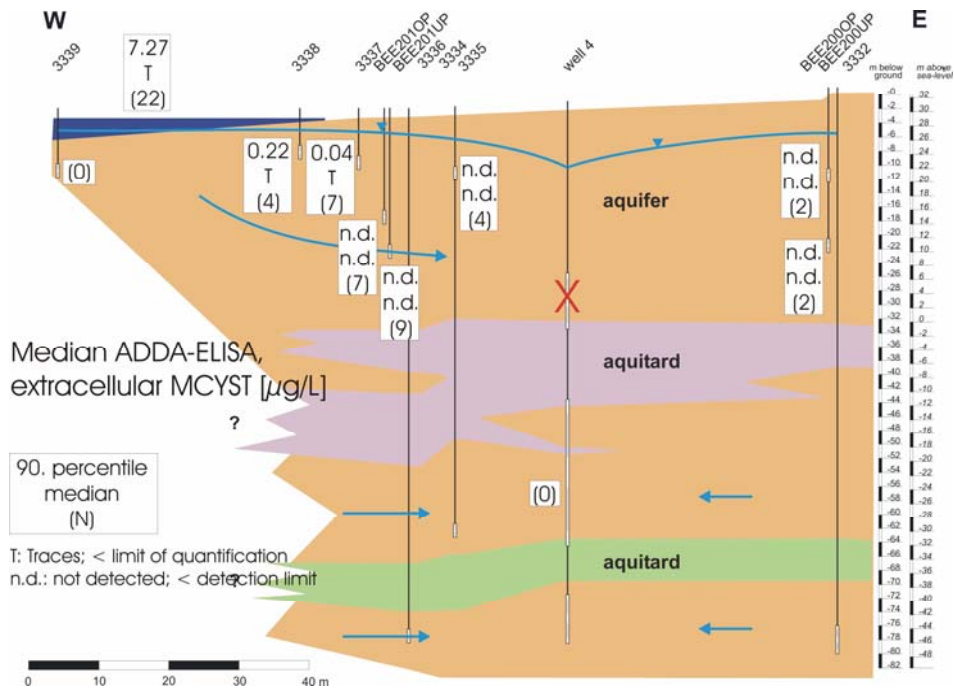
Figure 10: Results of extracellular MCYST at transect 1 and 2, analysed by ADDA-ELISA (May 2002 to August 2004).

About one month after a bloom of cyanobacteria in 2003, weekly sampling of selected shallow observation wells of the transects was started to observe potential breakthrough of MCYST. For this campaign, samples were analysed both by HPLC and by ELISA. Figure 11 shows the results of this intensive sampling campaign.

In contrast to other investigations maximum extracellular MCYST concentrations in the surface water were detected during the initial phase of the bloom (until the beginning of September). In this phase nearly one third of the total MCYST was extracellular. The bloom reached maximum values of 8.8 µg/L intracellular MCYST, which is not very high compared to the other years. The bloom, however, prevailed for a month (end of August to end of September) and then slowly broke down. MCYST concentrations around 1 µg/L were observed until the middle of November.
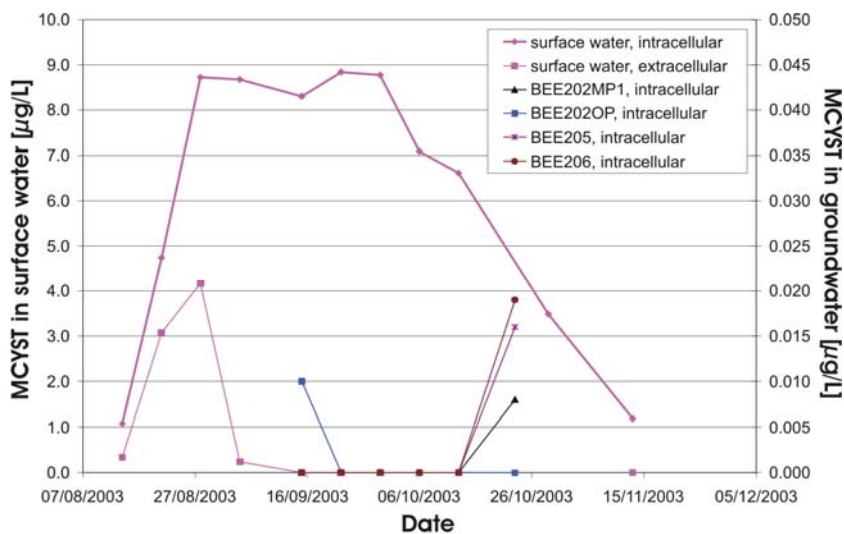
Figure 11: MCYST concentrations in surface- and groundwater analysed during the intensive sampling campaign in autumn 2003 (extracellular MCYST was not detected in the groundwater samples).

In the groundwater traces slightly above the limit of quantification were analysed by HPLC for intracellular MCYST. With exception of observation well BEE202OP these occurred a month later than previously assumed (so that only the last sample of this campaign contained MCYST). This as well as the fact that no extracellular MCYST was detected leads to the assumption that processes other than degradation or adsorption of extracellular MCYST might prevail. MCYST occurrence might be a function of a variety of factors including toxin release from the cells, adsorption onto carrier substances, flow velocity etc.

3.3   Conclusions

Cyanobacteria were present in the surface water every summer during the time period of the investigations. The blooms were similar to those during the last few years, however, not as severe as in other regions, where cyanobacterial densities can reach 10- to 100-fold higher values because of scum accumulation, which is not pronounced at the site of the transects. Highest MCYST concentrations (at times more than 20 µg/L) were observed during the bloom of Planktothrix agardhii in September and October 2003. Concentrations determined by ADDA-ELISA were usually higher than those measured by HPLC, and also indicated higher shares of extracellular MCYST. This is probably due to the fact that the ADDA-ELISA also responds to ADDA-containing degradation products of MCYST, which would usually occur outside the cyanobacterial cells.

In the groundwater MCYST and ADDA-containing substances were sometimes detectable in traces by ELISA only in the observation wells closest to the shore. Due to the minimal concentrations and due to the fact that the detection limit of the ELISA varies from analysis to analysis (see methods) the occurrence of positive signals might rather be a function of sensitivity of the ELISA than of input and transport in the groundwater.

Nevertheless some basic conclusions can be drawn:

- maximum elimination of MCYST and ADDA-containing substances occurs during the first few meters of underground passage,

- concentrations after 0.5 to 1 month of underground passage (BEE205, BEE206, 3339) usually lie well below 1 µg/L,

- the only observation well that showed ADDA-containing substances above quantification limit was BEE207UP, where sampling was difficult and no representative sample could be taken.

As quantification of MCYST concentrations in the bank filtrate was limited in face of the extremely low values, degradation rates could not be estimated from these field observations. Therefore, the investigations on this topic focussed on the experiments on UBA's experimental field in Berlin, Marienfelde.

4 Artificial Recharge Pond

4.1   Introduction

As cyanobacterial biovolume in Lake Tegel did not exceed 1 mm³/L (which is less than a tenth of the amount found in Lake Wannsee), it was not expected to find cyanobacteria in large quantities in the artificial recharge pond Tegel (which is fed with surface water from Lake Tegel). To ascertain this, however, the surface water of the pond was monitored for cyanobacteria in the first year of the project and toxins were analysed in case of positive findings.

4.2   Methods and Materials

Monthly samples of the surface water were first analyzed by microscope according to Lawton et al. (1999) to determine if cyanobacteria were present. In presence of cyanobacteria HPLC-PDA (High Pressure Liquid Chromatography – Diode Array) analyses for cell-bound microcystins were carried out after filtration and extraction according to Fastner et al. (1998).

Results

The results of the microscopic examination and the HPLC analyses are shown in Table 2. Only few cyanobacteria were found in the surface water of the AR pond. The highest biovolumes were observed during winter in December and January. During this time cyanobacterial biovolume reached values around 0.3 mm³/L. These are normal background concentrations for Lake Tegel and may be due to the fact that the microfiltration unit, which filters lakewater fed to the AR pond, was shut off during winter.

Cell-bound Microcystin concentrations of 0.05 and 0.14 µg/L were detected in the December and January samples, respectively. However, extracellular Microcystin could not be detected in any of these samples.

Table 2:   Results of microscopic and HPLC-analysis of surface water at the artificial recharge pond in Tegel (GWA Tegel).

Date	Cyanobacteria detected by microscopic analysis	Biovolume (mm³/L)	cell-bound Microcystins variants (HPLC) in µg/L
24.05.2002	none	not determined	no analysis
18.07.2002	none	not determined	< 0.01*
15.08.2002	few (Microcystis sp.)	0,06	< 0.01*
17.09.2002	few (Microcystis sp.)	0,05	< 0.01*
18.10.2002	very few (Planktothrix agardhii)	< determination limit	< 0.01*
21.11.2002	very few (Microcystis sp., Planktothrix agardhii, cf. Limnothrix sp.)	< determination limit	no analysis
12.12.2002	very few (Planktothrix agardhii, Limnothrix redeckii)	0,35	0,05
16.01.2003	some (Planktothrix agardhii, Limnothrix sp., Limnothrix redeckei, Pseudoanabaena sp.)	0,27	0,14
13.02.2003	some (Planktothrix agardhii, Limnothrix sp., Limnothrix redeckei, Pseudoanabaena sp.)	0,07	< 0.01*
13.03.2003	very few	< determination limit	< 0.01*
24.04.2003	very few (Limnothrix redeckei)	< determination limit	< 0.01*

* detection limit for individual MCYST variants.

During a dry phase in July 2003 three cores (10 cm) were taken from the infiltration pond. One core was examined by microscope. The surface layer (1 mm) showed a high content of green algae (Cladophora sp.) and diatoms (Navicula sp.). Cyanobacteria were not visible. Beneath the surface layer the amount of live organisms decreased rapidly.

Due to these low concentrations no groundwater samples were taken for toxin analysis and the investigations for cyanobacteria and microcystins in the surface water were not continued after April 2003.

4.3 References

Fastner J., Neumann U., Erhard M. (1998): Patterns of different microcystins in field samples dominated by different species of cyanobacteria, In: Chorus I. (ed.): Cyanotoxins – Occurences, Causes, Consequences.,190 - 199, Springer Verlag Berlin.

Lawton, L., Marsalek, B., Padisak, J. & Chorus, I. (1999): Determination of cyanobacteria in the Laboratory. - in: Chorus, I. & Bartram, J. (eds): Toxic cyanobacteria in water - a guide to their public health consequences, monitoring and management: p. 347 - 367, E & FN Spon, London.

5 Laboratory Experiments: Batch Experiments on MCYST-Degradation

5.1 Introduction

Previous studies have shown that biological degradation is the most important elimination process for microcystins in porous media without significant clay content as it is usually used for bank filtration or artificial recharge. As part of the research project NASRI (natural and artificial systems for recharge and infiltration) laboratory batch experiments were therefore conducted by the working group "environmental microbiology" of the Technical University Berlin in cooperation with the drinking water section of the Federal Environmental Agency (UBA). The aim was to study the kinetics of microcystin (MCYST) degradation under aerobic and anoxic conditions with the emphasis on the processes that lead to anoxic degradation of microcystins (anoxic meaning in this case that no free oxygen is present).

A preliminary experiment with an aerobic and an anoxic batch aimed to compare degradation under these different conditions and to enrich micro-organisms capable of degrading MCYST under anoxic conditions for further experiments. In the main series all batches were conducted under anoxic conditions with the objective of learning about processes leading to anoxic degradation of MCYST. The preliminary experiment was carried out with the crude extract of the Planktothrix agardhii mass culture, the main series with a purified stock solution of demethylised MCYST-RR.

5.2 Materials and Methods

5.2.1 Experimental setup

5.2.1.1 Preliminary experiment

The preliminary batch experiment was conducted with a crude extract of a mass culture of Planktothrix agardhii HUB 076 cultivated at the UBA's experimental field in Marienfelde (Berlin). Microcystins were extracted by repeated freeze-thawing a cell concentrate obtained by centrifuging the culture. After centrifuging the extract to remove all solid cell contents it contained up to 50 mg/L microcystins amongst other water soluble cell components.

This centrifuged extract was then brought into contact with an inoculum derived from natural sandy bank material from a lake in Berlin with frequent cyanobacterial blooms (Lake Wannsee) together with a fresh sample of the cyanobacterial mass culture in a ratio 5:5:1. The resulting concentration of demethylated MCYST-RR (main variant of Planktothrix agardhii HUB 076) was 49.48 mg/L (± 0.05 µg/L variation between the two batches).

One parallel was kept aerobic by allowing contact to the natural atmosphere (A), the other was held anoxic under N2/CO2-atmosphere (B).

- Aerobic approach (A): 550 ml batch volume incubation on a rotary shaker (120 rpm), at room temperature in the dark,

- Anoxic approach (B): 55 ml batch volume, at room temperature in the dark, serum bottle under N2/CO2 atmosphere.

Samples were taken daily during the first 10 days of the experiment, later weekly, filtered (membrane filter 0.45 µm pore size) and stored deep frozen until analysis.

5.2.1.2 Main series of batch experiments

The common basis of all batches run during this series was:

- 50 mL sulfide reduced anoxic medium, reduced by volume of added solutions, prepared according to Widdel & Bak (1992) and Tschech & Pfennig (1984),

- 1 mL demethylated MCYST-RR stock solution, about 800 mg/L and 600 mg/L in sum in the first and second series, respectively,

- 0.5 mL anoxic pre-culture (obtained in the anoxic preliminary experiment),

- 0.5 mL Planktothrix agardii HUB 076 culture.

The redox indicator resazurin was added to indicate oxidizing conditions by pink colour (Figure 12) and dithionite (reductive agent) was added when needed.

Three parallels were run for each of the following compounds in order to study the microorganisms and metabolic pathways involved in the transformation of microcystin with different electron acceptors/donors:

- KNO3 (0.1 mM), in oder to find out if nitrate can serve as electron donator,

- glucose (0.03 mM), in order to simulate high nutrient conditions (and thus co-metabolism as the prominent degradation process),

- casaminoacids (0.5 %), in first series only, in order to find out if MCYST is degraded simultaneously to chemically similar substances.

The experiments were carried out with a purified dem. MCYST-RR extract that was prepared in order to rule out co-metabolism as a degradation process. The purification was carried out by semi-preparative HPLC application (appendix VII-1). During the second main series an additional control without pre-culture and Planktothrix agardhii culture as inoculum was carried out.

Figure 12: Screw cap tubes filled with sulfide reduced anoxic medium supplemented with KNO3. The pink bottle shows an example of oxidized medium.

Samples were taken every 2 to 3 days and glass beads were added to the tubes in exchange in order to compensate for the loss in batch volume (Figure 12). The samples were then stored frozen in glass test tubes until analysis by HPLC.

5.2.2 Analytical Methods

MCYST-analyses were carried out by HPLC (High Performance Liquid Chromatography) with a photodiode array detector according to Lawton et al. (1994). The samples were thawed, diluted with methanol (1:1) and analyzed directly, without further pre-treatment.

5.3 Results

5.3.1 Preliminary experiment

The results of the two batch experiments (Figure 13) show complete transformation of microcystins (< 40 µg/L) under aerobic as well as under anoxic conditions with more rapid degradation under aerobic conditions. A lag phase of 2 days with only little degradation (10 %), however, can even be observed under aerobic conditions. Nevertheless, after the 2nd day 99.9 % of the microcystin present was degraded within 2 days. Under anoxic conditions the MCYST concentrations remained on a high level (> 44.85 mg/L) for the first nine days of the experiment. A sample taken on day 21 after the beginning of the experiment, however, showed complete degradation (MCYST-RR < 40 µg/L).
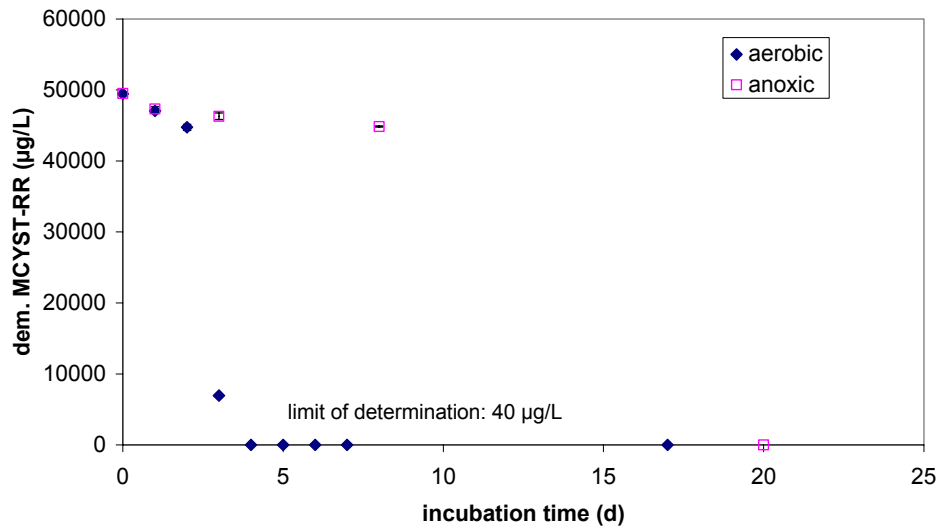
Figure 13: Degradation of dem. MCYST-RR under aerobic and anoxic conditions during first batch series.

These results show that transformation is also possible under anoxic conditions, although the lag phase seems to be distinctively longer. A contamination with oxygen during sampling, however, can not be ruled out completely so we decided to change the experimental setup and use an anoxic sulfide reduced medium with a redox indicator in further experiments.

5.3.2   Main series of batch experiments

The sum of MCYST analysed in the samples of the first batch series is given in Figure 14. All three different experiments showed a similar trend in MCYST concentration: Starting from values around 10 to 12 mg/L there is an immediate decline until values around 1 mg/L are reached on day 15. After this the MCYST concentration remains constant in all batches.

The residual concentrations of MCYST are, however, not demethylated MCYST-RR but are composed of substances that show different retention times in the HPLC chromatogram (Figure 15) but can be identified as MCYSTs due to their characteristic UV-spectra (see final report working group algae, part IIX). Dem. MCYST-RR is reduced to below detection limit after 5 to 8 days.

39
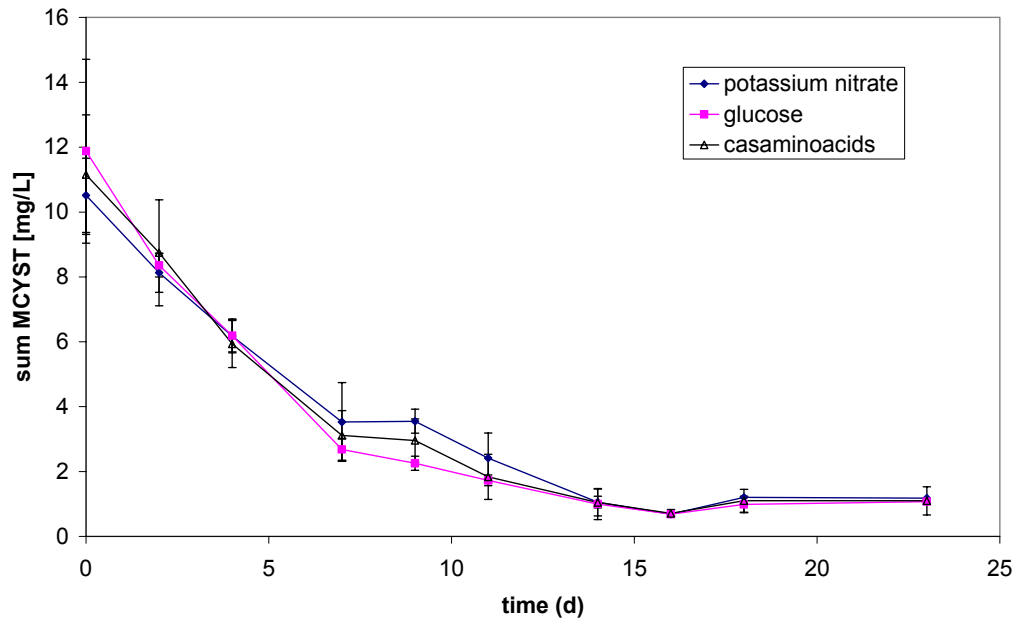
Figure 14: MCYST (sum of all variants) during the first main series of degradation experiments under anoxic conditions with addition of KNO3, glucose and casaminoacids (average values and standard deviation of three parallels each).
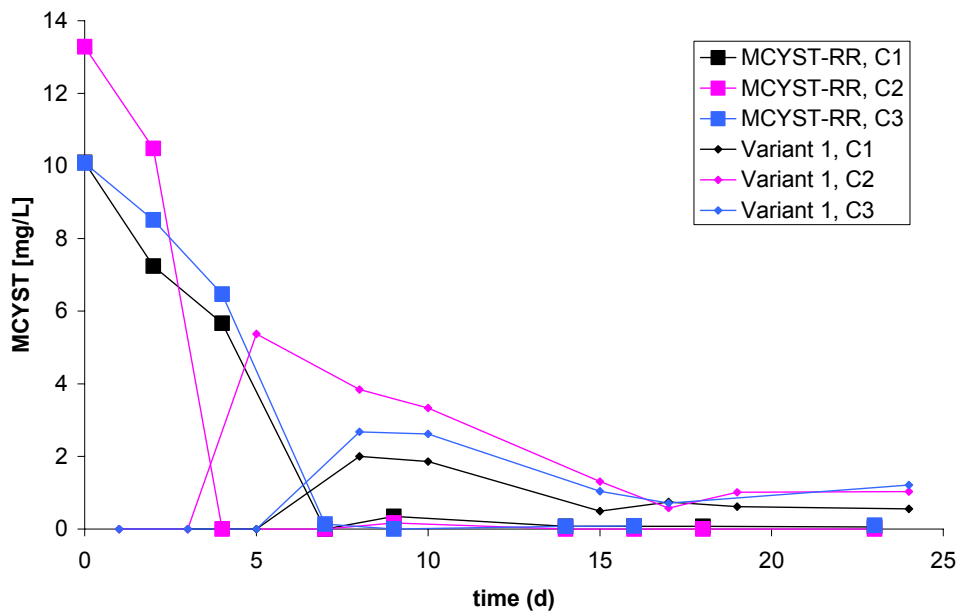
Figure 15: Concentrations of dem. MCYST-RR (full squares) and an unidentified MCYST variant (retention time: 10.5 min, small diamonds) during the three parallel experiments with casaminoacids in the first main series.

The HPLC analysis of the stock solution used for the second series already showed traces of other MCYST peaks: additionally to 98.7 % dem. MCYST-RR, 1 % was found at a retention time of 11.8 min and 0.3 % at 10.2 min. This indicates that transformation might have already taken place in the stock solution prior to the beginning of the experiment.

The results of the MCYST analyses of the second batch series are shown in Figure 16. In this series the drop in MCYST concentrations in all batches is even more rapid than in the first series (compare Figure 14). This might be due to lower initial concentrations (11.2 mg/L average in the first and 3.2 mg/L in the second series). Like in the first series, however, a residual concentration of about 1 mg/L is remained all batches with exception of those without inoculum and additional substances.
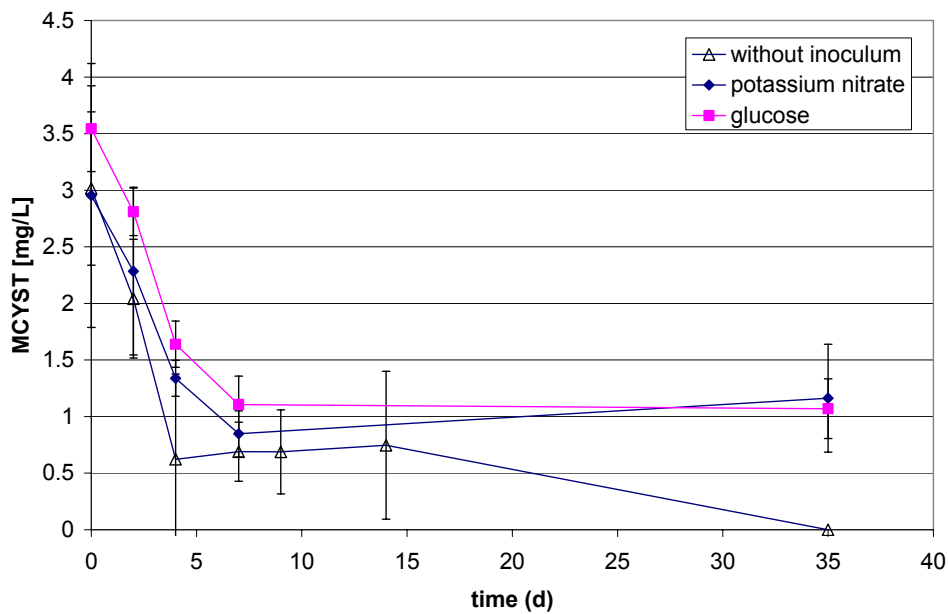
Figure 16: **MCYST (sum of all variants) during the second main series of degradation experiments under anoxic conditions with addition of KNO3, glucose and without inoculum (average values and standard deviation of three parallels each).**
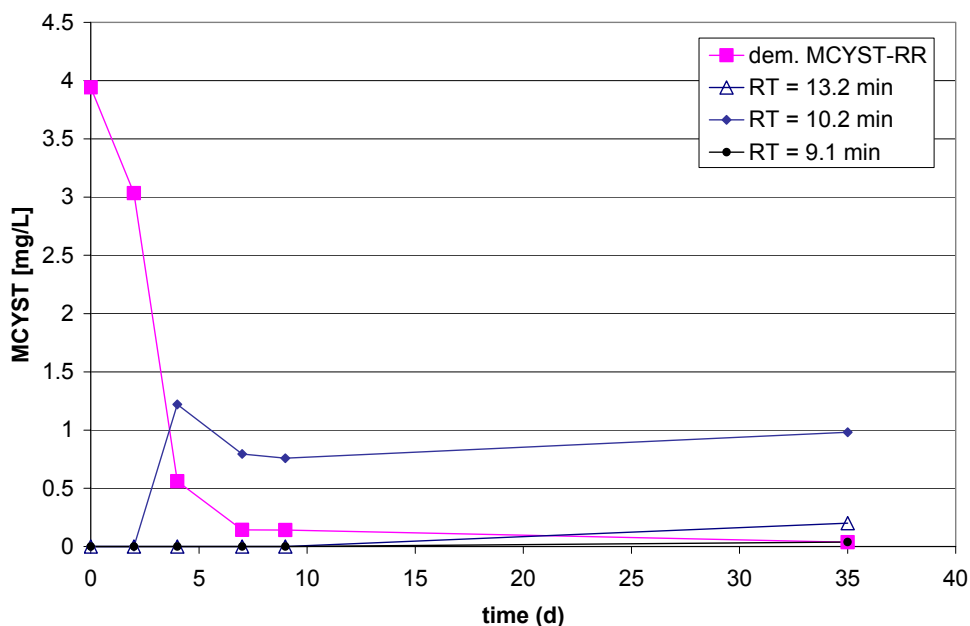
Figure 17:   Concentrations of dem. MCYST-RR and unidentified MCYST variants during one series with glucose in the second main series (RT = retention time).

A closer look at the different peaks of the HPLC chromatogram (Figure 17) reveals that the concentration of the main MCYST variant (dem. MCYST-RR) declined to values below 0.2 mg/L after day 8 and to around 0.04 mg/L (limit of determination) on day 36. Other substances with a typical MCYST-spectrum and other retention times were not detectable in the beginning of the experiment. For the variants previously identified in the undiluted stock solution this is in agreement with the theoretical concentration calculated from the dilution factor, which would be less than 0.01 mg/L whereas the detection limit is clearly higher (0.04 mg/L). After five days one variant with a retention time of 10.2 min appeared in concentrations around 1.2 mg/L. This had a molecular mass of m/z 1106 [M+H]+ (identified by LC-MS), some fragments characteristic for MCYSTs and remained detectable until the experiment was terminated at concentrations around 1.0 mg/L.

5.3.3 Summary of the Results

In summary, the batch experiments carried out on MCYST degradation showed the following results:

In the preliminary experiment aerobic degradation was more rapid than anoxic degradation due to a shorter lag phase. (However, as mentioned above, it could not be ruled out that degradation in the further course of the experiment was due to oxygen contamination).

In strictly anoxic experiments of the main batch series with pure MCYST and the anoxic pre-culture no lag phase was observed. This was, however, also true for a batch without any pre-culture - this indicates that the lack of adapted microorganisms was not the limiting factor in the preliminary series. Another possibility might be that degradation is not due to biological processes.

Addition of KNO3, glucose or casaminoacids did not accelerate or retard anoxic degradation of pure MCYST.

Surprisingly, during MCYST-transformation additional peaks appeared in the HPLC chromatogram, that showed a typical MCYST UV-spectrum and characteristic fragments. These appeared to be more stable than the variant present initially (dem. MCYST-RR) and are detectable at constant concentrations around 1 mg/L from day 5 until the end of the experiment (after 36 days).

5.4 Interpretation and Discussion

Taking these results of the preliminary and the main batch series into account the following conclusions can be drawn:

- Demethylated MCYST-RR can be transformed under aerobic and anoxic conditions.
- The presence of other, possibly more readily degradable substances (BDOC) in the crude extract seems to promote a lag phase before rapid degradation commences.
- Under the conditions used in the preliminary experiment (presence of high amounts of BDOC) the lag phase is shorter under aerobic than under anoxic conditions.
- Pure demethylated MCYST-RR is degraded rapidly (without lag phase) under anoxic conditions in the main series with half lives of less than 5 days.
- Under these conditions other substances with UV-spectra and mass fragments characteristic of MCYST emerged.
- These substances are less easy to degrade under the conditions mentioned above and are still present in solution 36 days after the beginning of the experiment.

Although a number of investigations on the aerobic degradation of MCYST have been published (e.g. Bourne et al. 1996, Christoffersen et al. 2002, Cousins et al. 1996, Jones et al. 1994, Lahti et al. 1997, Saitou et al. 2002, Welker et al. 2001), experiments on anoxic degradation are limited (Holst et al. 2003).

43

Holst et al. (2003) postulated that degradation of MCYSTs (in their case MCYST-LR) was restricted to situations in which a strong electron acceptor such as oxygen or nitrate was present. This was shown in batch experiments under microaerophilic conditions (O2 < 0.3 %), where degradation was only observed if NO3 and / or glucose was added. Although this seems to contradict our own experimental results, there are two important differences: a) the MCYST variant used by Holst et al. (2003) was mainly MCYST-LR, while our experiments were carried out with demethylated MCYST-RR and b) the conditions in our experiments were strictly anoxic (-51 mV, at pH 7), whereas Holst et al. (2003) stated microaerophilic conditions.

In conclusion, these findings leave the following open questions:

- Which are the factors influencing the occurence of a lag phase prior to rapid MCYST degradation (adapted microbiology, presence of BDOC or others?)

- Apart from the lag phase, is there a difference in aerobic and anoxic degradation rate?

- Do degradation rates differ between MCYST variants? Are there variants that are persistent?

- Can degradation transform MCYSTs from one variant to another?

- Which bacteria are involved in MCYST degradation?

In order to assess the rate and reliability of anoxic MCYST degradation under the conditions commonly occurring during infiltration, a broader, systematic approach to further experiments is needed. This is important as in most cases microaerophilic, anoxic and anaerobic conditions prevail during artificial recharge or bank filtration.

5.5   References

Bourne D.G., Jones, G.J., Blakeley R.L., Jones A., Negri A.P. & Riddles P. (1996): Enzymatic Pathway for the Bacterial Degradation of the Cyanobacterial Cyclic Peptide Toxin Microcystin LR., Appl. Env. Microbiology, 62 (11): 4086 – 4094.

Christoffersen K., Lyck S. & Winding A. (2002): Microbial activity and bacterial community structure during degradation of microcystins., Aq. Microb. Ecology, 27: 125 – 136.

Cousins I.T., Bealing D.J., James H.A. & Sutton A. (1996): Biodegradation of Microcystin-LR by Indegenous Mixed Bacterial Populations., Wat. Res., 30(2): 481 – 485.

Holst, T., Jörgensen, N.O.G., Jörgensen, C. & Johansen, A. (2003): Degradation of microcystin in sediments at oxic and anoxic, denitrifying conditions. - Wat. Res. 37: 4748 - 4760.

Jones G.J., Bourne D.G., Blakeley L. & Doelle H. (1994): Degradation of cyanobacterial hepatotoxin microcystin by aquatic bacteria., Natural Toxins, 2: 228-235

Lahti K., Rapala J., Färdig M., Niemelä M., Sivonen K. (1997): Persistence of cyanobacterial hepatotoxin, microcystin-LR, in particulate material and dissolved in lake water, Wat. Res., 31 (5): 1005 – 1012.

Lawton, L.A., C. Edwards, G.A. Codd (1994): Extraction and high-performance liquid chromatographic method for the determination of microcystins in raw and treated waters, Analyst, 119: 1525 – 1530.

Saitou T., Sugiura N., Itayama T., Inamori Y., Matsumura M. (2002): Degradation of Microcystin by Biofilm in Practical Treatment Facility., Wat. Sci. Techn. 46(11-12): 237 – 244.

Tschech, A. & Pfennig, N. (1984) Growth yield increase linked to caffeate reduction in Acetobacterium woodii. Arch. Microbiol. 137, p 163-167.

Welker M., Steinberg C. and Jones G. (2001): Release and Persistence of Microcystins in Natural Waters, In: (I. Chorus ed.): Cyanotoxins - Occurrence, causes, consequences., Springer Verlag Berlin, 83-101

Widdel, F. & Bak, F. (1992) Gram-negative mesotrophic sulfate-reducing bacteria. In: The Prokaryotes: a handbook on the biology of bacteria: ecophysiology, isolation, identification and applications, 2nd ed. (Balows, A., Trüper, H. G., Dworkin, M., Harder, W. and Schleifer, K.-H. Eds.) p 3353-3378. Springer-Verlag, New York.

6 Column Experiments to assess Effects of Temperature on MCYST-Degradation

6.1 Introduction

In order to transfer the results of laboratory and field experiments to the field setting, the influence of temperature on substance removal has to be regarded closely, as this is one of the physico-chemical parameters that varies distinctively throughout the year in natural settings. Concerning the elimination of cyanobacterial toxins, only few publications have so far addressed this topic.

Some publications suggest that a reduced degradation of microcystins (MCYST) could be the result of lower temperatures as biodegradation is known to decrease with sinking temperatures. This was the result of field experiments in late autumn for example (Grützmacher et al. 2002). Holst et al. (2003) carried out experiments with two different temperatures, 10 and 21°C, showing that elimination was better at 21°C. In order to confirm these findings experiments with MCYST were carried out on columns run by the NASRI working group "organics" (Technical University of Berlin) as part of a diploma thesis by Charlotte Garing, supported by the working group "algae" under supervision of Dr. Birgit Fritz and Prof. Behra (ENSIACET, France).

6.2 Materials and Methods

6.2.1 Microcystin extract

The microcystins were extracted from a mass culture of Planktothrix agardhii HUB 076, currently run by UBA, by centrifugation and freeze-thawing. The extracts were homogenated, centrifuged and stored frozen. The undiluted microcystin extract had a concentration of 61.85 mg/L.

6.2.2 Soil column experiments

6.2.2.1 General characteristics

Three acryl glass columns with a diameter of 0.14 m and height of 0.5 m were filled with an industrial sand, consisting mainly of quartz sand with a grain size ranging from 0.7 to 1.2 mm and with a poor organic content (loss on ignition = 0,13%). Water from Lake Tegel and microcystin were pumped into the column. The flow rate was estimated to be about 840 mL/d for each column and the pore velocity about 0.2 m/d. The installation is summarized in Figure 18 and Figure 19 gives an illustration of one of the columns. Further details can be taken from the final report of the NASRI working group "organics".
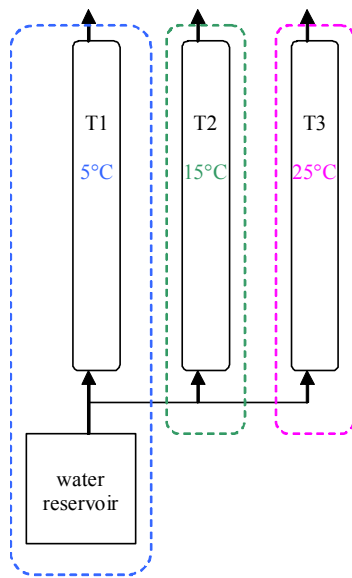
Figure 18 Simplified diagram of the installation.

The columns were kept at different temperatures: 5°C for the first column, 15°C for the second one and 25°C for the third one (see Table 3 for details on average temperatures of the columns during both experiments).

Table 3 Average temperature of each column during experiment 1 (a) and experiment 2 (b). The number of measurements was 23 and 7 for a) and b), respectively.

a)	T1 (°C)	T2 (°C)	T3 (°C)	b)	T1 (°C)	T2 (°C)	T3 (°C)
mean	4,83	15,65	25,67	mean	5,30	15,28	26,34
deviation	1,12	0,89	0,81	deviation	0,83	0,46	0,48

47
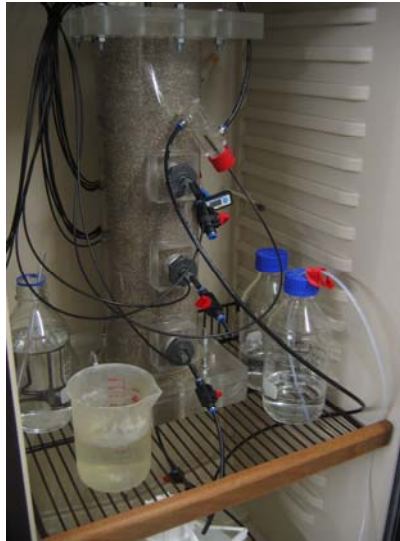
Figure 19 Photograph of one of the columns.

6.2.2.2   Experiment 1

For the first experiment, 5 mL of the microcystin extract and about 20 L of Lake Tegel water were added to the water reservoir each week in order to maintain a microcystin input concentration of around 15 µg/L.

The experiment lasted 47 days. The water reservoir was sampled daily, to check the development of its microcystin content. During the first four days, two samples of the effluent from each column were taken per day and then one per day until the end of the experiment. The samples were kept frozen in glass test tubes until analysis.

6.2.2.3   Experiment 2

In the second experiment, the diluted extract (40.5 mL in 1000 mL Lake Tegel water) was injected directly into each column just after having been mixed with Lake Tegel water from the water reservoir with a dilution factor of 1/50. This different mode of application was chosen in order to avoid variations in the input concentration due to degradation and / or incomplete mixing as observed in experiment 1. The resulting concentration was targetet at 50 µg/L.

The experiment lasted 35 days. The effluent of each column was sampled daily. Samples from the microcystin input solution were also taken, approximately once a week, in order to check the correct microcystin input concentration. The samples were kept frozen in glass test tubes until analysis.

6.2.2.4   Analytical methods

All samples were analyzed by ELISA in order to determine their total microcystin content. During the second experiment, one sample from the output water of each column and one from the input microcystin solution were additionally analyzed by HPLC to check the microcystin concentration and to distinguish the different microcystin variants present in the water. Further details on MCYST analysis can be taken from the final report of the working group "algae" part IIX.

6.2.2.5   ELISA

The concentration of microcystin in the samples was quantified by a competitive ELISA (enzyme-linked immunosorbent assay). This method is based on the reaction between microcystins and antibodies. It is an efficient method in detecting concentrations down to 0.1 µg/L with only a small volume of solution and no need for sample pre-treatment.

The ELISA used was a generic microcystin immonuassay based on monoclonal antibodies against the unusual Adda group characteristic for microcystins, nodularins and certain peptide fragments (Zeck et al. 2001). The range of determination lies between 0.1 µg/L and 1.0 µg/L, and thus samples from the water reservoir had to be diluted with deionized water. Each value was determined as the average of two parallels taken from the same sample.

6.2.2.6   HPLC

The microcystin variants and their concentrations were analyzed by HPLC with photodiode array detection. The samples were first filtered by membrane filters RC 55 with a pore size of 0.45 µm. They were then enriched by solid phase extraction over C18-cartridges: three cartridges were filled with the three samples from the column water outflow and one cartridge with the sample of the microcystin input solution. After one day the cartridges were submitted to washing, elution and evaporation (details are given in final report working group "algae" part IIX).

6.2.2.7   Numerical methods

Retardation and degradation rates were estimated by fitting a numerical model to the measured values obtained from the column experiments. The model used was an inverse model created by E. Holzbecher (IGB, Berlin), using basic MATLAB package in connection with the optimization toolbox. This model is represented in Appendix VIIb-1.

The function representing degradation was modified in order to obtain a better description of the processes in the columns:

for c ≠ 0, $\lambda = 1 / [\exp(-cT)-1] * [(\lambda 2-\lambda 1)\exp(-ct) + \lambda 1 \exp(-cT) - \lambda 2]$

for c = 0, $\lambda = \lambda 1+(\lambda 2- \lambda 1) t / T$

λ : loss rate [1/d]

t: time [d]

T: duration of the experiment [d]

λ1, λ2 and c: parameters of λ [1/d]

Figure 20 shows the evolution of λ with the time, for different values of c, as calculated by this model.
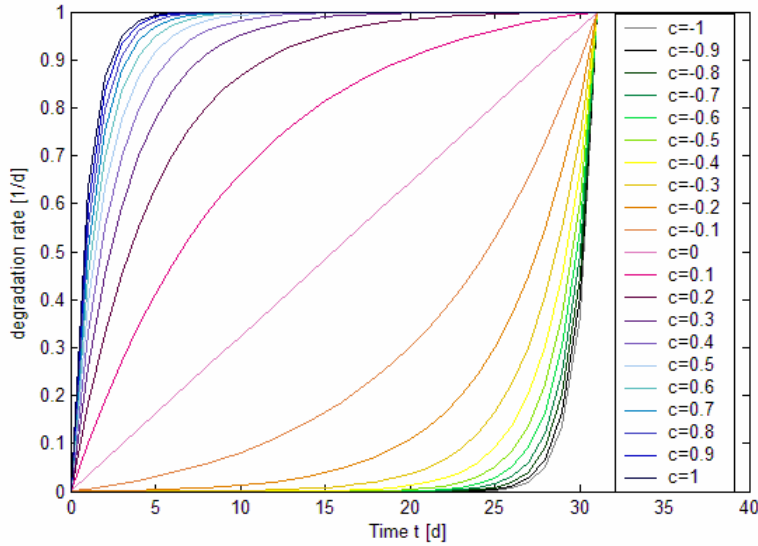
Figure 20 Evolution of loss rate (λ) with the time for c from -1 to 1. Parameters for the given situation are: λ1 = 1e-10, λ2 = 1 and T = 31.

The modelling was done with a pore velocity of 0.2 m/d and a value of the longitudinal dispersivity assumed equal to 0.05 m.

For the first experiment, a constant input microcystin concentration of 19.18 µg/L was taken and the modelling was done with the first 31 points.

For the second experiment, the model used a constant input microcystin concentration of 63.5 µg/L.

6.3 Results

6.3.1 Experiment 1

6.3.1.1 Soil column results

Although the evolution of microcystin input concentration was quite unstable, it could be separated into two main phases: the first 31 days the concentration in the water reservoir had an average value of 19.2 µg/L (± 4.7) and then from day 31 to day 47 the average concentration was around 7.6 µg/L (± 2.8) (Figure 21).
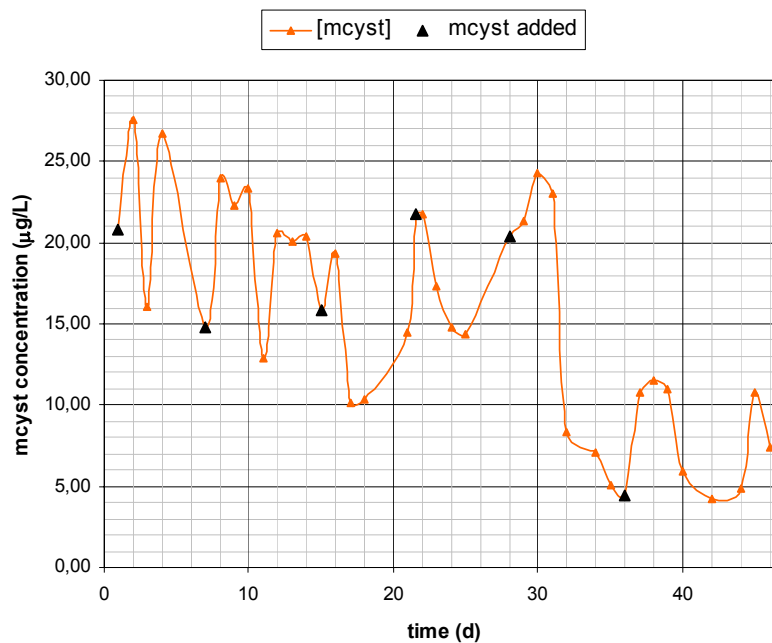
Figure 21 Microcystin concentration in the water reservoir.

The concentration of microcystin in the output water had the same tendency for each column, regardless of the experimental temperature, i.e. 5°C, 15°C and 25°C (Figure 22).
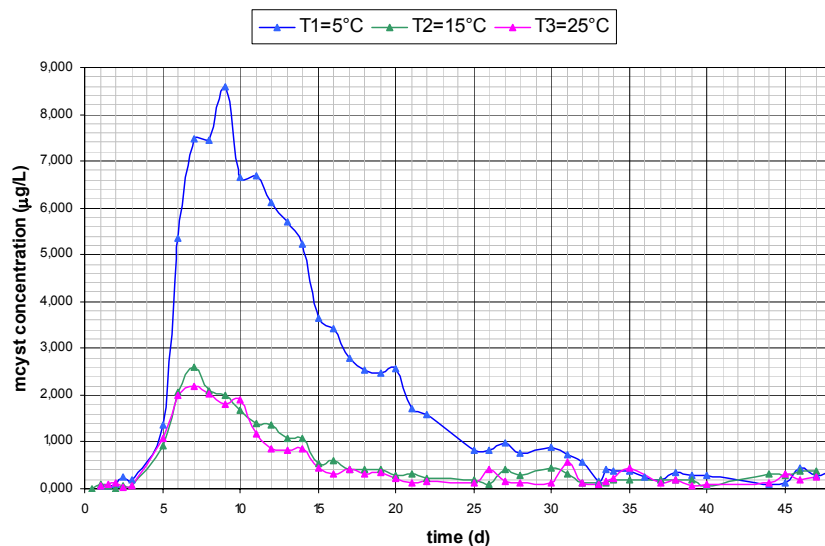
Figure 22 Microcystin concentrations at column outlets investigated at three experimental temperatures, T1 = 5°C, T2 = 15°C and T3 = 25°C for an input concentration around 19.2 µg/L.

During the first 3 to 4 days, no microcystin was observed in the outlet. Then the microcystin concentration increased rapidly until reaching a maximum value at day 7 for column 2 and 3, with 2.61 and 2.18 µg/L respectively, and at day 9 at 5°C in column 1 with 8.6 µg/L. Then it decreased in all columns until the end of the experiment. The concentration of microcystin in the output water reached values under detection limit after day 21 for column 3 at 25°C, day 26 for column 2 at 15 °C and day 44 for column 3 at 5 °C, and all the values after day 25 remained lower than 1 µg/L, the provisional WHO guideline value for MCYST-LR in drinking water (WHO 1998). From day 35 until day 47, the end of the experiment, the microcystin concentration was between 0.05 µg/l and 0.455 µg/L for all the columns.

In terms of elimination, the percentage of microcystin eliminated at the end of the columns compared to the input, column 1 at 5 °C showed an average elimination of 88.3%, whereas in the columns both at 15 and at 25 °C it amounted to 96.6% (Figure 23).

52
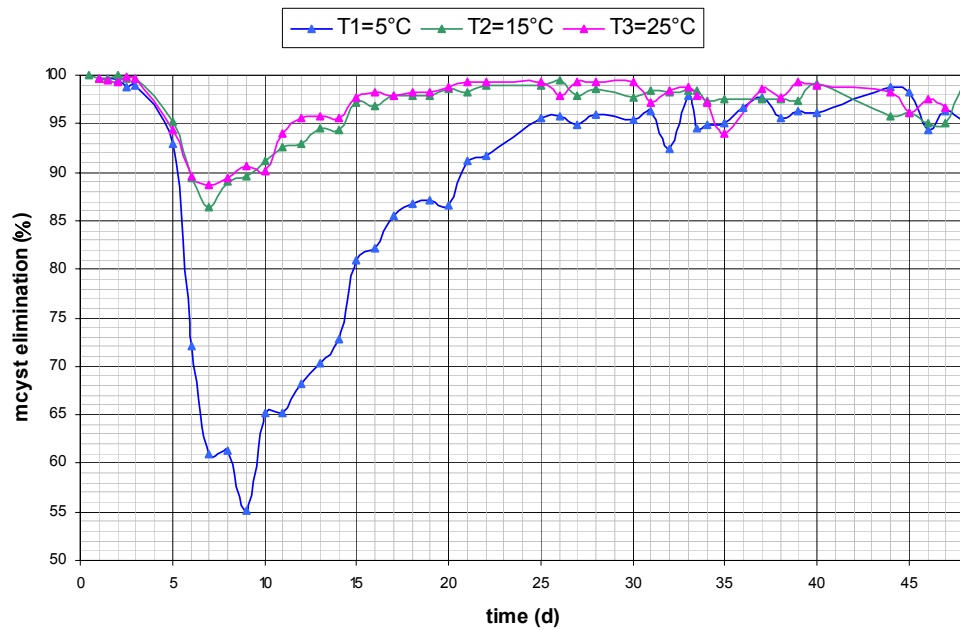
Figure 23 Microcystin elimination during experiment 1 (input concentration 19.2 µg/L for days 0 to 31 and 7.6 µg/L for days 32 to 47).

6.3.1.2 Modelling Results

For the first column at 5°C, the best fit of the microcystin outlet concentration curve was achieved with the set of parameters represented in Table 4. The modelled curves are shown Figure 24 and the corresponding degradation rates in Figure 25.

Table 4 Fitting parameters for experiment 1 (v = 0.2 m/d, αL = 0.05 m, T = 31 d).

	5 °C	15 °C	25 °C
R	3.44	4	4
λ_1 [d-1]	2.e-9	2.e-10	2.e-10
λ_2[d-1]	0.8	0.86	0.9
c [d-1]	-0.029	0.043	0.039

53
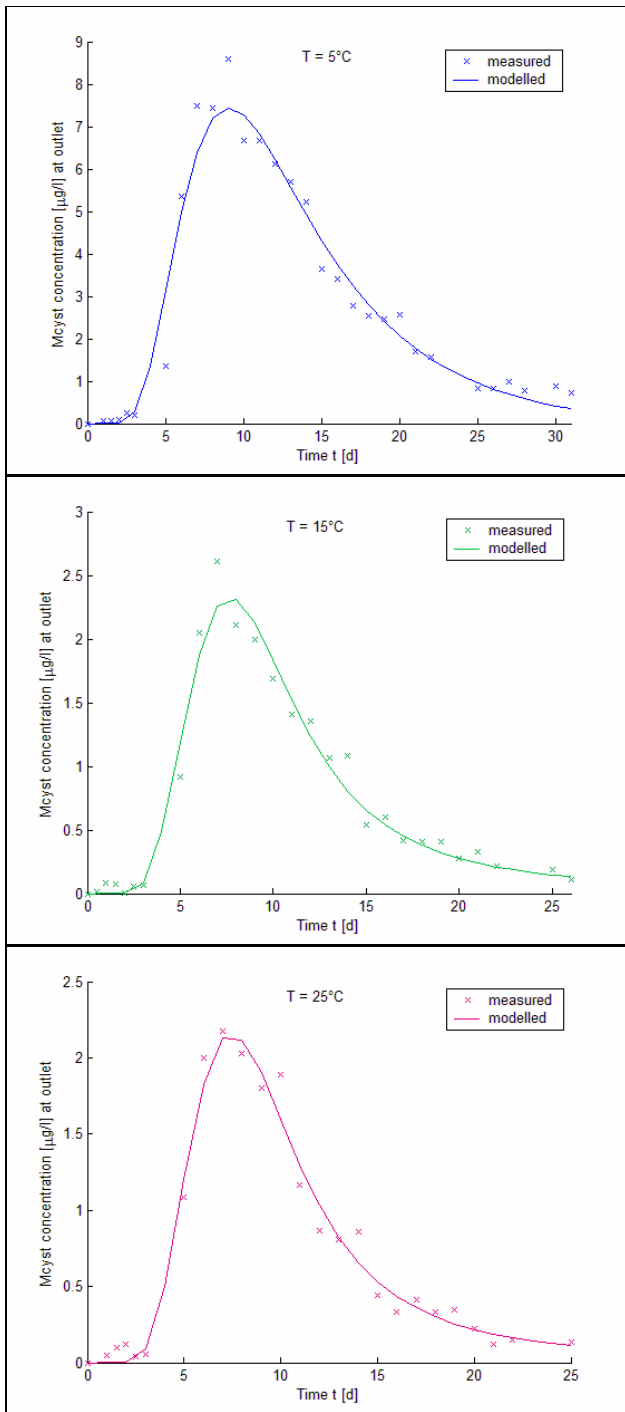
Figure 24 Measured and modelled microcystin outlet concentration for experiment 1.
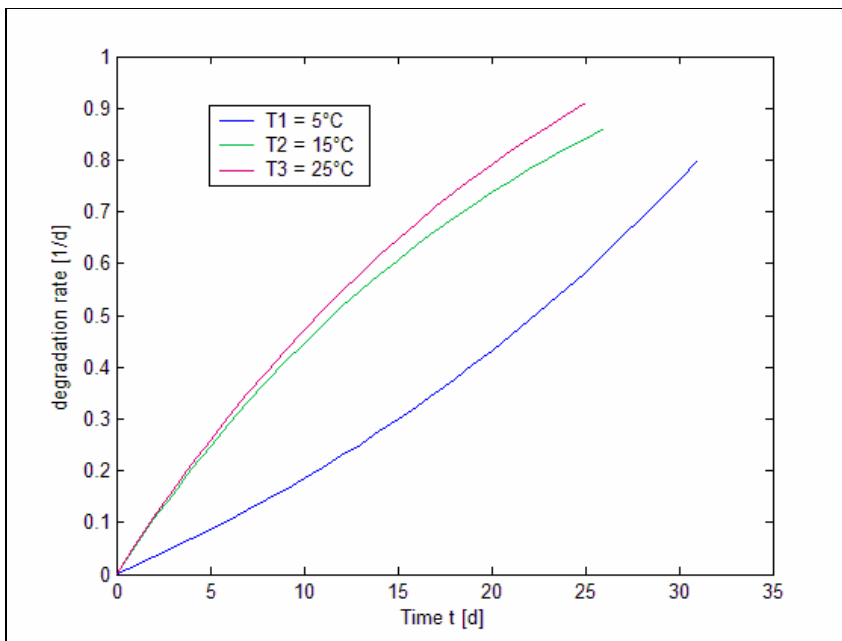
Figure 25 Microcystin degradation rates over time at 3 different temperatures.

6.3.2   Experiment 2

6.3.2.1   Soil column results

An HPLC analysis of the microcystin input solution was carried out at day 26. Eight different peaks corresponding to three types of microcystin variants (Table 5) were detected, amounting together to an overall microcystin input concentration of 96 µg/L.

Table 5 Microcystin variants in the input solution with their concentration in the solution and the calculated concentration injected into the column (dilution of 1/50).

MCYST variant	Concentration in MCYST-solution	MCYST input concentration
	µg/L	µg/L
LR 237.0	3583.55	71.67
YR 229.9	1219.64	24.39
MC_Tryp	4.53	0.09

Throughout the experiment, the ELISA analyses detected input concentrations ranging from 30 to 78 µg/L, with an average of 63.5 µg/L (± 20.8). The concentration of microcystin in the output water had the same tendency for each column (Figure 26).

55

During the first 5 to 7 days, microcystin was not present in the outlet samples. Then the concentration increased rapidly until a maximum value was reached at day 11 for all the columns, with 60.3 µg/L for column1, 18.1 µg/L for column 2 and 30 µg/L for column 3. Then the microcystin concentration decreased until the end of the experiment. For the first column the decrease of the concentration showed some fluctuations. The concentration of microcystin in the effluent reached values under 1 µg/L after day 14 for column 2, day 15 for column 3 and day 34 for column 1. For the column 2 and 3, from day 21 until the end of the experiment, the microcystin concentration stayed between 0.17 µg/l and 0.40 µg/L, which was very low but still above the detection limit of the ELISA. However, the HPLC analyses made by day 26 showed no microcystin in the effluent of any of the columns, not even for even for column 1.
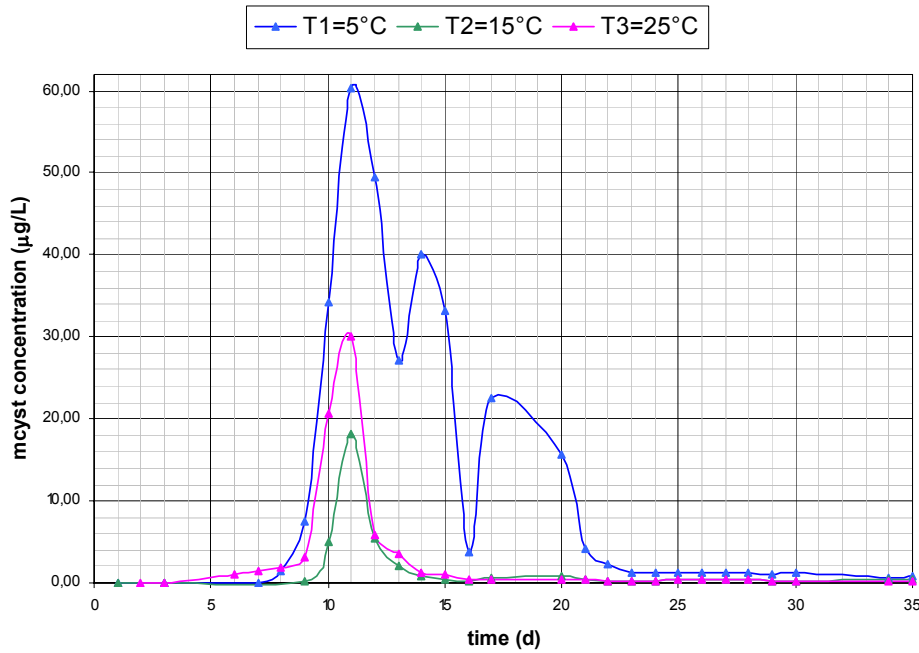
Figure 26 Microcystin concentration at T1 = 5°C, T2 = 15°C and T3 = 25°C for an input concentration of about 63.5 µg/L.

In the first column (5°C), the microcystin was eliminated by 81% in average. The mean value of microcystin elimination for columns 2 (15 °C) and 3 (25 °C) were 97.5% and 95.6%, respectively (Figure 27).
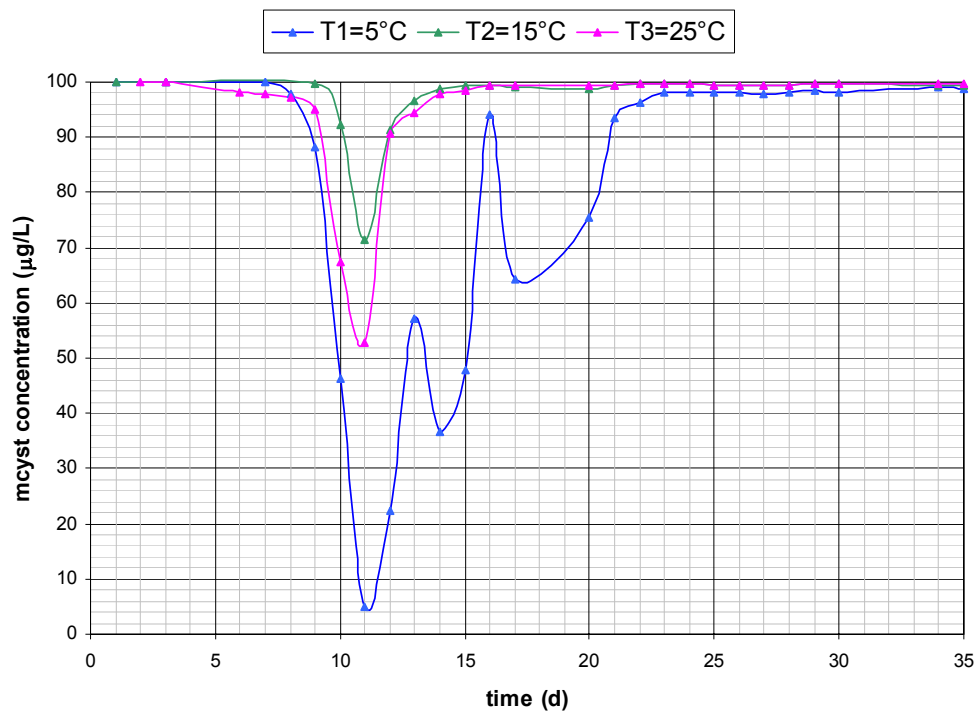
Figure 27 Microcystin elimination during the time of the experiment for each column (input concentration about 63.5 µg/L).

6.3.2.2   Modelling results

The parameters estimated for the first experiment were tested on the second one, changing the input microcystin concentration to 63.5 µg/L and the time of the experiment to 35 days. The three resulting curves are shown in Figure 28.

On the basis of these results, an adjustment of the parameters was attempted, in order to fit the microcystin outlet concentration curve better. However, no satisfactory fitting was achieved with this model: The major breakthrough peak for all columns was far too tight to be fitted closely.

The introduction of a lag phase T_0 in the λ function managed to yield better results but was still not satisfactory. The results for columns 2, with the addition of a lag phase of 5 days, are presented in Figure 29. This was the best fitting achieved for this column.
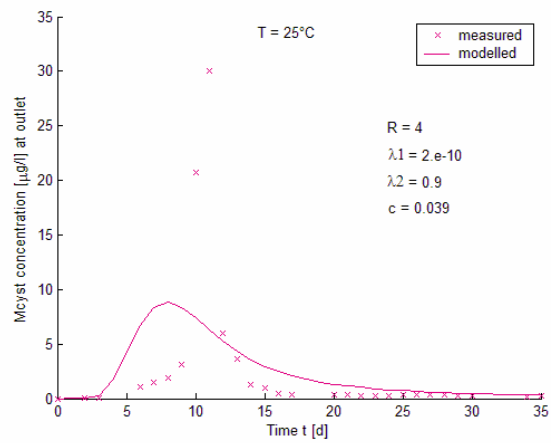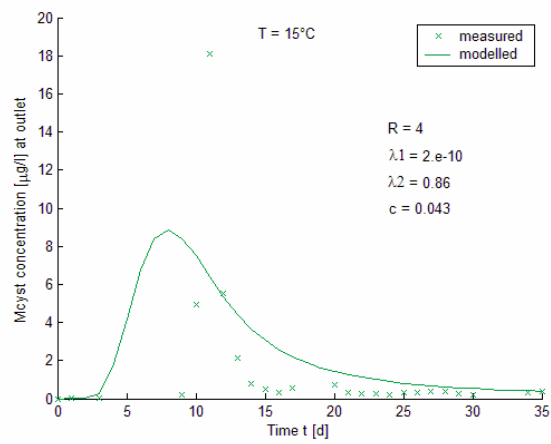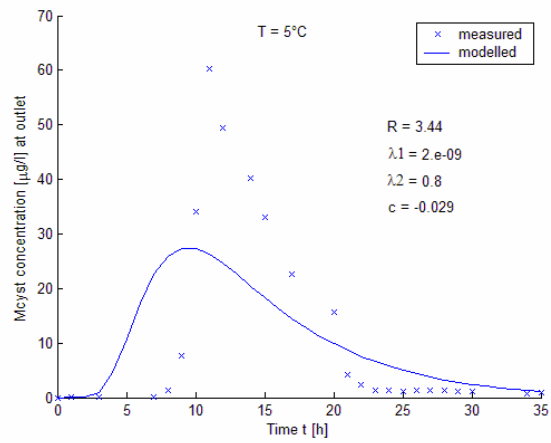
Figure 28 Measured and modelled microcystin outlet concentration for experiment 2 with the parameters estimated for the experiment 1.
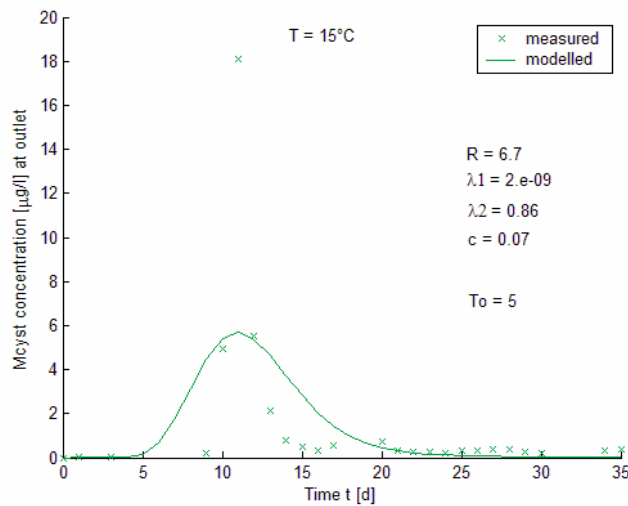
Figure 29 Measured and modelled microcystin outlet concentration for experiment 2 (column 2 at 15°C) with a lag phase for the degradation T$_0$ = 5 d.

6.4 Interpretation and Discussion

6.4.1 Elimination

The following table summarizes the mean value for the elimination obtained in both experiments.

Table 6 Mean value of the elimination for each temperature and experiment. Experiment 1: MCYST added to the water reservoir feeding the columns, Experiment 2: MCYST injected directly on column.

	Experiment 1	Experiment 2
MCYST input concentration	19.2 µg/L	63.5 µg/L
	elimination (%)	
5 °C	88.3	81
15 °C	96.6	97.5
25 °C	96.9	95.6

In the second experiment MCYST was still detectable after 35 days by ELISA. The HPLC analysis detected no microcystin after 26 days for all columns. The difference between both results can be explained by two methodological aspects: (i) The Adda-ELISA does not distinguish between microcystins and degradation products. When microcystin is degraded, it is transformed into a linear substance (Bourne et al. 1996) which also contains the Adda-

59

group. Thus some of the microcystin detected by the ELISA might result from degradation products. (ii) Differences between both methods may be due to differences in sensitivity of detection, particularly as the ELISA reacts to all microcystin variants in a sample in unison, whereas HPLC detects individual peaks for each variant.

The values found for microcystin elimination are in the same order of magnitude as those reported by Holst et al. (2003), who found an elimination of 93 % at 10°C and 97.5 % at 21°C for a 66 days experiment for an input concentration of 70 μg/L. In the experiments conducted by Lahti et al. (1998) with soil and sediment columns consisting mainly of gravel, an elimination of 97.9 % was achieved with two soil columns at 14°C during 7 days with an input microcystin concentration of 0.7 μg/L to 3.1 μg/L.

So far microcystin elimination was usually reported to increase with rising temperature (eg. Holst et al. 2003, see above). In both our experiments also, the rise in temperature from 5 to 15°C increased the percentage of microcystin eliminated. However, there was no significant difference between 15 and 25°C: in the first experiment column 3, run at 25 °C, showed a slightly better elimination, however, in the second experiment the tendency was the opposite with a better elimination for column 2 at 15°C. This can be explained by different processes influencing the degradation rate between the two experiments. In the first experiment the rise in degradation was surely due to the adaptation of the bacteria degrading microcystin. When a higher input concentration was applied, the bacteria may have first been overstrained, leading to the observed breakthrough in all columns. The rapid acceleration of degradation which then occurred is not likely to be due to further adaptation, but rather to population growth and / or higher activity of the bacteria in order to cope with this higher microcystin concentration. A growth optimum around 15°C for the microbial population in the Lake Tegel water would then explain the better elimination occurring at 15°C in the second experiment.

6.4.2 Degradation rates

In the first experiment, the degradation rates increased during the runtime of the experiment for all columns, with values ranging from 0 to 0.8 d-1, 0.86 d-1 and 0.9 d-1 for column 1, 2 and 3, respectively, with an average of 0.34 d-1 for column 1 (5°C) , 0.51 d-1 for column 2 (15°C) and 0.52 d-1 for column 3 (25°C) as shown in figure 8.

For an input microcystin concentration of 10 μg/L at 17°C and during 12 days, Cousins et al. (1996) reported a degradation rate of 0.17 to 0.23 d-1. These results are very similar to those of our experiment, where the mean value of the degradation rate on 12 days was 0.17 d-1 for 15°C and 0.18 d-1 for 25°C. For 4°C, during 7 days, Jørgensen (2001) found a degradation rate of 0.027 d-1, which is also quite similar to the value of the degradation rate at 5°C for 7 days that we estimated as 0.05 d-1.

The first experiment also showed that the degradation rate increased with the temperature. Like for the elimination, there was almost no difference between the degradation rate at 15°C and the one at 25°C compared to the much lower degradation rate found for 5°C. One conclusion from these results is that 20°C ± 5°C makes no substantial difference for the microbiology to degrade MCYST quite rapidly. For lower temperature such as 5°C, the

activity of the bacteria may be hindered, lengthening the time necessary to degrade the microcystins as efficiently as with higher temperatures. Holst et al. (2003) also reported a higher microcystin degradation at 21°C than 10°C. Schoenheinz et al. (2005) studied the DOC degradation at 5, 15 and 25°C and found a similar influence of temperature on DOC removal, with degradation rates of 0.9, 1.1 and 1.3 d-1 for 5, 15 and 25°C respectively.

6.4.3   Retardation factor

In the first experiment retardation coefficients varied between 3.44 (5°C) and 4 (15 and 25 °C), see table 2. Few retardation coefficients for MCYST are mentioned in the literature. Miller et al. (2001) determined retardation coefficient from breakthrough curves constructed from column experiments for different soil: 1.07 for a high sand soil, 4.40 for a high clay soil and 5.87 for an intermediate soils. Those values have the same order of magnitude as the one found by fitting the microcystin outlet concentration of the first experiment, maybe a little higher than what would have been expected with sand.

The influence of the temperature on the retardation factor was noticeable between 5 °C and 15°C but the same value was obtained for 15 and 25°C. Thus, higher temperatures may lead to higher retardation coefficients.

No retardation factors were calculated for the second experiment but the plot of the modelled curves with the fitting parameters of experiment 1 and the microcystin input concentration of experiment 2 showed that a much higher retardation coefficient would be appropriate. From the fitting tried on column T2 = 15°C, with the introduction of the lag phase in the λ function, a retardation factor of 6.7 was calculated instead of 4 for the first experiment. The tendency would be the same for the other temperatures as well. These results are surprising, taking into account that the flow rate was the same than for the first experiment. The microcystin outlet concentration curves showed that the breakthrough of microcystin appeared by day 8 or 9. The results and data available did not suggest any explanation for these observations.

6.5   Conclusions

The experiments conducted on three soil columns at different temperatures (5, 15 and 25°C) with two different microcystin input concentrations (19.2 and 63.5 µg/L) yielded the following conclusions:

Concerning reversible adsorption microcystin was quite mobile in the soil used, with higher mobilities at lower temperatures (retardation factor of 3.4 at 5°C instead of 4 at 15°C and 25°C). However, degradation was the most important process for microcystin elimination. This was also the conclusion of Bartel & Grützmacher (2002) and Lahti et al. (1998). Thus residence time is an important factor for MCYST removal during bank filtration.

Degradation rates increased during continuous application of microcystin, suggesting an adaptation and / or growth of the bacteria capable of degrading microcystin.

Microcystin elimination and degradation increased with temperature but for temperatures above 15°C, a rise in temperature had no relevant further impact on microcystin removal

processes. Microcystin degrading bacteria may have optimal conditions in the range of 15 – 25 °C.

With an input microcystin concentration of about 20 µg/L, a complete removal of microcystin was achieved in 21, 26 and 44 days at 25°C, 15°C and 5°C respectively. With a higher MCYST input the concentrations reached very low levels by day 35.

These results show that the use of underground passage in order to remove microcystin from water may be very effective, especially at moderate temperatures. However the efficiency of the toxin elimination strongly depends on many different factors such as the properties of the soil, the concentration of toxin applied, the behaviour of bacteria and microbiology and the filtration distance. Therefore, local validation of these results is important for candidate bank filtration sites.

6.6 References

BARTEL H., GRÜTZMACHER G., 2002: Elimination of Microcystins by slow sand filtration at the UBA Experimental Field, C. RAY (ed): Understanding Contaminant Biogeochemistry and pathogen Removal, 123-133, Kluwer Academic Publishers.

BOURNE D.G., JONES G.J., BLAKELEY R.L., JONES A., NEGRI A.P., RIDDLES P., 1996: Enzymatic Pathway for the Bacterial Degradation of the Cyanobacterial Cyclic Peptide Toxin Microcystin LR, Applied and Env. Microcbiology, 62 (11): 4086-4094.

COUSINS I.T., BEALING D.J., JAMES H.A., SUTTON A., 1996: Biodgradation of microcystin-LR by indigenous mixed bacterial populations, Wat. Res., 30 (2): 481-485.

GRÜTZMACHER G., BÖTTCHER G., CHORUS I., BARTEL H., 2002: Removal of microcystins by slow sand filtration, Environm. Tox, 17: 386-394, John Wiley & Sons.

HOLST T., JØRGENSEN N.O.G., JØRGENSEN C, JOHANSEN A., 2003: Degradation of microcystin in sediments at oxic and anoxic, denitrifying conditions, Wat. Res. 37: 4748-4760.

JØRGENSEN C., 2001: Removal of algae toxins during artificial recharge – column and batch studies, Artificial Recharge of Groundwater, EC project ENV4-CT95-0071, Final report, 6.6: 133-135.

LAHTI K., VAITOMAA J., KIVIMÄKI A.L., SIVONEN K., 1998: Fate of cyanobacterial hepatotoxins in artificial recharge of groundwater and in bank filtration, Artificial Recharge of Groundwater, Peters et al. (eds), Balkema, Rotterdam.

MILLER M.J., HUTSON J., FALLOWFIELD H.J., 2001: An overview of the potential for removal of cyanobacteria hepatotoxin from drinking water by riverbank filtration, Env. Health, 1 (1): 82-93.

SCHOENHEINZ D., BÖRNICK H., WORCH E., 2005 : Temperature effects on organics removal during river bank filtration, Proceedings of the 5th International Symposium on Management of Aquifer Recharge, ISMAR-5, Berlin, 12-17 june 2005.

World Health Organisation, 1998: Guidelines for drinking water quality, 2nd edition, Addendum to Volume 2, Health criteria and other supporting information, WHO, Geneva.

ZECK A, WELLER M.G., BURSILL D., NIESSNER R., 2001: Generic microcystin immunoassay based on monoclonal antibodies against Adda, Analyst, 126: 2002-2007.

7 Clogging Column Experiments

7.1 Introduction

The experiments carried out on the clogging column by the working group „algae" had the aim to examine the elimination of dissolved and extra-cellular microcystin (MCYST) in a setting typical for the Berlin situation. Experiments carried out on the UBA's experimental field (see final report working group algae, part IV and part V) had covered the setting relevant for many artificial recharge and bank filtration sites with mostly sandy sediments. These left a gap regarding settings with fine to medium grained sand with some portions of silt and clay as well as organic material, as are found partially in Berlin and elsewhere. Also, the observation wells at the transects with contact times of 2 weeks minimum did not cover the time span relevant for elimination of microcystins in detail (maximum half life only a few days). Therefore, experiments using the clogging column set up at the FU Berlin provided the opportunity to fill this gap.

Two experiments were carried out with MCYST:

- CC1: Continuous dosing of dissolved MCYST over 9 days, sampling water at different depths,

- CC2: Pulsed application of cyanobacterial cells with subsequent sampling of water and sediment.

7.2 Materials and Methods

7.2.1 Sediment chemistry

Further descriptions can be taken from the final report working group FUB, part I (see chapter 1.2.2).

7.2.2 Water chemistry

Further descriptions can be taken from the final report working group FUB, part I (see chapter 1.2.3)

7.2.3 Experimental Methods

7.2.3.1 Column setup

Further descriptions of the experimental design can be taken from the final report working group FUB, part I (see chapter 1.2.3)

7.2.3.2 Experiment with dissolved MCYST (CC1)

The crude extract of MCYST obtained from the UBA's mass culture (extract # 5 with 62 mg/L MCYST) was diluted 1: 500 with water from Lake Wannsee (see final report working group FUB, part I). Prior to the experiment the water reservoir at the top of the column as well as all tubing was emptied and filled with the prepared MCYST solution. The inlet was then connected to a water reservoir with MCYST solution that was permanently stirred (for oxygen saturation) and the bottle was wrapped with aluminium foil to avoid photochemical decay of MCYST.

A tracer experiment with NaCl was carried out in parallel to the first application of MCYST with continuous measurement of the electrical conductivity (EC) at the outlet (see final report working group FUB, part I, chapter hydraulics). The experiment commenced on 8th Dec. 2004. On 17th Dec. dosing with MCYST solution was terminated and the column was flushed with lake water. The last sampling was carried out on 27th Dec. 04. Thus, the experiment was carried out 246 to 265 days after column setup.

During the experiment the flow rate through the column amounted to 350 to 550 mL/d, corresponding to a filtration velocity of 0.091 m/d to 0.142 m/d and a flow velocity (considering an effective pore volume of about 30 %) of 30 cm/d to 48 cm/d (see final report working group FUB, part I).

Samples for MCYST analysis by ELISA were taken from the water reservoir (before and after the reservoir was exchanged every 2 to 3 days) as well as from the sampling ports at 4, 8, 12, 25, 60, 80, 90 and 99 cm every 2 to 3 days. The samples were stored frozen in glass test tubes and analysed using the Adda-ELISA (see chapter MCYST analyses).

7.2.3.3 Experiment with cyanobacterial cells (CC2)

The experiment with cyanobacterial cells was carried out together with the working group "microbiology" of the TU Berlin, which applied fluorescent particles (d = 2.44 µm) simultaneously. The particles and the cyanobacterial cells (taken from the UBA's mass culture of Planktothrix agardhii HUB 076) were applied in a pulse by exchanging the water above the column with Lake Wannsee water (300 mL) to which the substances had been added beforehand (200 mL mass culture, 10 mL NaCl solution and 10 µL particle suspension). The resulting initial concentration in the water reservoir was 165 µg/L total MCYST of which 39 µg/L (or 24 %) were extracellular. The biovolume amounted to 34 mm³/L, which is about the maximum concentration of cyanobacteria found in Lake Wannsee during 2002 to 2004 (see final report working group algae, part I).

The column was then flushed with water from Lake Wannsee at a constant flow rate of 600 mL/d which corrensponds to a filtration velocity of 15.6 cm/d (1.8*10-6 m/s) and a flow velocity of 52 cm/d (6*10-6 m/s). The experiment commenced on 3rd March 2005 and was terminated on 17th March 2005 (331 to 345 days after start of operation).

Similarly to the procedure for the dissolved microcystins, samples for MCYST analysis by ELISA were taken from the water reservoir and from the sampling ports in 4, 8, 12, 25, 60,

80, 90 and 99 cm depth twice a week. Parallel samples were taken for total MCYST (i.e. cell-bound and extra-cellular) and for extra-cellular MCYST (sample filtered by membrane filter, pore size 0.45 µm). The samples were stored frozen in glass test tubes and analysed using the Adda-ELISA (see chapter MCYST analyses). Biovolume of cyanobacteria was additionally determined in the samples from the water reservoir by microscope according to Utermöhl (1958).

After the experiment had been terminated the sediment was extracted from the column and samples were taken on 19th April 2005, 33 days after the last water samples had been taken, for biovolume determination and MCYST analysis. Biovolume of cyanobacteria in the sediment was determined by suspending a known volume of sediment (previously conserved with formolaldehyde) with deionized water with a ratio of 1:10, shaking and centrifuging for homogenisation and sedimentation of the particulate anorganic matter. The supernatant was then examined by microscope following the method described by Utermöhl (1958). The ELISA was carried out from a parallel sample that had been deep frozen and thawed in order to release cell-bound MCYST and also brought into suspension with a known volume of deionized water. This method detects the sum of cell-bound MCYST released from cells trapped within the sediment together with MCYST adsorbed to the sediment and desorbed by addition of deionized water.

7.3   Results

7.3.1   Experiment with dissolved MCYST (CC1)

Samples from the water reservoir were taken directly after preparation of the MCYST solution and before it was disconnected 2 to 3 days later. The results given in Figure 30 show a dramatic drop in concentration over the 2 to 3 days during which the water reservoir was connected to the column (the lines mark samples taken from the same flask, concentration developments would surely follow an exponential decay curve). This drop is most probably due to degradation in the water reservoir. This had not been expected, as previous experience during field experiments had never shown this rapid decline in concentration. The reason for this may lie in the constantly high temperatures of 20°C to 22°C, well above those reached during the field experiments. Hence the input concentration for the experiment was highly variable, making it difficult to draw quantitative conclusions.
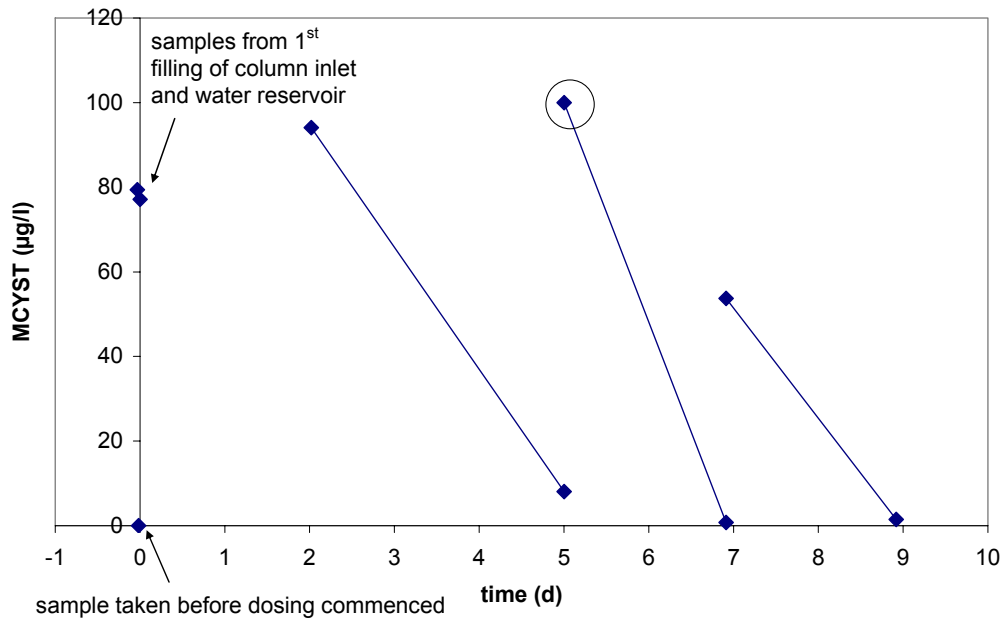
Figure 30: **Concentrations of MCYST in the water reservoir during the experiment with dissolved MCYST. Lines indicate samples taken from the sampe flask, not concentration developments (circle marks MCYST concentration calculated from extract concentration and dilution factor).**

The concentrations at the different sampling ports during the experiment are given in Figure 31. Due to the highly variable input (see above) the results are limited to the following points:

Concentrations of initially about 78 µg/L (water reservoir, day 0) decrease to 16 µg/L in 25 cm depth after 2 days (although higher values cannot be ruled out between 25 and 60 cm), a conservative tracer would be expected to reach 61 to 96 cm during this time (see chapter 7.2.3.1). This would imply a retardation coefficient roughly between 1.0 and 3.9.

After additional 3 days (5 d after first toxin application) a maximum in concentration was observed in 80 cm and 90 cm depth with 7.9 µg/L in both of the sampling ports. This maximum most probably traces back to the high concentrations in the water reservoir after it had been exchanged 3 days before. On the basis of these data, retardation coefficients amount roughly to values between 1.0 and 1.7.

After additional 2 days (7 d after first toxin application) a concentration peak of 4.5 µg/L was observed in 80 cm and 90 cm depth. Considering a water reservoir maximum 2 days prior to this sampling event retardation coefficients reach about 0.6 to 1.1. As values < 1 are not likely to occur for MCYST these low MCYST concentrations in 80 to 90 cm may be due to toxins originating from the peak applied on day 2 and only slowly desorbing from the fine particles occurring at the basis of the column (compare final report working group FUB, part I). This would also mean that the peak applied on day 5 has been degraded to values < 0.1 µg/L by this time.

Without taking dispersion and retardation into account the elimination rates amount to values between 80 % in two days (1st peak) and 92 % in three days (2nd peak). For peaks 3 and 4 (applied on day 5 and day 7) these rates lie well over 99 % in two days.
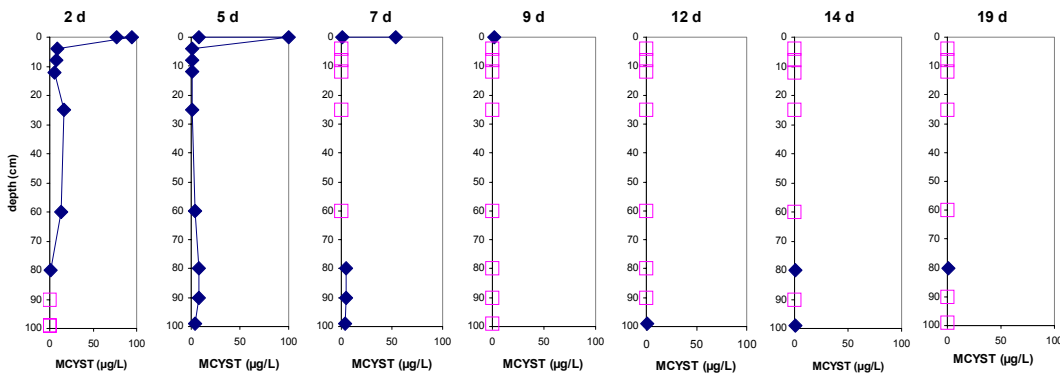
Figure 31: MCYST concentrations in the water reservoir (depth = 0) and in the sampling ports during experiment CC1 (two values at depth = 0 correspond to two samples taken before and after exchange of reservoir; open squares: values below detection limit).

These figures show that in spite of very high input concentrations (5 fold higher than the maximum total (i.e. extra-cellular and cell-bound) concentrations in Lake Wannsee during 2002 to 2004) only traces were detectable at the column effluent in 1 m depth, and elimination must be assessed as highly effective. This underpins the field observations of the concentrations measured along the transsects at Lake Tegel and Lake Wannsee which were usually below detection limit.

Formatiert: Nummerierung und Aufzählungszeichen

7.3.2   Experiment with cell-bound MCYST (CC2)

Experiment CC2 carried out with live cells of Planktotrix agardhii had the aim to asses the elimination of cyanobacterial cells through lake Wannsee shore sediment and the possible release of cell-bound MCYST from the strained cells. The biovolume of Planktothrix agardhii as well as the MCYST concentrations (total and extracellular) determined in the water reservoir are shown in Figure 32. There is a sharp drop in biovolume and total MCYST during the first day of the experiment. A comparison with the dilution curve calculated on the basis of a constant flow rate of 600 mLl/d (Figure 32), which drops even more steeply than the measured values of biovolume, shows that there must be some resuspension of the cells from the sediment surface as growth is unlikely to occur in darkness.

The absolute concentration of extracellular MCYST decreased only slightly during the first day of the experiment, and the relative share of extracellular MCYST increased from 24 % directly after application to 87 % and 86 % on day one. These initially high values might

already be an indication of cell stress or lysis, during which MCYST is released, as usually more than 90 % of the MCYST is cell-bound. This is indicated by changes in concentrations of MCYST per mm³ of cell volume, i.e. cellular MCYST content, decreased by 60 % from 3.7 µg/mm³ to 1.45 µg/mm³ during this time. It could, however, also be due to preferential sedimentation of the cyanobacterial cells, in contrast to extracellular, dissolved MCYST.
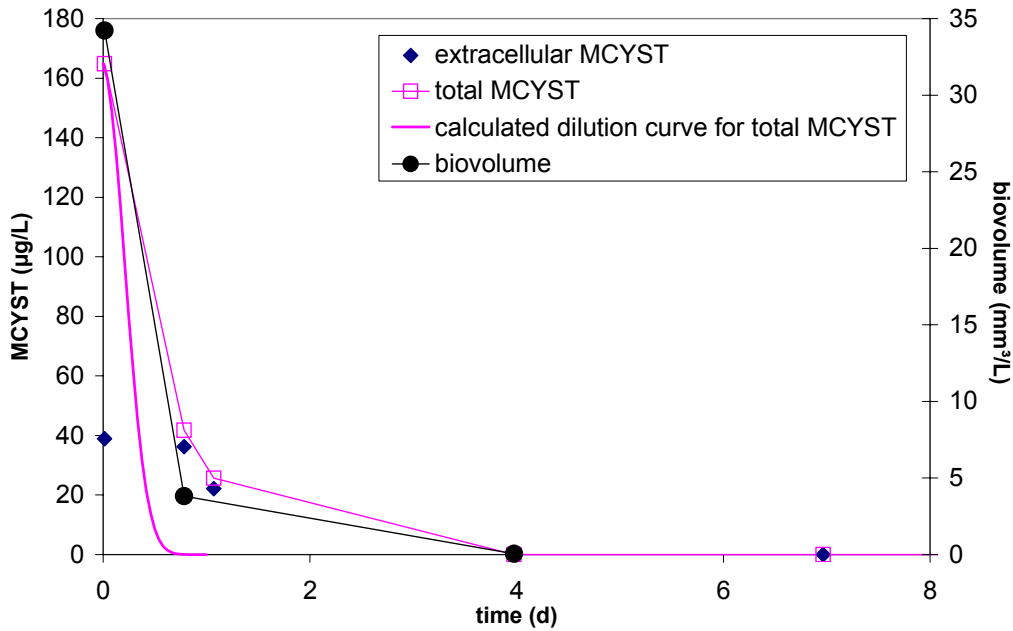
Figure 32: Total and extracellular MCYST as well cyanobacterial biovolume in the water reservoir during experiment CC2.

The extracellular MCYST concentrations measured and the cell-bound MCYST concentrations calculated from total and extracellular MCYST in the sampling ports are given in Figure 33 for day four after application. The curves show an increase of both concentrations with depth. No MCYST can be detected in the first 12 cm of sediment passage, cell-bound MCYST is not detectable in the uppermost 50 cm. From 50 cm on downwards extracellular MCYST was determined at concentrations between 0.43 µg/L and 0.48 µg/L. Cell-bound MCYST increases constantly with depth from 70 cm on downwards with a maximum of 1 µg/L in 99 cm depth. From the next sampling event (day 7) on, no MCYST was detectable in the sampling ports.
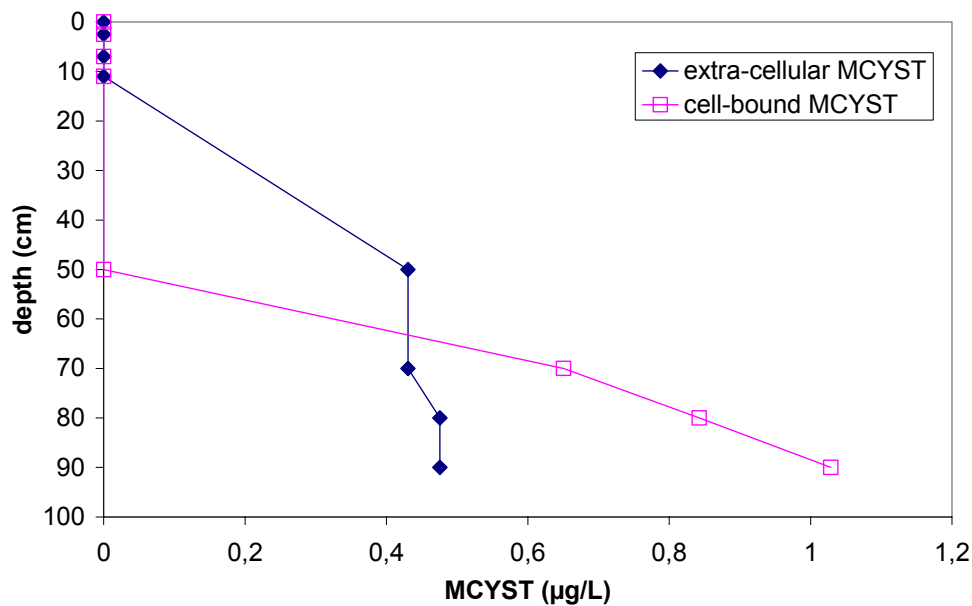
Figure 33: Cell-bound and extra-cellular MCYST in the sampling ports on day 4 after application.

Microscopic examination of the sediment after the column was sacrificed showed no filaments of Planktothrix agardhii throughout the column. The ELISA revealed low concentrations of extracellular MCYST (< 0.9 to 1.4 µg/L) in the pore water. As no MCYST had previously been detectable in the water samples these traces are probably due to MCYST released from particulate matter either by desorption or from lysed cells. The concentrations, however, are very low and distributed evenly across the entire depth of the column so that remobilisation does not seem to be a factor to be considered in the field setting.

7.4 Interpretation and Discussion

The experiment with dissolved MCYST in the clogging column (CC1) showed two important results:

In repeated pulsed applications retardation coefficients between 1.0 (no retardation compared to a conservative tracer) and 3.9 were observed. This is in agreement with field experiments carried out by our own working group (see final report working group algae, part IV and part V) as well as laboratory experiments carried out by Miller (2000).

Degradation could be observed, even under low oxygen conditions (no totally anoxic conditions were achieved during the experiment) and the elimination rates increased with time (from 80 % in the beginning to 99 % during the fourth pulsed application). Similar values

70

have also been published by other working groups (Lahti et al. 1996, Jørgensen 2001, Miller 2000). Although the adaptation of MCYST degrading bacteria with repeated contact has so far only been shown with lake water and without sediment contact (Christoffersen et al. 2002), this is the most likely mechanism causing enhanced elimination rates over time.

The second experiment with initially mostly cell-bound MCYST on the clogging column (CC2) showed the following results:

During the first day of application the ratio of extracellular MCYST in the water reservoir increased from 24 % to 86 % probably due to cell lysis under unfavourable conditions and / or sedimentation of cells. The assumption that release of MCYST from the cells is the main mechanism is supported by the fact that the concentrations of MCYST per mm³ of cell volume, i.e. cellular microcystin content, decreased by 60 % during this time.

After four days the uppermost 12 cm showed no detectable MCYST in the aqueous phase. This leads to the assumption that the cells accumulated on the sediment surface do not act as a continuous source for MCYST.

In greater depth, however, extracellular as well as cell-bound MCYST was detectable, mostly with greater cell-bound than extracellular concentrations. This shows that a breakthrough of cells may well be possible and has to be regarded more closely in further experiments.

In summary, the experiments with MCYST on the clogging column showed results that complement the observations on the transsects at Lake Wannsee and support the field results observed at these sites: Extracellular MCYST is degraded rapidly in the lake sediments even under conditions of low oxygen concentrations. Thus even maximum MCYST concentrations of 20 µg/L (greatest extracellular concentrations measured in Lake Wannsee surface water) would be reduced to at least 4 µg/L during the first day of sediment contact. Field observations showed that maximum values in observation wells with residence times of about 2 weeks amounted to less than 1 µg/L.

Concerning the complex question of interaction between extracellular and cell-bound MCYST the experiments still leave some uncertainties. Although an accumulation and subsequent continuous release of MCYST from sedimented cells could not be confirmed, the transport of cell-bound (possibly particle bound) MCYST through sediment has to be observed more closely in future experiments.

7.5   References

Christoffersen K., Lyck S. & Winding A. (2002): Microbial activity and bacterial community structure during degradation of microcystins., Aq. Microb. Ecology, 27: 125 – 136.

JØRGENSEN C., 2001: Removal of algae toxins during artificial recharge – column and batch studies, Artificial Recharge of Groundwater, EC project ENV4-CT95-0071, Final report, 6.6: 133-135.

Lahti, K., J. Silvonen, A-L. Kivimäki and K. Erkomaa (1996) Removal of cyanobacteria and their hepatotoxins from raw water in soil and sediments columns in Artificial Recharge

of Groundwater, Proceedings of an international symposium, A-L. Kivimäki and T. Suokko (eds.) Finnish Environment Institute, Helsinki, 187-195.

Miller M.J. (2000): Investigation of the removal of cyanobacterial hepatotoxins from water by river bank filtration . PhD Thesis, Flinders University.

Utermöhl H. 1958. Zur Vervollkommnung der quantitativen Phytoplanktonmethodik. Mitt Int Ver Limnol 9: 1 – 38.

8 Slow sand filter experiments

8.1 Introduction

The slow sand filter (SSF) experiments on the UBA's experimental field were carried out in order to investigate elimination processes during relatively short contact times and high flow velocities in comparison to the bank filtration sites. This was necessary especially for those substances that are usually readily removed by sediment contact (e.g. algal toxins, viruses and bacteria). For these substances the observation wells at the transects with contact times of 2 weeks minimum did not cover the time of interest. A second reason for conducting SSF experiments was the opportunity to observe substance removal during underground passage in settings likely to occur in other regions of the world and / or during artificial recharge. This was necessary as the bankfiltration sites in Berlin are not typical for most other settings and some of the investigated substances were not present in the artificial recharge basin at Tegel at sufficient level for detailed investigation. Additionally the slow sand filter offered the opportunity to investigate the formation of a clogging layer under well defined conditions by hydraulic, geochemical and microbiological methods.

Figure 34 gives an overview of all investigations and experiments carried out on the slow sand filter during the NASRI project.

	Jan.	Feb.	March	April		May	June	July	Aug.	Sept.	Oct.	Nov.	Dec.
	2002												
technical modifications									new drainage pipes, new sand				
	2003												
technical modifications				installation slide holders into sand								
average filtration velocity			2.4 m/d			1.2 m/d			0.9 m/d		0.6 m/d		
microbiol. Investigations			weekly sampling of clogging layer, LOI, DAPI										
experiments			SSF1	SSF2	SSF3	SSF4	SSF5					SSF6	
date of experiments			19.3.03	15.4.03	23.04.03	26.5.03	17.6.03					19.11.03	
applied substances			NaCl, phages	MCYST	NaCl, drugs	NaCl, phages	NaCl, MCYST, phages, drugs					NaCl, MCYST, phages, bact., drugs	
	2004												
technical modifications			installation of slide holders into piezzometers										
average filtration velocity							2.4 m/d	0.1 m/d			1.2 m/d		
microbiol. Investigations									analysis biofilm				
experiments							SSF7					SSF8	
date of experiments							14.6.04					22.11.04	
applied substances							NaCl, phages, bact.					NaCl, phages, bact.	
Legend:	SSF dry												
	SSF flooded (little or no clogging)												
	SSF flooded (visible clogging layer)												

Figure 34: Overview of the investigations and experiments carried out on the SSF.

The aim of the series of experiments conducted with MCYST was to test elimination under a combination of 3 worst-case conditions (experiment SSF2: virgin sand that had no previous contact to MCYST, missing clogging layer and with 2.4 m/d high filtration velocities) in order to test whether lower filtration velocities (experiment SSF5: 1.2 m/d and experiment SSF6: 0.6 m/d) and enhanced clogging can lead to better removal rates.

8.2   Materials and Methods

8.2.1   Technical scale slow sand filter on the UBA's experimental field

The slow sand filter (SSF) is fed with surface water from a storage pond of the facility and has a surface area of 73 m2 (Figure 35). As the pond narrows towards the bottom the average area of the filter sand is 60.4 m². The water reservoir above the filter bed has a depth of 30 cm to 60 cm and a volume of approximately 40 m³, depending on the water level adjusted for the respective experiment. Water percolates through the filter following gravitational flow. The filter bed has a depth of 80 cm with a gravel layer of 15 cm depth at the bottom and 65 cm of filter sand above. The drainage pipes form a double-H (Figure 36), ensuring almost vertical flow.

The filter sand was replaced in autumn 2002 in order to carry out experiments with virgin sand for the simulation of worst case conditions (Figure 37).
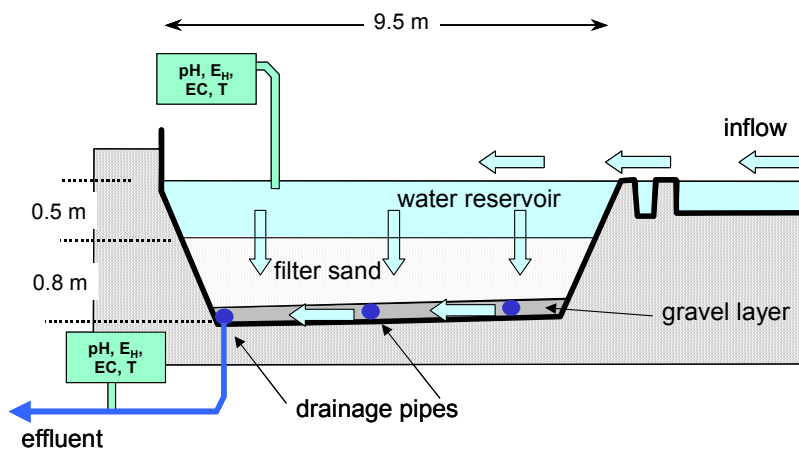
Figure 35:   **Schematical cross section of the slow sand filter**

Figure 36: Drainage pipes on the basis of the slow sand filter during sand exchange.

Figure 37: Preparation of the filter sand during sand exchange.

8.2.2 *Characterization of the virgin filter material*

The filter sand is medium to coarse sand with small amounts of fine sand. Silt and clay are not present. The gravel layer consists of fine gravel with large amounts of medium grained gravel (Figure 38).
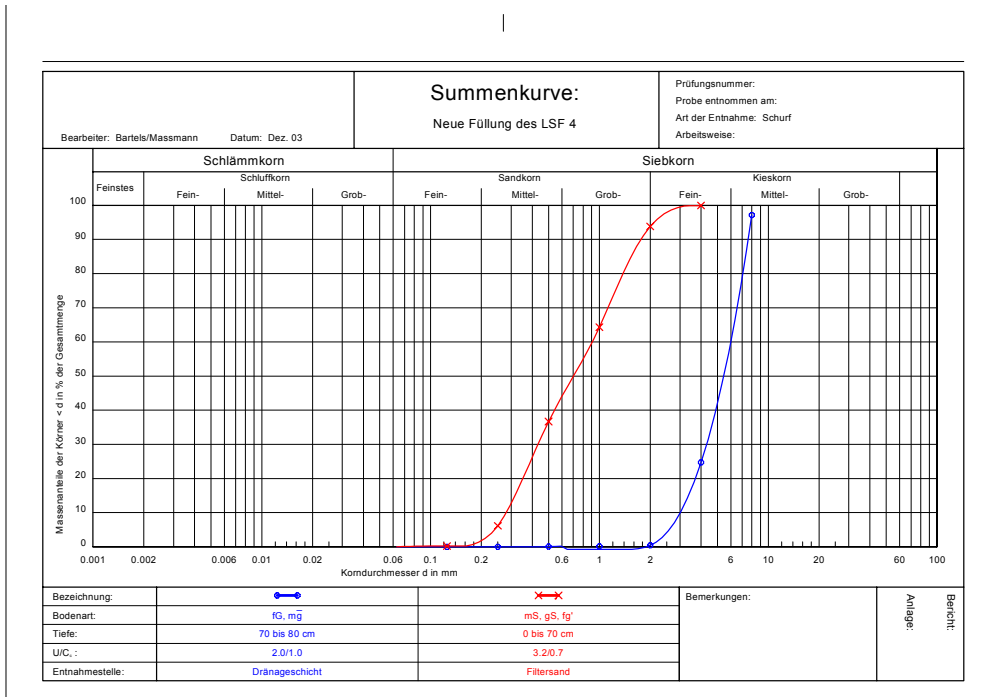
Figure 38: **Grain size distribution of the filter material in the SSF (data by FU Berlin).**

Table 7: **Geochemical properties of the virgin SSF sand in comparison to sand from Lake Wannsee's shore (data by FU Berlin).**

Parameter	virgin SSF sand	sand from Lake Wannsee shore (average of two samples taken by FU Berlin ± standard deviation)
Fe-ox [mg/kg]	275	457 (±140)
Fe-red [mg/kg]	850	838 (±88)
Fe-total [mg/kg]	1125	1295 (±52)
Mn-ox [mg/kg]	11.0	30 (±24)
Mn-red [mg/kg]	17.5	16.3 (±8.8)
Mn-total [mg/kg]	28.5	46 (±16)
C-org [weight %]	0.022	0.37 (±0.29)
C-inorg [weight %]	0.118	0.36 (±0.13)

The geochemistry resembles that of sand taken from the shore of Lake Wannsee fairly well (Table 7), with exception of the total Fe content (13 % less in the filter material) and the cation exchange capacity (CECeff: 82 % less in the filter material). This is probably due to the coarser grain size of the filter material (Massmann et al. 2004).

8.2.3 Hydrochemistry under normal operating conditions

The surface water used for the experiments originates from the surrounding aquifer and is treated for iron and manganese removal in the water works of the experimental field before being fed into the storage pond. Its high electrical conductivity (about 950 µS/cm) is due to relatively high concentrations of salts (HCO3-: 140 mg/L, SO42-: 230 mg/L, Cl-: 95 mg/L, Ca2+: 130 mg/L and Na+: 45 mg/L, average of 3 samples taken during 2002 and 2003, data is given in appendix IV-1). The DOC ranges from 5.5 mg/L in summer to 2.4 mg/L during winter. Calculations with PHREEQC show that in relation to the atmosphere the surface water is slightly oversaturated with CO_2 and O_2 (partial pressures 0.08 % and 28 %, respectively), probably due to biological activity of algae and water plants. This might also be the reason for the slightly alkaline pH in the water reservoir (pH 8.2 in average).

During sand passage a slight reduction of pH (to pH 7.9), O_2 (to a partial pressure of 20 %) and DOC (40 % reduction in summer and 15 % reduction in winter) can be observed. On the other hand, nitrate can be detected at values around 0.4 mg/L, while it cannot be detected in the surface water, due to nitrification inside the filter.

8.2.4 Experimental Methods

In preparation of the experiments the flow rate was adjusted to the desired amount, corresponding to the filtration velocities. The tracer and the trace substances were applied by spraying them evenly across the water reservoir with a hose from a barrel containing the concentrated substances diluted with 100 L of tap water. The tracer applied was sodium chloride (NaCl) so that the sampling intensity in the different sampling points could be adjusted by observing the electrical conductivity (EC). Care was taken not to increase the electrical conductivity by more than 10 %.

The MCYST applied was extracted from a mass culture of Planktothrix agardhii HUB 076 by centrifugation and freeze thawing in order to release the mainly cell-bound, highly water soluble microcystins. The freeze thawed extract was homogenized and then centrifuged to remove the cell debris and stored frozen. One day prior to each experiment the extract was thawed and partitioned into the required volume. The application to the water reservoir was carried out as mentioned above. The resulting MCYST concentrations in the water reservoir amounted to 10 µg/L ± 2 µg/L.

8.3 Results

Quantification of clogging by different methods

Hydraulic conductivity

Figure 39 gives the development of hydraulic conductivity (kf) determined by hydraulic head (i) and flow rate (Q) according to (1).

$$k_f = v_f / i = Q/(A*h/l)$$ (1)

With   A: average area of the SSF (60.4 m²),

       h: head loss between water reservoir and effluent,

       l: height of filter bed (0.8 m).
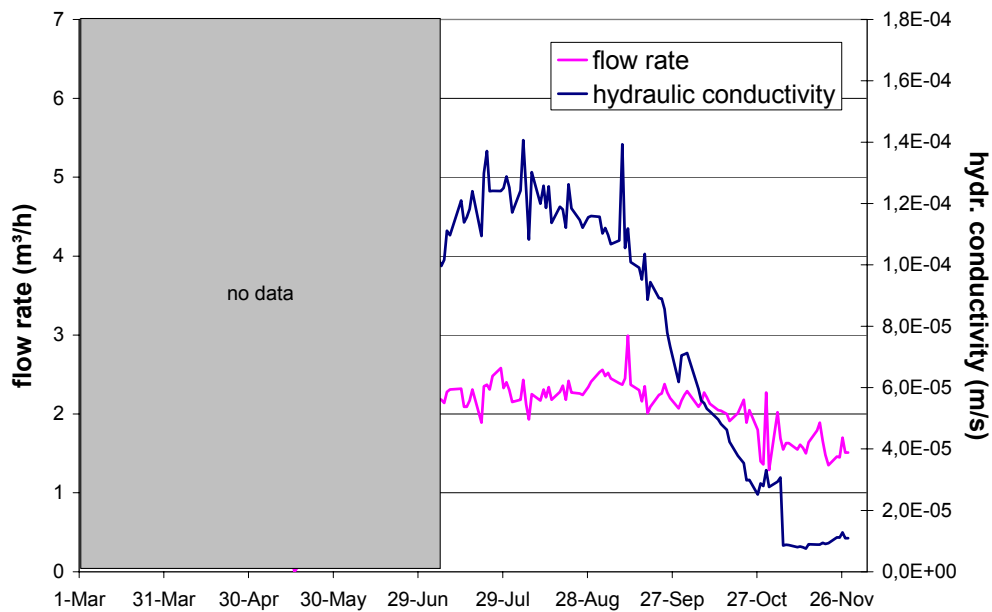
Figure 39: **Flow rate and hydraulic conductivity in the slow sand filter used for the SSF experiments during 2003 (time scale corresponding to Figure 41).**

The filter showed a substantial increase of clogging between August and November 2003. During this time hydraulic conductivity was reduced from 1.2 * 10-4 to 0.5 *10-4 m/s. Due to missing water table measurements before July 2003 no hydraulic conductivities could be calculated. As the observed water table was lower than during summer and the flow rate higher (up to 6 m³/h), we can conclude that the hydraulic conductivities must have been substantially higher.

In August 2004, after all SSF experiments had been carried out, the superficial layer of the slow sand filter was destroyed by raking. As can be seen on the picture taken during this

procedure (Figure 40), gas bubbles emerged, indicating that clogging had lead to partially unsaturated conditions due to trapped gas in the upper centimeters of the filter.

Figure 40: **Photograph taken during raking of the SSF in order to destroy the superficial clogging layer.**

8.3.1.1 Organic substance determined by loss on ignition (LOI)

The LOI-results of the 5 cm cores sampled weekly during 2003 (Figure 41) show high variations (minimum: 0.26 %; maximum: 4.4 %) in time and depth. The variations between different depth increased over time, as did some absolute values. In the beginning of 2003 when the measurements started the differences in LOI between the layers sampled did not exceed 0.5 %. In autumn 2003 the difference on some occasions reached 2 %. The highest values of LOI were measured in the uppermost millimeter of the filter in some samples taken during summer and autumn 2003. In other samples of this layer taken during that time, however, no relevant increase was observed compared to the values measured in March 2003. It was supposed that this may be due to a high spatial inhomogenity. In order to test this, six samples from different places distributed over the filter surface were taken on one occasion and analysed by the same method.
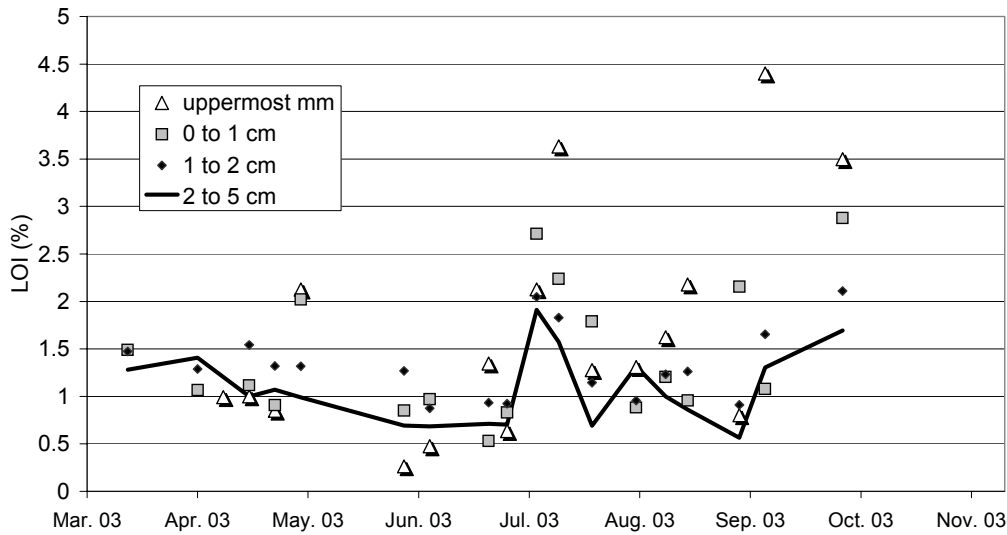
Figure 41:   Loss on ignition (LOI) as measure for organic substance in the filter bed of the SSF.

The results show a regional variation of up to 1 % LOI (95 % confidence interval) with highest variations in the uppermost centimeter (Figure 42). These variations, however, do not explain the differences of up to nearly 4 % between the different sampling events in 2003.
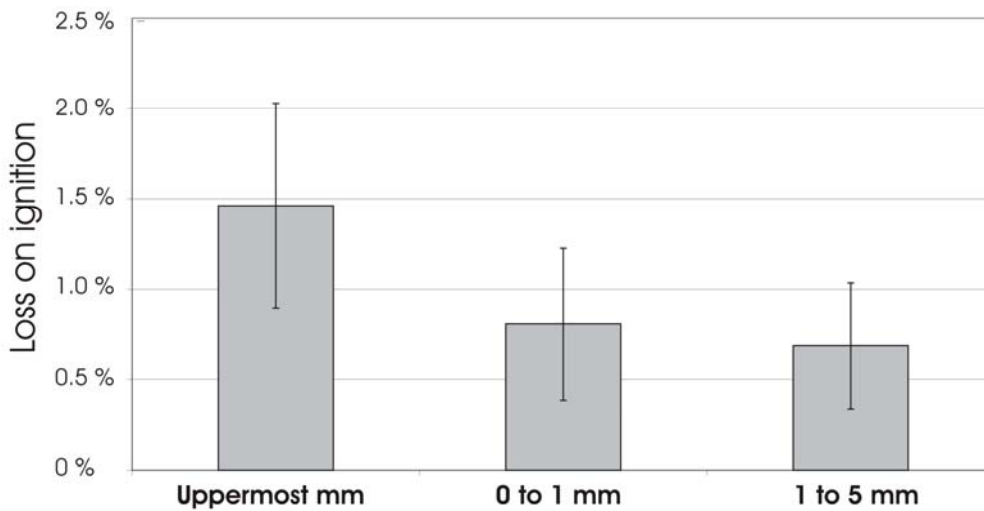
Figure 42:   Variation of LOI during one sampling event (error bars indicate the 95 % confidence interval, n = 6).

8.3.1.2 Geochemistry of the clogging layer

Table 8 gives the geochemical properties of the clogging layer in comparison to the values determined in the virgin SSF sand. The results show a clear increase of all the parameters measured. This is due to the accumulation of organic substance (debris and biomass lead to a 10-fold increase of Corg). There is, however, also a distinctive increase in inorganic carbon concentration (also more than 10-fold) as well as iron and manganese, probably due to the relative increase of fine mineral material.

Table 8: Geochemical properties of the clogging layer in comparison to virgin SSF sand. (Massmann et al. 2004).

Parameter	virgin SSF-material	clogging layer
Fe-ox [mg/kg]	275	605
Fe-red [mg/kg]	850	1700
Fe-total [mg/kg]	1125	2305
Mn-ox [mg/kg]	11.0	68.8
Mn-red [mg/kg]	17.5	100.0
Mn-total [mg/kg]	28.5	168.8
C-org [weight %]	0.022	0.343
C-anorg [weight %]	0.12	1.40

8.3.1.3 Hydraulic properties determined by tracer experiments

Figure 43 gives the conductivities measured in the effluent as well as the curves modelled by using Visual CXTFIT for all tracer experiments carried out in the course of 2003. Table 9 lists the modelled pore velocities, dispersion lengths as well as the filter resistance for each of the experiments conducted on the slow sand filters and enclosures.

Table 9: Pore velocities, dispersion lengths, effective pore volumes and hydraulic conductivities during the tracer experiments on slow sand filter.

Experiment No.	Filtration velocity	Pore velocity	Dispersion length	Eff. Pore-volume (ne)	Hydraulic conductivity
	[m/d]	[m/d]	[m]		[m/s]
SSF1	2.4	6.24	0.012	0.385	n.d.
SSF3	2.58	6.48	0.05	0.37	n.d.
SSF5	1.43	3.12	0.023	0.385	1.4*10-4
SSF6	0.59	1.68	0.01	0.357	7.4*10-6

The slow sand filter experiments were conducted with three different filtration velocities (about 2.5 m/d, 1.4 m/d and 0.6 m/d). Therefore pore velocities changed correspondingly. The reduction of the dispersion length between SSF3, SSF5 and SSF 6 can also be explained by the decline of flow velocities. A substantial disturbance of one part of the filter due to installation of microbial slide holders before SSF3 (see Figure 35) may be the reason for the increase in dispersion length between SSF1 and SSF3 with otherwise similar conditions. Effective pore volumes vary between 0.357 and 0.385, with a trend to smaller values with time. This is in line with the overall increase of hydraulic resistance. As to be expected average hydraulic conductivities dropped during 2003 due to clogging (see chapter 3.1).
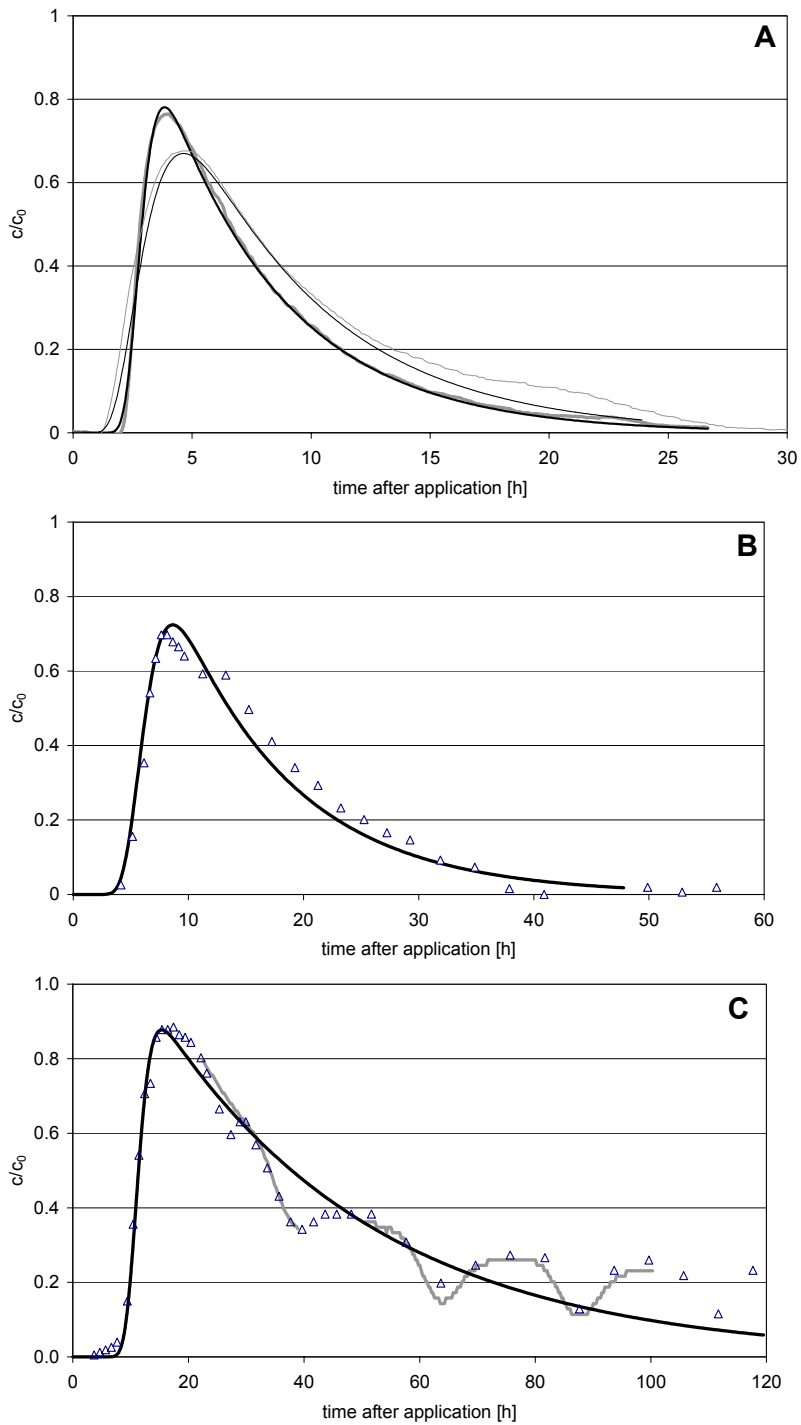
Figure 43: Measured electrical conductivity and modelled output function for SSF tracer experiments. Symbols: hand measurements, grey lines: online measurements, black lines: modeled curves. A: SSF1 (thick lines) and SSF3 (thin lines); B: SSF 5; C: SSF6 (note different time scales on x-axis for A, B and C).

8.3.1.4   Assessing the clogging situation of the slow sand filter during the experiments

Different methods were used to assess the clogging situation of the slow sand filter in 2003:

- Calculating hydraulic conductivities from daily measurement of water table and flow rates,

- Calculating effective porosities from pore velocities obtained by modeling breakthrough curves during tracer experiments,

- Measuring the organic content in the upper centimeters of the filter bed from weekly sampling,

- Determining the biomass by total cell count in weekly samples from the upper centimeters of the filter bed,

The hydraulic conductivities showed a clear and constant decrease in the course of September ($1.2*10-4$ m/s) to November 2003 ($0.2*10-4$ m/s) with previous short term variations (probably due to higher flow rates during rainfall) of $0.2*10-4$ m/s between June and September (Figure 39). Effective porosities, calculated from tracer breakthrough curves, show a similar pattern of quite constant values between 0.37 and 0.385 during the first few experiments (SSF1 through SSF 5) until June 2003. No tracer tests were performed from July to October, but in November the effective porosities had decreased significantly to 0.357 (Table 9).

The bio- and geochemical processes leading to this decrease in hydraulic conductivity (or clogging) were assessed with the two other methods mentioned above (LOI measurement and total cell count).

As expected, the measured values for organic content (loss on ignition, LOI) showed an increase from values around 1.5 % ($\pm$ 0.5 %) in March, April and May to 2 % ($\pm$ 1 %) after July (Figure 41). There are, however high temporal variations in all layers sampled (uppermost millimeter, 0 to 1 cm, 1 to 2 cm and 2 to 5 cm) with the temporal variations increasing in time and exceeding the vertical and horizontal spatial variations. These results imply that high organic content usually concurs with lower hydraulic conductivities. Lower organic content, however, does not necessarily mean high conductivities.

An indication of which processes take place during clogging can be derived from the observation of gas bubbles during raking of the filter surface (Figure 40). The formation of gas bubbles is due to biological activity inside the filter bed without the possibility of escaping to the water surface (which may be due to physical clogging by fine organic and inorganic particles).

During the enclosure experiments carried out with the same filter material, substances and water quality further results concerning clogging processes in this setting were obtained. They will be discussed in part V of this report.

8.3.2   Changes in general hydrochemistry during the experiments

Table 10 shows the results of the main cation and anion analysis carried out by the FU Berlin on samples taken during SSF 5.

Table 10:   Main anions and cations during TV 6 (data by FU Berlin).

	Time after application	Sodium	Potassium	Calcium	Magnesium	Chloride	sulfate	Nitrate	Phosphate
		Mmol/L							
Water reservoir	-0.6	2.02	0.11	3.13	0.74	2.82	2.46	0.005	< 0.001
	0.1	4.67	0.12	3.25	0.75	5.61	2.50	0.005	< 0.001
	5.1	3.61	0.12	3.20	0.74	4.51	2.35	0.005	< 0.001
	25.1	2.22	0.11	3.25	0.74	3.05	2.38	0.006	< 0.001
Effluent	0.7	2.02	0.11	3.30	0.77	2.82	2.36	0.006	< 0.001
	6.1	2.94	0.12	3.40	0.81	4.09	2.35	0.006	< 0.001
	34.9	2.27	0.10	3.15	0.74	3.07	2-43	0.006	0.003

In the course of the experiment no relevant change in inorganic hydrochemistry can be seen with exception of sodium and chloride that were added for tracer reasons together with the trace substances. The slight increase in calcium and magnesium in the effluent compared to the water reservoir before the experiment may indicate some cation exchange with the sodium added.

Simultaneously, DOC was analysed in a few representative samples. The results are shown in Figure 44. They indicate an increase in DOC removal during the course of the experiment that may be due to the addition of highly biodegradable polysaccharides together with the algal extract.
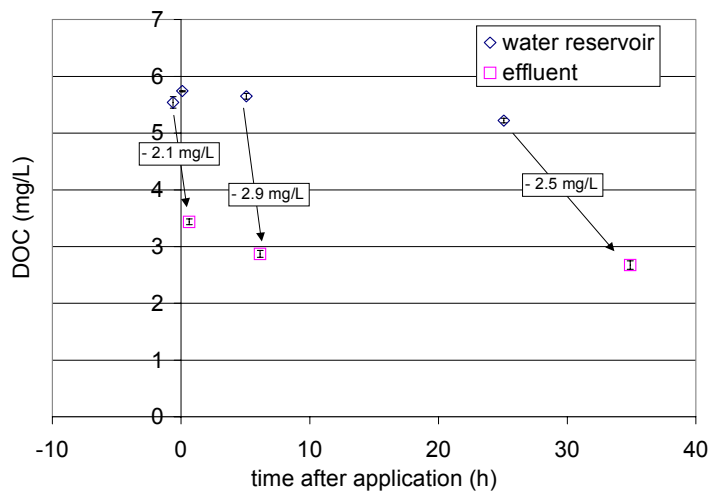
Figure 44: DOC values during SSF5 (data by TUB). Polysaccharides were reduced substantially through the filtration process, as indicated by the pronounced reduction of the peak at 39 min. in LC-OCD chromatograms (Fig. 12).
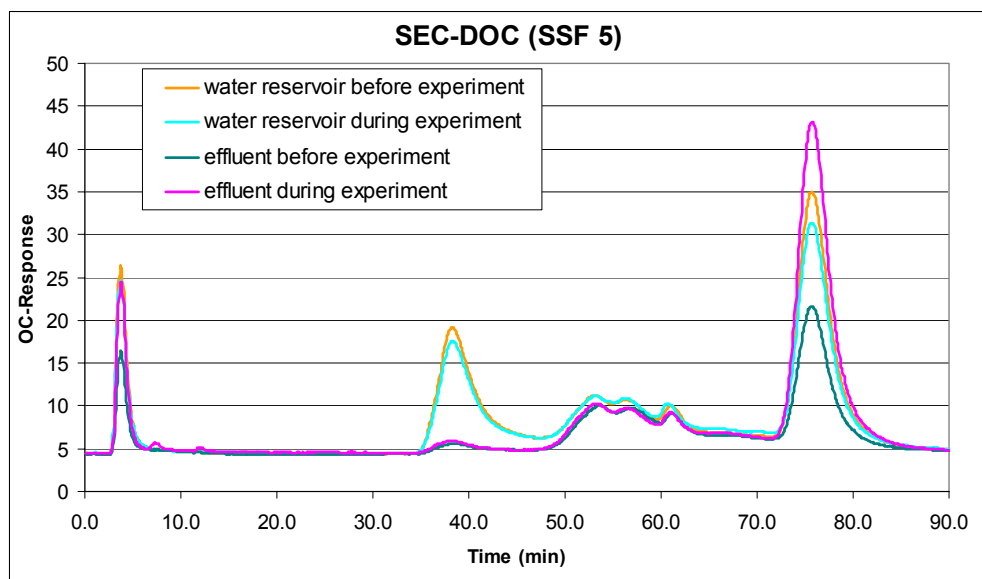
Figure 45: LC-OCD Chromatogram of samples taken before and during experiment SSF 5 (data by TUB).

8.3.3 *Elimination of trace substances during the experiments*

8.3.3.1 Cyanobacterial Toxins

Table 11 gives a summary of the initial parameters during the three SSF experiments conducted with MCYST. The MCYST concentrations were determined by HPLC and refer to the main MCYST variant (demethylated MCYST-RR). Two other peaks with UV spectra characteristic for MCYST were visible in some the HPLC chromatograms of water reservoir samples at retention times of 21.7 min and 14.2 min during SSF2 and SSF6. The concentrations, however, were below the limit of quantification (< 0.1 µg/L).

The mean residence times in Table 11 were obtained by modeling the tracer experiments conducted before and after the MCYST experiments (for SSF2) or simultaneously (for SSF5 and SSF6). They represent the half life of the fitted exponential decay function.

Table 11: Initial parameters of the SSF experiments with MCYST.

Experiment no.	Minimum and maximum air temp. [°C]	Average filtration velocity [m/d]	Clogging layer visible?	MCYST applied [mg] determined by HPLC	Initial concentration of MCYST determined by HPLC [µg/L]	Mean residence time in water reservoir [h]
SSF2	8 – 19.5	2.49	No	462	10.5	3.6
SSF5	14.7 – 25	1.43	Yes	301	8.6	6.3
SSF6	4.8 - 13	0.59	Yes	190	5.95	16.8

The relative concentrations of the main MCYST variant (demethylated (dem) MCYST-RR, determined by HPLC) measured in the water reservoir during SSF2 as well as the calculated dilution curve (confirmed by two tracer tests) are shown in Figure 46. These data confirm that there is no relevant degradation of this MCYST-variant in the water reservoir during the mean residence time of about 3 hours. Similar results were obtained in SSF5 and SSF6 with mean residence times in the water reservoir of 6.3 h and 16.8 h, respectively (see appendix IV-1).
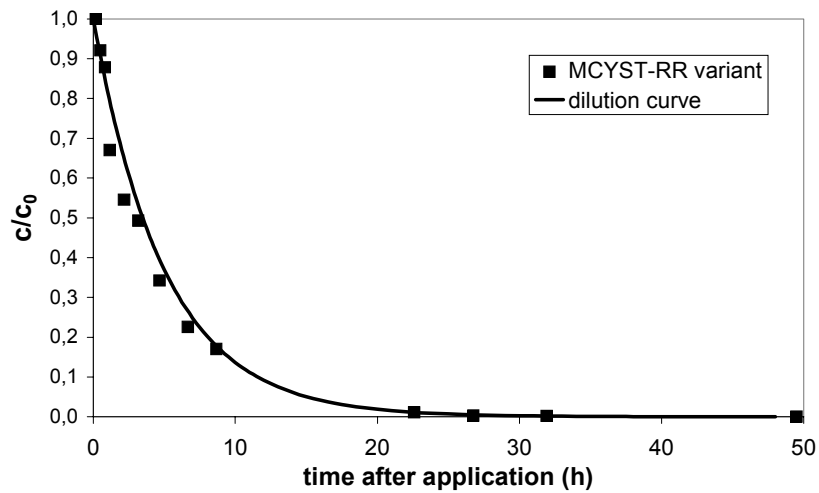
Figure 46: Concentration of demethylated MCYST-RR (main MCYST variant of mass culture) in the water reservoir during the slow sand filter experiment SSF2).

Figure 47 through Figure 49 show the effluent concentrations of MCYST during the three experiments (as sum of all MCYST variants determined by HPLC) in relation to the calculated dilution curve for the water reservoir concentrations and the tracer breakthrough curves (obtained by modeling the tracer results with VCXTFIT).

Compared to the tracer peak MCYST shows a clear retardation and decrease in concentration in all three experiments.
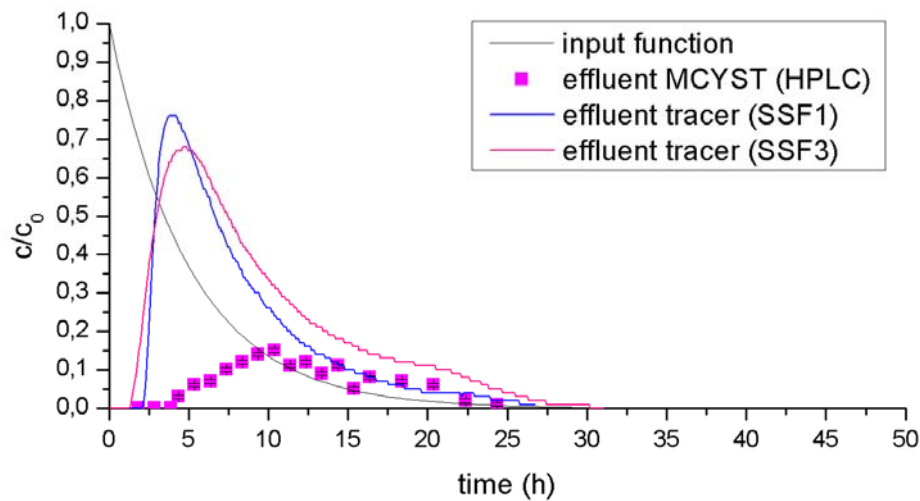
Figure 47: Effluent concentrations of MCYST in experiment SSF2 (tracer results refer to separate tracer experiments, before and after SSF2).
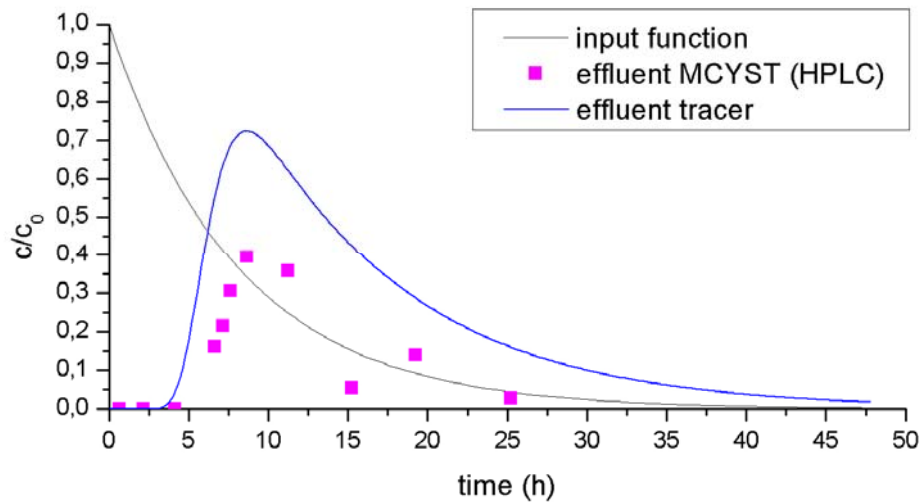
Figure 48: Effluent concentrations of MCYST in experiment SSF5.
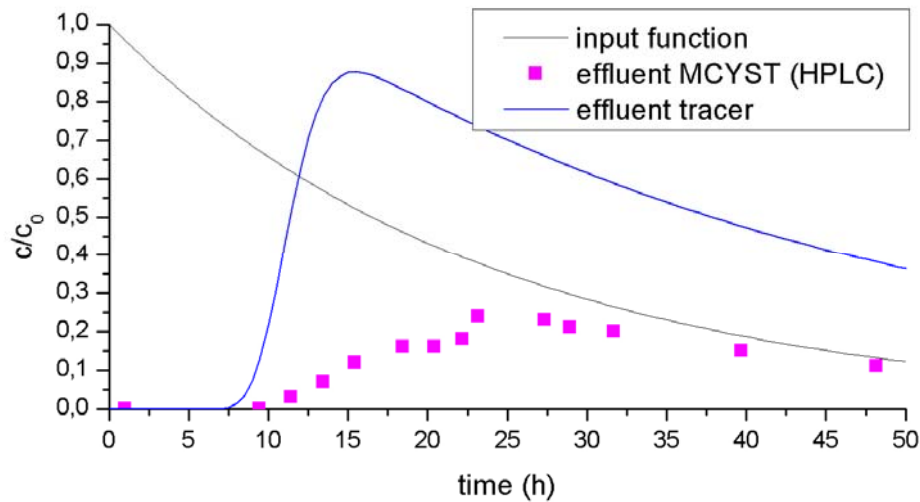
Figure 49: Effluent concentrations of MCYST in experiment SSF6 (after 50 h MCYST concentrations were no longer detectable).

Table 12 gives the amounts of MCYST recovered in the effluent during the SSF experiments. Concerning the recovered shares of MCYST there is a distinctive difference between SSF2 and SSF5 on the one hand (22.5% and 26.5%, respectively) and SSF6 on the other hand with a higher recovered share of 37.2 % of the initially applied MCYST. This shows that higher residence times in the filter do not necessarily lead to higher removal rates. Other parameters like temperature, see final report part V (enclosures) and part VII (laboratory

experiments) may have a far stronger influence. Surprisingly, the results also indicate that the worst case conditions simulated in SSF2 (virgin sand, no visible clogging layer, high flow velocity) did not lead to lower removal rates.

Table 12: Recovered amounts of MCYST the experiments SSF2, SSF5 and SSF6.

Experiment no.	Minimum and Maximum air temperature [°C]	Measured mean filtration velocity [m/d]	Clogging layer visible?	Mean residence time in filter [h]	MCYST recovered by HPLC [mg]	Share of recovered MCYST by HPLC [mg]
SSF2	8 – 19.5	2.49	No	3.0	104	22.5 %
SSF5	14.7 – 25	1.43	Yes	6.2	79,9	26.5 %
SSF6	4.8 - 13	0.59	Yes	11.4	70,7	37.2 %

In the HPLC chromatograms of the effluent samples up to 7 different peaks of substances were identified that show UV-spectra typical for microcystins. Figure 50 shows the distribution of the different peaks in effluent samples from SSF2, characterized either by MALDI-TOF (as [Asp³]MCYST-RR and [Asp³]MCYST-LR) or by their retention time (RT). Of these only the [Asp³]MCYST-RR had been detected in the water reservoir. Similar results, however with some different MCYST-peaks in the effluent, were observed in SSF5 and SSF6 as well as in the enclosure and laboratory experiments. The reasons for this are still unclear and will be discussed in part IIX (analytics).
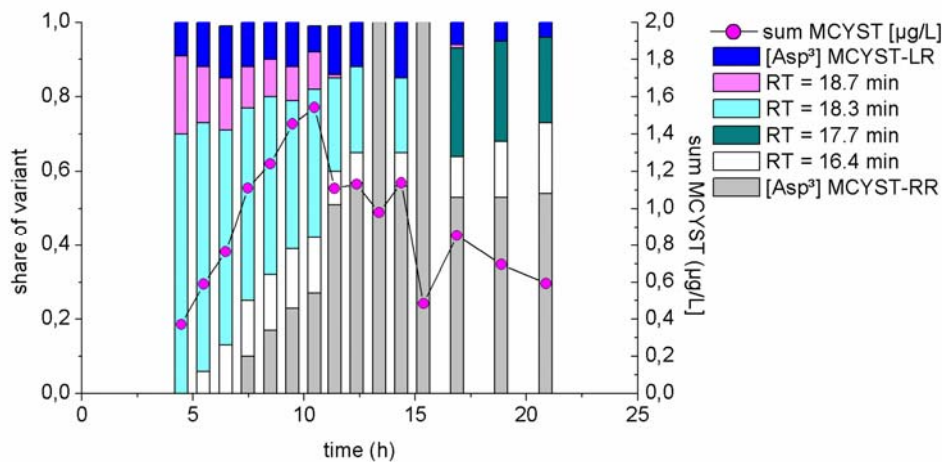
Figure 50: HPLC chromatogram peaks identified as microcystins in the SSF2 effluent samples (RT: retention time). Columns refer to left y-axis and represent the relative shares of the different peaks in relation to the sum of MCYST (dots, right y-axis).

The MCYST breakthrough curves were subsequently modelled with VCXTFIT with the hydraulic parameters (pore velocity and dispersion coefficient) obtained from the tracer breakthrough curves (Table 9). The resulting retardation coefficients and degradation rates are given in Table 13. While the retardation coefficients and degradation rates in SSF5 and SSF6 are similar (R = 1.3 to 1.5 and λ = 0.04 to 0.05 h-1), those obtained from experiment SSF2 are substantially higher (R = 2.6 and λ = 0.17).

Table 13: **Retardation coefficients (R) and degradation rates (λ) obtained by modeling SSF experiments with MCYST.**

Experiment #	filtration velocity	R	λ	remarks
	[m/d]		[h-1]	
SSF2	2.4	2.6	0.17	virgin sand, no clogging
SSF5	1.2	1.3	0.04	some clogging
SSF6	0.6	1.5	0.05	clogged

8.4 Interpretation and Discussion

The slow sand filter experiments had the aim to compare MCYST elimination under assumed worst case conditions with elimination under optimal conditions on a field scale in order to assess which parameters are crucial to prevent toxin breakthrough.

The first experiment (SSF2) was carried out under conditions assumed to be quite unfavourable for degradation, i.e. virgin sand and high flow velocity (pore velocity: 6.2 to 6.5 m/d, filtration velocity: 2.4 to 2.6 m/d). The results did not show a reduced elimination of MCYST compared with the other scenarios tested in SSF 5 and SSF 6 (preconditioned sand, and lower filtration velocities with 1.4 and 0.2 m/d). In contrast, under the presumably unfavourable conditions, higher elimination was observed (recovered amounts: 22.5 % in SSF2 and 26.5 to 37.2 % in SSF 5 and SSF 6, respectively).

Modelling the MCYST breakthrough yielded a possible reason for this unexpected result: Retardation coefficients and degradation rates in SSF 5 and 6 amounted to similar values (R = 1.3 to 1.5 and λ = 0.04 to 0.05 h-1) and are comparable to the values obtained by modelling the effluent data of the enclosure experiments (see final report, part V, table 11). In experiment SSF 2, however, with virgin sand and high flow velocity the retardation coefficient was 2.6 and the resulting degradation rate 0.17 h-1, i.e. 2 to 4 times the values obtained in the two other experiments. Thus, elimination processes during this first experiment seem to differ from those that occurred during the following experiments on the SSF and the enclosures.

A possible explanation might be irreversible sorption of MCYST onto the virgin grain surfaces and subsequent saturation, so that no or little further adsorption can occur. While the original working-hypothesis was that MCYST-elimination would be lower due to the lack of adapted bacteria (leading to lower degradation rates in virgin filter material), these results indicate that this effect is more than compensated by irreversible adsorption processes that can only occur with virgin filter material. Differentiation between irreversible adsorption and degradation is difficult to verify in experiments and has so far not been investigated. Further studies could therefore comprise laboratory experiments addressing this topic, e.g. with radio-labelled MCYST.

Enclosure experiments with MCYST were carried out subsequently to the SSF experiments in order to assess the influence of varying conditions (clogging, temperature, redox potential) onto MCYST elimination (see final report working group "algae" part V).

8.5 References

Massmann, G., Taute, T., Bartels, A. & Ohm, B. (2005): Characteristics of sediments used for Batch- Enclosure and Column-Studies. – report by the Free University of Berlin, NASRI working group Hydrogeology (unpublished).

9 Enclosure experiments on UBA's experimental field

9.1 Introduction

The enclosures were constructed as semi-technical scale filter columns that allowed experiments on a smaller scale and therefore under conditions easier to change and to control than in the technical scale slow sand filters. The enclosure experiments with relatively short contact times were necessary especially for substances that are usually readily removed by sediment contact (e.g. cyanotoxins, viruses and bacteria). For these substances the observation wells at the transects with contact times of at minimum 2 weeks did not cover the time scale of interest. Figure 51 and Figure 52 give an overview of all investigations and experiments carried out on the enclosures during the NASRI project.

	January	February	March	April	May	June	July	August	September	October	November	December
2002												
EI, EII, EIII											Installation, Filling	
2003												
EI												
Filtration velocity			0 m/d								1,1 m/d	
Experiment No.												E6
Date												17.12.03
Substances												NaCl
EII												
Filtration velocity			0 m/d							1,0 m/d	1,2 m/d	
Experiment No.											E4	E5
Date											11.11.03 NaCl, MCYST, Phages, Drugs	25.11.03 NaCl, MCYST, Phages, Drugs
Substances												
EIII												
Filtration velocity			0 m/d			1,2 m/d			1,0 m/d			0 m/d
Experiment No.							E1	E2	E3			
Date							27.7.03	5.8.03 NaCl, Phages, MCYST, Drugs	9.9.03 NaCl, Phages, MCYST, Drugs			
Substances							NaCl	Drugs	Drugs			

Figure 51: Overview of the investigations and experiments carried out on the enclosures in 2002 and 2003. Legend: yellow fields: enclosures dry; light-blue: flooded with little or no clogging; darker blue: flooded with pronounced clogging; hatched fields: flooded, but no experiment.

	2004											
EI												
Filtration velocity	0 m/d			ca. 0,7 m/d						0 m/d	0,3 m/d	
Experiment No.									E 10		E12	
Date									12.10. - 1.11.04		19.11.04 - 9.12.04	
Substances									NaCl, MCYST, Phages		NaCl, *Planktothrix agardhii*	
EII												
Filtration velocity	0 m/d	ca. 0,7 m/d		ca. 1,2 m/d	ca. 0,7 m/d	0,4 m/d	0 m/d	0,4 m/d	0 m/d			
Experiment No.				E7	E8	E9		E11				
Date				8/6/04	27.07.2004 - 11.08.04	30.8.04 - 03.09.04		2.11.04 - 17.11.04				
Substances				NaCl, Gd	DOC	DOC, NaCl, MCYST, Phages		DOC				
EIII												
Filtration velocity	0 m/d	0,7 m/d			0,4 m/d	0,6 m/d		0,6 m/d	0,3 m/d			
Experiment No.								E13				
Date												
Substances								primary effluent				
	Enclosure dry			stagnant conditions								
	Enclosure flooded (little or no clogging)											
	Enclosure flooded (visible clogging layer)											

Figure 52: Overview of the investigations and experiments carried out on the enclosures in 2004.
Legend: yellow fields: enclosures dry; light-blue: flooded with little or no clogging; darker blue: flooded with pronounced clogging; hatched fields: flooded, but no experiment.

Aim of experiments with cyanobacterial toxins (microcystins, MCYST): The aim of the first series of experiments was to investigate elimination processes and to quantify degradation rates of dissolved MCYST

- under "normal" conditions (aerobic, clogged and not clogged) and compare the results to those obtained in the SSF experiments (E2 to E5, see chapter 3.2.1),

- under anaerobic conditions (E9, see chapter 3.3),

- during continuous dosing over 3 weeks (E10, see chapter 3.4.1).

A final experiment with living cells of cyanobacteria (E12, see chapter 3.4.2) was conducted in order to obtain results most representative for the complex, natural system of extra-cellular and cell-bound MCYST during sediment passage.

Formatiert: Nummerierung und Aufzählungszeichen

9.2   Materials and Methods

9.2.1   Semi technical scale enclosures on the UBA's experimental field

9.2.1.1   Experimental design

The enclosures were constructed as semi-technical scale columns and were placed in the center of one of the open infiltration ponds of the UBA's experimental field (Figure 53). They were installed with the upper edge about 0.1 m below the upper edge of the basin's rim, i.e. their bottom 1.3 m below sand surface, so that surface water can enter through the openings without additional pumping. The enclosures were filled from bottom to top with 0.3 m of gravel and 1 m of filter sand (the same as in the slow sand filter experiments) leaving about 0.4 m depth of the water reservoir at the top. Small sampling tubes were installed in different depths according to Table 14 and Figure 54.
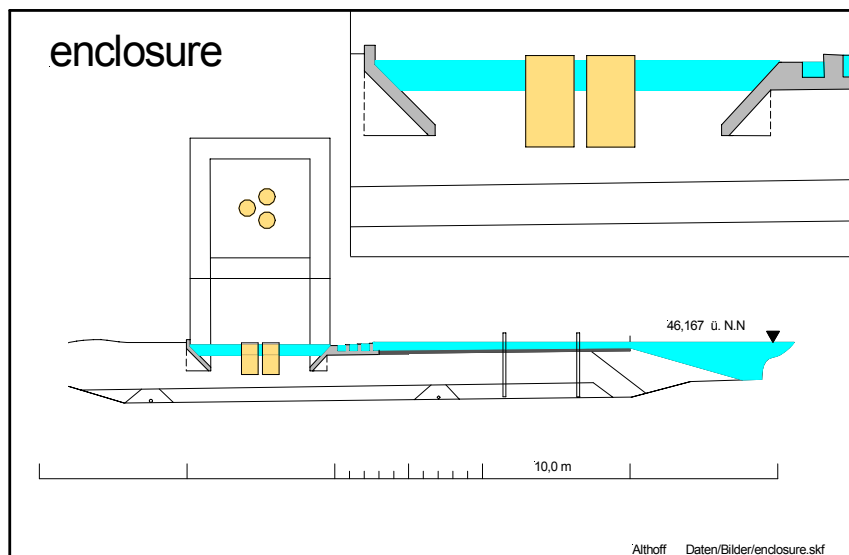
Figure 53:   **Position of the enclosures inside the infiltration ponds (cross section; dotted boxes show bird's-eye view and magnification), without tubing, pumps and sampling ports.**
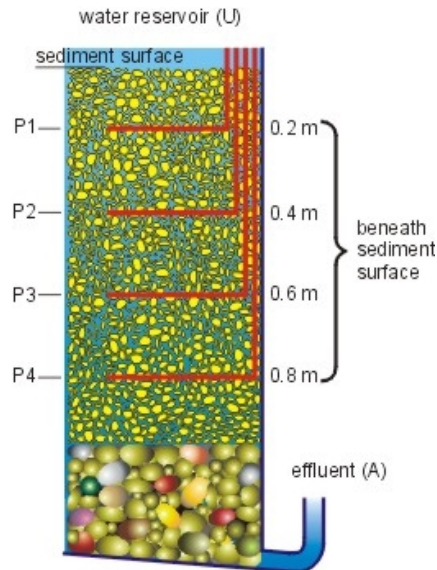
Figure 54: **Cross section of enclosure III with sampling ports.**

Table 14: Distribution of sampling tubes inside the enclosures.

Number of enclosure	Sampling tube in depth below sediment surface (m)			
	0.2	0.4	0.6	0.8
I	no sampling tubes, only outlet sampling			
II	no	yes	no	yes
III	yes	yes	yes	yes

9.2.1.2 Hydro- and geochemical conditions

9.2.1.2.1 Geochemical properties of the virgin filter material

The filter sand used for the enclosures was the same as for the slow sand filter (for details see final report working group algae, part IV). The filter sand is a medium to coarse sand with small amounts of fine sand. Silt and clay are not present. The gravel layer consists of fine gravel with large amounts of medium grained gravel.

The geochemistry resembles that of sand taken from the shore of Lake Wannsee fairly well, with exception of the total iron content (13 % less in the filter material) and the cation exchange capacity (CECeff: 82 % less in the filter material). This is probably due to the coarser grain size of the filter material (Massmann et al. 2004).

9.2.1.2.2 Hydrochemistry under normal operating conditions

The surface water used for the experiments originates from the surrounding aquifer and is treated for iron and manganese in the water works of the experimental field before being fed into the storage pond. Its high electrical conductivity (about 968 µS/cm) is due to relatively high concentrations of salts (HCO_3^-: 132 mg/L, SO_4^{2-}: 254 mg/L, Cl^-: 99 mg/L, Ca^{2+}: 127 mg/L and Na^+: 46 mg/L, average of 8 samples taken during 2003 and 2004; more detailed data are given in appendix V-1). DOC ranges from 3.2 mg/L in summer (experiments E2 and E3) to 2.1 mg/L in late autumn (experiment E5). Calculations with PHREEQC show that compared to the atmosphere the surface water is slightly oversaturated with CO_2 and O_2, probably due to biological activity of algae and water plants. This is also the reason for the slightly alkaline pH in the water reservoir (pH 8.0 in average).

During sand passage a reduction of pH (down to pH 7.7), O_2 (by 50 %) and DOC (by 28 % in summer and by 14 % in late autumn) was observed. These reductions take place in the uppermost 20 cm and are more pronounced in summer than in winter.

Nitrate is usually not detectable in the water reservoir, during filter passage or in the effluent. In one case, however, during experiment E3, an increase in the nitrate concentrations during the filter passage from 0.1 mg/L in the water reservoir up to 1.1 mg/L in 60 cm depth was observed (Figure 55). After 80 cm of sand passage and in the effluent the concentrations dropped again to values around 0.5 mg/L.
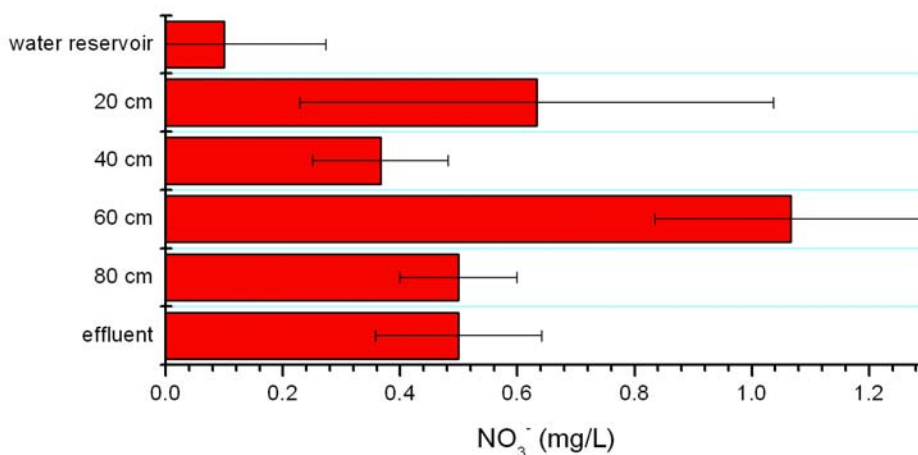
Figure 55: Average nitrate concentrations during experiment E3 (error bars indicating standard deviations of 3 samples).

9.2.2   Experimental Methods

9.2.2.1   Experiments with pulsed application (E1 to E7)

The experiments E1 to E7 were carried out on enclosures II and III. In preparation of the experiments the flow rate was adjusted to the desired amount, corresponding to the filtration velocities given in Figure 51 and Figure 52. The tracer and the trace substances were applied by pouring them evenly across the water reservoir (in which a pump had been installed for better mixing) from a watering can containing the concentrated substances diluted with 10 L of surface water from the water reservoir. The tracer applied was sodium chloride (NaCl) so that the sampling intensity in the different sampling points could be adjusted by observing the electrical conductivity (EC). Care was taken not to increase the EC by more than 10 %.

Samples were taken from the water reservoir, from the sampling ports and from the effluent. The sampling intervals were adjusted to the expected change in concentration and the amount needed by the different working groups for the analyses. As the flow rate in the sampling ports amounted to only 1 mL/min (in order to minimize hydraulic disturbances inside the enclosure) and the volume needed for analyses in some cases added up to 1.5 L, samples from these locations could sometimes not be taken as frequently as desired. With exception of the samples for virus and bacteria detection, samples were usually collected in a mutual flask for all working groups and then divided into the different subsamples for subsequent analysis.

Physico-chemical parameters (EC, pH, redoxvalue, oxygen and temperature) and alkalinity were measured on three occasions at the different sampling locations: a) before the experiment, b) when the tracer peak was expected to break through and c) after the tracer had reached its background level again. The analytical methods for these measurements are described in chapter 2.3. Simultaneously samples were taken for analysis of main anions and cations (Na^+, Ca^{2+}, Mg^{2+}, K^+, Cl^-, SO_4^{2-}), nutrients (NO_3^-, PO_4^{2-}) as well as DOC and immediately filtered by membrane filter (RC 55, Schleicher & Schuell, 0.45 µm pore size), conserved by addition of HNO_3 (cation samples only) and stored cool at 4 °C or frozen (for determination of DOC) until analysis. The analysis of the main cations and anions as well as of the nutrients was carried out by the FU Berlin. The DOC was determined by the TU Berlin. For description of analytical methods refer to the respective reports.

Cyanobacterial Toxins (Microcystins): The MCYST applied was extracted from a mass culture of Planktothrix agardhii HUB 076 by centrifugation and freeze thawing in order to release the mainly cell-bound, highly water soluble microcystins. The freeze thawed extract was homogenized and then centrifuged to remove the cell debris, stored frozen and thawed over night prior to the experiment. The resulting MCYST concentrations in the water reservoir amounted to values between 6.1 µg/L and 9.0 µg/L. For details on analytical methods see final report working group algae, part IIX.

9.2.2.2 Experiments under anaerobic conditions (E8, E9, E11)

The experiments under anaerobic conditions were carried out in enclosure II (sampling ports in 40 cm and 80 cm depth). Initially the flow rate was adjusted to 30 L/h ± 5 %, corresponding to 0.7 m/d filtration velocity. Due to clogging the flow rate decreased to 26 L/h (0.63 m/d filtration velocity) during the course of the experiments.

In order to eliminate oxygen from the infiltrating water, highly biodegradable DOC (acetic acid) was added continuously with a resulting concentration of 0.3 mmol/L additional DOC (resulting DOC concentration in water reservoir: 9.6 ± 0.5 mg/L, i.e. approximately 3-fold higher than under aerobic conditions).

During experiment E8 DOC dosing commenced on 29th July 2004. Oxygen concentration and redox-values were measured every day until 23rd August, when they had reached stable anaerobic conditions (O2 < detection limit (0.1 mg/L) and EH < 0 mV).

Then experiment E9 was conducted (30th Aug. to 3rd Sept. 2004) by adding trace substances and tracer using the same method as in experiments E2 to E5 (pulsed application, see chapter 2.2.1). Measurement of physico-chemical parameters and sampling were also carried out in a similar way, in order to obtain comparable results.

After a period of aerobic flow, a second attempt was made to establish anaerobic conditions in enclosure II (experiment E11) with dosing of DOC in November 2004. Probably due to lower temperatures oxygen was detectable in the sampling ports and in the effluent throughout the experiment which lasted 15 days, even though the DOC-dosing was increased to 0.5 mmol/L additional DOC. For this reason no second anaerobic experiment with trace substance application could be carried out.

9.2.2.3 Experiments with continuous application (E10, E12, E13)

The experiments with continuous application were carried out on enclosure I (no sampling ports besides the effluent) and enclosure III (4 sampling ports plus effluent). Phages, dissolved microcystin and cyanobacterial cells were added to enclosure I during E10 and E12, whereas primary effluent was dosed to enclosure III during E13 (see also Figure 52). Care was taken to achieve constant flow rates within the full time of an experiment by adjusting the pump when flow rates decreased due to clogging. Hydraulic conductivity was observed by monitoring the suction pressure changes .

Tracer experiments with NaCl were conducted prior to each experiment in the same way as for the earlier experiments (see chapter 2.2.1).

Experiment E10 was carried out from 12th Oct. 2004 until 1st Nov. 2004. The stock solution was prepared each day from the frozen crude extract of the Planktothrix agardhii mass culture (MCYST concentration determined by HPLC: 62 mg/L). Prior to the experiment 15 aliquots of 96 mL each had been prepared so that only one had to be thawed per day. The stock solution was adjusted to the target concentration of 4 mg/L by adding 1.5 L of deionized water. It was then dosed continuously with 1.08 ± 0.05 mL/min to the water reservoir of 350 L. In order to achieve a constant level of MCYST in the water reservoir as

quickly as possible, 300 mL of the undiluted MCYST extract were added at the same time as the continuous dosing commenced at the beginning of the experiment.

The stock solution was sampled after preparation and shortly before it was exchanged the next day and analyzed for MCYST content by ELISA. Daily samples were taken from the water reservoir and the effluent. Each sample was tested by ELISA for MCYST content and selected ones analyzed by HPLC. Shortly before dosing was terminated on the 27th October hourly samples were taken from the water reservoir and from the effluent for 24 h in order to assess short term changes in elimination.

Electrical conductivity and temperature were determined daily, the other parameters (pH, O2, EH, alkalinity, main anions and cations as well as DOC) prior to the beginning of the experiment and then on two occasions during the experiment.

9.2.2.4 Experiment with continuous application of cell-bound MCYST (E12)

Experiment E12 was carried out from 23rd Nov. until 9th Dec. 2004 and had to be terminated earlier than planned due to temperatures below 0 °C. Live cells of Planktothrix agardhii from the mass culture (total MCYST: 240 µg/L) were added to the water reservoir (350 L), first as a pulse of 15 L in order to achieve a concentration of about 10 µg/L total MCYST as quickly as possible and subsequently continuously at a rate of 20 mL/min from a 30 L tank containing material from the mass culture that was replenished daily for four days (until 26th Nov.). Technical problems lead to a flow interruption between 23rd Nov. and 24th Nov., so on 24th Nov. another pulse of 15 L mass culture was added. After 26th Nov. dosing was terminated, sampling however continued until 9th Dec.

Water samples were taken from the mass culture, from the water reservoir and from the effluent for determination of total and extracellular MCYST by ELISA, for cell-bound and extracellular MCYST by HPLC at regular intervals (twice daily at the beginning to once every two days in the end). Biovolume was determined additionally in the samples from the water reservoir. Physico-chemical parameters (pH, T, EC, oxygen, alkalinity and DOC) were determined in selected samples from water reservoir and effluent as described in chapter 2.3.

Before the beginning of the experiment, after 1, 3, 7 and 13 days sediment samples were taken from the uppermost 10 cm of the filter sand. The cores were obtained with a 2.5 cm diameter syringe from which the tip had been cut off or with a pipe (3.6 cm diameter). Two centimeter subsamples were taken, subsequently homogenized for biovolume determination and deep frozen for semi-quantitative analysis of total MCYST by ELISA.

9.2.3 Analytical Methods

The analytical methods used for the on-site determination of hydrochemical and -physical parameters are given in Table 15. Methods for sediment analysis and other hydrochemical

parameters can be taken from the final report working group FU Berlin, and details on MCYST analysis can be taken from the final report working group algae, part IIX.

Table 15: Overview of the analytical methods used for on-site water analysis.

Parameter	Method	Instrument	Measuring Range	Error
Electrical conductivity (EC), (temperature)	electrometric (temp.-corrected to 25°C)	Lf 325, Tetra-Con 325-sonde with integrated temperature sonde (WTW)	1 to 10.000 µS/cm (0 to30 °C)	± 1 µS/cm (0.1 °C)
pH	Potentiometric (autom. temp.-compensation)	CG 837, N 6480-sonde with integrated temperature sonde (Schott)	1 to 13	± 0.1
Redox potential	Potentiometric (Ag/AgCl-standard)	CG 837, Pt 6880-sonde (Schott)	-200 - 1000 mV	± 10 mV
Oxygen	polarographic measurement	Oxi 325, CellOx 325-bzw. EO90-sonde (WTW)	1 % - 100 %	± 5 %

9.2.4 *Modeling*

For inverse modelling two different software tools are applied, VisualCXTFIT and MATLAB®, corresponding to the inversion of different parameters in two steps. Modelling is based on the general transport equation, a partial differential equation for the unknown fluid phase concentration c:

$$\theta R \frac{\partial c}{\partial t} = \nabla \mathbf{D} \nabla c - \mathbf{v} \nabla c - \theta R \lambda c \qquad (1)$$

with the parameters: porosity θ, retardation R, dispersion tensor D, Darcy-velocity v and degradation rate λ. For column or enclosure experiments it may be assumed that flow can be treated as one-dimensional (1D). Then the transport equation can be formulated in a simpler form:

$$R \frac{\partial c}{\partial t} = \frac{\partial}{\partial x} \alpha_L u \frac{\partial c}{\partial x} - u \frac{\partial c}{\partial x} - \lambda R c \qquad (2)$$

with longitudinal dispersivity αL and interstitial 'real' flow velocity u. Altogether there are four parameters: αL, u, R and λ. Instead of u one may use the porosity θ =v/u as parameter, because the Darcy-velocity v is given implicitly by the applied flow rate. In the literature one often finds the combination $\mu = \lambda R$ used in estimation runs, for example in CXTFIT (1995).

The first two of the four parameters are species independent, the latter two are usually species dependent. The first two parameters can be best obtained from tracer experiments, because for tracers the 1D transport equation reduces to:

$$\frac{\partial c}{\partial t} = \frac{\partial}{\partial x} \alpha_L u \frac{\partial c}{\partial x} - u \frac{\partial c}{\partial x}$$
(3)

Within the project the inversion procedure was divided into two steps. In the first step species-independent parameters are determined from the tracer experiments, followed by the second step for the remaining parameters for each specie separately:

- Determination of velocity u and dispersivity αL from tracer experiments

- Determination of retardation R and degradation rate λ from experiments with non-tracers.

Step (1) was performed using VisualCXTFIT, which is a graphical user interface (GUI) for the CXTFIT code for parameter estimation. CXTFIT was developed at the U.S. Salinity Laboratories (Toride et al., 1995) and is based on analytical solutions of the 1D transport equation. Analytical solutions have the advantage that direct solutions of the differential equation have no problems with discretization errors, as they appear in numerical solutions. On the other hand analytical solutions exist only for specific conditions and can not be given for general boundary and initial conditions. However for the given experimental set-up in the enclosures as well as in the columns it was possible to use CXTFIT.

The VisualCXTFIT user interface for CXTFIT was developed within the NASRI project. An EXCEL-Add-in is produced, which allows the input and manipulation of measured data, as well as the specification of the inversion parameters and options. Moreover a graphical representation of the results is produced in the EXCEL sheet. A detailed description as well as application examples are given by Nützmann et al. (2005).

Step (2) was performed using a newly developed tool for parameter inversion, written as a m-file module in MATLAB® (2002). The module has been used for inversions of transport processes only, but could be used for other applications as well. The MATLAB® module works also for the inversion of temperature time series. For such an application the module is described in detail by Holzbecher (2005).

Within the MATLAB® module direct simulations of the transport equation are performed. The direct solution is obtained by using the 'pdepe'-solver, which is part of core MATLAB®. The direct solver is called within an inversion procedure, which is based on the MATLAB® optimization module. There are various options, concerning the search algorithm and the numerical parameters can be specified.

In the module the user can specify the parameters, which are to be estimated. Within the automatic inversion procedure it is attempted to modify the selected parameters from their initial values, in order to obtain a better fit with the remaining time-series in the input-data set. The objective function is sum of the squares of the deviations between measured and modelled values, which is usually known as least squares optimization. Parameters not selected for the estimation procedure remain at their initial value.

103

Formatiert: Nummerierung und Aufzählungszeichen

Input into the MATLAB® inversion module requires time series, measured at least at two positions along the flowpath. The first time series, given in the input data-set, is treated as a boundary condition; the other time series are used for the parameter estimation procedure. When several time-series are given there is the additional option to estimate parameters from various possible estimation intervals. For example, in case of three time series, the first can be treated as boundary condition and either the second, or the second and the third can be used for the estimation. Moreover, the second time series can be used as boundary condition, in order to use the third for the estimation. In that way it is possible to obtain an impression of the variability of the parameters with the spatial intervals.

For each estimation run MATLAB® finally produces a plot, visualizing the following:

- Measurements used as boundary conditions (one time series)

- Measurements used for parameter estimation

- Modelled concentration curve based on best-fit parameters.

In the estimation runs for the enclosures, slow sand filters and column experiments performed during the NASRI project, it turned out that the automatic inversion procedure did not deliver optimal results. The problem is well-known, as the algorithms find local minima of the objective function, which are not necessarily global minima. When the user suspects that the automatic solver has not found the global minimum yet, the algorithm is usually re-started again with a new starting set, which differs both from the obtained local minimum parameter set and from the previous starting values. Such 'fine-tuning' was required in almost all reported simulations.

Moreover the comparison of parameter values, obtained for different spatial intervals (as described above) mostly revealed substantial differences. It can be concluded that parameters are obviously not constant, but change with space. A more detailed description, concerning phage transport in the enclosures, is presented by Holzbecher et al. (2005).

9.3 Results

9.3.1 Tracer experiments

9.3.1.1 Differences between the enclosures

In the course of every experiment conducted on the enclosures a tracer experiment was carried out in order to determine the exact hydraulic conditions. Table 16 gives and overview of the hydraulic parameters measured or obtained by modelling.

104

Table 16: Hydraulic properties of the enclosures determined by tracer experiments (effluent data only).

Experiment No.	Date of experiment	Filtration velocity [m/d]	Pore velocity [m/d]	Dispersion length (αL) [m]	Eff. Pore-volume (ne)	Hydraulic conductivity [m/s]
Enclosure I						
E6	17th Dec. 2003	0.86	2.40	0.020	0.360	0.95*10-5
E10	12th Oct. 2004	0.73	1.78	0.027	0.410	0.4*10-5
E12	19th Nov. 2004	0.48	1.32	0.013	0.363	0.1*10-5
Enclosure II						
E4	11th Nov. 2003	1.09	2.88	0.016	0.379	1.5*10-5
E5	25th Nov. 2003	1.22	3.07	0.023	0.398	1.7*10-5
E7	8th June 2004	1.20	2.88	0.032	0.420	4.4*10-5
E9	30th Aug. 2004	0.64	1.75	0.049	0.366	1.2*10-5
Enclosure III						
E2	5th Aug. 2003	1.25	3.36	0.011	0.37	1.8*10-5
E3	9th Sept. 2003	1.12	2.76	0.013	0.40	1.6*10-5

Enclosure I shows distinctively lower hydraulic conductivities in comparison to enclosure II and enclosure III. In enclosure I the values lie between 0.1*10-5 m/s and 0.95*10-5 m/s, whereas the conductivities observed in enclosure II and enclosure III were greater than 1.2*10-5 m/s, reaching a maximum of 4.4*10-5 m/s. This might be due to the fact that there are no sampling ports installed in enclosure I, so that preferential flow paths can not develop as easily as in enclosure II and enclosure III. Additionally, in 2004 the experiments carried out in enclosure I were characterized by continuous application of microcystin extract and live cyanobacterial cells, thus adding considerable amounts of organic load. This will surely have enhanced clogging.

All enclosures show decreasing hydraulic conductivities over time with exception of enclosure II where the uppermost centimeter was removed in preparation of experiments E5 and E7. Highest conductivities were observed in experiment E7, which was also the only experiment carried out during early summer while the other experiments took place between August and December.

In summary, the following parameters seem to influence hydraulic conductivities in the enclosures:

- constructional details (existence of sampling ports),

- history (application of any clogging enhancing substance or material beforehand),

- previous removal of a clogging layer.

9.3.1.2 Differences within the enclosures

Figure 56 and Figure 57 show the spatial variability of the effective porevolume calculated on the basis of the tracer breakthrough curves for different experiments carried out in 2003 and 2004.
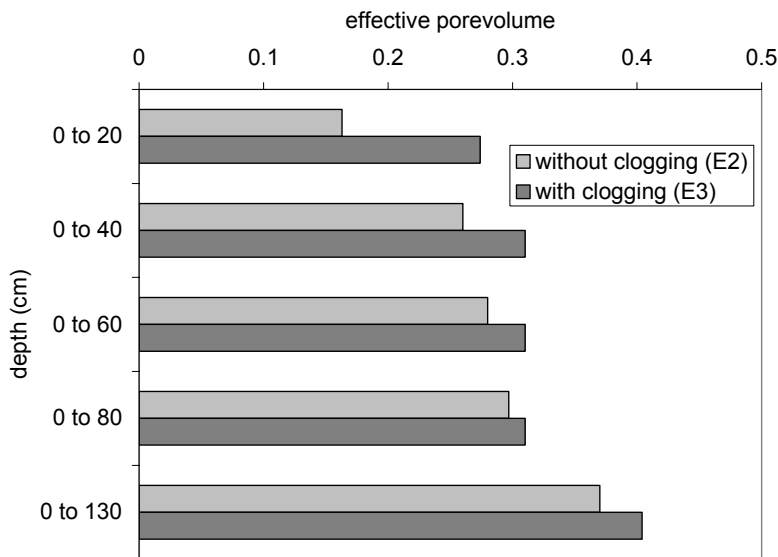
Figure 56: **Effective pore volumes in enclosure III calculated from tracer breakthrough curves ("clogging" refers to the existence of a visible, superficial "schmutzdecke" on the filter).**

The results show a distinctive increase in pore volume with depth. In the lower section between 80 cm and 120 cm this is due to the existence of a gravel drainage layer with higher porosity than the filter sand above. The surprisingly low values for effective porosity in the

106

upper section can, however, not be derived from initial differences in grain size. Here processes associated with clogging are likely to lead to diminished porosities. These processes are:

- physical clogging by sedimentation of small size organic and inorganic particles,

- biological and / or chemical clogging by growth of biofilm or precipitation of solids,

- formation of partially unsaturated conditions by degassing of the water passing through the filter due to high under-pressure.

-
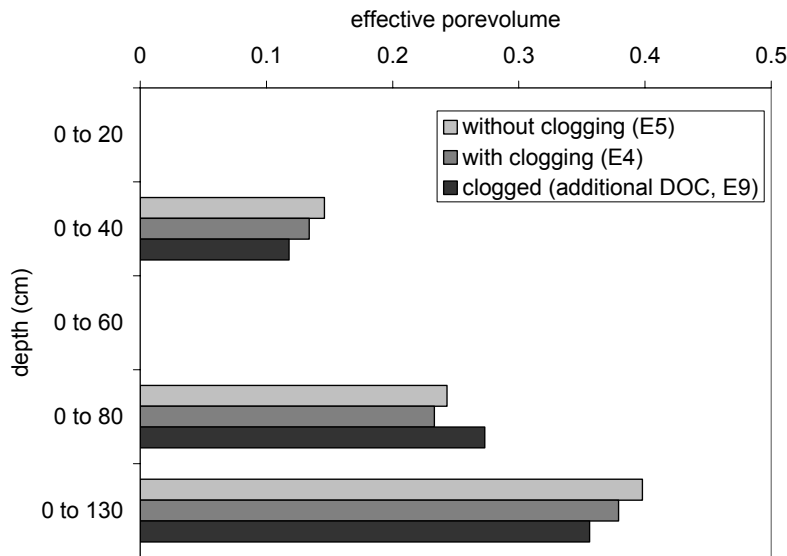
Figure 57: **Effective pore volumes in enclosure II calculated from tracer breakthrough curves ("clogging" refers to the existence of a visible, superficial "schmutzdecke" on the filter).**

Unsaturated conditions due to clogging were found to exist at least once in enclosure III after experiment E12 when gas bubbles appeared during clogging layer removal (Figure 58).

Figure 58: Gas bubble formation during removal of clogging layer on enclosure III in December 2004.

9.3.2 Experiments with pulsed application of trace substances

The aim of the series of experiments with pulsed application of dissolved MCYST, phages, bacteria, drugs and Gd-DTPA was to investigate elimination processes and quantify degradation rates under "normal" conditions (aerobic, clogged and not clogged) and compare the results to those obtained in the SSF experiments.

9.3.2.1 Changes in hydrochemistry

With exception of the electrical conductivity, chloride and sodium concentrations no significant changes (> 99 % level of significance) in hydrochemistry compared to the hydrochemistry under normal operating conditions (chapter 2.1.2.2) were observed during the experiments.

Significant differences in hydrochemical parameters between the experiments are limited to the temperatures (averages for experiments were: E2: 27°C, E3: 19°C, E4: 2.6°C and E5: 7.4°C) and some temperature related parameters (e.g. oxygen and alkalinity).

9.3.2.2 Cyanobacterial Toxins (Microcystins)

9.3.2.2.1 Experimental Results

Table 17 gives a summary of the initial parameters during the four aerobic enclosure experiments conducted with MCYST as pulsed application experiments. The MCYST concentrations were determined by HPLC and refer to the sum of all MCYST-variants. The

108

mean residence times were obtained by modeling the behavior of the tracer applied simultaneously. They represent the half life of the fitted exponential decay function.

Table 17: Initial parameters of the enclosure experiments E2 to E5.

Experiment no.	Water temperature (min – max in °C)	Measured mean filtration velocity (m/d)	Clogging layer visible?	MCYST applied (mg) analyzed by HPLC	Initial concentration of MCYST analyzed by HPLC (µg/L) in the reservoir	Mean residence time in water reservoir (h)
E2	23.6 - 31.6	1.23	No	2.8	6.1	5.4
E3	16.4 - 23.1	1.04	Yes	2.7	6.2	4.7
E4	0.6 - 4.7	1.03	Yes	3.9	9.0	6.3
E5	6.3 - 11.2	1.22	No	2.8	7.6	5.3

The data show that the mean filtration velocity was slightly lower during the two experiments with a visible clogging layer (1.0 m/d in contrast to 1.2 m/d without clogging layer). Additionally, as mentioned above, there are major differences in temperature with values around 25 °C during E2 and below 5 °C during E4. This may have had some impact already on the initial concentrations of MCYST which were highest (9 µg/L) in the experiment with the lowest temperatures (E4) and lowest (6.1 µg/L and 6.2 µg/L) in those with temperatures above 16 °C. This indicates that some degradation might already have taken place during thawing of the frozen extract before application.

Figure 59 and Figure 60 show the relative MCYST concentrations in the water reservoir during the experiments E2 and E5. All experiments conducted at low to moderate temperatures (E3 through E5) show a decrease in MCYST concentration similar to that of the tracer, so that degradation in the water reservoir can be ruled out and the decrease can be attributed solely to dilution. During E2, however, the MCYST concentrations decreased by a third more rapidly (half life 3.6 h compared to 5.4 h). This may be due to enhanced degradation of MCYST at the extremely high temperatures between 24 and 32 °C during this experiment.
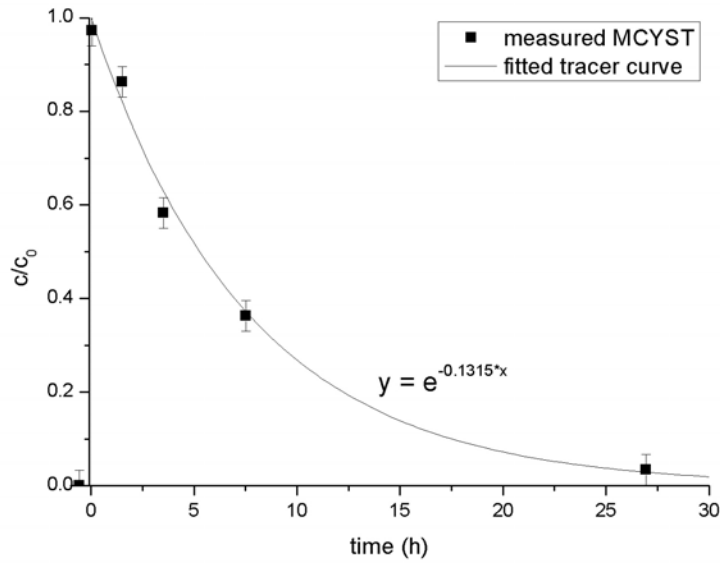
Figure 59: Measured MCYST concentration in the water reservoir and fitted tracer curve during experiment E 5 at moderate temperatures (< 23.5°C).
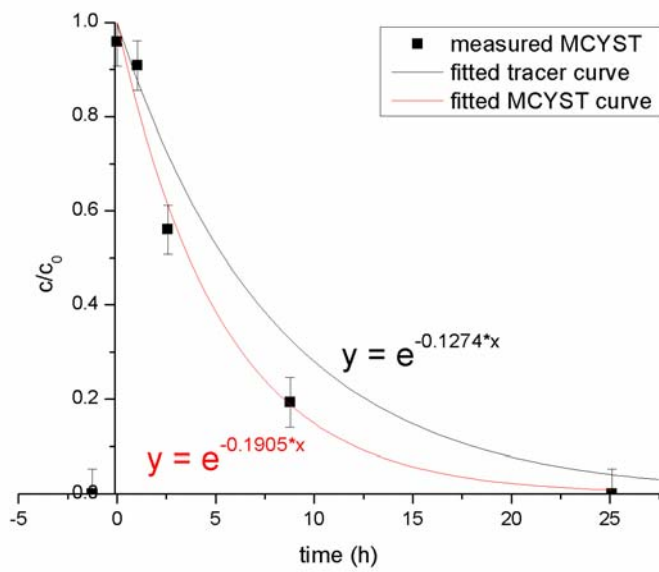
Figure 60: Measured MCYST concentration in the water reservoir, fitted decay function and fitted tracer curve during experiment E 2 at temperatures of 24 to 32°C.

Figure 61 to Figure 64 show the concentrations of MCYST during the experiments with pulsed application (as sum of all MCYST variants determined by HPLC) as well as the tracer

breakthrough curves (obtained either by measuring (E4 and E5) or by fitting the tracer results with VCXTFIT; see chapter 2.4). In all four experiments MCYST shows a clear retardation and decrease in concentration compared to the tracer.
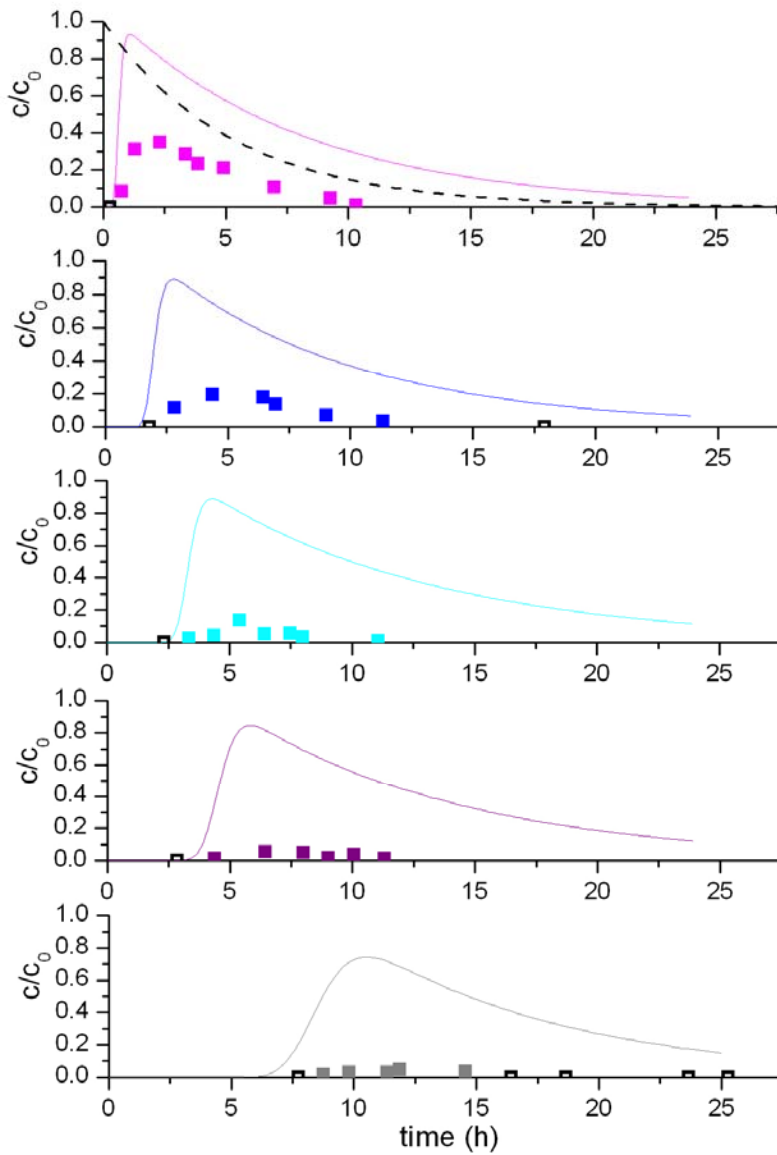
Figure 61: MCYST concentrations and modeled tracer breakthrough curves at sampling ports in 20 cm, 40 cm, 60 cm and 80 cm depth as well as in the effluent (from top to bottom) during E2 (c0 = 6.1 µg/L). Dotted curve: MCYST in water reservoir (modeled); Solid curves: tracer modeled at the respective port; solid squares; MCYST measured at the respective port; open squares: MCYST below detection limit, i.e. < 0.01 µg/L.
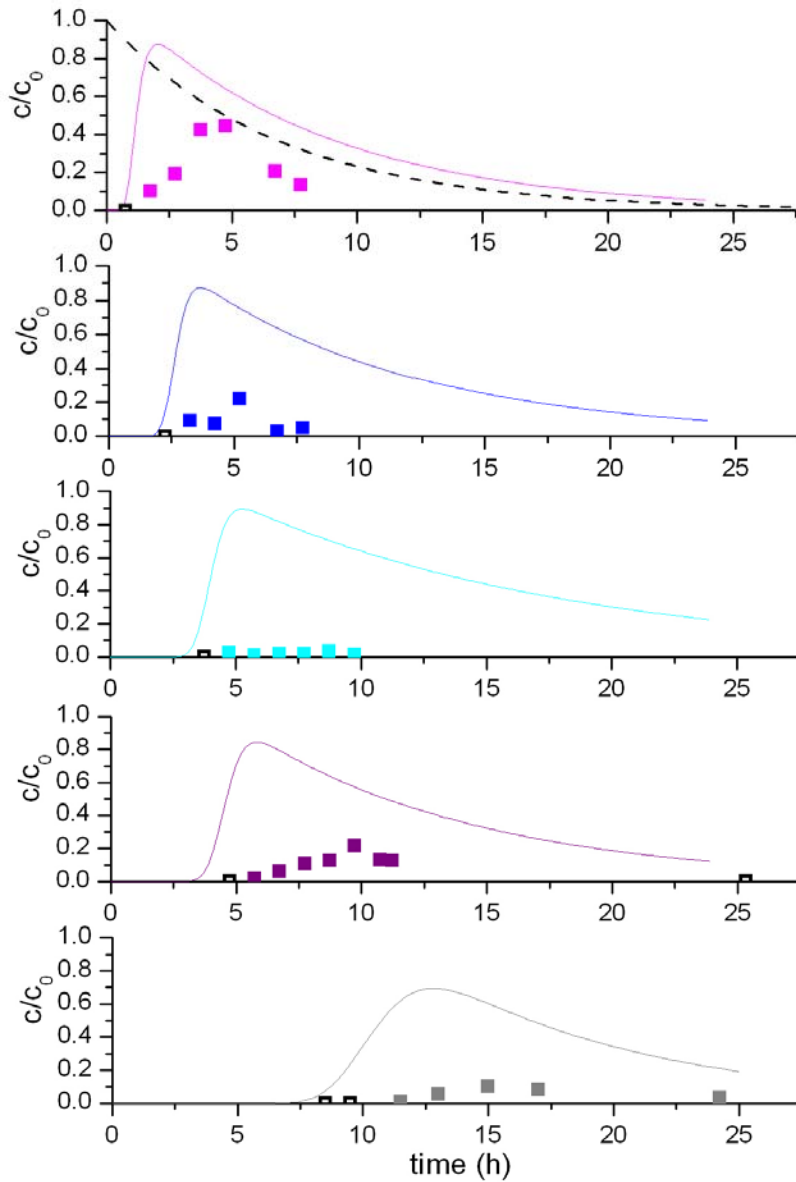
Figure 62: MCYST concentrations and modeled tracer breakthrough curves in sampling ports in 20 cm, 40 cm, 60 cm and 80 cm depth as well as in the effluent (from top to bottom) during E3 (c0 = 6.15 µg/L). Dotted curve: MCYST in water reservoir (modeled); Solid curves: tracer modeled at the respective port; solid squares; MCYST measured at the respective port; open squares: MCYST below detection limit, i.e. < 0.01 µg/L.
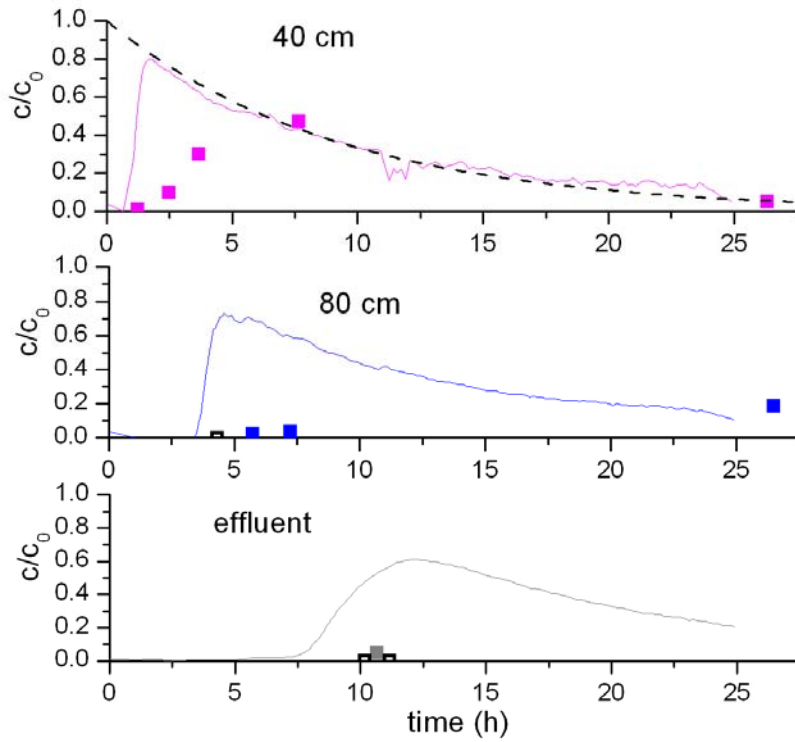
Figure 63: MCYST concentrations and measured tracer breakthrough curves in sampling ports in 40 cm and 80 cm depth as well as in the effluent during E4 (c0 = 9.0 µg/L). Dotted curve: MCYST in water reservoir (measured); Solid curves: tracer measured at the respective port; solid squares; MCYST measured at the respective port; open squares: MCYST below detection limit, i.e. < 0.01 µg/L.
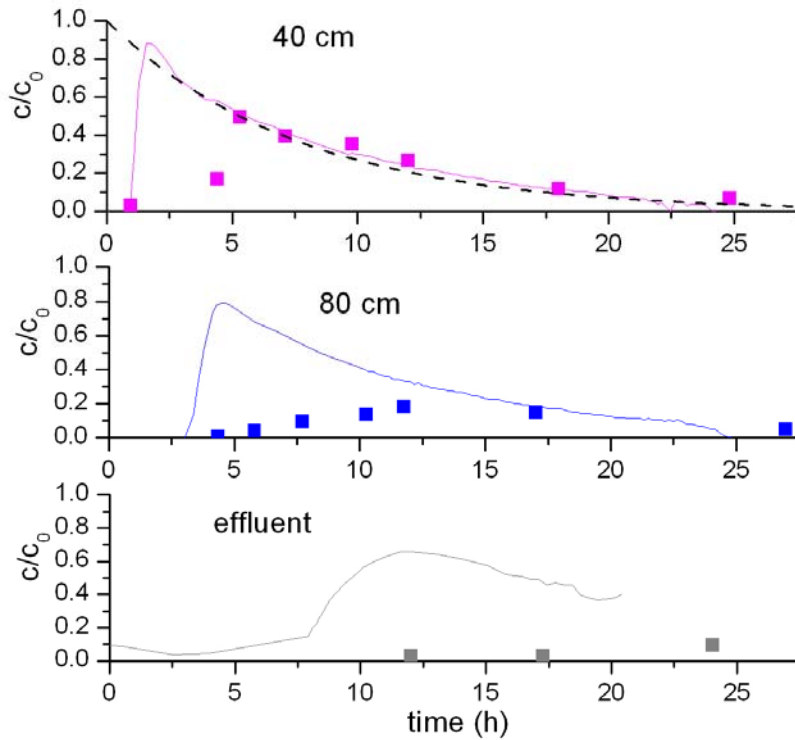
Figure 64: MCYST concentrations and measured tracer breakthrough curves in sampling ports in 40 cm and 80 cm depth as well as in the effluent during E5 (c0 = 7.6 µg/L). Dotted curve: MCYST in water reservoir (measured); Solid curves: tracer measured at the respective port; solid squares; MCYST measured at the respective port; open squares: MCYST below detection limit, i.e. < 0.01 µg/L.

Quantification of retardation and degradation rates was obtained by modeling the breakthrough curves, which was carried out by the working group "models" (IGB), see chapter 3.2.2.2.

Table 18 gives the shares of recovered MCYST (as the sum of all identified MCYST variants) for all four enclosure experiment with pulsed application. Both experiments carried out on enclosure III (four sampling ports), E2 and E3, show recovery rates between 2.5 % and 19 % and declining values with increasing depth. The existence of a visible clogging layer does not seem to be decisive – temperature probably plays a more important role. This can be derived from the fact that experiment E3, carried out with a visible clogging layer but at average

114

temperatures 10 °C lower than E2, shows higher recoveries, i.e. lower elimination rates. If the clogging layer had been decisive, the reverse result would have been expected.

Experiments E4 and E5, carried out on enclosure II (with 2 sampling ports), show clearly higher recoveries (i.e. lower elimination rates) with values ranging from 10 % to 82 %. Highest recoveries were obtained in experiment E5 which was conducted after the removal of the clogging layer and at higher temperatures than E4. Here the clogging layer seems to play a more important role.

Table 18: Recovered amounts of MCYST in experiments E2 through E5.

Experiment no.	Water temperature (min – max) [°C]	Clogging layer visible?	Share of recovered MCYST (by HPLC; %)				
			20 cm	40 cm	60 cm	80 cm	effluent
E2	23.6 - 31.6	No	19	13	4.2	2.5	2.7
E3	16.4 - 23.1	Yes	17	15	(1)*	15	9.8
E4	0.6 - 4.7	Yes		66		21	(0.5)*
E5	6.3 - 11.2	No		82		44	10

* uncertain value due to insufficient data

As all four experiments were conducted at similar filtration velocities and the same experimental setup the only explanation for the great differences in elimination rates between E2 / E3 and E4 / E5 are the varying water temperatures under which they were carried out. For further investigations laboratory experiments concerning this topic were conducted in cooperation with the TU Berlin in 2005 (see final report working group algae, part VII).

9.3.2.2.2 Modeling Results

The following figures show best fit results for enclosure experiments E2 and E3 for different intervals of the flow path. Depicted are

- Measured concentrations at the top position of the respective spatial interval, here denoted as 'inlet'; used as boundary condition for inverse modelling

- Measured concentrations at the bottom position of the respective spatial interval, here denoted as 'outlet' used for objective function in inverse modelling

- Modelled concentrations at the bottom position; simulated using best-fit parameter values.

Parameters given in the figures are: velocities v and longitudinal dispersivities αL, obtained from inverse modelling using VisualCXTFIT as well as retardation R and degradation rate λ, obtained form MATLAB® inverse modelling.

The results of the inversion modeling procedure are depicted Figure 65 to Figure 77. For some simulations an additional start was performed, in which one or two outliers, observed in the measurements, were not considered in the parameter estimation procedure (curves not shown). In all cases the restart improved the fit substantially and some parameter values changed significantly.

The plot shows the following parameters:

$v = 0.32$ m/h $\alpha_L = 0.0063$ m

$R = 1.97$ $\lambda = 0.74$ 1/h
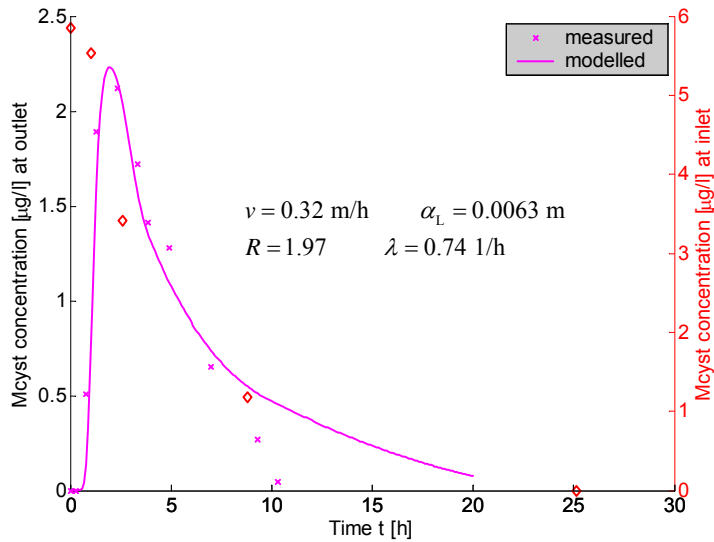
Figure 65: **Inverse modeling result for experiment E2, inlet to 20 cm (solid curve, left scale); measured inlet values: diamonds, right scale; measured values in 20 cm depth: crosses, left scale.**
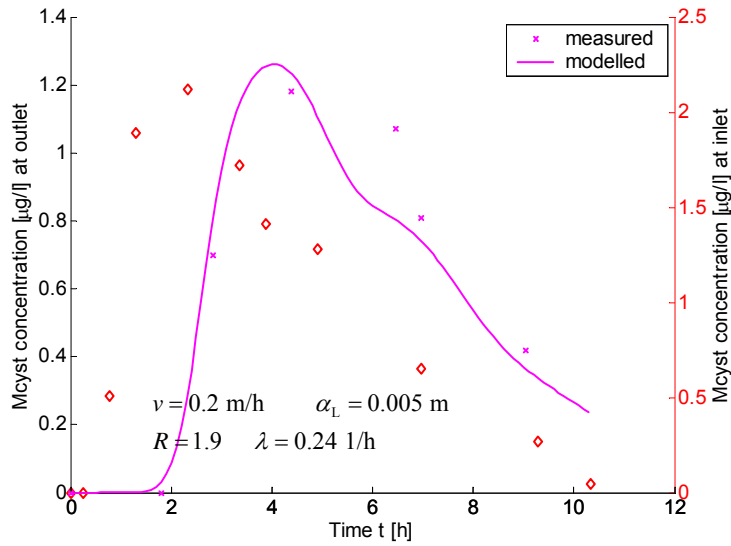
Figure 66: Inverse modeling result for experiment E2, 20 cm to 40 cm (solid curve, left scale); measured values in 20 cm depth: diamonds, right scale; measured values in 40 cm depth: crosses, left scale.
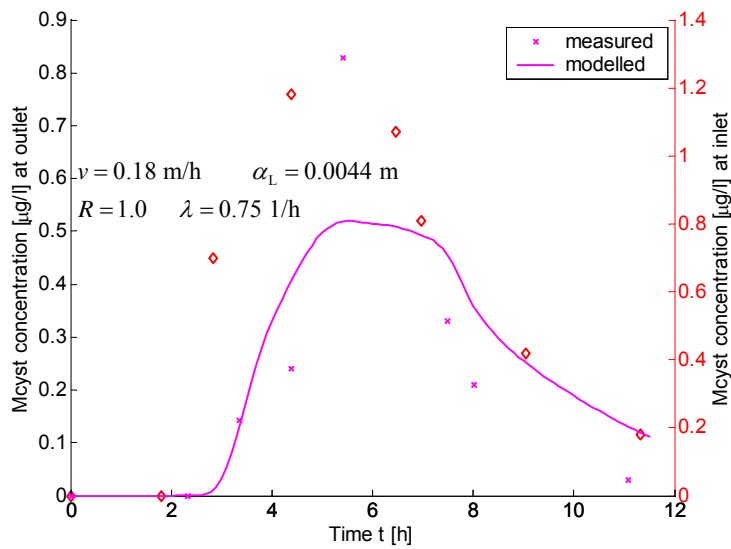
Figure 67: Inverse modeling result for experiment E2, 40 cm to 60 cm (solid curve, left scale); measured values in 40 cm depth: diamonds, right scale; measured values in 60 cm depth: crosses, left scale.

117
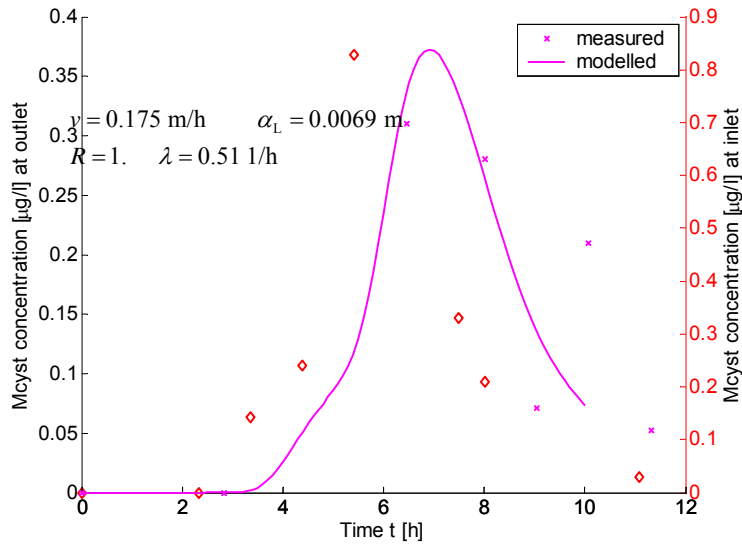
Figure 68: Inverse modeling result for experiment E2, 60 cm to 80 cm (solid curve, left scale); measured values in 60 cm depth: diamonds, right scale; measured values in 80 cm depth: crosses, left scale.
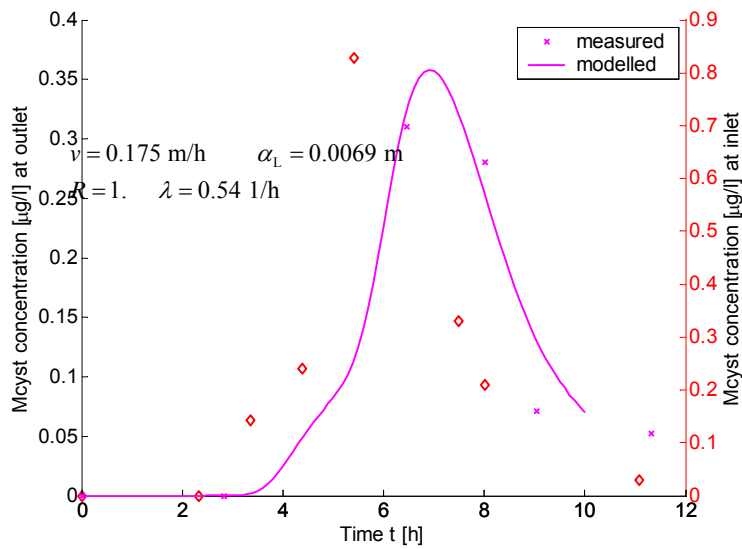
Figure 69: Inverse modeling result for experiment E2, 60 cm to 80 cm without outlier (solid curve, left scale); measured values in 60 cm depth: diamonds, right scale; measured values in 80 cm depth: crosses, left scale.
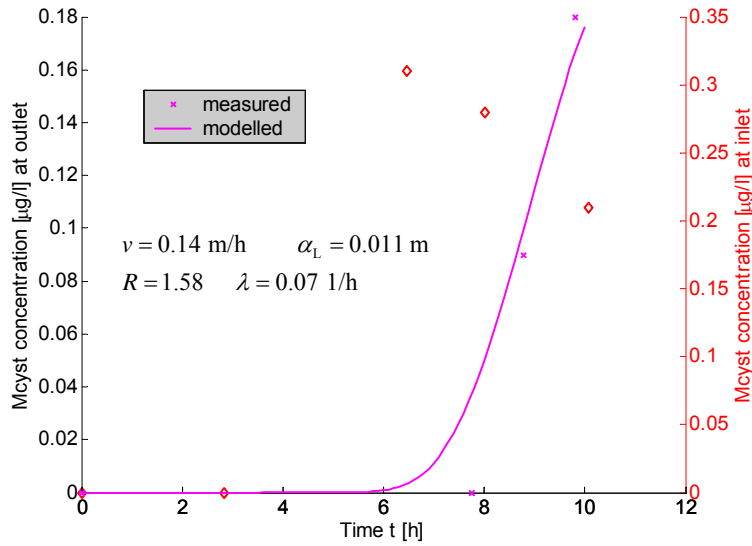
Figure 70: Inverse modeling result for experiment E2, 80 cm to effluent (solid curve, left scale); measured values in 80 cm depth: diamonds, right scale; measured values in effluent: crosses, left scale.
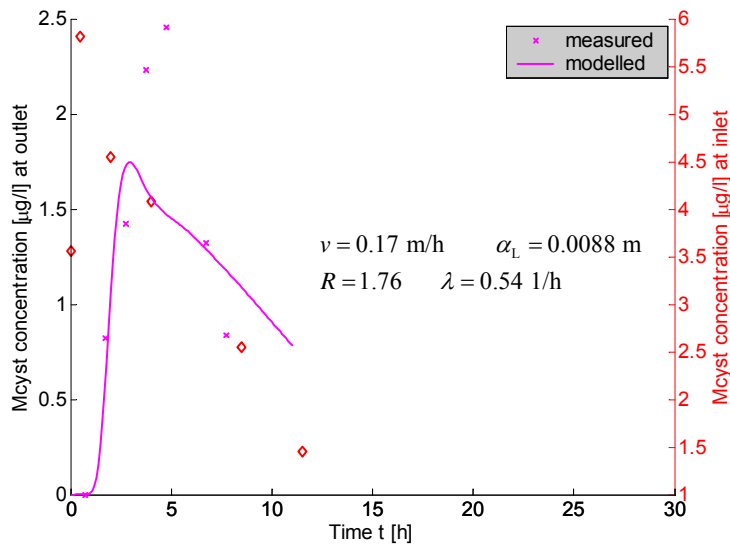
Figure 71: Inverse modeling result for experiment E3, inlet to 20 cm depth (solid curve, left scale); measured values in inlet: diamonds, right scale; measured values in 20 cm depth: crosses, left scale.
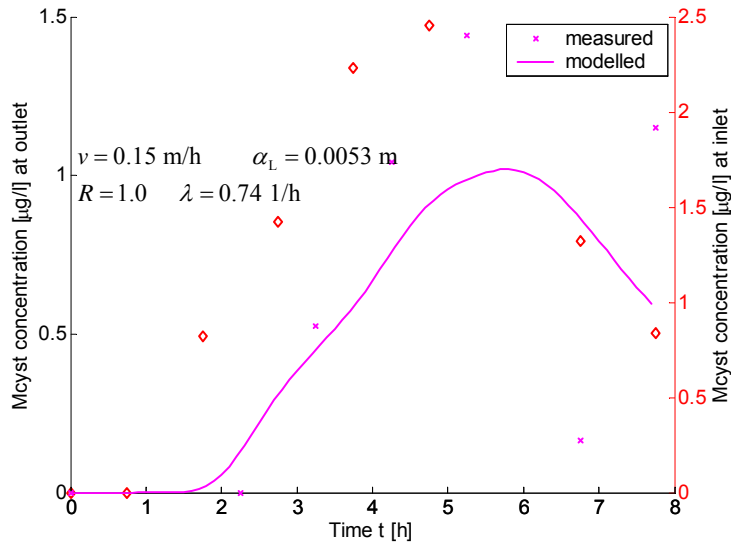
Figure 72: Inverse modeling result for experiment E3, 20 cm to 40 cm depth (solid curve, left scale); measured values in 20 cm depth: diamonds, right scale; measured values in 40 cm depth: crosses, left scale.
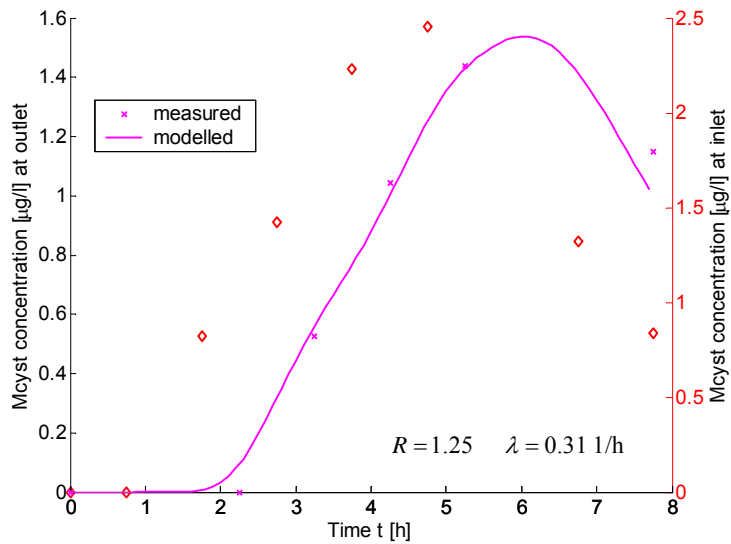
Figure 73: Inverse modeling result for experiment E3, 20 cm to 40 cm depth without outlier (solid curve, left scale); measured values in 20 cm depth: diamonds, right scale; measured values in 40 cm depth: crosses, left scale.
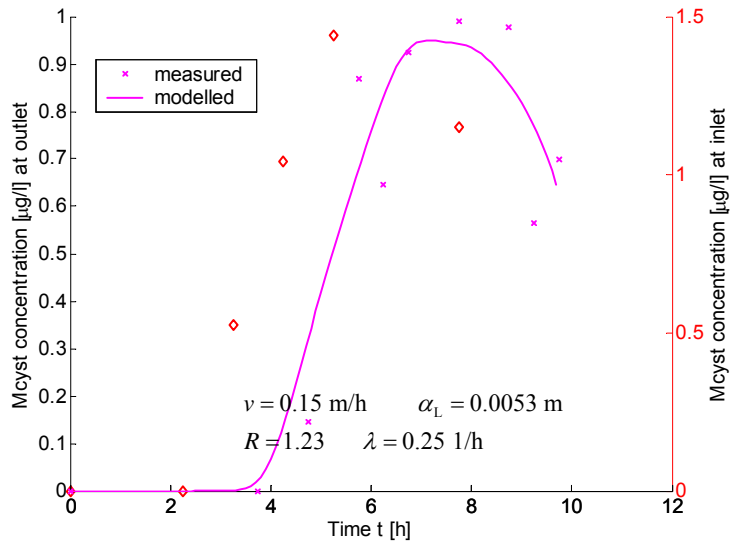
Figure 74: Inverse modeling result for experiment E3, 40 cm to 60 cm depth (solid curve, left scale); measured values in 40 cm depth: diamonds, right scale; measured values in 60 cm depth: crosses, left scale.
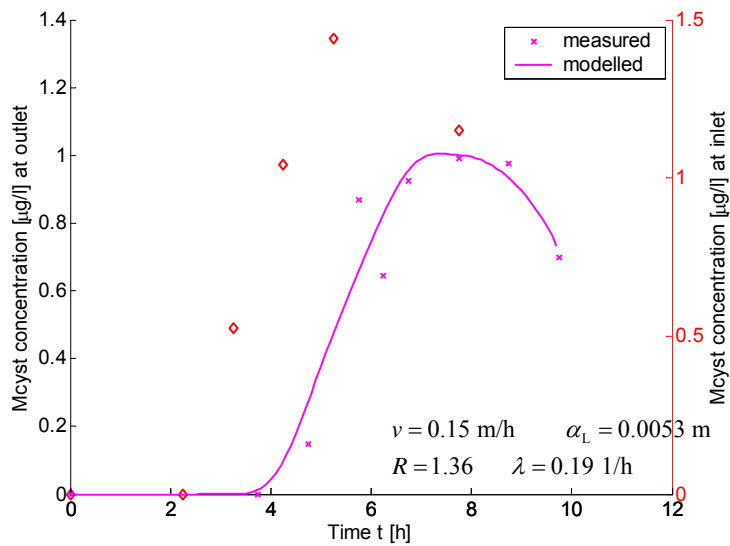
Figure 75: Inverse modeling result for experiment E3, 40 cm to 60 cm depth without outlier (solid curve, left scale); measured values in 40 cm depth: diamonds, right scale; measured values in 60 cm depth: crosses, left scale.
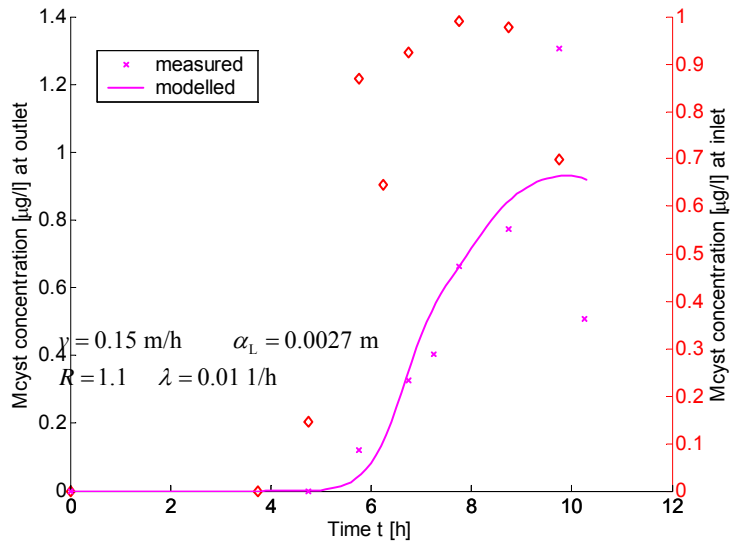
Figure 76: Inverse modeling result for experiment E3, 60 cm to 80 cm depth (solid curve, left scale); measured values in 60 cm depth: diamonds, right scale; measured values in 80 cm depth: crosses, left scale.
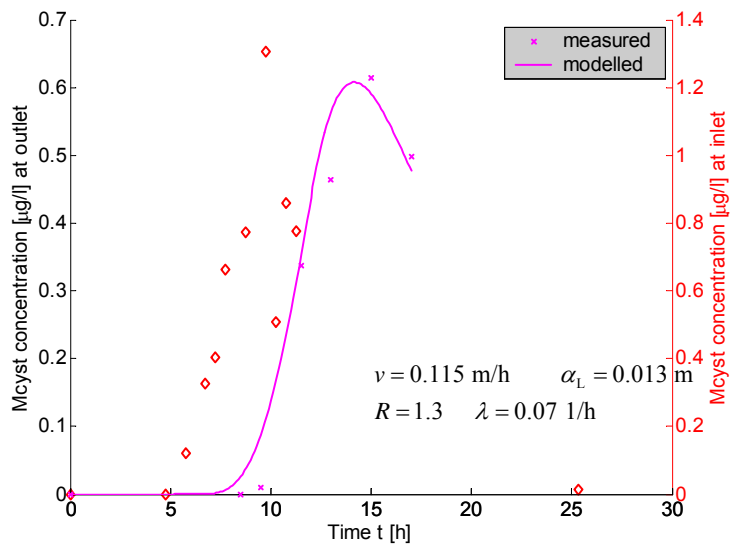
Figure 77: Inverse modeling result for experiment E3, 80 cm depth to effluent (solid curve, left scale); measured values in 80 cm depth: diamonds, right scale; measured values in effluent: crosses, left scale.

9.3.3   Experiments under anaerobic conditions

9.3.3.1   Changes in hydrochemistry

After 4 days of continuous dosing of additional DOC oxygen could not be detected in 40 cm depth and after 9 days, no more oxygen was found in the effluent (Figure 78). After 3 weeks the redoxpotential (EH) had dropped to values < 0 mV in both sampling points and in the effluent. Additionally iron and manganese reduction was observed (0.1 to 0.2 mg/L in all sampling ports), thus implying strictly anaerobic conditions after 40 cm of sand passage. Due to nitrate concentrations below detection limit in the inlet (< 0.1 mg/L) denitrification not was observed.
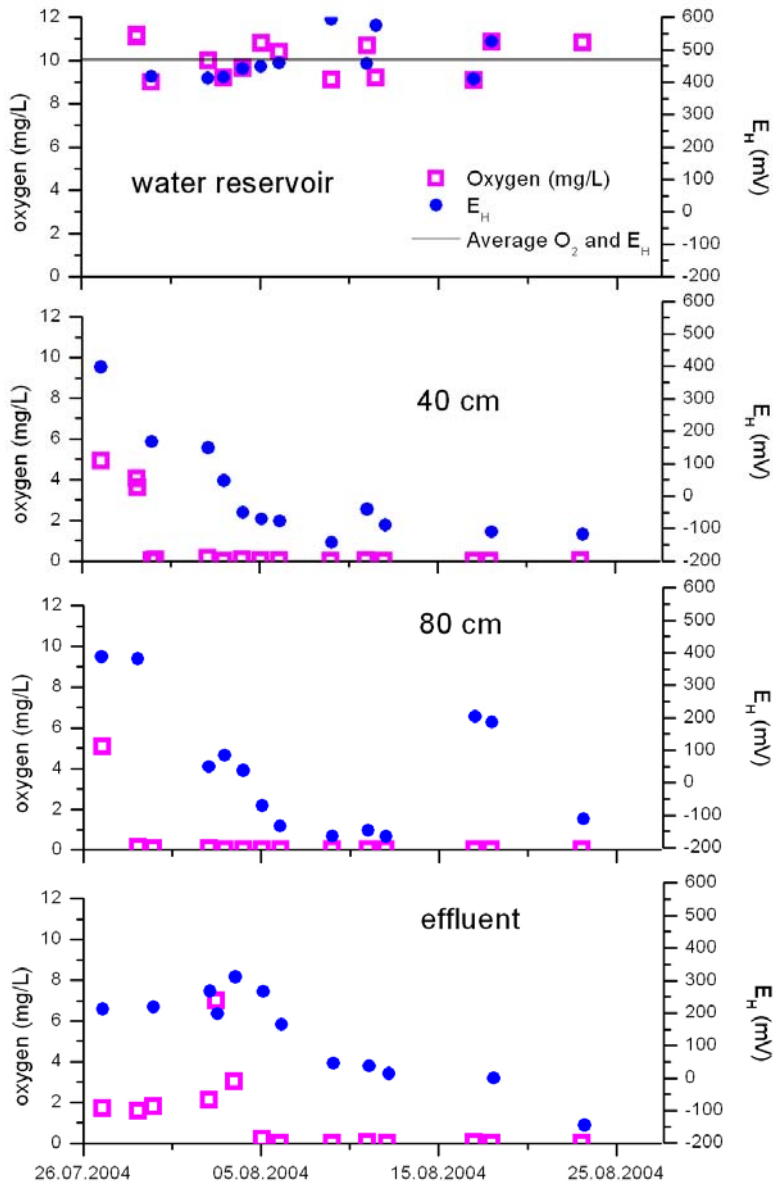
Figure 78: Development of oxygen concentrations and redoxpotential during additional DOC dosing (experiment E8).

For the anaerobic experiment E9 slightly less MCYST was applied than in comparable aerobic experiments (see Table 19). Filtration velocity reached values of only 0.6 m/d, which was about half as high as during the aerobic experiments. Thus the residence time in the

water reservoir was distinctively greater. Nevertheless no relevant degradation was observed prior to infiltration (Figure 79).

Table 19: Initial parameters of the anaerobic enclosure experiment E9 in comparison to minimum and maximum values of similar aerobic experiments E2 to E5 (see Table 17).

Experiment no.	Water temperature (min – max) [°C]	Measured mean filtration velocity [m/d]	Clogging layer visible?	MCYST applied [mg] measured by HPLC	Initial concentration of MCYST by HPLC]µg/L] in water reservoir	Mean residence time in water reservoir (h)
E9	23.0 – 27.0	0.62	Yes	2.34	6.03	7.6
E2 to E5	0.6 – 31.6	1.03 – 1.22	Partly	2.69 – 3.87	6.1 – 9.0	4.74 – 6.31

Figure 80 gives the relative MCYST concentrations measured in the sampling ports (40 cm and 80 cm depth) and the effluent as well as the relative tracer concentrations. In 40 cm depth the MCYST concentrations follow the tracer curve closely, showing only little retardation and degradation. Forty centimeters deeper only two samples showed MCYST values above the limit of determination (> 0.1 µg/L). However, the results show that a higher sampling density would have better depicted the processes during the time span that proved to be of interest, also for the analyses done by ELISA (see appendix V-6). It is likely that maximum MCYST concentrations may have passed the sampling point during 12 to 20 h after MCYST application, when no samples were taken.
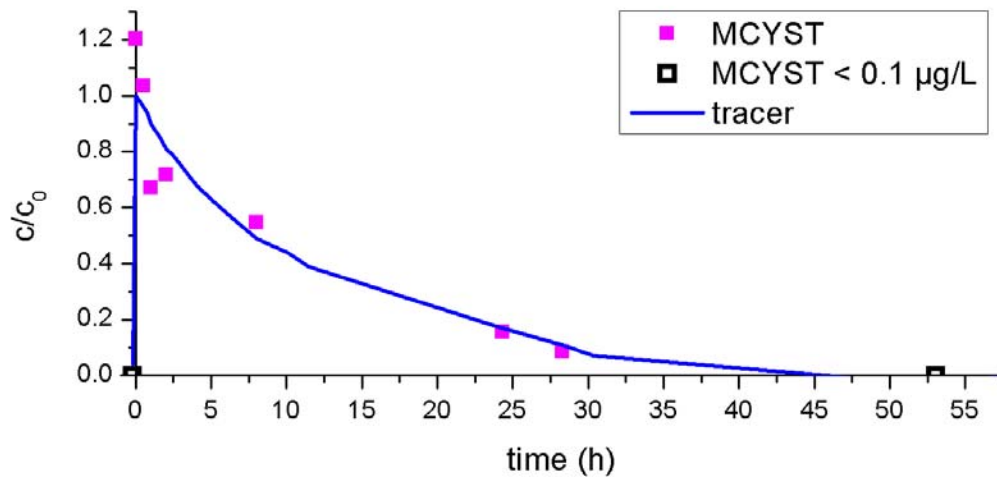
Figure 79: MCYST and tracer concentrations in the water reservoir during experiment E9. Due to the missing samples between 12 and 22 h maximum MCYST

concentrations were probably also missed in the effluent. Two unusually high MCYST values obtained by HPLC at 23 and 24 h could not be confirmed by ELISA, so they may bias the results towards higher recovery rates.
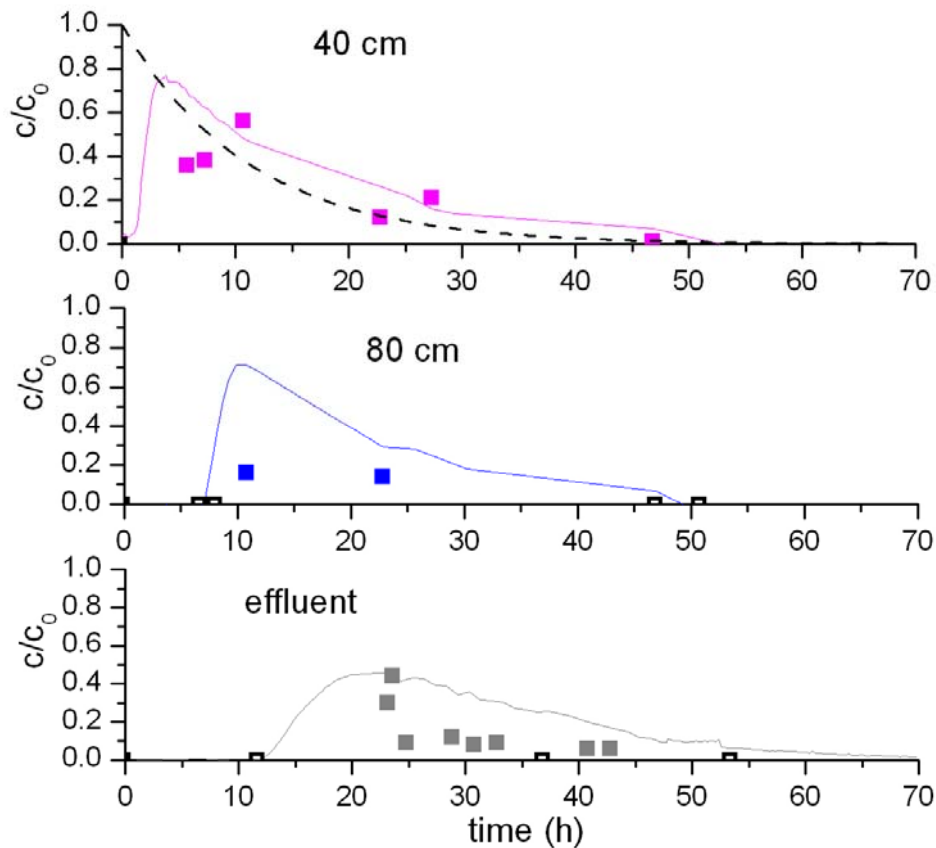
Figure 80: MCYST concentrations and tracer breakthrough curves in 40 cm and 80 cm depth as well as in the effluent (from top to bottom) during E9 (c0 = 6.031 µg/L). Dotted curve: MCYST in water reservoir (measured); Solid curves: tracer measured at the respective port; solid squares; MCYST measured at the respective port; open squares: MCYST below detection limit, i.e. < 0.01 µg/L.

Table 20 gives the shares of recovered MCYST (as the sum of all identified MCYST variants) for the anaerobic enclosure experiment in comparison with the aerobic experiments E2 to E5. Experiments E2 and E3 that were carried out at similar temperatures as experiment E9 show distinctively lower recoveries, i.e. higher elimination rates than the latter. Even experiments E4 and E5 that were conducted at clearly lower temperatures and showed higher amounts of MCYST in the effluent did not reach the recovery rates obtained during

the anaerobic experiment. Taking into account the uppermost 40 cm anaerobic conditions represent the worst case concerning MCYST elimination of all experiments carried out on the enclosures. The difference in elimination between the different aerobic experiments is, however, greater than between the anaerobic experiment and the worst case aerobic experiment (no clogging layer, low temperature, E5).

Table 20: **Recovered amounts of MCYST during experiments E9 (anaerobic) and E2 through E5 (aerobic).**

Experiment no.	Water temperature (min – max) [°C]	Clogging layer visible?	Share of recovered MCYST by HPLC [%]				
			20 cm	40 cm	60 cm	80 cm	effluent
Anaerobic							
E9	23 – 27	Yes		92		(33)*	42 / 15**
Aerobic							
E2	23.6 - 31.6	No	19	13	4.2	2.5	2.7
E3	16.4 - 23.1	Yes	17	15	(1)*	15	9.8
E4	0.6 - 4.7	Yes		66		21	(0.5)*
E5	6.3 - 11.2	No		82		44	10

* uncertain value due to insufficient data.
**2nd value without outliers.

9.3.4 *Experiments with continuous application (E10, E12 and E13)*

9.3.4.1 Changes in hydraulics and hydrochemistry during the experiment

Flow rate, water table and suction pressure in front of the pump at enclosure I during experiment E10 are given in Figure 81. As the flow rate was maintained at a constant level, the suction pressure rose distinctively, probably due to clogging. The hydraulic conductivity declined from 4.7*10-6 m/s on 13th Oct. to 1.95*10-6 m/s on 3rd Nov.
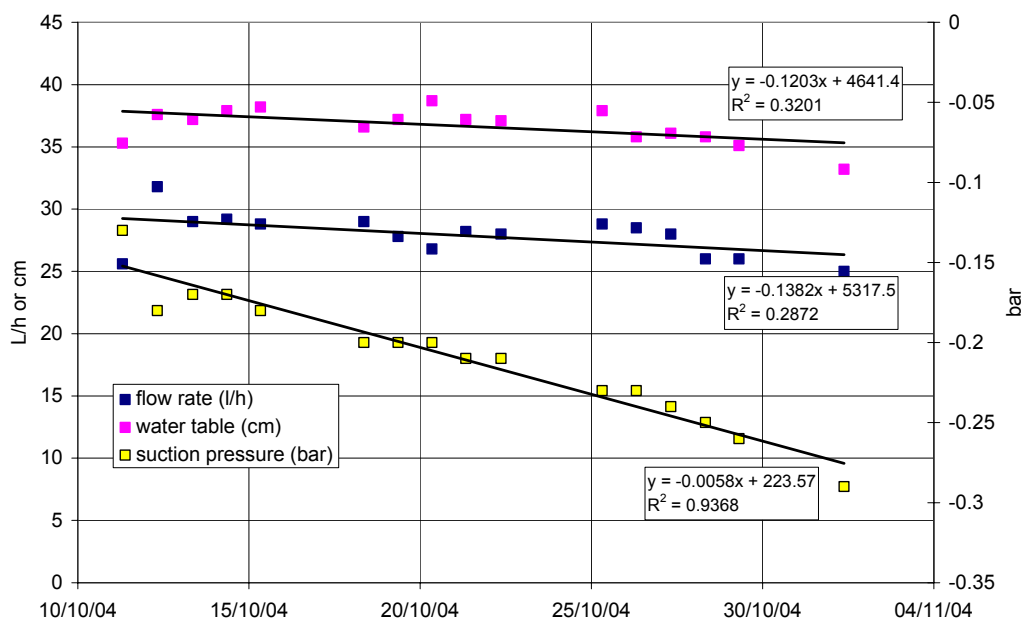
Figure 81: **Hydraulic parameters during experiment E10 (12th Oct. 04 to 1st Nov. 04).**

Hydrochemical parameters showed only very little variation during the experiment. The differences between water reservoir and effluent reflect the conditions that were observed under normal operating conditions (compare chapter 2.1.2.2).

Table 21: Average values of hydrochemical parameters during experiment E10.

Parameters	Water reservoir Average ± stand. dev. (number of samples)	Effluent Average ± stand. dev. (number of samples)
EC (µS/cm) without tracer experiment	878 ± 16 (14)	907 ± 30 (12)
Temperature (°C)	8.8 ± 2 (15)	10.6 ± 1.6 (10)
pH	8.5 ± 0.2 (6)	7.8 ± 0.1 (6)
Oxygen (mg/L)	12.1 ± 0.2 (2)	7.3 (1)
Oxygen (%)	97 ± 1.6 (2)	64 (1)
Alkalinity (mg/L)	50.8 ± 2.7 (5)	60.6 ±4.5 (5)
DOC (mg/L)	4.4 ± 1.9 (7)	2.4 ± 0.5 (7)

Figure 82 shows the concentrations of MCYST measured by ELISA in the stock solution (average of two samples taken before connection to the water reservoir and after disconnection one day later) and in the water reservoir of the enclosure. In order to be able

to adapt the the experimental design to MCYST-concentrations, ELISA was chosen as rapid method to follow these, with occasional confirmation by HPLC-analyses (see final report, part IIX). The error bars of the stock solution data points indicate minimum and maximum values of the two samples taken within these 2 days. High errors are due to analytical variations in two cases (16th and 25th Oct.) or, on one occasion (24th Oct.), some degradation may have taken place, as the stock solution was prepared and kept connected over two days, i.e. 1 day longer than otherwise.

The MCYST concentrations measured in the stock solution and in the water reservoir by ELISA show parallel fluctuations (Figure 82). This may be due to inhomogeneous distribution in the frozen and then thawed MCYST extract prior to the partitioning into aliquots. Very low concentrations in the water reservoir between 16th and 18th Oct. are due to a flow interruption from the stock solution to the water reservoir caused by technical problems.

The samples taken during the intensive sampling campaign on 26th to 27th Oct. show no trend with time. The 12 measurements distribute evenly around a value of 11.6 µg/L with a standard deviation of 1.1 µg/L (which in this case could be interpreted as the standard error for analyses and sampling).
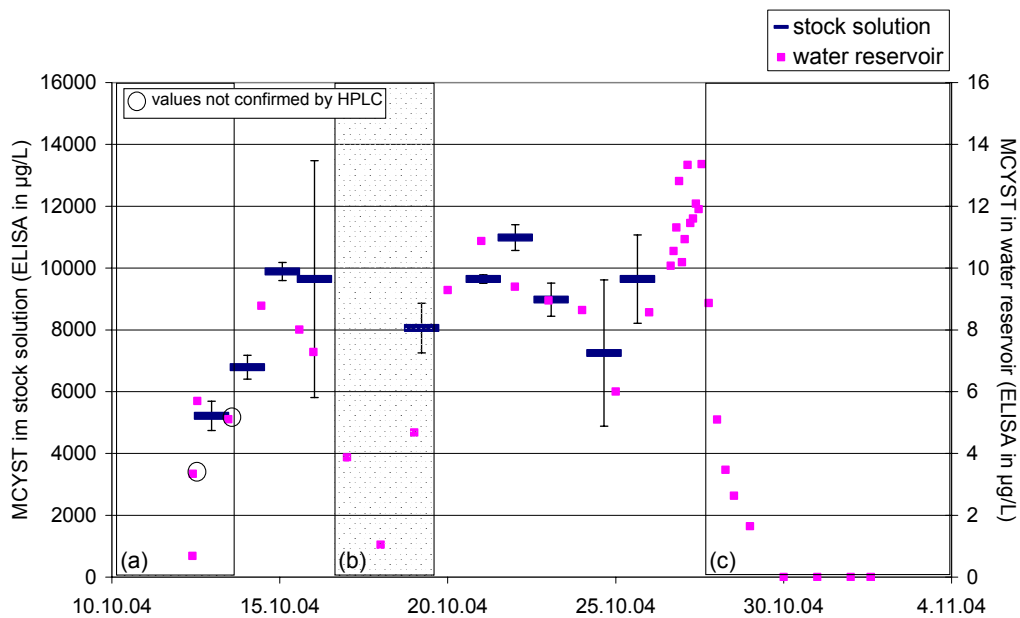
Figure 82: **MCYST concentrations in stock solution and water reservoir during experiment E10, measured by ELISA (error bars indicate minimum and maximum values) (a): starting phase with lower concentrations due to dilution and adsorption, b): low concentrations due to technical problems, c): end phase with declining concentrations).**

Taking these uncertainties into account two phases with relatively constant experimental conditions can be defined (Figure 82):

- 14th to 16th Oct.,

- 20th to 27th Oct..

During this time the MCYST concentrations lie roughly between 8 µg/L and 11 µg/L with a tendency towards higher values with time.

Figure 83 shows the MCYST concentrations measured in the effluent together with the related, interpolated values for the water reservoir (considering a residence time of 16.25 h in the filter bed). The elimination was calculated as the ratio of effluent to related water reservoir concentration. Values below the limit of determination were replaced by half the limit of determination.

During the starting phase MCYST concentrations in the effluent rise to values of about 4 µg/L and elimination rates decline from values of 80 % on the first day after dosing started to 45 % on day two. The initially high elimination rate may be due to a retardation of the MCYST by adsorption. In average elimination rates during this initial phase are around 60 %, however influenced by unusually high elimination during the first day.

The first phase of constant experimental conditions (without shading in Figure 83) is characterized by more or less constant effluent concentrations between 1 and 2 µg/L. The elimination rates lie around 48 %, which is clearly below the rates observed during previous enclosure experiments.

After a short flow interruption (shaded area (b) in Figure 83) elimination rates rise to over 80 % and remain at this level even though input concentrations increase steeply after 26th Oct.. The difference between the two phases of constant experimental conditions (i.e. the two areas without shading in Figure 83) in arithmetic mean is significant (probability of error in t-test < 1%).

During the 24 h intensive sampling campaign the elimination rates varied between 79 % and 96 %, showing slightly higher recoveries during the night and early morning (2 am to 9 am average: 16.6 ± 5.8 %, n = 5) than during the day (11 am to 9 pm average: 10.8 ± 3.6 %, n = 7). The difference in arithmetic mean is, however, not significant (probability of error in t-test > 5 %).
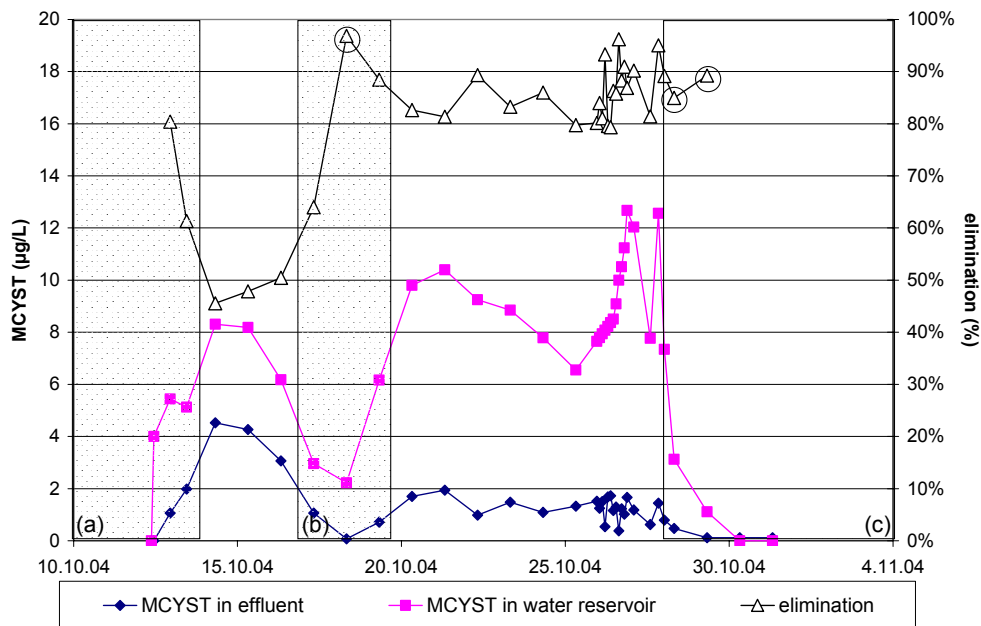
Figure 83: MCYST concentration in effluent and water reservoir as well as elimination rate during experiment E10 (shaded areas, see Figure 32, encircled values: effluent concentrations below limit of determination).

With the exception of 3 values, marked in light blue in Figure 84, the MCYST concentrations obtained by HPLC analysis confirm those measured by ELISA, although the HPLC values are generally lower (see final report working group algae, part IIX).
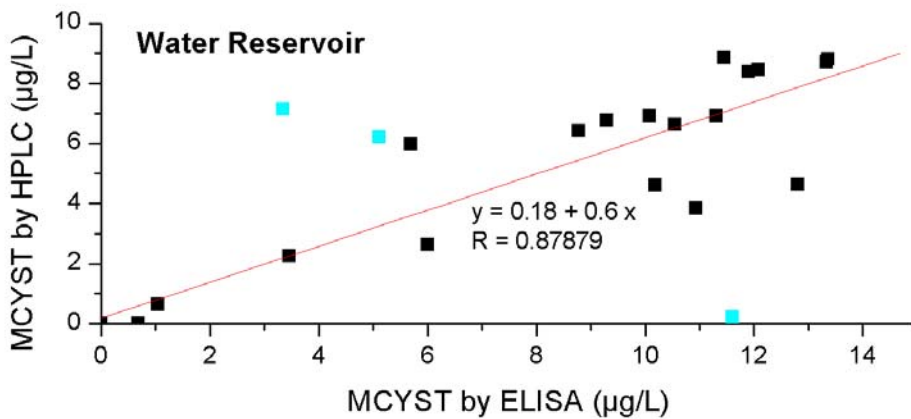
Figure 84: Correlation between MCYST concentrations measured by HPLC and by ELISA in the water reservoir during E10 (masked values in light blue).

In summary, the elimination rates obtained after eight days of continuous application under aerobic conditions show similar values as those calculated from the total recovered amounts of MCYST for pulsed application (90 % to 97.5 %, see Table 18).

9.3.4.2 Experiment with cyanobacterial cells (E12)

9.3.4.2.1 Changes in hydrochemistry and hydraulics during the experiment

During the first days of the experiment dosing of cyanobacterial cells, the flow rate in enclosure I decreased rapidly from an initial value of 34 L/h to about 15 L/h after 3 days, where it remained constant until the end of the 16-day experiment. Hydraulic conductivity of the enclosure showed the same development with initially 2.7 *10-6 m/s and later values around 1.0*10-6 m/s.
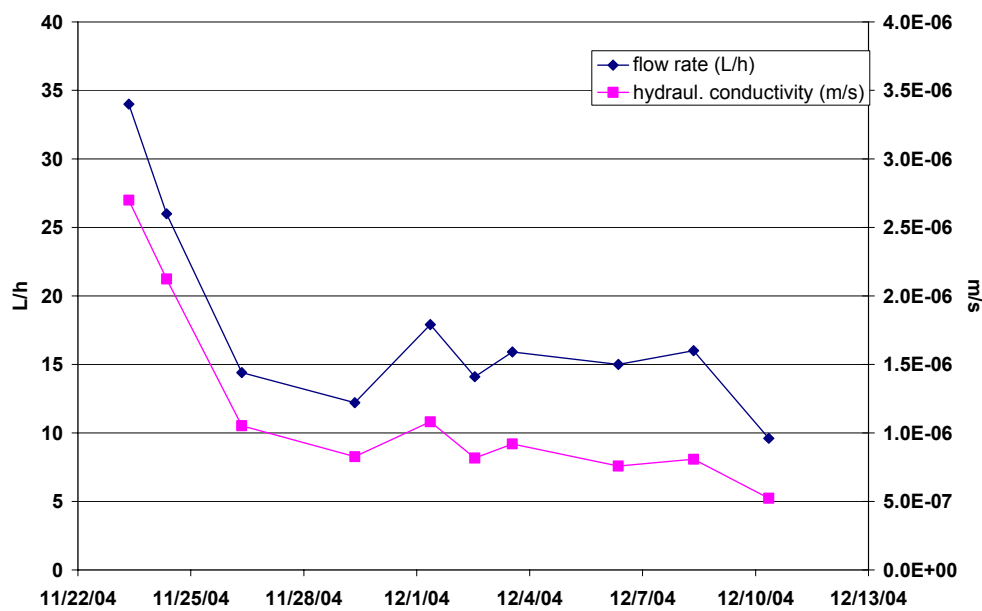
Figure 85: **Development of flow rate and hydraulic conductivity during experiment E12.**

Hydrochemical parameters showed only very little variation during the experiment. The differences between water reservoir and effluent reflect the conditions that were observed under normal operating conditions (compare chapter 2.1.2.2).

Table 22:   Average values of hydrochemical parameters during experiment E12.

Parameters	Water reservoir Average ± stand. dev. (number of samples)	Effluent Average ± stand. dev. (number of samples)
EC (µS/cm) without tracer experiment	872 ± 12 (8)	869 ± 21 (5)
Temperature (°C)	3.6 ± 0.8 (9)	5 ± 1.1 (5)
pH	8.3 ± 0.1 (5)	7.8 ± 0.03 (3)
Oxygen (mg/L)	13.8 ± 0.3 (3)	10.2 ± 0.3 (2)
Oxygen (%)	111 ± 4.1 (3)	80.9 ± 4.5 (2)
Alkalinity (mg/L)	95 ± 3 (3)	98 ± 5.7 (5)
DOC (mg/L) (see Figure 86)	3.4 ± 1.8 (8)	2.5 ± 0.8 (4)

The only exception is the DOC (Figure 86), which rose from 2.2 mg/L in the water reservoir before the experiment to 7.3 mg/L on the last day of dosing (26th Nov.) and then declined slowly to 2.7 mg/L on 6th Dec.. In the effluent values around 2 mg/L were observed before the experiment, 3.8 mg/L on the last day of dosing (26th Nov.) and 2.5 mg/L on 6th Dec..
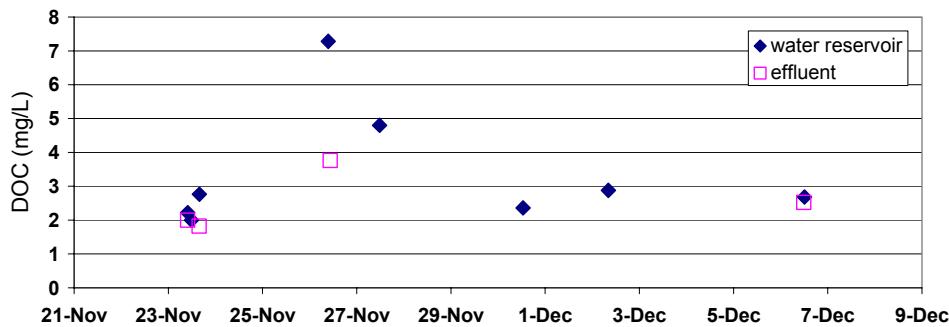
Figure 86:   **Concentrations of dissolved organic carbon (DOC) in water reservoir and effluent during experiment E12.**

9.3.4.2.2   Microcystins (MCYST)

Average MCYST values in the water reservoir during dosing amounted to 7.4 ± 2.9 µg/L (MCYST by ELISA) or 9.0 ± 3.4 µg/L (MCYST by HPLC). Average biovolume of Planktothrix agardhii was determined as 7.5 ± 2.5 mm³/L. One day after dosing was terminated the biovolume had declined to 3.7 mm³/L and the MCYST concentrations amounted to 1.3 µg/L and 1.4 µ/L by ELISA and HPLC, respectively (Figure 87).

From 31st Nov. on the biovolume remained quite constant at 0.6 mm³/L and MCYST determined by HPLC amounted to 0.3 µg/L. After dosing had been terminated the ELISA showed detectable MCYST only in one case with 0.2 µg/L on 6th Dec..
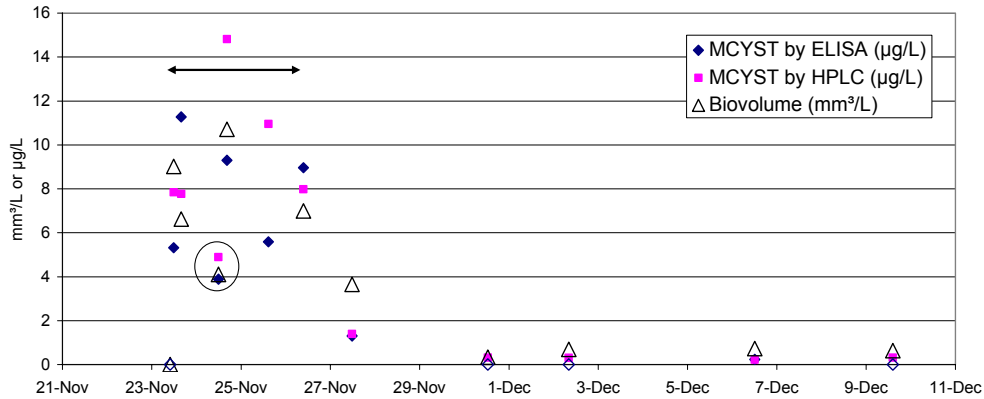
Figure 87: **MCYST (by HPLC and ELISA) and Planktothrix biovolume in the water reservoir during experiment E12 (circle: values influenced by flow interruption, arrow: time span of dosing; open diamonds indicate values below detection limit).**

In the effluent MCYST was not determined at any time, neither by ELISA, nor by HPLC.

The sediment cores showed an accumulation of MCYST in the uppermost 2 cm of the filter sand (Figure 88) at the end of the dosing phase (Nov. 26th). After dosing ceased, however, MCYST concentrations decreased rapidly so that no more MCYST was detected in the uppermost 2 cm after 10 days.
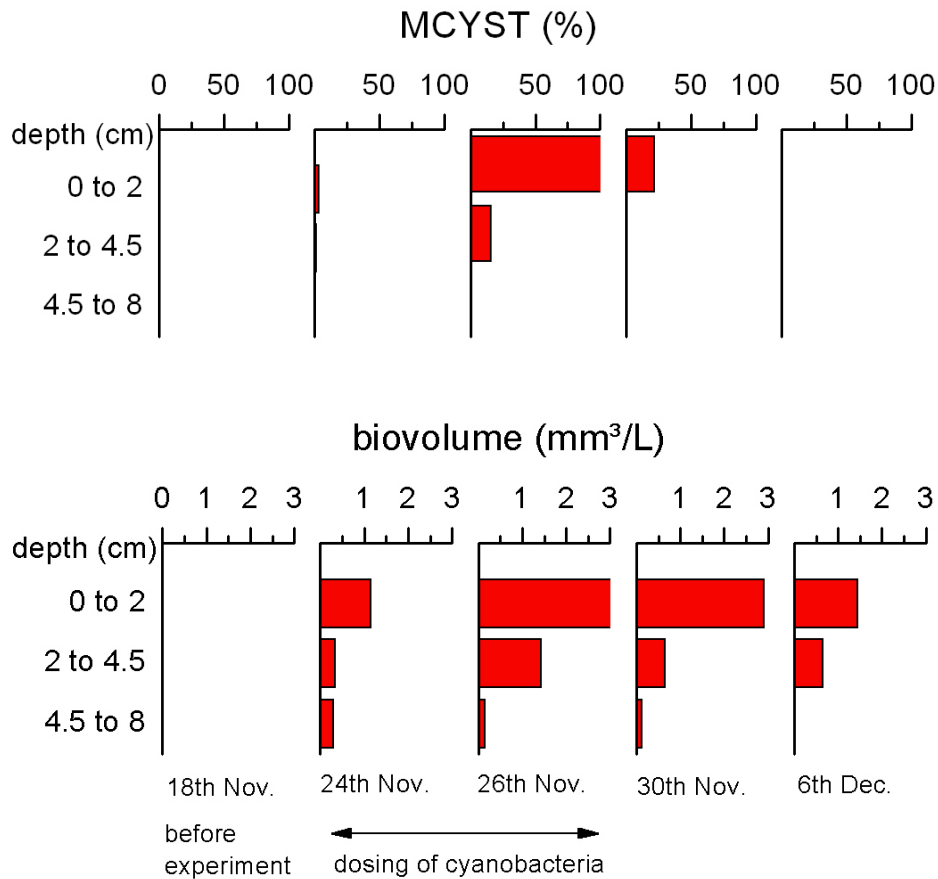
Figure 88: Total MCYST (in percent of maximum concentration - 1023 µg/L - at the end of the dosing phase) in the pore water of sediment cores during experiment E12.

Biovolume in the upper sediment layers, however, did not show any substantial decrease after dosing had been terminated (Figure 88). This leads to the assumption that although accumulated cells persist on the sediment surface and within the top few cm, no accumulation of MCYST takes place. This might be due to a) rapid degradation and / or b) release and rapid transport of dissolved MCYST, though at levels in the effluent that range below the detection limit.

9.4 Interpretation and Discussion

9.4.1 Clogging of the enclosures

The tracer experiments carried out simultaneously with the different enclosure experiments yielded varying effective pore volumes (calculated from measured filtration velocity and modeled pore velocity) and dispersion coefficients (obtained by modeling) in the course of the two years in which the experiments were carried out (Table 10). Effective pore volumes ranged from 36 % to 41 % for the total enclosure. In the uppermost 20 cm to 40 cm of the filter, however, effective pore volumes reached a minimum value of 12 % (experiment in enclosure II under anaerobic conditions, see Figure 57). Between 40 cm and 80 cm effective pore volumes usually ranged from 23 % to 31 %. Below 80 cm values ranged from 36 % to 40 %, probably influenced by the gravel drainage layer beneath 100 cm.

Values below 20 % were observed in different experiments in the uppermost part of the enclosures and seem to relate directly to clogging, with one exception: one tracer experiment in enclosure III yielded similar effective pore volumes directly after the uppermost centimeters had been removed (see Figure 56, experiment E2). This is probably explicable by partially unsaturated conditions, as this was the first experiment to be carried out after the water table had been lowered in order to remove the clogging layer, so that incomplete saturation during the rising of the water level is likely.

In all other cases, low effective pore volumes developed with increasing run time after removal of the clogging layer and reached minimum values during experiment E9. During this experiment additional DOC was dosed in order to reach anoxic and anaerobic conditions by oxygen consumption due to high biological activity, and this further enhanced clogging.

The processes that lead to diminished pore volumes or clogging can be (Schwarz 2004):

- physical clogging (caused by fine particles or gas bubbles),

- chemical clogging (e.g. by precipitation of carbonate or iron and manganese),

- biological clogging (by growth of biofilms, or by trapped gas bubbles produced by biological activity).

Evidence for all three processes can be found during the experiments:

- gas bubble formation was observed during removal of the uppermost centimeter in enclosure III (Figure 58) as well as visible accumulation of organic detritus indicating physical clogging by gas and fine organic particles,

- accumulation of inorganic carbon (i.e. chemical clogging) was detected during analysis of the SSF clogging layer (as chemistry of water and sediment resemble that of the SSF, a similar reaction for the enclosures seems reasonable),

- although no relevant increase in total cell count by DAPI was observed in the SSF clogging layer (see final report working group algae, part IV) the gas bubbles

observed during disturbance of the clogging layer are probably produced by biological activity (indirect biological clogging),

On the basis of the different measurements and observations all experiments carried out were characterized concerning the clogging situation as given in Table 23. This shows that, although the uppermost layer was destroyed prior to experiments E2 and E5 no totally unclogged conditions were generated. Clogging might therefore be not only due to "outer" clogging (e.g. due to a "schmutzdecke"-formation), but also due to "inner" clogging, i.e. reduction of effective porosity inside the filter (Grombach et al., 2000).

Table 23: **Hydraulic data of all enclosure experiments with resulting assessment of the clogging situation.**

Experiment No.	Date of experiment	Filtration velocity [m/d]	Pore velocity [m/d]	Dispersion length (αL) [m]	Eff. Pore-volume (ne)	Hydraulic conductivity [m/s]	Clogging situation
Enclosure I							
E6	17th Dec. 2003	0.86	2.40	0.020	0.360	0.95*10-5	Not clogged
E10	12th Oct. 2004	0.73	1.78	0.027	0.410	0.4*10-5	Clogged
E12	19th Nov. 2004	0.48	1.32	0.013	0.363	0.1*10-5	Clogged
Enclosure II							
E4	11th Nov. 2003	1.09	2.88	0.016	0.379	1.5*10-5	Clogged
E5	25th Nov. 2003	1.22	3.07	0.023	0.398	1.7*10-5	Partially clogged
E7	8th June 2004	1.20	2.88	0.032	0.420	4.4*10-5	Not clogged
E9	30th Aug. 2004	0.64	1.75	0.049	0.366	1.2*10-5	Clogged
Enclosure III							
E2	5th Aug. 2003	1.25	3.36	0.011	0.37	1.8*10-5	Partially clogged
E3	9th Sept. 2003	1.12	2.76	0.013	0.40	1.6*10-5	Clogged

For the interpretation of the enclosure experiments this means that no totally unclogged situations were simulated (with exception of experiments E6 and E7).

9.4.2 Cyanobacterial Toxins (Microcystins)

The first series of enclosure experiments carried out with cyanobacterial toxins (pulsed application, aerobic conditions) had the aim to identify and quantify processes related to short term microcystin transport through sediment with and without visible clogging and to compare these results to those obtained on technical scale slow sand filters (SSF).

Previous laboratory and field scale experiments had shown that biodegradation is the most important elimination process for microcystin removal in sandy material (Grützmacher et al., 2004, Miller, 2000). Degradation was confirmed as the most important process in the enclosure experiments as only little retardation was observed in relation to the tracer applied simultaneously. Modeling yielded R-values between 1.0 and 1.97 (Table 24). The existence of more or less visible clogging did not seem to have a relevant effect on retardation, as R-values with clogging (E3) ranged from 1.25 to 1.76 and were only slightly less with only partial clogging (E2: from 1.0 to 1.95). The retardation coefficients lie in the same range as those described previously for sandy material (Miller, 2000: R = 1.07; Grützmacher et al., 2002: R = 1.23).

Table 24: Summary of retardation coefficients and degradation rates obtained by modeling.

Depth segment of enclosure	Retardation		Degradation [h-1]	
	Experiment E2 (no clogging visible)	Experiment E3 (visible clogging)	Experiment E2 (no clogging visible)	Experiment E3 (visible clogging)
water reservoir to 20 cm	1.97	1.76	0.74	0.54
20 cm to 40 cm	1.90	1.25	0.24	0.31
40 cm to 60 cm	1.00	1.36	0.75	0.19
60 cm to 80 cm	1.00	1.14	0.54	0.01
80 cm to effluent	1.58	1.30	0.07	0.07

For elimination of MCYST over the depth profile of the enclosures, (Table 24) the following statements summarize key results:

- For all experiments highest retardations and degradation rates are observed in the upper 20 cm.

- Retardation coefficients and degradation rates show a tendency to decline along the flow paths.

- Most peculiar is the flow path between 20 and 40 cm, with either a reduced degradation (E2), or reduced retardation (E3); a possible explanation is variable water saturation, which could occur in that horizon, as the applied negative pressure reaches a maximum near to the top of the filter bed.

- Also the last depth segment (80 cm to effluent) shows some peculiarities, which may be explicable by column-end-effects as the final part of the flow path is located in a gravel layer and the measurements were made in the outlet tube.

The portions of MCYST recovered in the effluent ranged from 2.7 % to 10 % (elimination rates 90 % to 97.3 %) and the development of MCYST amounts in the different sampling ports showed a distinct difference between experiments E2/E3 on the one hand and E4/E5 on the other hand (Figure 89) even though the uppermost layer ("schmutzdecke") had been removed prior to experiments E2 and E5. The following differences can be determined between these two sets of experiments:

- different enclosures with different pretreatment:

    o E2/E3 were conducted in enclosure III (4 sampling ports, continuous operation since July 2003, four weeks prior to first experiment),

    o E4/E5 in enclosure II (2 sampling ports, continuous operation since November 2003, four days prior to first experiment),

- different temperature ranges:

    o E2/E3 were carried out in August and September with temperatures between 16.4°C and 31.6 °C,

    o E4/E5 were carried out in November with temperatures between 0.6°C and 11.2 °C.
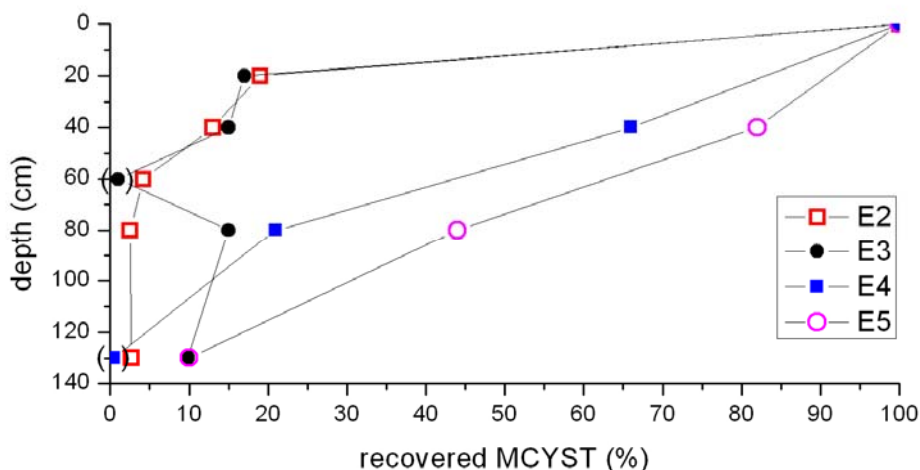
Figure 89: Recovered portions of MCYST during aerobic enclosure experiments E2 through E5.

These results support the hypothesis that the existence of a visible, superficial clogging layer or "schmutzdecke", is not of decisive importance concerning biodegradation of MCYST. Temperature as well as pretreatment of the filter as a whole (conditioning or maturation) play a much more important role. This is supported by Ellis (1975) who states that the "schmutzdecke" or organic filter adds substantially to the effectiveness of the straining process. Biological activity, however, is observed up to a depth of 40 cm or more.

Further experiments concerning temperature effects on MCYST degradation carried out in the laboratory (see final report working group algae, part VII) confirm this finding.

Figure 90 shows that the recovered amounts of MCYST in the anaerobic experiment, that was conducted in September 2004 after continuous operation for 4 months, are only slightly higher than in aerobic experiments carried out in the same enclosure, E4 and E5 (however without preconditioning and under lower temperatures). Experiments E2 and E3 that were conducted at similar temperatures and on a well preconditioned filter yielded distinctively lower recoveries (compare Figure 89). This leads to the assumption that there is MCYST degradation under anaerobic conditions and the degradation rates are comparable to those obtained under unfavorable, aerobic conditions (no preconditioning, low temperatures). This is in agreement with laboratory experiments carried out by Holst et al. (2003) that had shown that MCYST degradation was possible under anoxic conditions and could be accelerated by addition of nitrate and glucose. As true for aerobic conditions, there are, however, reported cases in which MCYST degradation is not detectable (Holst et al., 2003, Miller, 2000). The reasons for this will be discussed further on.
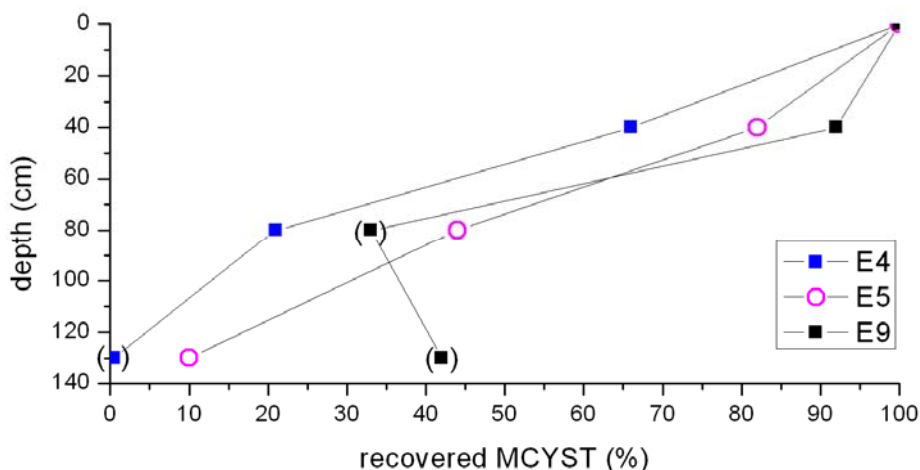
Figure 90: Recovered portions of MCYST during anaerobic (E9) and aerobic enclosure experiments (E4 and E5).

Continuous application of MCYST yielded a reduction of recovered portions (100 % minus eliminated portion) in the effluent ranging from 52 % during the first phase of constant experimental conditions (2 to 4 days), to 14 % during the second phase (day 8 to 15).

Compared to the experiments with pulsed application the recovered amounts during the first phase seem unusually high. Enclosure I, in which the experiment was carried out, had been in operation for 7 months before the beginning of the experiment. Therefore incomplete preconditioning, as for experiments E4 and E5, can be ruled out as a cause. Temperatures were also in the same range as during the experiments with pulsed application. Higher recoveries / lower elimination might explained by different elimination processes dominating only during short term, pulsed application and are less relevant for continuous application (e.g. irreversible sorption). In contrast, higher elimination rates / lower recoveries in the further course of the continuous dosing experiment (phase 2 and phase 3) would be compensated by the further adaptation of microbiology, leading to elimination rates around 90 % at the end of the experiment. These rates are in agreement with many previous publications with clearly higher contact times (e.g. Gützmacher et al., 2002, Lahti et al., 1997, Lahti et al., 1998).

In experiment E12 with continuous dosing of cyanobacteria a realistic scenario with cell-bound MCYST (7.4 µg/L by ELISA and 9 µg/L by HPLC) was simulated. In spite of low temperatures (clearly < 10°C) no MCYST could be detected in the effluent. The total amount of cell-bound MCYST during the dosing phase was 15.2 mg (ELISA) or 18 mg (HPLC), the total biovolume applied was 17 cm³. Four days after dosing has ceased, the biovolume in the uppermost 2 cm of sediment had not shown a relevant reduction. The concentrations of total MCYST in the porewater had, however, decreased to 22 % of the maximum concentration at the end of the dosing phase (this being the worst case, as degradation during the dosing

phase itself was not taken into account). 10 days after dosing was terminated no more MCYST was detectable in the porewater, biovolume, however, still amounted to 48 % of the maximum value.

These results show that even at low temperatures MCYST, though primarily cell-bound, is degraded by far more readily than the cells of the cyanobacteria themselves, indicating a) that MCYST may be released from the intact cells (thus being available for rapid extra-cellular degradation) and / or b) degradation may also take place within the cyanobacterial cells (there have been no reported indications for this so far, though senescent cells under poor growth conditions have not been studied).

Although no worst-case scenario was simulated (maximum biovolumes of cyanobacteria may reach values 10-fold higher than the ones generated in the water reservoir), it can be concluded that although accumulation of cyanobacterial cells on the sediment surface may take place, MCYST accumulation is unlikely to occur in the same manner, probably due to rates of degradation being more rapid than rates of MCYST release from the cells, even in a population under detrimental growth conditions, i.e. dark and cold.

There have been, however, indications that in some cases MCYST degradation rates are not sufficient for complete elimination of toxin being released from cyanobacterial cells during sand filtration (e.g. Grützmacher et al., 2002). This is probably due to conditions unfavorable for toxin biodegradation (low temperatures) while in other cases cyanobacterial cells were transported through coarsely grained material (e.g. Bricelj & Sedmak, 2001) thus protecting the mainly cell-bound MCYST from biodegradation. Furthermore our experiment did not totally simulate the situation of a senescent population at the very end of the growing season, as the cells used were derived from very good growth conditions in our large-scale culture.

Other investigations on interactions between cell-bound and extracellular MCYST are limited to observations in lake water without sediment contact. While experiments conducted by Kirivanta et al. (1991) yielded low degradability of MCYST-LR released by lysed cells in contact with river water (initially the batch culteres were run axenic), many other experiments (e.g. Jones et al., 1994, Christoffersen et al., 2002) showed very rapid degradation of initially already extracellular MCYST.

In summary, the enclosure experiments confirmed the importance of biodegradation for MCYST elimination in sandy material and yielded generally high degradation rates (0.01 h-1 to 0.75 h-1) under optimal conditions. Optimal conditions can be defined as the following:

- Previous conditioning of the filter for more than 4 days, better for several weeks,
- aerobic conditions,
- moderate temperatures (> 10 °C).

Lower degradation rates can be due to the following circumstances:

- Previous flushing of the filter for less than 4 days,
- low temperatures (< 10 °C),
- anoxic conditions.

142

Continuous application of dissolved MCYST can lead to an increase in elimination rates, although under optimal conditions this is not necessary for nearly complete elimination within less than 1 day. Under suboptimal conditions this may be a method to achieve better elimination.

MCYST is unlikely to accumulate on the surface of a filter or sediment in the same way as cyanobacterial cells do, due to rapid degradation, probably more rapid than release.

9.5 References

Bricelj, M. & Sedmak, B. (2001): Transport of biologically active substances through gravel strata. - in: Seiler & Wohnlich (eds.): New Approaches Characterizing Groundwater Flow, p. 25 - 29, Swets & Zeitlinger Lisse.

Christoffersen K., Lyck S. & Winding A. (2002): Microbial activity and bacterial community structure during degradation of microcystins., Aq. Microb. Ecology, 27: 125 – 136.

Ellis K.V. (1985): Slow sand filtration., CRC Critical Reviews in Environmental Control, 15 (4): 315 – 354.

Grombach, P., Haberer, K., Merkl, G., & Trueb, E.U. (2000): Handbuch der Wasserversorgungstechnik. Oldenbourg Verlag, München. 3. Auflage.

Grützmacher, G., Wessel., G., Chorus, I. & Bartel, H. (2004): Strategien zur Vermeidung des Vorkommens ausgewählter Algen- und Cyanobakterienmetabolite im Rohwasser, Teilprojekt: Wirksamkeit der Infiltration / Bodenpassage für die Retention von Algen- und Cyanobakterienmetaboliten. – Abschlussbericht des BMBF-Forschungsvorhabens, Förderkennzeichen: 02 WT9852/7.

Grützmacher, G., G. Böttcher, I. Chorus & H. Bartel (2002): Removal of microcystins by slow sand filtration. Environm. Tox. , 17: 386 – 394, John Wiley & Sons.Holst et al. 2003.

Holst, T., Jørgensen, N.O.G., Jørgensen, C. & Johansen, A. (2003): Degradation of microcystin in sediments at oxic and anoxic, denitrifying conditions. - Wat. Res. 37: 4748 - 4760.

Holzbecher E., Inversion of temperature time series from near-surface porous sediments, Journal of Geophysics and Engineering, Vol. 2, 343-348, 2005.

Holzbecher E., Dizer H., Grützmacher G., Lopez-Pila J., Nützmann G., The influence of degradation and sorption within biogeochemical cycles, submitted to: Environmental Engineering Science, 2005.

Jones G.J., Bourne D.G., Blakeley L. & Doelle H. (1994): Degradation of cyanobacterial hepatotoxin microcystin by aquatic bacteria., Natural Toxins, 2: 228-235

Lahti K., Rapala J., Färdig M., Niemelä M., Sivonen K. (1997): Persistence of cyanobacterial hepatotoxin, microcystin-LR, in particulate material and dissolved in lake water, Wat. Res., 31 (5): 1005 – 1012.

Lahti K., Vaitomaa J., Kivimäki A.L., Sivonen K. (1998): Fate of cyanobacterial hepatotoxins in artificial recharge of groundwater and in bank filtration, Artificial Recharge of Groundwater, Peters et al. (eds.) Balkema, Rotterdam.

Massmann, G., Taute, T. , Bartels, A. & Ohm, B. (2004): Characteristics of sediments used for batch-, enclosure- and column-studies. Internal Report, FU Berlin.

MATLAB® Version 6.5, Release 13 (2002). The MathWorks, Inc., 3 Apple Hill Drive, Natrick, MA 01760-2098, USA.

Miller M.J. (2000): Investigation of the removal of cyanobacterial hepatotoxins from water by river bank filtration . PhD Thesis, Flinders University.

Nützmann G., Holzbecher E., Strahl G., Wiese B., Licht E., Knappe A., Visual CXTFIT – a user-friendly simulation tool for modelling one-dimensional transport, sorption and degradation processes during bank filtration, Proceedings ISMAR 2005.

Schwarz, M. (2004): Mikrobielle Kolmation von abwasserdurchsickerten Bodenkörpern: Nucleinsäuren zum Nachweis von Biomasse und Bioaktivität. - Schriftenreihe des ISWW Karlsruhe: Band 116.

Toride N., Leij F.J., van Genuchten M. Th., The CXTFIT code for estimating transport parameters from laboratory or field tracer experiments, U.S. Salinity Lab., Agric. Res. Service, US Dep. of Agric., Research Report No. 137, Riverside (CA), 1995.

6

Using bacteriophages, indicator bacteria, and viral pathogens for assessing the health risk of drinking water obtained by bank filtration.

"bacteria"; Federal Environmental Agency of Germany (UBA)

Responsible Project leader: Dr. Juan Lopez-Pila, Dr. Regine Szewzyk

Content

Figure 44: Various cell morphologies in a four week old biofilm at site one as detected by DAPI staining. Scale bar in (A) equals 5µm and belongs to all images. (A) microcolony of small rod shaped bacteria attached to an alga body. (B) single rod shaped bacteria and

1 Bank filtration field sites

1.1 Introduction

Indicator bacteria and coliphages along the transects of Lake Tegel, Lake Wannsee and the artificial recharge pond Tegel

The indicator microorganims, E. coli, intestinal enterococci, and coliphages were analysed in water samples from both transects for bank filtration at the Lakes Tegel and Wannsee as well as from the artificial recharge pond of Tegel. Surface water samples of both lakes were examined from May 2002 to December 2004. In addition, samples were analysed from four shallow observation wells and three pumping sites for drinking water supply along the transect Wannsee, as well as four deep and seven shallow observation wells and 2-3 pumping sites along the transect of Lake Tegel. Sampling at the artificial recharge pond of Tegel was carried out during four field surveys (August 2002-December 2002) in two shallow, three deep wells and one pumping well for drinking water supply. In addition, the microbial flora was studied in the sand filter of the recharge pond in Tegel.

1.2 Results

1.2.1 Bank filtration field site Lake Tegel

1.2.1.1 Surface water

During the field surveys from May 2002 to December 2004, lake water samples were taken in monthly intervals and investigated for the indicator bacteria E. coli, intestinal enterococci and somatic coliphages. The concentration of indicator bacteria in lake water samples was very low and ranged from below detection limit (<1/100ml) to about 100 cfu/100 ml. Coliphages were detected in concentrations of 1 to 160 pfu/100 ml. No clear seasonal pattern of the concentration of indicator organisms was observed (Figure 1).

Lake Tegel receives faecally contaminated water from two sources: Canal Nordgraben discharging secondary effluent and Creek Tegel draining run off water from agricultural fields. These waters are, however, treated by a phosphate elimination plant (PEA Tegel) before entering the lake. The hygienic quality of the water was, therefore, higher than expected. The effect of this advanced treatment process (flocculation) on the reduction of indicator organisms was investigated during the sampling period from February to August 2004. Concentrations of E. coli, intestinal enterococci, and coliphages were determined in influent and effluent samples of the PEA Tegel (see Table 1).
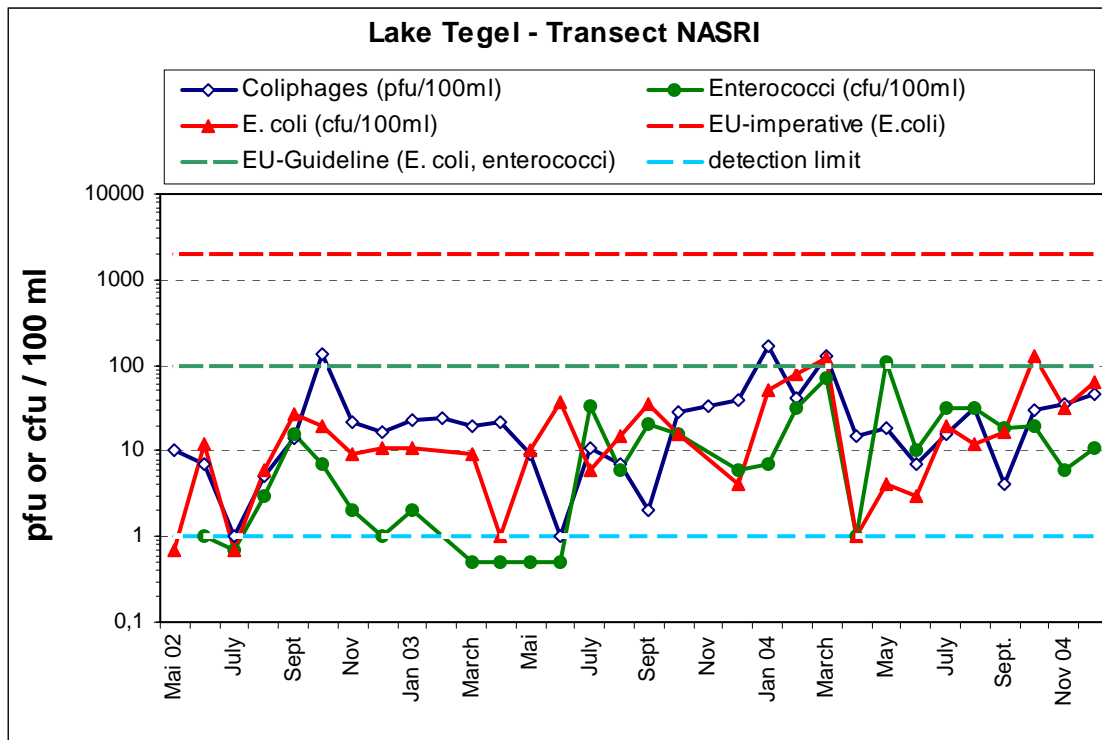
Figure 1 Occurrence of indicator organisms in surface water samples from Lake Tegel

Table 1 Reduction of indicator micro organisms in the PEA Tegel by flocking and rapid sand filtration. (* additional sampling at the same day)

Sampling	Coliphages (pfu/100ml)			E. coli (cfu/100ml)			Enterococci (cfu/100 ml)		
	influent	effluent	Reduction	influent	effluent	Reduction	influent	effluent	Reduction
Jan. 04	1653	232	0,86	1000	150	0,85	175	24	0,86
Jan. 04*	1511	209	0,86	1200	97	0,92	312	10	0,97
Feb. 04	2800	999	0,64	12483	725	0,94	1689	78	0,95
March 04	1032	51	0,95	500	120	0,76	273	72	0,74
April 04	1310	560	0,57	100	50	0,50	49	10	0,80
May 04	3100	100	0,97	3552	122	0,97	42	1	0,98
June 04	1170	172	0,85	438	22	0,95	42	1	0,98
Aug 04	1040	90	0,91	-	-	-	-	-	-
mean	-	-	0,82 + 0,13	-	-	0,84 + 0,15	-	-	0,9 + 0,09

Reduction of all test organisms was on average about one log unit. The reduction rates variied between 57 % and 97 % for somatic coliphages, 50 % and 97 % for E. coli, 74% and 98% for intestinal enterococci. Despite these relatively low elimination rates, the PEA Tegel contributes substantially to the reduction of indicator organisms and probably also of hygienically relevant microorganisms in the Lake Tegel.

1.2.1.2 Transects

1.2.1.2.1 Investigation on the transect of Lake Tegel in the year 2002

Water samples were taken from the deep observation wells (3301, 3302, 3303 and 3304) using a MP1-pumping module and accessories with a flow capacity of 200 L/min and directly from the faucets of 2 or 3 pumping wells for the regular drinking water supply (12, 13 and 14). The MP1-pumping module was not disinfectable and was used for all sampling points. Sampling of the shallow wells along the transect Tegel was started on August 2002 also using non sterile MP1 or Eijkelkamp pumping module. Sterilized Eijkelkamp pumps and equipments were used for each of the seven shallow observation wells during the last four field surveys (September-December 2002).

Apart from one positive sample from the deep observation well 3302, somatic coliphages were never detected in samples from deep wells (Table 2A). Samples from the shallow observation wells were also negative for coliphages (Table 2B). Only one sample from the first well (3311) located on the lake basin contained coliphages at a low concentration of 2 pfu/100 ml.

Table 2 Occurrence of somatic coliphages (pfu/100ml) in water samples from the transect of Lake Tegel (detection limit: 1 pfu/100ml)

A: deep observation wells and pumping wells

Sampling time	Lake Tegel	3301	3302	3303	3304	Well 12	Well 13	Well 14
16.05.02	10	<1	<1	<1	<1	<1	n.a.	<1
11.06.02	7	<1	<1	<1	<1	<1	n.a.	<1
09.07.02	1	<1	<1	<1	<1	<1	n.a.	<1
21.08.02	5	<1	<1	<1	<1	<1	n.a.	<1
23.09.02	14	<1	<1	<1	<1	<1	n.a.	<1
22.10.02	44	<1	1	<1	<1	<1	n.a.	<1
28.11.02	22	<1	<1	<1	<1	<1	<1	<1
19.12.02	15	<1	<1	<1	<1	<1	<1	<1

B: shallow observation wells

Sampling time	Lake Tegel	3311	3310	3309	3308	3307	3306	3305
22.08.02**	5	<1	<1	<1	<1	<1	<1	<1
23.09.02***	2	<1	<1	<1	<1	<1	<1	<1
22.10.02***	44	<1	<1	<1	<1	<1	<1	<1
27.11.02***	18	<1	*	<1	<1	<1	<1	n.a.
17.12.02***	17	<1	*	<1	<1	<1	<1	n.a.
28.01.03***	23	2	<1	<1	<1	<1	<1	<1

* no sample, ** sampling with non sterile instruments, *** sampling with sterilized instruments
n.a. = not analysed

Apart from one sample from well 3301, non of the water samples from deep wells contained intestinal enterococci (Table 3A).

All water samples were free from intestinal enterococci in 100 ml with the exception of the field survey on October 2002. During this survey intestinal enterococci were detected in 6 out of 7 water samples from the shallow wells in concentrations of 3 - 108 cfu/100ml (source of contamination unknown).

Table 3 Occurrence of intestinal enterococci (cfu/100ml) in water samples from the transect of Lake Tegel (detection limit: 1 cfu/100ml)

A: deep observation wells and pumping wells

Sampling time	Lake Tegel	3301	3302	3303	3304	Well 12	Well 13	Well 14
16.05.02	3	1	<1	<1	*	<1	n.a.	<1
11.06.02	1	<1	<1	<1	<1	<1	n.a.	<1
09.07.02	<1	<1	<1	<1	<1	<1	n.a.	<1
21.08.02	2	<1	<1	<1	<1	<1	n.a.	<1
23.09.02	6	<1	<1	<1	<1	<1	n.a.	<1
22.10.02	7	<1	<1	<1	<1	<1	n.a.	<1
28.11.02	2	<1	<1	<1	<1	<1	<1	<1
19.12.02	<1	<1	<1	<1	<1	<1	<1	<1

B: shallow observation wells

Sampling time	Lake Tegel	3311	3310	3309	3308	3307	3306	3305
22.08.02**	3	<1	<1	<1	<1	<1	<1	<1
23.09.02***	16	<1	<1	<1	<1	<1	<1	*
22.10.02***	6	22	3	108	14	<1	26	31
27.11.02***	1	<1	*	<1	<1	<1	<1	*
17.12.02***	1	<1	*	<1	<1	<1	<1	*
28.01.03***	2	<1	<1	<1	<1	<1	<1	*

* no sample, ** sampling with non sterile instruments, *** sampling with sterilized instruments
n.a. = not analysed

E. coli was not detected in water samples from deep wells during the field surveys in May and December. During all other surveys E. coli was detected in one or several samples in concentrations between 2 cfu/100 ml and 6 cfu/10 ml. In total 2 samples from the pumping sites 12 and 14 were also positive for E. coli (

Table 4a).

Table 4 Occurrence of E. coli (cfu/100ml) in water samples from the transect of Lake Tegel (detection limit: 1 cfu/100ml)

A: deep observation wells and pumping wells

Sampling time	Lake Tegel	3301	3302	3303	3304	Well 12	Well 13	Well 14
16.05.02	<1	<1	<1	<1	*	<1	n.a.	<1
11.06.02	12	<1	<1	<1	1	<1	n.a.	<1
09.07.02	<1	2	2	<1	<1	6	n.a.	<1
21.08.02	3	6	<1	<1	2	<1	n.a.	<1
23.09.02	5	9	<1	<1	<1	<1	n.a.	3
22.10.02	8	6	5	1	<1	<1	n.a.	<1
28.11.02	<1	<1	<1	1	<1	<1	<1	<1
19.12.02	5	<1	<1	<1	<1	<1	<1	<1

B: shallow observation wells

Sampling time	Lake Tegel	3311	3310	3309	3308	3307	3306	3305
22.08.02**	6	27	35	<1	<1	<1	<1	30
23.09.02***	27	<1	<1	<1	<1	<1	<1	n.a.
22.10.02***	10	<1	<1	<1	<1	<1	<1	<1
27.11.02***	9	<1	*	<1	<1	<1	<1	n.a.
17.12.02***	11	<1	*	<1	<1	<1	<1	n.a.
28.01.03***	15	<1	<1	<1	<1	<1	<1	<1

* no sample, ** sampling with non sterile instruments, *** sampling with sterilized instruments

n.a. = not analysed, italic = in 10 ml of sample

During the field survey August 2002, samples from the shallow observation wells were taken using a non sterile Eijkelkamp pump and non sterile tubing at all sampling sites. High densities of E. coli were found in samples from the wells 3311 and 3310 located on the lake basin, as wells as in the sample of the last well (3305) of the transect (Table 4B). E. coli was not detected during all other surveys in September 2002 to January 2003 when sterile equipment was used.

Data on the occurrence of heterotrophic plate count bacteria (according to the German Drinking water Directive; colony counts according to DIN EN ISO 6022 were slightly higher) in water samples from deep wells are shown in Table 5. No retention pattern can be deducted from the data received from the samples of the deep observation wells. Colony counts at 20 °C as well as at 37 °C varied from < 10 cfu/ml to > 103 cfu/ml, indicating external contamination by the non disinfected sampling equipment. At the regularly pumping sites of Water Work Tegel, colony counts were usually less than 100 cfu/ml. High concentrations of up to 500 cfu/ml were detected in three samples.

Table 5: Occurrence of heterotrophic plate count bacteria (cfu/ml) in water samples from deep wells and pumping wells along the transect of Lake Tegel (detection limit: 1 cfu/ml) * no sample

A. incubation at 20 °C

Sampling	Lake Tegel	3301	3302	3303	3304	well 12	well 13	well 14
16.05.02	690	160	20	30	n.a.	3	*	1
11.06.02	200	30	50	8	20	<1	*	1
09.07.02	530	360	60	70	160	60	*	30
22.08.02	1370	120	40	30	50	1	*	<1
23.09.02	20	6	90	7	90	1	*	1
22.10.02	2300	650	1300	60	150	210	*	20
27.11.02	820	40	60	6900	10	<1	<1	9
17.12.02	250	170	6	100	40	<1	3	2

B. incubation at 37 °C

Sampling	Lake Tegel	3301	3302	3303	3304	well 12	well 13	well 14
16.05.02	241	9	5	5	n.a.	<1	*	<1
11.06.02	200	1100	590	490	300	1	*	2
09.07.02	300	650	260	360	150	170	*	530
22.08.02	230	310	160	6	240	1	*	<1
23.09.02	21	300	230	10	50	1	*	<1
22.10.02	1800	1060	820	120	200	<1	*	10
27.11.02	130	20	10	2000	10	1	1	1
19.12.02	130	30	1	100	20	2	1	<1

In water samples from the shallow wells, colony counts were lower than in the deep observation wells and ranged from below detection limit to 320 cfu/ml (Table 6). With exception of samples on August 2002, all these samples were taken by disinfected pumps and silicon tubing. These findings further support the possible contamination of the deep wells during sampling.

Table 6 Occurrence of heterotrophic plate count bacteria in water samples from the shallow wells along the transect of Lake Tegel (detection limit: 1 cfu/ml), n.a: not analysed]

Sampling	Lake Tegel	3311	3310	3309	3308	3307	3306	3305
22.08.02 (20°C)	580	60	80	40	4	8	30	80
(37°C)	310	80	100	20	2	3	3	30
23.09.02 (20°C)	150	30	30	9	4	5	2	n.a.
(37°C)	70	40	30	8	<1	<1	20	n.a.
22.10.02 (20°C)	250	20	20	60	8	40	320	50
(37°C)	160	20	20	30	4	20	140	5
27.11.2002 (20°C)	1100	10	n.a.	5	10	10	80	n.a.
(37°C)	130	10	n.a.	5	1	10	30	n.a.
17.12.2002 (20°C)	20	5	n.a.	9	10	20	20	n.a.
(37°C)	30	2	n.a.	9	20	20	20	n.a.

1.2.1.2.2 Investigation on the transect of Lake Tegel in the years 2003-2004

No further investigations were performed at the transect of Lake Tegel because of the low initial concentrations of indicator microorganisms in the lake water. These low concentrations did not allow to deduct retention characteristics of the organisms during subsurface passage along the transect. Investigations were continued at the transect of Lake Wannsee awaiting new shallow wells to be build near the lake shore (see below).

1.2.2 Bank filtration field site Lake Wannsee

1.2.2.1 Surface water

Data on the occurrence of indicator bacteria and coliphages in surface water of Lake Wannsee taken monthly from May 2002 up to December 2004 are shown in the Fig. 2.
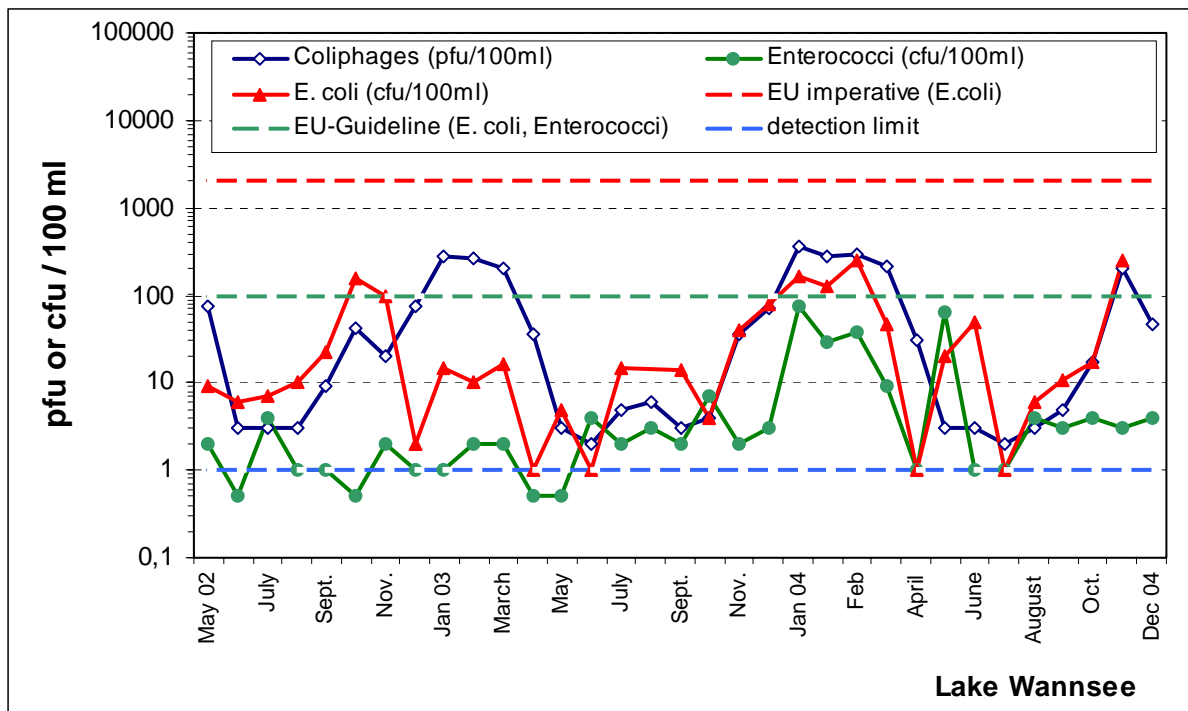
Figure 2 Occurrence of indicator organisms in surface water samples from Lake Wannsee

Concentrations of coliphages varied between 2 and 360 pfu/100 ml. Concentrations of indicator bacteria ranged from detection limit up to 38 cfu/100 ml for intestinal enterococci, and up to 250 cfu/100 ml for E. coli, respectively. A seasonal concentration pattern was observed with low concentrations in summer and higher concentrations in winter. Concentrations of intestinal enterococci were always below the guideline values of the EU bathing water Directive (Figure 2). Concentrations of E. coli were in some samples above the guideline value (100 cfu/100ml) but never reached the imperative value (2000 cfu/100ml).

On 17.3.2004 water samples were collected at 15 different sampling sites closed to the transect area to investigate the spatial variation in the concentration of indicator microorganisms . At one station (FU 9) samples were additionally taken from different depth down to 7 m (0, 2, 4, 6 and 7m).

High concentrations of coliphages (850 pfu/100ml), E. coli (50 mpn/100ml) and intestinal enterococci (32 mpn/100ml) were detected in the sample of station FU5 close to the Griebnitz Sea where water of the Teltow canal - contaminated with secondary effluent - is discharged into Lake Wannsee. Concentrations decreased with increasing distance to sampling site FU5 (see table 7, values above and below FU5) and were lowest at the sampling sites on the transects of Wannsee (Table 7).

Concentrations of coliphages at different depths of the lake were in the same order of magnitude ranging from 100 to 180 pfu/100ml. E. coli and intestinal enterococci were only sporadically detected at all sampling depths.

Table 7 Concentration of indicator organisms in Lake Wannsee at different sampling sites close to the transect area.

Sampling sites	Coliphages (pfu/100ml)	Enterococci (cfu/100ml)	E. coli (cfu/100ml)
FU10	70	1	0,1
FU11	80	<1	1
FU9 (0m)	100	<1	<1
FU9 (2m)	140	<1	<1
FU9 (4m)	100	<1	2
FU9 (6m)	150	<1	1
FU9 (7m)	180	1	3
FU8	110	<1	<1
FU7	220	3	2
FU6	240	<1	20
FU5	850	30	50
FU2	280	6	10
FU1	290	4	20
14	350	1	20
15	140	1	2
FU19	110	<1	<1
FU18	120	1	<1
18	70	<1	<1
19	70	<1	<1

1.2.2.2 Investigations on Transect 1 of Lake Wannsee in 2002.

Four shallow observation wells (3335, 3337, 3338 and 3339) and three pumping sites for drinking water supply (wells 3-5) along the transect Wannsee were sampled during the eight field surveys from March to December 2002. During the first four sampling dates, in May, June, July and August, the equipment of the Department of Hydrogeology in the Free University was used for sampling of the shallow observation wells. These samplings were carried out using one or two Eijkelkamp pumps connected in series and plastic tubing for all sampling sites. The flow capacity varied between 3-5 L/min depending on the depth of each sampling site. Sterilised Eijkelkamp pumps and silicon tubing were used for sampling the shallow wells in the last four sampling periods in September, October, November und December. Data on the occurrence of indicator microorganisms in water samples from the wells of transect Wannsee in the year 2002 are summarized in Table 8 - Somatic coliphages were sporadically detected in very low concentrations (1 and 4 pfu/100ml) in the first observation well (3339) located on the lake basin. All other samples located further along the filtration path were negative for coliphages (Table 8).

Table 8 Occurrence of somatic coliphages (pfu/100ml) in water samples from the transect of Lake Wannsee in the year 2002 (detection limit: 1 pfu/100ml)

Sampling time	Lake Wannsee	3339	3338	3337	3335	Well 3	Well 4	Well 5
15.05.2002*	75	4	<1	<1	<1	*	*	*
12.06.2002*	3	1	<1	<1	<1	<1	<1	<1
10.07.2002*	3	<1	<1	<1	<1	<1	<1	<1
21.08.2002*	3	*	<1	<1	<1	<1	<1	<1
25.09.2002**	9	<1	<1	<1	<1	<1	<1	<1
23.10.2002**	43	<1	<1	<1	<1	<1	<1	<1
26.11.2002**	20	*	<1	<1	<1	<1	<1	<1
18.12.2002**	73	<1	<1	<1	<1	<1	<1	<1

* sampling with a non sterilized pump, ** sampling with disinfected pumps

Intestinal enterococci were detected in two out of six samples from the first well 3339. No intestinal enterococci were detected in the other shallow sampling wells and regular pumping sites of the Water Work Beelitzhof (Table 9).

Table 9 Occurrence of intestinal enterococci (cfu/100ml) in water samples from the transect of Lake Wannsee in the year 2002 (detection limit: 1 cfu/100ml)

Sampling time	Lake Wannsee	3339	3338	3337	3335	Well 3	Well 4	Well 5
15.05.2002*	2	<1	<1	<1	<1	*	*	*
12.06.2002*	<1	<1	<1	<1	<1	<1	<1	<1
10.07.2002*	4	<1	<1	<1	<1	<1	<1	<1
21.08.2002*	1	*	<1	<1	<1	<1	<1	<1
25.09.2002**	1	1	<1	<1	<1	<1	<1	<1
23.10.2002**	<1	3	<1	<1	<1	<1	<1	<1
26.11.2002**	2	*	<1	<1	<1	<1	<1	<1
18.12.2002**	1	<1	<1	<1	<1	<1	<1	<1

* sampling with a non sterilized pump, ** sampling with disinfected pumps

In contrast to enterococci and coliphages, E. coli was detected in most samples (4) from wells 3339 and 3337. The detection frequency declined to 3 out of 8 samples in the second well on the sea basin (3338) or on the shore (3335), respectively. During the field survey in October 2002, E. coli was found in all shallow wells (Table 10). Only two out of 21 samples from the pumping sites (wells 3, 4, 5) contained E. coli. Using sterilized pumps and tubing had no effect on the detection frequency of E. coli in the shallow wells. Data on the occurrence of heterotrophic plate count bacteria (according to the German Drinking water Directive; colony counts according to DIN EN ISO 6022 were slightly higher) are summarized in Table 11.

Table 10 Occurrence of E. coli (cfu/100ml) in water samples from the transect of Lake Wannsee in the year 2002 (detection limit: 1 cfu/100ml)

Sampling time	Lake Wannsee	3339	3338	3337	3335	Well 3	Well 4	Well 5
15.05.2002*	9	5	<1	<1	<1	*	*	*
12.06.2002*	6	1	1	10	<1	<1	<1	5
10.07.2002*	7	<1	<1	<1	<1	<1	<1	<1
21.08.2002*	10	*	<1	<1	5	<1	<1	<1
25.09.2002**	22	2	<1	3	7	<1	<1	<1
23.10.2002**	160	2	2	33	11	1	<1	<1
26.11.2002**	100	*	3	<1	<1	<1	<1	<1
18.12.2002**	2	<1	<1	5	<1	<1	<1	<1

* sampling with a non sterilized pump, ** sampling with disinfected pumps

Non sterilized pump and tubing were used for sampling during the first four field surveys and sterilized equipment during the last four surveys. Colony counts in water samples from the shallow wells were usually low (< 100 cfu/ml) but single high concentrations were found especially during the first surveys when non sterilized equipment was used.

Table 11: Occurrence of heterotrophic plate count bacteria (cfu/ml) in water samples from the shallow wells and pumping sites (wells 3,4 and 5) of the Water Work Beelitzhof (detection limit: 1 cfu/ml)

A. incubation temperature 20°C

Sampling sites	Lake Wannsee	3339	3338	3337	3335	well 3	well 4	well 5
15.05.02*	220	50	7	12	6	n.a.	n.a.	n.a.
12.06.02*	80	40	9	500	50	320	60	200
10.07.02*	320	40	50	180	2400	<1	<1	120
21.08.02*	2040	n.a.	10	10	100	1	1	10
25.09.02**	100	50	70	110	110	2	<1	<1
23.10.02**	400	20	10	10	4	1	3	4
26.11.02**	60	n.a.	10	10	10	<1	<1	<1
18.12.02**	20	30	3	40	5	<1	<1	<1

B. Incubation temperature 37°C

Sampling sites	Lake Wannsee	3339	3338	3337	3335	well 3	well 4	well 5
15.05.02*	130	30	6	10	110	n.a.	n.a.	n.a.
12.06.02*	70	20	60	250	220	310	170	300
10.07.02*	200	130	180	270	3800	<1	17	230
21.08.02*	2300	*	10	10	100	1	1	10
25.09.02**	100	40	4	90	20	<1	<1	<1
23.10.02**	140	20	1300	240	20	<1	<1	1
26.11.02**	20	*	30	40	50	<1	<1	<1
18.12.02**	40	20	10	10	20	<1	<1	<1

* sampling with a non sterilized pump, ** sampling with disinfected pump

1.2.2.2.1 Investigations on transect 1 of Lake Wannsee in 2003-2004:

In the year 2003, water samples from transect 1 were taken monthly using sterilised pumps and silicon tubes separately for each station. Sampling concentrated on the shallow and less distant wells because no coliphages had been found after long filtration paths during the previous sampling period. A new observation well -well 201OP- was established additionally.

The observation wells 3337 and the new observation well 201OP were sampled at all sampling surveys. Sampling well 3339 was flooded with lake water and, therefore, not sampled. During some sampling times the shallow observation well 3338 was dry. Sampling at the observation well 3335 was carried out only four times during the intensive sampling period from 15.9.03 to 15.10.03 (data not shown).

Along transect 1 of Lake Wannsee (3338, 3337, 201OP, and well 4), no coliphages were detected in any of the samples (Table 12).

Table 12 Occurrence of somatic coliphages (pfu/100 ml) in water samples at different sampling sites along transect 1 of Lake Wannsee (detection limit: 1/ 100 ml), * no sample, n.a.: not analysed

Sampling time	Lake Wannsee	3338	3337	201OP	Well 4
20.02.2003	267	*	*	<1	n.a.
18.03.2003	290	<1	<1	<1	<1
08.04.2003	40	<1	<1	<1	<1
20.05.2003	3	<1	<1	<1	<1
17.06.2003	1	<1	<1	<1	<1
03.07.2003	5	<1	<1	<1	<1
19.08.2003	6	<1	<1	<1	<1
22.09.2003	2	*	<1	<1	<1
29.09.2003	2	<1	<1	<1	<1
06.10.2003	4	<1	<1	<1	<1
13.10.2003	6	*	<1	<1	<1
21.10.2003	36	*	<1	<1	<1
18.11.2003	n.a.	n.a.	n.a.	n.a.	n.a.
09.12.2003	71	*	<1	<1	<1
20.01.2004	362	<1	<1	<1	<1
17.02.2004	297	<1	<1	<1	<1
16.03.2004	157	<1	<1	<1	<1
20.04.2004	32	<1	<1	<1	<1
positive samples	17 / 17	0 / 12	0 / 16	0 / 17	0 / 16

As in 2002, intestinal enterococci were sporadically detected in water samples of transect 1 (Table 13). Four out of 12 samples contained intestinal enterococci in well 3338 located on the sea basin. The second well 3337 of transect 1 contained enterococci only in one out of 16 samples. No enterococci were detected in well 201OP and pumping station 4 of the Water Work.

E. coli was again detected more frequently than enterococci and coliphages. Three to four out of 12, 15 or 17 samples from wells 3338, 3337 and 201OP were positive, respectively (Table 14). E. coli was also detected in two samples from pumping well 4 in very low concentrations (1 cfu/100ml).

Table 13: Occurrence of intestinal enterococci (cfu/100 ml) in water samples at different sampling sites along the transect 1 of the Lake Wannsee

(detection limit <1 in 100 ml) * no sample, n.a.: not analysed

Sampling time	Lake Wannsee	3338	3337	201OP	Well 4
20.02.2003	2	*	*	<1	n.a
18.03.2003	1	<1	<1	<1	<1
08.04.2003	<1	<1	1	<1	<1
20.05.2003	<1	<1	<1	<1	<1
17.06.2003	<1	<1	<1	<1	<1
03.07.2003	<1	3	<1	<1	<1
19.08.2003	3	<1	<1	<1	<1
22.09.2003	20	*	<1	<1	<1
29.09.2003	34	<1	<1	<1	<1
06.10.2003	7	6	<1	<1	<1
13.10.2003	<1	*	<1	<1	<1
21.10.2003	1	*	<1	<1	<1
18.11.2003	n.a.	n.a.	n.a.	n.a.	n.a.
09.12.2003	3	*	<1	<1	<1
20.01.2004	29	1	<1	<1	<1
17.02.2004	38	1	<1	<1	<1
16.03.2004	<1	<1	<1	<1	<1
20.04.2004	<1	<1	<1	<1	<1
positive samples	10 / 17	4 / 12	1 / 16	0 / 17	0 / 15

Table 14 Occurrence of E. coli (cfu/100 ml) in water samples at different sampling sites along transect 1 of Lake Wannsee (detection limit: 1 cfu/100ml) *: no sample, n.a.: not analysed, >> invalid results]

Sampling time	Lake Wannsee	3338	3337	201OP	Well 4
20.02.2003	10	*	*	6	n.a.
18.03.2003	16	1	<1	<1	<1
08.04.2003	4	3	1	<1	<1
20.05.2003	5	<1	<1	<1	<1
17.06.2003	<1	<1	>>	<1	1
03.07.2003	15	<1	<1	<1	<1
19.08.2003	>>	1	<1	<1	<1
22.09.2003	19	*	<1	1	<1
29.09.2003	>>	<1	<1	<1	n.a.
06.10.2003	4	<1	8	<1	n.a.
13.10.2003	8	*	<1	<1	1
21.10.2003	8	*	1	<1	<1
18.11.2003	n.a.	n.a.	n.a.	n.a.	n.a.
09.12.2003	150	*	4	5	<1
20.01.2004	129	<1	<1	<1	<1
17.02.2004	250	<3	<3	<1	<1
16.03.2004	<3	<1	<1	<1	<1
20.04.2004	<1	<1	<1	<1	<1
positive samples	13 / 15	3 / 12	4 / 14	3 / 17	2 / 14

1.2.2.2.2 Investigations on transect 2 of Lake Wannsee in 2003-2004:

Four multi level wells were build in 2002 close to the lake shore in order to allow for shorter filtrations paths to be studied: well 207OP (30 cm), well 207MP1 (60 cm), well 207MP2 (120 cm), and well 207UP (180 cm). The new wells were integrated in transect 2 leading to pumping well 3. Unfortunately, three of the new observation wells (207OP, 207MP1, 207MP2) did not work during the sampling period. Well 207MP2 was permanently dry. Wells 207OP and 207MP1 did have water, but the water column in the wells remained at a constant level in spite of continuous pumping for 30 min and more. Obviously, surface water directly penetrated into the wells without infiltration through the filter matrix. The concentrations of indicator microorganisms in these wells were in the same range as in the lake water (Table 15 to Table 17). Sampling of these wells was, therefore, stopped in April 2003. During six field surveys in winter months, the deepest multi level well 207UP (180 cm) had a water column of only 30 cm, which was pumped out in intervals only for microbiological investigations.

Somatic coliphages were detected in five out of six water samples from well 207UP in concentrations of up to 9 pfu/100 ml. Coliphages occurred sporadically in the wells 203, 205 (620 cm depth), 206 and 202OP. No coliphages were detected in samples from pumping well 3.

Table 15 Occurrence of somatic coliphages (pfu/100 ml) in water samples along transect 2 of Lake Wannsee (detection limit 1 pfu/ 100 ml)

* no sample, n.a.: not analysed

Sampling time	Lake Wannsee	205	206	207OP 30 cm	207MP1 60 cm	207UP 180 cm	202OP	203	well 3
23.01.2003	276	1	<1	210	246	9	<1	<1	n.a.
20.02.2003	267	<1	<1	*	*	*	4	1	n.a.
20.03.2003	199	<1	<1	319	260	1	<1	<1	<1
10.04.2003	36	<1	<1	23	4	2	<1	<1	<1
22.05.2003	3	<1	<1	*	*	*	<1	<1	<1
19.06.2003	2	<1	<1	*	*	*	<1	<1	<1
03.07.2003	2	<1	<1	*	*	*	<1	<1	<1
21.08.2003	6	<1	<1	*	*	*	<1	<1	<1
15.09.2003	6	<1	<1	*	*	*	<1	<1	<1
24.09.2003	3	<1	<1	*	*	*	<1	n.a.	<1
29.09.2003	4	<1	<1	*	*	*	<1	n.a.	<1
06.10.2003	4	<1	<1	*	*	*	<1	n.a.	<1
20.10.2003	47	<1	<1	*	*	*	<1	n.a.	<1
11.12.2003	168	<1	<1	*	*	*	<1	n.a.	<1
22.01.2004	276	3	<1	*	*	1	<1	n.a.	<1
19.02.2004	382	1	<1	*	*	2	<1	n.a.	<1
18.03.2004	270	<1	<1	*	*	<1	<1	n.a.	<1
22.04.2004	31	<1	<1	*	*	*	<1	n.a.	<1
positive samples	18 / 18	3 / 18	0 / 18	3 / 3	3 / 3	5 / 6	1 / 18	1 / 9	0 / 16

Concentrations of intestinal enterococci in the lake water were very low and intestinal enterococci were only sporadically detected in water samples from wells 205, 207UP and 202OP (Table 16). No enterococci were detected in samples of wells 203, 206 and pumping well 3.

Table 16: Occurrence of intestinal enterococci (cfu/100 ml) in water samples along transect 2 of Lake Wannsee (detection limit: 1 cfu/100 ml)
* no sample, n.a.: not analysed,

Sampling time	Lake Wannsee	205	206	207OP 30 cm	207MP1 60 cm	207UP 180 cm	202OP	203	well 3
23.01.2003	1	<1	<1	<1	<1	<1	<1	<1	n.a.
20.02.2003	2	<1	<1	*	*	*	<1	<1	n.a.
20.03.2003	2	<1	<1	<1	<1	<1	<1	<1	<1
10.04.2003	<1	<1	<1	n.a.	n.a.	n.a.	<1	<1	<1
22.05.2003	<1	<1	<1	*	*	*	<1	<1	<1
19.06.2003	4	<1	<1	*	*	*	<1	<1	<1
03.07.2003	2	<1	<1	*	*	*	1	n.a.	<1
21.08.2003	<1	<1	<1	*	*	*	<1	<1	<1
15.09.2003	<1	<1	<1	*	*	*	<1	<1	<1
24.09.2003	2	<1	n.a.	*	*	*	<1	n.a.	<1
29.09.2003	34	<1	<1	*	*	*	<1	n.a.	n.a.
06.10.2003	7	<1	<1	*	*	*	2	n.a.	n.a.
20.10.2003	2	<1	<1	*	*	*	<1	n.a.	<1
11.12.2003	2	<1	<1	*	*	*	<1	n.a.	<1
22.01.2004	74	<1	<1	*	*	*	1	n.a.	<1
19.02.2004	9	1	<1	*	*	9	<1	n.a.	<1
18.03.2004	<1	<1	<1	*	*	<1	<1	n.a.	<1
22.04.2004	<1	<1	<1	*	*	*	<1	n.a.	<1
positive samples	12 / 18	1 / 18	0 / 18	0 / 2	0 / 2	1 / 4	3 / 18	0 / 8	0 / 14

E. coli was found in higher concentrations in the lake water than intestinal enterococci and more frequently in the shallow observation wells of transect 2 (Table 17). Several samples from wells 205, 202OP and 203 contained E. coli at concentrations ranging from 1 to 50 cfu/100 ml. E. coli was not detected in samples from the lake basin site 206 and from pumping well 3.

Table 17: Occurrence of. E coli (cfu/100 ml) in water samples along transect 2 of Lake Wannsee (detection limit: 1 cfu/100 ml)
* no sample, n.a.: not analysed, >> invalid result

Sampling time	Wannsee	205	206	207OP 30 cm	207MP1 60 cm	207UP 180 cm	202OP	203	well 3
23.01.2003	4	<1	<1	<1	<1	<1	2	1	n.a.
20.02.2003	10	<1	<1	*	*	*	<1	<1	n.a.
20.03.2003	16	<1	<1	21	27	<1	<1	<1	<1
10.04.2003	12	<1	<1	n.a.	n.a.	n.a.	<1	<1	<1
22.05.2003	<1	8	<1	*	*	*	<1	<1	<1
19.06.2003	1	1	<1	*	*	*	<1	<1	<1
03.07.2003	15	<1	<1	*	*	*	<1	n.a.	<1
21.08.2003	>>	<1	<1	*	*	*	<1	<1	<1
15.09.2003	8	<1	<1	*	*	*	<1	n.a.	<1
24.09.2003	14	<1	n.a.	*	*	*	52	n.a.	<1
29.09.2003	>>	<1	<1	*	*	*	1	n.a.	n.a.
06.10.2003	4	6	<1	*	*	*	<1	n.a.	n.a.
20.10.2003	40	<1	<1	*	*	*	<1	n.a.	<1
11.12.2003	11	<1	<1	*	*	*	<1	n.a.	<1
22.01.2004	165	<1	<1	*	*	>>	14	n.a.	<1
19.02.2004	46	12	<1	*	*	< 15	<1	n.a.	<1
18.03.2004	<1	1	<1	*	*	*	<1	n.a.	<1
22.04.2004	<1	<1	<1	*	*	*	<1	n.a.	<1
positive samples	13 / 16	5 / 18	0 / 17	1 / 2	1 / 2	0 / 4	4 / 18	1 / 7	0 / 14

2 Artificial recharge pond Tegel

2.1 Investigations on the transect of the recharge pond in 2002

The recharge pond is continuously filled with water from Lake Tegel (influent). Microbiological investigations were carried out in water samples from the pond, from two shallow wells (well 365 and well 366), three deep wells (wells 247, 248, 342) as well as from one regular pumping well of Water Work Tegel (well 20) located at a transect of the groundwater enrichment plant of Tegel. During the first three surveys, samples were taken by one MP1 pump. The same equipment was used at all sampling sites without any pre or post disinfection of instruments. During the field surveys in November and December, sterilized Eijkelkamp modules and silicon tubing were used for sampling of the two shallow wells 365 and 366.

Coliphages were found in pond water samples at concentrations between 2 and 26 pfu/100 ml, but were never detected in water samples from any of the wells (Table 18A). Concentrations of intestinal enterococci in pond water varied between 1 and 5 cfu/100ml. Only two samples from wells 247 and 342 contained enterococci in concentrations of 1 and 3 cfu/100 ml, respectively (Table 18B).

E. coli was detected in pond water samples in concentrations of up to 44 cfu/100 ml. About half of the water samples from the two shallow and three deep wells contained E. coli in concentrations of up to 45 cfu/ 100 ml (Table 16C). Samples of all wells taken on July 2002, as well as samples 4 of 5 samples of the pumping well 20 were free from E. coli in 100 ml volume.

Data on the occurrence of heterotrophic plate count bacteria (according to the German Drinking water Directive; colony counts according to DIN EN ISO 6022 were slightly higher) are shown in Table 18D. No retention pattern can be deducted from the data received. Colony counts at 20 °C as well as at 37°C varied from 1 cfu/ml to > 103 cfu/ml. At the regular pumping well 20, colony counts were usually below 100 cfu/ml. During the November and December surveys very low concentrations were found (1-2 cfu/ml). It is suspected that the well had been disinfected before.

Table 18: Occurrence of somatic coliphages (pfu/100 ml), intestinal enterococci (cfu/100 ml), E. coli (cfu/100 ml), and heterotrophic plate count bacteria (cfu/ml) in water samples from the wells of the groundwater enrichment plant of Tegel

(detection limit: 1 pfu or cfu/100 ml; for colony counts 1 cfu/ml)
* no sample, n.a.: not analysed

A: somatic coliphages

Sampling time	influent	pond water	365	366	247	248	well 20	342
18.07.02**	5	2	<1	<1	<1	<1	<1	<1
15.08.02**	n.a	4	<1	<1	<1	<1	<1	<1
21.09.02**	6	3	<1	<1	<1	<1	<1	<1
21.11.02***	15	19	<1	<1	<1	<1	<1	<1
12.12.02***	21	26	<1	<1	<1	<1	<1	<1
positive samples	4 / 4	5 / 5	0 / 5	0 / 5	0 / 5	0 / 5	0 / 5	0 / 5

B: Intestinal Enterococci

Sampling time	influent	pond water	366	365	247	248	well 20	342
18.07.02**	4	5	<1	<1	<1	<1	<1	<1
15.08.02**	*	1	<1	<1	<1	<1	<1	<1
21.09.02**	2	2	<1	<1	<1	<1	<1	<1
21.11.02***	1	1	<1	<1	3	<1	<1	<1
12.12.02***	2	2	<1	<1	<1	<1	<1	1
positive samples	4 / 4	5 / 5	0 / 5	0 / 5	1 / 5	0 / 5	0 / 5	1 / 5

C. E. coli

Sampling time	influent	pond water	366	365	247	248	20	342
18.07.02**	4	1	<1	<1	<1	<1	<1	<1
15.08.02**	*	44	<1	2	30	<1	1	45
21.09.02**	8	3	4	2	<1	<1	<1	4
21.11.02***	20	7	3	8	<1	2	<1	<1
12.12.02***	130	8	<1	3	3	2	<1	2
positive samples	4 / 4	5 / 5	2 / 5	4 / 5	2 / 5	2 / 5	1 / 5	3 / 5

D. Heterotrophic bacteria

Sampling	influent	pond water	366	365	247	248	well 20	342
18.07.02 (20 °C)	380	540	150	52	80	200	130	70
18.07.02 (37 °C)	140	340	140	30	30	40	100	40
15.08.02 (20 °C)	n.a.	760	3280	920	290	345	70	250
15.08.02 (37 °C)	n.a	230	3000	500	410	210	70	30
21.09.02 (20 °C)	870	1370	160	270	150	520	170	90
21.09.02 (37°C)	330	230	90	120	30	40	100	50
21.11.02 (20 °C)	70	2420	140	220	420	230	1	280
21.11.02 (37 °C)	10	400	60	120	60	330	1	110
12.12.02 (20 °C)	310	620	540	80	120	1440	2	110
12.12.02 (37 °C)	30	40	50	20	30	150	2	20

* no sample, ** sampling with non sterile instruments, *** sampling with sterilized instruments

 italic = in 10 ml of sample

2.2 Investigations in the filter bed of the recharge pond

Core samples were taken from the sand filter of the recharge pond to determine the distribution of bacteria in the filter. Sampling was performed when the filtration site was drained to remove the clogging layer. Sub-samples of the sand core from different depth (2-80 cm) were analysed using cultivation methods as well as cultivation independent methods.

Cultivation was performed using two different colony count agars: i) DEV-agar, according to the German Drinking Water Directive and ii) the agar given in DIN EN ISO 6222 (ISO-agar). For the ISO-agar, the highest concentration of cultivable bacteria was found in the upper 5 cm of the sand core (Figure 3). With DEV-agar no difference in concentration was detected over the whole cell core. No consistent difference in colony counts was observed between DEV and ISO-agar (Figure 3).
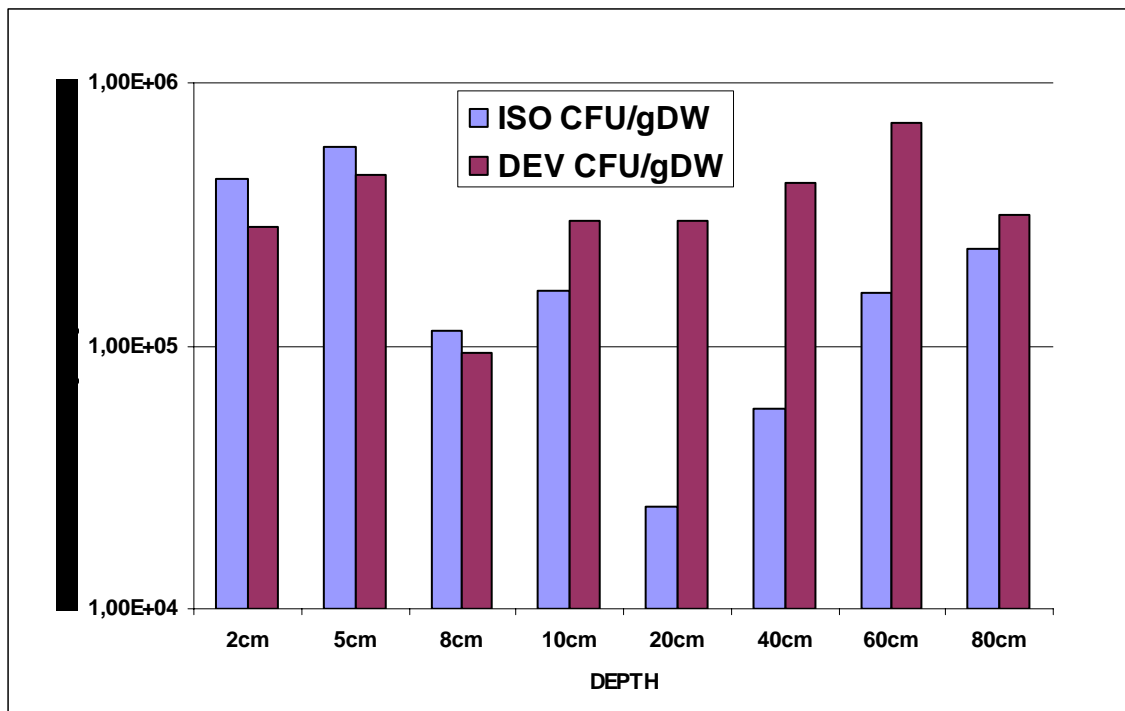
Figure 3 Cultivation of samples from the recharge pond on drinking water media. ISO= agar according to DIN EN ISO 6222, DEV= agar according to the German Drinking Water Directive. Colony forming units (CFU) are based on 1g dry weight (gDW).

Extraction methods with enzymes were used to enhance detachment of the bacteria from the sand. Samples were incubated in a Tris/sodium pyrophosphate solution with the enzymes Alfa-glucosidase, Beta-galactosidase and Lipase. No significant increase in the number of cultivable bacteria was found in the enzyme extracted samples compared to the extraction with buffer only (Figure 4).
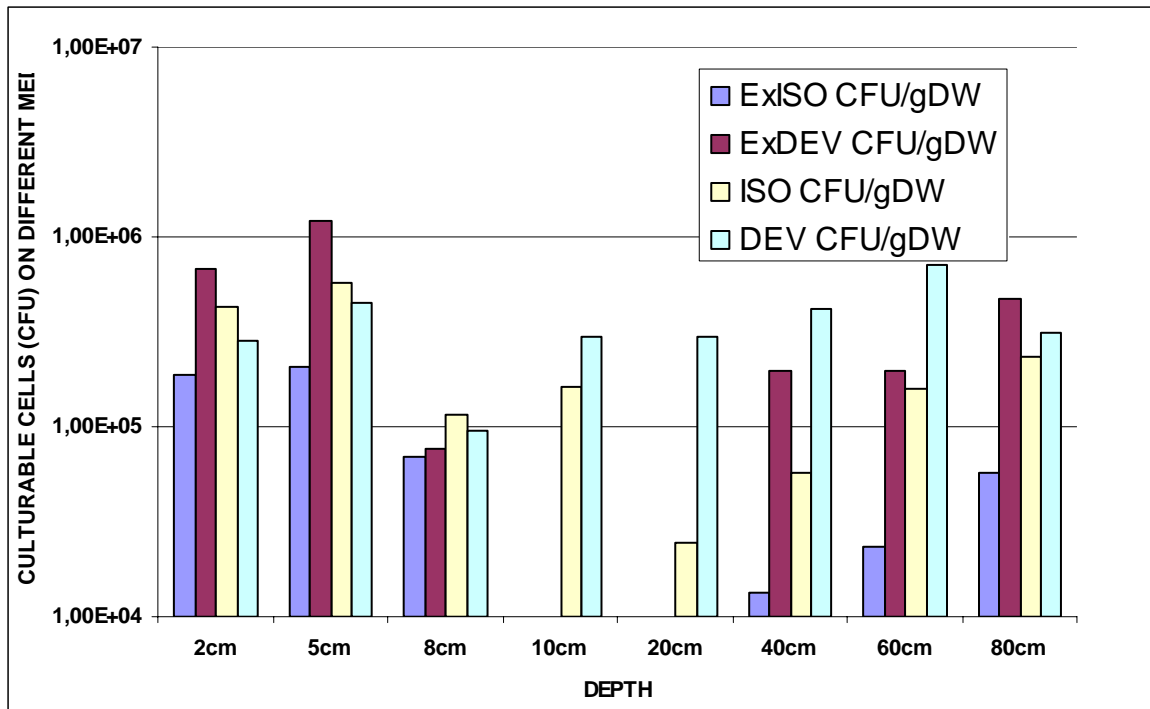
Figure 4 Comparison of extraction with and without enzymes. ISO= agar according to DIN EN ISO 6222, DEV= agar according to the German Drinking Water Directive. ExISO, ExDEV=enzyme extracted samples; ISO, DEV=samples treated without enzymes. Colony forming units (CFU) are based on 1g dry weight (gDW).

Total cell counts were determined microscopically after staining with DAPI. The total concentration of bacteria detected was in the range of 108 to 109 cells per gram dry weight in all depth of the filter core (Figure 5).

The fraction of cultivable bacteria was calculated from the comparison between the total cell count and the colony counts (Figure 6). Cultivability was between 0,01 and 0,5 %. No consistent difference was obtained on the two different media.

No further examinations of the sand core were performed since the transect at the recharge pond was not further investigated due to very low concentrations of bacteria and coliphages in the pond water.
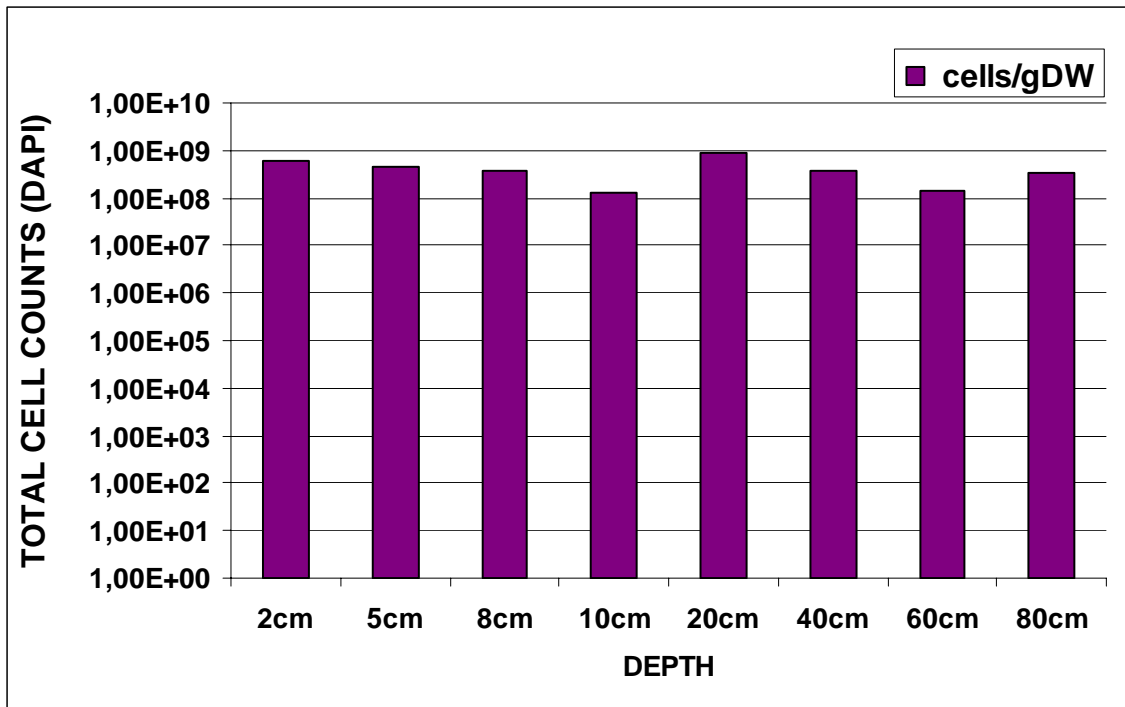
Figure 5 Total cell counts of core samples from the recharge pond determined by DAPI staining. Cells/gDW=cells per 1g dry weight

Fi
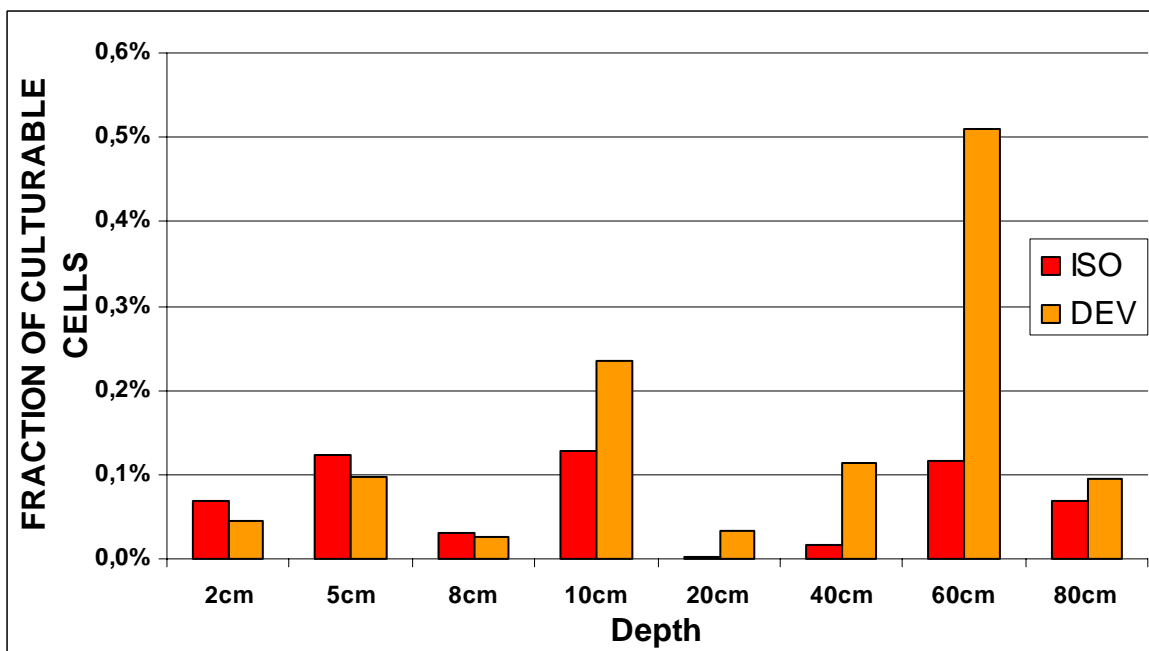
Figure 6 Percentage of culturable cells on two different media in core samples from the recharge pond. Fraction determined in relation to DAPI counts. ISO= agar according to DIN EN ISO 6222, DEV= agar according to the German Drinking Water Directive

2.3 Discussion

2.3.1 Surface water

The results of the microbiological investigations indicated a high hygienic quality of the surface water at both transects and at the artificial recharge pond Tegel. In the surface waters of Lake Tegel and Lake Wannsee, the concentration of intestinal enterococci never exceeded 100 cfu/100 ml (guideline value of the EU Bathing Water Directive), and that of E. coli only occasionally was higher than 100 cfu/100 ml (guideline value of the EU Bathing Water Directive) but never reached 2000 cfu/100 ml (imperative value of the EU Bathing Water Directive). The highest concentration of coliphages was 850 pfu in 100 ml (Fig. 1, 2, Tab.7). Concentrations of coliphages were at some sampling surveys more than 100 x higher than the concentrations of E. coli. This points to a more rapid inactivation of bacteria compared to coliphages under environmental stresses.

Concentrations of the indicator microorganisms examined were lower in Lake Tegel than in Lake Wannsee and showed less seasonal fluctuations during the field surveys between May 2002 and December 2004. An explanation for this is the improvement in hygienic quality of the surface water in Lake Tegel due to treatment of discharges (e.g. Creek Nordgraben) in the flocking and filtration plant of Tegel prior to entering the lake. With flocculation and rapid sand filtration of the inflow to Lake Tegel, an elimination of 84 % for E. coli, 92 % for intestinal enterococci, and 84 % for somatic coliphages was achieved.

Concentrations of indicator microorganisms in Lake Wannsee were higher than in Lake Tegel and clearly showed seasonal fluctuations with highest concentrations in the winter months. High biological activity of aquatic microorganisms and UV irradiation in the summer months are probably responsible for the rapid inactivation of indicator organisms that are not able to proliferate under environmental conditions. Rapid inactivation of coliphages and indicator bacteria by UV irradiation were also observed in a river simulation plant (Dizer et al. 2005).

The Teltow canal discharging a large amount of secondary effluent from the sewage treatment plants in Berlin flows through the Griebnitz Lake into Lake Wannsee. Concentrations of indicator microorganisms were elevated close to the inflow from the Griebnitz Lake. Concentrations decreased, however, with distance from the inflow and reached background close to the transect area.

2.3.2 Pumping wells

No somatic coliphages or enterococci were detected in any of the samples from regular pumping wells of the water works. E. coli was sporadically detected in samples from all but one well in concentrations near the detection limit of 1 cfu/100ml. Sampling was performed from especially installed taps. Although this procedure strongly reduces the risk of contamination, sporadic external contamination cannot be completely ruled out.

2.3.3 Deep observation wells

Deep observation wells were sampled at the transect of Lake Tegel and at the artificial recharge pond Tegel during the surveys in the year 2002. Somatic coliphages and enterococci were detected in one sample each from the four wells at the transect of Lake Tegel. In deep wells from the artificial recharge pond, no coliphages were detected and only 2 out of 15 samples contained enterococci. E. coli was detected in about one third of the samples from deep observation wells in concentrations of between 2 cfu/100 ml and 6 cfu/10 ml (Table 18, 19). Sampling from these wells was only possible using unsterile pumps and equipment which are not optimal for microbiological sampling. Only one MP1 pump and accessories were used during all field surveys for all sampling sites without any treatment before or after operations. The contamination of wells was reduced through pre-pumping groundwater for 20-30 min from each well at a relatively high flow rate of 100 L/min before taking samples. Nevertheless, the problem with possible contamination of the wells remained. Sampling of deep observation wells was not continued in 2003 because of the sterility problems and the very low detection frequency of coliphages not allowing the deduction of retention patterns.

Table 19 Frequency of positive findings of test organisms in deep observation wells sampled by non sterile MP1 pump and equipment along the transect of Lake Tegel.

	Coliphages	Intestinal enterococci	E. coli
MP1 pumps	1 / 32	1 / 32	10 / 31

2.3.4 Shallow observation wells

Seven shallow observation wells were sampled from the transect of Lake Tegel. Somatic coliphages were only detected in one sample of the well closest to the lake. Intestinal enterococci were not detected in the shallow wells except for the survey in October where all but one wells contained enterococci. E. coli was detected in three wells in concentrations of about 30 cfu/ml during the survey in August when non sterilized equipment was used. In all following surveys - when sterile equipment was used – no E. coli was detected in any of the samples. It is, therefore, assumed, that the high concentrations of E. coli found in August were due to contamination of the wells by sampling.

No retention pattern along the transect flow paths can be obtained from these results. The concentrations of indicator microorganisms in the lake were relatively low and – with a few exceptions –indicator bacteria and coliphages were not or only sporadically detected in the observation wells.

Two shallow wells were sampled at the transect of the artificial recharge pond Tegel. No enterococci or coliphages were detected in samples from these wells. In contrast, E. coli was

detected in most of the samples. Using disinfected equipment did not lower the frequency of positive findings.

Similar results were obtained for the shallow wells at the transects 1 and 2 of Lake Wannsee. Nine shallow wells from transect 1 and transect 2 were sampled. Enterococci and coliphages were only sporadically detected while E. coli was found in 70 out of 135 samples in concentrations of 1-50 cfu/ 100 ml. Again there was no difference in the frequency of positive findings when using non sterile compared to disinfected equipment.

The source of E. coli found in the shallow wells remains unclear. External contamination during sampling cannot be ruled out. Although sampling for microbiological investigations was carried out using disinfected pumps and tubing, other sampling and measurement tasks at the wells were performed using non sterile equipment. Furthermore, the disinfected pumps and tubing could not be introduced in the groundwater without contact with biofilm layers at the inside of the wells which might act as a source of contaminants. Swap samples were taken from the wall of some wells (3337, 3335, 207, and 201OP) as well as from the surface of several non disinfected instruments (tubing, sensors) used by other working groups. No E. coli were detected in biofilm samples from inside the wells. E. coli was, however, detected in one sample from the instruments.

False positive results in the detection method for E. coli might also explain positive findings especially in samples where other indicators were not detectable. To reduce the risk for false positive results, three different detection methods were used - partly in parallel. Aeromonades - identified in one method as giving false positive results - were thereby excluded. Therefore, this explanation for the occurrence of E. coli seems unlikely.

Since external contamination cannot be ruled out, the concentration of E. coli in the wells cannot be used to deduct retention characteristics. The concentration of the other indicators was too low to be able to see log reduction rates. A clear reduction in positive findings with length of filtration path is, however, obvious when compiling all results (see Table 20).

Table 20 Frequency of positive findings in shallow observation wells and pumping wells at the Lake Wannsee

A. Transect 1

Parameters	3339	3338	3337	201OP	3335	Well 4
depth	5	5	7	15	12	25
located	in the lake (40m)	in the lake (9 m)	at the shore 2 m	at the shore (7 m)	at the shore (15 m)	33 m
percolation time	< 1 month	30 d	27 d	?	30 d	90 d
Coliphages	2 / 6 (33%)	0 / 20	0 / 16	0 / 17	0 / 12	0 / 16
Enterococci	2 / 6 (33%)	4 / 20 (20%)	1 / 16 (6%)	0 / 17	0 / 12	0 / 15

B. Transect 2

Parameters	207 UP	205	206	202 OP	203	Well 3
depth (m)	1,8	5	7	12	12	25
located	in the lake (10 m)	in the lake (30 m)	in the lake (20 m)	at the shore (3m)	at the shore (20 m)	42 m
percolation time	a few days	1 month	25 d	72 d	3 month	3 month
Coliphages	5 / 6 (83%)	3 / 18 (2%)	0 / 18	1 / 18 (0.5%)	1 / 9 (1%)	0 / 16
Enterococci	1 / 4 (25%)	1 / 18 (1%)	0 / 17	3 / 18 (2%)	0 / 8	0 / 14

The highest frequency of positive results was found in the observation wells closest to the lake (3338, 3339, 207UP). The number of positive samples declined clearly with increasing distance from the lake along the shore. No positive samples were obtained from the pumping wells even when one liter of sample was analysed.

The data presented indicate a weak migration of indicator microorganisms along the filtration path to the shallow wells of the transects. The concentrations of indicator bacteria and coliphages in both, lake Wannsee and lake Tegel, were, however, never high enough to allow a quantitative approach for the elimination of microorganisms along the transects.

Therefore, further investigations focused on the three model filtration plants of Marienfelde: the sandy soil column of 5 m length, the enclosure and the slow sand filtration pond with a filtration path of 100 or 80 cm, respectively (see chapter XXX).

2.3.5 Microorganisms in the filter bed

Core samples were taken from the sand filter of the artificial recharge pond Tegel to determine the distribution of bacteria in the filter. The bacteria were evenly distributed over the whole length of the filter bed. The concentration was not higher in the upper zone (clogging layer) than in 80 cm depth. Colony counts as well as total cell counts were in the same order of magnitude at all sampling depth. Culturability ranged from 0.01 to 0.5 %. These results indicate a high potential for biological activity – elimination and degradation – in the whole sand filter.

3 Batch experiments

3.1 Introduction

The elimination of bacteria and viruses by slow sand or bank filtration is to be regarded as a cumulative function of different physically, chemical and biological procedures. The inactivation of micro organism in capillary water of sandy soil and their reversible and irreversible adsorption on to solid particles along the filtration path determine their survival, retention and transport behaviour. The physically chemical characteristics of the filter matrix regulate the interactions between micro organisms and sediment surface. The goal of the batch attempts is therefore the experimental determination of the information, which can be consulted with differential explanation of these interactions and served as basis or factor value for statistical assessment or modelling of the column attempts.

3.2 Survival of test organisms in water and water soil suspension

As groundwater was applied by all experiences on enclosure and slow sand filtration basin, the batch experiments were also accomplished in groundwater taken in the Water Work of Marienfelde. Native sand applied by filling slow sand filtration pond and enclosure, top layer of filtration pond (< 1cm) consisting of clogging layer formed during continuously operation for one year, and upper layer of the sediment (0-5 cm) from bottom of Lake Wannsee were used for batch experiments. The sampling and preparation of the sediment from the Lake Wansee were carried out by the working group hydrogeology of FU Berlin. A part of the sand and sediment samples was sterilised by autoclaving at 120°C for 30 min, in order to eliminate the biological inactivation of test organisms in different sets of soil suspension.

In a large glass flask, 2 L groundwater was inoculated with a dilution of culture suspension (1ml) of test coliphages and indicator bacteria, respectively. After genteelly shaking of samples for 5 min on a horizontally shaker, the culture suspension was allocated in 200 ml volumes in sterile erlenmayer flasks. 50 g sand of each origin were added to an aliquot of culture suspension and incubated on a horizontal shaker (30 rpm) at room temperature for 7-30 d. Incubation of indicator bacteria in water and different soil suspensions was carried out for 7 d. The sampling took place in regular intervals without any settling and centrifugation directly from the liquid phase of sand suspension. Two parallel sets of samples were applied for testing survival of indicator bacteria in water and different soil suspensions.

The amount of viruses present in the water phase was measured as a function of time. Virus density in control container with or without sand was measured to calculate inactivation in liquid phase as function of time (y´= eat).

The concentrations of test organisms in different sets of samples and their exponential regression lines and equations were demonstrated in figures and tables. The decreasing constant of each line corresponds to the inactivation coefficient of test virus which can be calculated through the derivative function y' = eax with x=1d. The reduction of the phage density in 30d of incubation was also calculated and given as factor or log units in each tables.

The adsorption equilibrium of test organisms in virgin sand of the filter pond was also tested by kinetic batch experiments under shaking at 60 rpm for 6h. Five ml samples from liquid phase were taken in interval of 30 min. After centrifugation of sample at 3000 rpm, concentration of test organisms was detected in supernatant. A set of culture suspension without sand was used as control for determination of total amount of test organisms during operation time. Viruses partitioned between solution and sorbent phases was characterised as adsorption rate (dimensionless) and distribution coefficient, Kf, (g-1).

Adsorption rate was calculated through the relation: (Co – Cf) / Co [Co: Total amount of coliphages in water without sand as control (pfu/ml), Cf: amount of free, non adsorbed coliphages in supernatant of centrifuged water sand suspension (pfu/ml)].

Dispersion coefficient (Kf) was calculated: [(Co – Cf) / sand weigth (g)] / Cf. A semi-log plot of virus adsorption to sandy soil as a function of time suggests the adsorption equilibrium.

3.3 Survival of coliphages in water and water soil suspensions

F+ phage 138 and somatic coliphage 241 have shown high persistence in native groundwater from Marienfelde (
Table 21). After 30 d incubation at 20°C, survival ratio of both viruses was about 0,65 corresponding with an inactivation rate of 0,2 log units/30d.

In all sterile sandy soil suspensions, very low or no lost of virulent of both coliphages were observed too. Less than one log unit of F+phage 138 disappeared in the native sand or the sandy soil from clogging layer of filter pond. Inactivation rate of somatic coliphage 241 was found only 1,4 log units/30d in native sand while they were not inactivated in sand containing clogging layer. Both coliphages likewise survived fully in the sterile sediment from bottom of the Lake Wannsee (
Table 21).

Table 21 Survival and inactivation ratio of test coliphages in suspensions of different sandy soils at room temperature [SD: Schmutzdecke, *)50 g sandy soil + 200 ml culture suspension in groundwater]

Samples	F+ coliphage 138				Somatic coliphage 241			
	Derivation of regression line	survival ratio (x=1d)	survival ratio (x=30d)	inactivation rate (log / 30d)	y'=e-0,0x	survival ratio (x=1d)	survival ratio (x=30d)	inactivation rate (log / 30d)
Groundwater Marienfelde (non sterile)	y'=e-0,015x	0,98	0,64	0,2	y'=e-0,015x	0,99	0,65	0,2
Sandy soil* Marienfelde (sterile)	y'= e-0,037x	0,96	0,33	0,5	y'=e-0,106x	0,90	0,04	1,4
Sandy soil* Marienfelde (non sterile)	y'=e-0,09x	0,91	0,07	1,2	y'=e-0,1291x	0,88	0,02	1,7
Sandy soil* + SD Marienfelde (sterile)	y'=e-,0236x	0,98	0,49	0,3	y'=e0,1113x	1,01	1,40	< 0
Sandy soil* + SD Marienfelde (non sterile)	y'=e1,5278x	0,22	<0,00001	>5	y'=e-1,0865x	0,34	<0,00001	>5
Sandy soil* - Wannsee (sterile)	y'=e0,01x	1,01	1,35	< 0	y'=e0,0304x	1,03	2,5	< 0
Sandy soil* - Wannsee (non sterile)	y'=e-,4049x	0,67	0,00001	5	y'=e-0,3194x	0,73	0,001	3

In contrast to the high survival ratios in sterile sand suspensions, all test organisms were rapidly inactivated in non sterile suspension of each sandy soil. Survival rates of F+ phage 138 and somatic phage 241 in non sterile sand of clogging layer were about 0,2 and 0,3.d-1, respectively, resulted in absolutely inactivation of both phages, more than 5 log units within 30 d (

Table 21). Both coliphages have shown a survival rate of about 0,7.d-1 in upper layer of the sediment from Lake Wannsee corresponding an inactivation ratio of 3 or 5 lo units within 30d, respectively. In non sterile native sandy soil of filtration pond, low amount of F+ and somatic phages lost their virulent, 1,2 and 1,7 log units in 30d, respectively (

Table 21).

3.4 Survival of indicator bacteria in water and water soil suspensions

Both indicator bacteria, E. coli A and E. faecalis, have shown high persistence in native groundwater. Survival ratios were calculated 0,74.d-1 for E. coli A (Table 22), and 0,61.d-1 for E. faecalis (Table 23). Less than one log unit of indicator bacteria was inactivated during an incubation time of 7d. Results of two parallel sets of samples have shown no or low deviation (Table 22 and Table 23).

Concentration of E. coli A significantly enhanced in sterile suspensions of native sandy soil and top layer of filter pond containing clogging layer (Table 22). An increase of the amount of E. faecalis was observed only in sterilized sand with clogging layer (Table 23). These results point to the growth of both indicator bacteria, if there is no biological stress in their aquatic or terrestrial environment.

In the non sterile sets of both sand suspensions, E. coli A was strongly inactivated within 7d. The survival ratios were found 0,57.d-1 in the native sand, and 0,53.d-1 in the top layer of filter pond with colmation layer. The inactivation ratio of E. coli A reached approximately 2 log units after 7 d of exposition in both soil suspensions (Table 22).

Table 22   Survival of E. coli A in groundwater and different water-sand suspensions during incubation for 7 d at a temperature of 20 + 2°C

Samples	Parallel experiments	Derivation of regression line	Survival rate (d-1)	Survival rate (in 7 d)	Inactivation (log / 7 d)
Groundwater Marienfelde (non sterile)	a	y'=e-0,2951x	0,74	0,13	0,9
	b	y''=e-0,2972x	0,74	0,12	0,9
	mean		0,74	0,10	0,9
native sandy soil - Marienfelde (sterile)	a	y'=e0,4247x	1,5	>1	0
	b	y'=e0,2733x	1,3	>1	0
	mean		1,4	>1	0
native sandy soil - Marienfelde (non sterile)	a	y'=e-0,6099x	0,54	0,01	1,9
	b	y'=e-0,5268x	0,59	0,03	1,6
	mean		0,57	0,02	1,8
Clogging layer of filtration pond (sterile)	a	y'=e0,842x	2,3	>1	0
	b	y'=e0,7892x	2,2	>1	0
	mean		2,3	>1	0
Clogging layer of filtration pond (non sterile)	a	y'=e-0,6082x	0,54	0,014	1,8
	b	y'=e-0,6563x	0,52	0,01	2,0
	mean		0,53	0,01	1,9

E. faecalis was also strongly inactivated in both non sterile sandy soil suspensions (Table 23). After one week of exposition 2,3 log or 3,2 log units of E. faecalis disappeared in native or sandy soil with clogging layer, respectively. In contrast to E. coli A, there was no clear

difference between relative high inactivation ratios of E. faecalis in sterile or non sterile native sand of filter pond.

These results point to the importance of the biological activity of native microorganism population of sandy soil by elimination of hygienic related bacteria and viruses which are not adapted to the biological stress conditions in capillary water of filtration units.

Table 23 Survival of E. faecalis in groundwater and different water-sand suspensions during incubation for 7 d at a temperature of 20 + 2°C

Samples	Parallel experiments	a (y'=e-ax)	Survival rate (x = 1)	Survival rate (x =7 d)	Inactivation (log / 7 d)
Groundwater Marienfelde (non sterile)	a	-0,588	0,556	0,016	1,8
	b	-0,401	0,670	0,060	1,2
	mean		0,61	0,04	1,5
native sandy soil - Marienfelde (sterile)	a	-1,048	0,351	0,0007	3,2
	b	-0,912	0,402	0,0017	2,8
	mean		0,38	0,0012	3,0
native sandy soil - Marienfelde (non sterile)	a	-1,041	0,353	0,0007	3,2
	b	-1,060	0,346	0,0006	3,2
	mean		0,35	0,0006	3,2
Clogging layer of filtration pond (sterile)	a	2,242	9,410	> 1	0,0
	b	2,009	7,452	> 1	0,0
	mean		8,43	> 1	0
Clogging layer of filtration pond (non sterile)	a	-0,754	0,470	0,0051	2,3
	b	-0,690	0,502	0,0080	2,1
	mean		0,49	0,0065	2,2

3.5 Adsorption of test organisms on sandy soil

Adsorption of F+ phage 138 and somatic phage 241 were tested in soil water suspensions, containing 50 g sterile sand and 200 ml groundwater.

Each of test organisms were separately inoculated in soil samples from there selected origins. After an incubation on a horizontally shaker at 60 rpm for 6h, and room temperature, 5 ml of each samples were centrifuged at 3000 rpm for 10 min. The free, not adsorbed phages in supernatant were quantified. Relation of the free phage density to the amount of phages in control sample without sand served the adsorption rate.

Both coliphages have shown a low adsorption on all sterilized sandy soil samples. Highest adsorption of F+ coliphage 138 was found factor 0,86 on the native sand of filter pond, and factor 0,75 on the sediment of Lake Wannsee (Table 24). Adsorption on the sandy soil of

filter pond containing clogging layer was about 0,32. Relatively high kf value (0,12.g-1) was calculated for F+ phage 138 adsorbed per g of native sand of filter pond.

Less adsorption of somatic coliphage 241 was found than those of F+ phage 138 ranging from 0,15 on sandy soil with clogging layer to 0,25 on the native sand of filter pond (Table 24). Correspondingly low kf values varied between 0,004 and 0,007.g-1 in all soil samples.

Table 24 Adsorption ratios and dispersion coefficients (kf values) of test coliphages in different water - sand suspensions (SD= clogging layer)

Samples (survival)	F+ phage 138		Somatic phage 241	
	Adsorption	Kf value	Adsorption	Kf value
native sandy soil - Marienfelde (sterile)	0,86	0,12	0,25	0,007
sandy soil + SD Marienfelde (streile)	0,32	0,01	0,15	0,004
sandy soil - Wannsee (sterile)	0,75	0,06	0,17	0,004

Low adsorption of both coliphages on sandy soil from colmation layer of filter pond points to the dispering effect of water soluble organic clogging matter on viruses which obviously reduced sorptive interaction between virus and grain surface.

Due to growth of indicator bacteria in sterile sets of sandy soils and sediments we could not analyse their adsorption on sand by batch experiments. In non sterile sets of soil-ground water suspensions, coliphages and indicator bacteria were differently inactivated during the incubation time. Therefore, the physically chemical adsorption may not be differed from biological inactivation of test organisms in non sterile water-soil suspension.

For testing adsorption of indicator bacteria, sand suspensions containing each bacteria culture was set up for 5 min, after shaking samples for 30 min. The still murky supernatant with colloid particles was used for estimation of the free non adsorbed bacteria. In spite of the short-term sedimentation, 67% or 96% of respective E. coli or E. faecalis remained on the sediment particles of the virgin sand of filtration units (Table 25).

Adsorption ratio of indicator bacteria was found in the same order of magnitude in the soil suspension containing clogging layer of the filter pond (Table 25). In compliance with high adsorption ratio, high dispersion coefficients were found in both soil suspensions of E. faecalis.

Table 25 Adsorption ratios and dispersion coefficients (kf values) of indicator bacteria in different water - sand suspensions (SD= clogging layer)

Samples (pH 7)	E. coli		E. faecalis	
	Adsorption	Kf value	Adsorption	Kf value
native sandy soil - Marienfelde	0,67	0,04	0,96	0,48
sandy soil + SD Marienfelde	0,76	0,06	0,89	0,16

4 Laboratory Experiments: Column studies

Retention and migration behaviour of indicator organisms during sand filtration was investigated in different laboratory columns in addition to the experiments in the semi technical plants of Marienfelde. Laboratory columns of UBA, Technical University of Berlin and Free University of Berlin were used for the investigations.

4.1 Experiments with laboratory columns of UBA

Two experiments were carried out to compare retention of test organisms under aerobic and anaerobic conditions.

4.1.1 Materials and methods

For test organisms, sampling, cultivation and detection see chapters "Enclosure" and "Slow Sand Filtration Pond". Concentrations of test organisms in each surface water and filtrate fractions were used for calculation of relative breakthrough ratios through the quotient of $C_{filtrate}$ to C_{input}. The mean value of all fractional breakthrough ratios was used for further calculations as described previously.

4.1.1.1.1 Column

An acrylic glass column with a diameter of 14 cm and a length of 110 cm was filled with the same sandy soil which was used for the enclosures of Marienfelde. Native sandy soil - free from organic matter - was not previously used for experiments. Four perforated drain tubes enabled sampling at 20, 40, 60 and 80 cm depths of column. Outlet samples were collected from the end of the column at 100 cm. After upwards saturation of the sandy soil column, tap water was percolated top down at a filttration velocity of 30 cm/d corresponding to a pore velocity of 100 cm/d for one week to stabilise the hydraulic conditions.

At a pore velocity of 100 cm/d, the following percolation or residence times were calculated at five sampling sites: 4,75 h at 20 cm; 9,5 h at 40 cm; 14,25 h at 60 cm; 19 h at 80 cm; and 24 h at 100 cm.

4.1.1.1.2 Anaerobic conditions

Further experiments in the same laboratory column were carried out after filling total volume of column with biologically active sandy soil in a length of 110 cm. Because of the higher filling, sampling sites were displaced to 30, 50, 70, 90 and 110 cm. During continuous percolation of tap water in this prolonged sandy soil column, anaerobic conditions developed in the filter bed. The filter matrix became black and the redox potential tropped to -100 mV.

Inoculation: For peak inoculation (4.1.2.1), suspensions of laboratory cultures of test organisms - F+ phage 138, somatic phage 241, E. coli A and E. faecium - were mixed in a total volume of 500 ml and put onto the surface of the sand filter. After gentle percolation of the suspension into the surface layer of the filter bed, pore water velocity was set on 100 cm/d by means of a regulatory pump. For continuous inoculation (4.1.2.2), culture suspensions were mixed with 50 L water in a reservoir tank from which the filter column was fed.

4.1.2 Results

4.1.2.1 Experiment I - 05.05.2004 (aerobic conditions)

Concentrations of test organisms in the initial suspension were about 7.10^7 pfu/100 ml for F+ phage 138, 5.10^5 pfu/100 ml for somatic phage 241, $8 .10^7$ mpn/100 ml for E. coli A, 2.10^7 mpn/100 ml for Enterococcus faecium.

After inoculation of $3,5.10^8$ pfu/500 ml, F+phages 138 were detected in filtrates after 4 h at 20 cm, 9 h at 40 cm, 14 h at 60 cm, 20 h at 80 cm, and 26 h at 100 cm (Figure 7). Following this early breakthrough, filtrate concentrations rapidly increased and reached the peak at 30 cm after 6h, at 60 cm after 17h, and at 100 cm after 30h (Figure 7).

Figure 7: Cocentration of F+phage 138 in the laboratory column of UBA at a pore velocity of 100 cm/d under aerobic conditions (Input of F+phage 138: 3,52.108 pfu/500ml, not demonstrated)

Breakthrough ratio was 0,0001 for the total effluent, 0,01 at 60 cm, and 0,07 at 40 cm depth. (Table 26). There was no removal of F+phages in the surface layer within 20 cm. Log-

retention increased with increasing depth to 1,2 log units within 40 cm and 4 logs within 100 cm. No homogenous removal of phages was observed along the filtration path between successive sampling sites. Δ log retention varied from 0,4 to 1,6 log units. Elimination rate coefficients (λA) were calculated for the different sampling sites ranging from 0,28 to 0,37 logs.h[-1] (Table 26). Based on the retention rate of F+phage at 100 cm depth, an elimination of one log unit would occur in a filter path of 26 cm.

Table 26: Retention of F+ phage 138 in the laboratory column of UBA at a pore velocity of 100 cm/d under aerobic conditions

sampling sites (cm)	Cumulative breakthrough ratio*	Retention (log)	Δ log Retention+ (heterogeneity)	Specific retention (Δ log) / cm	λA (log.h-1)*
20	1,1	0	-	-	-
40	0,07	1,2	1,2	0,06	0,28
60	0,01	1,9	0,7	0,04	0,30
80	0,005	2,3	0,4	0,02	0,28
100	0,0001	3,9	1,6	0,08	0,37

[*] Calculation by integrative balancing virus concentrations in influent and filtrate samples, +) Retention of phages between two neighbours sites, λA : elimination rate coefficient)]

Initial concentration of somatic coliphage 241 in the inoculum was about ($2,6.10^6$ pfu/500 ml). The behaviour of somatic coliphage 241 in the column was similar to that of F+phage 138. Highest concentrations of phages were found in filtrate samples from 20 cm after 6 h, 40 cm after 11 h, 60 cm after 16 h, 80 cm after 22h, and in the effluent after 30 h (Figure 8). Retention of phage 241 was distinctly less than observed for F+phage 138. Breakthrough ratios were about 0,03 in the effluent and 0,4 in filtrates from 80 cm. There was no retention in the upper filter paths of 60 cm (Table 27). After a moderate virus retention in the filter path between 60 and 80 cm, highest virus removal of 1,5 logs was observed in the end of the filter path from 80 cm to 100 cm. Correspondingly, elimination rate coefficients of somatic phage 241 were 0,04 and 0,14 logs.h[-1] at the sampling sites from 80 cm and 100 cm depth. For elimination of one log unit, water would have to be filtered through a filter path of 67 cm.

Figure 8: Concentration of somatic coliphage 241 in the laboratory column of UBA at a pore velocity of 100 cm/d under aerobic conditions (Input of phage 241: $1,6.10^6$ pfu/500ml, not demonstrated)

Initial concentration of E. coli A was 4.108 mpn/500ml. An early breakthrough of E. coli was observed at all sampling sites. It appeared with the front of percolating water after 8 h at 40 cm and after 25 h in the effluent (Figure 9). After this rapid break through, highest concentrations were found in the next filtrate samples. After an operation time of 84 h, cumulative breakthrough ratios of E. coli A were 0,3 at 20 cm, 0,004 at 60 cm and 0,00002 in the effluent (Table 28). Correspondingly, log-retention increased with filtration path from 0,5 to 4,8 log units. A filter path of 21 cm would enable to reduce E. coli A for one log unit.

Table 27: Retention of somatic phage 241 in the laboratory column of UBA at a pore velocity of 100 cm/d under aerobic conditions.

sampling sites (cm)	Cumulative breakthrough ratio*	Retention (log)	Δ log Retention+ (heterogeneity)	Specific retention (Δ log) / cm	λA (log.h-1)*
20	1,6	0	-	-	-
40	1,5	0	-	-	-
60	1,1	0	-	-	-
80	0,4	0,3	0,4	0,02	0,04
100	0,03	1,5	1,1	0,06	0,14

* Calculation by integrative balancing virus concentrations in influent and filtrate samples,
+ Retention of phages between two neighbouring sites, λA : elimination rate coefficient)]
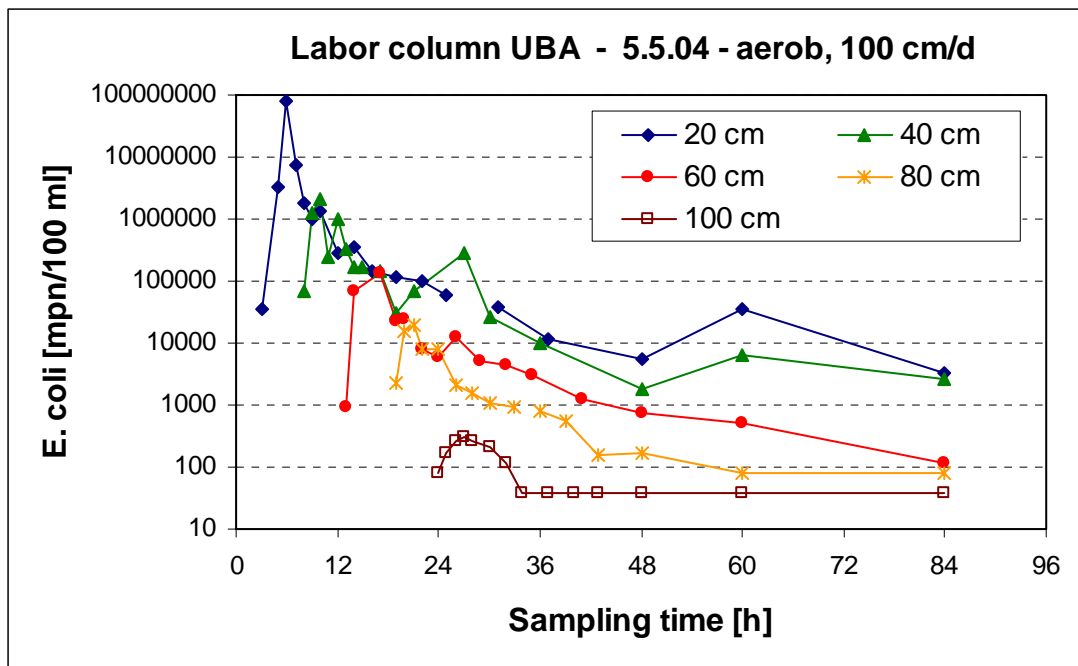
Figure 9: Concentrations of E. coli A in the laboratory column of UBA at a pore velocity of 100 cm/d under aerobic conditions (Input of E. coli A: 4,76.107 pfu/500ml, not demonstrated)

After inoculation of 9.10^7 mpn/500ml E. faecium was detected in the first filtrate samples at all sampling sites (Figure 10). Highest concentrations were observed two or four hours after its early breakthrough, e.g. $5,6.10^6$ mpn/100 ml after 6 h at 20 cm, $2,5.10^6$ mpn/100 ml after 17 h, and $1,6.10^5$ mpn/100 ml after 28 h at the end of column (100 cm). During further percolation of the column, concentrations of E faecium slightly decreased to detection limit within 84 h. Cumulative breakthrough ratios were calculated approximately 0,1 up to 80 cm and 0,006 in the effluent, corresponding with a retention ratio of 1 and 1,7 log units, respectively. (Table 29).

Table 28: Retention of E.coli A in the laboratory column of UBA at a pore velocity of 100 cm/d under aerobic conditions

sampling sites (cm)	Cumulative breakthrough ratio*	Retention (log)	Δ log Retention+ (heterogeneity)	Specific retention (Δ log) / cm	λA (log.h-1)*
20	0,3	0,5	0,5	0,03	0,23
40	0,05	1,3	0,8	0,04	0,10
60	0,004	2,4	1,1	0,05	0,39
80	0,0005	3,3	0,9	0,04	0,40
100	0,00002	4,8	1,5	0,07	0,46

* Calculation by integrative balancing virus concentrations in influent and filtrate samples,
+ Retention of phages between two neighbouring sites, λA : elimination rate coefficient)

Retention of intestinal enterococci was low and not homogenous in all part of the filter bed.

Highest retention (0,02-0,04 log/cm) was observed in the surface layer of 20 cm and at the end of the filter path between 80 and 100 cm. Log-retention over the whole filter was 1,7 log units. (Table 29). A filter path of 57 cm would be necessary for elimination of one log unit.
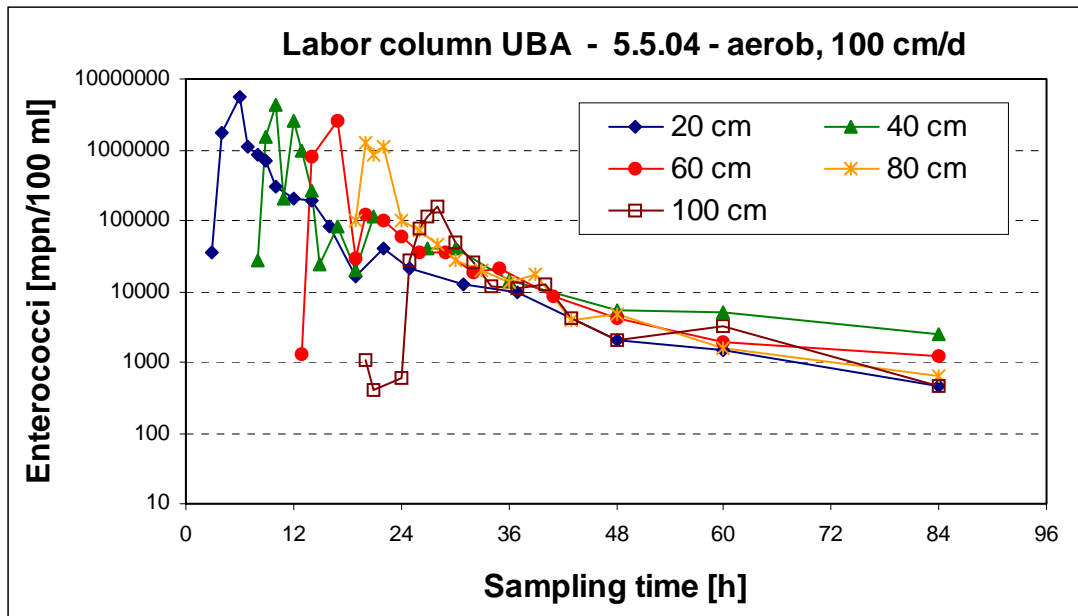
Figure 10: Concentrations of E. faecium in the laboratory column of UBA at a pore velocity of 100 cm/d under aerobic conditions (Input of E. faecium: 2.108 pfu/500ml, not demonstrated)

Table 29: Retention of E. faecium in the laboratory column of UBA at a pore velocity of 100 cm/d under aerobic conditions

Sampling sites (cm)	Cumulative breakthrough ratio*	Retention (log)	Δ log Retention+ (heterogeneity)	Specific retention (Δ log) / cm	λA (log.h-1)*
20	0,4	0,4	0,4	0,02	0,21
40	0,3	0,5	0,1	0,005	0,13
60	0,2	0,7	0,2	0,006	0,10
80	0,1	1,0	0,3	0,016	0,12
100	0,02	1,7	0,7	0,04	0,17

* Calculation by integrative balancing virus concentrations in influent and filtrate samples,
+ Retention between two neighbours sites, λA : elimination rate coefficient)]

4.1.2.2 Experiment II - 12.7.2005 (anaerobic conditions)

In the first part of the experiment F+phage 138 and somatic phage 241 were continuously inoculated into the column. Sampling was carried out in daily intervals from drain tubes at 30, 50, 70, 90 and 110 cm.

Concentrations of F+phage 138 in the water reservoir varied between $2,2.10^5$ and $1,2.10^6$ pfu/ml during the experiment. Average concentrations of F+phage 138 were $7,2.10^5$ pfu/ml in input, $4,4.10^5$, 2.10^5, and $3,1.10^5$ pfu/ml in filtrate fractions at 30, 70 and 110 cm, respectively (Figure 11). Correspondingly, mean breakthrough ratios of F+phages were in the same order of magnitude at all sampling sites, 0,07 at 20 cm; 0,05 at 70 cm; and 0,06 in the total effluent (Table 30). In comparison to the first experiment under aerobic conditions, relatively low retention of F+ phages was observed under anaerobic conditions (Table 26 and Table 30).

Figure 11: Concentrations of F+phage 138 in the laboratory column of UBA at a pore velocity of 100 cm/d under anaerobic conditions

Highest virus retention was about 1,2 log units in the top filter layer of 30 cm which resulted in a specific retention factor of 0,04 log/cm. Retention of F+phage declined in the deeper filtration path. Elimination rate coefficients decreased significantly from 0,37 log.h-1 at the surface layer to 0,11 log.h-1 in total effluent (Table 30).

Table 30: Retention of F+phage 138 in the laboratory column of UBA at a pore velocity of 100 cm/d under anaerobic conditions,

sampling sites (cm)	Breakthrough ratio*	Retention (log)	Δ log Retention+ (heterogeneity)	Specific retention (Δ log) / cm	λA (log.h-1)*
0,3	0,07	1,2	1,2	0,04	0,37
0,5	0,03	1,4	0,2	0,02	0,28
0,7	0,05	1,3	0	-	0,18
0,9	0,06	1,2	0	-	0,13
1,1	0,06	1,2	0	-	0,11

* Calculation by integrative balancing virus concentrations in influent and filtrate samples,
+ Retention of phages between two neighbours sites, λA : elimination rate coefficient

Concentrations of somatic phage 241 in the influent ranged from $1,4.10^5$ to $5,1.10^5$ pfu/ml, (average 3.10^5 pfu/ml). Mean concentrations in filtrate samples were $5,3.10^4$ pfu/ml at 20 cm, $2,2.10^4$ pfu/ml at 70 cm, and $1,2.10^4$ pfu/ml at 110 cm (Fig. 6). Correspondingly, breakthrough ratios of phage 241 were about 0,2, 0,1, and 0,05 at the sampling sites of 30, 70 and 110 cm depth, respectively (Table 6). The highest elimination rate coefficient of 0,22 log.h^{-1} was determined in the top layer of 30 cm which decreased with increasing filter depth to 0,12 log.h^{-1} at 100 cm (Table 31).

Figure 12 Concentrations of somatic coliphage 241 in the laboratory column of UBA at a pore velocity of 100 cm/d under anaerobic conditions

In the second part of the experiment, suspensions of E. coli A and E. faecium were inoculated as peak in the top layer of the filter bed. Percolation was continued at a pore velocity of 100 cm/d. Samples were taken in regularly intervals according to movement of frontal filtrate fraction. Redox potential was –190 mV in the effluent of the column at 110 cm.

Table 31 Retention of somatic coliphage 241 in the laboratory column of UBA at a pore velocity of 100 cm/d under anaerobic conditions

sampling sites (cm)	Cumulative breakthrough ratio*	Retention (log)	Δ log Retention+ (heterogeneity)	Specific retention (Δ log) / cm	λA (log.h-1)*
0,3	0,2	0,7	0,7	0,02	0,22
0,5	0,1	1	0,3	0,01	0,18
0,7	0,1	1	0	0,005	0,14
0,9	0,1	1	0	0,005	0,12
1,1	0,05	1,4	0,4	0,01	0,12

* Calculation by integrative balancing virus concentrations in influent and filtrate samples,
+ Retention of phages between two neighbours sites, λA : elimination rate coefficient

Initial concentration of inoculated E. coli A was about 8.10^9 pfu/100 ml. Relatively high concentrations were detectable in all frontal fractions of percolating water at all sampling sites. Following this early breakthrough, concentrations of E. coli A were highest in the next two or three filtrate fractions at all sampling sites. In further filtrate samples, E. coli A concentrations decreased slightly to detection limit (Figure 13).
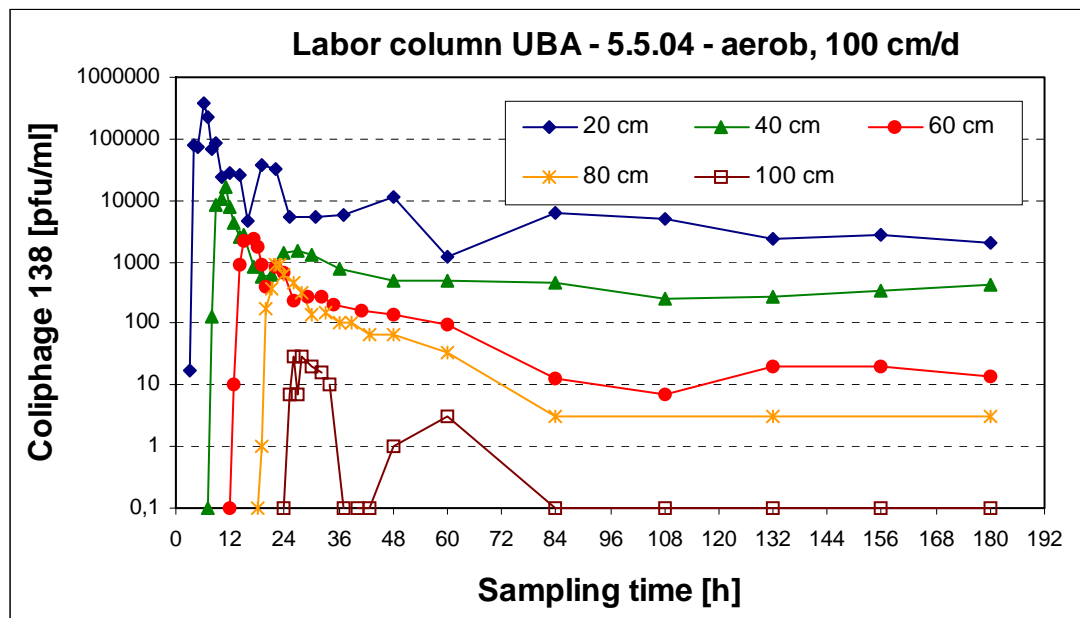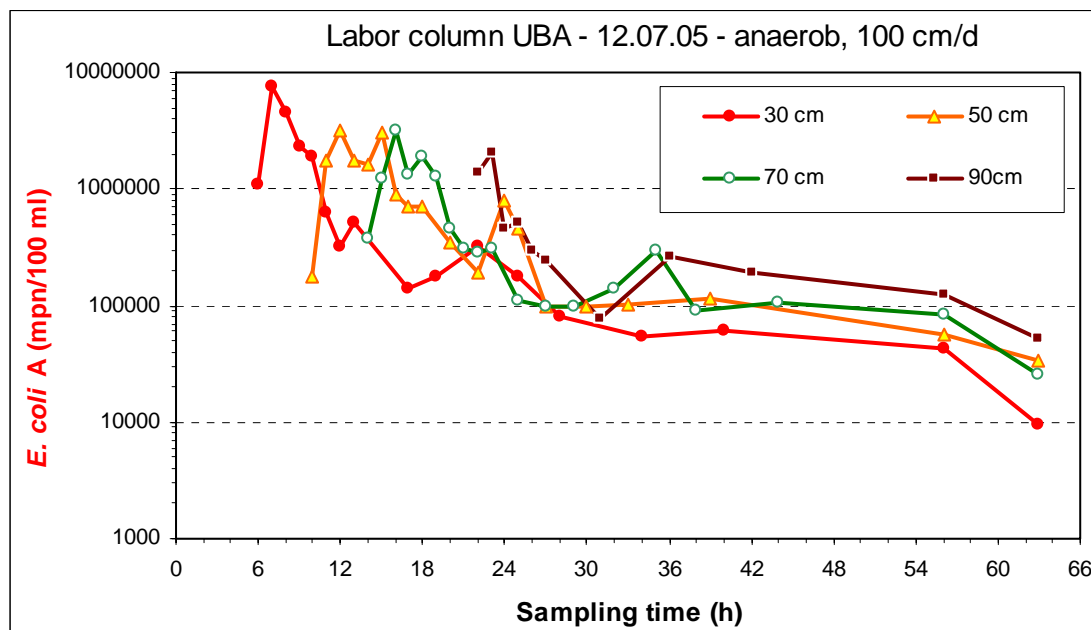

Figure 13: Concentrations of E. coli A in the laboratory column of UBA at a pore velocity of 100 cm/d under anaerobic conditions (Input of E. coli A: 8,3.109 pfu/100ml, not demonstrated)

Relatively high breakthrough ratios were calculated for all sampling sites compared to aerobic conditions. Cumulative breakthrough ratios were 0,5 in the upper filter path of 50 cm;

0,4 at 70 cm; and 0,2 at 90 cm depth (Table 32). Elimination rate coefficients were similar (0,07 log.h^{-1}) at all filter paths of this anaerobic filter column.

Table 32: Retention of E. coli A in the laboratory column of UBA at a pore velocity of 100 cm/d under anaerobic conditions

sampling sites (cm)	Cumulative breakthrough ratio*	Retention (log)	Δ log Retention+ (heterogeneity)	Specific retention (Δ log) / cm	λA (log.h-1)*
0,3	0,5	0,3	0,3	0,009	0,08
0,5	0,5	0,3	0	-	0,06
0,7	0,4	0,5	0,2	0,006	0,06
0,9	0,2	0,6	0,1	0,009	0,07

* Calculation by integrative balancing virus concentrations in influent and filtrate samples,
+ Retention of phages between two neighbours sites, λA : elimination rate coefficient

Concentration of E. faecium was about 6.109 mpn/100 ml in the inoculated culture suspension. Synchronic with the frontal fraction of percolating water, E. faecium was detected in all filtrate samples at all sampling sites (Figure 14). Highest concentrations were found in the following filtrate fractions within one hour.
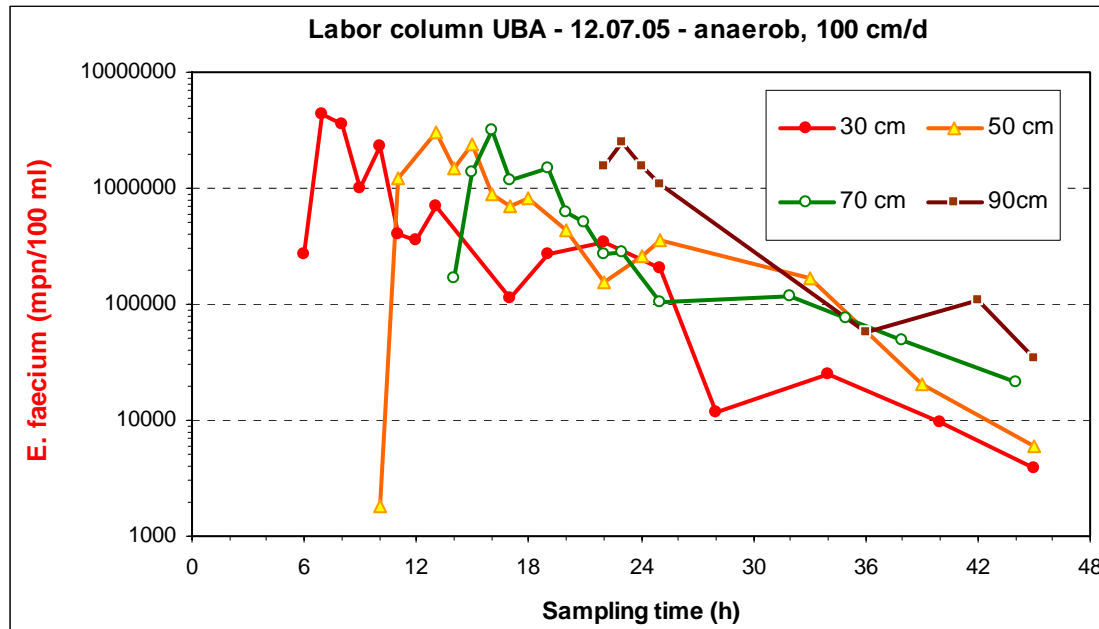
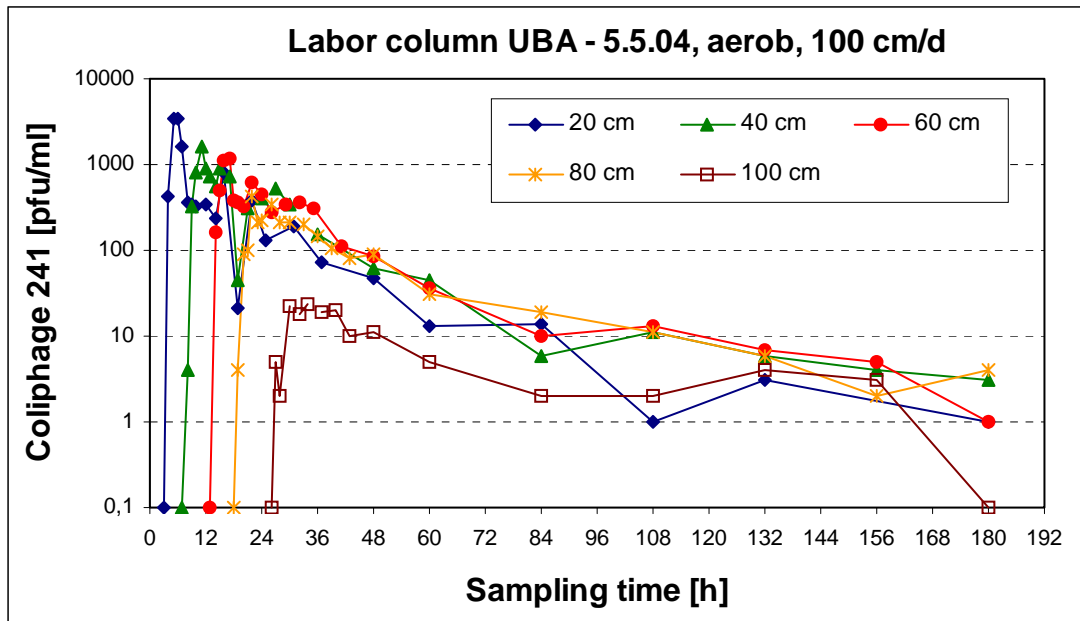**Figure 14: Concentrations of E. faecium in the laboratory column of UBA at a pore velocity of 100 cm/d under anaerobic conditions (Input of E.faecium: 6,7.109 pfu/100ml, not demonstrated)**

Retention of E. faecium was even lower under anaerobic conditions compared to aerobic conditions. High relative breakthrough ratios of intestinal enterococci were determined at all

sampling sites: 0,5 at 30 cm; 0,6 at 50 cm; 0,4 at 70 cm; 0,3 at 90 cm; and 0,2 at 110 cm (Table 33). Log-retention over the whole column was only 0,7 log units. Specific retention was 0,01 log/cm over the whole length of the filtration path. An elimination rate coefficient of 0,09 log.h^{-1} was calculated for the surface layer while it was about 0,06 log. h^{-1} in the further filtration paths of the column.

Table 33: Retention of E. faecium in the laboratory column of UBA at a pore velocity of 100 cm/d under anaerobic conditions

sampling sites (cm)	Cumulative breakthrough* (log)	Retention (log)	Δ log Retention+ (heterogeneity)	Specific retention (Δ log) / cm	λA (log.h-1)*
0,3	0,5	0,3	0,3	0,01	0,09
0,5	0,6	0,3	0	-	0,05
0,7	0,4	0,4	0,1	0,01	0,06
0,9	0,3	0,6	0,2	0,01	0,06
1,1	0,2	0,7	0,1	0,01	0,06

* Calculation by integrative balancing virus concentrations in influent and filtrate samples,
+ Retention of phages between two neighbours sites, λA : elimination rate coefficient

4.2 Experiments with the clogging column (FU-Berlin)

The aim of this experiment was to test adsorption and transport behaviour of test coliphages in a native and non destroyed sandy soil column from a lake basin consisting of natural layers of filter matrix.

Addition of bacteria was not possible in this experiment due to concerns about possible interactions between the bacteria and the trace chemicals added by the "chemical group".

4.2.1 Materials and methods

A filtration column was prepared with non destroyed sandy soil taken directly in an acryl glass cylinder from the bottom of Lake Wannsee.

After placing horizontal drain tubes in this plexi glass column at different depths, it was percolated with surface water from Lake Wannsee at a pore velocity of 100 cm/d. The length of the column was 100 cm. Seven drain tubes enabled continuous sampling at different sampling sites of the filter matrix using a multi canal peristaltic pump. Consecutive filtrate samples (à 3 ml) were continuously pumped out from each drain tube within a percolation time of 12 h and separately collected by means of an auto sampler over 6 weeks. Samples were taken from the reservoir and the drain tubes at 4, 12, 25, 50, 60 80 and 90 cm as well

as from the total outlet at 100 cm, respectively. (Fig. x, Chapter X). Samples were daily analysed.

Culture suspensions of the test coliphages F+ phage 138, and somatic phage 241 were added to the reservoir filled with 10 L of lake water. The reservoir was weakly refilled with lake water and inoculated with both phage cultures at the same concentrations.

4.2.2 Results

Initial concentrations of F+ phage 138 in the input varied between $1,1.10^4$ and $5,7.10^4$ pfu/ml during the operation time of two weeks. F+ phages were detected in all filtrate samples at 4 cm depth. Phages were not detected in filtrate samples at 25 cm and only very sporadically in filtrate samples at 12 cm. Phage concentrations increased to 480 pfu/ml in the filtrate sample at 4 cm after 12 h. Concentration varied synchronic with the concentrations in the water reservoir (Figure 15). Retention of F+ phage was very high. A log-retention of 2,7 log units was calculated within the top 4 cm of the filter bed. Retention of F+ phage was at least 4 log units within the upper 12 cm. Correspondingly, the highest elimination rate coefficient was found in the surface layer of 4 cm (6,4 log. h^{-1}) which decreased to 3,1 log.h^{-1} within a filter path of 12 cm (Table 34).
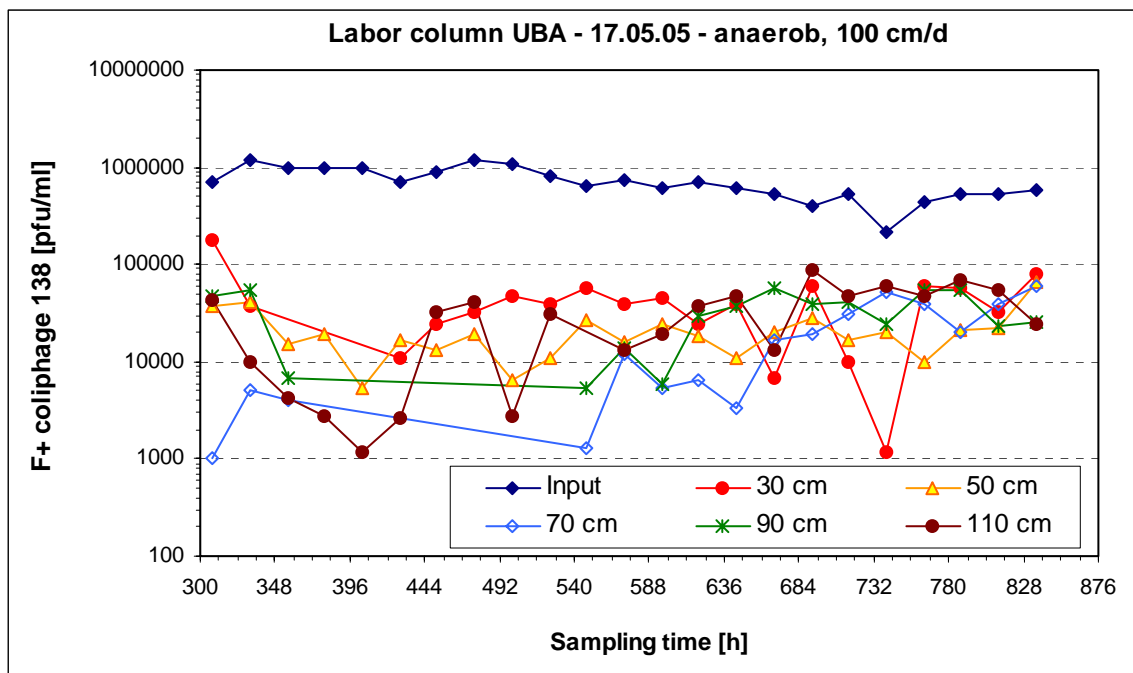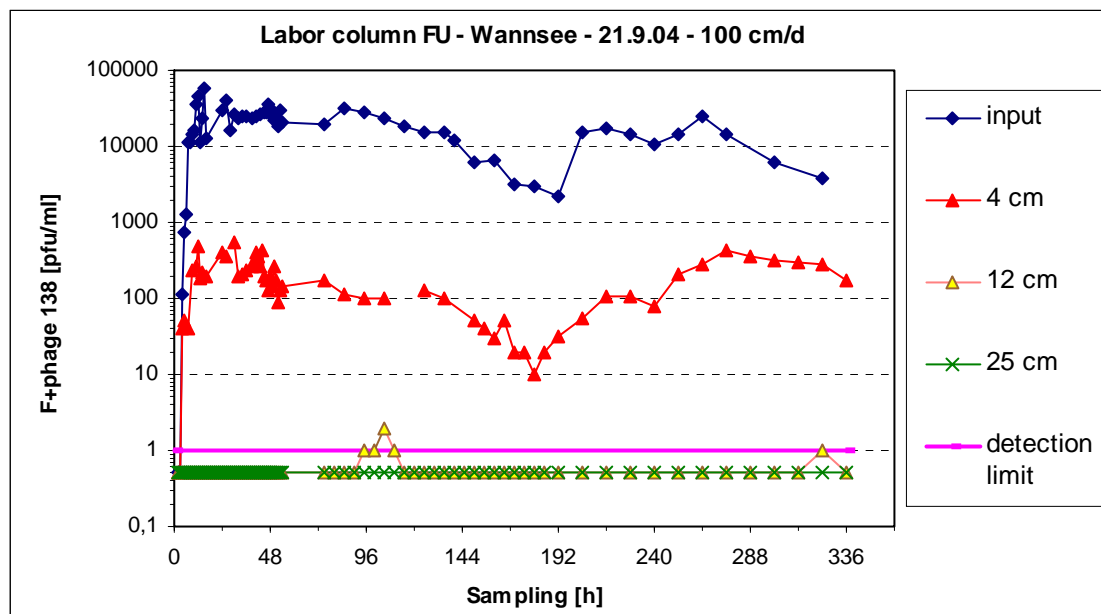

Figure 15 Concentrations of F+phage 138 in the laboratory column of FU Berlin at a pore velocity of 100 cm/d under aerobic conditions

Table 34 Retention of test coliphages in the laboratory column of the FU-Berlin (Pore velocity; 100 cm/d; filter path 100 cm, 21.9 – 1.11.2004)

Test organisms	sampling sites (cm)	Break-through ratio*	Retention (log)	Δ log Retention+ (heterogeneity)	Specific retention (Δ log) / cm	λA (log.h-1)*
F+ phage	4	0,002	2,7	2,7	0,67	6,4
138	12	< 0,0001	> 3,9	> 1,2	> 0,15	3,1
somatic	4	0,08	1,1	1,1	0,28	2,7
phage 241	12	< 0,00006	> 4,2	> 3,1	> 0,39	3,4

* Calculation by integrative balancing virus concentrations in influent and filtrate samples,
+ Retention between two neighbours sites, λA : elimination rate coefficient

Initial concentrations of somatic phage 241 ranged from $1,9.10^4$ to $4,6.10^4$ pfu/ml during the continuous inoculation of the filter column for two weeks (Figure 16). Coliphages were detected in all filtrate samples from the first drain tube at 4 cm in concentrations around 1000 pfu/ml. Phages were only very sporadically detected at the second sampling site at 12 cm. No phages were detected in the filtrate samples at 25 cm. Log-retention was relatively high and increased from 1,1 log units in the upper 4 cm to more than 4 log units within the upper 12 cm. (Table 34). Correspondingly, high elimination rate coefficients were found in both filter layers (2,7 and 3,4 $log.h^{-1}$).
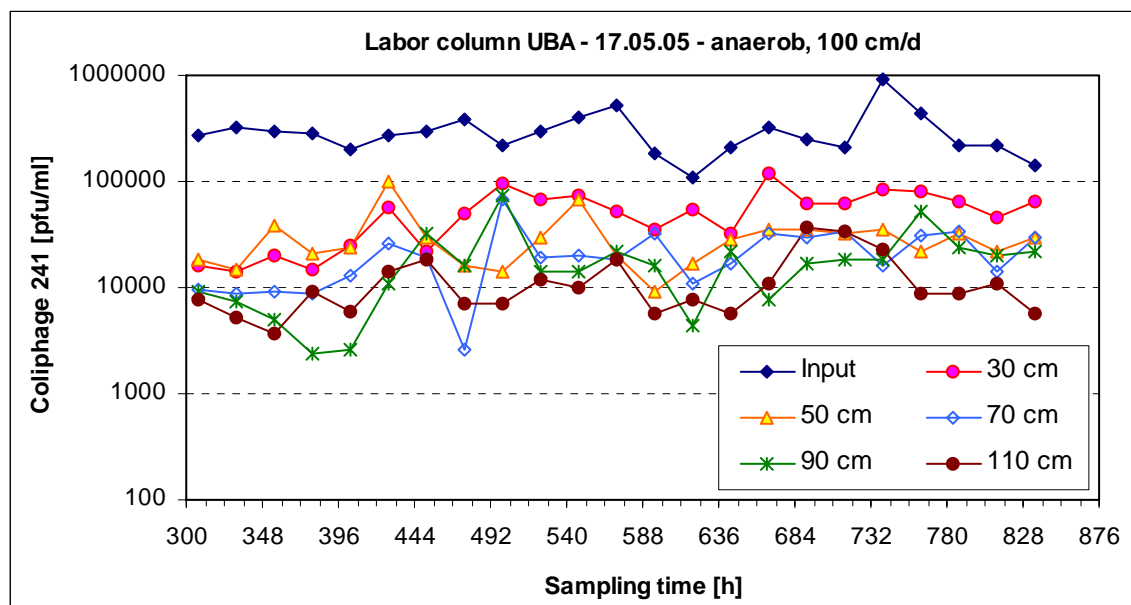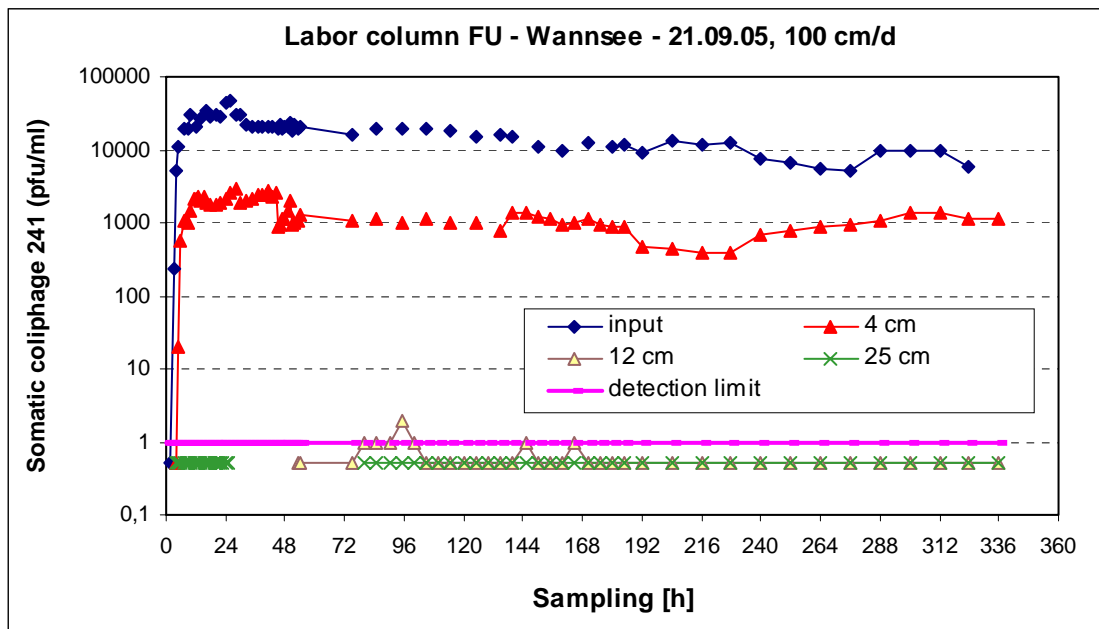

Figure 16: Concentrations of somatic coliphage 241 in the laboratory column of FU Berlin at a pore velocity of 100 cm/d under aerobic conditions

4.3 Experiments with the column system (TU-Berlin)

Columns operated at different temperatures were used to study the effect of temperature on phage retention.

Addition of bacteria was not possible in these experiments due to concerns about possible interactions between the bacteria and the trace chemicals added by the "chemical group".

4.3.1 Materials and methods

Three acryl glass columns, each of them with a length of 50 cm and a diameter of 10 cm were filled with sandy soil and saturated with water from Lake Tegel. Each column was placed in an incubator at a temperature of 5°C, 15°C and 25°C, respectively. Retention of test coliphages was tested at a pore water velocity of 30 cm/d at three different temperatures. Phages were added to the water reservoir of the columns. This enabled a continuous inoculation of the columns. Samples were taken daily from the input and the effluent of the columns.

4.3.2 Results

Input concentrations of F+ phage 138 varied between 1.10^4 and 8.10^4 pfu/ml during the total operation time of 6 weeks. At a temperature of 5 °C, F+ phages appeared in filtrate fraction after three days. The first breakthrough at 15 °C and 25 °C was observed in filtrate fractions after 4-5 days (Figure 17).

Relatively high amount of F+ phages broke through the filter column at 5°C. Breakthrough ratio reached the highest level of 0,15 in the filtrate fraction at day 7 (Figure 17). During further operation time, the retention of F+ phages moderately increased resulting in a lower breakthrough ratio of 0,02 which remained stabile at this order of magnitude up to end of the experiment. Mean breakthrough ratio of samples from 12th to 42th day was calculated 0,02 (Table 35).

At 15° and 25°C, F+ phage was detected in low concentrations in the filtrate during the first 12 days. This resulted in a high log-retention of more than 4 log units. After two weeks, breakthrough of phages increased, and the log-retention declined to about 3 log units. In the further run of the experiment, retention of phages was very variable resulting in log-retentions of 3-5 log units.
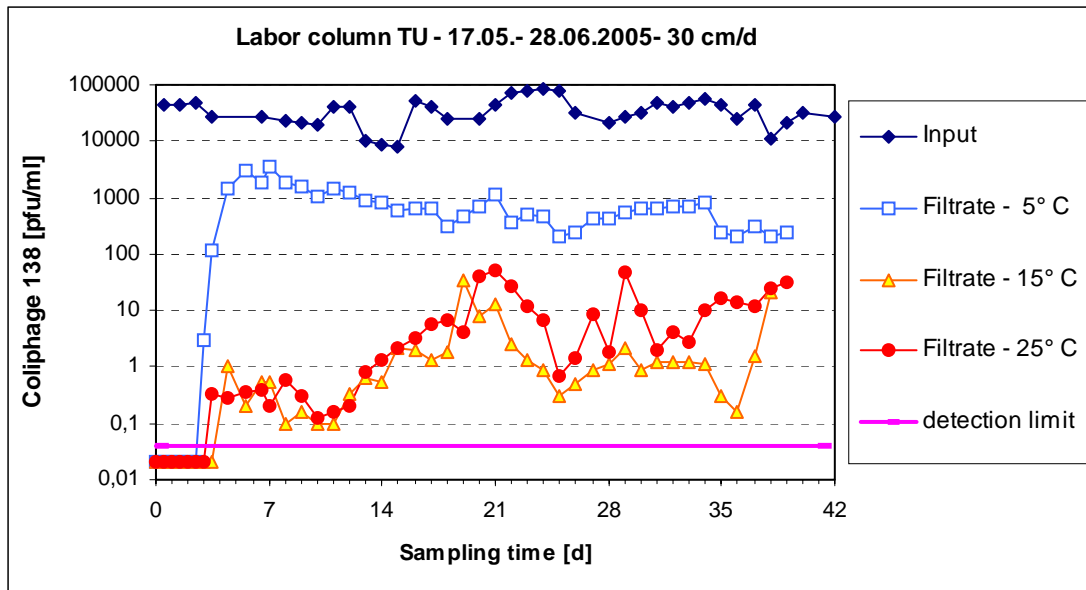
Figure 17: Effect of temperature on retention of F+phage 138 in the laboratory column of TU Berlin at a pore velocity of 100 cm/d under aerobic conditions

Taking into account all results of experiment during last 4 weeks all results of the experiment during 4 weeks the mean retention ratio of F+phage at 5°C was 1,7 log units corresponding to an elimination rate coefficient of 0,6 log.h-1. Retention ratios averaged 3,4 log units at 25°C and 3,8 log units at 15°C (Table 35). Both specific retention and elimination rate coefficient were slightly higher at 15°C than at 25°C.

Table 35: Retention of coliphages by slow sand filtration in dependence on temperature in laboratory column of Technical University Berlin (Pore velocity; 30 cm/d; filter path 50 cm; 29.5 – 28.6.2005)

Phages	Temperatur (°C)	Breakthrough ratio*	Retention (log)	specific retention (log/cm)	λ^* (log . h-1)
F+ coliphage 138	5	0,02	1,7	0,03	0,57
	15	0,0002	3,8	0,08	1,30
	25	0,0004	3,4	0,07	1,16
somatic coliphage 241	5	0,2	0,8	0,02	0,26
	15	0,01	2,0	0,04	0,70
	25	0,003	2,5	0,05	0,86

* Calculation by integrative balancing virus concentrations in influent and filtrate samples,
+ Retention of phages between two neighbours sites, λA: elimination rate coefficient

The concentration of somatic coliphage 241 in the water reservoir was relatively constant ranging from $1{,}6.10^4$ to $5{,}6.10^4$ pfu/ml. Phage 241 occurred at first in the filtrate fraction which was collected at day 3 at 5°C and at day 4 at 15°C and 25°C. The breakthrough ratio of phage 241 increased rapidly, and remained at a mean ratio of 0,2 up to the end of the experiment (Figure 18, Table 35).
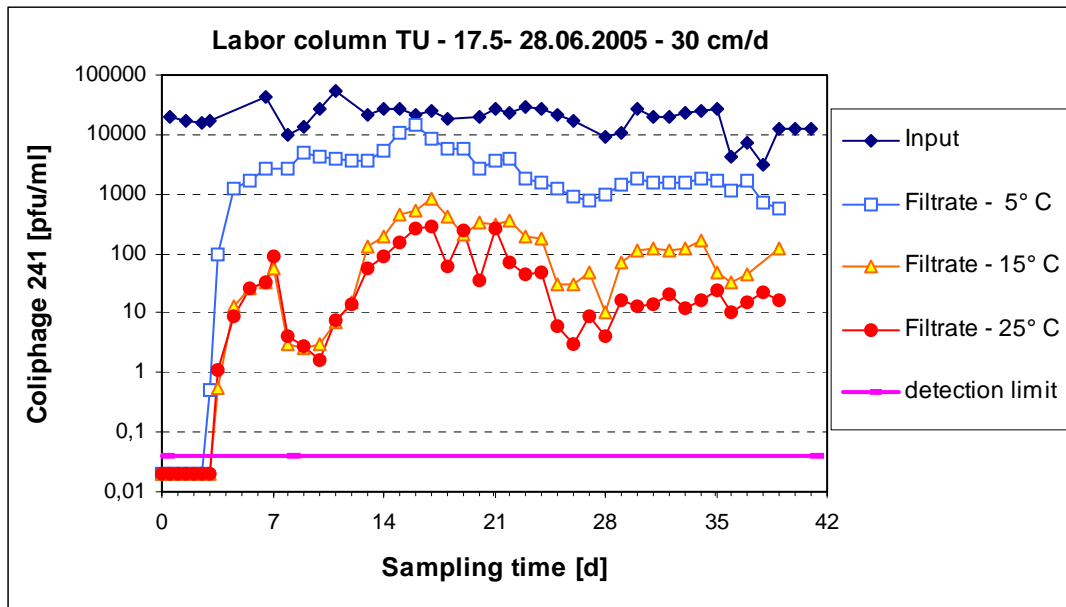
Figure 18: Effect of temperature on retention of somatic coliphage 241 in the laboratory column of TU Berlin at a pore velocity of 100 cm/d under aerobic conditions

At 15°C and 25°C, breakthrough of phage 241 was significantly less than at 5°C. Based on the results from 12 up to 42 d, mean retention ratios of phage 241 were 2,2 logs at 15°C and 2,6 logs at 25°C, respectively (Table 35).

4.4 Long filtration column (UBA)

Simultaneous addition of coliphages and bacteria was not possible in the experiments with the long column due to concerns about possible interactions between the bacteria and the trace chemicals added by the "chemical group".

4.4.1 Materials and Methods

For test organisms, sampling, cultivation and detection see chapters "Enclosure" and "Slow Sand Filtration Pond". For assessment of retention, relative breakthrough ratio was calculated through the quotient of phage concentrations in each fraction of filtrate and input samples. The mean value of all fractional breakthrough ratios was used for further calculation as described previously.

In the first experiment under aerobic conditions somatic coliphage 241 was directly injected in the input tube as sluggish pick. The amount of phage 241 in this inoculum was used as basis for calculation of phages broke through the column at different sampling sites. In comparison to this approach, densities of phage 241 in the filtrate samples from 20 cm depth were taken as basis for calculation breakthrough ratio in deeper sampling sites.

The long sandy soil column - for simulation of ground water stream in an aquifer for 50 d - was inoculated with both coliphages and percolated continuously with water from Lake Tegel.

Percolation rate of lake water was adjusted to 0,5 L/h corresponding to a filtration velocity of 33 cm/d or a pore water velocity of 100 cm/d for about 4 weeks (see Chapter xx). After four weeks the flow rate was increased to 4 L/h (pore water velocity 800 cm/d) for two weeks and to about 12 L/h for 3 weeks (pore water velocity 24 m/d). Subsequently, percolation of the column was continued at a flow rate of 100 cm/day for further 8 months (see 1.4).

In the year 2005 the long filter columns were operated under "anoxic" conditions (see 1.4). Experiments were carried out with coliphages at a pore velocity of 100 cm/d for 3 months.

4.4.2 Results

4.4.2.1 Short term experiment during 35 days

Somatic coliphage 241 was added as a peak whereas F+phage 138 was continuously added to the column. To achieve this, a suspension (500 ml) of coliphage 241 was directly inoculated into the inlet of the column within 30 minutes. A suspension of coliphage 138 was added into the lake water reservoir of 500 L. Sampling was carried out daily from the water reservoir and all drain tubes of the first column (20 cm, 40 cm, 80 cm, 160 cm, 340 cm and 500 cm).

At a pore velocity of 100 cm/d, the following percolation times are calculated for each filtration path: 16 h for 20 cm, 32 h for 40 cm, 64 h for 80 cm, 5 days for 160 cm, 11,3 days for 340 cm and 16,6 days for 5 m.

Inoculation of the lake water reservoir with a suspension of F+ phage 138 resulted in an initial concentration of 2 x10 5 pfu/ml which decreased to 550 pfu/ml after 35 d percolation time (Figure 19). At 20 cm and 40 cm, F+ phage 138 was found in relatively high concentrations of about 300 pfu/ml already at the second day. The first breakthrough of phage 138 at 80 cm and 160 cm, was observed at the days 3 and 7, respectively.
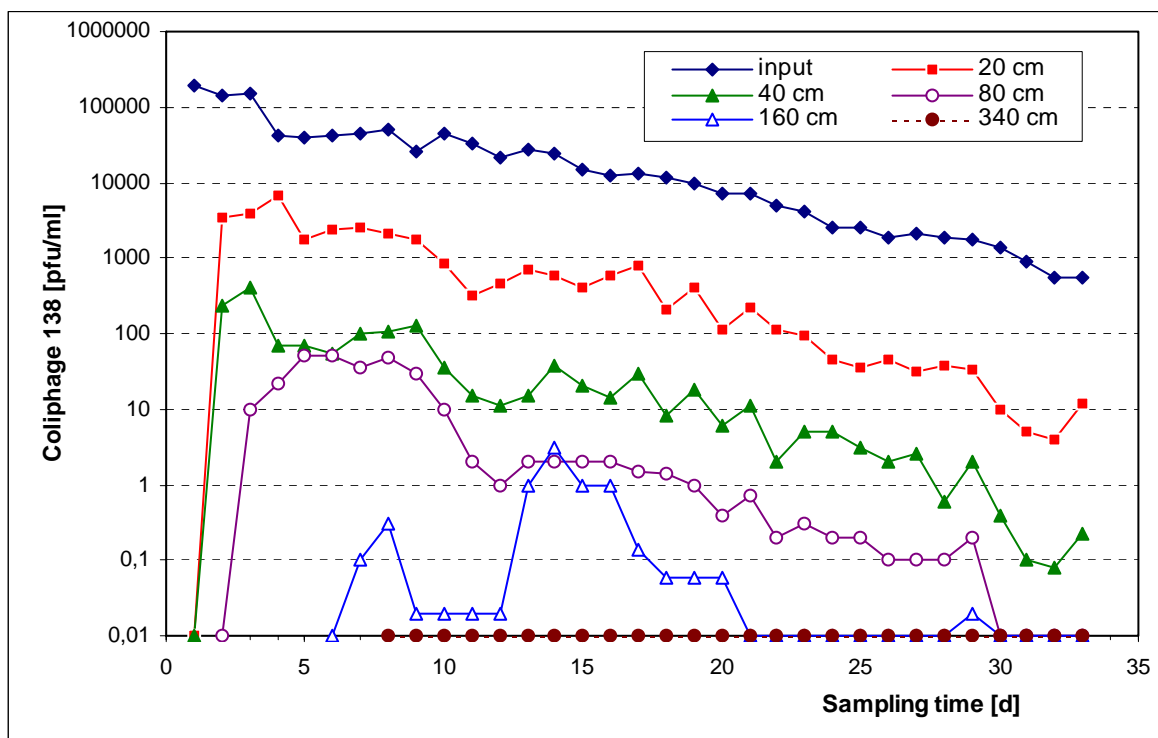
Figure 19: Concentration of coliphage 138 in different levels of the sandy soil column at a pore velocity of 100 cm/d; detection limit = 0.01 pfu/ml

After 35 d, the concentration of coliphage 138 was about 10 pfu/ml at 20 cm and less than 1 pfu/ml at 40 cm. At 80 cm and 160 cm coliphage 138 was no longer detected in 100 ml of samples collected after 30 d (Figure 19). No coliphage 138 was found at 340 cm during the entire experiment.

Breakthrough of phages in each fraction was calculated through integrative balancing virus concentrations in influent and filtrate samples (Table 36). During an operation time of 35 days, breakthrough ratios were 0,03 at 20 cm and 0,0003 at 80 cm depth (Figure 20, Table 36). Adequately, removal of F+ phage was found 1,5 log units within the upper 20 cm, 2,8 log units within 40 cm and 5,1 log units within 160 cm. Results of specific retention (log/cm) suggested that the removal of F+phage was not homogenous in all section of the filter matrix. Highest specific retention factor of 0,08 log.cm^{-1} was detected in the surface layer of 20 cm which clearly diminished with increasing filter path and amounted to 0,02 log.cm^{-1} within 40 and 160 cm.
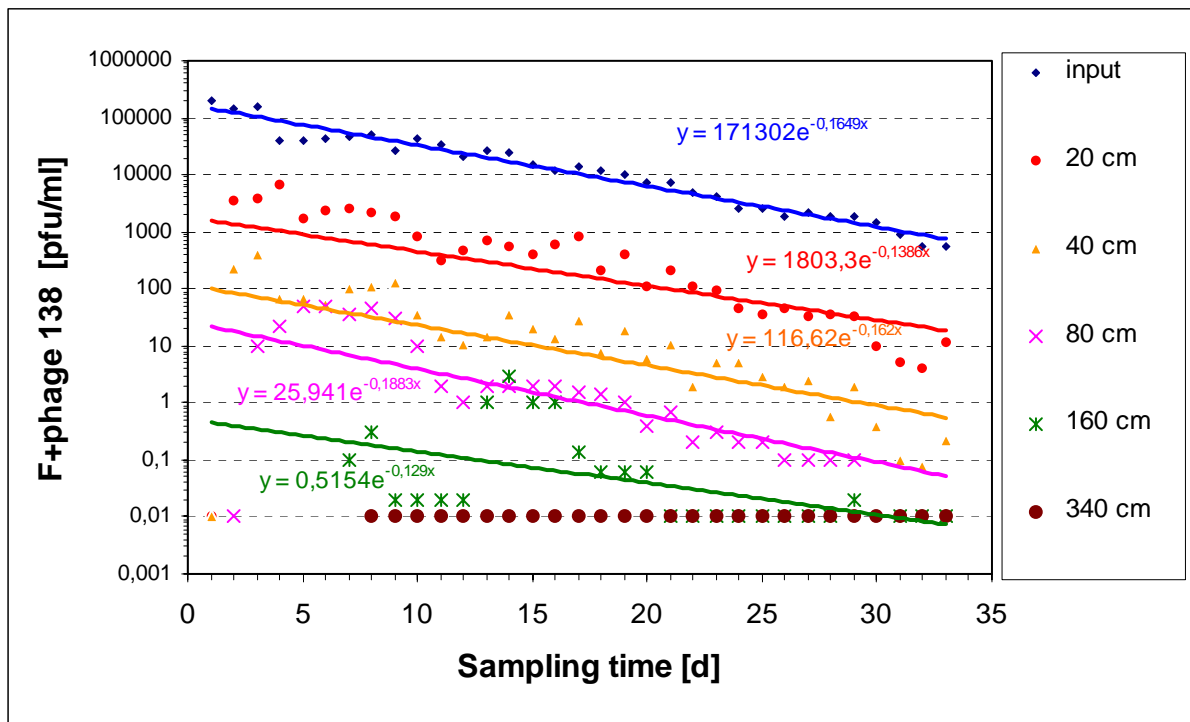
Figure 20 : Regression lines of F+phage 138 in different levels of the sandy soil column at a pore velocity of 100 cm/d

Correspondingly, the highest elimination rate coefficient (λ) was calculated as 0,72 log.h^{-1} in the upper 20 cm. In deeper parts of the filter λ-values decreased clearly to 0,3 log.h^{-1} at 160 cm (Table 36).

Table 36: Retention of F+ coliphage 138 in the long sandy soil column at a pore velocity of 100 cm/d.

Sampling sites (cm)	Breakthrough ratio*	Retention (log)	Δ log Retention+ (heterogeneity)	Specific retention (Δ log) / cm	λA (h-1)*
20	0,03	1,5	1,5	0,08	0,72
40	0,001	2,8	1,3	0,07	0,68
80	0,0003	3,6	0,7	0,02	0,42
160	0,00001	5,2	1,6	0,02	0,31
340	-	-	-	-	-

* Calculation by integrative balancing virus concentrations in influent and filtrate samples,
+ Retention of phages between two neighbours sites, λA : elimination rate coefficient

Additionally, regression lines were fitted for phage concentrations measured in samples from each sampling site (Figure 20). Interception point of these regression lines (a values) were also used for determination of breakthrough and retention of phages at each filter path tested (Table 37). Similar breakthrough ratios were estimated as detected by integrative balancing of virus densities (Table 36 and Table 37).

Table 37: Calculation of breakthrough and retention ratios of F+phage 138 using regression lines (Fig. 2) from each sampling sites

Sampling sites (cm)	a (pfu/ml)	log a	Breakthrough ratio*	Retention (log)	Δ Retention+ (Δ log a)	Specific retention (Δ log) / cm	λB (log.h-1)**
input	171302	5,2	-	-	-	-	-
20	1803	3,4	0,01	2	2	0,10	0,95
40	117	2,1	0,0007	3,2	1,2	0,06	0,76
80	26	1,4	0,0002	3,8	0,6	0,02	0,46
160	0,5	-0,3	0,000003	5,5	1,7	0,02	0,33
340	-	-	-	-	-	-	-

a: interception point of each regression line; *) Calculation through the relation of a values
+) Retention of phages between two neighbours sites; λB: elimination rate coefficient

The concentration of somatic coliphage 241 in the stock suspension was 5,8 x 10^{7} pfu/ml corresponding to a total peak inoculum of 2,9 x 109 pfu (500 ml). Somatic phages broke through the upper filter paths of 20 and 40 cm already in the first day of operation, and detected at deeper filter sections time delayed e.g. after 6 d at 160 cm, and after 9 d at 340 cm. Less concentrations of phage 241 were found in effluent of the first column (500 cm) after 23 d. No phage was detectable in the second column at a filter path of 660 cm (Figure 21).
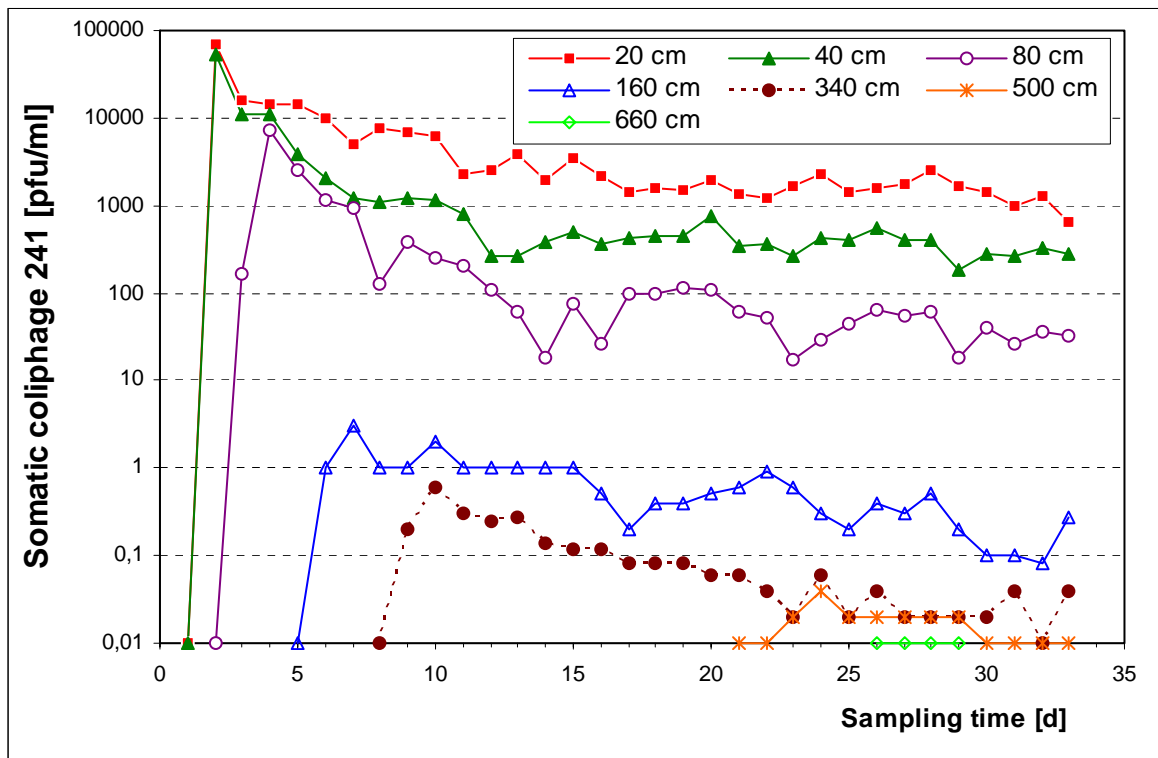
Figure 21: Concentration of somatic coliphage 241 in different levels of the sandy soil column at a pore water velocity of 100 cm/d (detection limit = 0,01 pfu/ml)

In a first attempt, the total amount of phages in the inoculum was used as basis for estimation of breakthrough and retention ratio of phages in filter matrix (Table 38). In comparison with F+phage 138, migration of somatic phage 241 in the column was relatively high. Breakthrough ratios were 0,08 within 20 cm and factor 0,006 within 80 cm (Table 38, Figure 21). Nevertheless, specific retention factor of phages in the surface filter path of 20 cm was clearly higher (0,06 log/cm) than in the filter path between 20 and 80 cm (0,02 log/cm). Log-retention of somatic phage 241 was 5, 6 or 7 log units in the deeper filter paths within 160, 340 or 500 cm, respectively. A relatively high specific retention of 0,04 log/cm was found only in the filter path between 80 and 160 cm. Significantly less specific retention was calculated for the deeper filter passages from 160 cm to 500 cm.

Correspondingly, the highest elimination rate coefficient λ (0,53 log.h^{-1}) was detected in the surface filter layer of 20 cm. Virus elimination remained at about 0,3 log.h^{-1} between 20 and 160 cm, and clearly declined in deeper filter paths to 0,13 log.h^{-1} between 340 and 500 cm (Table 38).

Table 38: Retention of somatic coliphage 241 in the long sand filtration column at a pore velocity of 100 cm (Inoculum concentration of phages was taken as 1)

Sampling sites (cm)	Breakthrough ratio*	Retention (log)	Δ log Retention+ (heterogeneity)	Specific retention (Δ log) / cm	λA (h-1)*
20	0,08	1,1	1,1	0,06	0,53
40	0,04	1,4	0,3	0,02	0,34
80	0,006	2,2	0,8	0,02	0,27
160	0,00001	5,1	2,9	0,04	0,30
340	0,000001	6	0,9	0,005	0,17
500	0,0000001	7,0	1,1	0,007	0,13

*) Calculation by integrative balancing virus concentrations in influent and filtrate samples,
+) Retention of phages between two neighbours sites, λA : elimination rate coefficient)]

As a second way for calculating virus retention in the filter column, we used the virus concentrations in filtrate samples from the first drain tube at 20 cm as basic input values which were continuously measured during the operation time of 35 days. In comparison to the first calculation model (Table 38), we found a relatively high breakthrough ratio of 0,28 in the upper filter path between 20 and 40 cm (Table 39). Removal of phages was relatively homogenous in a filter path between 20 and 160 cm with relatively stable specific log-retentions varying only between 0,02 and 0,03 log.h⁻¹. In contrast, log-retention was significant less (0,005 log/cm) in deeper filter paths up to 500 cm.

Adequately, relative high elimination rate coefficient was found in upper filter matrix between 40 and 160 cm ranging from 0,19 to 0,29 log.h⁻¹. Virus elimination rate declined to 0,13 or 0,11 log.h⁻¹ in a filter path of 320 or 480 cm, respectively (Table 39).

Table 39: Integrative balancing of the migration and retention of somatic phage 241 by slow sand filtration at a pore velocity of 100 cm (concentrations of phages in filtrates from 20 cm were taken as 1)

Sampling sites (cm)	Breakthrough ratio*	Retention (log)	Δ log Retention+ (heterogeneity)	Specific retention (Δ log) / cm	λA (h-1)*
20	-	-	-	-	-
40	0,28	0,6	0,6	0,03	0,27
80	0,06	1,2	0,6	0,02	0,19
160	0,0002	3,6	2,4	0,03	0,25
340	0,00003	4,5	0,9	0,005	0,13
500	0,000004	5,3	0,9	0,005	0,11

* Calculation by integrative balancing virus concentrations in influent and filtrate samples;
+ Retention of phages between two neighbours sites, λA : elimination rate coefficient

Breakthrough and retention ratios were also calculated by means of regression lines as demonstrated in Figure 22. Results of both calculation approaches, integrative balancing and comparison of regression lines, resulted in similar breakthrough and retention ratios (Table 39 and Table 40.

Table 40: Calculation of breakthrough and retention ratios of somatic coliphage 241 using regression lines from each sampling sites (Fig. 5),

Sampling sites (cm)	a* (pfu/ml)	log a	Break-through ratio*	Retention (log)	Δ log Retention+ (log a)	Specific retention (Δ log) / cm	λB (h-1)*
20	14632	4,2	-	-	-	-	-
40	4300	3,6	0,29	0,5	0,5	0,03	0,25
80	850	2,9	0,06	1,2	0,7	0,02	0,30
160	3,0	0,5	0,0002	3,7	2,5	0,03	0,44
340	0,50	-0,3	0,00003	4,5	0,8	0,004	0,27
500	0,1	-1	0,000007	5,2	0,7	0,004	0,62

a: interception point of each regression line; *) Calculation through the relation of a values
+ Retention of phages between two neighbours sites; λ: elimination rate coefficient
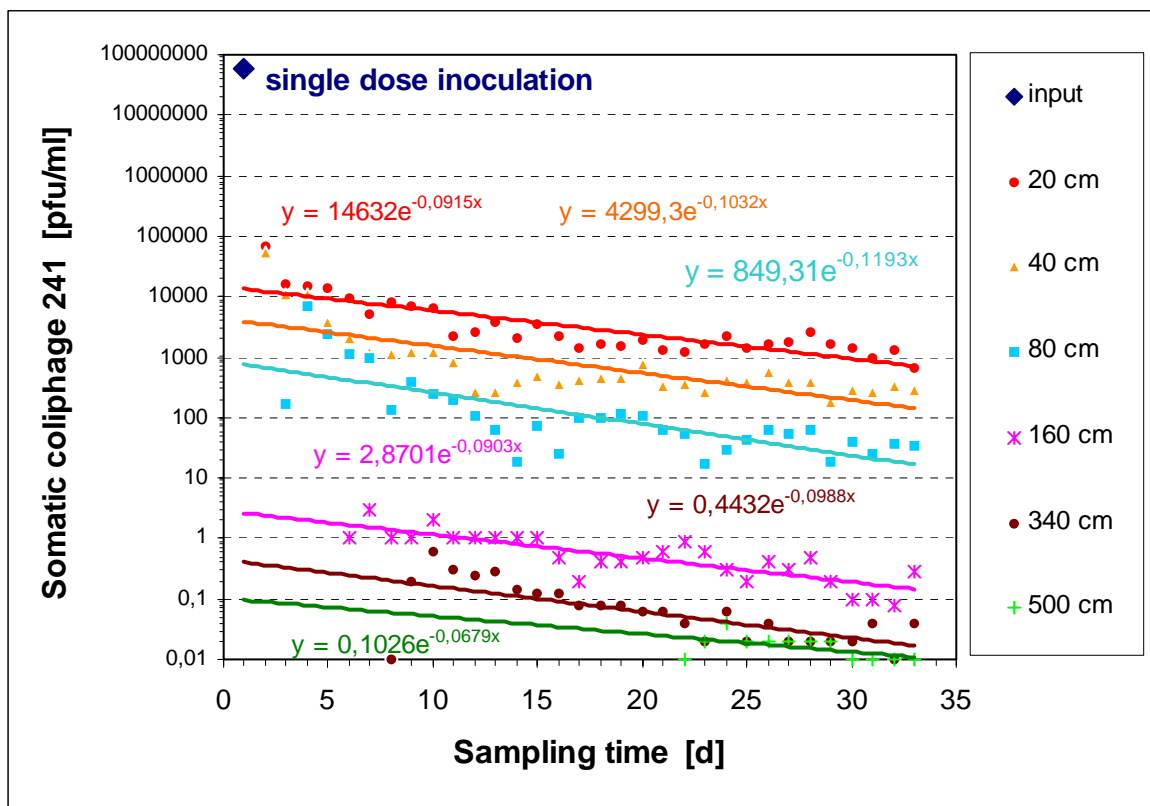
Figure 22: Regression lines of somatic phage 241 in different levels of the sandy soil column at a pore velocity of 100 cm/d

Modelling approach for determination of retention factor and deactivation rate coefficient (λC) of both test organisms will be separately reported by modelling group.

4.4.2.2 Effect of long term percolation on the migration of coliphage 241

Percolation of the sandy soil column with lake water was continued at a flow rate of 100 cm/d for 8 months without further inoculation of test coliphages in the column. Sampling was carried out weekly from 7.4.03 up to 7.12.03 from all drain tubes of the first column (20 cm, 40 cm, 80 cm, 160 cm, 340 cm and 500 cm).

F+coliphage 138 was only sporadically detected in the water samples from different sampling sites of the column during this long term experiment.

Somatic phage 241 was detected in all water samples during the 8 months of investigation. Concentrations of coliphage 241 were in the range of 103 to 104 pfu/ml in water samples from 20 and 40 cm within the first months, and declined about one log unit during the experiment (Figure 23). Similar behaviour at lower concentration levels was observed for the other sampling sites of 80, 160, and 340 cm of the column. At 500 cm coliphage 241 was only sporadically detected in low concentrations up to week 27.
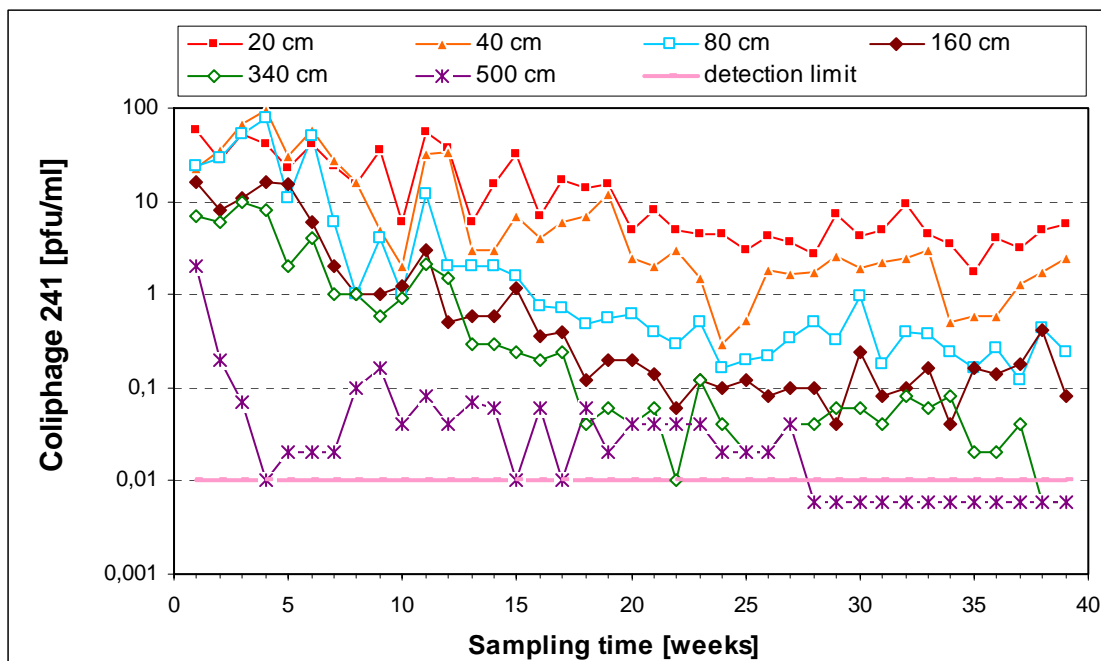
Figure 23: Concentration of coliphage 241 in the long sandy soil column during 8 months at a flow rate of 100 cm/d; detection limit: 0.01 pfu/ml

For the estimation of virus retention, the concentrations of phage 241 in samples from the first drain tube at 20 cm were taken as input values and compared with concentrations of phages at other sampling sites.

During this operation time of about 42 weeks, breakthrough ratios were 0,6 0,2 or 0,1 at the filter depths of 20, 60 or 140 cm, respectively. In deeper filtration paths at 340 cm 500 cm, breakthrough ratios were lower (0,04 and 0,01). In the upper filtration paths between 20 and 80 cm, retention of phages was relatively high with a specific retention of 0,01 log/cm. In deeper filter paths between 60 and 320 cm, relatively high virus migration was observed resulting in a low specific retention of 0,002 or 0,003 log/cm between 140 and 480 cm (Table 41) Elimination rate coefficients were 0,1 log.h^{-1} in the upper filter path up to 80 cm and slightly decreased to 0,07 log.h^{-1} within 160 cm and to 0,04 log.h^{-1} at the end of the first column (500 cm).

Table 41: Retention of somatic coliphage 241 (inoculated in the first experiment) during a further operation time of 8 months at a pore velocity of 100 cm/d

Sites (filtepaths) (cm)	Breakthrough ratio*	Retention (log)*	Δ log Retention+ (heterogeneity)	Specific retention (Δ log) / cm	λA (h-1)*
20 (-)	1	0	-	-	0,11
40 (20)	0,6	0,2	0,2	0,012	0,11
80 (60)	0,2	0,6	0,4	0,010	0,10
160 (140)	0,1	1,1	0,5	0,005	0,07
340 (320)	0,04	1,4	0,3	0,002	0,04
500 (480)	0,01	1,9	0,5	0,003	0,04

* Calculation of breakthrough and retention ratios by integrative balancing of virus concentrations in filtrate samples; virus concentrations in samples from 20 cm depth was taken as 1;
+ Retention of phages between two neighbours sites, λA : elimination rate coefficient

4.4.2.3 Effect of flow rate on migration of coliphages in the sandy soil column

After 35 d of percolation, the flow rate through the column was increased from 0,5 L/h (1 m/d) to 4 L/h (8 m/d) for the next three weeks without any additionally inoculation of the column with coliphages. Subsequently, the flow rate was further increased to 12 L/h (24 m/d) for a further 3 weeks.

The concentrations of coliphage 138 were very low after the first 35 h of operation. Nevertheless, an increase in concentration was detected at all sampling points after increase in flow rate (Figure 24). After two weeks, concentrations of coliphages 138 further decreased to values close to the detection limit. Therefore, the possible effects of a further increase in flow rate could not be detected.
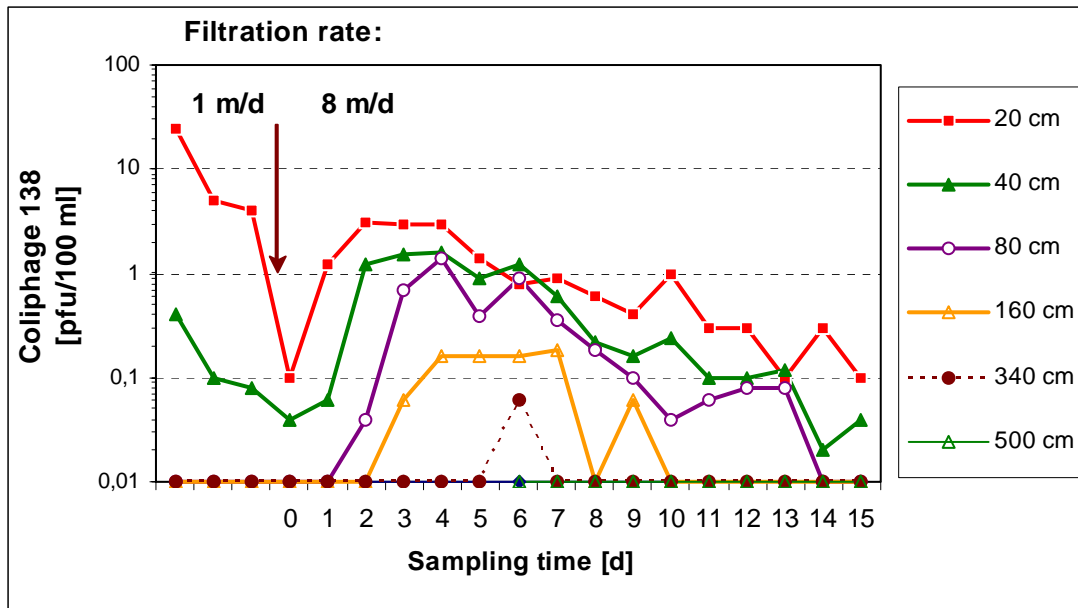
Figure 24: Concentration of F+ coliphage 138 in the sandy soil column after an increase of pore water velocity to 8 m/d.

Concentrations of coliphages 241 within the column high of 20 cm did not change by increasing the flow rate to 8 m/d (Figure 25). But migration of coliphages significantly increased in all other filtrates. At the sampling sites of 40 cm and 80 cm, coliphage 241 concentrations reached highest concentrations following a percolation of 2 and 3 days. At all other sampling sites, concentrations continuously increased up to 7 days and remained at this level until the end of experience.

A further increase in flow rate to 24 m/d did not alter the concentrations of coliphages 241 in the water samples from the drain tubes of 20, 40 and 80 cm high, but clearly induced coliphage mobilisation at a column high of 340 and 500 cm (Figure 25).
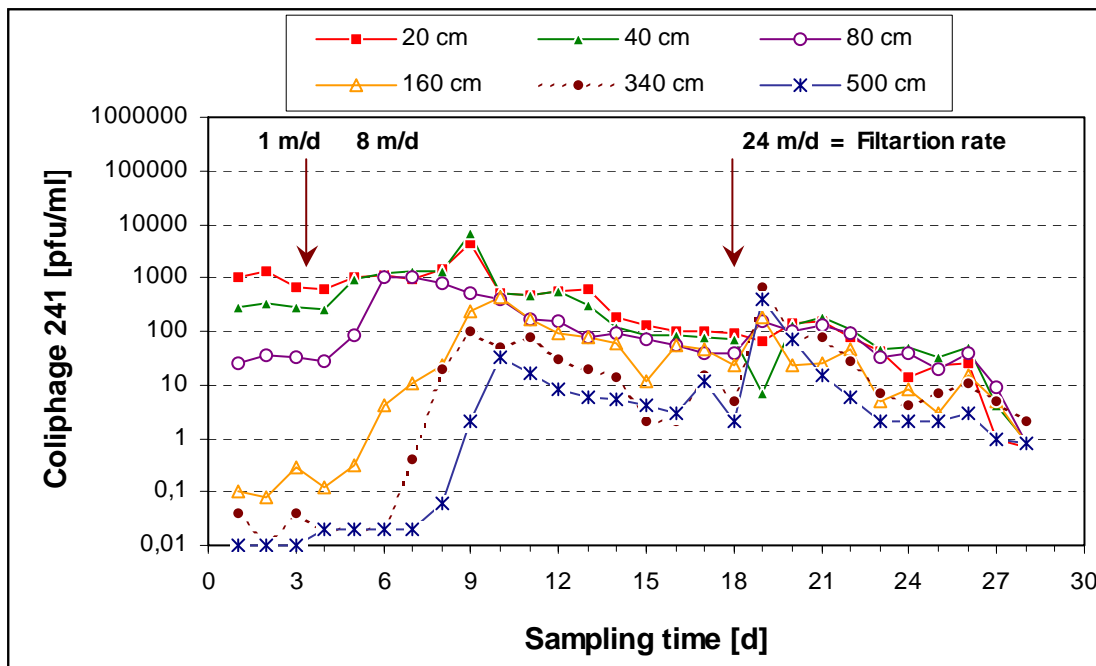
Figure 25: Concentration of coliphage 241 in the sandy soil column after increasing pore water velocity to 8 m/d and 24 m/d.

4.4.2.4 Effect of "anoxic" conditions on the retention of test coliphages

In the year 2005 reduced oxygen conditions (O2 < 0,1 mg/L) were introduced at the long sandy soil column. This was achieved by gassing the influent with nitrogen in the reservoir tank. Pore water velocity was regulated to 100 cm/d.

Both test coliphages were continuously added to the column. The initial concentration of coliphages was adjusted at different levels during the operation time of 90 days.

During the initial 7 weeks of the experiment, relatively low concentrations of F+ phage 138 were inoculated in the influent. Concentrations of phages in the influent varied between 10 and 100 pfu/ml (Figure 26). Phages were detected in all filtrate samples from 20 cm and 40 cm depth. They were sporadically detected at 80 cm depth but not in deeper sampling sites (Figure 26). Mean breakthrough ratio was 0,03 or 0,006 at 20 and 40 cm depths, corresponding to a log-retention of 1,5 or 2,2 log units, respectively (Table 42A).

Concentrations of F+ coliphage 138 were increased weakly up to 5x106 pfu/ml during the operation time between weeks 7 and 13 weeks. Phages were found in all filtrate samples up to 160 cm. In filtrates from 340 or 500 cm they did not appear before week 47 or 63, respectively (Figure 26).
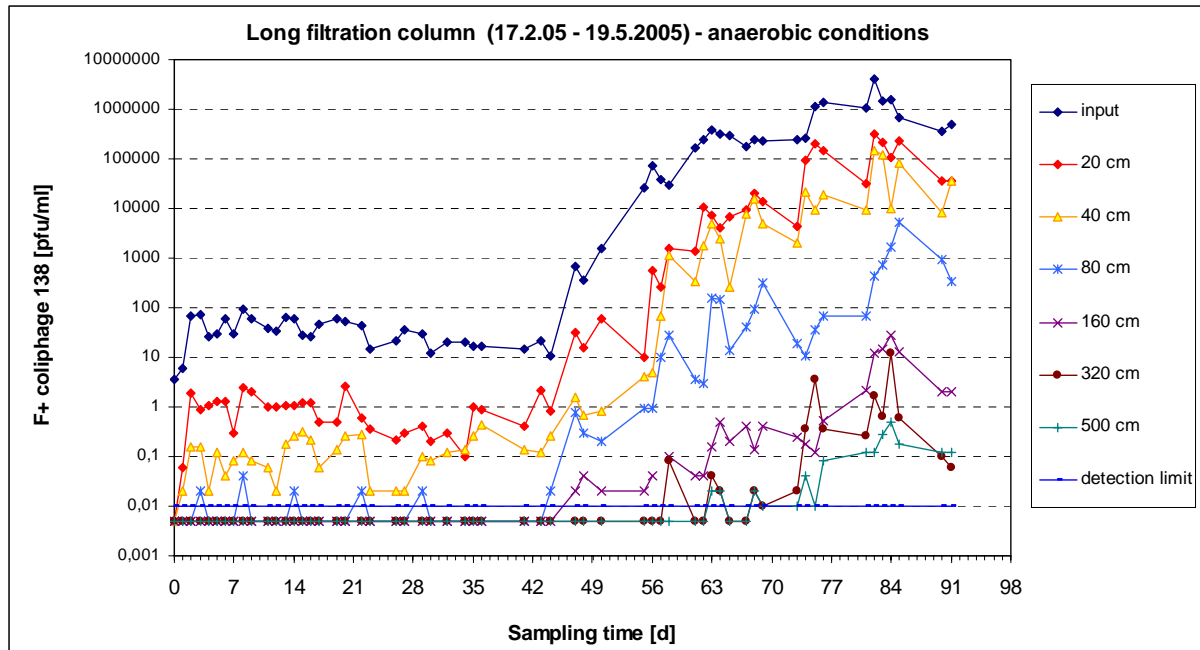
Figure 26: Concentrations of F+ coliphage 138 in influent and filtrate samples from different depths in the long column under "anoxic" conditions at a pore water velocity of 100 cm/d.

Table 42 : Retention of F+ coliphage 138 in long sandy soil column by anaoxic conditions: A. operation at low concentrations of phages in input (0-42 d)

Sampling sites (cm)	Break-through ratio	Retention (log)	Δ log Retention+ (heterogeneity)	Specific retention (Δ log) / cm)	λA (log.h-1)
20	0,03	1,5	1,5	0,08	0,72
40	0,006	2,2	0,7	0,035	0,53

+ Retention of phages between two neighbours sites, λA : elimination rate coefficient]

B. operation at high concentrations of phages in input (45-91 d)

Sampling sites (cm)	Break-through ratio	Retention (log)	Δ log Retention+ (heterogeneity)	Specific retention (Δ log) / cm))	λA (log.h-1)
0,2	0,08	1,1	1,1	0,06	0,52
0,4	0,03	1,5	0,4	0,02	0,37
0,8	0,0008	3,1	1,6	0,04	0,37
1,6	0,000004	5,5	2,4	0,03	0,33
3,4	0,000001	6	0,5	0,003	0,17
5	0,0000001	7	1	0,006	0,13

+ Retention of phages between two neighbours sites, λA : elimination rate coefficient]

Log- retention of F+phage138 was one to two log units within the upper 20 or 40 cm. Log-retention increased to 3 log units after 80 cm, 6 log units after 340 cm, and 7 log units after 5 m filtration path (Table 42B). Compared to the results of obtained in experiments under aerobic conditions, retention ratios of F+ phage from the first and the second filter paths (20 and 40 cm) were relatively low (Table 1 and 7B). Retention of phages in deeper filter paths up to 340 cm was found at a similar order of magnitude under aerobic and "anoxic" conditions.

Removal of F+phages was not homogenous in all sections of the filter column. Highest specific retention rate (0,06 log/cm) was found within the first 20 cm of filter (Table 42B). It decreased to 0,03 log/cm within 160 cm, and to 0,003 log/cm between 160 and 340 cm.

Correspondingly, the highest elimination rate coefficient (0,52 log.h^{-1}) was found in the first 20 cm which decreased with increasing filter paths to 0,13 log.h^{-1} at 5m filtration path.

Concentrations of somatic coliphage 241 in the influent of the filter column varied between 80 and 800 pfu/ml during the initial seven weeks of the experiment. Somatic phages were detected in all filtrate samples from 20, 40 cm, and 80 cm. After week 10 they appeared in filtrates from 160 and – sporadically - 160 cm (Figure 27).

Log-retention was especially low at 20 and 40 cm depths, with 0,7 log units and 1,2 log units, respectively (**Table 43**A). Log-retention increased to 2,8 log units at 80 cm, and 3,5 log units at 160 cm depth.
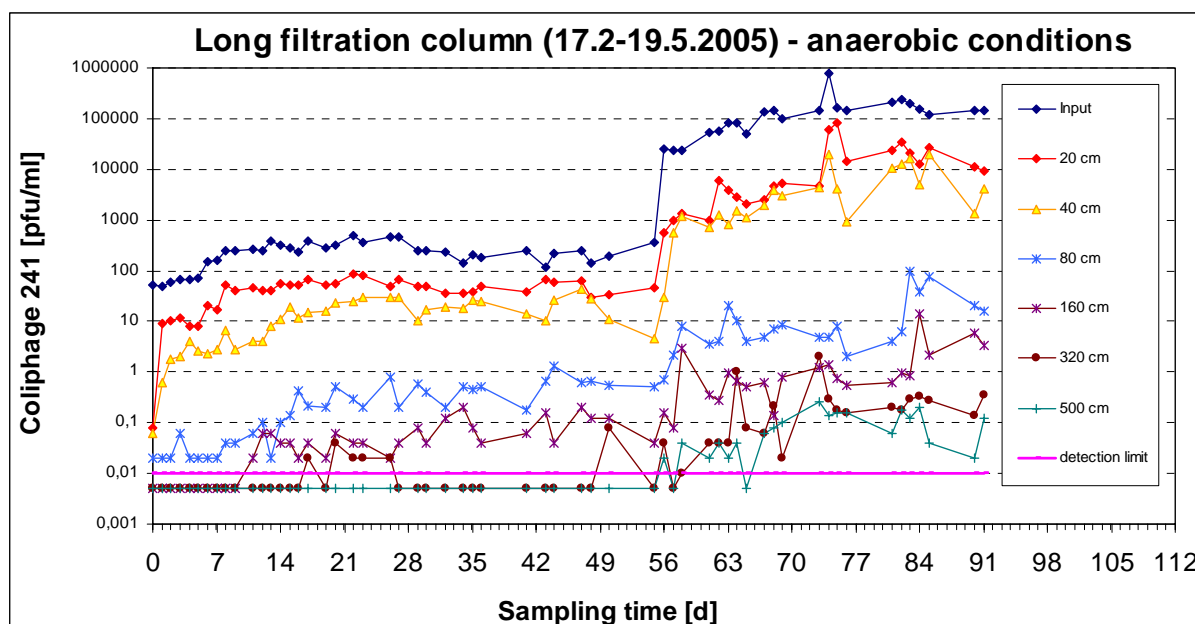
Figure 27: Concentrations of somatic coliphage 241 in influent and filtrate samples from different sampling sites by slow sand filtration under "anoxic" conditions at a pore water velocity of 100 cm/d.

Concentrations of coliphage 241 in the influent were increased up to 1×10^6 pf/ml during further operation between weeks 7 and 13. Coliphage 241 was subsequently detected in all filtrate samples up to 500 cm filtration path (Figure 27).

Table 43 : Retention of somatic phage 241 in long sandy soil column under "anoxic" conditions

A. operation at low concentrations of phages in input (0-45 d)

Sampling sites (cm)	Break-through ratio	Retention (log)	Δ log Retention+ (heterogeneity)	Specific retention (Δ log) / cm)	λA* (log.h^{-1})
20	0,2	0,7	0,7	0,04	0,35
40	0,06	1,2	0,5	0,03	0,30
80	0,002	2,8	1,6	0,04	0,34
160	0,0003	3,5	0,7	0,01	0,21

+ Retention of phages between two neighbours sites, λA : elimination rate coefficient]

B. operation at a high concentration of phages in input (55-91 d)

Sampling sites (cm))	Break-through ratio	Retention (log)	Δ log Retention+ (heterogeneity)	Specific retention (Δ log) / cm)	λA* (log.h^{-1})
20	0,1	1,1	1,1	0,05	0,50
40	0,03	1,5	0,4	0,02	0,35
80	0,0001	3,9	2,4	0,06	0,46
160	0,00002	4,7	0,9	0,01	0,28
340	0,000002	5,6	0,9	0,005	0,16
500	0,0000007	6,2	0,5	0,003	0,12

+ Retention of phages between two neighbours sites, λA : elimination rate coefficient]

Log-retention of somatic phages was 1,1 log units at 20 cm, 4 log units at 80 cm 4,7 log units at 160 cm and 6,2 log units at 500 cm. There was no clear difference between removal of coliphage 241 under aerobic and "anoxic" conditions (Table 38 and Table 43B).

Highest log-retention of phages (2,4 log units) was observed in the filter section between 40 and 80 cm with a specific retention rate of 0,06 log/cm comparable to the rate of 0,05 log/cm at 20 cm (Table 43B). In deeper filter sections specific retention rate decreased clearly to 0,003 log/cm.

Elimination rate coefficient was 0,5 log.h^{-1} in the upper 20 cm und decreased clearly with increasing filter path to 0,12 log.h$^-$1 at 500 cm (Table 43B).

5 Slow sand filtration experiments

5.1 Material and Methods

5.1.1 Test organisms.

see Part enclosure

5.1.2 Filtration pond

The slow sand filtration pond in is a semi technical plant with a quadratic filtration surface of 60,4 m2, filled with sandy soil of a depth of 80 cm. Effective (d_{10}) and median grain sizes of sand were 0,28 mm and 0,7 mm, respectively. As the d_{60}/d_{10} ratio was about 3,28 which is more than 2, the grain size is not considered as uniform (Clement, 2002). The nominal porosity of the sand was measured as 0,335. The experimental set up is shown in Part 6. Some physical and chemical characteristics of the sandy soil are listed in Table 44

Table 44: Selected characteristics of the native sandy soil in the filtration pond

Characteristics of sandy soil in filtration pond	
effective grain size	0,15 - 0,30 mm
uniformity coefficient	3
water charging particles	< 1%
Porosity	31,90%
Dispersion	0,04
dispersion coefficient	0,036 m2/d
average residual time	2,25 - 9 h

Ground water from the water work Marienfelde was used for filling and continuous percolation of the sand filter. During filling of the filter pond, ground water flowed upwards. At a water level of 45 cm corresponding 40 m^3 surface water volume, filtration process was started and stabilised four weeks at each flow adjusted. The flow velocity was regulated to 1,5, 3 and 6 m^3/h corresponding to a filtration velocity of 60, 120 and 240 cm water columns per day or a pore water velocity of 180, 360 and 720 cm/d. Theoretical detention time of water for the total length of the filtration path was measured as 2,25 h, 4,5 h or 9 h at the three filtration velocities, respectively. Table 45 shows some characteristics of the surface water percolated in the filtration pond. Selected geochemical properties of the sediments are listed in Table 46.

Table 45: Selected characteristics of surface water in the filtration pond

Characteristics of percolated water	
Natrium	46,4 mg/L
Kalium	4,3 mg/l
Calcium	125 mg/L
Magnesium	17,7 mg/L
Sulphate	236 mg/L
Nitrate	0,3 mg/L
Phosphate	<0,1mg/L
DOC	5,5 mg/L
pH	7,8
Conductivity	963 µS/cm

Table 46: Selected geochemical properties of the sediments

Parameters	Native	Clogging layer
Fe-ox [mg/kg]	275	605
Fe-red [mg/kg]	850	1700
Fe-total [mg/kg]	1125	2305
Mn-ox [mg/kg]	11.0	68.8
Mn-red [mg/kg]	17.5	100.0
Mn-total [mg/kg]	28.5	168.8
C-org [weight %]	0.022	0.343
C-inorg [weight %]	0.118	1.395
S-total [weight %]	0.010	0.048
CECeff [mmol(eq)/100g	0.127	1.127

5.1.3 Inoculation

Experiments with chemicals and coliphages were performed simultaneously. Reference compounds of all working groups were mixed in a stock solution of 100 L volume and added as a sluggish peak to the surface water of the filter pond (see 5.2.1.1, 5.2.2.1). Bacteria were not added simultaneously with chemicals because of possible interactions.

Inoculation of coliphages 138 and 241 and indicator bacteria in the reservoir was started in separate experiments synchronic with the tracer salt NaCl (5%) after completion of the experiments with chemical compounds (see 5.2.1.2, 5.2.2.3, 5.2.3). Approximate

concentrations of test organisms in the stock solution were 1×10^{11} pfu/ml for F+ coliphage 138, 1×10^{10} pfu/ml for somatic coliphage 241, and 1×10^9 mpn/ml for indicator bacteria.

After mixing, the solution of all reference compounds was evenly sprayed to the surface water of the filter pond within 5 min. The chloride concentration of surface water increased from 150 mg/L up to 500 mg/l, whereby an increase of conductivity from 895 to about 1400 µS/cm was measured. A water pump operated continuously to homogenize the reference contaminants in the surface water.

5.1.4 Sampling

Sampling was only possible from the water reservoir above the filter and from the outlet of the filter. Samples from reservoir water were collected 20 cm below the water surface in sterile flasks at regular intervals. Sampling from the effluent of filter pond was carried out in short intervals (30 – 60 min.) during the first 12 h after inoculation and were prolonged to several hours and days during the further course of the experiment. An auto sampler was used for sampling the outlet over night.

Core samples from the filter bed were taken before and after one of the experiments to investigate the survival of bacteria and coliphages in the filter.

The first experiment in the filtration pond was carried out on the native sandy soil without any apparent formation of biomass or clogging layer on the surface. During continuous operation, biomass rapidly developed in the filter pond in particular through algae growth which was apparent on the surface of the sand filter ("clogging layer"). After formation of a clogging layer, the filtration experiment was repeated with the same flow rate. At the end of all experiments - approximately after an operation time over 10 months – the filter bed was drained dry and samples from the clogging layer up to 1 cm depth was collected for batch experiments and chemical analysis. Some chemical properties of the clogging layer are given in Table 46.

5.1.5 Assessment of the retention of test organisms

5.1.5.1 Cumulative breakthrough ratio A - CBTA

Concentrations of test organisms in surface water and filtrate samples were used for calculation of relative breakthrough ratios. The quotient of the concentration in each filtrate sample to the total concentration of test organisms in pond water corresponds to the relative breakthrough of each filtrate fraction. The addition of these single relative breakthrough ratios as a function of time over the whole experiment resulted in a cumulative breakthrough ratio (CBT) of test organisms at a given time according to equation (1):

$$CBTA = \sum \frac{C \text{ filtrate}}{C \text{input}} \qquad (1)$$

Multiplication of the CBT values by 100 gives the breakthrough as percentage of the input concentration.

<u>Log-Retention.</u> The negative decade logarithm of the CBT gives the retention or removal of test organisms in the filter pond as log units.

5.1.5.2 Specific retention rate (filter factor F).

The specific retention rate demonstrates retention of test organisms per cm of filter path.

Retention as log unit per cm filter path has also been defined as filter factor F (Pang et al., 2005).

$$F = \frac{(-)\log CBT}{\text{Filter path (cm)}} \quad --- \qquad (2)$$

5.1.5.3 Elimination rate coefficient (λA)

On the basis of the filtration theory of Yao et al. (1971), transport of colloid particles through saturated porous media can be represented by a connective dispersion equation, augmented by adsorption and desorption terms to account for bacterial interaction with the collector surface. In a column with characteristic length L (m), operated by a constant flow rate V(m/h), assuming steady state conditions, and neglecting dispersion (<0,001), virus inactivation and detachment or virus transport is described by (Schijven and Hassanizadeh, 2001):

$$(-)\log (CBT) = [\lambda \cdot L] / [2,3 \cdot V]$$

The elimination rate coefficient λ can be derived from this equation:

$$\lambda = \frac{(-)\log (CBT) \cdot V \cdot 2,3}{L} \qquad (3)$$

5.1.5.4 Modelling parameter: λc(h-1), Retardation factor (R)

The adsorption and transport behaviour of test organisms was simulated using a one-dimensional, one-site kinetic model under following assumptions (see also Chapter XXX). Deactivation or elimination rate coefficient λC (h^{-1}), and retardation factor (R) were taken from the calculation model of Dr. Holzbecher. The λ obtained by modelling is listed as λC in the tables. λC was in the same order of magnitude as λA in all experiments.

5.1.5.5 One log removal distance (D) and time (T)

The elimination rate coefficient (λ) and filter factor (F) are the mean parameter to use to determine setback time or distances for removal of microorganisims in the aquifer. From equation 4, it can be deduced that virus removal in a saturated sand filter under steady state conditions with a constant attachment, detachment and inactivation coefficient, should decline in a linear fashion with travel distance. One log removal distance (D) may be calculated from the log retention of test organisms in the total length of filtration unit (L):

D (m) = log removal / L (m)   (4)

or

D = F / 0,01

The reciprocal of the filter factor gives also the distance (D) for one log unit reduction of the test organisms:

D = 1 / F   D= 1 log removal per m   (5)

One log retention time (T) of test organisms in each filter unit is the reciprocal of the elimination rate coefficient (λ)

T (h) = 1 / λ (6)

Distance or filtration time required for e.g. 8 log removal of test organisms are 8 time higher product of the D and T values.

5.1.5.6 Biofilm investigations

Biofilm investigations were made in the slow sand filtration pond at three different sites. Plastic pipes were installed in three different depth (10 cm, 30 cm and 60 cm). In each pipe a holder with four glass slides was introduced and left there for a period of several weeks. Sampling of glass slides with biofilms was done by pulling the glass slides out of the pipes

and immersing them in 50 ml Falcon tubes either with 3.7 % formaldehyde or water from the reservoir.

5.1.5.6.1 Determination of total cell counts (DAPI staining) and fluorescent in situ hybridization

For the determination of total cell counts different areas (at least 6 points) on the glass slide with biofilm were covered with 10 µl DAPI solution (4`6-diamidino-2-phenylindole, Sigma, Deisenhofen; Germany, 10 µg/ml) for 5 min, in the dark. After rinsing with water and air-drying DAPI cell signals were counted. At least 10 microscopic fields (100 x 100 µm) were chosen randomly and a minimum of 1000 cells were enumerated microscopically.

For in situ hybridization, the glass slides with the biofilms were fixed in 50 ml formaldehyde solution (3.7%) in Falcon tubes (Kisker, Germany), for 4 h at 10°C. Subsequent removal of the formaldehyde solution was performed by washing the slides in 50 ml 1 x PBS solution 3 times for 3 min each. After this, samples were air-dried and could be stored at room temperature in the dark at this step of the procedure for several weeks. To prepare wells for the hybridization five to eight grommets were sticked on each slide as shown in Figure 28.

Figure 28: glass slide with a two week old biofilm with grommets used as hybridization chambers

All custom synthesized oligonucleotide probes used in this study are listed in Table 47. They were 5'-labelled with the indocarbocyanine dye Cy3 (Metabion, Planegg, Germany) and stored in TE buffer (10 mM Tris, 1 mM EDTA, pH 7.5) at –20°C prior to usage. Hybridization solutions were adjusted to a final concentration of 5 ng probe/µl. The pre-warmed (46°C) hybridization solution (0.9 M NaCl, 20 mM TRIS/HCl, pH 7.2, 0.01% SDS, 35% v/v formamide) was mixed in a ratio of 9:1 with the fluorescently labelled oligonucleotide. To each well of the slides 10 µl hybridization solution was added and hybridized for at least 2 h at 46°C in the dark. To prevent evaporation the slides were put into Falkon tubes with a piece of wet paper. After the hybridization unbound oligonucleotides were carefully removed by a washing steps with 50 ml pre-warmed washing buffer (20 mM TRIS/HCl, 0.01% SDS, 88 mM NaCl) for 20 min.

After air-drying, the slides were counterstained with 10 µl DAPI solution (10 µg/ml) for 5 min, in the dark for the detection of total cell counts.

Table 47: oligonucleotide probes used for biofilm analysis

Probe	Target organisms	Reference
EUB338	Eubacteria	Amann et al. 1990
EUB338 II	Eubacteria	Daims et al. 1999
EUB338 III	Eubacteria	Daims et al. 1999
ALPHA1b	alpha-Proteobacteria	Manz et al. 1992
BETA42	beta-Proteobacteria	Manz et al. 1992
GAM42	gamma-Proteobacteria	Manz et al. 1992
CF319	Cytophaga-Flavobacteria	Manz et al. 1996
PLA46	Planctomycetales	Neef et al. 1998
HYPHO1241	Hyphomicrobiaceae	Layton et al. 2000
AQUA841	Aquabacteriaceae	Kalmbach et. al 1999
AERO1244	Aeromonadaceae	Böckelmann et al. 2000
FLAVO1004	Elbe river snow isolate 8	Böckelmann et al. 2000
BETA21	Elbe river snow isolate 21	Böckelmann et al. 2000
Probe D	Enterobacteriaceae	Gutell et al. 1994

5.1.5.6.2 Microscopy and documentation

FISH signals were detected by epifluorescence microscopy using a Zeiss Axioskop (Oberkochen, Germany) equipped with Zeiss light fliter set no. 01 for DAPI (excitation 365 nm, dichroic mirror 395 nm, suppression 397 nm), and HQ light filter 41007 (AF Analysentechnik, Tübingen, Germany) for CY3-labelled probes (excitation 535-550 nm, dichroic mirror 3565 nm, suppression 610-675 nm). Pictures were taken with the digital camera ColorView12 (SIS, Münster, Germany).

5.1.5.6.3 CTC and LIVE/DEAD staining

The 5-cyano-2,3-ditolyl tetrazolium chloride (CTC, Polysciences, Eppelheim, Germany) is a monotetrazolium redox dye which produces a fluorescent formazan (CTF) when it is chemically or biologically reduced. Four week old glass slides were sampled and washed in 1 x PBS to remove non-adherent or loosely-attached bacteria, and then stained by dipping the slides alternatively in 15 ml of a 4 mM solution of CTC or CTC solution plus R2A medium in a petridish for 2 h. After incubation the slides were rinsed in 1 x PBS and air-dried before microscopical examination.

For the determination of live and dead bacterial cells kit no. L7007 from Molecular Probes, Heidelberg, Germany was used. The kit contains the green-fluorescent nucleic acid stain SYTO9 and the red-fluorescent nucleic acid stain propidium iodide. SYTO9 stains generally all bacteria in a population those with intact membranes and those with damaged

membranes. In contrast, propidium iodide penetrates only bacteria with damaged membranes, causing a reduction in SYTO9 stain fluorescence when both dyes are present. Therefore live cells fluoresce green and dead cells red. Glass slides with biofilms were divided into six squares by pencil drawing. 10 µl of staining solution A (SYTO9, 1:1000 diluted) and staining solution B (propidium iodide, 1:1000 diluted) were pipetted on each square and incubated at room temperature in the dark for 15 min. After that slides were rinsed gently with water, air-dried, and covered with mounting oil and coverslips before microscopical examination.

5.2 Results

Experiments with coliphages and chemicals were performed simultaneously (see 2.1.1 and 2.2.1). Bacteria were not added in these experiments because of possible interactions. Inoculation of coliphages and indicator bacteria was started in separate experiments after completion of the experiments with chemical compounds (see 5.2.1.2, 5.2.2.3, 5.2.3).

The following three filtration velocities were tested:

- 240 cm/d corresponding to a pore water velocity of 720 cm/d and a flow rate of 6000 L/h (see 5.2.1)

- 120 cm/d corresponding to a pore water velocity of 360 cm/d and a flow rate of 3000 L/h (see 5.2.2)

- 60 cm/d corresponding to a pore water velocity of 180 cm/d and a flow rate of 1500 L/h (see 5.2.3)

Biofilm investigations were performed during experiment SSF8 (see 2.4).

5.2.1 Experiments with a filtration velocity of 240 cm/d

The heterogeneity of the filtration in the filter was tested in a first experiment using one coliphage (see 5.2.2.1). Two further experiments were conducted with both coliphages and chemicals (5.2.1.1) or bacteria (5.2.1.2) added simultaneously.

5.2.1.1 Experiment SSF1 – 19.3.03 (240 cm/d, without clogging layer)

In the first experiment with the slow sand filtration pond - during a continuous operation time for one week - the function of the six drainage tubes and pumps was tested. After inoculation of F+ phage 138 and tracer salt NaCl into the reservoir water, concentration of phages was about 2 x 105 pfu/ml. Concentrations decreased to 1,6x104 pfu/ml after 5 h and about1 x 103 pfu/ml after 22 h (Figure 29 and Figure 30).
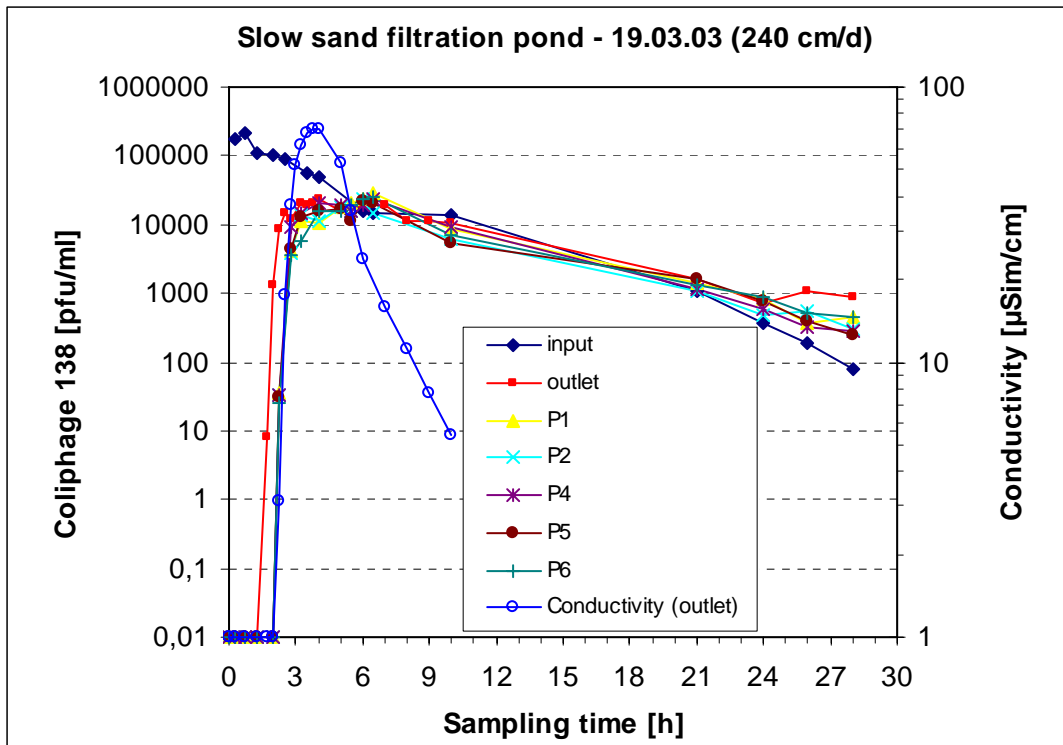
Figure 29: Concentration of F+ phage 138 in influent and filtrate samples from different drain tubes (P1-P6) and total effluent of the filtration pond, electro conductivity (µSim.cm-1) of total effluent samples (operation time: 11 – 28 h, pore water velocity: 720 cm/d, without clogging layer
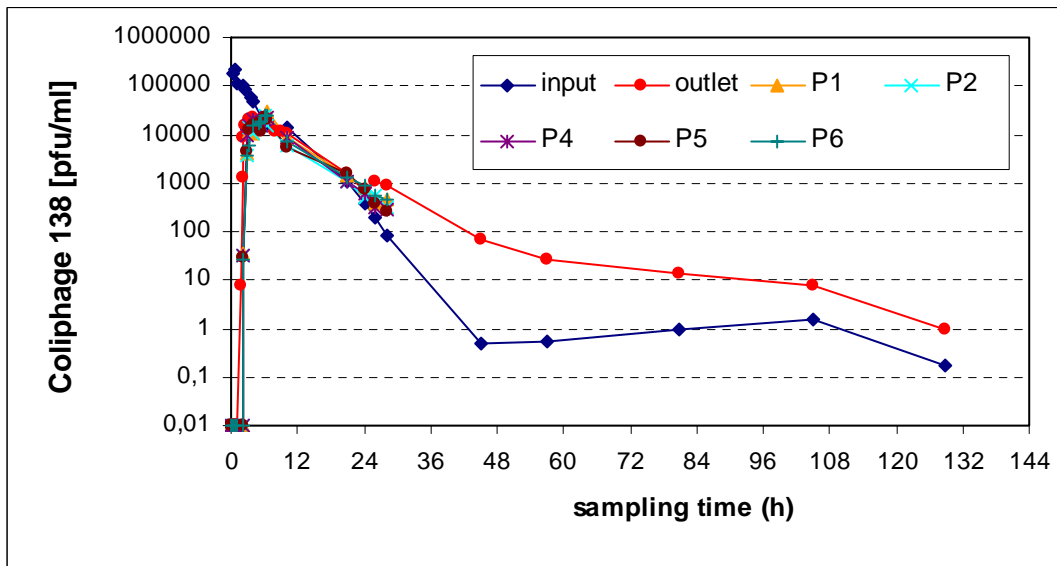
Figure 30: Concentration of F+ phage 138 in influent and filtrate samples from different drain tubes (P1-P6) and total effluent of the filtration pond (operation time: 128 h)

In filtrate samples, F+ phage 138 was already detectable synchronic with tracer salt NaCl in the initial filtrate fractions sampled after 2 h (Figure 29). Breakthrough of phages was

observed in the total effluent approximately 30 min earlier than in the single drainage tubes P1, P2, P4, P5 and P6 (tube P3 was blocked). Concentrations in samples from the six drainage tubes were comparable over the whole run of the experiment.

Concentrations increased to the highest concentration (about 2 x 104 pfu/ml) after 4 h in all filtrates samples and moderately decreased to to 5 x 102 pfu/ml after 24 h.

Breakthrough ratio and log retention of F+ phage 138 were calculated (Table 48). A breakthrough ratio of 0,69 was found for the total effluent. For the 5 drain tubes, relative breakthrough ratios varied between 0,43 and 0,52. Due to this relative low variation in migration of coliphages, samples in further experiments were not taken from single drain tubes but only from the total outlet tube of the filtration pond.

Table 48: Cumulative breakthrough of F+ coliphage 138 in filtrate samples from different drain tubes and total effluent during an operation time of 28 h

(P1-P6: different drain tubes at 100 cm depth)

Parameters	total effluent	P1	P2	P4	P5	P6	mean
Breakthrough ratio	0,7	0,5	0,4	0,5	0,5	0,5	0,5
Retention (log)	0,16	0,29	0,37	0,29	0,33	0,31	0,29

Sampling from the total effluent was continued in regular intervals during further filtration up to 7 d. Concentrations of coliphages were 100 pfu/ml after 2 days and 10 pfu/ml after 5 days (Figure 30). At the end of operation a cumulative breakthrough ratio of 0,41 was calculated corresponding to a log-retention of 0,39 logs and a filter factor of 0,005 logs/cm (Table 49). Elimination rate coefficient was determined as 0,33 log.h^{-1}. The results were not analysed by modelling approaches.

Table 49: Retention of F+ coliphage 138 in the sand filtration pond of Marienfelde by a pore water velocity of 720 cm/d (filter velocity 240 cm/d, SSF1 – 19.3.03)

Test organisms	Breakthrough ratio (CBTA)	Retention (log)	Specific retention (log)/cm	λA* (log.h-1)	Retardation (R)**	λC** (h-1)
F+Phage 138	0,4	0,4	0,005	0,33	-	-

*) Calculation according to integrative balancing of total virus concentrations in surface water and
filtrate samples, ** calculation according to modelling approaches

5.2.1.2 Experiment SSF7 - 14.6.04 (240 cm/d, without clogging layer)

After completion of the investigations of other working groups in the slow sand filter, retention of coliphages and indicator bacteria could be analysed. The first experiment was conducted with a filtration velocity of 240 cm/d corresponding to 720 cm pore water column per day.

Culture suspensions of test organisms (F+ phage 138, somatic coliphage 241, E. coli and intestinal enterococci) were simultaneously added into the reservoir water and mixed with a surface water pump.

Concentration of F+ phage 138 in the reservoir water was $1,1x10^5$ pfu/ml in the beginning of the experiment. Concentrations decreased to $2,1x10^4$ pfu/ml after 3 h, 2,6.103 pfu/ml after 5h, and $2x10^2$ pfu/ml after 8 h. Phages were no longer detected after 24h (Figure 29). In filtrate samples, coliphage 138 was already detected in the effluent fraction collected after 2h, synchronic with the tracer salt NaCl. Concentrations increased to the highest concentration of $1,7x10^3$ pfu/ml after 4 h and moderately declined to $1x10^2$ pfu/ml up to 24 h (Figure 31).

Cumulative breakthrough ratio was 0,3 after an operation time of 192 h. The breakthrough of phages, already in the initial phase of filtration was relatively high. Breakthrough ratios were 0,2 after 6 h and 0,3 after 24h (Figure 32). The retention equilibrium obviously occurred within 12-24 of filtration process.

Figure 31: Concentration of F+ phage 138 and somatic coliphage 241 in influent and effluent of the filtration pond without clogging layer at a pore velocity of 720 cm/d.

Figure 32: Cumulative breakthrough of test organisms by slow sand filtration without clogging layer at a pore velocity of 720 cm/d.

Corresponding to this relative high breakthrough ratios, a low retention of 0,5 log units was found at the end of the experiment, resulting in a specific retention ratio of 0,006 log/cm filter path (Table 50). The elimination rate coefficient (λA) of F+phage 138 at this high filtration velocity calculated by equation (3) was 0,44 log units.h-1. Statistical analysis of input and filtrate concentrations by modelling resulted in a retardation factor of 1,25 and a λc value of 0,4 h^{-1}.

Table 50: Retention of test organisms in the sand filtration pond of Marienfelde with a pore water velocity of 720 cm/d (filter velocity 240 cm/d, SSF7 – 14.6.04) *) Calculation according to integrative balancing total virus concentrations in surface water and filtrate samples, ** calculation according modelling approaches

Test organisms	Breakthrough ratio (CBTA)	Retention (log)	Specific retention (log)/cm	λA* (log.h-1)	Retardation (R)**	λC** (h-1)
F+Phage 138	0,3	0,5	0,006	0,44	1,25	0,40
somatic Phage 241	0, 7	0,2	0,002	0,15	1,36	0,17
E. coli	0,2	0,7	0,008	0,56	-	-

A relatively low concentration of somatic coliphage 241 (2.103 pfu/ml) was found in the reservoir water after inoculation. Concentrations decreased to 100 pfu/ml after 3h, and 10 pfu/ml after 6h (Figure 31). Somatic coliphages appeared in the effluent at a concentration of 13 pfu/ml after a percolation time of 2,5 h simultaneous with the tracer salt. The highest concentration of coliphage 241 was about 250 pfu/ml in the filtrate fraction taken after 4 h.

Concentrations decreased moderately up to less than 1 pfu/ml after an operation time of 100 h.

Cumulative breakthrough ratios were relatively high with 0,3 at 6 h, 0,5 at 12h and 0,6 at 24h (Figure 32). Cumulative breakthrough ratio was 0,7 after a filtration time of 150 h. Correspondingly, retention of F+ phage was low (0,18 log), with a specific retention rate of 0,002 log/cm filter path (Table 50).

The elimination rate coefficient λA of phage 241 was 0,15 log units.h-1 which was clearly less compared to phage 138. The modelling approach revealed a retardation factor of 1,36 and also a low elimination rate coefficient λc of 0,17.h-1.

The concentration of E. coli reached $1,5x10^4$ mpn/100 ml in the reservoir water which gradually decreased to 100 mpn/100ml after 24 h and 1 mpn/100ml after 48h (Figure 33). In the filtrate samples, E. coli was detected for the first time (6 mpn/100ml) after 1 h. The concentration increased rapidly in the next filtrate fractions, and reached the highest level of $4x10^4$ mpn/100 ml already in the sample taken after 2,5 h (Figure 32). Concentrations of E. coli decreased in further filtrate fractions, to 98 mpn/100 ml after 5 h, 10 mpn/100 ml after 24h and 1 mpn/100 ml after 48h.
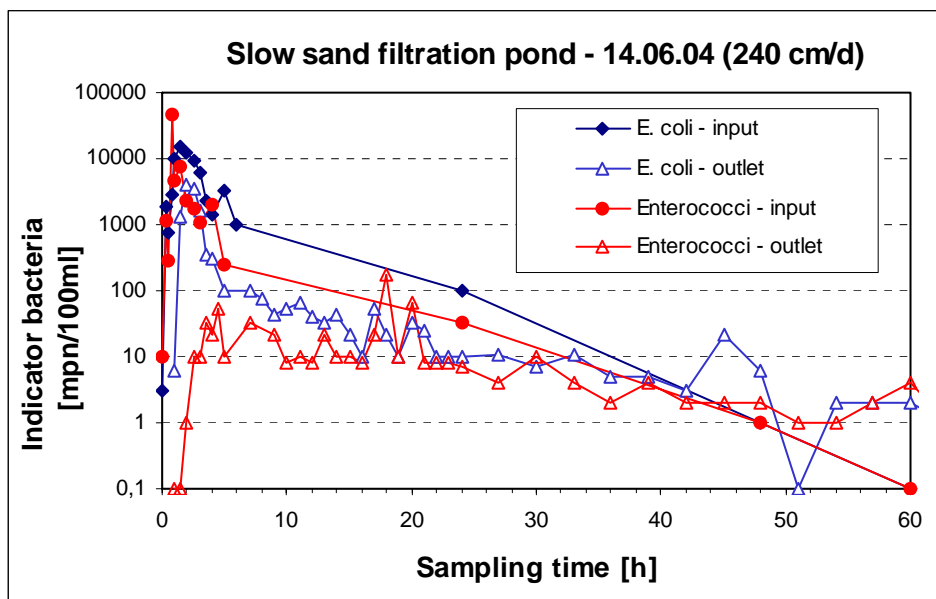
Figure 33: Concentrations of E. coli and Enterococcus sp. in influent and effluent of the filtration pond without clogging layer at a pore velocity of 720 cm/d.

Due to the rapid breakthrough of E. coli in high concentrations in the initial filtrate fractions, the cumulative breakthrough ratio was 0,2 % already after 3h. Similar breakthrough ratios were calculated after 12 h and at the end of operation after 150 h (Figure 33). Consequently, retention of E. coli was high (about 0,65 logs) with a specific retention rate of 0,008 log/cm (Table 50

The elimination rate coefficient (λA) was 0,56 log units.h-1. No modelling was carried out on these results. The highest concentrations of Enterococcus faecalis in reservoir water was 4,6.105 mpn/100ml declining to 250 mpn /100 ml after 5 h, and 32 mpn/100 ml after 24h

(Figure 33). In the filtrate samples, they were mostly detected in concentrations less than 100 mpn/100ml. Two high densities were observed with 54 mpn/100 ml after 5 h and 170 mpn/100 ml at 18 h.

Cumulative breakthrough ratio of enterococci was 0,005 after 6h, 0,01 after 12h, 0,03 after 24 h and 0,04 at the end of experiment after 150h (Figure 32). The retention of enterococci was, therefore, relatively high (1,4 log units) and resulted in a specific retention rate of 0,02 logs/cm filter path.

Correspondingly, the highest elimination rate coefficient (1,2 log units. h-1) was found for intestinal enterococci (Table 50). No modelling was carried out on these results.

5.2.2 Experiments with a filtration velocity of 120 cm/d

5.2.2.1 Experiment SSF4 – 26.05.03 (120 cm/d, without clogging layer)

In this experiment only phages were tested and the filtrate flow velocity was reduced to 120 cm/d water column or 360 cm/d pore water velocity. Immediately after inoculation of the reservoir water, the concentration of F+ coliphage 138 reached 6,1.105 pfu/ml and then gradually decreased to 5,2.104 pfu/ml after 6 h (Figure 34). After 48 h of operation 100 pfu/ml were detected in the reservoir water. After a rapid breakthrough, the concentration of coliphage 138 in the effluent reached 258 pfu/ml after 6 h and remained at a relatively constant level between 200 and 300 pfu/ml up to 24 h. Concentration subsequently declined to a level of 1 pfu/ml during further operation up to 90 h. Detection of coliphage 138 in the filtrate samples was synchronic with the increase in conductivity.

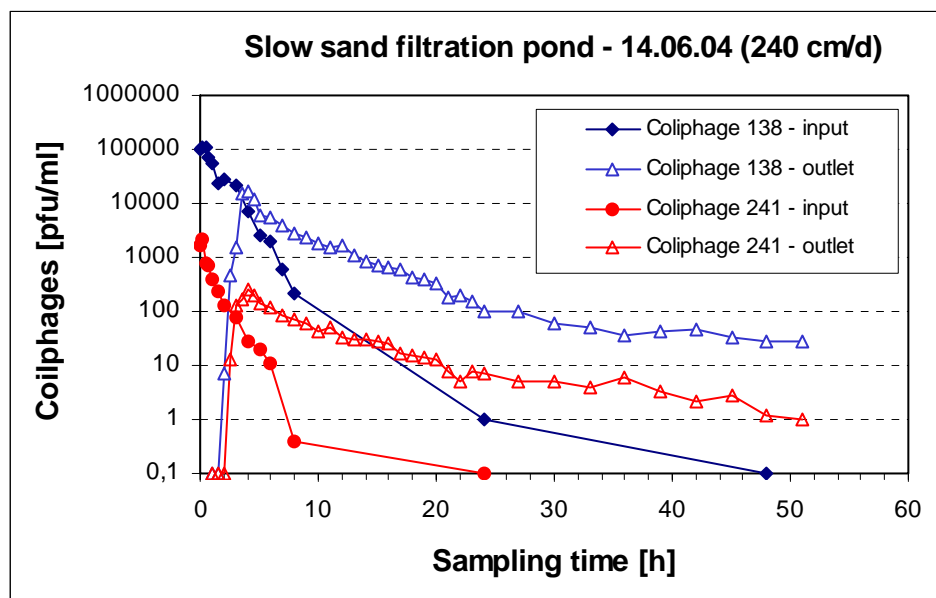**Figure 34: Concentration of F+ phage 138 and somatic phage 241 in influent and effluent of the filtration pond without clogging layer at a pore water velocity of 360 cm/d.**
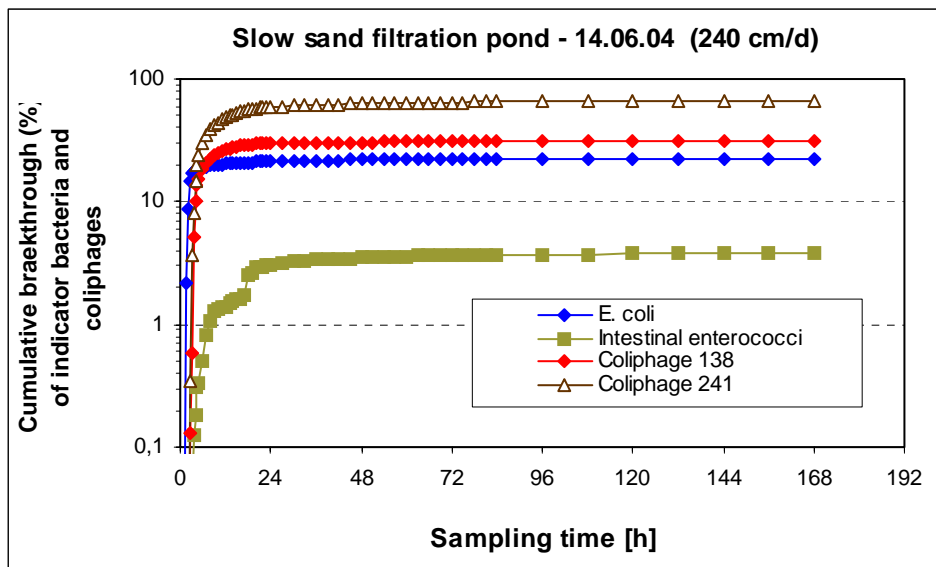
Cumulative breakthrough ratio of phage 138 was calculated as 0,001 after a filtration time of 12 h which increased marginally to 0,004 in the further run of the experiment (Figure 35, Table 51). Based on this total virus retention of 2,4 log units, a specific retention rate of 0,03 log units per cm filter length was calculated.

With a filtration velocity of 0,05 m.h-1 and a cumulative breakthrough of 0,004, the elimination rate coefficient was calculated (equation 3) as 1,02 log units.h-1 (Table 51). No modelling was carried out on these results.

After inoculation of the reservoir water, concentrations of coliphage 241 were much lower (103 pfu/ml) than that of coliphage 138. Concentrations decreased to 170 pfu/ml during an operation time of 6 h (Figure 31). Despite these relatively low concentrations in the reservoir water, coliphage 241 appeared synchronic with the tracer salt in the initial filtrate samples (Figure 32). Coliphage 241 was detected in all filtrate samples at low concentrations (10 - 200 pfu/100 ml) during the further run of the experiment.

Retention of coliphage 241 in filter pond was not as good as for coliphage 138. Cumulative breakthrough ratios reached 0,004 and 0,01 after a percolation time of 12 or 24 h, respectively. At the end of experiment the ratio increased up to 0,024 (Figure 32, Table 51). With a relative retention of 1,6 log units, the specific retention rate amounted to 0,02 log units per cm filter path. Correspondingly, an elimination rate coefficient of $0,7 \log h^{-1}$ was determined at this filter velocity of $0,05 \ mh^{-1}$ which was clearly less than that of phage 138 (Table 52). The results were not analysed by modelling approaches.
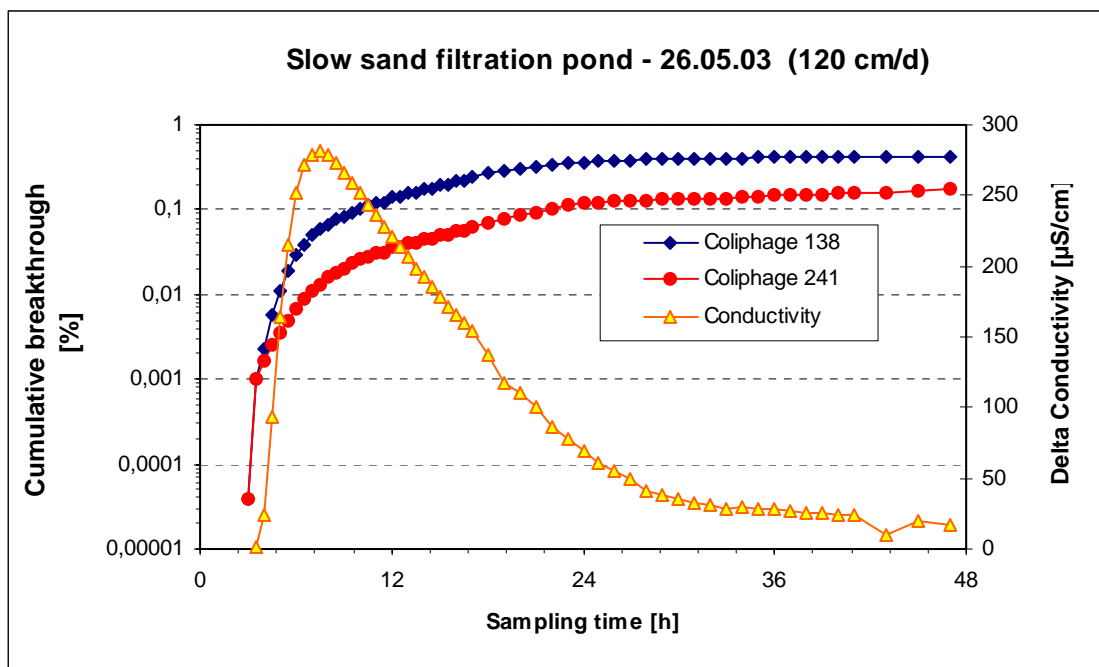
Figure 35: Cumulative breakthrough of test phages and mobility of tracer salt NaCl in slow sand filtration pond without clogging layer at a pore water velocity of 360 cm/d (3000 L/h).

Table 51: Breakthrough ratio of F+ phage 138, somatic coliphage 241 and E. coli in slow sand filtration pond at a filtration rate of 120 cm/d (360 cm pore water/d) before and after formation of a clogging layer

time (h)	26.05.03 (see 2.2.1) without clogging layer		17.06.03 (see 2.2.2) with clogging layer		22.11.04 (see 2.2.3) with clogging layer		
	f+ phage 138	Phage 241*	f+ phage 138	Phage 241*	f+ phage 138	Phage 241	E.coli
6	0,0003	0,001	0,0008	0,003	0,0001	0,0001	0,0003
12	0,0014	0,004	0,0013	0,012	0,0005	0,0004	0,0010
24	0,0036	0,012	0,0015	0,017	0,0008	0,0009	0,0014
48	0,0042	0,018	0,0016	0,024	0,0012	0,0018	0,0017
72	0,0042	0,021	0,0016	0,024	0,0014	0,0031	0,0018
96	0,0043	0,023	0,0016	0,024	0,0016	0,0041	0,0019
120	0,0043	0,024	0,0016	0,024	0,0017	0,0055	0,0019
144	0,0043	0,024	0,0016	0,024	0,0018	0,0064	0,0020
168	0,0043	0,024	0,0016	0,024	0,0019	0,0074	0,0020

5.2.2.2 Experiment SSF5 - 17.06.03 (120 cm/d, with clogging layer)

The experiment was repeated with both coliphages after an apparent biomass or clogging layer had formed on the filter surface. The clogging layer was not uniform but patchy with different thickness and structure.

F+ coliphage 138 reached a concentration of about 105 pfu/ml in the reservoir water after inoculation which rapidly declined to 1000 pfu/ml within 12 h (Figure 36). In the initial filtrate samples, concentration of F+phage increased synchronic with conductivity and reached the highest level of 100 pfu/ml after 6 h of operation. Concentration of phages declined gradually to 1 pfu/ml or 10 pfu/100ml after 36 h or 100 h, respectively.

Cumulative breakthrough ratios were calculated as 0,0013 after 12 h and 0,0016 after 60 h which did not change up to the end of the experiment (Figure 37, Table 52). Retention of phage 138 was about 2,79 log units and therewith in the same order of magnitude as in the experiment without clogging layer. A specific retention ratio of 0,035 logs per cm filter length was calculated. Consequently, a similar elimination rate coefficient of 1,2 log.h^{-1} was calculated like in the experiment before formation of an apparent biomass. Modelling of results showed no retardation (R=1) but a moderate elimination rate coefficient of 1,36.h^{-1} (Table 52).

The initial concentration of somatic coliphage 241 in the reservoir water was very low (about 100 pfu/ml). Nevertheless, phages were rapidly observed in the initial filtrate samples. Only low concentrations were detected in the effluent with a maximum of 24 pfu/100 ml in the effluent sample after 7 h of operation. Coliphage 241 was sporadically detected in 100 ml of other filtrate samples up to the end of operation at 180h (Figure 36).

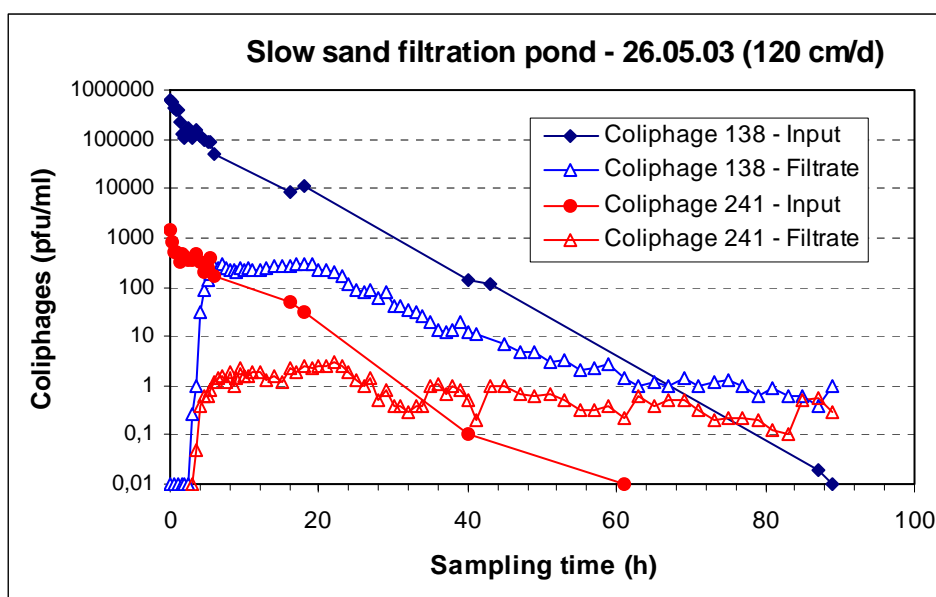**Figure 36: Concentration of coliphages 138 and 241 in influent and effluent of the filtration pond with clogging layer at a pore water velocity of 360 cm/d.**
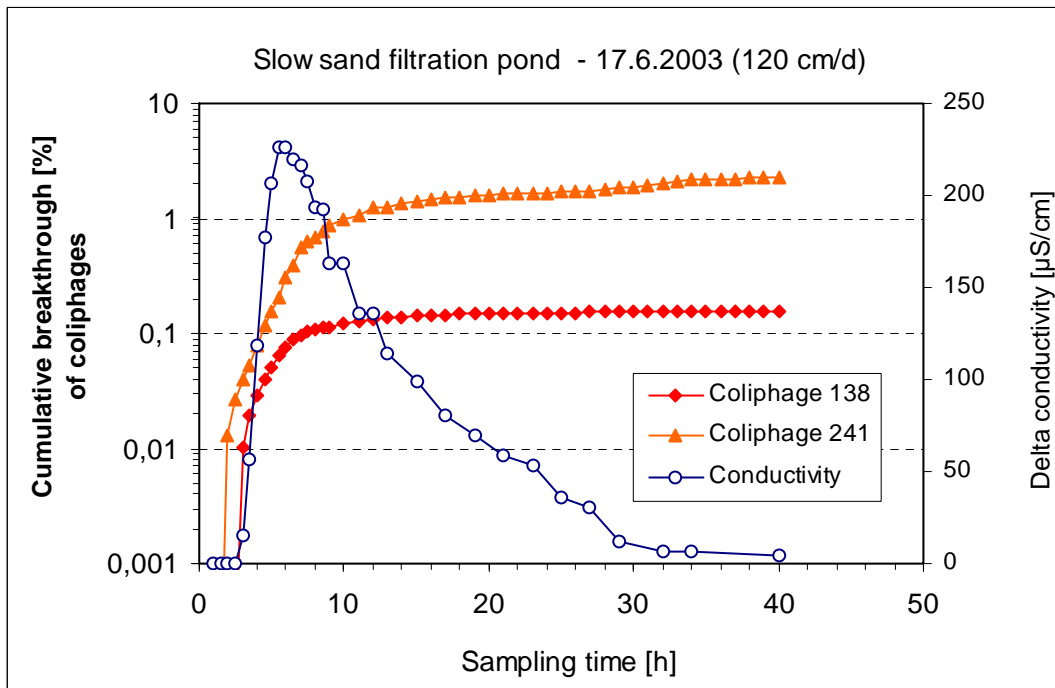
Figure 37: Cumulative breakthrough of coliphage 138, 241 and mobility of tracer in slow sand filtration pond with clogging layer at a pore water velocity of 360 cm/d.

Breakthrough ratios of somatic phage 241 were calculated as 0,012 after 12 h and as 0,024 at the end of the experiment after 150 h (Figure 35, Table 51). The same breakthrough ratio of 0,024 was also found in the previous experiment without clogging layer. The specific

retention ratio of 0,02 log/cm and the elimination rate coefficient of 0,70 were also similar to those of the previous experiment (Table 52). Adaptation of results by modelling approaches showed an elimination rate coefficient of 0,81 log.h^{-1} and a retardation factor of 1,3.

Table 52: Retention of test organisms in the sand filtration pond of Marienfelde before (-) and after (+) formation of an apparent biomass at a filtration velocity of 120 cm/d (360 cm pore water/d),)

Test organisms	Date	Clogging layer	Breakthrough ratio (CBTA)	Retention (log)*	Specific retention (log)/cm	λA* (log.h-1)	Retar-dation**	λC** (h-1)
F + phage 138	26.05.03	(-)	0,004	2,4	0,03	1,02		
	17.06.03	(+)	0,002	2,8	0,03	1,20	1,0	1,36
	22.11.04	(+)	0,002	2,7	0,03	1,16		
somatic coliphage 241	26.05.03	(-)	0,024	1,6	0,02	0,70		
	17.06.03	(+)	0,024	1,6	0,02	0,70	1,3	0,81
	22.11.04	(+)	0,012	1,9	0,02	0,83		
E. coli	22.11.04	(+)	0,002	3,3	0,04	1,44		

*) Calculation according to integrative balancing total virus concentrations in surface water and filtrate samples (equation 3), ** calculation according modelling approaches, λ: elimination rate coefficient

5.2.2.3 Experiment SSF8 – 22.11.2004 (120 cm/d, with clogging layer)

Coliphages and bacteria were applied simultaneously in this experiment with a filtration velocity of 120 cm/d or 360 cm pore water per day and the results were compare to the results of previous experiments at the same flow rate (see 5.2.1.1, 5.2.2.2). An apparent, thick, and uniform biomass had developed on the sandy soil surface.

F+ coliphage 138 reached an initial concentration of $1,27x10^6$ pfu/ml and decreased slowly to $4,5x10^4$ pfu/ml after 24 h, $1,8x10^3$ pfu/ml after 72 h, and 1 pfu/ml after 192 h (Figure 38). In the effluent, F+ phages appeared in filtrate sample after 3 h at a concentration of 14 pfu/100 ml before the tracer salt NaCl was detectable. Concentrations of phages in filtrate samples increased to a maximum value of 1250 pfu/ml after 6 h of operation and remained relatively long time at a high level similar to steady state conditions. After 72 of operation, concentration of F+ phage 138 declined to 100 pfu/ml. Phages were still detectable at the end of operation after 384 h in concentrations of approximately 10 pfu/ml.

Despite relatively high initial concentrations of F+ phage 138 in the reservoir water, cumulative breakthrough was low increasing from 0,0005 after 12 h, to 0,0009 after 24 h, and to 0,0016 after 10 days (Table 51, Figure 39). Similar breakthrough ratios were found in the

experiment in June 2003 (see 5.2.2.2, Table 51). Retention of F+ phage 138 was about 2,7 log units, corresponding to a specific retention rate of 0,034 log/cm filter path (Table 52).

Elimination rate coefficient (λ) was calculated as 1,16 log unit.h^{-1} which was also similar to that of the experiment in June 2003 (Table 52).
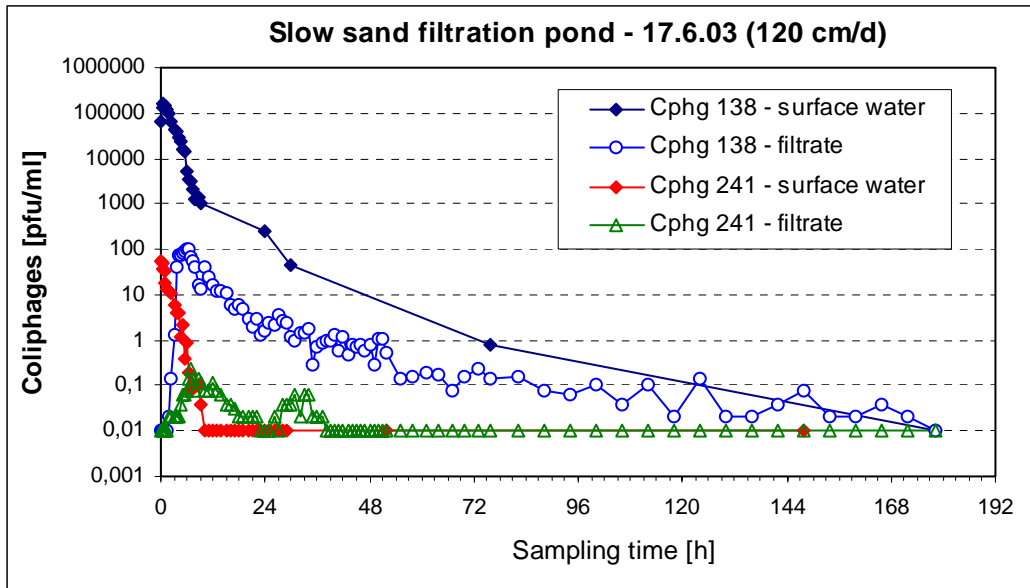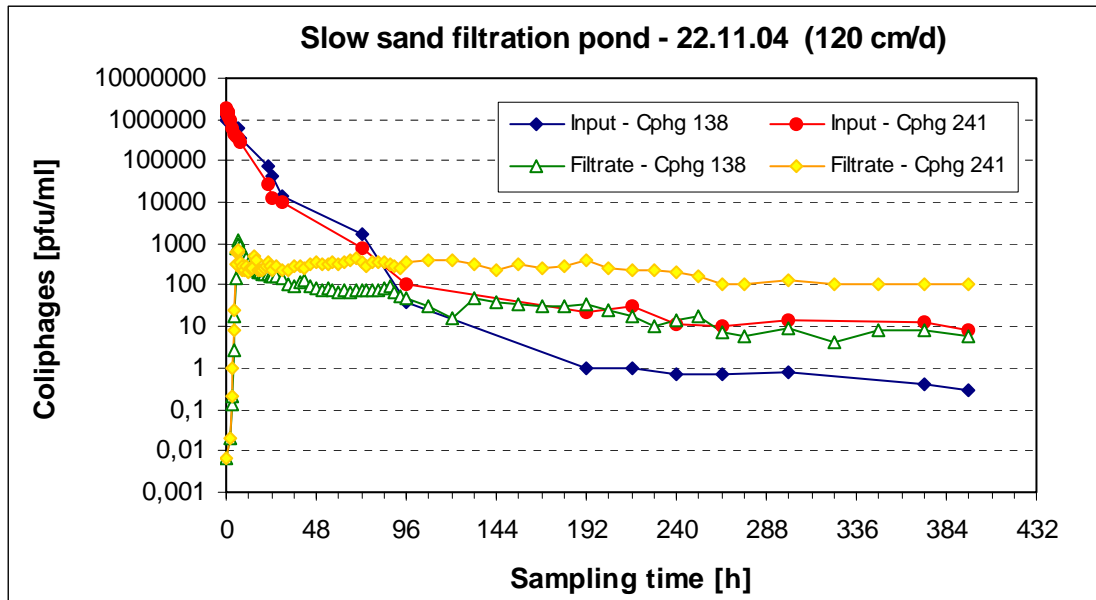

Figure 38: Concentration of coliphages 138 and 241 in influent and effluent of the filtration pond with clogging layer at a pore water velocity of 360 cm/d

Concentration of somatic phage 241 in the reservoir water was $1,9 \times 10^6$ pfu/ml directly after inoculation declining to $3,4 \times 10^5$ pfu/ml after 6 h, $1,3 \times 10^4$ pfu/ml after 24h and 10^2 pfu/ml after 96h of operation (Figure 38). Phage 241 was still detectable in pond water after 10 -18 days at concentrations of about 10 pfu/ml.

Effluent samples were already positive after 3 h of filtration. Highest concentration (700 pfu/ml) in the filtrate was found after an operation time of 3,5 h. Concentrations of phage 241 in all other filtrate samples varied between 210 and 360 pfu/ml within the next 10 days and marginally declined to 105 pfu/ml at the end of experiment after 396 h.

Cumulative breakthrough ratio increased slightly from 0,0004 within 6 h to 0,0008 after 12 h, and 0,005 after 120 h. After 15 d of operation the cumulative breakthrough ratio was 0,012 (Figure 39).

Retention of somatic phage 241 was 2 log units resulting in a specific retention rate of 0,024 log/cm filter path. Elimination rate coefficient was calculated as 0,83 log.h-1 which was slightly higher than those of other experiments at the same filtration velocity (Table 52).
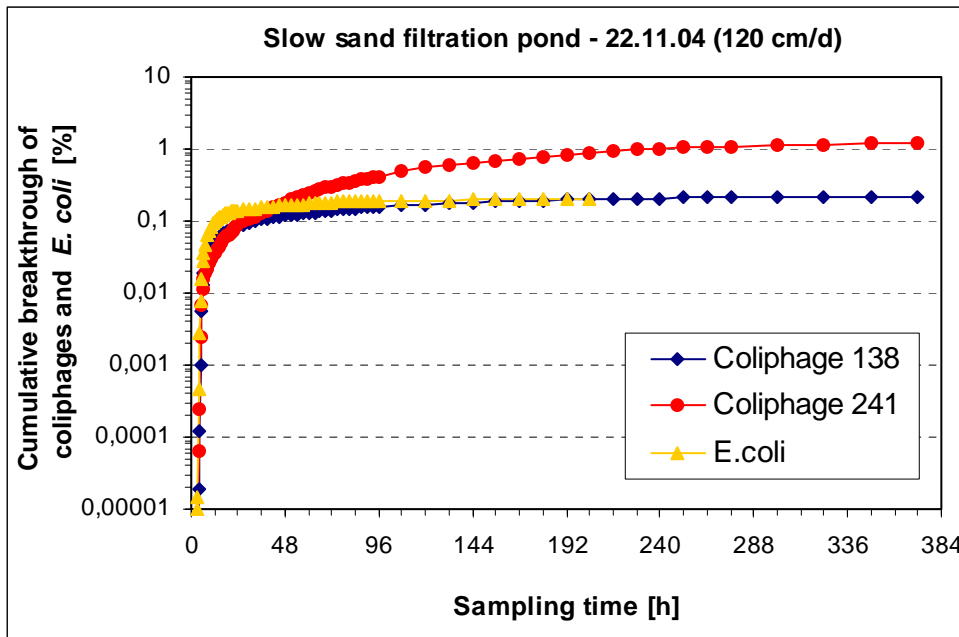
Figure 39: Cumulative breakthrough of the test coliphages and E. coli in slow sand filtration pond with clogging layer at a pore water velocity of 360 cm/d (3000 L/h)

Initial concentration of E. coli was 3,5.106 mpn/100 ml in the reservoir water which rapidly decreased to 3,8.105 mpn/100 ml after 6 h, and 575 mpn/100 ml after 24. E. coli was sporadically detected in reservoir water after 96h (Figure 37). Synchronic with other test organisms, E. coli was found in the effluent sample collected after 3 h of operation. Concentrations of E. coli were highest (2446 mpn/100 ml) already after 6h and decreased to 122 mpn/100 ml within 24 h. Concentrations remained at a stable level between 10 – 100 mpn/100ml during the further run of the experiment (Figure 40).
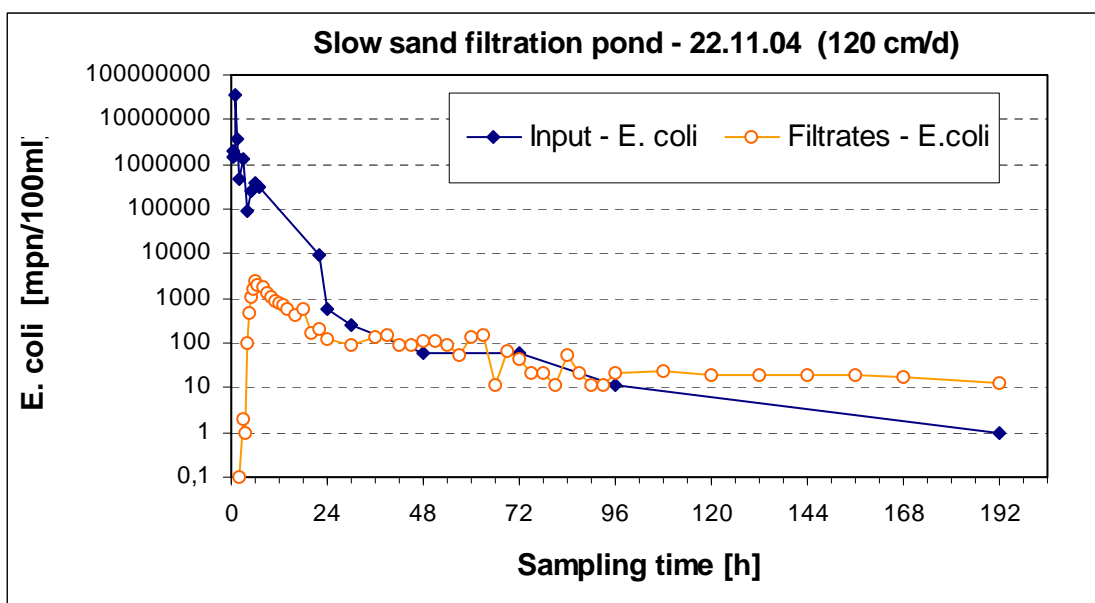
Figure 40: Concentration of E. coli in influent and effluent of the filtration pond with clogging layer at a flow rate of 360 cm pore water column per day

Despite early and continuous breakthrough, retention of E. coli in the slow sand filter was relatively high. Cumulative breakthrough ratios were about 0,001 at 12 and 24 h. Cumulative breakthrough ratio increased to 0,002 after 240 h of operation (Figure 39). Based on the relative high retention of 3,3 logs, specific retention capacity of filter pond was calculated as 0,042 log/cm corresponding to a relative high elimination rate coefficient of 1,44 log.h-1 (Table 52). The initial concentration of enterococci in the reservoir water was too low to deduct any retention behaviour.

5.2.3 Experiment SSF6 – 19.11.2003 (60 cm/d, with clogging layer)

Indicator bacteria and coliphages could be applied after completion of the experiments of other working groups at the end of the year 2003. The surface of the sandy soil was covered with a thick and homogenous biomass which reduced the filtrate volume significantly. The pore water velocity was set to 60 cm/d corresponding to a pore velocity of 180 cm/d.

F+phage 138 reached an initial concentration of 2.105 pfu/ml which declined one log unit after 5 h, and remained at a relatively stable level during the next two days. Concentration in reservoir water was 6,2.104 pfu/ml after 48 h, and 2 pfu/ml after 72 h Figure 42). Relatively low concentrations of F+ phage 138 were found in filtrate samples. However, they appeared in the initial filtrate samples. Concentrations reached a maximum of 6 pfu/ml after 18 h and slightly decreased to 1 pfu/ml after 48 h (Figure 41).

Retention of phage 138 was high. Cumulative breakthrough ratio was about 0,0001 after 24 h and at the end of the experiment after 150 h (Figure 42). Based on the total retention of 3,8 log units, a specific retention ratio resulted in a value of 0,05 logs/cm filter length (Table 53) Elimination rate coefficient was calculated as 0,82 log units.h-1 which was clearly less than at a flow rate of 120 cm/d. Modelling approach also showed a similar elimination rate of 0,89.h-1 and a retardation factor of 1,3 (Table 53).

Table 53: Retention of test organisms in the sand filtration pond with a filtration velocity of 60 cm/d (180 cm pore water/d),

Test organisms	Breakthrough ratio (CBTA)	Retention (log)	Specific retention (log)/cm	λA * (log.h-1)	Retardation (R) **	λC** (h-1)
F+ phage 138	0,0001	3,8	0,05	0,82	1,3	0,89
somatic phage 241	0,004	2,4	0,03	0,53	1,1	0,68
E. coli	0,0001	4	0,05	0,83		

[λ : elimination rate coefficient, *) calculation according to integrative balancing total virus concentrations in surface water and filtrate samples (equation 3),
** calculation according modelling approaches]

Initial concentrations of somatic phage 241 were low (about 6 x 10^2 pfu/ml) after inoculation into the reservoir and further decreased to 14 pfu/ml after 48 h (Figure 41). Phages rapidly appeared in the initial filtrate samples and reached a maximum concentration of 18 pfu/100ml in the effluent after 12 h of operation. Concentrations ranged from 1 to 10 pfu/100ml during the further run of the experiment.

A low cumulative breakthrough of phage 241 was calculated with 0,0002 after 12 h that slightly increased to 0,004 at the end of experiment after 150 h (Figure 42). High retention of phage 241 (2,4 logs) resulted in a specific retention ratio of 0,03 logs/cm.

In contrast to the low breakthrough ratio a moderate elimination rate coefficient of 0,53 log units.h^{-1} was determined. Modelling approaches also showed an elimination rate coefficient of 0,68.h^{-1} and retardation factor of 1,1.
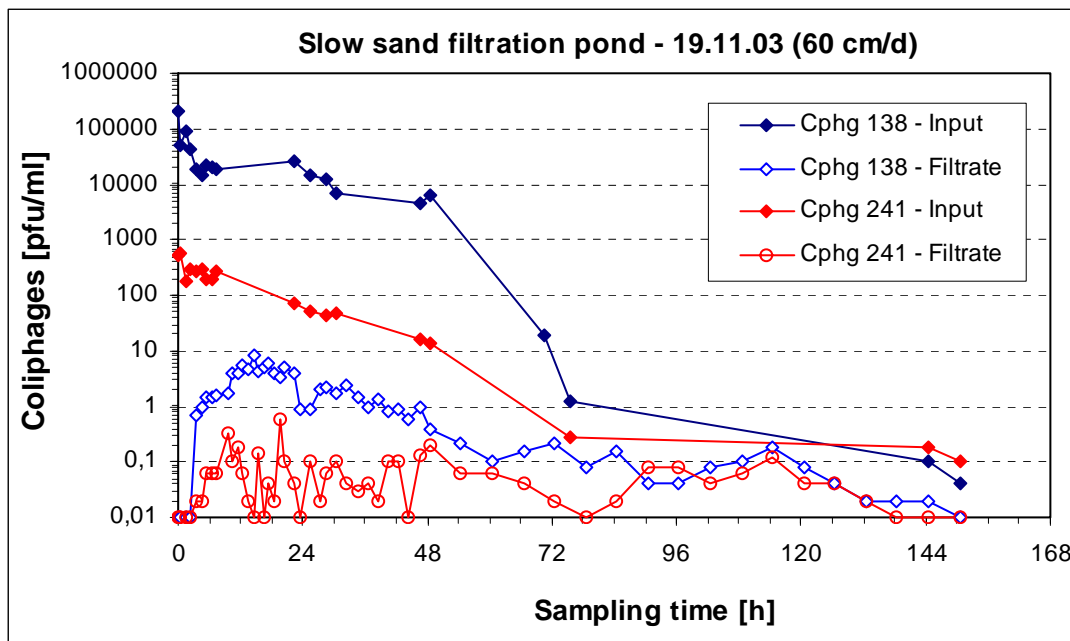
Figure 41: Concentration of F+ phage 138 and somatic coliphage 241 in influent and effluent of the filtration pond with clogging layer at a pore water velocity of 180 cm/d (1500 L/h)
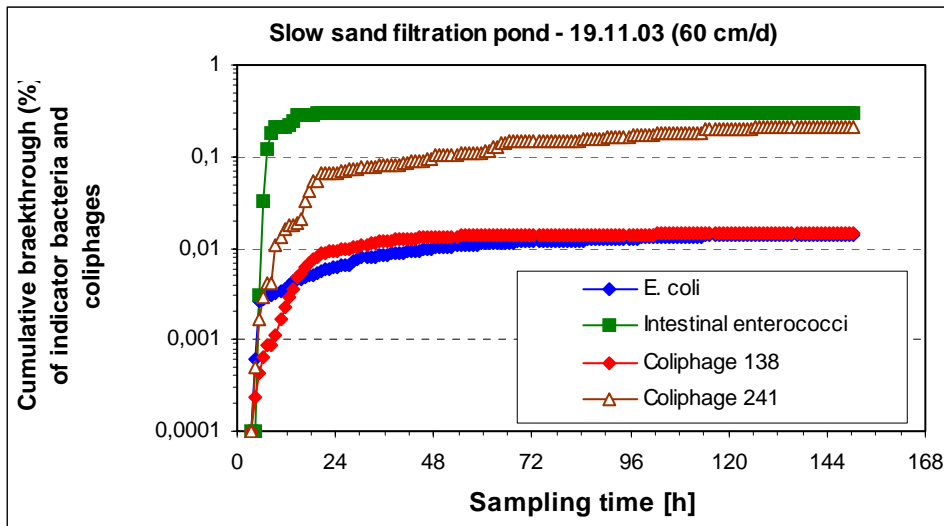
Figure 42: Cumulative breakthrough of test organisms by slow sand filtration with clogging layer at a pore water velocity of 180 cm/d (1500 L/h).

The initial concentration of E. coli in pond water was about $4,4 \times 10^7$ mpn/100 ml and decreased to $5,2 \times 10^5$ mpn/100 ml within 8 h of percolation. E. coli concentrations further decreased to 382 mpn/100ml or 42 mpn/100ml after 12 h or 24h, respectively. E. coli was already detected in the filtrate sample taken after 4 h despite a calculated percolation time of 9 h for water at this low flow rate to reach the effluent. Following this rapid breakthrough, the highest concentration of E. coli (240 mpn/100 ml) was detected after 5 h. Concentrations of E. coli varied between 15 and 75 mpn/100 ml in other effluent fractions collected within a filtration time of 48 h. After 60 h it was detected in all filtrate samples in concentrations below 10 mpn/100 ml (Figure 43).
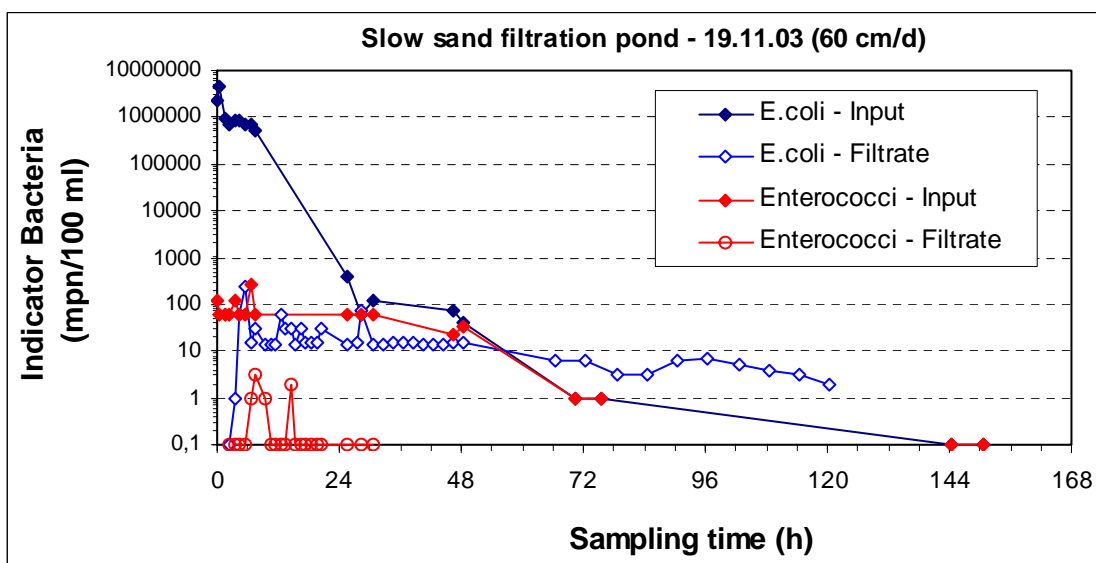
Figure 43: Concentration of E. coli and Enterococcus faecium. in influent and effluent of the filtration pond with clogging layer at a pore water velocity of 180 cm/d (1500 L/h)

Cumulative breakthrough ratio was 0,00004 within a filtration time of 12 h and increased to 0,0001 at the end of experiment after 150 h (Figure 42). The high retention of E.coli at this flow rate (4 log units) resulted in a high specific retention ratio of 0,05 log/cm filter length. Elimination rate coefficient reached 0,83 log unit.h^{-1} (Table 53).

After inoculation of filter pond, the concentration of Enterococcus faecium was extremely low (about 100 mpn/100 ml). After 6 h of operation it was no longer detectable in the reservoir water (Figure 43). As enterococci were only sporadically detected in filtrate samples, a reliable estimation of their removal or retention could not be carried out.

5.2.4 Biofilm Investigations before and after Experiment SSF8

Total bacterial cell counts were determined by DAPI staining (see 1). Counts in the biofilms varied between $1,8 \times 10^5$ and $6,3 \times 10^{106}$ cells/cm2 slide. A variety of different cell morphologies was detected in the biofilm; a selection is shown in Figure 44 (A-F).
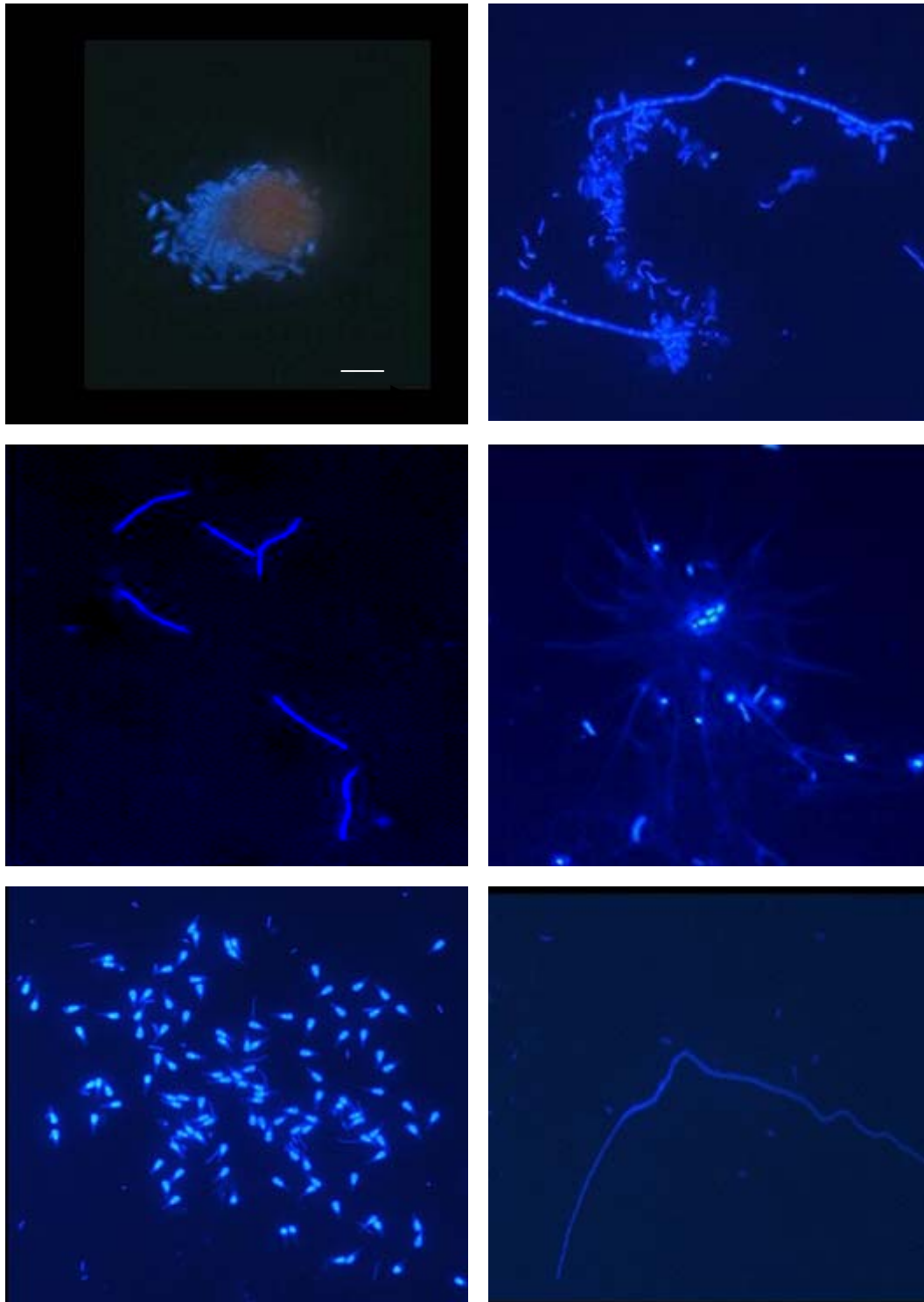
Figure 44: Various cell morphologies in a four week old biofilm at site one as detected by DAPI staining. Scale bar in (A) equals 5μm and belongs to all images. (A) microcolony of small rod shaped bacteria attached to an alga body. (B) single rod shaped bacteria and long chains of rod shaped bacteria. (C) slightly curved bacteria, the dominant type in the two, four and five week old biofilms in 10 cm and 30 cm depth. (D) a remarkable microcolony with a center of encapsulated bacteria with radial branches of a material around it. (E) bacterial cells composed of a "head" and a "tail". (F) thin and long filamentous bacterium.

Cell counts on the slides increased with increasing age of the biofilm and decreased with sampling depth. Figure 45 shows the results of one sampling site. Cell counts in the young, two week old biofilm were 2×10^6 cells/cm2 at 10 cm depth decreasing to 2×10^5 cells/cm2 at 30 cm and 60 cm depth. Cell counts of the four week old biofilm were higher than in the younger biofilm at 10 cm and 30 cm (about 3×10^6 cells/cm2). In 60 cm depth low concentrations were detected even after four weeks.
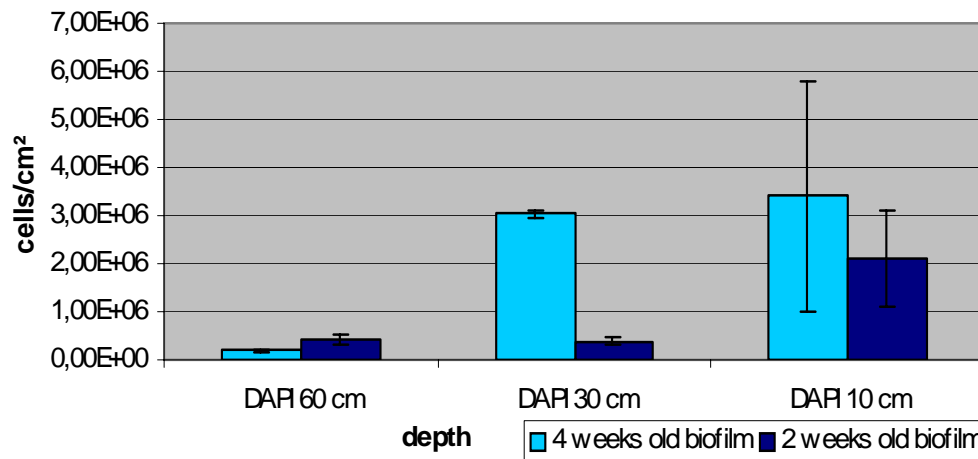
Figure 45: DAPI counts of biofilm bacteria at site one

No big differences in cell counts were found between the three sampling sites. Differences were highest at 10 cm depth were cell counts varied between 5×10^5 cells/cm2x and 2,5 x 10^6 cells/cm2 (Figure 46). At all three sampling sites cell counts decreased with depth to 3,5 x 10^5 cells/cm2 in 30 cm and even lower counts in 60 cm. Slides at 60 cm depth at site three were lost during the experiment because of a technical defect and, therefore, no values could be achieved for this point.

Phylogenetic characterization of the bacterial biofilm population (Figure 51) was performed in addition to DAPI total cell counts. The bacterial biofilm population was characterized with regard to (i) depth profile within 10 cm, 30 cm and 60 cm depth; (ii) biofilm age with two, four and seven week old biofilms and (iii) three different sites within the slow sand filter pond.
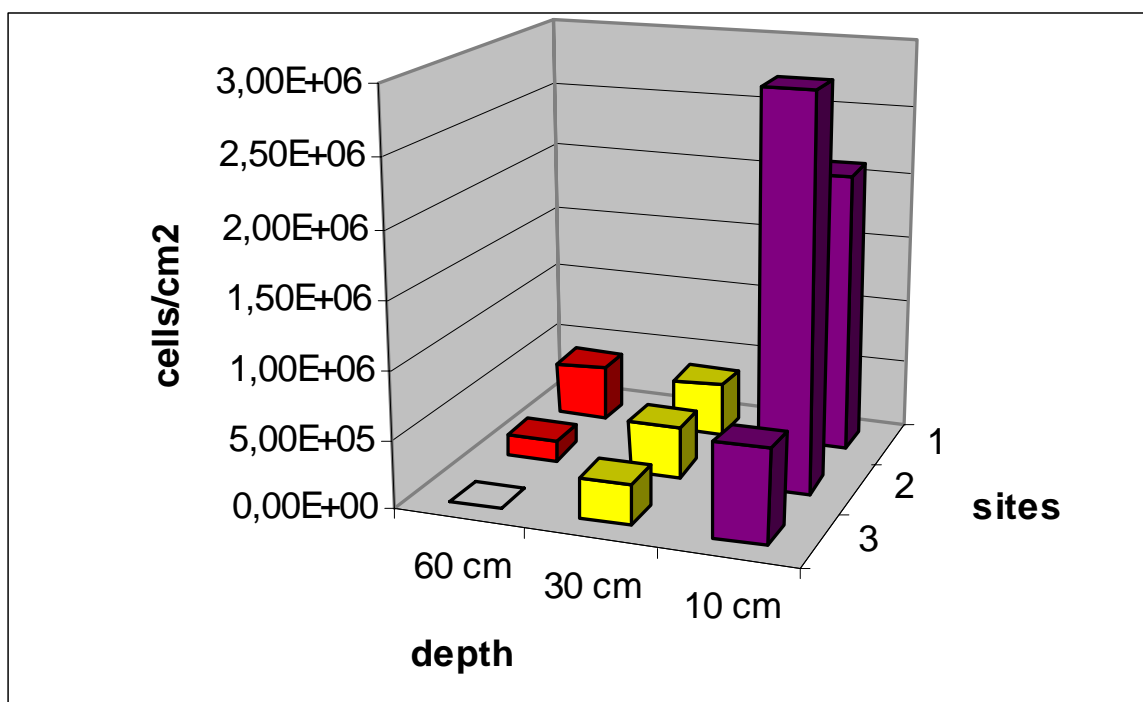
Figure 46 DAPI counts of biofilm bacteria at different sites

A high percentage of total cell counts was detectable with the Eubacteria probe. As exemplarily shown in a four week old biofilm (Figure 47) about 60 % of total cell counts in 10 cm and 30 cm depth and 40 % in 60 cm depth were detected. Within the Proteobacteria the alpha-group was dominant in the two upper layers with remarkable 22 % of total cell counts in 30 cm depth. In contrast to this, the alpha-Proteobacteria nearly disappeared in the deepest layer. Beta-Proteobacteria were only rarely detected in the top layer in contrast to 13 % in 30 cm depth and 8 % in 60 cm depth. Gamma-Proteobacteria were nearly equally distributed within the depth profile with values ranging between 3 % and 9 % of total cell counts. The group of Cytophaga-Flavobacteria was detected in the same range as the gamma-Proteobacteria with their highest amount of 9 % in the 30 cm depth. Planctomycetales were only detected in the top layer in low amounts.

The phylogenetic composition of the two week old biofilms was similar to the four week old biofilms (Figure 48). Alpa- and beta-Proteobacteria were, however, dominant in the 10 cm layer in the young biofilm and in the 30 cm layer in the older biofilm.

The phylogenetic characterization of two week old biofilms at the three different sites in the slow sand filter pond revealed a great diversity of the detected bacterial groups (Figure 49).
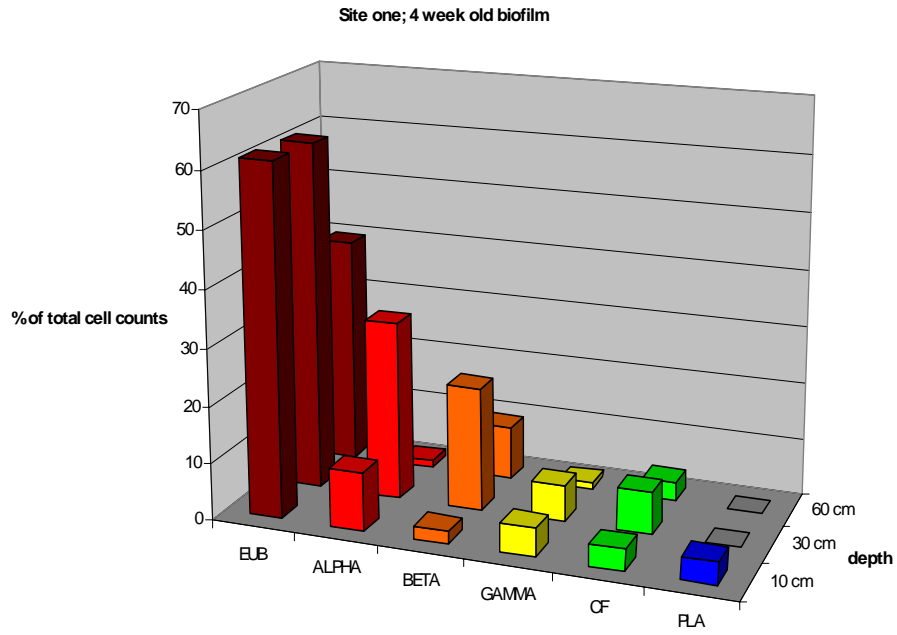
Figure 47: **Phylogenetic characterization of four week old biofilms at site one at different depths**
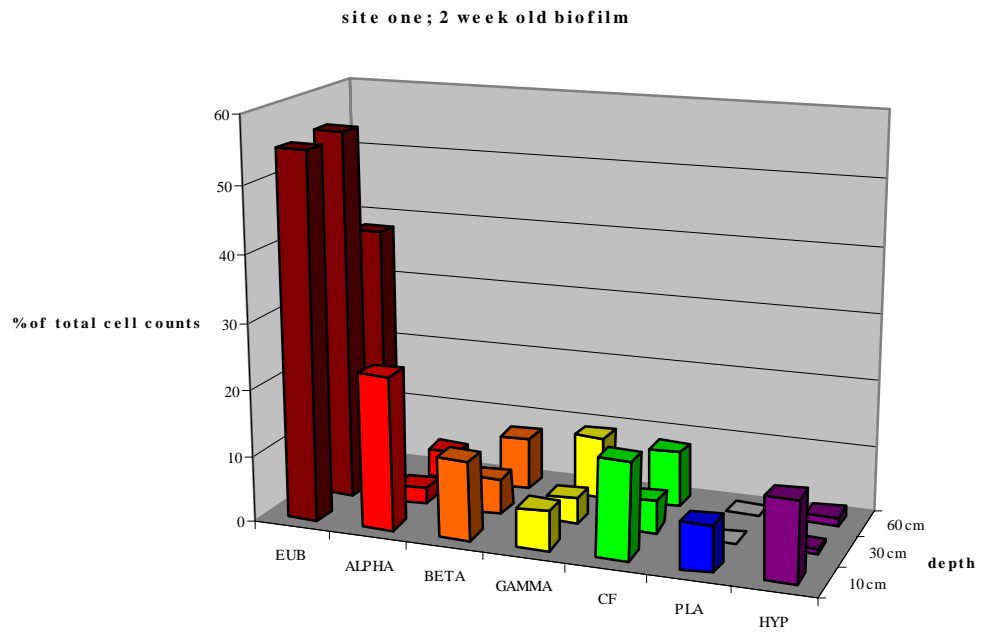
Figure 48: Phylogenetic characterization of two week old biofilms at site one at different depth

Eubacteria were nearly equally distributed at all three sites and depths ranging from 30 % to 60% of total cell counts. Within the Eubacteria the alpha-Proteobacteria were the dominant group at all three sites in 10 cm depth but not in deeper layers. In contrast to this the amount of beta-Proteobacteria remained constant over depth. Gamma-Proteobacteria were only rarely present at all three sites with up to 5 % of total cell counts. Cytophaga-Flavobacteria showed their highest amount at site one in all depths. Planctomycetales were only detected in the 10 cm layer at site one and two.
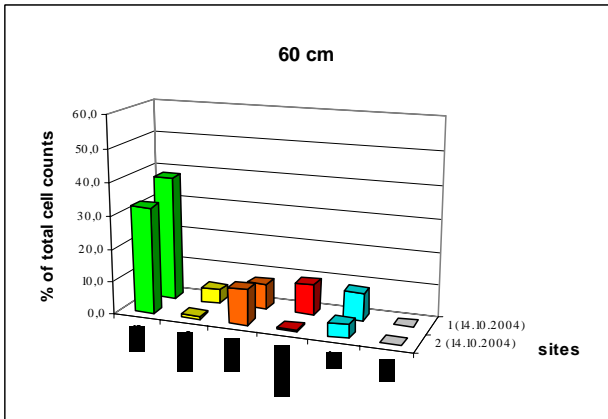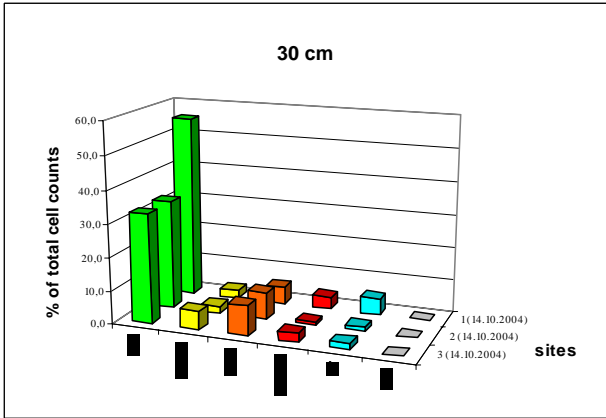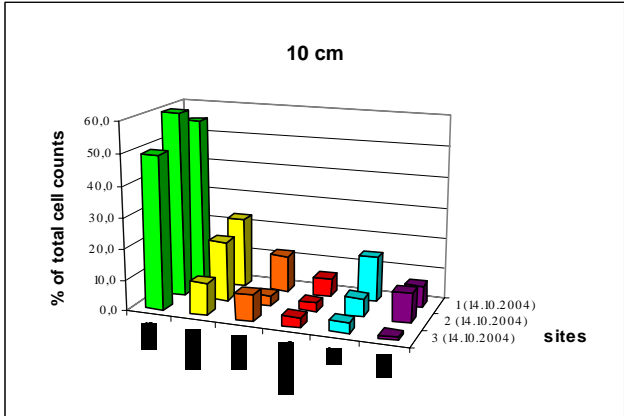
Figure 49: Phylogenetic characterization of two week old biofilms at different sites and different depths

A two and a five week old biofilm were hybridized with various probes targeting specific organisms within the Proteobacteria. Interestingly, bacteria hybridizing with probe HYPHO1241 in the dominant alpha-group accounted for 12 % of total cell counts in the two weeks old biofilm (see Figure 48). These bacteria had not the typical cell morphology of Hyphomicrobium but were slightly curved bacteria as shown in Figure 44.

Within the beta-Proteobacteria the amounts of Aquabacterium and those bacteria which hybridized with probe ISO21, a dominant bacterial member in the river Elbe, were nearly the same with 2 % -3 % of total cell counts. Within the gamma-Proteobacteria the specific probe for Aeromonadaceae detected an amount 2 % of total cell counts, whereas probe FLAVO1004 showed no signal in any depth of the biofilm (data not shown). After experiment SSF8, the presence of Enterobacteriaceae in the biofilms – the slides had been introduced in the filter 4 weeks prior to the experiment - was tested. Two weeks after the beginning of the experiment glass slides with biofilms were sampled and hybridized with probe D, specific for members of the Enterobacteriaceae (Figure 50). No signals were detected at site one at any depth. At site two 1 % of total cell counts gave positive signals with this sample in 10 cm depth and even remarkable 3 % of all DAPI stained cells hybridized with sample D at site three in 10 cm depth. No signals were detected in the deeper layers of the filter.
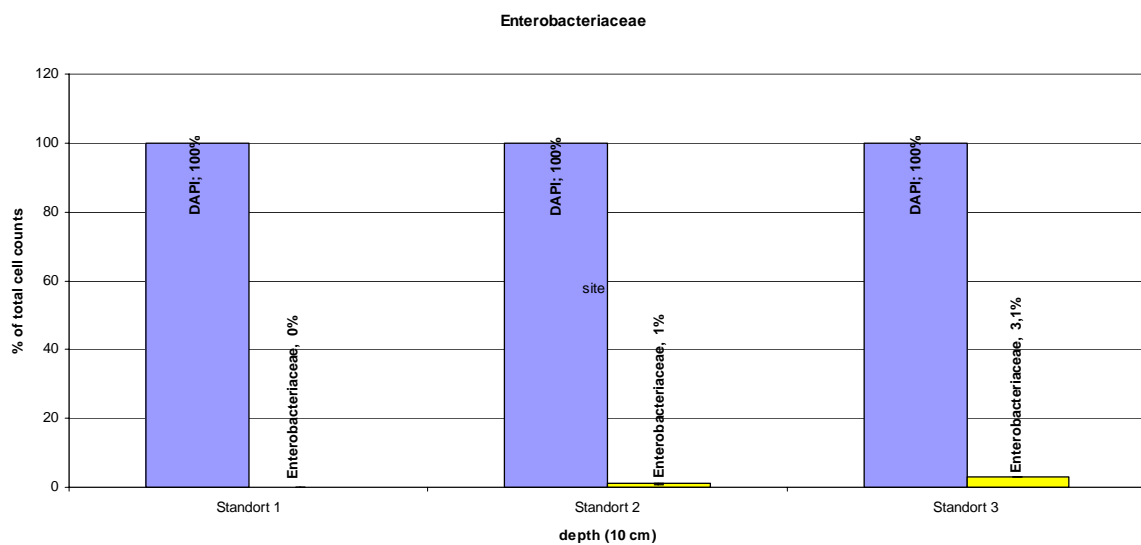
Figure 50: Detection of Enterobacteriaceae at the three different sites in the slow sand filter pond after deploying strain E.coli A3 and a retention period of two weeks

The amount of actively respiring bacteria in the biofilm (Figure 52A) was relatively low and decreased with increasing depth from 20 % of total cell counts in 10 cm depth to 9 % in 60 cm depth. No significant differences could be detected for the use of pure CTC or CTC with carbon supplementation due to high standard deviations. LIVE/DEAD staining of biofilm bacteria (Figure 53) revealed that the ratio of live and dead bacteria were similar in all biofilms examined. In 10 cm depth about 55 % of all bacteria were detected as living and 45 % were detected as dead cells. In 30 cm depth 65 % were detected as living cells and 35 % as dead. In the deepest layer of 60 cm live and dead cells were nearly equally distributed.
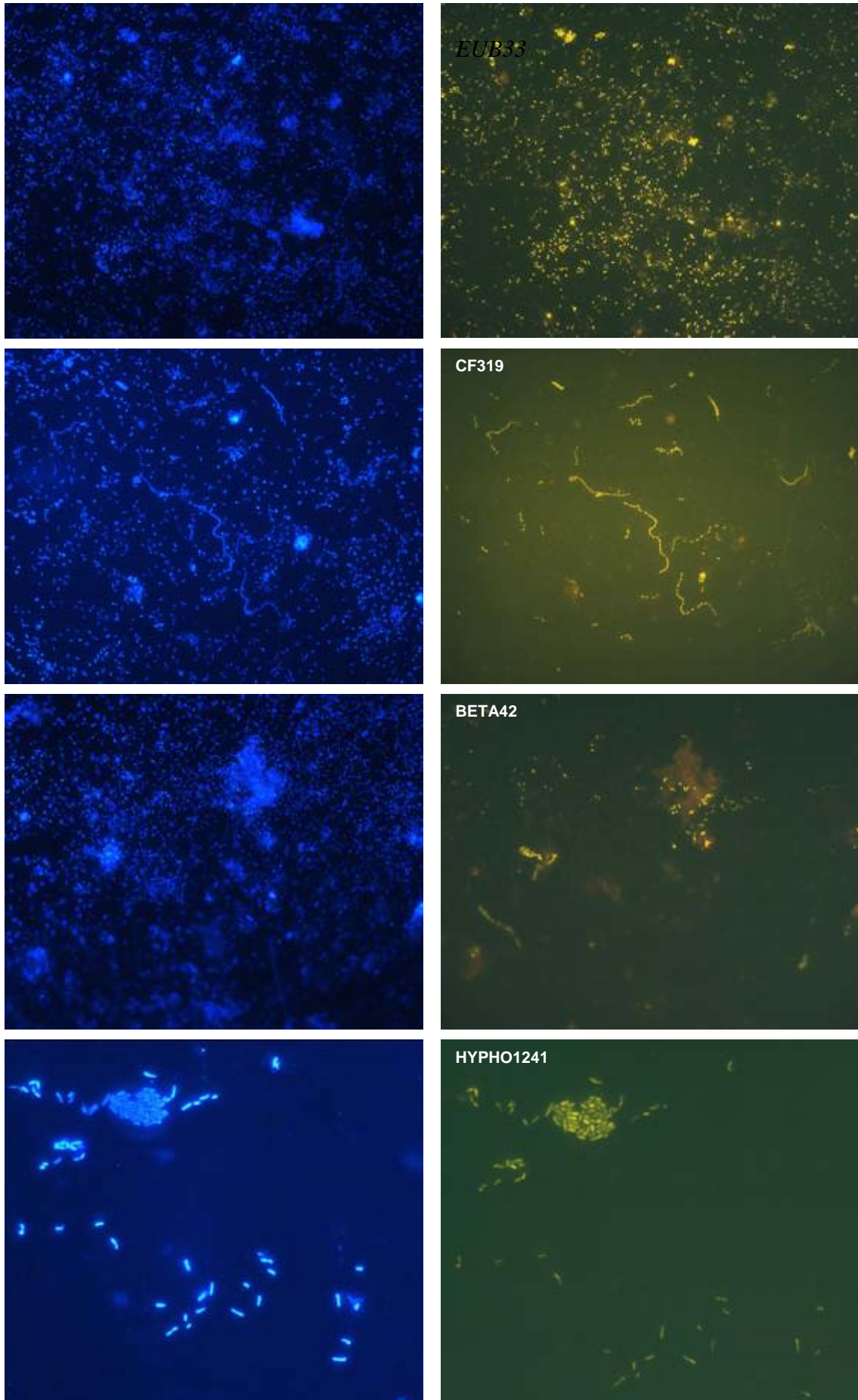
Figure 51: DAPI staining and probe signals of biofilm bacteria from the slow sand filter
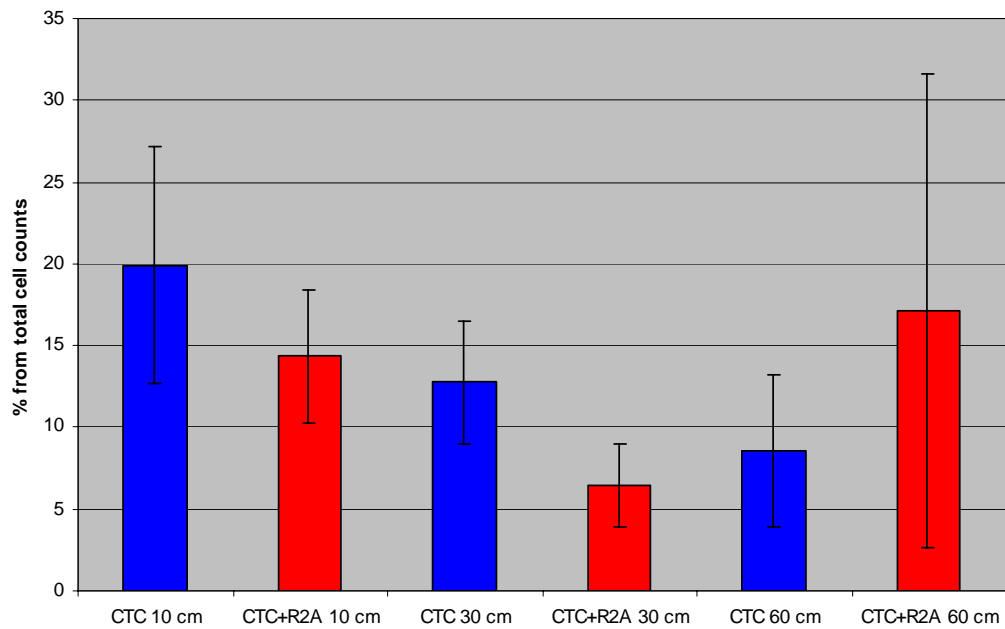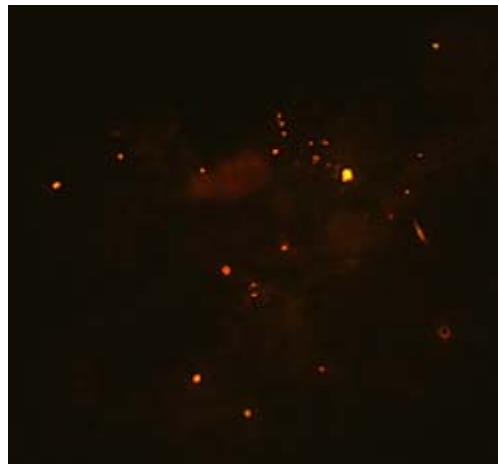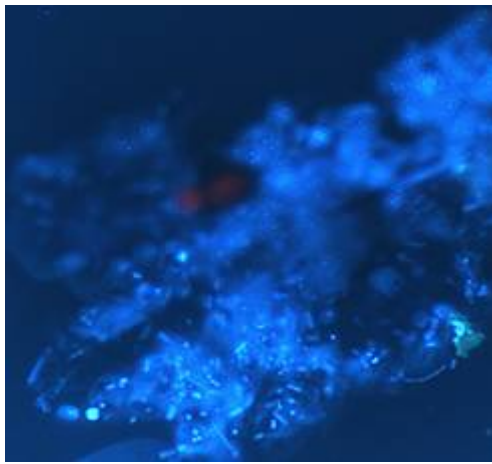
Figure 52: A: Epifluorescence photomicrographs of biofilm bacteria on glass slides in the slow sand filter pond (1) bacterial cells stained with DAPI (2) corresponding micrograph with CTC signals of active cells B. Percentage of actively respiring cells after incubation with 4mM CTC (blue) and 4mM CTC plus R2A medium (red)
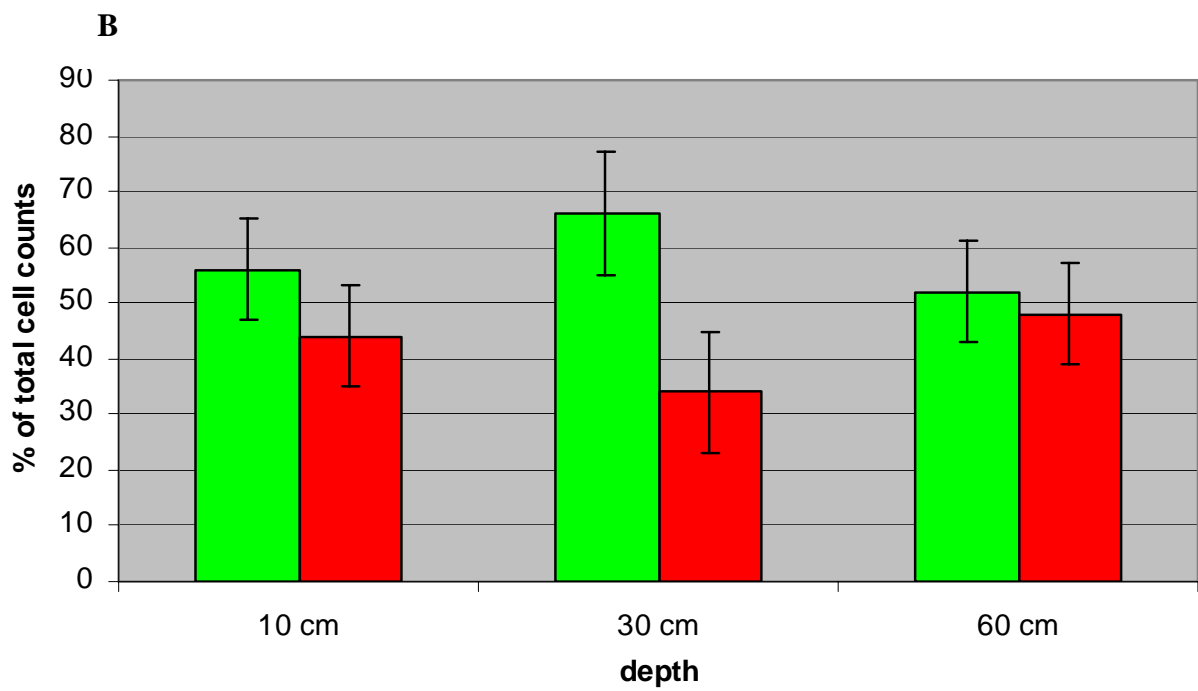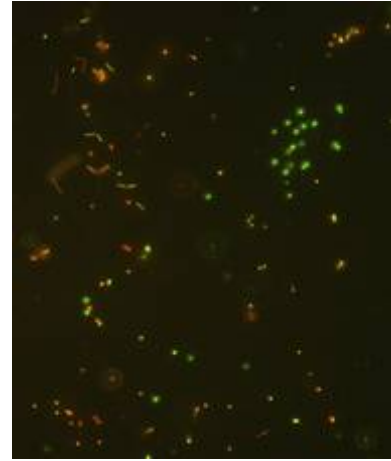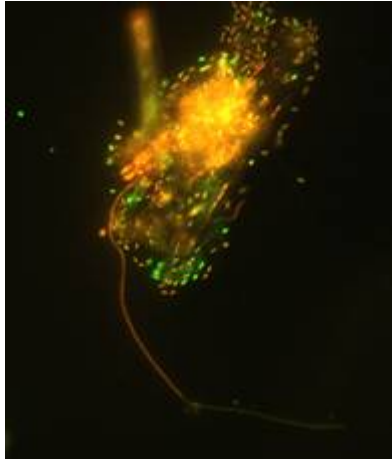
Figure 53 A: Epifluorescence photomicrographs of biofilm bacteria on glass slides in the slow sand filter pond after LIVE/DEAD staining (1) accumulation of different bacterial cells (2) single cells within the biofilm: green: live cells; red: dead cells. B: Percentage of live and dead cells in the biofilm after Live/Dead staining: green: live cells; red: dead cells

6 Enclosure experiments

Retention of coliphages and indicator bacteria by slow sand filtration in the enclosure

6.1 Material and Methods

6.1.1 Test organisms.

Both test coliphages were isolated from the Teltow canal discharging secondary effluent and run off water in Berlin. For isolation, cultivation and detection of somatic coliphage 241, the host bacterium E. coli WG5 was used as described in ISO 10705-2 (2000b). E. coli K13 was used as host for the phage 138 as described in EPA-methods 1601 (2001).

Detection limit was 1 plaque forming unit (pfu)/ 100 ml for both test coliphages.

The environmental E. coli strain A3 was obtained from the Department of Environmental Microbiology of the Technical University Berlin (Prof. Dr. Szewzyk). Enterococcus faecalis strain Teltow 11 was isolated from the Teltow canal. Detection and enumeration of E. coli and E. faecalis in water samples were carried out according to DIN EN ISO 9308-3, DIN EN ISO 7899-1 and DIN EN ISO 7899-2. Detection limit was 1-15 colony forming units (cfu)/100 ml or most probable number (mpn)/100 ml depending on the method used. All test organisms were selected for high survival potential in aquatic environments.

6.1.2 Enclosures.

Enclosures were cylindrical sand filtration units with a length of 200 cm and a diameter of 120 cm. Three enclosures were installed in an open infiltration pond and were filled from bottom to top with 0,3 m of gravel and 1 m of filter sand leaving about 0.8 m depth of water reservoir at the top. The effective (d_{10}) and median grain size of the sand was 0.28 mm and 0.7 mm, respectively. The d_{60}/d_{10} ratio was 3.28. The sand was, therefore, not considered uniform (ratio > 2, Clement, 2002). The porosity of the sand was measured to be 0.335. In Enclosure I, sampling sites were located at horizontal drain tubes at 20, 40, 60, and 80 cm depth as well as at the outlet at 100 cm depth (Fig. X in Chapter X). Enclosure II had three sampling sites at 40 cm, at 80 cm depth, and at the outlet tube at 100 cm depth. Sampling in Enclosure III was carried out only from the outlet tube at 100 cm depth. The water work Marienfelde regularly delivers ground water to all filtration ponds of the research area that was also used for filling and continuous percolation of the enclosures. By means of a hydraulic gradient, surface water in the reservoir of enclosure was maintained at a level of 70 cm corresponding to a volume of 500 L. The outlet of the enclosure had to be connected to a suction pump to regulate the filtration velocity to 50 L/h corresponding to 360 cm pore water per day (Vp) or 120 cm water column per day (Vf). Theoretical elapsed time of water during enclosure passage was calculated 6,6 h. Table Table 54 ,Table 55 and Table 56 show some characteristics of the surface water and sand used for the experiments in the enclosure.

Table 54: Selected characteristics of surface water in the filtration pond

Characteristics of percolated water	
Natrium	46,4 mg/L
Kalium	4,3 mg/l
Calcium	125 mg/L
Magnesium	17,7 mg/L
Sulphate	236 mg/L
Nitrate	0,3 mg/L
Phosphate	<0,1mg/L
DOC	5,5 mg/L
pH	7,8
Conductivity	963 µS/cm

Table 55: Selected characteristics of the native sandy soil in the filtration pond

Characteristics of sandy soil in filtration pond	
effective grain size	0,15 - 0,30 mm
uniformity coefficient	3
water charging particles	< 1%
Porosity	31,90%
Dispersion	0,04
dispersion coefficient	0,036 m2/d
average residual time	2,25 - 9 h

Table 56: Selected geochemical properties of the sediments

Parameters	Native	Colmation layer
Fe-ox [mg/kg]	275	605
Fe-red [mg/kg]	850	1700
Fe-total [mg/kg]	1125	2305
Mn-ox [mg/kg]	11.0	68.8
Mn-red [mg/kg]	17.5	100.0
Mn-total [mg/kg]	28.5	168.8
C-org [weight %]	0.022	0.343
C-inorg [weight %]	0.118	1.395
S-total [weight %]	0.010	0.048
CECeff [mmol(eq)/100g	0.127	1.127

6.1.3 Inoculation

Experiments with chemicals and coliphages were performed simultaneously. Reference compounds of all working groups were mixed in a stock solution of 10 L volume and added as a sluggish peak to the surface water reservoir of the enclosure containing 500 L of ground water. Bacteria were not added simultaneously with chemicals because of possible interactions. Inoculation of coliphages 138 and 241 and indicator bacteria in the reservoir was started in separate experiments synchronic with the tracer salt NaCl. Approximate densities of test organisms in the stock solutions were 1×10^{11} pfu/ml for f+ coliphage 138, 1×10^{10} pfu/ml for somatic coliphage 241, and 1×10^9 mpn/ml for indicator bacteria, respectively. The stock solutions of the test organisms were diluted in 10 L groundwater percolated and added into the water reservoir simultaneously with tracer salt solution of NaCl.

In the experiment Enclosure I-10 (see 6.2.5) both test coliphages were continuously injected into the reservoir water over a time period of 6 weeks.

During the experiment in the Enclosure III-13 (see 6.2.6), primary effluent from the sewage treatment plant of Berlin was daily added into the water reservoir in concentrations ranging from 2 % to 10 %.

6.1.4 Sampling

Samples from reservoir water were collected 20 cm below the water surface in sterile flasks at regular intervals. Sampling from drain tubes was carried out in sterile flasks separately from the other groups. Sampling intervals were short (30 – 60 min) during the first 12 h after inoculation and were prolonged to several hours and days during the further course of the experiment. An auto sampler was used for sampling the outlet over night.

Core samples from the filter bed were taken before and after one of the experiments to investigate the survival of bacteria and coliphages in the filter (see 6. 2.7).

After an operation time of over one year, filter bed was drained, and samples from the clogging layer up to 1 cm depth was collected for chemical analysis.

6.1.5 Assessment of the retention of test organisms

6.1.5.1 Cumulative breakthrough ratio A - CBTA

Concentrations of test organisms in reservoir water and filtrate samples were used for calculation of relative breakthrough ratios. The quotient of the concentration in each filtrate sample to the total concentration of test organisms in the reservoir water corresponds to the relative breakthrough of each filtrate fraction. The addition of these single relative breakthrough ratios as a function of time over the whole experiment resulted in a cumulative breakthrough ratio (CBT) of test organisms at a given time according to equation (1):

$$CBTA = \sum \frac{Cfiltrate}{CInput} \quad (1)$$

An example for the calculation of the cumulative breakthrough using phage 138 in experiment 1 of Enclosure III is given in Figure 67.

6.1.5.2 Cumulative breakthrough ratio B - CBTB

The breakthrough ratio was also calculated using the actual concentrations of microorganisims reached at each sampling point during the first 12 h of the experiment. Best fit straight lines were used to obtain the intersection points "a" for each sampling site (see Figure 66). These were used to determine the retention and the breakthrough of microorganisims after different filtration paths according to equation 2.

$$CBTB = \sum \frac{afiltrate}{ainput} \qquad (2)$$

Examples for the use of best fit straight lines of the equilibrium stage at five sampling sites are demonstrated in figure 1b for F+phage 138 and in Figure 69 for coliphage 241.

The values obtained for CBTB using this calculation method (see Table 57) were comparable to the CBTA-values (not shown in all tables) calculated as described above.

Multiplication of the CBT values by 100 gives the breakthrough as percentage of the input concentration.

6.1.5.3 Δ-Log-Retention (Δ-log a values, heterogeneity)

The decade logarithms of the concentrations of test organisms resulting from the interception points "a" of each regression line at each sampling site are demonstrated in tables 1-6 as log a values. The differences between two log a values from two neighbour sampling sites can be used to assess the heterogeneity of removal of test organisms in different path of the filter matrix.

6.1.5.4 Specific retention rate (filter factor F)

Retention of test organisms was also calculated through the (-)log10 of CBT values. The specific retention rate demonstrates the retention of test organisms per cm filter path.

Retention as log units per cm filter path has also been defined as filter factor F (Pang et al., 2005).

$$F = \frac{(-)LogCBT}{\text{Length of filter path (cm)}} \qquad (3)$$

The specific retention rate can also be calculated for the different parts of the filter by dividing the heterogeneity (Δ log a) through 20 cm.

6.1.5.5 Elimination rate coefficient (λ)

On the basis of the filtration theory of Yao et al. (1971), transport of colloid particles through saturated porous media can be represented by a connective dispersion equation, augmented by adsorption and desorption terms to account for bacterial interaction with the collector surface. In a column with characteristic length L (m), operated by a constant flow rate V(m/h), assuming steady state conditions, and neglecting dispersion (<0,001), virus inactivation and detachment or virus transport is described by (Schijven and Hassanizadeh, 2001):

$$(-)Log(CBT) = \frac{\lambda L}{2,3V} \qquad (4)$$

The elimination rate coefficient λ can be derived from this equation:

$$L = \frac{(-)Log(CBT)*V*2,3}{L} \qquad (5)$$

λ was calculated using both cumulative breakthrough ratios CBTA and CBTB (see λA and λB in the tables).

6.1.5.6 Modelling parameter: λC (h-1), Retardation factor (R)

The adsorption and transport behaviour of test organisms was simulated using a one-dimensional, one-site kinetic model (see also Chapter XXX). The λ obtained by modelling is listed as λC in the tables. λC was in the same order of magnitude as λA and λB in all experiments.

6.1.5.7 One log removal distance (D) and time (T)

Elimination rate coefficient (λ) and filter factor (F) are the main parameters to characterise removal of microorganisms in the aquifer. From equation 6, it can be deduced that virus removal in a saturated sand filter under steady state conditions with a constant attachment, detachment and inactivation coefficient, should decline in a linear fashion with travel distance.

One log removal distance (D) may be calculated from the log retention of test organisms in the total length of the filtration unit (L):

$$D\ (m) = L\ (m)\ /\ \log\ removal \qquad\qquad (6)$$

Or as reciprocate of filter factor (F) $D = 1\ /\ F$

One log retention time (T) of test organisms in each filter unit is the reciprocal of the elimination rate coefficient (λ)

$$T\ (h) = 1\ /\ \lambda \qquad\qquad (7)$$

Distance or filtration time required for e.g. 8 log removal of test organisms are 8 time higher than the D and T values.

6.2 Results

Four experiments (experiments 1, 3, 3 cont. and 13) were conducted in Enclosure III (6.2.1-6.2.3 and 6.2.6) and one experiment each in Enclosure II (experiment 9, 6.2.4) and Enclosure I (experiment 13, 6.2.5). Core samples were taken before and after experiment 3 in Enclosure III and analysed for coliphages and bacteria (6.2.7).

6.2.1 Experiment in enclosure III without apparent biomass on the filter surface (Enc.III-1 - 05.08.03)

The first experiment in Enclosure III - with five sampling sites at 20, 40, 60, 80 and 100 cm depth - was carried out directly after saturation of the native sandy soil with groundwater that was used for percolation of the enclosure. Filter velocity was adjusted to 120 cm/d or 50 L/h corresponding to a pore velocity of 360 cm/d. The surface layer of the enclosure was free from visible biomass.

After inoculation of the reservoir, the concentration of F+phage 138 was 8×10^5 pfu/ml decreasing to 2×10^5 or 4.7×10^4 pfu/ml after a percolation time of 5 or 12 h, respectively (Figure 65, Figure 66). An early breakthrough of F+phage 138 was observed synchronic with the tracer salt NaCl at all sampling sites. Concentrations in the filtrate samples increased rapidly, achieving highest levels after 4 h. Concentrations remained stable up to 24 h before gradually decreasing (Figure 66). Despite the rapid breakthrough in the initial filtrate fractions, retention of phages in the column was relatively high. Retention ratios were found 0,96 0,99 or 0,999 in filtrate samples from 20 cm, 60 cm or in the effluent, respectively, after 12 h of percolation time (Figure 67). After an operation time of 278 h, cumulative breakthrough of coliphage 138 at each sampling site remained at the same level as observed after 12 h.

Log-Retention was highest in the upper and lower part of the sand filter (1,3 and 1,1) and lower (0,5-0,8) in the middle part of the filtration path (Table 57).

The elimination rate coefficients (λ) calculated in three different ways - balancing total virus concentrations in reservoir and filtrate samples, using regression lines of each sampling site at their equilibrium stage as well as by two site kinetic adsorption modelling - were found to be in the same order of magnitude (Table 57). The highest elimination rate coefficients (about 5 log units.h^{-1}) were calculated for the filtration path in the upper 20 cm of the sand filter. With increasing filter length, elimination rates declined to about 2 log units.h-1 after 40 cm and to about 1,5 log units.h^{-1} in 60 cm or 80 cm filter path.

Table 57: Retention of F+phage 138 in Enclosure III without apparent biomass on the filter surface (pore velocity: 360 cm/d, 5.8.2003)

sampling sites	a (pfu/ml)	log a	log-Retention (total) +	Δ log-Retention (Heterogeneity) (Δ log a)++	λB* (log.h-1)	Break-through ratio (CBTA) **	λA** (log.h-1)	Retardation (R)***	λC*** (h-1)
surface water	514471	5,7	-	0	-	-	-	-	-
P1 (20 cm)	25486	4,4	1,3	1,3	4,8	0,04	5,4	2,1	5,5
P2 (40 cm)	8371	3,9	1,8	0,5	2,1	0,01	2,3	1,1	2,3
P3 (60 cm)	3210	3,5	2,2	0,4	1,5	0,004	1,7	1,1	1,5
P4 (80 cm)	550	2,7	3,0	0,8	1,5	0,001	1,6	1,1	1,6
effluent (100 cm)	43	1,6	4,1	1,1	1,3	0,0001	1,3	1,1	1,2

+) Retention of phages between surface and each sampling site
++) Retention of phages between two neighbour sites
*) Calculation according to the best fit straight line of the equilibrium phase,
**) Calculation according to balancing total virus concentrations in surface water and filtrate samples,
***) Calculation by modelling

The concentration of somatic coliphage 241 was much lower in the reservoir after inoculation compared to coliphage 138. Only 2000 pfu/ml were detected and concentration decreased to 40 pfu/ml during a percolation time of 24 h (Figure 68).

The detection of coliphage 241 in filtrate samples was also synchronic with the tracer NaCl at all sampling sites. After a rapid increase the densities of phages achieved maximum levels of 64 pfu/ml or 3 pfu/ml at the sampling sites 20 cm or 80 cm after a percolation time of 2 h or 6 h, respectively (Figure 68, Figure 69). The stationary phase of phage density in filtrate samples at all sampling sites occurred within a filtration time of 12 h. These characteristic events, early breakthrough and filtration equilibrium within 12-24 h, were observed in all further experiments in the enclosures.

Table 58: Retention of somatic phage 241 in Enclosure III without apparent biomass on the filter surface (pore velocity: 360 cm/d, 09.03.03)

sampling sites	a (pfu/ml)	log a	log-Retention (total) +	Δ log-Retention (Heterogeneity) (Δ log a)++	Break-through ratio (CBTA)*	λA* (log.h-1)	Retardation (R)***	λC** (h-1)
surface water	532	2,7	-	-	-	-	-	-
P1 (20 cm)	74	1,9	0,9	0,9	0,12	3,3	1,5	2,4
P2 (40 cm)	16	1,2	1,5	0,7	0,03	1,7	1,2	1,6
P3 (60 cm)	5	0,7	2,0	0,5	0,01	1,1	1,1	1,1
P4 (80 cm)	-	-	-	-	0,004	1,2	1,1	1,2
effluent (100 cm)	-	-	-	-	-	-	n.a.	n.a.

+) Retention of phages between surface and each sampling site
++) Retention of phages between two neighbour sites
*) Calculation according to balancing total virus concentrations in surface water and filtrate samples,
**) Calculation by modelling

Despite the low initial concentration of coliphage 241 in the influent, retention was lower than for F+phage 138. After a percolation time of 12 h, retention ratios of 0,92 and 0,99 were observed after 20 cm or in the effluent, respectively, (Figure 69). Coliphage 241 was detected in all filtrate samples during continued operation of the filter up to 278 h, but at relatively low concentrations (Figure 68).

As with F+phage 138, the highest log-retention (0.9) was found in the upper 20 cm of the sand filter (Table 58). Retention in the middle part of the filter was reduced (Log-Retention: 0,5-0,7). Due to very low concentrations of coliphage 241 in filtrate samples at 80 cm and 100 cm it was not possible to calculate the retention in the lower part of the filter.

High elimination rate coefficients (about 2-3 log units.h^{-1}) were calculated for the first 20 cm depth. Elimination rate coefficients clearly decreased to about 1 log unit.h^{-1} with increasing filtration path.

6.2.2 Experiment in enclosure III after visible biomass had formed on the filter (Enc.III-3 –10.09.2003)

The second experiment with coliphages in the enclosure was started after formation of apparent biomass on the filter surface. Some characteristics of sediment from the surface layer of enclosure (up to 1 cm depth) is summarised in table B. The accumulation of biomass on the surface reduced the flow rate at the same hydraulic conditions to 42 L/h corresponding to 100 cm water column or 300 cm pore velocity per day.

In the first part of the experiment, all reference chemicals and F+phage 138 were inoculated into the water reservoir of enclosure. The initial concentration of F+phage in the reservoir water was 6.8 x 10^4 pfu/ml and decreased by about 4 log units during the 140 h of operation. Similar curves were obtained at the different filtration levels at lower concentrations (Figure 71).

The retention of F+ phage 138 was slightly better than in the previous experiment without apparent biomass on the filter surface. After an operation time of 12 h, the retention of coliphage138 amounted 97 % or 99 % at a filtration path of 20 or 40 cm, respectively (Figure 72).

The elimination rates of coliphages attained 3 or 4 log units at the sampling sites of 80 cm and 100 cm depths (Table 59). Similar relative retentions were obtained at the end of operation after 140 h. The highest log-retentions were detected in the upper (1,5 log units) and lower (1,0 log units) filtration path of the enclosure. In the middle part lower log-retentions of 0,5-0,8 log units were calculated.

Elimination rate coefficients (λ) were highest (about 2-3 log units.h^{-1}) in the first 20 cm and decreased to 1.2-1.8 in the further filtration path. Due to the early breakthrough of phages, low and relatively constant retardation factors were found at all sampling sites of the enclosure, ranging between 1,1 and 1,2.

Table 59: Retention of F+ coliphage 138 in Enclosure III with apparent biomass on the filter surface (pore velocity: 300 cm/d, 10.09.03)

sampling sites	a* (pfu/ml)	log a*	log-Retention (total) +	Δ log-Retention (Heterogeneity) (Δ log a)++	λ B * (log.h-1)	Break-through ratio (CBTA)**	λA** (log.h-1)	Retardation (R)***	λC*** (h-1)
surface water	68211	4,8	-	-	-	-	-	-	-
P1 (20 cm)	2443	3,4	1,5	1,5	2,1	0,03	2,1	1,1	3,2
P2 (40 cm)	741	2,9	2,0	0,5	1,4	0,01	1,6	1,1	1,8
P3 (60 cm)	131	2,1	2,7	0,8	1,3	0,001	1,4	1,2	1,8
P4 (80 cm)	12	1,1	3,8	1,0	1,3	0,0002	1,3	1,1	1,5
effluent (100 cm)	-	-	-	-	-	0,00001	1,4	1,1	1,1

+) Retention of phages between surface and each sampling site
++) Retention of phages between two neighbour sites
*) Calculation according to the best fit straight line of the equilibrium phase,
**) Calculation according to balancing total virus concentrations in surface water and filtrate samples,
***) Calculation by modelling (R: retardation factor, λ: elimination rate coefficient)

6.2.3 Experiment in enclosure III with indicator bacteria cultures (Encl.III-3 continued - 17.09.2003)

In the second part of experiment Enclosure III-3, coliphage 241 and indicator bacteria (E. coli and enterococci) were inoculated together into the water reservoir of Enclosure III. Core samples of the sand filter were taken before and after the experiment and analysed for bacteria and coliphages (see 6.2.7). The initial concentration of coliphage 241 in the water reservoir was 2,1 x 10³ pfu/ml (Figure **73**). Concentration decreased about 3 log units during the first 100 h of operation. Similar curves were obtained at the different filtration levels at lower concentrations. Coliphage 241 was detected in low numbers from all filtrate samples up to an operation time of 800 h. The retention of coliphages 241 at all sampling sites was lower than in the previous experiment without apparent biomass on the filter surface (see 6.2.1). This may be due to preferential flow phenomena due to the core samples taken at the beginning of the experiment. Breakthrough ratios (51 h of operation) were 0,6 within 20 cm, 0,2 within 40 cm, and 0,004 in total effluent of the enclosure at a depth of 100 cm (Figure 74, Table 60). Highest retention was measured with 0,84 log units in the surface filtration path. It decreased to 0,42 log units between 20 and 40 cm. In the further filtration paths up to 80 cm depth, retention rates were measured as 0,65 and 0,8 log units. Relatively low elimination rate coefficients of 0,4-0,8 were calculated for all parts of the filtration path. Modelling

approaches showed a high retardation factor of 2,80 but very low λ value of 0,4.h^{-1} within the surface layer of 20 cm.

Table 60: Retention of the somatic coliphage 241 Enclosure III with apparent biomass on the filter surface (pore velocity: 300 cm/d, 17.09.03)

sampling sites	a* (pfu/ml)	log a*	log-Retention (total) +	Δ log-Retention (Heterogeneity) (Δ log a)++	Break-through ratio (CBTA)**	λA** (log.h-1)	Retardation (R)***	λC*** (h-1)
surface water	1655	3,2	-	-	-	-	-	-
P1 (20 cm)	241	2,4	0,8	0,8	0,6	0,5	2,8	0,4
P2 (40 cm)	92	2,0	1,3	0,4	0,2	0,6	1,6	0,5
P3 (60 cm)	21	1,3	1,9	0,6	0,07	0,8	2,1	0,5
P4 (80 cm)	3	0,5	2,7	0,8	0,02	0,8	1,5	0,5
effluent (100 cm)	-	-	-	-	0,004	0,6	n.a.	n.a.

+) Retention of phages between surface and each sampling site, ++) Retention of phages between two neighbour sites *) Calculation according to the best fit straight line of the equilibrium phase, **) Calculation according to balancing total virus concentrations in surface water and filtrate samples, ***) Calculation by modelling (R: retardation factor, λ: elimination rate coefficient)

The indicator bacteria E. coli and Enterococcus faecalis were added to the enclosure at the same time as coliphage 241. The addition of bacteria was possible for this experiment since the investigations with the trace chemicals had already been completed. Simultaneous addition of trace chemicals and bacteria was previously not allowed due to expected interactions.

Initial concentration of E. coli in the reservoir water was 108 cfu/100 ml (Figure 75, Table 61). It decreased about one log unit during the first 14 h of the experiment. The indicator bacteria also occurred synchronic with the tracer NaCl in all filtrate samples. Concentration in the effluent stabilized at about 1000 cfu/ 100 ml during the stationary phase of the filtration process within 24 h.

Retention of E. coli in the enclosure was higher than that of coliphages. About 99 % of the inoculated E. coli was eliminated after 20 cm of filtration after 14 h of operation. Elimination increased to 4 log units after 80 cm and 5 log units in the effluent at a depth of 100 cm (Figure 76).

Retention of E. coli was highest (2,1 log) in the upper part of the sand filter and lowest (0,6 log) between 60 cm and 80 cm (Table 5). Correspondingly, the elimination rate coefficient was 2-3 log units.h^{-1} in the upper part and lower (1,3 - 1,7 log units.h^{-1}) in the further filtration path.

Table 61: Retention of E. coli in Enclosure III with apparent biomass on the filter surface (pore velocity : 300 cm/d, 17.09.03)

sampling sites	a* (pfu/100ml)	log a*	log-Retention (total) +	Δ log-Retention (Heterogeneity) (Δ log a)++	λB* (log.h-1)*	Break-through ratio (CBTA)**	λA** (log.h-1)	Retardation (R)***	λC*** (h-1)
surface water	236000000	8,4	-	-	-	-	-	#	#
P1 (20 cm)	1963800	6,3	2,1	2,1	3,0	0,01	2,8	#	#
P2 (40 cm)	-	-	-	-	3,0	0,0002	2,6	#	#
P3 (60 cm)	58823	4,8	3,6	1,5	1,7	0,0002	1,8	#	#
P4 (80 cm)	14441	4,2	4,2	0,6	1,5	0,0001	1,4	#	#
effluent (100 cm)	1748	3,2	5,1	0,9	1,5	0,00002	1,4	#	#

+) Retention of phages between surface and each sampling site , ++) Retention of phages between two neighbour sites, *) Calculation according to the best fit straight line of the equilibrium phase,, **) Calculation according to balancing total virus concentrations in surface water and filtrate samples, ***) Calculation by modelling (R: retardation factor, λ: elimination rate coefficient), #) in preparation.

The concentration of enterococci in the reservoir water was about 106 cfu/100 ml after inoculation (Figure 77). Survival potential of enterococci was much lower than that of the E. coli strain. Concentration in the reservoir water decreased rapidly within a few hours and only 1000 cfu/100 ml were detected after 3 h. As for E. coli, the retention of enterococci was higher than that for coliphage 241. Only 0,9 % or 0,1 % of inoculated enterococci were found in filtrates at 20 or 80 cm depth, respectively. No enterococci were detected in the effluent (Figure 78).

Table 62: Retention of intestinal enterococci in Enclosure III with apparent biomass on the filter surface (pore velocity: 300 cm/d, 17.09.03)

sampling sites	a* (pfu/100 ml)	log a*	log-Retention (total) +	Δ log-Retention, Heterogeneity (Δ log a)++	λB* (log.h-1)*	Break-through ratio (CBTA)**	λA** (log.h-1)	Retardation (R)***	λC*** (h-1)
surface water	6095830	6,8	-	-	-	-	-	#	#
P1 (20 cm)	4082	3,6	3,2	3,2	4,6	0,01	4,0	#	#
P2 (40 cm)	378	2,6	4,2	1,0	3,0	0,002	2,3	#	#
P3 (60 cm)	125	2,1	4,7	0,5	2,5	0,001	2,0	#	#
P4 (80 cm)	10	1,0	5,8	1,1	2,1	0,0003	1,5	#	#
effluent (100 cm)	-	-	-	-	-	0,00001	1,3	#	#

+) Retention of phages between surface and each sampling site
++) Retention of phages between two neighbour sites
*) Calculation according to the best fit straight line of the equilibrium phase,
**) Calculation according to balancing total virus concentrations in surface water and filtrate samples,
***) Calculation by modelling (R: retardation factor, λ: elimination rate coefficient), #) in preparation.

Retention was more than 6 log units over the total filter path of 100 cm. Retention was highest (3,2 log) in the upper part of the sand filter and lowest (0,5 log) between 40 cm and 60 cm (**Table 62**).

Elimination rate coefficient were highest (about 4 log units.h^{-1}) within the top layer of 20 cm. It decreased to 2-3 log units.h^{-1} for a filtration paths of 40 and 60 cm and to 1,3 log units.h^{-1} in the total length of filter path.

6.2.4 Experiment in Enclosure II under microaerophilic conditions (Enc.II-9 – 30.08. 04)

Enclosure II - with two drain canals at 40 and 80 cm as well as the outlet at 100 cm depth - was continuously percolated with 0.1 M acetic acid for three weeks to reduce the oxygen content of the percolation water and to obtain micro aerophilic or anoxic conditions. At a relatively constant level of < 0,1 mg/L oxygen in effluent samples we inoculated the water reservoir with culture suspensions of coliphages and E. coli. Enclosure II was operated with a filtration velocity of 72 cm/d corresponding to a pore velocity of 210 cm/d.

Concentration of F+ phage 138 was 2×10^6 pfu/ml in the reservoir water directly after inoculation. Due to a relatively low filtration velocity, dilution of phages in the water reservoir was low and the concentration of phages did not decreased rapidly. After 10 h or 26 h, 1.106 or 1×10^5 pfu/ml phages were found, respectively (Figure 79). Retention of phages under micro- aerophilic filtration conditions in Enclosure II was very low. All filtrate samples contained more than 10^4 pfu/ml within the first 48 h. The highest concentration ($8,6 \times 10^5$ pfu/ml) was detected in the filtrate sample at 40 cm after 7 h of operation. In correspondence with the pore velocity, the highest phage concentrations were observed after 9 h at 80 cm and after 24 h at 100 cm . Concentrations in filtrate samples decreased slightly in the further course of the experiment. F+ phages were still detectable in all filtrate samples after 3 weeks.

Breakthrough of F+ phage 138 under micro aerophilic conditions was much higher than under aerobic conditions. Cumulative breakthrough ratios were 0,5 in the upper part of the enclosure and decreased to 0.2 in the lower part compared to 0,0002 under aerobic conditions (Table 59, Table 63). Correspondingly, low elimination rate coefficients (λ) were calculated at all sampling sites. Highest λ values of 0,4-0,6 log units.h^{-1} were calculated for the upper part of the filtration path decreasing to 0.6-1,0 in the lower part (Table 63). Statistical analysis of the results indicated no retardation of the coliphages (R = 1).

Table 63: Retention of F+ phage 138 in Enclosure II under micro-aerophilic conditions at a pore velocity of 210 cm/d (30.08.04).

sampling sites	a* (pfu/ml)	(log a)*	log-Retention (total) +	Δ log-Retention, Heterogeneity (Δ log a)++	Break-through ratio (CBTA)**	λA** (log.h-1)	(R)***	λC (h-1)***
surface water	1968000	6,3	-	-	-	-	-	-
P2 (40 cm)	784048	5,9	0,4	0,4	0,47	0,42	1,1	0,67
P4 (80 cm)	548000	5,7	0,6	0,2	0,32	0,13	1,0	0,16
Effluent (100 cm)	201446	5,3	1	0,4	0,17	0,13	1,0	0,06

+) Retention of phages between surface and each sampling site , ++) Retention of phages between two neighbour sites, *) Calculation according to the best fit straight line of the equilibrium phase,, **) Calculation according to balancing total virus concentrations in surface water and filtrate samples, , ***) Calculation by modelling (R: retardation factor, λ: elimination rate coefficient)

The initial concentration of somatic phage 241 was about $5,4 \times 10^4$ pfu/ml in the water reservoir of the enclosure. Concentration decreased to 104, 103, and 10^2 pfu/ml after a percolation time of 10, 24 and 48 h (Figure 80). After a rapid breakthrough of phages in the filtrate fractions at 40 cm the highest concentration of $8,5 \times 10^4$ pfu/ml was found after a percolation time of 4 h. Highest concentrations at other sampling sites were observed after 10 h at 80 cm and 28 h at 100 cm depth.

Retention of somatic phage 241 was much lower in the enclosure under micro-aerophilic conditions compared to aerobic conditions and even lower than for F+ phage 138. Highest retention was determined in the upper part with 0,6 log units which significantly decreased to

0.05-0.08 log units in the lower part of the enclosure. Accordingly, the highest elimination rate coefficient (0,3-0,4 log units.h^{-1}) were calculated for the upper part. In the lower part, the elimination rate coefficient decreased to 0,07-0,1 log units.h-1 in the lower part (Table 64). Modelling results showed a moderate retardation in the surface filter layer (R=1,5) but no retardation (R = 1) in the lower part.

Table 64: Retention of somatic coliphage 241 in the Enclosure II under micro aerophilic conditions at a pore velocity of 210 cm/d (30.08.04).

sampling sites	a* (pfu/ml)	(log a)*	log-Retention (total) +	Δ log-Retention, Heterogeneity (Δ log a)++	Break-through ratio (CBTA)**	λA** (log.h-1)	(R)***	λC (h-1)***
surface water	38170	4,6	-	-	-	-	-	-
P2 (40 cm)	9019	4,0	0,6	0,6	0,55	0,33	1,50	0,43
P4 (80 cm)	7531	3,9	0,7	0,08	0,40	0,11	1,04	0,14
Filtrate (100 cm)	6784	3,8	0,8	0,05	0,30	0,09	1,00	0,07

+) Retention of phages between surface and each sampling site
++) Retention of phages between two neighbour sites
*) Calculation according to the best fit straight line of the equilibrium phase,
**) Calculation according to balancing total virus concentrations in surface water and filtrate samples,
***) Calculation by modelling (R: retardation factor, λ: elimination rate coefficient)

After inoculation of E. coli, a high initial concentration of 7×10^9 mpn/100 ml was measured in the reservoir of the enclosure. Concentration of E. coli decreased to 1×10^7 mpn/100 ml after 12 h and $1,4 \times 10^6$ mpn/100 ml after 24 h (Figure 81). Highest concentrations of E. coli were found in filtrate samples already after 3 h at 40 cm, after 8 h at 40 cm, and after 24 h in the effluent of the enclosure. Concentrations of E. coli in filtrate samples reduced slightly during the further run of the experiment. E. coli was detectable in all filtrate samples over 3 weeks of operation.

Breakthrough of E. coli was also much higher under micro aerophilic conditions of this experiment compared to aerobic conditions. Cumulative breakthrough ratios were 0,84 in the upper part of the enclosure and decreased to 0,01 in the lower part compared to 0,00002 under aerobic conditions (Table 61, Table 65).

Breakthrough was again lower for E. coli than for coliphages.

Table 65: Retention of E. coli in Enclosure II under micro aerophilic conditions at a pore velocity of 210 m/d (30.08.04).

sampling sites	a* (mpn/100 ml)	(log a)*	log-Retention (total) +	Δ log-Retention, Heterogeneity (Δ log a)++	Break-through ratio (CBTA)**	λA** (log.h-1)	(R)***	λC (h-1)***
surface water	70341000	7,8	-	-	-	-	-	-
P2 (40 cm)	949126	6,0	1,9	1,87	0,84	0,19	#	#
P4 (80 cm)	263826	5,4	2,4	0,56	0,08	0,3	#	#
Filtrate (100 cm)	94105	5,0	2,8	0,45	0,01	0,33	#	#

+) Retention of E. coli between surface and each sampling site
++) Retention of E. coli between two neighbour sites
*) Calculation according to the best fit straight line of the equilibrium phase,
**) Calculation according to balancing total virus concentrations in surface water and filtrate samples,
***) Calculation by modelling (R: retardation factor, λ: elimination rate coefficient) #) in preparation

6.2.5 Experiment in Enclosure I with continuous inoculation (Enc.I-10 - 12.10.04)

A suspension of test coliphages was continuously injected into the surface water reservoir of Enclosure I - simultaneously with the reference suspension of microcystin - by means of a two canal pump. Filter velocity was regulated to 70 cm water column or 210 cm pore water column per day. Sampling was only possible in the water reservoir and at the outlet after a filtration path of 100 cm.

Mean concentration of F+ phage 138 in the water reservoir was $1,3 \times 10^5$ pfu/ml during the first part of the experiment for 15 days (Figure 54, Table 66). The cumulative breakthrough ratio (0.0001 log units) was similar to the ratios obtained for pulse experiments under aerobic conditions (see 6.2.1, 6.2.2). Based on a retention of 3,9 log units, an elimination rate coefficient (λ) of 0,67 log unit.h^{-1} was calculated for a filtration path of 100 cm.
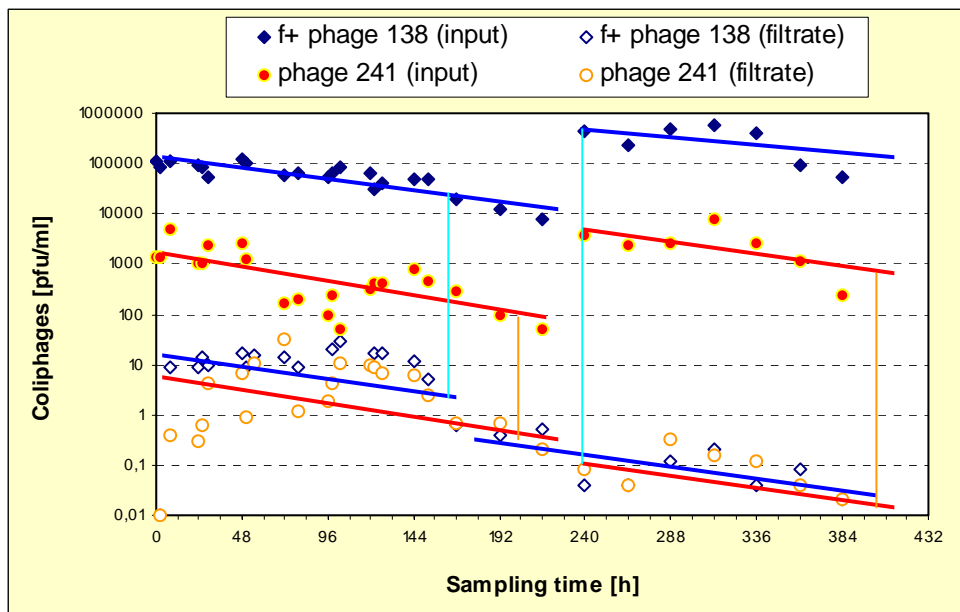
Figure 54: Retention of coliphages in Enclosure I (with clogging layer) during continuous inoculation at a pore water velocity of 210 cm/d

After 15 days of operation, inoculation dose of phages was increased to $1,2 \times 10^7$ pfu/ml . Nevertheless, F+ phage 138 was still only sporadically detected in the filtrate samples. Retention was, therefore, 7 log units and the elimination rate coefficient increased to 1,28 log units per h (Table 66). In the modelling approach, all results of this experiment were analysed as a block. No or only weak retardation (R=1,1) and also a relatively low elimination rate coefficient (λC) of 0,72 h^{-1} were found.

The concentration of somatic coliphage 241 averaged $1,7 \times 10^3$ pfu/ml in the reservoir water during the initial phase of experiment. Mean concentration of phages in filtrate samples was 14 pfu/ml corresponding to a retention of 2,1 log units. The elimination rate coefficient of phage 241 was calculated as 0,36 logs. h^{-1}.

After 15 days the concentration of somatic coliphage 241 was increased more than 2 log in the water reservoir to $1,7 \times 10^5$ pfu/ml. Concentrations in the filtrate samples were even lower than with lower initial concentrations in the beginning of the experiment. Retention, thereby, increased significantly to 5,2 log units resulting in a specific elimination rate of 0,92 logs. h -1. Modelling approach of results showed a relatively high retardation factor of 3,5, but extremely low elimination rate coefficient (λC) of 0,13 logs. h^{-1}.

Table 66: Retention of test coliphages in Enclosure I with continuous inoculation at a pore velocity of 210 cm/d (12.10.04)

F+ phage 138	a (pfu/ml)*	log a *	Δ log-Retention, Heterogeneity (Δ log a) +	Break-through ratio (CBTA)**	λA** (log.h-1)	(R)***	λC (h-1)***
surface water	128986	5,11	-	-	-	-	-
Filtrate (100 cm)	15	1,18	3,9	0,00012	0,67	1,1	0,72
surface water	11983696	7,08	-	-	-	-	-
Filtrate (100 cm)	1	0,00	7,1	0,00000003	1,28	-	-
somatic coliphage 241	a (pfu/ml)*	log a *	Δ log-Retention, Heterogeneity (Δ log a) +	Break-through ratio (CBTA)**	λA** (log.h-1)	(R)***	λC (h-1)***
surface water	1691	3,23	-	-	-	-	-
Filtrate (100 cm)	14	1,14	2,1	0,008	0,36	3,5	0,13
surface water	171509	5,23	-	-	-	-	-
Filtrate (100 cm)	1	5	5,2	0,000004	0,92	-	-

+) Retention of phages between two neighbour sites
*) Calculation according to the best fit straight line of the equilibrium phase,
**) Calculation according to balancing total virus concentrations in surface water and filtrate samples,
***) Calculation by modelling (R: retardation factor, λ: elimination rate coefficient)

6.2.6 Experiment in Enclosure III with primary effluent – (Enc.III-13 - 26.10 – 18.12.04, pore velocity: 210 cm/d)

In the last experiment with Enclosure III, surface water was continuously infected with domestic primary effluent from the sewage treatment plants of southern Berlin. The primary effluent was treated by sieving through 0,1 mm mesh size before usage. The concentration of primary effluent was regulated between 2 and 10 % to obtain a constant level of coliphages and indicator bacteria.

The concentration of F+ phages in the reservoir water varied between 2.105 – 2.106 pfu/100 ml in the first four days when 2 % of primary effluent was added to the water reservoir (Figure 55). After one week, the density of F+ phages declined to about 7.103 pfu/100ml in spite of permanent addition of 2 % waste water. Therefore, the amount of primary effluent was increased to 4 % which caused a moderate rise in the concentration of concentration F+ phages up to $9x10^4$ pfu/100 ml, but concentrations decreased again to $1x10^4$ pfu/100ml during the third week of operation. After four weeks, 10 % of primary effluent was added. Concentrations of F+ phages did not increase but remained at a similar level as measured previously (Figure 55).

Despite increasing volume of primary effluent, concentrations of coliphages remained at a relatively stable concentration. One explanation might be a high daily fluctuation of contaminants in the primary effluent added to the enclosure. The chemical and physical characteristics of the primary effluent were, however, similar over the whole run of the experiment. Some chemical parameters of primary effluent are demonstrated in Fig. 11A. Mean concentrations of these selected parameters averaged 638+217 mg/L for chemical oxygen demand (COD), 5,04 + 1,19 mg/L for total organic carbon (TOC), 64,6 + 12,4 mg/L total nitrogen (total N), and 0,95 + 0,23 g/L for dry matter. Constant concentrations of phages in the reservoir water despite increasing amount of primary effluent, might be explained by changing microbial activity or increasing deactivation of phages in water reservoir of Enclosure III.
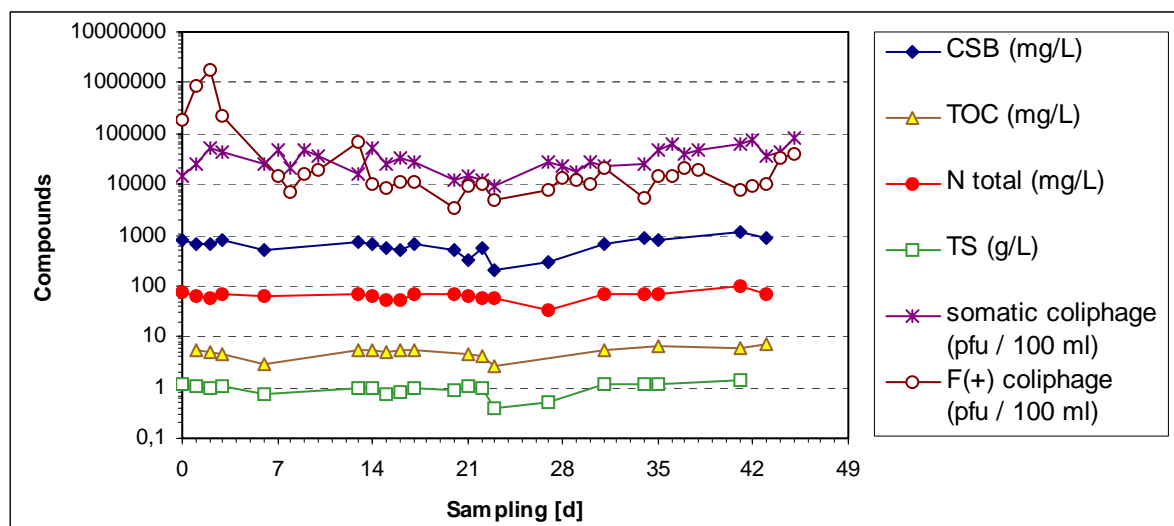
Figure 55: Concentrations of selected chemical parameters (mg/L) and coliphages (pfu/100 ml) in primary effluent spiked to the reservoir of Enclosure III
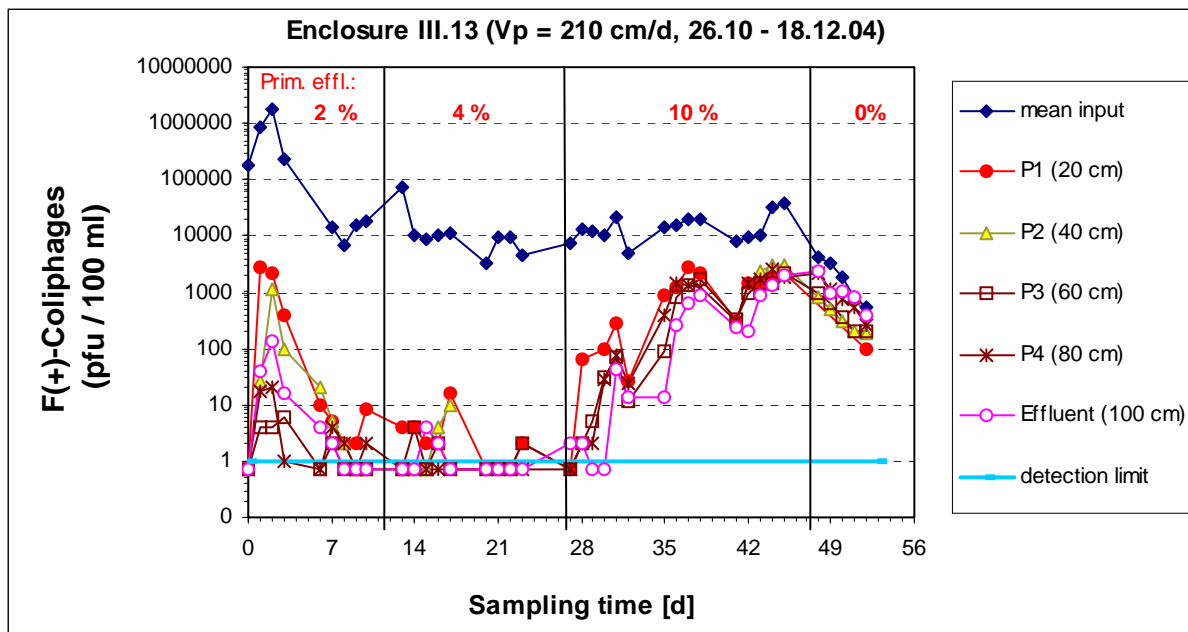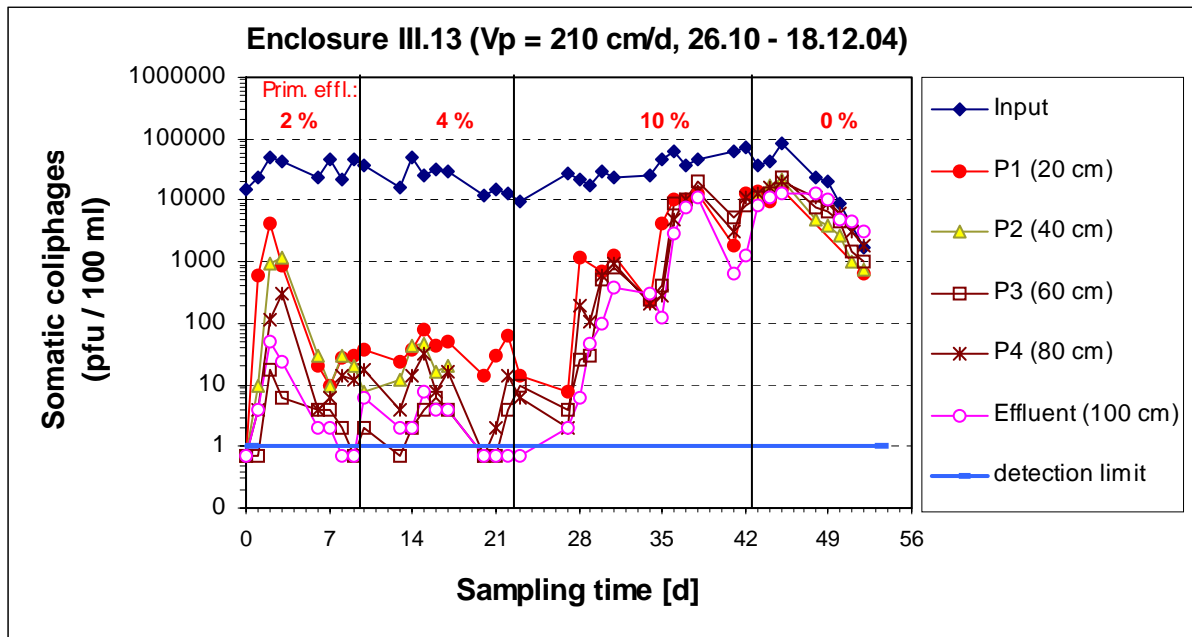
Figure 56: Retention of F+phages in Enclosure III with continuous percolation of primary effluent at different concentrations (pore velocity = 210 cm/d)

Relatively high concentrations of F+ phages were found in filtrate samples taken after 2 or 3 days (Figure 56). Consequently, breakthrough ratios of F+ phages during the initial phase of the experiment were relatively high, e.g. 0,002 or 0,0004 (corresponding to a log-retention of 2,7 and 3,4 log units) after a filtration path of 20 or 40 cm, respectively (Figure 56, Table 67). Retention increased to 3,5 or 3,7 log units in the further run of the experiment, during an operation time of 10 days. After rising of wastewater portion in the reservoir to 4 %, removal of F+ phages persisted at a high level of 4 log units during the further percolation time of two weeks. As the amount of waste water in the reservoir increased to 10 %, concentrations of F+ phages increased about three log units in filtrate samples at all sampling sites. Correspondingly, retention of F+ phages decreased to about one log unit at all sampling sites.

Table 67: Retention (log10) of F+ coliphages in Enclosure III during continuous filtration of primary effluent at different concentrations (pore velocity 210 cm/d, 26.10. – 18.12.04)

Wastewater (%)	P1 (20 cm)	P2 (40 cm)	P3 (60 cm)	P4 (80 cm)	Effluent (100 cm)
2 (initial)	2,7	3,4	3,6	4,9	4,2
2 (after 10 d)	3,5	3,7	3,6	3,5	3,0
4	3,5	3,5	3,8	4,1	3,8
10	1,2	1,2	1,4	1,3	1,7
0	0,9	0,6	0,6	0,3	0,2

The concentration of somatic phages in reservoir water varied between 1.104 and 8.104 pfu/ml during continuously contamination with primary effluent in increasing portions up to 10 % (Figure 57). Less retention of somatic coliphages has been observed than that of F+ phages. During the first three days, a relatively high amount of phages were detected in filtrate samples at all sampling sites that resulted in a breakthrough ratio of 0,04 at the upper part of the enclosure (20 cm), and 0,0006 in the total effluent at 100 cm depth. These breakthrough ratios were comparable to the ratios found when a sluggish peak inoculum of coliphages was applied (see 6.2.1-6.2.3).

During further percolation of the enclosure with 2 % primary effluent, retention of somatic phages increased clearly to 3,1 log units within 20 cm, and more than 4 log units in the effluent samples. A relatively high and stable retention of somatic phages in the enclosure was still observed when the amount of primary effluent was increased to 4 %. Log-retentions were 2,7 log at 20 cm and about 4 log units in the effluent (Table 68).

When the amount of primary effluent was increased to 10%, concentration of somatic phages was increasing by three log units in all filtrate samples (Figure 57). Correspondingly, retention decreased to about one log unit at all sampling sites (Table 68). Breakthrough ratios were 0,14 at the surface filter path, and 0,08 in the total effluent of the enclosure.

Table 68: Retention (log10) of somatic coliphages in Enclosure III during continuous filtration of primary effluent at different concentrations (pore velocity 210 cm/d, 26.10. – 18.12.04)

| Wastewater (%)	P1 (20 cm)	P2 (40 cm)	P3 (60 cm)	P4 (80 cm)	Effluent (100 cm)
2 (initial)	1,4	1,8	3,7	2,5	3,6
2 (after 10 d)	3,1	3,2	4,1	3,5	4,2
4	2,7	3,0	3,6	3,3	4,0
10	0,9	0,8	0,9	0,9	1,1
0	0,6	0,6	0,4	0,2	0,04

Figure 57: Retention of somatic coliphages in the Enclosure III with continuous percolation of primary effluent at different concentrations (pore velocity = 210 cm/d)

Following continuously spiking of primary effluent, concentration of E. coli in the reservoir water varied between 2.104 and 2.105 mpn/100 ml at the initial phase of the experiment with 2 % of primary effluent and slightly enhanced up to 1.106 mpn/100 ml as the amount of primary effluent was increased to 4 % and 10 % (Figure 58). Retention of E. coli was high during the first four weeks of operation with 2 % to 4 % of primary effluent. Most of the filtrate samples were free from E. coli in 100 ml volume. E. coli was only sporadically detected in filtrate samples from different sampling sites at concentrations of 3-100 mpn/100 ml. During this part of the experiment retention of E. coli varied between 3 and 5 log units (Table 69).

Increase of primary effluent concentration to 10 % led to a breakthrough of E. coli in filtrates at all sampling sites. Concentrations of E. coli in filtrate samples increased with percolation time up to concentration levels in the reservoir water. Correspondingly, log-retention decreased to 0,3 to 0,7 log units (Table 69). Breakthrough ratios averaged to 0,35 at 20 cm, 0,31 at 60 cm, and 0,19 in effluent from 100 cm.

Table 69: Retention (log10) of E. coli in the Enclosure III during continuous filtration of primary effluent at different concentrations (pore velocity 210 cm/d, 26.10. – 18.12.04)

Wastewater (%)	P1 (20 cm)	P2 (40 cm)	P3 (60 cm)	P4 (80 cm)	Effluent (100 cm)
2	3,9	5,0	3,0	3,6	3,7
4	4,9	5,7	5,3	4,2	4,3
10	0,5	0,3	0,5	0,8	0,7
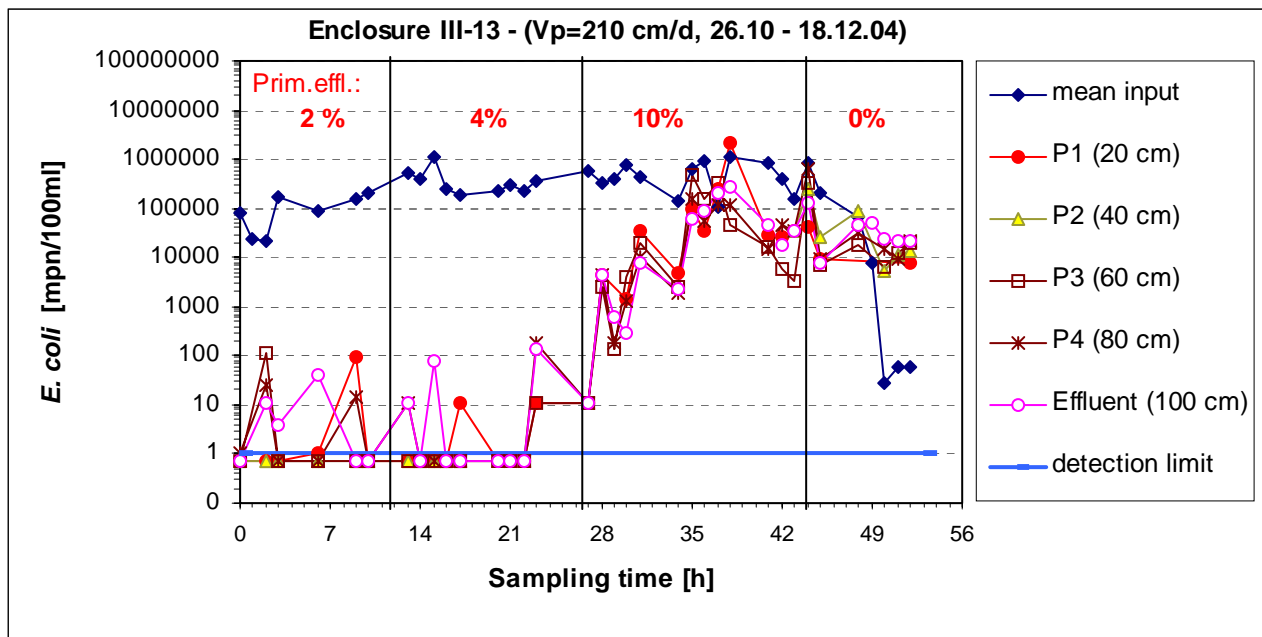
Figure 58: Retention of E. coli in the Enclosure III with continuous percolation of primary effluent at different concentrations (pore velocity = 210 cm/d)

Concentrations of intestinal enterococci in the water reservoir of the enclosure were in most cases between 104 and 105 mpn/100 ml. Filtrate samples from different sampling sites were sporadically positive for enterococci during the infiltration of 2 % and 4 % primary effluent (Figure 59). About 4 log units of intestinal enterococci were removed in the enclosure during this part of the experiment (Table 14). After increasing the amount of primary effluent to 10 %, enterococci were detected in filtrates from all sampling sites. The removal of enterococci diminished to about one log unit at most sampling sites (Table 70).

Table 70: Removal of intestinal enterococci (log10) in Enclosure III during continuous filtration of primary effluent at different concentrations (pore velocity 210 cm/d, 26.10. – 18.12.04)

Wastewater (%)	P1 (20 cm)	P2 (40 cm)	P3 (60 cm)	P4 (80 cm)	Effluent (100 cm)
2	3,0	4,3	3,6	4,4	4,4
4	4,1	4,9	3,5	3,4	3,6
10	0,2	1,1	1,1	1,2	1,0
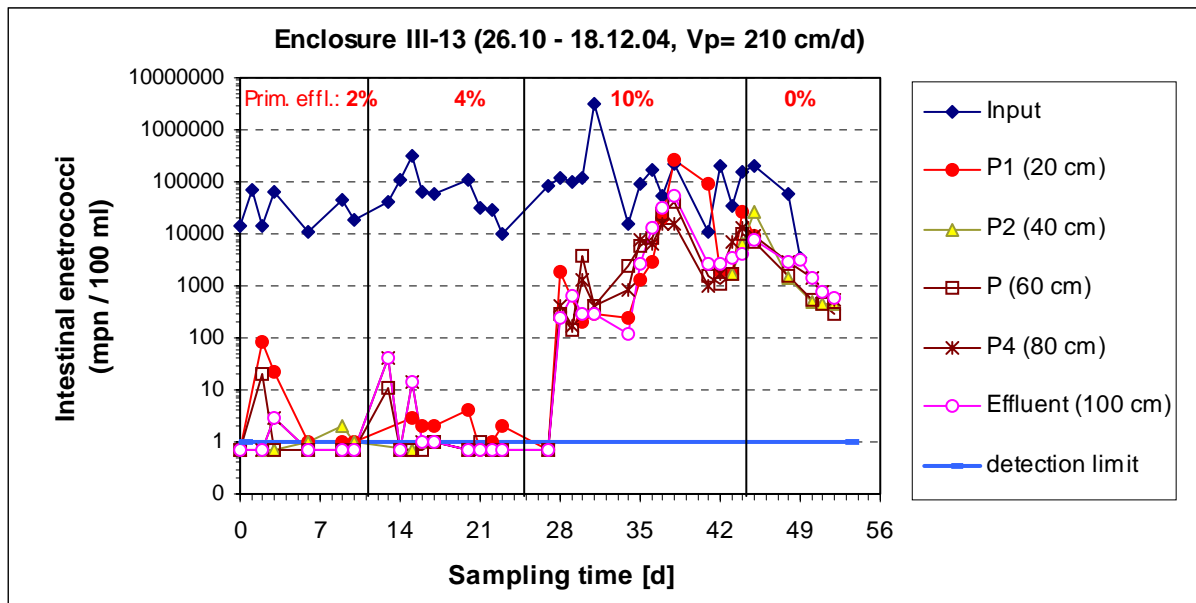
Figure 59: Retention of intestinal enterococci in Enclosure III with continuous percolation of primary effluent at different concentrations (pore velocity = 210 cm/d)

6.2.7 Core samples

Seven cores of the filter material in the enclosure were taken during and after experiment 3 in Enclosure III (days 1, 3, 4, 11, 23, 53, and 71. The cores were divided into 5-10 cm sections which were analysed for total bacteria (DAPI), E. coli, enterococci as well as the two coliphages. Additionally, the clogging layer and the core samples were examined microscopically.

Both, bacteria and coliphages survived in the filter sand for extended periods of time. Concentrations of 1-100 cfu/g E. coli were, for example, detected in core samples from all depths 71 days after inoculation. This long term survival potential in the filter bed may explain the sporadicac appearance of indicator bacteria and coliphages in the effluent of the filters several weeks after inoculation.

6.2.7.1 Characterisation of the clogging layer

The dominating organisms found in the clogging layer were algae of different groups (diatoms, gold and green algae) together with amoebae. Occasionally higher organisms (e.g. gastrotrichs) were found (Table 71, Figure 60). Cyanobacterium microcystis, which had been applied to the filter together with the microcystin was found in the clogging layer at all sampling times.

Table 71: organisms identified in the clogging layer

Cyanobacteria :   Microcystis spec.

Diatoms :   Navicula spec.
                     Synedra spec.
                     Anomoeoneis spec.
                     Nitzschia spec.

Gold algae :   Dinobryon spec.

Green algae :   Chlorococcum spec.
                     Euastrum spec.

Amoebae :   Actinosphaerium spec.
                     Testacea , ambiguous

Gastrotichs :   Chaetonotus spec.

„Schmutzdecke" enclosure
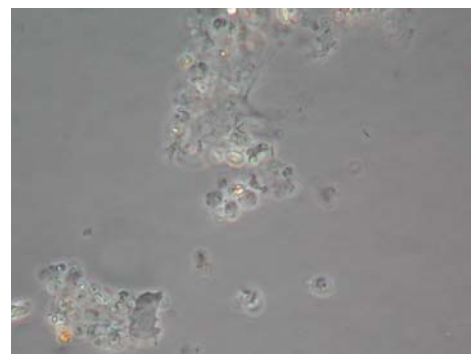
Amoeba, sediment et al.
magnification1000

Diatoms and single cell greenalgae
magnification 400
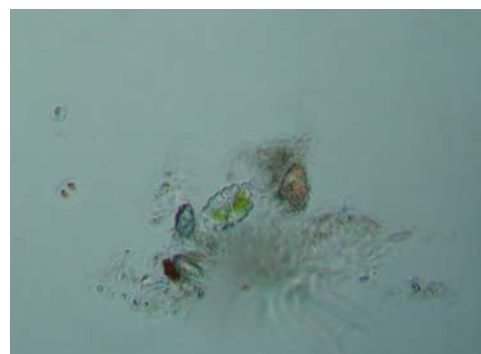
„Jochalge" Euastrum spec.
magnifigation 1000

Figure 60: typical organisms in the upper sand layers of the enclosure

6.2.7.2 Examination of the filter cores

Filter cores were analysed for total bacteria using DAPI staining and fluorescence microscopy. Concentrations between 10^8 and 10^9 cfu/g dry weight were found in all samples (Figure 61). No correlation between the concentration of the bacteria and the depth of the filter was detected. Similar results were obtained from the GWA Tegel (results not shown).
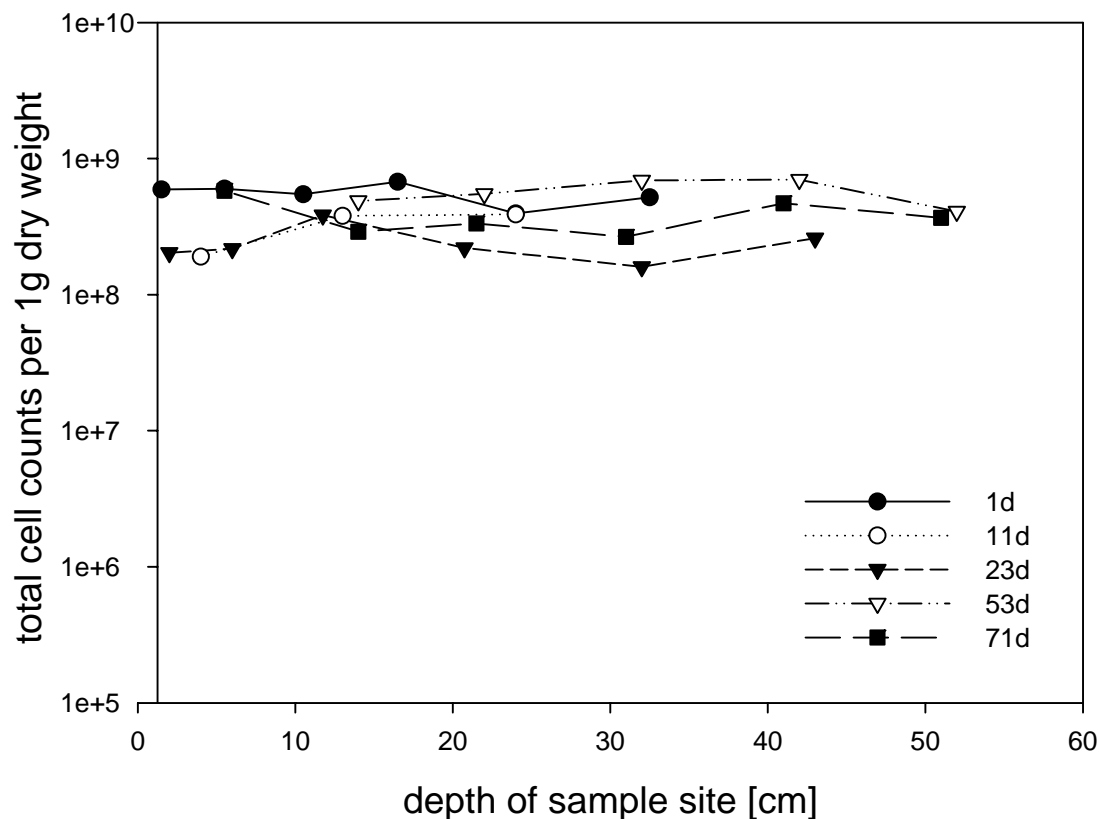
Figure 61: Total cell counts per 1g dry weight determined by DAPI staining in sediment samples taken from the enclosure during the filtration experiment.

The filter cores were analysed for both bacteriophages since the previous experiment had been carried out with coliphage 138. Coliphage 138 was still detected in concentrations of 10-70 pfu/g wet weight in the beginning of the experiment. After 23 days, these coliphages were only detected sporadically in very low numbers (< 1-3 pfu/ g, data not shown).

Coliphage 241 was detected in very low concentrations (1-5 pfu/g wet weight) before the start of the experiment in all sampling depths. High concentrations were found at day 3 and 4 after inoculation. Concentrations decreased with depths (Figure 62). In the upper layers concentrations ranged from $3 \times 10^3 - 1.5 \times 10^4$ pfu/g wet weight. In the lower layers,

concentrations increased from day 2 to day 3 from 10 to several hundred pfu/g. Coliphage 241 was still present after 23 days in all sampling depth at concentrations of 100-300 pfu/g.
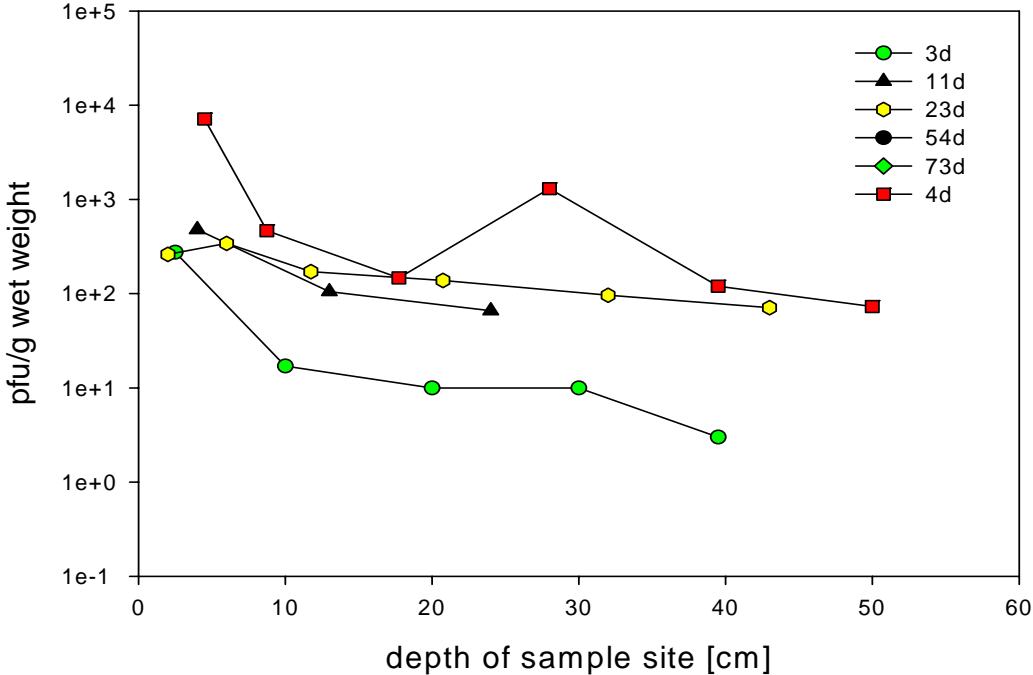
Figure 62: Concentration of coliphage 241 in sediment samples taken from the enclosure during the experiment (no data at day 54 and 73).
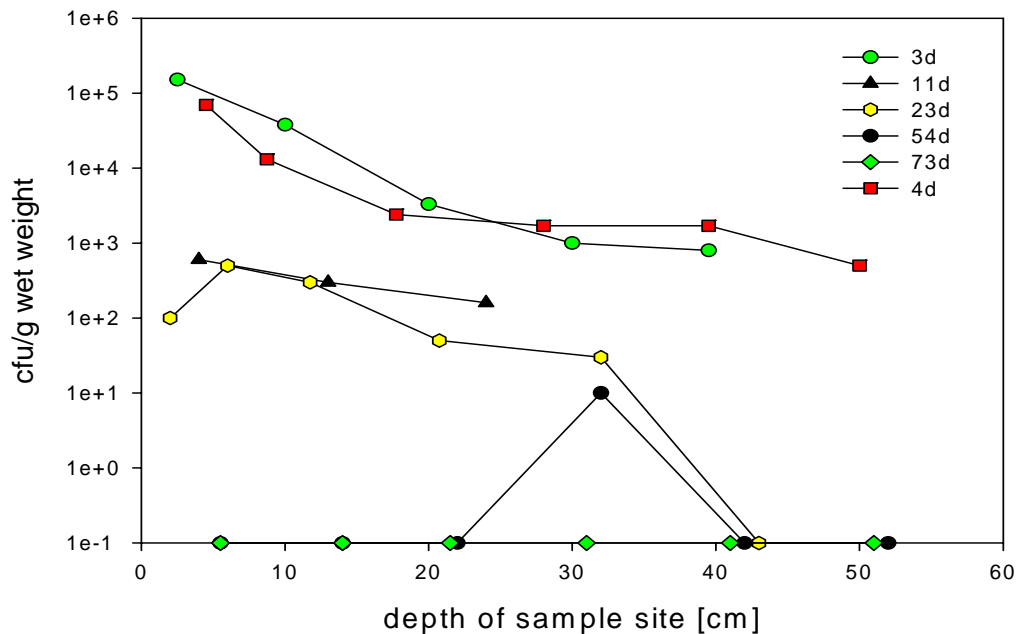
Figure 63: Concentration of enterococci in sediment samples taken from the enclosure during the filtration experiment (detection limit 1 cfu/g).

Enterococci were not detected in core samples before inoculation. After inoculation, concentrations were in the range of $1\text{-}8 \times 10^4$ cfu/g wet weight in the upper layers and decreased to about 1000 cfu/g in a depth of 40-50 cm (Figure 63). Concentrations decreased after 2-3 weeks to 100-600 pfu/g in the upper layers and to below detection limit in 40-50 cm depth. Enterococci were detected in only one core sample at day 53 and in none of the core samples at day 71.

E. coli was not detected in core samples before inoculation. Concentrations were above the detection limit at day 3 after inoculation (data not shown). At day 4 very high concentrations of 10^5 cfu/g wet weight were detected in the upper layers of the filter (Figure 64). Concentrations decreased with depths and were in the range of $10^3\text{-}10^4$ cfu/g in 20-50 cm. E. coli survived better in the filter than the enterococci. Concentrations of 1-100 cfu/g were detected in all core samples even after 71 days of percolation.
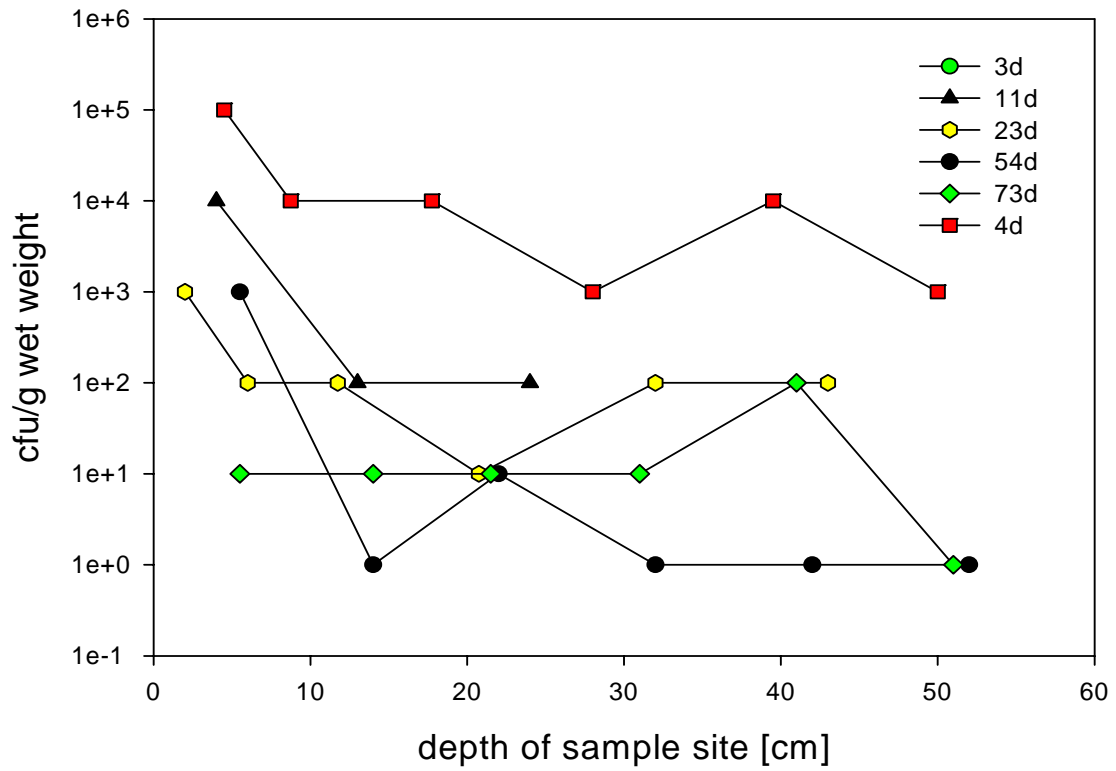
Figure 64: Concentration of E. coli in sediment samples taken from the enclosure during the experiment (no data at day 3, detection limit 1 cfu/g).

6.3 Summary

After a bloc injection, a part of test organisms break through the filter column synchronic with tracer salt NaCl. The filtration (retention) equilibrium occurred (was observed) within a percolation time of 12 h. The cumulative breakthrough of test organisms has marginally increased during the further operation time up to two weeks.

Despite to this early breakthrough, high retention of test organisms was determined in the enclosure by aerobic conditions which averaged to 3 log units for both coliphages and 2 log units for the indicator bacteria.

Developing a clogging layer had no clear effect on removal or mobility of test organisms.

The elimination of test organisms in the filter column was not homogenous, the highest level of retention was detected in the top layer of filtration column which declined significantly in the deeper layers tested.

On continuously contamination of enclosure with test organisms and by micro aerophile conditions corresponding to a dissolved oxygen content less than 0,2 mg/L, the removal of all test organisms decreased significantly.

Continuously inoculation of primary effluent at a concentration ranged from 2 - 10 % of filtrate volume has shown a moderate elimination rate of coliphages, approximately 2 log units during the initial phase of process. The retention of phages increased significantly, up to four log units during an operation time of 4 weeks. Removal of indicator bacteria was measured not less than four log units within this phase of operation. An increase of primary effluent rate to 10 % abruptly led to a breakthrough of all test organisms. Less than one log unit viral and bacterial contaminants were removed by further operation in enclosure.

Annex – ENCLOSURE
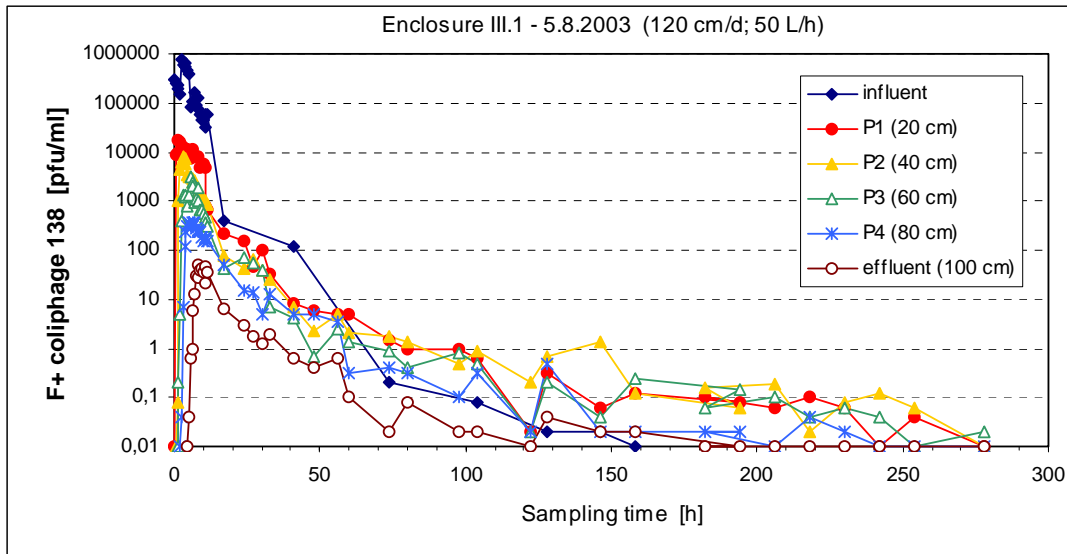
Figure 65 Concentration of F+phage 138 at different sampling levels of the enclosure by absence of an apparent biomass on the filter surface and at a pore velocity of 360 cm/d.
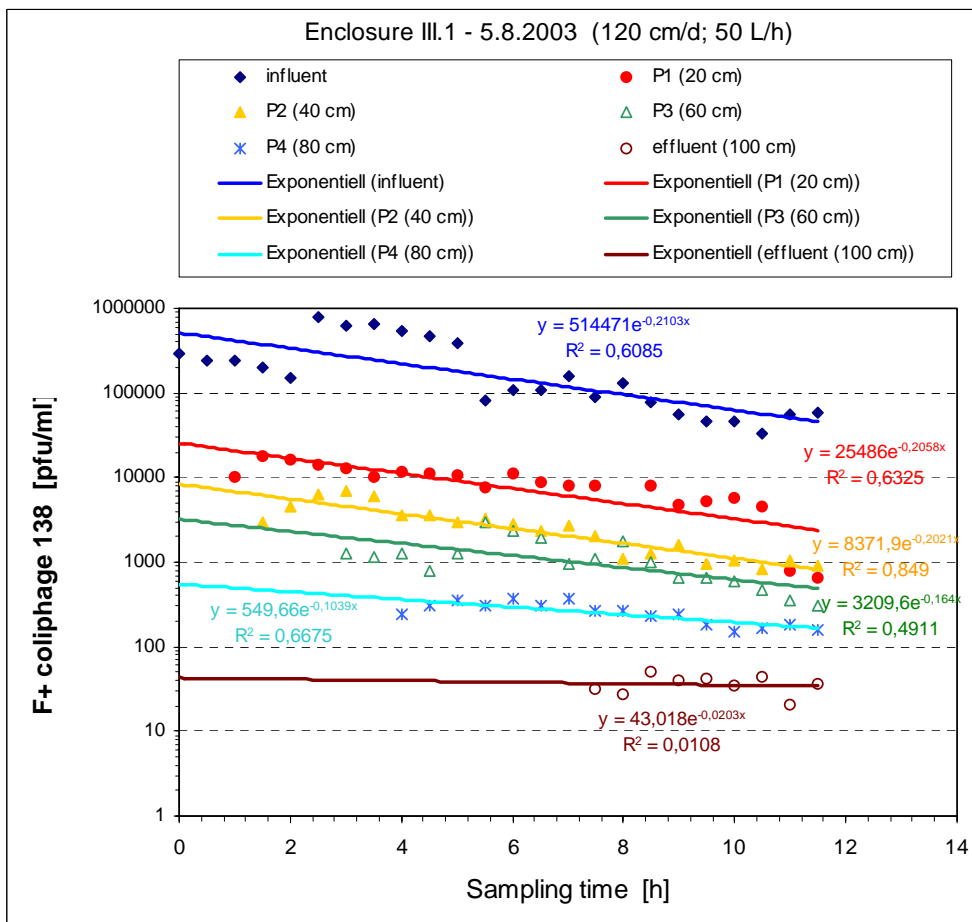
Figure 66 Regression lines of the F+ coliphage 138 concentrations at different sampling levels of the enclosure before forming any apparent biomass and at a pore velocity of 360 cm/d.
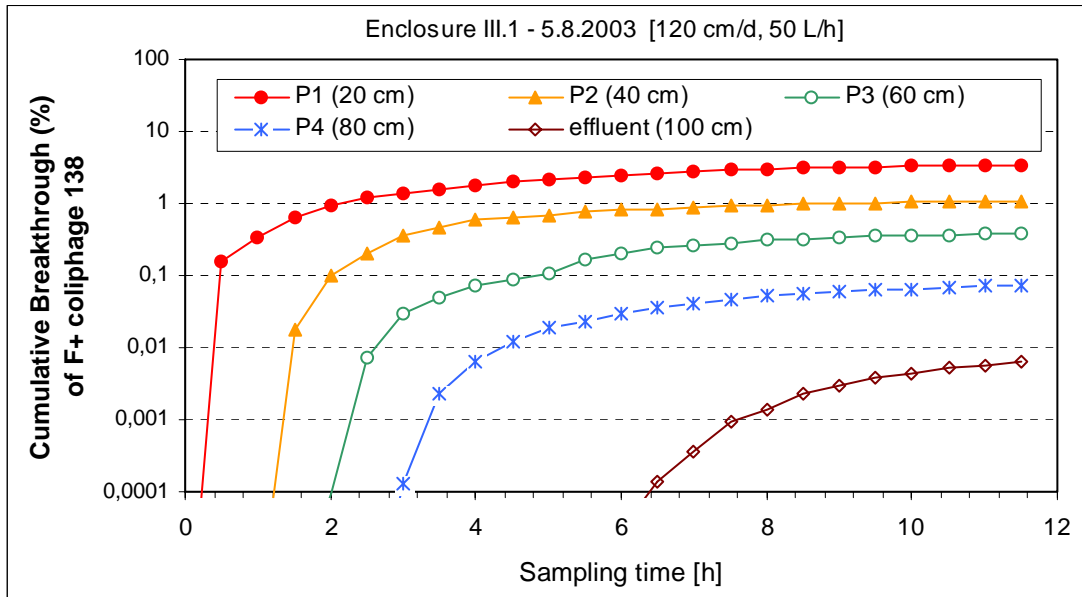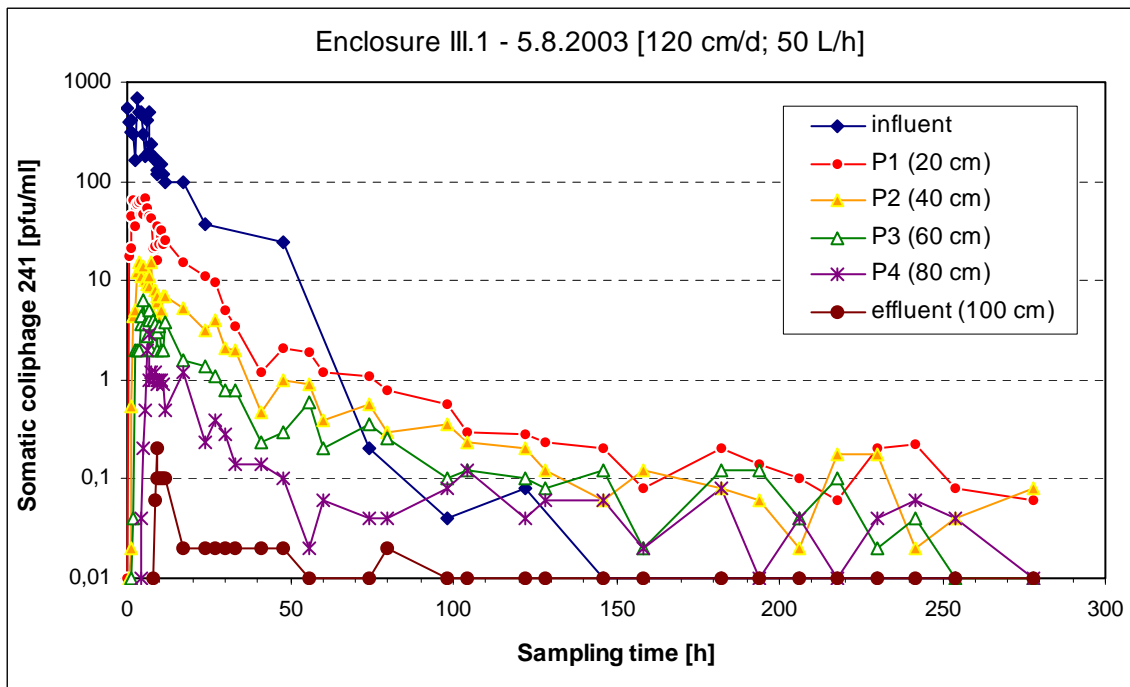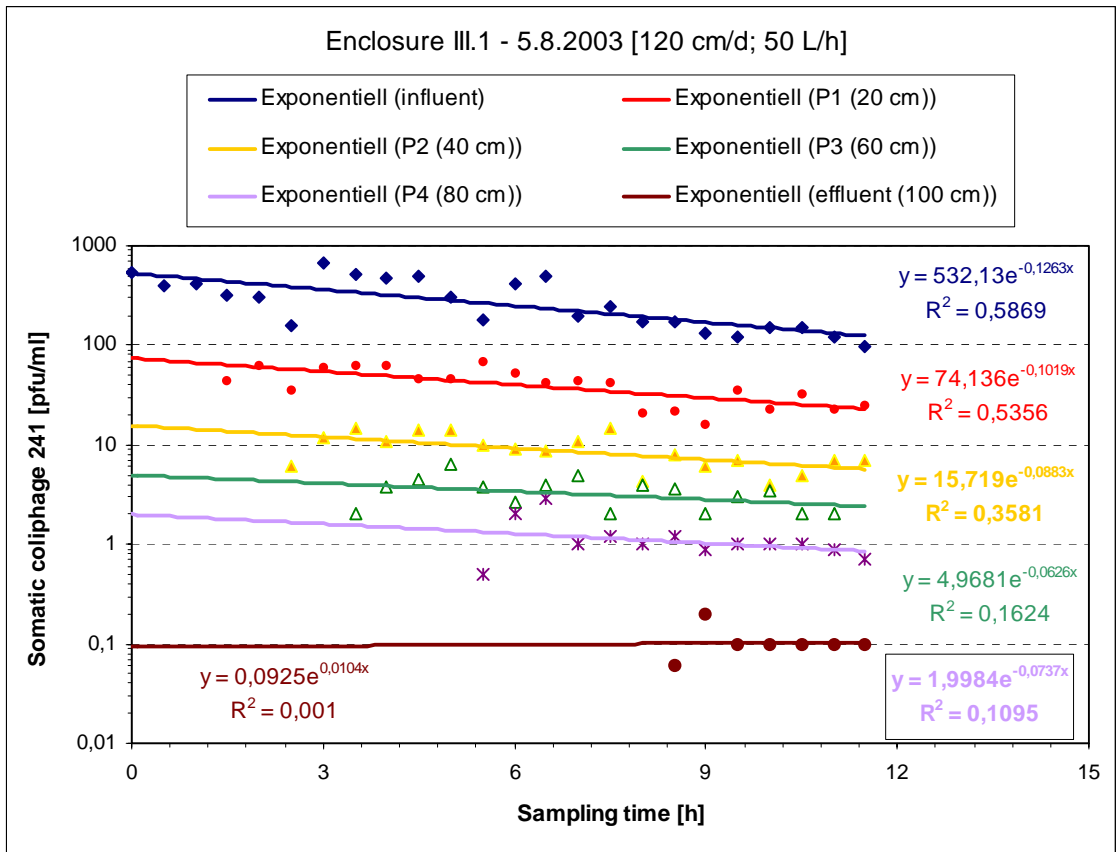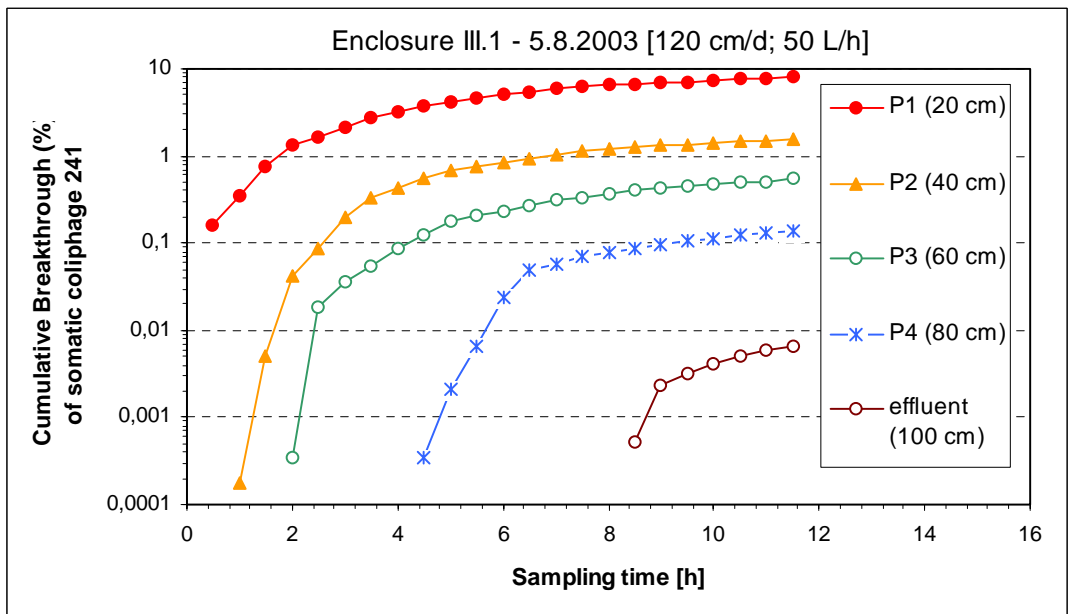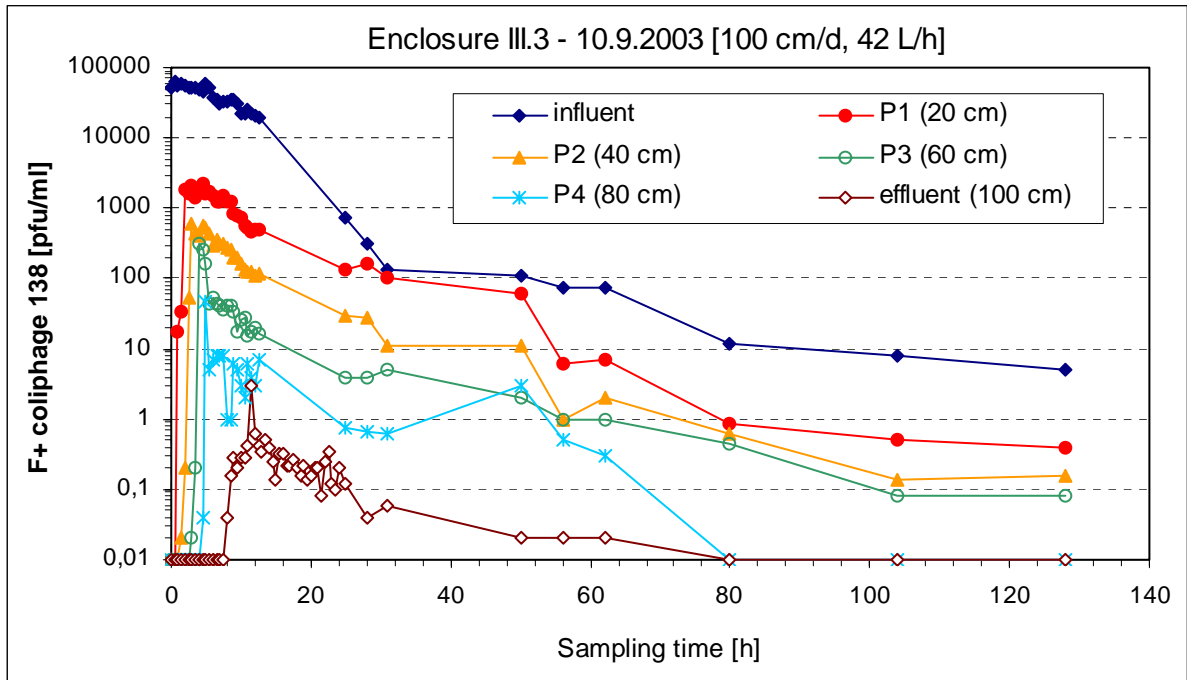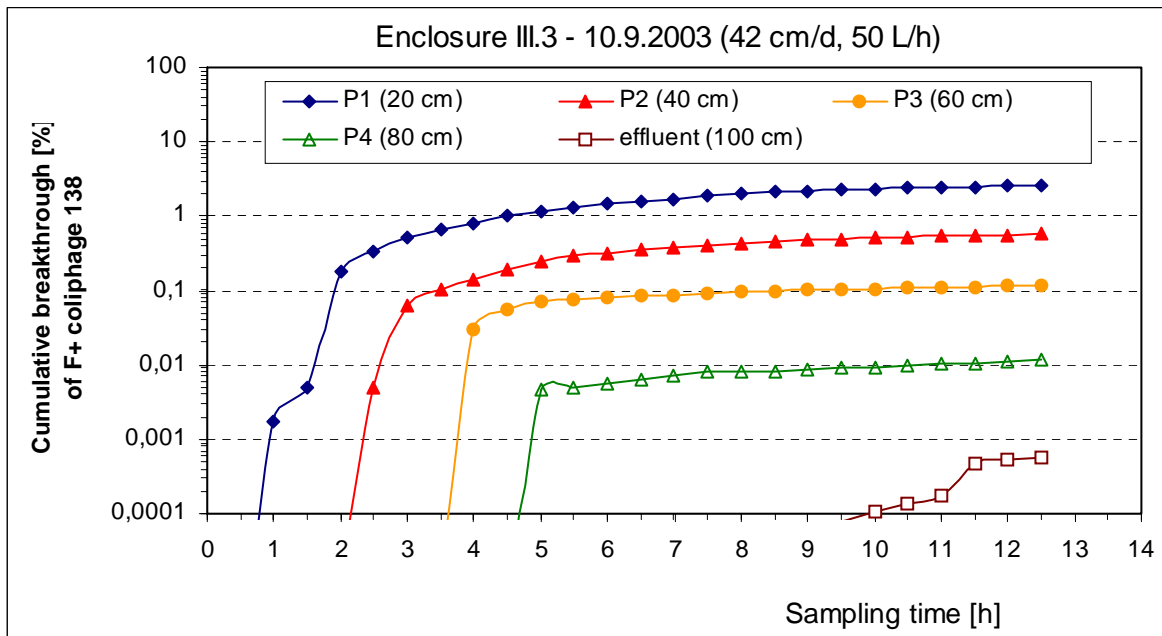
Figure 67: Cumulative breakthrough of F+ coliphage 138 at different sampling sites of the enclosure before forming any apparent biomass and at a pore velocity of 360 cm/d.
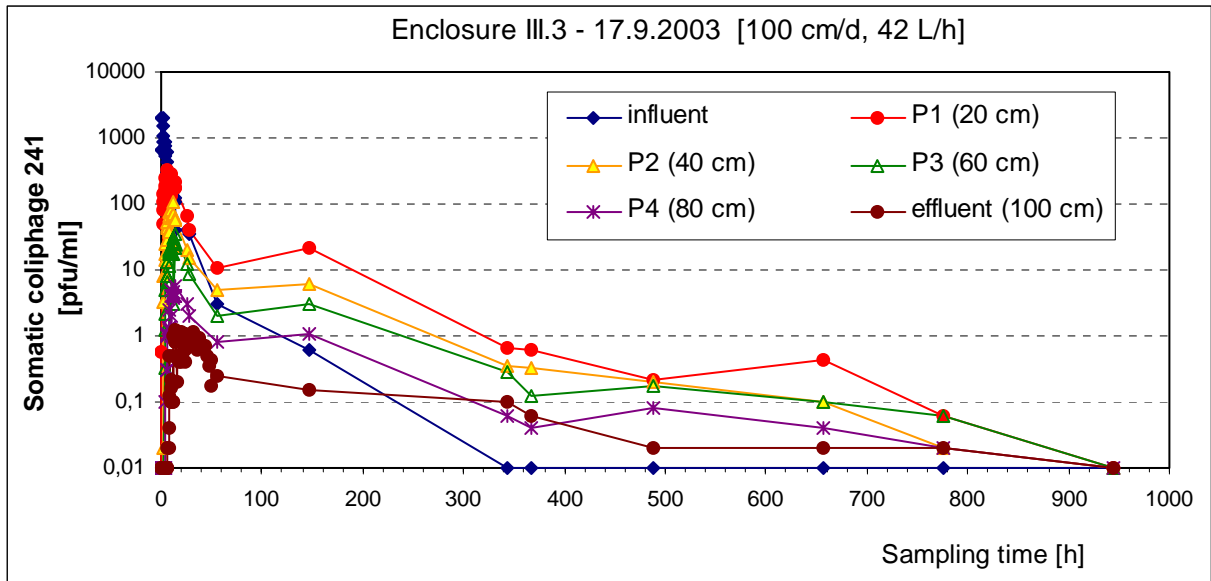

Figure 68: Concentration of somatic coliphage 241 in different sampling levels of the enclosure before forming any apparent biomass and at a pore velocity of 360 cm/d.
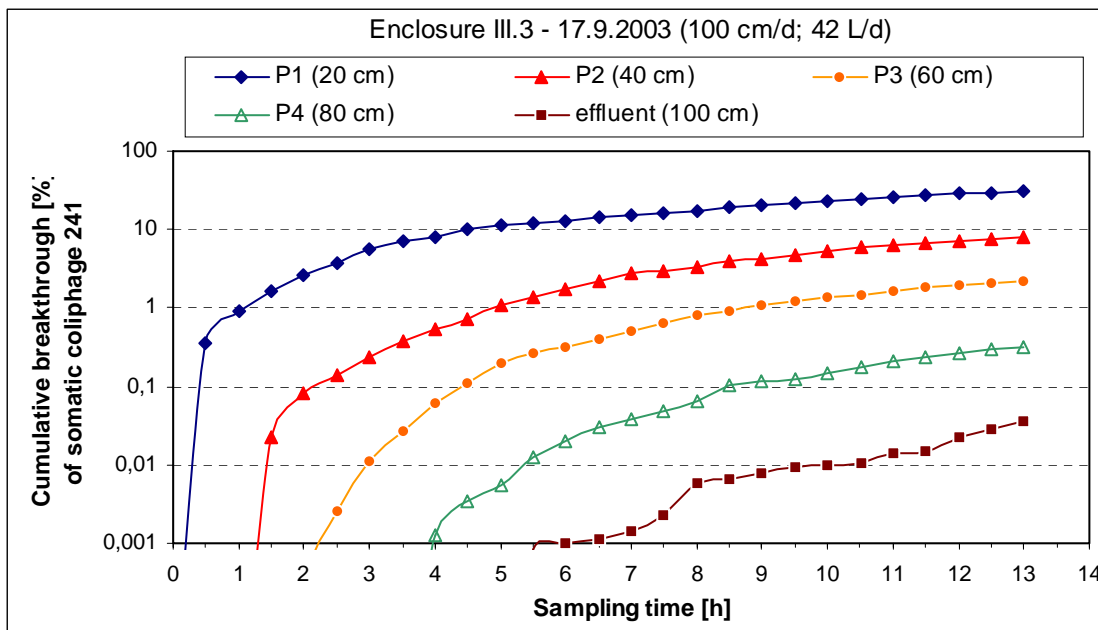
Figure 69 Regression lines of somatic coliphage 241 concentrations at different sampling levels of the enclosure before forming any apparent biomass and at a pore velocity of 360 cm/d.

Figure 70: Cumulative breakthrough of somatic coliphage 241 at different sampling sites of the enclosure before forming any apparent biomass and at a pore velocity of 360 cm/d.
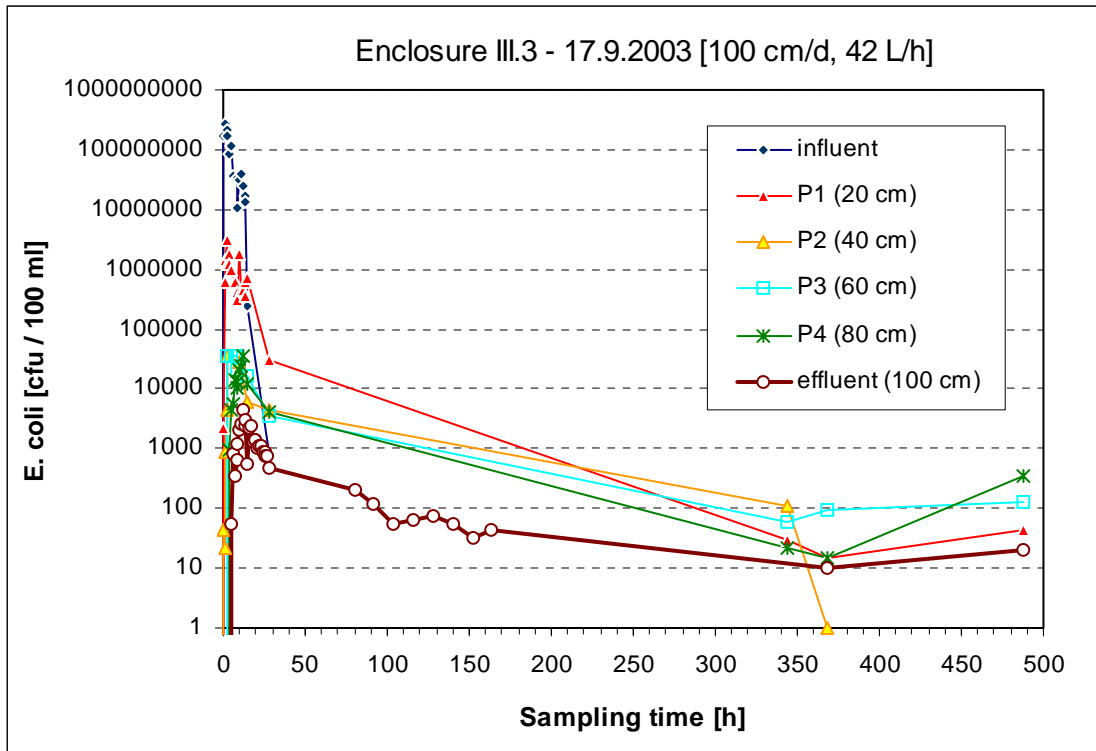
Figure 71 Concentration of F+ coliphage 138 in different sampling levels of the enclosure after forming an apparent biomass and at a pore velocity of 300 cm/d.
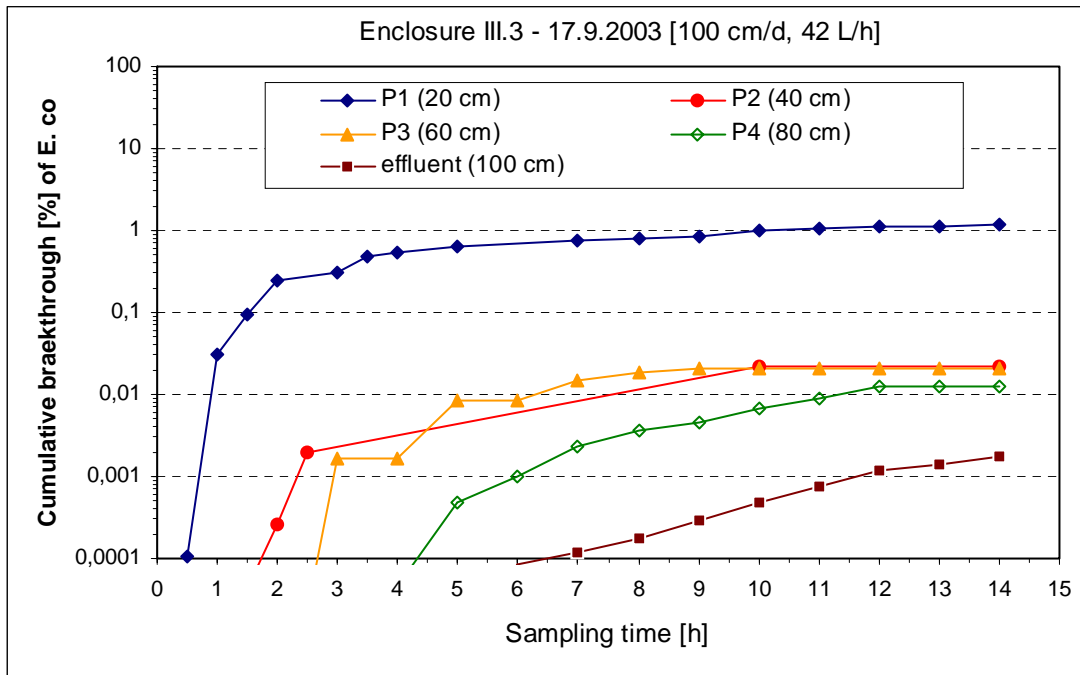

Figure 72 Cumulative breakthrough of F+ coliphage 138 at different sampling sites of the enclosure after forming an apparent biomass and at a pore velocity of 300 cm/d.

Figure 73 Concentration of somatic coliphage 241 in different sampling levels of the enclosure after forming an apparent biomass and at a pore velocity of 300 cm/d.

Figure 74 Cumulative breakthrough of somatic coliphage 241 at different sampling sites of the enclosure after forming an apparent biomass and at a pore velocity of 300 cm/d.

Figure 75 Concentration of E. coli in different sampling levels of the enclosure after forming an apparent biomass and at a pore velocity of 300 cm (detection limit 10-15 cfu/100 ml)

Figure 76 Cumulative breakthrough of E. coli at different sampling sites of the enclosure after forming an apparent biomass and at a pore velocity of 300 cm/d
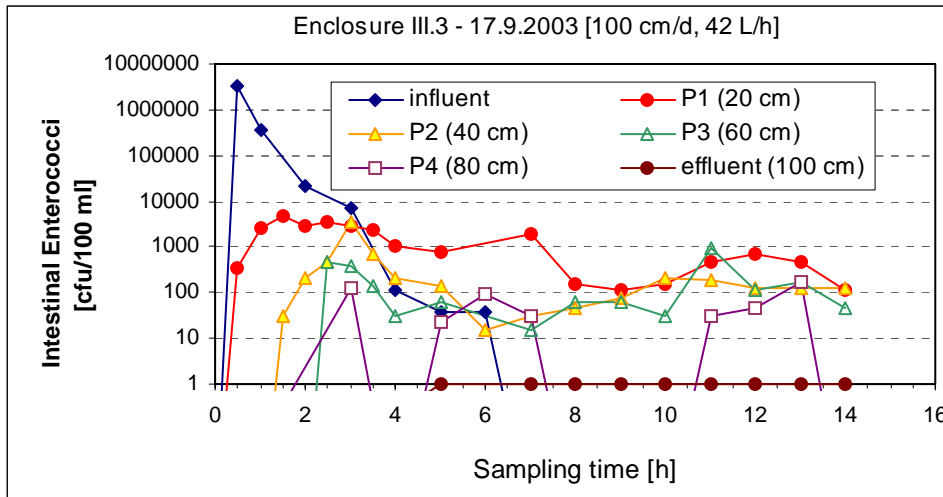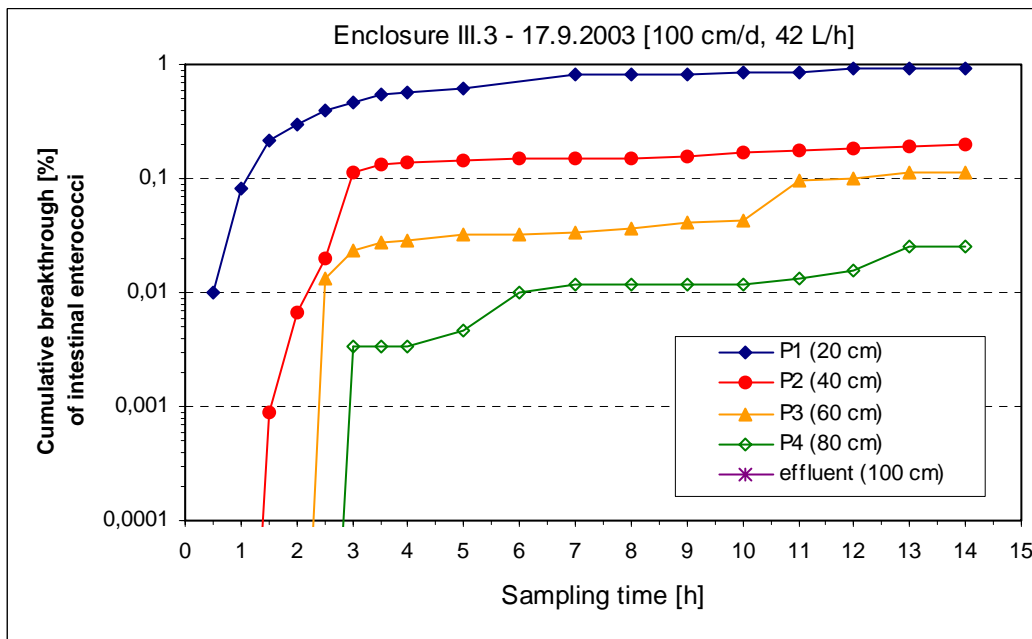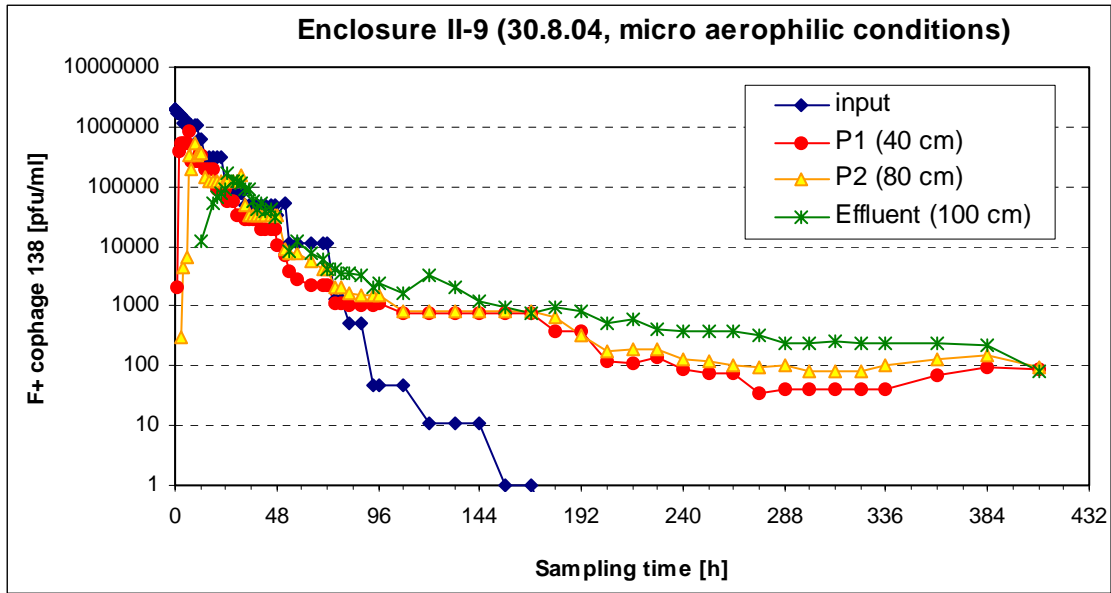
Figure 77 Concentration of E. faecium in different sampling levels of the enclosure after forming an apparent biomass and at a pore velocity of 300 cm (detection limit 10-15 cfu/100 ml)

Figure 78 Cumulative breakthrough of E. faecium at different sampling sites of the enclosure after forming an apparent biomass and at a pore velocity of 300 cm/d

Figure 79 Retention and transport behaviour of F+ coliphages in the enclosure II under micro aerophilic conditions at a pore velocity of 210 cm/d.
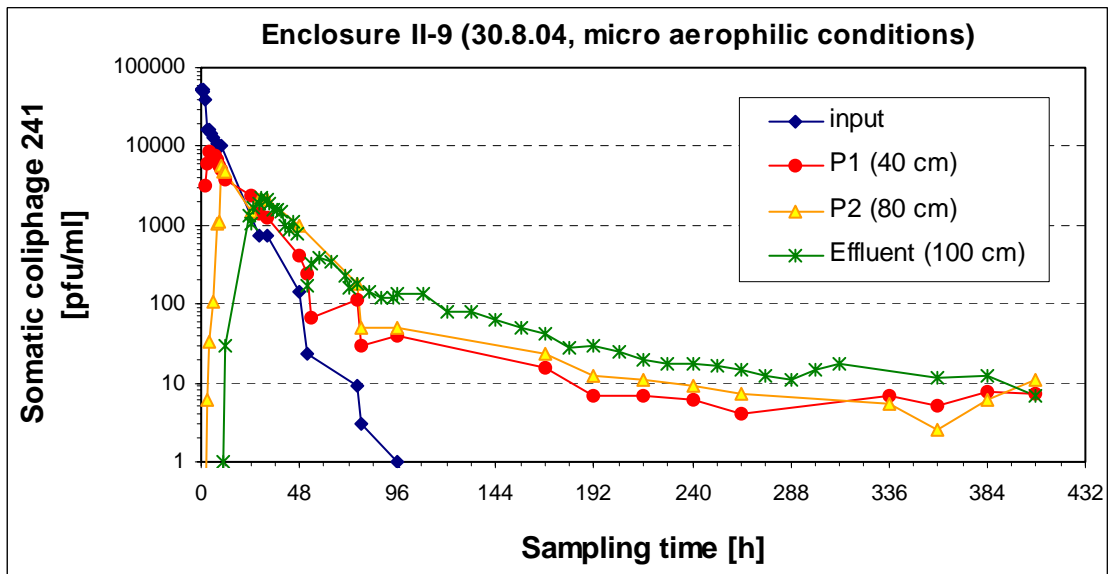

Figure 80 . Retention and transport behaviour of somatic coliphages in the enclosure II under micro aerophilic conditions at a pore velocity of 210 cm/d.
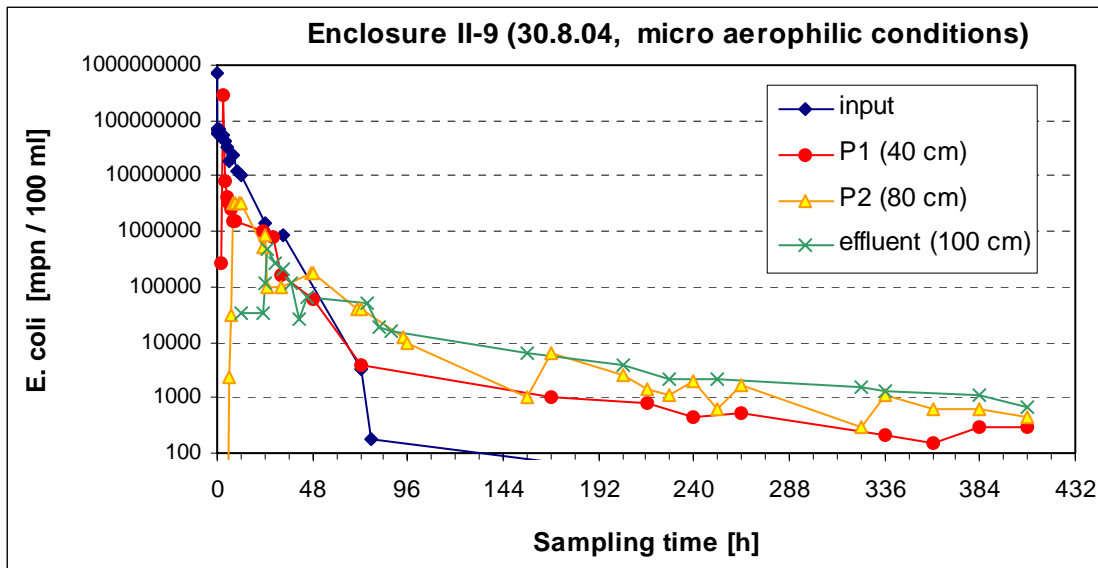
Figure 81 Retention and transport behaviour of E. coli in the enclosure II under micro aerophilic conditions at a pore velocity of 210 cm/d.